



Cryogenic On-Orbit Liquid Depot–Storage, Acquisition and Transfer (COLD-SAT) Experiment Conceptual Design and Feasibility Study

Edward Kramer, Editor
Lewis Research Center, Cleveland, Ohio

National Aeronautics and
Space Administration

Lewis Research Center

Acknowledgments

The work presented here was performed by a large number of people, both contractor employees and civil servants, associated with the NASA Lewis Research Center. Only a few are identified as authors of the various chapters in this report. Without the dedicated efforts of all of these people, both named and unnamed, the large amount of work presented here could never have been accomplished.

In addition, the quality of the presentation of this information has been greatly enhanced by the efforts of the NASA Lewis Research Center Publishing Services group. Of this group, Kathleen M. Healey, Editor; John Jindra and Nancy C. Mieczkowski, Graphic Artists; Denise A. Easter and Theresa C. Young, Manuscript Preparation; and Athina D. Crawford, Layout Artist, deserve special mention for their fine and patient work.

Trade names or manufacturers' names are used in this report for identification only. This usage does not constitute an official endorsement, either expressed or implied, by the National Aeronautics and Space Administration.

Available from

NASA Center for Aerospace Information
7121 Standard Drive
Hanover, MD 21076
Price Code: A99

National Technical Information Service
5287 Port Royal Road
Springfield, VA 22100
Price Code: A99

Contents

Contributors	xvii
Chapter 1—Introduction	1
1.0 Introduction	1
1.1 Scope	1
1.2 Related Documents	2
1.3 Relationship to Other Studies	3
1.4 Goals of COLD-SAT Program	3
1.5 Goals of In-House Study	3
Chapter 2—Requirements and Constraints	5
2.0 Introduction	5
2.1 Experiments	5
2.1.1 Low-Gravity Tank Pressure Control	5
2.1.1.1 Experiment Description	6
2.1.1.2 Experiment Requirements	6
2.1.2 No-Vent Fill and Refill	6
2.1.2.1 Experiment Description	6
2.1.2.2 Experiment Requirements	7
2.1.3 Cryogenic Tank Chillover	7
2.1.3.1 Experiment Description	7
2.1.3.2 Experiment Requirements	7
2.1.4 Fill and Refill of Liquid Acquisition Devices	7
2.1.4.1 Experiment Description	7
2.1.4.2 Experiment Requirements	7
2.1.5 Cryogenic Mass Gaging	8
2.1.6 Slosh Dynamics	8
2.1.7 Tank Thermal Performance	8
2.1.8 Pressurization of Cryogenic Tankage	8
2.1.8.1 Experiment Description	8
2.1.8.2 Experiment Requirements	8
2.1.9 Outflow and Vented Fill With Settling	8
2.1.9.1 Experiment Description	8
2.1.9.2 Experiment Requirements	9
2.1.10 Liquid Acquisition Device Performance	9
2.1.10.1 Experiment Description	9
2.1.10.2 Experiment Requirements	9
2.1.11 Transfer Line Chillover	9
2.1.12 Control of Thermodynamic State During Outflow	9
2.1.12.1 Experiment Description	9
2.1.12.2 Experiment Requirements	9
2.1.13 On-Orbit Cryogenic Fluid Dumping	10
2.1.13.1 Experiment Description	10
2.1.13.2 Experiment Requirements	10

2.1.14 Advanced Instrumentation	10
2.1.15 Partial Communication Liquid Acquisition Device (LAD) Performance	10
2.2 Orbital Requirements	10
2.3 Flight Communications	11
2.4 Schedule	11
2.5 Reliability	11
2.6 Safety	11
2.7 Testing	11
2.8 Policy	11
2.9 System Design Decisions	12
2.9.1 Mass Margin	12
2.9.2 Modular Design	12
2.9.3 Electromagnetic Compatibility	12
References	12
Appendix A—Pressure Control Experiment Requirements	13
Appendix B—No-Vent Fill Experiment Requirements	14
Appendix C—Chilldown Experiment Requirements	15
Appendix D—Fill and Refill of Liquid Acquisition Device (LAD) Experiment Requirements	17
Appendix E—Settled Outflow/Vented Fill Requirements	17
Appendix F—Liquid Acquisition Device (LAD) Performance Experiment Requirements	18
Appendix G—Tank Dumping Experiment Requirements	19
Chapter 3—System Overview	21
3.0 Introduction	21
3.1 Overall System Concept	21
3.2 Spacecraft Concept	21
3.2.1 Experiment System	23
3.2.2 Spacecraft Systems	25
3.2.2.1 TT&C System	25
3.2.2.2 Electric Power System	25
3.2.2.3 Attitude Control	26
3.2.2.4 Propulsion System	27
3.2.2.5 Thermal Control System	27
3.2.2.6 Structure and Configuration	27
3.2.2.7 Software	27
3.3 Ground Segment	28
3.4 Launch Vehicle	28
3.5 Operations	29
Chapter 4—Mission	31
4.1 Introduction	31
4.2 Orbit Selection Criteria	31
4.3 Attitude Selection	32
4.3.1 Disturbance Torques	34
4.3.2 Orbit Perturbations Due to Thrusting	35
4.3.3 Other Factors in Spacecraft Attitude Selection	37
4.3.4 Final Selected Attitude	38
4.4 Expendable Launch Vehicle Selection	41
4.4.1 Payload Volume Considerations	41
4.4.2 Launch Vehicle Lift Capability	41
4.4.3 Constraints on Mass Properties	41
4.4.4 Launch Pad Capabilities	42
4.4.5 Final Selection	43
4.5 Selected Orbit	43
References	45

Chapter 5—COLD-SAT Experiment System	47
5.1 Experiment System Design and Requirements	47
5.1.1 Introduction	47
5.1.2 Requirements	48
5.1.3 Interfaces	49
5.1.4 Overall Description	52
5.1.5 Ground rules	52
5.1.6 Design History and Decisions	55
5.1.6.1 Supply Tank Sizing and Liquid Hydrogen Requirements	55
5.1.6.2 Flow System and Flow Control	56
5.1.6.3 Cryogenic Tank Design	56
5.1.6.4 Modular Design	57
5.1.6.5 Pressurant Storage and Generation	57
5.1.6.6 Liquid Acquisition Devices	57
5.1.6.7 Thermodynamic Vent System	58
5.1.6.8 Design Considerations for Cryogenic Tankage	58
5.2 Experiment Flow System	58
5.2.1.1 Liquid Transfer	59
5.2.1.2 Venting	61
5.2.1.3 Pressurization	61
5.2.1.4 Thermodynamic Vent Systems	62
5.2.2 Design Details	62
5.2.2.1 Major Plumbing Components	62
5.2.2.2 Liquid Hydrogen Transfers	62
5.2.2.3 Vertical Schematic	63
5.2.2.4 Experiment Safe State	63
5.2.2.5 Venting Systems	64
5.2.3 Components and Selection	64
5.2.3.1 Plumbing Lines	64
5.2.3.2 Major Components	65
5.2.4 Analyses	67
5.2.4.1 Pressure Drop	67
5.2.4.2 Ground Venting (Worst Case)	68
5.2.4.3 Pump-Mixer Flow Requirements	69
5.3 Liquid Hydrogen Supply Tank Module	70
5.3.1 Description and Characteristics	70
5.3.1.1 Supply Tank Assembly	71
5.3.1.2 Purge Bag and MLI Blanket Configuration	76
5.3.1.3 Radiator Tray	79
5.3.1.4 Helium Pressurization System	81
5.3.1.5 Vent Panel	81
5.3.2 Analyses	81
5.3.2.1 Structural	81
5.3.2.2 Supply Tank Thermal Analysis	82
5.3.2.3 LAD/TVS Analysis	90
5.3.2.4 Ground Fill Level	91
5.4 Gaseous Hydrogen System	91
5.4.1 Description and Characteristics	91
5.4.2 Analyses	93
5.4.2.1 Thermodynamic Analysis	93
5.4.2.2 Thermal Analysis	93
5.4.2.3 Structural Analysis	94

5.5 Receiver Tank Modules	95
5.5.1 Large Receiver Tank Description and Characteristics	95
5.5.1.1 Thermal Mass	96
5.5.1.2 Large Receiver Tank MLI Can/MLI Insulation Blanket	96
5.5.1.3 Tank Internals	97
5.5.1.4 Liquid Acquisition Device (LAD) Configuration	97
5.5.1.5 Instrumentation Tree	98
5.5.1.6 Valve Panels	98
5.5.1.7 External Heater	98
5.5.1.8 Final Assembly	98
5.5.2 Small Receiver Tank Description and Characteristics	100
5.5.2.1 Thermal Mass	101
5.5.2.2 Internals	101
5.5.2.3 External Heat Exchanger	101
5.5.2.4 External Heater	102
5.5.2.5 Valve Panels	102
5.5.2.6 Final Assembly	102
5.5.3 Analysis of The Receiver Tanks	103
5.5.3.1 Structural	103
5.5.3.2 Receiver Tank Thermal Analysis	103
5.5.4 Manufacturing	104
5.6 Experiment Instrumentation and Electronics	104
5.6.1 Telemetry, tracking, and Command (TT&C) Interface	104
5.6.2 Electrical Systems Interface	105
5.6.3 Signal Conditioning Systems and Limitations	105
5.6.3.1 Basic Instrumentation and Signal Conditioning Operation	105
5.6.3.2 Experimental Data Units (EDU's)	107
5.6.4 Experiment Measurement Requirements	107
5.6.5 Instrumentation Selection	107
5.6.6 Instrumentation Description and Analysis	107
5.6.6.1 High Resolution Liquid Hydrogen and Gaseous Hydrogen Temperature Measurement Requirements	109
5.6.6.2 Surface Temperature Measurements	110
5.6.6.3 Discrete Point Liquid/Vapor Detection Requirement	110
5.6.6.4 Absolute Pressure Measurement Requirements	111
5.6.6.5 Liquid Hydrogen Flow Rate Measurement Requirements	112
5.6.6.6 Thermodynamic Vent System Flow Rate Measurement Requirements	113
5.6.6.7 Supply and Receiver Tank Flow Rate Measurement	113
5.6.6.8 Acceleration Measurement Requirement	114
5.6.6.9 Mixer Flow Rate Measurement Requirement	114
5.6.6.10 Valve Status Indicators	114
5.6.7 Harnessing	115
5.7 Operations, Consumables, Inventory, and Experiment Timeline	115
5.7.1 Introduction	115
5.7.2 Inventory and Timeline Layout	116
5.7.3 Operations	117
5.7.3.1 Experiment Sequencing	117
5.7.3.2 Pressure Control	118
5.7.3.3 Chillydown	118
5.7.3.4 No-Vent Fill	119
5.7.3.5 Vented Fill	120
5.7.4 Description of Analyses	120
5.7.4.1 Boiloff	120
5.7.4.2 Liquid Hydrogen Tank Ullage Calculation	120

5.7.4.3	Liquid Hydrogen Tank Pressure Rise Calculation	120
5.7.4.4	Pressure Control Experiment Calculation	121
5.7.4.5	Line/Tank Chillydown and Fill Experiment Calculation	121
5.7.4.6	Pressurization of Hydrogen Tanks in Low Gravity	122
Appendix A—	Experiment System Mechanical and Structural Analyses	123
Appendix B—	Analysis of LAD/TVS Heat Exchanger Operation	141
B.1	Description	141
B.1.1	Liquid Acquisition Device	141
B.1.2	TVS Heat Exchanger	141
B.2	Modeling and Performance Analysis	141
B.2.1	Operational Modes	141
B.2.2	Process Thermodynamics	142
B.2.3	Iterative Incremental Model	142
B.2.4	Passive TVS Model	143
B.3	Performance Calculation Results	144
B.3.1	Analysis of Active TVS	144
B.3.2	Analysis of Subcooler TVS	144
B.3.3	Analysis of Passive TVS	145
B.4	Discussion of Results	146
B.4.1	Active TVS	146
B.4.2	Subcooler TVS	147
B.4.3	Passive TVS	147
B.5	Vapor Condensation and Bubble Collapse	147
Appendix C—	Fluids Schematic Symbols	159
Appendix D—	Reference Figures	160
Appendix E—	Reference Tables	213
References		227
Chapter 6—	Spacecraft Structure and Configuration	229
6.1	Introduction	229
6.1.1	Spacecraft Description	229
6.1.2	Configuration Drivers	229
6.1.3	Modular Design	232
6.1.4	Spacecraft Structure	232
6.1.5	Design Process Overview	232
6.2	Major Requirements	232
6.2.1	Sources of Requirements	232
6.2.2	Atlas I Expendable Launch Vehicle (ELV)	232
6.2.3	Modularity	232
6.2.4	Configuration	233
6.2.4.1	Center of Gravity (CG)	233
6.2.4.2	Lateral Center of Gravity (CG) Offset and Moments and Products of Inertia	233
6.2.4.3	Sensor View Factors	233
6.2.4.4	Solar Arrays	233
6.2.4.5	Antennas	234
6.2.4.6	Experiment System Requirements	234
6.2.4.7	Propulsion System Requirements	234
6.2.4.8	Access	234
6.2.4.9	Thermal Requirements	234
6.2.5	Structural System	235
6.2.5.1	Materials	235
6.2.5.2	Assembly Methods	235
6.2.5.3	Openness/View Factors	235
6.2.5.4	Factors of Safety	235

6.2.6	Transportation and Handling	235
6.3	Interfaces	235
6.3.1	Atlas I Launch Vehicle	235
6.3.1.1	Payload Envelope	235
6.3.1.2	Relative Orientation	235
6.3.1.3	Fairing Access Doors	236
6.3.1.4	Spacecraft Adapter	236
6.3.1.5	Mass Properties	236
6.3.1.6	Launch Loads	242
6.3.1.7	Air Conditioning/Purge Gas and Duct	244
6.3.1.8	Liquid Hydrogen Loading	244
6.3.2	Experiment System	244
6.3.2.1	Experiment Tanks	244
6.3.2.2	Radiator Tray and Valve Panels	245
6.3.2.3	Pressurant Tanks	245
6.3.2.4	Electrical Harnessing	245
6.3.2.5	T – 4 Umbilical Panel	245
6.3.3	Electric Power System	245
6.3.3.1	Solar Arrays	245
6.3.3.2	Batteries	251
6.3.3.3	Boxes	251
6.3.3.4	Pyrotechnic Actuators	252
6.3.4	Telemetry, Tracking, and Command (TT&C) System	252
6.3.4.1	Antennas	252
6.3.4.2	Electronics Boxes	252
6.3.5	Propulsion System	252
6.3.5.1	Thruster Modules	253
6.3.5.2	Propellant Tanks	253
6.3.5.3	Pressurization System/Valve Panel	253
6.3.6	Attitude Control System	253
6.3.6.1	Attitude Sensors	254
6.3.6.2	Stability and Alignment	254
6.3.6.3	Electronics Boxes	254
6.3.7	Transportation and Handling	254
6.3.7.1	Handling Hardpoints	254
6.3.7.2	Transportation Loads	254
6.4	Alternate Configurations	254
6.4.1	Brief History	254
6.4.2	Final Delta Configuration	255
6.4.2.1	Description of Configuration	255
6.4.2.2	Mass Properties Verses Delta II Capabilities	259
6.4.3	Capabilities of Delta Versus Atlas	259
6.4.3.1	Comparative Payload Envelopes	261
6.4.3.2	Mass Properties Restrictions	261
6.4.4	Initial Atlas Configuration	261
6.4.4.1	Description of Configuration	261
6.4.4.2	Mass Properties	263
6.4.4.3	Alternative Solar Array Concepts	263
6.4.5	Summary of Subsequent Activities	263
6.5	Supporting Analyses	267
6.5.1	Spacecraft Balancing and Ballasting	267
6.5.2	Sensor Field of View	268
6.5.3	Solar Array Mounting	268
6.5.4	Expendable Launch Vehicle (ELV) Interface	268

6.5.4.1	Spacecraft Adapter	268
6.5.4.2	Vee-Band Clamp	270
6.5.5	Spacecraft Structure	270
6.5.5.1	Structural Member Shape	270
6.5.5.2	Material Selection	271
6.5.5.3	Methodology for Sizing Structural Members	272
6.5.5.4	Sizing of Hydrazine Tank Support Plate	275
6.6	Selected Configuration	279
6.6.1	Principles Guiding the Configuration	279
6.6.1.1	Minimum Lateral Center of Gravity (CG) Shift	279
6.6.1.2	Control of Axial Center of Gravity (CG) Location	279
6.6.1.3	Minimization of Solar Pressure Torques	279
6.6.1.4	Control of Moments and Products of Inertia	279
6.6.1.5	Large Volume Margin	279
6.6.1.6	Simple Supporting Structure	279
6.6.1.7	Use of Spacecraft as a Sun Shield	279
6.6.1.8	Accessibility	280
6.6.1.9	Summary	280
6.6.2	Final Design	280
6.6.2.1	Final Configuration	280
6.6.2.2	Structural System of Final Configuration	290
6.6.2.3	Mass Properties of Final Configuration	292
6.7	Operation	295
6.7.1	Separation	295
6.7.2	Solar Array Deployment	295
6.7.3	Variation in Mass Properties	295
6.8	Components	297
6.8.1	Solar Array Mechanism	297
6.8.2	Materials/Structural Shapes/Structures	297
6.9	Reliability	297
	References	297
Chapter 7	Attitude Control System	299
7.1	Introduction	299
7.2	Requirements	301
7.2.1	Orbit Altitude	301
7.2.2	Mass Properties	301
7.2.3	Center of Gravity Location	301
7.3	Disturbance Torques	301
7.3.1	External Disturbance Torques	303
7.3.2	Self-Induced Disturbance Torques	303
7.4	ACS Alternatives Considered	307
7.4.1	Attitude Determination	307
7.4.2	Attitude Control	308
7.4.2.1	Alternative 1	308
7.4.2.2	Alternative 2	308
7.4.2.3	Alternative 3	308
7.4.2.4	Alternative 4	308
7.4.2.5	Alternative 5	308
7.5	Tradeoff Analysis	308
7.5.1	Qualitative Evaluation	308
7.5.2	Quantitative Evaluation	309
7.5.3	Results of Evaluation	309
7.5.4	Selected System	325
7.6	Description of Selected System	325

7.6.1	Attitude Control System (ACS) Overview	325
7.6.2	Hardware Description	325
7.6.2.1	Inertial Reference Unit (IRU)	325
7.6.2.2	Digital Sun Sensors	331
7.6.2.3	Horizon Sensors	331
7.6.2.4	Magnetometers	331
7.6.2.5	Control Thrusters	332
7.6.2.6	Gimballed Thruster System	332
7.6.2.7	ACS Interface Electronics	332
7.6.3	Functional Description	333
7.6.3.1	Attitude Determination for Normal On-Orbit Operational Mode	333
7.6.3.2	Attitude Determination for Contingency Acquisition Mode	334
7.6.3.3	Attitude Control	334
7.6.4	ACS Performance Analysis	336
7.6.4.1	Control Torque Margins for Selected System	336
7.6.4.2	Spacecraft Dynamic Simulation	336
7.6.4.3	Simulation Results	338
7.6.4.4	180° Roll Maneuver	338
7.7	Components/Heritage	359
7.8	Reliability	359
7.9	Summary and Conclusions	359
7.10	COLD-SAT Dynamic Model	360
7.10.1	Translation Model	360
7.10.1.1	Orbit Simulation	360
7.10.1.2	Desired Attitude Computation	360
7.10.1.3	Axial Thrust Misalignment Torque	360
7.10.1.4	Greenwich Hour Angle (GHA) Computation	360
7.10.2	Rotation Model	364
7.10.2.1	Gravity-Gradient Torque	364
7.10.2.2	Magnetic Torque	364
7.10.2.3	Aerodynamic Torque	364
7.10.2.4	Solar Pressure Torque	364
7.10.2.5	Attitude Error Computation	364
7.10.2.6	Control Thruster Torque Computation	364
7.10.2.7	Gimballed Thruster Simulation	364
7.10.2.8	Kinematic Equations of Rotation	366
7.10.2.9	Disturbance Accelerations	366
7.10.3	Slosh Model	367
	References	367
Chapter 8	Propulsion System	369
8.1	Introduction	369
8.2	Requirements	369
8.3	Interfaces	369
8.4	Trade Studies	370
8.4.1	System Pressurization	370
8.4.1.1	Blow-Down Pressurization	370
8.4.1.2	Controlled Pressurization	372
8.4.2	Engine Configuration	372
8.5	System Description	373
8.5.1	Propulsion System Configuration	373
8.5.2	Pressurization	373
8.5.3	Propulsion System Operation	374
8.5.4	Propulsion System Components	375

8.6	Propellant Usage	376
8.7	Safety and Reliability	376
Chapter 9	Telemetry, Tracking, and Command System	379
9.1	Introduction	379
9.2	Major System Requirements	379
9.2.1	On-Orbit Requirements	379
9.2.1.1	Telemetry	379
9.2.1.2	Command and Data Uplink	380
9.2.1.3	Tracking	380
9.2.1.4	Spacecraft Control Computer	380
9.2.1.5	Spacecraft Control	380
9.2.2	Launch, Ascent, and Deployment Requirements	380
9.2.3	Prelaunch Requirements	380
9.2.4	System Test and Integration Requirements	380
9.2.5	Reliability	380
9.3	TT&C System Interfaces	380
9.3.1	External Interfaces	381
9.3.1.1	Tracking and Data Relay Satellite System (TDRSS) Interface	381
9.3.1.2	Launch Vehicle Interface	381
9.3.1.3	Ground Support Equipment (GSE) Interface	382
9.3.2	Internal Interfaces	382
9.3.2.1	TT&C-to-Spacecraft Structural System Interfaces	383
9.3.2.2	TT&C-to-Attitude Control System Interface	384
9.3.2.3	TT&C-to-Propulsion System Interfaces	384
9.3.2.4	TT&C-to-Electrical Power System (EPS) Interfaces	384
9.3.2.5	TT&C-to-Thermal Control System (TCS) Interfaces	386
9.3.2.6	TT&C-to-Experiment System Interfaces	386
9.4	TT&C System Design and Configuration	388
9.5	TT&C System Operation	388
9.5.1	Telemetry Downlink Operation	388
9.5.2	Uplink Operation	391
9.5.3	Autonomous Spacecraft Control Operation	391
9.5.4	Spacecraft Tracking Operation	392
9.5.5	Redundancy Implementation	394
9.6	Components	395
9.6.1	Flight Computer	395
9.6.2	Transponder	395
9.6.3	Remote Command Telemetry Unit (RCTU) and Command and Telemetry Unit (CTU)	395
9.6.4	Solid-State Recorder	395
9.6.5	Sequencers	397
9.6.6	Radiofrequency (RF) Processing Box	397
9.6.7	Antennas	397
9.6.8	High-Gain Antenna (HGA) Deployment Arm and Gimbal	397
9.6.9	Redundancy Control Unit	397
9.7	Supporting Analyses	397
9.8	Reliability	397
9.9	References	398
Chapter 10	Electric Power System	399
10.1	Introduction	399
10.2	Requirements	400
10.3	Power System Interfaces	402
10.3.1	Spacecraft Systems Electrical Interfaces	402

10.3.2	Other Spacecraft Interfaces	404
10.3.3	Ground Support Interfaces	404
10.3.4	Expendable Launch Vehicle (ELV) Interfaces	405
10.4	System Alternatives Considered	405
10.4.1	General	405
10.4.2	Solar Arrays	405
10.4.3	Batteries	406
10.4.4	Power Control and Distribution	407
10.5	Supporting Analyses	408
10.5.1	General	408
10.5.2	Solar Array Cant Angle	408
10.5.3	Solar Array Sizing	410
10.5.4	Batteries	413
10.6	Power System Configuration	415
10.6.1	General	415
10.6.2	Solar Arrays	415
10.6.3	Batteries	417
10.6.4	Power Control Unit	417
10.6.5	Power Distribution Unit	419
10.6.6	Pyro Control Unit	419
10.6.7	Harnesses	419
10.6.8	Instrumentation	419
10.6.9	Grounding and Bonding	420
10.6.10	Safety	420
10.7	Electric Power System Function	420
10.7.1	Power Generation and Storage	420
10.7.2	Power Distribution	421
10.7.3	Degraded Performance	422
10.8	Components/Heritage	422
10.9	Reliability	423
	References	423
Chapter 11	Thermal Control System	425
11.1	Introduction	425
11.2	Design Philosophy	426
11.3	Design Drivers and Requirements	426
11.3.1	Critical Design Goals	426
11.3.1.1	Experiment System Supply Tank Module	426
11.3.1.2	Propulsion System	426
11.3.1.3	Power System	426
11.3.1.1	Telemetry, Tracking, and Command (TT&C) System	426
11.3.2	Component Dissipations and Temperature Requirements	427
11.3.3	Safety	430
11.4	Thermal Control Subsystem Description	430
11.4.1	Exterior Thermal Control	430
11.4.1.1	Electronics Bays	430
11.4.1.2	Experiment Tankage	431
11.4.1.3	Spacecraft Structure	432
11.4.1.4	Plumbing Trays and Panels	433
11.4.1.5	Solar Arrays	433
11.4.1.6	Antenna	434
11.4.1.7	Components	434
11.4.2	Interior Thermal Control	436
11.4.2.1	Electronics Bays	436
11.4.2.2	Batteries	437

11.5 Thermal Control Subsystem Analysis	438
11.5.1 Analysis Overview	438
11.5.2 Thermal Design Issues and Trades	440
11.5.2.1 Spacecraft Thermal Bifurcation	440
11.5.2.2 Spacecraft Attitude Impacts	441
11.5.2.3 Supply Tank Purge Diaphragm Material	443
11.5.3 Analysis Results	444
11.5.4 Ascent Aerodynamic Heating	450
11.6 Thermal Control Subsystem Components	454
11.6.1 Multilayer Insulation	454
11.6.2 Optical Solar Reflectors	454
11.6.3 Heaters and Controllers	456
11.6.4 Passive Surfaces	456
11.6.5 Chocterm 1671	456
11.6.6 Thermal Control Subsystem Weight	456
11.6.7 Reliability	456
11.7 Operational Characteristics	459
11.8 Interfaces	459
11.9 References	459
Chapter 12—Software	461
12.1 Introduction	461
12.2 Major Requirements	461
12.3 Description	461
12.4 Interfaces	462
12.4.1 Command and Telemetry Unit (CTU)	462
12.4.2 Redundancy Control Unit (RCU)	462
12.4.3 Transponder	463
12.4.4 Launch Pad Electrical Ground Support Equipment (EGSE)	463
12.4.5 POCC Telemetry	463
12.5 Software Description	463
12.5.1 Attitude Determination and Control	464
12.5.2 Ground Command Processing	464
12.5.3 Command and Telemetry Unit Interface	464
12.5.4 Data Formatting	464
12.5.5 Critical Status Monitor and Safing	464
12.5.6 Electric Power Monitor	465
12.5.7 Antenna Pointing	465
12.5.8 Navigation	465
12.5.9 Thermal Monitor and Control	465
12.5.10 Propulsion System	465
12.5.11 Experiment Monitor and Control	465
12.5.12 Prelaunch Operations	465
12.5.13 Ascent Operations	466
12.5.14 Post-Separation Operations	466
12.6 Sample Rates	466
12.7 Safety	466
12.8 Onboard Computer (OBC) Software Size Estimate	466
12.9 Onboard Computer (OBC) Memory Requirements Estimate	466
12.10 Concluding Remarks	468
Chapter 13—Launch Vehicle, Launch, and Ascent Operations	469
13.0 Introduction	469
13.1 Spacecraft-ELV-Pad Interfaces	469
13.1.1 Mechanical Interfaces	470
13.1.2 Electric Power System Interfaces	470

13.1.3	Command and Telemetry Interfaces	471
13.1.4	Fluids Interfaces	473
13.1.5	Environment	473
13.1.6	Electromagnetic Compatibility	473
13.1.7	Destruct System	474
13.2	Launch Vehicle Capability	474
13.2.1	Introduction	474
13.2.2	Analysis and Ground Rules	474
13.2.3	Results and Conclusions	474
13.3	Launch Vehicle/Launch Pad Modifications	476
13.3.1	Introduction	476
13.3.2	Summary	476
13.3.3	Spacecraft-Pad-Expendable Launch Vehicle Interfaces	477
13.3.4	Vehicle and Pad Fluid Interfaces	478
13.3.5	Mechanical Interfaces	483
13.3.6	Liquid Hydrogen Loading Sequence	484
13.4	Launch and Ascent Operations	485
13.4.1	Introduction	485
13.4.2	Launch Operations	485
13.4.3	Ascent Operations	488
13.4.4	Separation, Deployment, and Acquisition	489
	References	489
Chapter 14	Ground Operations	491
14.1	Introduction	491
14.2	Requirements	492
14.2.1	Applicable Documents	492
14.2.2	Fluid Loading	492
14.2.3	Facilities	492
14.2.4	Communications	492
14.2.5	Assembly	492
14.2.6	Testing	493
14.3	Interfaces	493
14.3.1	Electrical Interfaces	494
14.3.2	Control, Communication, and Data Interfaces	494
14.3.3	Fluid Interfaces	494
14.3.4	Transportation and Handling Interfaces	495
14.4	Operations	495
14.4.1	Operational Timeline	495
14.4.2	Arrival	497
14.4.3	Payload Processing Facility Operations	497
14.4.4	Hazardous Processing Facility Operations	498
14.4.5	Encapsulation	499
14.4.6	Launch Complex 36 Operations	500
14.4.6.1	Launch Operations Timeline	500
14.4.6.2	Spacecraft Operations at the Launch Pad	500
14.4.6.3	Major On-Pad Tests	502
14.4.6.4	Launch Operations	503
14.5	Alternative Processing Considered	503
14.6	Ground Support Equipment	504
14.6.1	Mechanical Ground Support Equipment	504
14.6.2	Fluid Systems Ground Support Equipment	504
14.6.3	Electrical Ground Support Equipment	506
14.6.4	Safety Ground Support Equipment	506
14.7	Personnel	506

Chapter 15—Flight Operations	509
15.1 Introduction	509
15.2 Requirements	510
15.3 Interfaces	510
15.4 Nominal Operations	510
15.4.1 Initial Checkout	510
15.4.2 Experiment Operations	513
15.4.3 Spacecraft Operations	513
15.5 Redundancy Implementation and Spacecraft Autonomy	514
15.5.1 Redundancy Implementation	514
15.5.2 Failure Correction	514
15.6 Payload Operations Control Center (POCC)	516
15.6.1 Functions	516
15.6.2 Interfaces	516
15.6.3 Design	516
15.6.4 Personnel	520
Chapter 16—Reliability	523
16.1 Introduction	523
16.2 Requirements	523
16.2.1 Spacecraft Reliability Goal	523
16.2.2 Single-Point Failure Goal	524
16.2.3 Reliability Allocation	524
16.3 Reliability Activities	524
16.3.1 Spacecraft Design	524
16.3.2 System Design	524
16.3.3 Failure Rate Development	524
16.3.4 Single-Point Failure Analyses	524
16.4 Reliability Analysis Methodologies	525
16.4.1 System Reliability Allocation	525
16.4.2 System Reliability Analyses	525
16.4.3 Spacecraft Reliability Analysis	526
16.4.4 Failure Rate Estimation Methodology	526
16.5 Reliability Program Implementation	526
16.5.1 Individual System Reliability Analysis	526
16.5.1.1 Development of Failure Rate Data	526
16.5.1.2 System Block Diagram Development	530
16.5.2 Spacecraft Reliability Analysis	536
16.5.3 Intersystem Reliability Issues	537
16.5.4 Single-Point Failure Analyses	537
16.6 Conclusion	537
References	537
Chapter 17—Safety	539
17.1 Introduction	539
17.2 Preliminary Hazards Analysis	539
17.2.1 Hazard Matrix Description	539
17.2.2 Hazard Definition Approach	539
17.2.3 Classification Approach	542
17.2.4 Major Safety Concerns	544
17.3 System Design Approach to Major Safety Concerns	546
17.3.1 Structural System	546
17.3.2 Ground Support Equipment	546
17.3.3 Operations	546
17.3.4 Experiment System	546
17.3.5 Propulsion System	547
17.3.6 Power System	547

17.4 Specific Safety Issues	547
17.4.1 Structural Design Considerations	547
17.4.2 Launch Site Modifications	547
17.4.3 Gaseous Hydrogen, Gaseous Helium, and Hydrazene Loading Considerations	547
17.4.4 Pressure Vessel Design Considerations	547
17.4.5 Liquid Hydrogen Handling Considerations	547
17.4.6 Pyrotechnic Usage/Control Considerations	548
17.4.7 Flight Termination System	548
17.5 Conclusion and Recommendations	548
References	549
Chapter 18—System Development, Integration, and Test	551
18.1 Introduction	551
18.2 System Development	551
18.3 Development Philosophy	552
18.4 Integration and Test Flow	553
18.4.1 Electronics Integration and Test	553
18.4.2 Electronics Bay 1 Assembly and Test	554
18.4.3 Receiver Tank Module Assembly and Test	555
18.4.4 Supply Tank Module Assembly and Test	555
18.4.5 Spacecraft Assembly, Integration, and Test	558
18.5 Phase C/D Schedule	558
18.6 Test Facilities	561
18.7 Ground Support Equipment	561
18.7.1 Electronic Ground Support Equipment (EGSE) Trailer/Skid	561
18.7.2 Transport Trailer	561
18.7.3 Trunnion Support and Handling Dolly	562
18.7.4 Spacecraft Module EGSE	562
18.7.5 Other Ground Support Equipment	564
References	564
Appendix A—Nomenclature	565
Appendix B—Symbols	575
Appendix C—Bibliography	581

Contributors

Neil Adams, Analex Corporation, Cleveland, Ohio: Chapter 7, Attitude Control System

Hugh Arif, National Aeronautics and Space Administration, Lewis Research Center, Cleveland, Ohio: Chapter 11, Thermal Control System

Gary Bollenbacher, National Aeronautics and Space Administration, Lewis Research Center, Cleveland, Ohio: Chapter 7, Attitude Control System

Robert Dengler, Analex Corporation, Cleveland, Ohio: Chapter 5, COLD-SAT Experiment System, (Fluid Systems)

W. James Dorcey, Science Applications International Corp., Cleveland, Ohio: Chapter 16, Reliability

Lawrence Edwards, Analex Corporation, Cleveland, Ohio: Chapter 5, COLD-SAT Experiment System, (Instrumentation and Electronics)

Daniel Glover, National Aeronautics and Space Administration, Lewis Research Center, Cleveland, Ohio: Chapter 5, COLD-SAT Experiment System, (Experiment System)

George Harpster, National Aeronautics and Space Administration, Lewis Research Center, Cleveland, Ohio: Chapter 5, COLD-SAT Experiment System, (Fluid Inventory/Experiment Operations)

Richard Jacobs, Analex Corporation, Cleveland, Ohio: Chapter 13, Launch Vehicle, Launch and Ascent Operations; Chapter 14, Ground Operations

Edward Kramer, National Aeronautics and Space Administration, Lewis Research Center, Cleveland, Ohio: Editor; Chapter 1, Introduction; Chapter 2, Requirements and Constraints; Chapter 3, System Overview; Chapter 4, Mission; Chapter 13, Launch Vehicle, Launch and Ascent Operations; Chapter 15, Flight Operations; Chapter 18, System Development, Integration, and Test

Steven T. McHenry, Analex Corporation, Cleveland, Ohio: Chapter 17, Safety

John Mishic, Analex Corporation, Cleveland, Ohio: Chapter 5, COLD-SAT Experiment System, (Thermal Modeling)

Shigeo Nakaniski, Analex Corporation, Cleveland, Ohio: Chapter 5, COLD-SAT Experiment System, (Thermal and Fluid Analysis)

Kim Otten, Analex Corporation, Cleveland, Ohio: Chapter 6, Spacecraft Structure and Configuration

Don Perdue, National Aeronautics and Space Administration, Lewis Research Center, Cleveland, Ohio: Chapter 13, Launch Vehicle, Launch and Ascent Operations

Christopher J. Pestak, Analex Corporation, Cleveland, Ohio: Chapter 3, Telemetry, Tracking, and Command System

William Prati, Analex Corporation, Cleveland, Ohio: Chapter 5, COLD-SAT Experiment System, (Receiver Tank Module Design)

Dave Repas, National Aeronautics and Space Administration, Lewis Research Center, Cleveland, Ohio: Chapter 7, Attitude Control System

Jeff Samella, Analex Corporation, Cleveland, Ohio: Chapter 13, Launch Vehicle, Launch and Ascent Operations

Al Seigneur, National Aeronautics and Space Administration, Lewis Research Center, Cleveland, Ohio: Chapter 5, COLD-SAT Experiment System, (Supply Tank Module Design)

Tony D. Shook, National Aeronautics and Space Administration, Lewis Research Center, Cleveland, Ohio: Chapter 8, Propulsion System

Todd A. Tofil, National Aeronautics and Space Administration, Lewis Research Center, Cleveland, Ohio: Chapter 10, Electric Power System

Richard Verbus, Analex Corporation, Cleveland, Ohio: Chapter 5, COLD-SAT Experiment System, (Fluid Inventory/ Experiment Operations)

Daniel R. Vrnak, National Aeronautics and Space Administration, Lewis Research Center, Cleveland, Ohio: Chapter 12, Software

Frank Zimmerman, Analex Corporation, Cleveland, Ohio: Chapter 15, Flight Operations

Chapter 1

Introduction

Edward Kramer
National Aeronautics and Space Administration
Lewis Research Center
Cleveland, Ohio

1.0 Introduction

This report covers work performed at the NASA Lewis Research Center on the conceptual design of the cryogenic on-orbit liquid depot-storage, acquisition, and transfer (COLD-SAT) spacecraft and the planning of the COLD-SAT program. COLD-SAT was intended to provide sufficient data on the storage and handling of cryogenics (specifically liquid hydrogen) in the low-gravity environment of space to enable future space systems to be confidently and efficiently designed. NASA missions such as manned lunar/Mars exploration will require the safe storage of cryogenics in space for months or years and require the efficient transfer and handling of these fluids. In addition, this technology will greatly enhance the capability to perform a variety of near-Earth missions, such as transfers from low Earth orbit (LEO) to geosynchronous Earth orbit (GEO), in a more efficient manner.

Currently, no data is available on the long-term storage of liquid cryogenics (other than liquid helium) in low gravity. Essentially, all data on transfer and handling has been obtained from drop-tower or sounding-rocket experiments where the scale is measured in inches and the time is measured in seconds or minutes. COLD-SAT could extend the scale to feet and the times to weeks and months. No other approach is available to obtain this information.

This study shows that both the spacecraft and the program are feasible and that all required experiments can be accommodated on one relatively simple spacecraft. While the technology to be developed is new, the hardware to perform the experiments can be constructed by using existing designs and techniques and without major development of new components. The COLD-SAT spacecraft can be integrated and tested without constructing new facilities. In all, COLD-SAT would be a low-risk, high-return project.

1.1 Scope

This study covers all aspects of the COLD-SAT project including design, development, fabrication, integration, test, launch, and on-orbit operations. The level of detail in a given area of the study was tailored to the criticality of that area to the feasibility of the overall program. The design of the experiment system is new and was carried to considerable detail, beyond what is usual for a conceptual design. Other spacecraft systems are rather conventional and so the level of detail was reduced. However, unique or unusual aspects of these systems were given detailed coverage. For example, a detailed model of the attitude control system was developed because of the effects of that system on the acceleration environment of the experiment system and the potential effects of fluid slosh.

The handling of liquid hydrogen presents unique problems, especially when it must be integrated with other activities. In this study, special attention was given to the loading of the spacecraft with liquid hydrogen on the launch pad. The difficulties associated with liquid hydrogen also caused much attention to be focused on the integration and test of the spacecraft and experiment.

The COLD-SAT conceptual design studies were originally intended to be followed immediately by development and implementation (phase C/D) without intervening phase B studies. This enlarged the scope of the studies even further and increased the level of detail needed over that usually associated with conceptual design. Here, particular interest existed in the identification of components which could be used in the final design and in the initiation of development for those which could not be found. Thus, this design effort was expanded to a level approximating that of a preliminary design.

1.2 Related Documents

The work reported here is only part of a larger effort that sought to define the experimental systems required to develop the technologies needed to manage cryogenic fluids in the space environment. Significant work has been devoted to handling both normal and superfluid liquid helium. However, the unusual physical properties of liquid helium relegate these efforts to a position of only tangential interest. The major interest for large-scale space application is liquid hydrogen, with liquid oxygen and liquid nitrogen following behind. Only the former will be included here.

The present study is one of four COLD-SAT feasibility studies. The results of the other three have been reported in the following:

Rybak, S.C., et al. (Ball Aerospace Systems Group with McDonnell Douglas Space Systems Company and Boeing Aerospace and Electronics): Feasibility Study for a Cryogenic On-Orbit Liquid Depot Storage, Acquisition and Transfer (COLD-SAT) Satellite. NASA CR-185248, 1990.

Bailey, W.J., et al. (Martin Marietta Space Systems, Inc., Denver, CO (Astronautics Group)): Cryogenic On-Orbit Liquid Depot Storage, Acquisition and Transfer Satellite (COLD-SAT) Feasibility Study. NASA CR-185247, 1990.

Schuster, J.R. (General Dynamics Corp. Space Systems Division with Ford Aerospace Space Systems Division): Cryogenic On-Orbit Liquid Depot Storage, Acquisition, and Transfer Satellite (COLD-SAT). NASA CR-185249, 1990.

Schuster, J.R.; Wachter, J.P.; and Powers, A.G.: COLD-SAT, An Orbital Cryogenic Hydrogen Technology Experiment. NASA TM-102303, 1989.

Williams, G.E.; and Schuster, J.R.: Thermal Design Considerations for the Cryogenic On-Orbit Liquid Depot Storage, Acquisition and Transfer Satellite (COLD-SAT). AIAA Paper 90-0057, 1990.

Bailey, W.J.: The COLD-SAT Program: Advances in Cryogenic Engineering. Vol. 35B—Proceedings of the 1989 Cryogenic Engineering Conference, Plenum Press, 1990, pp 1669-1680.

Portions of the study presented here have been reported elsewhere either in preliminary or expanded form as follows:

Arif, H.; and Kroeger, E.W.: COLD-SAT: A Technology Satellite for Cryogenic Experimentation. NASA TM-102286, 1989.

Arif, H.: Spacecraft Attitude Impacts on COLD-SAT Non-Vacuum Jacketed LH₂ Supply Tank Thermal Performance. AIAA Paper 90-1672, June 1990 (also NASA TM-103158, 1990).

Arif, H.: Preliminary Thermal Design of the COLD-SAT Spacecraft. AIAA Paper 91-1305, June 1991 (also NASA TM-104440, 1991).

McHenry, S.T.; and Yost, J.M. (Analex Corporation): COLD-SAT Feasibility Study Safety Analysis. NASA CR-187042, 1991.

Adams, N.S. (Analex Corporation); and Bollenbacher, G.: COLD-SAT Dynamic Model. NASA TM-105185, 1992.

Edwards, L.G. (Analex Corporation): Cryogenic On-Orbit Liquid Depot Storage Acquisition and Transfer (COLD-SAT) Experiment Subsystem Instrumentation and Wire Harness Design Report. NASA CR-189172, 1992.

A number of cryogenic fluid handling flight experiments onboard the space transportation system (STS) were studied but abandoned because of the difficulties encountered with integration of liquid hydrogen payloads following the Challenger Space Shuttle incident. These are reported as follows:

Eberhardt, R.N., et al. (Martin Marietta Aerospace, Denver, CO): Cryogenic Fluid Management Facility Concept Definition Study (CFMF). NASA CR-174630, 1983.

Eberhardt, R.N., et al. (Martin Marietta Aerospace, Bethesda, MD): Cryogenic Fluid Management Experiment. NASA CR-165495, 1981.

Willen, G.S.; Riemer, D.H.; and Hustvedt, D.C. (Beech Aircraft Corporation, Boulder, CO): Conceptual Design of an In-Space Cryogenic Fluid Management Facility. NASA CR-165279, 1981.

Rudland, R.S.; Gille, J.P.; Eberhardt, R.N. (Martin Marietta Corporation, Denver, CO): Liquid Hydrogen Pressurization, Venting, and Resupply in Low-g. AIAA Paper 86-1251, 1986.

Eberhardt, R.N., et al. (Martin Marietta Aerospace, Denver, CO): Cryogenic Fluid Management Facility. AIAA Paper 84-1340, 1984.

The final report for the various studies of a shuttle-based liquid hydrogen experiment, which had a series of acronyms (CFMF, CFME, and CFMFE) was never published in a form that could be referenced.

One other study of interest, conducted by the Missile and Space Systems Division of Douglas Aircraft Company in the middle 1960's, is

Fredrickson, G.O.; and Schweikle, J.D.: Project Thermo—Phase B Prime. NASA CR-88712, 1967.

It produced a spacecraft design very similar to that resulting from the current study.

A full set of references to all cryogenic flight experiment efforts can be found in the following report:

Glover D.: NASA Cryogenic Fluid Management Space Experiment Efforts, 1960-1990. AIAA Paper 91-3538, 1991 (also NASA TM-103752, 1991).

1.3 Relationship to Other Studies

The work reported here is the result of a NASA Lewis in-house feasibility study, which was one of four parallel studies conducted for the COLD-SAT spacecraft. This effort continued on after the conclusion of the contractor studies and was conducted by government and support-service contractor personnel who had access to the work of all three groups of aerospace contractors. Many ideas which appear here are the result of borrowing, both deliberate and unconscious, from the work of the various contractors performing COLD-SAT feasibility studies. It was the specific intent of the second stage of the NASA Lewis study to use all available ideas to produce the best compromise design. Unfortunately, the genesis of all ideas in this report cannot be traced to their original source.

1.4 Goals of COLD-SAT Program

The ability to efficiently transfer and store cryogenics in the low-gravity environment of space is essential for a number of planned or proposed space missions. The primary cryogenics of interest are liquid hydrogen and liquid oxygen. Because of its thermophysical properties and its importance to space propulsion, hydrogen is a fluid of special interest. Currently, no data exist on the long-term storage of liquid hydrogen in low gravity, the longest attempt at storage being a few hours in space. Some problems in the handling, acquisition, and transfer of liquid cryogenics in low gravity have been investigated in very small scale, short-term experiments using sounding rockets and drop towers. The existing data would have to be extrapolated several orders of magnitude if used in the design of future space systems. In addition, only a small subset of the data is for liquid hydrogen.

The goal of the COLD-SAT project was to cure this dearth of data on cryogenic fluid handling by using one cost-effective spacecraft prior to the design of future space systems. Other design approaches, such as repeated development flights for a given space vehicle design, will cost orders of magnitude more than COLD-SAT and will only provide a small subset of the required data. In addition, fundamental information will not be available during this design process so the vehicles would be inherently less efficient.

COLD-SAT was intended to provide adequate data at reasonable dimensional scale and time scale for the following technologies:

- (1) Liquid cryogen storage
 - (a) Pressure control
 - (b) Thermal protection
 - (c) Settled venting
 - (d) Dumping and inerting
- (2) Liquid cryogen acquisition
 - (a) Settled outflow
 - (b) Screened channel capillary liquid acquisition devices
 - (c) Tank pressurization
- (3) Liquid cryogen transfer
 - (a) Transfer line chilldown
 - (b) Receiver tank chilldown
 - (c) No-vent fill in low gravity
 - (d) Vented fill
 - (e) Refill of partially filled tank

In addition, data will be taken in other areas of interest if it can be obtained at low cost without interfering with the primary goals of this project.

1.5 Goals of In-House Study

The basic goals of the NASA Lewis Research Center In-House Feasibility Study were to assess the technical feasibility and risk and to estimate the cost and schedule requirements of a spacecraft and associated ground segment that meets the COLD-SAT experimental requirements (detailed cost studies were performed but because of the sensitive nature of some of this information, it is not reported here). A major subsidiary goal was to provide a conceptual design as a basis for future development.

The tool used to meet these goals was the development of an expanded conceptual design (closer to a preliminary design) of the spacecraft and its supporting systems. Special emphasis was given to the problem of component development with its attendant cost and risk. Every effort was made in the design to minimize the use of developmental items and to minimize the risk associated with those which must of necessity be developed.

Chapter 2

Requirements and Constraints

Edward Kramer
National Aeronautics and Space Administration
Lewis Research Center
Cleveland, Ohio

2.0 Introduction

This chapter provides a summary of the top-level requirements and constraints that controlled the design of the cryogenic on-orbit liquid depot-storage, acquisition, and transfer (COLD-SAT) spacecraft and its related flight and ground systems and their operation and testing. It also summarizes certain system-level design decisions which were made to guide the design of the various subsystems and the planning of flight and ground operations.

2.1 Experiments

The COLD-SAT spacecraft exists only for the performance of a series of cryogenic fluid management experiments in low gravity. The requirements for these experiments drive all other features of the COLD-SAT design.

However, it should not be thought that experiment requirements were accepted as originally defined. The inclusion or exclusion of experiments and the details of their requirements were the subject of continuing negotiation between the spacecraft and experiment system designers and the various sources of experiment requirements. In fact, one of the primary goals of the COLD-SAT conceptual design effort was to define a practical and feasible set of experiments and to assure that the experiment requirements were adequately defined.

One requirement that was not open for negotiation was the choice of experimental fluid. Liquid hydrogen is the cryogenic fluid of interest. Future NASA space missions will require the storage and transfer of vast quantities of liquid hydrogen (measured in tons). The development of fluid storage and handling technology for liquid hydrogen will provide by far the greatest return. In addition, because of its thermodynamic

properties, liquid hydrogen is the most difficult of the cryogenic fluids to handle (with the possible exception of liquid helium).

Extensive studies were conducted in connection with the design of the shuttle-based Cryogenic Fluid Management Flight Experiment (CFMFE) on the scaling of data for other cryogenics to liquid hydrogen. Both in-house and contracted studies (e.g., ref. 1) concluded that while individual experiments that were scalable to liquid hydrogen could be defined, it was impossible to define a set of experiments with a referee fluid that would provide all needed technologies. One of the primary reasons for considering COLD-SAT on an expendable launch vehicle (ELV) is the difficulty of integrating liquid hydrogen payloads into the space transportation system (STS).

The initial COLD-SAT experiment set is shown in table 2.1, which also shows the final disposition of the individual experiments. Experiments were classified as class I or class II, depending on their priority. All Class I experiments were required to be integrated. Five experiments were deleted and some tests associated with other experiments were modified or eliminated. Because it is necessary to perform such activities to conduct the remaining experiments, COLD-SAT will provide some data for three: (1) Transfer Line Chillydown, (2) Tank Thermal Performance, and (3) SLOSH Dynamics. Mass gaging could be reinstated if a suitable mass gage is developed.

In the remainder of this section, a brief description of each experiment and its requirements is provided. All discussion covers the experiments as finally integrated into the COLD-SAT conceptual design.

2.1.1 LOW-GRAVITY TANK PRESSURE CONTROL

The goals of the tank pressure control experiment are to study the process of thermal stratification in cryogen-filled

TABLE 2.1.—COLD-SAT INITIAL EXPERIMENT SET

Experiment number	Title	Class	Disposition
1	Low-gravity tank pressure control	I	Integrated
2	No-vent fill and refill of cryogenic tanks in low gravity	I	Integrated
3	Cryogenic tank chilldown in low gravity	I	Integrated
4	Fill of liquid acquisition devices in low gravity	I	Integrated
5	Cryogenic mass gaging	II ↓	Deleted
6	Slosh dynamics		Deleted
7	Tank thermal performance		Deleted
8	Pressurization of cryogenic tankage in a low-gravity environment		Integrated
9	Direct liquid outflow and vented fill with low-gravity settling		Integrated
10	Liquid acquisition device performance in the on-orbit environment		Integrated
11	Transfer line chilldown under low-gravity conditions		Deleted
12	Control of fluid thermodynamic state during liquid outflow		Integrated
13	On-orbit cryogenic fluid dumping		Integrated
14	Advanced instrumentation for in-space cryogenic systems		Partially integrated
15	Partial communication liquid acquisition device performance		Deleted

tanks, to investigate the mixing of stratified tanks, and to study the operation and effectiveness of passive and active thermodynamic vent systems (TVS) for removing heat from cryogenic tanks.

2.1.1.1 Experiment Description

In the basic experiment, a tank containing a known quantity of cryogen is heated at a known rate by a uniformly distributed wall heat flux under controlled acceleration conditions. Fluid temperature is measured at various points within the tank. The critical data is the tank pressure. Following stratification, the fluid in the tank is mixed by an external pump and jet mixer, while temperature, pressure, and flow data is acquired. A heat exchanger is used to cool the return fluid from the mixer pump. The primary side of the heat exchanger is provided with cryogen cooled by expansion through a Joule-Thompson (J-T) expander (a thermodynamic vent system). For passive pressure control, a heat exchanger is provided inside the tank mounted to the tank wall. The primary side of this heat exchanger is also fed by a TVS system. Tank pressure and selected temperatures are measured with known heat fluxes under mixed and unmixed conditions.

2.1.1.2 Experiment Requirements

At least two tanks with known uniform wall heat flux are required. The heat flux must be variable for at least one of the tanks. This tank must be equipped with a jet mixer and active and passive TVS heat exchangers. The mixer must be capable of operating at regions I and IV as defined by Aydelott in

reference 2. Uniform acceleration of suitable quality must be applied during some tests, and the tank fill level varied between tests. Pressure, temperature, and mixer and TVS flow-rate data must be collected. More detailed requirements are provided in appendix A.

2.1.2 NO-VENT FILL AND REFILL

The goal of the no-vent fill and refill experiment is to characterize the performance of several techniques for filling or refilling tanks with subcritical cryogenics without venting of the ullage. The effects of (1) fluid position in relation to the inflow, (2) centrifugal techniques for positioning the fluid, and (3) droplet-to-ullage heat transfer for ullage gas condensation, will be investigated. Parametric investigations of inlet flow rate, inlet flow direction (radial, tangent into/onto liquid), inflowing fluid thermodynamic state, supply pressure, and tank size will be performed to allow subsequent modeling of the fill process.

2.1.2.1 Experiment Description

In the basic experiment, the tank to be filled is prechilled to conditions that provide suitable scaling to target systems as a substitute to providing similarity between the actual tank thermal-heat-capacity to liquid-volume ratio of the receiving tank and that of target systems. The liquid hydrogen source is thermodynamically conditioned to required conditions and the supply tank is pressurized. The transfer line between the tanks is prechilled. If necessary, the required acceleration is established to position the fluid in the receiving tank. The tank is then filled

using a variety of techniques while pressure, temperature, and flow data are recorded. The outflow from the supply tank may be subcooled as required by using a TVS system and associated heat exchanger to control the thermodynamic state.

2.1.2.2 Experiment Requirements

The experiment requires a source of subcooled cryogen with variable flow rate and two receiver tanks to be filled with the cryogen. Except during refill, the receiver tanks must be prechilled to a specified thermodynamic state. Each receiver must be equipped with multiple spray systems for introducing the fluid into the tank. One receiver tank must be of essentially cylindrical geometry with elliptical or hemispherical ends and the other tank of nearly spherical geometry. Steady low-g acceleration is needed to position the fluid during certain tests. The thermodynamic state of the incoming fluid and its flow rate must be measured, as well as receiver tank pressure, and liquid, vapor, and wall temperatures. Additional requirements are presented in appendix B to this chapter.

2.1.3 CRYOGENIC TANK CHILLDOWN

The goal of the tank chilldown experiment is to characterize a variety of methods for prechilling cryogenic tanks prior to filling, with a view to optimizing the chilldown process. It is desirable to minimize the quantity of cryogen used, the peak pressure in the tank, and the time required for the chilldown to occur.

2.1.3.1 Experiment Description

In the basic experiment, liquid cryogen in a known thermodynamic state is introduced into the tank to be chilled by using either axial, radial, or tangential spray systems (or a combination) or is introduced simply as an axial jet of fluid. The tank is then closed up for a certain length of time or until tank pressure reaches a preset maximum. Next, the tank is vented to remove some or all of the presumably vaporized cryogen. When all residuals from a given initial charge are vented, the process is repeated until the tank wall reaches the target chilldown temperature.

A variety of methods and flow rates are used to introduce fluid into the tank and vent the resulting gas. Two tanks of different sizes and thermal-heat-capacity to volume ratios are used to gather data under a variety of circumstances and conditions. Most testing occurs at the microgravity background acceleration but a few tests are conducted at imposed low-g accelerations to identify any effects of higher acceleration levels.

Basic measurements are the incoming fluid thermodynamic state (pressure and temperature), flow rate and quantity, overall thermodynamic state of the tank pressure vessel (wall temperature), and the thermodynamic state (temperature and pressure)

and quantity of the vented fluid. Tank pressure, internal temperature, and overall acceleration are also recorded.

2.1.3.2 Experiment Requirements

At least two tanks having ratios of thermal-heat-capacity to volume that will allow the extrapolation of results to potential space systems are required. These tanks must be equipped with axial, radial, and tangential spray systems and an axial jet to allow the investigation of various chilldown methods. A source of liquid cryogen at known thermodynamic state and controlled flow rate is needed. It must be possible to vent the experimental tanks to vacuum in a controlled manner while measuring the thermodynamic state, flow rate, and quantity of the vented fluid. The temperature of the tank pressure vessel and its contents must be measured. Requirements are summarized in appendix C to this chapter.

2.1.4 FILL AND REFILL OF LIQUID ACQUISITION DEVICES

The goal of this experiment is to verify that a screen-type liquid acquisition device (LAD) can be refilled completely with liquid (i.e., all vapor bubbles removed) in low gravity. The method to be verified is the selective cooling of the LAD channel.

2.1.4.1 Experiment Description

The presence of vapor bubbles within a screen-type LAD may prevent proper operation of the LAD by allowing the screen to dry out and permit ullage vapor to invade the LAD before the tank is emptied of liquid. The method used here is to first flow liquid into a chilled LAD and tank and then remove any residual vapor bubbles by cooling the LAD channel and its entrained liquid and vapor below the saturation temperature (and pressure) in the tank, thereby condensing the vapor bubbles.

The complete filling of the LAD will be verified by liquid-vapor sensors inside the LAD channel and by examining subsequent outflows from the tank through the LAD for bubbles. In addition, residual measurements made in connection with experiment 10 (LAD performance) will reveal serious failures in the operation of the LAD.

2.1.4.2 Experiment Requirements

The experiment requires a cryogenic tank with a low heat leak equipped with a screen-type total communication LAD. A source of vapor-free liquid is needed to fill the LAD. Internal liquid-vapor and temperature sensors are required within the LAD as well as vapor detection in the outflow from the LAD. Careful measurement of the quantity of liquid entering and

leaving the tank and the measurement of any remaining residuals are required. Requirements are summarized in appendix D to this chapter.

2.1.5 CRYOGENIC MASS GAGING

This experiment aims to demonstrate the operation and accuracy of a cryogenic mass gage in a microgravity environment. However, no mass gage concept has been developed to the extent required to allow integration into the experiment system. Hence, this experiment was deleted from the list.

No difficulty is anticipated in integrating a mass gaging experiment, once gauge concept development has proceeded to the prototype hardware stage so that interfaces and operating conditions can be defined.

2.1.6 SLOSH DYNAMICS

Significant effort was expended to define a meaningful slosh dynamics experiment that was compatible with the experiment system. Design of a system to measure slosh forces on the tank pressure vessels and installation of slosh baffles that would not interfere with other experiments was very difficult.

Since there is nothing inherently different about liquid hydrogen slosh or even cryogenic slosh, it was most efficient to delete the experiment from COLD-SAT and obtain the required information from experiments using a referee fluid on the space shuttle. However, the dynamic behavior of the COLD-SAT spacecraft during imposed accelerations and fluid repositioning will provide some data on sloshing of cryogenics in the various tanks.

2.1.7 TANK THERMAL PERFORMANCE

The goal of this experiment is to characterize the long-term behavior of high-performance liquid hydrogen tanks in the space environment, which include the effects of atomic oxygen and space debris. The development of cryogenic tankage with thermal performance that far exceeded the requirements of the remainder of the experiment set would have been required to integrate this experiment. In addition, there is a fundamental conflict between the instrumentation and flow system requirements of other COLD-SAT experiments and the requirements for the high thermal performance demanded by this experiment. Finally, to obtain long-term degradation data the duration of the COLD-SAT mission would have had to be extended considerably.

Since there is little microgravity effect on the performance of tank thermal control systems, the major portion of the data of interest can be obtained on the ground. On the basis of cost-effectiveness, the decision was made to delete this experiment and allow this area to be investigated using ground-based tests.

2.1.8 PRESSURIZATION OF CRYOGENIC TANKAGE

The quantity of pressurant gas required to increase the pressure of a tank containing cryogenics above the saturation pressure is difficult to calculate, because it depends on heat and mass transfer phenomena which are strongly influenced by the acceleration field. The quantity of gas required can be significant. The goal of this experiment is to characterize the pressurization process under a variety of acceleration and gas-flow conditions.

2.1.8.1 Experiment Description

The basic experiment is quite simple. Gas in a known thermodynamic state is introduced into a tank partially filled with a cryogen which is also in a known state. The quantity of gas required to initially increase the pressure and maintain it with time and outflow are measured. Fluid position and acceleration level are varied. The internal temperature of the tank (liquid and ullage) are measured as is the tank pressure and all flow rates. Pressurization is conducted using both non-condensable gas and vaporized propellant.

2.1.8.2 Experiment Requirements

At least two cryogenic tanks of various sizes with acceptably low heat leak and various fill levels of cryogenic fluid are required. A controlled source of noncondensable gas (helium) and condensable gas (hydrogen) are also required. Acceleration is required create a Bond number greater than 4 to settle the fluid for some experiments.

Required measurements are tank pressure; tank liquid, tank wall, and tank vapor temperatures; thermodynamic state; flow rate; and total injected mass of incoming gas.

2.1.9 OUTFLOW AND VENTED FILL WITH SETTLING

The goal of this experiment is characterization of the filling and subsequent outflow of cryogenics from tanks using low levels of acceleration to position the liquid. The effects of tank size and flow baffles will be investigated as well as variations in flow rate.

2.1.9.1 Experiment Description

In the vented fill, an acceleration field is established to settle the fluid away from the tank vent and over the inlet, and the tank is cooled to the desired condition. Fluid is then introduced into the tank while pressure is controlled by venting the tank ullage to space. The fill continues until liquid is detected in the tank vent line. The most significant measurements are the quantity of fluid transferred to the tank and the losses determined by

measurement of the total quantity of fluid introduced into the tank and the total venting. Filling takes place through both a straight inlet pipe and a baffled inlet to determine the effect of a baffle.

The settled outflow is essentially the inverse of the settled fill. At the beginning of the test, an acceleration field is established to settle the fluid over the outlet and the tank is pressurized to drive the fluid from the tank. The outflow is initiated at various flow rates and continues until vapor is detected in the outflow. The prime measurements of interest are the initial fill level, the quantity of fluid removed from the tank, and the tank residuals. Outflow takes place from tanks with both straight and baffled outlets to investigate the improvement in efficiency that results from use of a baffle.

2.1.9.2 Experiment Requirements

This experiment requires two different cryogenic tanks: one with an outflow baffle and one without. Both tanks require a vent to vacuum and a source of liquid (vapor-free) cryogen. Basic to the experiment is the detection of vapor in the liquid outflow and liquid in the vented vapor. The fundamental quantities to be measured are the quantity of liquid transferred into the tank during the fill and the quantity of residual cryogen remaining in the tank after the outflow is terminated. Acceleration is needed to position the fluid in the tank. More details may be found in appendix E to this chapter.

2.1.10 LIQUID ACQUISITION DEVICE PERFORMANCE

The purpose of this experiment is to quantify the performance of total communication LAD's in the microgravity environment. The principal areas of interest are the residuals remaining in the tank and the pressure drop that occurs in the LAD.

2.1.10.1 Experiment Description

Properly conditioned fluid is withdrawn from the tank through the LAD at varying flowrates until vapor appears in the outflow. The tank is then locked up and the residual fluid is measured by vaporizing the fluid and measuring the boiloff. A number of outflow rates are used to gather data under a variety of circumstances in order to determine the effect on performance.

2.1.10.2 Experiment Requirements

This experiment requires two tanks equipped with total communication (screen-type) LAD's and the pressurization

and outflow systems needed to expel the fluid from the tank through the LAD. Outflow systems must be equipped to detect two-phase flow (vapor). The tanks must also be equipped to measure the total quantity of gas generated as the residual liquid is vaporized in the tank following outflow. More detailed requirements are listed in appendix F to this chapter.

2.1.11 TRANSFER LINE CHILLDOWN

To be realistic, the transfer line chilldown experiment would have required a separate transfer line in addition to those needed to conduct the various other transfer experiments because proposed flight-type transfer lines are all lightweight, low thermal mass devices. Required pressure, flow, and temperature data rates would have impacted the telemetry design significantly.

It was not expected that low-gravity effects would have a major influence on the behavior of fluid near its saturation temperature in a transfer line so that Earth-based testing could provide most of the required data. A multitude of transfers would, in fact, take place on COLD-SAT so that any gross differences in behavior from one-g to low gravity would likely be observed. For these reasons, integration of the transfer line chilldown experiment was deemed not cost-effective and it was deleted from the experiment set.

2.1.12 CONTROL OF THERMODYNAMIC STATE DURING OUTFLOW

The purpose of this experiment is to verify the operation of a subcooler on the outflow from a cryogenic tank in low gravity. Subcooling allows transfers of cryogenics to take place without prior conditioning of the fluid in the supply tank and/or minimizes the quantity of pressurant or pump power required.

2.1.12.1 Experiment Description

In this experiment, the fluid to be transferred flows through the secondary side of a heat exchanger located at the outlet of a cryogenic tank before entering the transfer line. The primary side of the heat exchanger is cooled by a thermodynamic vent system also using cryogen from the tank. The efficiency of this process is measured and compared with other methods for controlling thermodynamic state.

2.1.12.2 Experiment Requirements

The basic requirements are for a supply of cryogen and a transfer system, an in-line heat exchanger, and a thermodynamic vent system. The heat exchanger must provide cooling as outlined in table 2.2.

TABLE 2.2—HEAT EXCHANGER COOLING

Flow rate, lbm/hr	Subcooling, °R
50	5
100	2

Measurements are required of (1) primary and secondary heat exchanger flow rates, (2) primary and secondary fluid thermodynamic state at both inlet and outlet, and (3) internal heat exchanger temperatures at sufficient points to characterize the operation of the heat exchanger.

2.1.13 ON-ORBIT CRYOGENIC FLUID DUMPING

The goal of this experiment is to obtain data on the quantity of saturated cryogen that can be removed from a tank by simple venting of the tank to vacuum without settling, LAD's, pressurization, or pumping. The data will be used for model verification.

2.1.13.1 Experiment Description

A tank at least half full of a cryogenic fluid in equilibrium with its vapor is vented to space through a path having minimum flow restrictions. When the flow is reduced to a minimal level, the venting is stopped and the tank is locked up. The tank is then allowed to warm to a temperature that would guarantee vaporization of any residuals and the quantity of gas is measured. The experiment takes place in a minimum acceleration environment in which background acceleration is desired. However, the venting itself may perturb the acceleration environment.

2.1.13.2 Experiment Requirements

Basic requirements are a tank of suitable size and negligible heat leak, filled with a known quantity of cryogen at equilibrium with its vapor, and a valve-controlled dump line to vacuum. Basic measurements are the quantities of fluid in the tank before and after the dumping takes place. Acceleration in the microgravity background range is required. In addition, the dump event itself must cause only minimal perturbation to the acceleration environment. More details are provided in appendix G to this chapter.

2.1.14 ADVANCED INSTRUMENTATION

A number of measurements are critical to the effective management of cryogenic fluids in the low-gravity environment. The principal need is to obtain techniques to measure the

mass of cryogen in a tank and the true mass flow rate of cryogens in a line. The purpose of this experiment is to verify operation of instruments that perform these types of measurements in low gravity.

Two instruments were originally considered for this experiment: (1) a true, two-phase mass flowmeter and (2) a tank mass gage. At the time of this study, no tank mass gage had been developed to a point where integration into the COLD-SAT experiment system could begin; therefore, the mass gage was dropped. There is no reason to believe that a gage could not be successfully integrated at a later date, but lack of information prevents further progress at this time.

A two-phase hydrogen mass flowmeter is being developed by Quantum Dynamics under contract with the NASA Lewis Research Center (ref. 3). This flowmeter could be integrated into the COLD-SAT experiment system.

In addition to the flowmeter, all that is required is a flow of liquid and two-phase hydrogen with means of verifying flowmeter operation. The hydrogen flow is readily provided by other COLD-SAT experiment operations. The verification is provided by both alternative flow-measuring devices and by determining the quantity of fluid in various tanks following a transfer.

The only additional requirements imposed are the accurate calibration (on liquid or gas only) of alternative flow measurement devices and the occasional settling of liquid in various tanks to allow an independent level determination.

2.1.15 PARTIAL COMMUNICATION LIQUID ACQUISITION DEVICE (LAD) PERFORMANCE

The purpose of this experiment was to verify the performance of a partial communication LAD with liquid hydrogen in low gravity. However, it proved difficult to integrate with the other COLD-SAT experiments. The physical structure of the device interfered with the performance of other experiments in the same tank, and so in the end, would have required the addition of another cryogenic tank to COLD-SAT for the sake of this experiment. This approach did not appear cost-effective and would have severely impacted already tight volume restrictions; hence, this low-priority experiment was deleted.

2.2 Orbital Requirements

A number of requirements were placed on the COLD-SAT mission that affected the selection of an orbit. The three principal requirements were:

- (1) Orbital life greater than 500 years
- (2) No launch window
- (3) Peak background (drag) acceleration less than $1 \mu g$

Each of these requirements requires some explanation.

Major portions of a spacecraft of COLD-SAT's size and type will survive reentry into the atmosphere (ref. 4). Uncontrolled reentry of the COLD-SAT spacecraft would present a non-negligible risk of death or injury (ref. 5).

Provisions for performing a controlled reentry of the spacecraft would have a significant impact on spacecraft cost and capability. However, it appears that in the future, with construction of Space Station Freedom, operations in low Earth orbit (LEO) will become commonplace and retrieval of a quiescent spacecraft straightforward. Hence, the decision was made, for purposes of this study, to place the spacecraft into a long-life orbit until it could be retrieved at a later date.

The presence of the spacecraft in orbit presents the potential for generation of orbital debris. However, if the spacecraft is placed in a quiescent state with all pressurants and propellants depleted, the possibility of self-fragmentation is negated. As NASA has not, to date, developed a clear policy on orbital reentry or on generation of additional space debris, this was the approach adopted for COLD-SAT.

Because of the possibility of programmatic schedule slips and potential problems with liquid hydrogen loading, a launch window appears to present an unnecessary risk. The only real effect of requiring there be no launch window is to possibly require a somewhat higher orbit than needed to meet the last requirement, microgravity background acceleration, during periods of maximum solar activity. This decision should not have a serious impact on launch vehicle selection.

The microgravity background acceleration guarantees that surface tension effects will predominate in all experiment hardware onboard COLD-SAT.

2.3 Flight Communications

All communications with the spacecraft in flight are required to take place using the Tracking and Data Relay Satellite System (TDRSS). This is the only guaranteed source of communications available to date. To prevent possible disruption of experiment operations because of tracking and data relay satellite (TDRS) unavailability, the spacecraft is also required to operate normally with communications, both forward and return links, limited to 13 min per orbit of TDRS multiple-access (MA) service. This level of coverage is compatible with projected TDRSS usage.

For critical spacecraft operations, such as attitude acquisition and subsequent solar array deployment, TDRSS single-access (SA) coverage is assumed to be available. Enhanced or continuous MA coverage is assumed available during critical experiment operations. As a backup, capability for Spaceflight Tracking and Data Network (STDN) coverage is also included.

The spacecraft and experiment are required to operate satisfactorily without loss of data if at least one orbit's communications period is missed. This allows for potential problems with the TDRSS, ground communications, schedule conflicts, etc.

2.4 Schedule

The total time from the initiation of phase C/D (design, development, and test of the spacecraft) until delivery of the spacecraft for integration with the ELV is limited to 4 years.

2.5 Reliability

The base reliability requirement imposed was that the probability for the proper operation of all class I experiments should be greater than 0.92. For reliability purposes, the design life of COLD-SAT is 6 months. This reliability number is applicable to the launched and separated spacecraft. It does not include potential failures external to the spacecraft, such as TDRSS failures or problems with the ground support equipment.

Excluded from this number is possible damage from space debris or micrometeoroids. There is little about a spacecraft of the COLD-SAT type that is particularly susceptible to this type of damage, orbital life is short (about 6 months), and there is no known case of an operational spacecraft being disabled by collision with debris or micrometeoroids. In addition, while the micrometeoroid environment is somewhat predictable, the space debris population is purely conjectural, making any realistic numerical estimate difficult.

2.6 Safety

All COLD-SAT operations are required to conform to NHB 1700.1 (Vol. B) of the NASA Basic Safety Manual (ref. 6). All operations at the launch site and the launch itself are required to conform to Range Safety EWR 127-1 (ref. 7).

In addition, a tailored system safety program must be implemented for the entire COLD-SAT program. OSHA requirements must be met as well as DOT requirements covering transportation.

Electromagnetic compatibility is included in the safety area. The spacecraft must be compatible with the environment at the launch site and with the launch vehicle.

2.7 Testing

An overall system test in a properly simulated thermal-vacuum environment with liquid hydrogen and flight software is required prior to delivery of the spacecraft.

2.8 Policy

A number of requirements are imposed on all NASA flight hardware. These include:

(1) All electrical, electronic, and electromechanical (EEE) components must be selected by using the criteria of NASA Standard Electrical, Electronic, and Electromechanical (EEE) Parts List (ref. 8).

(2) All software must be developed in accordance with a plan compatible with NASA Management Instruction NMI 2410.10 (ref. 9).

(3) A full reliability, quality, and configuration management program is required.

2.9 System Design Decisions

In addition to the numerous requirements that needed to be met, a number of system-level design decisions were made and imposed on the design of the COLD-SAT system. These include decisions on design margins, modularity, and electromagnetic compatibility.

2.9.1 MASS MARGIN

A 20-percent margin on spacecraft dry weight against launch vehicle capability will be maintained. That is, the dry weight of the spacecraft is increased by 20 percent, the weight of consumables and launch vehicle payload chargeable weight are added, and the result must be within the capability of the selected launch vehicle for the required orbit. This margin is compatible with weight growth of similar systems following preliminary design (ref. 10). Because the nature of COLD-SAT is that the predominant mass is in structure and tankage and mass can be predicted easily and conservatively, a weight margin on the low side of average was judged acceptable. However, reasonable margins on propellant, power, and telemetry capability are to be maintained by the various subsystems.

Also, because the selected launch vehicle has excess capability, the decision was made to trade increased mass, which in turn leads to increased strength margins and higher factors of safety, in return for simplified design, reduced analysis and testing, and ease of fabrication.

2.9.2 MODULAR DESIGN

The decision was made to modularize the experiment system and its associated spacecraft structure into testable units,

because of the difficulties associated with testing and debugging liquid hydrogen systems. This allows complete assembly, checkout, and test before integration into a complete system. A similar approach is used for the electronics. This approach was intended to minimize problems during the (very expensive) system test.

2.9.3 ELECTROMAGNETIC COMPATIBILITY

The total operating magnetic dipole moment of the spacecraft will be held at less than 30 A-m². This will hold disturbance torques generated by Earth's magnetic field to a minimum and will allow use of magnetometers for some attitude sensing functions.

For internal design purposes, the spacecraft electronics will be held to the requirements of MIL-STD-461D (ref. 11) and related documents.

References

1. Bowles, E.B.; Dodge, F.T.; and Green, S.T.: Scaling Trades Study of the Cryogenic Fluid Management Flight Experiment. Final report, contract AC-86-002, Southwest Research Institute, 1987.
2. Aydelott, J.C.: Modeling of Space Vehicle Propellant Mixing—Cryogenic Propellants. NASA TP-2107, 1983.
3. Final report, contract NAS3-25057, Quantum Dynamics Inc.
4. Drago, V.J.; and Edgecombe, D.S.: A Review of NASA Orbital Decay Reentry Debris Hazard, Appendix A: BMI-NLVP-TM-74-1, Battelle Columbus Laboratories, March 7, 1974.
5. Crafts, J.L.; and Lindberg, J.P.: Procedure for Estimating Orbital Debris Risks. NASA TP-2507, 1985.
6. NASA Safety Policy and Requirements Document. NHB 1700.1 (Vol. B), NASA Headquarters, June 1993.
7. Eastern and Western Range ESMCR 127-1 Range Safety Requirements (US Air Force 30th Space Wing and US Air Force 45th Space Wing). Range Safety Office, Patrick Air Force Base, Florida, March 31, 1995.
8. MIL-STD-975M (2) (1995). NASA Standard Electrical, Electronic, and Electromechanical (EEE) Parts List. US Department of Defense, Naval Publications and Forms Center, Philadelphia, PA.
9. NASA Software Management Requirements for Flight Projects. NMI 2410.10, Jan. 22, 1992.
10. Hawkins, K.: Space Vehicle and Associated Subsystem Weight Growth. SAWE Paper 1816, May 1988.
11. MIL-STD-461D (1996). Requirements for the Control of Electromagnetic Interference and Susceptibility. US Department of Defense, Naval Publications and Forms Center, Philadelphia, PA.

Appendix A

Pressure Control Experiment Requirements

Two experiment tanks—primary and secondary

Primary tank

- Cylindrical tank
- Length of cylindrical section to diameter ratio (L_c/D) >0.7
- Diameter >4 ft
- Average heat leak <0.1 Btu/hr-ft²
- Imposed wall heat flux levels: 0.1, 0.3, and 0.6 Btu/hr-ft²
- Passive thermodynamic vent system (TVS) with wall-mounted heat exchanger capable of controlling a wall heat flux of 0.3 Btu/hr-ft²
- Active TVS with jet mixer capable of controlling imposed heat fluxes of 0.1, 0.3, and 0.6 Btu/hr-ft²
- Mixer with 2 speeds: nozzle diameter 1/20 to 1/60 tank diameter
- Fill level tests, approximately 90, 75, and 50 percent full
- No helium in system
- No contamination with other condensable fluids
- High-resolution temperature rakes near wall
- High-resolution absolute tank pressure measurement
- Fluid (liquid and vapor) temperature sensors
- Internal liquid level sensors
- Tank wall temperature sensors
- TVS heat exchanger temperatures, active and passive
- Jet mixer flow rate
- TVS thermodynamic state (temperature, absolute pressure, and flow rate)

Secondary tank

- Cylindrical tank with elliptical or hemispherical ends
- Heat leak <0.5 Btu/hr-ft²
- Volume approximately 1/3 to 1/2 that of primary tank
- Passive TVS with wall-mounted heat exchanger
- Temperature and pressure instrumentation

Acceleration

- Three acceleration levels to provide Bond numbers in the primary tank from <0.25 to 20
- Lowest acceleration level may be provided by background acceleration of spacecraft
- Minimize disturbances during applied accelerations

Appendix B

No-Vent Fill Experiment Requirements

Transfer

- Essentially pure liquid at entrance to receiver tank (prechilled transfer line)
- Receiving tank prechilled to remove 90 to 95 percent of internal energy at 300 K (target temperature of approximately 78 K)
- Liquid hydrogen subcooled a variable amount of up to 3 K below saturation temperature at delivery pressure (delivery pressure 15 to 20 psia)
- Flow rates of 50, 100, and 200 lb/hr
- Selection of spray system to be used

Receiver tank 1

- Cylindrical shape with hemispherical or elliptical ends
- Length >4.3 ft
- Length-to-diameter ratio (L/D) >1.6
- Heat leak <0.5 Btu/hr-ft²
- Four spray nozzles tangential to cylindrical section with 10 percent of maximum flow
- Axial spray nozzle(s) situated so fluid may be settled over or away from active spray nozzle
- Diffused liquid inlet

Receiver tank 2

- Approximately spherical tank
- Diameter >3 ft
- L/D : $0.8 < L/D < 1.2$
- Heat leak <0.5 Btu/hr-ft²
- Two spray nozzles mounted tangentially to tank wall and perpendicular to axial spray
- One axial spray nozzle
- Radial spray bar on tank axis providing full spray coverage of tank interior

Acceleration

- Acceleration along tank axes to produce Bond number >4 during some fills (settled fluid condition)

Measurements

- Flow rate and thermodynamic state (temperature and pressure) of incoming fluid
- Receiver tank pressure
- Tank wall and internal temperatures

Appendix C

Chiltdown Experiment Requirements

Fluid transfer/venting

- Liquid at tank inlet
- Inlet flow rates of 50, 100, and 200 lbm/hr
- Tank vacuum vent
- Tank initially at vacuum
- Controlled vent in 5-psi increments

Experimental tanks

- At least two receiver tanks with different sizes and fluid-volume to tank-wall-thermal-heat-capacity ratios
- Tank material of aluminum or stainless steel
- Tank heat leak $<0.5 \text{ Btu/hr-ft}^2$
- Axial and tangential spray systems in all tanks
- Radial spray system in one tank
- Axial jet inlet in at least one tank
- No liquid acquisition device or other obstructions near wall in one tank
- Peak pressure capability $>50 \text{ psia}$
- Initial tank temperature $>400 \text{ }^\circ\text{R}$

Acceleration

- Microgravity background acceleration
- $1.0 \times 10^{-4} g$ acceleration during one test
- $3.0 \times 10^{-5} g$ acceleration during one test

Measurements

- Internal energy (temperature) of tank pressure vessel and associated hardware
- Tank pressure
- Tank internal fluid temperature
- Incoming fluid thermodynamic state (temperature and pressure), flow rate, and quantity
- Vented fluid thermodynamic state (temperature and pressure), flow rate, and quantity

Appendix D

Fill and Refill of Liquid Acquisition Device (LAD) Experiment Requirements

Flow system

- Provisions for the inflow and outflow of liquid cryogen
- Detection of two-phase flow during outflow
- Measurement of fluid thermodynamic state, flow rate, and quantity during inflow and outflow

Tank

- Single cryogenic tank
- Heat leak $<0.5 \text{ Btu/hr-ft}^2$
- Screen type total communication LAD
- Heat exchanger supplied from thermodynamic vent system (TVS) to cool LAD and entrained fluid at least 2 K below saturation temperature
- Capability to vaporize residuals, vent residual gas to space, and measure mass of residual fluid vented

Measurements

- Liquid-vapor detectors in the LAD channel
- TVS flow rate and inflow and outflow thermodynamic state (temperature and pressure)
- Tank pressure
- Tank fluid and wall temperatures

Appendix E

Settled Outflow/Vented Fill Requirements

Transfer

- Inflow-outflow transfer system
- Single-phase liquid at tank inlet
- Transfer rates of 50, 100, and 150 lbm/hr

Experimental tank 1

- Baffled liquid inlet/outlet
- Oriented so liquid may be settled away from vent over inlet-outlet
- Controlled vent to vacuum
- Autogenous pressurization system for expulsion
- Heat leak $<0.5 \text{ Btu/hr-ft}^2$

Experimental tank 2

- Jet (straight pipe) liquid inlet-outlet
- Oriented so liquid may be settled away from vent over inlet-outlet
- Controlled vent to vacuum
- Autogenous pressurization system for expulsion
- Heat leak $<0.5 \text{ Btu/hr-ft}^2$

Acceleration

- Bond number in both tanks ranging from 2 to 10 for settling

Measurements

- Two-phase flow detection in liquid transfer lines
- Liquid detection in each tank vent line
- Tank pressure
- Tank liquid, vapor, and wall temperatures
- Tank liquid level sensors
- Liquid transfer line flow rate and liquid mass
- Vent line gas flow rate and vented mass
- Thermodynamic state of incoming fluid (temperature and pressure)

Appendix F

Liquid Acquisition Device (LAD) Performance Experiment Requirements

Flow system

- Flow rates of 50, 100, and 200 lbm/hr
- Two-phase flow detection for tank outflow

Pressurization system

- Autogenous gas pressurization system supplying vaporized propellant to maintain a tank pressure sufficient to force required flow rates

Primary tank

- Total communication LAD
- LAD cooling via thermodynamic vent system (TVS) heat exchanger
- Liquid/vapor detection in LAD channel
- Heat leak $<0.5 \text{ Btu/hr-ft}^2$
- Capability to vaporize liquid residuals and measure quantity of gas produced

Secondary tank

- Total communication LAD
- LAD cooling via TVS heat exchanger
- Liquid/vapor detection in LAD channel
- Heat leak $<0.5 \text{ Btu/hr-ft}^2$
- Capability to vaporize liquid residuals and measure quantity of gas produced

Acceleration

- Background

Measurements

- Tank wall, LAD, and fluid temperatures
- Fluid outflow rate, total mass, and thermodynamic state
- Tank pressure, LAD differential pressure
- Thermodynamic vent system (TVS) performance (inlet and outlet temperature and pressure; flow rate)
- Total mass of vaporized residuals as gas flow rate, pressure, and temperature
- Mass of pressurant gas injected
- Pressure, temperature of injected gas

Appendix G

Tank Dumping Experiment Requirements

Tank

- Volume at least 10 ft³
- More than half full of saturated cryogen at equilibrium with its vapor (no noncondensables)
- Heat leak <0.5 Btu/hr- ft³
- Dump system providing minimal flow restriction to vacuum
- Capability to vent and measure vaporized residuals

Acceleration

- Background
- Vent system designed to minimize any direct acceleration of spacecraft

Measurements

- Initial fluid mass in tank
- Dump-line flow detection
- Tank pressure
- Tank wall and internal temperatures
- Residual vent gas flow rate, total flow, and thermodynamic state

Chapter 3

System Overview

Edward Kramer
National Aeronautics and Space Administration
Lewis Research Center
Cleveland, Ohio

3.0 Introduction

The purpose of this chapter is to provide an overview of the complete COLD-SAT system so that the detailed descriptions provided in the following chapters may be understood in relation to the whole. It is intended to provide a brief summary of the capabilities and characteristics of the various elements and subsystems.

3.1 Overall System Concept

Figure 3.1 provides an overall block diagram of the COLD-SAT launch and flight systems. COLD-SAT will be launched on an Atlas I (Centaur) expendable launch vehicle (ELV). Prior to launch it will be loaded with liquid hydrogen using a COLD-SAT unique loading system which is adapted to the Centaur liquid hydrogen loading system. The ELV will require some modifications to accommodate COLD-SAT loading requirements.

Loading of COLD-SAT will be controlled at the launch site and monitored by the COLD-SAT Payload Operations Control Center (POCC), another COLD-SAT system. COLD-SAT will be launched in an active state and will control its liquid hydrogen cargo during ascent. This process will be synchronized with ELV activities and monitored at the POCC using information included in the ELV telemetry downlink.

Following separation from the ELV upper stage (Centaur) the spacecraft will control its liquid hydrogen cargo, stabilize itself in the proper attitude, and deploy its solar arrays and antenna. This process will be monitored (and if necessary controlled) from the POCC using Tracking and Data Relay Satellite System (TDRSS) single-access (SA) service. Following successful attitude acquisition and deployment, the space-

craft will be controlled from and data returned to the POCC using TDRSS multiple-access (MA) service.

At the Goddard Space Flight Center (GSFC), the Network Control Center (NCC) will schedule and coordinate communications with the COLD-SAT spacecraft. The GSFC will provide tracking information and orbit predictions to the COLD-SAT POCC. Communication between TDRSS, NCC and the COLD-SAT POCC will use the NASCOM system.

3.2 Spacecraft Concept

Figure 3.2 is an artist's conception of the COLD-SAT spacecraft showing its principal features. As can be seen, the main portion of the spacecraft volume is occupied by three liquid hydrogen tanks for experimental use. These tanks and the remainder of the spacecraft systems are supported by an external spaceframe structure. The spacecraft is equipped with two solar arrays and a deployable high-gain antenna. Figure 3.3 provides a cross sectional view of the spacecraft and a summary of its characteristics. COLD-SAT is a large spacecraft, over 25 ft long, which weighs over 5700 lb at launch. The launch vehicle payload fairing and allowable payload envelope are also shown in figure 3.3. One of the continuing challenges during the design of the COLD-SAT system was fitting experiment tanks of adequate size within the available payload envelope; COLD-SAT is a fundamentally volume-limited payload.

COLD-SAT is a fully modularized spacecraft. This was done to allow completed functional units to be fully tested prior to spacecraft integration and so minimize the risks associated with debugging a complex liquid hydrogen system at final assembly and test. Figure 3.4 identifies the various modules of the spacecraft.

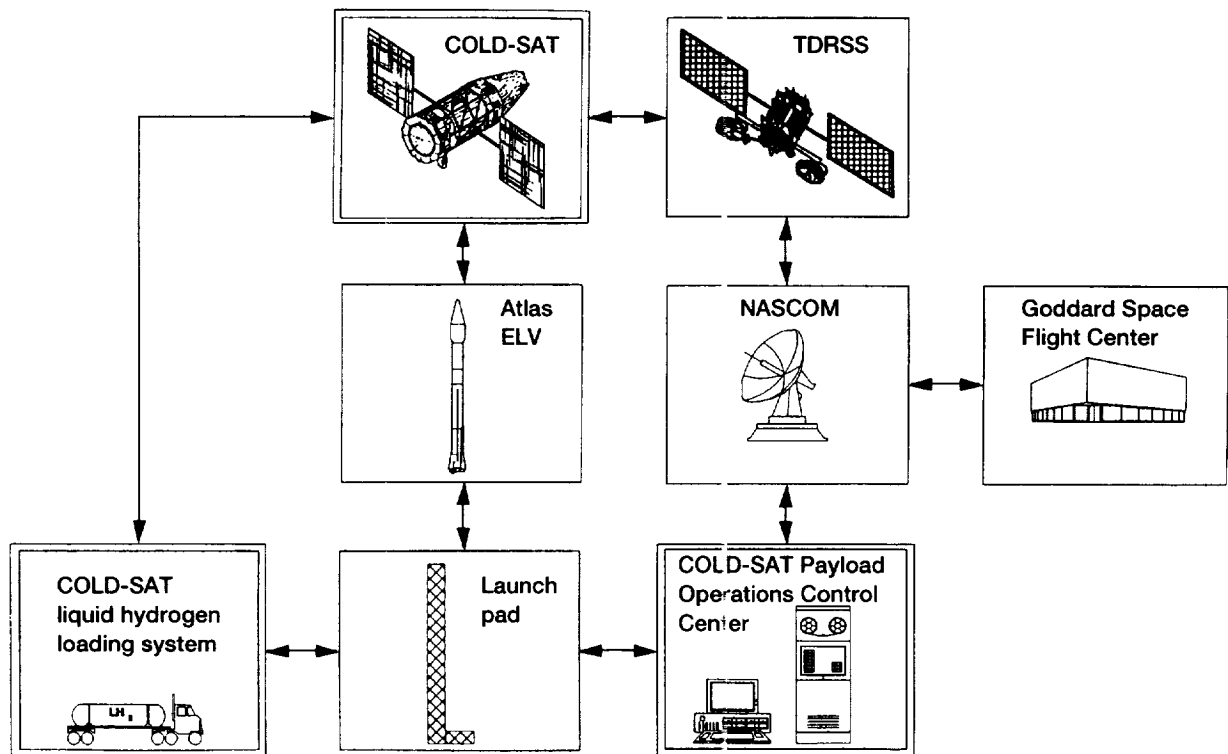


Figure 3.1.—COLD-SAT launch and flight systems (double boxes indicate new equipment for COLD-SAT).

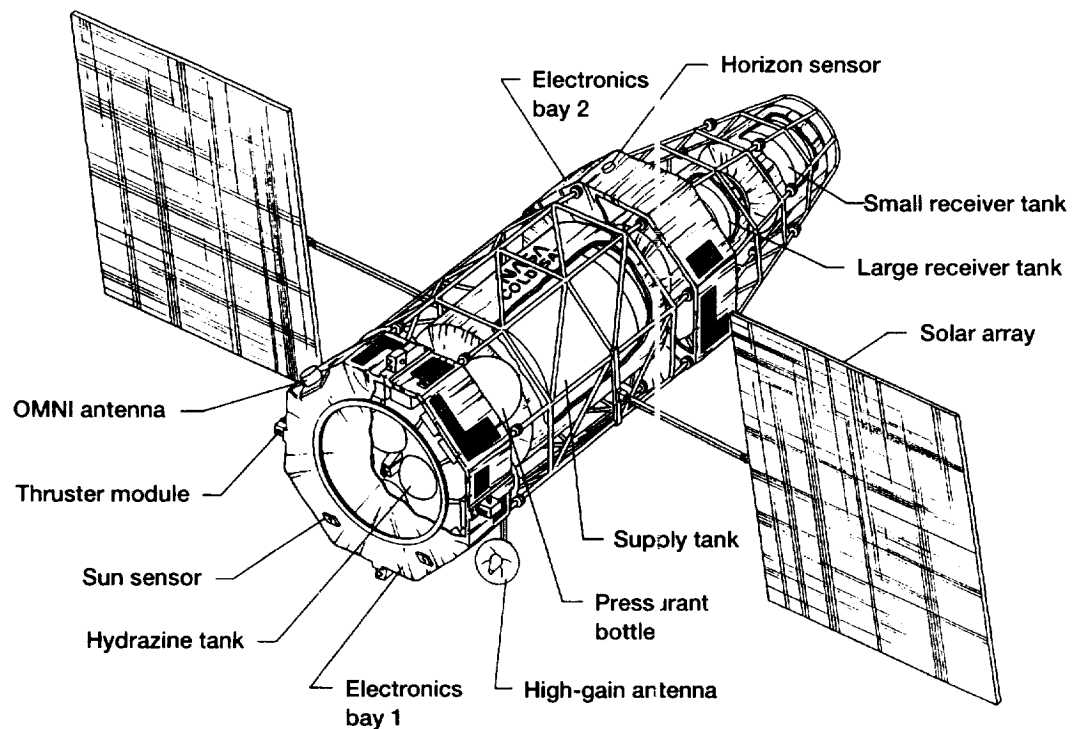


Figure 3.2.—Artist's conception of COLD-SAT spacecraft.

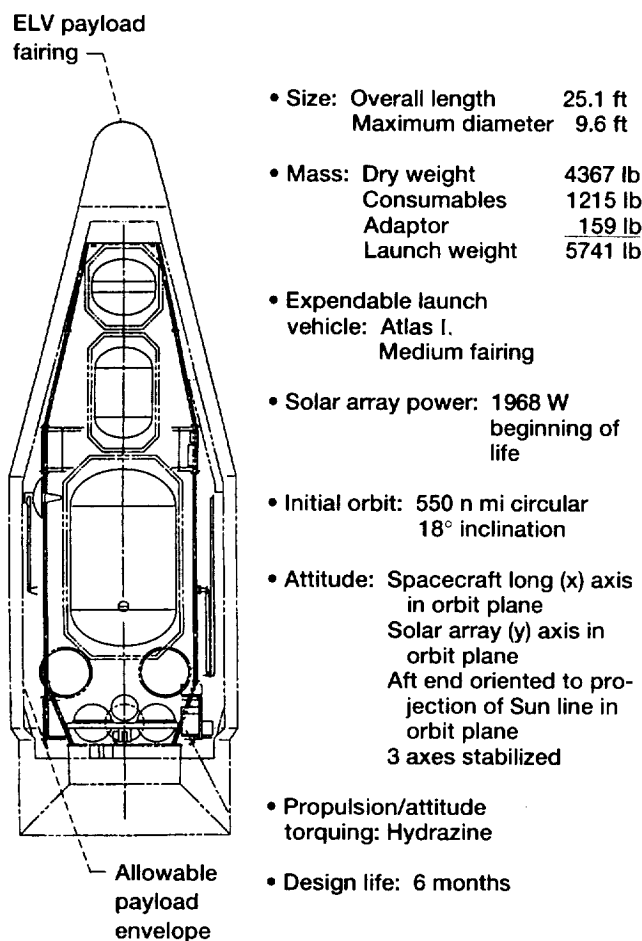


Figure 3.3.—Summary of COLD-SAT characteristics.

Module 1 contains the majority of the purely spacecraft systems. The payload adaptor, which connects the spacecraft to the launch vehicle is attached to the lower end of this module as are all of the propulsion and attitude control thrusters. The interior of this module contains the remainder of the propulsion subsystem. The majority of the spacecraft electronics are attached to electronics bay 1 which surrounds the exterior of the module.

Module 2, the supply module, contains the liquid hydrogen supply tank, launched full of liquid hydrogen, the gaseous hydrogen and helium supplies, and associated plumbing and instrumentation. The module structure provides support for the solar arrays and the high-gain antenna. Module 3 attaches to module 2 and houses the remainder of the COLD-SAT electronics and the horizon sensors. Modules 4 and 5 each contain one liquid hydrogen experimental tank and its associated plumbing and instrumentation.

Figure 3.5 defines the spacecraft coordinate system. The positive x-axis follows the long axis of the spacecraft from the payload adaptor up. The y-axis lies along the axis of the solar arrays normal to the x-axis. The positive z-axis forms a right-hand system with the other two axes and points in the direction

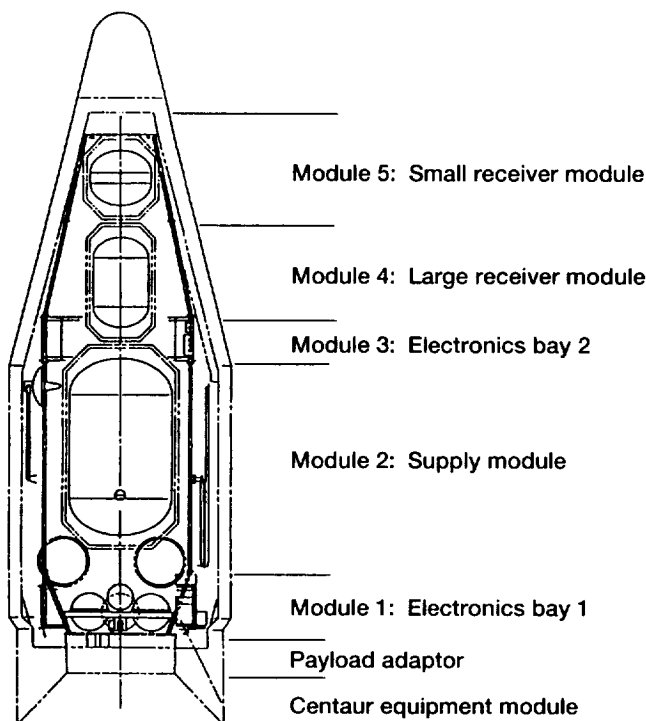


Figure 3.4.—Spacecraft module identification.

away from the high-gain antenna. In the selected attitude, the x-axis lies in the orbital plane and points away from the projection of the Sun line in that plane. This causes module 1 to act as a partial Sun shield for the cryogenic portions of the system. The spacecraft is rotated 180° as required to assure that the Sun always falls on the high-gain-antenna side of the spacecraft. This causes COLD-SAT to have a hot side and a cold side. The cryogenic piping and valving is confined to the cold side.

3.2.1 EXPERIMENT SYSTEM

The experiment system has the largest mass and volume (and cost) of any system on the spacecraft. Figure 3.6 is a (very) simplified schematic diagram of the fluid-handling portion of the experiment system. It is composed principally of three tanks interconnected by a liquid transfer system. There is also a gas supply (and generation) system for pressurizing the tanks and a vent system for each tank.

The supply tank is launched loaded with 565 lb of liquid hydrogen and serves as the source of all experiment fluid. None of the tanks is vacuum-jacketed. To allow handling of liquid hydrogen on the ground, the supply tank only is equipped with a purge bag and helium purge system. This results in a ground boil-off rate of up to 85 lbm/hr but the tank is continually topped off until 4 sec before launch. Once on orbit the tank insulation system is vented to space vacuum and the heat leak is reduced to acceptable levels.

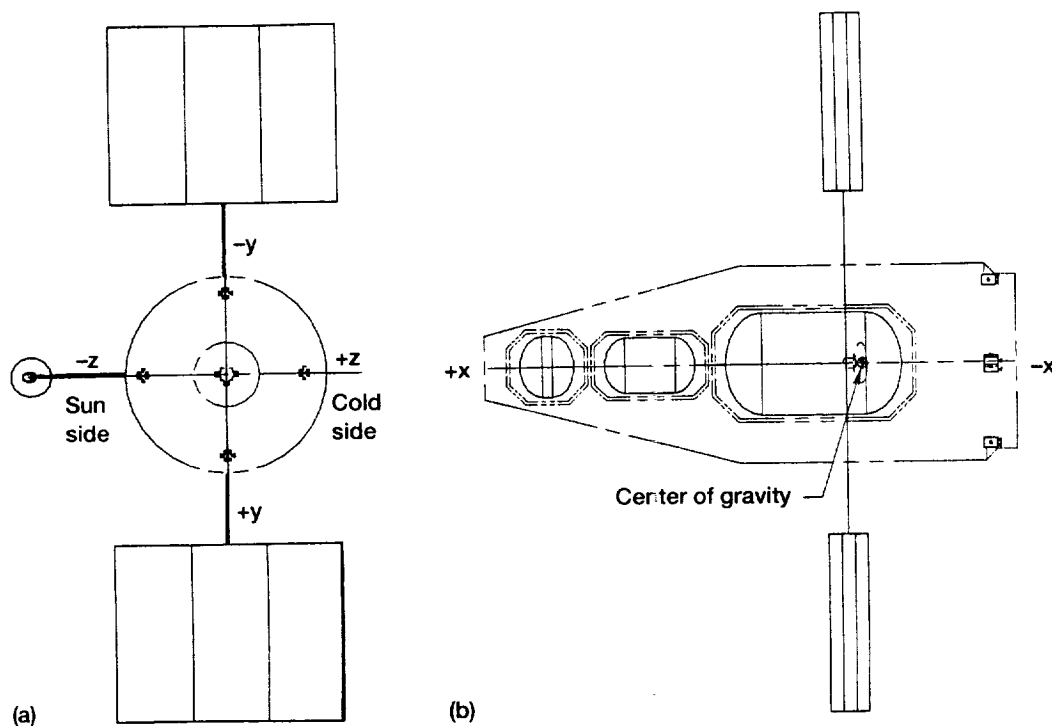


Figure 3.5.—Spacecraft coordinate system (a) End view (along x-axis in the negative x direction).
(b) Top view (along z-axis in the negative z direction).

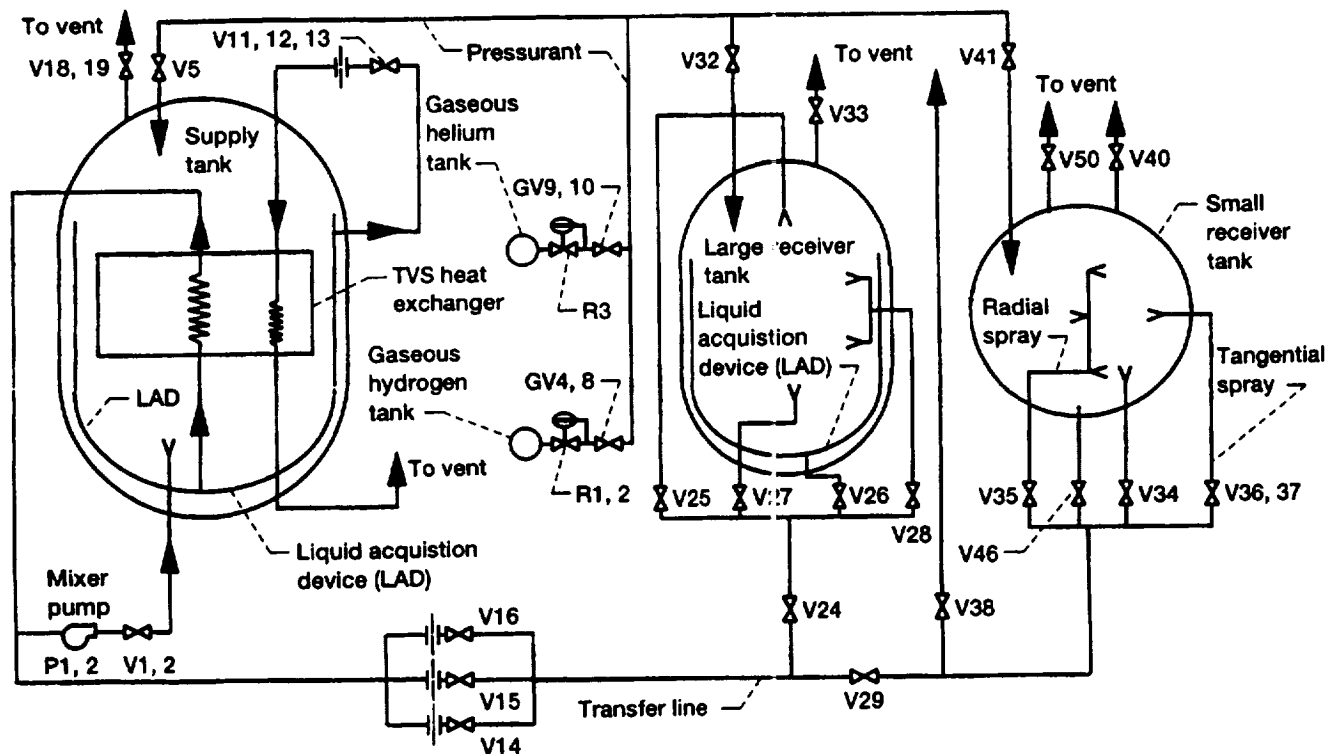


Figure 3.6.—Simplified fluid schematic of experiment system. [See table 3.1 for experiment system tank characteristics. See also figure D.1 for more detailed fluid schematics.]

TABLE 3.1.—EXPERIMENT SYSTEM TANK CHARACTERISTICS

	Supply tank	Large receiver tank	Small receiver tank
Volume, ft ³	144	21	13.5
Capacity, lb liquid hydrogen	565	84	54
Length, ft	8.6	4	2.6
Diameter, ft	5	2.7	3
Average heat flux, Btu/hr-ft ²	0.08	0.3	0.4
Surface area, ft ²	143	39	28

The experiment system tanks are all cylindrical with elliptical domes. However, the barrel section of the small receiver tank is rather short. The characteristics of the tanks are listed in table 3.1.

All tanks are equipped with thermodynamic vent systems and the supply tank is equipped with a mixer and heat exchanger for active pressure control. All tanks are insulated with multilayer insulation (MLI). The outer surface of the MLI is thermally conditioned to minimize absorption of the solar spectrum and maximize radiation.

The pressure vessel of each tank is instrumented for temperature. Each tank contains an instrument rake equipped with temperature and liquid level sensors. Redundant instrumentation measures the pressure of each tank. The supply tank and large receiver tank are equipped with total-communication LAD's.

The three tanks are linked by a liquid hydrogen transfer system capable of controlled flow rates from 50 to 200 lbm/hr. Using the transfer line, any of the tanks can be filled with liquid hydrogen through a variety of inlets including jets, sprays, and baffles. They can be emptied using baffled or unbaffled outlets or LAD's. The outflow line from the supply tank is equipped with a heat exchanger and TVS to allow the outflowing liquid to be subcooled. This allows considerable savings of liquid hydrogen and pressurant gas when fluid is thermodynamically conditioned for various experiment conditions.

A pressurization system provides gaseous hydrogen and helium to the three tanks. Gas pressure is controlled as required to drive the various liquid transfer operations. The hydrogen gas storage tanks can be recharged with liquid hydrogen which reduces the mass of the system and allows for the difficulty of predicting the quantity of hydrogen required for pressurizing the liquid tanks. Each tank can also be vented to space in a controlled manner via free- and back-pressure vents. The liquid transfer, pressurization, and vent systems are equipped to measure the thermodynamic state and quantity of the flowing fluids so that a complete mass inventory can be maintained.

While the main data acquisition and signal conditioning task is carried out by the spacecraft telemetry, tracking, and command (TT&C) system, the experiment system includes the electronics required to perform some special signal conditioning and data acquisition functions. Included with the experiment system electronics are the accelerometers required to measure the experimentally important acceleration levels.

3.2.2 SPACECRAFT SYSTEMS

COLD-SAT is a very highly integrated spacecraft. Every effort was made to take advantage of the performance improvements possible by coordinating the design of the various subsystems.

3.2.2.1 TT&C System

Figure 3.7 is a block diagram showing the interrelationship of the various spacecraft systems with the TT&C and electric power systems. As can be seen, control and data acquisition is centralized on the spacecraft. The spacecraft computer, located in the TT&C system, provides control for all spacecraft functions including attitude control.

Other than certain functions associated with the high-gain antenna, the TT&C system is fully redundant, and includes a unique method for maintaining a "hot" backup spacecraft computer. The TT&C system is built around a redundant MIL-STD-1553 data bus.

The basic spacecraft data rate is 3900 bits per second (bps). Between TDRSS contacts, spacecraft data is stored in redundant solid state recorders capable of storing 512 Mb each. This provides storage for up to 20 orbits if required. For nominal operations data is played back via TDRSS at 32 000 bps during TDRSS contacts of 13 min each orbit. The uplink data rate for commands and reprogramming is 1000 bps.

Communications takes place using NASA standard transponders. The spacecraft is equipped with a deployable, two-axis-steerable, high-gain antenna for normal, high-data-rate communication with TDRSS. As a backup, two hemispherical coverage antennas are located on opposite sides of the spacecraft to provide communications before the high-gain antenna is deployed and during contingencies if the spacecraft loses attitude control or the high-gain antenna system fails.

3.2.2.2 Electric Power System

The average electric power required for the spacecraft is 646 W. This power is ultimately derived from two fixed solar panels. Each solar panel has an area of 91.5 ft² providing a maximum beginning-of-life (BOL) power of 1968 W. The plane of the solar arrays is canted 10° with respect to the x-y plane of the spacecraft which lies in the orbit plane. This

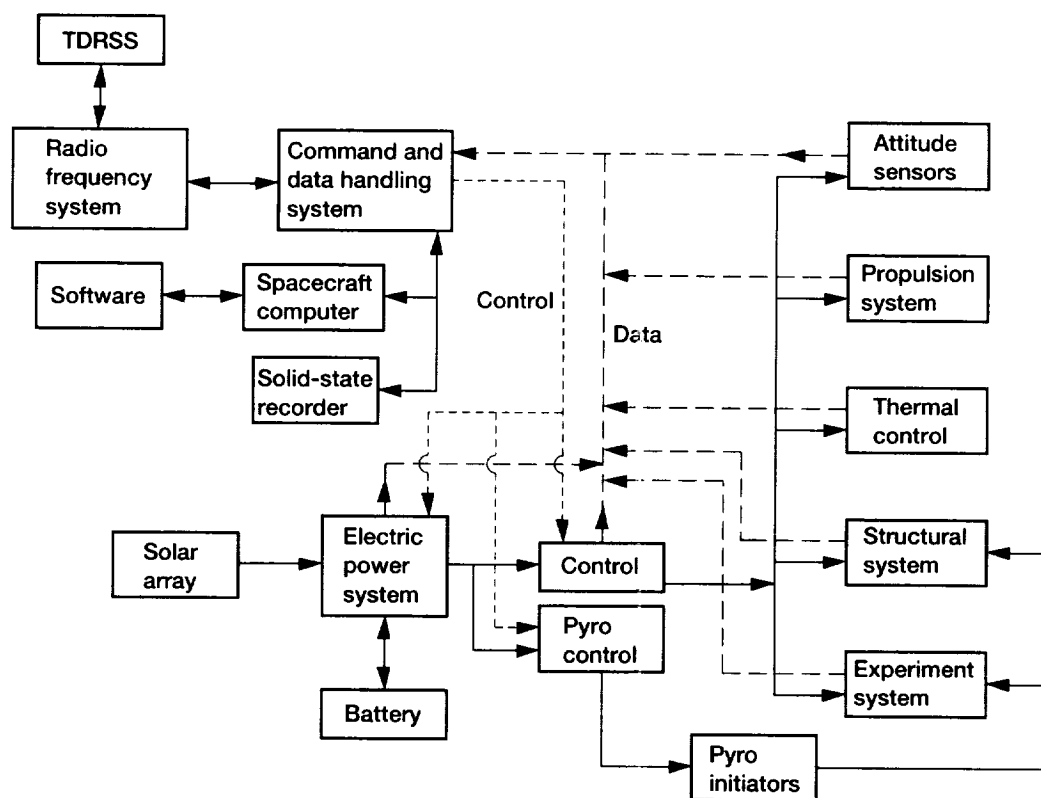


Figure 3.7.—Spacecraft command and control system and electric power system.

provides optimum output from the solar arrays as the angle to the Sun varies caused by the precession of the spacecraft orbit. As was indicated above, the entire spacecraft is rotated 180° when the Sun moves from one side of the orbit plane to the other. For operation during attitude acquisition and solar array deployment and during eclipse, power is stored in two 36 A-hr nickel cadmium batteries. During eclipse the depth of discharge is 24.7 percent, which assures more than adequate life for the 6-month mission.

The electric power system provides a nominal unregulated bus voltage of 28 V which floats on the spacecraft battery allowing the batteries to provide any necessary surge currents. Most detailed switching of electric power occurs in the TT&C system, but the electric power system does actuate all pyrotechnic devices on the spacecraft. The electric power system provides high-level fault protection and load shed using a system of prioritized power buses. This assures that any available electrical power will be supplied to essential loads during fault conditions.

3.2.2.3 Attitude Control

COLD-SAT is a three-axis stabilized spacecraft. The primary attitude reference is provided by three-axis rate gyros.

The gyros are updated using two-axis digital sun sensors and scanning horizon sensors. The spacecraft is also equipped with a three-axis magnetometer to provide assistance with rapid attitude acquisition.

In the selected spacecraft attitude, the axis of the solar arrays, the y-axis, and the long axis of the spacecraft, the x-axis, lie in the orbit plane (fig. 3.5). The positive z-axis forms a right-hand system with the other two axes and points away from the side of the orbit plane illuminated by the Sun. The attitude control system is required to perform a 180° roll maneuver periodically to maintain this condition as the orbit plane precesses. It is also required to automatically acquire and maintain the correct attitude.

In this attitude, the primary disturbance torque is a gravity gradient torque. The selected attitude is a compromise which allows fixed solar arrays and allows the aft end of the spacecraft to be used as a partial Sun shield at the expense of somewhat increased disturbance torques. The basic pointing accuracy requirement of 2° is driven by the requirements for pointing the high-gain antenna and by the need for reasonable predictability following long-term, low-level thrusting.

The attitude control system also controls the spacecraft during those periods of low-level thrusting required to position fluids for experimental purposes. Primary attitude control

torques are generated using fixed thrusters. The torques are applied in couples around the x-axis and single thrusters are used for control about the y- and z-axes. A gimballed thruster is used for control during long-term thrusting.

The attitude control system also handles the navigation functions required for the interpretation of horizon sensor data and the proper pointing of the high-gain antenna. All software functions of the attitude control system reside in the spacecraft computer which is part of the TT&C system.

3.2.2.4 Propulsion System

Hydrazine is used as the propellant for all thrusters. At launch, 428 lbm of propellant are loaded, an amount which includes 150 lbm of reserve. The hydrazine is stored in four spherical tanks equipped with bladders. It is expelled from the tanks using pressure-controlled helium.

The propulsion system is located completely within module 1 with thrusters located on the aft end of the spacecraft. This arrangement minimizes the problems associated with hydrazine plumbing and potential effects of thruster plumes on thermal control surfaces. All thrusters are contained in five thruster modules, one located on the center line and four located around the periphery. All attitude control thrusters are redundant. Some propulsion thrusters are redundant with degraded performance.

To provide controlled acceleration for experiment purposes, the propulsion system generates three thrust levels: 0.04, 0.16, and 0.52 lb. During these thrusting periods, attitude control is provided by a gimballed thruster located on the x-axis. This eliminates the impulsive action of the pitch and yaw attitude control thrusters and thus provides a superior acceleration environment.

3.2.2.5 Thermal Control System

Thermal control was a major issue in the design of COLD-SAT. The prime concern was to minimize the heat input into the cryogenic system and, as a result, to simplify the design. A number of key design decisions were made on the basis of their thermal impact such as the choice of spacecraft attitude. The thermal design had an especially large effect on the spacecraft configuration. Basically, the thermal control system is divided into a number of zones which are isolated from each other to the maximum extent possible. The two electronic bays, modules 1 and 3, contain those items which require a relatively narrow temperature range. The other (cryogenic) portions of the spacecraft are operated at as cold a temperature as possible.

The thermal control system relies primarily on passive techniques—paint, MLI, second-surface dielectric mirrors, etc. Heaters are used in the electronics bays to assure that minimum temperature requirements are met when the equipment is powered down.

3.2.2.6 Structure and Configuration

A number of basic constraints governed the configuration of the spacecraft. These were:

(1) The need to accommodate the experiment tanks within the launch vehicle payload envelope.

(2) The need to keep the center of mass (COM) as low as possible.

(3) The thermal requirement to provide the cryogenic tanks with a good radiative view factor to deep space while shielding them from the Sun and local heat sources.

(4) The modularization of the spacecraft with all that this implies in terms of thermal and structural constraints.

To satisfy these requirements a space-frame type of structure on the outside of the spacecraft was chosen. This allows the cryogenic tanks to be kept on axis but have good radiation view factors to space through the structure while accommodating modular design for ease of test and integration. To maintain a low COM, the densest items (batteries, hydrazine, electronics, etc.) were located in module 1, closest to the payload adaptor (figs. 3.2 and 3.4). With the large cryogenic tanks on axis this arrangement made it possible to maintain good symmetry about the spacecraft x-axis as well.

The structure is conventional, made out of standard shapes and welded except at access points where it is bolted. It does have a few unique features. A large honeycomb plate is used to mount the hydrazine tanks in the center of electronics bay 1 and all electronics boxes are mounted on modular plates located around the perimeter of the electronics bays.

Every effort was made in the design to minimize disturbance torques through the control of the spacecraft configuration and so of its mass properties. Spacecraft moments and products of inertia were controlled to the extent possible to minimize gravity-gradient torques. The solar arrays and high-gain antenna are located near the average location of the COM along the x-axis to minimize solar pressure torques. In addition, the design includes compensating weights to minimize the products of inertia.

3.2.2.7 Software

Control of essentially all operations, both spacecraft and experiment, is by software resident in the central spacecraft computer. Because of the restrictions imposed on TDRSS coverage and the long-term nature of some experiment operations, this software must provide a high degree of autonomy to the spacecraft. The nature of the liquid hydrogen payload, which cannot simply be allowed to sit until problems are discovered and diagnosed on the ground, requires that a number of corrective actions be attempted by the flight software in failure situations.

The operation of the software is centered around an executive which schedules and controls the operation of various control and calculation routines as required. For the experiment, execution of the various experiment sequences is scheduled by ground command and then executed by the spacecraft. An ongoing function of the software is to continuously monitor the experiment system to prevent or correct unsafe states. On the ground, the software will also control the loading of liquid hydrogen.

A considerable portion of the software will reside in read-only memory onboard the spacecraft to insure that it is not inadvertently corrupted. However, virtually all software is reprogrammable from the ground. To assure against changes in the software and proper functioning of the hardware, the software will continuously generate checksums and similar internal checks on operation and write the result to the redundancy control unit in the TT&C system. Failure to perform this function on schedule will result in a switch to the "hot spare" computer and software.

3.3 Ground Segment

On the ground, a variety of equipment is required to support the development, test and operation of the COLD-SAT spacecraft. A number of liquid hydrogen-compatible, thermal-vacuum facilities are needed for development and test, including one large enough to contain the entire spacecraft for system test. Testing must be supported by electrical and mechanical ground support equipment to control the spacecraft, acquire data from it, and service it with the required consumables. Handling fixtures and shipping containers are needed to transport it and support its integration, servicing, and installation.

At the launch site, equipment is needed to test the spacecraft and service it prior to launch. Immediately prior to launch the supply tank must be filled and continuously topped-off with liquid hydrogen using a ground-fill/drain/vent system adapted to the existing Centaur hydrogen loading system. Facilities are required at the launch site to control the spacecraft during the loading process until launch.

From lift-off until separation, spacecraft data is returned via the launch vehicle telemetry stream. This data must be transmitted to the COLD-SAT Payload Operations Control Center (POCC), processed, and recorded. Although there may be other alternatives, for purposes of this conceptual design it was assumed that the POCC would be constructed at the NASA Lewis Research Center. The POCC will control the spacecraft from separation through end-of-life through the NASCOM/TDRSS network. It will process all data returned from the spacecraft and both display and record it as required.

The POCC will produce historical data tapes. Final conversion of the data to engineering units and its subsequent analysis will take place offline using conventional computing facilities.

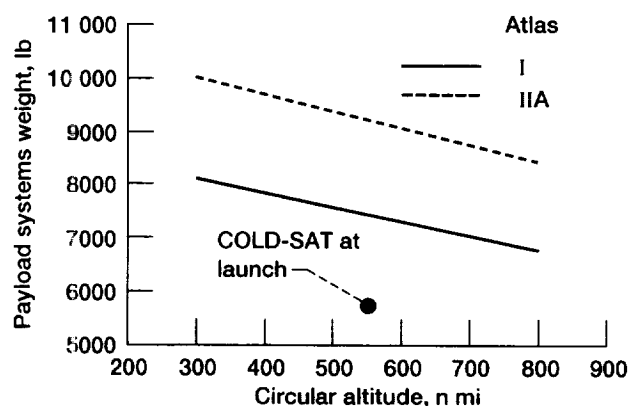


Figure 3.8.—Payload capability versus circular orbit altitude (18° circular orbit).

3.4 Launch Vehicle

COLD-SAT is designed to be launched on the Atlas I (Centaur) expendable launch vehicle supplied by General Dynamics. In the time frame of the COLD-SAT launch it is expected that the Atlas II will be in current production. However, complete data on the Atlas II was not available at the initiation of the conceptual design so the Atlas I was used for design purposes with the expectation of full upward compatibility.

COLD-SAT is to be placed into a 550 n mi, 18° inclination, nearly circular orbit. Figure 3.8 shows the capability of the Atlas I and Atlas IIA launch vehicles for 18°-inclination circular orbits. As can be seen there is more than adequate margin.

A number of launch vehicle modifications and some mission-peculiar equipment will be required. Venting of gaseous hydrogen will occur through the Centaur hydrogen vent; some minor modifications to the Centaur vent and the payload fairing will be required to accommodate this. In addition, a number of access doors will be required in the fairing, including one for the COLD-SAT T-4 umbilical. Modification of an existing payload-attach fitting will be required to handle the COLD-SAT spacecraft.

During ascent, power will be supplied to the spacecraft from the launch vehicle. This will require a mission-peculiar battery and associated electrical equipment (a standard service). The Centaur will also carry a destruct charge to guarantee safe reentry of the spacecraft in the event of inadvertent separation or intentional destruction of the launch vehicle. In addition, the launch vehicle will also provide a number of discrete signals to the spacecraft to synchronize its activities with those of the ELV. COLD-SAT telemetry will be included in the launch vehicle telemetry stream to provide monitoring during ascent.

3.5 Operations

Onboard COLD-SAT, the initial 565 lb of liquid hydrogen is a wasting asset. On the pad, before the supply tank multi-layer insulation (MLI) is evacuated by the vacuum of space, the boiloff rate is 85 lbm/hr. In space, using active methods to control tank pressure the loss rate is approximately 1.5 lbm/day. If pressure control is lost and uncontrolled venting takes place through the relief system, a major fraction of the stored hydrogen could be dumped. These facts drove the planning of COLD-SAT operations.

Prior to the beginning of the launch count the spacecraft will be serviced with hydrazine, gaseous helium, and gaseous hydrogen. On the pad, the spacecraft computer is loaded with software and checked. The computer and its software remain operational from before the initiation of liquid hydrogen loading until the completion of the mission. Liquid hydrogen is loaded and the supply tank is continuously topped-off until $T - 95$ sec when the supply tank is locked up to assure that no venting will take place while in the atmosphere during the initial ascent phase. The 2-in. motion signal from the launch vehicle initiates the ascent phase. In general, venting is inhibited unless required and required venting is coordinated with the launch vehicle. However, a scheduled settled vent takes place during powered flight to condition the fluid in the supply tank so that it may be locked up for the subsequent attitude acquisition and deployment phase. No ground intervention is possible from lift-off to separation but telemetry is returned in the ELV data stream.

Immediately prior to separation, the Centaur upper stage is placed in the desired attitude and a discrete signal from the launch vehicle causes the spacecraft computer to use this known attitude to initialize the onboard attitude reference. Following separation, a breakwire causes the spacecraft to begin to automatically stabilize and seek its required attitude. If the attitude is confirmed by sensor readings, the solar arrays

and high-gain antenna are deployed and on-orbit operations begin. Two additional backup methods for attitude acquisition are provided which assure that the Sun will be acquired and battery charging initiated within 2.83 hr from separation. Worst-case time for final acquisition is 11.4 hr. During this time the spacecraft is monitored from the POCC (and controlled if required) using TDRSS single-access communications.

Following a 2-week checkout period, experiment operations are started. Experiments are grouped in interrelated sequences which last for up to a week. In general, the end of a sequence leaves the experiment system in a quiescent state. Several days of contingency are then allowed which will also allow ground personnel to rest if necessary. Many of the individual experiments are of considerable duration, up to 50 hr. As communications time is limited, experiment operations will be controlled by software which will be loaded at launch (or uploaded) and then initiated from the ground. For planning purposes, communications will be limited to 13 min of TDRSS multiple-access (MA) coverage per orbit although as much MA return service as is practical will be sought during operations.

Periodically, as the precession of the orbit causes the Sun to move from one side of the orbit plane to the other, the spacecraft must be rotated 180° to prevent the Sun from falling on the cold side of the spacecraft and to keep a satisfactory angle with the solar arrays. There is no critical scheduling of this event which is initiated by ground command and controlled by software and it can be easily accommodated during contingency periods between groups of experiments. Active experiment operations will be completed within 62 days of launch. Following this, all residuals will be vaporized and all experiment system consumables will be vented to space. The remaining hydrazine will be depleted to raise the spacecraft orbit and increase its life. The spacecraft will then be shut down.

Following the completion of operations, the data will be archived and analysis performed. The POCC and other ground-segment equipment will be closed out and the project terminated.

Chapter 4

Mission

Edward Kramer

National Aeronautics and Space Administration

Lewis Research Center

Cleveland, Ohio

4.1 Introduction

The selection of orbit, launch vehicle, and spacecraft attitude have a strong influence on the design of a spacecraft and related systems; the decisions are significantly interrelated. Orbital requirements are basically driven by orbital life and drag considerations, but once minimum requirements are met, the final orbit is selected with a view to the capabilities of the expendable launch vehicle (ELV). The ELV must be selected to meet minimum orbital requirements but once it is selected every effort is made to maximize the use of its capabilities to simplify the design of the spacecraft. The selected ELV fixes the maximum allowable launch weight, launch center of mass (COM), and, once a payload fairing is selected, overall spacecraft envelope. In addition, the experimental requirement for long-term, low-level accelerations causes an interaction between spacecraft attitude and final spacecraft orbit. This chapter presents the rationale which led to the selection of an 18° inclination, a 550-n mi orbit, an Atlas II ELV with medium payload fairing, and a quasi-inertial spacecraft attitude that is Sun-oriented with the long axis of the spacecraft in the orbit plane. In reading this chapter it should be recognized that many of the calculations were made early on in the design process and some of the values used do not reflect the final COLD-SAT design values.

4.2 Orbit Selection Criteria

Of the two prime requirements affecting the orbit, the requirement for 500-year life dominates over the requirement for microgravity background acceleration levels. However, this orbital life requirement is effective at the end of the mission when the orbit has been perturbed by thrusting required by the experiment. The orbit perturbation caused by thrusting is dependent on the selected spacecraft attitude and thus, the initial spacecraft orbit is as well.

The lifetimes of long-lived spacecraft cannot be calculated with great accuracy. For COLD-SAT, spacecraft life was estimated by using the methods of D.G. King-Hele (ref. 1). The controlling parameters are spacecraft effective-mass-to-area ratio and orbit perigee height and eccentricity.

An uncontrolled spacecraft will eventually begin to tumble because of random disturbance torques. This tumbling affects the projected area along the velocity vector for drag calculations. For COLD-SAT, the worst case would occur if the spacecraft rotates about an axis normal to both the long axis of the spacecraft and the solar array axis with this axis of rotation perpendicular to the velocity vector. The average projected area of the solar arrays is then:

$$\hat{A}_{sa} = A_{sa} \frac{1}{2\pi} \int_0^{2\pi} |\cos \Theta| d\Theta = \frac{2}{\pi} A_{sa} = 116.5 \text{ ft}^2$$

where

A_{sa} solar array area = 183 ft²

\hat{A}_{sa} average projected area

The spacecraft body can be approximated as a right circular cylinder, 9.6 ft in diameter and 25.1 ft long, rotating perpendicular to its axis. Its average projected area is (ref. 1, p. 27):

$$\hat{A}_B = LD \left(0.818 + 0.25 \frac{D}{L} \right) = 220.15 \text{ ft}^2$$

where

L length of cylinder

D diameter of cylinder

The total projected area of the spacecraft is then:

$$\hat{A} = \hat{A}_B + \hat{A}_{sa}$$

For COLD-SAT, the worst-case average projected area is:

$$\hat{A} = 336.65 \text{ ft}^2$$

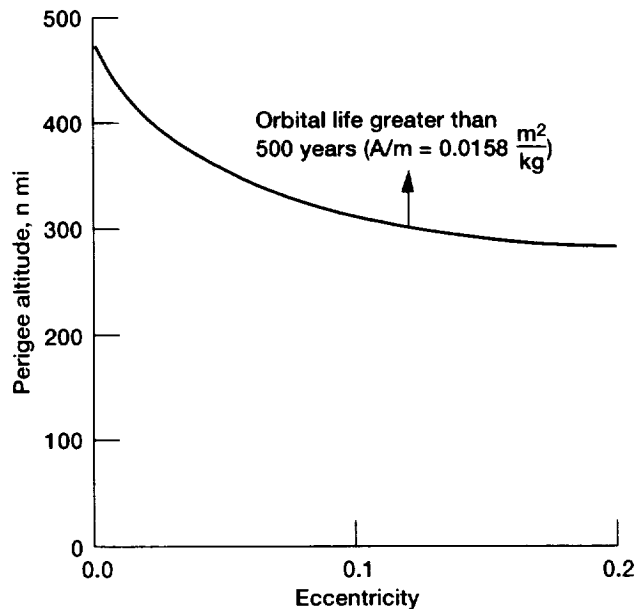


Figure 4.1.—Acceptable end-of-life orbits.

and the ratio of area to end of life (EOL) mass (M_{eol}) is:

$$\frac{\hat{A}}{M_{eol}} = 0.0771 \frac{\text{ft}^2}{\text{lbm}} = 0.0158 \frac{\text{m}^2}{\text{kg}}$$

For a spacecraft with this ratio of projected area to mass, figure 4.1 (adapted from ref. 1, fig. 12.19) shows those combinations of perigee altitude and orbital eccentricity which will give a 500-year life. This is an EOL condition which then becomes a constraint on the initial orbit as perturbed by the experiment thrusting.

4.3 Attitude Selection

Three goals drove the selection of the spacecraft attitude. They were:

- (1) Minimization of gravity gradient disturbance torques
- (2) Minimization of heating of the cryogenic systems by direct solar flux
- (3) Acceptable levels of orbital perturbation due to thrusting required to provide low-level accelerations for various experiments

These goals are not mutually compatible and trade-offs are required. Also considered in attitude selection were the level of drag torques, required view factors for the attitude sensors and high-gain antenna, and potential effects of the selected attitude on the various spacecraft systems, especially the solar arrays. Because of the increased cost and complexity and the potential for disturbance of the experiment, elimination of rotating solar arrays was considered very desirable. Extensive trade studies were performed early in the design effort to select the COLD-SAT attitude.

A total of eight potential spacecraft attitudes were considered. They are summarized in table 4.1 and illustrated in figure 4.2. Six of the candidate attitudes were quasi-inertial and oriented to the Sun, the ecliptic plane, or the orbit plane. These would undergo only slow, secular rotations with respect to a true inertial reference system. Two (attitudes three and four) are oriented to the velocity vector and so the spacecraft rotates 360° once each orbit. This rotation produces a centripetal acceleration which, at reasonable distances from the spacecraft COM, produces accelerations that are an appreciable fraction of a 1 μg . This effect is illustrated in figure 4.3.

TABLE 4.1.—SPACECRAFT ATTITUDE OPTIONS

Attitude option	Axis			Quasi-inertial	Solar array
	x	y	z		
1(a)	Sun-oriented	*	Normal to ecliptic	Yes	Fixed
1(b)	Normal to ecliptic	*	Sun-oriented	Yes	Fixed
1(c)	*	Normal to ecliptic	Sun-oriented	Yes	Fixed
2(a)	Normal to orbit plane	*	To projection of Sun line in orbit plane	Yes	Fixed
2(b)	To projection of Sun line in orbit plane	*	Normal to orbit plane	Yes	Fixed
2(c)	*	Normal to orbit plane	To projection of Sun line in orbit plane	Yes	Fixed
3	To spacecraft velocity vector	Normal to plane defined by velocity and Sun vectors	*	No	Rotating
4	To spacecraft velocity vector	Normal to orbit plane	*	No	Rotating

*Not specified.

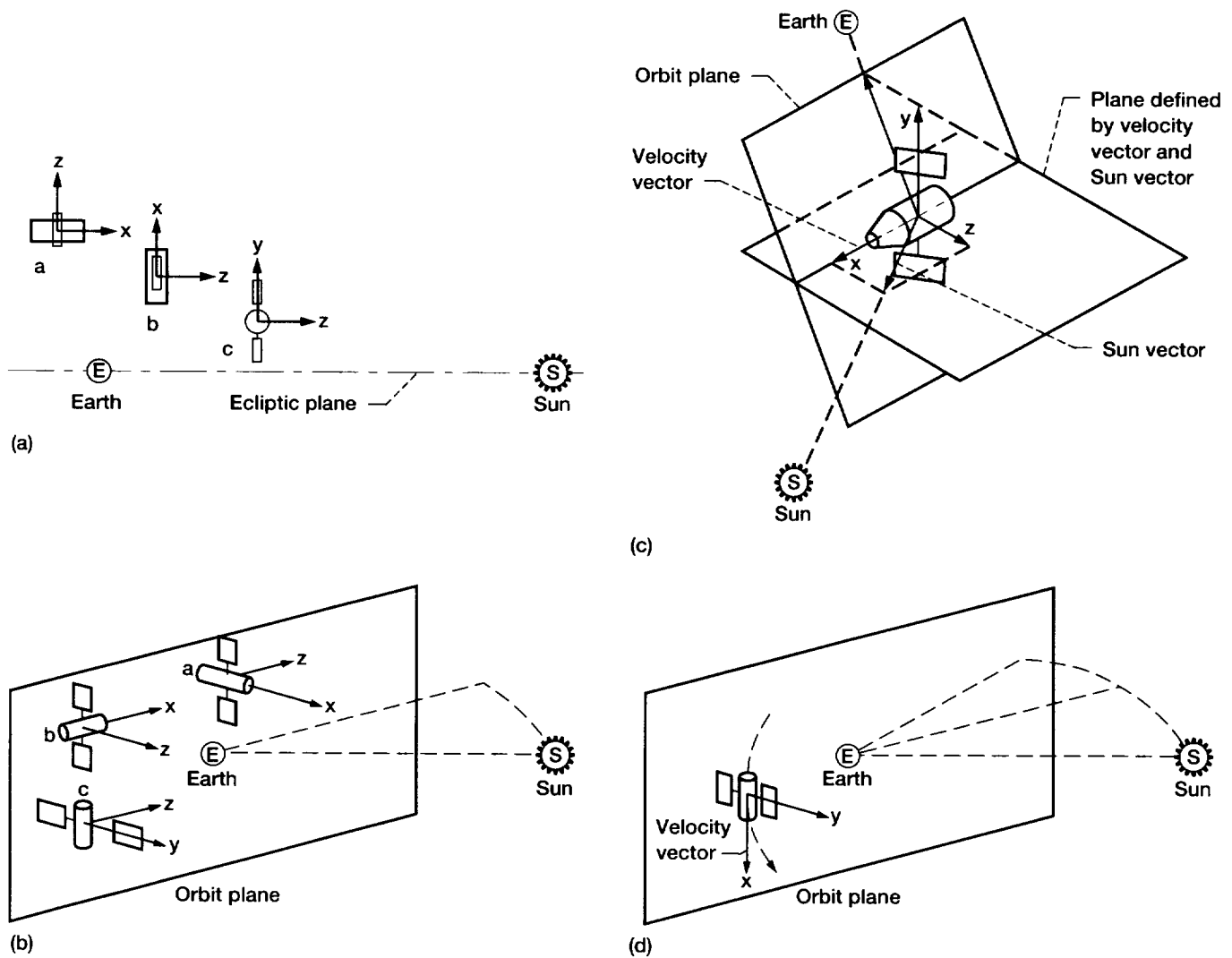


Figure 4.2.—Spacecraft attitude definition. (a) Option 1 (oriented to the ecliptic plane). (b) Option 2 (oriented to the orbit plane). (c) Option 3 (oriented to velocity-Sun vector plane). During each orbit Sun traces out a cone about the spacecraft. (d) Option 4 (oriented to velocity vector and orbit plane).

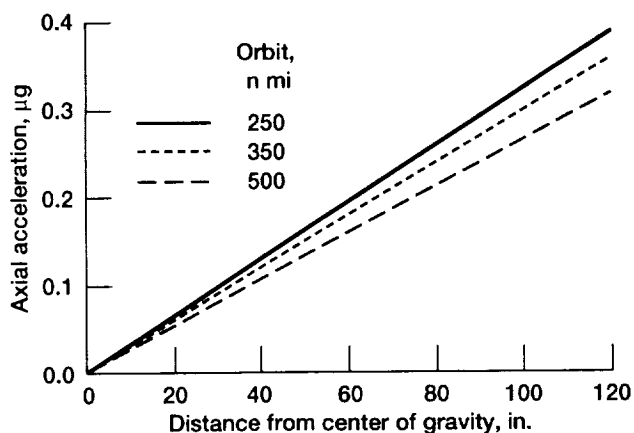


Figure 4.3.—Axial acceleration caused by spacecraft rotation (one rotation per orbit).

4.3.1 DISTURBANCE TORQUES

Disturbance torques are not in themselves important to the COLD-SAT spacecraft, their acceleration levels being far below the threshold which will disturb experiment operations. However, the effects of these torques must be removed by countervailing control torques to maintain spacecraft attitude. Generation of these control torques will either lead to increased spacecraft cost and complexity or cause accelerations that disturb the experiments or both.

Disturbance torques arise from a variety of sources; magnetic, aerodynamic, solar radiation, and gravity gradient torques are the main sources of perturbation. For COLD-SAT, gravity gradient torques are the principal disturbance torques. The gravity gradient torque is given by:

$$\begin{bmatrix} \tau_x \\ \tau_y \\ \tau_z \end{bmatrix} = 3 \frac{\mu}{R^5} \begin{bmatrix} R_x \\ R_y \\ R_z \end{bmatrix} \times \begin{bmatrix} I_{xx} & I_{xy} & I_{xz} \\ I_{xy} & I_{yy} & I_{yz} \\ I_{xz} & I_{yz} & I_{zz} \end{bmatrix} \begin{bmatrix} R_x \\ R_y \\ R_z \end{bmatrix}$$

where

$\tau_{x,y,z}$ elements of torque vector

$R_{x,y,z}$ elements of spacecraft position vector, \bar{R}

R $|\bar{R}|$

$I_{xx,yy,zz}$ spacecraft principal moments of inertia

$I_{xy,xz,yz}$ spacecraft products of inertia

μ GM_e = Earth gravitational constant

All elements are referred to the spacecraft coordinate system. The \times refers to the vector or cross product.

The results of gravity-gradient torque studies for the various attitudes considered are summarized in table 4.2 and illustrated in figures 4.4 and 4.5. These studies were performed by using the inertial properties shown in table 4.3. Values differ considerably from those of the final spacecraft but are used in a consistent manner, so the various trends illustrated are valid.

As can be seen from the figures, those attitudes which are oriented to the velocity vector (3 and 4) produce low peak and average disturbance torques. Those attitudes which are oriented to the Sun or the ecliptic plane (1(a), (b), and (c)) produce large peak and secular torques about all three axes and for this reason they were dropped from further consideration. Those

TABLE 4.2.—GRAVITY GRADIENT TORQUE SUMMARY

Attitude option	Worst-case peak gravity gradient torque, in.-lb		
	Axis		
	x	y	z
1(a)	0.0181	0.0632	0.0452
1(b)	.0206	.0680	.0473
1(c)	.0205	.0682	.0472
2(a)	.0206	.0010	.0015
2(b)	.0004	.0006	.0454
2(c)	.0009	.0684	.0014
3	.0206	.0010	.0015
4	.0003	.0005	.0000
Attitude option	Worst-case average gravity gradient torque, in.-lb		
	x	y	z
	x	y	z
1(a)	0.0088	0.0309	0.0109
1(b)	.0051	.0332	.0230
1(c)	.0100	.0163	.0230
2(a)	.0000	.0003	.0007
2(b)	.0001	.0003	.0000
2(c)	.0001	.0000	.0007
3	.0003	.0005	.0011
4	.0003	.0005	.0000

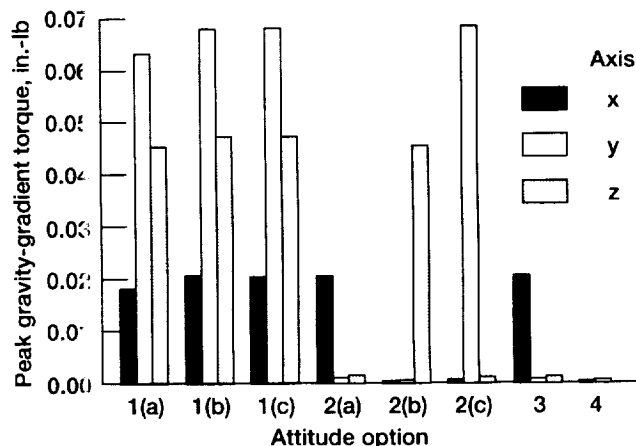


Figure 4.4.—Peak gravity-gradient torque.

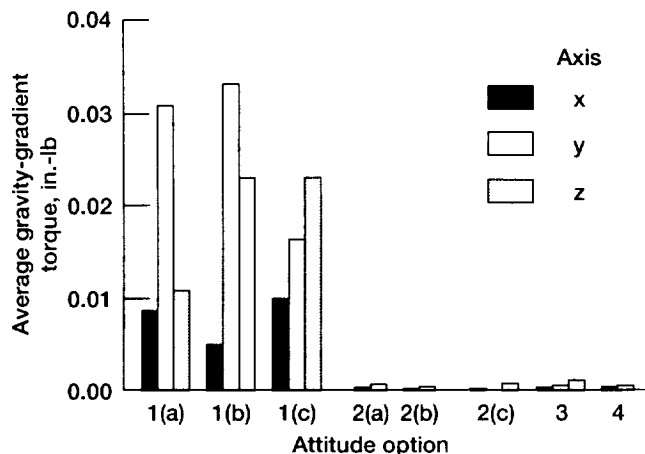


Figure 4.5.—Average gravity-gradient torque.

Attitude option	Moment, in.-lb-sec ²					
	I_{xx}	I_{yy}	I_{zz}	I_{xy}	I_{yz}	I_{xz}
1(a)	25643	49899	59667	-382	-140	-77
1(b)	24373		60937			
1(c)	24373		60937			
2(a)	24373		60937			
2(b)	25643		59667			
2(c)	24373		60937			
3	24373		60937			
4	24373		60937			

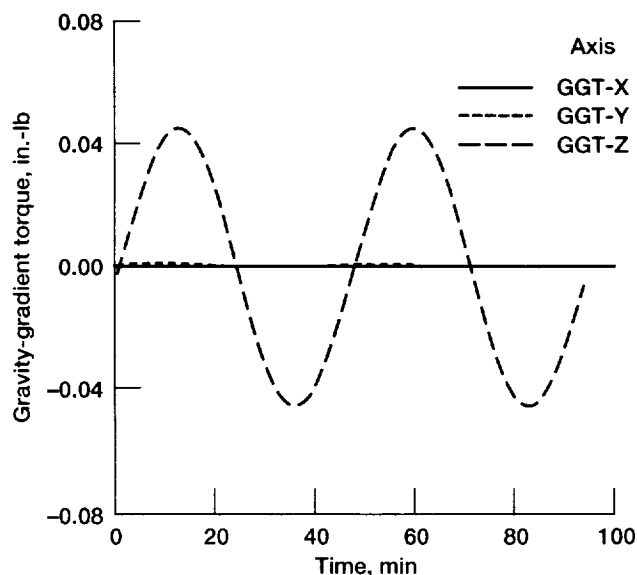


Figure 4.6.—Typical gravity-gradient torque (attitude option 2(b)).

attitudes which are oriented to the orbit plane and the Sun (2(a), (b), and (c)) have moderately large peak gravity-gradient torques about one axis only and low-average torques. For these latter attitudes, figure 4.6 illustrates the typical behavior of the gravity gradient torque with time as the spacecraft proceeds around its orbit.

4.3.2 ORBIT PERTURBATIONS DUE TO THRUSTING

COLD-SAT requires long-term, low-level thrusting to create controlled, low-level accelerations. The required accelerations are in general unidirectional, in the positive x direction. This thrusting will produce perturbations in the initial spacecraft orbit unless canceled by additional thrusting in a suitable direction. It would be possible to add additional experiment hardware to make the system symmetrical with respect to the spacecraft x-axis and add symmetrical thrusters to both ends of the spacecraft to allow balanced thrusting but this would add cost and complexity. It would also be possible to simply perform additional thrusting to cancel the effects of the thrusting required by the experiment but this would entail almost doubling the fuel load. Another option, the one selected, is to accept a certain amount of orbital perturbation and plan on it in the selection of the initial orbit.

The effect of thrusting on the orbit depends on the relation of the thrust vector to the current velocity vector. In the case of the COLD-SAT spacecraft, where all tanks that require experiment acceleration are grouped along the long axis to minimize disturbance torques caused by thrusting, the perturbations depend on the selected attitude. For those attitudes with the long axis along the velocity vector (attitudes 3 and 4) unidirectional thrusting will produce unacceptable perturbations to the orbit by either pushing it down to the point where orbital life becomes unacceptable or pushing it up into the Van Allen belts where radiation effects on the electronics would become significant. This occurs because the thrusting along the velocity vector performs work on the spacecraft that continually increases (or decreases) its energy. There is no cancellation due to the orbital motion.

Attitude 2(a) with the x-axis normal to the orbit plane has the least perturbation due to thrusting. For this attitude, the thrust is normal to the velocity vector so very little work is actually performed on the spacecraft. There is then little change in spacecraft energy; essentially all effort is exerted to precess the relatively large orbital angular momentum. As the spacecraft proceeds around the orbit there is almost complete cancellation of the effects of thrusting. From the point of view of orbit perturbations, this is the best spacecraft attitude. Unfortunately, it is not the best attitude from a thermal point of view.

Attitudes 2(b) and (c) are quasi-inertial, being oriented to the Sun and the orbit plane. In these attitudes, the thrust vector lies in the orbit plane and is essentially fixed in inertial space. As the spacecraft revolves in its orbit there is almost complete

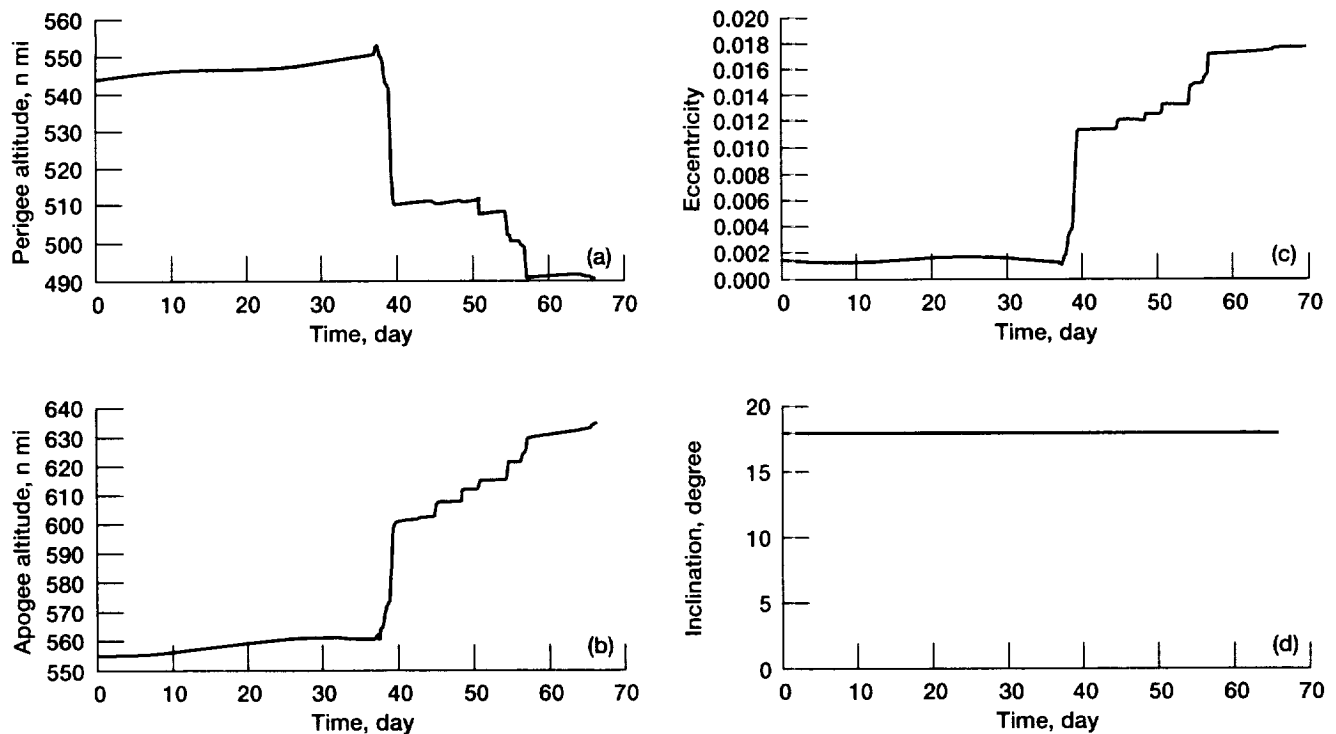


Figure 4.7.—COLD-SAT orbit perturbations (attitude option 2(b)). [Minimum beginning-of-life spacecraft weight (5610 lb)]. (a) Perigee altitude versus time. (b) Apogee altitude versus time. (c) Orbital eccentricity versus time. (d) Orbital inclination versus time.

cancellation of the effects of long-term thrusting. Thrust which is along the velocity vector at one point in the orbit is counter to the velocity vector at that point on the orbit which is symmetric with respect to the center of the orbital eclipse. However, during those portions of the orbit where the thrust vector has a component along the velocity vector, energy and angular momentum are added to the spacecraft placing it in a slightly different orbit. Then, during that portion of the (slightly different) orbit when the thrust vector has a component in opposition to the velocity vector, complete cancellation does not occur due to the slight loss of symmetry. The effect of the anticipated schedule of thrusting on a spacecraft with attitude 2(b) and the anticipated COLD-SAT orbit and weight is shown in figure 4.7. Figure 4.7 is calculated with the anticipated COLD-SAT orbit, thrust schedule, and variable mass. Figure 4.8 shows that the varying eccentricity and perigee altitude remain above that required for a 500-year life.

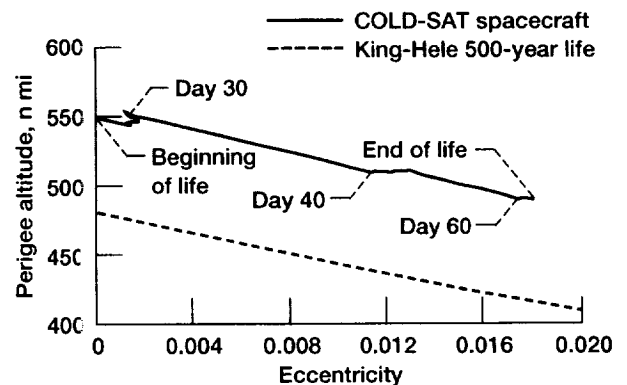


Figure 4.8.—Evolution of perigee altitude and eccentricity with time on orbit as a parameter (attitude option 2(b)).

4.3.3 OTHER FACTORS IN SPACECRAFT ATTITUDE SELECTION

The spacecraft attitude also affects a number of other spacecraft systems. These include the solar arrays and the thermal control system.

Attitude options 1(a), (b), and (c), which are oriented to the Sun and the ecliptic plane, assure that there is a solar array location and orientation where the angle between the Sun line and the solar arrays is 90° . There is then no cosine loss and the solar array size is at a minimum. This is also true for attitude option 3 but a rotating solar array is required. Attitude option 4 requires a rotating solar array but, in addition, the array must be canted to minimize the increase in size of the solar array.

For attitude options 2(a), 2(b), and 2(c) and option 4 the spacecraft axes are oriented to the orbit plane. Due to nodal regression of the spacecraft orbit and the obliquity of the ecliptic plane, the angle between the Sun line and the orbit plane can vary from $+51.5^\circ$ to -51.5° during a 1-yr period for an orbit with a 28° inclination. This requires an increase in size for a fixed solar array. If the angle between a spacecraft axis and the Sun line can be held in the range from 0° to 51.5° (i.e., by periodic rotation of the spacecraft) the size increase in the solar array can be reduced by canting the solar array with respect to the orbit plane. Figure 4.9 illustrates this effect. It shows the size of the solar array required relative to one held perpendicular to the Sun line for various cant angles between the array surface and the normal to the orbit plane. As can be seen, proper canting reduces the solar array size penalty to negligible proportions.

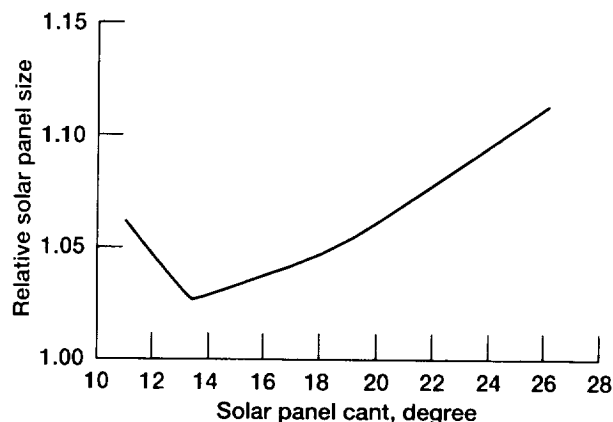


Figure 4.9.—Size penalty for fixed solar arrays. Penalty shown is for 350-n mi orbit altitude.

The reduction is possible because variations in the beta angle are accompanied by compensating changes in the duration of eclipse periods to allow more constant energy input per orbit.

The attitude selected can have a significant impact on the thermal design of the spacecraft. For COLD-SAT, the most critical thermal problems are associated with the cryogenic systems, specifically the supply tank. Those attitudes for which the solar flux falls primarily on the aft (negative x) end of the spacecraft yield considerable improvement in the performance of the cryogenic systems, as the aft end of the spacecraft acts as a Sun shield. Attitude 2(a) with the Sun essentially broadside to the spacecraft and attitude 2(b) with the Sun primarily on the aft end represent the limits of the problem. Figure 4.10 shows the

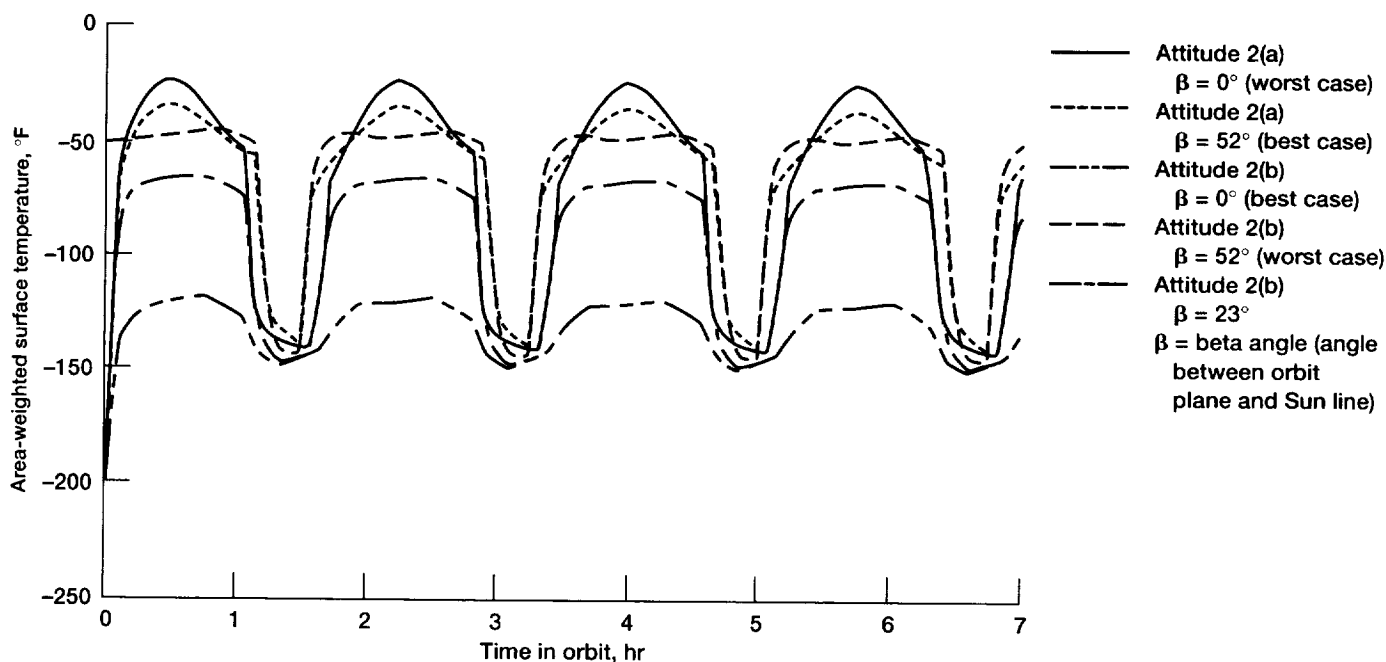


Figure 4.10.—Area-weighted supply tank purge diaphragm surface temperature. Comparison of attitude 2(a) (Sun essentially broadside to spacecraft) versus attitude 2(b) (Sun primarily on aft end of spacecraft). [Purge diaphragm material is layered 5-mill Teflon/VD silver/Kevlar cloth/Kapton VDA material with absorptivity of 0.09 and emissivity of 0.75 (end-of-life), is available from Sheldahl, Inc.]

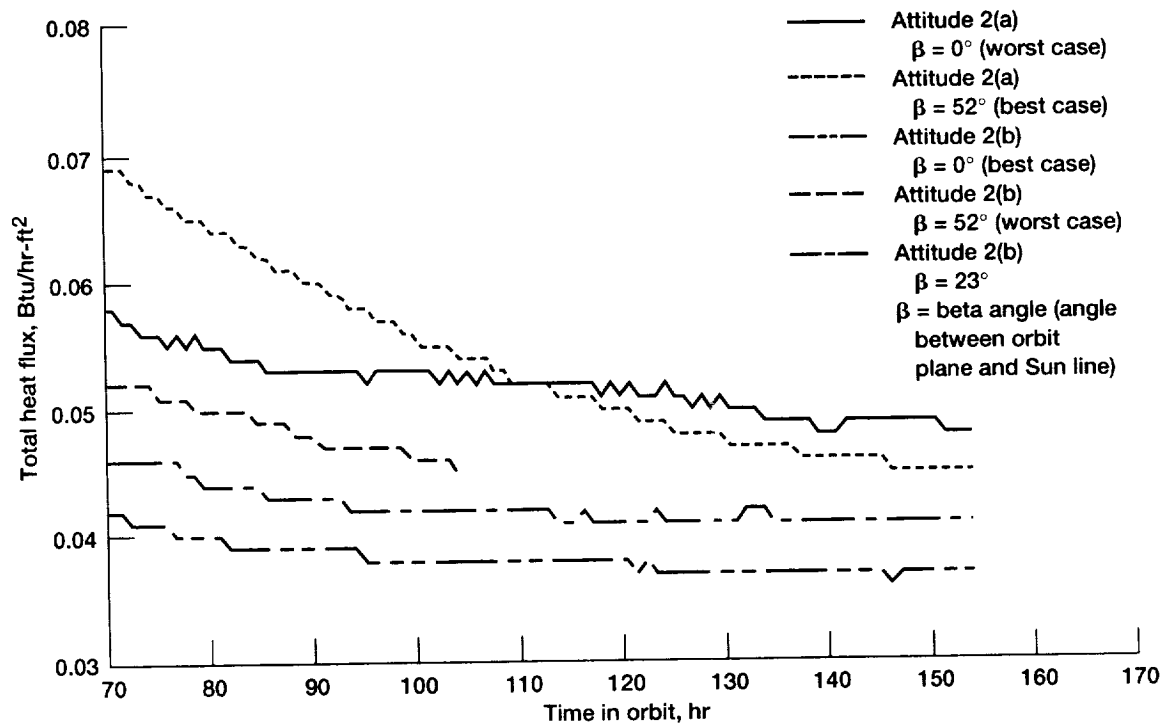


Figure 4.11.—Transient total heat flux on pressure vessel. Comparison of attitude 2(a) (Sun essentially broadside to spacecraft) versus attitude 2(b) (Sun primarily on aft end of spacecraft). [Honeycomb inner facesheet emissivity, 0.05; pressure vessel emissivity, 0.05; emissivity is for Kapton VDA.]

average surface temperature of the supply tank at various angles of incidence for the solar flux. As can be seen, the supply tank surface temperature for the 2(b) worst case is lower than the 2(a) best case and the 2(b) best case represents a major reduction in surface temperature. Figure 4.11 illustrates the effect on supply tank heat leak. Use of attitude 2(b) will result in a 10 to 20 percent improvement in the performance of the COLD-SAT supply tank if other factors remain constant.

With attitude 2(b), additional improvement can be obtained by allowing the Sun to shine on one side of the spacecraft only. This can be accomplished by periodically rotating the spacecraft about its x-axis as the Sun line goes through the orbit plane. If this is done the spacecraft will have a hot side and a cold side. Cryogenic lines can be routed along the cold side allowing further reduction in heat leak to the system. In addition, the solar arrays can be effectively canted to hold their size to a minimum.

4.3.4 FINAL SELECTED ATTITUDE

Attitude 2(b), with the positive x-axis pointing away from the Sun, was selected for the COLD-SAT spacecraft and is illustrated in figure 4.12. It has tolerable gravity gradient disturbance torques. The orbital perturbations due to thrusting are minimal.

The spacecraft will be rotated periodically to maintain the Sun on one side of the spacecraft as illustrated in figure 4.13. Figure 4.14 depicts the typical behavior of the angle between the orbit plane and the Sun line (the beta angle) with time for several values of initial right ascension of the ascending node. The spacecraft must be rotated each time the beta angle goes through zero. Control system simulations indicate that this maneuver can be accomplished easily. Statistics in table 4.4 indicate that the maximum expected number of rotations during a 6-month mission is five and that, for many launch dates, the first rotation can be postponed until the completion of all experimental operations by judicious selection of launch time. With this periodic rotation, the fixed solar arrays can be canted so that there is a minimal increase in size over a true Sun-pointing array and one side of the spacecraft will always remain in shadow. The cryogenic systems are partially shielded from the Sun by the aft end of the spacecraft.

This attitude allows easy positioning of attitude sensors. Sun sensors are mounted on the aft end of the spacecraft and have an unobstructed field of view. Conical Earth sensors with their axis of rotation along the spacecraft z-axis (i.e., normal to the orbit plane) have an unobstructed view of the Earth. Side-mounted solar arrays (along the y-axis) allow nearly unobstructed viewing of TDRS by the high-gain antenna.

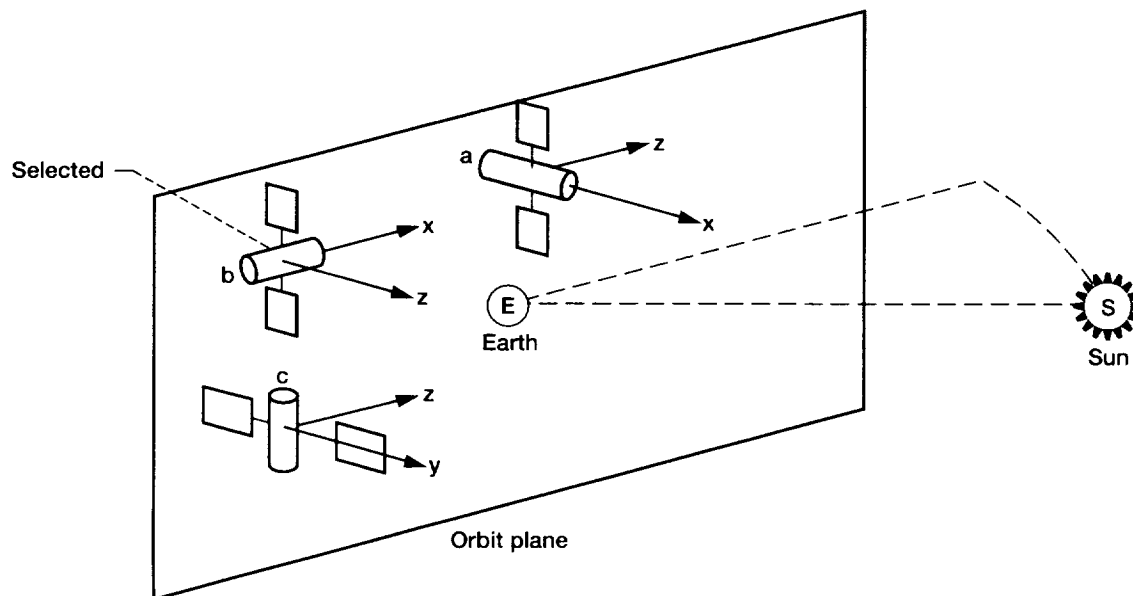


Figure 4.12.—Final selected spacecraft attitude.

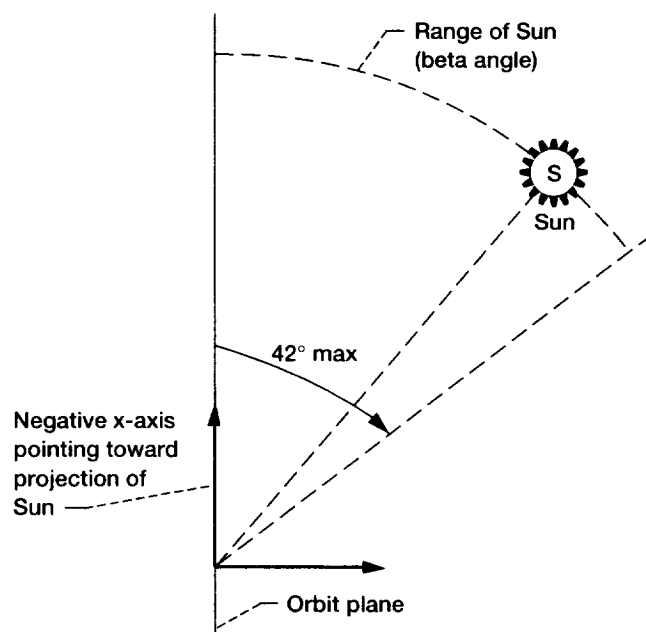


Figure 4.13.—Maximum range of angle between spacecraft x-y plane and Sun line (beta angle) for selected attitude (option 2(b)).

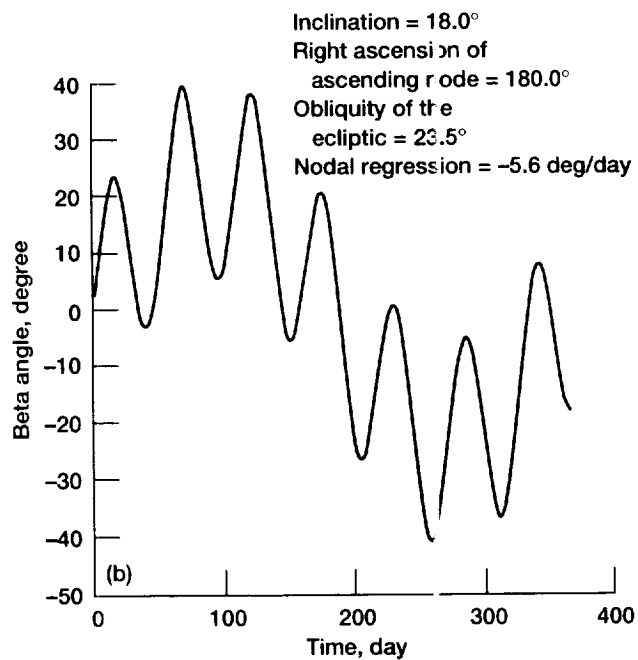
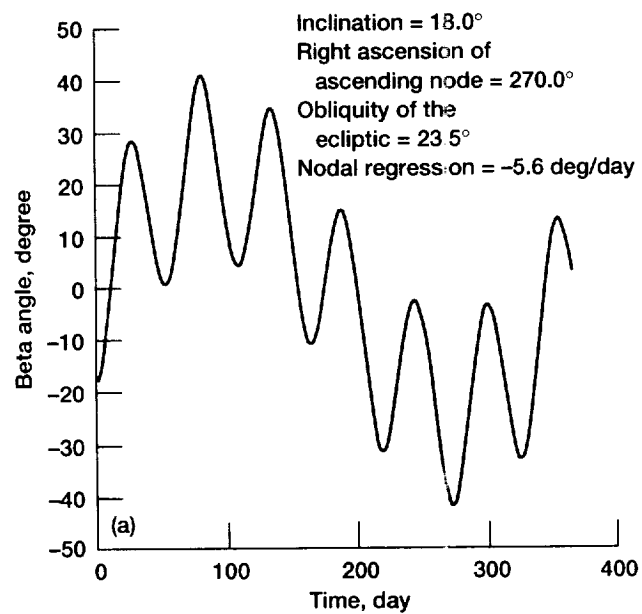


Figure 4.14.—Angle between spacecraft x-y plane and Sun line (beta angle) versus time. (a) Right ascension of ascending node at 270° . (b) Right ascension at ascending node 180° .

TABLE 4.4—ROTATION CHARACTERISTICS VERSUS LAUNCH DATE AND TIME

Launch date	Launch time	Time to first rotation, day	Time between rotations, day		Number of rotations
			Minimum	Maximum	
October 1, 1997	00:00	22.1	10.89	98.98	5
	06:00	142.59	20.38	142.59	2
	12:00	11.33	11.33	142.87	3
	18:00	4.51	4.51	94.47	5
December 1, 1997	00:00	87.13	19.3	87.13	3
	06:00	86.84	23.09	86.84	3
	12:00	110.4	19.64	110.4	3
	18:00	64.97	11.01	64.57	5
February 1, 1998	00:00	20.04	20.04	117.56	3
	06:00	31.47	19.98	103.9	3
	12:00	5.93	5.93	92.83	4
	18:00	8.16	5.48	82.72	5
April 1, 1998	00:00	11.04	11.04	143.06	3
	06:00	4.24	4.24	98.95	5
	12:00	21.56	11.04	98.39	5
	18:00	142.37	19.93	142.37	2
June 1, 1998	00:00	98.79	18.19	98.79	3
	06:00	64.93	10.65	64.93	5
	12:00	75.65	17.15	75.65	3
	18:00	87.09	23.04	87.09	3
August 1, 1998	00:00	5.15	5.15	92.45	4
	06:00	9.14	7.40	82.13	5
	12:00	19.65	19.65	114.6	3
	18:00	31.63	20.64	103.1	3

4.4 Expendable Launch Vehicle Selection

While all available ELV's were considered, two (Delta and Atlas) were examined in detail. All others were rejected because of cost or because they were obviously incapable of doing the job. Between the Atlas and the Delta, the principal selection factors were lift capability, payload volume constraints within existing fairings, and constraints on payload COM. Pad modifications required to load the spacecraft with liquid hydrogen were also considered.

4.4.1 PAYLOAD VOLUME CONSIDERATIONS

Figure 4.15 shows the allowable payload dynamic envelopes for the various payload fairings now available on the Atlas and Delta launch vehicles. As can be seen, the Delta payload volume for the largest available fairing is much more restrictive than that for the Atlas. The initial COLD-SAT concepts were all based on the Delta launch vehicle with the large fairing but available volume proved to be a continuing problem. Even if the spacecraft could be forced into this fairing there would be no volume contingency to accommodate future changes. A later switch to the Atlas medium fairing eased most volume and configuration problems and added a certain amount of contingency.

4.4.2 LAUNCH VEHICLE LIFT CAPABILITY

Total payload-chargeable weight at lift-off (including 20-percent weight margin on the spacecraft systems) of COLD-SAT was estimated to be 6715 lb. To meet EOL orbit requirements this weight must be launched into a 550-n mi, nearly circular orbit. The initial orbit requirement is derived from the orbit perturbation calculations of the type illustrated in figure 4.7.

The weight quoted above is a little misleading as it applies to the final COLD-SAT design. Because of the absence of facilities for handling liquid and gaseous hydrogen on the Delta launch pad, it was the conclusion of this study that a Delta-launched COLD-SAT would require a vacuum-jacketed supply tank which would increase the launch weight by 1500 lb.

A Delta 7920 is capable of placing 9000 lb into a 28°, 550-n mi, nearly circular orbit (ref. 2). The Atlas II launch vehicle is capable of placing 12 100 lb in the same orbit (ref. 3). Either launch vehicle is capable of placing a spacecraft of the COLD-SAT weight class into the required orbit.

4.4.3 CONSTRAINTS ON MASS PROPERTIES

All launch vehicles require that the spacecraft COM be located close to the vertical axis. This does not present a problem for COLD-SAT which is nearly axisymmetric.

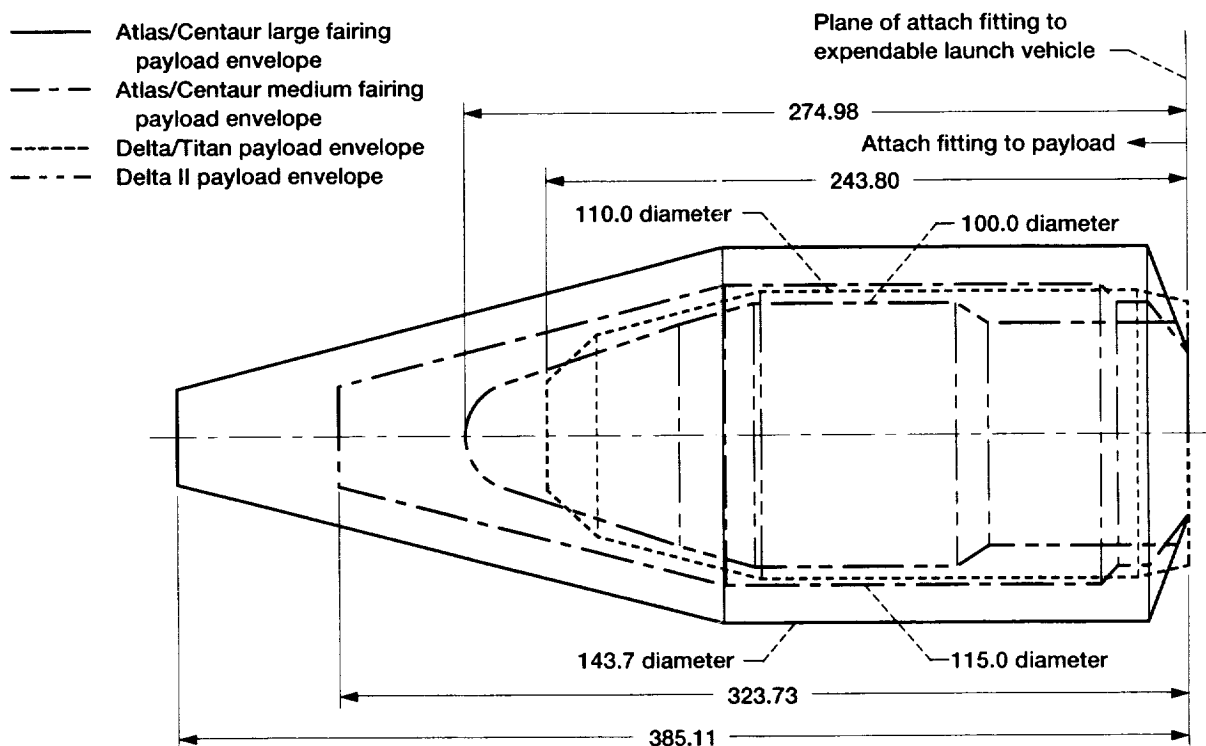


Figure 4.15.—Delta and Atlas II payload envelopes. Dimensions are in inches.

The other principal constraint is on the vertical location of the spacecraft COM. This is dependent on both the structural properties of the launch vehicle and on the payload attach fitting. No qualified attach fittings exist for a spacecraft in COLD-SAT's weight class for either the Atlas II or the Delta. However, there are existing attach fitting designs for both launch vehicles which appear to be adaptable to the COLD-SAT launch. The spacecraft COM is located approximately 81 in. above the spacecraft-ELV separation plane. The Atlas II launch vehicle would restrict a 6500-lb spacecraft to 112 in. so there is more than adequate margin.

Things are more complex for the Delta. The Delta would require the COM to be below 90 in. from the separation plane. Again, there is some margin. However, because of complexities associated with handling liquid hydrogen on the Delta pad it was concluded that a vacuum-jacketed supply tank would be required. This increased the weight of the spacecraft to approximately 8000 lb and increased the height of the COM. At the increased weight, the standard Delta limits the COM to about 84 in. and COLD-SAT exceeds this limit. There are relatively simple modifications to the Delta which would allow it to accommodate the higher COM but they have not yet been implemented.

Again, although either ELV is capable of launching COLD-SAT to the required orbit, the Delta has much less margin and the integration is much more complex and risky.

4.4.4 LAUNCH PAD CAPABILITIES

COLD-SAT must be loaded with liquid hydrogen prior to launch and, in the event of a launch vehicle or spacecraft contingency, it must be drained of liquid hydrogen as well. The Centaur upper stage of the Atlas II is fueled with liquid hydrogen. The Atlas pad is fully prepared and qualified for handling liquid hydrogen. Relatively simple modifications to this existing system will allow filling and draining of COLD-SAT. A simple plumbing attachment to the Centaur vent system will allow venting of gaseous hydrogen and liquid hydrogen both on the ground and during ascent.

The Delta pad is not equipped to handle liquid hydrogen. The facilities on the pad must be modified to assure compatibility. Complete liquid hydrogen fill, drain, vent, and storage systems must be installed. The required pad modifications and associated training are feasible but with increased cost and risk. Additional provisions may be necessary to handle hydrogen venting during launch.

4.4.5 FINAL SELECTION

Although COLD-SAT could be designed to fly on either the Atlas II or the Delta, in all cases, use of a Delta results in serious configuration problems, reduced margins, increased risk, and increased cost to the spacecraft. The early COLD-SAT designs were all performed assuming that the Delta ELV would be used and that idea was given up only reluctantly because of the lower cost of the Delta. The cost impact is difficult to quantify but, initial estimates of the cost reductions to the spacecraft and its ground support equipment resulting from the use of an Atlas do not fully compensate for the higher cost of an Atlas.

Risk is another factor to consider. The Atlas provides large margins in lift capability, payload fairing volume, COM location, and liquid hydrogen loading capability. The Delta is marginal on fairing volume and must be modified to handle the COLD-SAT COM location. COLD-SAT is early in its development and has the potential for significant changes in its configuration and mass properties, undoubtedly in an adverse direction. The Delta pad requires extensive modifications to handle liquid hydrogen.

In the end, the Atlas II was chosen over the Delta because (1) it was not felt that the relatively small cost savings of the Delta justified the increased risk to the project, and (2) because it appeared that significant simplifications to the spacecraft were possible by using the margin available on the Atlas II.

4.5 Selected Orbit

The performance of the thermal control system and the solar arrays can be improved by using the excess lift capability of the Atlas II to place the spacecraft in a lower inclination orbit. The initial COLD-SAT orbit is then 550 n mi, nearly circular, with an 18° inclination. There is no launch window but, if possible, the launch time during a given day (and with it the right ascension of the orbit's ascending node) will be selected to minimize the number of spacecraft rotations and/or to control their timing during the flight. An 18° orbital inclination also reduces the on-orbit radiation dose caused by the South Atlantic anomaly.

The initial spacecraft orbit has the characteristics listed in table 4.5.

Following perturbation by experiment-required thrusting, the orbit will have a perigee altitude of 490 n mi and an eccentricity of 0.018. The inclination will remain at 18° . In this latter orbit the predicted lifetime is 696 years.

Figure 4.16 shows the worst-case atmospheric density along the worst-case EOL orbit. Maximum drag occurs at the perigee of this EOL orbit. The worst-case drag with this $+3\sigma$ atmosphere is $3.29 \times 10^{-8}g$. Atomic oxygen effects should be negligible.

In this orbit the spacecraft will make one rotation per year in inertial space about an axis normal to the orbit plane as

TABLE 4.5.—CHARACTERISTICS OF INITIAL SPACECRAFT ORBIT

Nodal regression rate	5.66 deg/day
Period	105.46 min
Maximum eclipse	35 min
Minimum eclipse	28 min
Spacecraft velocity	24 083 ft/sec
Geometric TDRSS blockage	<2 percent

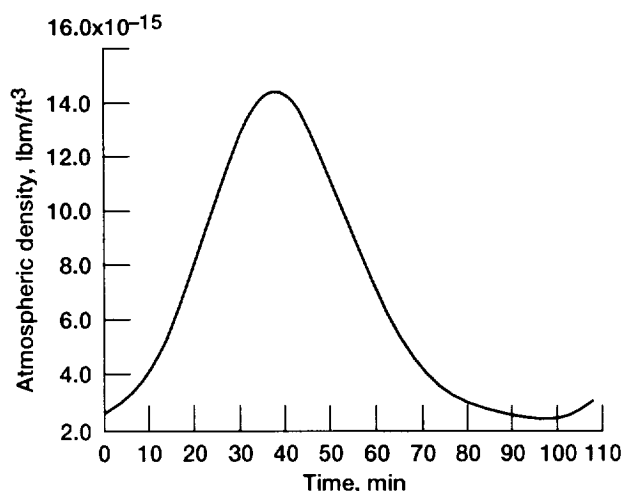


Figure 4.16.—Atmospheric density along orbit, worst-case solar, and magnetic activity. Lowest end-of-life orbit, 490.4 n mi.

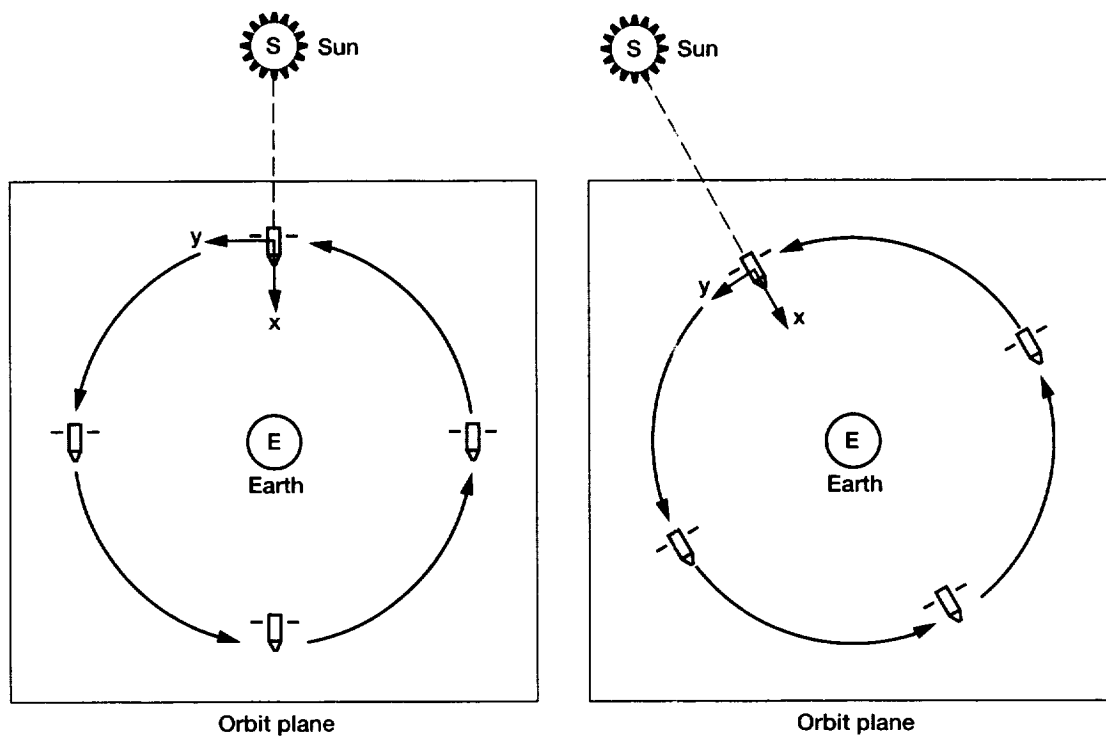


Figure 4.17.—Sun tracking with COLD-SAT attitude. [COLD-SAT spacecraft rotates about z-axis at 1 rev/yr to track Sun.]

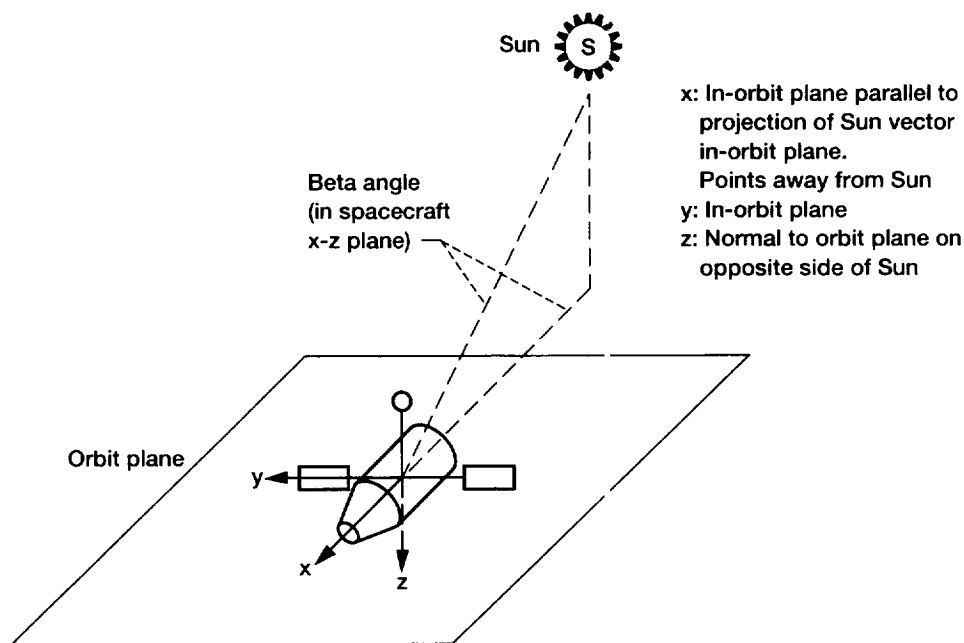


Figure 4.18.—COLD-SAT attitude and beta angle.

illustrated in figure 4.17. The angle between the Sun line and the orbit plane (the beta angle; fig. 4.18) will vary $\pm 41.4^\circ$. With rotation of the spacecraft about its long axis the angle seen by the spacecraft will be limited from 0 to 41.4° .

The orbit remains below the Van Allen belts. The total integrated radiation dose for the entire 6-month mission is estimated to be less than 1000 rads silicon with 690 mg/cm^2 (0.1 in.) aluminum shielding. At this level, radiation effects on semiconductors should be minimal and radiation-hardened electrical, electronic, and electromechanical (EEE) parts should not be required.

References

1. King-Hele, D.G.: *Satellite Orbits in an Atmosphere: Theory and Applications*, Blackie and Son, Ltd., Glasgow, 1987.
2. *Delta II Commercial Spacecraft Users Manual*, MDC H3224, McDonnell-Douglas Astronautics Company, July 1987.
3. *Mission Planners Guide for the Atlas Launch Vehicle Family*, General Dynamics Commercial Launch Services, Inc., March 1989.

Chapter 5

COLD-SAT Experiment System

Daniel Glover¹ (*Experiment System*), George Harpster (*Fluid Inventory/Experiment Operations*),
Al Seigneur (*Supply Tank Module Design*)
National Aeronautics and Space Administration
Lewis Research Center
Cleveland, Ohio

and

Robert Dengler (*Fluid Systems*), Lawrence Edwards (*Instrumentation and Electronics*), John Mishic
(*Thermal Modeling*), Shigeo Nakaniski (*Thermal and Fluid Analysis*), William Prati (*Receiver Tank*
Module Design), and Richard Verbus (*Fluid Inventory/Experiment Operations*)
Analex Corporation
Cleveland, Ohio

5.1 Experiment System Design and Requirements

5.1.1 INTRODUCTION

The COLD-SAT experiment system is the part of that spacecraft which can be considered to be the payload. It consists of tanks, pressurant bottles, their interconnecting plumbing, valves, associated instrumentation, and signal conditioning electronics. The experiment system is designed to store liquid hydrogen with low boiloff losses by minimizing the heat input to the tanks from the surrounding environment. During the 3-month mission, experiments concerned with controlling tank pressure and transferring liquid hydrogen between tanks will be performed.

This chapter presents the experiment system design and discusses the configuration and rationale behind the fluid system and tank design approach. Details of the interfaces with other systems, fluid system design, supply tank design, receiver tank designs, instrumentation, and operations will also be

covered. First, a general overview of the requirements, interfaces, ground rules, and design history is given. A description of the flow system, which is the heart of the experiment system, is given in section 5.2. The supply tank design, presented in section 5.3, was the most technically challenging part of the effort. Section 5.4 covers the gaseous hydrogen pressurant system, which is a close second to the supply tank in terms of design challenge. Section 5.5 presents the receiver tank module designs; section 5.6 covers instrumentation; and section 5.7 gives operations information. Analyses of the mechanical and thermal aspects of the experiment system and a discussion of the liquid acquisition device (LAD) and thermodynamic vent system (TVS) heat exchange are presented in appendixes A and B, respectively. Appendix C illustrates the fluids schematic symbols used most frequently throughout this chapter. Reference figures and tables are located in appendixes D and E, respectively.

The key design issue for the tanks and plumbing is keeping the heat input to a minimum. This requires careful insulation and mounting techniques, use of low thermal conductivity materials, minimization of penetrations of the insulation

¹Project engineer.

system, use of TVS, evacuation of pipes not in use, careful location of components, reduction of instrumentation, lead wires, and so forth. The best thermal performance is required in the largest tank, known as the supply tank, which is the only tank containing liquid hydrogen at launch. The supply tank is the site of most pressure control experiments because of its well-controlled thermal performance.

Tank pressure control in low gravity needs special technology because the location of the vapor (ullage) in the tank cannot easily be determined or predicted. Even small heat leaks will result in liquid being vaporized with a resulting pressure rise. The vapor that is generated may not be near a vent, so that an attempt to simply vent the tank would probably result in liquid being dumped—an extremely inefficient way of lowering pressure.

Pressure control techniques that will be used in the supply tank include mixing and thermodynamic venting. The thermal stratification of the tank contents will be investigated under different applied heat fluxes and induced acceleration environments and the resulting pressure rises will be removed by mixing or by using the TVS.

Transfer-related problems in low gravity include pressurization of the source tank, chilldown of the transfer plumbing and receiver tank, and fill of the receiver tank by collapsing (no-vent fill) or venting (vented fill) the vapor generated during the fill. Transfers will be attempted with different spray systems, flow rates, and acceleration environments.

Many aspects of the COLD-SAT experiment system design are based on the best available engineering information about cryogenic fluid management systems in space, which is to say that engineering estimates and judgement frequently had to be used in place of hard data and experience. The results of this design are believed to be a sound first step, but there are many aspects which necessarily are preliminary. This problem is inevitable when designing a system such as this. Until COLD-SAT is flown and its data analyzed, the design of its fluid system must be subject to much uncertainty.

This experiment system design should serve as an example of a design approach rather than as a source of detailed design information. The assumptions and estimates used herein may not, in general, be optimal. Although we have tried to identify our assumptions, they may not always be evident and numerical results in this chapter should be used with caution.

The reader is directed to the bibliography of this report for a collection of references which may be of assistance in understanding the design and operation of the COLD-SAT experiment system.

5.1.2 REQUIREMENTS

The experiment system is designed to perform the experiments listed in table E.1 in appendix E to this chapter. The individual tests for each experiment are also listed there. Based on the size of the receiver tanks and the number of experiments,

the total amount of liquid hydrogen required for all experiments is 565 lbm. This is used as a nominal ground-fill mass. The on-orbit inventory calculations described in section 5.7 assume a starting mass of 525 lbm to account for worst case boiloff losses and other uncertainties during ground operations, ascent, and deployment. Tank flow system and acceleration requirements are given in table E.2. Measurement requirements are given in the COLD-SAT Instrumentation and Wire Harness Design Report, which is a separate report by L. Edwards (ref. 1).

The COLD-SAT experiments can be divided into two general types: (1) pressure control and (2) transfer-related experiments. The pressure control experiments are performed for the most part in the supply tank. They require application of uniform heat fluxes to the tank of 0.1, 0.3 and 0.6 Btu/hr-ft² to the tank and measurement of the temperature response throughout the inside of the tank. Pressure control tests also investigate the effect of a passive (no mixing) and an active (with mixing) TVS which requires heat exchangers and mixers. The mixer is used with and without the TVS. Some of the tests require the application of a small acceleration (10⁻⁵ to 10⁻⁴g).

The transfer-related experiments require receiver tanks with geometric variation, a transfer line connecting the tanks, flow control, different types of spray systems, pressurization systems, vents, and applied accelerations. Data requirements are for temperature distributions on and in the tanks, pressures, and flow rates. The receiver tank requirements are for one nearly spherical tank and one cylindrical tank with axial, tangential, radial, and diffuse spray systems. The flow rates for transfer are 50 to 350 lbm/hr. Helium and hydrogen gas will be investigated as pressurants. The acceleration requirements are given in terms of the Bond number, which is a dimensionless parameter equal to the ratio of gravitational-to-surface tension forces. A Bond number of 4 is generally considered sufficient for settling liquid to one end of the tank (ref. 2). The equation for the dimensionless Bond number, *Bo*, is

$$Bo = ar^2/b$$

where

a acceleration

r characteristic length of the tank (usually taken to be the tank radius)

b specific surface tension (1.66 in.³/sec² for liquid hydrogen).

In addition to experiment requirements, other requirements, such as safety and reliability, were imposed on the design. Ground rules for the design evolved as time went on into the final design approach given in table 5.1. A key plumbing ground rule is to have at least two barriers between the tanks and space vacuum to avoid inadvertently dumping hydrogen.

TABLE 5.1.—EXPERIMENT SYSTEM DESIGN APPROACH/GROUND RULES

- Keep large margins
- Use standard materials, pipe sizes, etc.
- Incorporate available sensors, and components
- Build in component accessibility and maintainability (e.g., MLI can disassembling, no moving parts inside tanks)
- Use modular design: assemble and test subassemblies (e.g., valve panels, LAD)
- Design for easy manufacturing (e.g., MLI layup)
- Design tanks and bottles to MIL-STD-1522 or ASME boiler code
- Use hydrogen-compatible materials in hydrogen systems (aluminum for tanks and bottles, SS316 for fluid systems components)
- Include relief devices on all hydrogen pressure vessels and potential trapped volumes (except helium bottles)
- Place at least two barriers between liquid hydrogen and space (except dump vent)
- Make all fluid components accessible
- Keep reliability allocation of 0.958 for class I experiments
- Determine supply tank size by hydrogen use predictions for experiments, given receiver tank size requirements
- Use two receiver tanks to provide variation in geometry and thermal mass/volume for transfer experiments
 - Provide degraded redundancy with two receivers
 - Provide redundant isolation valve for each tank
- Make receiver tank designs similar to supply tank designs, to simplify analysis and manufacturing
 - Trade slight weight increase for lower cost
- Use hot side/cold side of spacecraft to optimize external interface temperatures
- Utilize pressurized transfers for simplest, low-cost approach
 - Select vaporizers for volume efficiency and operational flexibility
 - Use only hydrogen pressurant in supply tank to avoid helium contamination
- Use solenoid-actuated valves
- Provide flow variation by parallel legs with different flow restrictions
- Combine active TVS, passive TVS, and subcooler heat exchangers in supply tank

Another important ground rule is to keep all components accessible (i.e., not put any active components inside the tanks).

Tanks are designed to ASME Boiler and Pressure Vessel Code standards (ref. 3), and pressurant bottles are designed to MIL-STD-1522, to minimize testing requirements and safety concerns at the cost of a small weight increase. Mechanical relief devices protect all potential trapped volumes except the helium bottles. Pressurized transfers will be used to avoid the need for developing a transfer pump, but this ground rule can be revisited if a reliable pump becomes available. Solenoid-actuated valves are used exclusively. Flow-rate variation is achieved by using parallel legs with different flow restrictions.

If a flow-control valve becomes available, this ground rule can also be revisited.

5.1.3 INTERFACES

The experiment system interfaces with all of the other spacecraft systems. The experiment system is physically large and constrained by the volume of the payload envelope rather than by the lift capability of the launch vehicle. The hardware is divided into modules, which correspond to the experiment tanks, to allow assembly and test of individual tank systems before integration of the entire system. The primary structure

TABLE 5.2.—EXPERIMENT SYSTEM POWER REQUIREMENTS

Item	Number	Power requirement, W	Duty cycle, percent
Experiment data units	3	15	100
Accelerometer	1	10	10
Mixer motor power unit	1	15	10
Signal conditioning unit	1	15	10
Heaters			
Pressure control	1	21	1
Tank warmup	2	50	2
Vaporizer	2	100	2
Vent	2	10	10
Thermal control	2	6	50
	2	2	50
Valves			
Cryo	50	5 A, 28 V	200 msec pulses
Gas	12	2 A, 28 V	200 msec pulses

TABLE 5.3.—EXPERIMENT MEASUREMENTS SUMMARY

Type	Number	Sample rate, Hz	Resolution
Temperature			
Type A ^a	139	0.1	8-bit
Type Ab ^b	162	0.1	8-bit
Pressure	42	0.1	8- to 12-bit
Liquid/vapor	116	0.1	On/off
Flow	12	0.1 to 10.0	8- to 12-bit
Acceleration (3-axis)	1	1	12-bit
Valve status	61	0.1	On/off
Mixer speed	2	0.1	12-bit
Current	6	0.1	8-bit
Capacitance level sensor (ground only)	1	-----	-----

^a29 to 40 °R.^b29 to 540 °R (dual range).

of the spacecraft has to accommodate this modular configuration and allow for removal of failed modules. Module breakpoints, secondary structure attach points, tank assembly envelopes, valve panel envelopes, and the plumbing tray envelopes had to be negotiated with the spacecraft configuration engineer.

The experiment system's 28-V power requirements are given in table 5.2. The loads include four electronics boxes, an ac inverter for mixer motor power, heaters, and solenoid valves. Nominal average power required is 125 W.

Telemetry and command requirements are summarized in tables 5.3 and 5.4. Some 450 measurements are taken directly by the telemetry, tracking, and command (TT&C) system while others require special processing in the experiment system before the data are passed to the TT&C system because of high accuracy, sampling, or signal conditioning requirements. The TT&C system also reads the status of the valves, pumps, and

heaters. The experiment system has three data acquisition boxes of its own which pass data to the TT&C system on serial digital links. The control requirements are for operation of 61 valves, 2 pumps, 11 heaters, and control of power to 6 electronics boxes. Four pyrotechnic actuators for operation of the supply tank vent doors are controlled by the electric power system.

There are three different types of valves which the TT&C system has to actuate: (1) four-wire cryogenic, (2) two-wire cryogenic, and (3) four-wire gas. The cryogenic valves require up to 5 A actuation current for at least 200 msec, while the gas valves only need 2 A. The four-wire valves have two solenoid coils, one for open and one for close. The two-wire, cryogenic valves are the same as the four-wire version except that only one actuation coil is used so current polarity must be switched to open and close the valve. This type of valve hook up is used where thermal conduction down the wires results in significant

TABLE 5.4.—EXPERIMENT SYSTEM
CONTROLLED COMPONENTS LIST

Item	Quantity
Cryogenic valves	49
Gas valves	12
Pumps	2
Heaters	11
Pyros	4
Electronics boxes (on/off)	6

heat-leak to a cryogenic system (e.g., a valve mounted on the supply tank). The two-wire valves require special current polarity selection circuitry in the TT&C system.

In order to avoid redundant actuation driver circuits for each valve, groups of valves that are independent from a reliability standpoint are driven by a common, redundant actuation circuit. These groups of valves are called redundancy clusters. The clusters are organized such that, if an actuation circuit fails and the valves in that circuit fail, there are other valves that can bypass the failed valves driven by other actuation circuits (i.e., no two valves in any one cluster perform the same function). Redundancy cluster identification is given in table E.3 in appendix E to this chapter, which is a summary of all experiment system fluid components. This redundancy may be a degraded redundancy; for example, for reliability purposes the two receiver tank systems are considered redundant even though loss of one tank would result in loss of data.

The experiment system places two basic requirements on the attitude control and propulsion systems: (1) provide a minimum perturbation acceleration environment during certain tests, and (2) provide a controlled micro-g acceleration environment during certain other tests. The average background acceleration must be less than $10^{-6}g$. The required induced acceleration levels are 3×10^{-5} and $10^{-4}g$. The total thrust duration is 52 hr for all experimental thrusting. A summary is given in table 5.5.

Thermal system interfaces are primarily intended to isolate the cryogenic systems from the rest of the spacecraft. The

experiment system has the responsibility of insulating the tanks and plumbing to meet heat-leak requirements. The resulting heat fluxes are very low, which makes the thermal interface somewhat easier than might be expected. However, care must be taken with cryogenic attach points, radiation onto cryogenic systems, and plumbing that may only be at cryogenic temperatures intermittently. Plumbing that interconnects the tanks must run the length of the spacecraft and so may be in proximity to electronics boxes at some point. Another concern is that the hydrogen vents be kept warm to prevent frozen hydrogen from clogging the outlets or plumbing. This is done with passive environmental control and with heaters.

Thermal problems include keeping the outer surfaces of cryogenic systems as cold as possible and the noncryogenic systems warm. Experiment system items that require cold outer surfaces include the cryogenic tanks and the plumbing tray. The plumbing tray is a structure that supports the transfer and plumbing lines that run between the tanks, bottles, vents, ground interfaces, and so forth. The tray is located on the cold side of the spacecraft and has a radiator mounted on its outside surface to keep the plumbing as cold as possible thus minimizing the heat-leak into the tanks. Items that need to be kept warm include the pressurant bottles, pressurization valve panels, and vents.

Software residing in the TT&C computers controls experiment operations. There are software modules that provide constant oversight of the experiment system to prevent damage or loss of liquid (e.g., caused by overpressurization or inadvertent valve actuation). Experiments are broken up into individual tests which are stand-alone operations. Many tests are similar and differ only by parameter changes which can be handled by one software module that looks up valves or settings in a table for different test configurations.

Tests are initiated by ground command. Constant monitoring is required for the first test of a particular type and desired for all test runs, but the software should be able to handle most contingencies on its own, ultimately by putting the hardware in a safe state and waiting for ground intervention.

TABLE 5.5.—EXPERIMENT SYSTEM ACCELERATION
REQUIREMENTS SUMMARY^{a,b,c}

Operation	Bond number, ^d B_0	Total thrust acceleration, g	Duration
Experiment 1, mixing	Supply tank > 4	3×10^{-5}	25 min
Experiment 1, test 23 to 28	Supply tank > 0.1	3×10^{-5}	16 hr 16 hr
Experiment 2, test 1, 2 4 to 9	Large receiver tank ≥ 4	10^{-4}	40 min
Experiment 2, test 3, 10, 11	Small receiver tank ≥ 4	10^{-4}	70 min
Experiment 3, test 9, 10	NA	10^{-4}	2 hr
Experiment 9, test 1, 3, 4	Large receiver tank ≥ 4	3×10^{-5}	3 hr
Experiment 9, test 2, 5	Small receiver tank ≥ 4	10^{-4}	1 hr
Operational transfers	Small receiver tank ≥ 4	10^{-4}	12 hr

^aAll applied acceleration is in +x direction.

^bPerturbations shall be minimized during applied accelerations.

^cNormal spacecraft disturbances are acceptable during background acceleration.

^dBond number (B_0) calculated by using the characteristic length appropriate for tank.

The requirements on the software are to open and close valves, turn heaters and pumps on and off, and take measurements. The controlled items are all controlled on the basis of time, temperature, or pressure. The response time of the system in most cases is quite slow, on the order of seconds to hours.

The hardware ground interfaces include a liquid-hydrogen fill/drain line, a vent line, two helium purge lines for supply-tank-insulation ground purge, and pressurant bottle fill lines. The COLD-SAT hydrogen vent ties into the Centaur launch vehicle vent for ground and ascent venting.

5.1.4 OVERALL DESCRIPTION

The major characteristics of the final conceptual design of the experiment system are shown in tables 5.6 to 5.14. The system hardware consists of 3 cryogenic tank assemblies, 4 pressurant bottles (2 of which are rechargeable), transfer and vent plumbing, 49 cryogenic valves, 12 gas valves, 2 cryogenic pumps, 2 regulators, and 19 relief valves. Instrumentation includes 301 temperature sensors, 42 pressure sensors, 116 liquid-vapors, 12 flowmeters, and a 3-axis low-g accelerometer. The total system weight estimate is 2206 lb (dry). The system will be launched with 565 lbm of liquid hydrogen in the largest tank, 7.4 lbm of helium, and 17.4 lbm of hydrogen gas for a total wet weight of 2796 lb.

Table 5.6 gives the primary locations for the conduct of the various experiments. Table 5.7 lists the major hardware items needed to perform the experiments. Table 5.8 gives the pressure vessel geometries at room temperature for the last design iteration. Table 5.9 presents the pressure vessel characteristics for the tanks and bottles. Table 5.10 shows the thermal performance characteristics of the tanks, and table 5.11 presents a summary of the thermodynamic vent system design data. Tables 5.12 and 5.13 outline a breakdown of the 2796-lb mass of the experiment system. Table 5.14 lists the experiment system's electrical/electronics boxes.

5.1.5 GROUND RULES

The experiment system design took place in two major iterations. The first was designed to fit into a Delta payload fairing and included a vacuum-jacketed Dewar as the liquid hydrogen supply tank to simplify ground operations. Because the Delta launch vehicle does not use liquid hydrogen and the launch pad is not equipped to deal with large quantities of liquid hydrogen, a Dewar approach seemed easiest to implement.

The second iteration was designed to fit into an Atlas I medium fairing and does not include a vacuum jacket on the supply tank, but rather has a bag purged with helium that surrounds the tank to prevent condensation of air. The vent system design ties into the Centaur ground-flight vent fin. The Centaur upper stage is a liquid-hydrogen-fueled vehicle which offers some advantages as far as pad and vehicle accommodations are concerned (e.g., explosion-proof pad facilities).

As the design work progressed, several ground rules were developed to guide the design. These ground rules and the key features of the second iteration were mainly directed at keeping the cost of designing, building, and testing the experiment system as low as possible while still meeting primary experiment requirements. The key ground rule is component accessibility. A major cost in space cryogenic systems is the repair or replacement of failed components following assembly. In the second design iteration, no active components were allowed inside the tanks so that tanks would not have to be cut open to fix a failed part. The vacuum jacket was eliminated in part to provide easier access to components mounted on the tank (although the primary motivation was weight reduction), and the purge bag was designed to be removable.

Another related ground rule mandated the use of modular assemblies wherever possible. Components were designed into subassemblies (e.g., valve panels) that could be built and tested before being integrated into the next larger assembly, to allow earlier problem detection and to minimize rework costs. Other ground rules included using standard materials and components where possible, loosening tolerances, and avoiding space-flight practices where standard industrial practices would suffice.

The experiment system was designed as a unit to meet all of the experiment requirements rather than designing separate pieces of hardware for each experiment. Because of the interdependence of different tests, it did not make sense to have completely isolated test rigs for individual experiments; however, certain tanks were optimized for certain experiments.

TABLE 5.6.—EXPERIMENT LOCATIONS

Experiment	Primary location
Pressure control	Supply tank
No-vent fill	Large receiver tank Small receiver tank
Vented fill	Large receiver tank Small receiver tank
Low-gravity outflow	Small receiver tank
Chiltdown	Large receiver tank Small receiver tank
Dumping	Small receiver tank
LAD performance	Large receiver tank
Pressurization	Large receiver tank Small receiver tank

TABLE 5.7.—EXPERIMENT SYSTEM CONFIGURATION

Design feature	Criteria
Supply tank, capacity 565 lbm	Sufficient liquid hydrogen to perform minimum experiment set
Two receiver tanks, capacity 86 and 55 lbm	Variation in geometry
Two hydrogen vaporizers, capacity 3.5 lbm each	Ability to generate pressurant is most economical response to variability in autogenous pressurant quantity predictions
Two helium bottles, capacity 8.5 lbm each	Provides helium for pressurization experiment, enough for minimum number of fills
Three fluid system flow legs, 50, 100, and 200 lbm/hr	Combinations cover all required rates
Subcooler	Provides subcooling for transfers
TVS	Passive TVS, active TVS
Two-speed mixer	Provides region 1 and region 4 regimes
Wall-mounted heaters on supply tank	Provide three heat flux levels
High performance LAD in supply tank	Minimize residuals
Axial spray at both ends of large receiver tank (LRT)	Provide covered or uncovered spray
Tangential spray in LRT	Chilldown, fill
LAD-mounted heat exchanger in LRT	LAD fill bubble collapse
Cone diffuser in LRT	Pressurization
Axial, radial, tangential sprays in small receiver tank (SRT)	Chilldown, fill
Baffled outlet in SRT	Settled outflow/fill
Wall-mounted heat exchanger on SRT	Pressure control comparison with internal heat exchanger in other tanks
Pipe diffuser in SRT	Pressurization
Dump vent on SRT	Minimize dump losses

TABLE 5.8.—EXPERIMENT SYSTEM PRESSURE VESSEL GEOMETRIES^a

Parameter	Supply tank	Large receiver tank	Small receiver tank
Volume, ft ³	144	21	13.5
Length, ft	8.6	4	2.6
Outside diameter, ft	5	2.7	3
Surface area, ft ²	143	39	28
Capacity, lbm liquid hydrogen	565	84	54

^aDimensions are at room temperature, capacity is 92 percent of available volume 20-psia saturated liquid.

TABLE 5.9.—EXPERIMENT SYSTEM PRESSURE VESSEL CHARACTERISTICS

Pressure vessel	Ground maximum operating pressure, psia	Relief pressure, psia	Proof pressure, psia	Burst pressure, psia	Factor of safety at ground maximum operating pressure in 1 atm at operating temperature, based on indicated stress		Factor of safety at relief pressure in 1 atm at operating temperature, based on indicated stress	
					Ultimate	Yield	Ultimate	Yield
Supply tank	49	52	63	121	5.4	1.9	5.0	1.8
Gaseous hydrogen bottles	2000	2180	3800	4400	2.2	1.9	2.0	1.7
Gaseous helium bottles	3000	NA	5000	6000	2	1.7	NA	NA
Large receiver tank ^a	52	52	82	165	4.0	1.8	4.0	1.8
Small receiver tank ^a	52	52	82	163	4.0	1.8	4.0	1.8

^aLaunched with gaseous helium pad pressure.

TABLE 5.10.—EXPERIMENT SYSTEM TANK THERMAL PERFORMANCE SUMMARY

System	Supply tank	Large receiver tank	Small receiver tank
On-orbit heat flux, Btu/hr-ft ²	0.08	0.3	0.4
MLI thickness, in.	1	1	1
Layers	80	80	80
Penetration count			
Plumbing-to-pressure vessel (PV)	6	7	5
Struts	16	10	10
Manganin wires-to-PV	429	293	264
Manganin wires-to-MLI can	96	72	88
Phosphor-bronze wires-to-PV	52	40	44
Heaters, quantity	1	1	1
Ground heat flux, Btu/hr-ft ²	110	NA	NA

TABLE 5.11.—THERMODYNAMIC VENT SYSTEMS (TVS) DESIGN DATA SUMMARY

System	Design heat load, Btu/hr	Heat exchanger flow rate, lbm/hr		Expected heat load, Btu/hr
		TVS vent side	Liquid side	
Supply, active	1030	5.6	440	14.4 43.2 86.4
Supply, passive	86.4	0.48	NA	14.4 43.2 86.4
Subcooler	665	3.5	50.0 100.0 200.0	665
Large receiver tank	38.9	.21	NA	19.5
Small receiver tank	27.7	.15	NA	13.9

TABLE 5.12.—EXPERIMENT SYSTEM MASS SUMMARY

Experiment system	Mass, lb
Dry weight	
Supply tank module	1504
Large receiver tank module	207
Small receiver tank module	178
Electronics	46.5
Total dry weight	1935.5
Consumables	
Liquid hydrogen	565
Gaseous hydrogen	7.4
Gaseous helium	17.4
Total consumables weight	589.8
Experiment system weight	2525.3

TABLE 5.13.—EXPERIMENT SYSTEM TANK MASS SUMMARY

System	Supply tank, lbm	Large receiver tank, lbm	Small receiver tank, lbm	Vaporizer, lbm	Gaseous helium, lbm
Pressure vessel mass	207	38	29	144	74
Struts	30	16	16	5	5
Tank internals	208	13	11	26	NA
Mounted plumbing and harnessing	255	82	75	NA	NA
MLI (including purge bag and support assembly)	190	58	47	<1	<1
Total assembly	890	207	178	175(×2)	79(×2)

TABLE 5.14.—EXPERIMENT ELECTRICAL/ELECTRONICS BOXES

Item	Number	Weight (each), lb	Power (each), W
Experiment data units	3	7	15
Accelerometer	1	6	10
Mixer motor power unit	1	7.5	15
Signal conditioning unit	1	12	15

5.1.6 DESIGN HISTORY AND DECISIONS

Experiment requirements dictate a minimum of three tanks—one supply tank and two receiver tanks. Two receiver tanks are needed for geometric variation—one cylindrical tank and one nearly spherical. Early in the design process a third receiver tank was included to provide a control case, (i.e., it did not include spray systems and had minimal instrumentation). This tank was eventually dropped from the design because of volume constraints and the added disadvantage (caused by acceleration perturbations) of having the small receiver tank off-axis.

The supply tank was configured to perform most of the pressure control experiments. It includes a TVS with selectable flow rates, a mixer, and instrumentation (temperature, pressure, and liquid-vapors) to perform the various tests. Heaters mounted on the outside of the pressure vessel provide controlled heat fluxes for the experiments. The supply tank is the only tank loaded with liquid hydrogen at launch. Since it is well-equipped for cooling the fluid, it is the tank that is best suited for thermally conditioning (i.e., removing heat from) the liquid. It also includes a LAD and a subcooler for conditioning the liquid to be transferred. The supply tank is the source for subcooled liquid to perform the experimental transfers to the receiver tanks. Liquid that has been used in experiments will be returned to the supply tank for thermal conditioning.

The receiver tanks are outfitted with various spray systems which are used to investigate different types of transfer and chilldown processes. The large receiver tank contains a LAD for acquisition experiments and demonstrations. The small receiver tank has a special vent for dumping. Both tanks have a TVS.

5.1.6.1 Supply Tank Sizing and Liquid Hydrogen Requirements

The supply tank was sized to perform the minimum number of experiments required for mission success while assuming worst-case conditions. The smallest possible receiver tank sizes were chosen that met the experiment requirements. A fluid inventory spreadsheet was developed to track liquid hydrogen use through the planned set of tests. Losses caused by boiloff, chilldown, residuals, and so forth, were tracked with worst-case assumptions. The supply tank size was adjusted to provide enough hydrogen to do the tests as assumptions were refined.

Individual tests were grouped to optimize the use of liquid hydrogen by attempting to have the final conditions of one test provide the initial conditions for the next. For example, a typical group of tests consists of a set of pressure control tests that is followed by a set of transfer tests that reduce the fill level in the supply tank for the next set of pressure control tests. The pressure control tests are groups of four basic test types: (1) stratification, (2) mixing, (3) active TVS, and (4) passive TVS. These are repeated at different fill levels, heat fluxes, and acceleration levels. To vary the fill level it is necessary to remove liquid, and this is done most economically by performing transfers. A transfer may include several different kinds of tests and operations such as tank chilldown, LAD fill, no-vent fill, pressurization, direct liquid outflow, and vented fill. Since the pressure control and transfer experiments have the highest priority, the combination of alternating sets of these two types of tests forms the basic structure of the timeline.

5.1.6.2 Flow System and Flow Control

The tanks are interconnected by a number of plumbing systems. A transfer line provides various flow restrictions and paths between all three tanks for transfer of liquid. All the tanks are connected to the system flight vent, and all the TVS's are connected to a backpressure vent. A pressurization system provides either helium or hydrogen pressurant to each tank. The plumbing is located predominantly in a tray on the cold side of the spacecraft while the vents are on the hot side.

A solenoid-actuated latching valve is the basic flow control device used. Flow rate is varied by placing different flow restrictions (e.g., differently sized orifices) in parallel legs and selecting the proper leg or combination of legs as desired.

There are two possible types of transfers: pressure-driven and pumped. Both types can meet the experiment requirements. Pressurized transfers can be accomplished with simple hardware, but require pressurant gas. The amount of gas required to pressurize a tank in low-g with low outflow rates is not easily predicted with any accuracy because of the uncertainty of pressurant collapse or condensation rates. A noncondensable pressurant (gaseous helium) would provide better predictability, but would contaminate the tank and ruin the pressure control experiment. Helium is not allowed in the supply tank because of the pressure control tests, but will be used in some receiver tank transfers where the tank can be evacuated before the next fill. Care was taken in the design of the pressurization system to prevent helium contamination of the supply tank.

Pumped transfers require a liquid-hydrogen pump. The cost and risk of developing a reliable pump was deemed to be too high to include a separate transfer pump or pumps at this time. It may be that the mixer pump that must be developed for the pressure control experiment can be modified to provide the proper specific speed for a transfer pump. The mixer pump was originally envisioned as an axial pump (fanlike) that would be mounted inside the tank (submerged). As part of the "design cost-and-simple-manufacturing" philosophy that was imposed in the second iteration of the design, it was decided to remove all active components from inside the tanks.

The pump was moved to a panel mounted outside the tank on the lower dome. A second pump was added for redundancy. Two penetrations of the tank dome for the pump inlet and outlet were added. A change was also made to integrate all TVS heat exchangers in the supply tank into a single heat exchanger. The additional pressure drop from the pipes and valves required a change to a centrifugal pump. The mixer now consists of two pumps (to provide different flow rates along with redundancy), which circulate liquid through the heat exchanger in a 2.4-in.-diameter straight pipe (jet nozzle) and back into the tank. It may be possible to use the same pump design for transfers.

5.1.6.3 Cryogenic Tank Design

The supply tank was originally conceived of as a Dewar consisting of a pressure vessel surrounded by insulation and a vapor-cooled shield enclosed in a vacuum jacket. The vacuum space prevents convective heat transfer and condensation on the pressure vessel and enables the multilayer insulation (MLI) to work. The Dewar approach simplified tank operations on the ground.

Eventually an alternative approach was adopted that eliminated the massive vacuum jacket, which saved approximately 800 lbm. The vacuum jacket, was replaced by a purge bag, which is filled with helium gas on the ground to prevent condensation. The heat leak to the tank on the ground is much greater with the purge bag since convective and conductive heat transfer occurs and the MLI is rendered ineffective. However, the boiloff rate is reasonable (around 85 lbm/hr), and the tank can be locked up for the launch and ascent phases. During ascent, vent doors are opened in the purge bag to allow the pressure to equalize across the bag and to evacuate the MLI.

With a vacuum-jacketed supply tank, the MLI is protected from distortion caused by the ascent venting of the purge gas. The vacuum jacket also provides a uniform boundary temperature for the tank (through thermal conduction). There is some concern that the purged MLI will suffer distortion from ascent venting, so plenty of support pins and seam length are provided. However, support pins and seams also degrade the thermal performance of the MLI so a trade is required. On the purge bag there is a hot side and cold side. Most seams and penetrations are located on the cold side of the tank.

Initial estimates of the purge-bag-tank concept indicated that a 1-in.-thick MLI blanket could be sufficient to meet the experiment goal for the tank heat leak of 0.1 Btu/hr-ft². It also appeared that conduction heat leaks might be larger than originally expected, and that the experiment requirement for uniform heat leak into the fluid could be difficult to meet. Extensive thermal modeling was done to help the design meet these goals, but the uniformity problem was not completely resolved. It may be necessary to take further steps to reduce conduction heat leaks, such as thermally shorting harnesses to the MLI can or routing TVS heat exchangers to hot spots.

Early tank concepts followed standard space cryogenic tank practices for design, such as using aluminum alloys 6063 or 2219 and keeping margins low (e.g., a factor of safety on yield less than 1.5). As the design progressed and it became obvious that CCLD-SAT was limited by volume and center of gravity rather than by weight, a more unconventional (albeit conservative) approach was investigated. It was determined that significant cost savings could be achieved by designing the tanks to the ASME Boiler and Pressure Vessel Code (ref. 3). Because of

the large safety factors and prior history, analysis and testing requirements are much less severe with “boiler code” tanks as compared to typical flight tanks. The additional weight added by applying the boiler code amounted to approximately a 50 percent increase for the supply tank pressure vessel (80 lbm increased to 120 lbm), but a relatively modest increase to the total supply tank assembly. The material called out by the boiler code for cryogenic use is aluminum 5083 and that became the selected tank material for all three tanks. This alloy has excellent fracture toughness.

A trade of additional weight for decreased cost is intuitively unsettling to most space engineers to whom cost is usually directly proportional to weight. In this case, however, weight is not an active constraint since volume constraints are reached first. There are cost savings arising from reduced design analysis and easier manufacturing since margins are not cut to the bone. In addition, less testing is required. Risk of a failure that could postpone system integration and test is also reduced.

5.1.6.4 Modular Design

For design and assembly simplification, the experiment system was divided into the following four modules: (1) supply tank module, (2) large receiver tank module, (3) small receiver tank module, and (4) electronics module. A transfer and vent module was incorporated into the supply tank module after it was decided that the two modules overlapped enough that separation was not justified.

The supply tank module consists of the supply tank assembly, gaseous helium pressurant bottles, liquid hydrogen vaporizers, vent panels, a ground interface panel, valve panels, and a portion of the plumbing tray. The supply tank assembly consists of the tank, insulation, supports, purge bag, valves, plumbing, and harnessing.

Two vents are located on the supply tank module: the flight balanced vent and the TVS backpressure vent. The TVS vent maintains a backpressure to prevent hydrogen from freezing in the vent system. The triple-point pressure of hydrogen is 1.02 psia so the TVS vent backpressure was selected as 2 psia to avoid freezing. The flight balanced vent provides venting to hard vacuum and handles much larger flow rates from operations such as chilldowns.

The ground interface panel (also known to the design team as the “T – 0 panel,” although the launch pad connection to this panel is actually pulled at T – 4 sec) provides the interfaces to the ground loading system. The loading interfaces include a liquid hydrogen fill-and-drain line and a helium purge line for the purge bag. Pressurant bottle interfaces are located on another panel. The ground vent is not located on the T – 0 panel in the current design; it is tied into the Centaur flight vent.

This provides safe venting on the ground until liftoff and an emergency vent path on ascent in the event of a failure.

The modular approach was taken down to even small subassemblies. Valves are installed on valve panels that can be assembled and tested before being integrated with the rest of the module.

The plumbing tray (also known as the radiator tray or cold tray) provides a structure for routing plumbing lines and cable harnesses. The tray runs the length of the spacecraft from the T – 0 panel to the small receiver tank module.

5.1.6.5 Pressurant Storage and Generation

Two gaseous helium pressurant bottles contain ambient temperature, high-pressure helium gas for use as pressurant. The vaporizers are hydrogen gas storage bottles that can be recharged with liquid. The pressurization experiment calls for helium and hydrogen pressurant, the former classified as noncondensable and the latter as autogenous. Most pressurization will be done with hydrogen gas. There is uncertainty as to how much hydrogen gas will be needed to perform a pressurization since it is possible for the gas to condense into liquid. At one point in the design there were over a dozen pressurant spheres providing enough gas to reach the desired experiment pressures with the worst-case collapse factor for condensing gas. There was not enough room to fit all the bottles required to take the worst-case amount of gas. It was not clear how likely the worst case was. The decision was made to put enough gas to do one transfer under worst-case assumptions in one bottle and to recharge the bottle by using liquid hydrogen. A second vaporizer bottle was added for redundancy and to allow experiment operations to continue while one bottle was recharging.

5.1.6.6 Liquid Acquisition Devices

Screen-channel liquid acquisition devices (LAD’s) are used to provide single-phase liquid (no bubbles) for transfer to another tank. A LAD uses surface tension to separate liquid and vapor. In the supply tank, the LAD consists of four channels running the length of the tank near the tank walls with the side of the channel which faces the tank wall being composed of a fine-mesh, woven screen. The screen allows liquid to pass but filters out bubbles or vapor as long as the screen is wet. The LAD in the supply tank is designed not to break down and is not used for any LAD experiments. An experiment LAD is included in the large receiver tank. It was originally designed with a coarse-mesh screen so an attempt to break it down could be made. Later changes in the experiment objectives resulted in a fine-mesh screen being used with residual tests replacing breakdown tests.

5.1.6.7 Thermodynamic Vent System

A thermodynamic vent system (TVS) is essentially an open loop refrigeration system. Liquid is taken from the tank at a low flow rate and expanded isentropically to provide cooling. The flow is passed through a heat exchanger and vented overboard. There is no vapor-acquisition device for low-g that would allow venting of vapor only, and venting liquid or two-phase fluid is very inefficient. Tank pressure is controlled thermally by intercepting and removing heat that would cause, or has caused, a pressure rise.

There are three different TVS functions that need to be accommodated in the supply tank: active TVS, passive TVS, and liquid outflow subcooling. In the early designs, these three functions were handled by separate heat exchangers and Joule-Thompson (J-T) devices. The active TVS used a compact heat exchanger to cool liquid that is pumped back into the tank. The cold side of the compact heat exchanger was supplied with liquid taken from the tank and expanded through a J-T device, passed through the compact heat exchanger, and vented overboard. The passive TVS was a distributed heat exchanger whose cold side was a low flow-rate TVS and whose hot side was the tank wall and bulk liquid. The subcooler used a concentric tube counterflow heat exchanger to cool liquid being removed from the supply tank for transfer.

The subcooler and active TVS flow rates were similar so it seemed possible to combine the functions into a single piece of hardware. The next logical step was to include all of the TVS functions into the same hardware. Combining all the TVS functions and integrating the LAD with the TVS hardware saved weight and simplified tank assembly. The LAD-TVS can be built and tested as a unit and then placed inside the tank. It was also decided to incorporate the experiment sensor racks on the integrated LAD-TVS.

5.1.6.8 Design Considerations for Cryogenic Tankage

The tank designs were driven primarily by thermal considerations. Because liquid hydrogen must be stored near its boiling point, it is important to minimize the heat entering the tank to keep liquid from vaporizing and to control pressure rise. Conduction paths via support struts, plumbing, and harnesses were minimized by materials selection and routing (e.g., using long runs thermally shorted at the hot end to the MLI can). The radiator tray that runs along the length of the anti-Sun side of the spacecraft is used to provide a low-temperature boundary on the warm end of the plumbing and harnesses. Radiation is minimized through the use of MLI blankets with a minimum amount of seam length.

Uniformity of the heat leak into the supply tank is an important requirement for some experiments. This means minimizing the conduction heat leaks and distributing the conduction paths over the tank surface as much as possible. Plumbing penetrations are fairly large, with up to a 1 1/2-in. diameter,

but the heat leak was kept down by using thin-walled pipe made of stainless steel (which is a good thermal insulator compared to aluminum and most other metals). Explosively welded transitions of stainless-steel-to-aluminum are used to attach the piping to the aluminum tanks. Each plumbing penetration has one or more valves associated with it located nearby. These valves have actuation wires and position indication wires that are conduction heat sources. The plumbing penetrations are located on the domes of the tanks to simplify assembly (also because the tops and bottoms of the tanks are logical places for most penetrations when the tanks are tested on the ground).

The valves that form the first barrier to fluid-flow in the piping system are located on the tank. This placement keeps the valves cold, which prevents vaporization of the liquid inside the tank. The danger of locating the valves where they would be warm is that liquid could wick up the sides of the pipe, vaporize, and allow warm vapor to travel back down the center of the pipe, thus acting like a heat pipe and dumping large amounts of heat into the tank. Another danger is thermoacoustic oscillation where a liquid-vapor interface in a pipe closed at the warm end oscillates through a cycle of vaporization-pressure-rise and condensation-pressure-drop, which dumps heat into the tank. With the valve right on the tank, the pipe that comes into the tank can be evacuated to remove the residual vapor and thereby stop all heat transfer by means of the vapor in the pipe.

Several locations for the valves were examined, including inside the tank, directly on the tank domes, on panels mounted to the domes, and on the MLI can. Locating them inside the tank was rejected for reliability reasons leading to the ground rule that no active components are allowed inside the tank. Valve panels mounted to the tank domes were chosen because the panel assemblies can be built and tested in modular fashion, and the panels help spread out the thermal and mechanical loads on the dome.

A concern in running chilldown and fill tests in the receiver tanks was the transient response of the MLI. A quick check was done with the supply tank thermal model, which roughly resembles a scaled-up large receiver tank, and the chilldown time of the MLI can was estimated. The tank was set at liquid hydrogen temperature and the MLI can was started at -50°F and then allowed to equilibrate. The time to equilibrium was 5 hr.

5.2 Experiment Flow System

The experiment flow system performs three basic functions: (1) liquid transfer, (2) tank venting, and (3) tank pressurization. These functions are performed not only in space for experimentation, but also on the ground for loading, under much different circumstances. We will consider the flight and ground functions separately, although some common hardware is used for both purposes. Detailed flow system schematic information is shown in figures D.1(a) to (e), and D.2 (in appendix D to this

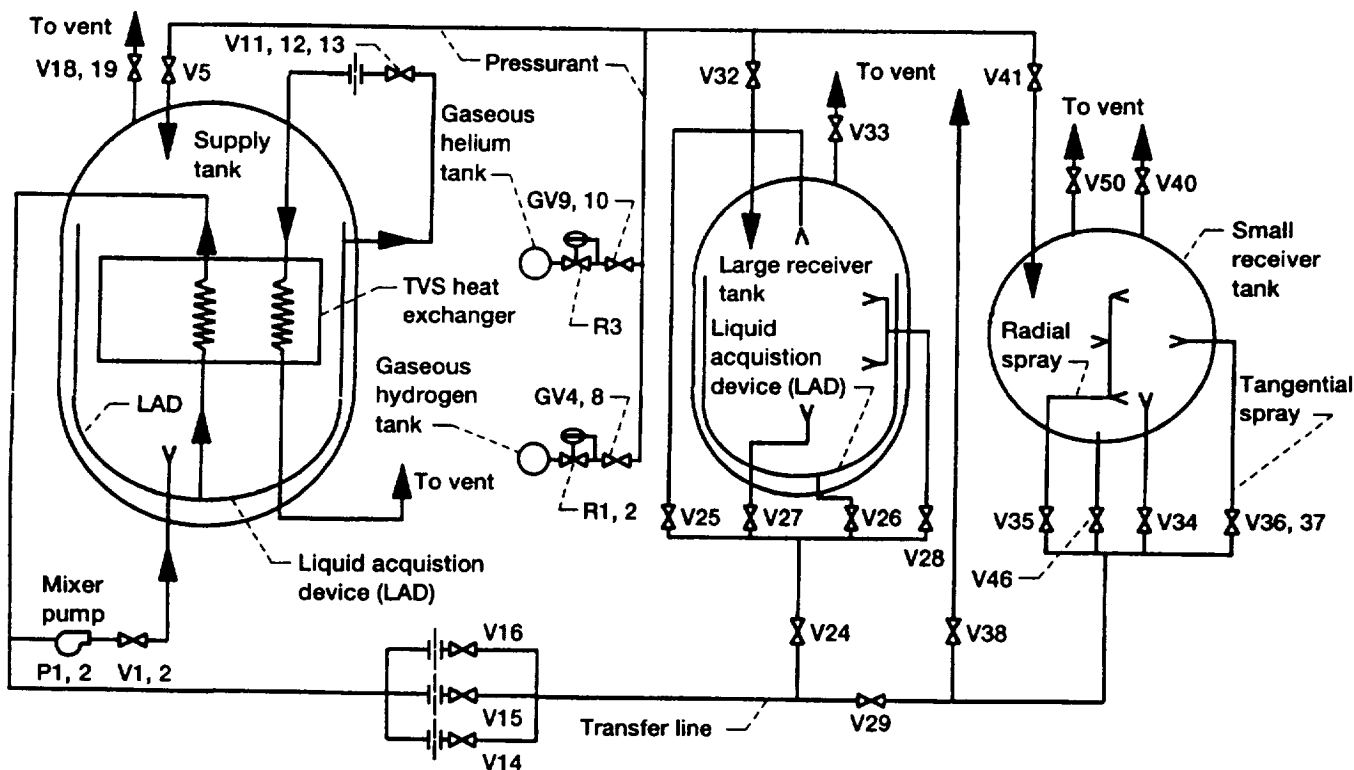


Figure 5.1.—Simplified fluids schematic of experiment system. (See table 3.1 for experiment system tank characteristics. See also figure D.1 for more detailed fluid schematics.)

chapter). Figure 5.1 provides a simplified fluid schematic. A simplified ground interface schematic is also given in figure 5.2.

5.2.1.1 Liquid Transfer

Most of the experiments, and operations preparatory to experiments, require the ability to transfer liquid between any two of the three tanks. The required flow rates of 50 to 350 lbm/hr between supply and receiver tanks are provided by selecting flow legs with different flow restrictions. The flow rate accuracy requirements are not severe, and the experiments can be performed with a constant flow restriction in the line even though the flow rate will vary as the pressures in the supply and receiver tanks change during the transfer. The leg with V14 (fig. D.1(a) in appendix D to this chapter) provides a nominal 50 lbm/hr restriction, the V15 leg is sized for 100 lbm/hr, and the V16 leg is sized for 200 lbm/hr. The transfer line between the large and small receiver tanks doesn't have a flow restriction, but is limited to about 400 lbm/hr by the flow drops in the system, assuming a 30-psia pressure in the source tank and 18 psia in the receiving tank. The pressure in the receiving tank depends on the amount of subcooling of the liquid, heat transfer to the liquid from the transfer line, and the thermal state of the receiving tank.

Subcooled liquid is required for transfer experiments. In the supply tank, subcooling can be achieved with an outflow heat exchanger which is an integral part of the TVS. In the receiver tanks, subcooling is achieved by pressurizing the tank from initial saturated conditions and performing the fill before significant heat is transferred to the liquid. After a transfer or after a long storage period in the receiver tanks (with a heat leak of around 0.5 Btu/hr-ft²), the liquid will have to be cooled to achieve a saturation pressure of 15 psi. This cooling can be accomplished by settling the liquid away from the tank vent outlet, opening the vent (V33 or V40; fig. D.1(d)) to space, and boiling the liquid to remove heat. The experiment TVS could also be used to aid this process.

To perform a transfer, it is necessary to first chill down the transfer line (including valves, relief valves, dead-end legs, etc.) and the receiver tank. This is done by flowing liquid hydrogen through the lines. The warm items may be at ambient temperatures or already somewhat cooled depending on the time since the last operation. Transfer lines will be chilled with a continuous flow chilldown through V8, V14, V29, and V38 (figs. D.1(a) and (e)) (for supply tank source) to the flight balanced vent. This method uses the heat of the vaporization of hydrogen with very little sensible heating of the boiloff gas. For a thermal mass of 20 lbm of stainless steel (approximating the transfer line), it is estimated that it will take 4 lbm of liquid

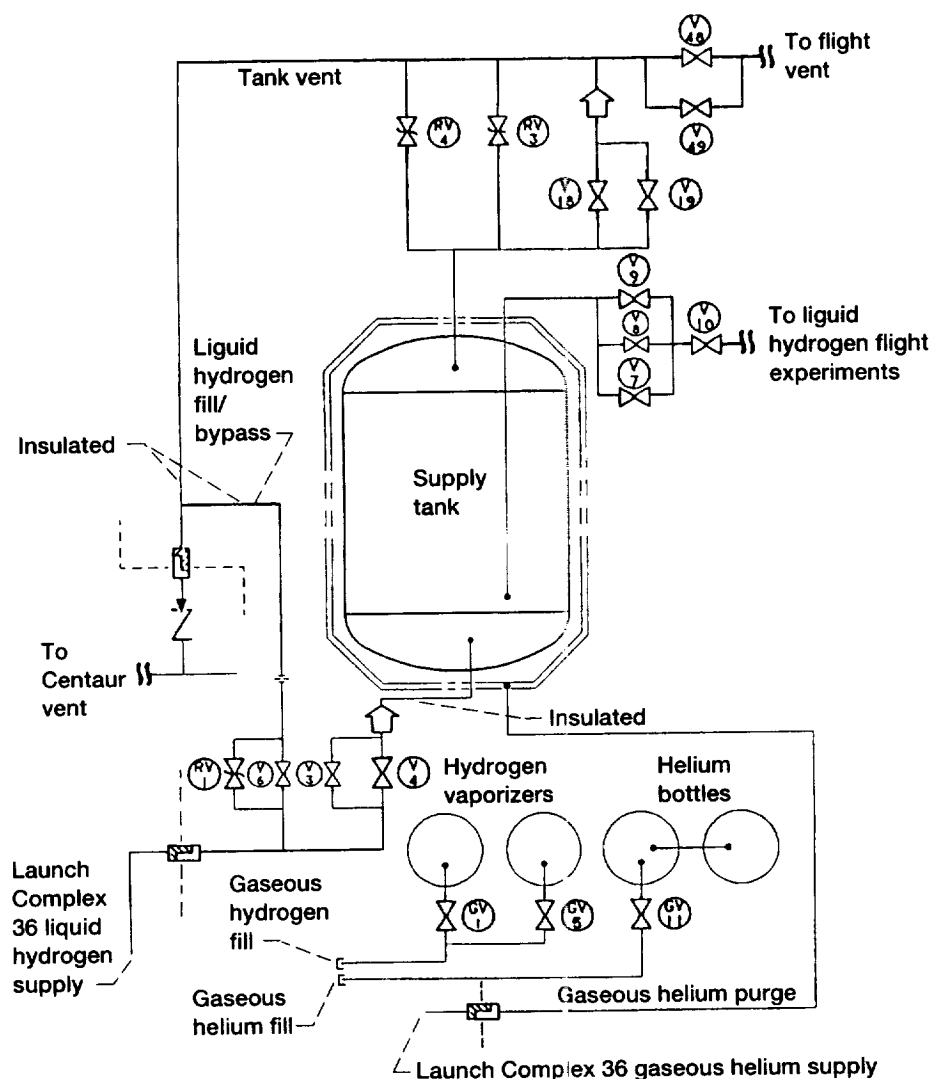


Figure 5.2.—Simplified ground interface schematic. (Not to scale; valving not shown in true or actual position.)

hydrogen to chill the transfer line from 540 °R and 1.4 lbm of liquid hydrogen to chill from 300 °R.

To chill the transfer line right up to the tank without affecting the tank temperature is a little more tricky, but fortunately is not currently a requirement. It might be possible to chill down the lines and valves on the tank by venting through the tank without chilling the tank below its initial temperature requirement for a tank chilldown experiment or heating the tank back up. Alternately, a charge-hold-vent chill procedure could be used where a charge of liquid is introduced into a sealed off section of line and heat transfer is allowed to take place until the pressure rises to the point where the line has to be vented. Since the burst pressure for the valves is 240 psia, the allowable pressure must be less than this, perhaps 120 psia.

Tank chilldown is done primarily by charge-hold-vent procedures. The charge can be introduced into the tank through one of the spray systems that exist for fill operations. The passive TVS system (V31 and V39; figs. D.1(d) and (e)) heat exchanger can be used to increase heat transfer to the tank, but the flow rate for gas through the J-T device is slow.

There are two types of fills: no-vent fill and vented (settled) fill. The plumbing hardware for performing either type is the same with the exception of the vent status (open for vented fill and closed for no-vent fill). The large receiver tank, shown in figure D.1(d), has a LAD which can be used to transfer liquid to or from the tank (V26), a tangential spray system (V28) used to set up a swirling motion, and two axial sprays, one at each end of the tank (V25 and V27). The two axial sprays are located at

opposite ends of the tank such that, when the spacecraft thrusters are fired to settle the liquid, one sprays through the liquid and one sprays through the vapor. The LAD acts as a diffuser when used as a tank inlet. As illustrated in figure D.1(e), the small receiver tank has a tangential spray (V36 and V37 provide different flow restrictions), an axial spray (V34), a radial spray (V35), and a baffled outlet (V46).

Transfers of liquid to the vaporizers are needed for gas generation. The purpose of the vaporizers is to convert liquid hydrogen to pressurant gas. The vaporizer must first be chilled to guarantee that liquid can be injected into it. Then liquid is sealed in the vaporizer and heated until it becomes gas. These chilldowns and transfers take place through V47, V21, GV2, and GV3 for vaporizer B or V20, GV6, and GV7 for vaporizer A, as illustrated in figure D.1(c).

When the supply tank is the source of liquid, the LAD outlet is connected to the flow rate selection bank (V14 to V16) by means of V7, V8, or V9. A turbine flowmeter is in the V9 leg and the V7 leg provides an unrestricted bypass in case the flowmeter fails and blocks flow. The V8 leg has a flow restriction that will be optimized for line chilldown. The LAD transfer outlet (V7 to V9) is closed for backtransfers into the supply tank via V17 to avoid getting vapor into the LAD. The transfer outlet is also closed when the active TVS is being run (V1 and V2). A TVS connection to the transfer line via V10 allows TVS vapor to be vented through the transfer line to help keep it cold between transfers. After a transfer, residual liquid in the line is dumped to space via V38 (fig. D.1(e)).

Loading the supply tank on the ground is done through V3 and V4 (figs. D.1(a) and 5.2). These valves are in parallel to provide an adequate flow rate for chilldown and fill and not for reliability reasons although the parallel combination does provide some redundancy for draining the tank. A bypass to the vent line through V6 is provided to allow the fill line to be kept cold during the time between tank fill and top-off. The fill/drain line will have a sealing disconnect to provide the second barrier between liquid hydrogen and space required by design ground rules. The ground helium purge is controlled on the ground side. Lines that see cryogenic temperatures on the ground are foam-insulated.

5.2.1.2 Venting

Venting can be divided into four types: (1) ground, (2) flight vacuum (3) flight backpressure (for TVS), and (4) relief. On the ground, all venting is routed through the Centaur vent system to a burn stack on the pad. COLD-SAT post-chilldown vent rates are low enough that they do not interfere with the backpressure required by Centaur in its vent system. The COLD-SAT relief valves (except for RV18 (fig. D.1(b) in appendix D to this chapter), are routed through the ground vent until liftoff. The flight vacuum vents (direct to space) are the flight balanced vent and the small receiver tank dump vent. The

backpressure vent prevents freezing in the low flow TVS lines and is known as the balanced TVS vent.

The ground vent must handle a nominal maximum flow of 200 lbm/hr and a worst-case (purge bag failure) flow of 4200 lbm/hr. This latter requirement drove the use of 1 1/2-in. line for the ground vent. As noted previously, all vent lines that see cryogenic temperatures on the ground are foam-insulated to prevent the formation of liquid air. The ground vent is isolated from the flight vent by V48 and V49 (for redundancy) (fig. D.1(b)) which are opened after fairing jettison. The ground vent is attached to the Centaur payload fairing. When the fairing is jettisoned, the disconnect that is provided opens to release the fairing and at the same time seals the vent pipe from COLD-SAT. Ground venting is due to the supply tank chilldown, fill, and normal boiloff and takes place through V18 and V19 (fig. D.1(a)). These valves are in parallel to provide a low pressure drop and not for redundancy. The nominal tank pressure after fill is 20 psia and the nominal boiloff rate is 90 lbm/hr.

The relief devices are tied into the ground vent so that any failure results in venting to the burn stack. Relief devices are required on all potential trapped volumes of hydrogen. The helium bottles do not have relief devices, but rely on temperature control to prevent overpressure. The supply tank relief pressure is 52 psia, and worst-case flow is 4200 lbm/hr. Plumbing relief valves are set at 100 psia. The isolation valves V48 and V49 (fig. D.1(b) in appendix D to this chapter) might be used to control a leaky relief valve to some degree. Relief valve RV18 (fig. D.1(a)) (which bypasses the flight balanced vent valves) is set at a low pressure (15 psia) so that upstream relief valves can function at a trapped pressure that is low enough to prevent damage.

The flight balanced vent and the balanced TVS vent are similar in that the three tanks vent into a manifold with parallel redundant shutoff valves (V44-V45 and V42-V43 (fig. D.1(b)), respectively) at the vent panel. The small receiver tank dump vent (V50; fig. D.1(e)) was originally envisioned as a straight pipe to space on the spacecraft long axis. The dump vent is the only place where the two-barrier ground rule would have been broken. However, after discussions with the experimenters, it was decided that another valve can be added in series and that this vent can be balanced. The perturbations of the spacecraft attitude caused by a high flow-rate dump are large, and the dump experiment can be designed so that the plumbing complications do not interfere with the data analysis.

5.2.1.3 Pressurization

Pressurant gas acts as the driving force for liquid transfers. Hydrogen gas is the primary source of pressurant for the experiments. A concern with hydrogen (or autogenous) pressurization is that the gas will condense and dump its heat into the liquid rather than provide a pressurized ullage. Helium

pressurant is planned to be used for only a few experiments, and helium is not desired in the supply tank because it would interfere with the pressure control experiment. Enough helium is carried to provide some redundancy for performing critical experiments if the primary hydrogen pressurization technique develops problems.

The integrated plumbing schematic (figs. D.1(a) to (e) in appendix D to this chapter) identifies the three tanks as the supply tank, the large receiver tank, and the small receiver tank which are of different sizes or shapes in order to satisfy specific experiment requirements and constraints. The supply tank is equipped with heaters to provide uniform heating at the required heat flux levels of 0.1, 0.3, and 0.6 Btu/hr-ft². The receiver tanks have heaters to warm the tanks up to required initial temperatures for experiments. The design allows for the supply tank to be launched "wet" (i.e., containing liquid hydrogen) and the receiver tanks to be launched "dry" (i.e., with only a pad pressure of gaseous helium). Prior to any liquid hydrogen transfer in space, the receiver tank vent valve will be opened to the vacuum of space in order to evacuate all traces of helium gas.

Helium and hydrogen pressurant gas are supplied to the tanks through a common pressurization manifold. A helium supply consisting of two bottles containing 7.4 lbm and two separate, rechargeable hydrogen supplies, which initially contain 17.4 lbm of hydrogen gas, are the pressurant sources. All sources are regulated. The helium supply is isolated by two series-redundant valves (GV9 and GV10; fig. D.1(c)) to prevent helium contamination of the supply tank through inadvertent operation or leakage.

The pressurant manifold is connected to the supply tank through V5 (fig. D.1(a)), the large receiver tank through V32 (fig. D.1(d)), and to the small receiver tank through V41 (fig. D.1(e)). After pressurization, the manifold will be vented to vacuum in order to reduce the heat leak to the tanks. A separate vent was not added to the manifold so that the number of valves would be kept low and to reduce failure modes. The manifold can only be vented through an empty receiver tank.

5.2.1.4 Thermodynamic Vent Systems

The experiment system design incorporates thermodynamic vent systems (TVS's) with their associated heat exchangers as the primary means of pressure control. Each of the three tanks has a passive TVS. The supply tank also has an active TVS that incorporates a pump to provide a mixing jet of recycled liquid that can be subcooled for destratification purposes. In addition, the supply tank includes a subcooler for thermal conditioning of the liquid being transferred.

For operation of either the TVS system or subcooler of the supply tank, liquid hydrogen from the LAD is directed to a parallel branching of valves (V11, V12, and V13; fig. D.1(a) in appendix D to this chapter) in combination with J-T flow restrictor devices sized to provide the required flow rates. The

leg with V11 is sized at 0.48 lbm/hr for passive TVS, the leg with V12 is sized at 3.5 lbm/hr for the subcooler, and the leg with V13 is sized at 5.6 lbm/hr for the active TVS. Upon flowing through the selected valve, the fluid expands isenthalpically through a J-T flow device to a two-phase condition. It is then directed back to another heat exchanger channel on the LAD to provide cooling before it exits the LAD assembly and is vented to space.

For the active TVS, subcooled liquid from the LAD is directed to one of the redundant pump and valve (either V1 or V2; fig. D.1(a)) combinations. From here the liquid is returned to the tank through a 2.4-in.-diameter nozzle (the 0.5-in. penetration flares out to 2.4 in. inside the tank) to provide destratification and pressure control.

5.2.2 DESIGN DETAILS

Figures 5.1 and D.1 (in appendix D to this chapter) are schematic representations of the plumbing design that evolved for fulfilling the functional requirements. The plumbing was divided up among the three experiment system modules, namely, the supply tank module, the large receiver tank module, and the small receiver tank module. The boundaries of the individual modules is indicated on the fluid schematic with dashed lines. The supply tank module includes the helium bottles, the hydrogen vaporizers, and various valve panels in addition to the supply tank and its associated components.

5.2.2.1 Major Plumbing Components

Table 5.15 indicates the types of fluid components incorporated in the design and provides a summary of the quantity of components utilized in each module. The plumbing components are further grouped for assembly as panels which are mounted directly to, or in close proximity to, their respective tank or bottle. Table E.3 in appendix E to this chapter provides a list of candidate valving used in this design.

During the planning stages and early design phase, the philosophy with respect to valving was to require single-fault tolerance which led to considerable redundancy. As the design progressed and reliability analyses were performed, it became evident that some redundant valving was not providing a significant improvement in reliability. In those particular cases the redundancy was deleted in the interest of cost and weight reduction. The philosophy of providing two barriers between hydrogen and space was maintained throughout the entire design phase.

5.2.2.2 Liquid Hydrogen Transfers

The driving force for transfer operations will be pressurized gas. Two gases are available: hydrogen, a condensable gas at 20 K, and helium, a noncondensable gas at 20 K. Prior to launch,

TABLE 5.15.—EXPERIMENT SUBSYSTEM FLUID COMPONENTS SUMMARY

Components	Supply module						Large receiver module			Small receiver module			Totals
	In tank	Tank panels	Hydrogen vaporizer panels	Helium panels	Tray	Vent panel	In tank	Tank panels	Tray	In tank	Tank panels	Tray	
Cryogenic valves	0	18	4	0	4	4	0	9	1	0	9	0	49
Gas valves		0	8	4	0	0		0	0		0	0	12
Relief valves		3	7	0	1	2		2	2		1	1	19
Cryogenic check valves		0	2	0	0	2		1	0		0	0	5
Pressure regulators		0	2	1		0		0			0		3
Pumps		2	0	0		0		0			0		2
Joule-Thompson devices		3		0		0		1			1		5
Flow meters		4		1	2	3		0	3		0	2	15
Spray nozzles		0		0	0	0	6	0	0	15	0	0	21
LAD	1	0		0	0	0	1	0	0	0	0	0	2

the two helium bottles will be filled with gas to a pressure of 3000 psi, and the hydrogen vaporizer bottles will be filled with gaseous hydrogen to a pressure of 2000 psi.

When the hydrogen bottles are depleted to a pressure of about 200 psi, the bottles will be vented to space and otherwise prepared for admitting liquid hydrogen to an internal coil of the vaporizer bottle. The liquid in the coil will be allowed to vaporize and expand into the bottle proper and further heated until the pressurant supply is replenished.

Prior to any transfer, the lines and components that the liquid hydrogen will encounter must be chilled down. An estimate of the mass outside of the MLI can requiring chilldown for this purpose is contained in table 5.16.

5.2.2.3 Vertical Schematic

The diagram in figures D.2(a) and (b) is called the vertical schematic because it depicts the three tanks in the orientation they will have at launch. This schematic provides a more realistic indication of the relative position of plumbing subassemblies with respect to individual tanks or bottles. The octagonal shape that encircles each tank is representative of the MLI can that surrounds the respective tank and its associated panels of plumbing components. Each MLI can is encased in a blanket of multilayer insulation for thermal protection.

All fill and vent lines used on the ground outside of the MLI can for the supply tank will be covered with a thickness of foam insulation and have a certain number of layers of MLI over that. While on the ground, the foam will provide the necessary insulating properties to prevent air or its constituent gases from condensing on cold plumbing, and the MLI will provide the necessary insulating qualities for on-orbit operations. Since neither of the receiver tanks will contain a cryogen until on-orbit operations, all lines that do not have a possibility of reaching cryogenic temperatures in the atmosphere will be wrapped with MLI only.

TABLE 5.16.—ESTIMATED TRANSFER LINE CHILLDOWN MASS

Items	Chilldown mass, lb
Cryogenic valves V47, V24, and V29 (3.5 lb each)	10.5
Relief valves RV11 and RV12 (1.65 lb each)	3.3
2 pressure transducers and 1 thermocouple	1.0
20 ft of 1/2-in. diameter tubing (0.174 lb/ft)	3.5
Total chilldown mass (stainless steel)	18.3

In general, all plumbing lines leaving the MLI cans will be routed to a plumbing tray which is located on the "cold" side of the spacecraft and acts as a radiator to space. This tray, which houses plumbing lines and associated plumbing components, is indicated by a dashed line enclosure in figure D.2. In the case of the flight balanced vent and the TVS balanced vent, these lines are first routed to the plumbing tray before continuing on to the "warm" side of the spacecraft for venting.

5.2.2.4 Experiment Safe State

In the event of an unexpected failure or interruption of the spacecraft control systems, the COLD-SAT experiment system will be put in a safe standby condition (safe state) with the expectation of a near term recovery. The basic ground rules require that there be no damage to the system, a minimization of fluid losses, and the potential for recovering and continuing experimentation. This safe state will be self or ground initiated and will be required to hold for a minimum of 4 to 6 orbits (about 12 hr) until data can be analyzed and necessary fixes transmitted to the spacecraft. The safe state column entries listed in table E.3 in appendix E to this chapter indicate the correct position for all the solenoid-actuated valves. These valve positions will seal off all tanks, activate the passive TVS's of all tanks, and activate the venting of all transfer lines.

In this condition, at least one barrier is provided between the liquid hydrogen and space. All heaters and pumps will be in the off position for a safe-state condition.

5.2.2.5 Venting Systems

Table 5.17 lists the venting requirements for the supply tank, the large receiver tank, the small receiver tank, and the transfer lines, respectively. Ground tank boiloff will be vented to atmosphere (through the Centaur vent system) until T - 95 sec, at which time the supply tank is locked up for launch. All ground and ascent venting, if required, will be accomplished through the Centaur vent fin (fig. 5.3) until the payload fairing is jettisoned. This includes all relief valves except the relief valve for the flight vent manifold (panel O). Venting will be switched over to the flight balanced vent following this jettison procedure by an automatic sealing disconnect and the opening of the redundant valves, V48 and V49 (fig. D.1(b)) in appendix D to this chapter.

While on-orbit there will be three different vent systems for accommodating the venting requirements: the flight balanced vent, the balanced TVS vent, and a fluid-dump vent. The flight balanced vent (V44 and V45; fig. D.1(b)) will be activated during chilldown and vented-fill operations and will accommodate any relief venting. The balanced TVS vent (V42 and V43; fig. D.1(b)) will accommodate venting when any of the passive thermodynamic vent systems are in operation, or when the supply tank's active TVS or subcooler features are being used.

TABLE 5.17.—VENTING REQUIREMENTS

Supply tank, lb/hr	
Ground vent	
Normal ground boil-off vent	140
Emergency ground vent	4200
Chilldown	220
Flight vent	
Planned ascent vent	30
Relief vent	200
TVS vent	
Passive	0.48
Active	5.6
Subcooler	3.5
Large receiver tank, lb/hr	
Flight vent	
Vented fill	10
Chilldown	50
Relief	50
TVS vent	
Passive	0.21
Small receiver tank, lb/hr	
Flight vent	
Vented fill	10
Chilldown	20
Relief	20
TVS vent	
Passive	0.15
Dump vent	100
Transfer lines, lb/hr	
Chilldown	20
Relief	20

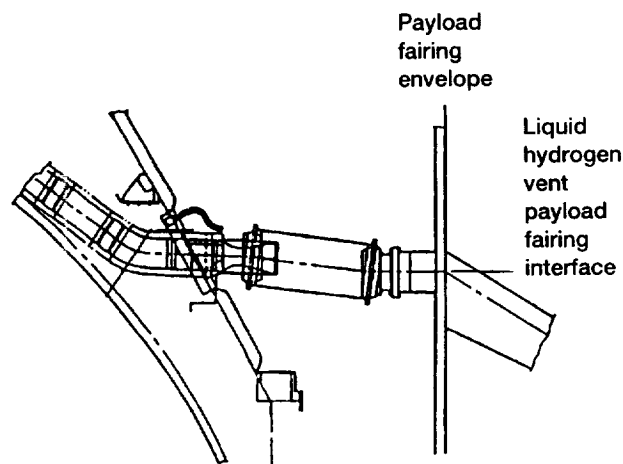


Figure 5.3.—Supply tank gaseous hydrogen interface to central vent fin.

The balanced TVS vent has a check valve in the system to assure a backpressure of 2 psi to prevent formation of frozen hydrogen. The fluid-dump vent is provided for accommodating the fluid dumping experiment that is planned for the small receiver tank.

5.2.3 COMPONENTS AND SELECTION

A great deal of effort went into identifying specific components for the COLD-SAT design to minimize cost and risk. When specific models are identified in this report, such identification only indicates potential availability and not NASA endorsement of specific commercial products. Areas where off-the-shelf components were not readily available include the following: cryogenic valves, cryogenic disconnects, large cryogenic relief valves, and liquid hydrogen pumps.

5.2.3.1 Plumbing Lines

Table 5.18 shows the general tubing sizes for the main plumbing lines in the experiment system design. All tubing was sized in accordance with standard practices. The Crane Handbook (ref. 4) was used for obtaining many of the flow characteristics such as friction factors, flow resistance factors, and flow coefficients for determining flow capability for tubing.

TABLE 5.18.—LINE SIZE SUMMARY

Line description	Tubing size, diameter, in.
Fill/drain	3/4
Pressurization	1/4
Transfer lines	1/2
On-orbit vent	3/8
Ground vent	3/4, 1 1/2
Passive TVS	1/4
Pump/mixer	1/2

fittings, plumbing components, and flow control devices like orifices and venturi. No line size smaller than 1/4 in. in diameter was selected even if a smaller size was adequate, in order to alleviate any potential fabrication or assembly problems. Two sizes of tubing are listed for tank ground vent—3/4 in. and 1 1/2 in. The 3/4-in. tubing accommodates the normal boiloff that is expected from the supply tank and is controlled by redundant valves V18 and V19 (fig. D.1(a) in appendix D to this chapter). The 1 1/2-in. tubing is provided to accommodate venting in a worst-case type failure, which assumes a ruptured purge bag and loss of power, and is controlled by relief valve RV3 (fig. D.1(a)). As indicated on the integrated system schematic (fig. D.1), the 3/4-in. line ties into the 1 1/2-in. line just beyond the valving. In general, flow velocities were limited to under 20 ft/sec for liquid hydrogen and to a Mach number less than 0.20 for gaseous hydrogen conditions.

Attachment of tubing to fittings, components, and so forth, will be accomplished by an orbit arc welder to provide reliable and consistent weld quality. This type of system is especially adapted for welds of tubing systems that require close component spacing and will be ideal for the experiment system's modular concept with subassemblies and various panels containing several components in confined spaces.

5.2.3.2 Major Components

Table E.3 in appendix E to this chapter lists the major components employed in the experiment system design. The following sections provide a description of components selected for use in the design.

5.2.3.2.1 Cryogenic Latching Valve.—Valves capable of operation with liquid hydrogen are required in 49 different locations throughout the system for flow control purposes. A cryogenic latching valve planned for use in the experiment system was being developed at the time of this design effort by Moog, Inc. under NASA contract NAS3-25056. Some of the more pertinent requirements and features of the cryogenic latching valve design are listed in table 5.19 and illustrated in

figure 5.4. The valve is a two-coil, solenoid-operated component for flow control that latches in the last position commanded. The valve is capable of bidirectional flow and has a flow capacity of an equivalent square-edged orifice (ESEO) that has a diameter of 0.3 in. This particular valve has been designated as -020 and is in the latter stages of development. It has already been subjected to the required proof pressure testing of 240 psi. The valve weighs approximately 2.5 lb. and therefore has met another requirement of being less than 5 lb. It has also met the requirement for current draw of less than 5 A at the temperature of liquid hydrogen, and the unit opens or closes in less than 100 msec at the cryogen temperature. Upon completion of the development stage the valve will undergo qualification testing.

With the completion of the development of the -020 version, modifications will be made to the present design for producing another version (-030) that will provide a flow rate that is double that of the present version for a given pressure drop. This new valve configuration will have an ESEO with a 0.42-in. diameter. Both versions of this cryogenic valve are being used in this system design as indicated in the valve list (table E.3). Thirty-four of the -020 models and fifteen of the -030 models are required.

5.2.3.2.2 High Pressure Gas Valves.—Valves capable of operation with gaseous hydrogen and helium at high pressures are required for tank pressurization purposes, and for operation of the hydrogen vaporizers. In addition, some gas valves will be exposed to liquid hydrogen temperatures. Two different gas valves were selected to accommodate these requirements. One valve identified is capable of operation at temperatures as low as -425 °F. This type of valve is designated for use in six different locations shown in figure D.1(c), in appendix D to this chapter, as GV1, GV2, GV3, GV5, GV6, and GV7. This valve design is pilot-operated, weighs 2.5 lb. and is capable of flow that is comparable to a 0.35-in.-diameter ESEO. It is solenoid-actuated, but is not a latching valve design. Modification to make this a latching type valve for conserving power is anticipated. This valve design has already been used for space

TABLE 5.19.—CRYOGENIC LATCH VALVE

Required item	Minimum requirements (if any)	Moog 020 valve capability
Working fluid	Liquid hydrogen, gaseous hydrogen	Liquid hydrogen, gaseous hydrogen
Pressure	49 psi maximum expected operating pressure	120 psi
Proof pressure	-----	240 psi
Operating temperature	-435 to 140 °F	-435 to 150 °F
Leakage (external)	-----	<10 ⁻⁹ standard cm ³ /sec helium
Leakage (internal, at liquid hydrogen temperature)	-----	0.1 standard cm ³ /sec helium
Input power (at 70 °F)	24 to 32 V at <5 A	28 V at 2.5 A
Latch in position driven	Yes	Yes
Flow capacity	-----	Equivalent square-edged orifice, 0.3-in. diameter
Position indication	Yes	Yes
Weight	-----	2.5 lb
Cycle life	1000	10 000

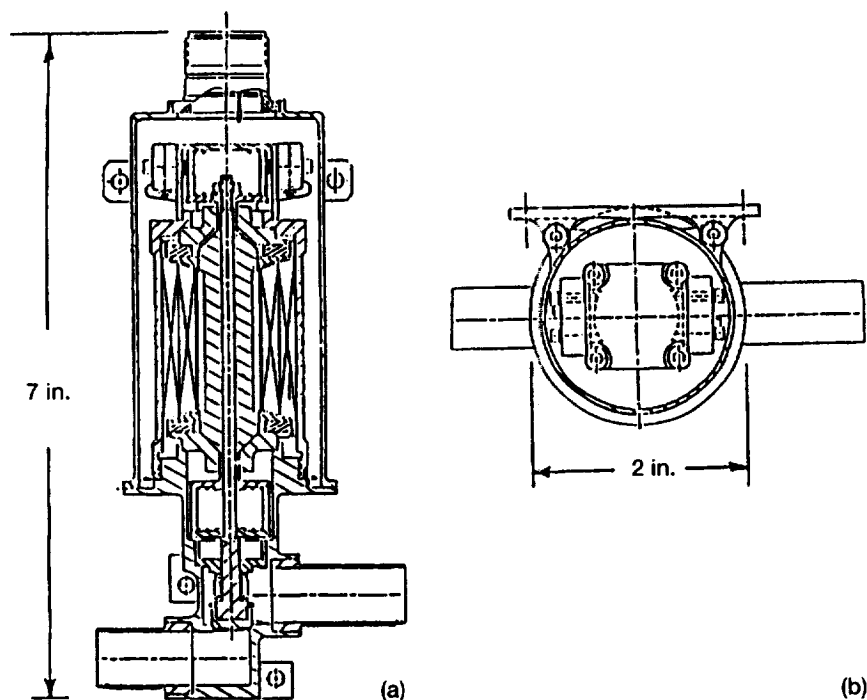


Figure 5.4.—Cryogenic latching valve. (See also table 5.19.) (a) Side view. (b) Top view.

application using gaseous helium as the media in connection with the Saturn vehicle, but the design will have to be checked out for compatibility with gaseous hydrogen.

The gas valve selected for the six other locations (GV4, GV8, GV9, GV10, GV11, and GV12; fig. D.1(c)) is solenoid-actuated and is a latching valve. It weighs only 0.65 lb and has been used in a space application. Although it meets other requirements, the media used with this valve was gaseous nitrogen, and some modification may be required to make it compatible with gaseous hydrogen.

5.2.3.2.3 Pressure Regulator.—Pressure regulators will be required for operation with both helium and hydrogen gas to control tank pressures to 30 psi, particularly during transfer processes. The regulator design selected is typical of a single-stage design and is capable of handling source pressures from 3530 psi down to 145 psi with regulated pressure of 37.5 psi. The COLD-SAT design requires source pressures from 2000 to 200 psi be regulated to a pressure of 30 psi. In addition, this particular design is capable of flowing about 2 lb/hr of helium gas which is roughly half of the maximum requirement for COLD-SAT. The changes or modifications required do not appear impractical or extensive. This design has seen an application with helium on the space shuttle.

Two separate pressure regulator designs could be used to regulate pressure to the required pressure level in two stages. A candidate high-pressure regulator decreases the source pressure from levels as high as 4500 psi to a controlled pressure of 225 psi and has more than adequate flow capability. The low-

pressure regulator reduces the intermediate pressure of 225 psi down to a regulated pressure between 20 and 30 psi which meets the requirements of COLD-SAT but modifications would be necessary to meet the flow capacity requirement.

5.2.3.2.4 Relief Valves.—As indicated in table E.3 in appendix E to this chapter, the relief valves incorporated in the experiment system design require five different relief pressure levels varying from 15 to 2200 psi. Candidates capable of pressures up to 2400 psi and capable of cryogenic service application have been identified. Valves of this type have seen applications on the Shuttle Orbiter and the Atlas II vehicle. Candidate models have been identified that will accommodate the needs and requirements of all but one application for the COLD-SAT design. The one exception is that the supply tank relief valves RV3 and RV4 (fig. D.1(a) in appendix D to this chapter) accommodate a high flow rate for a worst-case ground boiloff scenario, in which the helium purge bag has suffered a rupture and all power has been lost. The flow rate for this scenario, will require a 1 1/2-in. relief valve and the largest valve of this design produced to date has been 1 1/4 in.

5.2.3.2.5 Check Valves.—The experiment system design incorporates five check valves. Candidates have been identified that can be used in cryogenic applications where operating pressures are as high as 3000 psi which is much greater than the experiment requirement. The valve design is capable of being sized for any cracking pressure up to 8 psi which is more than adequate for the COLD-SAT system. The identified valve design has been used in space applications.

TABLE 5.20.—JOULE-THOMPSON (J-T) FLOW DEVICES

[Lee Visco jet flow restrictor application.]

Tank	Feature	Liquid hydrogen flow rate lb/hr	Lee part number	Minimum passage, in.	Weight, lb
Supply	Passive TVS	0.48	VDCB1835240H	0.01	0.06
	Active TVS	5.6	VDLA68 series ^a	.062	.17
Supply	Subcooler	3.5	or VXLA2500210D (axial)	.04	.1
			VDLA68 series ^a	.062	.17
Large receiver	Passive TVS	.21	or VXLA2500330D (axial)	.035	.1
	Small receiver		VDLA4326460H	.015	.09
	Passive TVS	.16	VDLA4326650H	.015	.09

^aStandard size does not quite match requirements.

TABLE 5.21.—PUMP-MIXER DESIGN PARAMETERS

Parameter	Speed	
	High	Low
Flow rate, cfm	1.7	0.4
Delta pressure, psid	1.0	0.06
Rotational speed, rpm	4000	960
Power required, W	6.7	0.1

5.2.3.2.6 Cryogenic Disconnects.—Cryogenic disconnects are required in the fill/drain line and the ground vent line for the supply tank. These disconnects provide an interface with the ground support equipment (GSE) and are composed of a flight half-coupling and a latching or nonlatching ground half-coupling. Both halves are required to be self-sealing when unmated.

5.2.3.2.7 Joule-Thompson (J-T) Flow Devices.—The experiment system design utilizes J-T devices for expanding liquid hydrogen to a two-phase, subcooled condition to cool the tank liquid for pressure control and thermal conditioning purposes. The required flow rates for the passive TVS, the active TVS, and the subcooler operations are presented in table 5.20. Candidates include flow restriction devices and pressure regulators.

5.2.3.2.8 Pump-Mixer.—A pump-mixer has been incorporated in the warm side of the supply tank active thermodynamic vent system (TVS). In this location, the pump-mixer can supply the energy to overcome flow resistance in the active TVS warm-side tubing as well as provide the desired level of mixing within the tank.

The determination of pump-mixer type (centrifugal, mixed-flow, or axial) and the definition of operational characteristics can be described by the specific speed parameter. The specific speed is defined as follows (ref. 5):

$$\text{specific speed} = \frac{(\text{rpm})(\text{gpm})^{0.5}}{[H]^{0.75}}$$

where

rpm pump rotational speed in revolutions per minute

gpm liquid hydrogen flow rate through the pump in gallons per minute

H pressure rise across the pump in feet of liquid

Two of the three terms on the right side of the specific speed equation have been determined. These terms are

(1) Two suitable pump-mixer flow rates (1.7 and 0.4 cfm) based on the results listed in section 4.2.4.3 and NASA TP-2107 (ref. 6)

(2) The estimation of pressure drop through the active TVS warm-side tubing at these two flow rates (1 and 0.06 psid for the high and low flow rates, respectively)

A maximum rotational speed of 4000 rpm was selected at the high pump-mixer flow rate in order to maintain both the pump suction pressure and electric motor speed requirements at reasonable values. Based on this value for rotational speed, the pump-mixer specific speed is calculated to be 1030. This value for specific speed indicates that a centrifugal pump is the best choice for the active TVS pump-mixer. Parameters for both high- and low-speed operation of the COLD-SAT pump-mixer design are shown in table 5.21.

This type of pump is discussed in reference 7. The impeller features a screw type of inducer at the inlet to provide operating capability at low net positive suction pressure.

5.2.4 ANALYSES

A number of analyses were performed in support of the design of the COLD-SAT experimental plumbing system. This section provides a summary of some of these.

5.2.4.1 Pressure Drop

The driving force for accomplishing liquid transfers between tanks is pressurized gas. Because of design consider-

TABLE 5.22.—SPRAY NOZZLES AND SPRAY PATTERNS

Tank	Spray application	Spraying systems part number	Number required	Flow rate (per nozzle of liquid hydrogen, lb/hr	Pressure drop, psid	Spray pattern	Spray angle, degree
Large receiver	Axial	3/8-G-SS-22	2	90	1.41	Full cone	90
Large receiver	Tangential	1/8-K-SS-1	4	5	↓	Flat fan	109
Small receiver	Radial	1/8-G-SS-1.5	12	7.5		Full cone	58
Small receiver	Axial	1/4-G-SS-10	1	50		Full cone	67
Small receiver	Tangential	1/8-K-SS-1	2	5		Flat fan	109

ations and system requirements, the available pressure head for conducting these liquid transfers may be very limited. Therefore, the pressure drop in the fluid system lines can have a significant impact on system performance and must be considered when arranging or selecting system components.

Pressure drop estimates have been made for the system layout as it is presently represented. The results of the pressure drop analyses have been used to further refine system design, including redundancy determinations, component specifications and selection, and system performance evaluations.

Table 5.22 lists the spray nozzles used in the experiment tanks. Table 5.23 presents the system pressure loss estimates for a liquid hydrogen transfer from the supply tank to the large receiver tank for the desired flow rate of 200 lb/hr. Estimates of pressure loss associated with each component, fitting, or tubing is presented along with the quantity of those items used or encountered in a typical transfer from the supply tank to the large receiver tank. The total pressure drop for the typical liquid hydrogen transfer is about 4 psi for the desired flow rate of 200 lb/hr.

The general equation for pressure drop is commonly known as the Darcy formula (ref. 4) and when expressed in feet of fluid is as follows:

$$h_1 = (f L/D) (v^2/2g) = K(v^2/2g)$$

where

h_1	loss of static pressure head caused by fluid flow, feet of liquid
f	friction factor
L/D	equivalent length of a flow resistance in pipe diameters
v	mean velocity of flow, ft/sec
g	acceleration of gravity, 32.2 ft/sec ²
K	resistance coefficient or velocity head loss

TABLE 5.23.—PRESSURE LOSS ESTIMATES FOR LIQUID HYDROGEN TRANSFER FROM SUPPLY TANK TO LARGE RECEIVER TANK

[Liquid hydrogen flow rate of 200 lb/hr.]

Item/component	Pressure drop (each), psi	Quantity	Total pressure drop, psi
Tee-through branch	0.110	4	0.44
Tee-through run	.037	6	.22
Moog valve (030)	.20	4	.80
Flowmeter	.23	1	.23
Standard bend	.056	8	.45
Supply tank LAD	.003	1	— — —
Spray nozzle	1.41	—	1.41
Tubing length	.022/ft	20 ft	.44
Total			3.99

While some pressure drop characteristics were supplied by vendors, the majority of the pressure drop estimates presented in table 5.23 were determined through use of the Darcy formula. Friction factors for various sized drawn tubing were obtained from Crane's "Flow of Fluids" handbook (ref. 4) to generate the family of curves for pressure losses of respective tubing sizes shown in figure 5.5. Representative values of L/D for various tube fittings were obtained to generate similar pressure loss curves. The pressure loss curves for the two valve designs used in the system (fig. 5.6) are based on information supplied by the manufacturer. The pressure drop characteristics for the spray nozzles using water as the fluid were obtained from the vendor and accordingly converted for use with liquid hydrogen as the fluid. If need be, the final system design will use a venturi for measuring flow during transfers because of its inherently lower pressure losses. The flowmeter pressure losses listed in table 5.23 were estimated for an orifice with a ratio of inside tube diameter-to-orifice diameter of 0.6.

5.2.4.2 Ground Venting (Worst Case)

The venting system has been designed to accommodate ground venting for the expected normal boiloff and also provides for emergency conditions. The 3/4-in.-diameter lines can

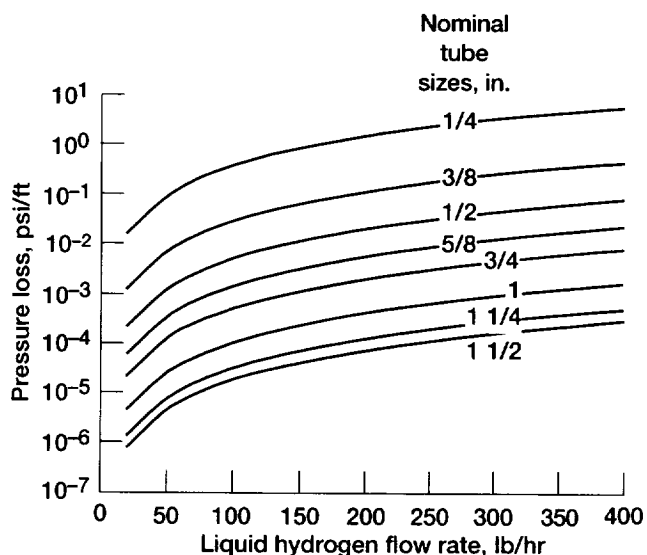


Figure 5.5.—Liquid hydrogen pressure drop estimates for tubing (tubing wall thickness, 0.028 in.).

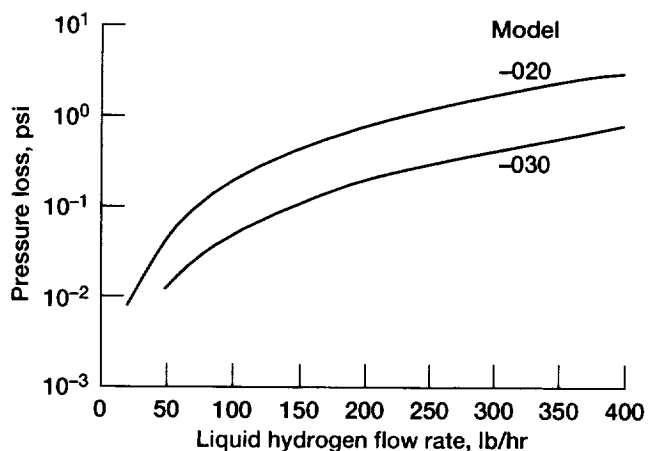


Figure 5.6.—Moog valve pressure drop estimates.

handle the expected normal boiloff venting on the ground, but 1 1/2-in. lines are needed to meet the requirements for emergency conditions. For a worst-case emergency condition, the scenario assumed was that of a rupture of the helium purge bag surrounding the MLI can in addition to a loss of power.

From the Van Gundy/Uglum report entitled "Heat Transfer to an Uninsulated Surface at 20 K" (ref. 8), indications are that the heat transfer to a bare tank containing liquid hydrogen could be as high as 5000 Btu/hr/ft². This extreme condition of high heat transfer can occur when frost does not accumulate, and liquid air continually runs down the tank wall.

For the heat transfer rate of 5000 Btu/hr/ft² to the supply-tank which has a surface area of 144 ft², and for a tank relief valve cracking pressure of 55 psia, the boiloff rate could be 4260 lb/hr. By using the Darcy formula and the Crane hand-

TABLE 5.24.—PRESSURE DROP DETERMINATIONS
FOR EMERGENCY VENT SYSTEM
[At 4260 lb/hr.]

System component	Pressure drop, psid
Relief valve	10.0
15 ft of 1.5-in. tubing	5.5
Four 90° bends	6.5
Enlargement (1.5- to 3-in. line)	2.3
Total	24.3

book (ref. 4) and a typical relief valve path, pressure drop throughout the emergency vent system was determined. A summary of the pressure drops through the emergency vent system is presented in table 5.24.

Therefore, with a cracking pressure of 55 psia for the tank relief valve, it can be seen that the required pressure at the interface where the 1 1/2-in. line transitions to the 3-in. Centaur vent line is 30.7 psia or less.

5.2.4.3 Pump-Mixer Flow Requirements

Information from NASA TP-2107 (ref. 6) was used as a guide for sizing the COLD-SAT pump-mixer. This report identifies four distinct low gravity tank mixing flow patterns based on drop tower test data that covered a range of flow conditions. These flow patterns are described in table 5.25.

Experimental results presented in NASA TP-2107 (ref. 6) indicate that flow patterns II and III are inefficient for tank bulk fluid mixing. Flow pattern I is considered to be the most efficient for mixing the bulk liquid, and flow pattern IV is effective for cooling the ullage and tank wall. Therefore, COLD-SAT mixing tests should concentrate on flow patterns I and IV.

Based on analyses presented in NASA TP-2107 (ref. 6), calculations were performed to determine the required mixer flow rates for investigating mixing patterns I and IV. The mixing flow pattern is shown to be a function of a nondimensional flow characterization parameter F . For turbulent liquid jets (Reynolds number > 1250), F is defined as follows:

$$F = \frac{0.5 + 1.6 We}{1 + 0.6 Bo}$$

where

We is the Weber number, a ratio of pressure or flow forces to surface tension forces, and is defined as

$$We = \frac{\rho v^2 Ro^2}{\sigma D}$$

TABLE 5.25.—LOW-GRAVITY TANK MIXING FLOW PATTERNS

Pattern	Description
I	Dissipation of liquid jet in bulk liquid region
II	Geyser formation
III	Collection of liquid jet in end of tank opposite jet outlet
IV	Liquid circulation over aft end of tank and down tank wall

where

Bo is the Bond number, the ratio of gravitational or acceleration forces to capillary or surface tension forces, and is defined as

$$Bo = \frac{a\rho R_j^2}{\sigma}$$

and where

- ρ liquid density
- v nozzle exit velocity
- Ro nozzle exit radius
- R_j liquid jet radius at liquid-vapor interface
- D liquid jet diameter at liquid-vapor interface
- σ surface tension
- a acceleration

The relationship between flow characterization parameter F and the observed flow pattern is shown in figure 5.7. For a given nozzle diameter, a flow rate can be selected to provide the desired mixing pattern. A value of 25 for the ratio of tank diameter to nozzle-jet-diameter was found to produce effective mixing. With the COLD-SAT supply tank diameter being 60 in., a jet nozzle diameter of 2.4 in. was established. Table 5.26 presents the results for the two selected flow rates (0.4 and 1.7 ft³/min) at three tank fill levels. These two flow rates will allow investigation of mixing regimes I and IV as

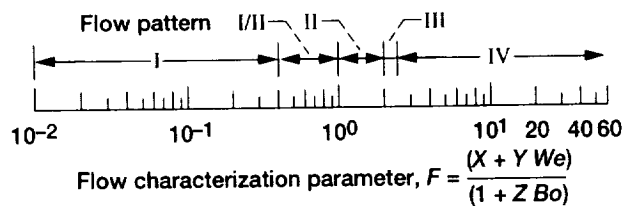


Figure 5.7.—Relationship between flow characterization parameter, F , and flow pattern. (See reference 6 for definitions of flow patterns and symbols.)

TABLE 5.26.—SUPPLY TANK MIXING PARAMETERS

Fill level, percent	50		65		90	
Flow rate, cfm	0.4	1.7	0.4	1.7	0.4	1.7
Weber number	0.8	15	0.5	10	0.34	6.4
Bond number	0.12		0.28		0.66	
F^a	0.7	21.8	0.3	13.2	0.03	7.0
Flow pattern	I/II	IV	I	IV	I	IV

^aFlow characterization parameter.

defined in NASA TP-2107 (ref. 6). The active TVS warm-side design flow rate is coincident with the high mixer flow rate.

The expected pressure drop through the active TVS warm-side heat exchanger and tubing was estimated. The calculated values for pressure drop are 1 and 0.06 psid for the high and low flow rates, respectively. The majority of the pressure drop occurs across the active TVS warm-side isolation valve. It should be noted that the calculated pressure drop, the required pump power, and the heat input from pump-mixer operation significantly decreases if the isolation valve is eliminated. This valveless arrangement is possible with an internal pump-mixer configuration. An external placement of the pump-mixer was made necessary, however, by the requirement that all active components be outside the tanks for easy access.

5.3 Liquid Hydrogen Supply Tank Module

5.3.1 DESCRIPTION AND CHARACTERISTICS

This section describes the design of the supply tank module and discusses some of the requirements which drove that design. Following is a list of the principal experiment requirements which controlled the design of the supply tank module:

(1) Pressure control:

- Thermal performance < 0.1 Btu/hr-ft
- Uniform heat flux levels of 0.1, 0.3, and 0.6 Btu/hr-ft for 5 psi rise
- Passive TVS capable of controlling 0.1 Btu/hr-ft
- Active TVS capable of controlling all applied heat fluxes

- Mixer with two speeds, nozzle 1/20 to 1/60 of tank diameter
- (2) Pressurization:
 - Straight pipe diffuser
 - (3) No-vent fill:
 - Sufficient liquid hydrogen to perform a minimum of two fills of each of two receiver tanks
 - Liquid acquisition device for supply tank
 - (4) Thermodynamic state:
 - Subcooler to provide 5 °R cooling at 50-lb/hr flow rate

In addition to the experiment requirements, the following design requirements were added to limit the cost and complexity of the module:

- (1) Design the supply tank to the ASME boiler code (ref. 3) to limit the analysis and testing required
- (2) Allow “easy” access to active components, in particular the valves mounted on tank domes
- (3) Use a modular concept to allow for assembly and checkout of modules prior to integration with other modular components of the spacecraft

The supply tank module (fig. D.3 in appendix D to this chapter) consists of the following components:

- (1) Liquid hydrogen supply tank that supplies hydrogen to other experiment system components
- (2) Multilayer insulation (MLI) assembly to shield the supply tank from radiation losses and provide a more uniform heat flux to the tank
- (3) Helium purge system for ground purging of the external tank surface and MLI
- (4) Radiator tray to support plumbing and wiring harnesses and to allow them to radiate heat prior to penetrating the tank insulation systems
- (5) Redundant gaseous hydrogen systems for vaporizing liquid hydrogen that will be used in pressurization experiments (two bottles, two valve panels)

- (6) Helium pressurization system for pressurizing the supply tank and receiver tanks
- (7) Vent panel for balanced TVS and relief venting
- (8) Ground interface panel for supply tank fill/drain and helium purge operation
- (9) Ground/ascent vent interface with the Centaur vent system

On-orbit, the spacecraft attitude will be controlled so that the same side of the spacecraft is always facing the Sun. Consequently, one side is always warmer relative to the other. In all drawings the “cold side” is designated as a positive z coordinate while the “hot side” is designated by a negative z coordinate. Certain components such as the radiator tray and ground interface panel will be located on the cold side of the spacecraft to allow plumbing, wiring harnesses, and disconnects to radiate to space. On the other hand, such components as the vent panel, vaporizer valve panels, and vaporizer bottles are located on the spacecraft hot side to take advantage of warmer temperatures and higher heat fluxes. In addition, components such as the ground interface, helium valve panel, vaporizer valve panel, and vent panels are located to allow access when solar arrays are in place during ground operations.

5.3.1.1 Supply Tank Assembly

The supply tank (fig. D.3(c) in appendix D to this chapter) is designed to provide liquid hydrogen for all COLD-SAT experiments. The 5083 aluminum pressure vessel is cylindrical in shape with 1.41:1 elliptical domes and has a volume of 144 ft³. When filled to the 92-percent fill level, the tank will contain 565 lb of liquid hydrogen at 20 psia saturated condition. The tank has a surface area of 143 ft². The 0.080 in. (minimum) thick shell is reinforced by two girth rings located fore and aft on the cylindrical section of the tank.

The tank is supported off the spacecraft structure by 16 fiberglass struts, 8 fore and 8 aft, which attach to the girth rings and are evenly spaced around the circumference of the tank for structural and thermal symmetry. The tank contains instrumentation racks for monitoring temperatures and determining fluid levels and a liquid acquisition device (LAD) for collecting fluid in the low-acceleration environment of space. Electrical harnesses for the instrumentation are routed through six electrical feedthroughs located in the aft dome. This location was chosen because of limited space between the MLI can and tank cylinder and for ease of tank assembly.

In an effort to minimize the need for access, no active plumbing components are located inside the tank. Instead, valves are mounted on six valve panels which are mounted on the outside of the tank, four on the forward dome and two on the aft dome. Five plumbing lines penetrate the aft dome while

three more lines penetrate the forward dome. In addition, strip and patch heaters are attached to provide the required experiment heat fluxes.

The supply tank is enclosed by a cylindrical honeycomb structure with truncated cone ends, the MLI can. The purpose of the MLI can is to support the multilayer insulation (MLI), thermally isolate the MLI from the pressure vessel, spread out heat gain for better uniformity, and act as a heat sink for penetrations. The MLI can is assembled in sections to allow easy access to plumbing components underneath. The can is supported by the same struts that support the tank. Two 1/2-in. blankets of MLI cover the MLI can. The blankets are held in place by hook-and-loop (e.g., Velcro) fasteners and nylon pins. External to the MLI layers is the purge bag which contains the gaseous helium used to purge the tank exterior and MLI during ground loading operations. Ascent vent doors are located near the fore and aft domes.

5.3.1.1.1 Thermal Design.—A key element in the success of the mission will be the thermal performance of the supply tank assembly. In an effort to minimize heat leaks to the supply tank, stainless steel plumbing will be used because of its lower conductivity relative to that of aluminum. In addition, plumbing and wiring lengths inside the multilayer insulation have been maximized (average length = 96 in.) to reduce heat conduction to the tank. The length is achieved by having all plumbing and wiring harnesses penetrate the MLI can at or near the tank equator and then run along the tank wall to the appropriate dome. The only exception to this is the 1.5-in. diameter ground ascent vent line. Because of the limited space (approximately 1/2 in.) between the supply tank girth rings and the MLI, this line penetrates at the seam between the truncated cone and cylinder of the MLI can. It then runs around the circumference of the tank to achieve some thermal length before attaching to a valve panel. Plumbing and wiring are attached to the tank wall with fiberglass fairleads to limit conduction. To improve the uniformity of heat gain to the tank, each dome-mounted valve panel has six legs and each leg has 6 in.² of contact area.

Struts are made of low thermal conductance S-2 glass-epoxy with stainless steel end fittings. The struts, as well as all plumbing and wiring, are thermally grounded to the can supporting the multilayer insulation. This reduces the heat conducted directly to the supply tank and, since the can is made of highly conductive aluminum, it provides a more uniform radiative heat transfer to the tank.

5.3.1.1.2 Valve Panel Design.—To limit the need for accessing the inside of the supply tank, all active components are located outside of the tank. Valves, pumps, and plumbed instrumentation other than resistance temperature detectors (RTD's) and level sensors are grouped and attached to panels which are then attached directly to the tank domes as shown in figure 5.8. This method allows the panels to be assembled and checked out prior to installation.

Four panels are mounted to the forward dome and two to the aft dome. Panels are made of 5083 aluminum, and each is attached to the dome by six support legs which not only support but also spread out the heat conducted to the tank from the wiring and plumbing. Support legs are welded to the dome surface, and panels are mechanically fastened to the legs.

Figures D.4(a) and D.5(a) in appendix D to this chapter show the panel layout on the forward and aft domes. Panels E and F, shown in figure D.4(b) and (c), will be mounted to the aft dome while panels G, H, I, and J (fig. D.5) will be mounted to the forward dome. Table E.4 in appendix E to this chapter lists the instrumentation and valves for each panel.

Because the plumbing schematic was not finalized at the time these valve panels were laid out, there may be some differences between the panel and the corresponding portion of the schematic. However, the panels presented are still considered to be a good representation of the approximate size and location of panels and their components. Fairleads attach the plumbing and wire harnesses to the tank wall rather than to the MLI can. This method for supporting the wiring and plumbing was chosen to simplify the assembly and disassembly of the can sections.

5.3.1.1.3 Strut Design.—Sixteen struts support the supply tank, MLI can, MLI, and purge bag. Eight struts attach at each of the fore and aft girth rings. The struts are evenly spaced (fig. D.6 in appendix D to this chapter) around the circumference to provide structural and thermal symmetry to the supply tank. Struts are made of filament-wound, S-2 glass epoxy with stainless steel ends for reduced thermal conductivity between the spacecraft structure and the tank.

The struts are connected to the tank and spacecraft structure by spherical rod ends which allow the struts to pivot. Each strut is initially aligned at right angle to a line that contains both the geometric center of the supply tank and the strut attachment point at the girth ring. As the tank contracts during chilldown, the attachment point moves toward the center of the tank. This arrangement allows the strut to pivot slightly and minimizes elongation of the strut which, in turn, minimizes the bending and axial stress induced in the strut. The stress induced will be a tensile stress which is preferable to a compressive stress since the strut material is considerably stronger in tension than in compression.

The multilayer insulation, MLI can, and purge bag assembly are also supported off the struts. A sleeve of aluminum is mechanically fastened to the MLI can at one end. The other end of the sleeve is clamped at approximately the mid-span of the strut. This design is intended to shunt some of the heat transmitted through the strut from the spacecraft structure into the MLI can rather than into the supply tank.

5.3.1.1.4 Heater Design.—Heaters are required to provide the desired heat fluxes for the pressure control experiments. Thin flexible heaters consisting of etched, metal foil, resistive elements laminated between layers of Kapton insulation will be

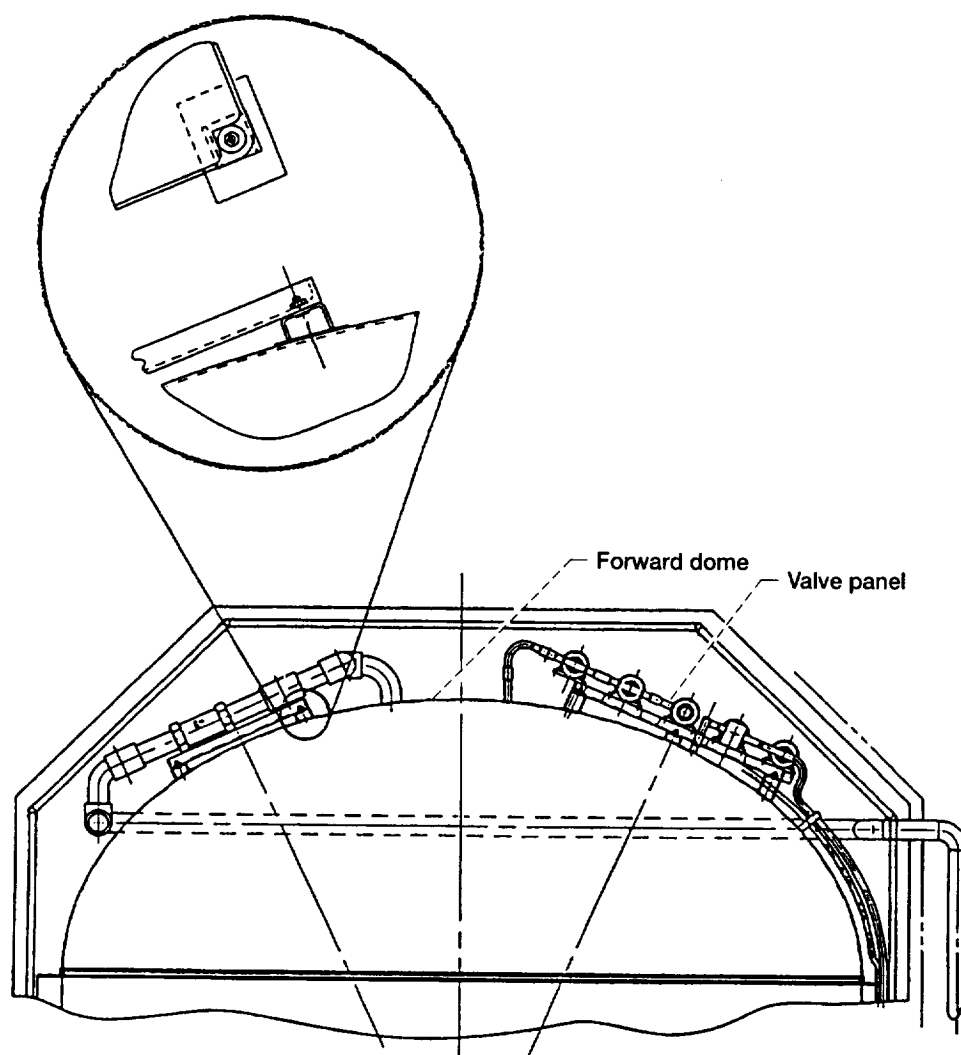


Figure 5.8.—Valve panel design.

applied to the tank with an adhesive such as American Cyanamide HT-424. Strips of heaters (fig. D.7 in appendix D to this chapter) will be attached to the cylindrical portion of the tank with patch heaters (fig. D.4(a)) applied to the domes. These Thermofoil heaters, currently used on the space shuttle, are thin (0.01 in.) and very lightweight (0.081 lb/ft²). It was determined to be more efficient to place the heaters directly on the tank rather than to heat up the MLI can to provide the experimental heat fluxes needed for the experiments.

5.3.1.1.5 Liquid Acquisition Device (LAD).—In the low acceleration environment of space, the location of bulk fluid in a tank with respect to the outlet cannot be predicted. Therefore, a liquid acquisition device (LAD) is needed in the supply tank to acquire vapor-free liquid hydrogen for transfer to other experiment components.

The ability of screen-covered channels to function as LAD's is based on their ability to remain filled even when not completely submerged in the bulk fluid of the tank. Once the

channel is exposed to the ullage, a liquid-vapor interface is established at the screen due to surface tension. This interface resists the passage of vapor into the channel. The strength of the interface is defined by the bubble point which is characterized by the liquid surface tension and the screen pore size. When the pressure difference across the LAD exceeds the bubble point, the liquid-vapor interface breaks down allowing vapor to pass into the LAD which generally terminates liquid acquisition.

Liquid Acquisition Device/Thermodynamic Vent System (LAD/TVS)

The LAD shown in figure D.8 in appendix D to this chapter is a state-of-the-art, integrated LAD/TVS design which incorporates the functions of the LAD with those of the active and passive TVS and subcooler heat exchangers. An additional function is to condense bubbles in the LAD. The all-aluminum supply tank LAD has four legs or channels which are joined at

the fore and aft domes by manifolds. Aluminum was chosen over stainless steel to limit the LAD weight and to minimize the stresses induced by differential thermal contraction between the LAD and the aluminum tank.

A cross section of the LAD channel is shown in figure 5.9(b). Each channel consists of three concentric tubes welded together to form the heat exchanger as well as the back wall of the flow channel. Flat plates are welded to the tubes to form the sidewalls of the channel, and screen-covered perforated plate makes up the remaining side of the channel.

To maintain dependable performance under all COLD-SAT conditions, a high bubble-point pressure is required. To this end, a fine screen of aluminum 200 by 1400 Dutch twill configuration was selected. Although not a standard item, the Dutch twill screen can be made from nearly any material including aluminum.

As shown in figure D.8, the LAD is supported in the supply tank by two circumferential structural channels which are attached to the barrel section of the tank. The LAD is also supported by four brackets which attach it to the aft dome.

LAD Schematic

Figure 5.9(a) shows schematically how the integrated LAD/TVS functions. Liquid hydrogen flows through the fine mesh screen and toward manifolds in the fore and aft domes of the supply tank. Liquid hydrogen from the forward manifold is expanded by using J-T devices. The cooled fluid is then used in a counterflow, concentric tube heat exchanger to cool the transfer fluid flowing from the aft manifold to the forward manifold. A cross section of one of the LAD legs (fig. 5.9(b)) shows the concentric tube arrangement with the TVS fluid flowing through the annulus and the relatively warm transfer fluid flowing through the small tube. The TVS fluid exits the tank at the aft manifold.

Forward LAD Manifold and Tank Penetrations

The forward manifold (fig. 5.10) consists of three concentric manifolds. Fluid is drawn off the middle manifold and circulated through the Joule-Thompson device. The cooled fluid

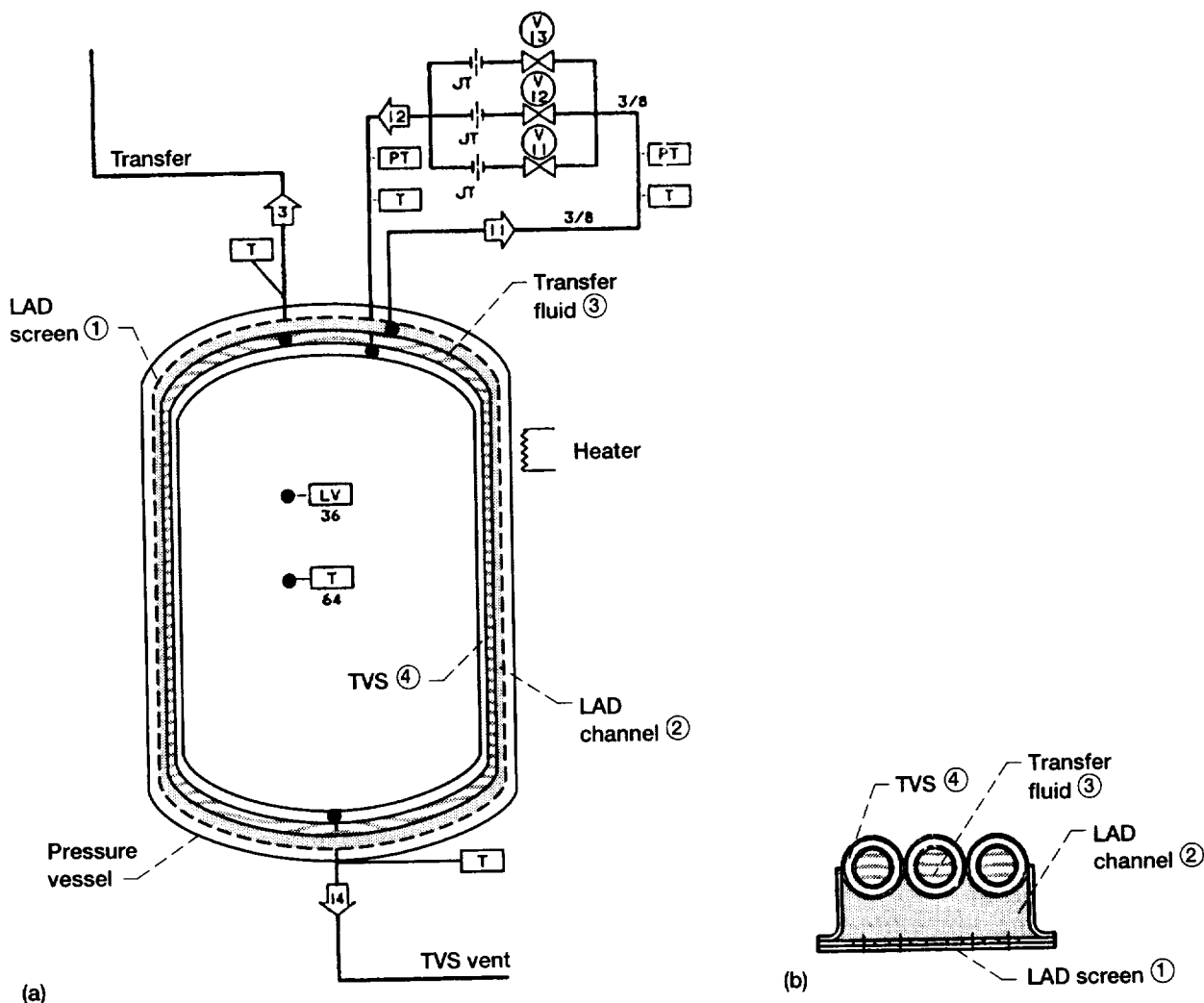


Figure 5.9.—Supply tank liquid acquisition device (LAD). (a) Interconnection schematic. (b) LAD cross section.

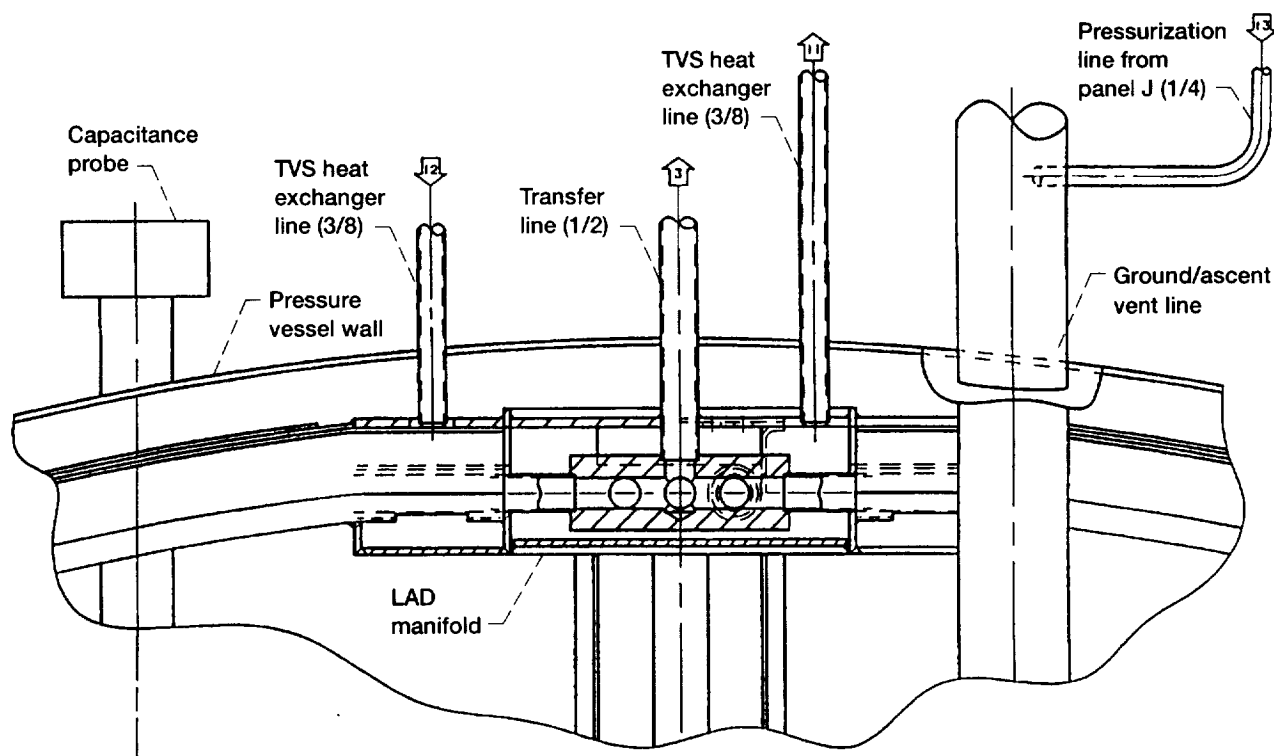


Figure 5.10.—Supply tank forward dome—LAD manifold plumbing penetration. Tube dimensions are in inches.

flows back into the outer manifold to be used in the heat exchange with the transfer fluid. The inner portion of the manifold collects the transfer fluid from each LAD leg before it is transferred out of the tank.

The following are forward dome penetrations:

- (1) The 3/8-in.-o.d. TVS heat exchanger lines penetrate the dome and attach to the LAD manifold.
- (2) The 1/2-in. transfer line penetrates the dome and enters the manifold.
- (3) The 1 1/2-in. ground/ascent vent line penetrates the tank wall and extends down to the 92-percent fill level of the tank.
- (4) A capacitance probe for measuring the liquid hydrogen level is also shown penetrating the wall and extending to the 85-percent level.

Aft LAD Manifold and Tank Penetrations

The aft manifold (fig. 5.11) consists of an inner and outer manifold. The inner manifold collects the fluid from the LAD channel and distributes it among the 1/2-in. tubes in the LAD legs where the heat exchange with the cooled TVS fluid takes

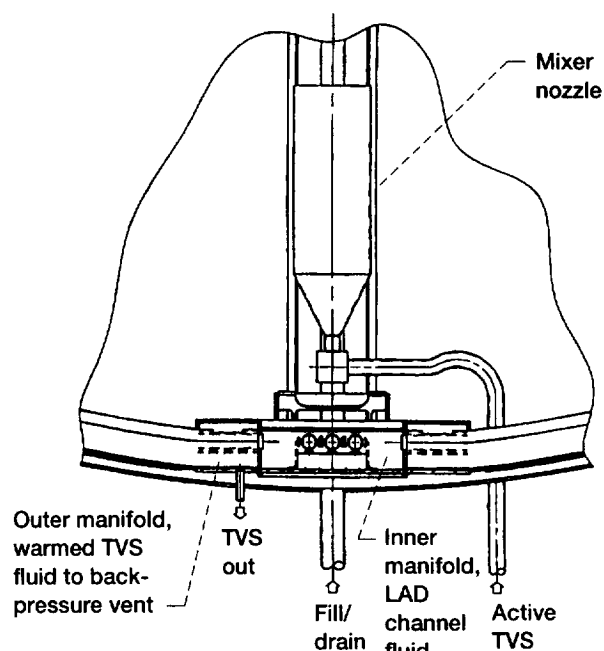


Figure 5.11.—Supply tank aft dome/LAD manifold plumbing penetrations.

place. The outer manifold collects the TVS fluid as it exits the heat exchanger and before it passes to the TVS vent.

The following are aft dome penetrations:

- (1) The 1/4-in. TVS vent line penetrates the dome and attaches to the outer manifold.
- (2) The 3/4-in. ground fill/drain line penetrates the dome and is nearly flush with the inside surface of the tank wall.
- (3) The 1/2-in. active TVS line penetrates the dome and attaches to the forward side of the manifold where it transitions to a 2.5-in.-diameter mixer nozzle.

LAD Instrumentation Rakes

The supply tank LAD has 46 temperature sensors and 33 liquid-vapor sensors. As illustrated in figure 5.12, most sensors are attached to instrumentation rakes which consist of 1-in. square structural aluminum tubing, which is mechanically attached at the top and bottom to the LAD channel. The sensors are attached to the tip of stainless steel cones which tend to wick the liquid away from the sensor and improve the accuracy of measurements. Some sensors are also mounted on rakes attached to the tank wall to take measurements at various levels close to the wall.

5.3.1.1.6 Fabrication and Assembly Sequence.—The supply tank fabrication and assembly sequence is illustrated in figure 5.13. The cylindrical section of the tank will be fabricated complete with girth rings, strut attachment brackets, LAD mounting brackets and plumbing and wiring fairleads welded in place. The fore and aft domes will be spun and machined to provide a uniform thickness and smooth finish on both the inside and outside surfaces. Valve panel mounting legs and plumbing and wiring fairleads will be welded in place. The aft dome will also include four LAD mounting brackets and six electrical feedthroughs for the instrumentation wiring. Domes will be welded to the cylinder using a butt weld and backing plate. The tank is designed with no moving parts inside to limit the need to gain access to the tank internals. However, should it ever become necessary to open the tank, the weld can be cut, the backing plate replaced, and the dome rewelded to the cylinder.

The LAD will be fabricated and assembled complete with fore and aft manifolds and instrumentation rakes and sensors. The LAD assembly will be attached to the aft dome by four mounting brackets, one for each leg. The tank cylinder will be welded to the aft dome using a backing ring and butt weld. The LAD support channels are then mechanically fastened to the LAD mounting brackets. At this point the LAD instrumentation will be checked out before welding the forward dome in place.

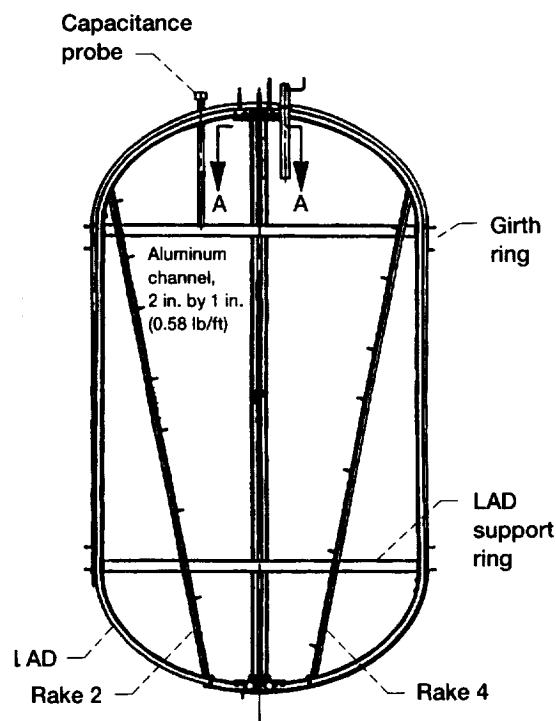
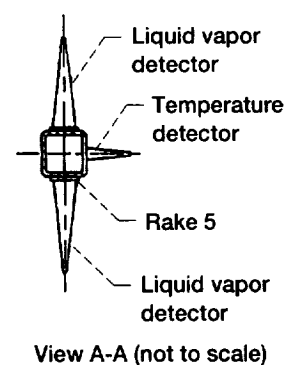


Figure 5.12.—Supply tank LAD—Illustration of instrumentation rakes.

5.3.1.2 Purge Bag and MLI Blanket Configuration

The purge bag for helium-purging the supply tank insulation is similar to the one designed for shuttle/Centaur (fig. 5.14). The purge bag is outside the MLI and consists of two Kevlar-cloth reinforced shields separated by an embossed Kapton shield. The outer shield has a layer of silverized Teflon. The high-strength reinforced shields are required to withstand a purge system design pressure of 0.5 psid. These shields are actually laminates with the high-strength Kevlar cloth sandwiched between two layers of Kapton. All shield surfaces have a vacuum-deposited layer of aluminum applied to achieve emittances of 0.05 or less.

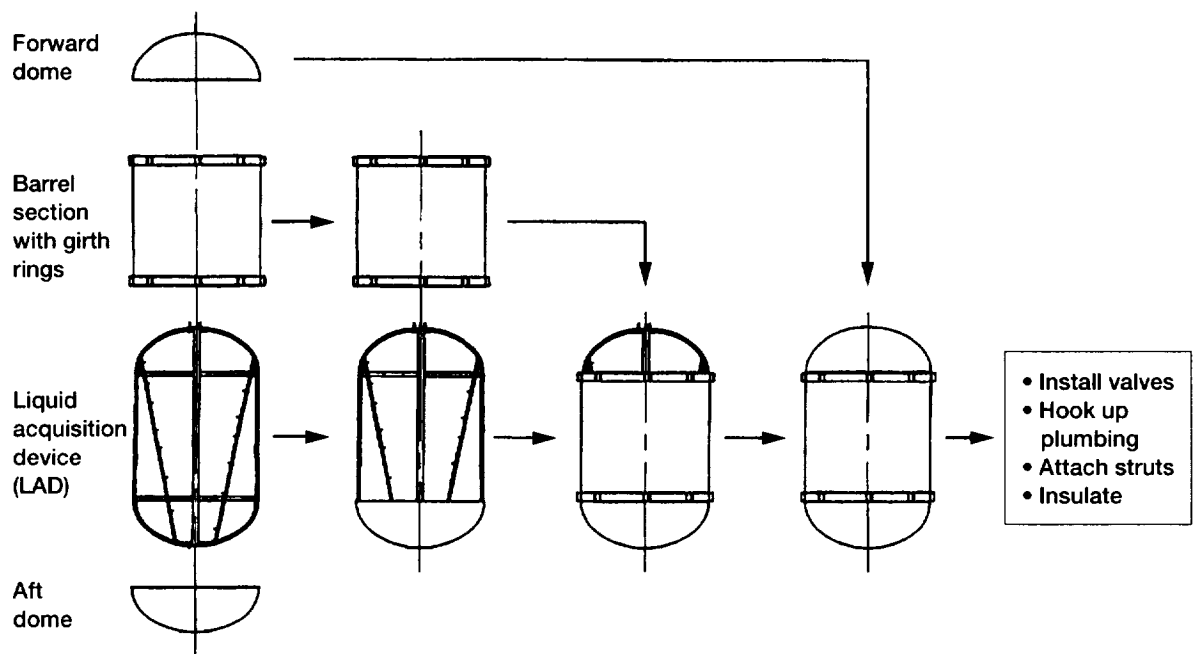


Figure 5.13.—Supply tank assembly sequence.

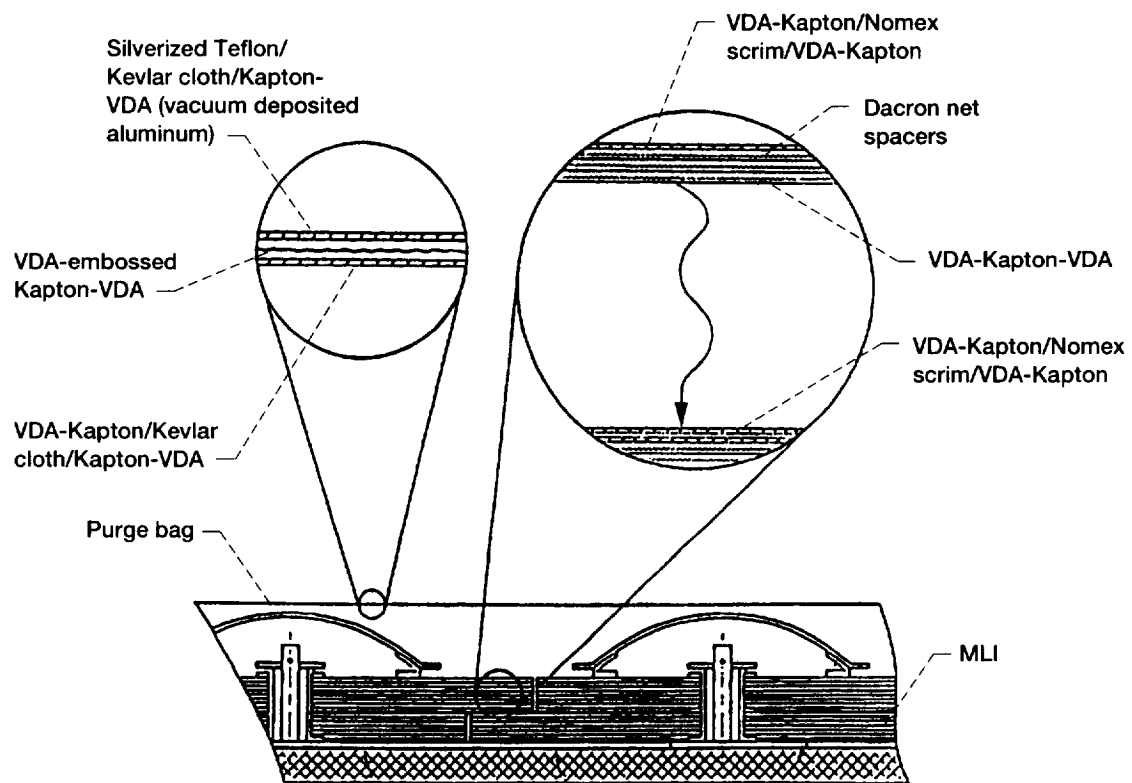


Figure 5.14.—Purge bag and multilayer insulation (MLI) configuration.

The multilayer insulation (MLI) for the supply tank consists of two blankets each approximately 1/2 in. in thickness. Each blanket has 40 layers.

5.3.1.2.1 Multilayer Insulation Assembly.—Figure 5.15 shows a cross section of the tank and MLI assembly.

MLI Can: The MLI can supports the multilayer insulation (MLI) and purge bag system and helps to provide uniform radiative heat gain to the supply tank. The can (fig. D.9 in appendix D to this chapter) consists of a 3/8-in. 5056 aluminum honeycomb core bonded to 0.020 in. 2024 aluminum facesheets with an epoxy-polyamide resin. The honeycomb cell size is 1/4 in. and the foil thickness is 0.001 in. The can is configured to facilitate its removal as needed to gain access to valve panels during installation and check out operations. The MLI can is made up of cylindrical and truncated cone sections which are mechanically fastened together. The simple geometry (no doubly curved surfaces) will allow MLI blankets to be made of flat patterns (no gore sections). The MLI can is supported by sleeves attached to the supply tank struts and designed to distribute the load of the can, MLI, and purge bag over the strut. The sleeve also thermally grounds the struts to the MLI can to shunt heat into the can instead of into the supply tank.

The MLI can has two vent doors (fig. D.9) located fore and aft on the cold side (positive z) of the spacecraft to limit radiation losses through these openings. The doors are spring-loaded closed and held open at launch by pyrotechnic pin

pullers. These doors, in conjunction with vent doors in the purge bag (see section 5.3.1.2.2), allow the helium from the ground purge to vent during ascent thus equalizing the pressures that are internal and external to the can. Approximately 14 hr after launch, the doors, which are covered with blankets of MLI, will be closed to reduce radiation losses. Door stops will keep the doors from closing completely to allow a gap for residual helium to migrate out.

Multilayer Insulation: The MLI for the supply tank, shown in figure 5.14, consists of two blankets, each approximately 1/2 in. thick. Each blanket has 40 layers. The outer and innermost layers consist of a laminate of Nomex scrim sandwiched between two layers of Kapton. This material was selected for its low weight and rip-resistant features. The other layers are Kapton with vacuum-deposited aluminum on both surfaces. The layers are separated by Dacron net spacers.

Figure D.10 in appendix D to this chapter shows the MLI can covered with multilayer insulation. The blankets overlap at all seam locations and are held in place by nylon positioning pins and grommets. Five-layer MLI blanket patches are also used to cover the positioning pins and seams. In addition to pins and grommets, hook-and-loop fasteners are used between the MLI can and blankets and to hold seams together. The MLI is electrically grounded to the spacecraft.

MLI Venting: The purge bag ascent vent doors will remain open throughout the mission to allow residual helium from the

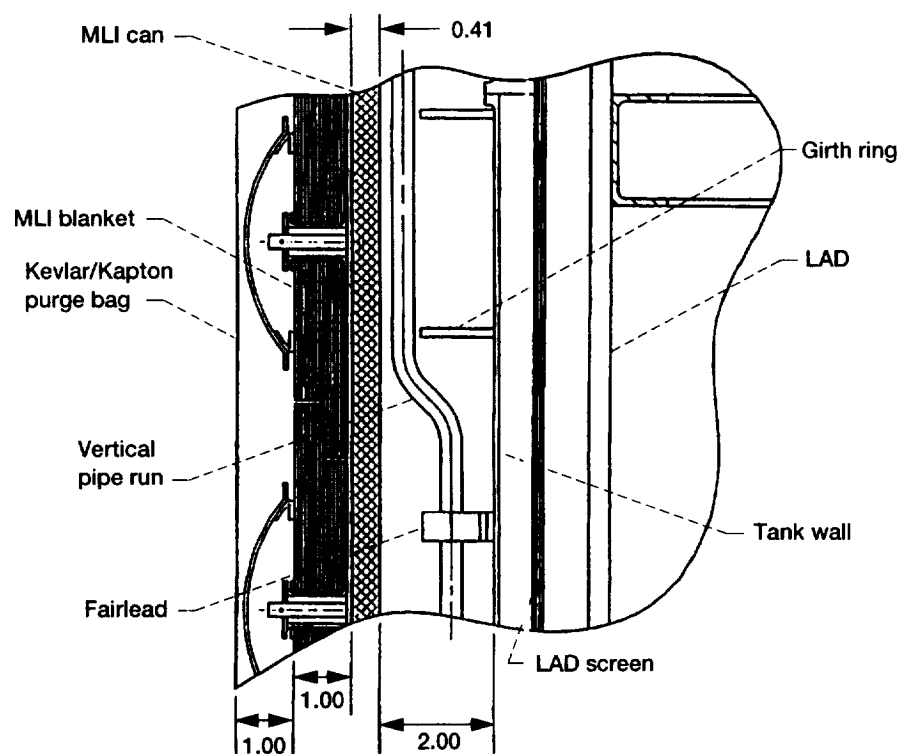


Figure 5.15.—Cross section of liquid acquisition device (LAD), supply tank wall, multilayer insulation (MLI) can, and insulation system. Dimensions are in inches.

purge system to vent to space. Trapped helium will be able to vent from the MLI layers continuously through the 105 ft of MLI seams. The maximum distance a molecule of trapped helium will have to travel to find a seam is 2.1 ft. Although the vent doors in the MLI can close at T + 14 hr, a door stop will prevent the vent doors from closing completely. This will allow helium trapped inside the MLI can to vent continuously as well.

Thermal Design: The following design features were included to improve thermal performance and limit MLI degradation:

- (1) The simple geometry of the MLI and MLI can helps to minimize the seam length and facilitate the overlapping of blankets at all seams.
- (2) The good thermal conductivity of aluminum will improve the uniformity of radiative heat gain from the MLI can to the supply tank and plumbing.
- (3) All plumbing and wiring penetrations and vent doors are located on the cold side of the spacecraft to limit radiation losses.
- (4) MLI blankets will be held in place by fastening pins and grommets made of nylon to limit the heat conduction through the blankets to the MLI can.
- (5) All MLI fastening pins will be covered with a five-layer MLI patch to limit the blanket degradation resulting from these penetrations.
- (6) Vent doors in the purge bag and MLI can are clocked 90° from each other to eliminate a direct view of the tank and valve panels.

5.3.1.2.2 Purge and Ascent Venting System

Purge Bag Functional Requirements

The volume between the purge bag and the supply tank will be purged with helium prior to filling the tank with liquid hydrogen. This prevents the condensation of payload-fairing nitrogen purge gas on the tank and related components. The volume to be purged is approximately 72 ft³. A positive purge pressure will be maintained during prelaunch activities to prevent ingress of payload-fairing atmosphere. During ascent, the purge bag, MLI, and MLI can will be vented to allow the helium to escape. Once vented, doors in the MLI can will close on-orbit to reduce radiative losses.

Purge System

The helium purge system is similar to the one designed for shuttle/Centaur. As shown in figure D.11 in appendix D to this chapter, it consists of a purge bag, two relief valves, and two ascent vent doors. The purge bag is outside the MLI and consists of two Kevlar-cloth reinforced shields separated by an embossed Kapton shield. The outer shield has a layer of silverized Teflon. The high-strength reinforced shields are

required to withstand a purge system design pressure of 0.5 psid. These shields are actually laminates with the high-strength Kevlar cloth sandwiched between two layers of Kapton. All shield surfaces have a vacuum-deposited layer of aluminum applied to achieve emittances of 0.05 or less.

Sections of the bag are sewn and taped to minimize leakage. The assembled pieces are fastened to two support rings of 0.030-in. fiberglass by aluminum retaining rings. The retaining rings allow the fore and aft dome portions of the bag to be easily removed should access to the MLI, MLI can, and valve panels be required. Fiberglass brackets attach the support rings to the cylindrical portion of the MLI can. The relief valves (fig. D.12) are mounted to the aft support ring (ref. 9).

The valve in figure D.12 is shown in the static (closed) condition. As the pressure in the liquid hydrogen insulation blanket increases, so does the pressure behind the main poppet bellows assembly (via the control orifice) and against the sensing diaphragm. When the differential across the sensing diaphragm reaches cracking pressure (with reference to ambient pressure), the pilot poppet opens, relieves pressure behind the main poppet bellows assembly, and the main poppet opens. Valve operation, when open, is controlled by orifices in the sensing port which allow the valve to maintain a steady open differential pressure.

Gaseous helium will be introduced near the top or forward end of the purge bag for ground purging. A positive pressure of between 0.1 and 0.3 psid will be maintained. Burst pressure of the purge bag is estimated to be 0.5 psid.

Ascent/On-Orbit Vent Doors

The purge bag has two ascent vent doors (fig. D.13 in appendix D to this chapter) which are offset from the doors in the MLI can to reduce radiation losses. The ascent vent doors are supported off the fiberglass support ring and are spring-loaded open. They will be held closed during ground purging operations by the same type of pyrotechnic pin pullers used on the MLI can vent doors. Seconds after liftoff, the pin pullers will be activated and the door will open for helium ascent venting. Each door is sized for the full flow of the venting helium in case either pin puller should fail. Once open, the doors remain open for the duration of the flight which allows continuous venting and outgassing of the MLI.

5.3.1.3 Radiator Tray

The radiator tray (figs. 5.16 to 5.18 and D.14 and D.15 (in appendix D to this chapter)) is located just outside the spacecraft structure on the cold side until it approaches the electronics bay where it runs inside the spacecraft structure on its way to the receiver tanks. The lightweight aluminum tray contains the plumbing and wiring harnesses with sufficient space for the contraction-expansion bends. Its purpose is to allow the plumbing and harnesses to radiate to space before they penetrate the

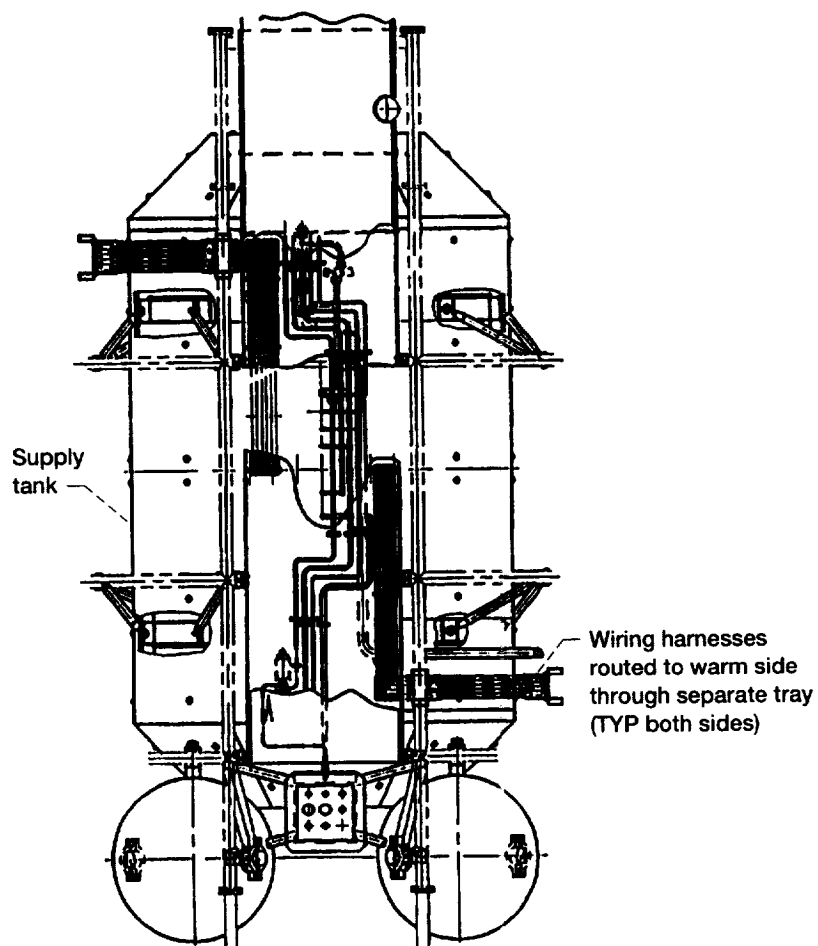


Figure 5.16.—Supply tank radiator tray.

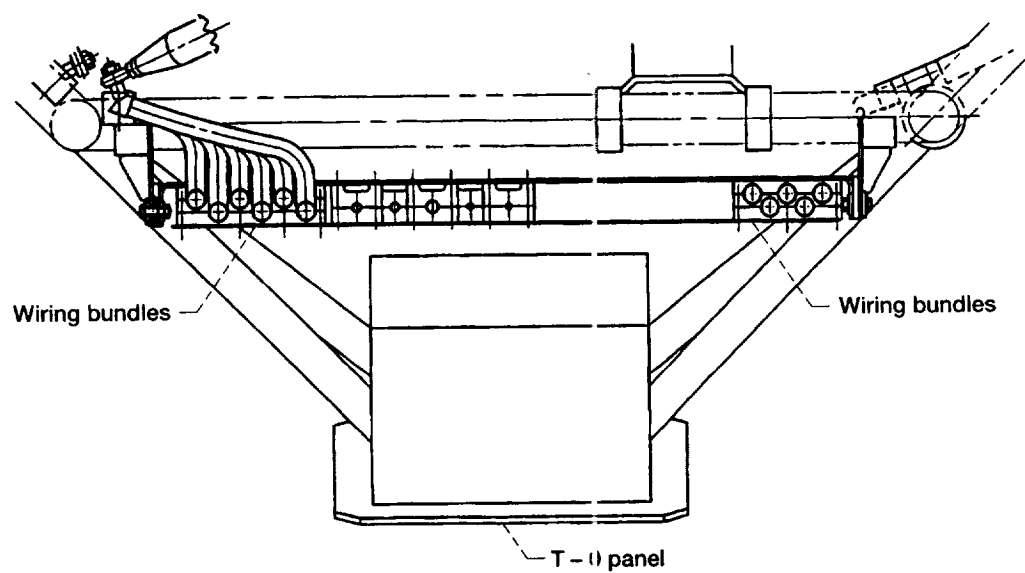


Figure 5.17.—Top view of radiator tray (cold side of spacecraft).

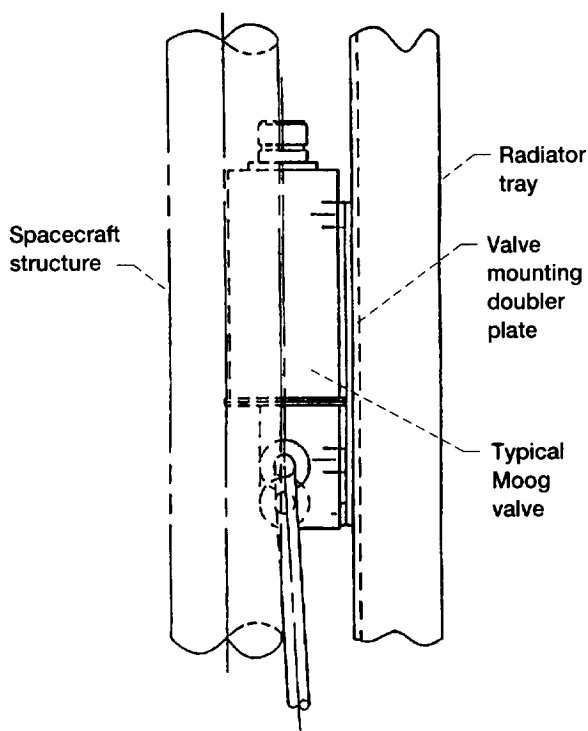


Figure 5.18.—Radiator tray mounted valve.

MLI and tank surfaces. The radiating surface (positive z side of tray) consists of a thin plate of aluminum covered with a highly emissive coating. Six support brackets (of 6061-T6 aluminum to match the spacecraft structure) are welded to cross members of the spacecraft structure. The tray is attached to the brackets with stainless steel bolts and G-10 fiberglass spacers to thermally isolate the tray from the spacecraft.

Fairleads secure the plumbing and harnesses to the tray. The portion of fairlead attached to the bottom or inboard side of the tray will be made of fiberglass while the portion of fairlead attached to the radiating surface will be made of aluminum. This allows the heat from plumbing and harnesses to be conducted directly to the radiating surface.

Table E.5 in appendix E to this chapter lists the valves and instrumentation to be mounted on the negative z face of the radiator tray within the supply tank module.

5.3.1.4 Helium Pressurization System

Two spherical helium-filled bottles (fig. D.16 in appendix D to this chapter) are provided for pressurant storage. The 8000-in.³ bottles are located on the cold side (positive z) of the spacecraft below the supply tank. The composite over-wrapped, (Kevlar/cryoform 301) load-sharing bottles were designed for Atlas/Centaur. Four struts of aluminum structural tubing support each bottle off the spacecraft structure. The struts attach to support posts built into either side of the bottles.

The associated valve panel (fig. D.17) is located on the positive y side of the spacecraft. It is positioned low enough in the module to allow access through a door in the spacecraft shroud without interference from the solar panels. Because the plumbing schematic was not finalized at the time these valve panels were laid out, there may be some differences between the panel and the corresponding portion of the schematic. However, the panel illustrations are still considered to be a good representation of the approximate size and location of panels and their components.

5.3.1.5 Vent Panel

The purpose of the vent panel, valve panel O (fig. D.18 in appendix D to this chapter) is to provide balanced TVS and relief venting. The panel is located on the hot side of the spacecraft to take advantage of warmer temperatures and higher heat fluxes and thus prevent freezing. In addition, strip heaters are wrapped around the plumbing. The panel is located between the solar arrays to allow access during ground operations. Because the plumbing schematic was not finalized at the time these valve panels were laid out, there may be some differences between the panel and the corresponding portion of the schematic. However, the panels presented are still considered to be a good representation of the approximate size and location of panels and their components. A list of panel components is given in table E.6 in appendix E to this chapter.

5.3.2 ANALYSES

5.3.2.1 Structural

The preliminary structural analysis of the liquid hydrogen supply tank includes the material selection and sizing of the tank wall, girth rings, supporting struts, and other primary structural members. Additional information on the structural analysis can be found in the appendices to this chapter.

5.3.2.1.1 Supply Tank Pressure Vessel.—The supply tank is designed in accordance with ESMCR 127-1 (ref. 10), MIL STD 1522a, and the ASME Boiler and Pressure Vessel Code Section VIII, Division I (ref. 3). The design philosophy was to meet the boiler code requirements for ground operations in order to limit the amount of analysis and testing required. Aluminum 5083-0 was selected from Part ULT, "Alternative Rules for Pressure Vessels Constructed of Materials Having Higher Allowable Stresses at Low Temperature," of the boiler code (ref. 3). Aluminum 5083 has good strength properties in the as-welded condition and has excellent ratings for weldability, formability, machinability, and hydrogen embrittlement. From Part ULT, the maximum allowable stress for temperatures not exceeding -320°F is 13.4 kpsi.

Maximum ground operating pressure will be limited to 49 psia (34.3 psid) with a relief valve setting of 52 psia

TABLE 5.27.—SUPPLY TANK PRESSURE VESSEL DESIGN CHARACTERISTICS

Temperature	Maximum operating pressure, psia	Relief pressure, psia	Proof pressure, psia	Burst pressure, psia	Factor of safety at maximum operating pressure		Factor of safety at relief pressure	
					Ultimate	Yield	Ultimate	Yield
Cryogenic								
On ground	49	52	82	201	5.4	1.9	5.0	1.8
On orbit	49	52	67	187	3.8	1.4	3.6	1.3
Room								
On ground	49	52	63	121	3.1	1.4	2.8	1.3
On orbit	49	52	48	106	2.2	1.0	2.0	0.9

(37.3 psid). By using equations from the boiler code (ref. 3) for internal pressure on cylindrical and elliptical shells and a minimum wall thickness of 0.08 in., the stress was calculated to be 12.9 kpsi in the cylinder and 8.5 kpsi in the ellipsoidal head. If a maximum stress of 12.9 kpsi is used, the safety factors are 5.4 and 1.9 for ultimate tensile and yield strengths of 70 and 25 kpsi, respectively.

Maximum on-orbit operating pressure is the same as the maximum ground operating pressure of 49 psia, but since atmospheric pressure is no longer present, the differential pressure for calculating tank stresses becomes 49 psi. Consequently, the stresses on orbit will be 18.4 kpsi in the cylinder and 12.1 kpsi in the ellipsoidal head. If a maximum stress of 18.4 kpsi is used, the safety factors become 3.8 on ultimate strength and 1.4 on yield. The safety factors as well as the calculated proof and burst pressures are summarized in table 5.27.

By using the boiler code (ref. 3), the collapse pressure for the tank was calculated to be 12 psia. In addition, external loads were applied to the tank to account for valve panels mounted on the forward dome. The launch and ascent accelerations of 6-g axial and 2-g lateral were also considered in the analysis. Maximum stress in the dome was determined to be 15 kpsi which is well below the yield stress of 25 kpsi.

It was determined early in the analysis that thermal stress was not significant because of the thin wall of the tank and the highly conductive nature of aluminum.

In accordance with the boiler code, materials will be inspected prior to fabrication. After inspection of welds, a pneumatic test of the vessel will be conducted at a test pressure calculated from boiler code Part UG-100 (approximately 35 psid). Joints and connections will be inspected at not less than four-fifths of the test pressure.

5.3.2.1.2 Supply Tank Strut.—The supply tank is supported from the spacecraft primary structure by sixteen struts attached at the fore and aft girth rings. Struts attach at evenly spaced positions to provide structural symmetry. In order to minimize stresses caused by uneven thermal contraction and expansion of the supply tank, struts have been positioned and oriented such that the axis of each strut is perpendicular to a line from the attachment point on the girth ring to the center of the tank. Consequently, as the tank shrinks, the struts pivot toward the

center of the tank thus minimizing induced stresses from elongation.

An S-2 glass-epoxy filament-wound strut was selected for the supply tank supporting struts because of its low thermal conductivity, high strength, and high stiffness for buckling resistance. The hollow tube struts are 19.1 in. long with a 1.375 in. diameter and a wall thickness of 0.04 in. They were analyzed for their ability to withstand the 6-g axial and 2-g lateral worst-case load conditions during ascent. Since the compressive strength of the glass is much less than the tensile strength (120 kpsi versus 235 kpsi), it was conservatively assumed that the total axial load of the supply tank and MLI assembly is evenly distributed among the eight forward struts thus putting them into compression. In addition, it was assumed that the lateral load is divided between two of the eight struts. The loads from the supply tank were applied to the end of the strut while the MLI assembly loads were placed in the middle of the strut. For a strut with combined axial and lateral loading, the safety factor was calculated to be 2.8. This factor takes into account the potential for buckling as a result of deflections created by the MLI assembly load.

Loads on the struts during ground transportation of the supply tank assembly were assumed to be less than the loads calculated for launch conditions since the dry weight of the tank assembly is 54 percent of the wet weight.

5.3.2.1.3 Plumbing.—Cryogenic tubing runs were analyzed to determine the dimensions of the tube bends required to accommodate the thermal expansion/contraction of the stainless steel plumbing lines. The main criterion was to limit the normal stress at the bend location to no more than 18 kpsi. Figure 5 19 shows the dimension selection for Z-bends and U-bends in the plumbing lines.

5.3.2.2 Supply Tank Thermal Analysis

5.3.2.2.1 Introduction.—A lumped-parameter nodal network thermal model of the supply tank, using the SINDA85 thermal analyzer program, was used to predict supply tank thermal performance. This model was used to calculate total heat flux, Q , to the tank, as well as supply tank module component temperatures. The model was run for three different on-orbit attitude cases to obtain the orbital steady state heat flux

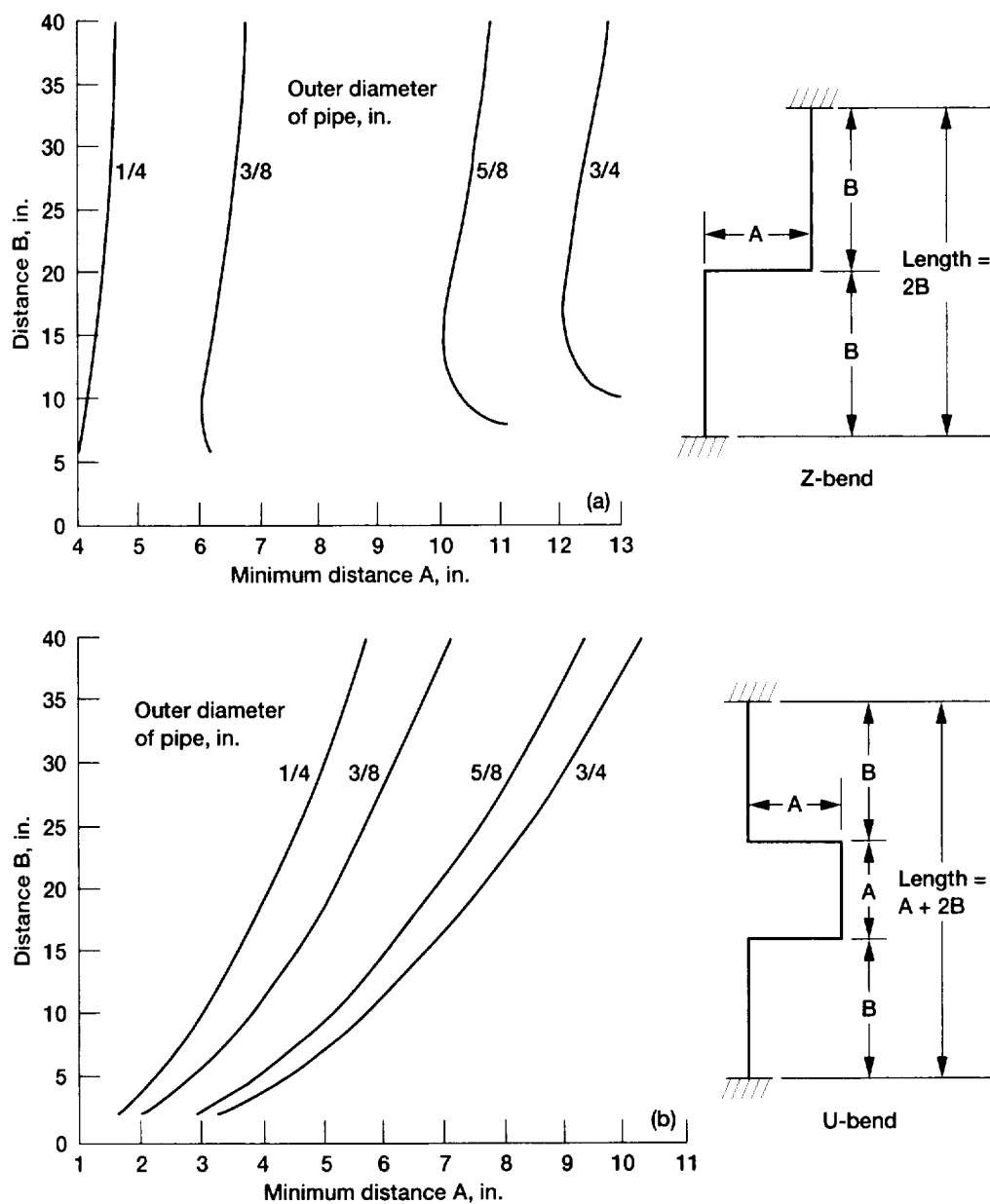


Figure 5.19.—Dimension selection for bends in plumbing lines. (a) Z-bends. (b) U-bends.

TABLE 5.28.—SUPPLY TANK THERMAL PERFORMANCE^a

Attitude	Heat flux (Btu/hr-ft ² to pressure vessel)
$\beta = 0^\circ$ (best case)	0.074
$\beta = 41^\circ$ (nominal worst case)	.084
$\beta = 0^\circ$, x-axis normal to orbit plane (loss of attitude)	.095

^aNominal heat flux is approximately 50 percent conduction and 50 percent radiation.

(Btu/hr-ft²) to the tank. A summary of these results (table 5.28) indicates that heat flux did not exceed the design limit of 0.1 Btu/hr-ft² in any case. The model was refined to include the conduction/convection effects of helium purge gas for the ground and ascent phase, providing an ascent heat flux profile from which the liquid hydrogen boiloff rate may be calculated.

5.3.2.2.2 Geometric Model.—Before the SINDA85 model could be constructed, geometric (TRASYS) models of the areas internal and external to the supply tank module were needed. These provided environmental (solar, planetary, albedo) heating data as well as surface-to-surface radiation conductors (RADK's), both of which were added to the SINDA85 input deck. Radiative heat transfer between surface 1 and surface 2 takes place according to the following equation (ref. 11):

$$Q_{12} = \sigma \epsilon F_{12} A_1 (T_1^4 - T_2^4)$$

where

σ Stefan-Boltzmann constant, 1.712×10^{-9} Btu/hr-ft² °R⁴

ϵ emissivity of surface 1

F_{12} view factor from surface 1 to surface 2, the fraction of energy leaving surface 1 which reaches surface 2

A_1 area of surface 1

The product $\epsilon_1 F_{12} A_1$ is known as a radiation conductor, or RADK.

An external TRASYS model (provided by the thermal system engineer) gave purge bag external heating rates, as well as RADK's to the purge bag from external surfaces included in the thermal model. It was run for three different orbital attitude cases, each assigning different heat rates to the external surfaces:

- (1) $\beta = 0^\circ$. Nominal best case; spacecraft spends more time in eclipse (50 percent) in this attitude than in any other; minimizes effect of solar heating
- (2) $\beta = 41^\circ$. Nominal worst case
- (3) $\beta = 0^\circ$ with Sun vector normal to side of spacecraft, directly opposite thermal tray; a loss of attitude control case; a worst-case loss of attitude study, with the Sun vector normal to the plumbing radiator tray, was not run

An internal TRASYS model was generated as well. It provided surface-to-surface RADK's between the inner facesheet of the honeycomb and the pressure vessel, as well as between different surfaces of the honeycomb itself. These

TABLE 5.29.—TRASYS INTERNAL GEOMETRIC MODEL SURFACE LISTING (HONEY-COMB-TO-PRESSURE VESSEL)

Surface type	Number of surfaces
Honeycomb inner facesheet	50
Pressure vessel	360
Valve panel	6
Total	416

surfaces were not directly exposed to external environmental heating, so there is no direct external source in the internal model. The breakdown of surfaces in the TRASYS internal model is identified in table 5.29. There were 416 surfaces in the TRASYS internal model.

Fine division of honeycomb and pressure vessel surfaces resulted in creation of over 35 000 internal RADK's. Excessive computer time would be needed to run a model containing this many RADK's, so the TRASYS model was rerun to eliminate RADK's with low gray-body factor to emittance ratio

$$F_{ij}/\epsilon_i < 0.001$$

where

F_{ij} gray-body factor, node i to node j

ϵ_i infrared emittance of node i

The reduced set of RADK's (5500) resulted in a thermal model which ran significantly faster without sacrificing accuracy.

Interactive TRASYS plots (TPLOT's) of the internal geometric model are given in figures D.19 and D.20 in appendix D to this chapter.

5.3.2.2.3 Thermal Model.—After appropriate TRASYS data were obtained, the SINDA85 model was developed. Nodes were selected to reflect the presence of thermal gradients and/or nonuniformity in local heat flux. This nodal breakdown is presented in table 5.30. There were 817 nodes in the SINDA85 model.

Once the nodal breakup of the model was established, the internodal heat conductors were included. These were classified as either linear conduction or radiation.

TABLE 5.30.—SINDA85 NODE SUMMARY

Purge diaphragm	14
Honeycomb.....	150
Pressure vessel.....	360
Struts.....	96
Plumbing.....	37
Wiring	112
Spacecraft, tray, space	3
Valve panels.....	6
External surfaces	39
Total nodes.....	817

Linear conduction:

- (1) Through wiring harnesses (8 by 48 wire bundles) and temperature sensor wires (4 wire groups)
- (2) Through plumbing
- (3) Through struts

Radiation:

- (1) From the purge diaphragm, through the MLI to the honeycomb outer facesheet
- (2) Through the honeycomb itself (ref. 12)
- (3) From the honeycomb inner facesheet to the pressure vessel, as provided by the internal TRASYS model

All plumbing and wiring harnesses were heat paths to the supply tank by linear conduction, whose governing equation for the total heat flux, Q , is

$$Q = \frac{kA}{L}(T_H - T_C)$$

where

- k material thermal conductivity
 A heat path cross-sectional area
 L heat path length
 T_H material hot side temperature
 T_C material cold side temperature

The majority of plumbing and wiring penetrations which reached valve panels, and hence the pressure vessel itself, entered through the honeycomb outer facesheet cold side (fig. 5.20). The model could have been oriented such that hot and cold sides would each correspond to one 90° wedge, instead of being spread out over two such wedges, but the coarse resolution of the model made this refinement meaningless. The honeycomb barrel was divided into 10 axial nodes (each 6 in. high) by 4 circumferential nodes (18.8-in. arc-length each).

All temperature sensors and wire bundles which penetrated the pressure vessel entered at two honeycomb node locations as indicated in figure 5.20 at 11025 and 11026. Although these wires will probably be dispersed more in the actual design, the

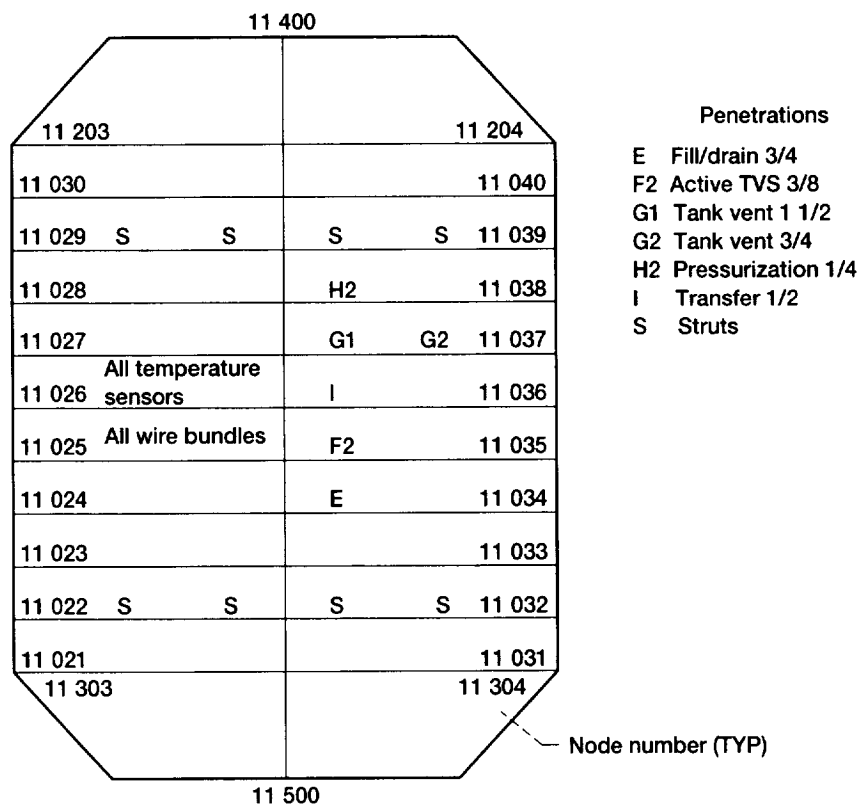


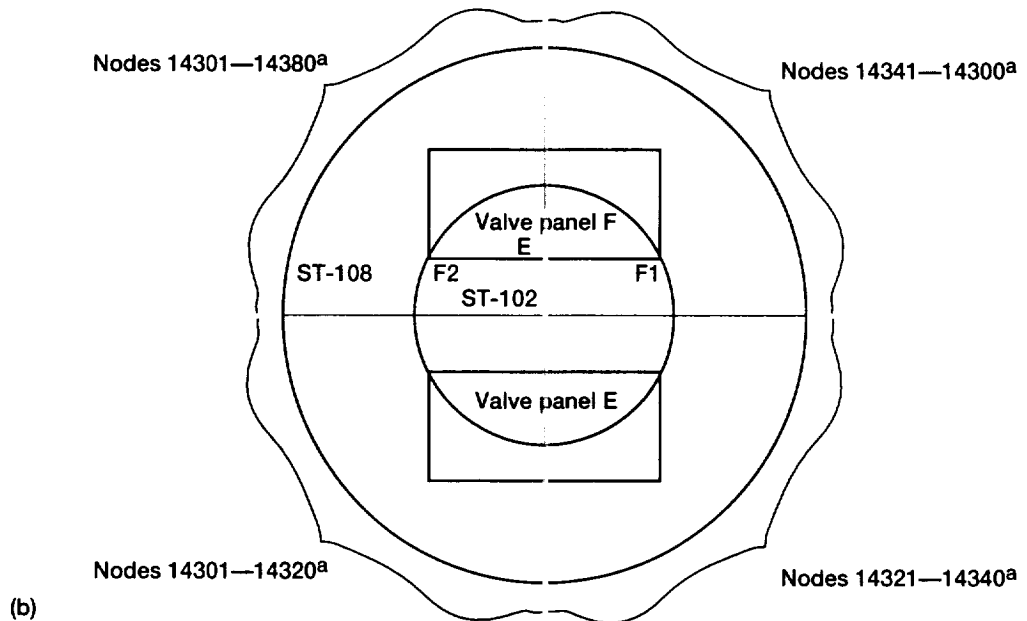
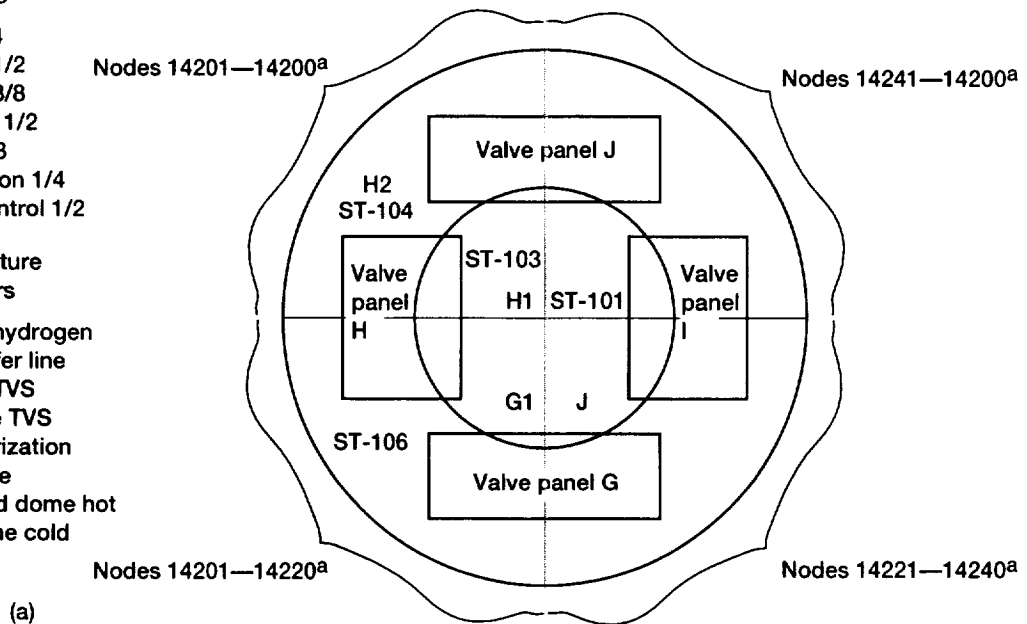
Figure 5.20.—MLI can honeycomb outer facesheet nodes, cold side. Dimensions are in inches.

Plumbing

E Fill/drain 3/4
 F1 Active TVS 1/2
 F2 Active TVS 3/8
 G1 Tank vent 1 1/2
 H1 TVS flow 3/8
 H2 Pressurization 1/4
 J Transfer control 1/2

Temperature sensors

ST-101 Liquid hydrogen transfer line
 ST-102 Active TVS
 ST-103 Passive TVS
 ST-104 Pressurization
 ST-105 Vent line
 ST-106 Forward dome hot
 ST-108 Aft dome cold



^aTwenty wedge-shaped nodes are not shown for clarity.

Figure 5.21.—Linear penetrations at PV dome. Dimensions are in inches. (a) PV forward dome. (b) PV aft dome.

resolution of the model and the fact that all heat flux to the honeycomb was evenly spread out by the time it reached the inner facesheet made this refinement unimportant. All eight strut locations on this side are shown. Pertinent plumbing attachments, with pipe outside diameters, are shown.

Locations of struts and temperature sensors that penetrate the pressure vessel barrel are shown in figure D.21 (in appendix D to this chapter), which shows two unrolled barrel section halves. The barrel was divided into 20 axial nodes (3-in. high each) by 10 circumferential nodes (18.8-in. arc-length each). This finer mesh size was used to show heat flux uniformity from node to node with a greater resolution than would be possible with the node sizes used for the outer layers.

Each pressure vessel dome was divided into two radial nodes (with diameters of 30 and 60 in., respectively), by 40 circumferential nodes (fig. 5.21). In figure 5.21 each quadrant is shown, but the individual nodes are not shown to simplify the drawing. Approximate positions of temperature sensors and plumbing lines direct to the pressure vessel are shown in boldface type. Valve panels were positioned as indicated in design drawings. All heat flux to the valve panels was divided equally among the six valve panel legs, located at the four corners and two middle points of the long side of each panel.

The S2 struts were important contributors to supply tank heat flux, as they were attached directly to the pressure vessel (fig. 5.22). Each 22-in. strut was divided into two aluminum end pieces and a three-node S2 fiberglass-epoxy composite section. A cylindrical aluminum section enclosed a 6-in. section of the strut and was joined to the honeycomb with an aluminum sleeve, which is a cone made of 1/8-in.-thick aluminum.

Because of the complexity of the model, there was some finite time (sometimes months) before design changes could be incorporated. The model used characteristics that lagged the design, and hence the end pieces of the struts were made of aluminum. The current design has stainless steel end pieces, which are good thermal insulators and give the struts a longer thermal length, thus reducing heat flux to the pressure vessel.

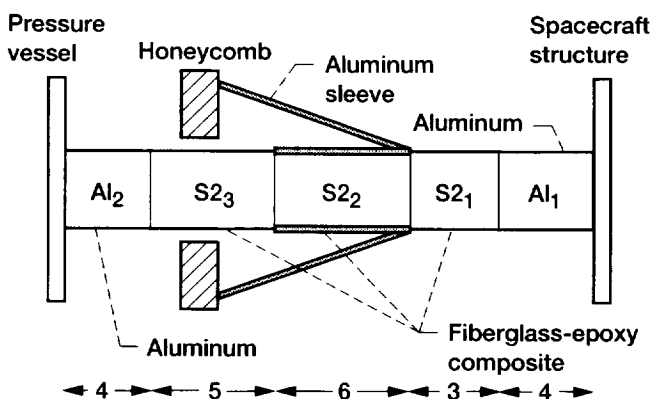


Figure 5.22.—Strut thermal model schematic. Dimensions are in inches.

The model as it stands thus gives conservative (higher than the most recent design) values of heat flux to the pressure vessel.

Accurate characterization of the multilayer insulation (MLI) surrounding the honeycomb was needed. The MLI insulated the honeycomb from quickly changing transient external heating effects and was the principal thermal insulation for the supply tank.

An effective MLI conductivity, k , was found using the Lockheed formulation (ref. 13), as follows:

Divide MLI heat flux into an "ideal" part and a "correction" part

$$Q_{TOTAL} = Q_{IDEAL} + Q_{CORRECTION}$$

where

$$Q_{IDEAL} = Q \text{ caused by linear conduction} \\ + Q \text{ caused by radiation}$$

$$Q_{IDEAL} = Q_{SOLID} + Q_{RAD}$$

and

$$Q_{CORRECTION} = Q \text{ caused by pins through MLI} \\ + Q \text{ caused by seams}$$

$$Q_{CORRECTION} = Q_{PINS} + Q_{SEAMS}$$

We have

$$Q_{SOLID} = (8.95 \times 10^{-8}) N^{2.56} (T_H^2 - T_C^2) / 2N_s$$

$$Q_{RAD} = (5.39 \times 10^{-10}) (0.031) (T_H^{4.67} - T_C^{4.67}) / (N_s - 1)$$

$$Q_{PINS} = K_{PINS} (T_H - T_C) / d_{MLI}$$

$$Q_{SEAMS} = \sigma (6.63 \times 10^{-4}) (T_H^4 - T_C^4),$$

which are all expressed in W/m^2 . From these we obtain

$$K = (Q_{TOTAL}) (d_{MLI}) / (T_H - T_C) \text{ in } W/m-K$$

where

Q heat flux, W/m^2

N blanket density, sheets/cm

T_H blanket hot temperature, K

T_C blanket cold temperature, K

N_s number of radiation shields

K_{PINS} conductivity of MLI pins, W/m-K

d_{MLI} MLI blanket thickness, m

σ Stephan-Boltzmann constant, $5.7 \times 10^{-8} \text{ W/m}^2 \cdot \text{K}^4$

The main advantage of the Lockheed equations is that degradation of MLI performance caused by seams and pins is accounted for by the $Q_{CORRECTION}$ terms. This formulation is more rigorous than the other commonly used approach of degrading MLI performance through an approximation derived empirically (refs. 14 to 16)

$$Q_{TOTAL} = (\text{arbitrary multiplicative constant}) \times Q_{IDEAL}$$

The Lockheed equation applies for any combination of $T(\text{inner})$ and $T(\text{outer})$. Although the outer layer is directly heated by the sun during part of the orbit, its temperature can swing below that of $T(\text{inner})$ as the spacecraft enters eclipse. These equations are plotted for a range of $T(\text{inner})$ and $T(\text{outer})$ values in figure 5.23.

The presence of helium in the supply tank MLI on the ground causes the temperatures throughout the MLI to be lower on the ground than on-orbit. This is because helium is not a good insulator, but it is used to prevent condensation. When the tank is on-orbit and the MLI is evacuated, it will have to warm up to get to equilibrium. Thus, equilibrium (or lower) heat flux should be reached very quickly. Figure 5.24 shows test data from Sumner and Maloy for a similar system (ref. 15).

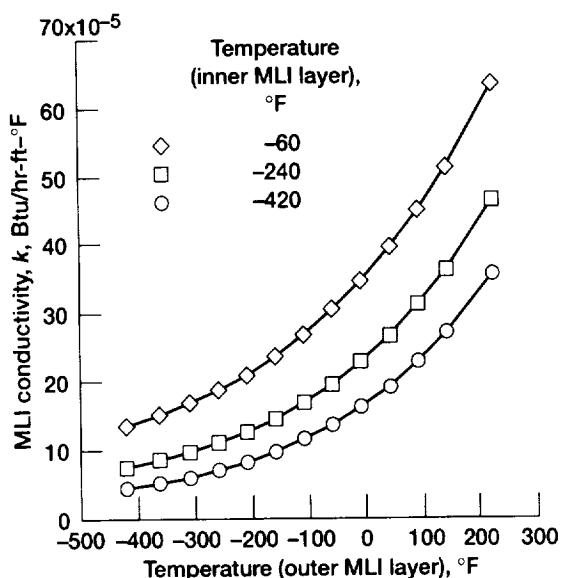


Figure 5.23.—Multilayer insulation (MLI) effectiveness model: MLI conductivity, k , versus temperature (outer MLI layer) (1.0-in. blanket, 80 sheets).

The ground and ascent stage, helium-purged supply tank thermal model used the altitude-versus-time profile from Atlas/Centaur flight A/C-68 with the "U.S. Standard Atmosphere" (ref. 17) pressure-versus-altitude data to obtain a helium purge gas pressure-versus-time profile (fig. 5.25). From this, the following purge gas properties were obtained:

- (1) Specific heat, $C_p(\text{He})$, versus time
- (2) Velocity (He) versus time
- (3) Thermal conductivity, $k(\text{He})$, versus time
- (4) Prandtl number, $Pr(\text{He})$, versus time
- (5) Reynolds number, $Re(\text{He})$, versus time

The pressure lag between the spacecraft interior and ambient pressure was neglected. These parameters were then used to obtain the linear conduction and convection through the supply tank structure caused by the helium gas. The Prandtl number for helium followed atmospheric pressure on ascent until it reached 0.1 psia (124 sec into ascent), and then linearly ramped off to 0.0 psia at 12 hr. In this way the pressure lag inside the spacecraft was approximated. Molecular conduction effects at low pressures were neglected in this model.

The ascent heat flux profile (fig. 5.26) was obtained once the pressure profile was established and conduction/convection effects caused by the helium gas were included. The ground-purge steady-state heat flux level was 110 Btu/hr-ft². This heat flux is large because of convection. The hot helium purge gas impinging on the supply tank is the dominant effect; MLI is relatively useless except in a vacuum. On ascent, conduction/convection heat inputs initially were large, but decreased gradually as less bulk helium was available for conduction. As the helium flow rate decreased, convection effects also became small. After 71 hr, supply tank heat flux decreased to the nominal best-case, steady-state value of 0.0841 Btu/hr-ft².

All supply tank module component temperatures were also obtained (table 5.31). The purge diaphragm, with low thermal mass, had the largest temperature gradient caused by external heating. The effect of localized external heating was diluted somewhat at the MLI layer, and local heat sources were totally dispersed at the honeycomb, which had no temperature gradient. The honeycomb thus provided a uniform radiative heat flux background to the supply tank, to which was added heat input from local penetrations (valve panel legs and struts). These penetrations were laid out to improve total heat flux uniformity. Background radiative heat flux served to smooth out local nonuniformities caused by penetrations. The struts were thermally shorted to the honeycomb at the sleeve, and thus were at the honeycomb temperature. The temperature profile along typical wiring harnesses and plumbing was different because

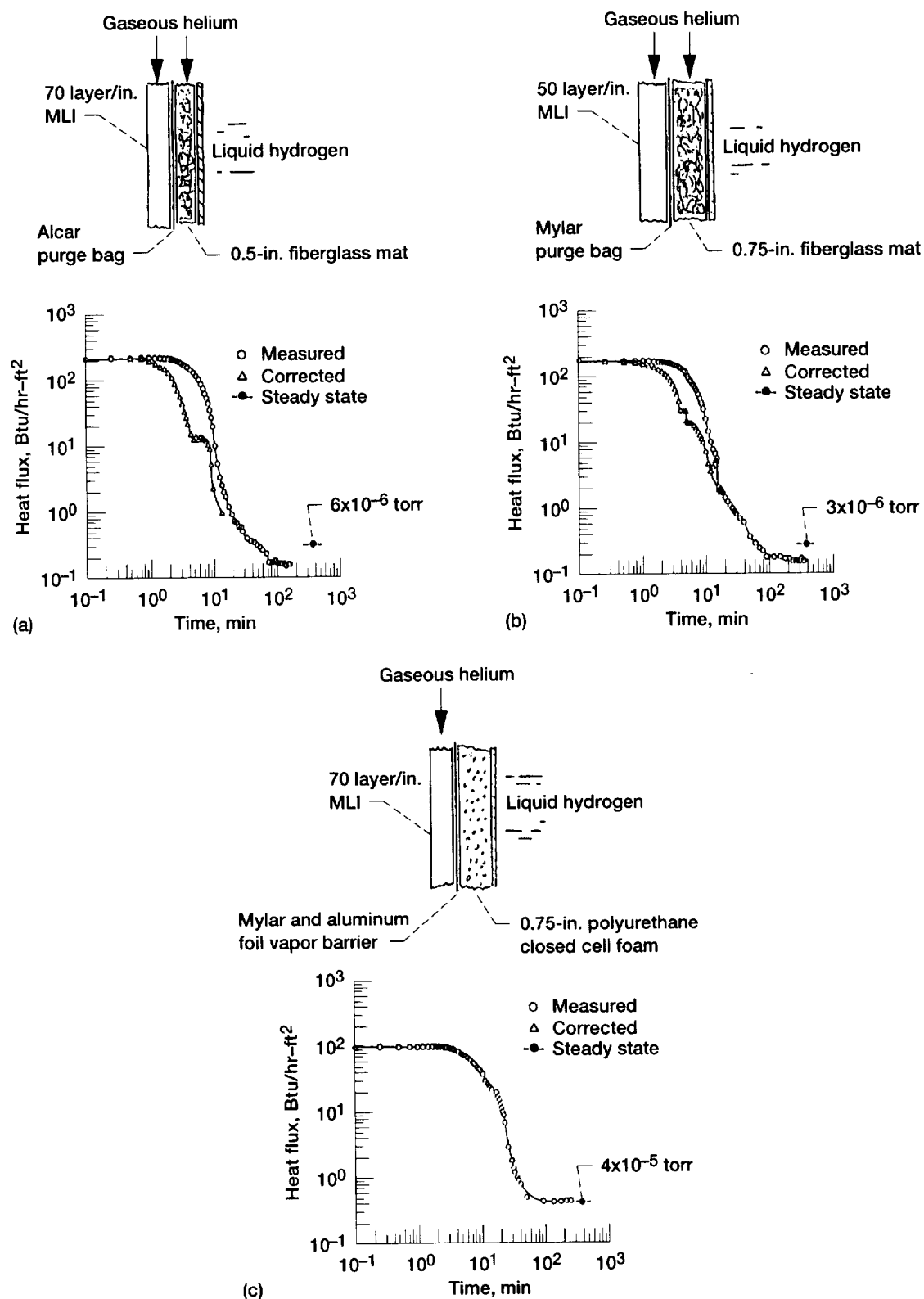


Figure 5.24.—Transient performance of 30-layer, helium-purged MLI systems during simulated ascent (ref. 15). (a) Dense MLI/purged fiberglass. (b) Lower density MLI/thick purged fiberglass. (c) Dense MLI/closed cell polyurethane foam.

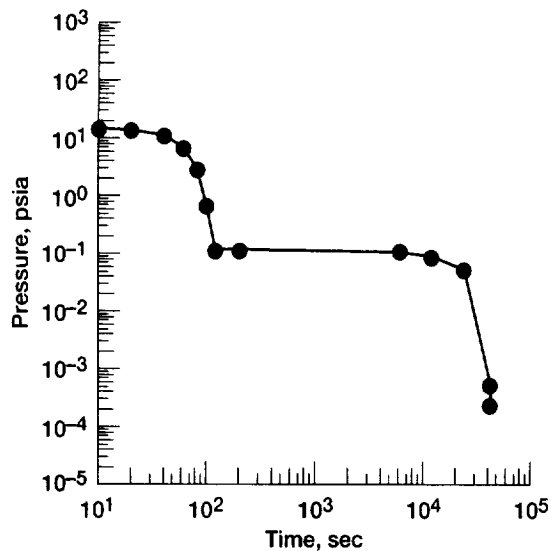


Figure 5.25.—Thermal model pressure profile for ground and ascent from Atlas-Centaur 68 flight telemetry.

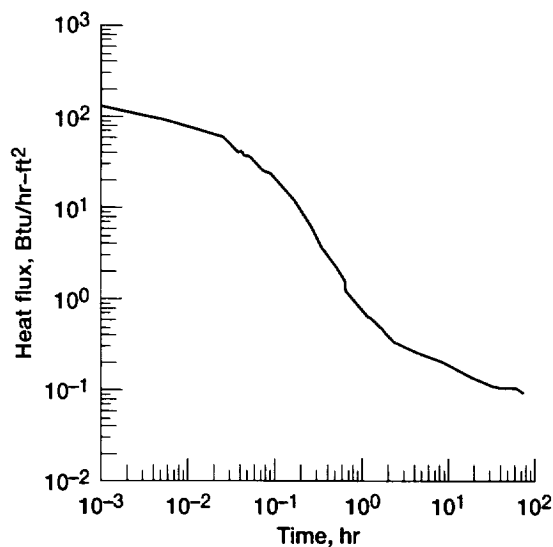


Figure 5.26.—Ascent heat flux profile from ground and ascent supply tank thermal model.

the materials used were stainless steel (plumbing) and manganin or phosphor-bronze (wiring) rather than fiberglass.

5.3.2.3 LAD/TVS Analysis

The LAD/TVS heat exchanger designed for the COLD-SAT experiment system supply tank was modeled and analyzed to evaluate its thermal performance. An iterative method, described in appendix B to this chapter, was applied to incremen-

TABLE 5.31.—SUPPLY TANK COMPONENT TEMPERATURES (°F)

Purge diaphragm	
Hot	0
Cold	-150
MLI	
Hot	-100
Cold	-120
All honeycomb layers	-298
Struts	
Spacecraft-to-honeycomb	-240
Sleeve	-298
Sleeve-to-tank	-360
Wires and plumbing	
Spacecraft-to-honeycomb	-225
Sleeve-to-tank	-340
Valve panels	-421
Pressure vessel	-423
Thermal tray	-100
Spacecraft structure	0

tal segments of the heat exchanger length by using two-phase and single-phase heat transfer coefficients obtained from correlations.

Performance calculations were made for three modes of TVS operation as presented in appendix B. The temperature and quality profiles along the length of the heat exchanger were obtained for the active and subcooler modes for assumed steady-state conditions. Change in the supply tank pressure was calculated for a constant heat removal rate during active TVS operation. The passive mode was analyzed with a one-dimensional transient model to obtain the time-dependent temperature and pressure response in the supply tank under continuous and intermittent TVS operation.

The TVS heat exchanger design was adequate for the required operational conditions. At high liquid flow rates associated with the active mode, the heat exchange rate was sufficient to vaporize and superheat the TVS fluid and to lower the supply tank pressure at a rate of 2.5 psi/hr. In the subcooler mode, the liquid flow rate and degree of subcooling desired must be combined to match the heat exchange capacity and operating point. Under some operating conditions, the TVS flow rate had to be reduced to assure venting of 100 percent quality vapor. The passive TVS mode was found to be a long duration, slow response, pressure control process applicable to low heat flux conditions. Heat flux to the exchanger varied with time, and the TVS flow rate for 100-percent vapor venting was accordingly time-dependent. Other considerations concerning the analytical model and performance calculations for the TVS heat exchanger are discussed in section B.2.4.

Spherical and rectangular vapor bubbles trapped within the LAD channels of the supply tank and the large receiver were found to be condensible to liquid by their TVS systems. As discussed in more detail in section B.2.5, the collapse times were of the order of 3 min or less for any size bubble expected to be confined within the LAD.

The analytical models and methods used for evaluating the performance of the COLD-SAT LAD/TVS heat exchanger required many simplifying assumptions, and the results obtained should be viewed accordingly. More rigorous and sophisticated models are conceivable but at the expense of more time and cost. The assumptions used are considered reasonable and realistic, however, and do not invalidate the methodology adopted to perform the calculations. The main simplification is that the flow rate was allowed to be continuously variable, whereas in the actual design there are three discrete flow legs with constant flow restrictions.

5.3.2.4 Ground Fill Level

The ground fill level was selected to be 92 percent. This fill level should guarantee that there is some ullage in the tank at any point up to the relief pressure (the pressure at which the relief valve opens and vents to the atmosphere). The volume expansion of liquid hydrogen with temperature is significant.

A ground fill level of 92 percent of the volume of the tank (142 ft^3 at 20 K) with liquid hydrogen at 20 psia (tank saturated) conditions corresponds to a mass of 567 lbm of liquid hydrogen. A figure of 565 lbm is used to account for volume taken up inside the tank by the LAD, rakes, and so forth. This assumes that the liquid is uniformly saturated at 20 psia and there is no thermal stratification (colder liquid at the bottom of the tank) which is a reasonable assumption because of the uniform, high heat leak to the tank on the ground. Since the liquid will be boiling at this high heat flux level, some volume (less than 0.5 percent) will be taken up by vapor bubbles. This effect was ignored to make the analysis more conservative, but it is less than the error caused by a 1-psi change in saturation pressure.

If the tank is locked up with 565 lbm of liquid hydrogen and the liquid is allowed to rise to a saturation pressure corresponding to the relief pressure of 52 psia, the volume taken up by the liquid becomes 141.5 ft^3 . This is a worst-case number since thermal stratification is ignored and the liquid is assumed to be homogeneous. This number should be acceptable with reasonable relief valve accuracy. Thus, a 92-percent fill level guarantees that some ullage will be present at 52 psia.

5.4 Gaseous Hydrogen System

The purpose of the gaseous hydrogen system is to provide gaseous hydrogen on-orbit for expelling liquid hydrogen from the supply tank and transferring it to the receiver tanks and back again. Because of the difficulty of predicting accurately the amount of gaseous hydrogen required for transfer and the large mass and volume required to carry an assured gaseous hydrogen supply, on-orbit generation of gaseous hydrogen is used. The concept involves injecting liquid hydrogen into a pressurant bottle maintained at ambient temperature. As time passes and

heat is supplied, the liquid hydrogen vaporizes and the internal pressure rises.

An alternative to the proposed system would be to store the required gaseous hydrogen on board in additional ground-charged pressurant bottles. As our thermodynamic analysis will show, about 30.6 lbm of hydrogen will be required for cryogen transfer operations which equates to a storage volume of 50 ft^3 or about 11 pressurant bottles similar in size to our vaporizer bottles. This option appeared to be infeasible because of space limitations within the existing spacecraft fairings. Another disadvantage of this concept came from the uncertainty in calculating the amount of pressurant required for transfers. If requirements are overestimated, the result is unnecessary spacecraft mass and volume used for pressurant storage. On the other hand, if pressurant requirements are underestimated, the result is insufficient pressurant to complete the experiment sets.

Consequently, a more flexible and compact system which allows us to produce pressurant on an "as required" basis was selected. The vaporizer bottles will be charged with gaseous hydrogen during ground operations and then remaining pressurant requirements will be satisfied by on-orbit operation of the system.

One system requirement is to accurately meter the amount of liquid hydrogen injected into the bottle so the pressure rise can be safely predicted and at the same time minimize chilldown requirements. Our solution is to chill and fill a coiled tube inside the bottle and then allow the hydrogen to expand into the bottle. Consequently, as shown in figure 5.27, a vaporizer consists of a pressurant bottle with a coiled tube inside. More detail on this procedure is given in the following sections.

5.4.1 DESCRIPTION AND CHARACTERISTICS

The system designed is redundant with two vaporizer bottles, each serviced by its own valve panel and capable of generating, storing, and delivering gaseous hydrogen for experimental pressurization and transfer operations. Table 5.32 summarizes the physical and operational characteristics of the vaporizers.

Each vaporizer consists of a bottle and a coil. The 6061-T6 aluminum bottle (fig. 5.27) is spherical in shape with a volume of 5.7 ft^3 . The double coil inside consists of 3003-H14 aluminum tubing. The 1.5-in.-o.d. tubing transitions to 3/8-in.-o.d. tubing before penetrating the bottle. To limit heat conduction (and consequently chilldown mass) from the bottle to the coiled tubing, a hi-hat arrangement (fig. 5.28) with bimetallic junctions will be used to transition the 3/8-in. tubing from aluminum to stainless steel. Each coil is supported by six brackets that slip between the inner and outer coils and fit the contour of the bottle.

Figure D.22 in appendix D to this chapter shows the plumbing schematic for the system, and figure D.23 is a layout of valve panels B and C which service the vaporizers. Table E.7 in appendix E to this chapter is a list of components for valve

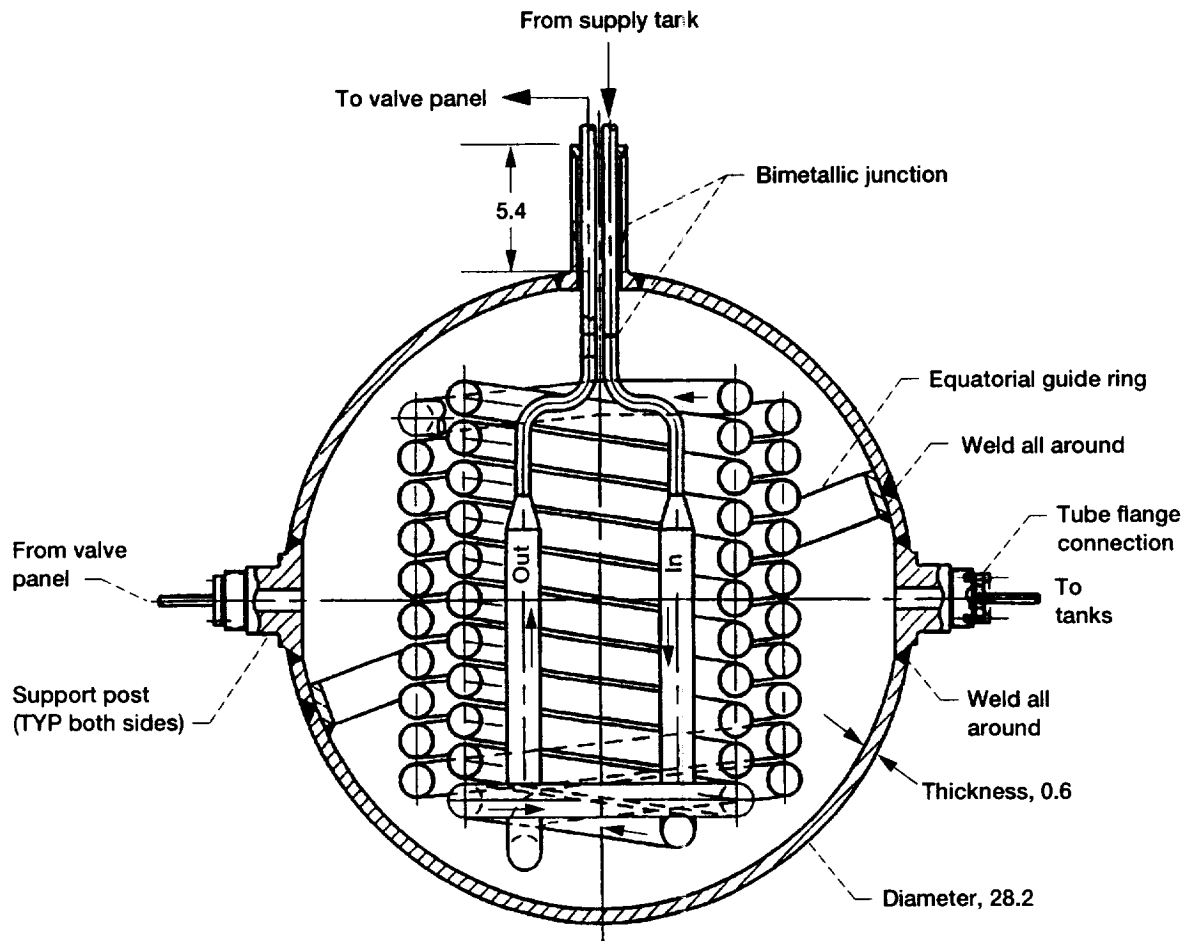


Figure 5.27.—Vaporizer bottle cross section. Dimensions are in inches.

TABLE 5.32.—HYDROGEN VAPORIZER CHARACTERISTICS

Physical	
Hydrogen mass capacity, lbm.....	3.5
Bottle internal volume, ft ³	5.7
Bottle material.....	6061-T6 Aluminum
Bottle outer diameter, in.	28.2
Bottle wall thickness, in.	0.6
Coil tube material.....	3003-H14 Aluminum
Tube outer diameter, in.	1.5
Tube wall thickness, in.	0.065
Operational	
Maximum operating pressure, psia.....	2000
Maximum operating temperature, °R.....	540
Vaporization time, hr	
Maximum.....	45
Minimum.....	20
Chilldown liquid hydrogen required—coil and vessel, lbm	
Maximum.....	51
Minimum.....	10

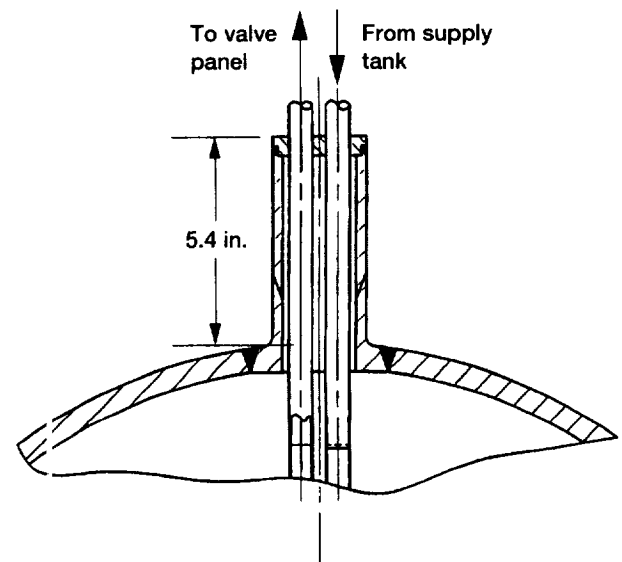


Figure 5.28.—Vaporizer hi-hat.

panels B and C. As previously mentioned, the bottles will be charged with gaseous hydrogen prior to launch. Vaporizer A is operated as follows. Hydrogen gas is drawn off the bottle for the pressurization experiments using gas valve GV8 and regulator R2. Once the pressurant is used up, the bottle will be readied for refilling by venting it to space through GV6 and GV7. The coil in the vaporizer, which acts as a measuring device for the liquid hydrogen, is then chilled and filled with 3.5 lbm of liquid hydrogen from the supply tank through cryogenic valves V47 and V20 as well as check valve CV2. Once a liquid sensor indicates a liquid condition at the coil outlet, gas valve GV7 and cryogenic valve V22 are closed and gas valve GV6 is opened to allow the hydrogen to pass into the gas bottle as it warms and vaporizes. The same procedure will be used for vaporizer B.

Both valve panels and vaporizer bottles are located on the warm side (negative z) of the spacecraft to take advantage of the warmer temperatures and higher heat fluxes. In addition, strip heaters are applied to the outside of the bottles to decrease vaporization time. Consequently, the maximum time it takes for vaporization is estimated to be 45 hr while the minimum time is around 20 hr.

The support post design for the vaporizer bottle is similar to that used for the helium bottles. Plumbing penetrations in the bottle support posts are piped to the associated valve panel. Each tank is supported off the spacecraft structure by four 6061-T6 aluminum struts as shown in figure 5.29. A G-10 epoxy-fiberglass ring fits around the post and serves to thermally isolate the tank from the struts and spacecraft structure.

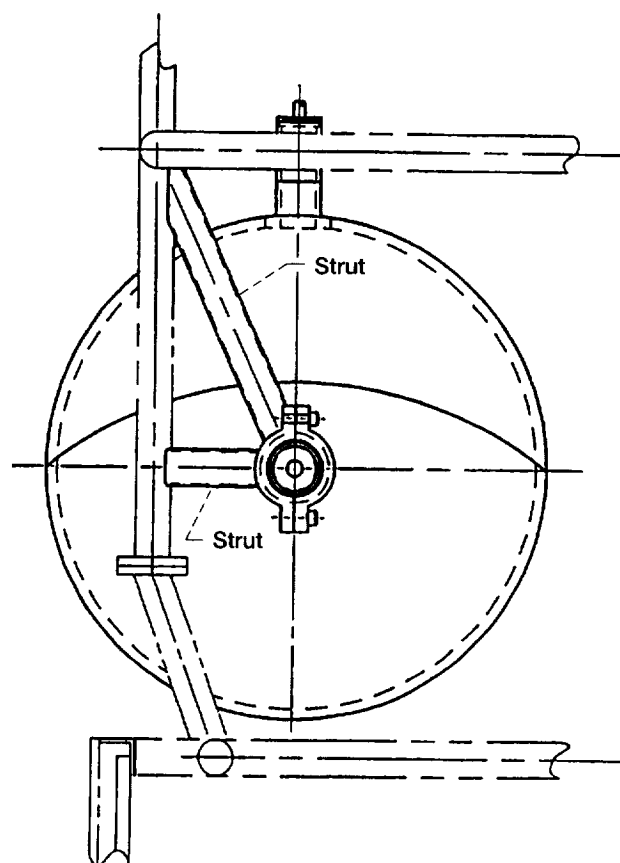


Figure 5.29.—Vaporizer support structure.

5.4.2 ANALYSES

5.4.2.1 Thermodynamic Analysis

Autogenous tank pressurization for liquid hydrogen expulsion involves the injection of gaseous hydrogen pressurant into the ullage space of a supply tank for the purpose of delivering liquid hydrogen to a receiving tank.

Because of uncertainty of such phenomena as the rate of heat transfer from pressurant to cryogen and condensation rate of the gaseous hydrogen pressurant, it is difficult to accurately estimate the amount of pressurant gas required for each transfer of liquid hydrogen. Two simple pressurization analyses were performed for each of the six different COLD-SAT pressurization and transfer operations including supply tank to large or small receiver tank, large receiver tank to supply or small receiver tank, and small receiver tank to supply or large receiver tank. The results of these analyses are shown in figure D.24 in appendix D to this chapter. These two analyses provide upper and lower bounds for the actual quantity of pressurant required to raise the pressure from 15 to 30 psia. The best case (minimum pressurant required) assumes that the bulk cryogenic liquid and the incoming warm pressurant gas each undergo reversible, adiabatic (isentropic) processes in reaching the final state. The isentropic case is characterized by total thermal stratification.

The worst case (maximum pressurant required) assumes that thermal equilibrium is maintained between the bulk liquid and the pressurant gas at all times during the process. The thermal equilibrium case is characterized by substantial condensation of the incoming pressurant gas.

Clearly, neither the isentropic nor thermal equilibrium models predict the actual COLD-SAT pressurant use. The nominal case pressurant mass required was chosen at the mid-point between the two extremes and has been plotted as a function of initial tank fill level in figure D.24 (a) to (f). Nominal hydrogen pressurant requirements for each of the six different COLD-SAT pressurization and transfer operations are summarized in table 5.33.

5.4.2.2 Thermal Analysis

A lumped-parameter, nodal-network, thermal model of the vaporizer using the SINDA85 thermal analysis program was developed to determine vaporizer thermal feasibility for the design configuration. The coil and bottle temperatures predicted by the model were then used as inputs for the thermodynamic calculations in the previous section.

A TRASYS geometric model of the vaporizer was developed to provide bottle wall-to-coil radiation conductors

TABLE 5.33.—LIQUID HYDROGEN REQUIRED FOR PRESSURIZATION AND TRANSFER

Operation	Amount per transfer, lbm	Number of transfers	Total liquid hydrogen, lbm
Supply tank to large receiver tank	2.0	6	12.00
Supply tank to small receiver tank	1.9	6	11.40
Large receiver tank to supply tank	0.56	6	3.36
Large receiver tank to small receiver tank	.5	2	1.00
Small receiver tank to supply tank	.36	6	2.16
Small receiver tank to large receiver tank	.36	2	.72
Total hydrogen pressurant required for COLD-SAT			30.60

(RADK's). A cross-sectional view of the model is shown in figure D.25 in appendix D to this chapter. The inner bottle wall was modeled as a sphere, and the coils were modeled as two rows of stacked tori. Inlet and outlet coil lengths were modeled as cylinders parallel to and equidistant from the coil axis. Large thermal gradients exist between the bottle wall and the coils and between the inner and outer coils, so bottle wall-to-coil and inner-to-outer-coil distances precisely match those given in design drawings. The spacing of coils within the same row required less precision, since temperature gradients between coils in the same row were relatively small and the contribution to radiation heat flux was insignificant.

It should be noted that the number of vaporizer coils in the model does not match the number in the current design. However, it is believed that changing the number of coils does not significantly affect the radiation heat flux.

After appropriate RADK data was obtained from the TRASYS model, a SINDA85 thermal model was then constructed (fig. D.26). The following items explain the assumptions and modeling philosophy used in constructing the model.

(1) The bottle wall was modeled as a cylindrical enclosure with a cross section that forms a square grid, which facilitates placement of nodes in the proper grid blocks.

(2) The thickness of the bottle wall was calculated such that the masses of the cylindrical and spherical (real) enclosures are equal.

(3) Individual coils were modeled as square toroids with the same mass as the actual coils. The cross sections of these square toroids correspond to blocks in the nodal grid.

(4) Hydrogen properties are used in spaces between coils. Though this leads to underestimation of heat transfer along vertical rows of coils by means of gas conduction, the effect is felt to be negligible compared to the radiative effects which are modeled precisely.

(5) Modeling of the inlet and outlet coils was straightforward, as each 1.5-in. section of coil occupied one grid element.

(6) All spaces in the grid not occupied by bottle wall or coil were filled with hydrogen gas, and gaseous conduction through these elements to adjoining nodes was included in the model.

(7) The 5-in. bimetallic connectors were included as additional linear conductors penetrating the appropriate bottle wall nodes.

Figure 5.30 shows the results of the thermal model for a vaporizer with chilled coils, giving the temperature profile for the top, middle, and bottom of the bottle. In 12 min, the average bottle wall temperature dropped from 80 to 56 °F. Since the nodes along the top of the bottle wall had a higher thermal mass than those at the bottom, their temperature dropped more slowly. The middle section of the bottle wall cooled most rapidly since it had more available coil area to radiate to. The profile of bottle wall temperature versus time for a vaporizer with chilled coils was then used to perform thermodynamic calculations of hydrogen usage during vaporizer chilldown.

5.4.2.3 Structural Analysis

Analysis of the bottle took into account the thermal stresses in the bottle wall created when liquid hydrogen contacts the relatively warm surface and the subsequent pressure rise as the liquid hydrogen vaporizes.

A wall thickness of 0.60 in. was used to calculate combined in-phase thermal and pressure stresses to be a maximum of 22 500 psi which occurs at a temperature of 540 °R and an internal pressure of 2000 psia. Room temperature yield and ultimate strengths for 6061-T6 aluminum determined factors of safety to be 1.8 and 2.0, respectively. The calculated proof and burst pressure are 3600 and 4000 psia, respectively.

Vaporizer bottles meet the requirements of MIL-STD-1522A, section 5.1.3, Pressure Vessels Designed Employing Strength of Materials. Safety factors required are a minimum proof pressure = $1.5 \times$ maximum effective operating pressure (MEOP) and a minimum design burst pressure = $2.0 \times$ MEOP. A safe-life analysis is required by section 5.1.1.2, but has not yet been done. Required qualification testing includes fatigue

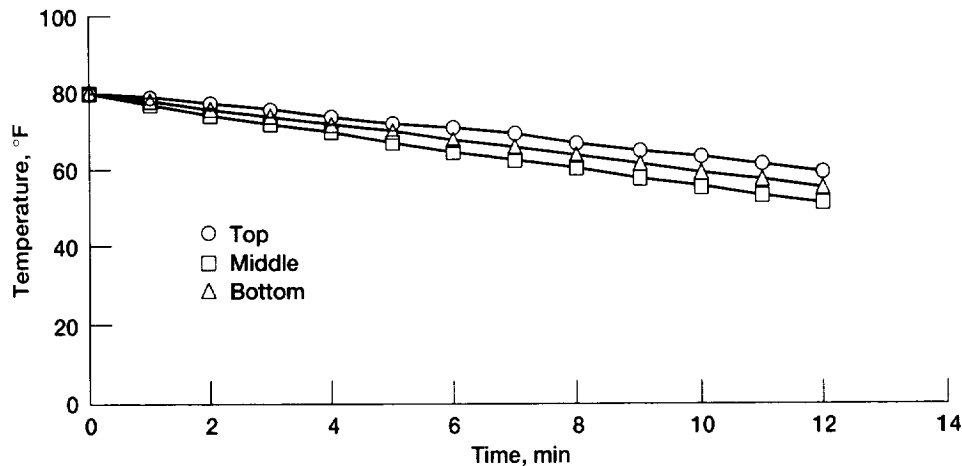


Figure 5.30.—Calculated vaporizer tank wall temperatures—coil temperature held constant.

life by cycle testing and random vibration testing and ultimate strength by burst testing. Acceptance testing requirements include nondestructive inspection and a proof pressure test at $1.5 \times \text{MEOP}$.

The vaporizer struts are 1.5- by 2-in. structural tubing of 6061-0 aluminum and are welded directly to the spacecraft structure. Each vaporizer has four struts, two horizontal and two nearly vertical. The struts were analyzed for their ability to withstand the 6-g axial and 2-g lateral load conditions during ascent. Axial loads were applied where the vertical and horizontal struts join (bottle support posts). For lateral loads, the deflection equations for the different length struts were used to determine the portion of load on each strut. Stress from combined loading was determined to be 1280 psi for the vertical strut and 3670 psi for the horizontal strut. Using a yield strength of 12 kpsi, the safety factors were 9.4 and 3.3 respectively.

5.5 Receiver Tank Modules

This section covers the design and analysis of the COLD-SAT Experiment System large and small receiver tank modules.

5.5.1 LARGE RECEIVER TANK DESCRIPTION AND CHARACTERISTICS

The large receiver tank was designed to meet the following requirements:

- (1) Cylindrical tank
- (2) Length-to-diameter ratio, L/D , 1.6
- (3) Length, 4 ft
- (4) Total communication liquid acquisition device (LAD)
- (5) Passive thermodynamic vent system (TVS)

- (6) Axial spray system (covered and uncovered)
- (7) Tangential spray system
- (8) Cone-shaped pressurant diffuser
- (9) Liquid-vapors
- (10) Temperature sensors
- (11) External heaters

The final configuration has the following characteristics (figs. D.27 and D.28 in appendix D to this chapter):

(1) The pressure vessel (PV) is cylindrical with ellipsoidal heads. Because the spacecraft system is basically restricted by volume instead of weight, this shape allows for a good trade-off in the strength-to-volume ratio of the vessel.

(2) The material selected for the PV is 5083-T0 aluminum. In order to reduce the required testing, the design of the vessel is in accordance with the ASME Boiler and Pressure Vessel Code Section VIII, Division I (ref. 3). One of the materials specified in this section is 5083 aluminum. The selection of 5083 was made on the basis of its superior strength properties in the untreated condition and fracture toughness relative to other aluminums. Untreated properties were used in the design of the vessel because of the difficulty of treating the final welded assembly to restore the welded areas to the prewelded strength. By meeting the boiler code, the factor of safety on ultimate is 4.0 and on yield, 1.8, during ground operations. While on orbit, the factor of safety on ultimate is 2.9 and on yield, 1.3. The reduction in the on-orbit factors of safety is due to the increase in the pressure differential across the vessel since the on-orbit ambient pressure is essentially zero. As noted, the on-orbit yield factor of safety is 1.3 instead of a possible minimum design factor of 1.1. Because of this difference, a weight penalty of approximately 18 percent is incurred. This translates to 6 lb and, as shown in section 5.5.1.1 of this report,

has a minimal effect on the thermal-mass-to-volume (M/V) ratio.

- (3) PV length = 51.5 in.
- (4) PV diameter = 32.5 in.
- (5) PV wall thickness = 0.061 in. (minimum)
- (6) PV volume = 21.04 ft³
- (7) Four electrical feedthroughs
- (8) Eight plumbing penetrations
- (9) External heaters

The receiver tank is attached to the spacecraft structure with 10 struts instead of 16 as in the case of the supply tank module. This is possible because the large receiver tank module is much lighter than the supply tank module. Eight struts (31.1 in. each) are used to stabilize the tank in the longitudinal and lateral directions, and two struts (33.9 in. each) are used to stabilize the tank in the torsional direction. The struts are made of S-2 glass (0.040-in. wall) with stainless steel end fittings. This configuration was selected to reduce weight and lower thermal conductivity. A goal of the design was to maintain the angle between the strut line of action and a line from the center of the tank near 90°. With the freedom in the end attach fitting and the angle approaching 90°, the stresses caused by contraction and expansion are reduced since the struts are able to rotate about the attachment pivot points. Also, the normal forces induced at the dome/fitting attach point are reduced since the strut force line of action is tangent to the dome.

Table 5.34 shows the weight estimate for the large receiver tank module including the tank, related plumbing and components, and the portion of the radiator tray that is attached to this module. See table A.3 (appendix A to this chapter) for a more detailed mass estimate.

5.5.1.1 Thermal Mass

A low ratio of thermal mass to volume is of interest for experiment purposes. The thermal mass is the mass of that portion of the system that affects chilldown and fill. The thermal mass is estimated by subtracting the mass of the MLI, MLI can, and half the mass of the struts from the tank assembly mass. By using the weights and vessel volume given in table 5.34, the thermal-mass-to-volume ratio, M/V, is estimated as noted in table 5.35.

If the pressure vessel were designed to a yield factor of safety equal to 1.1, the vessel would weigh 32 lb and the mass-to-volume ratio would be 6.4. As previously stated, the effect of

TABLE 5.34.—LARGE RECEIVER TANK WEIGHT ESTIMATE SUMMARY

Component	Weight, lb
Tank assembly	
Pressure vessel	38
MLI CAN	43
MLI	15
Internals	13
Valves, tubing, spray system, struts	98
Subtotal	207
Radiator tray	
Tray	24
Instrumentation, harnesses	21
Valves, tubing	11
Subtotal	56
Total module weight (without structure)	263

TABLE 5.35.—LARGE RECEIVER TANK THERMAL-MASS-TO-VOLUME RATIO ESTIMATES

Thermal mass, lb	141
Volume, ft ³	21.04
Mass-to-volume ratio, lb/ft ³	141/21.04 = 6.7

the difference in weight is minimal even though the design meets the boiler code specifications on the ground.

5.5.1.2 Large Receiver Tank MLI Can/MLI Insulation Blanket

The MLI can (figs. D.29 and D.30 in appendix D to this chapter) supports and thermally isolates the multilayer insulation (MLI) from the receiver tank. The can is very similar in design to the supply tank MLI can which simplifies the structural and thermal analyses. It consists of a 0.375-in. 5056-aluminum-honeycomb core bonded to 0.020-in. 2024 aluminum face sheets with an epoxy-polyamide resin. The honeycomb cell size is 0.25 in. and the foil thickness is 0.001 in. Additional detailed analysis may indicate that a thinner core is possible. Aluminum was selected for its high thermal conductivity. This characteristic is necessary to wash out any concentrated heat inputs to the can and subsequently to the receiver. The MLI can is cylindrical with truncated cone domes. The overall length is 64.5 in. and the diameter is 37.5 in. The can is supported by sleeves attached to the receiver struts and designed to distribute the load of the MLI can and insulation over the strut. The sleeves also thermally ground the struts to the MLI can to shunt heat into the can instead of directly to the tank. The MLI can has a vent door located aft on the cold side (positive z) of the spacecraft. The door is spring-loaded closed with a fixed flow area when closed to ensure a venting area at all times. The vent door is covered with blankets of MLI to reduce radiation loss.

The multilayer insulation for the large receiver consists of two blankets each approximately 0.5-in. thick. Each blanket

has 40 layers. The outer and inner most layers consist of a laminate of Nomex scrim sandwiched between two layers of Kapton. This material was selected for its low weight and rip-resistant features. The other layers are Kapton with vapor-deposited aluminum on both surfaces. The layers are separated by Dacron net spacers.

The blankets overlap at all seam locations and are held in place by nylon positioning pins and grommets. A five-layer MLI blanket is also used to cover the positioning pins and seams. In addition to pins and grommets, hook-and-loop (Velcro) fasteners are used between the MLI can and blankets to hold the seams together. The MLI is electrically grounded to the spacecraft.

5.5.1.3 Tank Internals

The large receiver tank contains a tangential and axial spray system, a pressurant diffuser, a vent line, and a liquid acquisition device (LAD) with an instrumentation tree attached (fig. D.31 in appendix D to this chapter).

The tangential spray system (fig. D.32 of appendix D to this chapter) consists of four nozzles, 0.25-in.-o.d. tubing, and tubing/LAD support clips. The spray tubing penetrates the tank at the aft dome of the tank, runs up the two aft instrumentation tree legs, and terminates at the LAD channel attach points. At these points, there are two sets of nozzles, two nozzles per set, 180° apart. The vertical distance between a pair of nozzles is

13 in. They are equally spaced on either side of the tank horizontal centerline. The spray pattern is planar and directed toward the tank wall, downstream of each LAD channel leg, at an angle of approximately 15°. There are two axial nozzles, one located in the forward dome and one located in the aft dome, to accommodate covered and uncovered flow with a unidirectional settling force. Each nozzle sprays with a full cone angle of approximately 60°. The pressurant diffuser is required to preclude direct impingement of high-velocity gas on the bulk liquid. The diffuser is conical which enables the axial spray inlet tube to be concentric with the diffuser and allow both the pressurant and axial spray inlets to be coincident with the tank centerline. Four 37-pin electrical feedthroughs are located on the aft dome of the receiver tank. These feedthroughs accommodate the many internal instrumentation sensors, both liquid/vapor and temperature.

5.5.1.4 Liquid Acquisition Device (LAD) Configuration

The LAD (fig. 5.31) consists of two legs that follow the internal surface of the pressure vessel. It is constructed from 5083 aluminum and contains two manifolds, a passive TVS, and a fine screen. Aluminum was selected for its light weight and compatibility with the aluminum tank.

The LAD is constructed by welding several triangular shaped channels together following the McDonnell-Douglas design outlined in reference 18. The bottom of the channel

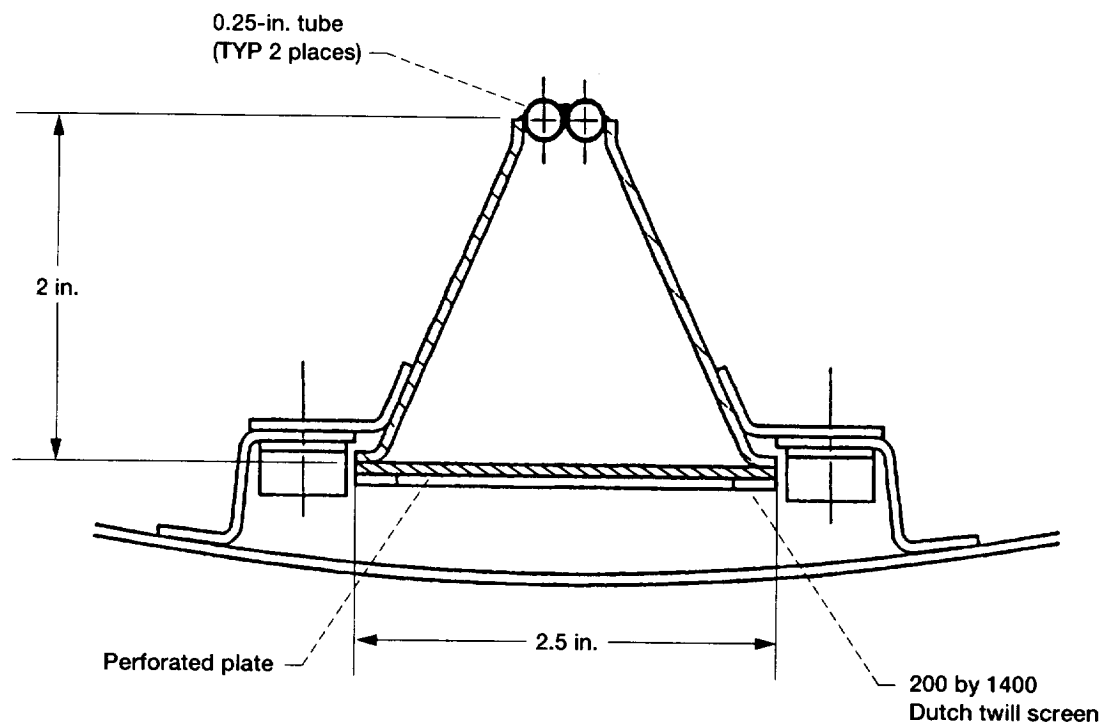


Figure 5.31.—Cross section of large receiver tank LAD.

includes a screen surface through which bulk fluid is acquired. The screen is supported by a beaded perforated plate. The TVS tubes are located at the channel apex. During assembly, the channel side walls of a single segment are formed with two pieces of aluminum welded together. All the segments of each channel leg are then connected and the TVS tubes are welded along the apex. Then the perforated plate is welded to the side walls along the length of the channel. The screen bottom will be constructed as a series of screen patch assemblies approximately 5.0 in. long. Each screen patch will be lined on its edges with a ribbon of 0.01-in. aluminum which extends approximately 0.25 in. outside its perimeter. This ribbon allows for welding of the patches to the side walls and to each other. The patches are attached to the channel one at a time. In order to maintain dependable performance, a fine screen (200 by 1400 Dutch twill) is used.

The LAD contains two manifolds, one at each of the domes. Both forward and aft manifolds are similar in design. The triangular channel legs are welded to the manifolds. The forward manifold includes the LAD fill and outlet, and the TVS inlet, and accommodates the pressurant diffuser and axial spray. The TVS flow proceeds around the legs of the LAD (counterflow), and exits at the forward dome. The bottom manifold accommodates a centerline axial spray tube.

5.5.1.5 Instrumentation Tree

The large receiver instrumentation tree (fig. 5.32) consists of 1- by 0.5-in. aluminum channels fastened to the LAD channels. By attaching the tree legs to the LAD channels, one creates an integral assembly that allows for system checkout and facilitates the final assembly process. The tree includes 31 liquid vapor sensors and 19 temperature sensors.

5.5.1.6 Valve Panels

There are two valve panels (fig. 5.33) associated with the large receiver tank. One panel is mounted to each dome. The panels are made of 5083 aluminum, and each is attached to the dome by six support legs which not only provide structural support but also distribute the heat input to the tank from the wiring and plumbing. The weight of each valve panel is approximately 20 lb. The forward dome valve panel is designated panel L and contains the following components: four cryogenic valves, two relief valves, one J-T device, one check valve, four pressure transducers, four temperature sensors, and one flowmeter. The aft dome valve panel is designated panel K and contains three cryogenic valves, two pressure transducers, and two temperature sensors.

The design of the experiment system has been through several iterations, so that the layout of the valve panels may not correspond to the latest fluid schematic. The valve panel designs are close enough in size, mass, and number of components that another design iteration was not deemed effective at

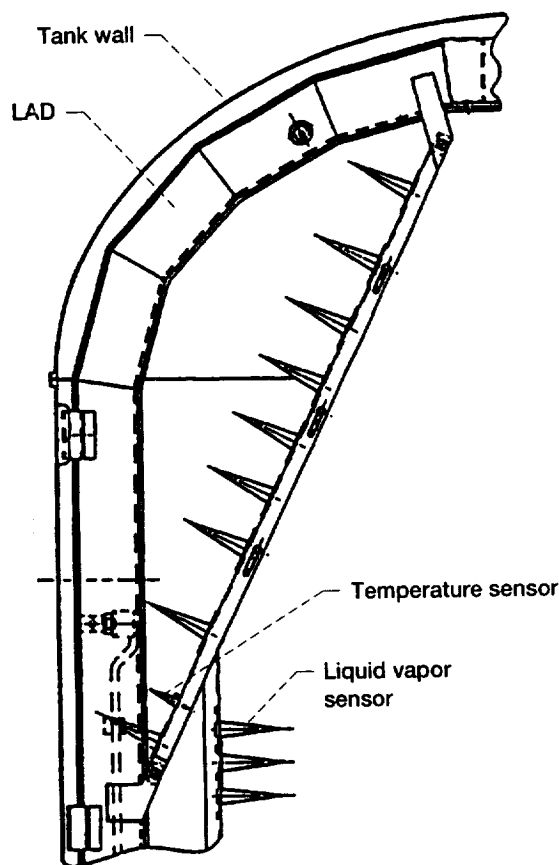


Figure 5.32.—Large receiver tank instrumentation tree (partial).

this stage. Sufficient margins have been included to make this design conservative.

5.5.1.7 External Heater

Heaters are required to provide the desired heat fluxes for the pressure control experiments. Thin flexible heaters with the same basic design as those on the supply tank are used on the large receiver tank. (See section 5.3.1.1.4.)

5.5.1.8 Final Assembly

The large receiver tank was designed in a modular fashion. The internals are prefabricated assemblies that can be test-verified prior to installation in the vessel. The valve assemblies are also prefabricated and test-verified prior to installation. The final installation sequence allows for continuous system checkout as the process continues. The final assembly sequence (fig. 5.34) is as follows:

- (1) Attach instrumentation tree and tangential spray system to LAD

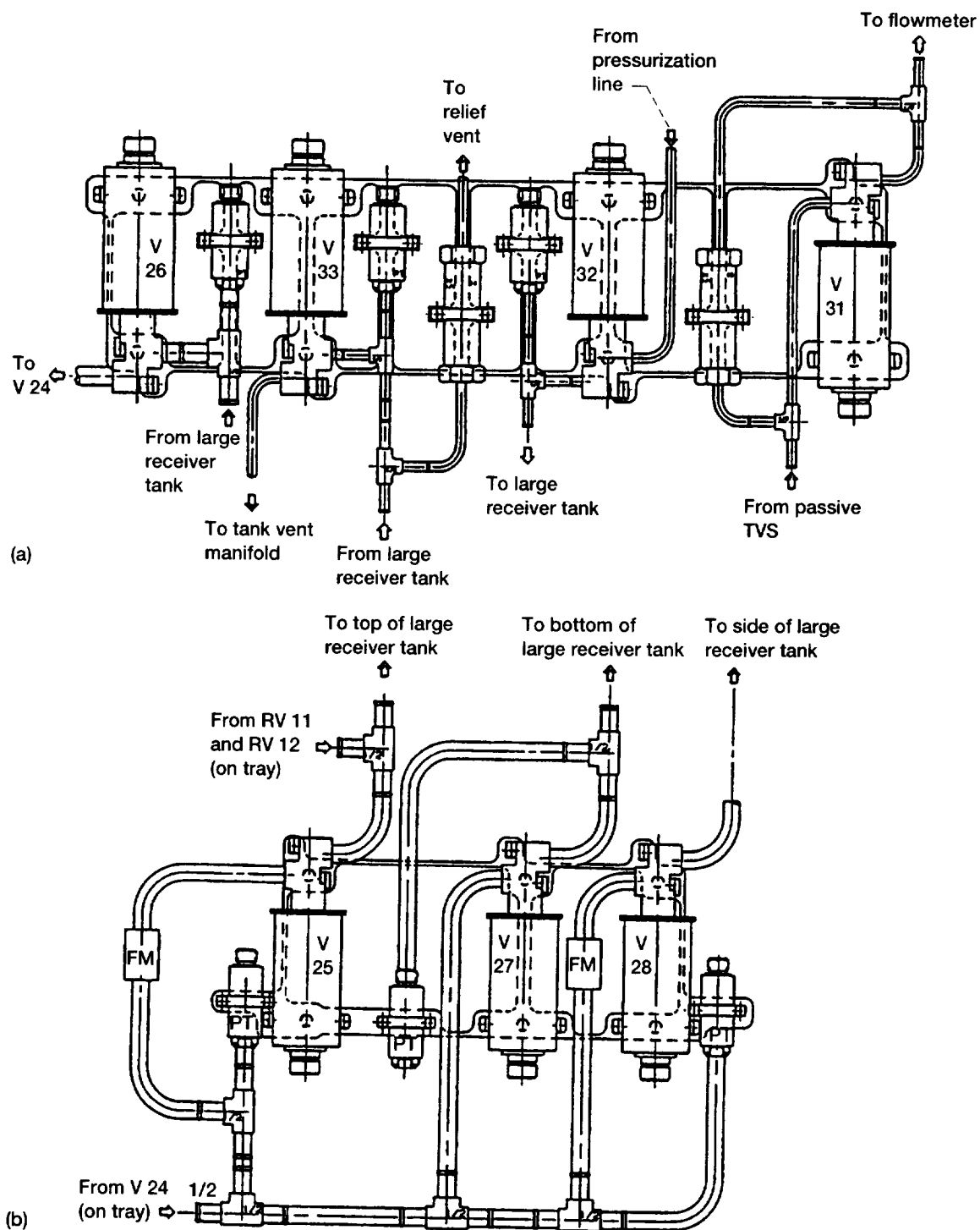


Figure 5.33.—Large receiver tank valve panels. Dimensions are in inches. (a) Panel L (forward dome). (b) Panel K (aft dome).

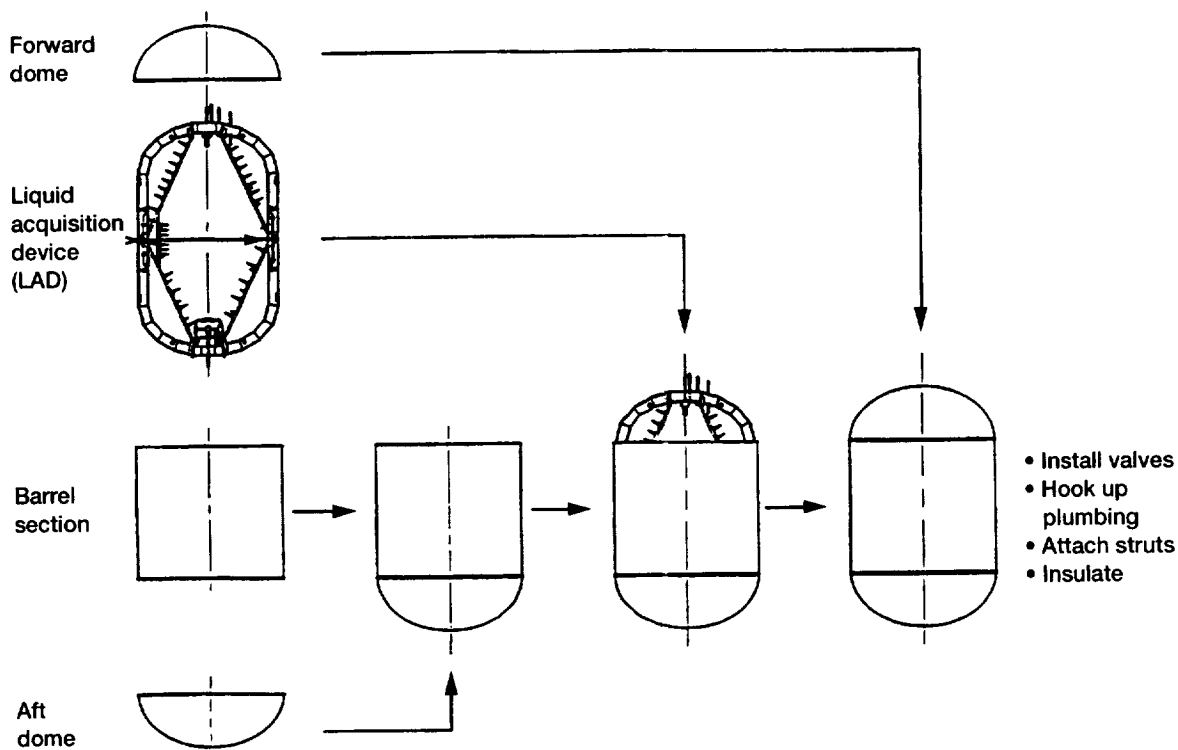


Figure 5.34.—Large receiver tank assembly sequence.

- (2) Weld aft dome to cylinder
- (3) Install LAD system and attach to tank wall
- (4) Mate electrical connectors
- (5) Perform electrical continuity check
- (6) Weld forward dome to cylinder
- (7) Complete plumbing penetration welds on domes
- (8) Leak check tank
- (9) Install external valve panels on domes

5.5.2 SMALL RECEIVER TANK DESCRIPTION AND CHARACTERISTICS

The following requirements controlled the design of the small receiver tank:

- (1) Nearly spherical
- (2) Length-to-diameter ratio, L/D , 0.8 to 1.2
- (3) Diameter, 3 ft
- (4) Tangential spray system
- (5) Radial spray system
- (6) Axial spray system
- (7) External wall-mounted heat exchanger
- (8) Direct vent to vacuum, minimum obstruction
- (9) Baffled hydrogen inlet/outlet
- (10) Straight pipe pressurant diffuser
- (11) Liquid/vapor sensors
- (12) Temperature sensors

The final configuration meets the requirements and has the following characteristics (figs. D.33 and D.34 in appendix D to this chapter):

- (1) Nearly spherical vessel short barrel section (6 in.) with ellipsoidal heads
- (2) Material, 5083-0 aluminum
- (3) Length, 31.5 in.
- (4) Diameter, 36.0 in.
- (5) Thickness, 0.067 in.
- (6) Volume, 13.55 ft³
- (7) Three electrical feedthroughs
- (8) Five plumbing penetrations

Like the large receiver tank, the design of the small receiver vessel is in accordance with the ASME Boiler and Pressure Vessel Code Section VIII, Division I (ref. 3). By meeting the boiler code standards, the amount of testing required is reduced with the penalty being a slight increase in the vessel weight. The effect of the weight increase is minimal as demonstrated in section 5.5.2.1 herein.

The receiver is attached to the spacecraft structure with 10 struts. The length of each strut is 15.4 in. Like the large receiver and supply tank, the struts are made of S-2 glass (0.040-in. wall) with stainless steel end fittings. This configuration was selected because of weight considerations and combined lower thermal conductivity. Also, the same design

TABLE 5.36.—SMALL RECEIVER TANK MODULE WEIGHT ESTIMATE SUMMARY

Component	Weight, lb
Tank assembly	
Pressure vessel	29
MLI CAN	35
MLI	12
Internals	11
Valve, harnesses, spray system, struts, instrumentation	91
Subtotal	178
Radiator tray	
Tray	9
Valves, tubing, instrumentation, harnesses, connectors	13
Subtotal	22
Total module weight	200

considerations for thermal stresses and dome/attach fitting normal forces were used for this receiver configuration.

Table 5.36 shows the weight estimate for the entire small receiver tank module including the tank, related plumbing and components, and the portion of the radiator tray that is attached to this module. See appendix A for a more detailed weight estimate.

5.5.2.1 Thermal Mass

The thermal mass is estimated by subtracting the mass of the MLI, MLI can, and half the mass of the struts from the tank assembly mass. The thermal mass-to-volume ratio, M/V , can be calculated as

Thermal mass, 123 lb

Volume, 13.55 ft³

Mass-to-volume ratio, M/V , $123/13.55 = 9.0 \text{ lb/ft}^3$

If the pressure vessel were designed to a yield factor of safety of 1.1, the vessel would weigh 25 lb and the M/V ratio would be 8.8. As previously stated, the effect of the difference in weight is minimal even though the design meets the boiler code specifications.

The MLI can and MLI blanket (figs. D.35 and D.36 of appendix D to this chapter) for the small receiver tank are the same configuration as for the large receiver tank with the exception of the size. The overall length of the can is 44.5 in. and the diameter is 40.0 in. The addition of the MLI blankets adds 2 in. to the overall length and diameter. The can is also supported from the struts in the same manner as the large receiver tank. (See section 5.5.1.2 herein.)

5.5.2.2 Internals

The small receiver tank contains tangential, axial, and radial spray systems, pressurant and vent lines, an inflow/outflow

baffle, and an instrumentation tree (fig. D.37 of appendix D to this chapter). The tangential spray system inlet penetrates the aft dome, and the tubing is supported internally by the radial spray support tube and cross-member channel. There are two spray nozzles 180° apart with a planar spray pattern directed toward the vessel wall at approximately 15°. There is a single axial nozzle penetrating the aft dome and baffle plate, which sprays with a full cone angle of approximately 60°. This nozzle is located 1.8 in. off the tank centerline. The radial spray inlet penetrates the aft dome, also 1.8 in. off the tank centerline.

Internally, the radial nozzles are attached to a 1-in. square tube. There are three sets of four nozzles, equally spaced longitudinally with each nozzle spraying with a full cone angle of approximately 60°. The pressurant inlet and vent are combined into a single line penetrating the forward dome. In accord with the requirements, the inlet is basically a straight pipe. The exit of this pipe is positioned at the 95-percent fill level and also acts as the inlet to the tank vent. One of the requirements for the vent is that it be capable of dumping the fluid to space as directly as possible with minimum restrictions in the line. To meet this requirement and to minimize the effects of a possible propulsive vent force, the vent line is exited at the forward dome along the x-axis of the spacecraft. To further reduce the effects of a potential propulsive vent force, a 360° fluid deflection cap is incorporated on the exit of the vent line to create a balanced vent.

The instrumentation tree is made from 1- by 0.5-in. aluminum channels attached to the baffle plate and the tangential spray tube support channel. The tree contains 24 temperature sensors and 40 liquid vapor sensors.

The flow baffle plate is 22.5 in. in diameter and has a two-fold purpose. One is to retard the ingestion of vapor at the tank outlet during a low-g fluid transfer. This enhances the outflow process and reduces the amount of residuals in the tank. The baffle also prevents a geyser from occurring during the tank filling process. The design of the baffle follows the guidelines of NASA TM X-2631 (ref. 19). The design philosophy of the internals was to maintain the vessel internal wall surface as bare as possible.

5.5.2.3 External Heat Exchanger

The external TVS system is sized at twice the receiver tank heat leak. The inlet side of the J-T device is located next to the pressure vessel wall to promote liquid delivery to the TVS. The flow exits the tank at the forward dome and is routed around the receiver tank through approximately 40 ft of 0.25- by 0.022-in. aluminum tube attached to the tank wall. The attachment is accomplished by welding the tube to the tank wall at prescribed locations with the same weld technique required for the dome strut pads. The flow should be completely vaporized at or above the 5-psia saturation temperature (30.8 °R) before it is routed to the 1.5-psia vent system.

5.5.2.4 External Heater

Heaters are required to provide the desired heat fluxes for the pressure control experiments. Thin flexible heaters with the same basic design as those on the supply tank are used on the small receiver tank. (See section 5.3.1.1.4.)

5.5.2.5 Valve Panels

There are two valve panels associated with the small receiver tank (fig. D.38 of appendix D to this chapter). One panel is mounted to each dome. The panels are made of 5083 aluminum, and each is attached to the dome by six support legs which not only provide structural support but also distribute the heat input to the tank from the wiring and plumbing. The weight of each valve panel is approximately 20 lb. The forward dome valve panel is designated panel N and supports the following components: five cryogenic valves, one relief valve, four pressure transducers, three temperature sensors, and two orifices. The aft dome valve panel is designated panel M and contains four cryogenic valves, four pressure transducers, four temperature sensors, and a J-T expansion device.

5.5.2.6 Final Assembly

The small receiver tank, like the large receiver tank, was designed in a modular fashion. The internals are prefabricated assemblies that can be test-verified prior to installation in the vessel. The valve assemblies are also prefabricated and test-verified prior to installation. The final installation sequence allows for continuous system checkout as the process continues. The final assembly sequence (fig. 5.35) is as follows:

- (1) Assemble the internal instrumentation tree, tangential spray system, and baffle plate
- (2) Install external TVS heat exchanger to forward dome, weld forward dome to cylinder
- (3) Install instrumentation tree assembly, mate internal electrical connectors, perform electrical continuity check
- (4) Install external heat exchanger to aft dome, weld aft dome to cylinder
- (5) Complete plumbing penetration welds on domes, leak-check tank, and install external valve panels on domes

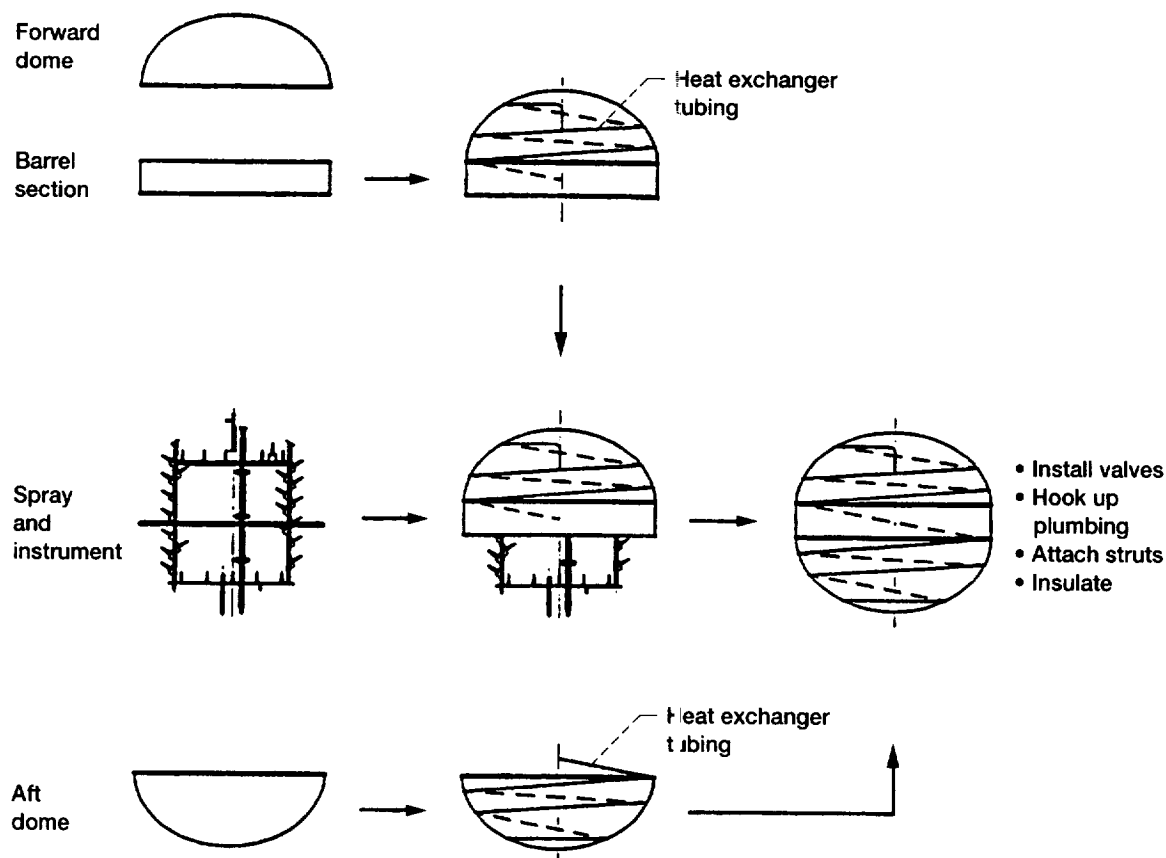


Figure 5.35.—Small receiver tank assembly sequence.

5.5.3 ANALYSIS OF THE RECEIVER TANKS

The following sections describe mechanical and thermal considerations used in the design of the two receiver tank assemblies.

5.5.3.1 Structural

Using the same rationale as for the supply tank (see section 5.3.2.1.1), aluminum 5083-0 was selected as the material for the receiver tanks and filament-wound S-2 glass/epoxy for the supporting struts.

The sizing of the receiver tank walls was done in accordance with ANSI/ASME BPV-VIII-1 (ref. 3) and governed by the internal pressure load of 52 psia for both the on-ground and on-orbit conditions. The tank wall thicknesses of 0.061 and 0.067 in. for the large receiver tank and small receiver tank, respectively, were determined using the room temperature allowable stress of 10 000 psi. The thermal stresses induced during the liquid hydrogen filling process were also accounted for in the tank wall sizing. The ground condition equivalent factors of safety are 1.8 for yield and 4.0 for ultimate. For the on-orbit condition, the factors of safety are reduced because of the reduction of the ambient pressure and consequent increase in the pressure differential across the vessel. The on-orbit values are 1.3 for yield and 2.9 for ultimate.

The large and small receiver tanks are both individually supported by ten struts. Four pairs of these struts form a "V" with the apexes attached to the spacecraft structure and the opposite ends attached to the forward and aft domes. These struts are used to support the tank in the longitudinal, lateral, and bending directions. The remaining two struts are horizontal, 180° apart, and are attached to the spacecraft structure and the cylindrical portion of the tank, nearly tangential to the shell. These struts are used to stabilize the tank in the torsional direction.

The tubular struts for both the large and small receivers have an outside diameter of 1.0 in. and a wall thickness of 0.04 in. The lengths of the struts from pin to pin are 31.1 and 33.9 in. for the large receiver tank, and 15.4 in. for the small receiver tank. The critical buckling force for the large receiver tank supporting struts is 1137 lb versus its maximum compressive

force of 356 lb during launch. Similarly, the critical buckling force for the small receiver tank supporting struts is 4635 lb versus its maximum compressive force of 268 lb during launch. At the same time, the maximum normal stress for all the struts is 16 000 psi during launch versus its compressive proportional limit stress of 63 000 psi. For more details on the structural analyses of the receiver tanks see table A.4 in appendix A to this chapter.

5.5.3.2 Receiver Tank Thermal Analysis

No detailed SINDA85 thermal model of either the large or small receiver tanks was developed. However, hand calculations of heat flux to both receiver tanks via all possible conduction paths were performed (tables 5.37 and 5.38).

Radiation heat flux to the receiver tanks came exclusively through the MLI layer. The Lockheed formulation (ref. 13) gave the values of k to be used in the linear heat transfer relation

$$Q = \frac{kA}{L}(T_H - T_c)$$

where

- Q heat transfer rate
- A area of MLI blanket
- L heat path length through MLI
- T_H obtained from external spacecraft thermal modeling data
- T_c temperature of receiver MLI can (assumed equal to supply tank can temperature)

All manganin wires and all phosphor-bronze wires were grouped together into single conductors. The endpoint temperatures of these bundles, which ran from the thermal tray (−100 °F) to the receiver tank (−423 °F) were known, so the T_H and T_c of the linear heat flux relation were known. The thermal conductivity k used was the average value along the wire length L . The cross-sectional area A of heat flow was the combined area of all wires in the bundle.

TABLE 5.37.—LARGE RECEIVER TANK THERMAL CHARACTERISTICS^a

Source	Heat leak, Btu/hr	Notes
Radiation	9.3	80 layers MLI, 1.1 in. thick
Struts	0.1	10 fiberglass struts; length, 30 in.
Manganin wires	.4	300 wires, 24 AWG; length, 4 ft
Phosphor-bronze wires	.2	22 wires, 18 AWG; length, 4 ft
Plumbing	1.6	Length, 6 ft stainless steel; 3 by 1/4 in.; 5 by 1/2 in.
Total	11.6	Tray temperature of −100 °F

^aBy using a pressure vessel area of 38.92 ft², we obtain an average heat flux of 0.3 Btu/hr-ft².

TABLE 5.38.—SMALL RECEIVER TANK THERMAL CHARACTERISTICS^a

Source	Heat leak. Btu/hr	Notes
Radiation	7.5	80 layers MLI, 1.1 in. thick
Struts	0.4	10 fiberglass struts; length, 12 in.
Manganin wires	.4	250 wires, 24 AWG; length, 3 ft
Phosphor-bronze wires	.3	20 wires, 18 AWG; length, 3 ft
Plumbing	1.9	Length, 4 ft stainless steel; 3 by 1/4 in.; 4 by 1/2 in.
Total	10.5	Tray temperature of -100 °F

^aBy using a pressure vessel area of 27.69 ft², we obtain an average heat flux of 0.4 Btu/hr-ft².

Plumbing attachments were treated similarly to the wire bundles, except a heat flux calculation was performed for each individual plumbing line.

Struts were treated similarly to wires and plumbing, except that they originated at the generalized spacecraft structure (boundary with $T = 0$ °F) rather than the radiator tray.

A coarse receiver tank model was developed, by using

- (1) A coarsely divided tank, honeycomb, and MLI layer
- (2) One gross plumbing attachment, spacecraft to pressure vessel
- (3) One gross wiring attachment, spacecraft to pressure vessel
- (4) Heat rates from the external TRASYS model
- (5) Radiation conductors from the internal TRASYS model

With the MLI can at -50 °F and the receiver tank at liquid hydrogen temperature, it took approximately 5 hr for the system to equilibrate, with $Q/A = 0.272$ Btu/hr-ft² and an MLI can temperature of -101 °F (fig. 5.36)

5.5.4 MANUFACTURING

The manufacture of the thin-walled pressure vessels was investigated and discussed at length with vendors. The responses indicated that these vessels can be fabricated as previously described. The domes will be spun to a given minimum thickness and machined to remove the spinning process ridges. This is necessary to attain a surface finish compatible with thermal radiation requirements and to remove possible contaminant entrapment regions. The cylindrical sections will be rolled, butt-welded along the seam, and machined for surface finish characteristics and thickness requirements. During the final assembly process, the domes will be butt-welded to the cylindrical sections by the use of fixtures and standard welding processes. This includes an internal thin ring at the weld joint to preclude weld contaminants from entering the tank. The ring then becomes an integral part of the weld joint. If the tank must be reopened subsequent to welding, the weld joint can be cut either through the weld seam or slightly off the seam on the cylinder and then rewelded using the same

initial process. The effect on the length of the tank and its volume by this reopening/closing process is determined by the width of the cut and is minimal. All other parts can be manufactured and assembled by using standard procedures and processes.

5.6 Experiment Instrumentation and Electronics

The experiment system instrumentation and electronics system design begins with the transducers required to convert physical process parameters such as temperature, pressure, flow rate, and acceleration into electrical equivalent signals. The transducers require electrical excitation signals which are provided by power supplies contained in the signal conditioning electronics. The output signal of the transducers must be conditioned to a form compatible for input to the spacecraft telemetry system. This is accomplished by signal converters, amplifiers, filters, and analog-to-digital converters. The experiment system contains three high-resolution, 12-bit, analog-to-digital converter signal conditioning units called experiment data units (EDU's). The instrumentation and electronics system also includes wire harnesses, sensor mounting hardware, heaters, a liquid level capacitive probe signal conditioning unit, accelerometers, and fluid mixer power unit. Table 5.39 lists the experiment system electronics boxes and their estimated properties.

5.6.1 TELEMETRY, TRACKING, AND COMMAND (TT&C) INTERFACE

The experiment instrumentation and electronic system interfaces with the spacecraft TT&C system. The TT&C system contains CTU's and RCTU's which provide sensor excitation, and 8-bit analog-to-digital signal conversion for the experiment instrumentation and electronics system. The TT&C system also contains relay sequencer units which distribute electrical power to the experiment system valves and heaters. Figure 5.37 is a block diagram of the COLD-SAT experiment system electronics and its interface with the TT&C system. The total number of sensors is listed and the number of sensors assigned to each signal conditioner is indicated.

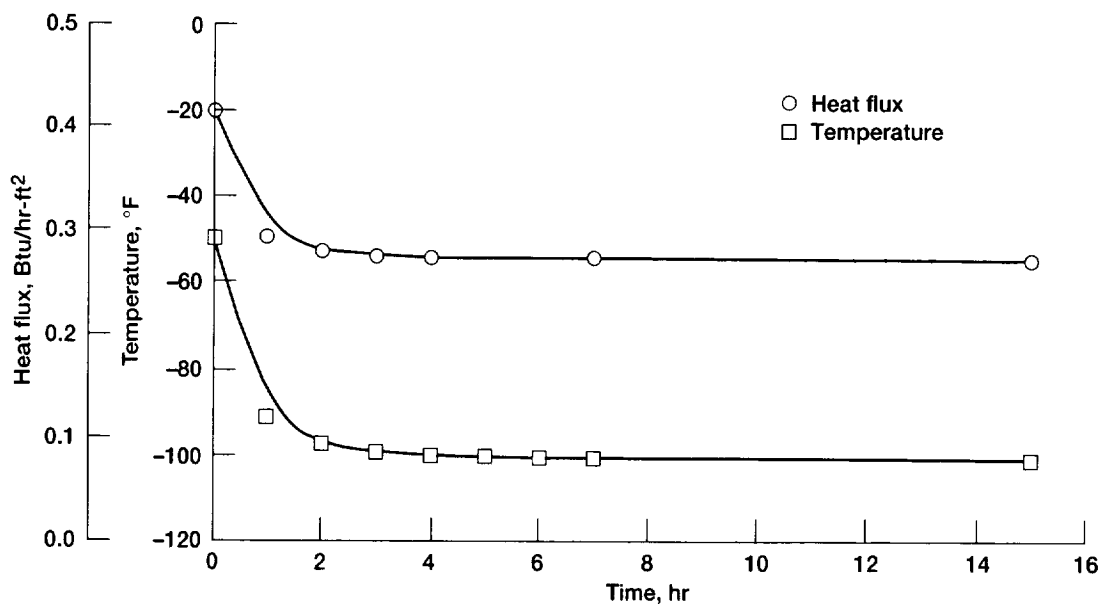


Figure 5.36.—Receiver tank multilayer insulation (MLI) can transient temperature and heat flux.

TABLE 5.39.—EXPERIMENT ELECTRICAL/ELECTRONICS BOXES

Item	Number	Location	Weight (each), lb	Power (each), W
Experimental data units	3	Electronics bay 2	7	15
Accelerometer data unit	1	Electronics bay 2	6	10
Mixer motor power unit	1	Electronics bay 2	7.5	15
Signal condition power unit capacitive probe	1	Electronics bay 1	12	15

5.6.2 ELECTRICAL SYSTEMS INTERFACE

The experiment electrical/electronic boxes receive power from the spacecraft electric power system. Heaters and instrumentation receive controlled and conditioned electrical power through the TT&C system which is powered by the electrical power system.

5.6.3 SIGNAL CONDITIONING SYSTEMS AND LIMITATIONS

The TT&C system's command and telemetry units (CTU's and RCTU's) provide the majority of the power and data acquisition electronics for the COLD-SAT experiment instrumentation. The inaccuracies of the measurement electronics must be considered in the selection of a sensor and included in the measurement error analysis. Table 5.40 lists the combined,

worst-case excitation and data acquisition errors of a typical flight-qualified data acquisition system. The errors are combined using the root sum square (RSS). These error values were utilized to approximate overall measurement accuracies obtainable for the transducer candidates used with space-flight-qualified signal conditioning systems.

5.6.3.1 Basic Instrumentation and Signal Conditioning Operation

Figure 5.38 shows a block diagram of a basic measurement system. Physical parameters such as temperature, pressure, flow, and acceleration are converted to electrical signal equivalents by the instrumentation transducers. Large numbers of similar transducer measurements are to be made, and the CTU's and RCTU's use multiplexers to electronically switch a specific sensor's output to the signal conditioning circuitry.

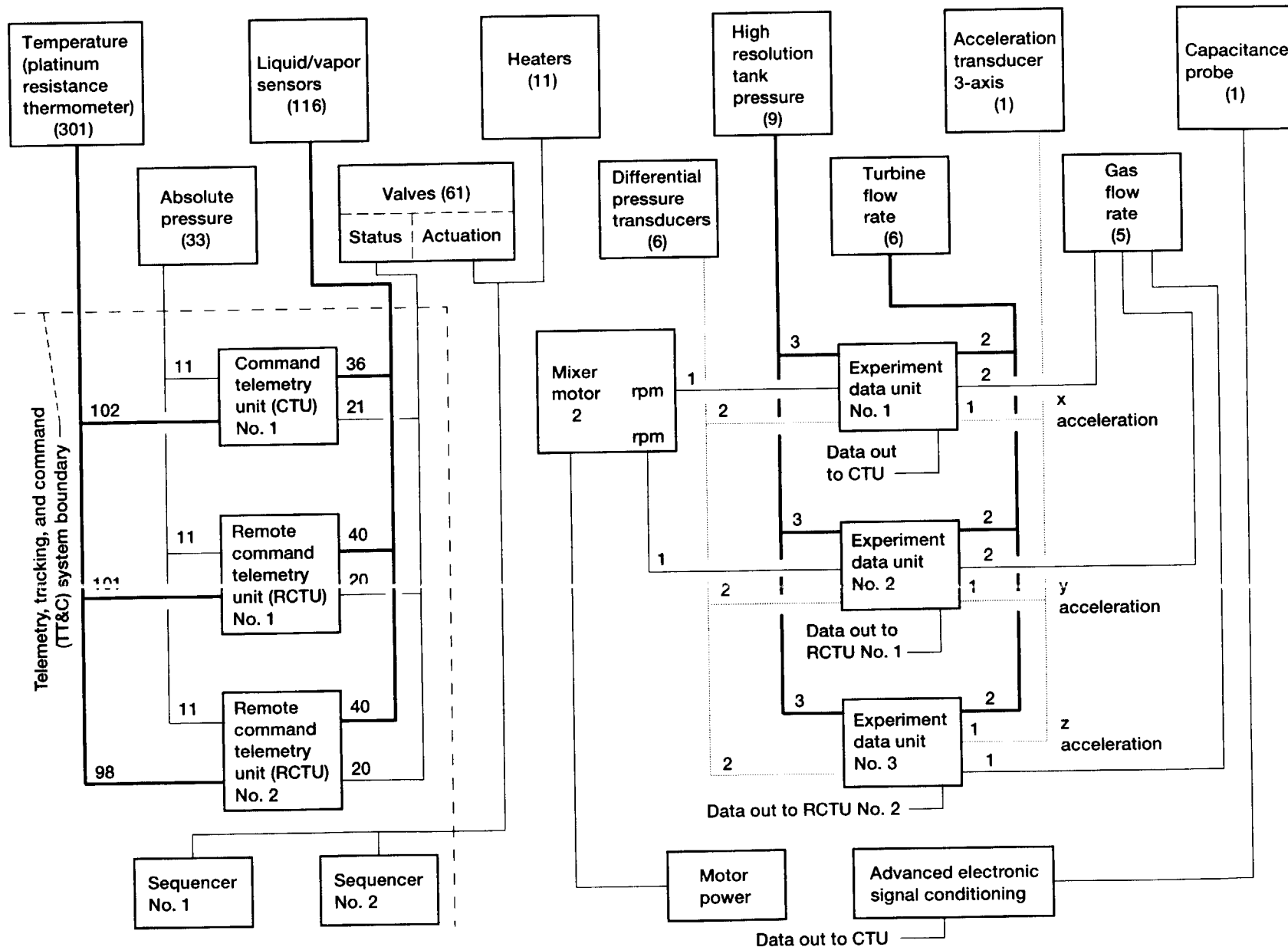


Figure 5.37.—Simplified block diagram of experiment system instrumentation and electronics. Numbers indicate number of signals except when in parentheses, which indicates total quantity.

TABLE 5.40.—TT&C VOLTAGE MEASUREMENT
ERROR RANGES

Voltage range	Root sum square error, percent of full scale	Root sum square error, mV
10 mV	1.79	0.179
30 mV	0.68	.204
125 mV	.36	.455
1.25 V	.27	3.340

This results in a reduction of hardware and savings in weight, power, and cost. The system uses eight dual 4-channel multiplexers per card which allow 32 double-ended measurement channels.

Multiplexers are not ideal and have leakage current components. The voltage drop developed across resistive components in the multiplexer circuits by these leakage currents contribute to the circuit measurement error. The multiplexed output level of the transducer is fed to an instrumentation amplifier stage where the signal is converted to a 0- to 5-V level. The analog output of the amplifier stage must be converted to an equivalent digital form for the telemetry system. This process is performed by analog-to-digital (A/D) converters. The system's use of 8-bit A/D converters sets the measurement resolution to 1 part in 256 of its nominal analog range. The measurement range can be thought of as being divided into 256 increments starting from zero and increasing in amplitude by increments of magnitude equal to the resolution. The maximum error between the analog input and its digitized equivalent can be as great as one-half the resolution value which is equivalent to ± 0.195 percent of the range. This error component is known as the quantization error.

5.6.3.2 Experimental Data Units (EDU's)

Three experimental data units were designed to provide improved accuracy and resolution to meet measurement requirements incapable of being met by an 8-bit data acquisition system. The hardware of the EDU was assumed identical to the TT&C system except for the use of a 12-bit A/D converter and only one multiplexer per circuit card. These changes would decrease the quantization error to ± 0.012 percent and reduce the multiplexer leakage current error by a factor of 1/8. Figure 5.39 shows pie chart representations of the 8- and 12-bit system error magnitudes for a 30-mV measurement range.

The EDU's provide excitation and signal conditioning electronics for the flow measurement systems, accelerometer, and high-resolution tank pressure measurement transducers as indicated in the block diagram of figure D.39 in appendix D to this chapter. The qualification of a 12-bit A/D converter for space flight use has to occur for this system to be feasible.

5.6.4 EXPERIMENT MEASUREMENT REQUIREMENTS

The type and number of sensors selected was determined from the COLD-SAT experiment requirements. From the primary experiment data requirements the following types of measurements were identified to be necessary:

- (1) High-resolution liquid and gaseous hydrogen temperatures (identified as type A)
- (2) Tank structure temperatures (identified as type AB)
- (3) Hydrogen liquid/vapor level
- (4) Liquid/vapor two-phase flow detection
- (5) Tank pressures and flow device pressure drops
- (6) Liquid hydrogen flow rates
- (7) Mixer flow rates
- (8) TVS and vent flow rates
- (9) Spacecraft acceleration
- (10) Valve status indication
- (11) Electrical power supplied to heaters and mixers

5.6.5 INSTRUMENTATION SELECTION

Literature surveys, cryogenic instrumentation testing facilities, and instrumentation manufacturers were used to identify sources of instrumentation capable of fulfilling the COLD-SAT experiment measurement requirements. Space-flight-qualified instrumentation and hardware which has been used in, and shown to be reliable in, liquid and gaseous hydrogen environments was also sought and used when at all possible.

A primary transducer type was selected from the candidates for each measurement based on measurement range, accuracy, and reliability. Signal conditioning techniques were selected to achieve best possible measurement accuracy based on a measurement error analysis. Table E.8 in appendix E to this chapter lists the required measurements, measurement range, selected transducer type, and number of transducers proposed. Calculated measurement accuracies and proposed sampling rates are also listed. Detailed descriptions of the instrumentation candidates and measurement error analysis are presented in the COLD-SAT experiment system instrumentation report (ref. 1). A measurement list is also provided in the Instrumentation Report along with drawings of sensor locations.

The transducers, signal conditioning techniques, and electrical harnessing were selected and designed to minimize heat conduction to the cryogenic tanks which could result in excessive boiloff of hydrogen over the course of the mission.

5.6.6 INSTRUMENTATION DESCRIPTION AND ANALYSIS

To minimize cost and risk, during the design, every effort was made to identify existing components. In most cases,

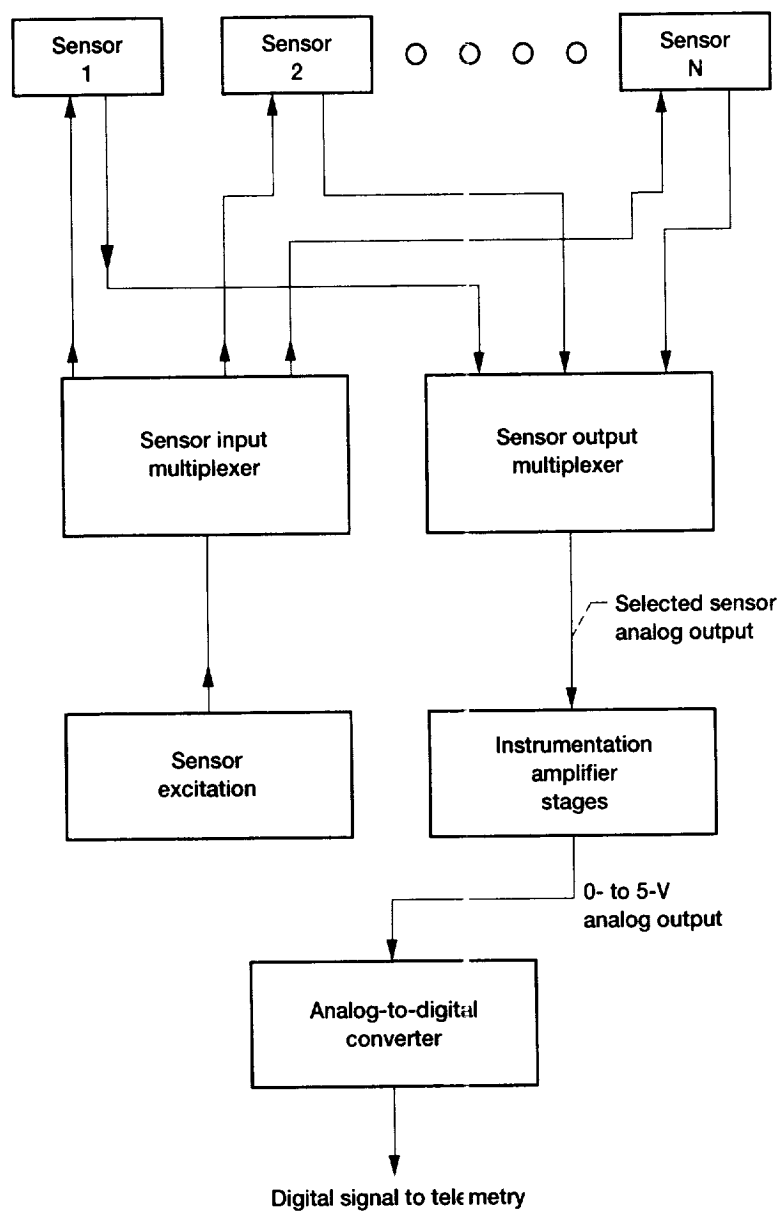


Figure 5.38.—Generic measurement system block diagram.

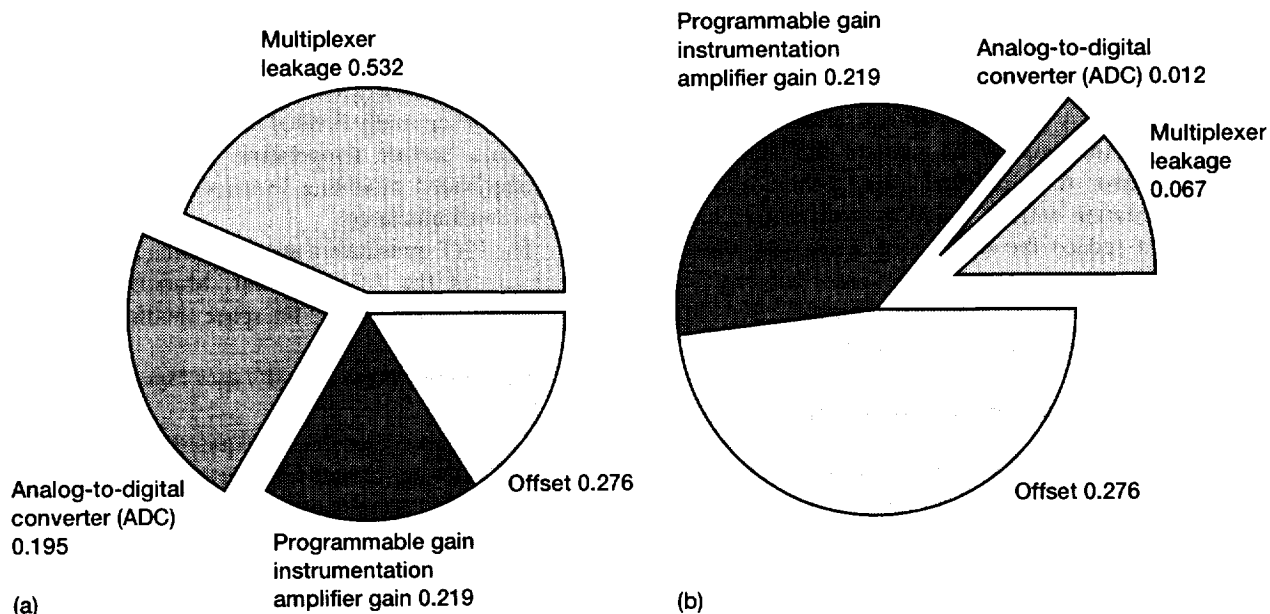


Figure 5.39.—Distribution of major signal conditioning errors of 8-bit TT&C system versus 12-bit EDU system in 30-mV measurement range. Numbers are percentages of error. (a) 8-bit system. (b) 12-bit system.

instrumentation was found that could meet COLD-SAT requirements with little or no modification. Flow measurement was identified as one area where some development was needed. More experience is needed with pressure transducers to determine repeatability over a mission with many thermal cycles. Specific models are not identified in this report to avoid the appearance of NASA endorsement of commercial products.

5.6.6.1 High Resolution Liquid Hydrogen and Gaseous Hydrogen Temperature Measurement Requirements

Measurement of the small temperature gradients that exist from the liquid hydrogen supply tank wall into the bulk of the fluid and also measurement of the temperature gradient existing at the liquid hydrogen-gaseous hydrogen interface is required. Accuracies on the order of ± 0.2 °R are desired. Temperature sensors capable of fulfilling this requirement would also be used for all temperature measurements of structure and fluid in the saturated and subcooled hydrogen temperature ranges. The saturation temperature of hydrogen varies from 30.8 °R at 5 psia to 45.4 °R at 50 psia. This range of pressure covers the operating range of the cryogenic tanks and TVS systems. The temperature measurement accuracy over this range was considered most critical.

Thermocouples, thermistors, diodes, germanium resistance thermometers (GRT's), and platinum resistance thermometers (PRT's) were considered for this measurement. Thermocouples were not recommended because of their low sensitivities ($\mu\text{V}/\text{deg}$) and poor accuracies. Thermistors were not recommended because of their rapidly changing sensitivities and the need for

elaborate signal conditioning systems. Platinum resistance thermometers were recommended over the other candidates because of their extensive space-flight histories and measurement accuracies of ≤ 0.2 °R using a space-flight-qualified 8-bit data acquisition system over the temperature range from 29 to 50 °R.

A modified version of a platinum resistance temperature probe was selected for immersion temperature measurements. This type of sensor has been qualified for space-flight use. It contains a platinum sensing element encased in a 316L CRES cone-shaped probe. The cone shape is designed to wick liquid films away from the sensor tip, minimizing false ullage temperature readings under low-gravity conditions. The probe is very rugged, and the threaded mounting attachment ensures a reliable mount to an instrumentation rake. The present model contains a 300- Ω , ice point (R_0) PRT. The sensor is also supplied with 3-conductor 22 AWG-shielded nickel-clad copper leads. Desired sensor modifications include changing the platinum sensor resistance to a 1000- Ω (R_0) value and changing the wiring to 4 conductors. These changes would increase the sensor sensitivity. Discussions with the manufacturer indicate that such changes are feasible. A similar platinum probe has also been used on Atlas-Centaur vehicles.

To achieve the desired measurement accuracy and resolution, the 1000- Ω ice point sensor will be excited by a 10-mA square wave current pulse provided by the RCTU's. The excitation time required to achieve a steady-state measurement must be experimentally verified but should be less than 1 msec. The sensor would be energized once every 10 sec and would produce a 30- to 150-mV peak output over the 28 to 50 °R temperature range. The effective power dissipated by the

sensor would vary from 0.03 to 0.150 μ W over this temperature range and so self-heating should not be a concern. The sensors will be installed in a four-wire configuration in which two wires provide current excitation and two wires sense the voltage drop directly across the sensor. This method eliminates the wire voltage drop error. A multiplexed wiring technique in which a common excitation wire is shared by four sensors has been developed to reduce the number of wires and connectors penetrating the cryogenic tanks. The sensor output voltage is conditioned to a 0- to 5-V level and digitized by the 8-bit A/D converter of a CTU or RCTU of the TT&C system.

5.6.6.2 Surface Temperature Measurements

High accuracy (± 0.2 $^{\circ}$ R) type A surface temperature measurements are required to monitor the temperature of the tank walls and thermally bonded structure. The information obtained will be analyzed to determine the heat energy conducted and radiated into the various tank systems. Liquid hydrogen transfer lines and TVS lines will require temperature measurements to determine the thermodynamic state of the fluid and the efficiency of the operating systems.

Less accurate surface temperature measurements of the cryogenic tanks, plumbing system, and structure components are required to provide experiment data and operation status information during chilldown experiments and periodically during the course of the COLD-SAT mission. A wide temperature range measurement from 36 to 540 $^{\circ}$ R is required.

Thermocouples, diodes, and PRT's were considered for this measurement and PRT's were recommended for the reasons given in section 5.6.6.1 of this report. Total temperature range measurements can also be made with an inaccuracy of less than ± 2 $^{\circ}$ R by using the dual-range measurement capability of the data acquisition system.

Platinum resistance temperature sensors were selected to perform the surface measurements. The sensor can also be used for immersion measurements such as monitoring the fluid temperature inside a LAD channel. The high-accuracy surface temperature measurements will be achieved by the same method used for the internal fluid measurements discussed previously.

The wide temperature range measurements will be obtained by using 1000- Ω ice point sensors excited by 1-mA current pulse inputs. The total temperature range was divided into two ranges, 29 to 110 $^{\circ}$ R, and 110 to 500 $^{\circ}$ R. The output of the PRT will vary from approximately 5 to 120 mV over the temperature range from 36 to 110 $^{\circ}$ R and 120 to 1100 mV over the temperature range from 110 to 530 $^{\circ}$ R. The input of the data acquisition system uses programmable gain amplifiers which will allow the two temperature spans to be monitored with inaccuracies of less than ± 1.52 $^{\circ}$ R.

Surface temperature sensors must be attached to the structure in a manner such that intimate thermal contact is obtained with adequate strength to withstand thermal cycling and stresses of launch. Sensors will be mounted with adhesives or mounted

in a high thermal conductivity holder that will be attached with screws or spot welded to the structure. The sensor leads can conduct heat energy to the sensor resulting in errors. The wires should be thermally bonded to the structure so that they are at the same surface temperature. Reference reports detailing recommended mounting techniques are available from the sensor manufacturers.

The PRT transducers are the standard surface temperature sensors of the Atlas-Centaur. Models have been flight-qualified for Skylab and the space shuttle.

5.6.6.3 Discrete Point Liquid/Vapor Detection Requirement

Liquid-level detectors are required to determine the level of tank fill during ground-fill operation. In-flight uses include liquid-level determination during periods of settling, two-phase flow detection, and liquid/vapor distribution of tank fluid during the overall course of the mission.

Point liquid/vapor detector candidates include thermoresistive elements such as thermistors, carbon resistors, or resistance thermometers that are operated at a self-heating level. Other methods of determining fluid level include capacitance probes and resistive tape strips. These detectors will give accurate liquid fill level measurement for systems with a well-defined liquid/vapor interface. Inaccurate measurements could result from use of these types of detectors with fluids of a very wetting nature especially while experiencing reduced-gravity conditions. Point-level sensors could also give erroneous indications of liquid presence under reduced-gravity conditions because of wicking of a liquid film over the sensor. To minimize this problem, cone-shaped sensor holders have been developed. The surface tension forces experienced by the fluid result in the wicking of the fluid film away from the sensor located at the tip.

Figure 5.40 shows a drawing of a candidate liquid/vapor detector. The conical shape of this sensor is required for low-gravity measurements. The sensor tip of this probe consists of a vacuum-deposited carbon film on a quartz substrate. A liquid/vapor detector based on this design is recommended for the COLD-SAT experiment system.

The detectors are excited at an electrical power level at which self-heating of the sensor will occur. This causes the resistance of the sensor to be significantly different when immersed in liquid from its resistance when immersed in vapor. The sensor is used in series with a 226- Ω resistor in a voltage divider circuit configuration and excited by a constant 5.15-V source. The change in the voltage at the center tap of the voltage divider is specified to be ≥ 0.6 V within 1 sec after the sensor is withdrawn from a liquid hydrogen state to a gaseous hydrogen state. This voltage level is detected by a comparator circuit located in the RCTU which produces either a high- or low-voltage output dependant on the liquid or vapor state of the measured fluid.

Large quantities of detectors are required to determine the fluid phase throughout the COLD-SAT tanks. To reduce the

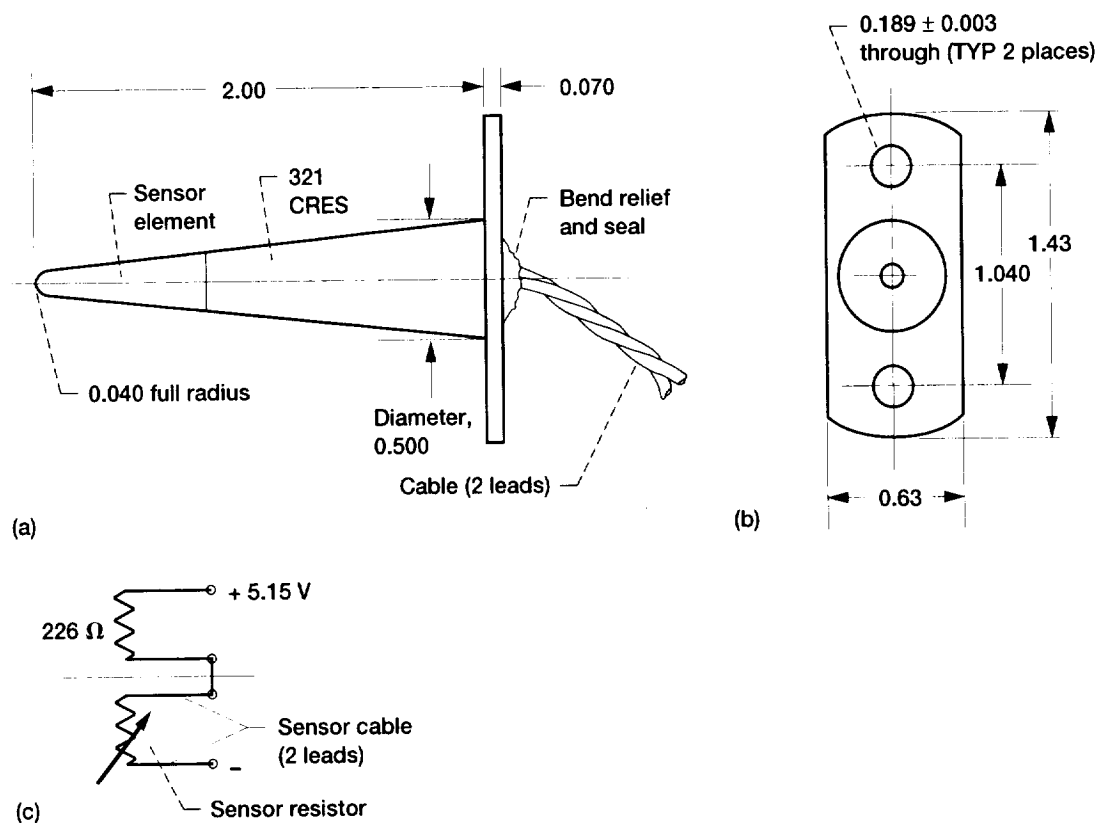


Figure 5.40.—Liquid/vapor sensor. Dimensions are in inches. (Tolerances (except when specified): .x = $\pm .1$, .xx = $\pm .03$, .xxx = $\pm .010$.) (a) Side view. (b) Mounting detail. (c) Electrical schematic.

number of wires and connectors penetrating the tanks, a multiplex wiring technique will be used. This method uses a common excitation wire for every four sensors inside the cryogenic tanks. The specific sensor to be measured is selected by addressing the appropriate switch positions of the multiplexers. The number of wires penetrating the tanks by this method would be one-fourth the number required for individually wired detectors.

The liquid hydrogen level must be monitored during the ground-fill operation. Ground test results indicate inaccuracies in point-level detectors for measuring hydrogen fill level caused by the vigorous boiling of the hydrogen. Capacitance probes however, have performed satisfactorily and are used for liquid hydrogen gauging for the space shuttle power reactant storage assembly. A capacitance probe that will monitor the fill level from 85 to 100 percent is proposed for the COLD-SAT ground-fill measurement.

Two-phase flow detection inside the LAD channels and also at the LAD and vent line exits is required. Thermistors which have very high sensitivities (mV/T) characteristics will be mounted inside the channels or at the entrances to the plumbing lines. The sensors will be excited at a power level such that sensor self-heating will occur. The rate and magnitude of sensor self-heating in vapor will be far greater than when

immersed in liquid because of the large differences in convection coefficients. The output of the sensor will be monitored by a comparator circuit which would indicate either liquid or vapor state.

The flowmeters used on the liquid hydrogen and vent lines should also give two-phase flow indications. Two-phase flow through a turbine meter is generally to be avoided and will cause noticeable speed increases. Two-phase flow through a differential pressure flow metering device should be detectable by pressure surges.

5.6.6.4 Absolute Pressure Measurement Requirements

The absolute pressure of the cryogenic tanks, plumbing systems, and gas pressure supplies must be monitored to determine experiment pressurization rates, system operational status, and fluid thermodynamic state information. Accuracies of ± 0.2 psia are desired for tank pressure control measurements. Accuracies of ± 0.5 psia are required for less critical measurements.

Absolute pressure measurements of the cryogenic tanks present unique problems. Standard temperature range transducers could be employed by tapping into the system with stainless steel tubes. This procedure could result in thermal

acoustic oscillations and also conduct large amounts of heat energy into the cryogen. A transducer capable of operating at the liquid hydrogen temperature range is therefore desired.

A number of companies manufacture cryogenic-rated, absolute pressure transducers. Four such companies which manufacture aerospace-qualified cryogenic transducers are IMO Delaval Inc., CEC Instrument Division, Teledyne Taber Corporation, and Schlumberger Satham Transducer Division. Sputtered, thin-film pressure transducers have been space-flight-qualified and can be compensated for use at liquid hydrogen temperatures.

Strain-gauge pressure transducers that use four strain gauges which are sputtered-deposited on an insulating substrate are suggested for pressure measurements above -65°F . The gauges are connected into a Wheatstone resistance bridge configuration. Pressure causes two of the gauges to tense and the other two gauges to compress resulting in bridge unbalance and a millivolt output that is proportional to applied pressure. The recommended excitation for the transducers is 10 V and the output is 30 mV at full-scale pressure.

Manganin wiring is to be used to minimize the heat energy that is thermally conducted into the cryogenic tanks. The voltage drop across the manganin wire is sufficient to change the voltage actually supplied to the transducer. A second voltage measurement directly at the transducer input terminals must be made to correct for this excitation error. This is undesirable because of the added wiring, weight, and measurements required. To overcome this problem, the transducers will be calibrated and excited by an equivalent current source equal to the recommended excitation voltage (10 V dc) divided by the transducers bridge resistance. A transducer with a bridge resistance of $1000\ \Omega$ would require a 10-mA excitation source, and the same current source design required for the PRT temperature sensors will be used.

The full-scale output of the candidate pressure transducer is 30 mV. Pressure measurements made by the 8-bit data acquisition system would result in a error of ± 0.365 psia for a 50-psia range measurement with a resolution of 0.196 psia. To improve the resolution and accuracy of the tank pressure measurements, three transducers will be dedicated to each cryogenic tank and the output of the transducers will be monitored by the EDU's. This will improve the measurement resolution to 0.012 psia and reduce the estimated measurement error to ± 0.23 psia. The sensor has Space Shuttle SRB/Titan/Arian/Atlas/Delta heritage.

5.6.6.5 Liquid Hydrogen Flow Rate Measurement Requirements

Liquid hydrogen flow rates of 50, 100, and 200 lbm/hr are required for the various tank chilldown, tank fill, and liquid hydrogen transfer experiments. Fluid inventories will also be

maintained by integrating the liquid hydrogen flow rates over the COLD-SAT experiment timeline.

Error analyses were performed on turbine, target, and differential pressure measurement systems based on manufacturer specifications and estimated signal conditioning errors. The influence of inaccuracy in fluid density measurement was also considered in the analysis. The target meter was not recommended because of its high pressure-drop versus flow-rate characteristic and low millivolt output.

Turbine flowmeters have been used extensively on ground test facilities to measure liquid hydrogen flow rates. Measurement inaccuracies of ≤ 1 percent were calculated for turbine meters from 50- to 100-percent rated flow rate. Over-speeding of the turbine meter by liquid flashing into a vapor is a concern with the use of turbine meters. Plumbing designs must be used that ensure that the meter and its plumbing is properly cooled prior to introduction of the rated cryogen flow.

The desired COLD-SAT flow rates will be obtained by sizing orifices or venturies to provide the required transfer-line pressure drops. The pressure drop across a flow control device is ideally proportional to the flow rate squared and can be used for flow-rate measurement. Measurement of liquid hydrogen flow rate by monitoring the pressure drop across the flow control device is attractive since no moving parts are placed in the flow path. The use of differential pressure transducers mounted to tubes which are tapped to the flow lines would conduct undesirable levels of heat into the system and present thermal acoustic oscillation problems. A differential pressure transducer capable of operating in liquid hydrogen is therefore required.

A variable reluctance differential pressure transducer has shown the capability of operating satisfactorily at cryogenic temperatures. The estimated liquid hydrogen mass flow rate error analysis based on the measurement of differential pressure drop across a flow control orifice by use of a variable reluctance transducer was estimated at ≤ 1 percent from 60 to 100 percent of rated flow rate.

Venturi or orifice flow control devices will be sized to provide the required flow rates. The differential pressure developed across the flow control devices will be monitored by differential pressure transducers. A turbine meter will also be used in the main liquid hydrogen transfer line for redundancy. The turbine meter is located immediately downstream of the supply tank and can be disconnected from the transfer line if desired.

A variable reluctance transducer contains two series-connected, impedance-matched coils. The differential pressure developed across the transducers diaphragm causes a change in the coil inductances and an output voltage which is proportional to the applied differential pressure. The liquid hydrogen volumetric flow rate would be determined from calibration data that relates flow rate to pressure drop across the flow control element.

The recommended excitation signal for the sensor is 5 V rms at 3 to 5 kHz. The output is 30 mV/V full scale nominal. The signal conditioning circuitry required for the sensor would be contained in the EDU's.

The basic construction of a turbine meter consists of a turbine suspended in the meter housing by rotor bearings. The flow of fluid through the meter imparts a torque on the turbine blades causing the turbine to rotate at a rate proportional to the fluid's volumetric flow rate over the designed operating range of the meter. The rotation rate of the turbine is detected by a pickoff assembly which produces a electrical pulse output at a frequency proportional to volumetric flow rate. The pulse output of the meter will be fed into frequency-to-voltage converter circuits located in the EDU's which will condition the meter's 30- to 2000-Hz output to a format compatible with the TT&C system. The pulse output can also be summed by a counter circuit for total volume transfer measurements. A serious problem with turbine meters is overspeed destruction of bearings during two-phase flow.

Differential pressure and turbine flowmeters measure volumetric flow rate, and the fluid density must be known to determine mass flow rate. The liquid hydrogen density will be determined from thermodynamic property tables by using the fluid's temperature and pressure, which are obtained at the flowmeter's inlet.

5.6.6.6 Thermodynamic Vent System Flow Rate Measurement Requirements

The thermodynamic vent system (TVS) flow rates will be monitored to determine system operational status and to quantify the hydrogen mass expelled. The flow rates will be obtained by the use of properly designed and sized flow control devices. The TVS systems will be designed to provide single-phase hydrogen vapor at their exit. Additional gaseous TVS flow rate measurements are required with an inaccuracy of ± 5.0 percent.

The TVS vent plumbing design uses tee connections located on the radiator tray where the individual tank vent lines join to a common TVS vent line. To individually meter each TVS line, flowmeters will be located on the radiator tray and must be capable of operating within a temperature range of -423 to -100 °F.

The proposed volumetric flowmeter for the TVS' is a turbine flowmeter. The turbine meters are designed for both liquid and gas measurements and are operable over the temperature range from -430 to 750 °F.

The turbine meter consists of a rotor mounted in a meter housing with bearings that attach the rotor to the housing. Fluid flow through the meter imparts a torque on the rotor blades causing the rotor to spin at a rate proportional to volumetric flow. Rotation rate is detected by a magnetic or carrier modulated pickup assembly that detects a change in motional inductance of the coil either as a voltage pulse or as a change in carrier

frequency. The meters are calibrated and a calibration constant k relating meter output frequency to volume is determined. The deviation of the k factor over the measurement range of the meter from its nominal value is given in the linearity specification. The candidate turbine flowmeters have a listed linearity of ± 1.0 percent of full scale over a normal 10-to-1 flow range. Other gas service meter specifications based on a gas density of 0.075 lb/ft³ at 14.7 psia and 60 °F are calibration accuracy of ± 0.3 percent, repeatability of ± 0.1 percent, and a dynamic response time of ≤ 6 msec. The calibration of the meters using gaseous hydrogen at the actual operating temperature and pressure conditions will be required.

Turbine meters measure volumetric flow, and in order to calculate mass flow rate the density must be determined. Temperature and pressure measurements made at the meter inlet will be used to determine density. Mass flow rate error is therefore a function of the uncertainty of the turbine's volumetric flow measurement and also the uncertainty in density determination based on the temperature and pressure measurement errors.

The influence of temperature and pressure on gaseous hydrogen density was determined by finding the best-fit equations which mathematically described the change in hydrogen density as a function of temperature and pressure over the temperature range of 180 to 360 °R and the pressure range of 5 to 20 psia. The results of this analysis indicate that a root sum square (RSS) density uncertainty of 3.66 percent could exist. The total RSS inaccuracy caused by flowmeter, data acquisition, and density measurement uncertainties was estimated at ≤ 5.0 percent from 50 to 100 percent of design range.

5.6.6.7 Supply and Receiver Tank Vent Flow Rate Measurement

Measurement of the vent flow rates of the supply and receiver tanks is required for fluid inventory management and receiver tank chilldown performance determination. Tank vent flow rates of approximately 50 lbm/hr are estimated.

A flow regulation device will be required to control the rate of tank pressure decrease so that valve actuation and tank pressure can be controlled. The tanks will be vented at pressures of approximately 50 psia to a near vacuum condition. This large pressure drop across a sonic flow nozzle will result in a choked flow condition at the throat section of the nozzle. The velocity of the gas will reach the sonic value and will not be influenced by changes in downstream pressure. The flow rate is dependent only on the upstream pressure. Temperature of the vented gas will also be measured so that density and mass flow rates can be calculated. Estimated measurement inaccuracies of ≤ 5.0 percent were calculated over the operating range of 50 to 5 psia.

Commercial suppliers have designed flow nozzles which develop sonic flow with downstream pressures as high as 80 percent of the nozzle inlet pressure.

5.6.6.8 Acceleration Measurement Requirement

The acceleration environment existing along all three axes will be measured. The influence of acceleration levels on the fluid dynamic and thermodynamic properties will be determined during the experiments by accelerating the spacecraft at levels from 10 to 100 μg .

A candidate system consists of three accelerometers. This unit also contains the required power conditioning, analog servo and signal conditioning electronics. The unit has been used on the space shuttle orbiter program to measure low level accelerations in the 1- to 10- μg range.

The three-axis 0- to 5-V acceleration output signals of the accelerometer will be measured at the experimental data unit boxes and converted to their digital equivalent by the high-resolution 12-bit analog-to-digital converters. A peak hold circuit will register peak transient acceleration levels. The peak detector will be read and reset every 1 sec.

Another candidate accelerometer is designed to measure acceleration in the range of 10^{-2} to 10^{-9}g . The listed worst-case accuracy is 1 percent of full scale. The lowest full-scale range for this model is 10 μg .

5.6.6.9 Mixer Flow Rate Measurement Requirement

A mixer is required for the active thermodynamic vent system in the supply tank. The mixer-pump must be capable of

supplying liquid hydrogen flow rates of 3.0 to 12.7 gal/min. The flow rate of the mixer can be obtained by calibrating the mixer shaft rotation rate with respect to flow rate. The mixer shaft rotation rate can be detected by a number of methods such as by use of a tachometer or by use of induction or magnetic pulse detecting sensors.

A speed sensor compatible with the liquid hydrogen environment will be required with the selected mixer-pump. The frequency of the pulse output of the mixer speed sensor will be proportional to the shaft rpm and so the flow rate. The frequency output of the speed sensor is supplied to an EDU for signal conditioning and fed to a RCTU/CTU of the TT&C system. A candidate design is similar to a rotational speed measurement design used in the Shuttle-Centaur design (ref. 20).

5.6.6.10 Valve Status Indicators

The cryogenic and standard valves proposed for the COLD-SAT plumbing system are manufactured with valve-position indicating switches. The status of the switches (open/closed) will be monitored by the RCTU's to verify operational status.

A candidate design is based on one proposed for the Shuttle/Centaur (ref. 20). A modification to the design would utilize manganin wiring for the cryogenic valve switches to minimize heat conduction.

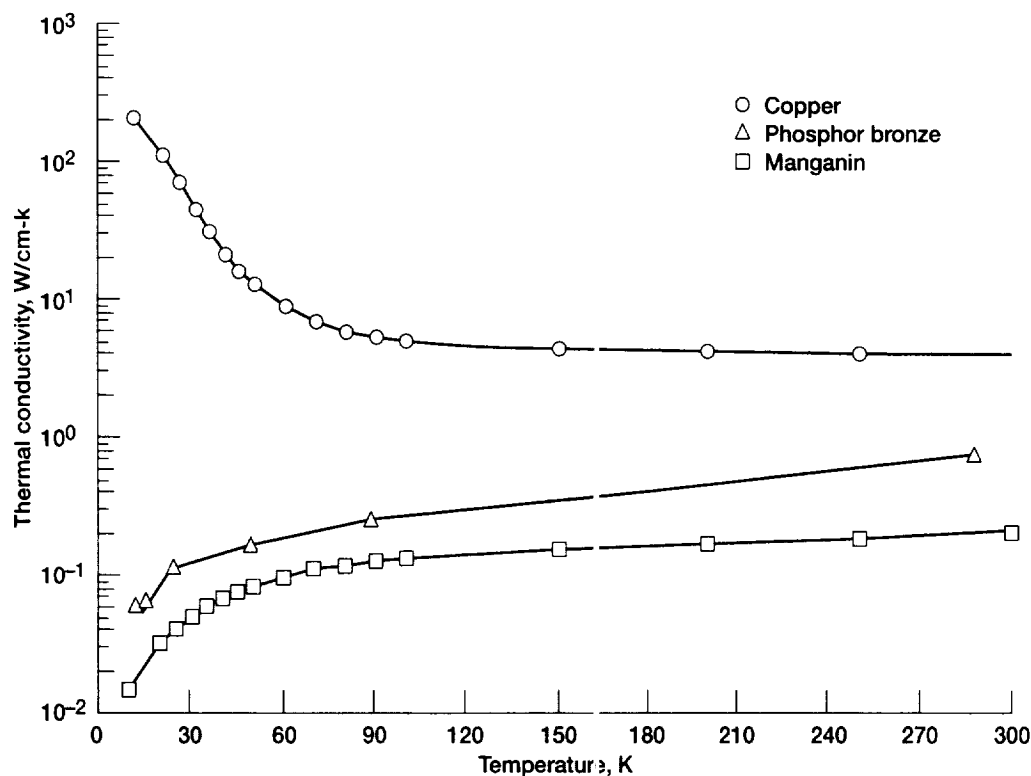


Figure 5.41.—Thermal conductivity of wire materials.

The voltage and current supplied to the COLD-SAT experiment system heaters and mixers will be measured to determine the power dissipated by the components. The measurements will be made at the relay sequencer units of the TT&C system.

5.6.7 HARNESSING

Electrical wiring is required to supply excitation power to the sensors and to couple the sensor's output signal to the data acquisition systems. The majority of the instrumentation will be thermally bonded to the cryogenic tanks and a large heat input to the tanks would occur if copper wire were used. To minimize this problem, manganin wire will be used for instrumentation wiring. Phosphor-bronze wiring will be used for valve and heater applications. The influence of temperature on the thermal conductivity of copper, manganin, and phosphor-bronze is shown in figure 5.41. Manganin has a distinct advantage over other wire materials for cryogenic use in that it has a very low thermal conductivity at low temperatures. This property helps to minimize heat leak into the system when manganin wire is used. Unfortunately, the advantage in thermal conductivity is offset by manganin's high resistivity, so that the use of manganin wire is not a panacea. For large current carrying capability (e.g., for valves, motors, heaters), phosphor-bronze provides a good mix of fairly low thermal conductivity combined with reasonable resistivity. The mechanical properties of these wire materials should be investigated more closely to determine their suitability for flight use.

Connectors and receptacles used for cryogenic tank wire feedthroughs will be similar to the type used on D-1A Centaur. Bulkhead connector assemblies exposed to temperatures below -55°F will be series 40M38294 (ref. 21). Connectors exposed to temperatures above -55°F will be series MIL-C-38999. Detailed descriptions of the wire harness can be found in the COLD-SAT Instrumentation Report (ref. 1).

5.7 Operations, Consumables Inventory, and Experiment Timeline

5.7.1 INTRODUCTION

This section describes the COLD-SAT experiment operations, consumables inventory, and experiment timeline. The consumables inventory and experiment timeline were used for mission planning and spacecraft design. The experiment set contains tests in each of the following categories:

- Low gravity tank pressure control
- No-vent fill and refill of cryogenic tanks in low gravity
- Cryogenic tank chilldown in low gravity
- Fill of liquid acquisition devices in low gravity

- Pressurization of cryogenic tankage in a low-gravity environment
- Direct liquid outflow and vented fill with low-gravity settling
- Liquid acquisition device performance in the on-orbit environment
- Control of fluid thermodynamic state during liquid outflow
- On-orbit cryogenic fluid dumping
- Advanced instrumentation for in-space cryogenic systems

The consumables inventory and timeline was developed by using a computerized spreadsheet. It tracks experimental event, liquid hydrogen use, tank pressures, tank fill levels, hydrogen mass vented, hydrogen mass transferred, applied thrust duration, hydrazine mass, and g-levels. A bookkeeping section of the spreadsheet tracks fluid losses by operation or experiment event. The inventory/timeline is essentially a simple thermodynamic model of the experiment system. It was used to determine how much of the experiment set could be accommodated by a given system design. The hardware design and the consumables inventory influenced each other in an iterative process.

Key areas that benefitted from the inventory included: test prioritization, number of tests accommodated, boiloff losses, pressurant requirements, operations sequencing and events, and identification of chilldown and other losses.

Supply, large receiver, small receiver, vaporizer and experiment system helium tank volume, surface area, and heat flux input data used in the spreadsheet calculations are shown below in table 5.41.

Other basic inventory and timeline assumptions include

- The supply tank contains 525 lbm of saturated liquid hydrogen as a worst-case (minimum) amount at the start of experiment operations.
- Experiment operations begin at $T + 2$ weeks.
- The large and small receiver tanks reach a fill level of 90 percent of total tank volume following a chilldown and fill process.

TABLE 5.41.—TANK DATA FOR SPREADSHEET CALCULATIONS

Tank	Volume, ft^3	Surface area, ft^2	Heat flux, Btu/hr-ft^2
Supply tank	144.0	142.7	0.1 0.3 0.6
Large receiver	20.9	38.9	0.5
Small receiver	13.4	27.7	0.5
Vaporizer	5.7	15.5	NA
Helium bottles	4.7	13.6	NA

- The receiver tank liquid hydrogen residuals following expulsion are assumed to be 5 percent by volume for the large receiver tank and 10 percent by volume for the small receiver tank. (This is considered to be a conservative estimate. Assumed receiver tank residual amounts have a great effect on spacecraft liquid hydrogen inventory as residuals are ultimately vented to space and are therefore lost for the purpose of future experimentation.)

- All transfer flow rates used in the analysis effort were assumed to be 200 lbm/hr.

The inventory was used to organize experiment operations and to determine how much of the experiment set could be accomplished under various conditions. At first, the inventory consisted of a simple allocation of liquid hydrogen to each experiment. As the design progressed it was possible to make better estimates of hydrogen use, for example, taking into account boiloff rates over time, or using the latest tank and plumbing masses for chilldown estimates.

As the hydrogen use estimates became more refined, it became necessary to use a computerized spreadsheet to do the accounting. A timeline was developed to keep track of hydrogen use over time. It was determined that the amount of pressurant required was an important design consideration (there being a large uncertainty in the amount needed with the worst-case amount causing severe mass and volume problems in the spacecraft configuration), so helium and hydrogen pressurant gas were added to the inventory for tracking. Later, hydrazine propellant was also added to the inventory to account for the experimental acceleration requirements over time as well as normal attitude control.

Once the timeline of operations was incorporated into the inventory, it was possible to make more refinements in the estimates of fluid use. Certain tests are best run in a particular order, such as a chilldown followed by a fill. One result from the inventory was that not all experiment tests could be accommodated in the worst case, and some prioritization of tests was needed.

High priority tests were scheduled early in experimental operations to maximize the data return in the event of a shorter mission than nominally planned. This called for storage of liquid hydrogen in the receiver tanks in order to reach the proper fill level for some pressure control tests. The higher boiloff rates caused by the higher heat leak into the receiver tanks could be accounted for more accurately with the computerized inventory/timeline. Another refinement was that instead of linking a chilldown with each fill, several fills could be accomplished while the system was cold.

It was determined by looking at the timeline that additional time would be required between tests for experimenters to analyze the data. Time was also added to allow the spacecraft operators and experimenters some rest after long experiment runs and to provide some time for problem solution. Time was also added in cases where a tank needed to warm up to get to

initial conditions for a test. This refinement of the operational timeline allowed more accurate accounting of boiloff losses and provided a more realistic estimate of experiment system life.

The inventory was expanded to track tank pressures as well as the mass of fluid in the tank. It became clear that the fluid would have to be "conditioned" in some cases to obtain the experiment requirements for fluid thermodynamic state. After introducing hot pressurant gas into a tank to perform a pressurized outflow, the removal of the added thermal energy to return the tank to its initial pressure could be accounted for more accurately with the computerized inventory. The inventory was updated to include the latest design volumes and masses of tanks and plumbing to better account for losses. It was planned to eventually track tank and plumbing temperature, but the inventory never reached that level of refinement, and worst-case estimates were used for chilldown losses. As the inventory became more refined, it began to resemble a model of the experiment system.

Because of the experimental nature of the operations, some of the engineering estimates used in the inventory are preliminary. In some cases, engineering assumptions are the only means available to quantify low-gravity cryogenic fluid behavior. The biggest uncertainty is the location and shape of the liquid/vapor interface(s) and its effect on liquid/pressurant heat transfer. Another problem is para-to-ortho conversion, which was not included in the inventory as a specific item, but was treated as an overall lump contribution to boiloff loss. Further refinements to the inventory to explicitly calculate these effects were begun, but not completed. To investigate their potential impact on the inventory, the spreadsheet was calculated twice, once with best-case assumptions and once with worst-case assumptions.

5.7.2 INVENTORY AND TIMELINE LAYOUT

Spreadsheet column headings are shown in table E.9 in appendix E to this chapter for a typical spreadsheet run. This figure shows the types of information that were included in the inventory. Each row corresponds to an operation or experiment event. The inventory tracks fluids in the supply tank, large receiver tank, small receiver tank, two hydrogen vaporizers, a lumped gaseous helium volume, and a lumped hydrazine mass.

The spreadsheet tracks experiment event, liquid hydrogen use, tank pressures, tank fill levels, hydrogen mass vented, hydrogen mass transferred thrust duration, and gravity levels. A bookkeeping section of the spreadsheet tracks fluid losses by operation or experiment event.

Table E.10 shows a simplified spreadsheet that gives an example of a possible timeline for a COLD-SAT mission. The figure lists item numbers, times, events, and the total amount of liquid hydrogen on board. The first column, "ITEM NUMBER," assigns a number to each line of the spreadsheet. This allows easy reference to a specific event across the

spreadsheet. It is calculated by adding one to the item number in the previous row.

The next two columns in the spreadsheet, "TIME" and "CHANGE IN TIME," keep track of the total mission time elapsed (in weeks) and the time used by the event (in hours). The "EVENT" columns list the events that are occurring in each of the tanks. The abbreviations used are:

Boiloff	An idle period with liquid in the tank that is being heated at the tank heat-leak rate
CD	Chilldown of a tank
Condition	Removal of thermal energy from the bulk liquid in preparation for a test
Dump	Dumping liquid hydrogen overboard to empty a tank
Empty	Empty tank, nothing happening
GH ₂ tank CD	Pressurant bottle chilldown for recharge (gaseous hydrogen)
GH ₂ tank VF	Pressurant bottle recharge (gaseous hydrogen)
Launch/orbit	Launch and deployment activities
LG	Large receiver tank
NVF	No-vent fill test
NVRF	No-vent refill
PC	Pressure control test
Preparation/checkout	System preparation and checkout after launch
Recondition	Removal of thermal energy from the bulk liquid following a test that may have added heat
SM	Small receiver tank
SU	Supply tank
VF	Vented fill test
VRF	Vented refill test
Transfer line CD	Transfer line chilldown operation

The order in which events occur is dictated by individual experiment requirements and operation efficiency. For example, pressure control experiments require specific tank fill levels. Transfer line chilldowns are needed before tank chilldowns or fills. Conditioning brings the liquid in a tank to specific thermodynamic conditions prior to a fill test. Reconditioning prepares a tank for a refill operation. A dump is used to evacuate a tank in preparation for the next sequence of tests. Some nonexperimental operations are needed to place the system into a state suitable for the next test.

The total liquid hydrogen on board versus time is plotted in figure 5.42 for a typical inventory run.

5.7.3 OPERATIONS

The supply tank will be chilled and filled on the ground several hours before launch. The tank will be vented to atmosphere until T - 95 sec when it will be locked up for launch. The tank should remain locked up until it reaches orbit, but the capability to vent through the Centaur vent system will exist for contingencies. The tank will vent through the passive TVS and the mixer will be run periodically to keep the tank pressure under control during deployment. No experimentation is planned during the first two weeks on orbit to allow for spacecraft deployment and checkout and thermal equilibration. Data on the supply tank will be taken throughout this time.

5.7.3.1 Experiment Sequencing

The order in which experiments are performed depends on the initial conditions required for one test and the final conditions provided by another. Certain sequences of tests naturally follow one another, for example, a chilldown test is followed by a no-vent fill.

The pressure control experiment tests are the drivers for the overall structure of the experiment sequence because of fill level requirements for the tests. Pressure control tests are run at three fill levels in the supply tank, designated 90, 65, and 50 percent. The 90-percent full tests have to be run soon after launch because the initial fill level is 92 percent and hydrogen

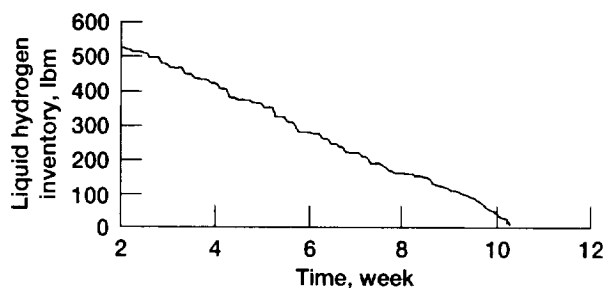


Figure 5.42.—Total COLD-SAT liquid hydrogen inventory (average liquid hydrogen use during experiment operations is 9.2 lbm/day).

is lost daily by boiloff at a rate of about 1.5 lbm/day. To perform the next set of tests, the fill level has to be dropped to around 65 percent by removing liquid hydrogen, which implies doing transfer experiments.

Transfer experiments usually require a transfer line chilldown operation, receiver tank chilldown test, and a fill test. The chilldowns involve a loss of liquid since heat is removed by vaporizing liquid hydrogen which is then vented overboard. After a fill there are additional losses caused by removal of energy added to the liquid during the transfer, higher boiloff rates in the receiver tanks, and residual liquid being trapped in the receiver tanks after a back transfer to the supply tank.

There are two possible approaches to achieving the required initial fill levels for pressure control tests in the supply tank: (1) use up the liquid by performing transfers, or (2) store the excess liquid in the receiver tanks while performing the pressure control tests in the supply tank. The second method is more convenient and provides for performance of the higher priority pressure control tests as soon as possible, but suffers from higher losses caused by boiloff (which is nonproductive) because of the higher heat leak in the receiver tanks. The nominal sequence is a combination of the two. Four transfers are performed and then some liquid is held in the receiver tanks while the 65-percent pressure control tests are run. The four transfers are the first four no-vent fill tests which are the highest priority transfer tests. Thus the relative priority of the various experiments and tests enters in as a factor in the sequencing of events with high priority tests being performed as soon as possible.

5.7.3.2 Pressure Control

The pressure control experiment primarily consists of parametric variations on a set of five tests. The basic test set is: (1) thermal stratification, (2) mixing, (3) passive TVS, (4) another mixing test, and (5) active TVS. The final conditions for one test provide the initial conditions for the next. This set of tests is repeated at different tank fill levels (90, 65, 50 percent), different applied heat fluxes (0.1, 0.3, and 0.6 Btu/hr-ft²) and different acceleration environments (background, $3 \times 10^{-5}g$, and $10^{-4}g$).

The tests are largely passive from a control standpoint. The thermal phenomenon have long time constraints. Some pressure spikes are possible during mixing especially if regions of superheated liquid have formed during the stratification tests. For the most part, it is anticipated that pressure control test conditions will be set up and the tank observed until the time limit or pressure limit of the test is reached. The passive TVS is oversized for low heat input so the TVS valve will be cycled to provide an average flow rate corresponding to the tank heat flux (e.g., 10 min on, 20 min off).

Supply tank pressure control tests typically occur in the sequence shown in figure 5.43. During thermal stratification tests, tank pressure rises at rates that depend on the experimen-

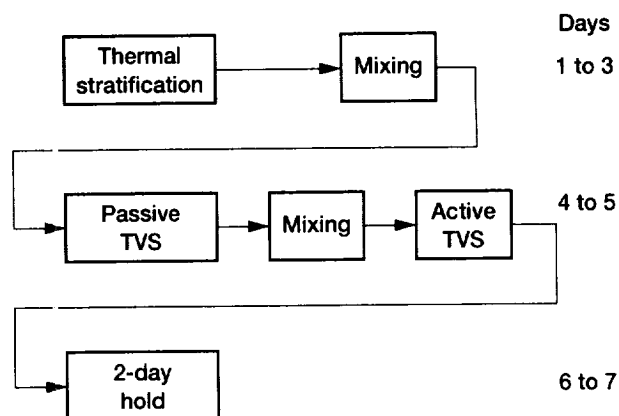


Figure 5.43.—Typical pressure control test sequence.

tal heat flux level (0.1, 0.3, or 0.6 Btu/hr-ft²) and the tank liquid hydrogen fill level. During mixing tests, supply tank pressure is lowered to that value which corresponds to a saturated, homogeneous pressure rise from the last mixing or active TVS operating event. During passive TVS tests, the tank is vented at the TVS vent rate shown in table 5.11 and energy removal is estimated to be at the rate shown in the design heat load column.

During active TVS tests, the supply tank is vented and energy removed at the rates shown in table 5.11 and the tank is brought to a saturated, homogeneous condition. Tank pressure reduction is a consequence of mixing and energy removal during active TVS operation.

5.7.3.3 Chilldown

Figure 5.44 shows a typical 7-day operating sequence for tank chilldown and fill experimentation. The cycle begins with a thermally conditioned supply tank (pressure less than 20 psia) and proceeds through a chilldown of the transfer line and a chilldown of either the large or small receiver tank. The subsequent no-vent fill of the receiver tank is followed by an operational transfer back to the supply tank where the liquid hydrogen can be reconditioned by the active thermodynamic vent system. The tank chilldown and fill sequence begins again with the reconditioned liquid hydrogen. A 2-day quiescent spacecraft period concludes the 7-day week.

The transfer lines and receiver tanks must be cold to perform a fill. Normally, a fill test will be preceded by chilldown tests. Chilldowns may not be needed for fills and refills that immediately follow one another. Heaters have been included on the receiver tank designs to provide a way of warming the tank to the desired initial temperature (e.g., $>400^{\circ}R$) without having to wait a week. If there are more chilldown tests desired than are needed for fills, the chilldowns can be done at the end of the mission by using the heaters to warm the tanks.

Transfer line chilldown is primarily a continuous flow process. The possibility of pressure spikes over 100 psi exists, so the vents must be sized to handle warm hydrogen gas at

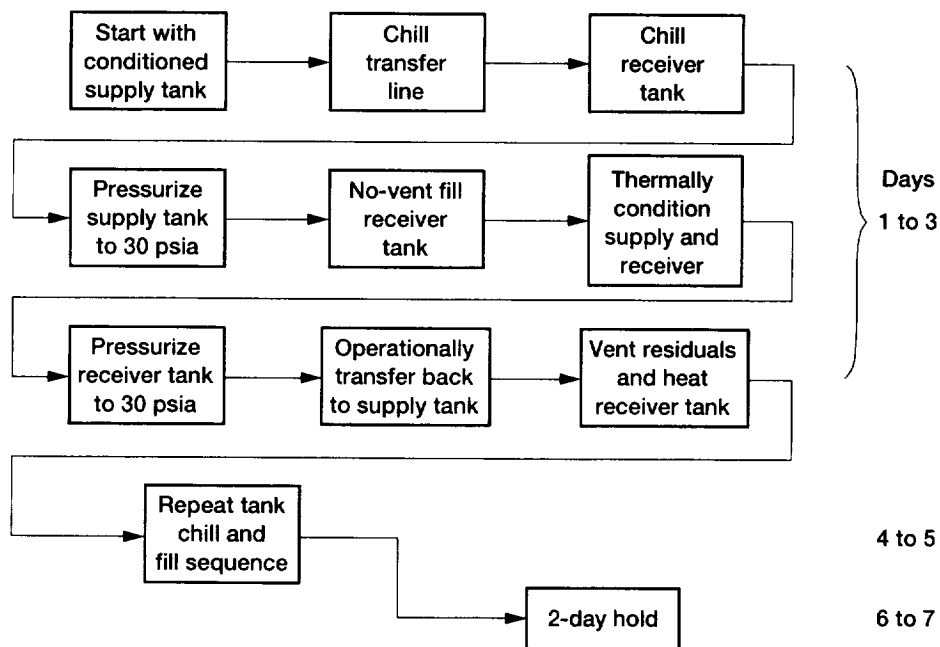


Figure 5.44.—Typical sequence of transfer-related tests.

chilldown flow rates. Pressure surges could cause backflow into the supply tank. An initial low flow rate or pulsed flow chilldown may be needed to reduce the initial pressure spike depending on the line temperature.

The COLD-SAT transfer line has many branches that will be difficult to chill with a continuous flow through only one leg. Branch shutoff valves must be located as close to the main transfer line as possible to allow easy chilldown of the shutoff valve, otherwise the heat leak to the transfer line will be large. The best approach would be to vent the line through the tank that is to be filled, but this must be done carefully to avoid chilling the tank below the initial starting temperature for the tank chilldown test.

Tank chilldown is primarily a charge-hold-vent procedure in which a charge of liquid is introduced into the tank and held, while heat is transferred between the tank and the liquid, generating vapor, and finally the vapor is vented out of the tank, removing the heat. The charge can be introduced through one of the spray systems used for fill; each of the types of sprays will be evaluated in separate chilldown tests.

A typical chilldown would consist of the following steps: (1) flow through the transfer line (low flow leg) to the selected spray of the desired receiver tank is initiated, (2) flow continues for approximately one minute until the desired charge mass (~1 lb) is injected, (3) the pressure in the locked-up receiver tank is allowed to rise to 30 psia as heat is transferred from the tank to the hydrogen, (4) the vent is opened for approximately 10 sec to reduce tank pressure by 5 psi, (5) steps 3 and 4 are repeated four times, and (6) the tank is vented to space and

another charge-hold-vent cycle is initiated until the target temperature of the tank is reached.

5.7.3.4 No-Vent Fill

No-vent fill in at least two tanks with different mass-to-volume ratios will be investigated. The tank will be initially chilled down to a target temperature, vented to near space vacuum, the vent valves closed, and liquid hydrogen will be introduced into the tank via a tangential spray system. The initial use of the tangential inflow nozzles is intended to promote mixing, thereby minimizing the rate of pressure rise and thus aiding the pressure-driven liquid transfer operations. Inflow through the tangential nozzles is also expected to cause centrifuging of the liquid to the tank walls with the resultant vapor region being centrally located in the tank. As the filling proceeds, the pressure will rise causing the liquid transfer rate to decrease. As the pressure continues to rise, it will be necessary to introduce a portion of the liquid hydrogen flow through the radial spray system into the vapor region to promote vapor condensation. The filling process will terminate when the source tank and receiver tank pressures are nearly equal. The TVS will be activated to maintain the tank pressure within acceptable limits following the transfer operation.

Key variables affecting the results are expected to be: the acceleration environment, the thermodynamic state of the inflowing liquid, the receiver tank initial temperature, the timing of the initiation of flow through the radial spray system, and tank mass and volume. The thermodynamic state of the test

fluid is primarily controlled by the operating conditions maintained in the source tank. However, heat addition and pressure loss in the transfer line will also contribute to the establishment of the thermodynamic state of the liquid hydrogen as it enters the tank.

No-vent fill through the LAD will follow an identical procedure with the exception that flow will be introduced into the tank via the LAD.

The refilling of tanks will follow an identical procedure with the addition of continuous TVS operation throughout the fill. Additional key variables are the quantity, position, and thermodynamic state of the residual hydrogen in the tank prior to the initiation of the refill.

For no-vent fills that employ an axial spray, a nozzle will be used which will break the flow into a spray of liquid droplets. The nozzle will be oriented so that the centerline of the spray and the long central axis of the tank are aligned (the configuration will be designated "axial spray"). Spacecraft maneuvers will be used to maintain the bulk liquid away from the nozzle for as long as possible. The tank is designed to be of sufficient size so that the spray volume is representative of the volume which a single nozzle would be expected to cover in a full-scale system. Flow will continue until tank pressure reaches within 5 psia of inflow pressure.

5.7.3.5 Vented Fill

An axial acceleration environment will be provided for this experiment. Numerical modeling predictions of liquid residuals following outflow from a tank will be compared with test results. The key variables affecting the results are expected to be the acceleration environment and liquid flow rate. The quality of the liquid outflow can be utilized to determine the effectiveness of the settling maneuver.

Following tank chilldown and evacuation, liquid hydrogen will be introduced through the end of the tank where liquid is located by applied acceleration while pressure-activated venting will be permitted at the other end of the tank. The vented fluid will be continuously monitored and the venting operation will be terminated when the source tank and receiver tank pressures are nearly equal. The on-the-wall TVS on the receiver tank will be activated following the transfer operation to maintain the tank pressure within acceptable limits.

5.7.4 DESCRIPTION OF ANALYSES

The fluid inventory and timeline is composed of a number of interdependent thermodynamic analyses. Basic thermodynamic principles were applied to COLD-SAT experimental and operational processes in an attempt to model experiment operations as accurately as possible. The operating range for the

supply, large receiver, and small receiver tanks is 15 to 30 psia. It was necessary for the model to have access to hydrogen thermodynamic data in this range. To fill this need, the least squares, best linear fit equations plotted in figures D.40a through f in appendix D to this chapter were incorporated either directly into the spreadsheet or indirectly through subsequent analysis. Data points for the linear representations of hydrogen properties were obtained from reference 22.

5.7.4.1 Boiloff

Boiloff is an idle period where the only occurrence is that heat leaking into the tank is adding thermal energy to the tank and its contents. This heat leak is assumed to be constant and is removed from the tank by the TVS. The TVS is assumed to remove heat at the rates given in table 5.11, which are assumed to include any TVS inefficiency. Boiloff losses are added to most events in which there is liquid in a tank.

5.7.4.2 Liquid Hydrogen Tank Ullage Calculation

The following equation was used for the supply tank ullage, large receiver tank ullage, and small receiver tank ullage columns:

Gaseous hydrogen ullage (lbm) =

$$\left(\text{tank volume} - \frac{\text{liquid hydrogen mass}}{\text{liquid hydrogen density}} \right) \times (\text{gaseous hydrogen density})$$

In the previous equation, liquid hydrogen density is calculated at the saturated, homogeneous pressure and gaseous hydrogen density is calculated at two times the saturated, homogeneous pressure. The use of two times saturation pressure is a compromise lumped estimate to account for thermal energy in the ullage. A completely homogeneous condition is not expected in low gravity except after mixing. The estimate of two times saturation was suggested by the experimenters. This is an area for further refinement.

5.7.4.3 Liquid Hydrogen Tank Pressure Rise Calculation

Hydrogen tank pressure rise rates were calculated from the saturated, homogeneous model of NASA TN D-4171 (appendix B) (ref. 23) for the supply tank pressure, large tank pressure and small tank pressure columns. The saturated, homogeneous rate was multiplied by two, and the resultant values for each tank at the assumed heat flux levels were plotted as a function of tank fill level. The second-order curve fits shown in figures D.41 to D.45 in appendix D to this chapter were incorporated directly into the spreadsheet.

5.7.4.4 Pressure Control Experiment Calculations

During thermal stratification experiments, tank pressure is estimated to rise at the rates shown in figures D.41 to D.43 in appendix D to this chapter depending on the experiment heat flux level (0.1, 0.3, or 0.6 Btu/hr-ft²) and the tank liquid hydrogen fill level. During mixing experiments, supply tank pressure drops to a value which corresponds to a saturated, homogeneous condition.

During passive TVS experiments, the following changes occur in the spreadsheet:

- (1) Tank is vented at the rate shown in table 5.11. (Supply passive, large receiver, and small receiver vent flow rates)
- (2) Energy is removed at the TVS design rate (given in table 5.11, design heat load column)

During active TVS experimentation, the following changes occur in the spreadsheet:

- (1) Supply tank is vented at the rate given in table 5.11.
- (2) Energy is removed at the rate given in table 5.11.
- (3) Tank is brought to a saturated, homogeneous condition.

The amount of liquid hydrogen vented during active and passive TVS operation is determined according to the following equation for both the active and passive thermodynamic vent systems:

$$\text{lbm of liquid hydrogen vented} = (\text{time of TVS operation}) \times (\text{vent flow rate})$$

Tank pressure reduction is a consequence of mixing and energy removal during active TVS operation. Liquid hydrogen temperature is reduced according to the following equation for both the active and passive thermodynamic vent systems:

$$T_f = T_i - \frac{(\text{design heat load}) \times (\text{TVS operation time})}{(\text{tank liquid hydrogen mass}) \times (\text{liquid hydrogen specific heat})}$$

The new tank pressure is the liquid hydrogen saturation pressure at the calculated final temperature.

5.7.4.5 Line/Tank Chillover and Fill Experiment Calculations

For fluid inventory purposes, the total mass of liquid hydrogen required for one chillover of the COLD-SAT transfer line

was calculated as the average between two extreme values. The low value represents the mass of liquid hydrogen that would be needed at the heat transfer rate expected at the beginning of the chillover process while the high value represents the mass of liquid hydrogen that would be needed at the heat transfer rate expected at the end of the process.

At the start of the process, the large amount of transfer line thermal energy is expected to completely vaporize the liquid hydrogen as it enters the hot line. The process uses both the heat of vaporization and subsequent sensible heating of the hydrogen vapor (to 100 °R) to cool the transfer line before venting to space. At the end of the process, the lower transfer line temperature is assumed to only vaporize the liquid hydrogen by the time it is vented; no subsequent sensible heating of the vapor is assumed. For cases where the transfer line has not had a chance to warm up to ambient temperature a cold chillover estimate using the heat of vaporization only was calculated from a starting line temperature of 300 °R.

The equation used for transfer line chillover is

$$\text{lbm of liquid hydrogen} = (H_v + H_s) \left(M_t \right) \int_{T_1}^{T_2} \frac{C(T)}{T} dT$$

where

H_v the enthalpy of vaporization of hydrogen

H_s the change in enthalpy caused by sensible heating of the vapor (41.3 to 100 °R at 30 psia); zero for no sensible heating

T_1 initial transfer line temperature; 540 °R (initial transfer line chillover); and 300 °R (subsequent chillovers)

T_2 the final transfer line temperature; 41.3 °R

$C(T)$ the specific heat of stainless steel as a function of temperature (fig. D.46 in appendix D to this chapter)

M_t transfer line mass (estimated to be 20 lbm)

Average values between process beginning results and process end results yield the following:

Warm line chillover: 4.0 lbm liquid hydrogen
Subsequent line chillovers: 1.4 lbm liquid hydrogen

The mass of liquid hydrogen used to chill the receiver tanks was estimated to be

TABLE 5.42.—HYDROGEN PRESSURANT REQUIREMENTS FOR TRANSFER OPERATIONS

Operation	Requirements, lbm/transfer
Supply tank to large receiver tank	2.0
Supply tank to small receiver tank	1.9
Large receiver tank to supply tank	0.56
Large receiver tank to small receiver tank	.50
Small receiver tank to supply tank	.36
Small receiver tank to large receiver tank	.36

Large receiver tank chilldown: 7.2 lbm liquid hydrogen
 Small receiver tank chilldown: 2.8 lbm liquid hydrogen

The previous values include an estimated 0.3 lbm of transfer line residuals for all operations. The tank chilldown requirements were obtained from the CRYOCHILL computer model for charge-hold-vent chilldowns which makes certain assumptions about the efficiency of heat transfer between the tank and the hydrogen.

For all fills it is assumed that the receiver tank will achieve a 90-percent fill level regardless of the filling method. Losses due to residual liquid in the tank after it is emptied are reflected in dump operations following the transfer.

5.7.4.6 Pressurization of Hydrogen Tanks in Low Gravity

Autogenous tank pressurization for liquid hydrogen expulsion involves the injection of gaseous hydrogen pressurant into the ullage space of a cryogenic tank for the purpose of expelling liquid hydrogen from the tank through a connecting line to a receiving tank. The phenomena involved in autogenous pressurization in low gravity are not well understood. The data supplied by the COLD-SAT experiments in this area will attempt to fill this void.

Two simple pressurization analyses were performed for each of the six different COLD-SAT pressurization and transfer operations. These two analyses represent extreme cases, which provide upper and lower bounds for the actual quantity of pressurant required. The set of operations characterized includes supply tank to large receiver tank or small receiver tank transfers; large receiver tank to supply tank or small receiver tank transfers; and small receiver tank to supply tank or large receiver tank transfers. The results of these analyses are shown in figures D.24(a) to (f) in appendix D to this chapter. The tanks were assumed to be pressurized to 30 psia from an initial saturated, homogeneous condition at 15 psia with gaseous hydrogen at 520 °R.

The best case (minimum pressurant required) assumes that the bulk cryogenic liquid and the incoming warm pressurant gas each undergo reversible, adiabatic (isentropic) processes in reaching the final state. The isentropic case is characterized by total thermal stratification. The worst case (maximum pressurant required) assumes that thermal equilibrium is maintained between the bulk liquid and the pressurant gas at all times during the process. The thermal equilibrium case is characterized by substantial condensation of the incoming pressurant gas. Clearly, neither the isentropic nor the thermal equilibrium models predict the actual COLD-SAT pressurant use. The nominal pressurant mass required was estimated as the midpoint of the two extremes.

Nominal hydrogen pressurant requirements for each of the six different COLD-SAT pressurization and transfer operations are given in table 5.42.

Accurate estimates of pressurant gas required for space-based transfer operations are important. Excess pressurant carries a substantial weight penalty (for high pressure bottles) while insufficient pressurant will result in an incomplete mission. This area (pressurization of hydrogen tanks in low gravity) has the most critical need for future research of all the problems faced by the COLD-SAT experiment system design team.

Appendix A

Experiment System Mechanical and Structural Analyses

This appendix contains summaries, generally in tabular form, of the following mechanical and structural analyses:

- (1) Dimensions of Principal Components and Structural Data Summary
- (2) Experiment System Mass Estimates
- (3) Structural Analyses
 - (a) Supply Tank Structure.
 - (b) Large Receiver Tank Structure
 - (c) Small Receiver Tank Structure
 - (d) Hydrogen Vaporizer Struts
 - (e) Helium Bottle Struts
- (4) LAD Pressure Drop Calculations

Table A.1 provides a summary of the dimensions of, and other structural data for, the major components of the experiment system, which are the supply tank, the two receiver tanks, the hydrogen vaporizers, and the helium pressurant bottles.

Table A.2 provides a summary of the experiment system mass. The organization of this table corresponds to the organization of the more detailed listing in Table A.3, which contains a listing of all components in the experiment system, the number of flight units, and an estimate of their mass.

Table A.4 summarizes structural analyses performed on various portions of the major components of the experiment system, specifically, the supply tank, the large and small receiver tanks, the hydrogen vaporizer struts, and the helium bottle struts.

Table A.5 liquid acquisition device pressure drop calculations are based on the methods of E. C. Cady's Study of Thermodynamic Vent and Screen Baffle Integration for Orbital Storage and Transfer of Liquid Hydrogen (ref. 24).

TABLE A.1.—COLD-SAT EXPERIMENT SYSTEM STRUCTURAL DATA SUMMARY
[Room-temperature dimension .]

Vessel	Supply tank	Vaporizers	Helium bottles	Large receivers	Small receivers
Number	1	2	2	1	1
Volume, ft ³	143.9	5.7	5.7	21.0	13.6
Shape		Sphere	Sphere		
Cylinder, ft	5.0-by 5.03			2.71-by 2.375	3.0-by 0.5
Elliptical ends	SR.2			SR.2	SR.2
Length, ft	8.6			4.3	2.6
Outside diameter, ft	5.0	2.4	2.2	2.7	3.0
Surface area, ft ²	142.7	17.4	15.2	38.9	27.7
Wall thickness, in.	0.080	0.60	0.364	0.061	0.067
Material	Aluminum 5083	Aluminum 6061-T6.	Aluminum 6061-T6, Kevlar 49-epoxy	Aluminum 5083	Aluminum 5083
Pressure vessel emissivity	0.05	-----	-----	0.05	0.05
Mass (dry), lb	194.0	143.6	73.5	38.0	29.0
Ground maximum expected operating pressure, psia	49.0	2000.0	3000.0	49.0	49.0
Safety factor on ultimate	5.4	2.2	2.0	4.4	4.3
Safety factor on yield	1.9	1.9	1.7	2.0	1.9
On-orbit maximum expected operating pressure, psia	49.0	2000.0	3000.0	49.0	49.0
Safety factor on ultimate	3.8	1.3	2.0	3.1	3.0
Safety factor on yield	1.4	1.1	1.7	1.4	1.4
Liquid hydrogen capacity at 20 psia saturated, lb	565.0 at 92 percent	3.5	-----	-----	-----
Tube coils	NA	2	NA	NA	NA
Tube o.d., in.	↓	1.5	↓	↓	↓
Wall thickness, in.		0.035			
Length, ft		75.0			
Number of coil supports		2.0			
Mass		14.5			
Material		Aluminum 3003-H14			
Supports					
Type	Struts	Struts	Struts	Struts	Struts
Number	16	4 per bottle	4 per bottle	10	10
Material	S-2 glass	6061-0 Aluminum	6061-0 Aluminum	S-2 Glass	S-2 Glass
Length, in.	19.3	2 at 8.0, 2 at 19.3	2 at 8.0, 2 at 19.3	8 at 31.1, 2 at 33.9	10 at 15.4
Outer diameter, in.	1.375	1.5 by 2.0	1.5 by 2.0	1.0	1.0
Wall thickness, in.	0.04	0.125	0.125	0.04	0.04
Ends	Stainless steel	Aluminum	Aluminum	Stainless steel	Stainless steel
Mass, lb	21.6	17.7	17.7	15.6	15.6
Thermal length, in.	13.1			8 at 25.1, 2 at 27.9	10 at 9.4
Thermal area, in.	0.168	0.813	0.813	0.062	0.062
Support brackets	8	-----	-----	6	6
Factor of safety	5.4	3.3	6.2	6.4	16.6
MLI can	Yes	N/A	N/A	Yes	Yes
Length, in.	114.8	↓	↓	64.5	44.5
Diameter, in.	65.2			37.5	40.0
Shape					
Cylinder, in.	65.18-by 84.77			37.5-by 49	40-by 28.5
Frustum ends, in.	65.18-by 35.5-by 15.0			37.5-by 22-by 7.75	40-by 24-by 8
Surface area, ft ²					
Inner	176.8			57.4	45.1
Outer	180.6			59.6	47.0
Can inner emissivity	0.05			0.05	0.05
Honeycomb					
Material	Aluminum 5056	NA	NA	Aluminum 5056	Aluminum 5056
Thickness, in.	0.375			0.3755	0.375
Facesheets					
Material	Aluminum 2024	NA	NA	Aluminum 2025	Aluminum 2024
Thickness, in.	0.020			0.020	0.020
Mass, lb	119.1	NA	NA	42.9	34.8

TABLE A.2.—COLD-SAT EXPERIMENT
SUBSYSTEM MASS SUMMARY

Subsystem	Weight. lb
SUPPLY TANK MODULE	
Liquid hydrogen supply tank assembly	890
Gaseous hydrogen supply	426
Helium supply	188
Total	1504
LARGE RECEIVER TANK MODULE	
Total	207
SMALL RECEIVER TANK MODULE	
Total	178
FLUID INTERFACE SUBSYSTEM	
Supply tank module	134
Large receiver tank module	56.4
Small receiver tank module	22.5
Vent system	49.1
Ground interface panel	9
Total	271
ELECTRONICS	
Total	46.5
CONSUMABLES	
Supply tank liquid hydrogen	565
Helium pressurant	17.4
Vaporizer hydrogen	7.4
Total	589.8
TOTAL SUBSYSTEM MASS	2796.3

TABLE A.3.—COLD-SAT EXPERIMENT SYSTEM COMPONENTS LIST AND MASS SUMMARY

Item	Number of flight units	Unit mass, lb	Total mass, lb	Assembly mass, lb
SUPPLY TANK MODULE	-----	-----	-----	1504
Liquid Hydrogen Supply Tank (subtotal)	-----	-----	-----	890
Pressure vessel (Aluminum 5083, 0.096 lb/in. ³)	-----	-----	-----	-----
Elliptical domes (10 percent margin)	2	39	78.0	-----
Cylinder (10 percent margin)	1	95.5	95.5	-----
Girth rings	4	5.09	20.4	-----
Panel supports	18	0.75	13.5	-----
Heaters	-----	-----	-----	-----
Strips (1.25 in. by 15.7 ft)	9	.13	1.2	-----
Patches (10 in. diam)	8	.0433	0.3	-----
Struts	-----	-----	-----	-----
Glass	16	.188	3.0	-----
Aluminum ends	32	.256	8.2	-----
Spacecraft brackets	8	1.094	8.8	-----
Tank brackets	16	.1	1.6	-----
LAD assembly	-----	-----	-----	-----
Channels	4	22.95	91.8	-----
1/2-in. tubing (0.035-in. wall), ft	130	^a .0609	7.9	-----
3/4-in. tubing (0.049-in. wall), ft	130	^a .1285	16.7	-----
Sidewalls (0.050-in. thick)	8	.549	4.4	-----
Perforated plate (0.05-in. thick)	4	.78	3.1	-----
Screen (Dutch twill)	4	.421	1.7	-----
Manifolds	2	7.89	15.8	-----
Structural rings	2	26.1	52.2	-----
Brackets	-----	-----	-----	-----
Rings	8	.29	2.3	-----
LAD	4	.33	1.3	-----
Instrumentation rakes	-----	-----	-----	-----
Support rods	4	2.2	8.8	-----
Temperature cones	51	.0066	.3	-----
Liquid-vapor cones	35	.0432	1.5	-----
Pump	2	2.0	4.0	-----
MLI can	-----	-----	-----	-----
Facesheets - 2024 Aluminum - 0.020 in.	-----	-----	-----	-----
Inner (176.8 ft ²)	1	49.9	49.9	-----
Outer (180.64 ft ²)	1	51	51.0	-----
Honeycomb (3/8-in. 5056 Aluminum)	1	10.71	10.7	-----
Vent doors	2	.5	1.0	-----
Pyrotechnic pin pullers	2	1.0	2.0	-----
Fasteners and doublers	30	.25	7.5	-----
Thermal insulation	-----	-----	-----	-----
MLI	1	46.1	46.1	-----
Nylon pins	130	.03125	4.1	-----
Purge bag	-----	-----	-----	-----
Bag (130 in. ³)	1	13.0	13.0	-----
Vent doors	2	.3	.6	-----
Pyrotechnical pin pullers	2	1.0	2.0	-----
Support rings	2	1.25	2.5	-----
Relief valves	2	.156	.3	-----
Valves	-----	-----	-----	-----
Cryogenic valves	18	3.5	63.0	-----
Relief valves	3	.156	.5	-----

^aMeasured in lb/ft.

TABLE A.3.— Continued.

Item	Number of flight units	Unit mass, lb	Total mass, lb	Assembly mass, lb
Harnesses				
Fairleads	16	0.1250	2.0	-----
Phos-bronze wires (25 ft)	38	.15	5.7	-----
Mangnin wires (25 ft)	57	.0675	3.8	-----
Connectors				
61-pin	16	1.0	16.0	-----
37-pin	10	2	20.0	-----
5-pin	24	.25	6.0	-----
Instrumentation				
Harnesses				
Internal tank wires (4 ft)	186	.0108	2.0	-----
External tank wires (5.2 ft)	289	.01404	4.1	-----
External MLI can (6.5 ft)	20	.01755	4	-----
Fairleads	35	.125	4.4	-----
Connectors				
61-pin	16	2	32.0	-----
Tank feedthroughs	10	2	20.0	-----
Flowmeters				
Turbine	3	.5	1.5	-----
Venturis	3	.8	2.4	-----
Joule-Thompson device	3	.09	.3	-----
Pressure sensors				
Absolute	14	.3125	4.4	-----
Differential	3	.688	2.1	-----
Temperature sensors	116	.003	.3	-----
Burst disk	1	2	2.0	-----
Piping (lengths in feet)	12	°.054	0.7	-----
1/4-in. o.d.	10	°.104	1.0	-----
3/8-in. o.d.	21	°.174	3.7	-----
1/2-in. o.d.	15	°.476	7.3	-----
3/4-in. o.d.	14	°.996	13.9	-----
1 1/2-in. o.d.	35	.25	8.8	-----
Fairleads				
Panels	1	4.0	4.0	-----
E - Fill/drain	1	4.0	4.0	-----
F - Active TVS/TVS vent	1	4.0	4.0	-----
G - Tank vent	1	5.6	5.6	-----
H - TVS flow	1	7.2	7.2	-----
I - Transfer	1	4.0	4.0	-----
J - Transfer control				
Gaseous Hydrogen Supply	-----	-----	-----	426
Vaporizer				
Bottles	2	143.6	287.2	-----
Coils	2	26.4	52.8	-----
Struts				
Horizontal (8.0 in.)	4	.65	2.6	-----
Vertical (19.3 in.)	4	1.57	6.3	-----
Tubing 1/4-in. o.d. (length in feet)	25	.054	1.4	-----
Instrumentation				
Sensors				
Temperature	9	.003	.03	-----
Absolute pressure	9	.3125	2.8	-----

°Measured in lb/ft.

TABLE A.3.— Continued

Item	Number of flight units	Unit mass, lb	Total mass, lb	Assembly mass, lb
Fairleads	9	0.125	1.1	-----
Harnesses (7 ft)	136	.0189	2.6	-----
Connectors				
61-pin	1	1.5	1.5	-----
37-pin	2	2.0	4.0	-----
Pressure sensors	9	.05	.5	-----
Valving				
Cryogenic valves	4	3.5	14.0	-----
Check valves	2	.156	.3	-----
Gas valves	8	2	16.0	-----
Relief valves	7	.2	1.4	-----
Regulators	2	2.6	5.2	-----
Valve harnesses				-----
Phos-bronze wires (7.5 ft)	8	.045	4	-----
Manganin wires (7.5 ft)	12	.0203	.2	-----
Fairleads	3	.125	4	-----
Connectors (at valves)	16	.25	4.0	-----
Connectors (at sequencers)	16	.25	4.0	-----
Panels (22 by 20)	2	8.8	17.3	-----
Helium Supply	-----	-----	-----	188
Helium bottles	2	73.5	147.0	-----
Struts				
Horizontal (8.0 in.)	4	0.65	2.6	-----
Vertical (19.3 in.)	4	1.57	6.3	-----
Tubing 1/4-in. o.d.	25	.054	1.4	-----
Panel				
Plate (16- by 16- by 0.1-in.)	1	2.6	2.6	-----
Regulator	1	2.6	2.6	-----
Gas valves	4	2	8.0	-----
Instrumentation				
Harnesses (7 ft)	36	.0189	.7	-----
Pressure sensors	2	.31	.6	-----
Flowmeters	1	.5	.5	-----
Miscellaneous structure, fasteners, and fittings	-----	-----	15.7	-----
LARGE RECEIVER TANK MODULE	-----	-----	-----	207
Pressure vessel				
Elliptical domes (10 percent added)	2	9.02	18.0	-----
Cylinder (10 percent added)	1	19.72	19.7	-----
Panel supports	12	.75	9.0	-----
Supporting structure				
Struts				
Glass-tension	8	.188	1.5	-----
Glass-torsion	2	.188	.4	-----
Aluminum ends	20	.256	5.1	-----
Spacecraft brackets	6	1.094	6.6	-----
Tank brackets	10	.2	2.0	-----
LAD assembly				
Channels				
Sidewalls (144- by 2.2- by 0.06-in.)	2	1.9	3.8	-----
Screen (1400 by 200)	1	.47	.5	-----
Perforated plate (0.05 in.)	1	.9	.9	-----
Tubing 1/4 in.	26	.0236	.6	-----

TABLE A.3.— Continued.

Item	Number of flight units	Unit mass, lb	Total mass, lb	Assembly mass, lb
Manifolds (6- by 6- by 2-in.)	2	.25	.5	-----
Ring-to-wall brackets	12	.05	.6	-----
Instrumentation racks				
Support rods	4	.62	2.5	-----
Temperature cones	19	.00655	.1	-----
Liquid-vapor cones	40	.0432	1.7	-----
Tangential spray system				
Tubing (1/4-in.)	8	.0236	.2	-----
Nozzles	4	.0625	.3	-----
Tubing support brackets	6	.03	.2	-----
Axial spray system				
Nozzles	2	.0625	.1	-----
Pressurant diffuser	1	.3	.3	-----
Insulation system				
MLI	1	15.2	15.2	-----
MLI can				
Facesheets - 2024 Aluminum				
Inner (57.4 ft ²)	1	16.5	16.5	-----
Outer (59.6 ft ²)	1	17.2	17.2	-----
Honeycomb (3/8 in. 5056 Aluminum)	1	4.2	4.2	-----
Valving	-----	-----	-----	-----
Viscojets	1	.095	.1	-----
Check valve	1	.156	.2	-----
Cryogenic valves	9	3.5	31.5	-----
Relief valves	2	.156	.3	-----
Harnesses				
Fairleads	6	.125	.75	-----
Phos-bronze wires (7.5 ft)	18	.045	.81	-----
Manganin wires (7.5 ft)	27	.0203	.548	-----
Connectors				
55-pin	2	1	2.0	-----
5-pin	9	.25	2.3	-----
Instrumentation				
Harnesses				
Valve panel (6 ft)	72	.0162	1.2	-----
Internal tank wires (5 ft)	120	.0135	1.6	-----
External tank wires (8 ft)	225	.0216	4.9	-----
External MLI can (8 ft)	24	.0216	.5	-----
Fairleads	40	.125	5.0	-----
Connectors				
55-pin	7	1	7.0	-----
Tank feedthroughs	4	2	8.0	-----
Flowmeters				
Venturis	1	.8	.8	-----
Pressure sensors				
Absolute	9	.31	2.8	-----
Differential	1	.688	.7	-----
Temperature sensors	86	.0033	.3	-----
Tubing				
1/4-in. o.d.	17	.054	.9	-----
1/2-in. o.d.	23	.174	4.0	-----
Miscellaneous fittings and fasteners	-----	-----	3.1	-----

TABLE A.3.— Continued.

Item	Number of flight units	Unit mass, lb	Total mass, lb	Assembly mass, lb
SMALL RECEIVER TANK MODULE	-----	-----	-----	178
Pressure vessel				
Elliptical domes (10 percent added)	2	12.13	24.3	-----
Cylinder (10 percent added)	1	4.98	5.0	-----
Panel supports	12	.83	10.0	-----
Supporting structure				
Struts				
Glass-tension	8	.188	1.5	-----
Glass-torsion	2	.188	.4	-----
Aluminum ends	20	.256	5.1	-----
Spacecraft brackets	6	1.094	6.6	-----
Tank brackets	10	.2	2.0	-----
Spray system				
Radial tube	1	.8	.8	-----
Nozzles	15	.0625	.9	-----
1/4-in. tangential tube (3 ft)	1	.06	.1	-----
Flow baffle (22-in. diameter)	1	3.8	3.8	-----
Insulation system				
MLI	1	12.0	12.0	-----
MLI can				
Facesheets - 2024 Aluminum - 0.020 in.				
Inner (45.1 ft ²)	1	13.0	13.0	-----
Outer (47.0 ft ²)	1	13.5	13.5	-----
Honeycomb (3/8 in. 5056 Aluminum)	1	3.3	3.3	-----
Valves				
Cryogenic valves	9	3.5	31.5	-----
Relief valves	1	.156	.2	-----
Harnesses				
Fairleads	6	.125	.75	-----
Phos-bronze wires (7.5 ft)	20	.045	.9	-----
Manganin wires (7.5 ft)	21	.0203	.426	-----
Connectors				
55-pin	1	1	1.0	-----
5-pin	8	.25	2.0	-----
TVS				
Viscojet	1	.095	.1	-----
1/4-in. tube	50	.0236	1.2	-----
Instrumentation				
Rake support rods	4	.3	1.2	-----
Brackets	2	.1	.2	-----
Harnesses				
Valve panels (4 ft)	68	.0108	.7	-----
Internal tank wires (6 ft)	96	.0162	1.6	-----
External tank wires (6 ft)	239	.0162	3.9	-----
Fairleads	35	.125	4.4	-----
Connectors				
55-pin	8	1	8.0	-----
Tank feedthroughs	3	2	6.0	-----
Pressure sensors				
Absolute	8	.31	2.5	-----
Temperature sensors	24	.00655	.2	-----
Liquid/vapor sensors	40	.0432	1.7	-----
Tubing				
1/4-in. o.d.	8	.054	.4	-----
1/2-in. o.d.	13	.174	2.3	-----
Miscellaneous fittings and fasteners	-----	-----	4.5	-----

TABLE A.3.— Continued.

Item	Number of flight units	Unit mass, lb	Total mass, lb	Assembly mass, lb
FLUID INTERFACE SUBSYSTEM	-----	-----	-----	271
Supply Tank Module	-----	-----	-----	134
Radiator tray				
Tray	1	45	45.0	-----
Radiating surface	1	11	11.0	-----
Support brackets	8	0.5	4.0	-----
Valves				
Cryogenic	4	3.5	14.0	-----
Relief	1	.156	.2	-----
Harnesses	9	.0296	.3	-----
Connectors	1	.25	.3	-----
Instrumentation				
Harnesses (11 ft)	820	.0296	24.3	-----
Connectors (55-pin)	15	1.5	22.5	-----
Piping				
1/4-in. o.d. (13.3 + 13.3 ft)	26.6	.054	1.4	-----
3/8-in. o.d. (7.4 + 13.3 ft)	20.7	.104	2.2	-----
1/2-in. o.d. (3.3 ft)	3.3	.174	.6	-----
3/4-in. o.d. (5.6 ft)	5.6	.476	2.7	-----
1 1/2-in. o.d.	5.6	.996	5.5	-----
Large Receiver Tank Module	-----	-----	-----	56.4
Radiator tray				
Tray	1	17.8	17.8	-----
Radiating surface	1	4.1	4.1	-----
Support brackets	4	.5	2.0	-----
Valves				
Cryogenic	2	3.5	7.0	-----
Relief	3	.156	.5	-----
Harnesses	52	.0169	.9	-----
Connectors	1	.25	.3	-----
Instrumentation				
Harnesses (6.3 ft)	442	.0169	7.5	-----
Connectors	9	1.5	13.5	-----
Piping				
1/4-in. o.d. (6.0 + 6.0 ft)	12	^a .054	.6	-----
3/8-in. o.d. (6.0 + 6.0 ft)	12	^a .104	1.0	-----
1/2-in. o.d. (6.0 ft)	6	^a .174	1.0	-----
Small Receiver Tank Module	-----	-----	-----	22.5
Radiator tray				
Tray	1	5.8	5.8	-----
Radiating surface	1	1.2	1.2	-----
Support brackets	4	.5	2.0	-----
Valves				
Relief	1	.156	.2	-----
Harnesses	41	.0169	.7	-----
Connectors	1	.25	.3	-----
Instrumentation				
Harnesses	318	.00594	1.9	-----
Connectors	6	1.5	9.0	-----
Piping				
1/4-in. o.d. (3.0 + 3.0 ft)	6	^a .054	.3	-----
3/8-in. o.d. (3.0 + 3.0 ft)	6	^a .104	.6	-----
1/2-in. o.d. (3.0 ft)	3	^a .174	.5	-----

^aMeasured in lb/ft.

TABLE A.3.— Concluded

Item	Number of flight units	Unit mass, lb	Total mass, lb	Assembly mass, lb
Vent System	-----	-----	-----	49.1
Panel structure				
Panel	1	9	9.0	-----
Brackets	4	0.5	2.0	-----
Valves				
Cryogenic	4	3.5	14.0	-----
Relief	2	.156	.3	-----
Check	2	.156	.3	-----
Harnesses	22	.0296	.7	-----
Connector	1	1.5	1.5	-----
Instrumentation				
Flowmeter	2	2.2	4.4	-----
Temperature sensor	2	.003	.01	-----
Pressure sensor	2	.31	.6	-----
Harnesses	46	.0296	1.4	-----
Connector	1	1.5	1.5	-----
Vent heater	2	.1	.2	-----
Piping 3/8 in. (9.9 + 9.9 ft)	19.8	^a .104	2.1	-----
Heat exchanger				
Tubing 3/8-in. stainless steel (30 ft)	1	3.9	3.9	-----
Panel	1	5.2	5.2	-----
Brackets	4	5	2.0	-----
Ground Interface Panel	-----	-----	-----	9.0
Ground interface panel	1	3	3.0	-----
Disconnects	2	3	6.0	-----
EXPERIMENT SYSTEM ELECTRONICS	-----	-----	-----	46.5
Signal conditioner	1	12.0	12.0	-----
Experiment data unit	3	7	21.0	-----
Accelerometer	1	6	6.0	-----
Mixer motor	1	7.5	7.5	-----
Total Experiment System Mass, Dry	-----	-----	-----	2206.5
CONSUMABLES	-----	-----	-----	589.8
Supply tank liquid hydrogen	-----	-----	565	-----
Helium pressurant	-----	-----	17.4	-----
Vaporizer liquid hydrogen	-----	-----	7.4	-----
TOTAL EXPERIMENT SYSTEM MASS, LIFT OFF	-----	-----	-----	2796.3

^aMeasured in lb/ft.

TABLE A.4.—STRUCTURAL ANALYSES SUMMARIES

SUPPLY TANK	
Material - 5083-0 Aluminum	
Ground operation	
Relief pressure, psia	52.0
Maximum expected operating pressure (MEOP), psia	49.0
Design pressure (P), psi	34.3
Wall thickness (t), in.	0.080
Radius of tank (R), in.	30
Ultimate strength (at cryogenic temperature), psi	70 000
Yield strength (at cryogenic temperature), psi	25 000
Weld efficiency (E)	1.0
Allowable stress per ASME boiler and pressure vessel code, section VIII, division I, psi	13 400
For internal pressure on cylindrical shell	
Stress = $S = P (R + 0.6t)/(Et)$, psi	12 883
For internal pressure on ellipsoidal shell (1.4:1)	
Stress = $S = P (0.66D + 0.2t)/(2Et)$, psi	8470
Factor of safety on ultimate	5.4
Burst pressure, psia	201.1
Factor of safety on yield	1.9
Proof pressure, psia	81.3
On-orbit	
Relief pressure, psia	52.0
Maximum operating pressure, psia	49.0
Design pressure (P), psi	49.0
Wall thickness (t), in.	0.80
Radius of tank (R), in.	30
Ultimate strength, psi	70 000
Yield strength, psi	25 000
Weld efficiency (E)	1.0
For internal pressure on cylindrical shell	
Stress = $S = P (R + 0.6t)/(Et)$, psi	18 404
For internal pressure on ellipsoidal shell (1.4:1)	
Stress = $S = P (0.66D + 0.2t)/(2Et)$, psi	12 100
Factor of safety on ultimate	3.8
Burst pressure, psia	186.4
Factor of safety on yield	1.4
Proof pressure, psia	66.6
Structural analysis for supply tank struts	
Wet weight of supply tank, lb	1275
Weight of MLI, MLI can, and purge bag, lb	187
Vertical loading, g	6
Horizontal loading, g	2
Strut angle with respect to horizontal (θ), degree	28.5
Strut length	
Total length, in.	19.73
Length from spacecraft structure to honeycomb, in.	9.87
Length from honeycomb to pressure vessel, in.	9.87
Strut o.d., in.	1.375
Strut wall thickness, in.	0.04
Strut cross-sectional area, in. ²	0.1678
Moment of inertia (I), in. ⁴	0.03741
Z , in. ³	0.0544
E (S-2 glass epoxy strut), psi	8 000 000
Tensile strength, psi	235 000
Compressive strength, psi	120 000
(Assume all vertical load is taken by top eight struts, but horizontal load is taken by four struts. Analysis is for strut in compression from horizontal and vertical load combined.)	
For vertical loads	
$P_{ST} = (\text{supply tank weight})/8$, lb	159.4
$P_{MLI} = (\text{MLI weight})/8$, lb	23.4

TABLE A.4.—Continued

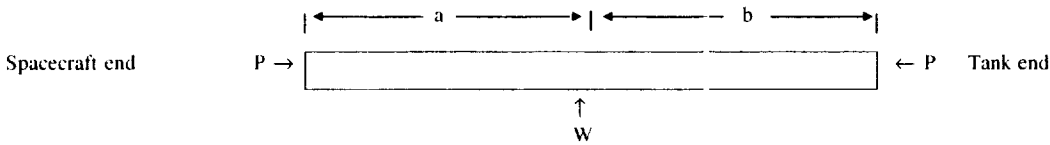
For horizontal loads	
P_{ST} = (supply tank weight, lb)/4	318.8
P_{MLI} = (MLI weight, lb)/4	46.8
W = load perpendicular to strut length, lb	167.9
P = axial load on strut, lb	1165.6
	
Displacement, in. = $(-Wa((L^2 - a^2)/3)^{1.5})/3EIL$	0.0898
Buckling = $P_{CR} = (\pi^2) EI/(L^2)$, lb	7587.3
Buckling amplification factor = $1/(1 - P/P_{CR})$	1.18
Total displacement, (Δ), in.	0.1060
$M_{max} = Wab/L$, lb-in.	828.9
Total bending moment = $M_{max} + (P\Delta)$, lb-in.	925.5
Bending stress = M/Z , psi	17 505
Axial stress = P/A , psi	6948
Total stress = $(P/A) + (M/Z)$, psi	22 181
Factor of safety in compression	5.4
LARGE RECEIVER TANK	
Material - 5083-0 Aluminum	
Ground operation	
Relief pressure, psia	52.0
Maximum operating pressure, psia	49.0
Design pressure (P), psi	34.3
Wall thickness (t), in.	0.061
Radius of tank (R), in.	16.25
Ultimate strength (room temperature), psi	40 000
Yield strength (room temperature), psi	18 000
Weld efficiency (E)	1.0
Allowable stress per ASME boiler and pressure vessel code, section VIII, division I, psi	10 000
For internal pressure on a cylindrical shell	
Stress = $S = P(R + (0.6t))/(Et)$, psi	9158
For internal pressure on ellipsoidal shell (1.4:1)	
Stress = $S = P(0.66D + 0.2t)/(2Et)$, psi	6537
Factor of safety on ultimate	4.4
Burst pressure, psia	164.5
Factor of safety on yield	2.0
Proof pressure, psi	82.1
On-orbit operation	
Relief pressure, psia	52.0
Maximum operating pressure, psia	49.0
Design pressure (P), psi	49.0
Wall thickness (t), in.	0.061
Radius of tank (R), in.	16.25
Ultimate strength (room temperature), psi	18 000
Weld efficiency (E)	1.0
For internal pressure on cylindrical shell	
Stress = $S = P(R + (0.6t))/(Et)$, psi	13 083
For internal pressure on ellipsoidal shell (1.4:1)	
Stress = $S = P(0.66D + 0.2t)/(2Et)$, psi	8588
Factor of safety on ultimate	3.1
Burst pressure, psia	149.8
Factor of safety on yield	1.4
Proof pressure, psi	67.4

TABLE A.4.—Continued

Structural analysis for large receiver tank struts

Dry weight of large receiver tank, lb	153
Weight of MLI and MLI can. lb	58
Vertical loading, g	6
Horizontal loading, g	2
Strut angle with respect to horizontal (θ), degree	39
Strut length	
Total length, in.	25.1
Length from spacecraft structure to honeycomb, in.	12.55
Length from honeycomb to pressure vessel, in.	12.55
Strut o.d., in.	1.00
Strut wall thickness, in.	0.04
Strut cross-sectional area, in. ²	0.1206
Moment of inertia (I), in. ⁴	0.01392
Z , in. ³	0.0278
E (S-2 glass epoxy strut), psi	8 000 000
Tensile strength, psi	235 000
Compressive strength, psi	120 000

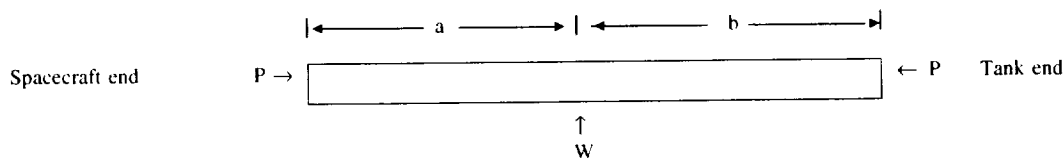
(Assume all vertical load is taken by top four struts, but horizontal load is taken by two struts. Analysis is for strut in compression from horizontal and vertical load combined.)

For vertical loads

P_{LR} = large receiver tank weight/4, lb	38.3
P_{MLI} = MLI weight/4, lb	7.3

For horizontal loads

P_{LR} = large receiver tank weight/2, lb	76.5
P_{MLI} = MLI weight/2, lb	29.0
W = load perpendicular to strut length, lb	70.3
P = axial load on strut, lb	335.8



Displacement, in. = $(-Wa((L^2 - a^2)/3)^{1/2})/(3EIL)$	0.2080
Buckling = $P_{CR} = (\pi^2 EI)/(L^2)$, lb	1744.7
Buckling amplification factor = $1/(1 - P/P_{CR})$	1.24
Total displacement, (Δ), in.	0.2575
$M_{max} = Wab/L$, lb-in.	441.2
Total bending moment = $M_{max} + P\Delta$, lb-in.	527.6
Bending stress = M/Z , psi	18 951
Axial stress = P/A , psi	2783
Total stress = $(P/A) + (M/Z)$, psi	18 628
Factor of safety in compression	6.4

SMALL RECEIVER TANK

Material - 5083-O Aluminum

Ground operation

Relief pressure, psia	52.0
Maximum operating pressure, psia	49.0
Design pressure (P), psi	34.3
Wall thickness (t), in.	0.067
Radius of tank (R), in.	18
Ultimate strength (room temperature), psi	40 000
Yield strength (room temperature), psi	18 000
Weld efficiency (E)	1.0
Allowable stress per ASME boiler and pressure vessel code, section VIII, division I, psi	10 000

TABLE A.4.—Continued

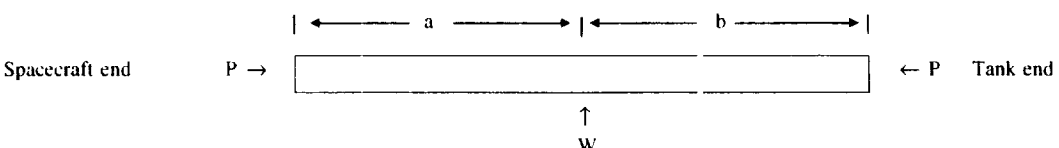
For internal pressure on cylindrical shell	
Stress = $S = P (R + (0.6t))/(Et)$, psi	9 236
For internal pressure on ellipsoidal shell (1.4:1)	
Stress = $S = P (0.66D + 0.2t)/(2 Et)$, psi	6 593
For MOP	
Factor of safety on ultimate	4.3
Burst pressure, psia	163.3
Factor of safety on yield	1.9
Proof pressure, psi	81.6
On-orbit operation	
Relief pressure, psia	52.0
Maximum operating pressure, psia	49.0
Design pressure (P), psi	49.0
Wall thickness (t), in.	0.067
Radius of tank (R), in.	18
Ultimate strength (room temperature), psi	40 000
Yield strength (room temperature), psi	18 000
Weld efficiency (E)	1.0
For internal pressure on cylindrical shell	
Stress = $S = P (R + (0.6t))/(Et)$, psi	13 194
For internal pressure on ellipsoidal shell (1.4:1)	
Stress = $S = P (0.66D + 0.2t)/(2 Et)$, psi	8 661
Factor of safety on ultimate	3.0
Burst pressure, psia	148.6
Factor of safety on yield	1.4
Proof pressure, psi	66.9
Structural analysis for small receiver tank struts	
Dry weight of small receiver tank, lb	122
Weight of MLI and MLI can, lb	47
Vertical loading, g	6
Horizontal loading, g	2
Strut angle with respect to horizontal (θ), degree	50
Strut length	
Total length, in.	9.4
Length from spacecraft structure to honeycomb, in.	4.7
Length from honeycomb to pressure vessel, in.	4.7
Strut o.d., in.	1.00
Wall thickness, in.	0.04
Strut cross-sectional area, in. ²	0.1206
Moment of inertia (I), in. ⁴	0.01392
Z , in. ³	0.0278
E (S-2 glass epoxy strut), psi	8 000 000
Tensile strength, psi	235 000
Compressive strength, psi	120 000
(Assume all vertical load is taken by top four struts, but horizontal load is taken by two struts. Analysis is for strut in compression from horizontal and vertical load combined.)	
For vertical loads	
P_{SR} = small receiver tank weight/4, lb	30.5
P_{MLI} = MLI weight/2, lb	5.9
For horizontal loads	
P_{SR} = small receiver tank weight/2, lb	61.0
P_{MLI} = MLI weight/2, lb	23.5
W = load perpendicular to strut length, lb	58.7
P = axial load on strut, lb	275.8
	

TABLE A.4.—Continued.

$Y_{\max} = (-Wa((L^2 - a^2)/3)^{1/3})/(3 EIL)$	0.0091
Buckling = $P_{CR} = \pi^2 EI/(L^2)$, lb	12 440.0
Buckling amplification factor = $1/(1 - P/P_{CR})$	1.02
Total displacement = Δ , in.	0.0093
$M_{\max} = Wab/L$, lb-in.	137.9
Total bending moment = $M_{\max} + p \Delta$, lb-in.	140.4
Bending stress = M/Z , psi	5044
Axial stress, P/A , psi	2286
Total stress = $(P/A) + (M/Z)$, psi	7238
Factor of safety in compression	16
HYDROGEN VAPORIZER STRUTS	
Wet weight of vaporizer, lb	171
Vertical loading, g	6
Horizontal loading, g	2
Strut angle with respect to horizontal (θ), degree	65
Strut length	
Near vertical strut, in.	19.3
Horizontal strut, in.	8
Strut dimensions	
Height, in.	2
Width, in.	1.5
Wall thickness, in.	0.125
Strut cross-sectional area, in. ²	0.8125
E , psi	10 000 000
Yield strength (6061-0 Aluminum), psi	12 000
Ultimate strength (6061-0 Aluminum), psi	22 000
(Analysis is for combined horizontal and vertical load on struts.)	
For vertical loads	
P_{SI} = vaporizer weight/two sides, lb	513.0
Load on near vertical strut, lb	566.0
Axial stress in vertical strut, psi	696.7
Load on horizontal strut, lb	-239.2
Axial stress in horizontal strut, psi	-294.4
For horizontal loads	
P_{SI} = vaporizer weight/two sides, lb	171.0
Using cantilever beam equations	
I_{xx} , in. ⁴	0.2836
$Z = I/c$, in. ³	0.3781
Load on vertical strut, lb	11.4
Moment on near vertical strut, lb-in	219.4
Deflection in near vertical strut, in.	0.010
Bending stress in near vertical strut, psi	580
Load on horizontal strut, lb	159.6
Moment on horizontal strut, lb-in	1277.049
Deflection in near horizontal strut, in.	0.10
Bending stress in near horizontal strut, psi	3 378
Total stress in near vertical strut, psi	1 277
Total stress in horizontal strut, psi	3 672
Yield strength factor of safety	
Vertical strut	9.4
Horizontal strut	3.3
Ultimate strength factor of safety	
Vertical strut	17.2
Horizontal strut	6.0
HELIUM BOTTLE STRUTS	
Wet weight of helium bottle, lb	89.5
Vertical loading, g	6
Horizontal loading,	2
Strut angle with respect to horizontal (θ), degree	65

TABLE A.4.—Concluded

Strut length	
Near vertical strut, in.	19.3
Horizontal strut, in.	8
Strut dimensions	
Height, in.	2
Width, in.	1.5
Wall thickness, in.	0.125
Strut cross-sectional area, in. ²	0.8125
E , psi	10 000 000
Yield strength (6061-T6 Aluminum), psi	12 000
Ultimate strength (6061-T6 Aluminum), psi	22 000
(Analysis is for combined horizontal and vertical load on struts.)	
For vertical loads	
P_{S1} = Vaporizer weight/two sides, lb	268.5
Load on near vertical strut, lb	296.3
Axial stress in vertical strut, psi	364.6
Load on horizontal strut, lb	-125.2
Axial stress in horizontal strut, psi	-154.1
For horizontal loads	
P_{S1} = Vaporizer weight/two sides, lb	89.5
Using cantilever beam equations	
I_{xx} , in. ⁴	0.2836
$Z = I/c$, in. ³	0.3781
Load on vertical strut, lb	6.0
Moment on near vertical strut, lb-in	114.8
Deflection in near vertical strut, in.	0.005
Bending stress in near vertical strut, psi	304
Load on horizontal strut, lb	83.5
Moment on horizontal strut, lb-in	668.3972
Deflection in near horizontal strut, in.	0.005
Bending stress in near horizontal strut, psi.	1768
Total stress in near vertical strut, psi	668
Total stress in horizontal strut, psi	1922
Yield strength factor of safety	
Vertical strut	18.0
Horizontal strut	6.2
Ultimate strength factor of safety	
Vertical strut	32.9
Horizontal strut	11.4

TABLE A.5.—LIQUID ACQUISITION DEVICE PRESSURE DROP CALCULATIONS

SCREEN CONFIGURATION — 200 by 1400 DUTCH TWILL	
Total LAD flow rate, lb/h	350
Liquid hydrogen properties	
Density (ρ), lb/ft ³	4.3
Viscosity (μ), lbm/ft-sec	6.24×10^{-6}
Bubble point, lb/ft ²	4.432
Gravity constant (g), ft/sec ²	32.17
Gravity (on orbit), ft/sec ²	0.00001
LAD geometry	
Channel width, in.	2.25
Channel depth (tube on screen), in.	0.500
Channel length (one leg), in.	130
Tube outside diameter, in.	0.75
Screen area open to flow, percent	50
Drop-through screen	
Flow area, in. ²	585
Velocity (V), ft/sec	0.00557
Pressure drop = $(0.885V + 2.01(V^2))\rho$, lb/ft ²	0.01995
Dynamic drop in channel	
Flow area, in. ²	1.306
Velocity (V), ft/sec	0.623
Pressure drop = $\rho V^2/(2g)$, lb/ft ²	0.0260
Friction drop in channel	
Wetted perimeter = p_w , in.	7.53
Hydraulic diameter = $D_h = (4A)/p_w$, in.	0.6934
Reynolds number = $(\rho V D_h)/\mu$	24 815
e (roughness)	0.0009
e/D_h	0.0013
Friction factor = f	0.0275
Pressure drop = $(f\rho L V^2)/(2g D_h)$, lb/ft ²	0.134
Turning drop in channel	
L/D	20
Pressure drop = $(L/D)f\rho V^2/(2g)$, lb/ft ²	0.0143
Total drop in LAD, lb/ft ²	0.194
Hydrostatic pressure in channel	
Height, ft	7
Pressure, lb/ft ²	0.00001
Total pressure drop in LAD (including hydrostatic drop), lb/ft ²	0.194021

Appendix B

Analysis of LAD/TVS Heat Exchanger Operation

This appendix presents a description of the integrated liquid acquisition device/thermodynamic vent system (LAD/TVS) proposed for use in the COLD-SAT supply tank and an analysis of its various modes of operation.

B.1 Description

The integrated LAD/TVS is composed of two principal parts: a screen channel liquid acquisition device (LAD) and an integral counterflow heat exchanger which forms the major portion of the thermodynamic vent system (TVS).

B.1.1 LIQUID ACQUISITION DEVICE

The integrated LAD/TVS is a component part of the liquid hydrogen supply tank. Each of the four LAD channels extends fore and aft along a longitudinal line in close proximity to the inner wall of the tank. The LAD assures phase separation so that hydrogen vapor is excluded when liquid is withdrawn from the supply tank. The TVS component of the LAD/TVS provides a heat sink during its operation to enable preconditioning of the outflow liquid, cooling of the bulk liquid, or condensing of vapor inadvertently trapped within the LAD channel. The integrated design promotes direct and intimate contact of the surrounding fluid with the cold surfaces of the TVS heat exchanger, for maximum performance and structural integrity in addition to compactness for minimum weight penalty.

Figure B.1 shows a cross-section view of a typical LAD/TVS channel. Three heat exchanger tubes are welded together along their sides to form one face of the channel. The opposite face consists of the phase separation screen mounted between the two side walls of the channel. A specific requirement of this construction is that no part of the weld can have porosity or a leakage area larger than the mean pore size of the screen even though the pressure difference across the channel wall is negligible. The surface tension and wetting characteristics of liquid hydrogen are expected preferentially to fill and to cause flow along the valleys formed between the tubes. Intimate contact between the heat exchanger tubes and liquid is thus further assured.

B.1.2 TVS HEAT EXCHANGER

The heat exchanger is an integral part of the LAD channel. Each of the 4 channels has 3 heat exchanger tubes for a total of 12 tubes, each nominally 137 in. long. The dimensions of a typical heat exchanger tube are shown in the cross-section drawing of figure B.1. The inner tube has a 0.5-in. diameter with a 0.035-in. thick wall. The liquid hydrogen, or hot-side fluid, enters an aft manifold, flows through the inner tubes, and exits into a forward manifold. The outer tube has a 0.75-in. diameter with a 0.049-in. thick wall. The TVS, or cold-side fluid, usually two-phase, enters its own forward manifold, flows through the annulus between the inner and outer tubes in a direction counter to the hot-side liquid, and exits into the aft TVS manifold.

All parts are fabricated of 5083 aluminum alloy which has desirable physical and thermal properties at cryogenic temperatures. The alloy has a mean density of 0.096 lb/in.³. Specific heat is about 3×10^{-3} Btu/lb/°R over a temperature range of 36 to 40 °R.

B.2 Modeling and Performance Analysis

The LAD/TVS system was analyzed to evaluate its thermal performance. The overall operating requirements such as heat load, flow rates, pressure, and temperature were specified by the COLDSAT experiment requirements. Physical sizes and dimensions of the supply tank and LAD/TVS components were established by the experiment subsystem design. The adequacy of the LAD/TVS thermal design, however, remains to be verified over the full range of operation imposed by the experiments. Furthermore, the analytical model and method of analysis require verification before ultimate use in designing a full-scale system in the future.

B.2.1 OPERATIONAL MODES

In the active TVS mode, the primary objective is supply tank pressure control. The heat exchanger operates steady-state at constant TVS and liquid hydrogen flow rates. The cooled liquid

hydrogen is recirculated back to the supply tank to reduce the bulk liquid temperature and hence the tank pressure. For purposes of analysis, the fluid states in the supply tank are assumed to be uniform with liquid and vapor coexisting at saturation conditions.

The subcooler TVS mode is used to condition the liquid to be transferred from the supply tank to a receiver tank. Depending upon the degree of subcooling required, the TVS and liquid flow rates are set at steady-state levels to vent 100 percent quality vapor at the TVS outlet.

The passive TVS mode is intended for long-term control of the supply tank pressure. No bulk liquid is circulated, hence heat transfer from the tank liquid to the heat exchanger is by conduction only. Intermittent and continuous TVS operations are examined. Because the heat transfer rates are time-dependent, the flow rates are expected to vary with time. The temperature profiles throughout the bulk tank liquid and the resulting pressures will also be time-dependent.

In this appendix each of the modes of operation previously mentioned will be examined for their salient features and overall effect upon the fluid state. Where ever possible, uniform or one-dimensional analytical approximations are used to avoid the rigors of more realistic but complex multidimensional models.

B.2.2 PROCESS THERMODYNAMICS

The thermodynamic state of the TVS fluid can be defined by a temperature-entropy diagram for hydrogen, which is shown in figure B.2. The left and right boundaries are the saturated liquid and vapor lines, respectively. The region to the far left is sub-cooled liquid and, although not shown, lines of constant pressure run nearly parallel to and in close proximity to the saturated liquid line. The far right region is superheated vapor with curves that define the temperature-entropy relationship at various pressures. In the region between the liquid and vapor lines are the two-phase mixtures varying in quality from zero at the liquid line to 100 percent at the vapor line. In this region, temperature and pressure are not independent, that is, when one is specified so is the other. Hence, a line of constant temperature is also a line of the corresponding constant pressure.

To follow the thermodynamic vent process, saturated liquid at 15 psia, for example, is passed through a Joule-Thomson (J-T) device and expanded along a line of constant enthalpy to 5 psia. The vapor quality downstream of the J-T device, or at the inlet to the heat exchanger, is 6.4 percent at 5 psia. Assuming negligible pressure drop in the TVS channel, the two-phase fluid follows a constant-pressure, constant-temperature path while absorbing heat and increasing in quality. Beyond the saturated vapor condition, further addition of heat results in superheated vapor of increasing temperature along a constant pressure line, assuming negligible pressure drop during superheating. If nonnegligible pressure drop exists in the vent line, there will be a pressure difference between the exit of the heat

exchanger and the vent outlet. For analysis purposes, the pressure is assumed to be constant throughout the domain of the TVS heat exchanger.

B.2.3 ITERATIVE INCREMENTAL MODEL

The heat transfer calculation for the LAD/TVS heat exchanger is an iterative procedure. The inlet states of both the liquid hydrogen and the TVS fluid are known but at opposite ends of the counterflow heat exchanger. The total length is divided into a number of segments shown typically in figure B.3. Calculation is initiated at the TVS inlet end. If the TVS fluid is known to remain two-phase throughout the heat exchanger, its temperature remains constant, and calculation can be started at either end. The temperature of the liquid at its exit from the heat exchanger is first estimated by performing an overall heat balance between the liquid and the TVS fluid assuming that the TVS fluid exits as 100 percent saturated vapor. Other assumptions are that pressure drops in both channels are negligible and that hot-side and cold-side temperatures are uniform at any cross section. The overall heat transfer coefficient consists of the hot-side (liquid hydrogen) and cold-side (TVS) individual heat transfer coefficients, and the intervening wall resistance. For thin walls of high conductivity material, this resistance can be neglected although its inclusion does not add significantly to the computation procedure.

A flow chart of the computation procedure when the heat exchange occurs from single-phase liquid to a two-phase mixture of liquid and its vapor is shown in figure B.4a. A length increment of the heat exchanger over which the iteration occurs is represented in figure B.3. At station 1 of the first segment, the fluid states, individual heat transfer coefficients, overall temperature difference between the liquid side and TVS side, and the overall heat transfer coefficient are calculated. This overall coefficient is kept available to a later part of the computation. A guess is then made for the liquid temperature T_2 at station 2, which allows an estimate of properties and coefficients at the end of the segment. The heat transfer rate, Q , within the segment, is calculated, by using the following equation for heat transfer from single-phase liquid to two-phase flow:

$$Q = A \left[\frac{U_1 \times \Delta T_2 - U_2 \times \Delta T_1}{\ln \left(\frac{U_1 \times \Delta T_2}{U_2 \times \Delta T_1} \right)} \right]$$

$$\frac{1}{U} = \frac{2}{h_L} + \frac{1}{h_G}$$

where

Q	heat transfer rate
h_G	two-phase heat transfer coefficient
h_L	liquid heat transfer coefficient
A	heat transfer area
U	overall heat transfer coefficient
ΔT	hot-side to cold-side temperature difference
D	characteristic dimension
G	mass velocity
C_p	specific heat
k	conductivity
μ	viscosity
1, 2	denotes station position of the increment
h_G	two-phase heat transfer coefficient

This Q is then used to calculate the properties of both fluids at station 2. The properties thus calculated are not necessarily the same as the estimated values based on the guess temperature unless there is a balanced match of the fluid enthalpies, heat transfer coefficients, and temperature differences. Successively better guesses of the liquid temperature at station 2 lead to a converged solution which then becomes the inlet conditions for the next segment. In practice, the best guess for each iteration was found to be the calculated value from the preceding iteration. The TVS quality, X_2 , was monitored at each converged solution, and if greater than 100 percent, the calculation for that segment was repeated, using a smaller increment size to define the heat exchanger location at which the quality attained exactly 100 percent. Beyond the 100 percent quality location, the TVS flow is single-phase, and this second equation for Q , was used:

$$Q = UA \left[\frac{\Delta T_2 - \Delta T_1}{\ln \left(\frac{\Delta T_2}{\Delta T_1} \right)} \right]$$

$$h = 0.023 \left(\frac{D \times G}{\mu} \right)^{0.8} \left(\frac{C_p \mu}{k} \right)^{0.4} \left(\frac{k}{D} \right) \text{ for liquid or gas}$$

Fluid properties constantly change throughout the calculation. Computer programs for fluid properties are available, but it was found more convenient and faster to use curve-fitted polynomials of first to third degree over the limited temperature range of interest.

The two-phase heat transfer coefficients were calculated from a correlation method developed by Chen (ref. 25). The single-phase coefficients were calculated by the Dittus-Boelter equation (ref. 26) for liquid or gas.

When both heat exchanger passages contained single phase fluid, the second form of the equation for Q , shown previously, was used. A flow chart of the computation for single-phase fluids is shown in figure B.4(b). The iteration process is similar, but instead of temperature, a guess value of temperature difference, ΔT_2 , is used at station 2. The overall coefficient, U , is assumed constant over the segment, and iteration is repeated until the calculated temperature difference equals the guess value. As before, the computation algorithm must allow for variation of increment length, especially if the overall coefficient evaluated at the inlet of the next segment shows that the coefficient change was too large, in which case the assumption of constant U over the preceding segment had been violated. The allowable change for the coefficient is a matter of judgment and compromise to avoid excessive calculation time for increment sizes which are too small.

It should be noted that the first pass through the full length of the heat exchanger may not necessarily yield the correct solution. If the assumed exit temperature of the liquid side is too high at the start of the calculation pass, the calculated liquid inlet temperature may likewise end up higher than the actual inlet temperature. A second pass will then be necessary using a lower exit temperature. For a case in which the TVS fluid is known to be at constant temperature throughout the heat exchanger and exiting at exactly 100 percent vapor without superheat, the iterative incremental model calculation can be started at the liquid hydrogen inlet end. The computation algorithm should be checked to assure that heat is being removed from the liquid and added to the TVS fluid as the calculation proceeds from one increment to the next.

Clearly, the validity of the calculated results depends upon the correctness of the various heat transfer coefficients involved. Two-phase boiling heat transfer, especially of cryogenic fluids flowing at low mass velocity in a weightless environment, is a subject of much uncertainty and on-going research. The proposed COLDSAT experiment is a vital part of this research.

B.2.4 PASSIVE TVS MODEL

In the passive TVS mode, no bulk liquid is circulated through the heat exchanger. This mode requires a transient analytical model, not only because the operation might be intermittent, but also because the nature of the process itself is strongly time-dependent. Without liquid convection, the heat

transfer mechanism from the tank bulk liquid to the heat exchanger is by conduction only, which is relatively slow. The TVS heat exchanger temperature is assumed to be 30.8 °R whenever the TVS is in operation because the transients in the exchanger tubes are short compared to those of the liquid. If operated intermittently, the liquid adjacent to the heat exchanger is cooled and warmed cyclically as the TVS flow is started and stopped. Even with continuous operation from an initially uniform temperature, transient cooling of the adjacent liquid leads to progressively less heat transfer into the TVS fluid. Unless the TVS flow rate is varied to match the decreasing heat input rate, vapor efflux at 100-percent quality cannot be assured.

A simple one-dimensional cylindrical coordinate model shown in figure B.5 was used to analyze the problem. The size of the LAD is small relative to the rest of the tank, so that conducted heat flux is assumed to follow radial lines with uniform flux density at any given radius. In order to keep the model one-dimensional and transient, it was assumed that the radial heat flux density was constant along the length of the heat exchanger. This assumption is considered acceptable if the LAD cross-sectional dimensions are small relative to the liquid bulk in which there is no convection, and if the distance between the liquid/vapor interface and the LAD is nearly constant over its length. The liquid region between the heat exchanger and the liquid/vapor interface was divided into 30 equal increments. A time-dependent conduction equation was written for each node and solved simultaneously using a Runge-Kutta-Gill integration scheme.

The liquid confined within the LAD channel was set up as a transient one-dimensional conduction problem in Cartesian coordinates and divided into 5 equal increments. The corresponding 5 equations were included as a set with the other 30 and solved together. The governing equations and their boundary conditions are listed in figure B.5. By using suitable logical conditions, the computer program could also be used to solve the problem as a continuous TVS operation.

B.3 Performance Calculation Results

As mentioned earlier, three modes of TVS operation are being considered for the COLD-SAT flight experiment. Although essentially the same experiment hardware is used for each mode, the method of operation is varied to fulfill the specific objectives of the different experiments. The parameters of the experiment such as heat load and flow rates were considerably different in some cases and the calculation procedure needed to be adjusted accordingly. In particular, the passive TVS mode involved totally different heat transfer and process physics, so that the problem required a formulation much different from the active and subcooler modes.

In the following sections, the objectives, operating conditions, and results of each operating mode will be presented.

Characteristics unique to each mode will be shown and discussed in greater detail in a subsequent section.

B.3.1 ANALYSIS OF ACTIVE TVS

The active TVS mode is used primarily for pressure control in the supply tank. Liquid hydrogen from the tank is "actively" pumped through the heat exchanger and returned to the tank as cooled liquid. Operating parameters for this mode are shown in the conceptual diagram of figure B.6. The liquid pump rate and TVS flow rates were established at 440.1 lb/hr and 5.6 lb/hr, respectively, and held constant. The various inlet and outlet states are indicated in the figure and were either specified by the experiment requirements or calculated by the heat exchanger analysis method described earlier. The supply tank pressure was taken to be 15 psia with the liquid at saturation temperature. These conditions were input to the J-T device and to the aft manifold of the LAD channels. The circulation pump is shown downstream of the LAD heat exchanger, but system design modifications to locate the pump upstream have been considered. Energy addition to the liquid from the pump could thus be removed by the heat exchanger.

The constant-enthalpy expansion to 5 psia through the J-T device resulted in a quality of 6.4 percent and a saturation temperature of 30.8 °R at the inlet of the heat exchanger. The temperature and quality profiles throughout the exchanger are shown in figure B.7. The TVS flow was two-phase and at constant temperature for about 12 in. from its inlet. Most of the liquid cooling occurred over this length. Beyond this length, the heat removed from the liquid went into superheating of the TVS fluid which exited the heat exchanger at the same temperature as the incoming liquid.

The corresponding quality profile of the TVS fluid is shown as a broken line in figure B.7. Following a linear increase to 100 percent quality at about 12 in., the flow continued as superheated vapor to the exit at 137 in. from the inlet.

The time-dependent change in supply tank pressure under active TVS operation over a 2-hr period is shown in figure B.8. The heat rejection rate of 1021 Btu/hr was assumed to be constant and the cooled liquid was assumed to be uniformly mixed with the bulk liquid in the supply tank. The coexistence of liquid and its vapor as a uniform mixture of known enthalpy defines the temperature and pressure which decreased at a rate of about 2.5 psia/hr.

B.3.2 ANALYSIS OF SUBCOOLER TVS

The subcooler TVS mode is used to pre-condition the liquid hydrogen prior to pressurized transfer into a receiver. Figure B.9 shows the various parameters associated with this operating mode. Because the supply tank is pressurized rapidly within a short time period before transfer begins, the bulk liquid is essentially at saturation conditions corresponding to the initial tank pressures of 15 and 25 psia used in the analysis.

Flow rates ranging from 50 to 350 lb/hr were examined. The degree of subcooling varied from 8.8 to 1.1 °R depending on flow rate. The TVS fluid was drawn from the two initial conditions in the supply tank at flow rates which assured that no liquid would be vented. Under these conditions, the heat exchanger performance analysis was more exacting than was the case for the active TVS mode, because in the active TVS mode the heat transfer rates and liquid flow rates were interdependent.

Figure B.10 shows the temperature profile throughout the heat exchanger for a liquid flow rate of 50 lb/hr and a TVS flow rate of 5.6 lb/hr. Temperatures associated with the 25-psia initial tank conditions are shown as broken lines. The TVS fluid reached 100 percent quality at a distance of about 120 in. from the inlet, followed by some superheating before exiting the heat exchanger. The liquid entered at 40 °R and was subcooled 8.8 °R to exit at a temperature of 31.2 °R, or 0.4 °R above the TVS inlet temperature.

When liquid was drawn from the 15-psia initial tank conditions, the degree of subcooling was reduced, entering at 36.6 °R and exiting at 30.9 °R. Accordingly, a reduction in the TVS flow rate to 3.5 lb/hr was required to obtain 100-percent saturated vapor venting at the heat exchanger exit.

The TVS quality profile for the two flow rates are shown in figure B.11. With liquid drawn from the 25-psia initial condition, the full length of the heat exchanger was not required to vaporize all of the 5.6 lb/hr TVS flow. At the 15-psia initial tank conditions, a TVS flow rate of 5.6 lb/hr would have exited the heat exchanger at only 60.1-percent quality. Even at the reduced flow rate of 3.5 lb/hr, the full length of 137 in. was required to just reach 100-percent saturated vapor at the exit.

B.3.3 ANALYSIS OF PASSIVE TVS

Figure B.12 illustrates the conditions and assumptions associated with the passive TVS mode for intermittent operation over a period of 84 hr. As stated earlier, the tank bulk liquid was not circulated, and heat transport to the heat exchanger was by conduction only. Because of the time-dependent low heat flux, the TVS flow rate was less than 1 lb/hr and decreased with time. As the liquid in the tank is gradually cooled over time, the TVS fluid, expanding to a constant 5-psia pressure downstream of the J-T device, can be expected to decrease in quality, but this variation was neglected. The exterior surface of the heat exchanger was assumed to be liquid-wetted at all times without exposure to the ullage vapor. The TVS flow was varied to obtain 100 percent quality at the outlet before venting.

The intermittent passive TVS mode was analyzed for a tank liquid condition at 15-psia saturation pressure. The radial distance from the tank wall to the liquid-vapor interface, a significant parameter of the problem, was selected to correspond to a 95-percent full tank with axisymmetric ullage. Because the small TVS flow rate was the sole mechanism

for liquid mass loss, the radial distance to the interface was assumed constant throughout the analysis.

Intermittent passive TVS operation over an 84-hr period with a duty cycle of 12 hr on and 24 hr off was arbitrarily selected to examine its transient characteristics. A continuous passive TVS mode was also run for a pressure history comparison to be made later.

Figure B.13 shows a history of the TVS, liquid, and interface temperatures over the 84-hr period. Only 3 of the 35 nodal temperatures available in the model are presented in figure B.13 for the sake of clarity. The TVS temperature corresponds to a liquid node (node 1) within the LAD channel closest to and located 0.22 in. from the heat exchanger tube surface. The liquid temperature is node 1, located in the bulk tank liquid 0.45 in. from the heat exchanger tube surface. The interface (node 30), is at a radial distance of 15.35 in.

At the beginning of the cycle, at 0 hr, the TVS temperature dropped rapidly to approach the two-phase saturation temperature of 30.8 °R. A small lag is noticeable because this temperature is of a liquid node that is a finite distance removed from the heat exchanger surface. When the TVS flow was stopped at 12 hr, the temperature rose linearly during the off period. Because of the constant heat input from the tank wall nearby, the TVS temperature could exceed the liquid temperature if kept in the off condition too long. When the TVS flow was on again, the temperature dropped rapidly as before to repeat the cycle.

The liquid temperature exhibited characteristics similar to the TVS temperature but with a larger lag, presumably because this node was twice as far from the cold heat exchanger surface and surrounded by a radial expanse of bulk tank liquid. As the off period progressed, the temperature seemed to approach an asymptote without exceeding the interface temperature because the source for the heat conducted toward the heat exchanger was the interface, which was the farthest liquid node and presumably the warmest.

The interface temperature had the largest lag and because of the damping effect of the liquid thermal capacity, did not exhibit wide temperature excursions during the on/off periods. The interface temperature decreased monotonically because heat was being conducted continuously toward the heat exchanger whether the TVS was on or off. A small amount of nonlinearity existed and was observed to be out of phase with the TVS cycle. The total change in interface temperature over the 84-hr period was of the order of 1 °R.

The corresponding change in tank pressure during the intermittent passive TVS operation is shown in figure B.14. Also shown for comparison is the pressure history for a continuous passive TVS operation. The time-temperature profile for a passive TVS operation in continuous mode is shown in figure B.15, which requires little comment because of its apparent simplicity. As expected, the continuous mode resulted in a more rapid and eventually larger decrease in pressure (fig. B.14), because heat extraction was uninterrupted over the

entire period. The total decrease in pressure for the intermittent mode over the 84-hr period was about 2.5 psi, which corresponds to the saturation pressure change for a 1° change in interface temperature.

A requirement of the TVS operation was that the flow remain two-phase throughout the heat exchanger but exit without venting any liquid, that is, reach 100-percent vapor at the heat exchanger outlet. To meet this requirement during passive TVS operation, the TVS flow rate had to be varied according to the time-dependent heat load. The TVS flow rate variations throughout the 84-hr period under continuous mode and the intermittent mode of 12 hr on and 24 hr off are shown in figure B.14. At the beginning, the required flow rate was of the order of 0.8 lb/hr, but it decreased rapidly to approach 0.1 lb/hr at the 12-hr turn-off time. Note that the initial phase of the intermittent mode is identical with the initial part of the continuous mode because both start from identical initial conditions. When the TVS was turned on again at 36 hr, the required flow rate rose to nearly 0.6 lb/hr but rapidly dropped to about 0.1 lb/hr by the 48-hr turn-off time. Similar patterns repeated at 72 hr and 84 hr, except that the peak and minimum flow rates continued to decrease slightly because of the slowly decreasing heat load as the bulk liquid gradually cooled down.

For the continuous TVS operation, the first "on" cycle was identical to the intermittent mode. Thereafter, the continuous TVS flow rate decreased slowly as expected.

As an arbitrary alternative, a duty cycle of 1 hr on and 2 hr off was investigated, and the results are shown in figure B.16. The time scale is highly expanded so (comparisons with the 84-hr case should be made accordingly. Initial conditions and fill levels were kept identical. Quantitatively, the liquid temperature minimum in the first cycle was 32.8 °R after 1 hr compared with 31.7 °R after 12 hr in the 84-hr cycle. During the 2-hr off period, the temperature recovered to nearly the same level as in the longer 24-hr off part of the 84-hr cycle. The more noticeable difference between the two duty cycles was in the TVS temperature. In either case, the temperature minimum during the on period was nearly the same because the same TVS temperature of 30.8 °R was reached rather quickly. The recovery process was much slower and thus 2 hr off was insufficient time to cause a significant temperature rise. The short duty cycle thus tended to approach a continuous "on" mode. In terms of the interface temperature, after the first 7 hr of operation the continuous mode reached a temperature of 36.588 °R compared with 36.591 °R for the short duty cycle in which three "on" periods and two "off" periods had occurred.

B.4 Discussion of Results

The performance calculations presented above were obtained using various simplifying assumptions. Although the

results are not unreasonable, their accuracy cannot be verified without comparison against experimental data. Recalculations with different models or parameter values can determine the sensitivity of each assumption, but an effort of such magnitude was not considered justifiable at the time. As an alternative, the context and possible impact of various assumptions will be discussed to temper the results and possibly to obtain a better understanding of the experiment subsystem performance.

B.4.1 ACTIVE TVS

The heat exchanger performance calculations for the active TVS mode assumed liquid drawn from the supply tank at constant inlet conditions. Actually, the cooled liquid was returned to the tank at a flow rate of 440.1 lb/hr which would cause the supply tank liquid to cool down continuously. Two departures from the assumed conditions are expected to occur: (1) The liquid entering the heat exchanger changes continuously thus making its performance time-varying. (2) The TVS liquid drawn through the J T device also changes, and the exit quality therefore changes with time. These effects in turn affect the end-to-end performance of the heat exchanger and the cooling rate of the supply tank liquid. Another factor of greater uncertainty is the extent of mixing between the supply tank liquid and the recirculating cooled liquid from the heat exchanger. The present calculation assumed uniform mixing at all times. The actual mixture might have considerable nonuniformity which could manifest itself as irregular variations in tank pressure as liquid masses of varying temperature are convected to the liquid-vapor interface. An inclusive model representing all of the possible fluid physics would involve considerable effort and difficulty. A reasonable compromise may be to allow incremental changes in the heat exchanger operating point and to calculate its performance as a quasi-steady system. The supply tank pressure may then be assumed as a smoothed average from point to point.

Another related question is how the performance might be affected by the fact that the outer halves of the heat exchanger tubes are exposed to the bulk tank liquid while the inner halves face the liquid flowing within the LAD channel before entering the aft manifold. From an overall heat balance viewpoint, heat is being transferred from bulk tank liquid conditions to the TVS heat sink temperature. How the heat transfer is distributed between different sides of the tube, and where the exact boundary between bulk liquid and heat exchanger is located does not affect the overall process, although the details of local temperature gradients and heat flux density may be interrelated. Stated another way, the heat transfer rate depends upon the transfer coefficient, the effective area, and the temperature difference. If only one of the three factors is known, the overall heat balance can still be satisfied by appropriately defining and specifying the other two.

B.4.2 SUBCOOLER TVS

The liquid conditions under subcooler TVS operation are expected to be more like those assumed in the analysis. Because liquid is withdrawn but not recirculated, the bulk tank liquid is expected to remain essentially constant and unmixed. As the ullage volume increases, however, the supply tank pressure will decrease. Evaporation from the interface and lowering of the interface temperature would tend to maintain saturation conditions. Eventually as tank pressure drops below the saturation pressure of the warmest liquid in the bulk, nucleate boiling can be expected, thus promoting mixing and a trend toward a uniform mixture at a lower pressure.

A further refinement on the performance calculations would be to model the system as a transient problem similar to that suggested for the active TVS mode. The temporal changes are expected to be slower, and the point to point approximation should be sufficiently accurate.

B.4.3 PASSIVE TVS

The one-dimensional transient model used for analyzing the passive TVS performance was selected as a reasonable compromise considering realistic limitations of time and resources. Clearly, a transient model was needed to represent the strong time dependence. It was reasoned that the temporal variations would be of more concern than the spatial details because as heat transport through the bulk liquid was by conduction. Even using commercially available codes such as SINDA to analyze the problem, modeling and computing time would be considerable.

The one-dimensional model, as formulated, has some limitations which should be recognized. Whereas the uniform heat leak rate through the tank wall was included with the liquid confined within the LAD, it was not included for the bulk liquid in the tank. The boundary condition representing the wall heat leak could not be specified without using a second dimensional variable. The second variable would also have permitted establishing axes of symmetry for a better modeling of each of the four LAD channels. Such a refinement would prompt the addition of a third dimensional variable because of variations along the length of the LAD and the shape of the tank. Because the region of primary interest was the LAD/TVS heat exchanger and its transient behavior, external details were sacrificed for simplicity. The results are credible and indicative of the salient features of the passive TVS operation.

Another deviation inherent in the one-dimensional model is the curvature of the liquid/vapor interface which, in reality, should be concave as viewed from the tank centerline. Interface definition is necessary for determining the tank pressure. The boundary condition for the interface was specified as an adiabatic surface, and the significant parameter was its distance

from the heat sink. For an actual system, the interface is an isothermal surface, hence the temporal behavior of a leading, or most responsive, spatial point could be considered as representative of the entire interface.

The TVS flow rate calculated to obtain 100-percent vapor at the heat exchanger outlet varied with time over a wide range because of the time-varying heat load. Obtaining such a flow profile, hereafter referred to as ideal flow, would require a continuously variable flow controller at the TVS inlet. The COLD-SAT TVS system as presently configured does not include a continuously variable flow control valve. Instead, three on-off valves of different flow capacities are to be used singly or in parallel combinations to produce up to seven discrete levels of flow. These seven flow levels cannot be expected to match the infinite variability of a continuously variable flow control valve. If the discharge of even a small amount of unvaporized liquid at the TVS outlet is forbidden, the three on-off valves will have to be operated in a scheduled combination such that the heat transfer rate is always equal to or less than that calculated previously. There will thus be periods when the TVS outlet vapor is slightly superheated and the resulting overall heat removal will be less than for the ideal flow.

The other alternative is to cycle the on-off valves intermittently and rapidly in the correct combinations to obtain a time-integrated quantity of flow equal to the ideal flow. This approach assumes that a momentarily excessive amount, or slug, of TVS fluid, introduced during the valve-open period, will flow smoothly through the heat exchanger during the valve-closed period. Heat exchanger performance calculation will be considerably more difficult in this mode, and in practice, smooth flow of a vaporizing slug of liquid through the heat exchanger tubes may not be physically obtainable.

B.5 Vapor Condensation and Bubble Collapse

The purpose of the LAD is to separate the phases of hydrogen so that only liquid is drawn into the LAD channel. Inadvertently high pump-out rate and heat leak or incomplete initial venting could cause vapor bubbles to be trapped. It is of interest to evaluate the effectiveness of the TVS system in condensing the vapor and causing the bubble to collapse. Tegart and Dominick (ref. 27) performed an analysis and compared it with experiments in Freon 11 to determine the collapse time of spherical and rectangular bubbles. The analysis was applied to liquid hydrogen, and the results are shown in figure B.17 for tank pressures of 15 and 25 psia. The characteristic dimension, D , is the length of bubble in a rectangular channel with a cross section of 0.45 by 2.2 in. corresponding to the supply tank LAD. In the spherical bubble, the dimension, D , refers to the

bubble diameter. For the large receiver LAD having a triangular cross section, the maximum trapped spherical bubble diameter is limited to 1.5 in.

Both the rectangular and spherical bubbles were found to require less than 3 minutes for total collapse. The rectangular bubble, in particular, required moderate times even for lengths up to 100 in. These characteristics are believed to be due to the heat transfer areas available in the bubbles. A spherical bubble,

for any given volume, has the minimum surface to volume ratio, which vary as $6/D$ for a diameter, D . A rectangular bubble, on the other hand, has the same surface area per unit length of the bubble, however long. The analysis of Tegar and Dominick assumed that liquid at the condensing temperature totally surrounded the vapor bubble. To first order, conditions within a LAD channel cooled by the TVS heat exchanger were assumed to be amenable to the same assumption and analysis.

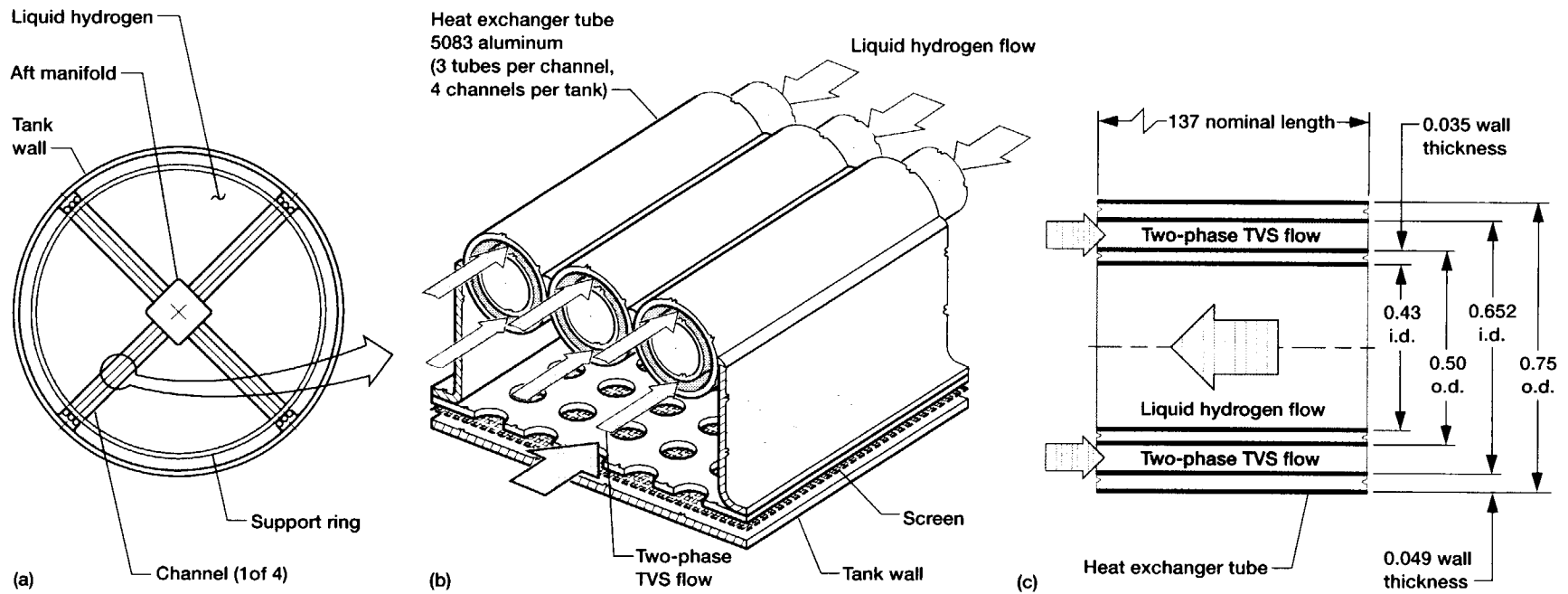


Figure B.1.—Typical LAD/TVS system channel. Dimensions are in inches.
 (a) LAD/TVS system channel in supply tank (top view).
 (b) Detail of LAD/TVS channel. (c) Cross section of one heat exchanger tube.

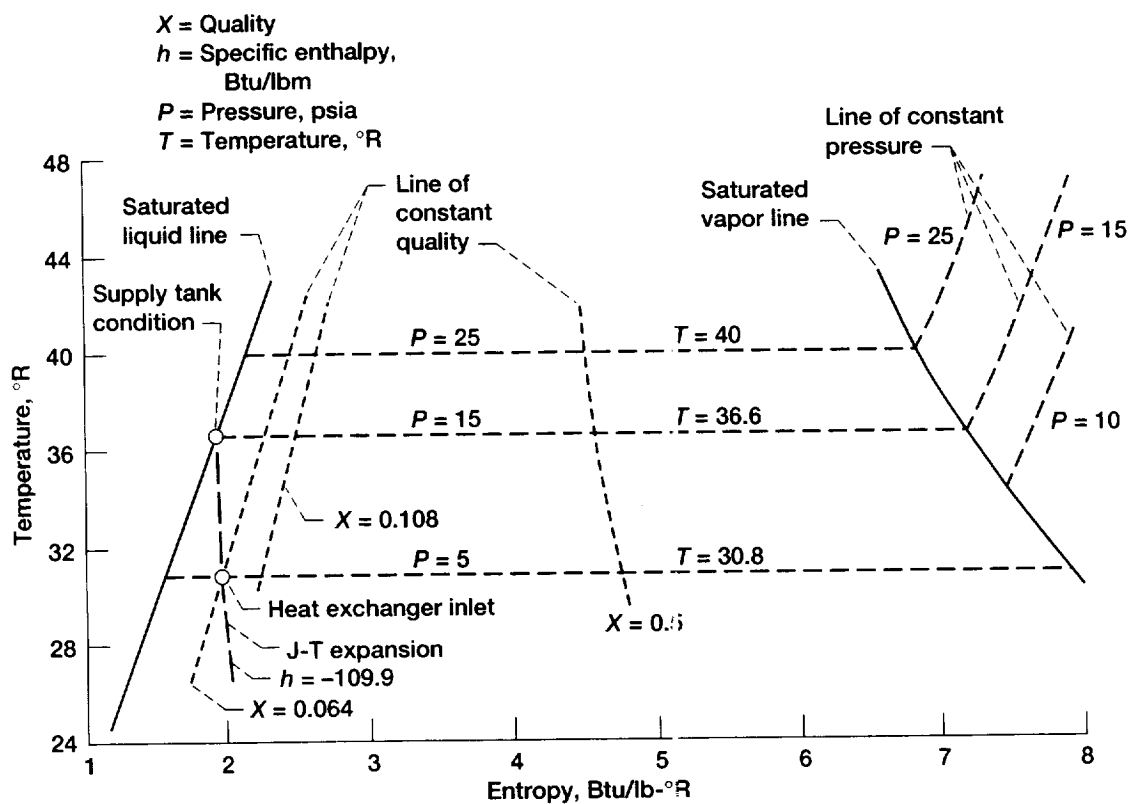


Figure B.2.—Hydrogen temperature-entropy diagram (Constant enthalpy Joule-Thompson (J-T) expansion).

Assumptions

- (1) Negligible pressure drop
- (2) Any given cross section hot-side cold-side temperatures uniform
- (3) Overall heat transfer coefficient, U
 $1/U = 1/h_L + \tau_w/k_w + 1/h_g$; but
 $k_w/\tau_w \ll h_L$ or h_g , thus
 $1/U = 1/h_L + 1/h_g$

where

τ_w Wall thickness
 k_w Thermal conductivity
 h_g Convective heat transfer coefficient for hydrogen gas
 h_L Convective heat transfer coefficient for hydrogen liquid

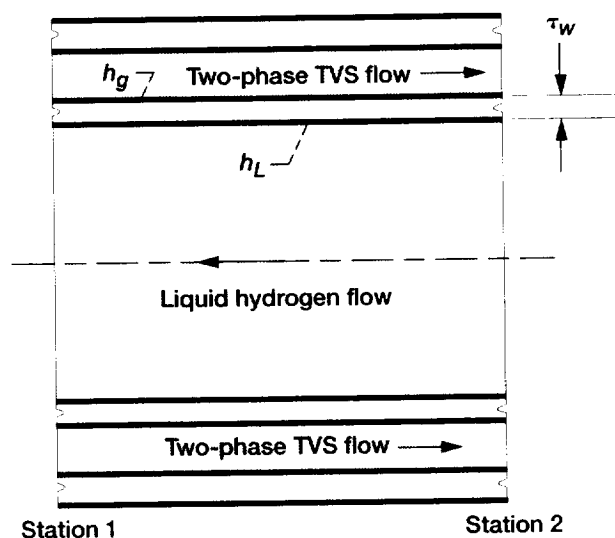


Figure B.3.—Counter-flow heat exchanger performance iterative incremental model, typical segment.

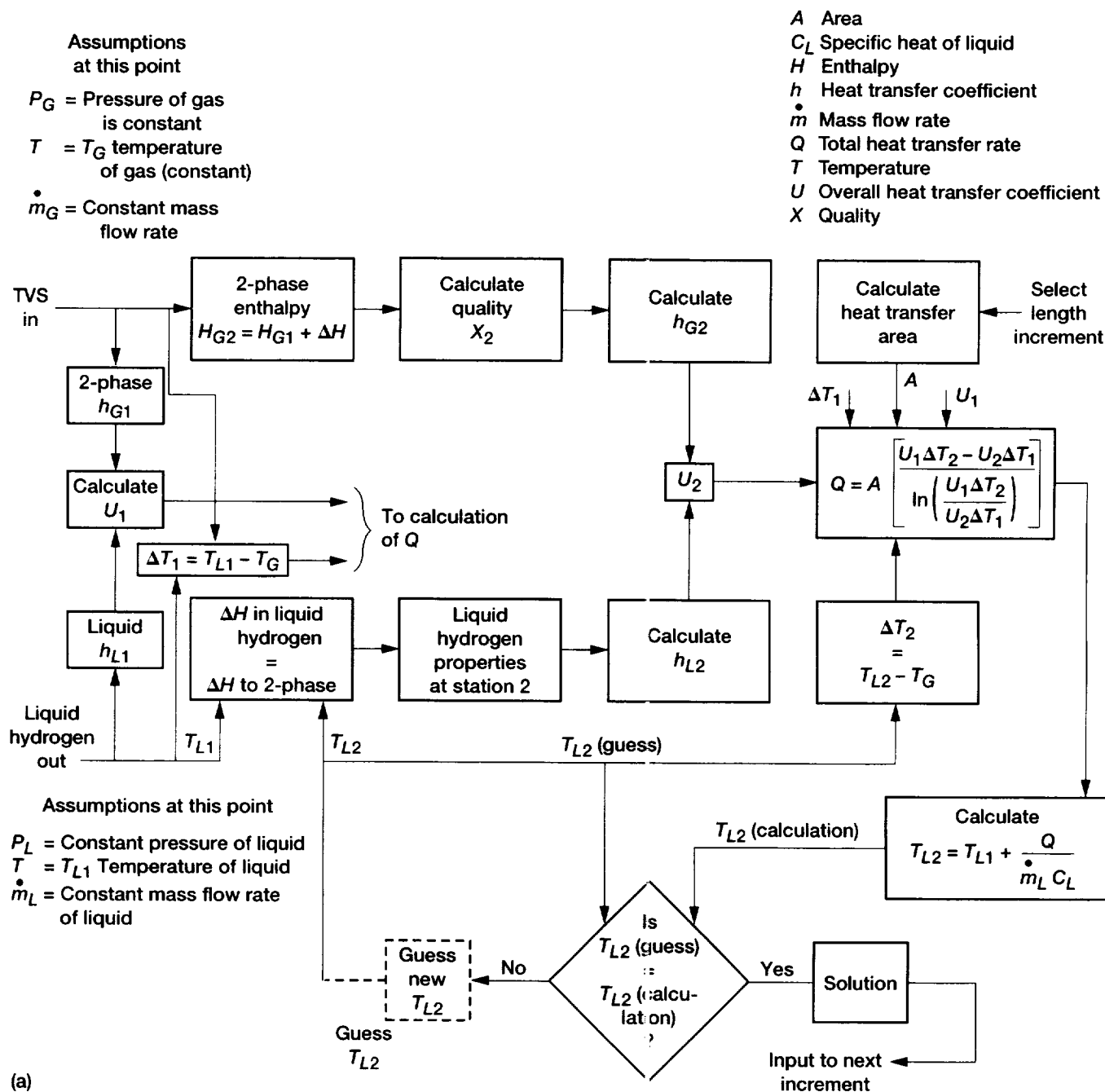


Figure B.4.—Heat exchange calculation flow charts. (a) Single-phase to two-phase liquid. (b) Single-phase liquid to single-phase vapor.

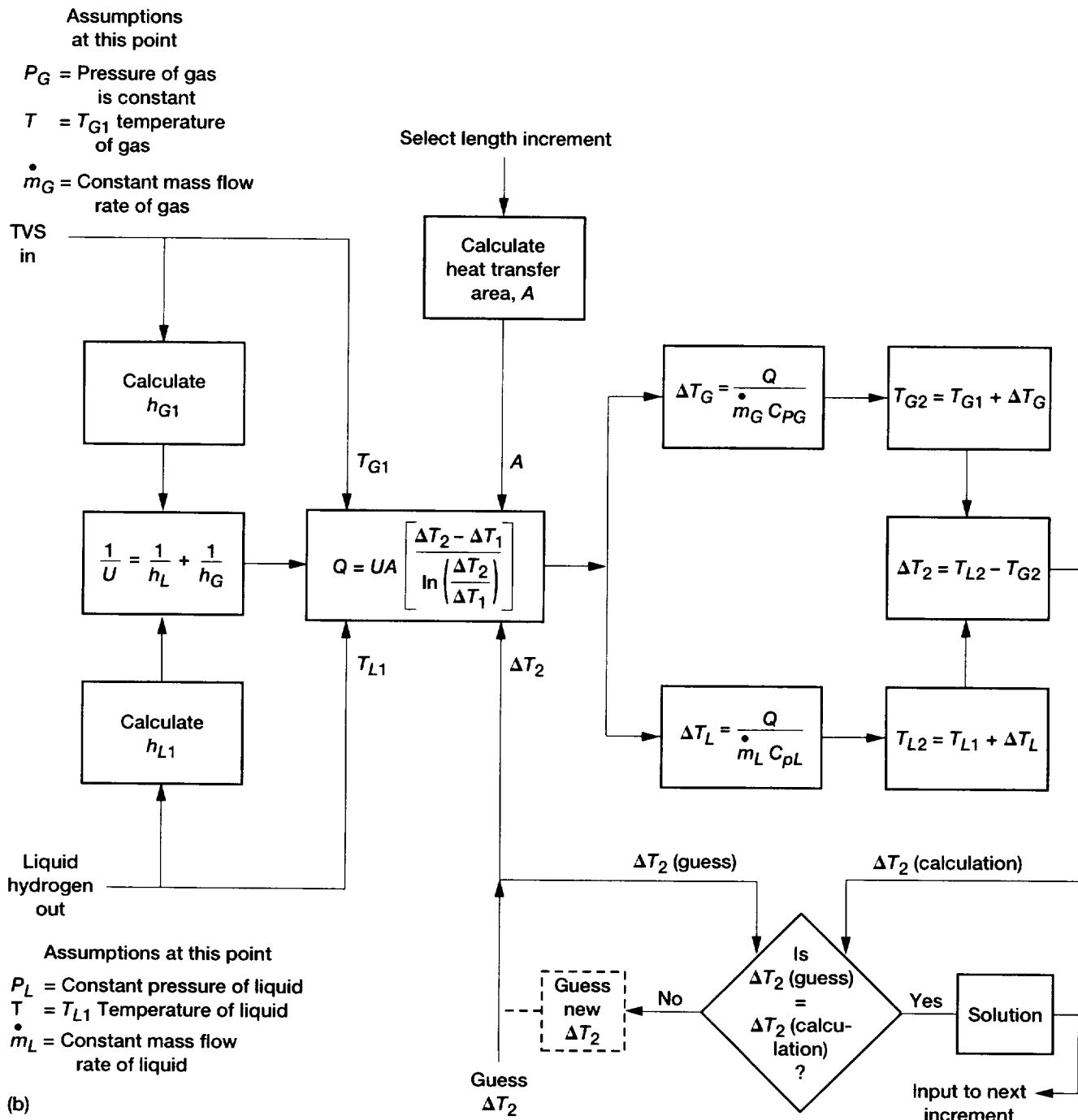
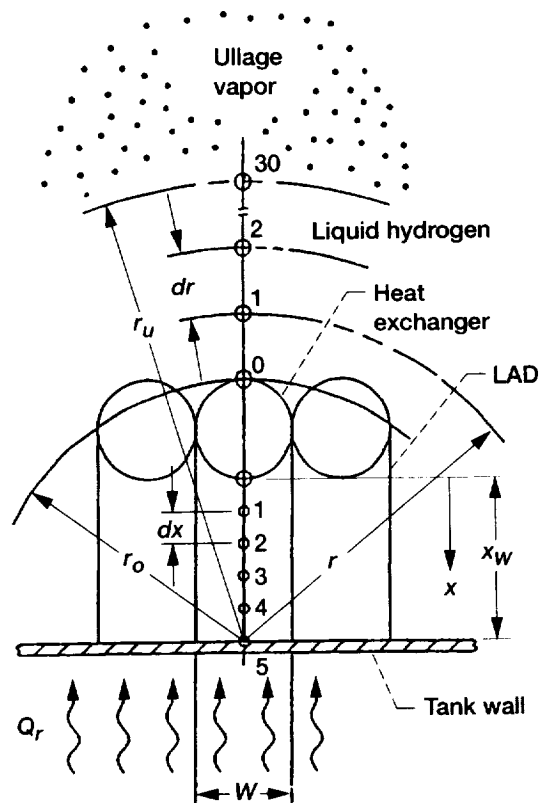


Figure B.4.—Concluded. (b) Single-phase vapor to liquid.



In liquid bulk, $r_o < r < r_{30}$

$$\rho C \frac{\partial T}{\partial t} = k \left(\frac{\partial^2 T}{\partial r^2} + \frac{1}{r} \frac{\partial T}{\partial r} \right)$$

Boundary conditions:

at r_o , $T_0 = T_{TVS}$, for TVS on
 $T_0 = T_1$, for TVS off

at r_u , $\frac{\partial T}{\partial r} = 0$

In the confined liquid within LAD,
 $0 < x < x_w$

$$\rho C \frac{\partial T}{\partial t} = k \left(\frac{\partial^2 T}{\partial x^2} \right)$$

Boundary conditions:

at $x = 0$, $Tx_0 = T_{TVS}$, for TVS on
 $Tx_0 = Tx_1$, for TVS off

at $x = x_w$, $k(\delta T / \delta x)_{x_w} = Q_r$

where

- ρ Liquid density
- C Liquid specific heat
- k Liquid conductivity
- Q Heat flux
- r_u Distance from wall to ullage
- r Radial distance
- T Temperature
- t Time
- W Width
- x Distance from heat exchanger internal to LAD

Figure B.5.—Passive TVS (intermittent model) (using one-dimensional transient model).

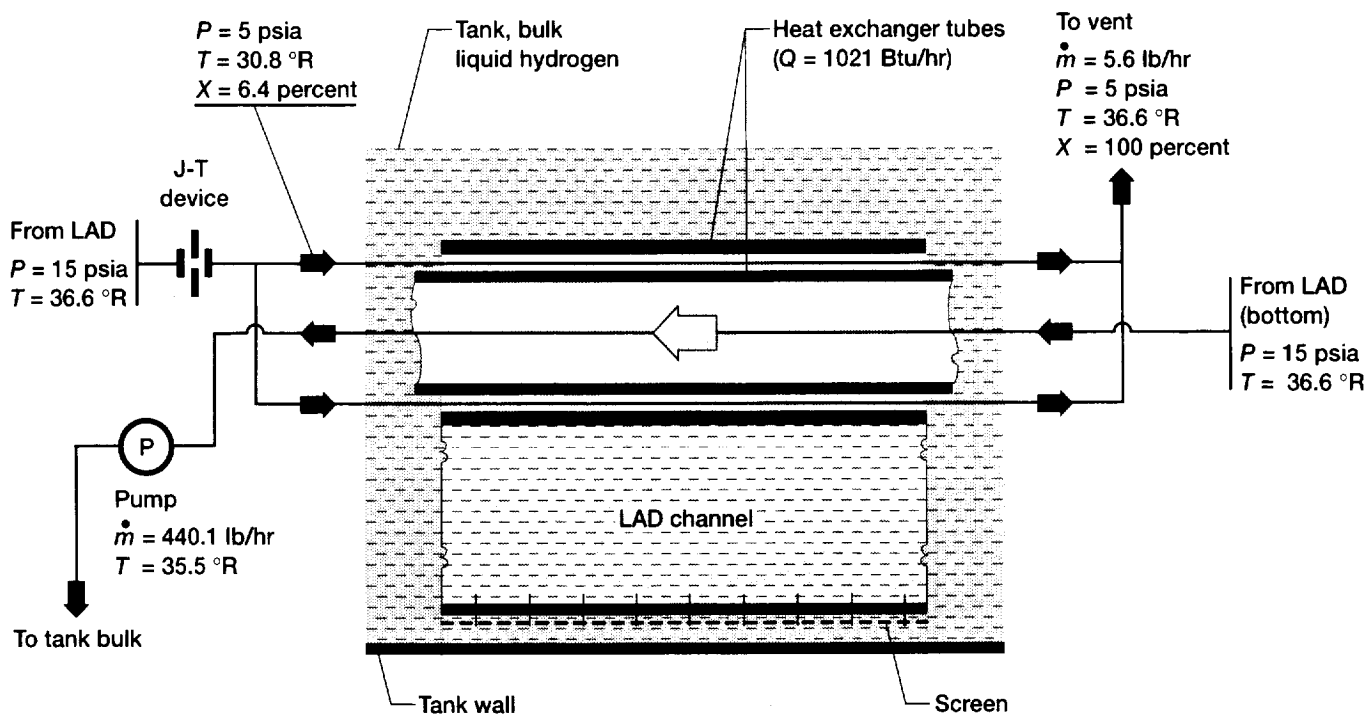


Figure B.6.—COLDSAT TVS system conceptual diagram, active TVS.

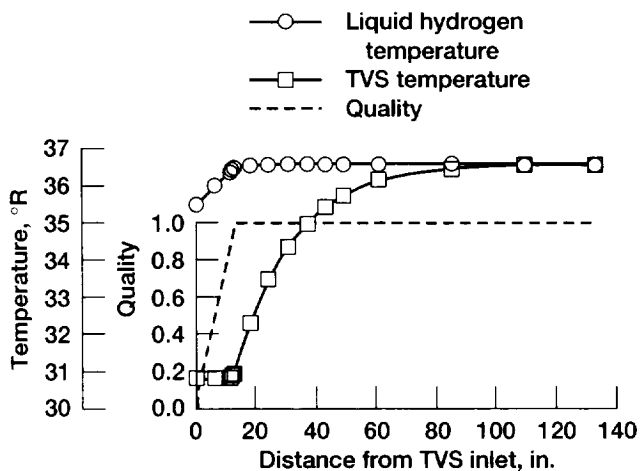


Figure B.7.—Temperature and quality profile of active TVS mode heat exchanger (TVS flow rate, 5.6 lb/hr from 15 psia; liquid hydrogen flow rate, 440.1 lb/hr).

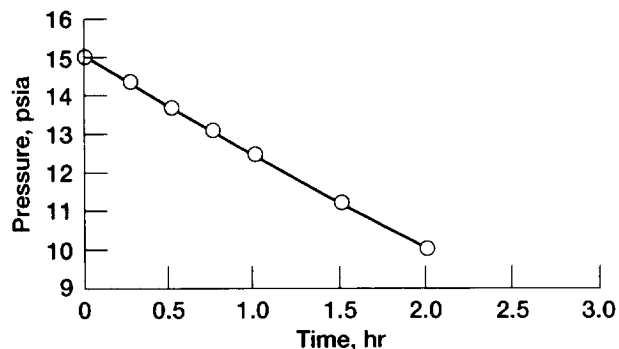
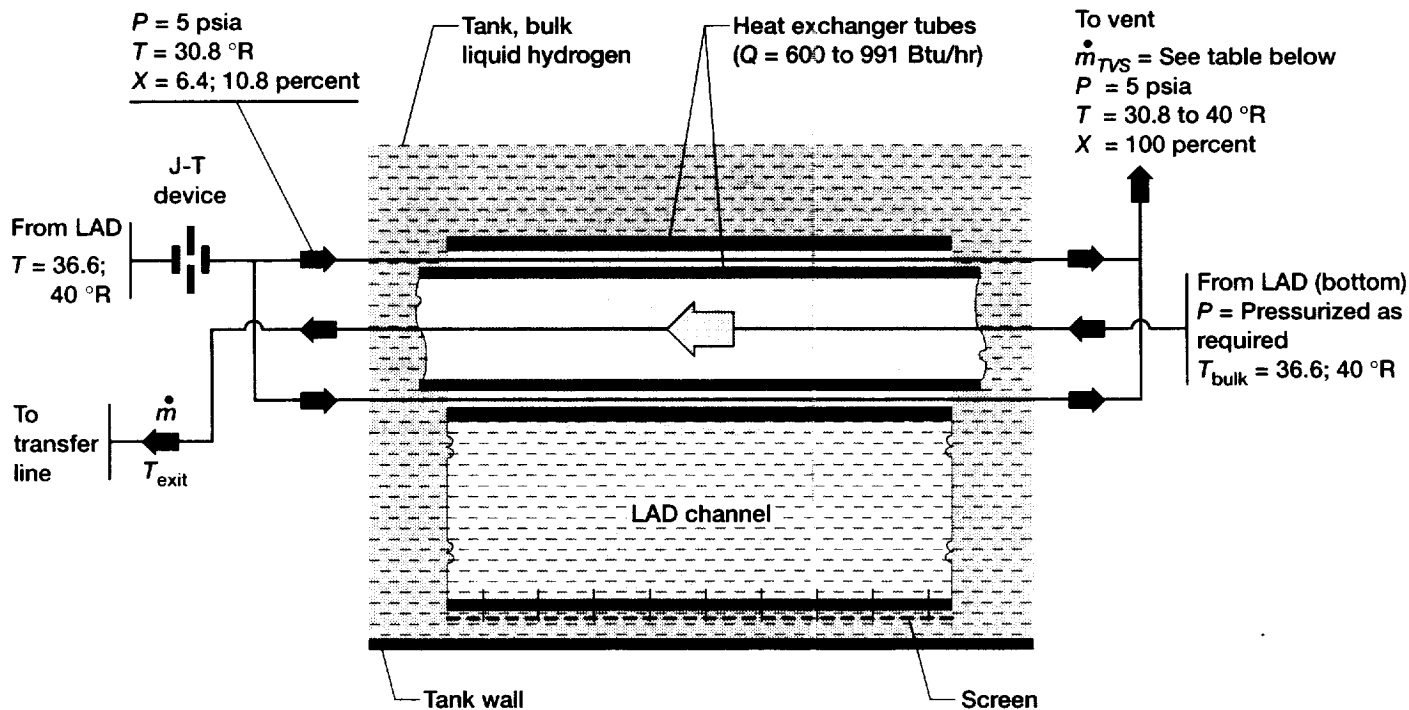


Figure B.8.—Supply tank pressure in active TVS mode. (144 ft³ tank, 95 percent full; TVS flow, 5.6 lb/hr; heat leak, 0.1 Btu/hr-ft²; uniform mixture assumed.)



Flow rate \dot{m} from LAD (bottom) to transfer line
(subcooler operating modes)

\dot{m} , lb/hr ^a	T_{exit} , °R	ΔT , °R ^b	\dot{m}_{TVS} , lb/hr	T_{bulk} , °R
50	30.9	5.7	3.5	36.6
50	31.2	8.8	5.6	40
100	32.6	4	4.75	36.6
200	34.6	2	5.0	36.6
350	35.5	1.1	5.6	36.6

^a \dot{m} = Flow rate from LAD to transfer line

^b ΔT = Degree of subcooling

Figure B.9.—COLDSAT TVS system conceptual diagram, subcooler TVS.

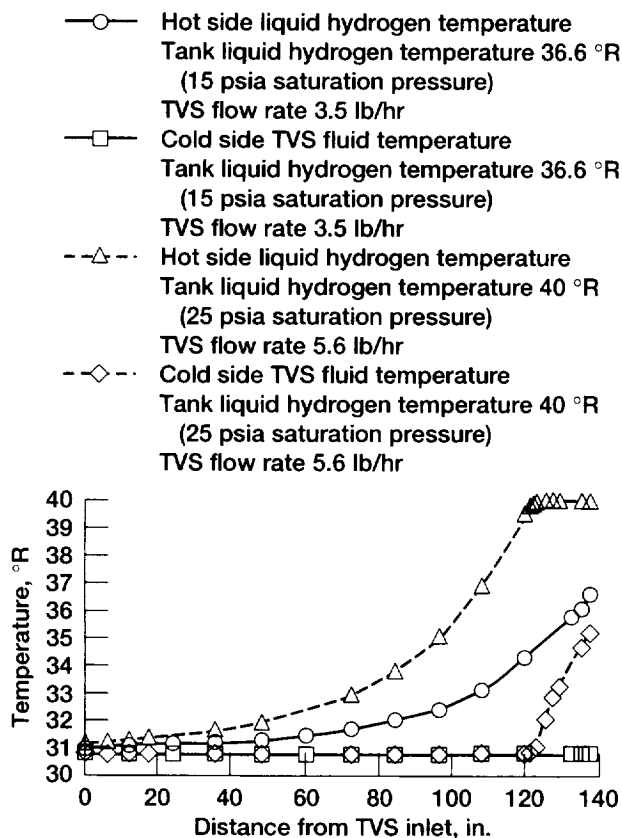


Figure B.10.—Heat exchanger temperature profile in subcooler TVS mode (liquid hydrogen flow rate, 50 lb/hr; TVS exit quality, 100 percent).

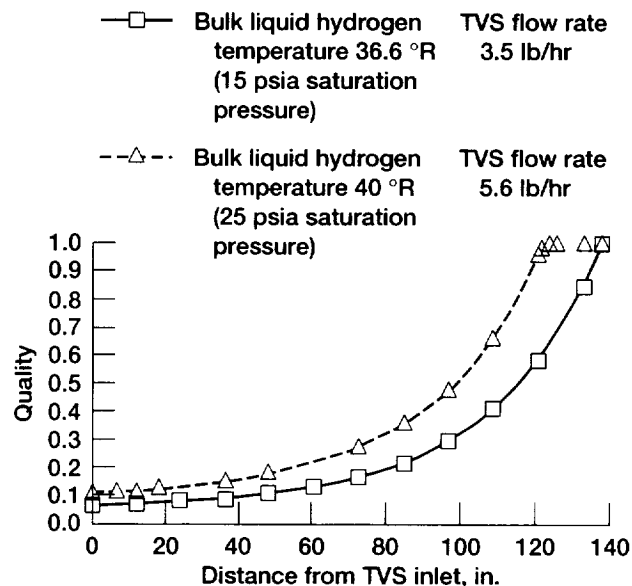


Figure B.11.—Heat exchanger quality profile in subcooler TVS mode (liquid hydrogen flow rate, 50 lb/hr).

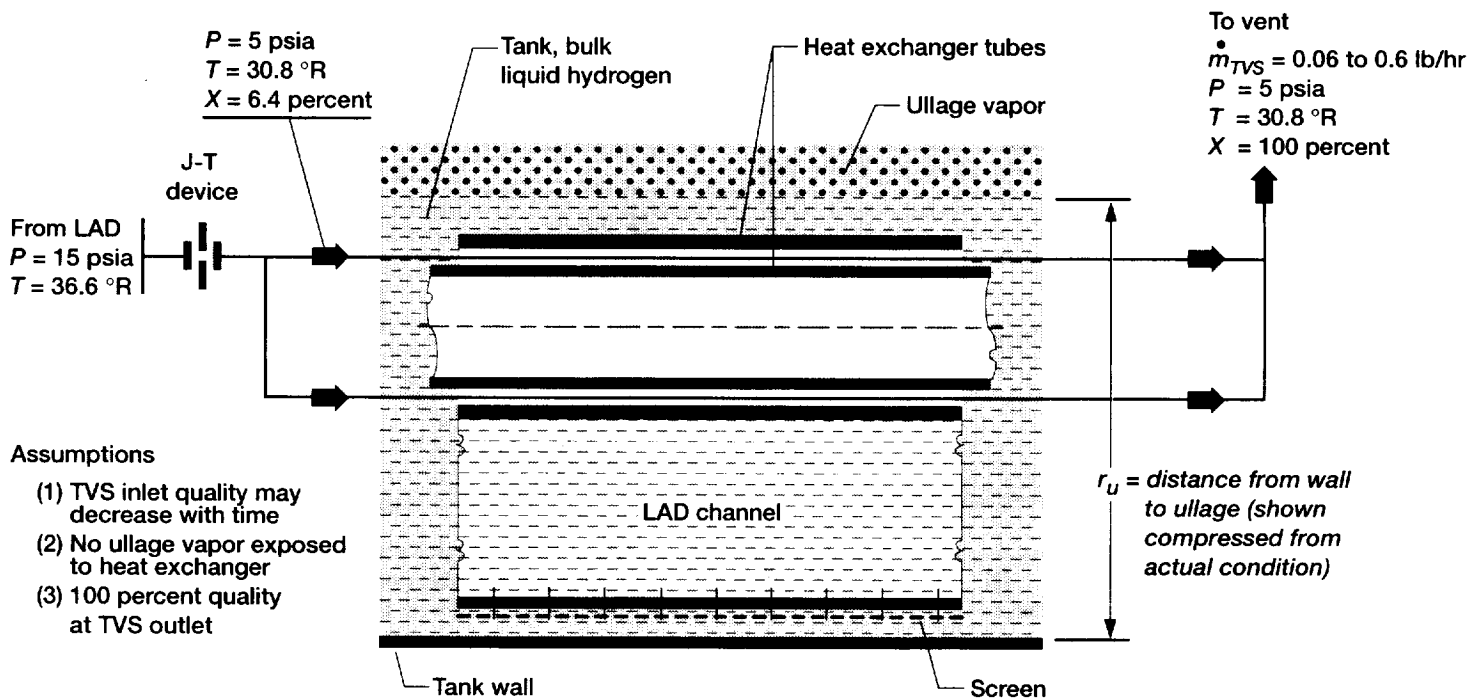


Figure B.12.—COLDSAT TVS system conceptual diagram, intermittent passive TVS.

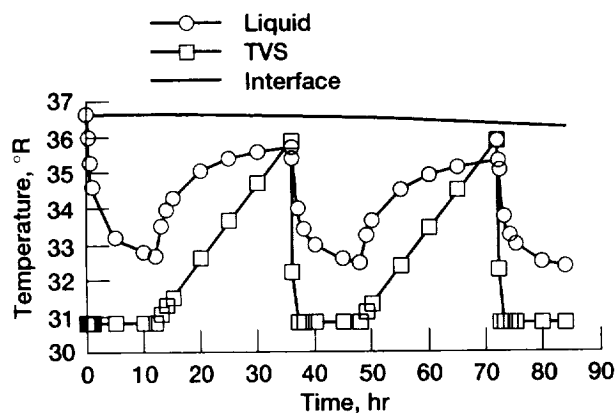


Figure B.13.—Transient temperature profile, 84-hr intermittent passive TVS mode (on, 12 hr; off, 24 hr; interface, 15.35-in. radial distance).

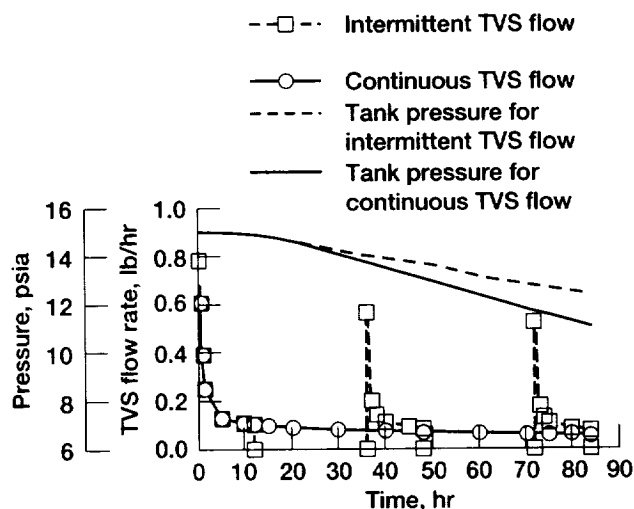


Figure B.14.—Supply tank pressure and passive TVS flow rates versus time (interface, 15.35-in. radial distance; intermittent cycle: on, 12 hr; off, 24 hr; TVS exit quality, 100 percent).

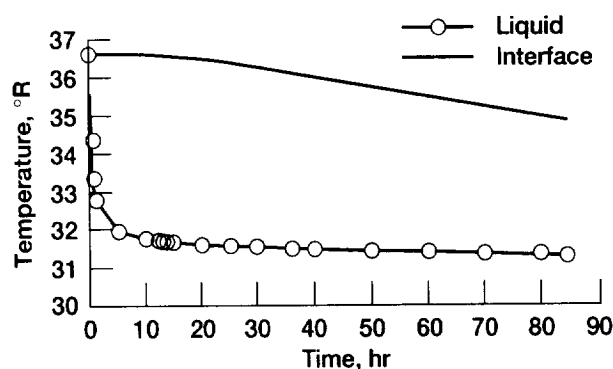


Figure B.15.—Transient temperature profile at 84-hr continuous on passive TVS mode (interface, 15.35-in. radial distance; liquid temperature, 2.3-in. radial distance).

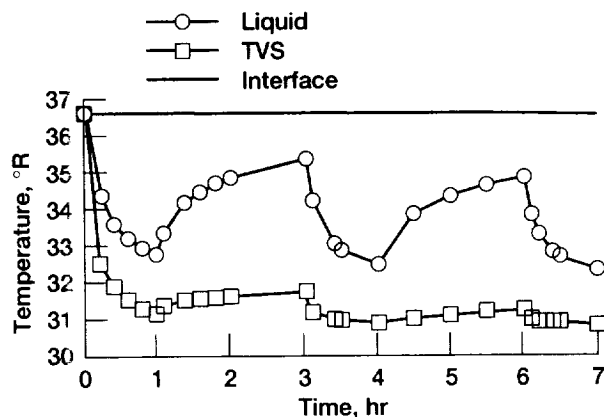


Figure B.16.—Transient temperature profile, intermittent passive TVS mode (on, 1 hr; off, 2 hr; interface, 15.35-in. radial distance; liquid temperature, 2.3-in. radial distance).

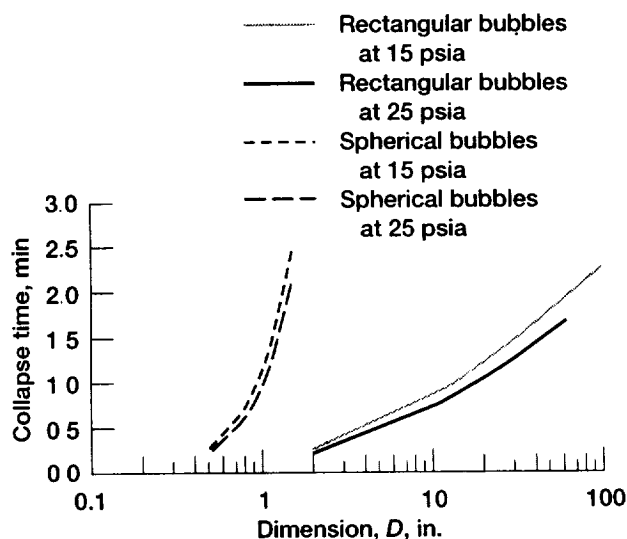


Figure B.17.—Vapor collapse time for rectangular and spherical bubbles (ref. 29; TVS temperature, 30.8 °R; rectangle, 0.45 by 2.2 by D (sphere diameter)).

Appendix C

Fluids Schematic Symbols

Piping component symbols			
Butterfly valve	Directional valves 3-way 4-way	Cylinder regulator	Pressure gauge
Check valve		Turbine flowmeter	Filter
Gate valve		Orifice	Strainer
Relief valve		Venturi	Heat exchanger
Ball valve	Pressure regulator Loader	Rupture disk	Pump
Globe valve		Flowmeter	Motor
3-way valve			Cap

Actuator symbols	Primary control element symbols		Item designations
Cylinders	EP Electron-pneumatic transducer	PS Pressure switch	Locally mounted
	EH Electron-hydraulic transducer	PT Pressure transducer	
Hand	LLS Liquid level switch	TC Thermocouple	Control room located
Pneumatic control	LLT Liquid level transducer	TS Temperature switch	
Rotary motor	LS Limit switch	LV Liquid/vapor sensor	Alternate control room located
	PDS Pressure differential switch	T Temperature sensor	
Solenoid	PDT Pressure differential transducer		Reference drawing

Instrument letter designations for				Instrument symbols	
First letter	B-burner	L-level	Z-position	General	Data collector facility
	E-emergency	P-pressure			
	F-flow	S-speed		Program logic controller	Program process controller
	H-hand	T-temperature			
Succeeding letters	A-alarm	I-indicate	S-shutdown		
	C-control	L-low	Y-datalog		
	D-differential	P-permissive			
	H-high	R-record			

Appendix D

Reference Figures

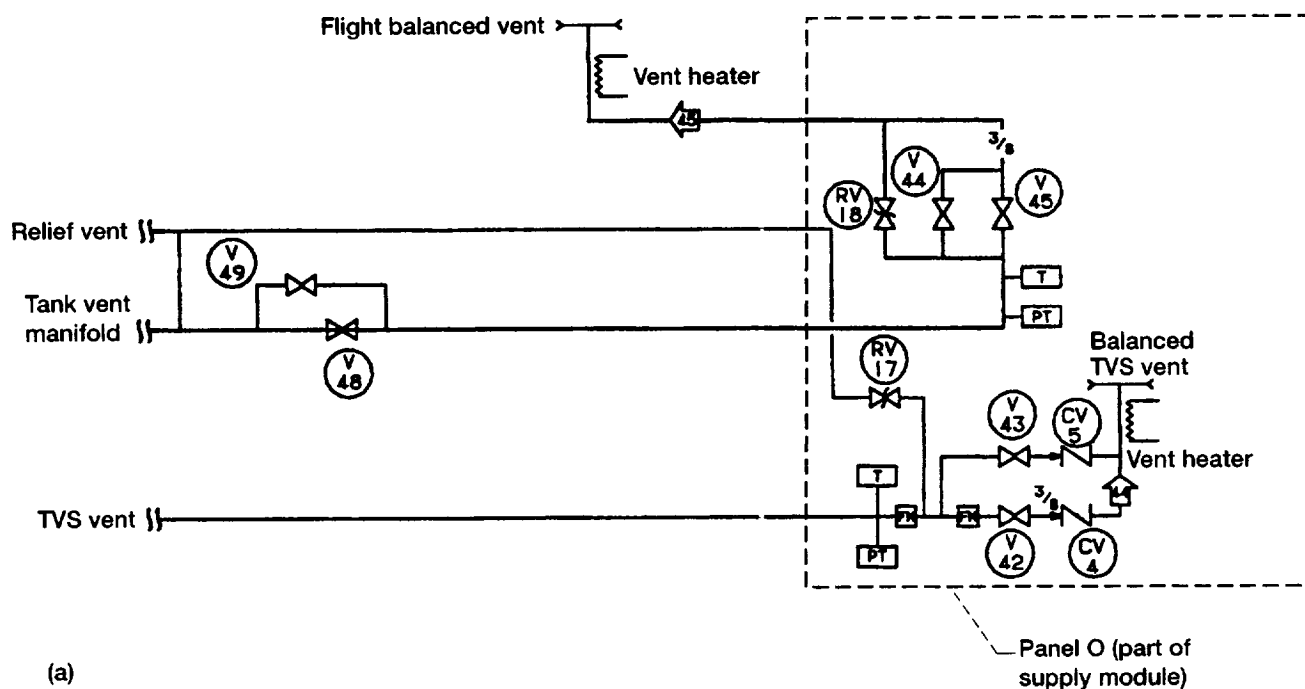


Figure D.1.—Experiment system plumbing schematic. Pipe dimensions are in inches. (See appendix C for interpretation of symbols.) (a) Vent panel. (b) Supply tank system of supply module. (c) Pressurant supply system. (d) Large receiver tank module. (e) Small receiver tank module.

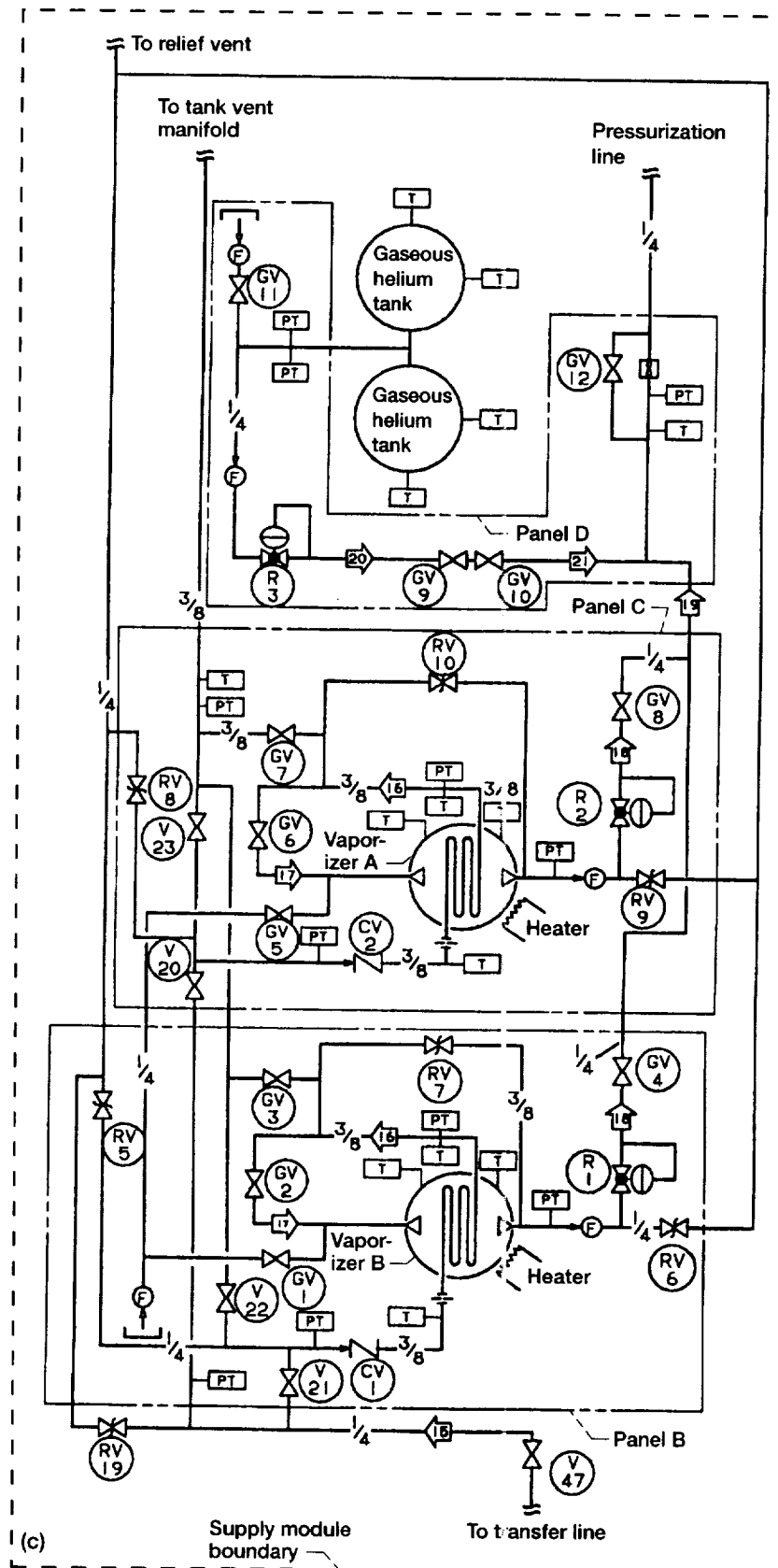


Figure D.1.—Continued. (c) Pressurant supply system.

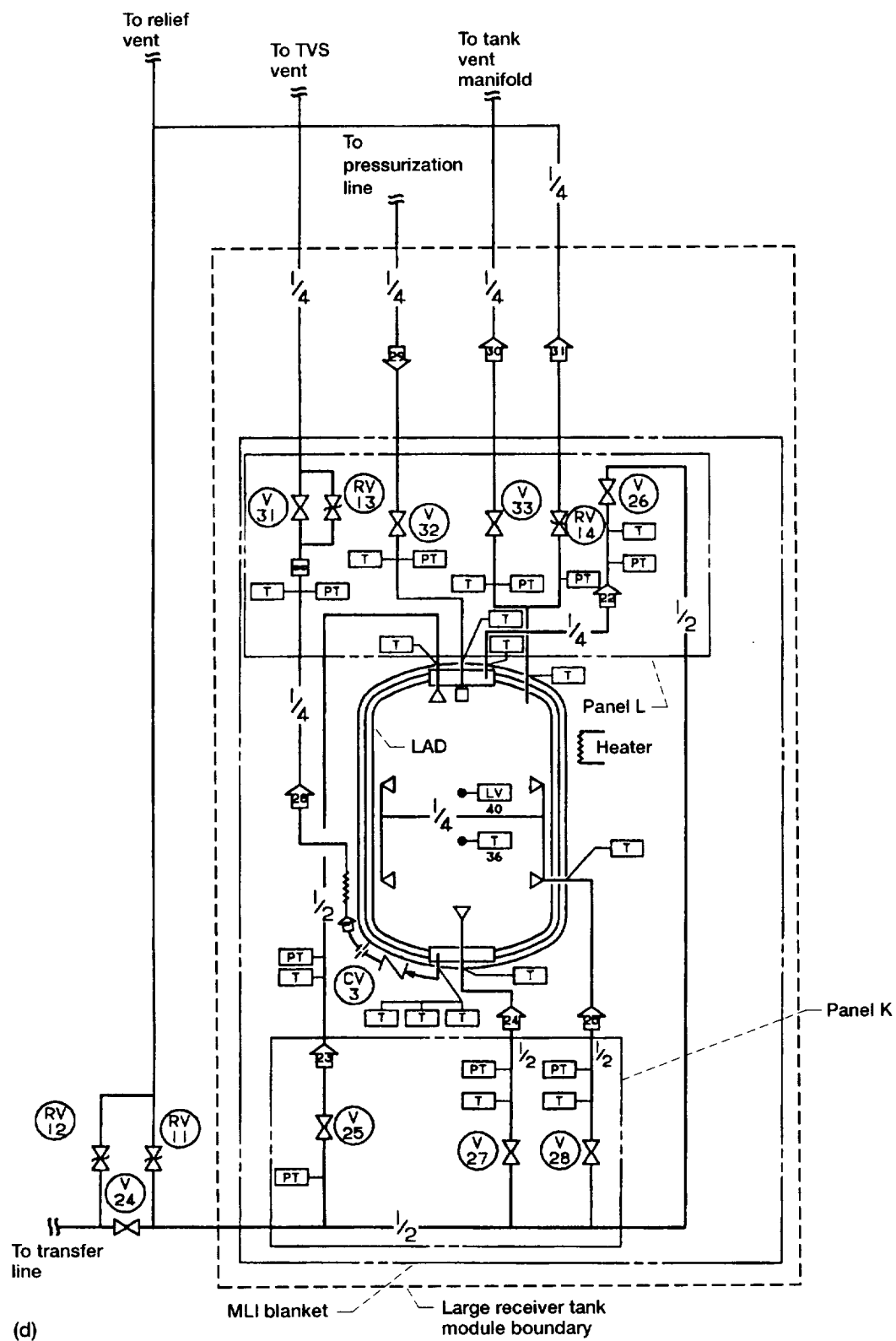
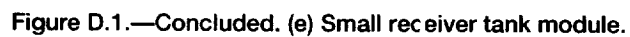


Figure D.1.—Continued. (d) Large receiver tank module.



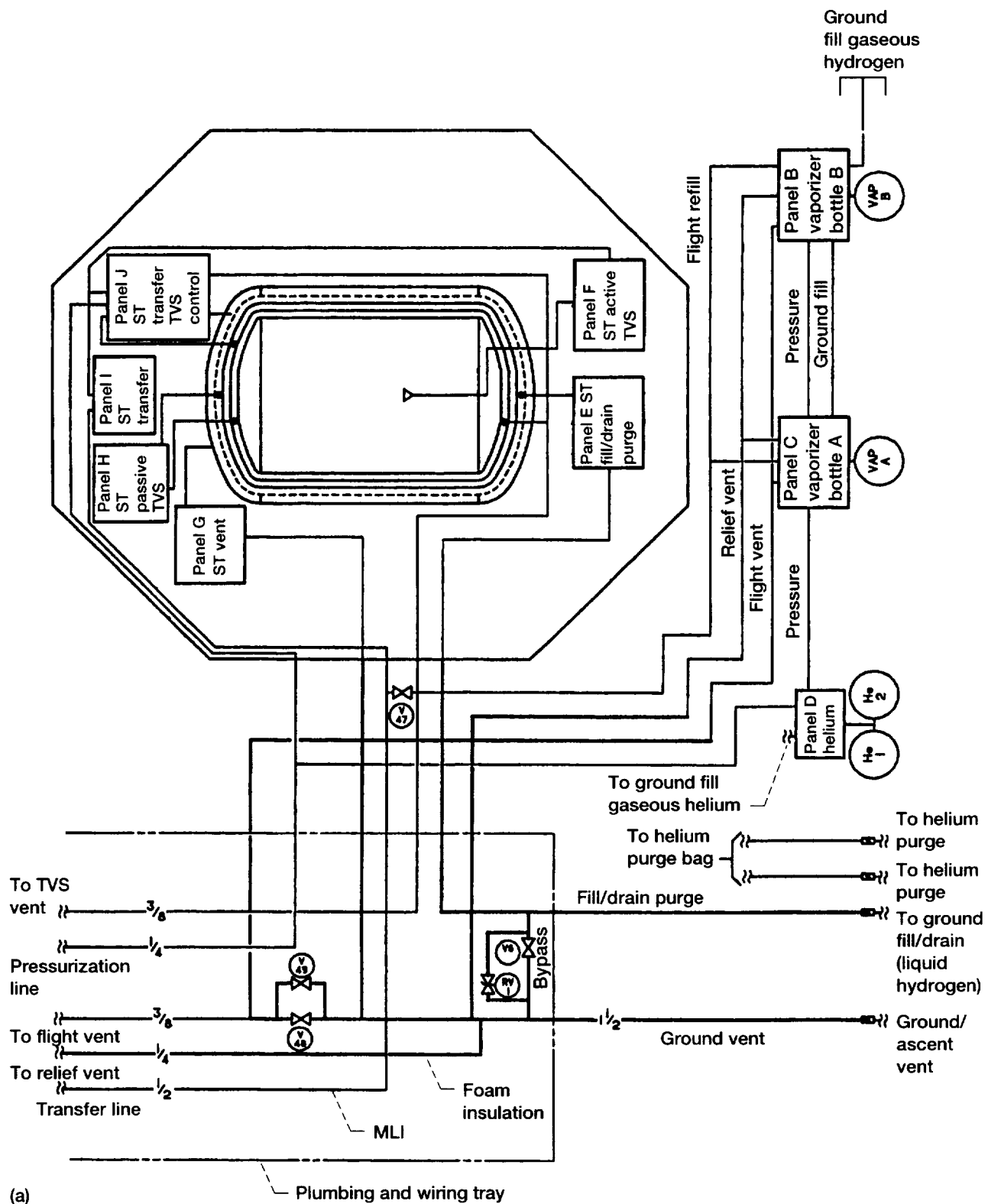


Figure D.2.—Experiment system vertical fluid schematic. Dimensions are in inches. (See appendix C for interpretation of symbols.) (a) Supply tank module (ST). (b) Large receiver tank module and small receiver tank module.

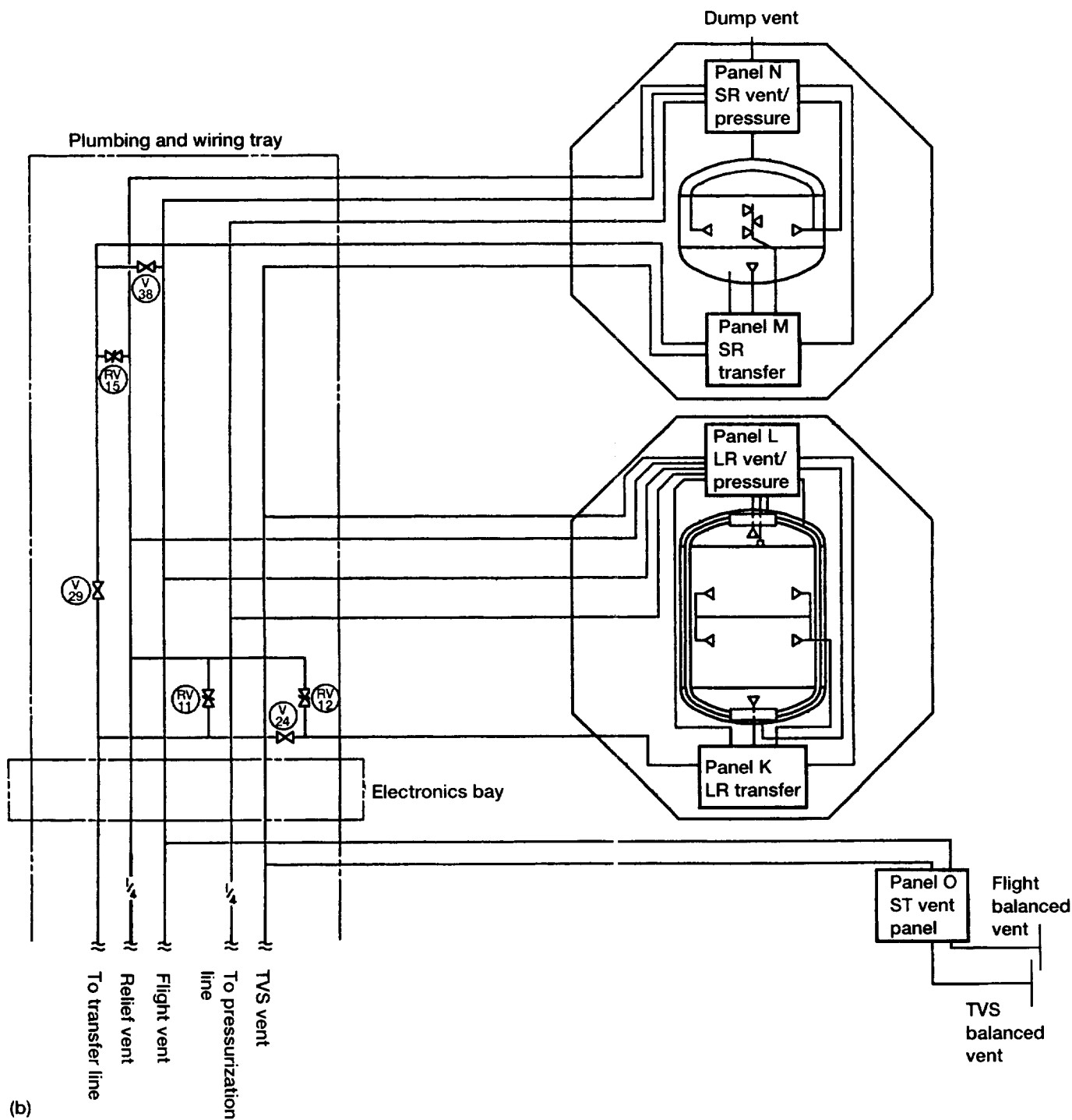


Figure D.2.—Concluded. (b) Large receiver tank module (LR) and small receiver tank module (SR).

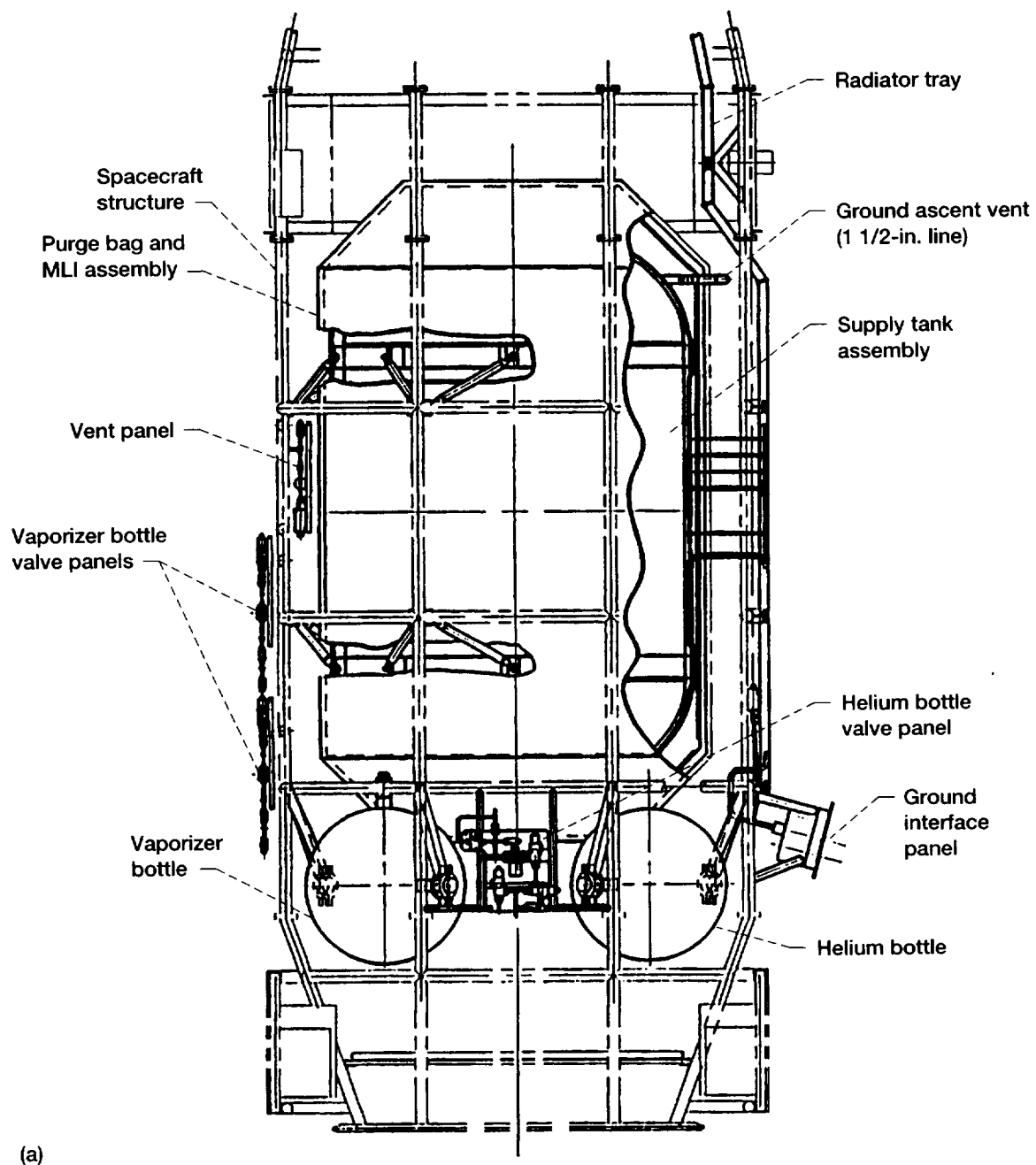
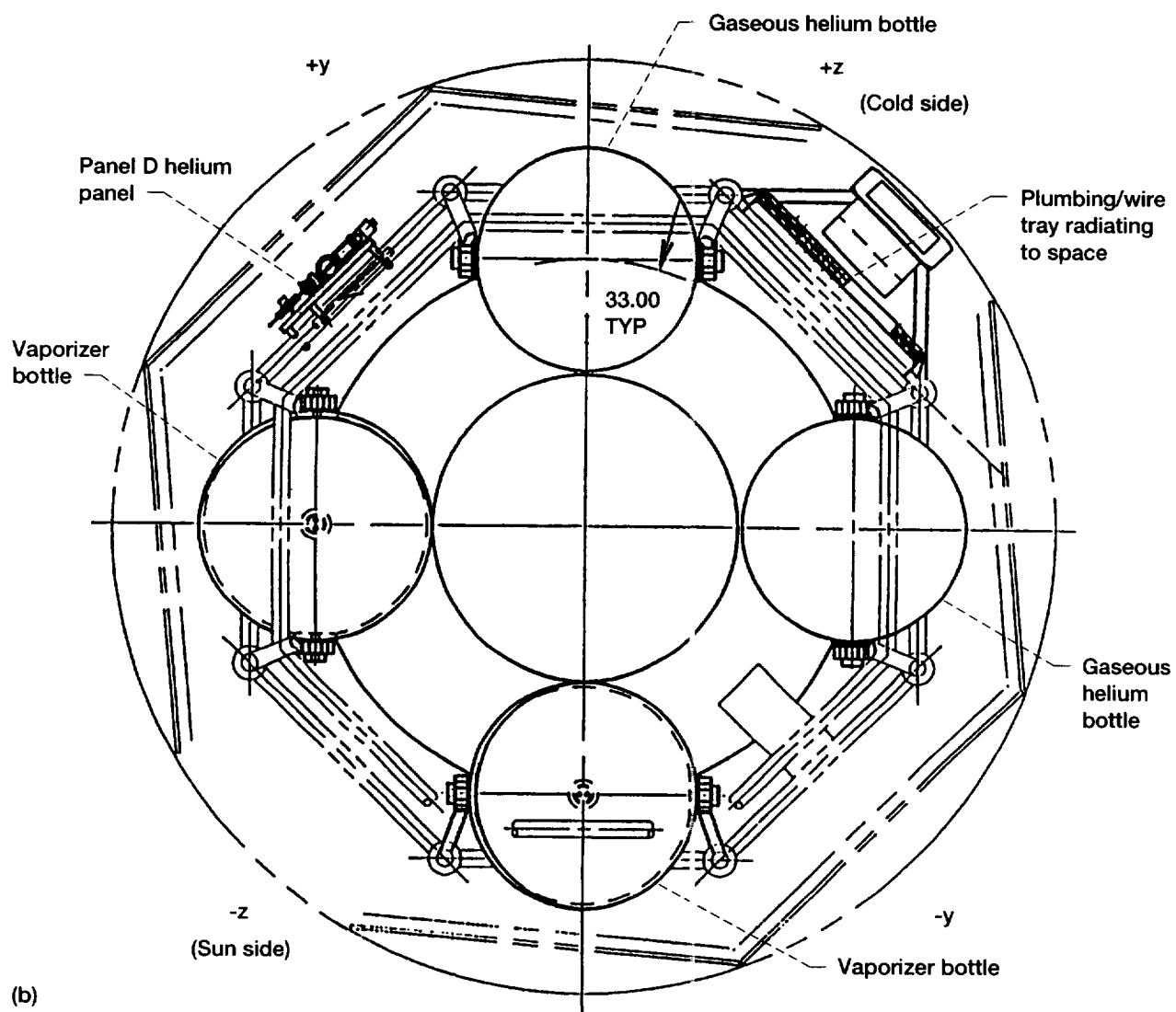


Figure D.3.—Supply tank module. (a) Side view. (b) Bottom view. (c) Cutaway view.



(b)

Figure D.3.—Continued. (b) Bottom view.

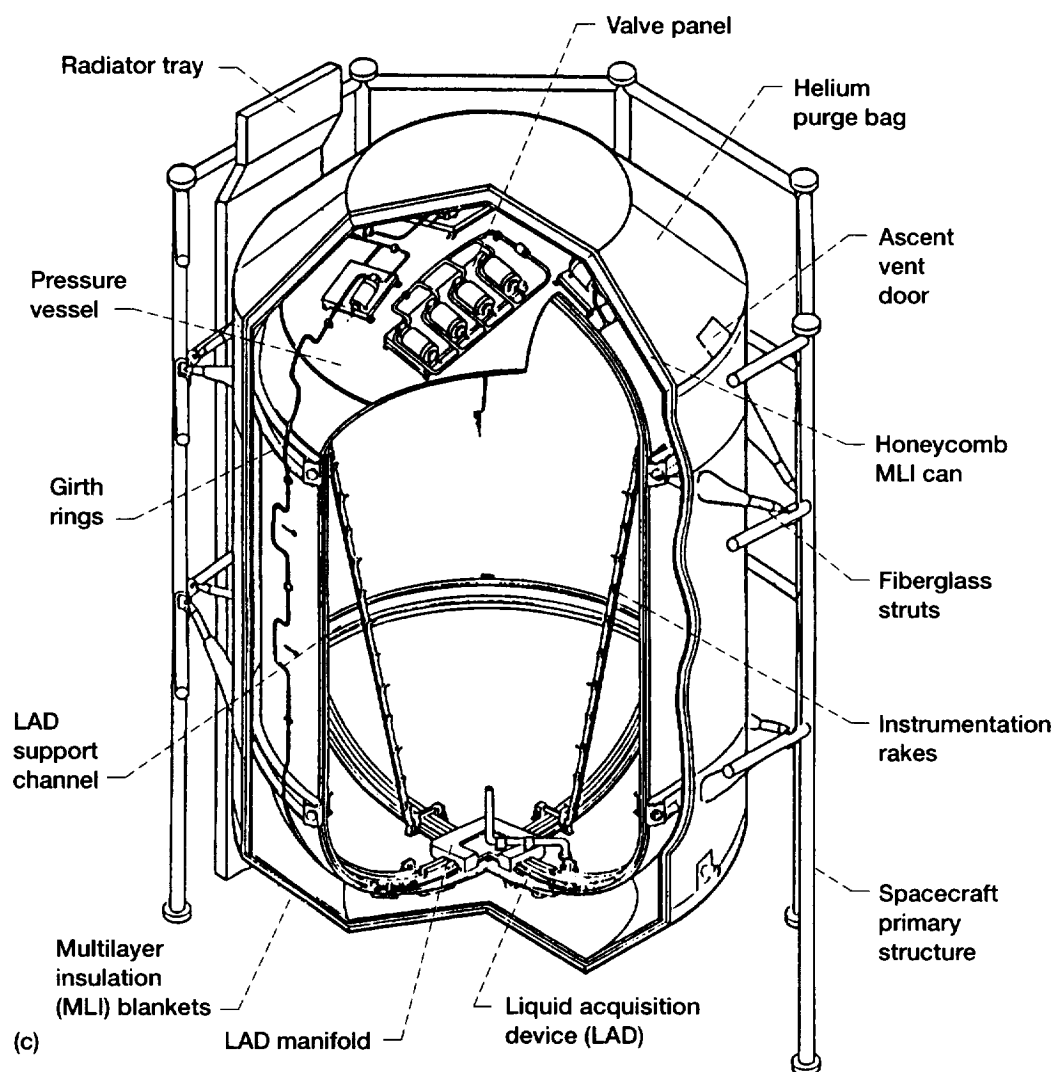


Figure D.3.—Concluded. (c) Cutaway view.

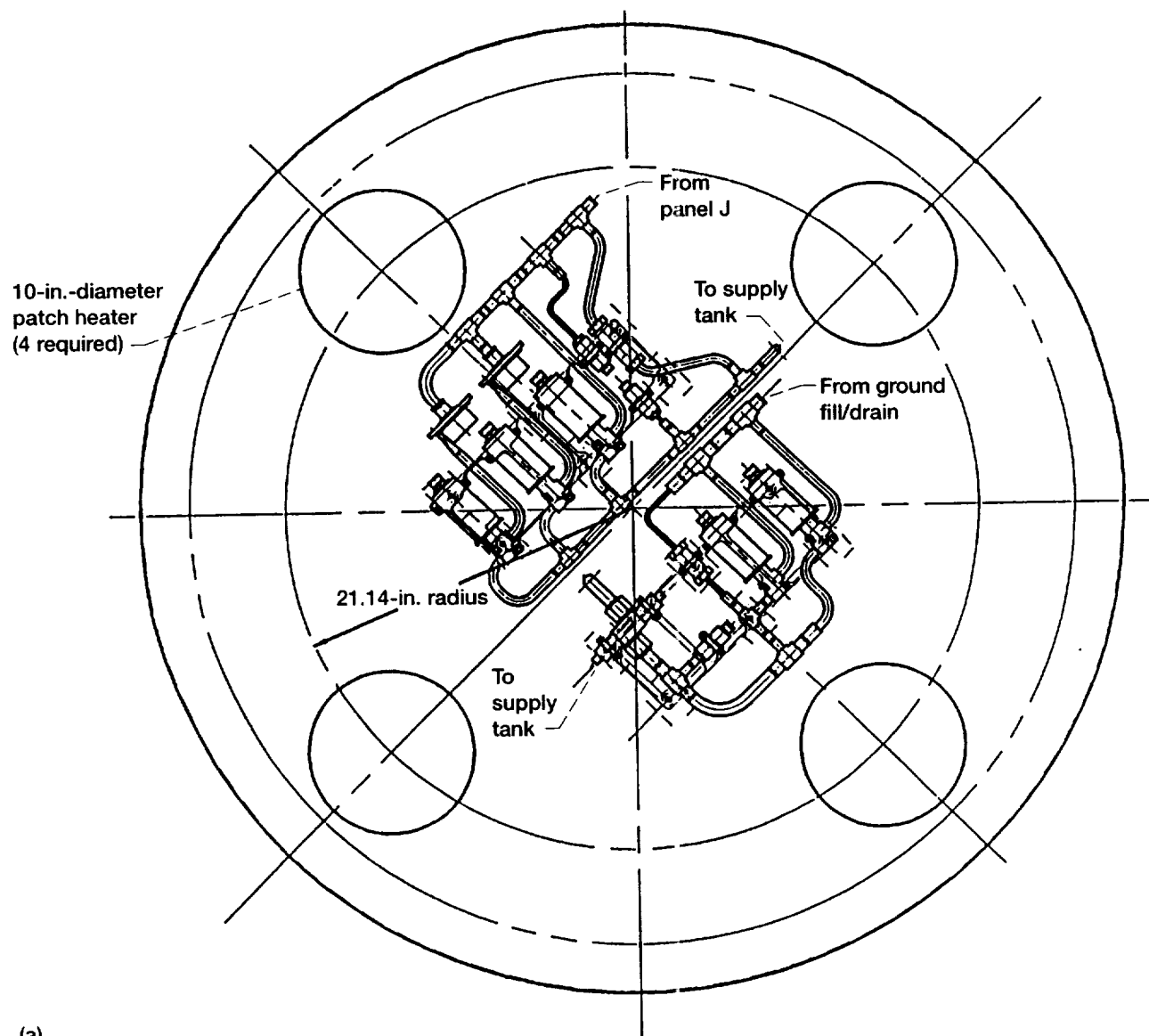


Figure D.4.—Supply tank aft dome panels. Dimensions are in inches. (a) Valve panel layout. (b) Panel E, ground fill/drain/purge. (c) Panel F, active TVS.

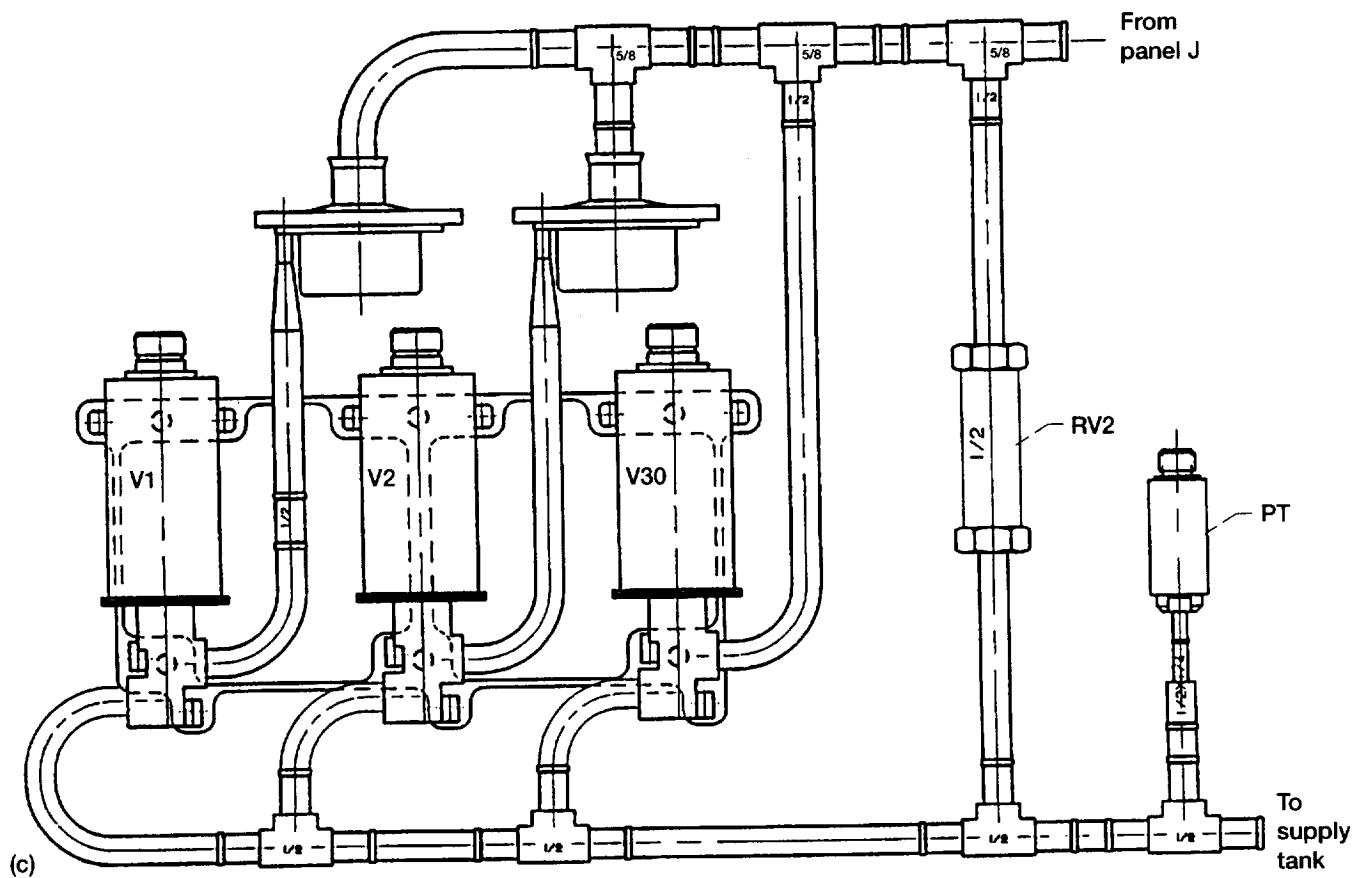
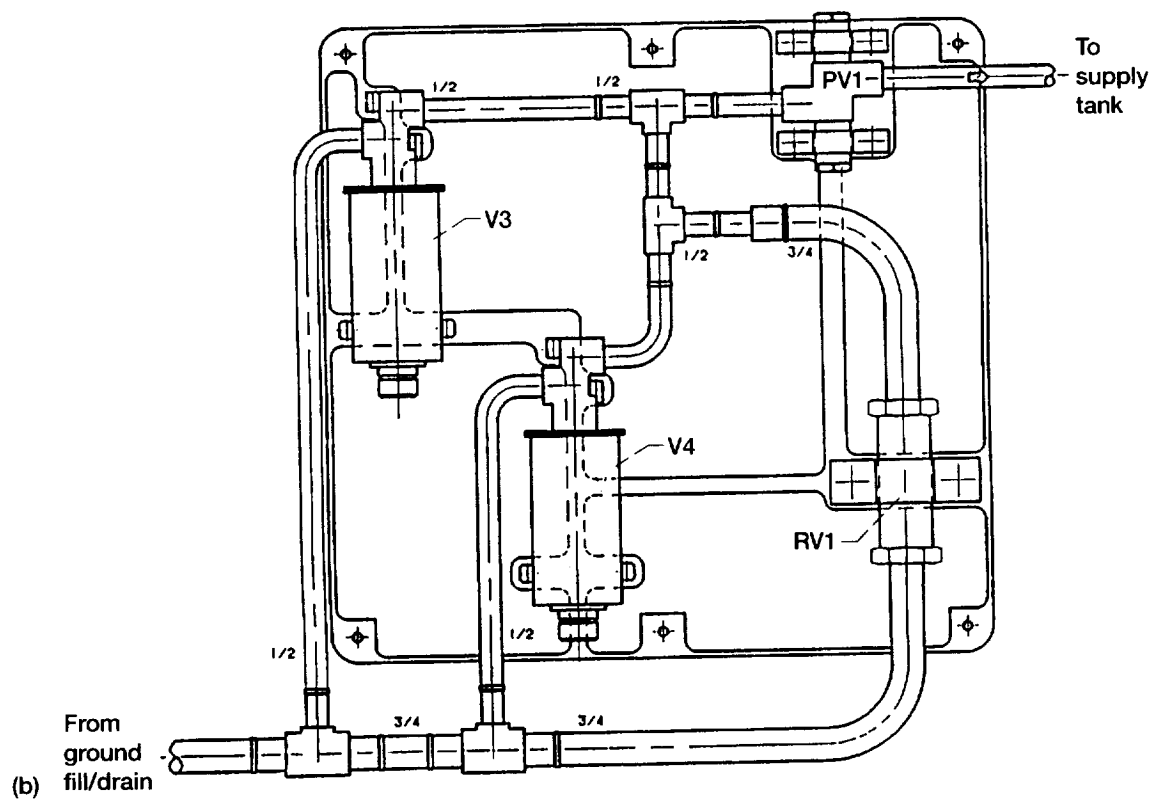


Figure D.4.—Concluded. (b) Panel E, ground fill/drain/purge. (c) Panel F, active TVS.

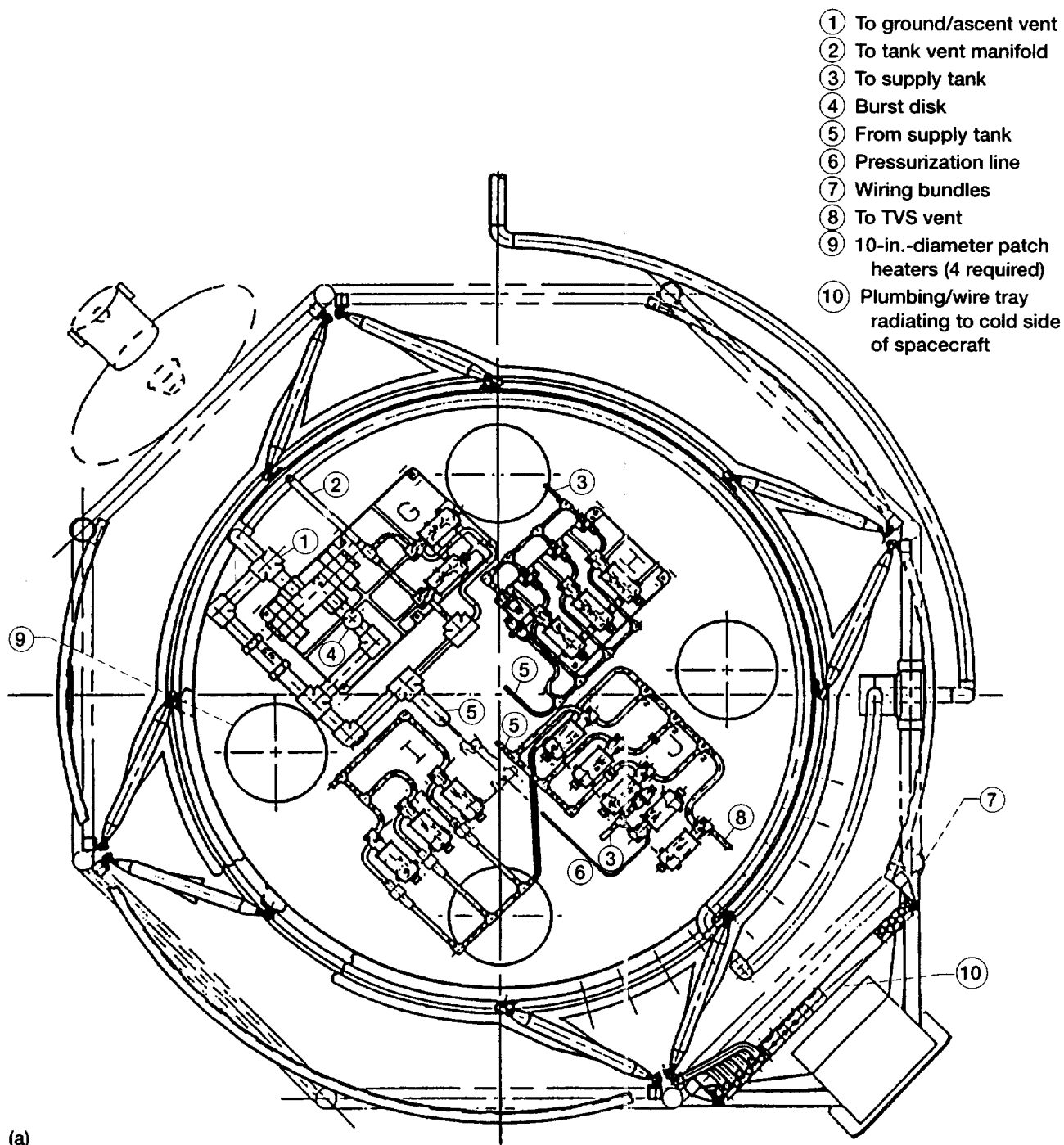


Figure D.5.—Supply tank forward dome panels. Dimensions are in inches. (a) Forward dome layout. (b) Panel G, tank vent. (c) Panel H, passive TVS panel. All panel H lines and fittings are 3/8 in. (d) Panel I, transfer. (e) Panel J, transfer/TVS control.

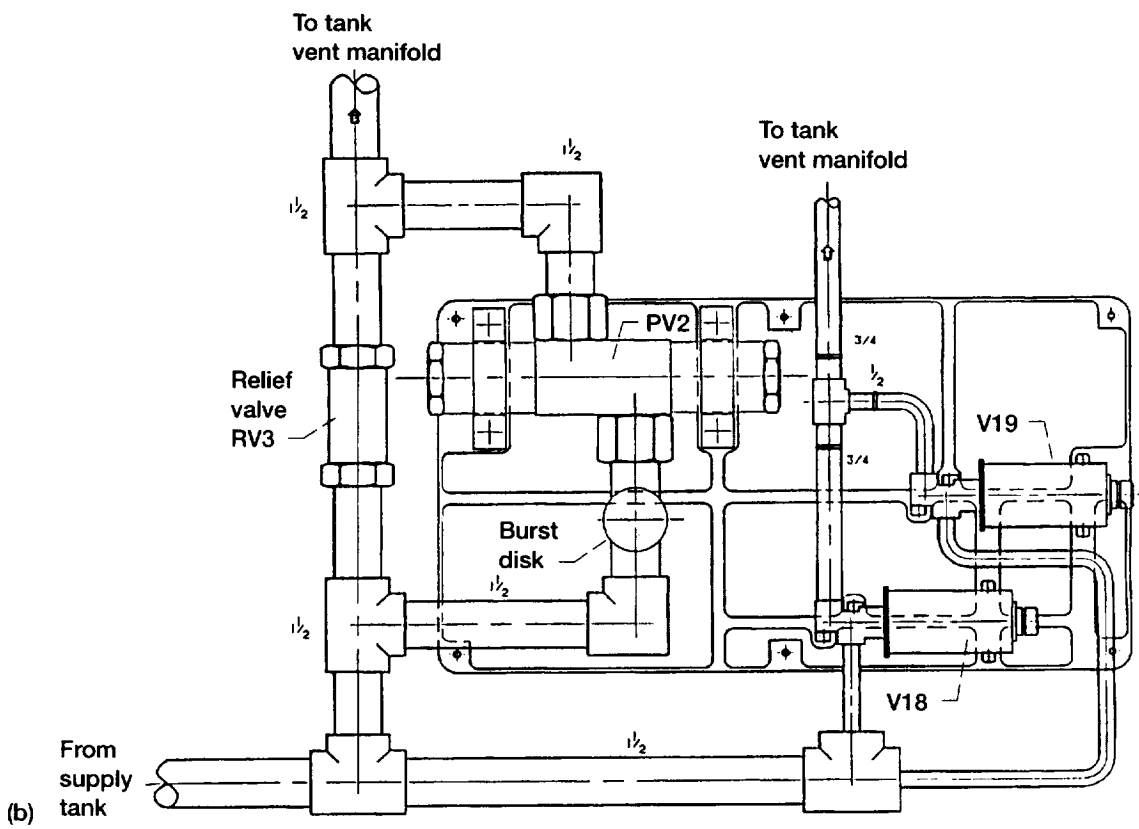


Figure D.5.—Continued. (b) Panel G, tank vent.

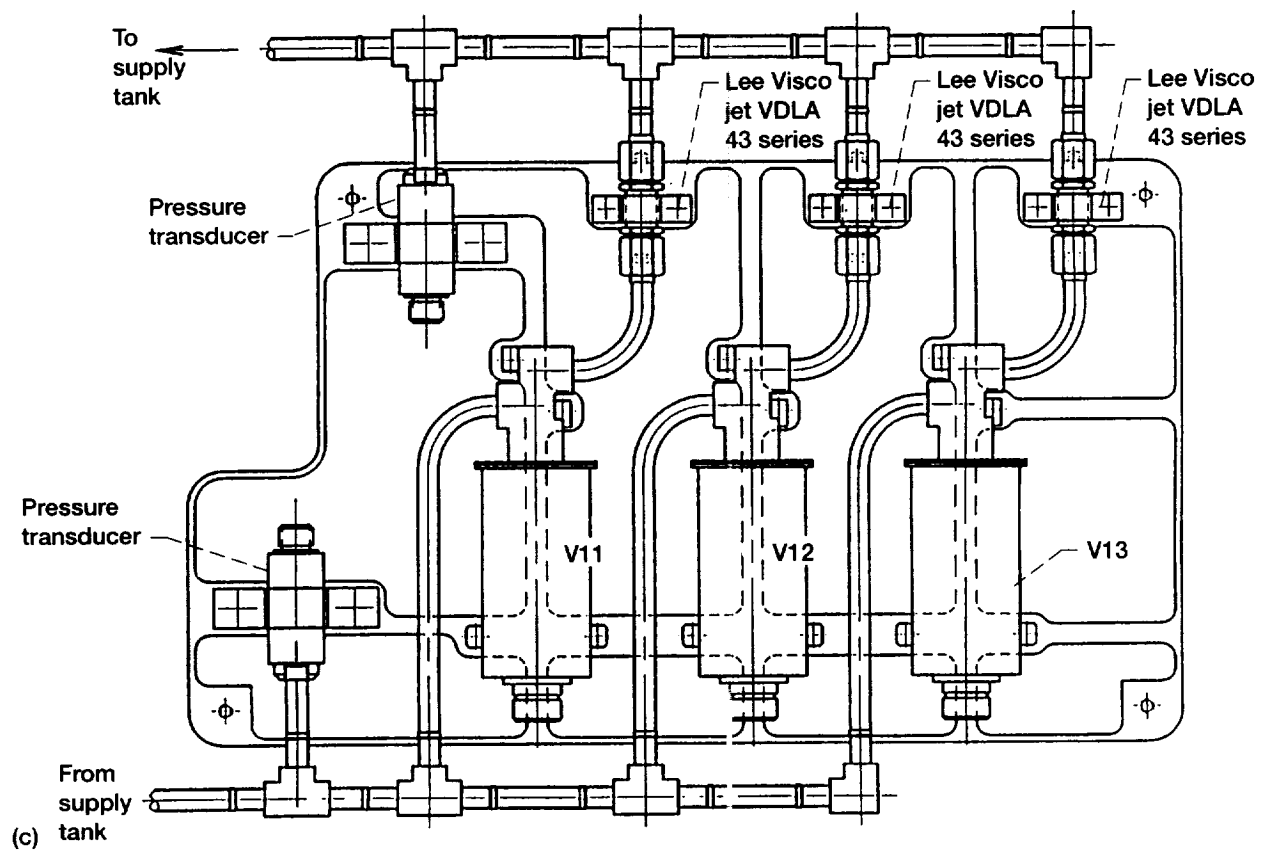


Figure D.5.—Continued. (c) Panel H, passive TVS panel. All panel H lines and fittings are 3/8 in.

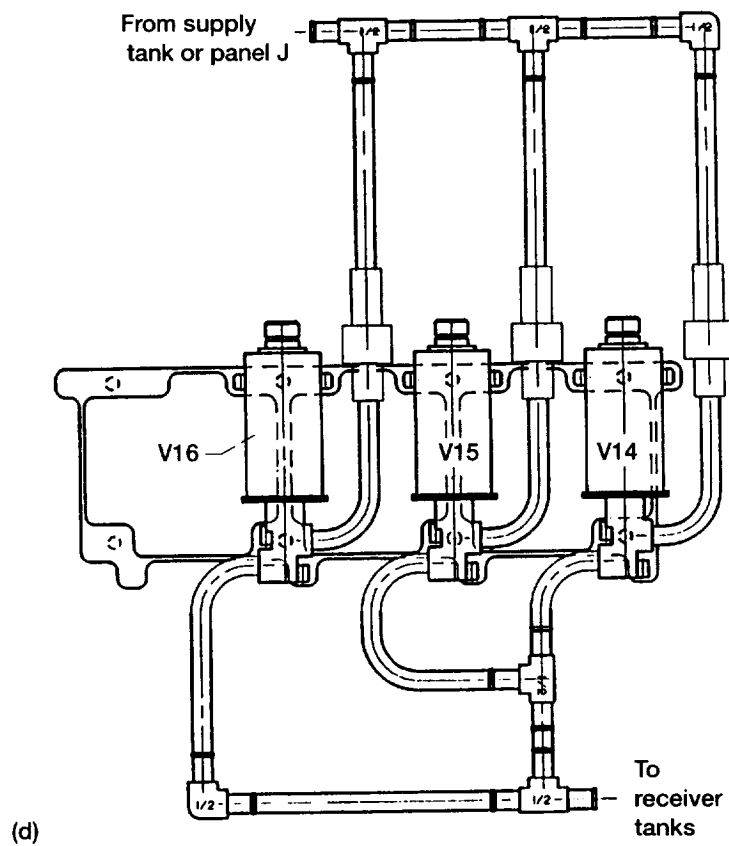


Figure D.5.—Continued. (d) Panel I, transfer.

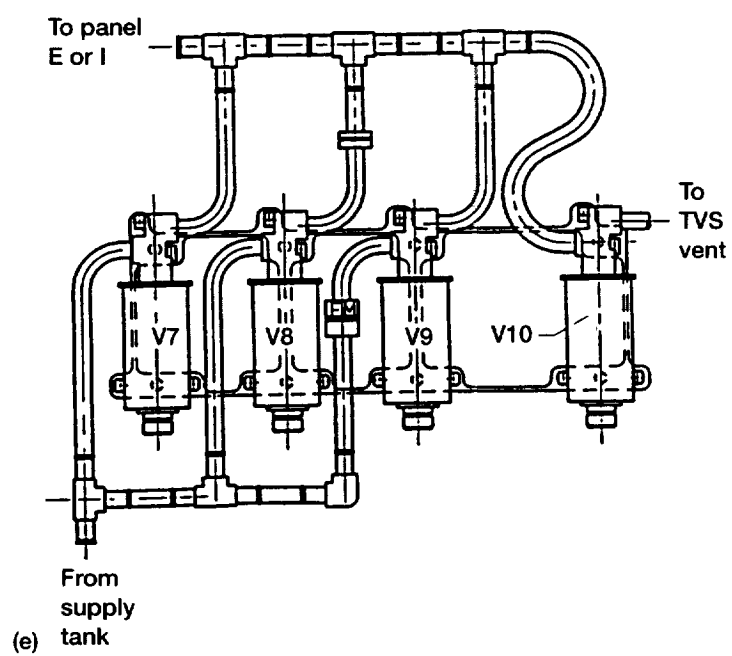


Figure D.5.—Concluded. (e) Panel J, transfer/TVS control.

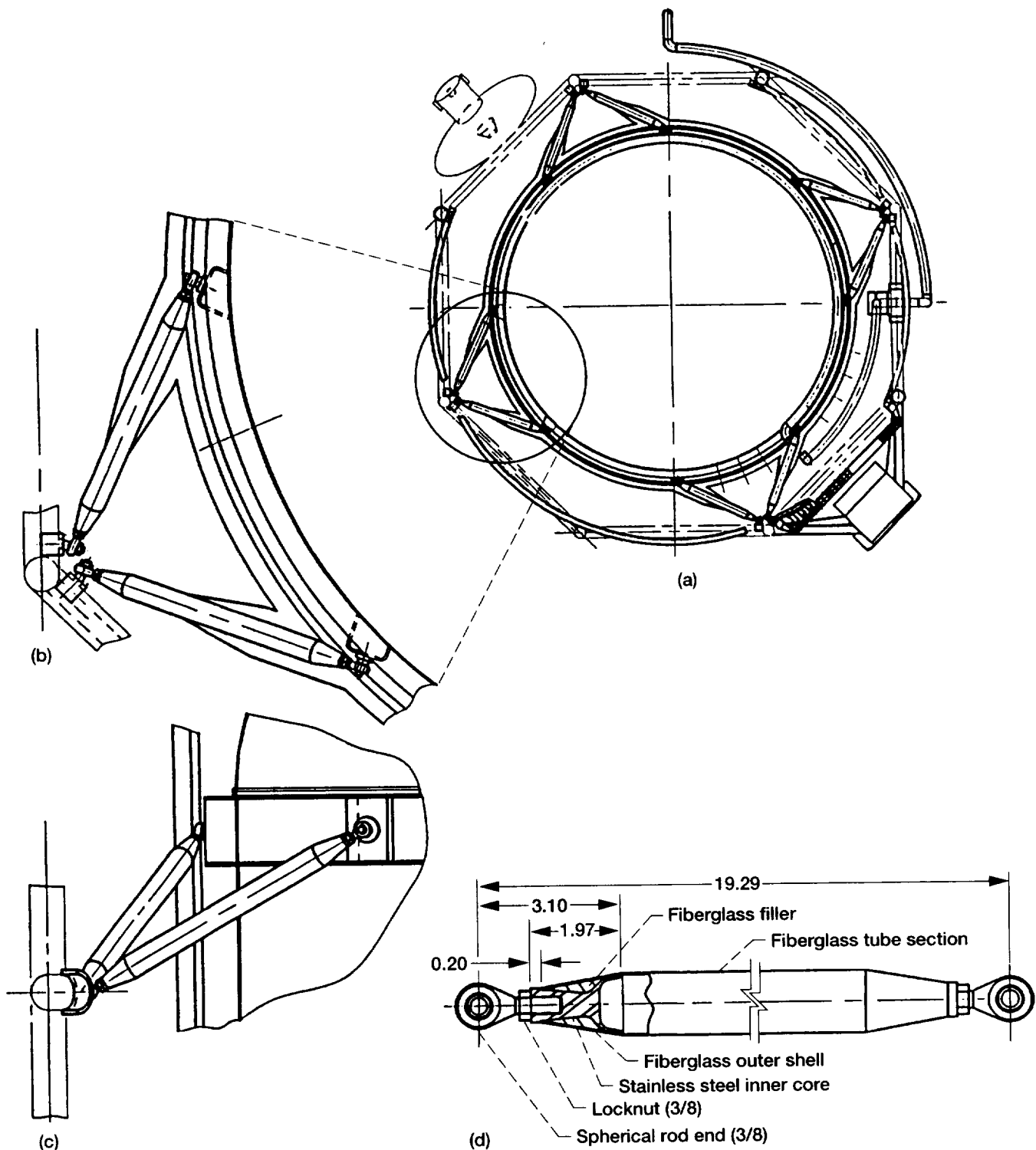


Figure D.6.—Supply tank strut detail. Dimensions are in inches. (a) Top view of tank supported by struts. (b) Enlargement of strut top view detail. (c) Side view of enlarged strut top view detail. (d) Side view of strut.

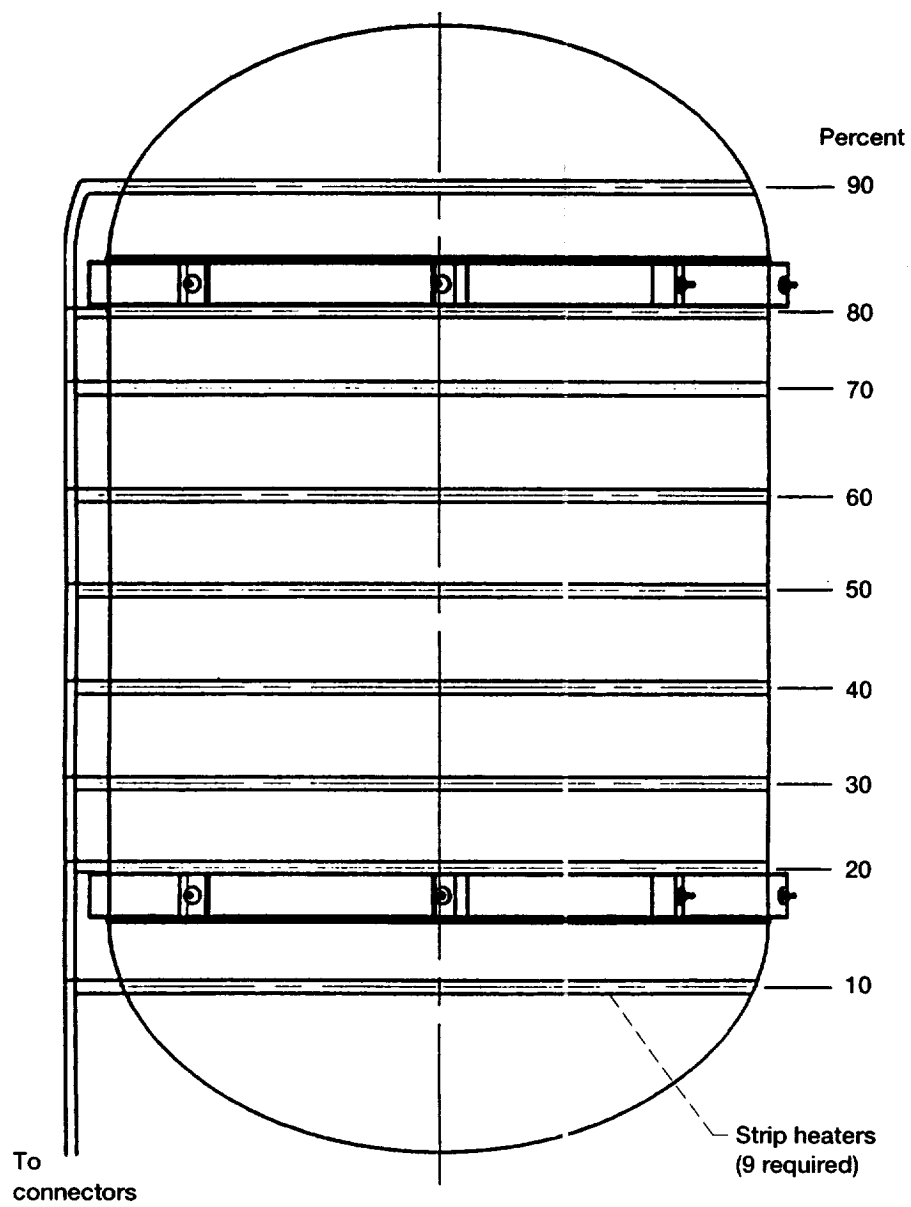


Figure D.7.—Supply tank strip heaters.

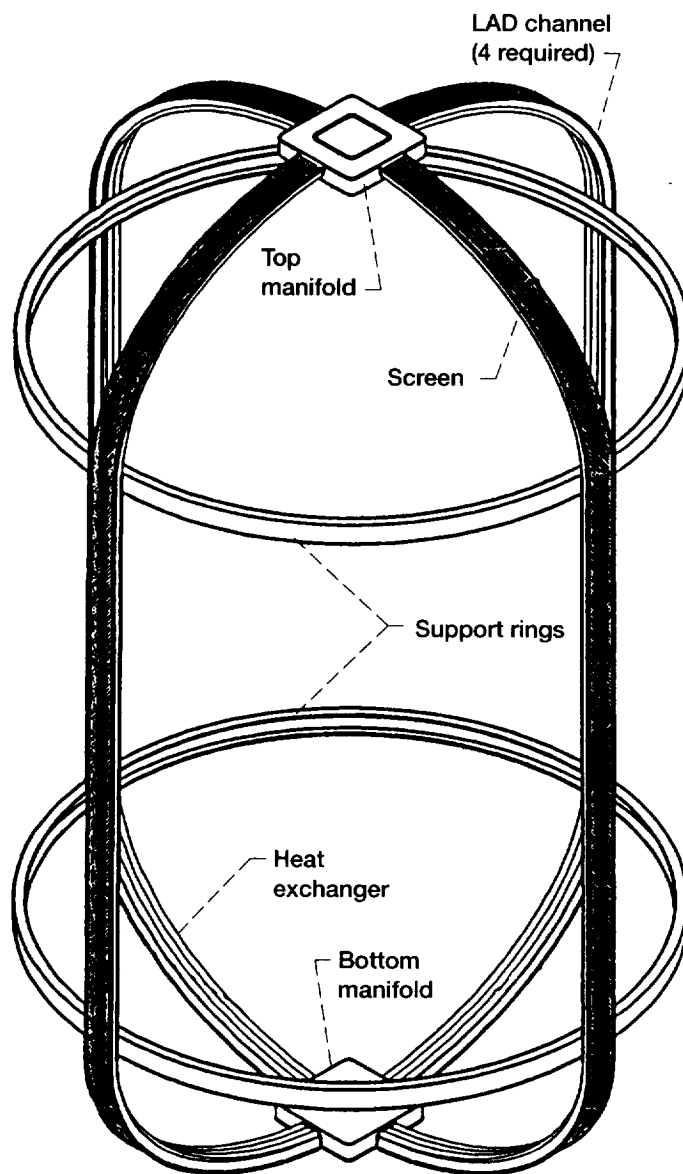


Figure D.8.—Supply tank LAD (isometric).

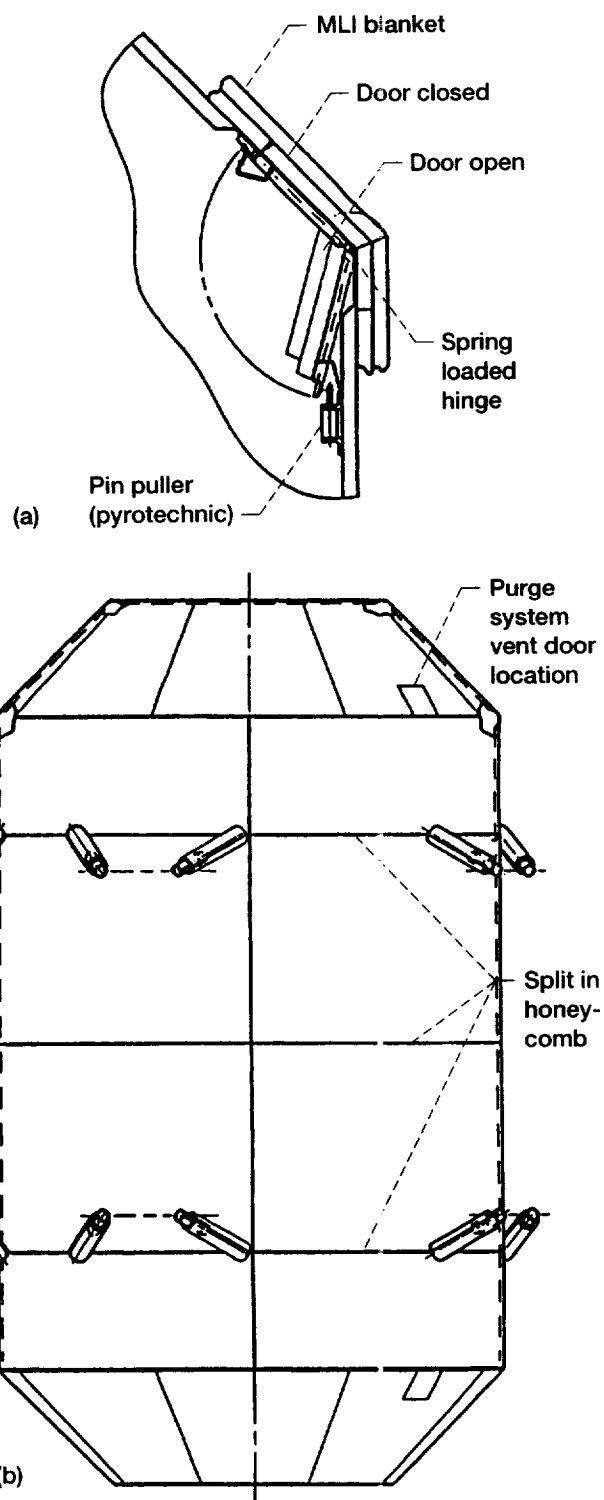


Figure D.9.—Supply tank MLI can. (a) MLI purge system vent door. (b) MLI can.

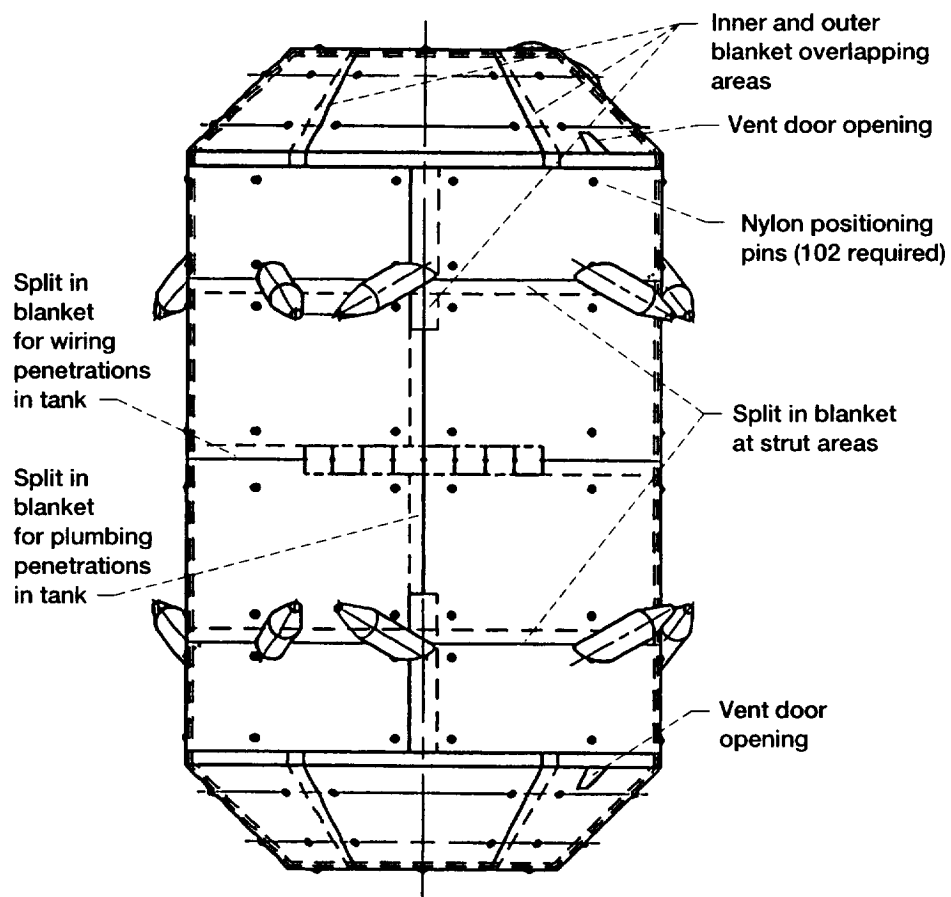


Figure D.10.—Supply tank MLI blanket.

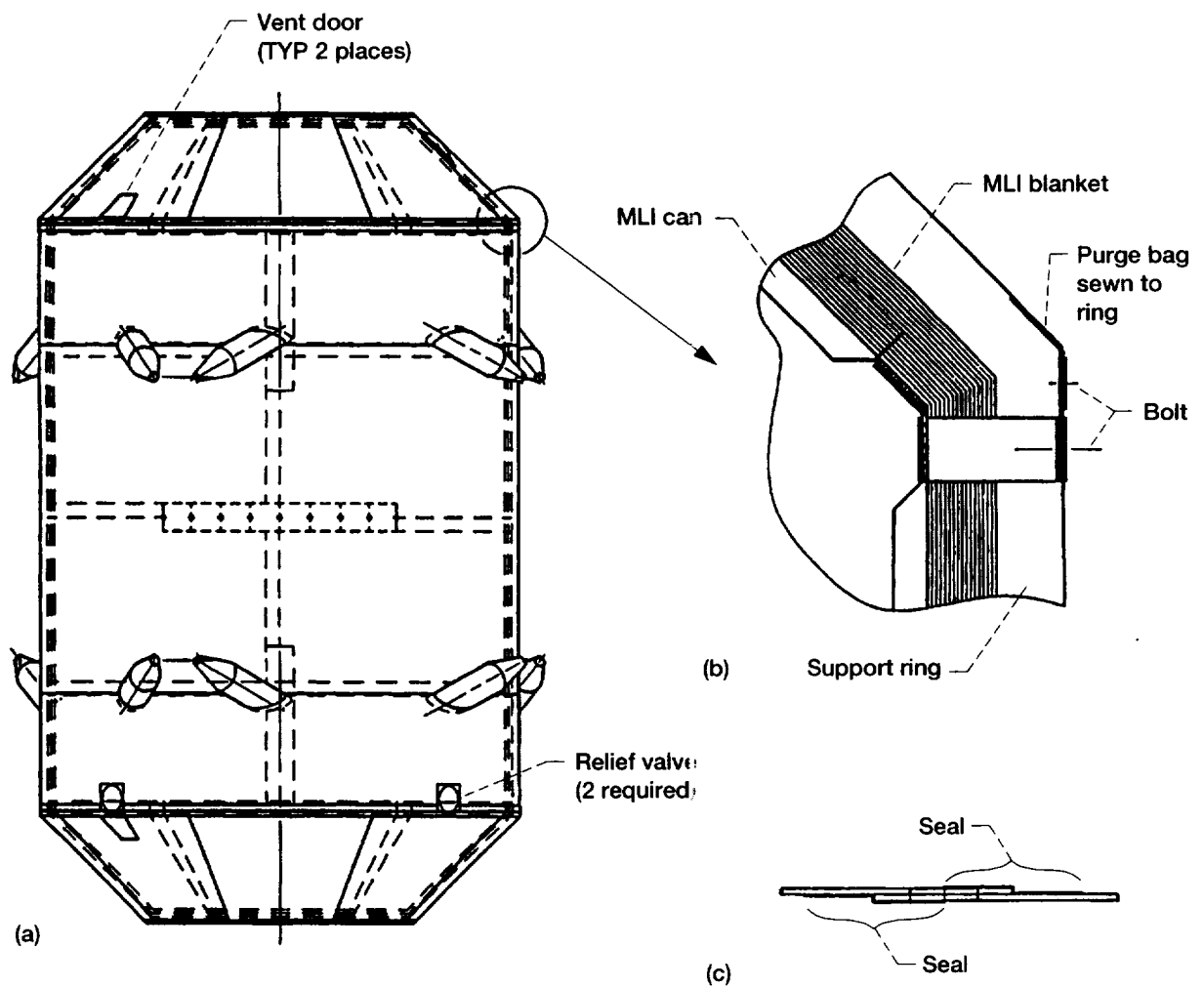


Figure D.11.—Supply tank purge bag. (a) Side view. (b) Enlargement of corner view. (c) Illustration of typical sewn seam.

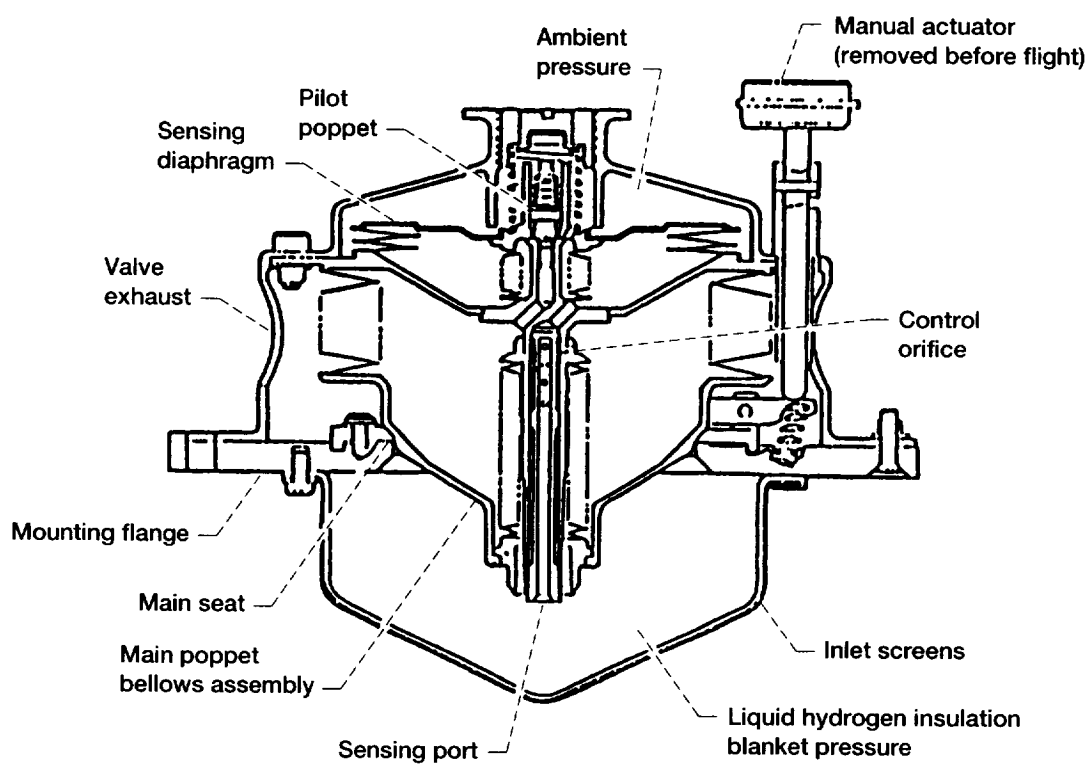


Figure D.12.—Supply tank purge bag relief valve.

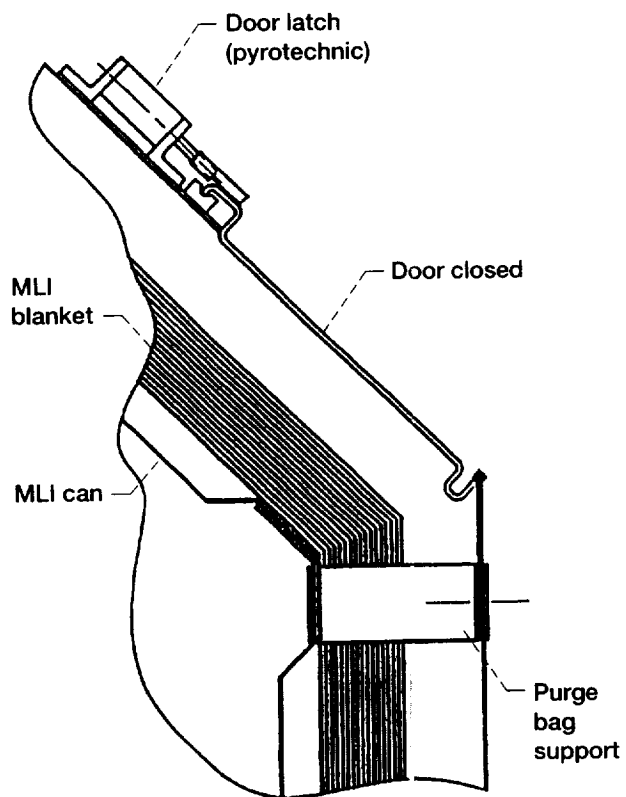


Figure D.13.—Purge bag vent door.

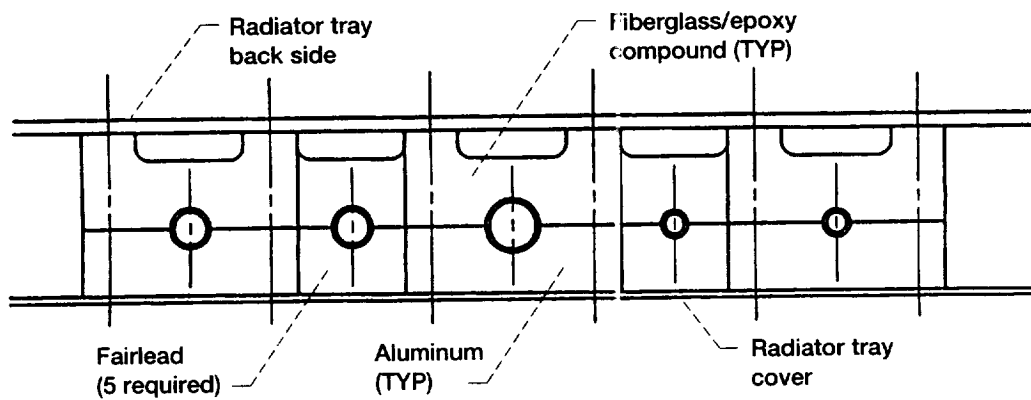


Figure D.14.—Radiator tray fairlead.

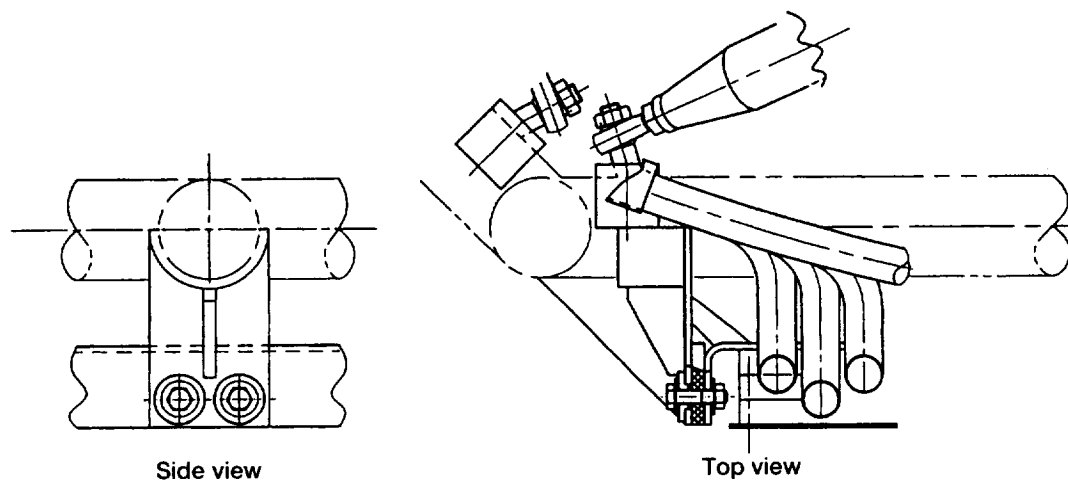


Figure D.15.—Radiator tray structural attachment.

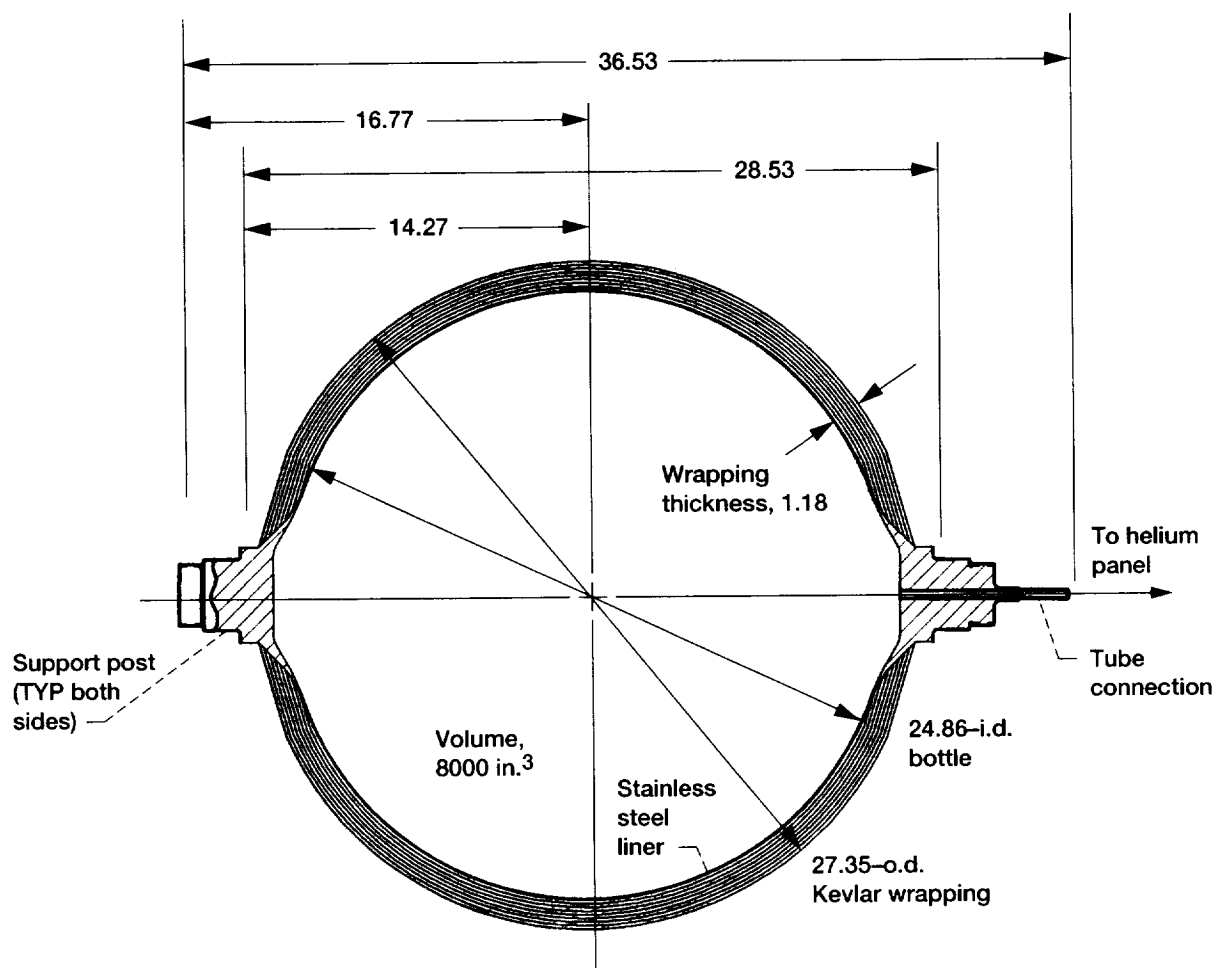


Figure D.16.—Helium bottle cross section. Dimensions are in inches.

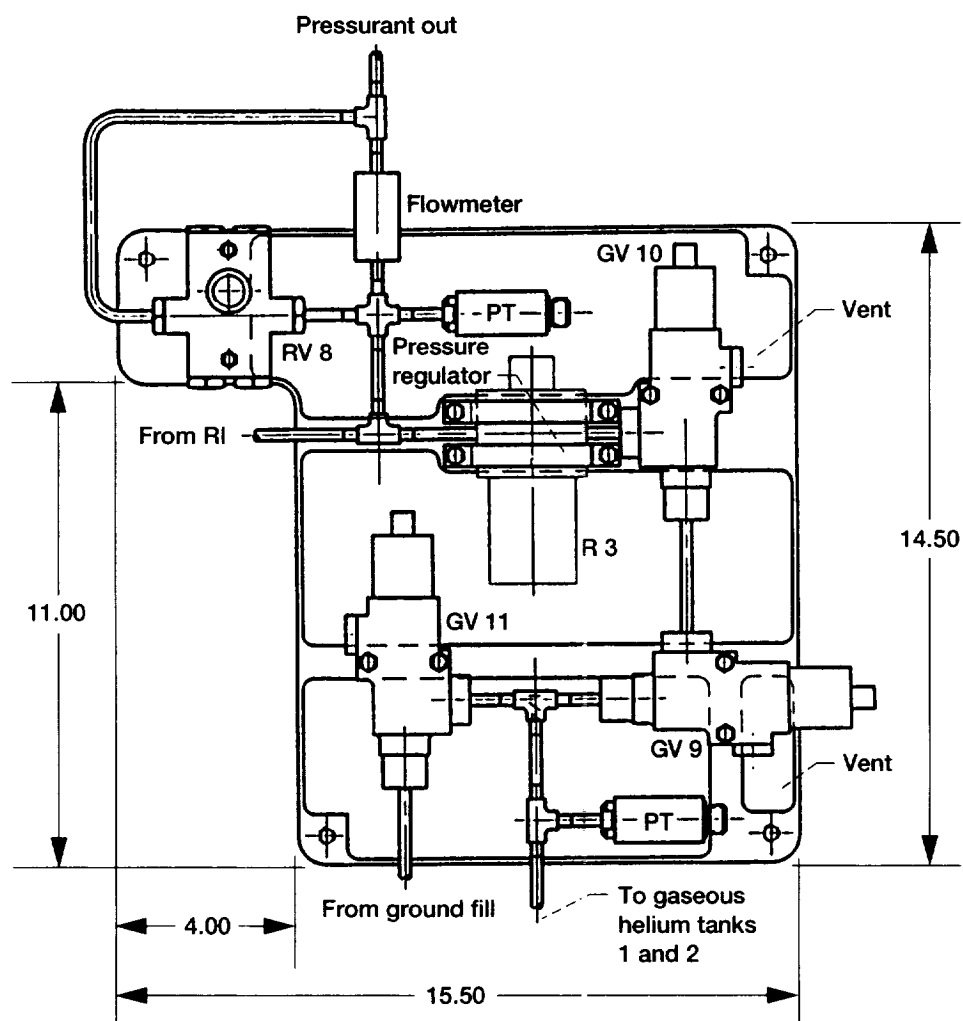


Figure D.17.—Valve panel "D" (helium bottles). Dimensions are in inches.

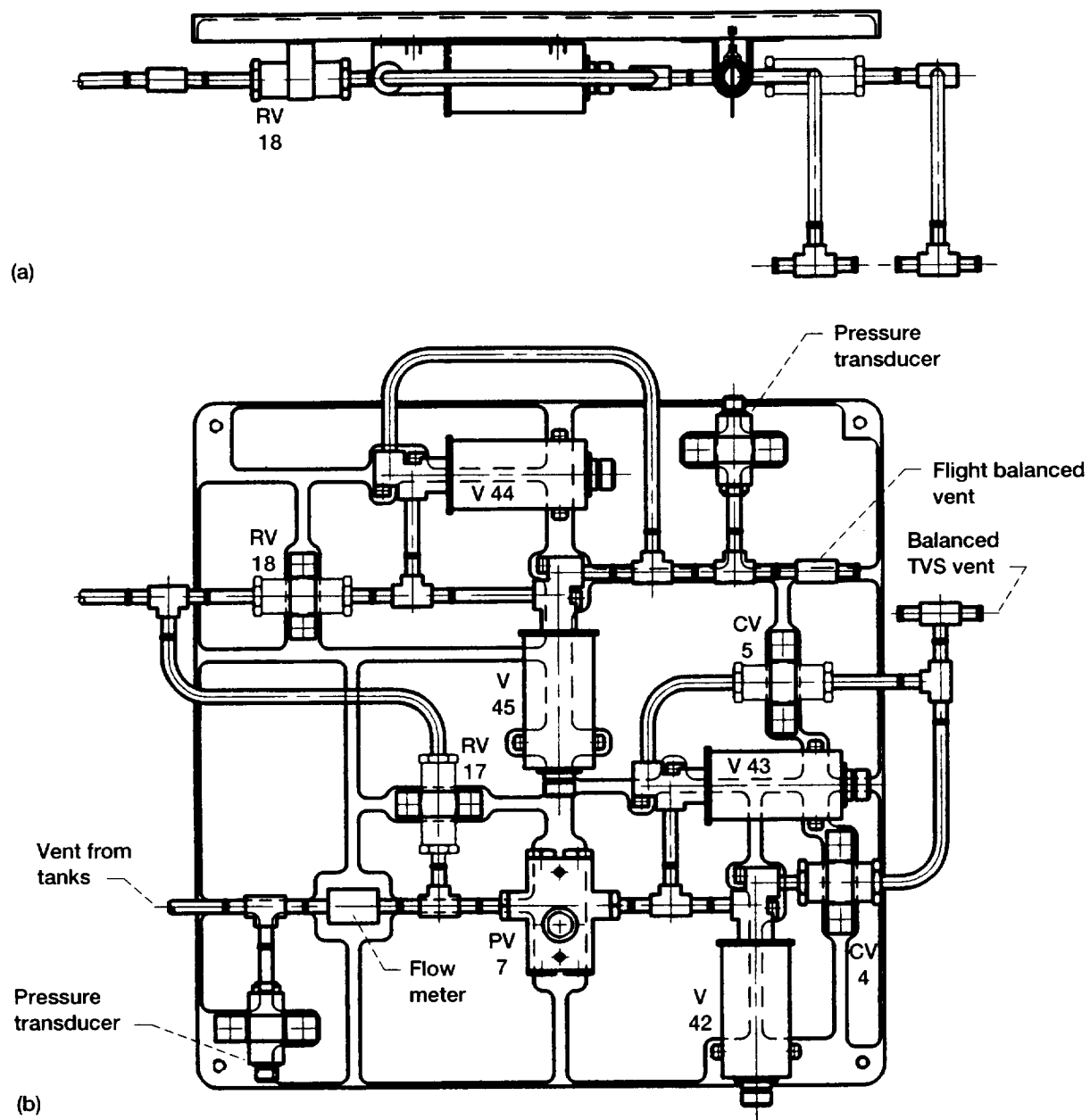


Figure D.18.—Valve panel "O" (vent panel). (a) Top view. (b) Side view.

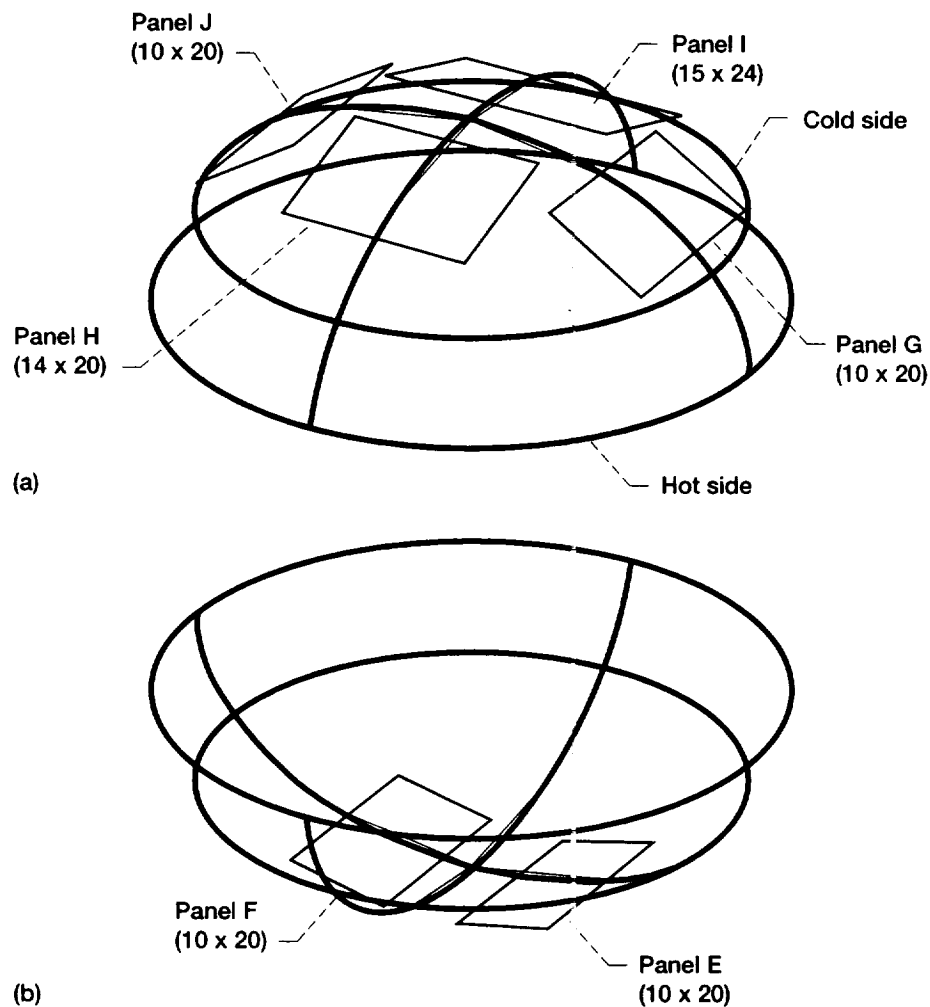


Figure D.19.—TRASYS supply tank model with valve panels; pressure vessel (PV) barrel and honeycomb removed. All valve panel corners placed 1.5 in. above point where panel legs attach. Dimensions are in inches. (a) Top, panels G to J. (b) Bottom, panels E and F.

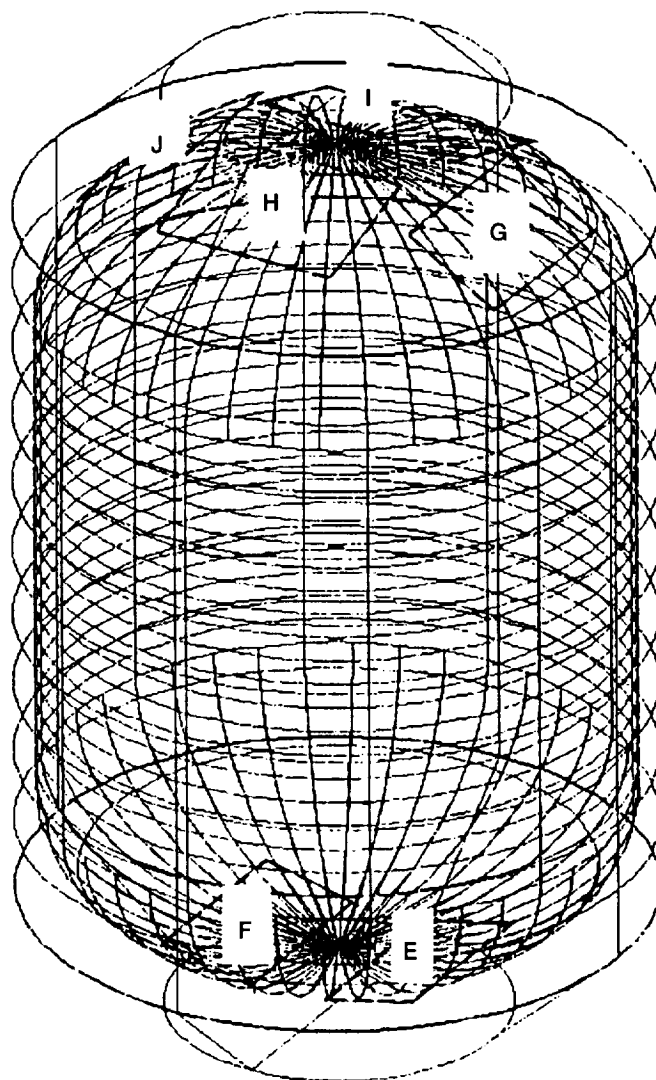


Figure D.20.—Full TRASYS internal supply tank model with valve panels.

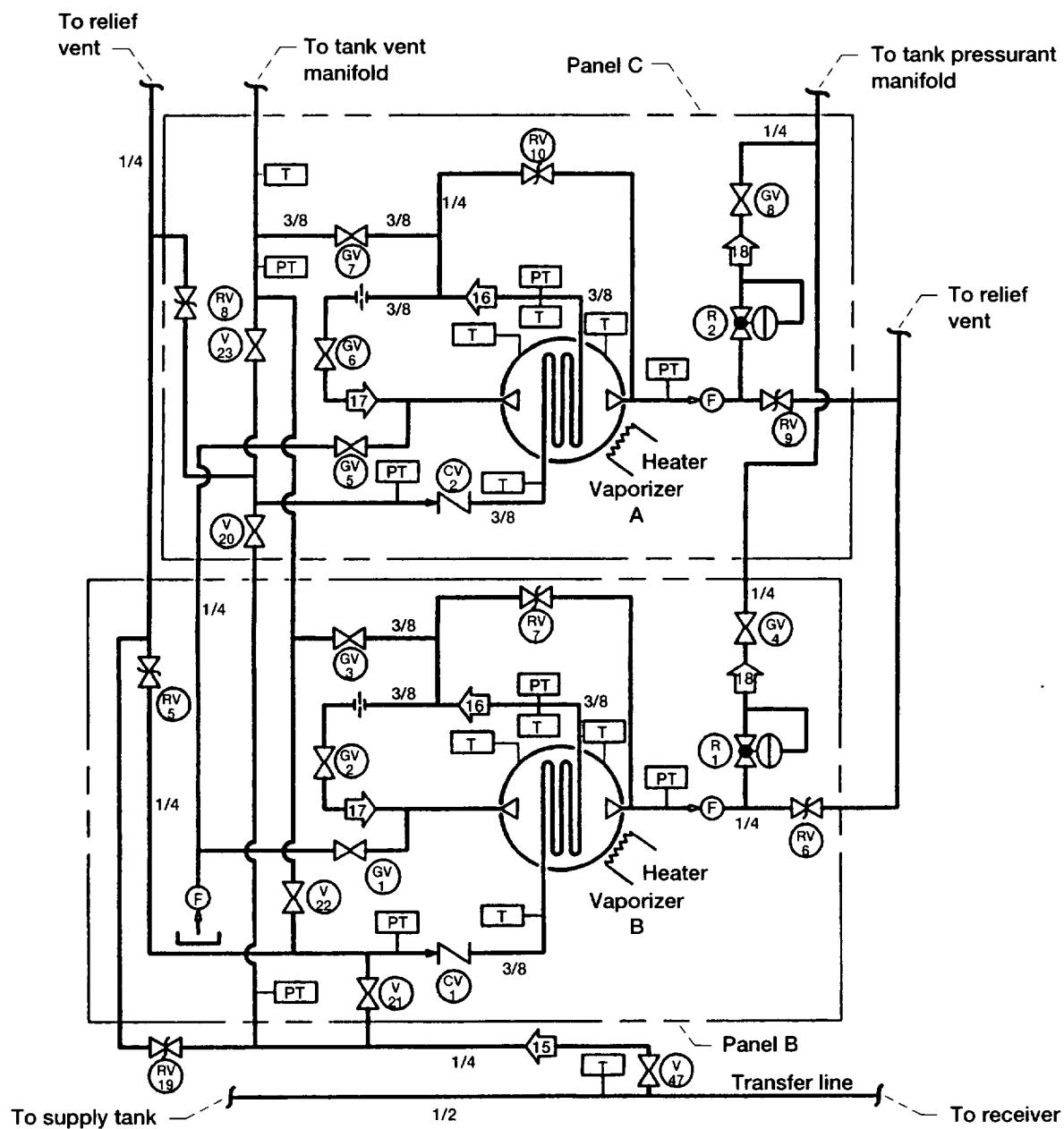


Figure D.22.—Hydrogen vaporizer system schematic. Dimensions are in inches.

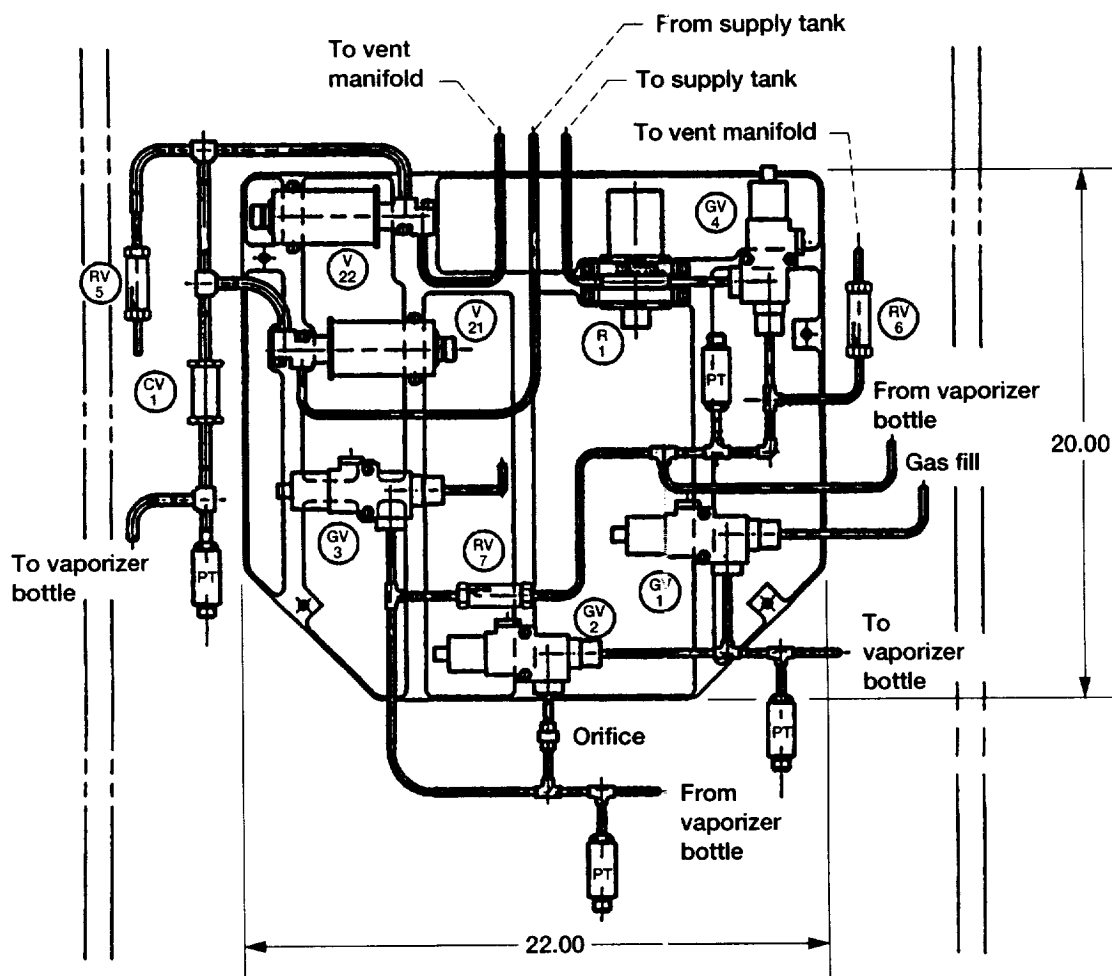


Figure D.23.—Vaporizer valve panel layout (valve panels B and C). Dimensions are in inches.

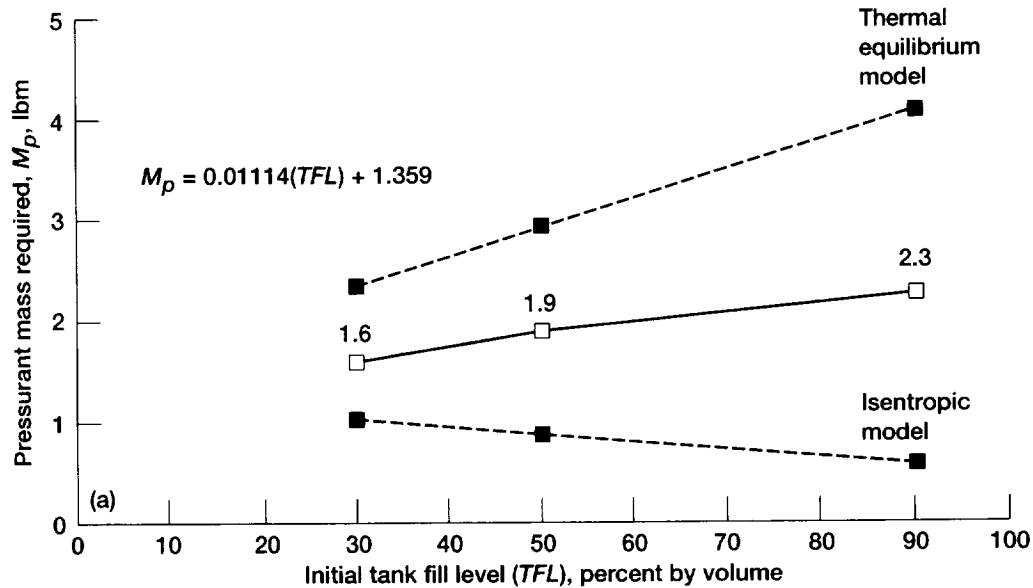


Figure D.24.—Pressurant mass required for transfers. (a) Supply tank to large receiver tank. (b) Supply tank to small receiver tank. (c) Large receiver tank to supply tank. (d) Large receiver tank to small receiver tank. (e) Small receiver tank to supply tank. (f) Small receiver tank to large receiver tank.

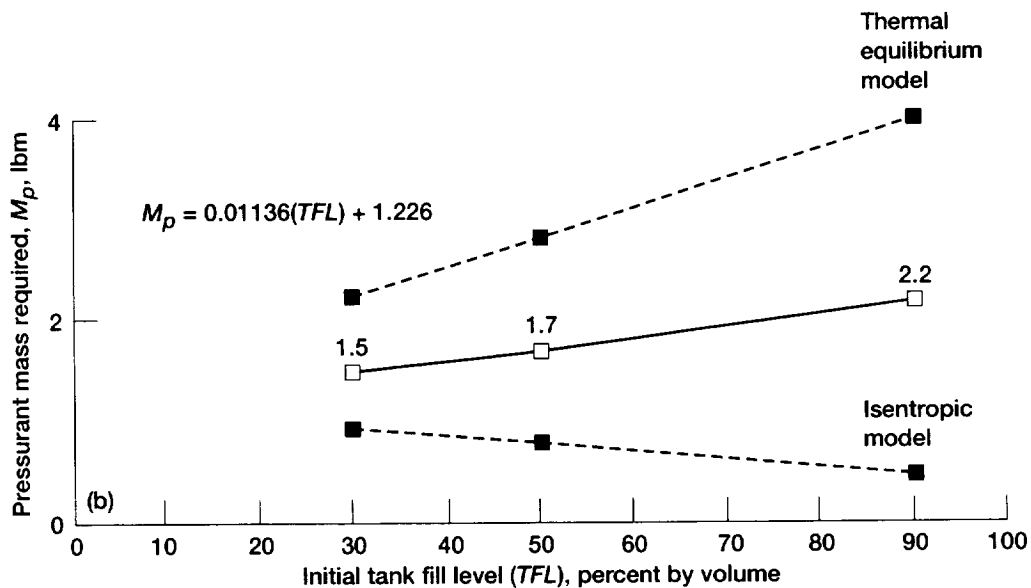


Figure D.24.—Continued. (b) Supply tank to small receiver tank.

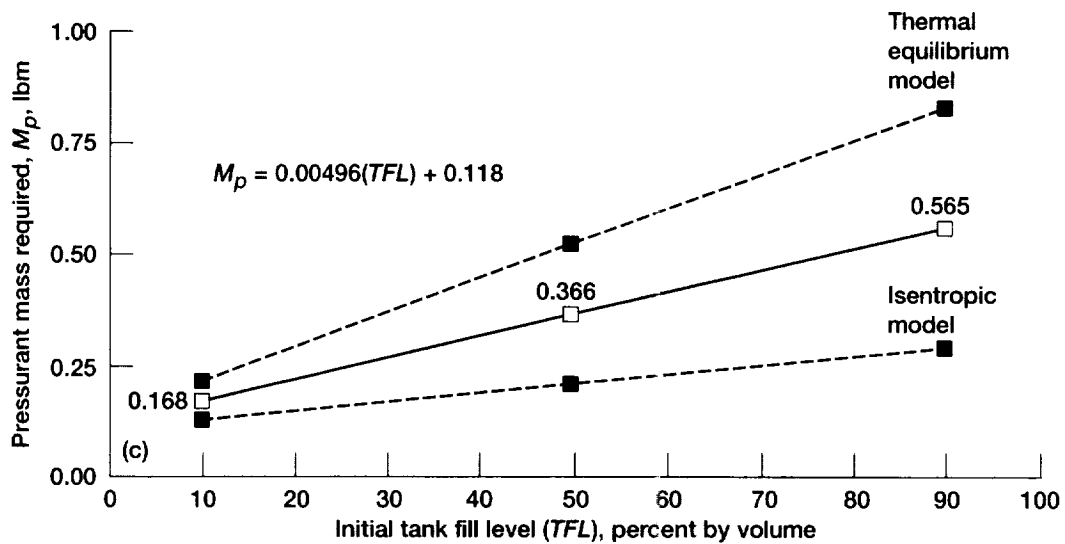


Figure D.24.—Continued. (c) Large receiver tank to supply tank.

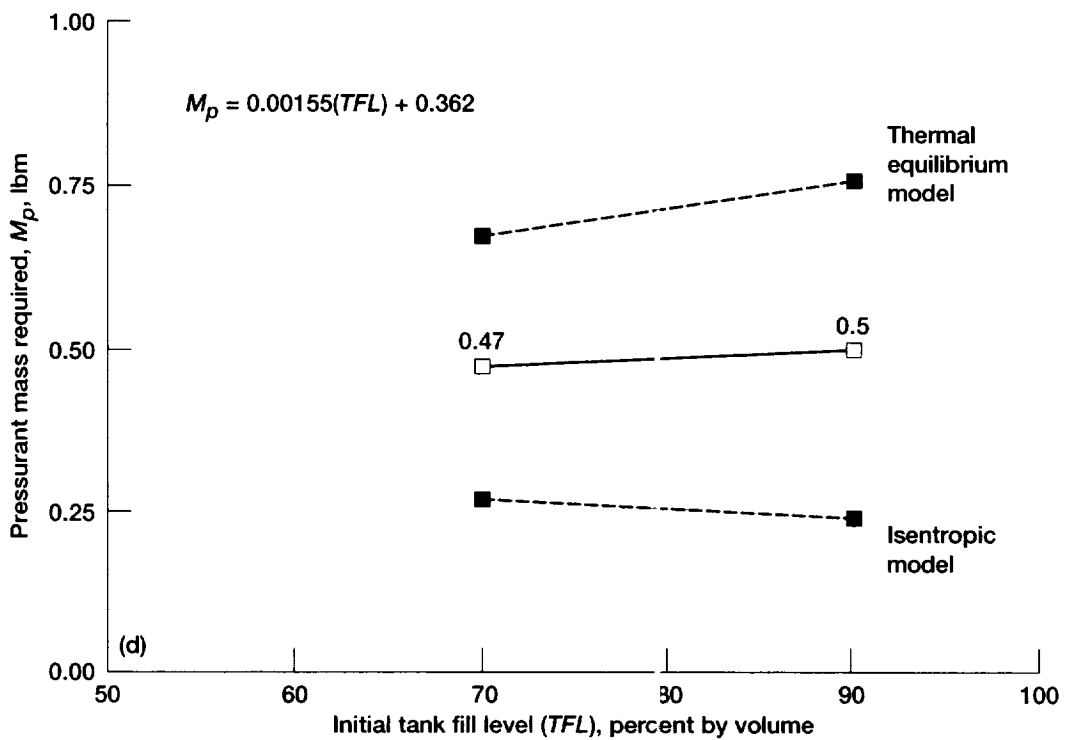


Figure D.24.—Continued. (d) Large receiver tank to small receiver tank.

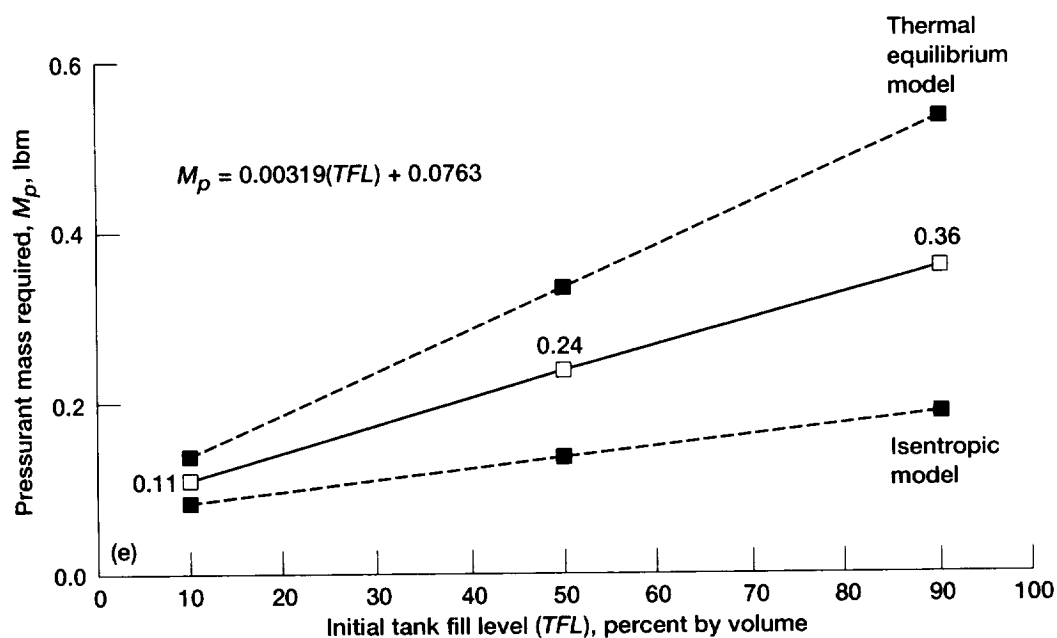


Figure D.24.—Continued. (e) Small receiver tank to supply tank.

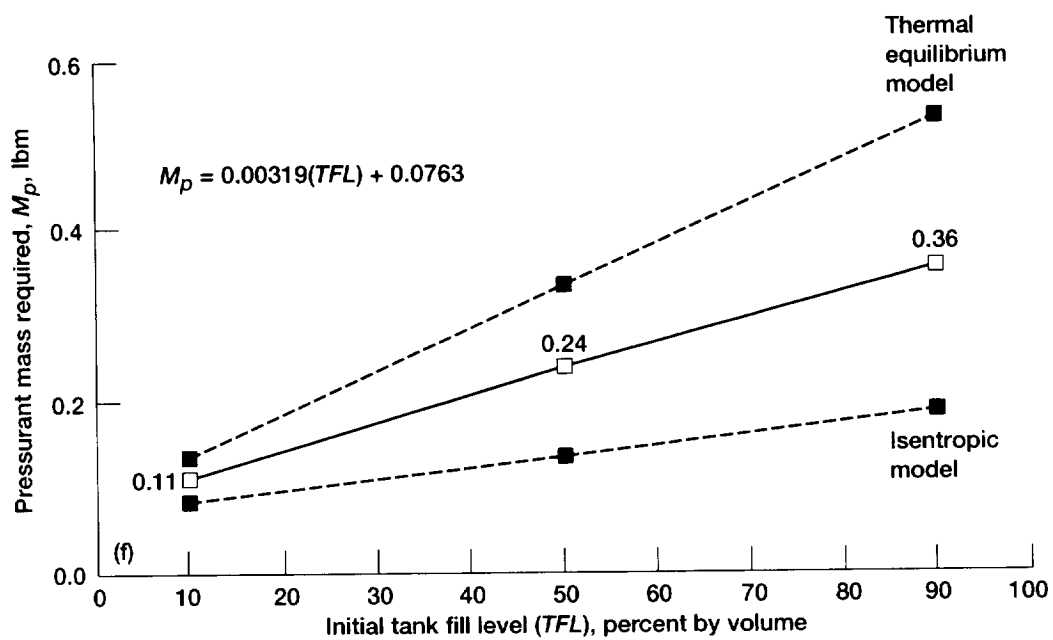


Figure D.24.—Concluded. (f) Small receiver tank to large receiver tank.

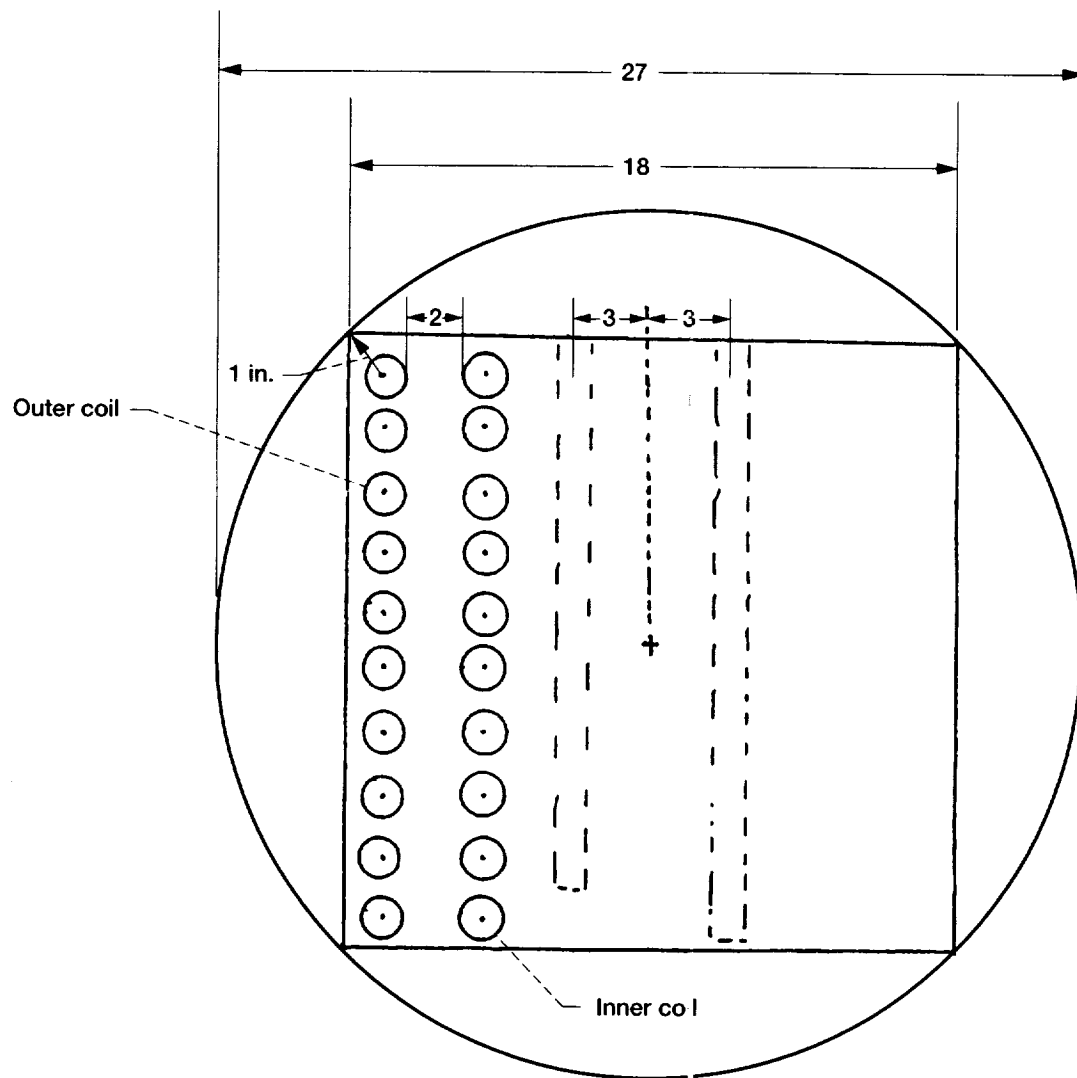


Figure D.25.—Vaporizer TRASYS surface model cross section. Dimensions are in inches.

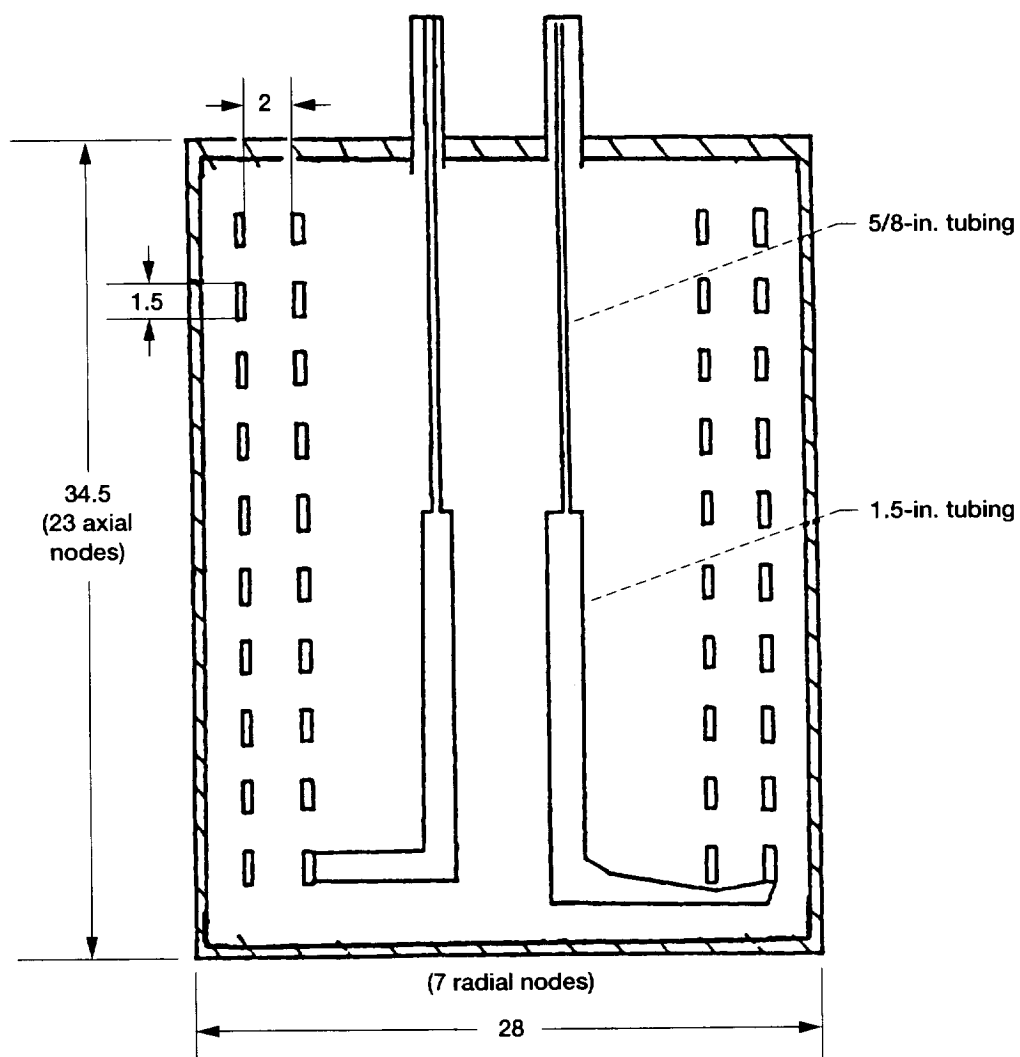


Figure D.26.—Vaporizer SINDA85 thermal model cross section. Dimensions are in inches.

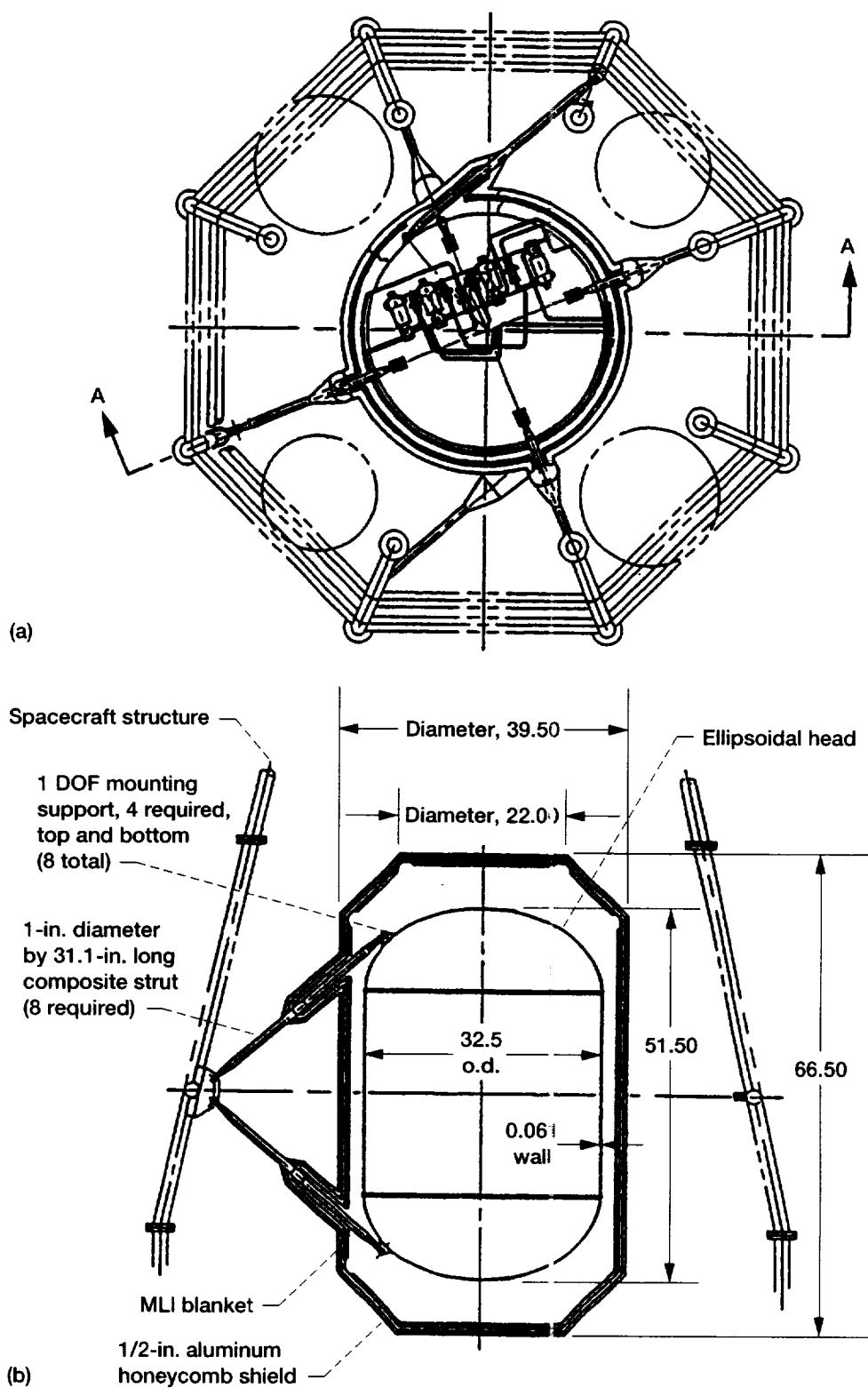


Figure D.27.—Large receiver tank module. Dimensions are in inches. (a) Top view. (b) Side view of (A-A).

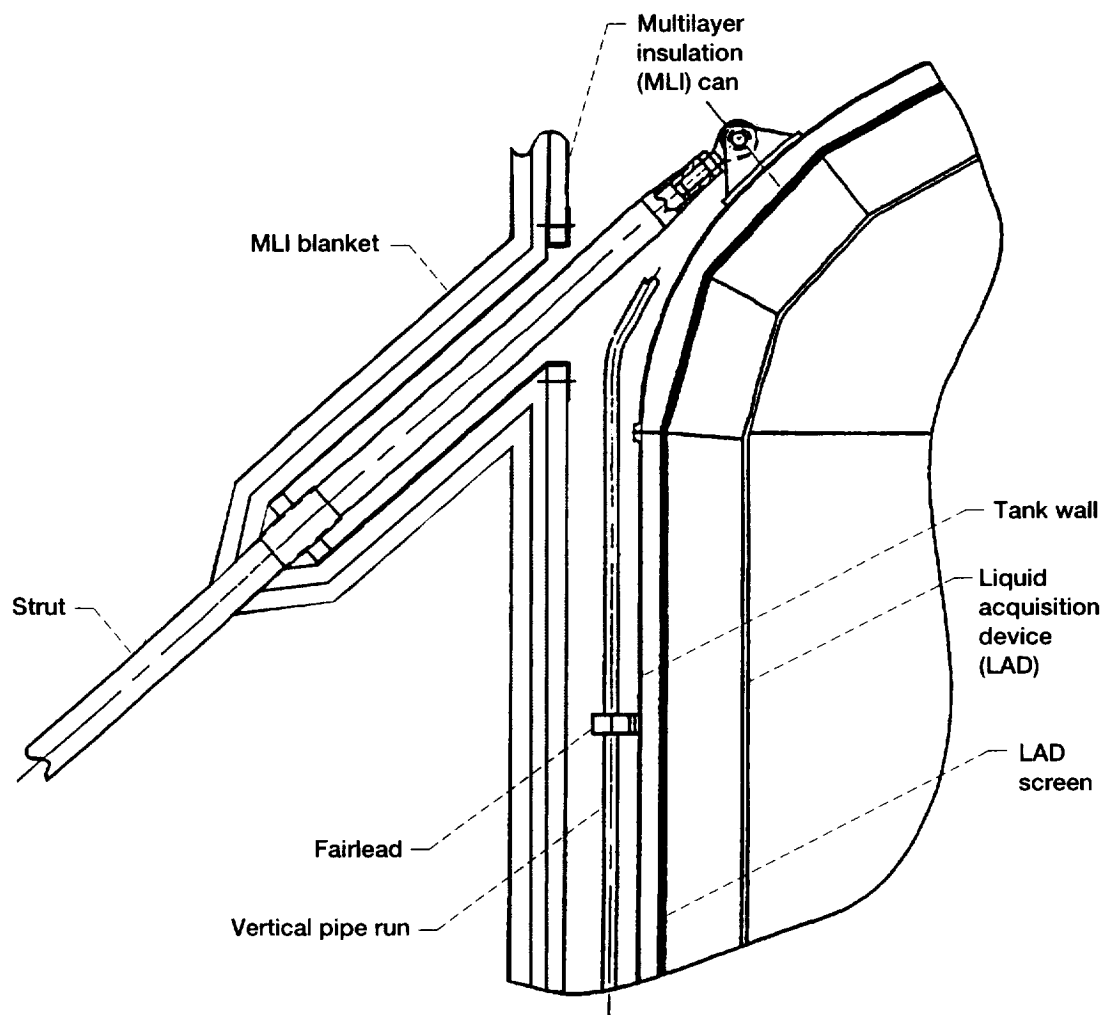


Figure D.28.—Large receiver tank cross section.

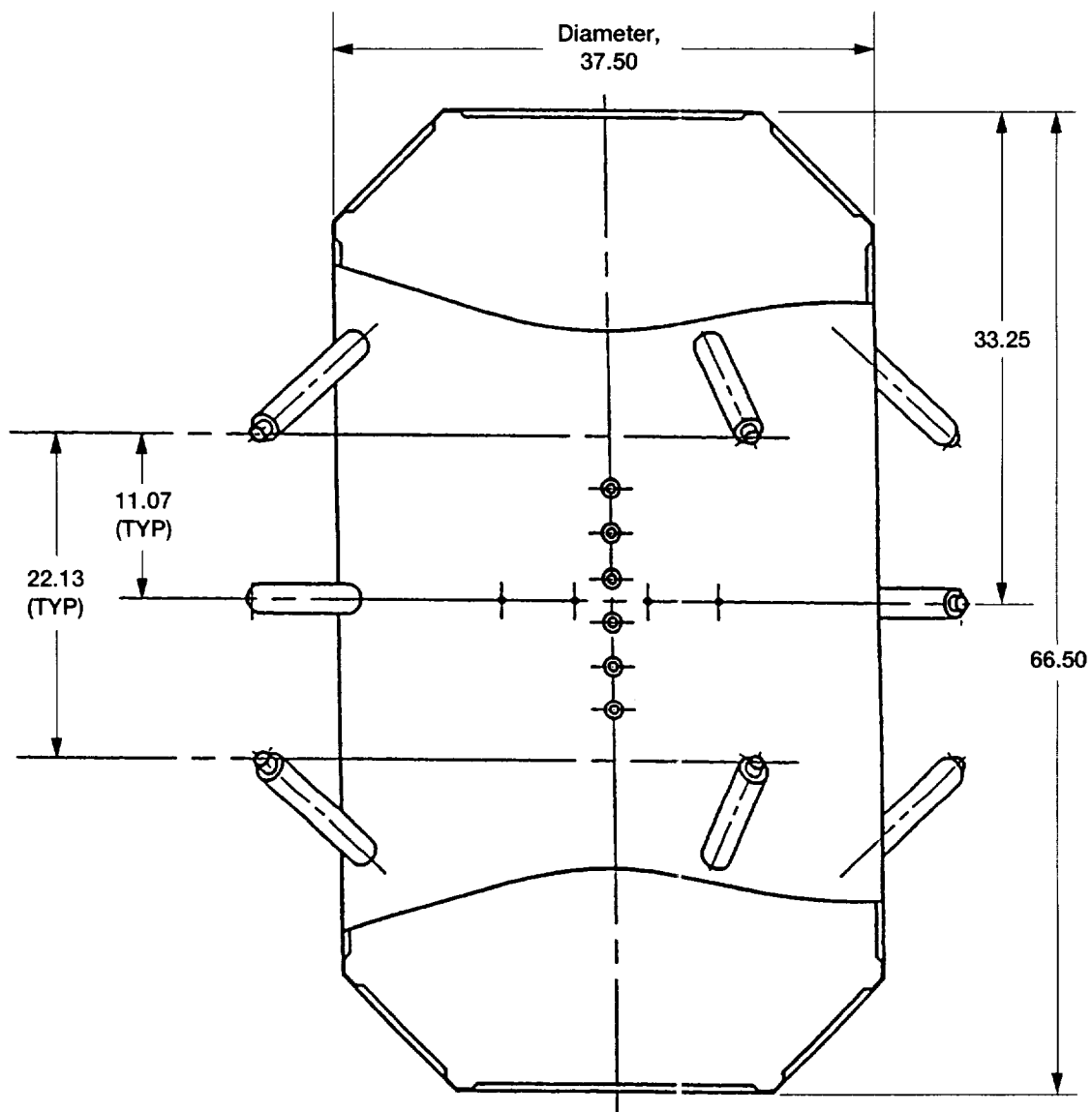


Figure D.29.—Large receiver tank multilayer insulation (MLI) can. Dimensions are in inches.

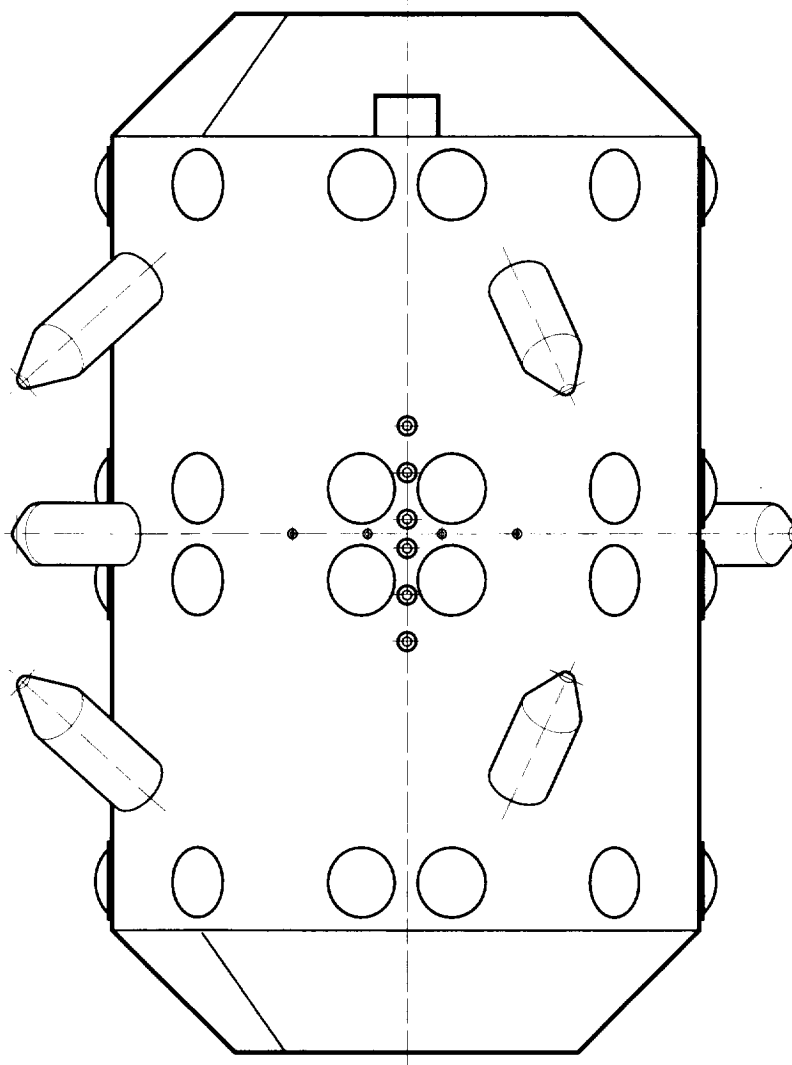


Figure D.30.—Large receiver tank multilayer insulation (MLI) blanket.

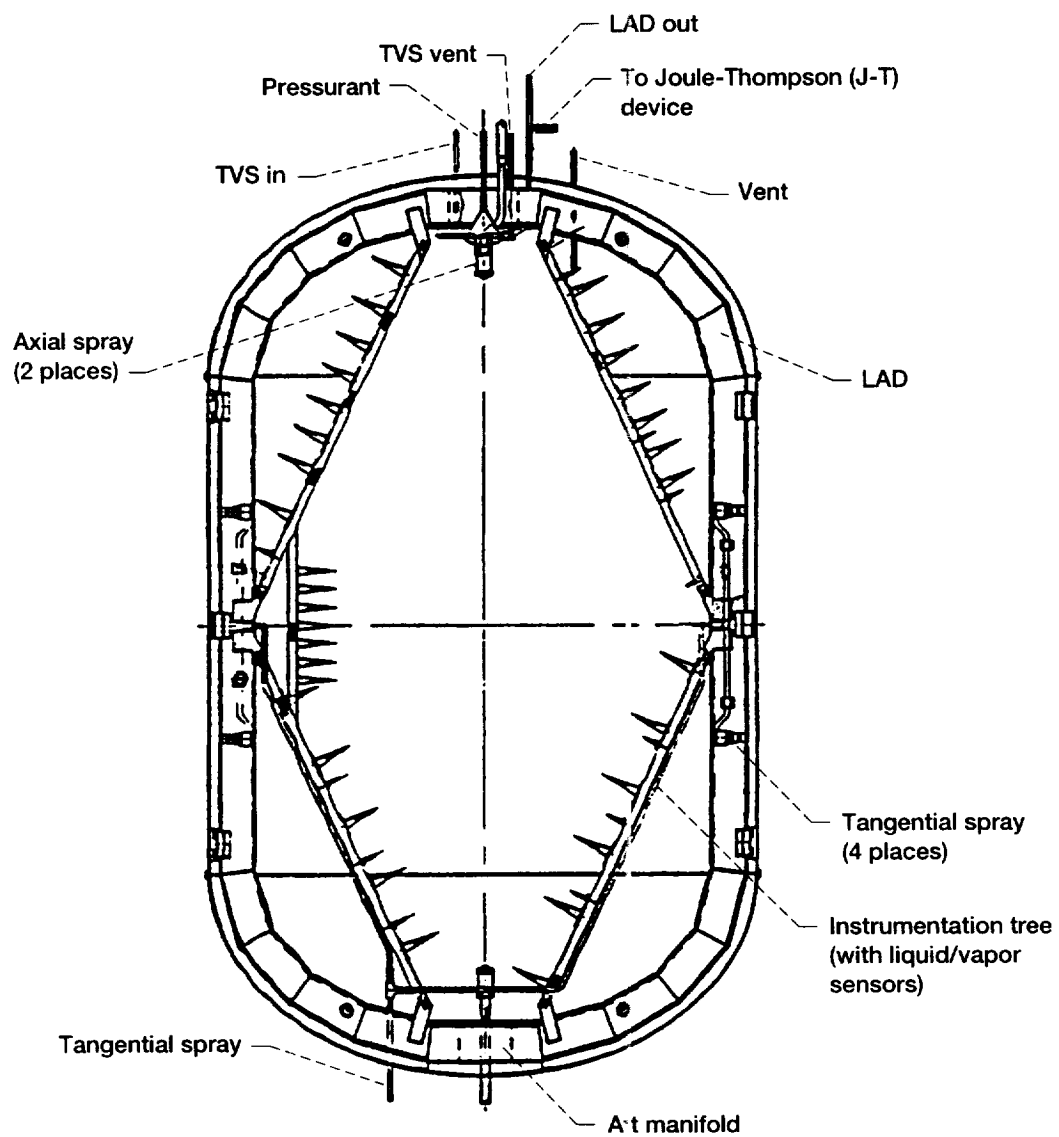


Figure D.31.—Large receiver tank internals.

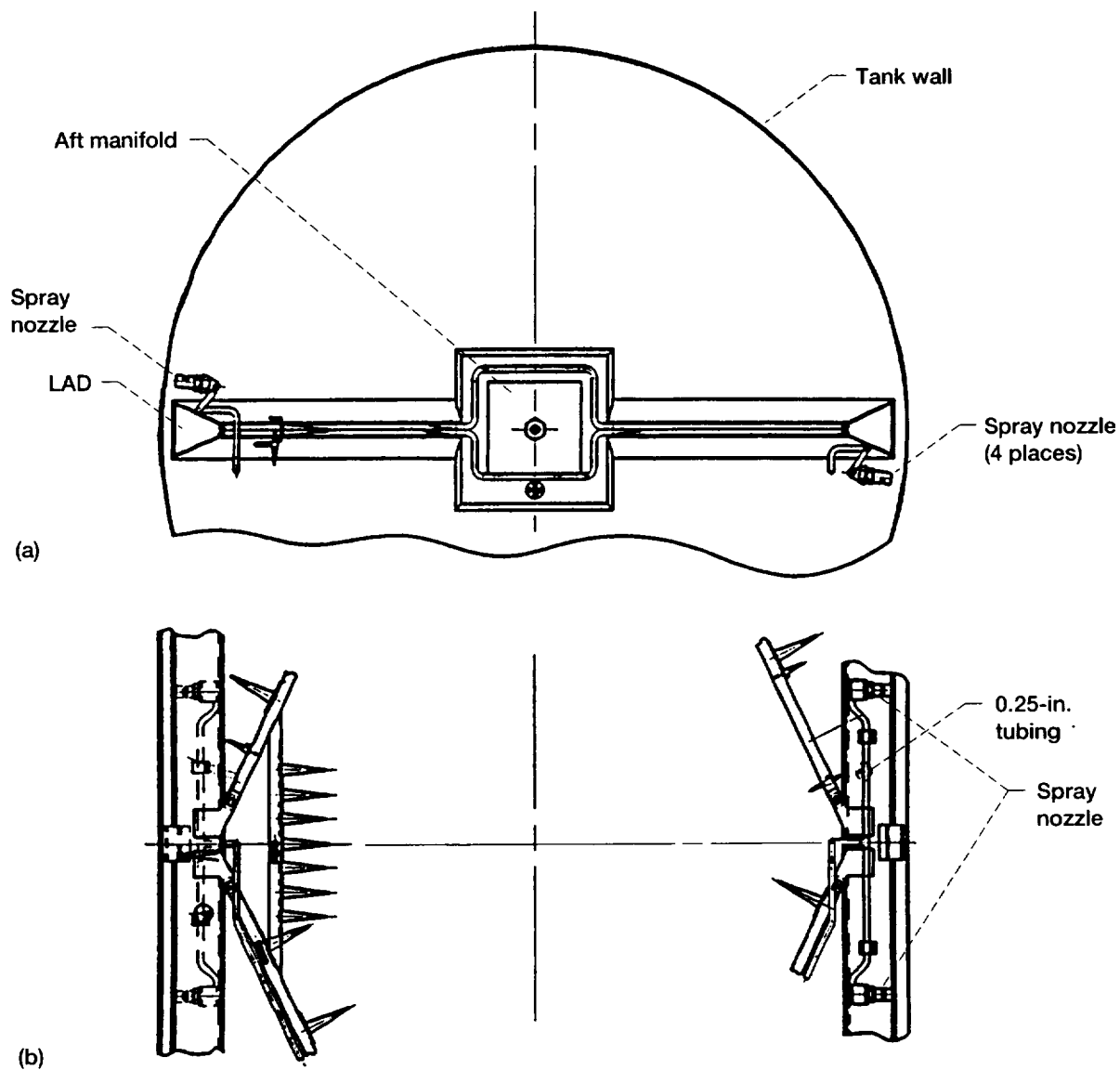


Figure D.32.—Large receiver tank tangential spray system. (a) Aft view from inside tank. (b) Center of tank—detailed view.

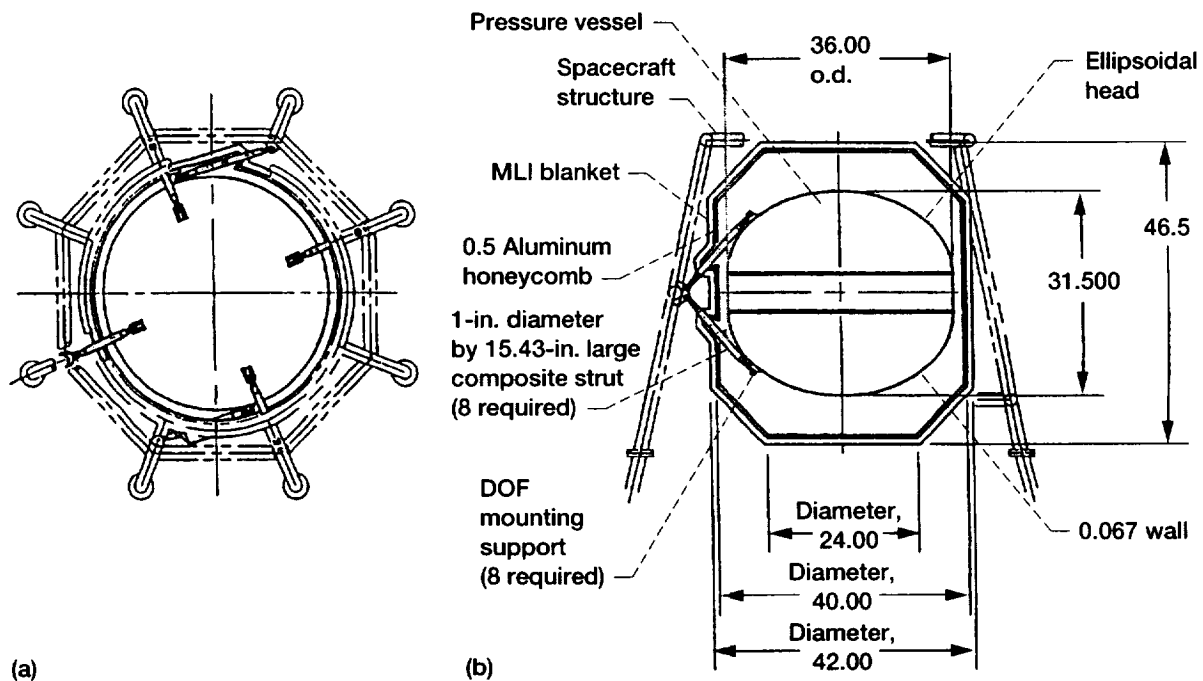


Figure D.33.—Small receiver tank module. Dimensions are in inches. (a) Top view with top of aluminum honeycomb shield removed. (b) Side view.

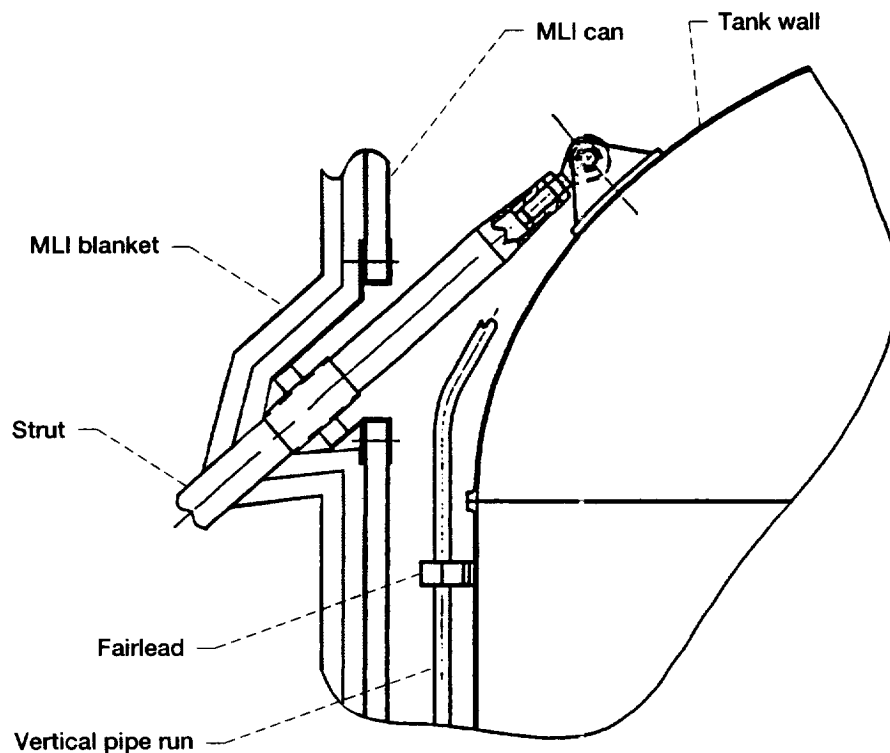


Figure D.34.—Cross section of small receiver tank.

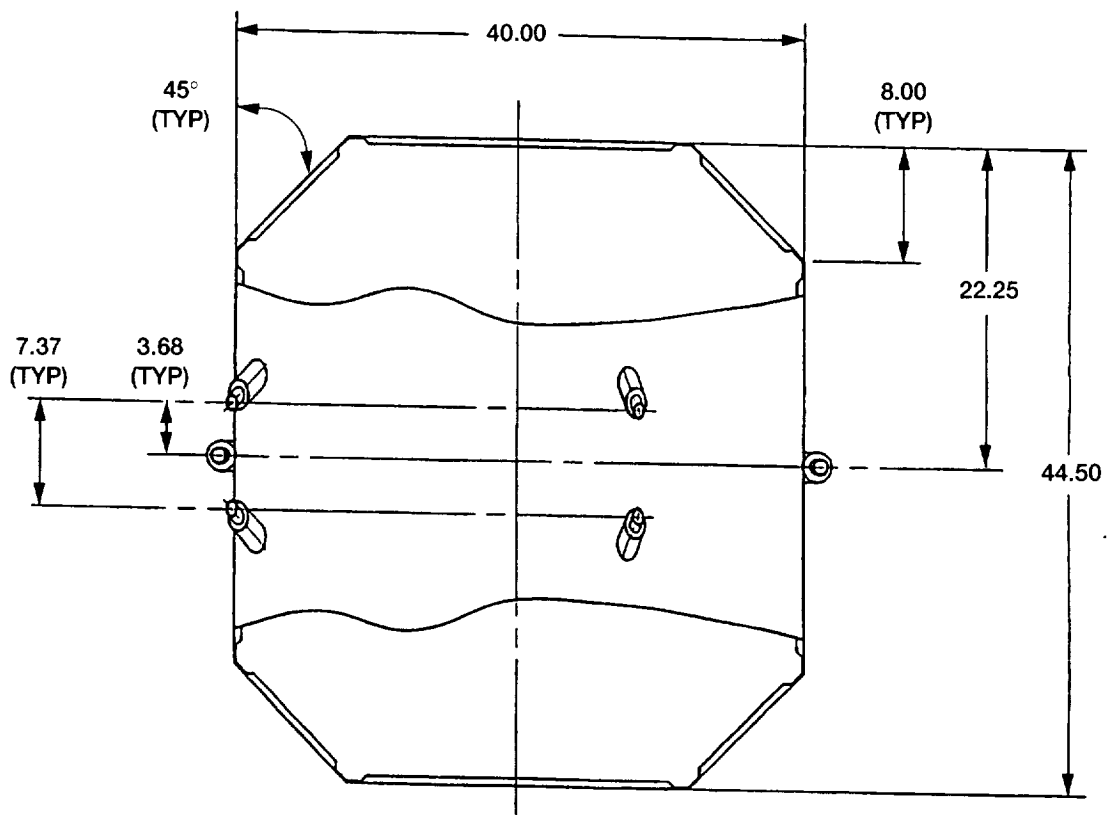


Figure D.35.—Small receiver tank MLI can. Dimensions are in inches.

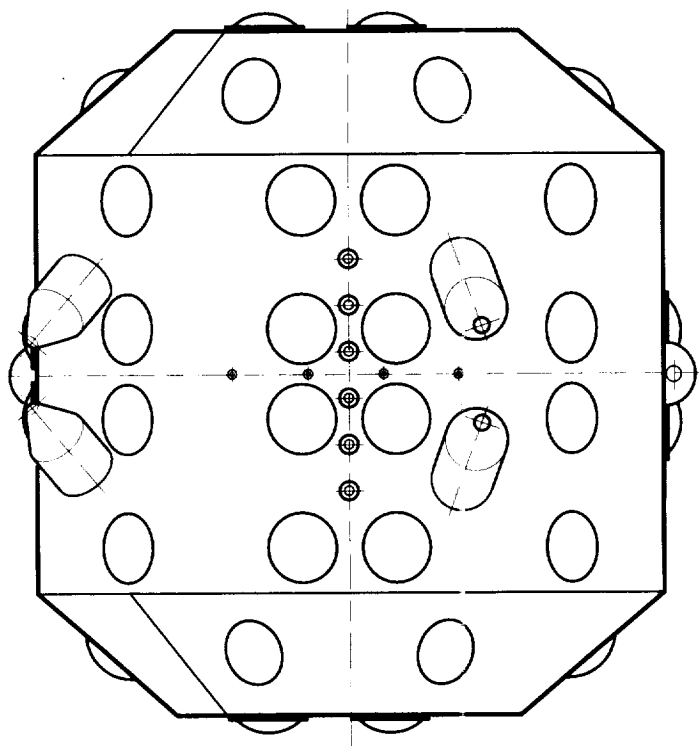


Figure D.36.—Small receiver tank multilayer insulation (MLI) blanket.

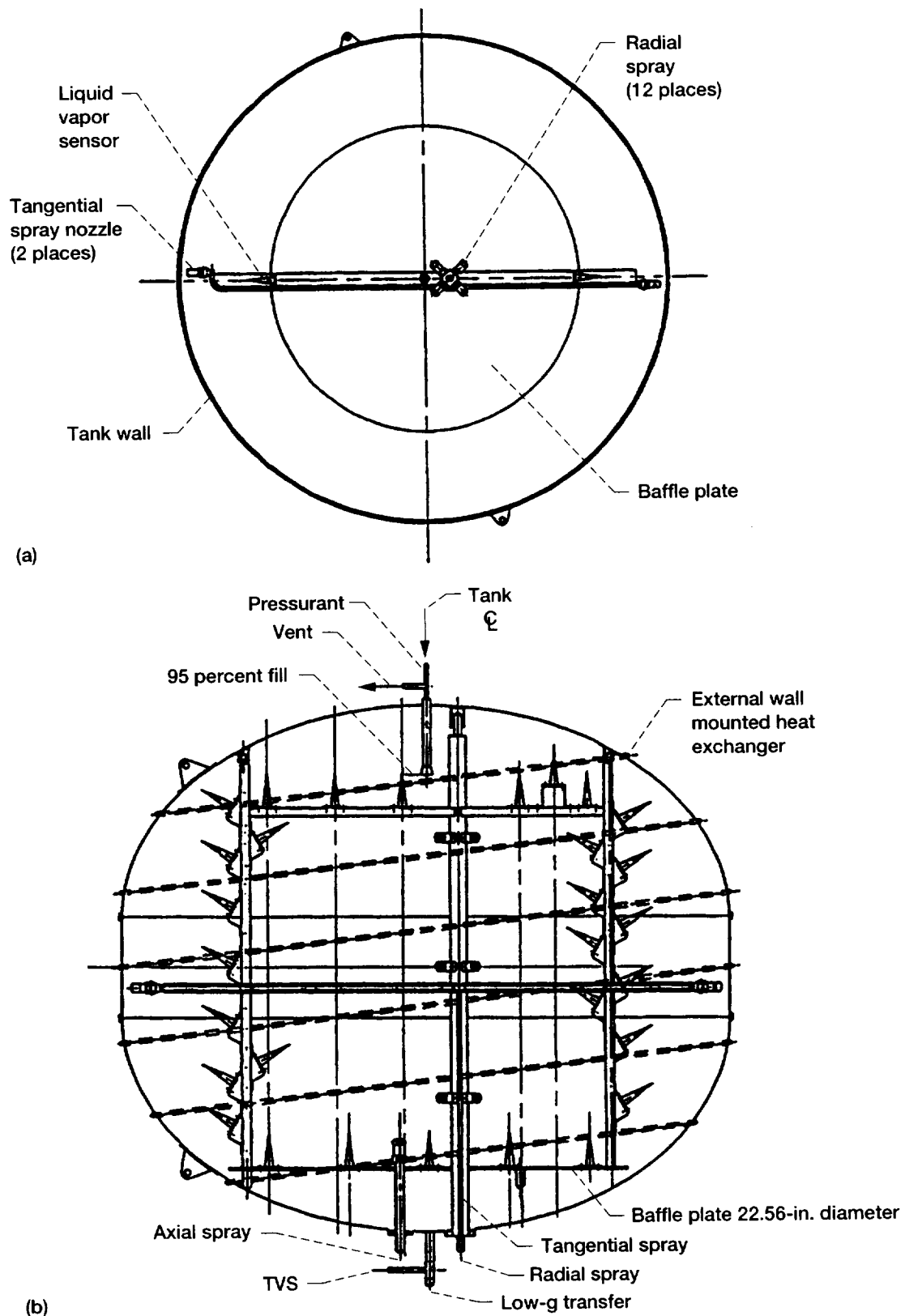


Figure D.37.—Small receiver tank internals. (a) Top view looking down inside tank. (b) Side view.

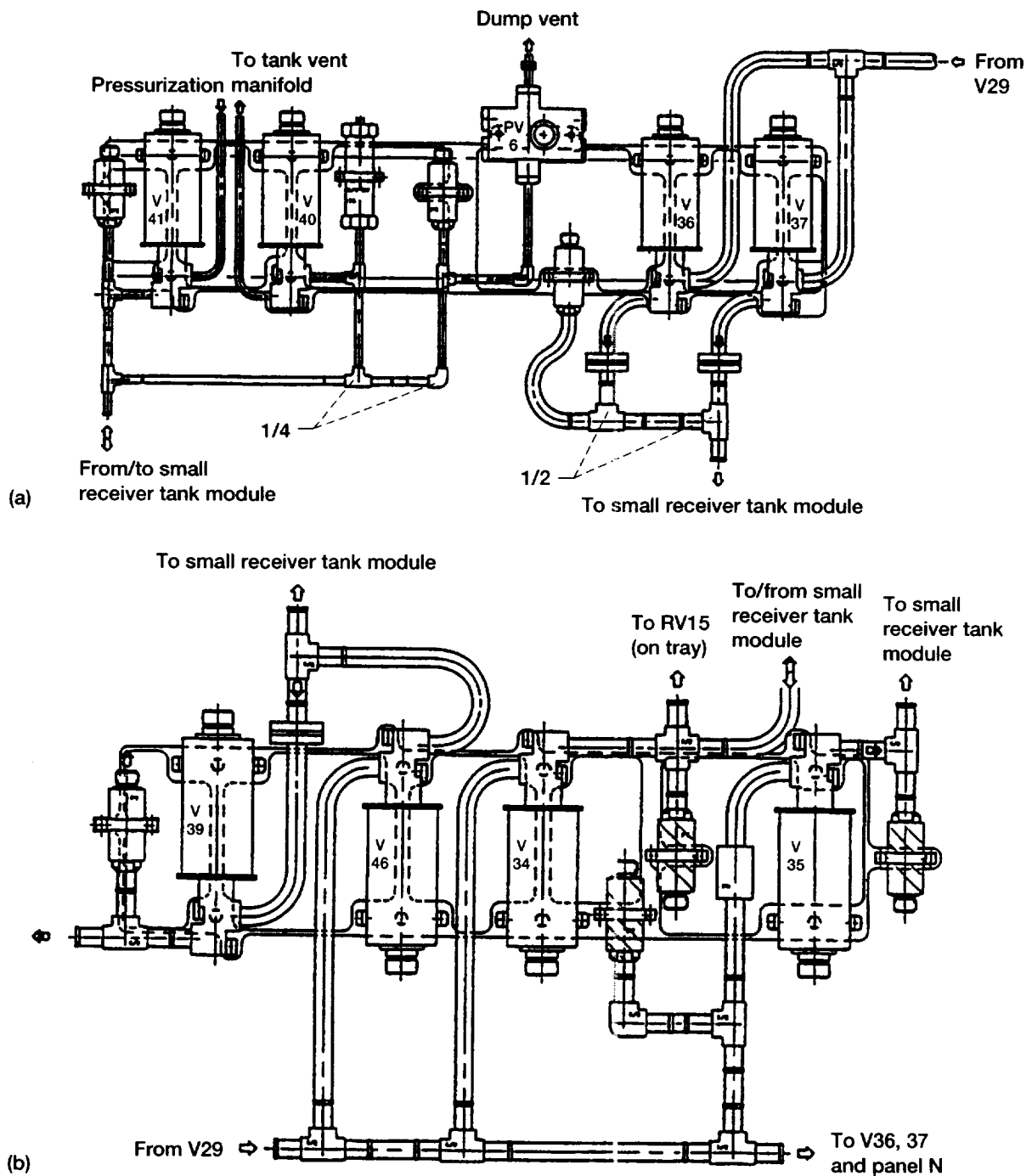


Figure D.38.—Small receiver tank valve panels. (a) Panel N (forward dome). (b) Panel M (aft dome).

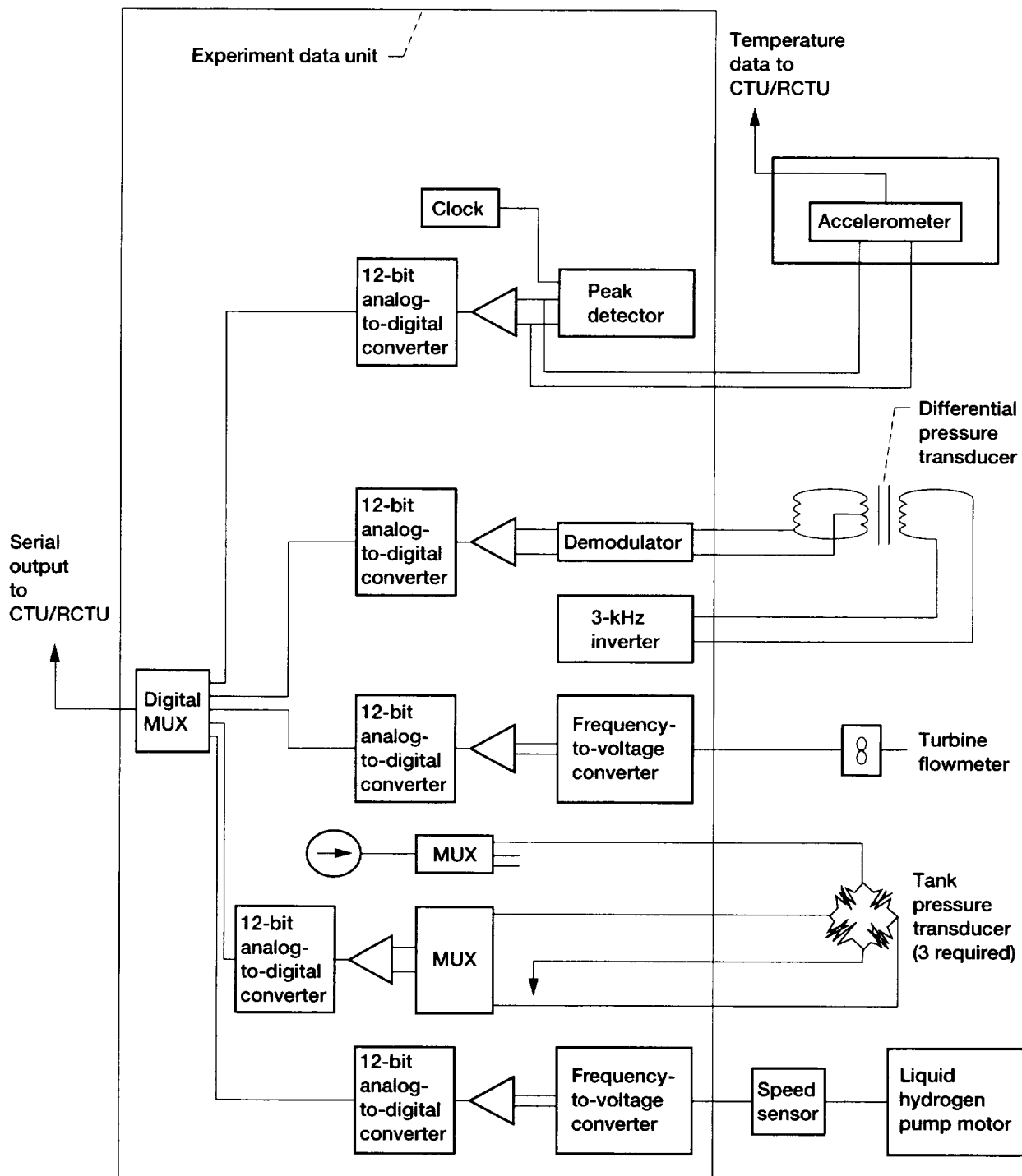


Figure D.39.—Experiment data unit block diagram.

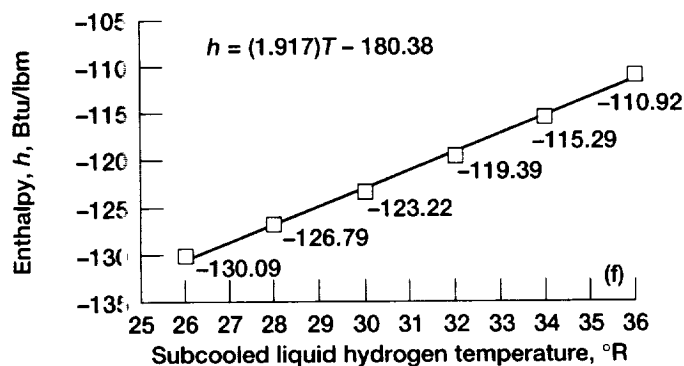
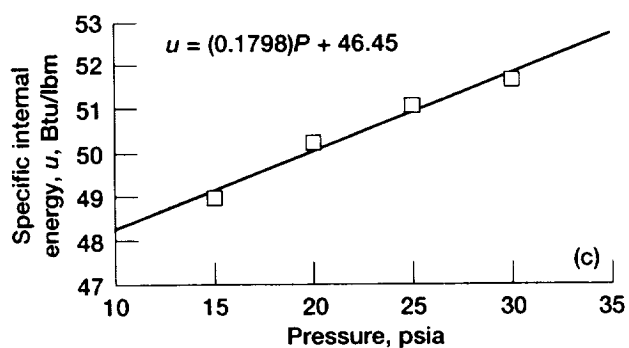
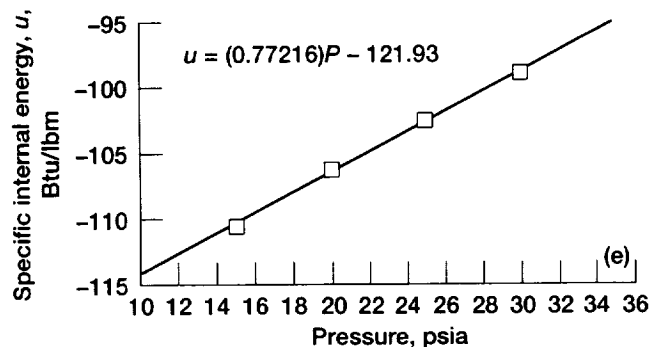
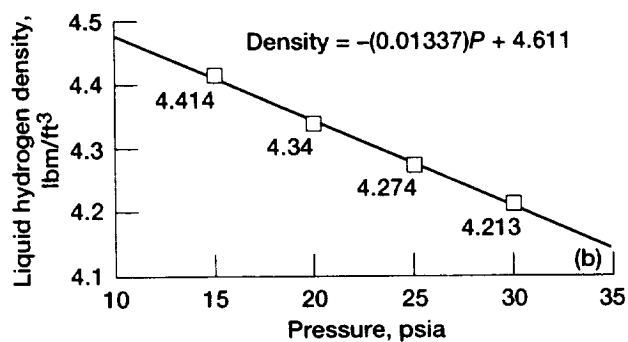
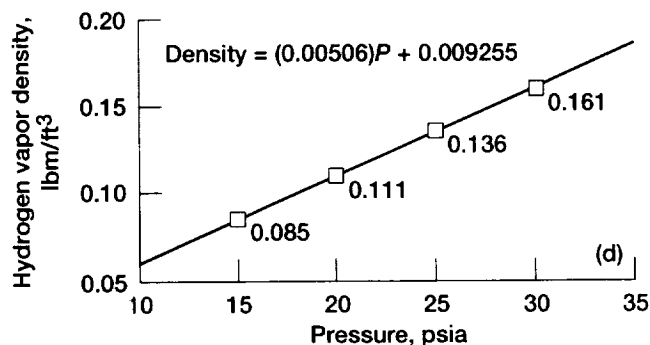
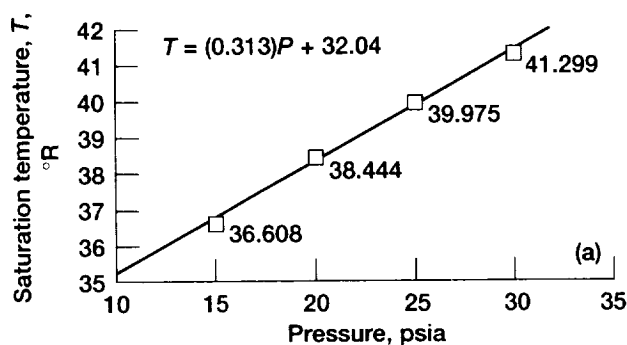


Figure D.40.—Thermodynamic properties of hydrogen. (a) Saturated liquid hydrogen temperature versus pressure. (b) Saturated liquid hydrogen density versus pressure. (c) Saturated hydrogen vapor internal energy versus pressure. (d) Saturated hydrogen vapor density versus pressure. (e) Saturated liquid hydrogen internal energy versus pressure. (f) Subcooled liquid hydrogen enthalpy versus temperature (pressure = 30 psia; saturation temperature = 41.3 °R).

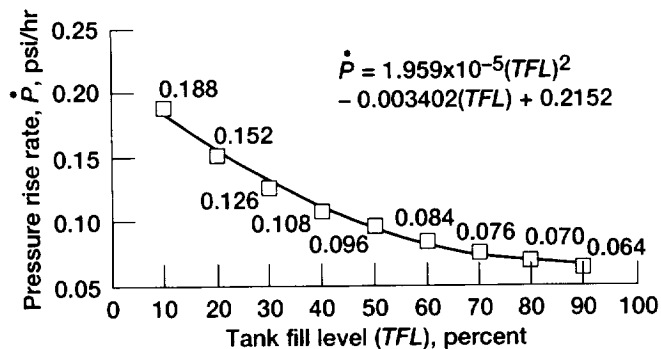


Figure D.41.—Supply tank pressure rise rate (2 x homogeneous model) 0.1 Btu/hr-ft².

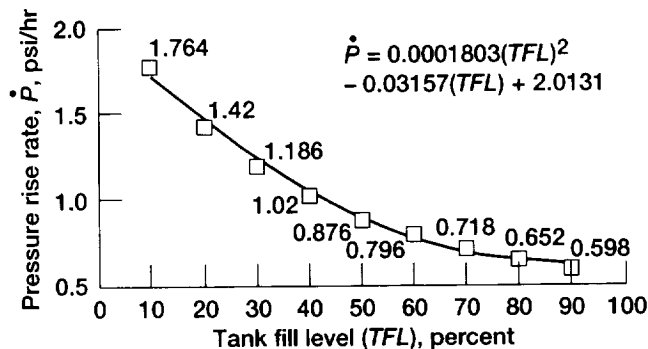


Figure D.44.—Large receiver tank pressure rise rate (2 x homogeneous model) 0.5 Btu/hr-ft².

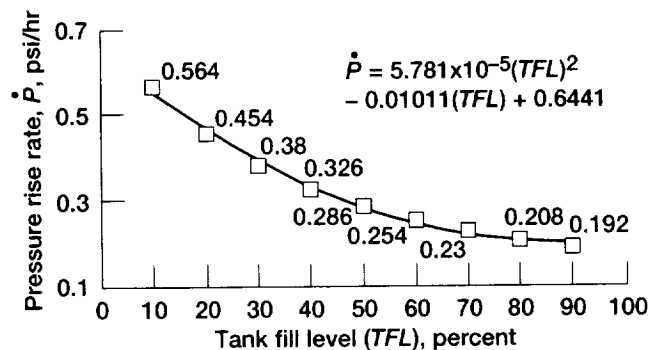


Figure D.42.—Supply tank pressure rise rate (2 x homogeneous model) 0.3 Btu/hr-ft².

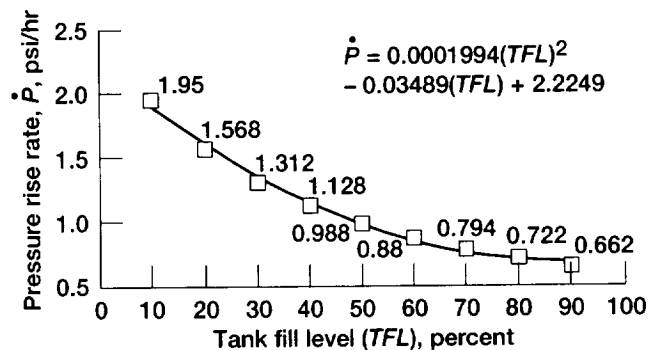


Figure D.45.—Small receiver tank pressure rise rate (2 x homogeneous model) 0.5 Btu/hr-ft².

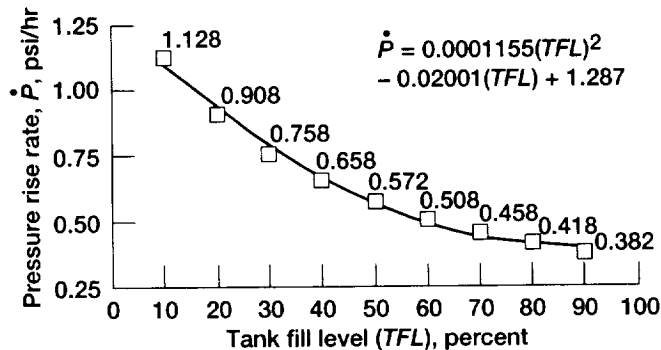


Figure D.43.—Supply tank pressure rise rate (2 x homogeneous model) 0.6 Btu/hr-ft².

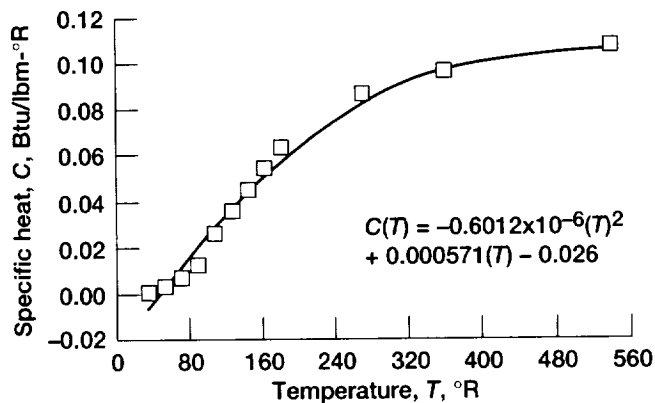


Figure D.46.—Specific heat of stainless steel.

Appendix E

Reference Tables

TABLE E.1—COLD-SAT EXPERIMENT SET

Test	Characteristics
Experiment 1—Low-gravity tank pressure control (class 1)	
1	Thermal stratification, low heat flux, 90 percent full
2	Mixing, low heat flux, 90 percent full
3	Passive TVS, low heat flux, 90 percent full
4	Mixing, low heat flux, 90 percent full
5	Active TVS, low heat input, 90 percent full
6	Thermal stratification, medium heat flux, 90 percent full
7	Mixing, medium heat flux, 90 percent full
8	Passive TVS, medium heat flux, 90 percent full
9	Mixing, medium heat flux, 90 percent full
10	Active TVS, medium heat input, 90 percent full
11	Thermal stratification, high heat flux, 90 percent full
12	Mixing, high heat flux, 90 percent full
13	Deleted (passive TVS, high heat flux, 90 percent full)
14	Active TVS, high heat input, 90 percent full
15	Thermal stratification, high heat flux, 65 percent full
16	Mixing, high heat flux, 65 percent full
17	Active TVS, low heat flux, 65 percent full
18	Passive TVS, low heat flux, 65 percent full
19	Mixing, low heat flux, 65 percent full
20	Active TVS, low heat input, 65 percent full
21	Thermal stratification, high heat flux, 50 percent full
22	Mixing, high heat flux, 50 percent full
23	Stratification, high heat flux, 50 percent full, low thrust
24	Mixing, high heat flux, 50 percent full, low thrust
25	Active TVS, high heat flux, 50 percent full, low thrust
26	Stratification, high heat flux, 50 percent full, high thrust
27	Mixing, high heat flux, 50 percent full, high thrust
28	Active TVS, low heat flux, 50 percent full, high thrust
29	Passive TVS, low heat flux, 50 percent full
30	Active TVS, low heat flux, 50 percent full
31	Deleted (passive TVS, low heat flux, 50 percent full)
32	TVS operation in large receiver tank
33	TVS operation in small receiver tank
34	Pressure rise in nearly empty tank
Experiment 2—No-vent fill and refill of cryogenic tanks in low gravity (class 1)	
1	No-vent fill of large receiver through axial spray
2	No-vent fill of large receiver through submerged spray
3	No-vent fill of small receiver through submerged spray
4	No-vent fill of small receiver through radial and tangential spray
5	No-vent refill of 70-percent full large receiver tank through submerged spray
6	No-vent fill of small receiver through radial spray
7	No-vent fill of large receiver through axial and tangential spray
8	Parametric fill of small receiver tank
9	Parametric fill of small receiver tank
10	Parametric refill of small receiver tank
11	Parametric refill of small receiver tank
12	Deleted (no-vent fill through LAD)

TABLE E.1.—Concluded.

Test	Characteristics
Experiment 3—Cryogenic tank chilldown in low gravity (class I)	
1	Tangential spray in small receiver tank
2	Radial spray in small receiver tank
3	Deleted
4	Combined spray in small receiver tank
5	Combined spray in small receiver tank
6	Combined spray in small receiver tank
7	Tangential then radial spray in small receiver tank
8	Deleted
9	Radial spray partial chilldown in low-g, small receiver tank
10	Radial spray partial chilldown in low-g, small receiver tank
11	Deleted
12	Deleted
13	Deleted
14	Axial jet in large receiver tank
15	Axial spray in large receiver tank
16	Deleted
17	Deleted
18	Large receiver heat exchanger chilldown
Experiment 4—Fill of liquid acquisition devices (LAD) in low gravity (class I)	
1	Collapse of vapor with TVS
Experiment 5—Mass gaging (deleted)	
Experiment 6—Slosh (deleted)	
Experiment 7—Tank thermal performance (deleted)	
Experiment 8—Pressurization of cryogenic tankage in a low-gravity environment	
1	Hydrogen pressurization, in microgravity, diffuser
2	Hydrogen pressurization, settled, diffuser
3	Hydrogen pressurization, in microgravity, pipe
4	Hydrogen pressurization, settled, pipe
5	Helium pressurization, in microgravity, diffuser
6	Helium pressurization, settled, diffuser
7	Helium pressurization, in microgravity, pipe
8	Helium pressurization, settled, pipe
Experiment 9—Direct liquid outflow and vented fill with low-gravity settling	
1	Vented fill of large receiver tank
2	Vented fill of small receiver tank, warm
3	Vented refill of large receiver tank, long pulse settling
4	Vented refill of large receiver tank, short pulse settling
5	Vented fill of small receiver tank, cold
Experiment 10—Liquid acquisition device performance in on-orbit environment	
1	Outflow through large receiver tank LAD
Experiment 11—Transfer line chilldown under low-gravity conditions (deleted)	
Experiment 12—Control of fluid thermodynamic state during liquid outflow	
1	Subcooler not active during fill
Experiment 13—On-orbit cryogenic fluid dumping	
1	Dumping of half-full small receiver tank
Experiment 14—Advanced instrumentation for in-space cryogenic systems (deleted)	
Experiment 15—Partial LAD (deleted)	

TABLE E.2.—EXPERIMENT REQUIREMENTS SUMMARY

Parameter	Characteristics
Pressure control requirements summary	
Supply tank characteristics	$L_c/D > 0.7$ (L_c = length of cylindrical section of tank (end caps excluded)) $D > 4$ ft (D = diameter of cylindrical section) Thermal performance < 0.1 Btu/hr-ft ² Uniform heat flux levels of 0.1, 0.3, 0.6 Btu/hr-ft ² for 5 psi rise Passive TVS capable of controlling 0.3 Btu/hr-ft ² Active TVS capable of controlling applied heat fluxes of 0.1, 0.3, and 0.6 Btu/hr-ft ² Mixer with 2 speeds, nozzle $\sim 1/20$ to $1/60$ tank diameter Tests at three fill levels: ~ 90 , 75, 50 percent No helium in system High-resolution temperature rakes near wall High-resolution pressure measurement Internal temperature and level sensors Heat exchanger temperatures Mixer flow rate, TVS flow rate
Receiver tank characteristics	Passive TVS with wall-mounted heat exchanger on at least one tank
Acceleration	Three acceleration levels between 10^{-6} and 10^{-4} g, one level may be "background" Minimize disturbances during applied accelerations
No-vent fill requirements summary	
Transfer	Subcooled liquid hydrogen, ~ 20 psia receiver tank pressure 50, 100, and 200 lb/hr flow rates
Receiver tanks	At least two different tanks with different length-diameter ratio (L/D) and shapes One cylindrical tank with $L/D \geq 1.6$, $L \geq 4$ ft 4 in. Tangential spray with 10 percent of maximum flow Axial spray, fluid settled over or away Diffused inlet One nearly spherical tank with $L/D = 0.8$ to 1.2, $D \geq 3$ ft Tangential spray with 10 percent of maximum flow Radial spray Axial spray Tank pressure, temperature throughout tank, inlet temperature and pressure, and fill level Target temperature of 140 °R
Acceleration	Bond number (Bo) > 4 during some fills
Chilldown requirements summary	
Transfer/vent	Flowrates of 50, 100, and 200 lbm/hr Vent to vacuum Controlled vent in 5 psi increments
Receiver tanks	At least two receiver tanks with different thermal mass/volume values Heat flux ≤ 0.5 Btu/hr-ft ² Axial, tangential spray systems in all receivers Radial spray in one tank Initial temperature ≥ 400 °R No LAD or obstructions near wall in one tank
Acceleration	Some chilldown at low-gravity
Liquid acquisition device (LAD) requirements summary	
Large receiver tank	Total communication LAD Measure residuals Channel temperatures, vapor sensors Channel cooling via passive TVS
Acceleration	$Bo \geq 4$ for some tests, others at background Liquid settled away from outlet
Transfer line	Two-phase flow detection

TABLE E.2.—Concluded.

Settled outflow/tank vented fill requirements summary	
Transfer	50, 100, and 150 lbm/hr
Small receiver tank	Baffled inlet/outlet Liquid settled away from vent cover inlet/outlet Tank pressure, internal and wall temperatures, level sensors, and tank vent liquid/vapor sensor
Acceleration	$2 \leq B_v \leq 10$
Transfer line	Two-phase flow detection
Thermodynamic state requirements summary	
Supply tank	Subcooler to provide 5 °R cooling at 50 lbm/hr flow rate, 2 °R at 100 lbm/hr Heat exchanger temperatures
Dumping requirements summary	
Small receiver tank	Direct vent to vacuum, (minimal restrictions) Initial fill level at least 50 percent Tank pressure, internal temperature and wall temperature measurements
Acceleration	Background
Advanced instrumentation requirements summary (deleted)	
Transfer line	Two-phase mass flowmeter

TABLE E.3.—EXPERIMENT SYSTEM FLUID COMPONENTS SUMMARY

Valve designation	Panel designation	Descriptive name (ST, supply tank; LRT, large receiver tank; SRT, small receiver tank)	Manufacturer/ part number	Relief pressure, psi	Current/time required	Coils	Redundancy cluster	Estimated cycles	Safe state
V1	F	ST – active TVS	Moog/-020	NA	5A/200 msec	1	B	<100	X ^a
V2	F	ST – active TVS (redundant)	Moog/-020			1	A	↓	
V3	E	ST – ground fill/drain/purge 1	Moog/-030			1	B		
V4	E	ST – ground fill/drain/purge 2	Moog/-030			1	A	↓	
V5	J	ST – pressurant control	Moog/-020			1	B	<500	
V6	Tray	ST – ground fill bypass	Moog/-020			2	E	<100	
V7	J	ST – LAD outlet transfer	Moog/-030			1	A	<500	
V8		ST – transfer line chilldown	Moog/-020			1	C	↓	
V9		ST – LAD outlet metered transfer	Moog/-030			1	B		
V10	↓	ST – TVS vent chilldown	Moog/-020			1	D	↓	
V11	H	ST – TVS (low flow)				1	A	<1000	
V12	H	ST – TVS (medium flow)				1	D	<1000	
V13	H	ST – TVS (high flow)				1	C	<1000	
V14	I	ST – bidirectional transfer (low flow)	Moog/-030			1	C	<500	
V15	I	ST – bidirectional transfer (medium flow)	Moog/-020			1	D	<500	
V16	I	ST – bidirectional transfer (high flow)	Moog/-020			1	D	<500	
V17	F	ST – return transfer	Moog/-020			1	D	<100	
V18	G	ST – tank vent 1	Moog/-030			1	G		
V19	G	ST – tank vent 2	Moog/-030			1	G		
V20	C	ST – vaporizer A liquid hydrogen supply	Moog/-020			2	F		
V21	B	ST – vaporizer B liquid hydrogen supply					L		
V22	B	ST – vaporizer B liquid hydrogen bypass					L		
V23	C	ST – vaporizer A liquid hydrogen bypass					F	↓	
V24	Tray	LRT – transfer	Moog/-030				E	<500	O ^a
V25	K	LRT – axial spray (top)					H	<100	X ^b
V26	L	LRT – LAD outlet transfer					↓	↓	
V27	K	LRT – axial spray (bottom)					↓	↓	
V28	K	LRT – tangential spray	Moog/-020				↓	↓	
V29	Tray	LRT – transfer bypass					K	<500	↓
V31	L	LRT – passive TVS vent					H	<500	O ^a
V32	L	LRT – pressurant control					H	<500	O ^a
V33	L	LRT – tank vent					H	<100	X ^b
V34	M	SRT – axial spray	Moog/-030				J	↓	
V35	M	SRT – radial spray	Moog/-030				↓	↓	
V36	N	SRT – tangential spray (low flow)	Moog/-020				↓	↓	
V37	N	SRT – tangential spray (high flow)					↓	↓	
V38	Tray	SRT – subsystem transfer chilldown bypass					M	<500	O ^a
V39	M	SRT – passive TVS					J	<500	O ^a
V40	N	SRT – tank vent					J	<100	X ^b
V41	N	SRT – pressurant control					J	<500	X ^b
V42	O	ST – subsystem TVS vent					K	<100	O ^a
V43	↓	ST – subsystem TVS vent (redundant)					E	↓	
V44		ST – subsystem primary vent					E		
V45	↓	ST – subsystem primary vent (redundant)					K	↓	
V46	M	SRT – low-gravity transfer	Moog/-030				J		X ^b
V47	Tray	ST – chilldown isolator	Moog/-020				K		X ^b
V48	Tray	ST – tank vent isolator	Moog/-020				H		O ^a
V49	Tray	ST – tank vent isolator (redundant)	Moog/-020				C		O ^a
V50	N	SRT – dump vent	Moog/-030	↓	↓	↓	D	↓	X ^b

^aO = open.^bX = closed.

TABLE E.3.—Concluded.

Valve designation	Panel designation	Descriptive name (ST: supply tank; LRT: large receiver tank; SRT: small receiver tank)	Manufacturer/ part number	Relief pressure, psi	Current/time required	Coils	Redundancy cluster	Estimated cycles	Safe state
CV1	B	ST – vaporizer B coil	Circle seal/K22OT	NA	NA	NA	NA	<500	NA
CV2	C	ST – vaporizer A coil	↓	↓	↓	↓	↓	↓	↓
CV3	Tank	LRT – passive TVS	↓	↓	↓	↓	↓	↓	↓
CV4	O	ST – subsystem TVS vent	↓	↓	↓	↓	↓	↓	↓
CV5	O	ST – subsystem TVS vent (redundant)	↓	↓	↓	↓	↓	↓	↓
GV1	B	ST – vaporizer B ground fill	Valcor/V27200	↓	2A/300 msec	2	E	<100	X ^b
GV2	B	ST – vaporizer B coil-to-bottle isolator	Ketema/548	↓	1A/15 min	1	L	<100	↓
GV3	B	ST – vaporizer B coil chilldown vent	Ketema/548	↓	1A/15 min	1	L	<100	↓
GV4	B	ST – vaporizer B pressurant supply	Valcor/V27200	↓	2A/300 msec	2	L	<1000	↓
GV5	C	ST – vaporizer A ground fill	Valcor/V27200	↓	2A/300 msec	2	E	<100	↓
GV6	C	ST – vaporizer A coil-to-bottle isolator	Ketema/548	↓	1A/15 min	1	F	<100	↓
GV7	C	ST – vaporizer A coil chilldown vent	Ketema/548	↓	1A/15 min	1	F	<100	↓
GV8	C	ST – vaporizer A pressurant supply	Valcor/V27200	↓	2A/300 msec	2	F	<1000	↓
GV9	D	ST – helium pressurant supply	↓	↓	↓	↓	K	<1000	↓
GV10	D	ST – helium pressurant supply (redundant)	↓	↓	↓	↓	K	<1000	↓
GV11	D	ST – helium ground fill	↓	↓	↓	↓	E	<100	↓
GV12	D	ST – pressurization (meter bypass)	↓	↓	↓	↓	D	<100	↓
R1	B	ST – vaporizer B pressurant control	Valcor/884000	↓	NA	NA	NA	<1000	NA
R2	C	ST – vaporizer A pressurant control	Valcor/884000	↓	↓	↓	↓	<1000	↓
R3	D	ST – helium pressurant supply	Valcor/884000	↓	↓	↓	↓	<1000	↓
RV1	E	ST – ground fill/bypass	Circle seal/K5120	100	↓	↓	↓	<100	↓
RV2	F	ST – return transfer	↓	52 ^c	↓	↓	↓	<100	↓
RV3	G	ST – tank ground vent	↓	52 ^c	↓	↓	↓	<500	↓
RV3	G	ST – tank ground vent (redundant)	↓	52 ^c	↓	↓	↓	<500	↓
RV5	B	ST – vaporizer B liquid hydrogen charge	↓	100	↓	↓	↓	<100	↓
RV6	B	ST – vaporizer B vessel	↓	2200	↓	↓	↓	<500	↓
RV7	B	ST – vaporizer B coil	↓	100	↓	↓	↓	<100	↓
RV8	C	ST – vaporizer A liquid hydrogen charge	↓	100	↓	↓	↓	<100	↓
RV9	C	ST – vaporizer A vessel	↓	2200	↓	↓	↓	<500	↓
RV10	C	ST – vaporizer A coil	↓	100	↓	↓	↓	<100	↓
RV11	Tray	LRT – transfer line	↓	↓	↓	↓	↓	↓	↓
RV12	Tray	LRT – transfer line/spray	↓	↓	↓	↓	↓	↓	↓
RV13	L	LRT – TVS vent	↓	↓	↓	↓	↓	↓	↓
RV14	L	LRT – tank vent	↓	46	↓	↓	↓	↓	↓
RV15	Tray	ST – transfer line	↓	100	↓	↓	↓	↓	↓
RV16	N	ST – tank vent	↓	46	↓	↓	↓	↓	↓
RV17	O	ST – subsystem TVS vent	↓	15	↓	↓	↓	<500	↓
RV18	O	ST – subsystem tank vents	↓	15	↓	↓	↓	<500	↓
RV19	B	ST – chilldown isolator	↓	100	↓	↓	↓	<100	↓

^b X = closed.^c Relief pressure in psia.

TABLE E.4.—PANEL COMPONENTS

Total components		Valve details		
Component name	Quantity	Valve designation	Description	Manufacturer/number
Valve panel E				
Pressure transducer	1	Valve 3	Supply tank-ground fill/drain/purge 1	Moog/-030
Temperature sensor	1	Valve 4	Supply tank-ground fill/drain/purge 2	Moog/-030
Valves	2			
Valve panel F				
Pressure transducer	1	Relief valve 2	Supply tank-return transfer	Circle Seal/K5120
Pump/mixers	2	Valve 1	Supply tank-active TVS	Moog/-020
Temperature sensors	2	Valve 2	Supply tank-active TVS (redundant)	Moog/-020
Relief valve	1	Valve 17	Supply tank-return transfer	Moog/-020
Valves	3			
Valve panel G				
Pressure transducers	3	Relief valve 3	Supply tank-tank ground vent	Circle seal/K5120
Temperature sensor	1	Relief valve 3	Supply tank-tank ground vent (redundant)	Circle seal/K5120
Relief valves	2	Valve 18	Supply tank-tank vent 1	Moog/-030
Valves	2	Valve 19	Supply tank-tank vent 2	Moog/-030
Valve panel H				
Pressure transducers	2	Valve 11	Supply tank-TVS (low flow)	Moog/-020
Visco jets	3	Valve 12	Supply tank-TVS (medium flow)	Moog/-020
Temperature sensors	3	Valve 13	Supply tank-TVS (high flow)	Moog/-020
Valves	3			
Valve panel I				
Venturis	3	Valve 14	Supply tank-bidirectional transfer (low flow)	Moog/-030
Differential pressure transducers	3	Valve 15	Supply tank-bidirectional transfer (medium flow)	Moog/-020
Pressure transducer	1	Valve 16	Supply tank-bidirectional transfer (high flow)	Moog/-020
Temperature sensors	2			
Valves	3			
Valve panel J				
Flow meter	1	Valve 5	Supply tank-pressurant control	Moog/-020
Pressure transducers	3	Valve 7	Supply tank-LAD outlet transfer	Moog/-030
Orifice	1	Valve 8	Supply tank-transfer line chilldown	Moog/-020
Temperature sensors	2	Valve 9	Supply tank-LAD outlet metered transfer	Moog/-030
Valves	5	Valve 10	Supply tank-TVS vent chilldown	Moog/-020

TABLE E.5.—RADIATOR TRAY PLUMBING COMPONENTS

Total components		Valve details		
Component name	Quantity	Valve designation	Description	Manufacturer/number
Pressure transducer	1	Relief valve 1	Supply tank—Ground fill/bypass	Circle seal/K5120
Temperature sensor	1	Relief valve 19	Supply tank—Chilldown isolator	Circle seal/K5120
Filter	1	Valve 6	Supply tank—Ground fill/bypass	Moog/-020
Orifice	1	Valve 47	Supply tank—Chilldown isolator	Moog/-020
Relief valves	2	Valve 48	Supply tank—Tank vent isolator	Moog/-020
Valves	4	Valve 49	Supply tank—Tank vent isolator (redundant)	Moog/-020

TABLE E.6—VALVE PANEL O COMPONENTS

Total components		Valves details		
Component name	Quantity	Valve designation	Description	Manufacturer/number
Pressure transducers	2	Check valve 4	Supply tank—Subsystem TVS vent	Circle Seal/K220T
Flowmeters	2	Check valve 5	Supply tank—Subsystem TVS vent (redundant)	Circle Seal/K220T
Balanced vents with strip heaters	2	Relief valve 17	Supply tank—Subsystem TVS vent	Circle Seal/K5120
Temperature sensors	2	Relief valve 18	Supply tank—Subsystem tank vent	Circle Seal/K5120
Check valves	2	Valve 42	Supply tank—Subsystem TVS vent	Moog/-020
Relief valves	2	Valve 43	Supply tank—Subsystem TVS vent (redundant)	↓
Valves	4	Valve 44	Supply tank—Subsystem primary vent	
		Valve 45	Supply tank—Subsystem primary vent (redundant)	

TABLE E.7.—VALVE PANEL B AND C COMPONENTS

Total components		Valve details		
Component	Quantity	Valve designation	Description	Manufacturer/number
Pressure transducers	3	-----	-----	-----
Filters	2	-----	-----	-----
Orifice	1	-----	-----	-----
Temperature sensors	2	-----	-----	-----
Check valves	2	Check valve 1	Supply tank—Vaporizer B coil	Circle SE
Gas valves	8	Check valve 2	Supply tank—Vaporizer A coil	Circle SE
		Gas valve 1	Supply tank—Vaporizer B ground fill	Valcor/V2
		Gas valve 2	Supply tank—Vaporizer B coil-to-bottle isolator	Ketema/54
		Gas valve 3	Supply tank—Vaporizer B coil chilldown vent	Ketema/54
		Gas valve 4	Supply tank—Vaporizer B pressurant supply	Valcor/V2
		Gas valve 5	Supply tank—Vaporizer A ground fill	Valcor/V2
		Gas valve 6	Supply tank—Vaporizer A coil-to-bottle isolator	Ketema/54
		Gas valve 7	Supply tank—Vaporizer A coil chilldown vent	Ketema/54
Regulators	2	Regulator 1	Supply tank—Vaporizer B pressurant control	Valcor/88
		Regulator 2	Supply tank—Vaporizer A pressurant control	Valcor/88
Relief valves	6	Relief valve 5	Supply tank—Vaporizer B liquid hydrogen charge	Circle SE
		Relief valve 6	Supply tank—Vaporizer B vessel	↓
		Relief valve 7	Supply tank—Vaporizer B coil	
		Relief valve 8	Supply tank—Vaporizer A liquid hydrogen charge	
		Relief valve 9	Supply tank—Vaporizer A vessel	
		Relief valve 10	Supply tank—Vaporizer A coil	
Cryogenic valves	4	Valve 20	Supply tank—Vaporizer A liquid hydrogen supply	Moog/-020
		Valve 21	Supply tank—Vaporizer B liquid hydrogen supply	Moog/-020
		Valve 22	Supply tank—Vaporizer B liquid hydrogen bypass	Moog/-020
		Valve 23	Supply tank—Vaporizer A liquid hydrogen bypass	Moog/-020

TABLE E.8.—COLD-SAT EXPERIMENT SUBSYSTEM MEASUREMENT REQUIREMENT SUMMARY

Measurement requirement	Measurement range	Candidate transducer	Measurement error	Resolution, bits	Sample frequency, Hz	Number requirement
High-accuracy fluid temperature	30 to 50 °R	Platinum resistance thermometer	$\leq \pm 0.2$ °R	8	0.1	90
Thermally bonded liquid hydrogen tank structure	30 to 50 °R	Platinum resistance thermometer	$\leq \pm 0.2$ °R	8	↓	49
Structure temperatures	36 to 540 °R	Platinum resistance thermometer	$\leq \pm 1.5$ °R	8		162
Hydrogen liquid/vapor level detection	Tank volume	Thermistor	± 1.0 percent	1		106
Two-phase flow detection	Liquid/vapor	Thermistor	NA	1		10
High-resolution tank pressures	0 to 50 psia	Strain gauge transducer	± 0.23 psia	12		9
Plumbing system pressures	2 to 5000 psia	Strain gauge transducer	± 1.0 percent	8		33
Liquid hydrogen transfer flow rates	50 to 200 lbm/hr	Venturi/ ΔP	± 2.0 percent	12		4
Mixer flow rate	960 to 4000 rpm	Mag speed sensor	TBD ^a	12		2
TVS flow rates	0.16 to 5.6 lbm/hr 0.21 lbm/hr 0.15 lbm/hr	Turbine Flow Meters	± 5.0 percent	12		2
Supply tank				12		1
Large receiver tank				12		1
Small receiver tank					↓	
Vent flow rates	5 to 50 lbm/hr	Sonic nozzle	± 5.0 percent	8	10	3
Acceleration	1 to 100 μg	HiRAP	TBD ^a	12	10	3
Valve status	open/close	Switch	NA	1	0.1	61

^aTo be determined.

TABLE E.9.—CONSUMABLE INVENTORY AND EXPERIMENT TIMELINE
[Representative segment for typical spreadsheet run. See section 5.7.2 for definitions of spreadsheet terms.]

A	B	C	D	E	F	G	H	I	J	K	L	M	N	O	P	Q
Item number	Time, week	Change in time, hr	Supply tank event	Experiment group number	Supply tank liquid hydrogen use, lb	Supply tank liquid hydrogen total, lb	Supply tank ullage, lb	Supply tank pressure, psia	Homogenous supply tank pressure, psia	Supply tank fill level, percent	Large tank event	Large tank liquid hydrogen use, lb	Large tank liquid hydrogen total, lb	Large tank ullage, lb	Large tank pressure, lb	Large tank fill level, percent
Typical pressure control experiment operation																
8	3.42	25.00	PC 6. Thermal stratification, medium heat flux, 90 percent full	2	-0.601	511.372	3.451	24.0	19.6	81.6	Empty	0.00	0.00	0.0000	0.0	0.0
9	3.43	3.00	PC 7. Mixing, medium heat flux, 90 percent full		0.573	511.945	2.878	19.9	19.9	81.8						
10	3.73	50.00	PC 8. Passive TVS, medium heat flux, 90 percent full		-4.00	507.945	3.208	21.5	19.8	81.2						
11	3.75	3.00	PC 9. Mixing, medium heat flux, 90 percent full		0.209	508.154	2.999	20.1	20.1	81.3						
12	3.78	4.50	PC 10. Active TVS, medium heat flux, 90 percent full		-12.88	495.274	2.713	15.1	15.1	78.0						
Typical tank chilldown and fill operation																
18	4.37	1.00	Transfer line chilldown	4A	-4.00	473.404	3.425	16.8	15.9	74.7	Empty	0.00	0.00	0.0000	0.0	0.0
19	4.42	8.00	Large receiver tank chilldown, experiment 3, test 14		-7.20	466.204	3.679	17.3	16.2	73.7	Large receiver tank chilldown, experiment 3, test 14	0.00	0.00	0.0000	0.0	0.0
20	4.43	2.00	No-vent fill, large receiver tank, experiment 2, test 1		-83.93	382.270	8.571	30.0	30.0	63.0	No-vent fill, large receiver tank, experiment 2, test 1	83.09	83.09	0.2004	21.5	91.9
21	4.43	1.00	Transfer line chilldown		-1.40	380.870	6.997	23.1	23.1	61.5	Operational large receiver tank thermal conditioning	-0.11	82.99	0.2038	21.9	91.9
22	4.44	1.00	Quiescent supply tank		-0.021	380.848	7.018	23.2	23.1	61.5	Hydrogenized pressurization, micro-g, diffuser-experiment 8, test 1	0.56	83.55	0.1724	30.0	94.9
23	4.45	1.00	Operational transfer, large receiver tank to supply tank		78.07	458.920	4.736	23.2	23.2	74.1	Operational transfer, large receiver tank to supply tank	-78.37	5.18	3.1706	30.0	5.9
24	4.46	2.00	Operational supply tank thermal conditioning		-11.20	447.720	4.160	17.9	17.9	71.1	Vent large receiver tank	-5.18	0.00	0.1936	0.0	0.0

TABLE E.9—Concluded.

TABLE E.9—Continued.														
R ¹	X	Y	Z	AA	AB ¹	AF ²	AJ ¹	AL	AM	AN	AO	AP	AQ	AR
Small tank event	Gaseous hydrogen tank 1 event	Gaseous hydrogen tank 1 use, lb	Gasous hydrogen tank 1 total, lb	Gaseous hydrogen tank 1 pressure, lb	Gaseous hydrogen tank 2 event	Gaseous helium tank event	Liquid hydrogen on-board total, lb	Time, week	Change in time, hr	COLD-SAT event	Hydrazine, tank use, lb	Hydrazine tank total, lb	Thrust level, lbf	Thrust duration, sec
Typical pressure control experiment operation														
Empty ↓	Quiescent vaporizer ↓	0.00 ↓	3.50 ↓	2000 ↓	Quiescent vaporizer ↓	Quiescent pressurant tank ↓	511.37	3.42	25.00	PC 6, thermal stratification, medium heat flux, 90 percent full	0.0	659.6	0.00	0.0
							511.95	3.43	3.00	PC 7, mixing, medium heat flux, 90 percent full	0.2	659.4	0.16	300.0
							507.95	3.73	50.00	PC 8, passive TVS, medium heat flux, 90 percent full	0.0	659.4	0.00	0.0
							508.15	3.75	3.00	PC 9, mixing, medium heat flux, 90 percent full	0.2	659.2	0.16	300.0
							495.27	3.78	4.50	PC 10, active TVS, medium heat flux, 90 percent full	0.0	659.2	0.00	0.0
Typical tank chilldown and fill operation														
Empty ↓	Quiescent vaporizer	0.00	3.50	2000	Quiescent vaporizer ↓	Quiescent pressurant tank ↓	473.40	4.37	1.00	Transfer line chilldown	0.0	659.0	0.00	0.00
	Quiescent vaporizer	0.00	3.50	2000			466.20	4.42	8.00	Large receiver tank chilldown, experiment 3, test 14	0.0	659.0	0.00	0.00
	No-vent fill, large receiver tank, experiment 2, test 1	-2.00	1.50	780			465.36	4.44	4.00	No-vent fill, large receiver tank, experiment 2, test 1	1.1	657.9	0.52	450.0
	Quiescent vaporizer	0.00	1.50	780			463.86	4.45	1.00	Transfer line chilldown	0.0	657.9	0.00	0.00
	Hydrogenized pressurization, micro-g, diffuser, experiment 8, test 1	-0.56	0.94	489			462.72	4.45	1.00	Hydrogenized pressurization, micro-g, diffuser, experiment 8, test 1	0.0	657.9	0.00	0.00
	Operational transfer, large receiver tank to supply tank	0.00	0.94	489			462.42	4.46	1.00	Operational transfer, large receiver tank to supply tank	1.1	656.8	0.52	450.0
	Quiescent vaporizer	0.00	0.94	489			446.04	4.47	2.00	Operational supply tank thermal conditioning	0.0	656.8	0.00	0.00

¹The following items, which would normally be included in a typical spreadsheet run, were not reproduced here in order to save space: small tank liquid hydrogen use (0.00 lb); T, Small tank liquid hydrogen total (0.00 lb); U, Small tank ullage (0.000 lb); V, Small tank pressure (0.00 psia); W, Small tank fill level (0.0 percent); AC, Gaseous hydrogen tank 2 use (0.00 lb); AD, Gaseous hydrogen tank 2 total (3.5 lbm); AE, Gaseous hydrogen tank 2 pressure (2000 psia); AG, Gaseous helium tank use (0.00 lb); AH, Gaseous helium tank total (10.58 lb); AI, Gaseous helium tank pressure (3000 psia).

TABLE E.10—SIMPLIFIED INVENTORY/TIMELINE

Item number	Time, week	Change in time, hr	Supply tank event	Large tank event	Small tank event	Liquid hydrogen on-board total, lb
1	0.00	0.00	Launch/orbit	Empty	Empty	576.04
2	2.00	336.00	Preparation/checkout			568.88
3	2.30	50.00	PC 1			565.33
4	2.45	25.00	PC 2			560.00
5	2.54	15.00	PC 3			553.60
6	3.00	78.00	Boiloff			551.94
7	3.14	24.00	Condition			517.73
8	3.29	24.00	PC 4			507.50
9	3.30	3.00	PC 5			506.22
10	3.45	24.00	PC 6			501.11
11	3.46	3.00	PC 7			500.47
12	4.00	90.00	Boiloff			498.55
13	4.14	24.00	PC 8			498.76
14	4.16	3.00	PC 9			498.55
15	4.17	0.75	Boiloff			498.53
16	4.17	0.25	Transfer line CD			494.54
17	4.17	1.00	CD 12 (LG)			487.32
18	4.19	2.46	Boiloff			487.26
19	4.20	1.54	VF 1 (LG)	VF 1 (LG)		486.48
20	4.25	9.00	Boiloff	Boil off		486.15
21	4.39	24.00	Condition			463.59
22	4.48	15.00	PC 13			456.96
23	4.57	15.00	PC 14			450.34
24	5.00	72.00	Boiloff			447.71
25	5.09	15.00	PC 15			441.08
26	5.23	24.00	Condition	PC 19		421.14
27	5.38	24.00	PC 16	Boil off		419.07
28	5.39	3.00	PC 17	Boil off		418.81
29	5.40	1.00	Boiloff	Boil off		418.77
30	5.54	24.00	Boiloff	Condition		410.08
31	5.55	0.75	Boiloff	Boil off		410.05
32	5.55	0.25	Transfer line CD	Boil off		406.05
33	5.55	1.00	Boiloff	Boil off		406.01
34	5.57	3.00	VRF 5a (SU)	VRF 5a (SU)		405.67
35	6.00	72.00	Boiloff	Boil off		403.03
36	6.14	24.00	Recondition			395.31
37	6.16	3.00	Boiloff			395.20
38	6.25	15.00	PC 10			388.58
39	6.39	24.00	PC 11			386.51
40	6.41	3.00	PC 12			386.25
41	6.43	3.00	Boiloff	Drup		381.05
42	6.57	24.00	Condition	Empty		371.86
43	7.00	72.00	Boiloff			370.33
44	7.00	0.25	Transfer line CD			366.33
45	7.01	1.00	CD 13 (LG)			359.11
46	7.01	0.75	Boiloff			359.09
47	7.02	1.54	NVF 18 (LG)	NVF 18 (LG)		358.31
48	7.03	1.46	Boiloff	Boil off		358.25
49	7.04	1.00	Boiloff			358.22
50	7.04	1.00	GH ₂ tank CD			348.18
51	7.05	1.00	Boiloff			348.14
52	7.05	1.00	GH ₂ tank VF			341.82
53	7.39	57.00	Boiloff			339.74
54	7.54	24.00	Condition	Condition		318.12
55	7.54	1.00	Boiloff	Boil off		318.08
56	7.54	0.25	Transfer line CD	Boil off		314.08
57	7.55	1.75	Boiloff	Boil off		314.02
58	7.57	3.00	VRF 5b (SU)	VRF 5b (SU)		313.67
59	8.00	72.00	Boiloff	Boil off		311.04
60	8.14	24.00	Recondition	Boil off		303.19
61	8.27	21.00	Boiloff	Drup		296.97
62	8.27	0.25	Transfer line CD	Empty		292.97
63	8.28	1.00	CD 14 (LG)	Empty		285.75

TABLE E.10.—Continued.

Item number	Time, week	Change in time, hr	Supply tank event	Large tank event	Small tank event	Liquid hydrogen on-board total, lb
64	8.29	1.75	Boiloff	Empty	Empty	285.71
65	8.29	1.54	NVF 16 (LG)	NVF 16 (LG)		284.93
66	8.40	17.46	Boiloff	Boiloff		284.29
67	8.54	24.00	Condition	Condition		266.06
68	8.55	1.00	Boiloff	Boiloff		266.02
69	8.55	0.25	Transfer line CD	Boiloff		262.02
70	8.55	0.75	Boiloff	Boiloff		261.99
71	8.57	3.00	VRF 5c (SU)	VRF 5c (SU)		261.65
72	9.00	72.00	Boiloff	Boiloff		259.01
73	9.14	24.00	Recondition	Boiloff		251.12
74	9.29	24.00	Boiloff	Dump		244.84
75	9.29	0.25	Transfer line CD	Empty		240.84
76	9.29	1.00	CD 15 (LG)	Empty		233.62
77	9.31	2.75	Boiloff	Empty		233.56
78	9.31	0.77	NVF 17 (LG)	NVF 17 (LG)		232.79
79	9.55	39.98	Boiloff	Boiloff		231.33
80	9.55	0.25				231.32
81	9.56	1.00				231.29
82	9.57	1.00				231.25
83	9.57	1.00				231.21
84	10.00	72.00				228.58
85	10.14	24.00		Condition		219.81
86	10.15	1.00		Boiloff		219.77
87	10.15	0.25		Transfer line CD		215.77
88	10.16	1.00		CD 1 (SM)		212.93
89	10.16	1.00		CD 2 (SM)		210.09
90	10.17	0.75		Boiloff		210.07
91	10.17	0.88		NVF 2 (SM)	NVF 2 (SM)	209.61
92	10.18	2.12		Boiloff	Boiloff	209.48
93	10.19	0.44		NVF 3 (SM)	NVF 3 (SM)	209.03
94	10.26	11.56		Boiloff	PC 18	208.08
95	10.40	24.00		Condition	Condition	199.40
96	10.41	1.75		Boiloff	Boiloff	199.26
97	10.41	0.25		Transfer line CD	Boiloff	195.25
98	10.42	1.00		VRF 2b (LG)	VRF 2b (LG)	194.90
99	10.42	0.75		Boiloff	Boiloff	194.84
100	10.56	24.00		Recondition	Boiloff	190.93
101	10.57	0.25		Transfer line CD	Boiloff	186.91
102	10.57	1.00		VRF 2a (LG)	VRF 2a (LG)	187.14
103	11.00	72.00		Boiloff	Boiloff	181.21
104	11.14	24.00	Condition	Recondition		171.46
105	11.14	0.08	Boiloff	Boiloff		171.45
106	11.14	0.25	Transfer line CD	Boiloff		167.44
107	11.15	0.08	Boiloff	Boiloff		167.43
108	11.15	0.47	NVRF 11 (LG)	NVRF 11 (LG)		167.12
109	11.15	0.28	Boiloff	Boiloff		167.10
110	11.29	24.00	PC 20	Recondition		161.90
111	11.29	0.13	Boiloff	Boiloff	Dump	159.26
112	11.29	0.25		Transfer line CD	Empty	155.25
113	11.30	1.00		CD 4 (SM)	Empty	152.42
114	11.30	0.08		Boiloff	Empty	152.41
115	11.30	0.44		NVF 7 (SM)	NVF 7 (SM)	151.97
116	11.30	0.06		Boiloff	Boiloff	151.97
117	11.45	24.00		Condition	Condition	143.20
118	11.45	0.13		Boiloff	Boiloff	143.19
119	11.45	0.25		Transfer line CD	Boiloff	139.19
120	11.45	0.08		Boiloff	Boiloff	139.18
121	11.46	1.00		VRF 3 (LG)	VRF 3 (LG)	138.86
122	11.46	0.13		Boiloff	Boiloff	138.86
123	11.46	0.25		Transfer line CD	Boiloff	134.85
124	11.46	0.08		Boiloff	Boiloff	134.84

TABLE E.10.—Concluded.

Item number	Time, week	Change in time, hr	Supply tank event	Large tank event	Small tank event	Liquid hydrogen on-board total, lb
125	11.46	0.22	Boiloff	NVRF 9 (SM)	NVRF 9 (SM)	134.55
126	11.46	0.16		Boiloff	Boiloff	134.54
127	11.60	24.00		Recondition	Recondition	131.16
128	11.60	0.17		Boiloff	Boiloff	131.15
129	11.61	0.25		Transfer line CD	Boiloff	127.14
130	11.61	0.17		Boiloff	Boiloff	127.13
131	11.61	1.00		VRF 2c (LG)	VRF 2c (LG)	126.81
132	12.00	65.00		Boiloff	Boiloff	122.94
133	12.14	24.00		Recondition	Boiloff	119.48
134	12.31	28.75		Boiloff	Dump	116.07
135	12.32	0.25		↓	Empty	116.06
136	12.32	1.00				116.03
137	12.33	1.00				115.99
138	12.33	0.22				115.98
139	12.42	14.78				115.44
140	12.56	24.00				114.56
141	12.56	0.25				114.56
142	12.56	0.25				114.55
143	12.57	0.50				114.53
144	12.57	1.00				114.49
145	13.00	72.00				111.86
146	13.14	24.00				110.98
147	13.14	0.25				110.97
148	13.15	0.25		Transfer line CD		106.97
149	13.15	1.00		CD 6 (SM)		104.13
150	13.15	0.25		Boiloff		104.12
151	13.16	0.44		NVF 13 (SM)	NVF 13 (SM)	103.68
152	13.16	0.06		Boiloff	Boiloff	103.68
153	13.30	24.00		Condition	Condition	97.45
154	13.30	0.25		Boiloff	Boiloff	97.44
155	13.30	0.25		Transfer line CD	Boiloff	93.43
156	13.30	0.25		Boiloff	Boiloff	93.41
157	13.31	1.00		VRF 4 (LG)	VRF 4 (LG)	93.10
158	13.31	0.25		Boiloff	Boiloff	93.08
159	13.45	24.00		Recondition	Condition	89.43
160	13.46	0.25		Boiloff	Boiloff	89.41
161	13.46	0.25		Transfer line CD	Boiloff	85.41
162	13.46	0.25		Boiloff	Boiloff	85.39
163	13.46	0.14		NVRF 10 (SM)	NVRF 10 (SM)	85.10
164	13.46	0.11		Boiloff	Boiloff	85.10
165	13.60	24.00		Condition	Recondition	81.68
166	13.60	0.25		Boiloff	Boiloff	81.66
167	13.61	0.25		Transfer line CD	Boiloff	77.65
168	13.61	0.25		Boiloff	Boiloff	77.64
169	13.61	1.00		VRF 2c (LG)	VRF 2c (LG)	77.32
170	14.00	65.00		Boiloff	Boiloff	73.45
171	14.14	24.00		Recondition	Boiloff	69.96
172	14.15	1.75		Boiloff	Dump 2	67.55
173	14.15	0.25		Transfer line CD	Empty	63.54
174	14.16	1.00		CD 7 (SM)		62.71
175	14.17	1.00		CD 9 (SM)		61.87
176	14.17	1.00		CD 10 (SM)		61.03
177	14.18	1.00		CD 12 (SM)		58.20
178	14.18	1.00		CD 5 (SM)		55.36
179	14.19	1.00		Dump		21.38
180	20.16	1003.18	↓	Empty	↓	0.00

References

1. Edwards, L.G.: (Analex Corp.) Cryogenic On-Orbit Liquid Depot Storage Acquisition and Transfer (COLD-SAT) Experiment Subsystem Instrumentation and Wire Harness Design Report. NASA CR-189172, 1992.
2. Sumner, I. E.: Liquid Propellant Reorientation in a Low-Gravity Environment. NASA TM-78969, 1978.
3. ASME Boiler and Pressure Vessel Code, Section VIII, Rules for Construction of Pressure Vessels, Division I. ANSI/ASME BPV-VIII-1. The American Society of Mechanical Engineers, New York, July 1980.
4. Flow of Fluids Through Valves, Fittings, and Pipe. Crane Co., Chicago, 1965.
5. White, F.M.: Fluid Mechanics. McGraw Hill, New York, 1979.
6. Aydelott, J.C.: Modeling of Space Vehicle Propellant Mixing—Cryogenic Propellants. NASA TP-2107, 1983.
7. Caine, G.H.; and Pradhan, A.V.: Pumps or Fans for Destratification of Hydrogen Liquid and Gas—Proceedings of the Advances in Cryogenic Engineering, vol. 13. Plenum Press, New York, 1968, pp 728-738.
8. Van Gundy, D.A.; and Uglam, J.R.: Heat Transfer to an Uninsulated Surface at 20 K. Advances in Cryogenic Engineering; vol. 7; K.D. Timmerhaus ed.; Plenum Press; New York, 1962. pp. 377-384.
9. Knoll, R.H.; MacNeil, P.N.; and England, J.E.: Design, Development, and Test of Shuttle/Centaur G-Prime Cryogenic Tankage Thermal Protection Systems. NASA TM-89825, 1987.
10. Eastern and Western Range ESMCR 127-1, Range Safety Requirements (U.S. Air Force 30th Space Wing and U.S. Air Force 45th Space Wing). Range Safety Office, Patrick Air Force Base, Florida, March 31, 1995.
11. Rohsenow, W.M.; and Hartnett, J.P.: Handbook of Heat Transfer. McGraw-Hill, New York, 1973.
12. Swann, R.T.; and Pittman, C.M.: Analysis of Effective Thermal Conductivities of Honeycomb-Core and Corrugated-Core Sandwich Panels. NASA TN D-714, 1961.
13. Keller, C.W.; Cunningham, G.R.; and Glassford, A.P.: Thermal Performance of Multilayer Insulation—Gas Evacuation in Characteristics of Three Selected Multilayer Insulation Composites. NASA CR-13477, 1974.
14. DeWitt, R.L.; and Mellner, M.B.: Experimental Evaluation of a Purged Substrate Multilayer Insulation System for Liquid Hydrogen Tankage. NASA TN D-6331, 1971.
15. Maloy, J.E.; and Sumner, I.E.: Transient Thermal Performance of Multilayer Insulation Systems During Simulated Ascent Pressure Decay. NASA TN D-6335, 1971.
16. Sumner, I.E.: Degradation of a Multilayer Insulation Due to a Seam and a Penetration. NASA TN D-8229, 1976.
17. U.S. Standard Atmosphere 5-77.
18. Rybak, S.C., et al. (Ball Aerospace Systems Group with McDonnell Douglas Space Systems Company and Boeing Aerospace and Electronics): Cryogenic On-Orbit Liquid Depot-Storage, Acquisition and Transfer (COLD-SAT) Satellite Feasibility Study. NASA CR-185248, August 1990.
19. Symons, E.P.: Outlet Baffles: Effect on Liquid Residuals From Zero-Gravity Draining of Hemispherically Ended Cylinders. NASA TM X-2631, 1972.
20. Shuttle/Centaur Functional Requirements Document SC1114-2. General Dynamics Convair Division.
21. MSFC Specification: Connector, Electrical, Circular, Cryogenic Environment Resisting, Drawing Number 40M38294, Marshall Space Flight Center, May 25, 1973.
22. McCarty, R.D.: Hydrogen Technology Survey: Thermophysical Properties. NASA SP-3089, 1975.
23. Aydelott, J.C.: Normal Gravity Self-Pressurization of 9-inch (23 cm) Diameter Spherical Liquid Hydrogen Tankage. NASA TN D-4171, 1967.
24. Cady, E.C.: Study of Thermodynamic Vent and Screen Baffle Integration for Orbital Storage and Transfer of Liquid Hydrogen. NASA CR-134482, 1973.
25. Chen, J.C.: Boiling Heat—Transfer Coefficients for Saturated Nonmetallic Fluids in Convective Flow. ASME 63-HT-34, 1963.
26. Dittus, F.W.; and Boelter, L.M.K.: Heat Transfer in Automotive Radiators of the Tubular Type. University of California Publications in Engineering, vol. 2, no. 13, 1930, pp 443-461.
27. Tegtart, J.; and Dominick, S.: Collapse of Large Vapor Bubbles. D.H. Lecroisette, ed. Proceedings of the Second International Colloquium on Drops and Bubbles. NASA CR-168848, 1982.

Chapter 6

Spacecraft Structure and Configuration

Kim Otten
Analex Corporation
Cleveland, Ohio

6.1 Introduction

This chapter addresses both the configuration and the structural system of the COLD-SAT spacecraft (see fig. 6.1). It also covers the mechanical and configurational interfaces and mass properties requirements which have significantly influenced the spacecraft design. The major challenge to the COLD-SAT design is fitting the required equipment into an available expendable launch vehicle (ELV) payload fairing while preserving an acceptable on-orbit configuration. The size and shape of the cryogenic tanks and their thermal control requirements are also a major constraint on the design of the structure. The spacecraft configuration and supporting structural system that have been developed meet the program, experiment, spacecraft, and launch vehicle requirements with more than adequate margins.

6.1.1 SPACECRAFT DESCRIPTION

COLD-SAT is 24.8 ft long (without payload adapter), 9.6 ft in diameter, and weighs 6615 lb. COLD-SAT is composed of five vertically stacked modules: two electronics bay modules, one supply tank module, and two receiver tank modules (see fig. 6.2). Starting aft and mating to the spacecraft adapter is electronics bay 1. This module houses the majority of the spacecraft electronics boxes as well as the propulsion system. The electronics bay itself is a 2-ft high octagonal framed structure that is 7 ft in diameter across a flat. Detachable honeycomb panels mounted across the flats of the structure are used for mounting electronics boxes. Inside the electronics bay are four 22-in. diameter hydrazine tanks. These tanks are supported on a honeycomb plate that spans the diameter of the bay and has cutouts to accommodate the tanks.

Forward of electronics bay 1 is COLD-SAT's largest module, the supply tank module. The supply tank module houses the liquid hydrogen supply tank and its associated pressurant bottles. The 145-ft³ supply tank is located on the spacecraft's longitudinal axis and four 30-in. pressurant bottles are located symmetrically in four quadrants immediately aft of the supply tank. The supply tank module also supports the spacecraft's deployable appendages, the high-gain antenna and the solar arrays. The stowed solar arrays are body-wrapped around the perimeter of the supply tank module and the antenna is located in a gap between the arrays (see fig. 6.3).

Forward of the supply tank module is electronics bay 2. This module is similar in configuration and construction to bay 1 but the two modules are different in detail. These differences pertain to the spacecraft structure within the module and the components enclosed by it.

Forward of electronics bay 2 are COLD-SAT's fourth and fifth modules, the large and small receiver tank modules. They house a 21- and a 13.5-ft³ receiver tank, respectively. Both tanks are located along the spacecraft's centerline and are supported by struts that extend to the spacecraft's enveloping structure.

6.1.2 CONFIGURATION DRIVERS

The objectives of the spacecraft configuration are derived from experiment, spacecraft, program, and expendable launch vehicle (ELV) requirements. The experiment requirements drove the number of experiment tanks, tank volumes, tank configurations, etc. The spacecraft requirements drove the size and location of the electronics bays; the location of the antennas; and the number, location, and weight of electronics boxes. Program requirements drove choice of hardware (flight

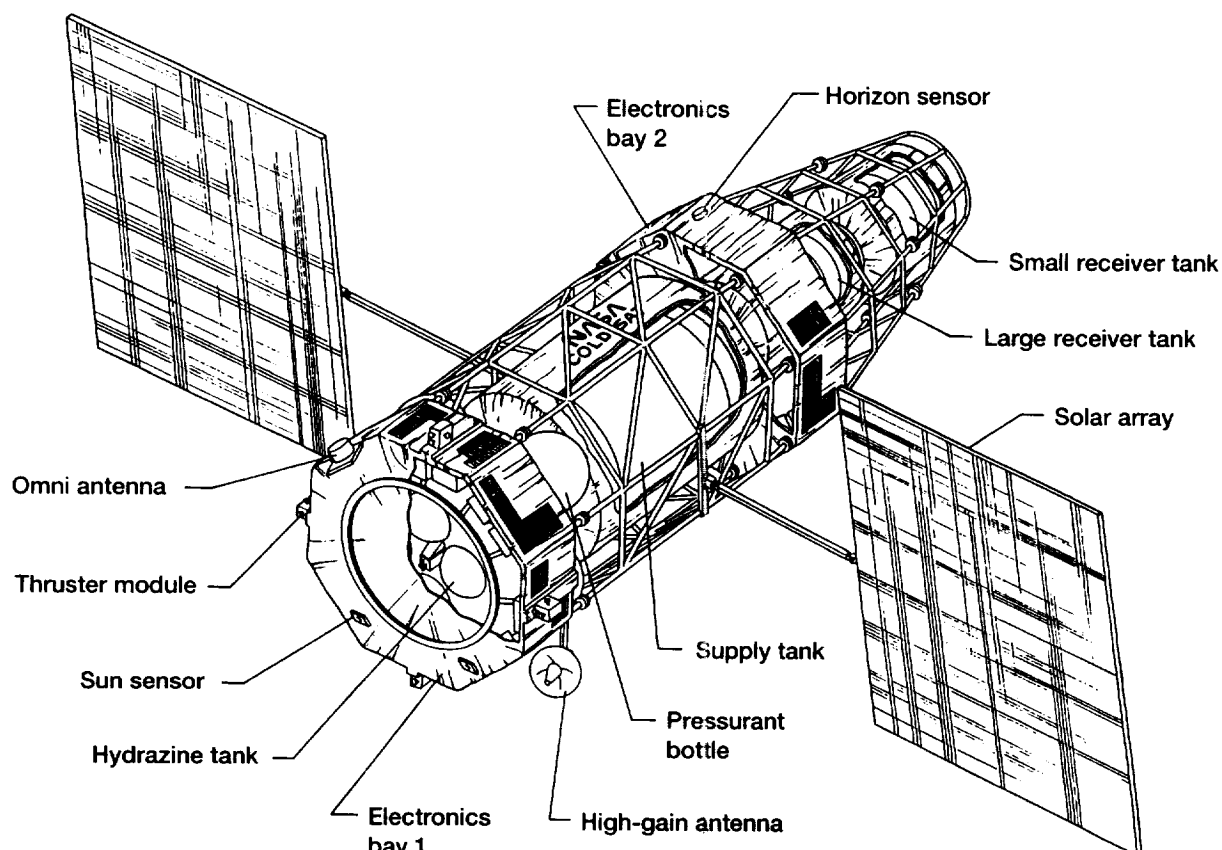


Figure 6.1.—COLD-SAT configuration and structural subsystem.

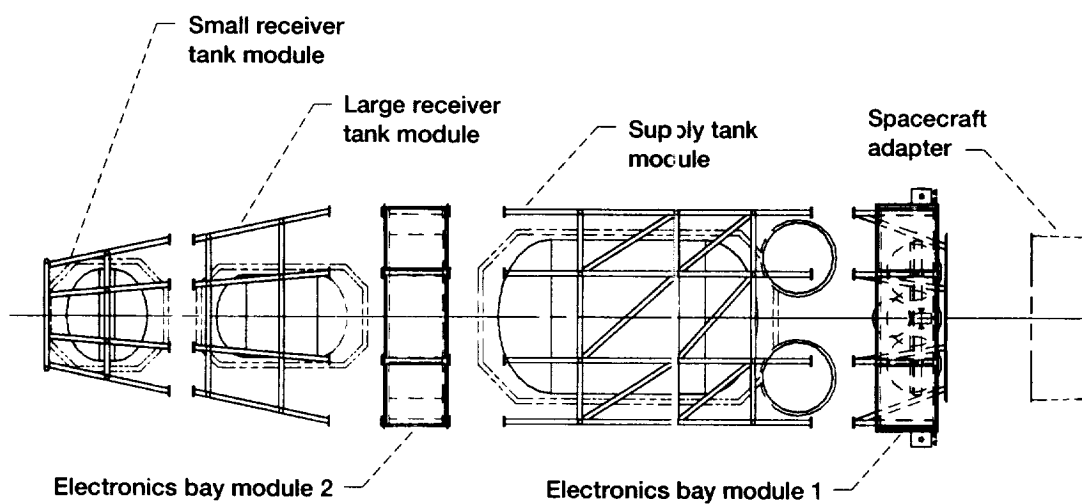


Figure 6.2.—COLD-SAT modular configuration.

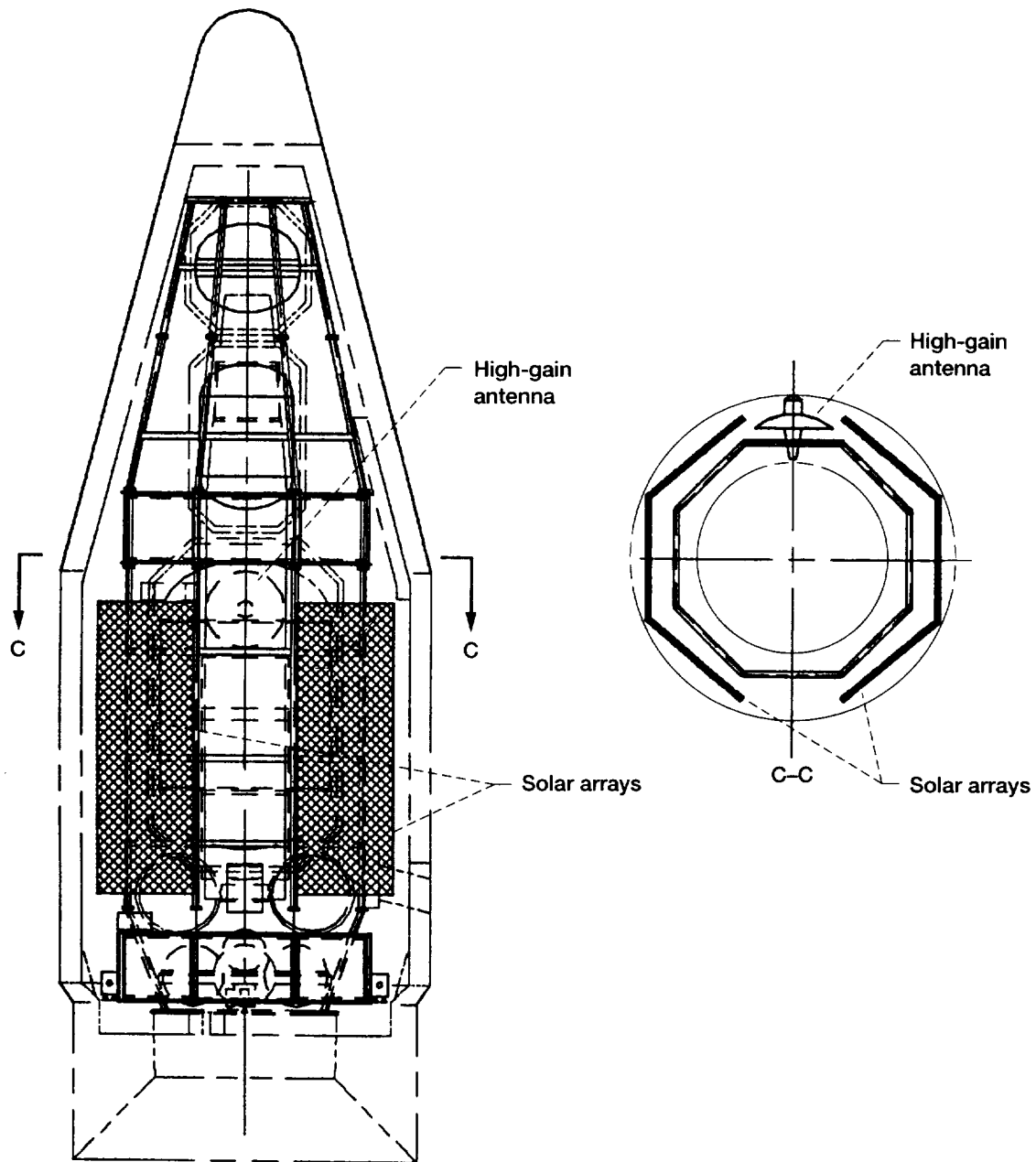


Figure 6.3.—Stowed arrays and high-gain antenna.

qualified), means of fabrication (low technology materials and standard manufacturing processes), means of assembly, margin for spacecraft growth (weight and mounting surfaces), etc. And finally, the ELV requirements drove the spacecraft configuration through the allowed payload fairing envelope, and the component distribution by launch vehicle weight and center of gravity restrictions.

6.1.3 MODULAR DESIGN

COLD-SAT's modular design was mandated by system design requirements. It caused certain complications in the configuration of the spacecraft but was deemed to benefit the overall system design. The benefits of a modular design include enhancement of the spacecraft's maintainability, accessibility, inspection, integration, assembly, and testing; and reduction in program cost and risk.

6.1.4 SPACECRAFT STRUCTURE

COLD-SAT's structure system uses a longeron-based external structure. This design is driven by thermal control requirements to keep the experiment tanks thermally isolated while having good view factors to deep space. The outside structure envelopes the tanks and provides long conduction paths between the experiment tanks and spacecraft structure, which thereby enhances the tank's thermal isolation. The longeron-based structure creates an open structure that permits view factors to deep space from the experiment tanks, which thereby capitalizes on the infinite heat sink of deep space and enhances the thermal performance of the tanks.

The structural system consists primarily of off-the-shelf aluminum hardware. Low technology manufacturing techniques and assembly practices are used to fabricate the design. The structural system design is conservative both in terms of safety factors and materials used.

6.1.5 DESIGN PROCESS OVERVIEW

COLD-SAT's design process started by developing a modest understanding of the experiment, program, spacecraft, and launch vehicle requirements. Based on this understanding, concepts for the various spacecraft systems were initially developed with an estimate of component characteristics (i.e., weight, volume, power consumption, quantity). Spacecraft configuration concepts were then generated from these system requirements. As the requirements were better defined and understood, changes and refinements were incorporated into the spacecraft's configuration, but not before careful investigation of the corresponding impacts on all spacecraft systems. Configuration changes were reviewed with the engineers for the various spacecraft systems and the lead project engineer prior to implementation.

The spacecraft design was a highly iterative process with a number of fundamentally different configurations and literally dozens of detailed layouts. Naturally, negotiations and compromises between the various spacecraft systems were common. Impasses were resolved by a committee of system engineers and the COLD-SAT project engineer. The committee resolved the disputes by determining what was in the best interest of COLD-SAT.

Initially, COLD-SAT configurations were developed for the Delta launch vehicle. However, because of configurational problems using available payload fairings and mass properties limitations, this configuration was eventually discarded and new configurations were developed for the Atlas I launch vehicle. This also occasioned major changes in the experiment hardware with one receiver tank being dropped and significant changes made in the volume- and weight-intensive gaseous hydrogen storage. It is this latter configuration, considerably changed in detail, which forms the basis of the COLD-SAT conceptual design.

6.2 Major Requirements

The major requirements which drove the selection of spacecraft configuration and the design of the structural system are found in this section. Additional details, in many instances, can be found in section, 6.3, Interfaces, of this report.

6.2.1 SOURCES OF REQUIREMENTS

Requirements that significantly impact COLD-SAT's configuration and structural system arise from the selection of launch vehicle, from various system level design decisions, from the individual spacecraft systems (especially the experiment system), and from general safety, ground handling, and qualification requirements. The specific requirements are delineated in the remainder of this section.

6.2.2 ATLAS I EXPENDABLE LAUNCH VEHICLE (ELV)

COLD-SAT requires an Atlas I or Atlas II launch vehicle with an 11-ft (medium) payload fairing. This launch vehicle is required largely because of its allowable payload volume, its performance, and its facilities for handling liquid hydrogen on the launch pad.

6.2.3 MODULARITY

COLD-SAT requires a modular spacecraft design. This was a system level design requirement. A modular design is required because it enhances spacecraft assembly, testing, integration, accessibility and maintainability, and because it minimizes program cost and risk.

This modular design needs to accommodate independent and/or parallel testing of the three major experiment tanks. As a result, the various spacecraft components must be grouped into modules to create functional units with straightforward interfaces. It specifically requires that virtually all mechanical and plumbing interfaces within the module be complete.

6.2.4 CONFIGURATION

There are several requirements that significantly impact COLD-SAT's configuration and they are identified below.

6.2.4.1 Center of Gravity (CG)

COLD-SAT is required to meet the launch vehicle's longitudinal CG restraint which is a function of the spacecraft weight. This requirement is imposed by the launch vehicle (see section, 6.3, Interfaces, of this report for additional details).

6.2.4.2 Lateral Center of Gravity (CG) Offset and Moments and Products of Inertia

COLD-SAT's lateral CG offset is required to be 0.5 in. or less from the spacecraft's axial centerline. This is a system-level requirement to minimize thrust vector misalignment torques and associated thruster compliance during thrusting. This requirement is well within the launch vehicle's lateral CG restriction.

COLD-SAT also requires the gravity gradient torques to be minimized. These are proportional to the difference in moment of inertia terms about the three axes and to the products of inertia which are influenced by the CG location. This requirement is imposed by the attitude control system.

6.2.4.3 Sensor View Factors

COLD-SAT requires two horizon sensors on opposite sides of the spacecraft along the spacecraft $\pm z$ -axis for attitude control (see fig. 6.4 for a definition of the spacecraft coordinate system). Each horizon sensor requires an unobstructed view of the Earth over a 90° cone angle.

COLD-SAT also requires two Sun sensors for spacecraft attitude determination. Each Sun sensor must be mounted on the spacecraft's aft end and have an unobstructed view of the Sun for a cone angle of 32° . The Sun sensor requires an angled mount to bisect the expected Sun angle (see fig. 7.19 in Chapter 7, Attitude Control System, of this report).

6.2.4.4 Solar Arrays

COLD-SAT requires two solar arrays with a total surface area of 190 ft^2 for power generation. The deployed arrays must be an adequate distance from the spacecraft to minimize the thermal radiation view factor of the arrays to the experiment system tanks, particularly the supply tank. The arrays must be located to minimize blockage of the high-gain antenna's

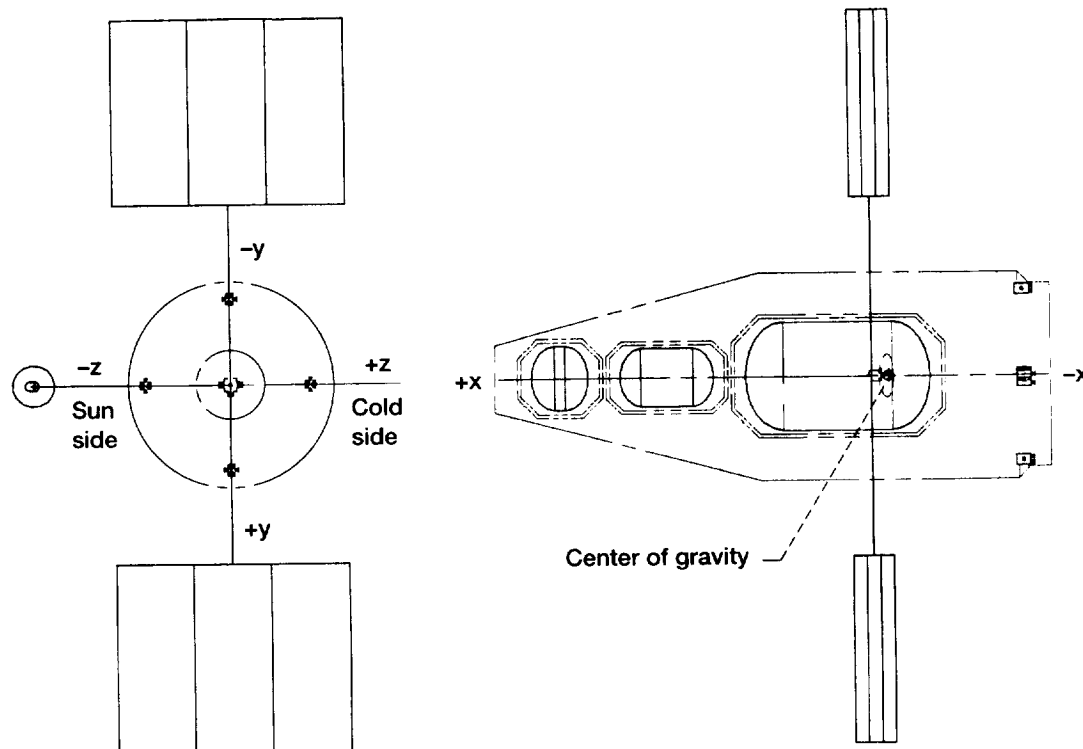


Figure 6.4.—Spacecraft coordinate system.

line-of-sight with the Tracking and Data Relay Satellite System (TDRSS). The arrays require canting with respect to the spacecraft long axis to provide more efficient use of the arrays (see Chapter 10, Electric Power System, of this report, for additional details).

6.2.4.5 Antennas

COLD-SAT requires a high-gain antenna for spacecraft communications. The antenna's final deployed position must be located on the spacecraft's $\pm z$ -axis such that blockage of the antenna's line-of-sight with TDRSS is minimized.

COLD-SAT also requires two low-gain, omnidirectional antennas for spacecraft communications. The low-gain antennas are used when the high-gain antenna is not deployed or is not functional. The antennas must be located in opposing positions where they collectively provide nearly continuous coverage irrespective of spacecraft attitude.

6.2.4.6 Experiment System Requirements

The COLD-SAT experiment system requires three cryogenic tanks having the dimensional requirements identified in table 6.1. The tanks must meet these minimum requirements, but are also to be adjusted to provide a balanced system with proper hydrogen consumption characteristics while meeting payload fairing volume restrictions and other spacecraft configuration requirements.

To minimize the heat leak to the cryogenic tanks, the tanks must be isolated from the warm portions of the spacecraft and provided with the maximum view factor to deep space. The tanks are to be located so that portions of the spacecraft can be used to shield the tanks from the Sun in the nominal attitude.

COLD-SAT also requires a pressurization system to facilitate fluid transfer between experiment tanks. Specifically COLD-SAT requires storage for 7.4 lb of gaseous helium and 3.7 lb of gaseous hydrogen pressurant. The pressurant system is required to be located immediately adjacent to the supply tank. The gaseous hydrogen supply is required to be located on the Sun side of the spacecraft and the gaseous helium supply is required on the anti-Sun side (see fig. 6.4 for definition of the Sun side). In addition, provisions must be made for the cryogenic and pressurant lines which interconnect the system.

TABLE 6.1.—EXPERIMENT TANK REQUIREMENTS

Experiment tank	Length-to-diameter ratio	Length or diameter requirement, ft
Supply	^a ≥ 0.7	$D > 4$
Large receiver	≥ 1.6	$L \geq 4$
Small receiver	0.8 to 1.2	$D \geq 3$

^aCylindrical portion.

6.2.4.7 Propulsion System Requirements

COLD-SAT requires 600 lb of hydrazine for spacecraft attitude control and experiment accelerations and 3.5 lbm of gaseous helium pressurant for hydrazine expulsion. The entire propulsion system requires thermal control and must be located in the same spacecraft module to permit system testing before final integration and to minimize weight and power consumption.

All hydrazine thrusters are to be located on the aft end of the spacecraft. They must be located so that their exhaust plumes do not contaminate any other component and render it nonfunctional (below specification) or obstruct the view of the Sun sensors. The control thrusters shall be located such that the lateral distance from the spacecraft centerline (moment arm) is maximized to produce the largest control torque for a given propellant utilization. Additional requirement details can be found in Chapter 8, Propulsion System, of this report.

6.2.4.8 Access

COLD-SAT requires access to spacecraft components during specific mission phases, namely, assembly/preflight and launch pad operations. The spacecraft access requirements are delineated below.

6.2.4.8.1 Assembly/Preflight.—During assembly and preflight, COLD-SAT requires access to electrical connectors for the power and the telemetry, tracking, and command system (TT&C), to the hydrazine panel for hydrazine fill/drain, to the gaseous helium and gaseous hydrogen fill/drain valves for supply tank pressurant, to the solar arrays for installation, to the attitude control components (sensors) for alignment, to the liquid hydrogen fill/drain/vent connections and for pyrotechnic installation.

6.2.4.8.2 Launch pad.—During launch pad operations, COLD-SAT requires access through the payload fairing to several spacecraft components. These components include the T-4 umbilical panel for fill and drain of liquid hydrogen; hydrazine fill and drain valves; electrical connections for the spacecraft batteries, for enabling the propulsion system, and for safing and arming the pyrotechnic devices; and the fill and drain valves for the vaporizer system and the pressurant supply.

6.2.4.9 Thermal Requirements

COLD-SAT requires that the heat leak to the experiment tanks be minimized to reduce liquid hydrogen boil-off. This requires the tanks to be thermally isolated from the spacecraft primary structure to the maximum extent possible and also requires that the view factors from the experiment tanks to deep space be maximized. The tanks must also be shielded to the maximum extent possible from the Sun and also from warmer portions of the spacecraft such as the electronics boxes and the solar arrays.

COLD-SAT requires the electronics boxes to be thermally conditioned on a volume basis rather than on an individual box basis to minimize the temperature control equipment, increase thermal control reliability, and minimize the power consumption. The boxes must be grouped appropriately to efficiently achieve this requirement.

6.2.5 STRUCTURAL SYSTEM

COLD-SAT's structural system is required to provide the mechanical interface with the launch vehicle, give mechanical support to all spacecraft systems, sustain launch loads, and provide precise alignment where needed, such as for antennas and attitude sensors. The structure shall also satisfy the minimum spacecraft frequency requirements defined by the launch vehicle.

6.2.5.1 Materials

Program requirements mandate that low technology aerospace materials and A-rated material properties be used to the maximum extent possible.

6.2.5.2 Assembly Methods

The structural system must be assembled by using standard methods such as welding and bolting.

6.2.5.3 Openness/View Factors

The structural system requires an open configuration that maximizes the view factor to deep space for the experiment tanks.

6.2.5.4 Factors of Safety

The structural system requires a feasible design with conservative factors of safety as identified in table 6.2. These safety factors are for feasibility and are not final program factors.

TABLE 6.2.—SAFETY FACTORS FOR FEASIBILITY

Article	Yield	Ultimate
Proof on FA ^a	1.6	2.0
TA ^b to ultimate	1.6	2.0

^aFA = flight article.

^bTA = test article.

6.2.6 TRANSPORTATION AND HANDLING

The structural system is required to accommodate the transportation loads for both truck and plane transportation.

6.3 Interfaces

This section describes the interfaces between the spacecraft configuration and structural system and those various entities that interact with them. Specific interfaces include those with: Atlas I launch vehicle, launch site, experiment system, electric power system, TT&C system, propulsion system, attitude control system, and transportation and handling.

6.3.1 ATLAS I LAUNCH VEHICLE

The interfaces with the Atlas I launch vehicle include the usable payload envelope inside the fairing, orientation and access while mounted at the launch pad, the launch vehicle/spacecraft adapter, spacecraft mass properties restraints, flight loads and environments, purge gas while on the launch pad, and liquid hydrogen loading and venting umbilicals. These interfaces are discussed below.

6.3.1.1 Payload Envelope

The payload fairing establishes the maximum allowable outside envelope for COLD-SAT's configuration. This envelope is commonly referred to as the usable static envelope and is established by accounting for the spacecraft dynamic deflections, the payload fairing static and dynamic deflections, the manufacturing tolerances, the out-of-round conditions, and misalignments. COLD-SAT surfaces are not permitted to protrude outside the usable static envelope without permission from the ELV contractor. Details of the usable static envelope are described in the Atlas Mission Planner's Guide (ref. 1), but are presented in figure 6.5 for reference.

It should be noted that the payload envelope is only valid when the spacecraft primary structure has fundamental frequencies in the axial and lateral directions above those specified in table 6.3.

TABLE 6.3.—MINIMUM SPACECRAFT
FREQUENCY REQUIREMENTS

Direction	Axial	Lateral
Frequency, Hz	10	15

6.3.1.2 Relative Orientation

COLD-SAT must be oriented on the launch pad so that its hardware is aligned appropriately relative to the payload fairing access doors and launch service tower. Items that require orientation on the pad include the liquid hydrogen fill/drain plumbing, electrical lines, propellant venting plumbing, payload fairing conditioned air/gaseous nitrogen line, battery connectors, hydrazine valve panel, and pyrotechnic control box.

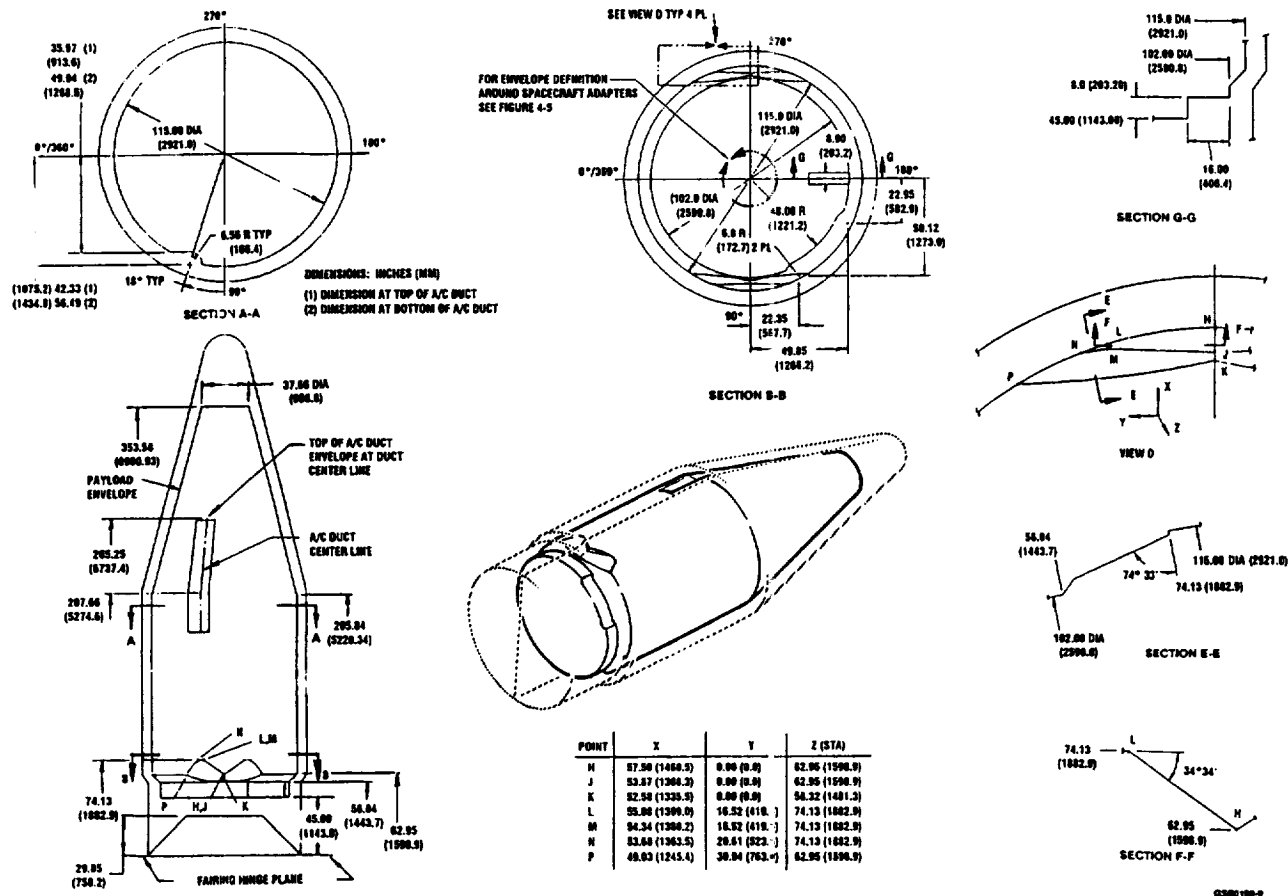


Figure 6.5.—Atlas launch vehicle payload fairing (ref. 1).

6.3.1.3 Fairing Access Doors

Fairing access doors are required because several COLD-SAT components require access capability after the spacecraft has been encapsulated in the payload fairing. COLD-SAT requires four mission-peculiar doors. These doors are described in table 6.4 and their relative orientation is shown in figure 6.6.

A chute is required for guiding the T-4 umbilical disconnect safely away from the spacecraft to outside the payload fairing after disconnect separation (four seconds prior to lift-off). The chute extends from the spacecraft's T-4 umbilical panel to the payload fairing's T-4 umbilical access door. COLD-SAT's chute is based on an existing chute used in the Centaur program and is shown in figure 6.7. The T-4 umbilical panel access door is spring-loaded so that it shuts automatically after the umbilical is pulled.

6.3.1.4 Spacecraft Adapter

COLD-SAT interfaces directly to the launch vehicle via the spacecraft adapter. The spacecraft adapter provides the hardware interface between the spacecraft and launch vehicle.

COLD-SAT's adapter requires the standard interfaces including a basic attaching with its securing provisions, two spacecraft rise-off electrical disconnects, and separation springs. The rise-off disconnects provide a spacecraft-dedicated umbilical interface between the spacecraft, ground support equipment, and the ELV. A typical adapter and interfaces are shown in figure 6.8. A vee-band clamp provides the latching interface between the spacecraft and adapter and is shown in figure 6.9.

6.3.1.5 Mass Properties

The Atlas launch vehicle places certain restraints on the COLD-SAT mass properties. The available launch vehicle performance restricts the overall mass of the spacecraft. In addition, launch vehicle structural and control limitations restrict the vertical location of the spacecraft center of mass and its deviation from the axial centerline. Spacecraft attitude control requirements limit the motion of the center of mass.

6.3.1.5.1 Launch weight.—The allowable spacecraft launch weight is dictated by the launch vehicle performance and the spacecraft orbit requirements. COLD-SAT requires a 550-n mi altitude orbit with a 18° inclination. Figure 6.10 shows the Atlas I performance for nearly circular orbits. This figure is

TABLE 6.4.—FAIRING ACCESS DOORS

Description	Door size required, in. ^a	Function	Size
T - 4 umbilical	12 by 12	Fill and drain	< Standard
Hydrazine	24 by 24	Drain	< Maximum
Electrical connections	24 by 24	Batteries and pyro's	< Maximum
Vaporizer	24 by 32	Fill and purge	= Maximum

^aMeasurement = width × height. Standard size access door: 18.4- by 15.6-in.

Maximum size access door: 24.4- by 32.2-in.

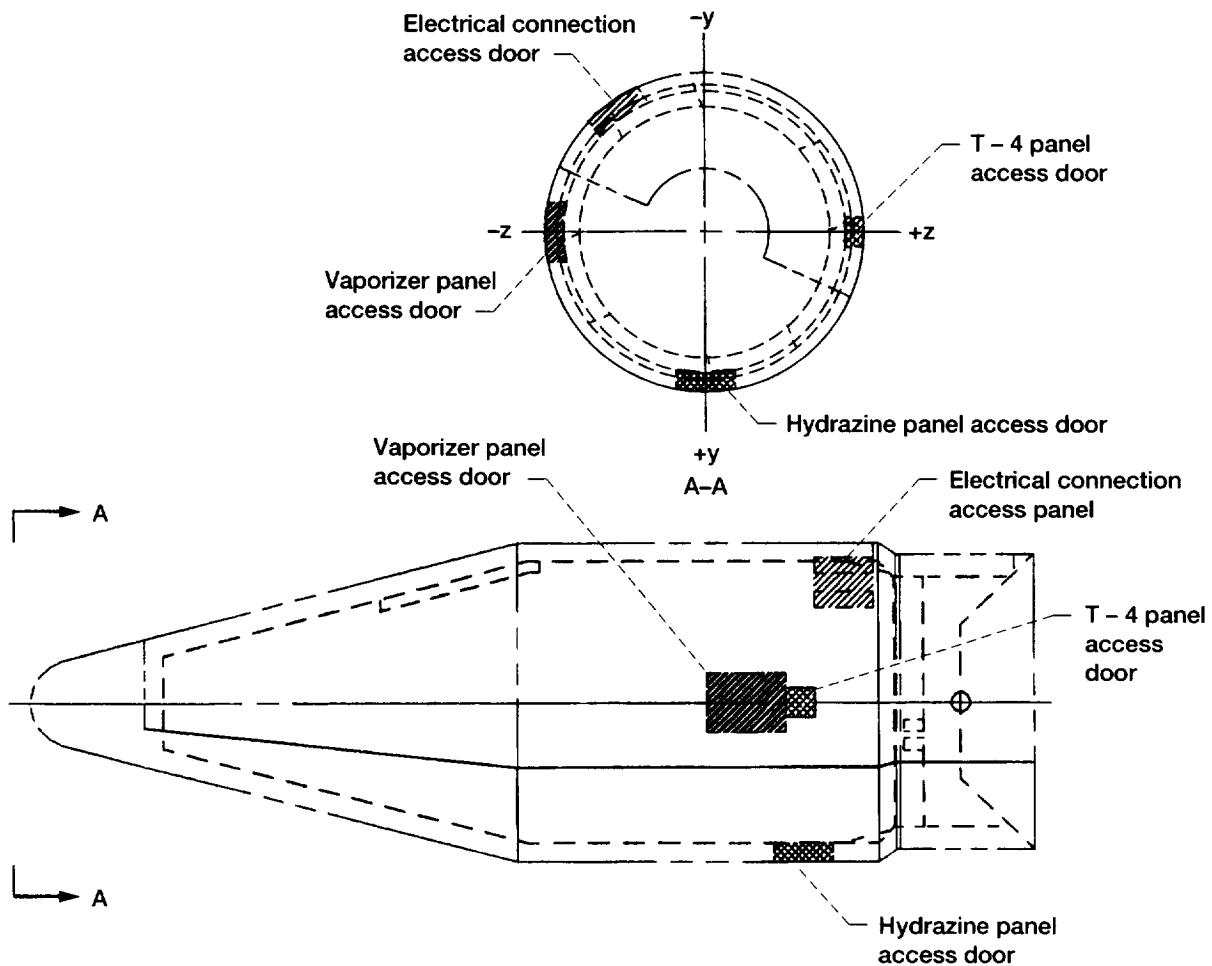


Figure 6.6.—Fairing access doors.

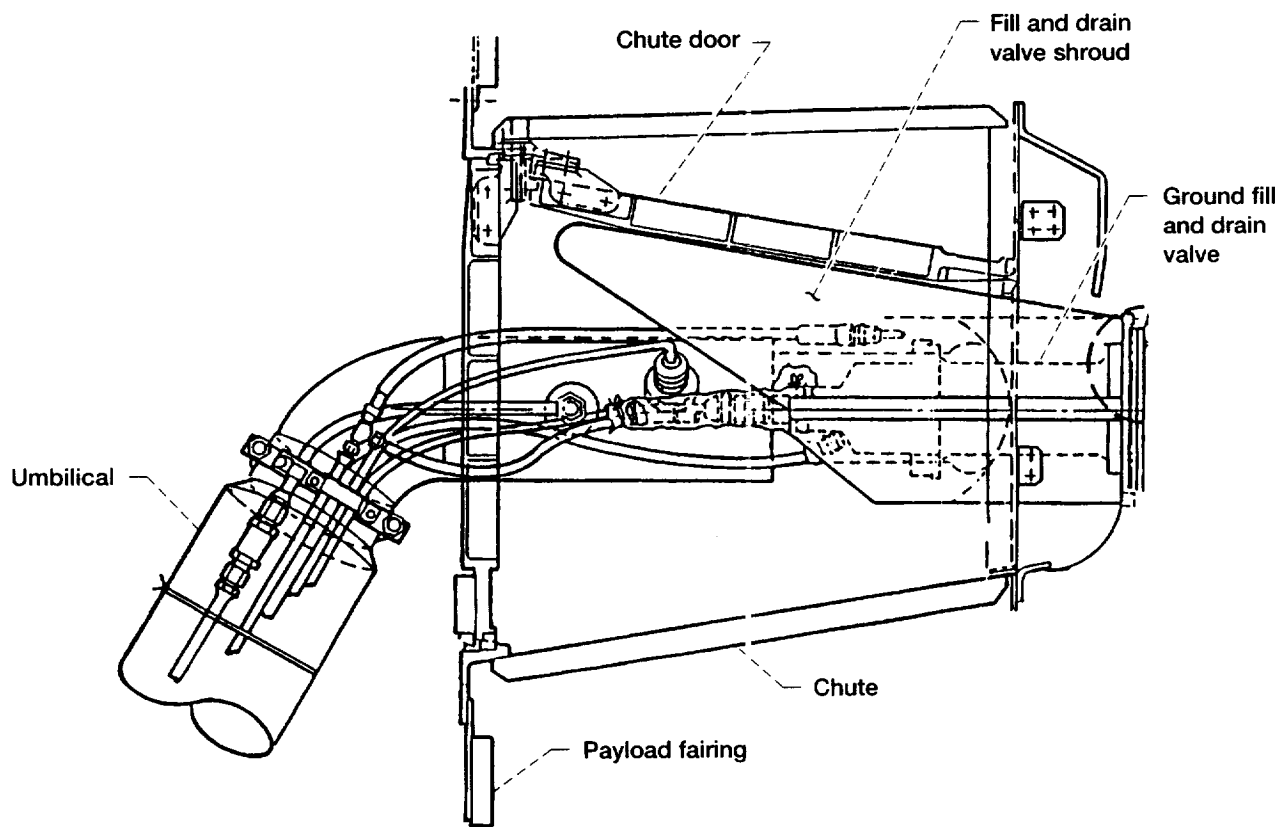


Figure 6.7.—T - 4 umbilical chute.

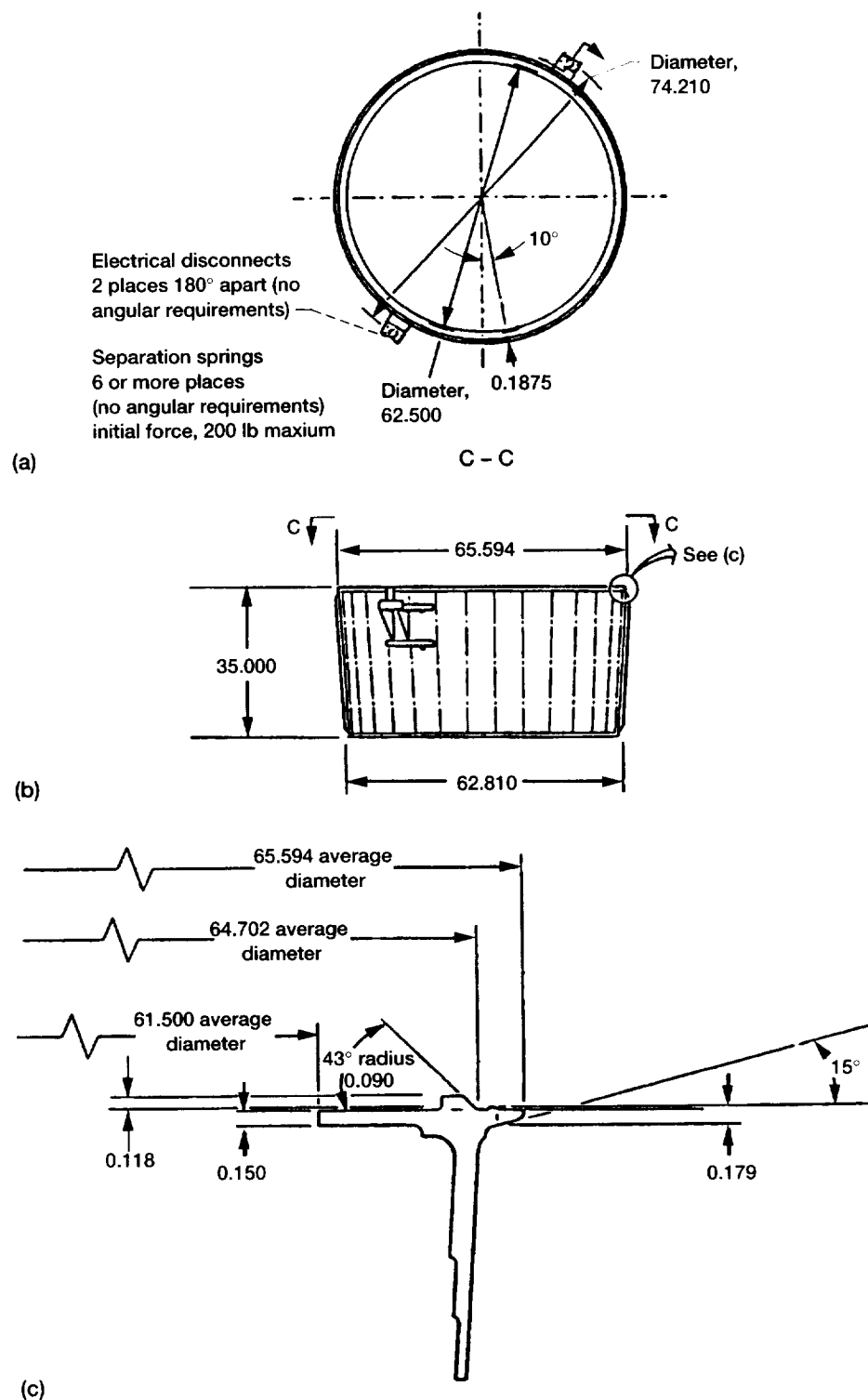


Figure 6.8.—Typical spacecraft adaptor. Dimensions are in inches. (a) Top view.
(b) Side view. (c) Spacecraft mounting surface.

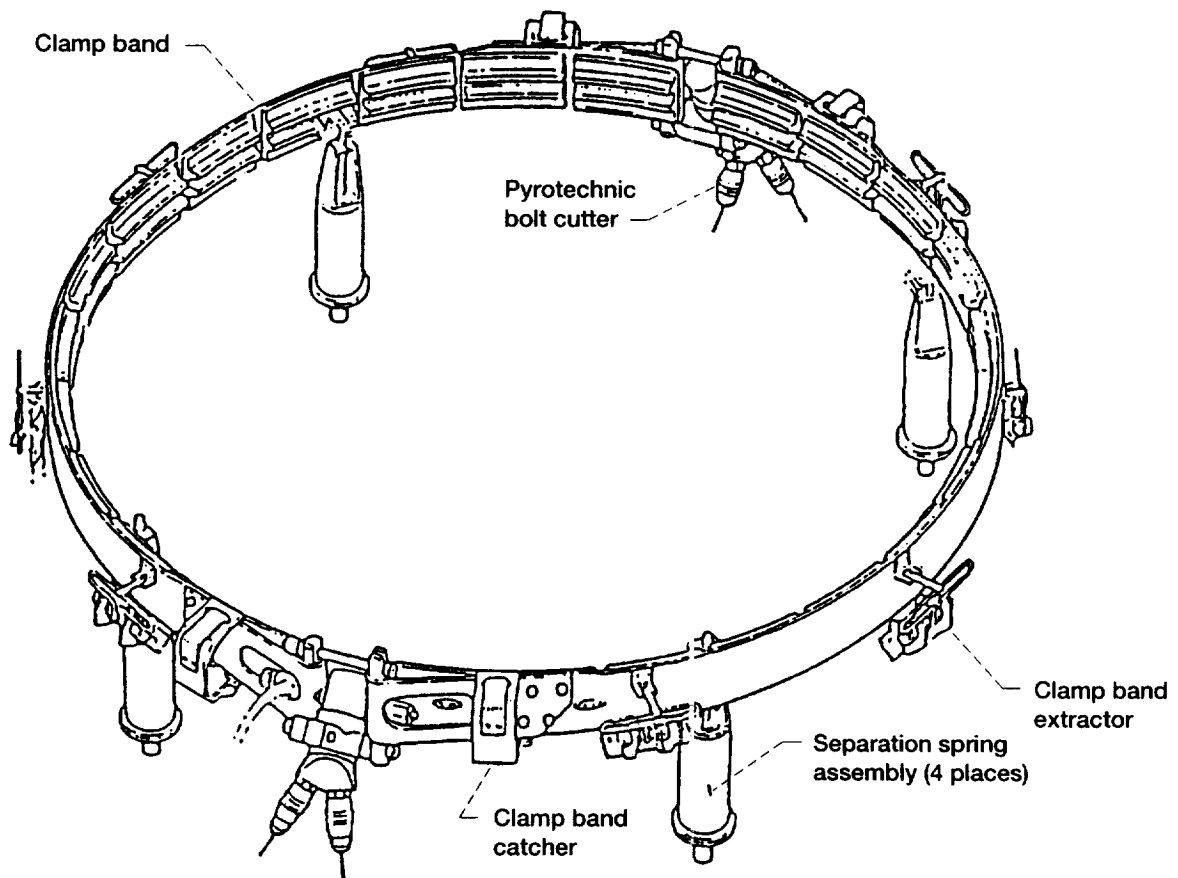


Figure 6.9.—Typical vee-band clamp separation system.

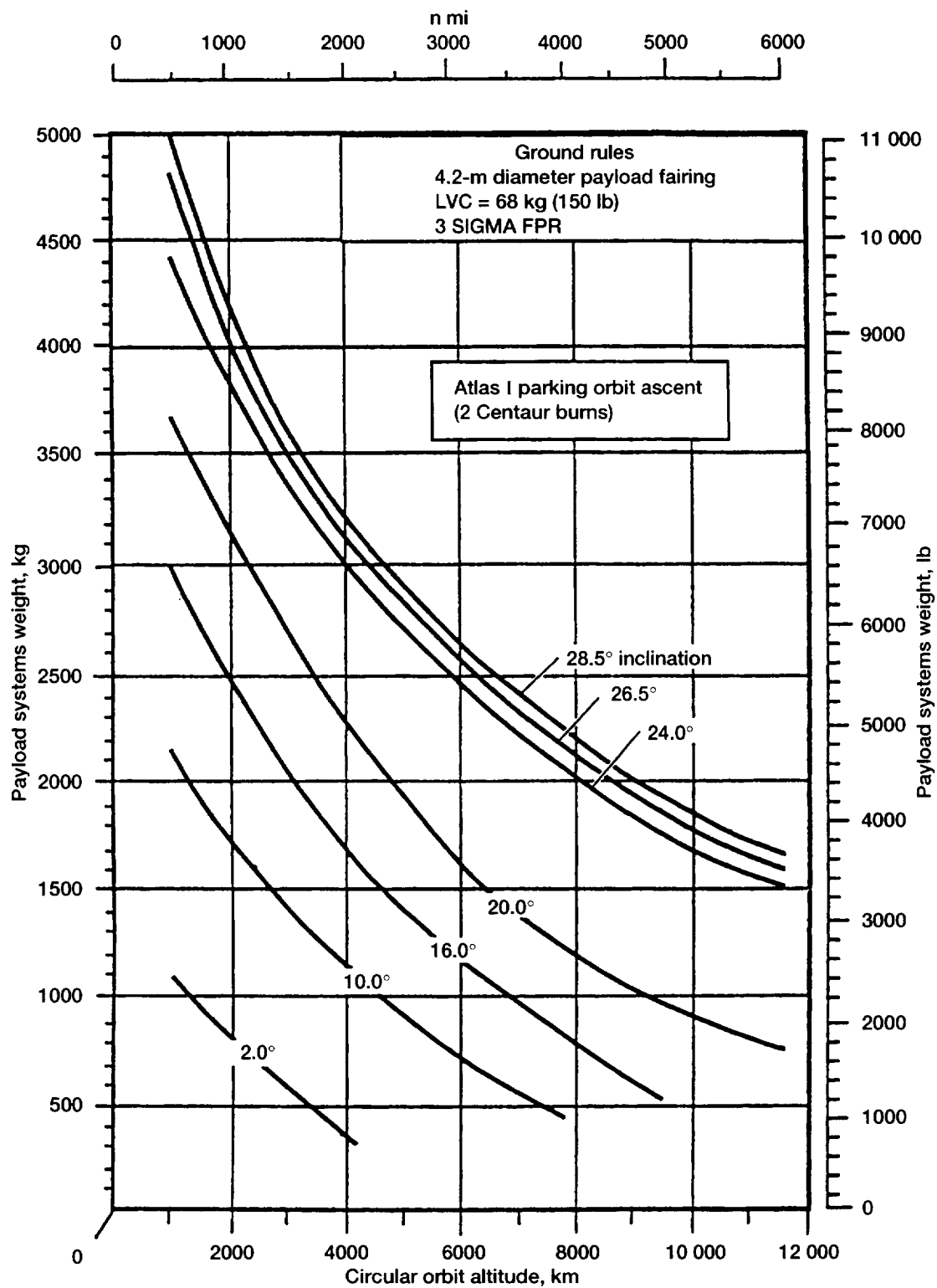


Figure 6.10.—Atlas launch vehicle capability (ref. 1).

reproduced from the Atlas Mission Planner's Guide (ref. 1) and is used to guide the preliminary design. A more refined analysis of launch vehicle capabilities can be found in Chapter 13, Launch Vehicle, Launch, and Ascent Operations, of this report.

6.3.1.5.2 Center of gravity (CG).—The spacecraft's longitudinal CG restraint is dictated by launch vehicle strength and spacecraft weight. The limiting hardware within the launch vehicle is the Centaur equipment module (since the spacecraft adapter is mission unique). This limitation is shown in figure 6.11.

6.3.1.5.3 Balance.—The balance requirements reflect COLD-SAT's allowable CG offset in the lateral direction. CG offset is the radial distance from the spacecraft's longitudinal axis to the spacecraft's center of gravity. The COLD-SAT balance requirement is 0.5 in. which is more stringent than the launch vehicle requirement of a couple of inches. This requirement is dictated by the spacecraft attitude control system.

6.3.1.6 Launch Loads

During the launch and ascent portion of the flight, the spacecraft structural system and other spacecraft hardware are subjected to a variety of loads and environments. These loads and environments are described by quasi-static and dynamic load factors, acoustic loads, random vibrations, and separation shock. The requirements are given below.

6.3.1.6.1 Load factors.—Quasi-static and dynamic loads interact with the spacecraft's structural system during various phases of launch and ascent. Load factors, developed by the ELV manufacturer, represent the acceleration load environment during powered flight and are to be used for the preliminary design of primary structure. The load factors provide a conservative design envelope for a typical spacecraft when its first lateral mode of vibration is above 10 Hz and the first axial mode of vibration is above 15 Hz. Table 6.5 illustrates the

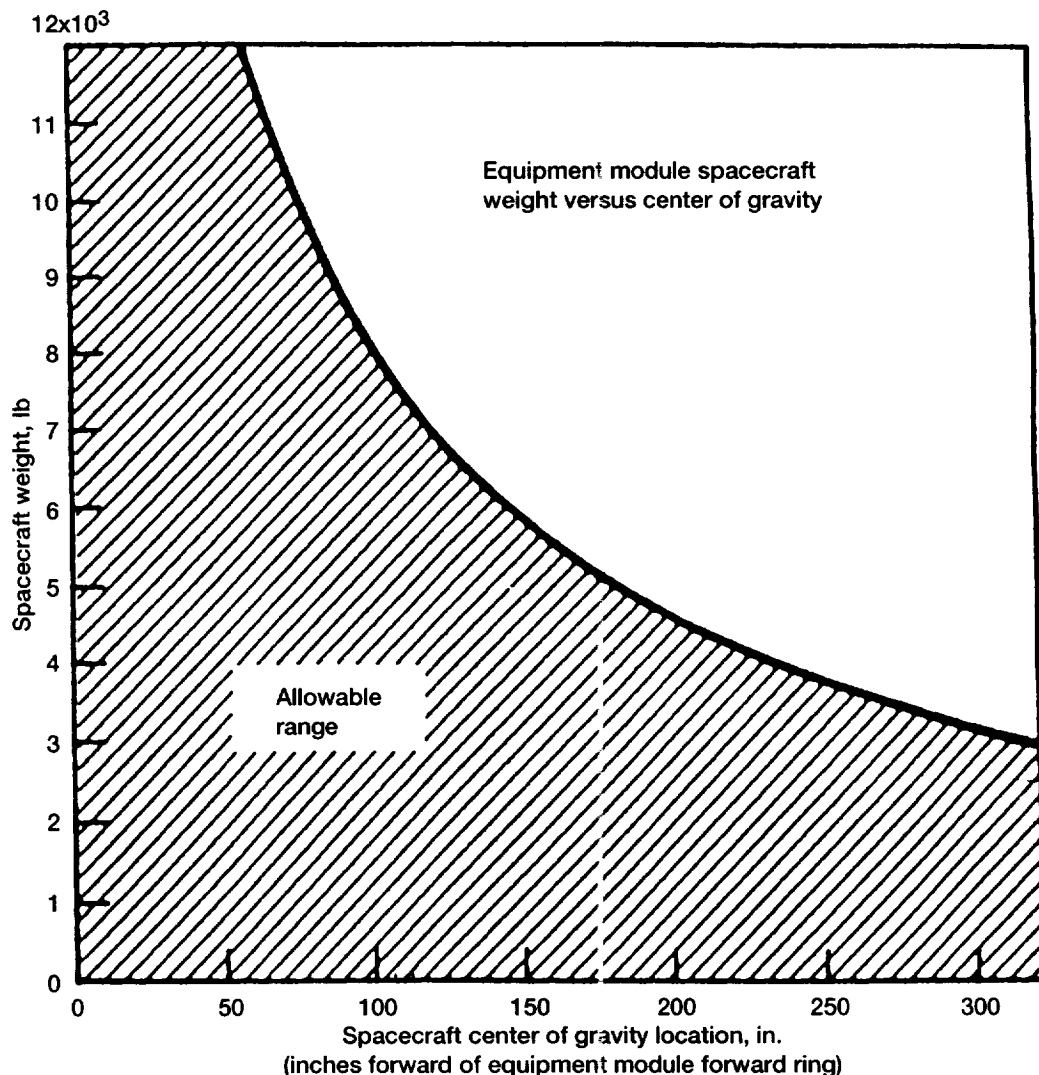


Figure 6.11.—Atlas launch vehicle center of gravity constraint.

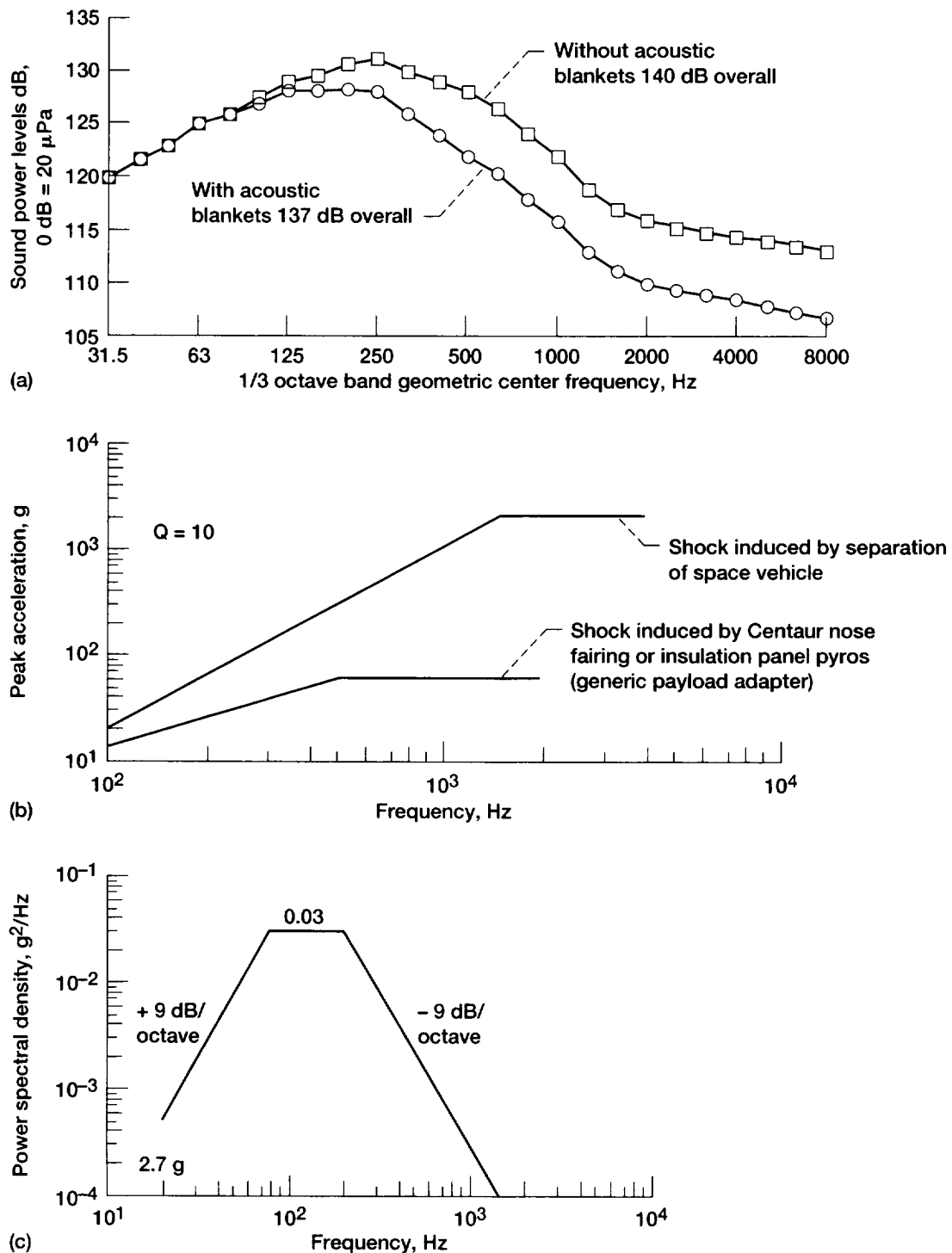


Figure 6.12.—Typical Atlas dynamic environments. (a) Acoustic levels for Atlas I with the 11-foot payload fairing. (b) Atlas I pyrotechnic shock levels. (c) Atlas I random vibration levels at payload adapter (ref. 1).

TABLE 6.5.—PRELIMINARY DESIGN LOAD FACTORS

Load condition	Direction	Steady-state, g	Dynamic, g
Liftoff	Axial	1.2	±1.5
	Lateral	NA	±1.0
Flight winds	Axial	2.2	±0.3
	Lateral	0.4	±1.2
Booster engine cutoff (BECO) (maximum axial)	Axial	5.5	±0.5
	Lateral	NA	±0.5
Booster engine cutoff/booster pod jettison (BECO/BPJ) (maximum lateral)	Axial	2.5 to 1.0	±1.0
	Lateral	NA	±2.0
Sustainer engine cutoff (SECO)	Axial	2.0 to 0.0	±0.4
	Lateral	NA	±0.3
Main engine cutoff (MECO)	Axial	4.0 to 0.0	±0.5
	Axial	0	±2.0
	Lateral	NA	±0.5

recommended load factors for the different phases of flight. The load factors are to be applied at the spacecraft CG.

6.3.1.6.2 Acoustic levels.—The launch vehicle acoustic environment impacts COLD-SAT, particularly the large surface areas. The acoustic environment starts at lift-off and continues through the boost phase of flight until the vehicle is out of the sensible atmosphere. The highest acoustic level occurs for approximately 5 sec during lift-off, when the acoustical energy of the engine exhaust is being reflected by the launch pad. The Atlas I acoustic levels for lift-off, with and without acoustic blankets, for the 11-ft payload fairing are shown in figure 6.12.

6.3.1.6.3 Random vibration.—Random vibrations are primarily caused by the acoustic noise field, with a very small portion being mechanically transmitted from the engines, and tends to be the design driver for components, small structure supports, etc. The random vibration levels and the acoustic pressures reach maximum at about the same time. Figure 6.12 identifies the expected flight random vibration interface levels for the spacecraft. This environment is to be applied to the mechanically coupled interface at the payload adapter.

6.3.1.6.4 Separation shock.—Four pyrotechnic shock events are coupled to the spacecraft during flight. These are insulation panel jettison, payload fairing jettison, Centaur separation from Atlas sustainer, and spacecraft separation. Spacecraft separation occurs at the spacecraft/Centaur interface and produces the highest shock levels for the spacecraft. The expected shock environment for spacecraft separation is shown in figure 6.12.

6.3.1.7 Air Conditioning/Purge Gas and Duct

After encapsulation, the payload fairing environment is continuously purged with filtered gases (nitrogen or air) to ensure cleanliness of the enclosed environment. The purge air/gas duct within the payload fairing interfaces with the

spacecraft's configuration. The duct is located on the inside of the payload fairing and impacts the configuration of the usable static envelope. The duct enters the fairing near the intersection of the fairing's cylindrical and conical section and runs along the conical section. The duct interface is shown in figure 6.5.

6.3.1.8 Liquid Hydrogen Loading

Liquid hydrogen loading hardware consists of the T-4 umbilical panel and its associated lines (fill, drain, and vent) and the liquid hydrogen/gaseous hydrogen vent. The umbilical panel dimensions are 12 in. by 12 in. and its interface is required along the lower end of the supply tank module on the anti-Sun (cold) side of the spacecraft to minimize heat leak into the supply tank. The vent interface is located further up the supply tank module and mates with launch vehicle mission-peculiar hardware supported off the payload fairing.

6.3.2 EXPERIMENT SYSTEM

The experiment system has a large number of interfaces with the spacecraft configuration and the structural system. These include interfaces for the three cryogenic tanks, the radiator tray and associated valve panels, pressurant tanks and liquid hydrogen vaporizers, electrical harnessing, and the T-4 umbilical. These interfaces are addressed below.

6.3.2.1 Experiment Tanks

The rather large envelopes of the experiment tanks and their associated insulation systems are one of the principal drivers for the spacecraft configuration. Their characteristics are summarized in table 6.6.

The mounting interface between the structural system and the experiment system is at the structural system (i.e., the experiment system is responsible for supporting their tanks and

TABLE 6.6.—MULTILAYER INSULATION (MLI) CAN DIMENSIONS

Description	Overall can dimensions, in.	Barrel portion, in.	Heads (truncated cones), in.
Supply tank MLI can	Length, 118.75 Diameter, 68	Length, 87.75 Diameter, 68	Height, 15.5 Large radius, 34 Small radius, 18.85
Large receiver tank MLI can	Length, 67.5 Diameter, 40.5	Length, 50.44 Diameter, 40.5	Height, 8.53 Large radius, 20.25 Small radius, 11.72
Small receiver tank MLI can	Length, 47.5 Diameter, 44	Length, 25.5 Diameter, 44	Height, 11 Large radius, 22 Small radius, 11

associated components from the structural system). The experiment system is responsible for the tanks' support struts and their interface with the tanks, whereas the structural system is responsible for the strut interface at the spacecraft structure. Additional details regarding the strut interfaces can be found in Chapter 5, Experiment System, of this report.

6.3.2.2 Radiator Tray and Valve Panels

The experiment system's radiator tray, valve panels, plumbing, and interconnects must be accommodated in the spacecraft configuration. The experiment system plumbing and radiator tray run nearly the entire length of the spacecraft (the tray supports the plumbing). The tray runs continuously from the base of the supply tank module to the middle of the small receiver tank module. The tray is required to be on the anti-Sun side of the spacecraft (to minimize heat leak). The volume allocated for the plumbing tray is constant from the bottom of the supply tank module through the electronics bay 2 module, and then tapers in accordance with the taper on the spacecraft structural system in the large and small receiver tank modules (fig. 6.13). As with the tank supports, the experiment system is responsible for mounting the plumbing tray to the structural system.

Two vent panels, two vaporizer panels, and a helium panel must be accommodated. The panels, whose configuration characteristics are summarized in table 6.7, must be located at the perimeter of the supply tank and large receiver tank modules for easy access (fig. 6.14).

6.3.2.3 Pressurant Tanks

The experiment system has four pressurant tanks whose configuration and mechanical characteristics are summarized in table 6.8. The four pressurant tanks are required to be immediately adjacent to the supply tank and equally spaced in four quadrants (because of the mass balance requirement) (fig. 6.15).

6.3.2.4 Electrical Harnessing

The electrical harnesses required for the experiment and power systems must be accommodated within the spacecraft

configuration. The harnessing runs between the two electronics bays and to the experiment tanks (for instrumentation). The harnessing is routed in the radiator tray to the maximum extent possible.

6.3.2.5 T – 4 Umbilical Panel

The T – 4 umbilical panel's layout and design is under the auspices of the experiment system. The spacecraft configuration must provide the interface volume at the aft end of the radiator tray in the appropriate orientation relative to the service towers at the launch pad. The interface is located at the lower end of the supply tank module (fig. 6.16).

6.3.3 ELECTRIC POWER SYSTEM

The major portions of the electric power system which must be accommodated within the spacecraft configuration are the solar arrays and their associated deployment mechanisms, the spacecraft batteries, and the various electronics boxes required for the system. The interfaces for these items are discussed below.

6.3.3.1 Solar Arrays

COLD-SAT has two symmetric array interfaces (to meet balance requirements) along the spacecraft's $\pm y$ -axis. The arrays are based on the Fleet SATCOM (FLTSATCOM) design which uses a three panel body-wrapped array in the stowed configuration. The solar cells are directed outward in the stowed configuration for power generation in the event of deployment difficulties. The arrays are configured so that they permit access to critical components and valve panels (on the launch pad) post encapsulation (fig. 6.17).

A total surface area of 190.6 ft² is required for the arrays. The arrays extend 99.8 in. from the spacecraft longitudinal axis (fig. 6.18) which is needed to minimize the view factors with the experiment tanks. The arrays must be located so that the center of pressure is near the spacecraft center of mass to minimize solar pressure torques. The arrays are fixed once deployed (and do not articulate). Table 6.9 summarizes the characteristics of the arrays. On deployment, the arrays are canted 10° to allow for a higher average incidence of sunshine

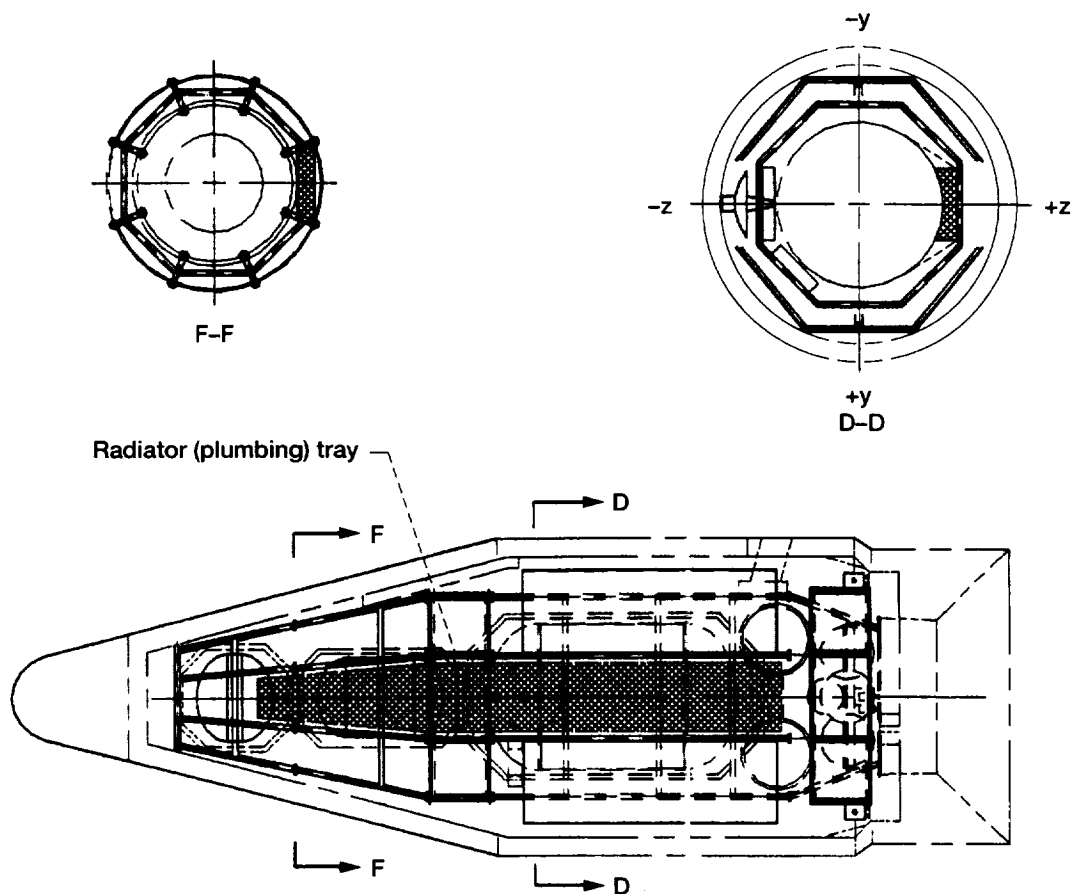


Figure 6.13.—Radiator (plumbing) tray.

TABLE 6.7.—VALVE PANEL CHARACTERISTICS

Description	Size, in.	Location
Vent panel A	30 by 22 by 6	Supply tank module Sun side
Vent panel B	22 by 20 by 6	Large receiver tank module Sun side
Vaporizer panel A	30 by 30.5 by 6	Supply tank module Sun side
Vaporizer panel B	30 by 30.5 by 6	Supply tank module Sun side
Helium panel	15 by 20 by 6	Supply tank module

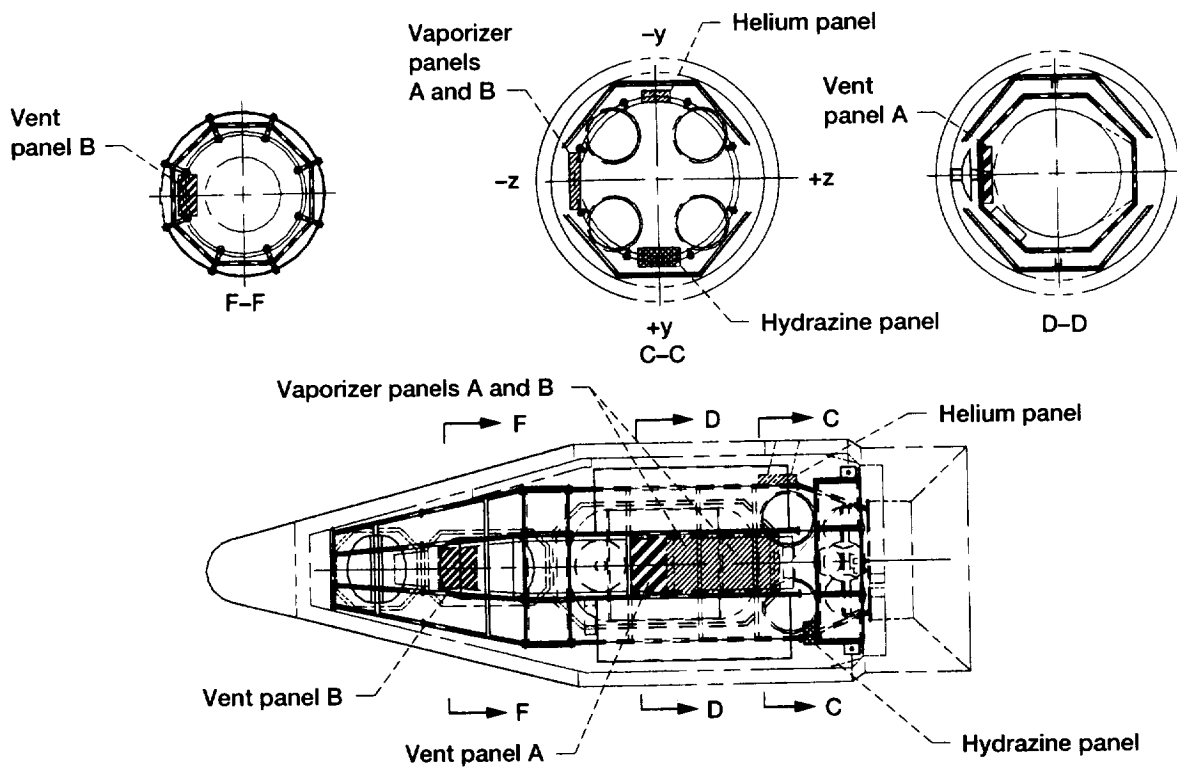


Figure 6.14.—Valve panels interface.

TABLE 6.8.—EXPERIMENT SYSTEM PRESSURANT BOTTLE CHARACTERISTICS

Description	Size	Volume, ft ³	Weight	Quantity
Helium pressurant	2-ft 6-in. sphere	5.7	105-lb tank	2
Vaporizer	2-ft 6-in. sphere	5.7	7.4-lbm gaseous hydrogen	2
			170-lb tank	
			3.7-lbm gaseous hydrogen	

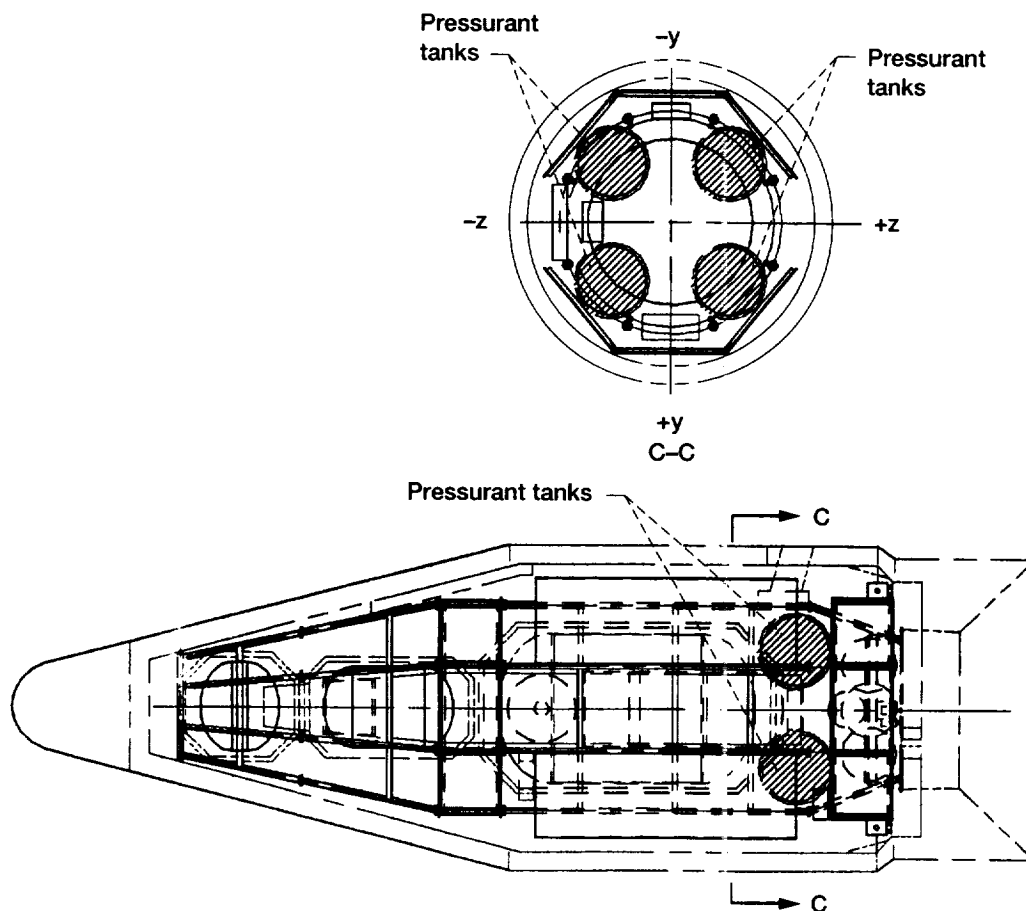


Figure 6.15.—Pressurant tanks.

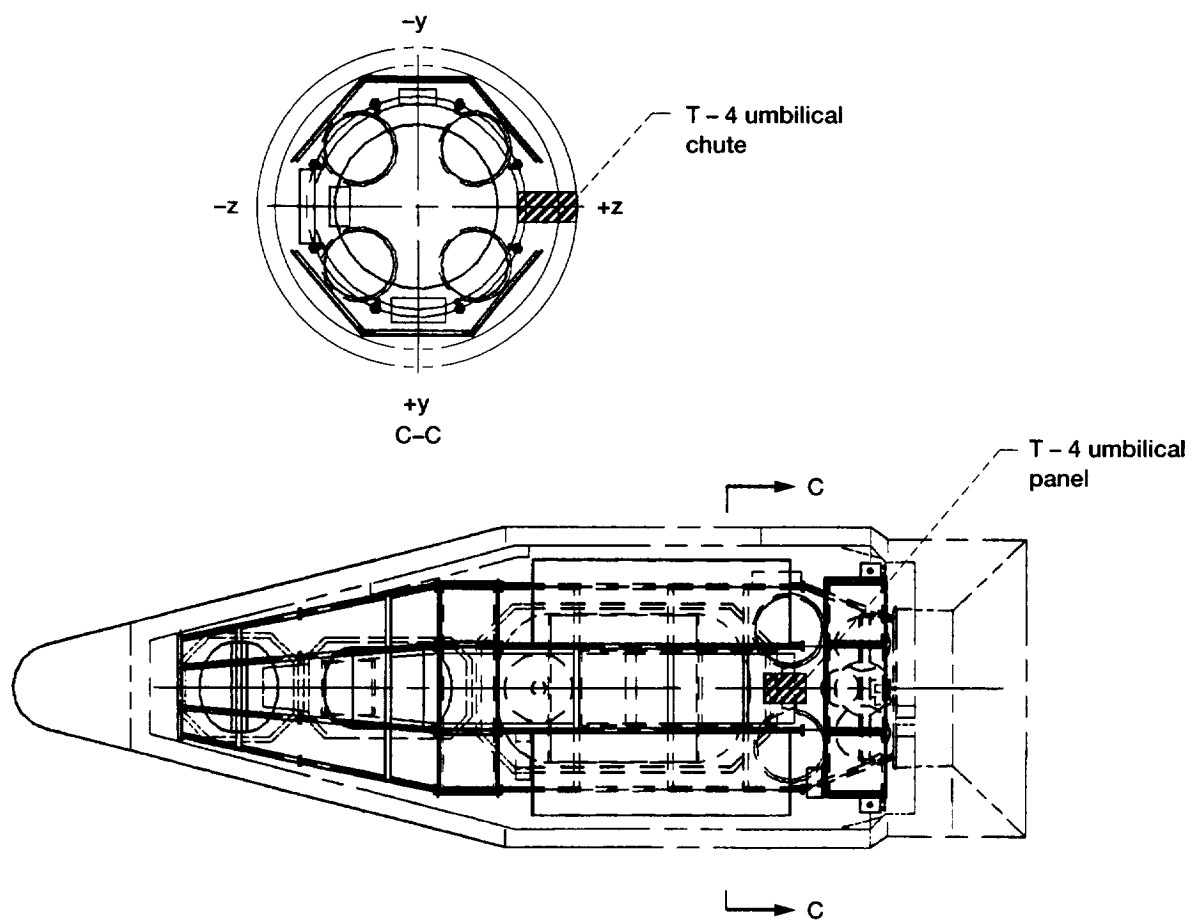


Figure 6.16.—T - 4 umbilical panel.

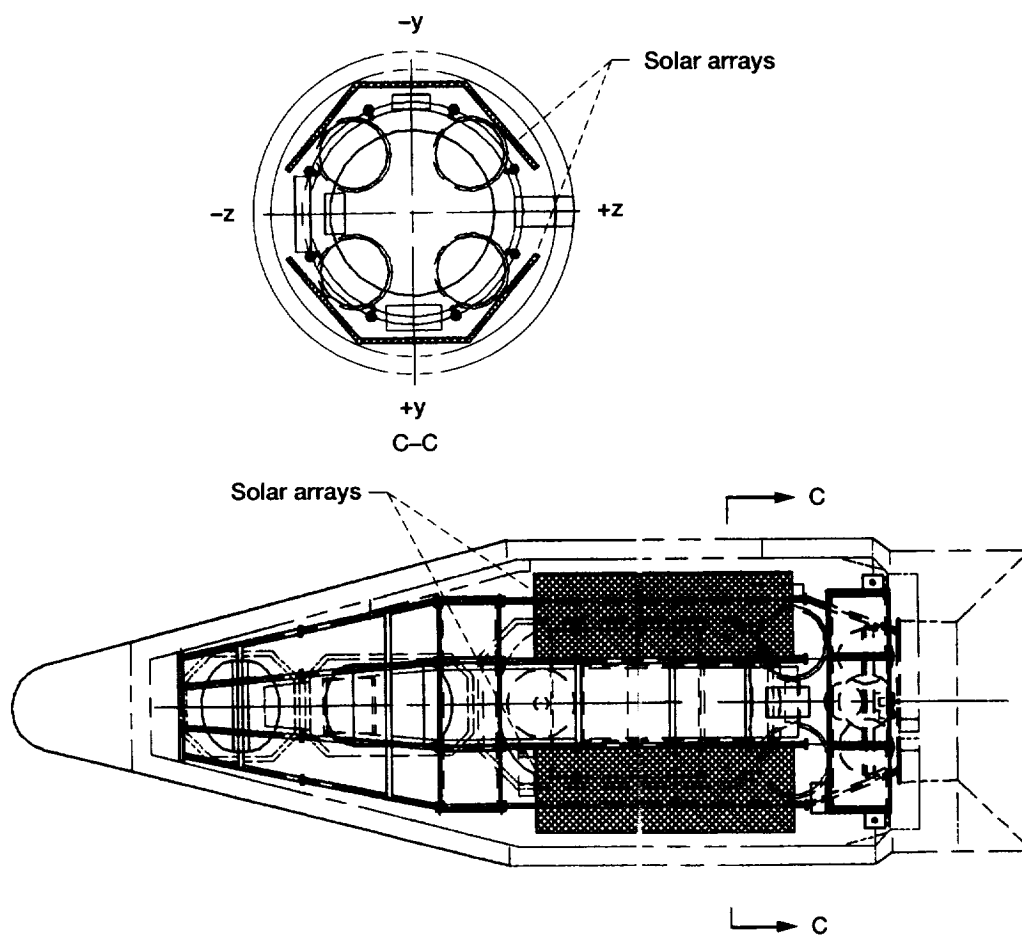


Figure 6.17.—Stowed solar arrays.

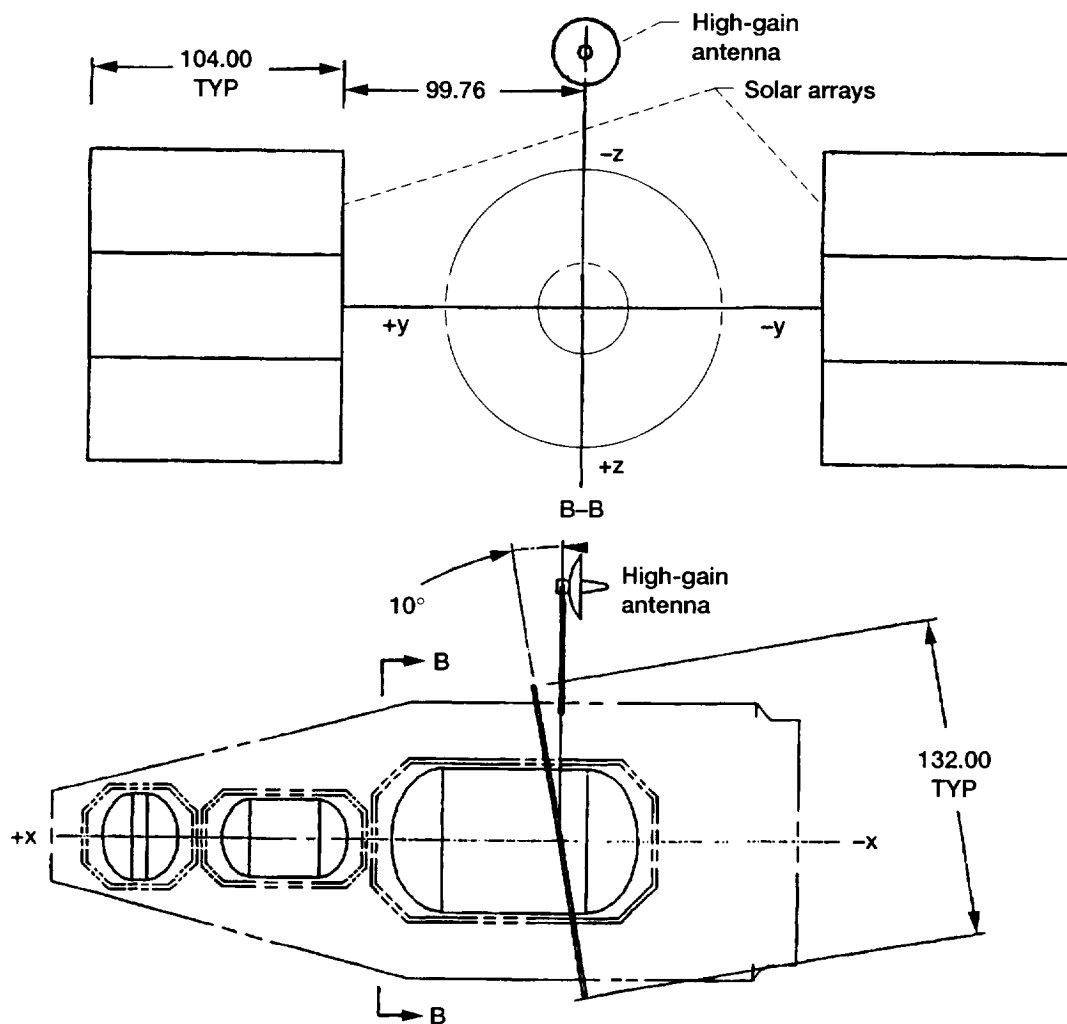


Figure 6.18.—Solar arrays. Dimensions are in inches.

TABLE 6.9.—SOLAR ARRAY CHARACTERISTICS
(Two panels)

Description	Size, ft ²	Weight, lb
Solar arrays	190.6	210

TABLE 6.10.—BATTERY CHARACTERISTICS

Description	Size, in.	Weight, lb	Quantity
Batteries	16 by 15 by 9	85	2

on the arrays (fig. 6.18). The solar array stowage and deployment requirements are based on the FLTSATCOM satellite design.

6.3.3.2 Batteries

The battery interface characteristics are summarized in table 6.10. COLD-SAT must accommodate the volume, weight, and quantity of the batteries. The batteries must be located in a

warm and thermally stable environment and in close proximity to one another as well to other power system boxes (to minimize cable runs). The batteries must be easily accessible for installation and removal.

6.3.3.3 Boxes

Three electrical boxes are required by the system. These boxes are the power control box, ordinance control box, and

TABLE 6.11.—POWER SYSTEM ELECTRONIC BOX DESCRIPTION

Box description	Size, in.	Weight, lb	Quantity
Power control	10 by 12 by 12	32	1
Ordinance control	4 by 5 by 4	5	1
Power distribution	8 by 12 by 5	25	1

TABLE 6.12.—TELEMETRY, TRACKING AND COMMAND SYSTEM ANTENNA CHARACTERISTICS

Description	Size, in.	Weight, lb	Quantity	Location
High-gain antenna	Diameter, 27.5; depth, 16	16	1	Sun side
Low-gain antenna	Diameter, 7; depth, 5	3	2	Forward and aft end of spacecraft

TABLE 6.13.—TELEMETRY, TRACKING, AND COMMAND SYSTEM REQUIREMENTS

Description	Size, in.	Weight, lb	Quantity
Flight computers	12 by 11 by 9	35	2
Sequencers	12 by 12 by 9	51	2
Data storage units	10 by 16 by 10	28	2
Radiofrequency processing box	10 by 4 by 10	10	1
Remote command and telemetry unit (RCTU)	12 by 9 by 5	11	2
Command and telemetry unit (CTU)	19 by 9 by 5	17	1
Antenna gimbal motor	Diameter, 9; depth, 5	5	1
Transponders	14 by 9 by 6	14	2
Motor drive electronics	8 by 11 by 6	11	1
Redundancy control unit	6 by 6 by 3	4	1

power distribution box. The boxes must be located in a thermally warm and relatively stable environment in the vicinity of the batteries. The structural interface is hard-mounted and positioned relatively low in the spacecraft. A summary of the electrical power system box characteristics is provided in table 6.11.

6.3.3.4 Pyrotechnic Actuators

Four pyrotechnic actuators are required for the deployment of each solar array. The interface will be similar to the FLTSATCOM design.

6.3.4 TELEMETRY, TRACKING, AND COMMAND (TT&C) SYSTEM

The interfaces between the TT&C system and the spacecraft structural system and spacecraft configuration are addressed below.

6.3.4.1 Antennas

The COLD-SAT configuration must accommodate the TT&C system's antennas, one high-gain and two low-gain. Their interface characteristics are summarized in table 6.12.

The high-gain antenna must be located on the spacecraft's perimeter where deployment can occur unencumbered. The antenna's final deployed position must be located where obstruction of the line-of-sight with TDRSS is minimized. The antenna interface is to be located in the same plane as the solar

arrays (to minimize line-of-sight blockage with TDRSS) and on the Sun side of the spacecraft.

The low-gain antennas are to be located on opposite ends of the spacecraft (fore and aft), 180° apart, and in open areas. With these mounting arrangements, the antennas can collectively provide nearly continuous coverage irrespective of spacecraft attitude.

6.3.4.2 Electronics Boxes

The TT&C system requires accommodation of several electronics boxes in the COLD-SAT configuration. Their interface characteristics are summarized in table 6.13.

The TT&C boxes are to be located in a thermally stable environment. The radiofrequency (RF) processing box and the two transponders are to be in close proximity to the high-gain antenna (to minimize RF loss). The mounting of the sequencers should minimize shock and vibration. One remote command and telemetry unit must be placed in each electronics bay (for data collection efficiency).

6.3.5 PROPULSION SYSTEM

A number of propulsion system components must be accommodated by the spacecraft configuration and the structural system. These include rocket engine modules, hydrazine propellant tanks, a gaseous helium pressurant tank (for hydrazine expulsion), and a hydrazine valve panel (for servicing). Details of these interfaces are discussed below.

TABLE 6.14.—THRUSTER MODULE CHARACTERISTICS

Description	Size, in.	Weight, lb	Location	Orientation
Rocket engine module 1	8 by 6 by 10	8	-z-axis at outside spacecraft radius	-x-axis +y-axis -y-axis
Rocket engine module 2			+z-axis at outside spacecraft radius	-x-axis +y-axis -y-axis
Rocket engine module 3			-y-axis at outside spacecraft radius	-x-axis +z-axis -z-axis
Rocket engine module 4			+y-axis at outside spacecraft radius	-x-axis +z-axis -z-axis
Gimbal thruster module	7 by 7 by 10	15	x-axis	-x-axis

TABLE 6.15.—PROPELLANT TANK CHARACTERISTICS

Description	Size	Volume, ft ³	Weight, lb	Quantity
Hydrazine propellant tank	22.125-in. sphere	3.2	14; Tank 150; Hydrazine	4

TABLE 6.16.—PROPULSION SYSTEM PRESSURANT BOTTLE CHARACTERISTICS

Description	Size	Volume, ft ³	Weight, lb	Quantity
Hydrazine pressurant bottle	15-in. diameter sphere	1.03	15	1

TABLE 6.17.—HYDRAZINE VALVE PANEL CHARACTERISTICS

Description	Size, in.	Location
Hydrazine valve panel	22 by 12 by 6	Electronics bay module 1, outside perimeter

6.3.5.1 Thruster Modules

The structural and configuration interface characteristics of the five rocket engine modules are summarized in table 6.14. The thruster modules interface shall be at the spacecraft's aft end.

The thruster modules must be so located that the thrusters' exhaust plumes are directed away from the spacecraft, particularly away from sensitive components such as sensors, solar arrays, and thermal control surfaces. The thruster modules must be located at the spacecraft's perimeter to maximize control torque and to minimize the component performance degradation.

6.3.5.2 Propellant Tanks

Four propellant (hydrazine) tanks are required for the propulsion system. The configuration and mechanical characteristics of the propellant tanks are summarized in table 6.15.

Since the hydrazine propellant tanks require a temperature-controlled environment, the tanks are to be located within the electronics bay 1 module. By locating the tanks aft, piping that

runs to the thruster modules is minimized and CG problems caused by the propellant weight are reduced.

6.3.5.3 Pressurization System/Valve Panel

The pressurant bottle and valve panel for the propulsion system must be accommodated in the spacecraft configuration and their interface characteristics are summarized in tables 6.16 and 6.17, respectively. The pressurant bottle must be located in close proximity to the valve panel and hydrazine supply. Likewise, the valve panel is located near the propellant tanks. The panel must be accessible for detanking hydrazine on the pad in the event of an extended launch delay. The panel's thermal requirements are similar to those for the hydrazine tanks.

6.3.6 ATTITUDE CONTROL SYSTEM

The principal elements of the attitude control system which must be accommodated in the spacecraft configuration are the attitude sensors, the inertial reference unit, and their associated electronics boxes.

TABLE 6.18.—ATTITUDE CONTROL SYSTEM CHARACTERISTICS

Description	Size, in.	Weight, lb	Quantity
Horizon sensors	Diameter, 4.1; length, 1.9	2.5	2
Sun sensors	3.3 by 4.3 by 0.94	0.7	2
Inertial reference unit	12.5 by 9 by 9	37	1
Horizon sensor electronics	10.3 by 5.8 by 4	7.5	2
Sun sensor electronics	4.5 by 7.8 by 2	2.3	2
Attitude control I/F electronics	8 by 15 by 4	15	1
Magnetometers	1.25 by 1.375 by 4	0.33	2

6.3.6.1 Attitude Sensors

Four different types of attitude sensors are required. These include Sun sensors, horizon sensors, magnetometers, and the gyros. Details of size, weight, and shape are given in table 6.18. Additional interface details are discussed below.

6.3.6.1.1 Sun sensors.—Two Sun sensors are required. They must be located on the spacecraft's aft end facing the Sun. The sensor requires a view of the Sun with a cone angle of 32° and tilting 20.5° (from the spacecraft's longitudinal axis in the spacecraft x-y plane) to bisect the Sun angle during various mission phases (see fig. 7.19 in Chapter 7, Attitude Control System, of this report). The sensor electronics are to be located in the immediate vicinity of the sensor.

6.3.6.1.2 Horizon sensors.—Two horizon sensors are required and their interface location is in electronics bay 2 facing outward perpendicular to the orbit plane. The horizon sensors are located 180° apart with one sensor facing parallel to the spacecraft's positive y-axis and the other sensor facing parallel to negative y-axis. Each sensor requires a view of the Earth with a cone angle of 90° .

6.3.6.1.3 Magnetometers.—Two magnetometers are required. The magnetometers must be isolated from interfering magnetic fields to the maximum extent possible.

6.3.6.1.4 Inertial reference unit (gyros).—The inertial reference unit has no peculiar mounting or view factor requirements. However, it requires a rigid mount and with a known orientation with respect to the remaining sensors.

6.3.6.2 Stability and Alignment

All of the sensors require a stable mount with access for alignment. Except for the Sun sensors, each sensor is to be located in an electronics bay for thermal stability and on the spacecraft's perimeter for ease of alignment and so that view factors are not obscured. The electronics associated with each sensor should be located immediately adjacent to that sensor.

6.3.6.3 Electronics Boxes

The Sun sensors and the horizon sensors have separate electronics boxes associated with them. In addition, there is the attitude control interface electronics box. The characteristics of the electronics boxes and the sensors are presented in table 6.18.

6.3.7 TRANSPORTATION AND HANDLING

The completed spacecraft must be transported between the various test sites and to the launch site. Hard points are required for attachment of the transportation and handling fixtures. The hardpoints must safely support the spacecraft under expected loading.

6.3.7.1 Handling Hardpoints

The handling hardpoints are to be located on the structural system and require enough strength and stiffness to handle the transportation and handling loads without damage to the spacecraft. Additional information on handling equipment and lifting rigs is given in Chapter 14, Ground Operations, of this report.

6.3.7.2 Transportation Loads

The transportation loads interface with the structural system and are identified in table 6.19.

TABLE 6.19.—TRANSPORTATION LOADS (g's)

Mode	Fore/aft	Lateral	Vertical
Truck	± 3.5	± 2.0	+3.5, -1.5
Plane	± 3.5	± 3.5	± 3.5

6.4 Alternate Configurations

COLD-SAT was originally configured for a Delta launch vehicle. At that time, COLD-SAT contained four cryogenic tanks and a large number of hydrogen pressurant bottles. The design path to an acceptable configuration was long and tortuous. Eventually configuration problems, among other factors, led to the switch to the Atlas launch vehicle. This section presents a brief overview of the COLD-SAT design process.

6.4.1 BRIEF HISTORY

The first COLD-SAT layout began 50 iterations ago. Initially, a small team of subsystem engineers and a lead project

engineer got together to identify the COLD-SAT requirements. System concepts were developed based on a modest understanding of experiment, spacecraft, program, and launch vehicle requirements. Component characteristics for these systems, such as volume, weight, power consumption, quantity, location restrictions, thermal requirements, etc. were estimated. The estimates were submitted to the spacecraft configuration team who laid out the initial spacecraft concepts. As the process continued, numerous configuration changes and refinements were made. Each change was reviewed by a team of lead system engineers and configuration modifications were made as appropriate. Configuration changes were fairly dramatic in the program's early stages, but gradually the dramatic changes transformed into refinements as the configuration matured.

COLD-SAT's configuration was initially developed for the Delta II Launch Vehicle with a 10-ft diameter payload fairing. Twenty-one iterations were performed using the Delta until some design problems became overwhelming. This situation prompted the investigation of an alternative launch vehicle. After the investigation, an Atlas I was selected to continue the feasibility study. Much of the work performed and experience gained while working on the Delta was carried over to the Atlas I.

6.4.2 FINAL DELTA CONFIGURATION

The final COLD-SAT configuration on a Delta was a viable configuration, but it had essentially no volume margin. Spacecraft CG restrictions also caused continuing problems. The final configuration on the Delta II is described below.

6.4.2.1 Description of Configuration

The final COLD-SAT configuration for a Delta launch vehicle evolved through 20 iterations. The design requirements used to establish this configuration are similar to the ones described in section 6.2, Major Requirements, of this report. Some requirement differences include the mass property restraints (for different launch vehicles), the payload fairing (the Delta II 10-ft (diameter) fairing versus the Atlas 11-ft fairing), the number and size of experiment tanks, the launch vehicle performance, the spacecraft loads and environments, and the payload stiffness requirements.

Figure 6.19 shows the final COLD-SAT configuration using a Delta launch vehicle. Table 6.20 identifies the various components shown in the figure. The usable payload envelope is 20 ft long and 10 ft in diameter. This configuration includes a 150-ft³ vacuum jacketed supply tank, a 36-ft³ large receiver tank, two 10-ft³ small receiver tanks, two 8.9-ft³ gaseous helium pressurant spheres, one 8.9-ft³ gaseous hydrogen accumulator, and one 8.9-ft³ vaporizer (see table 6.20 for the component number index and additional details). In addition, this configuration contains four reaction wheels, two electronics bays for housing electronics boxes, and four 3.2-ft³ hydrazine

spheres. The solar arrays are body-wrapped around the supply tank and mounted from the supply tank's vacuum jacket. The high-gain antenna is also mounted to the vacuum jacket and is located in the same plane as the deployed solar arrays. The attitude control thrusters are mounted fore and aft on the spacecraft.

The spacecraft's structural system (shown in fig. 6.20) uses a longeron-based outside structure. This design was driven by the experiment requirements of keeping the experiment tanks thermally isolated and as cold as possible. The outside structure envelopes the tanks and provides long conduction paths thereby enhancing thermal isolation to the experiment tanks. The longeron-based structure creates an open structure that permits view factors to deep space from the experiment tanks and thereby capitalizes on the very low temperature of deep space and enhances the tanks' thermal performance. The supply tank vacuum jacket was regarded as a primary structure. Other spacecraft structure and the deployable components were mounted to it.

The Delta configuration incorporates a modular design which is derived from the program requirements. The modular configuration enhances the spacecraft's maintainability, accessibility, inspection, integration, assembly, and testing producing reduced program costs. Flat rectangular cross-section rings are the mating interface between the modules. Both electronics bays can be detached and serviced during testing operations or during prelaunch checkout. Also, the framed electronics bay structure uses detachable honeycomb panels for mounting electronics boxes.

The Delta concept has five vertically stacked modules (i.e., two electronics bay modules, one supply tank module, a large receiver tank module, and a small receiver tank module that includes the pressurant). The aft module houses electronics bay 1 and the spacecraft's propellant. The next module is the supply tank module and it houses the supply tank, the solar arrays, and the high-gain antenna. The solar arrays completely envelope the supply tank module's perimeter.

Forward of the supply tank module is the small receiver tank module. This module houses two 10-ft³ tanks (small receiver tanks) in addition to two gaseous helium pressurant cylinders, a hydrogen system accumulator, and a hydrogen system vaporizer.

Forward of the small receiver tank module is the electronics bay 2 module which houses an appreciable portion of the electronics, and finally, forward of this module is the large receiver tank module which houses the large receiver tank and the gaseous helium for the propulsion system. The entire spacecraft is enveloped by a 10-ft payload fairing and mounted on top of a Delta II launch vehicle.

The structural system primarily consists of off-the-shelf aluminum shapes. Low technology manufacturing techniques and assembly practices are used to assemble the design. The design of the structural system is conservative both in terms of safety factors and materials used.

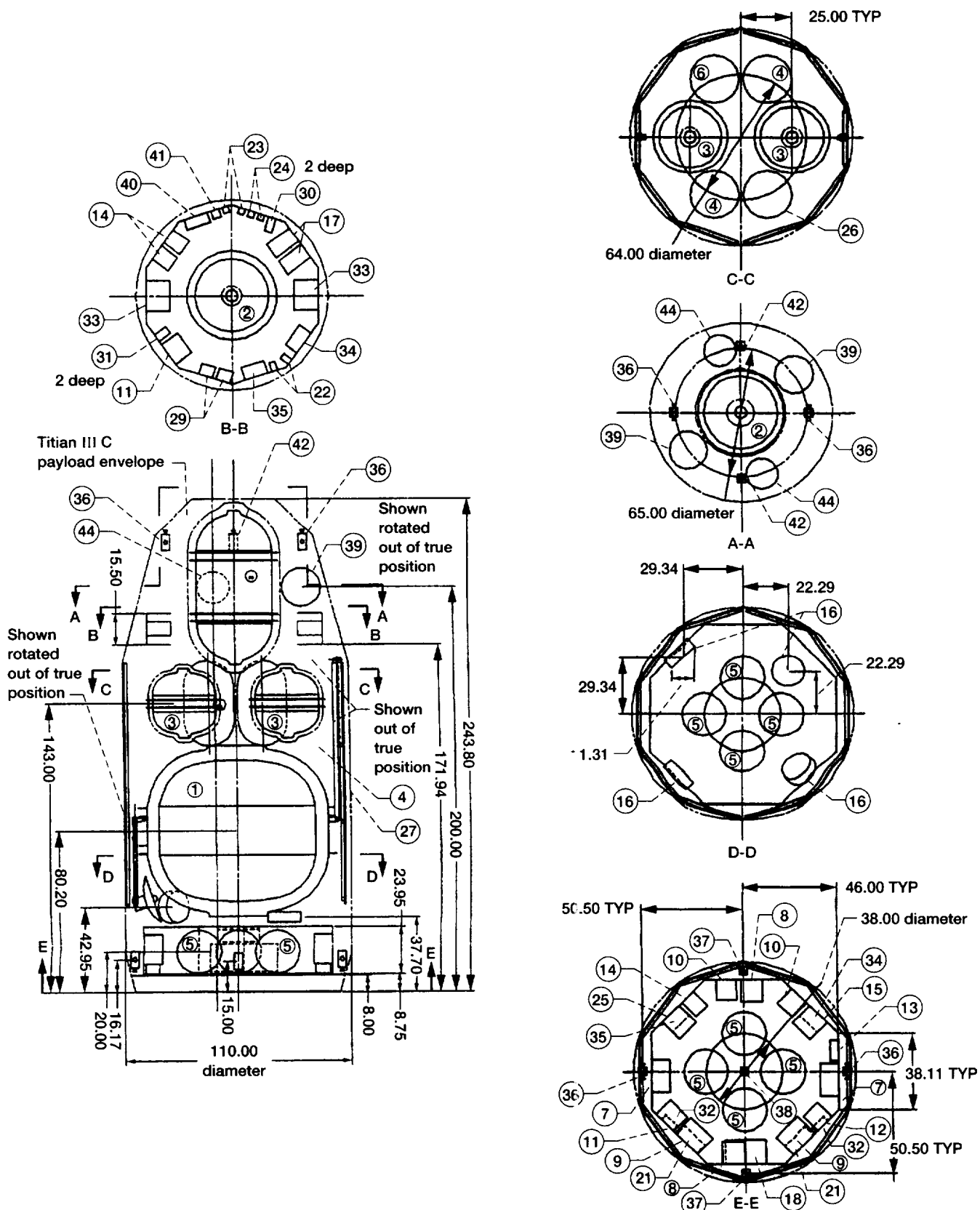


Figure 6.19.—Final spacecraft configuration for Delta launch vehicle. Dimensions are in inches. See table 6.20 for a list of components identified by numbered circles in this figure.

TABLE 6.20.—FINAL COMPONENT CHARACTERISTICS FOR DELTA LAUNCH VEHICLE

Item	Description	Size, in.	Volume	Weight, lb	Quantity
1	Tanker tank	6-ft-4-in. diameter by 5-ft-9.5-in. long Cassini heads; 6-in. all around for vacuum jacket	150 ft ³	1618 Tank 660 Liquid hydrogen	1
2	Depot tank	3-ft-0.5-in. diameter by 6-ft-1-in. long hemispherical heads; 4 in. insulation all around	36 ft ³	285	1
3	Orbit transfer vehicle tank	2-ft-7-in. diameter by 2-ft-6.25-in. long ellipsoidal heads; 2 in. insulation all around	10 ft ³	83	2
4	Helium pressurant cylinder	2-ft diameter by 3-ft-6-in. long hemispherical heads (2000 psia, 540 °R, 2.47 lb/ft)	8.9 ft ³	95 Tank 11.55 Helium	2
5	Hydrazine sphere	1-ft-10.125-in. diameter	3.2 ft ³	17.25	4
6	Hydrogen system (accumulator)	2-ft diameter by 3-ft-6-in. long hemispherical ends	9.9 ft ³	95	1
7	Batteries	16 by 15 by 9	2160 in. ³	102	2
8	Sequencers	11 by 8 by 11	968 in. ³	51/45	↓
9	Flight computers	15 by 10 by 12	1800 in. ³	25	
10	Data storage units	10 by 16 by 10	1600 in. ³	19	
11	Control data units	12 by 8 by 10	960 in. ³	15	
12	Command decoder	10 by 8 by 10	800 in. ³	10	1
13	Radiofrequency processing box	10 by 10 by 4	400 in. ³	5	1
14	Remote data units	8 by 12 by 10	960 in. ³	15	3
15	Power control	12 by 10 by 12	1440 in. ³	32	1
16	Reaction wheels; roll, pitch, and yaw	15-in. diameter by 5-in. long	1183 in. ³	21	4
17	Attitude control electronics	8 by 11 by 14	1232 in. ³	18	2
18	Propellant distribution assembly	20 by 6 by 12	1440 in. ³	10	1
19	High-gain antenna	24-in. diameter by 12-in. deep	-----	17	1
20	Antenna gimbal motor	8 by 6 by 6	288 in. ³	5	1
21	Transponders	14 by 6 by 6	504 in. ³	14	2
22	Earth sensors 1 and 2	3-in. diameter by 5-in. long	35.4 in. ³	2	↓
23	Coarse Sun sensor 1 and 2	3 by 1 by 3	9 in. ³	1	
24	Fine Sun sensor 1 and 2	3 by 1 by 3	9 in. ³	1	
25	Gyro assemblies 3-200F	12 by 9 by 12	1296 in. ³	37	1
26	Hydrogen system (vaporizer)	2-ft diameter by 3-ft-6-in. long, hemispherical ends	8.9 ft ³	95	1
27	Solar panels	2-ft-3 in. by 9-ft-10.75 in.	27.2 ft ²	21.5	10
28	Low-gain antenna	-----	-----	2	2
29	Electronics-Earth sensors 1 and 2	7 by 3 by 6	126 in. ³	4	↓
30	Electronics-coarse Sun sensors 1 and 2	4 by 6 by 7	168 in. ³	3	
31	Electronics-fine Sun sensors 1 and 2	4 by 6 by 7	168 in. ³	3	2
32	Uplink formatter 1 and 2	8 by 9 by 3	192 in. ³	9	↓
33	Flow meter electronics boxes	15 by 7 by 12	1260 in. ³	15	
34	Experimental signal conditioning boxes (transducer)	12 by 7 by 7	588 in. ³	15	
35	Experimental signal conditioning boxes (data)	12 by 7 by 7	588 in. ³	20	
36	Rocket engine modules 1 to 4 (4 thrusters each)	10 by 8 by 4	320 in. ³	8	4
37	Rocket engine modules (4 thrusters each)	10 by 4 by 4	180 in. ³	2	2
38	Rocket engine module 7 (4 thrusters)	10 by 4 by 4	400 in. ³	8	1
39	Hydrazine pressurant (gaseous helium)	19-in. sphere (low press)	2.08 ft ³	7.75	2
40	Power distribution box	12 by 8 by 5	480 in. ³	25	1
41	Ordnance control box	4 by 5 by 4	80 in. ³	5	1
42	Rocket engine module	10 by 4 by 4	160 in. ³	-----	2
44	Hydrazine pressurant (gaseous helium)	15.8-in. sphere	1.24 ft ³	21.5	2

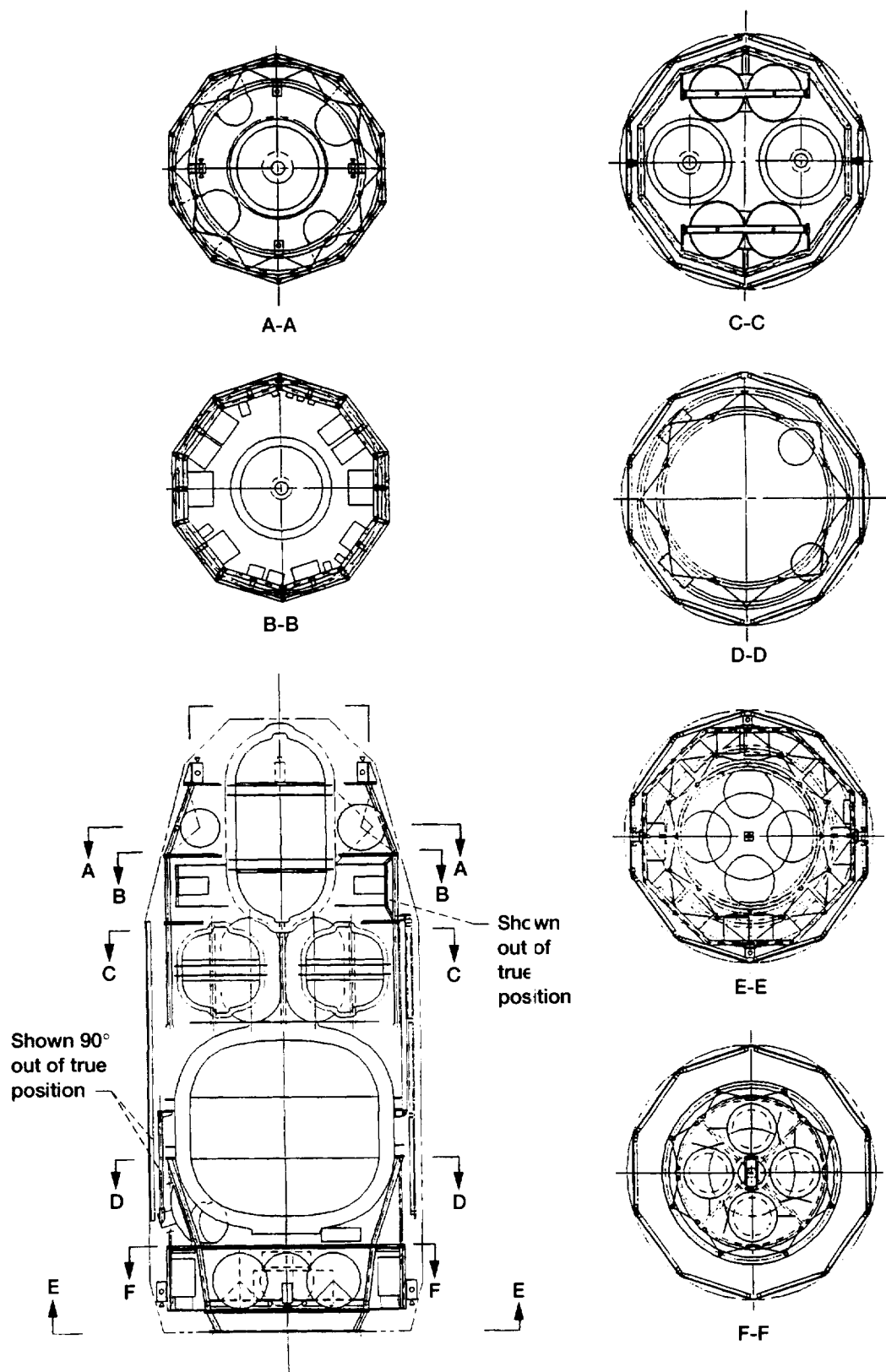


Figure 6.20.—Final spacecraft configuration for Delta, structural system.

6.4.2.2 Mass Properties Verses Delta II Capabilities

Spacecraft mass properties were tracked throughout the feasibility study. The properties tracked included the spacecraft's weight and CG (longitudinal axis). These properties were tracked because of concerns regarding compliance with the Delta's CG restraint. In fact, during most of the first 20 COLD-SAT iterations, COLD-SAT's configuration was not in compliance with the Delta's published CG capability.

Initially, the maximum Delta capability published was for a 4300 lb spacecraft, but COLD-SAT was an 8000 lb class spacecraft (see Delta II Commercial Spacecraft Users Manual, ref. 2). In addition, the 6019 payload attach fitting described in the users manual was only capable of supporting a 4800 lb spacecraft with a CG 82 in. above the separation plane (assuming a 2-in. radial CG offset). At the time, COLD-SAT's CG was in the 82-in. ballpark and it weighed significantly more than the published payload adapter weight capability. Until additional launch vehicle capability was published, COLD-SAT's configuration and corresponding mass properties were a major concern and put tremendous pressure on the COLD-SAT feasibility team.

COLD-SAT's final weight and CG location for the Delta configuration are shown in figure 6.21. COLD-SAT's final weight is 8007 lb (includes growth margin) and its CG is 76.9 in. from the spacecraft separation plane (station 494.37 which assumes a 6-in. spacecraft adapter). Figure 6.21 shows adequate margin in the launch vehicle without modification.

Other factors that provided impetus to consider alternative launch vehicles were the launch vehicle lift capability, the usable payload fairing volume, estimated COLD-SAT cost, and the experience base and ground capability to handle liquid hydrogen.

From figure 6.20 one can see that the last COLD-SAT concept on the Delta is severely volume-limited. In addition, at that time many components had not been incorporated into the configuration, including the plumbing trays, harnessing trays, valve panels, interface panels, secondary structure, etc. Serious doubts were raised about whether it was wise to proceed with a concept on a launch vehicle so volume-limited at this early design phase with all the missing components.

Another major concern was the estimated cost of COLD-SAT. A preliminary COLD-SAT cost estimate was deemed too expensive for the Agency. The size and cost of COLD-SAT had to be reduced. The vacuum jacketed supply tank was the most expensive single item on COLD-SAT and only useful on the ground. Therefore it was considered an ideal candidate for omission in subsequent iterations.

6.4.3 CAPABILITIES OF DELTA VERSUS ATLAS

As further configuration problems mounted for COLD-SAT on a Delta launch vehicle with little relief in sight, alternative launch vehicles were investigated for relief on CG, volume, and cost. Below, the capabilities of the Atlas/Centaur and the Delta launch vehicle are compared.

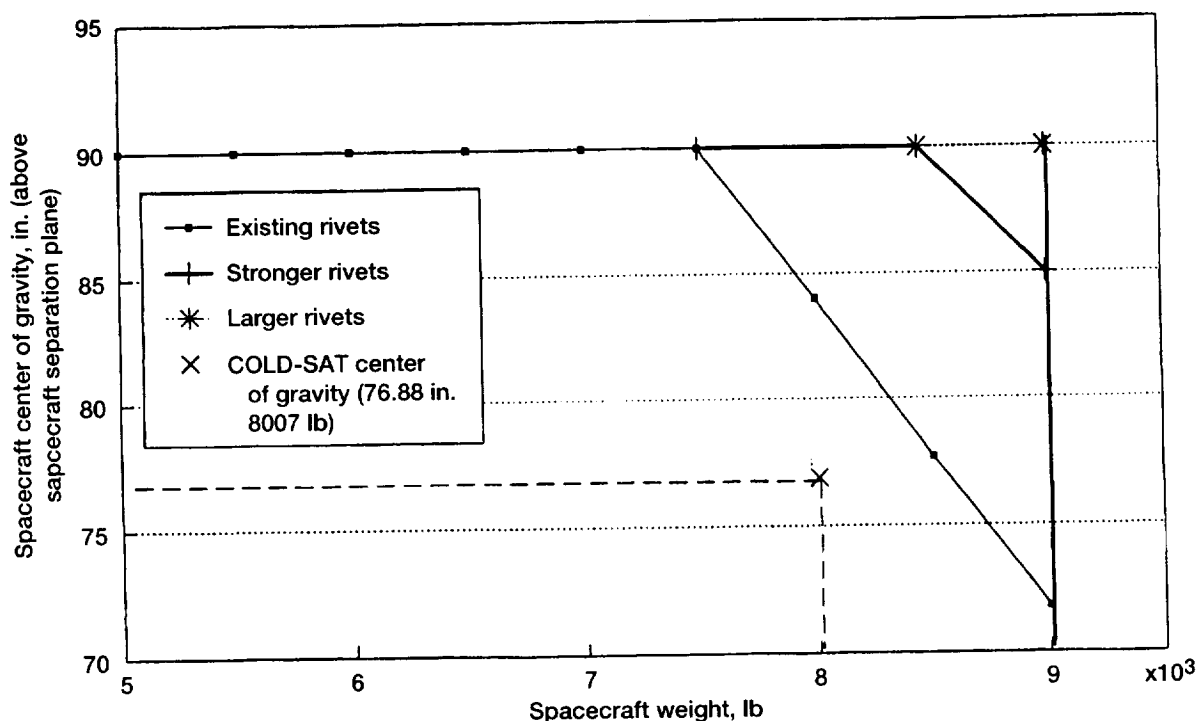


Figure 6.21.—Final COLD-SAT center of gravity relative to Delta launch vehicle capability.

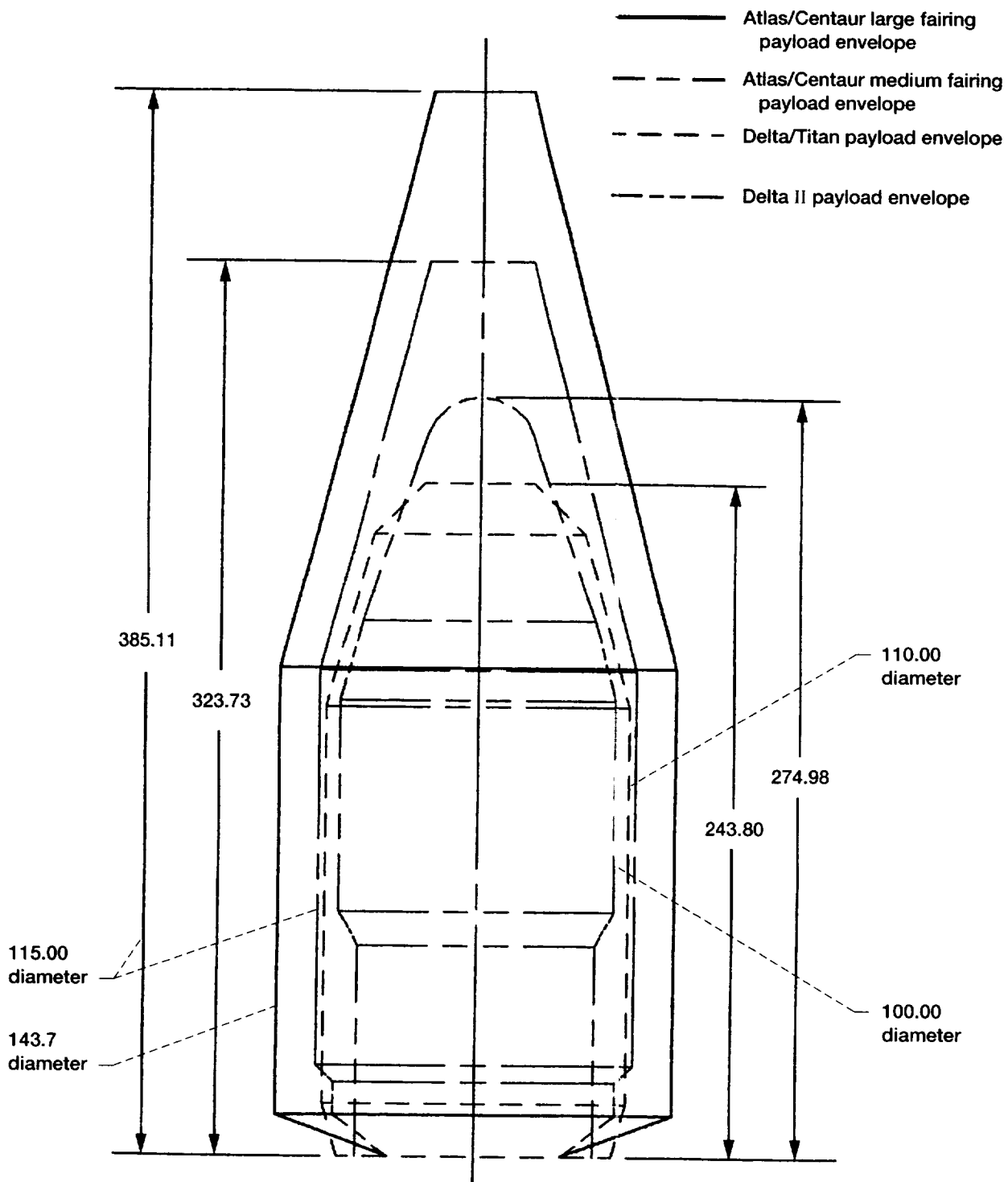


Figure 6.22.—Payload fairing usable envelope comparison. Dimensions are in inches.

6.4.3.1 Comparative Payload Envelopes

The usable payload envelope defines the volume available to the spacecraft developers using a given payload fairing. The usable payload envelopes for the Delta II and Atlas I are shown in figure 6.22. Two different size fairings are shown for the Delta (9.5- and 10-ft) and for the Atlas launch vehicle (11- and 14-ft). Clearly, the Atlas provides a larger usable envelope.

6.4.3.2 Mass Properties Restrictions

Figure 6.23 illustrates the launch vehicle CG restraint for the Delta II and Atlas I launch vehicles based on existing capability. Under no circumstance did the COLD-SAT team want to exceed the existing CG restraints for either launch vehicle because of the cost associated with modifying and requalifying the launch vehicle. Assuming the same size spacecraft adapter, the Atlas I provides additional CG capability.

6.4.4 INITIAL ATLAS CONFIGURATION

The first COLD-SAT concept laid out using the 11-ft medium Atlas/Centaur payload fairing is shown in figure 6.24. This iteration was based on the final COLD-SAT concept on a Delta and from the freshly revised experiment requirements.

Shortly after the transition to the Atlas I, a revised set of experiment requirements were issued. Four experiment tanks were no longer optional. Three tanks were mandated and the length-to-diameter ratios of the experiment tanks were changed along with the experiment acceleration requirements, etc. A summary of the differences between the final Delta configuration and initial Atlas configuration is given in table 6.21. These changes had a significant impact on COLD-SAT's configuration.

6.4.4.1 Description of Configuration

The first COLD-SAT layout in the 11-ft medium fairing includes a 145-ft³ supply tank, a 21-ft³ large receiver tank, a 13.5-ft³ small receiver tank, two 5.3-ft³ gaseous helium pressurant tanks, and two 5.3-ft³ gaseous hydrogen pressurant bottles. The spacecraft still has two electronics bays, propulsion thrusters located fore and aft, reaction wheels, hydrazine pressurant bottles, and body-wrapped solar arrays. The pressurant cylinders have been replaced by pressurant spheres. Additional component details (i.e., weight, quantity, size, volume, etc.) can be found in table 6.22.

The experiment tanks are aligned on the longitudinal axis of the spacecraft to minimize induced accelerations and hydrazine propellant usage. The experiment tanks have also added an MLI (multilayer insulation) can to simplify the insulation layup (fig. 6.24).

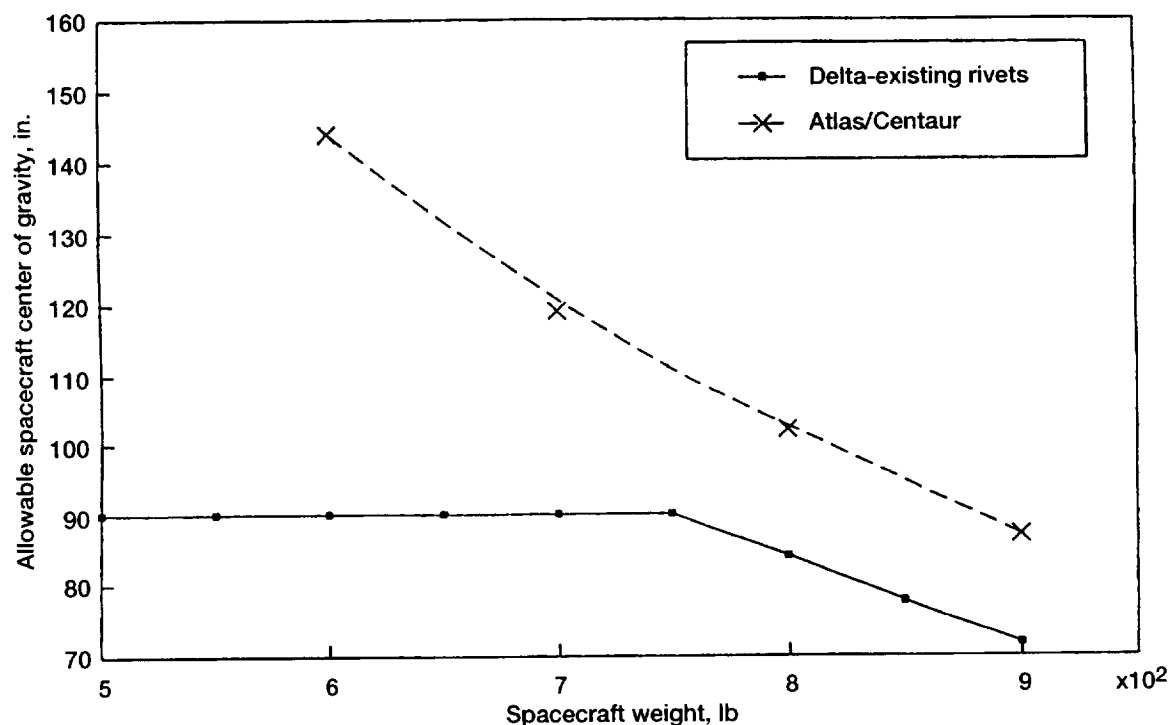


Figure 6.23.—Atlas and Delta launch vehicle center of gravity capability comparison.

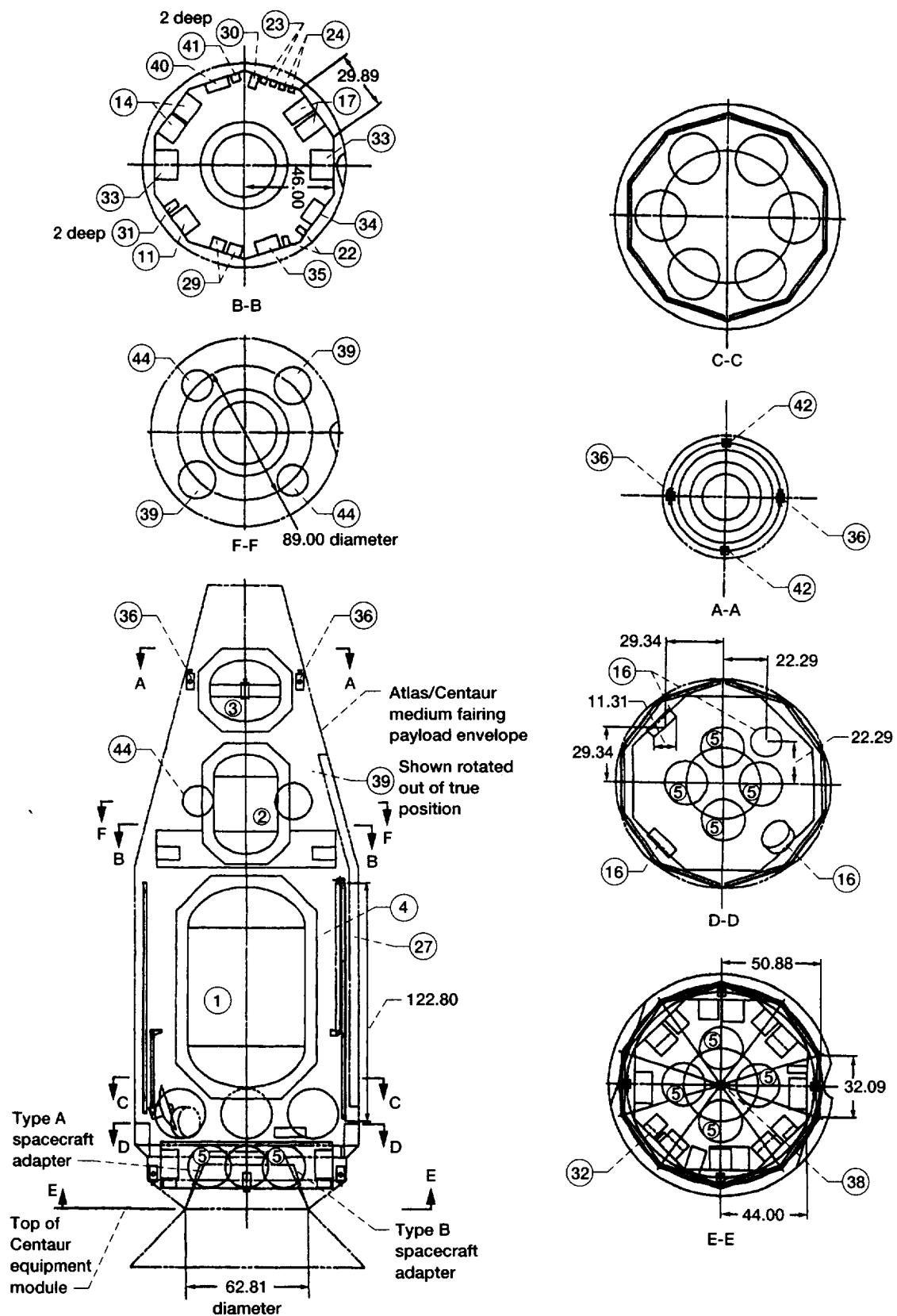


TABLE 6.21.—MODIFICATIONS TO INITIAL ATLAS CONFIGURATION

Component	Updated configuration (configuration 1600)	Previous configuration (configuration 01900)
Launch vehicle	Atlas/Centaur	Delta II
Fairing	11-ft diameter	10-ft diameter
Supply tank	Eliminated vacuum jacket	Vacuum-jacketed
	Decreased volume (145 ft ³)	150 ft ³
	Altered shape (length-to-diameter ratio)	-----
	Added MLI can	-----
	Eliminated vapor-cooled shield	Vapor-cooled shield
Receiver tank	Reduced volume (21 ft ³)	136 ft ³
Orbit transfer vehicle tank 2	Eliminated	Existed
Orbit transfer vehicle tank 1	Reoriented on-axis	Off-axis
Pressurant bottles	Altered bottle size	-----
	Added vaporizer	-----
Electronics bay 1	Contracted and lengthed	-----
Electronics bay 2	Lengthened and changed sides	10-sided
Avionics boxes	Reoriented and reshuffled	-----
Hydrazine thrusters	Diameters altered	-----
Sensors	Added	Missing
OMNI antenna	Added	Missing
Solar array deploy mechanics	Added	Missing
Power subsystem boxes	Added 2 boxes	Missing
Experiment system	Relabeled boxes	-----

One significant difference between the final Delta and the initial Atlas configurations is the elimination of the supply tank vacuum jacket. The vacuum jacket was eliminated to save 1000 lb of spacecraft weight and to significantly reduce the estimated cost of COLD-SAT. The deletion of the vacuum jacket comes at the expense of more sophisticated ground operations, but the Atlas I ground crew and launch site are well suited for the additional sophistication because of their experience and capability in handling liquid hydrogen associated with the Centaur upper stage.

6.4.4.2 Mass Properties

The dry spacecraft weight for the initial configuration on the Atlas was 2912 lb. However, this value did not include the weight of the spacecraft structure which would not be configured or sized for several more iterations (until the configuration began to settle down).

6.4.4.3 Alternative Solar Array Concepts

Two different configurations for stowing solar arrays (on the Atlas I) were investigated (figs. 6.25 and 6.26). Both

schemes employed the same sized arrays and used identical deployment mechanisms with one exception. The configuration shown in figure 6.25 requires a torsional spring for canting, whereas the concept in figure 6.26 does not. However, the concept shown in figure 6.26 contributes to unsymmetric mass properties during powered flight, but deploys the arrays into the canted position naturally. Both concepts are feasible, and in fact, remarkably similar. However, only one concept could be selected for COLD-SAT feasibility and the symmetric concept (figure 6.25) was selected.

6.4.5 SUMMARY OF SUBSEQUENT ACTIVITIES

Using the initial COLD-SAT configuration on an Atlas I as a baseline, subsequent iterations refined the configuration. After the tank and component sizes were relatively firm, additional detail was added. For example, the structural system was added, plumbing trays and valve panels were added, interface panels for fill/drain and electrical connections were added, the alignment and orientation with the launch pad was established, the propulsion system was consolidated in the spacecraft's aft end, etc. Twenty-odd iterations later, the final COLD-SAT concept for the Atlas launch vehicle arrived.

TABLE 6.22.—INITIAL ATLAS COMPONENT CHARACTERISTICS

Item	Description	Size, in.	Volume	Weight, lb	Quantity
1	Tanker tank	6-ft-4-in. diameter by 6-ft-1-in. long elipsoidal heads	145 ft ³	414 Tank	1
2	Depot tank	2-ft-1.5-in. diameter by 4-ft-3-in. long hemispherical heads; 4-in. insulation all around	20 ft ³	660 Liquid hydrogen 100	1
3	Orbit transfer vehicle	2-ft-7-in. diameter by 2-ft-6.25-in. long elipsoidal heads; 2-in. insulation all around	10 ft ³	83	1
4	Helium pressurant	2-ft-2-in. sphere (2000 psia, 540 °R, 2.47 lb/ft)	5.3 ft ³	57 tank	4
5	Hydrazine sphere	1-ft-10.125-in. sphere	3.2 ft ³	6.9 Gaseous helium 17.25	4
6	Hydrogen system (accumulator)	2-ft-2-in. sphere	5.3 ft ³	57	1
7	Batteries	16 by 15 by 9	2160 in. ³	102	2
8	Sequencers	11 by 8 by 11	968 in. ³	51/45	2
9	Flight computers	15 by 10 by 12	1800 in. ³	25	2
10	Data storage units	10 by 16 by 10	1600 in. ³	19	2
11	Control data units	12 by 8 by 10	960 in. ³	15	2
12	Command decoder	10 by 8 by 10	800 in. ³	10	1
13	Radiofrequency processing box	10 by 10 by 4	400 in. ³	5	1
14	Remote data units	8 by 12 by 10	960 in. ³	15	3
15	Power control	12 by 10 by 12	1440 in. ³	32	1
16	Reaction wheels: roll, pitch, and yaw	16-in. diameter by 5-in. long	1183 in. ³	21	4
17	Attitude control electronics	8 by 11 by 14	1232 in. ³	18	2
18	Propellant distribution assembly	20 by 6 by 12	1440 in. ³	10	1
19	High-gain antenna	24-in. diameter by 12-in. deep	-----	17	1
20	Antenna gimbal motor	8 by 6 by 6	288 in. ³	5	1
21	Transponders	14 by 6 by 6	504 in. ³	14	2
22	Earth sensors 1 and 2	3-in. diameter by 5-in. long	35.4 in. ³	2	2
23	Coarse Sun sensor 1 and 2	3 by 1 by 3	9 in. ³	1	2
24	Fine Sun sensor 1 and 2	3 by 1 by 3	9 in. ³	1	2
25	Gyro assemblies 3-200F	12 by 9 by 12	1296 in. ³	37	1
26	Hydrogen system (vaporizer)	2-ft-2-in. sphere	5.3 ft ³	57	1
27	Solar panels	2 ft 9 in. by 9 ft 10.75 in.	27.2 ft ²	21.5	10
28	Low-gain antenna	-----	-----	2	2
29	Electronics-Earth sensors 1 and 2	7 by 3 by 6	126 in. ³	4	2
30	Electronics coarse Sun sensors 1 and 2	4 by 6 by 7	168 in. ³	3	2
31	Electronics-fine Sun sensors 1 and 2	4 by 6 by 7	168 in. ³	3	2
32	Uplink formatter 1 and 2	8 by 8 by 3	192 in. ³	9	2
33	Flow meter electronics box	15 by 7 by 12	1260 in. ³	15	2
34	Experiment signal conditioning box (transducer)	12 by 7 by 7	588 in. ³	15	2
35	Experiment signal conditioning box (data)	12 by 7 by 7	588 in. ³	20	2
36	Rocket engine modules 1 to 4 (4 thrusters)	10 by 8 by 4	320 in. ³	8	4
37	Rocket engine modules (4 thrusters)	10 by 4 by 4	160 in. ³	2	2
38	Rocket engine module 7 (4 thrusters)	10 by 4 by 4	400 in. ³	8	1
39	Hydrazine pressurant (gaseous helium)	19-in. sphere (low pressure)	2.08 ft ³	7.75	2
40	Power distribution box	12 by 8 by 5	480 in. ³	25	1
41	Ordnance control box	4 by 5 by 4	80 in. ³	5	1
42	Rocket engine module	10 by 4 by 4	160 in. ³	-----	2
44	Hydrazine pressurant (gaseous helium)	15.8-in. sphere	1.24 ft ³	21.5	2

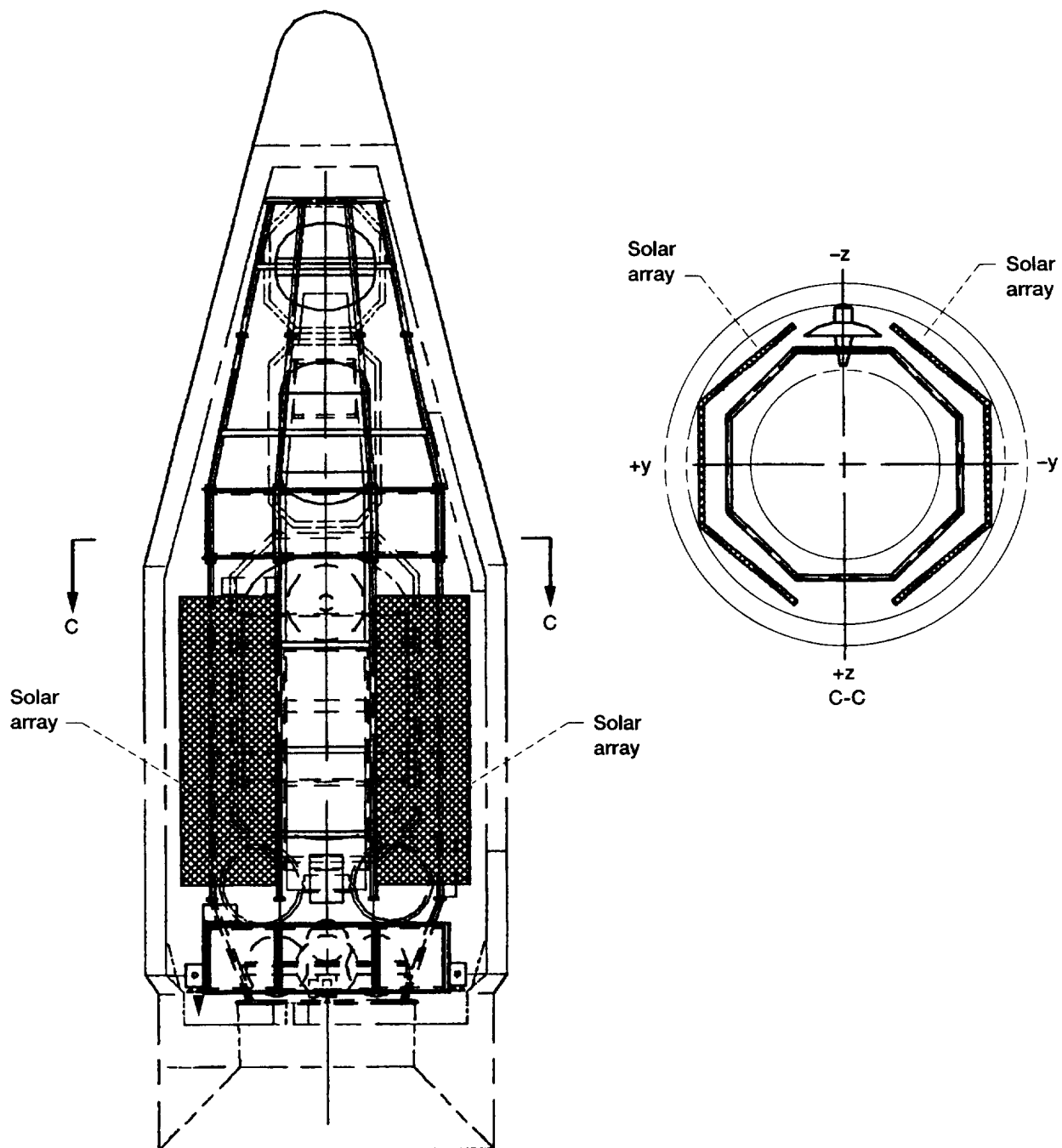


Figure 6.25.—COLD-SAT Atlas I solar array configuration.

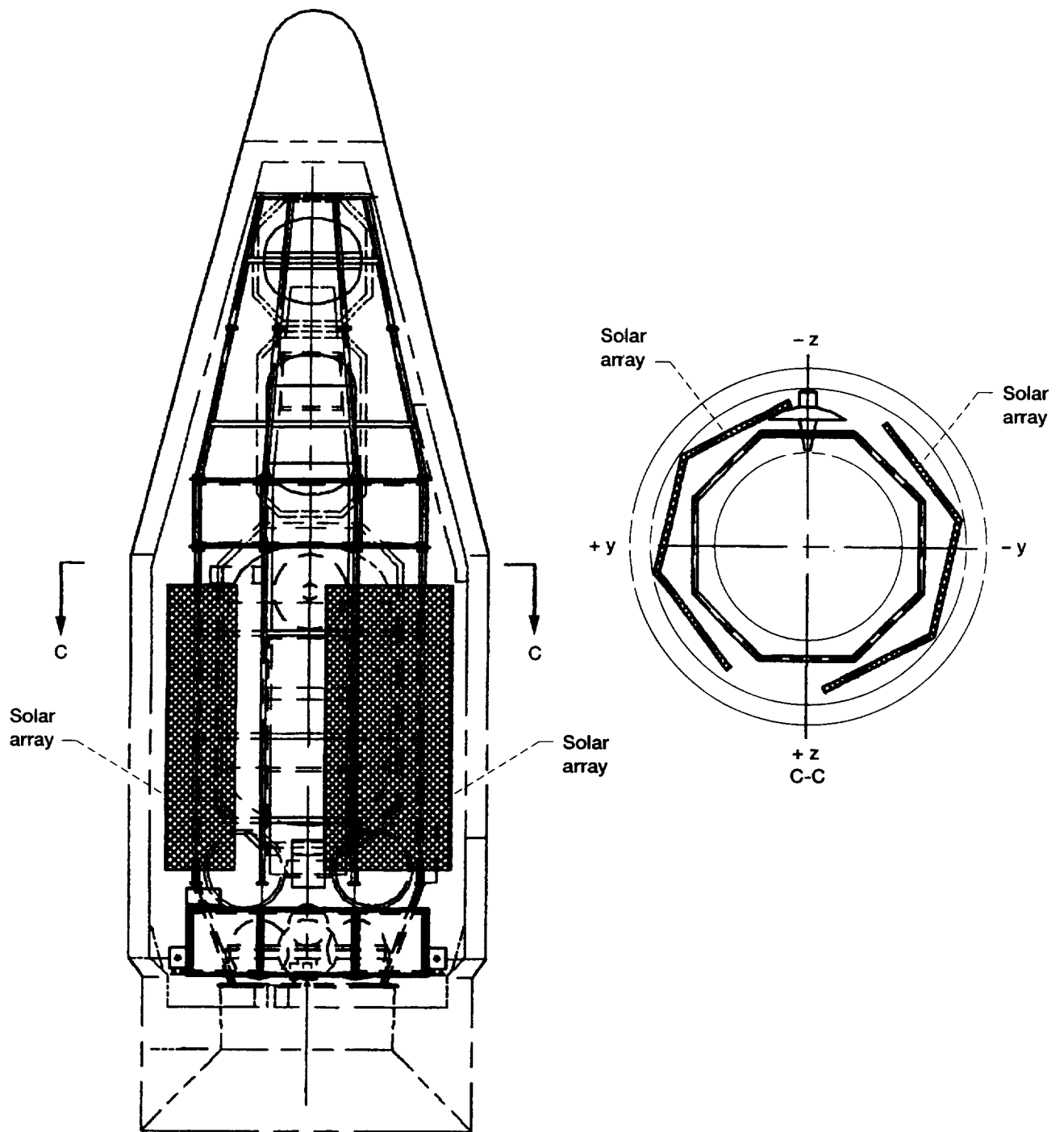


Figure 6.26.—Alternative Atlas I solar array configuration.

6.5 Supporting Analyses

This section describes some of the trade studies and analyses conducted in establishing COLD-SAT's Atlas I configuration and structural system. Topics investigated pertain to spacecraft balancing, sensor field of view, longeron sizing, hydrazine support plate sizing, payload adapter, and vee-band clamp.

6.5.1 SPACECRAFT BALANCING AND BALLASTING

During the development of COLD-SAT, the spacecraft was balanced periodically to insure the spacecraft CG was within launch vehicle and attitude control restraints. Balancing consisted of arranging the spacecraft components so that the spacecraft's axial CG and lateral CG offset were minimized and also complied with restraints. A reduced lateral CG offset reduces the hydrazine consumption and helps minimize products of inertia terms which contribute directly to the gravity gradient torques (GGT) acting on the spacecraft.

The spacecraft's lateral CG offset is strongly influenced by the arrangement of the boxes within the electronics bays. The major concentrated masses on the spacecraft are distributed symmetrically about the x-axis: three major experiment tanks are aligned along the spacecraft longitudinal axis (centerline); the four supply tank pressurant bottles and four hydrazine bottles are located equal distances radially away from the spacecraft's centerline and are equally spaced with respect to each other. The location of the nonsymmetric components (e.g., high-gain antenna) are relatively fixed. Consequently, by arranging the boxes in the electronics bays, the lateral spacecraft CG could be closely aligned with the spacecraft centerline. This exercise was performed with much success on several occasions (with various configurations). The mass properties of the spacecraft after realignment are identified in section 6.7, Operation, of this report.

The spacecraft's axial CG location was always a major concern during the initial stages of the feasibility study. During the first phase of the feasibility study, when COLD-SAT used the Delta launch vehicle, the configuration exceeded the allowable published axial CG restraint. Only after increased CG allowables were published by the Delta launch vehicle developer and enormous pressure placed on the system engineers for lighter systems did the axial CG issue resolve itself. However, the axial CG issue reappeared with the Atlas I because the major experiment tanks were stacked vertically on axis. The specified length-to-diameter ratios created longer tanks which were adjusted (lengthened) to capitalize on the volume within the payload fairing. Throughout the feasibility study, the spacecraft mass and CG location were constantly calculated and compared with the launch vehicle constraint. In addition, a 20 percent weight margin on dry spacecraft weight was allocated for COLD-SAT's growth from feasibility to actual hardware. To help insure the lowest possible axial CG, cross

sections of COLD-SAT's configuration were evaluated to insure that the greatest weight per vertical inch of spacecraft components were at the aft end of the spacecraft and that this number decreased as one ascended the spacecraft. This is illustrated in figure 6.27 (without structure).

A ballast analysis was conducted to minimize the disturbance torques on the spacecraft. The ballast analysis determined the ballast magnitude, the ballast locations, and the effectiveness in reducing the product of inertia terms which contribute directly to gravity gradient torques. The objective of the spacecraft ballast is to eliminate or very nearly eliminate the products of inertia terms. The results of the ballast analysis were forwarded to the attitude control system engineers to aid their decision process pertaining to which attitude control system to use for COLD-SAT.

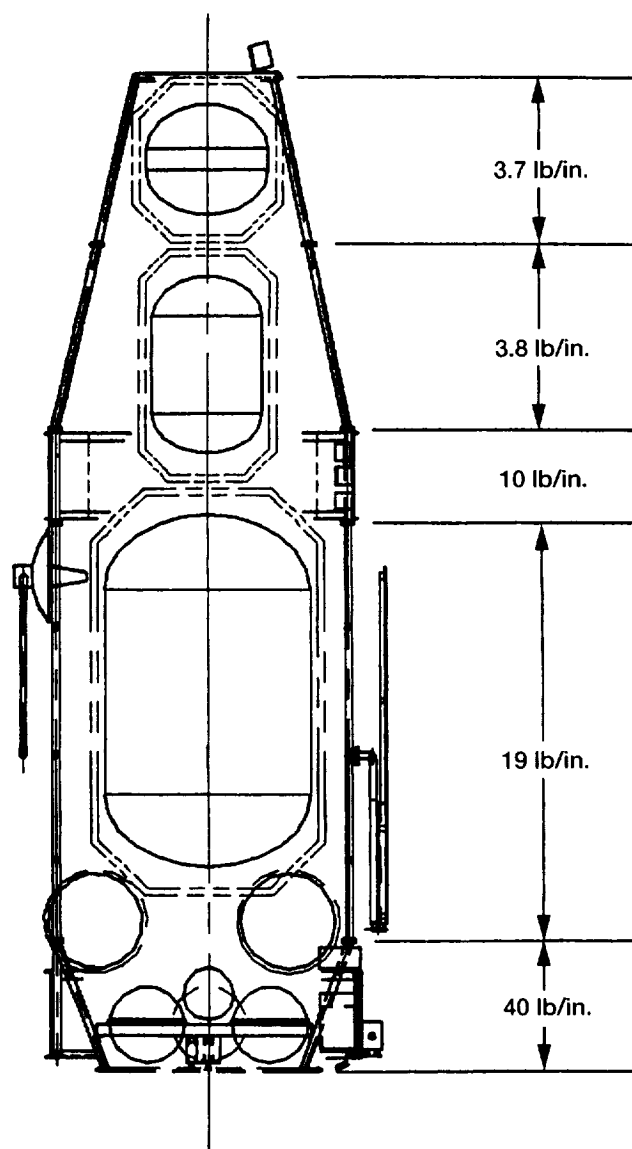


Figure 6.27.—COLD-SAT weight distribution.

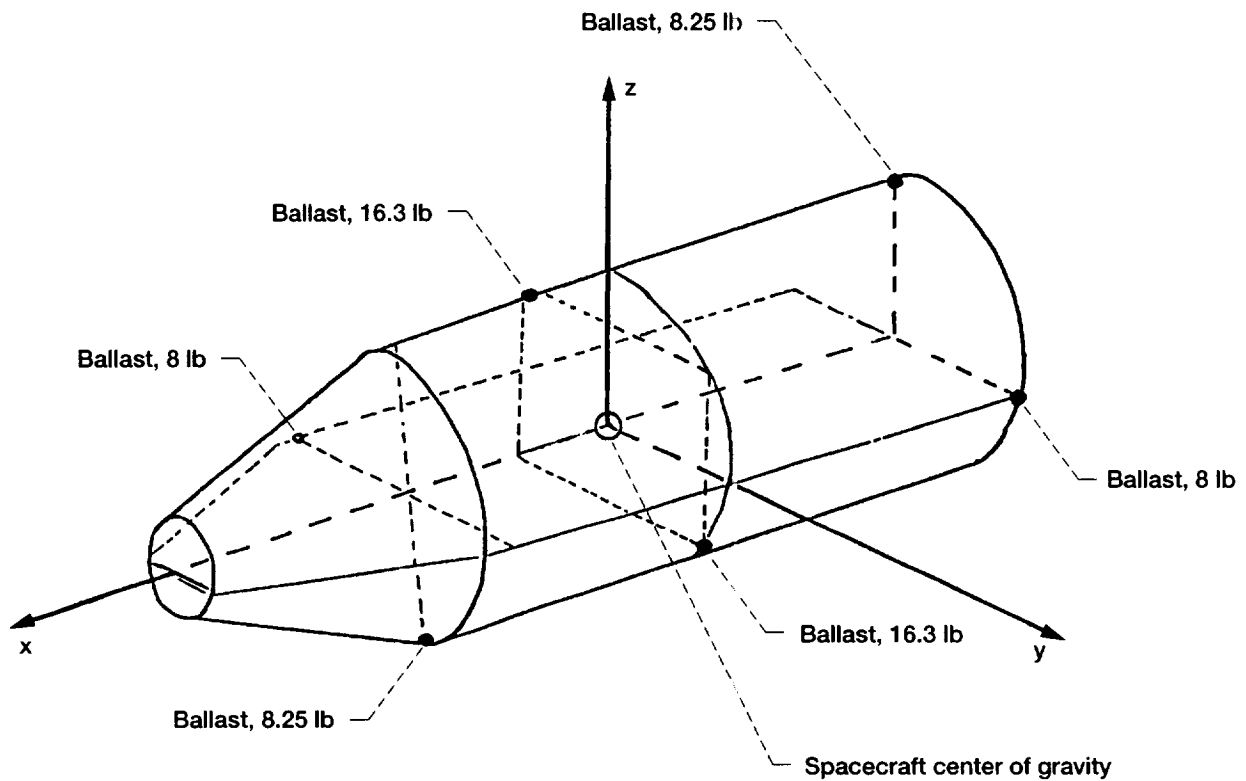


Figure 6.28.—Ballast locations.

The ballast magnitude was calculated so that it could be added to the spacecraft weight (65 lb). The ballast location was determined to insure volume availability within the spacecraft configuration (fig. 6.28).

6.5.2 SENSOR FIELD OF VIEW

The field of view (FOV) for the horizon and Sun sensors was investigated to insure that they were not obscured by the solar arrays or any other components. Figure 6.29 illustrates the available FOV for the horizon sensor in a two-dimensional sense. The minimum FOV requirement is satisfied for both sensors. The horizon sensor requires that unobstructed half-angles of 45° and 46° are available. The Sun sensor requires a unobstructed half angle of 16° and that is readily available. Hence, COLD-SAT's configuration is in compliance with the FOV requirements. A two-dimensional analysis was used to compute the available 46° FOV for the horizon sensor. A more accurate three-dimensional analysis would have resulted in an even larger computed FOV.

6.5.3 SOLAR ARRAY MOUNTING

The alternative mounting methods for the solar arrays are described in section 6.4.4.3, Alternative Solar Array Concepts, of this report, and will not be further elaborated upon here.

6.5.4 EXPENDABLE LAUNCH VEHICLE (ELV) INTERFACE

Two ELV interfaces, the spacecraft adapter and vee-band clamp, required investigation and are discussed below.

6.5.4.1 Spacecraft Adapter

The spacecraft adapter, which is the hardware interface between the spacecraft and the launch vehicle, was structurally sized by General Dynamics (ref. 3), the ELV contractor (see figure 6.30). The adapter was sized based on a spacecraft weight of 8078 lb (which is heavier than the current spacecraft, 6456 lb, even when margin is added) and CG 101 in. forward of the spacecraft separation plane (which is nearly the same as COLD-SAT CG location, 104 in.). Conservatively ignoring post-buckling load capability, the skin was sized for local buckling using a criterion of no buckling at ultimate. For these assumptions, a skin thickness of 0.090 in. was required. Ring sections were sized for twisting loads caused by load path eccentricities. Conservatively ignoring the stiffness contribution of the skin, sections sized for twisting strength required more material than existing adapter rings. Angle of twist may prove to be a more critical criterion for the ring gripped by the vee-band clamp, but allowable rotations are yet to be determined. Additional details can be found in reference 3, the final report for the General Dynamics COLD-SAT Feasibility Study.

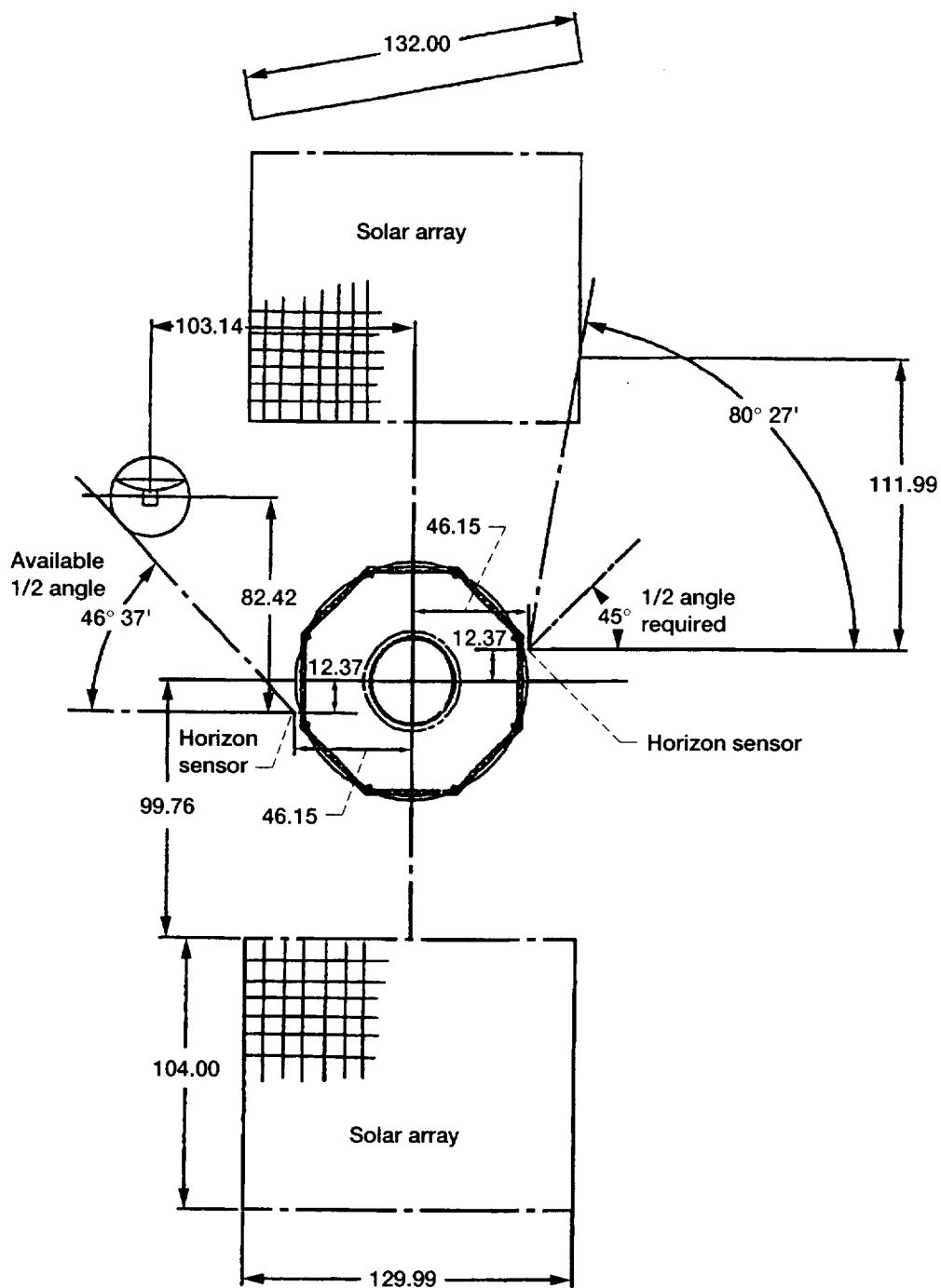
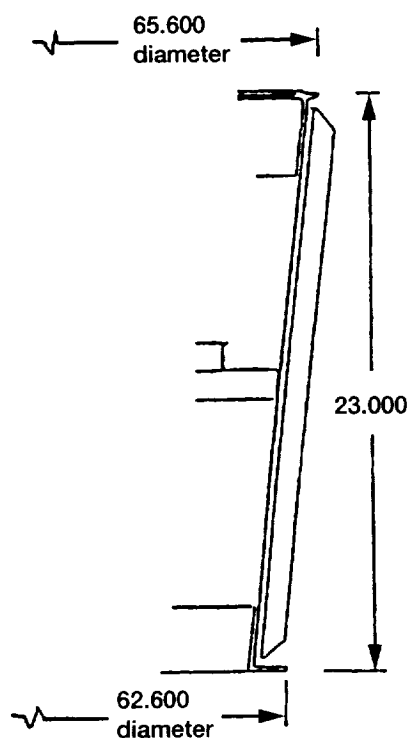


Figure 6.29.—Horizon sensor locations and unobstructed view. Dimensions are in inches.



Part	Weight, lb
Forward ring	28.35
Intermediate frame	5.74
Aft ring	13.60
Skin	22.69
Stringer (30)	19.92
Fasteners	7.48
Electrical disconnects	4.80
Total weight	123.10 (102.58 + 20 percent margin)

Figure 6.30.—Spacecraft adapter.

6.5.4.2 Vee-Band Clamp

Analysis by General Dynamics (ref. 3) indicates that an existing qualified vee-band clamp from Saab has sufficient strength to serve COLD-SAT's requirements. The vee-band clamp is used to hold the spacecraft onto the spacecraft adapter until separation. The loads acting on the clamp were calculated based on the predicted spacecraft weight plus 20 percent contingency. Tension loads acting normal to the plane of the clamp are the most critical, and side-load bending moments are the source of these loads. Loads at the interface plane were calculated for the maximum side-load condition, BECO/BPJ (booster engine cut off/booster pod jettison). See reference 3 for more details.

6.5.5 SPACECRAFT STRUCTURE

A number of studies were performed to assist in the design of the structural system. These studies addressed longeron cross-sectional properties, material selection, sizing of the primary structure, and sizing of the honeycomb plate that supports the hydrazine bottles. Details of these studies are found below.

6.5.5.1 Structural Member Shape

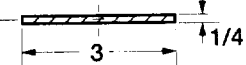
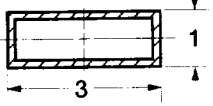
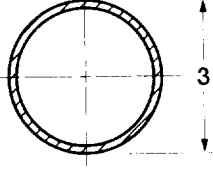
A trade study was conducted to evaluate the relative advantages of different longeron cross sections for the spacecraft's

primary structure. The cross sections were investigated with respect to their axial load capability, bending resistance, and weight-per-unit gross section. Three different configurations were investigated: a solid rectangular cross section, a rectangular hollow cross section, and a hollow circular cross section. Table 6.23 summarizes the results of the trade study.

For comparison basis, each cross section was normalized with respect to width and was limited to off-the-shelf hardware. A solid rectangular cross section, 3-in. wide and 0.25-in. high, was selected as the baseline cross section. This was compared to the 3-in. by 1-in. hollow rectangular cross section and a 3-in. diameter tube. Notice that the 3-in. width is common to every cross section and provides a common baseline for comparison. The 1-in. height was selected for the rectangular hollow cross section because it was the shortest 3-in. wide off-the-shelf cross section found. The tube's wall thickness was calculated such that its area moment of inertia term was identical to that of the hollow rectangular cross section, thereby establishing another basis of comparison between those two cross sections.

The cross sections were evaluated based on axial load resistance, bending resistance, and weight and the results are shown in table 6.23. Table 6.23 illustrates that the hollow rectangular cross section can withstand 15 percent less axial load, 2800 percent more bending load, while being 15 percent lighter than the baseline solid rectangular cross section. The hollow circular cross section, on the other hand, can withstand 87 percent less axial load, 2800 percent more bending load,

TABLE 6.23.—STRUCTURAL SYSTEM CROSS-SECTION INVESTIGATION RESULTS

Ring cross section	Section properties			Comments
	Area, in. ² (axial load)	Inertia, in. ⁴ (buckling)	Weight, lb/ft	
	0.75	0.0039	0.0735	Reference Proposed for Delta configurations
	0.6364 -15 percent	0.113 2800 percent	0.0624 15 percent	Off-the-shelf hardware Base on width for Delta configurations
	0.101 -87 percent	0.113 2800 percent	0.0099 87.00 percent	Representative Same area moment of inertia as hollow rectangular tube

while being 87 percent lighter than the solid cross section. The comparison between the two hollow cross sections reveal that the cross sections are identical in bending resistance. However, the circular cross section is 84 percent lighter, but can withstand 84 percent less axial load than the rectangular cross section. Since the bending resistances are the same, COLD-SAT's longerons for initial sizing would be selected on the basis of weight. Thus, the lighter tubular cross-section was selected. Note however, if the need arises the cross-sectional configuration can readily be changed in the COLD-SAT structure.

Obviously, the results from this trade study were not all inclusive, but do indicate general trends for particular cross sections. It should also be noted that a square hollow cross section (which was not investigated as part of the study) provides greater bending resistance for the same weight and axial strength when compared to a hollow circular cross section. So, if problems arise "downstream," other cross sections can be considered as a viable alternative.

6.5.5.2 Material Selection

A material selection trade study was conducted for COLD-SAT's structural system. The trade study consisted of two parts. First, determining the parent material for the primary structure, and then, the specific alloy and temper. The first phase of the trade study established the parent material. The criteria employed for evaluating the parent materials includes flight history, ability to be easily manufactured, strength-to-weight ratio, relative expense, etc. Because of the relatively high density of steel and the excessive cost of high-technology materials, aluminum was the obvious choice for the parent material. Aluminum has several advantages, including an extensive flight history, high strength-to-weight ratio, ease of fabrication, diversity of form, low density, ready availability, and relatively

low cost. The second phase of the material selection trade study determined the specific aluminum alloy and temper combination for the primary structure. Several different specific alloy/temper combinations were investigated including 5083-T0, 5083-H112, 6061-T0, 6061-T6, 2219-T0, 2219-T6, and 2219-T87. Each combination was evaluated for strength (yield and ultimate), fracture toughness, density, stress corrosion cracking, corrosion ratings, hydrogen embrittlement rating, weldability, formability, and common forms. The trade study results are summarized in table 6.24.

After considering several well-qualified candidates, aluminum 6061-T61 was selected for COLD-SAT's structural system for this conceptual design. Aluminum 6061-T61 has several excellent qualities including weldability, formability, stress corrosion resistance, and hydrogen embrittlement rating. The mechanical strength properties are also considered adequate. The only drawback to 6061-T61 occurs when the material is welded. The parent material immediately adjacent to the weld (i.e., in the heat-affected zone) changes state because of the high temperature from welding. The material within the heat affected zone assumes the annealed condition (6061-T0). The annealed material still retains the excellent characteristics (weldability, etc.), however the mechanical strength properties decline. A listing of material properties for 6061-T0 and 6061-T6 are provided in table 6.25. It should be noted that aluminum alloys with greater mechanical strength post-welding could have been selected for COLD-SAT's structural system, however for a feasibility study a conservative approach was deemed appropriate.

Therefore, to demonstrate feasibility of COLD-SAT's structural system, the material used for primary structure is 6061-T61 and sized using the 6061-T0 properties. If a problem were to develop in subsequent analyses, one option for relief would be changing the material.

TABLE 6.24.—COLD-SAT MATERIALS INVESTIGATION

Property ^a	Aluminum alloy and temper						
	5083-0	5083-H112	6061-T0	6061-T6	2219-0	2219-T6	2219-T87
Ultimate (ksi)	40	40	22	42	32	54	63
Yield-tension (ksi)	18	18	12	35	16	36	51
Yield-compression (ksi)	18	18	NA	35	NA	38	52
Young's modulus (psi × 10 ⁶)	10.2	10.2	9.9	9.9	10.5	10.5	10.5
KiC (ksi(in.) ^{1/2})	NA	NA	NA	27	NA	NA	32.5
Density (lb/in. ³)	0.096	0.097	0.098	0.098	0.102	0.102	0.102
Thermal expansion coefficient (1/°F)×10 ⁻⁶	13.2	13.2	12.75	12.75	12.4	12.25	12.25
Thermal conductivity, (Btu/hr-ft-°F)	67.5	67.5	104.2	89	99	72	72
SCC rating	B	A	A	A	A	A	A
Corrosion rating	B	B	B	B	B	B	B
Hydrogen embrittlement rating	A	A	A	A	A	A	A
Weldability	Excellent	Excellent	Excellent	Excellent	Good	Good	Good
Formability	Excellent	Excellent	Excellent	Excellent	Fair	Fair	Fair
Common forms	All	All	All	All	All	All	All

^aRoom temperature.TABLE 6.25.—MATERIAL CHARACTERISTICS OF 6061 ALUMINUM^a

Property	Temper	
	6061-T0	6061-T6
Ultimate (ksi)	22	42
Yield-tension (ksi)	12	35
Yield-compression (ksi)	NA	35
Young's modulus (psi × 10 ⁶)	9.9	9.9
KiC (ksi (in.) ^{1/2})	NA	27
Density (lb/in. ³)	0.098	0.098
Expansion coefficient (1/°F)×10 ⁻⁶	12.75	12.75
K (Btu-ft/hr-ft ² -°F)	104.2	89
SCC rating	A	A
Corrosion rating	B	B
Hydrogen embrittlement rating	A	A
Weldability	Excellent	Excellent
Formability	Excellent	Excellent
Common forms	All	All

^aRoom temperature.

TABLE 6.26.—COMBINED DESIGN LOAD FACTORS

Load condition	Direction	Combined loads, g
Launch	Axial	2.7
	Lateral	1
Flight winds	Axial	2.5
	Lateral	1.6
Booster engine cutoff (BECO) (maximum axial)	Axial	6
	Lateral	0.5
Booster engine cutoff/booster pod jettison (BECO/BPJ) (maximum lateral)	Axial	3.5
	Lateral	2
Sustainer engine cutoff (SECO)	Axial	2.4
	Lateral	0.3
Main engine cutoff (MECO)	Axial	4.5
	Axial	2
	Lateral	0.5

6.5.5.3 Methodology for Sizing Structural Members

A sizing analysis was performed for the longerons in the structural system. The longerons were sized for yield strength, ultimate strength, and buckling on a per module basis using hand calculations. It should be noted that the sizing analysis was not complete at the conclusion of this feasibility study, however it was complete enough to demonstrate feasibility of the structural system and to establish a reasonable weight for the structural system. More refined analyses will be conducted in later phases.

The sizing analysis for the structural system was conducted in a series of steps. First, the preliminary design load factors were established in the axial and lateral directions for the different flight events during powered flight. The static and dynamic load factors (described in section 6.3.1.6.1, Load Factors, of this report) were combined to form the total load factors in those axial and lateral directions (see table 6.26). The total load factors were then multiplied by the appropriate ultimate and yield safety factors (identified in section 6.2.5.4,

Factors of Safety, of this report) to establish the load to be applied to the structure for each flight event.

The second step in the sizing analysis is to develop a series of ball and stick models that represent that portion of the spacecraft seen at specific interfaces (fig. 6.31). The models allow one to determine the maximum axial, bending, and shear load at each module interface. A ball (lump mass) and stick model was developed at the base of each module (5 models in total). The weight of the ball (lumped mass) represents the weight of the spacecraft above the interface being modeled. The height of the stick represents the height of the axial CG of the portion of spacecraft above the interface being evaluated (fig. 6.31).

For example, the small receiver tank module is represented by a ball and stick model cantilevered from the interface between the large and small receiver tank modules. The height of the stick is equal to the height of the CG of the spacecraft mass above the interface being investigated (i.e., to the CG height of the small receiver tank module above the interface).

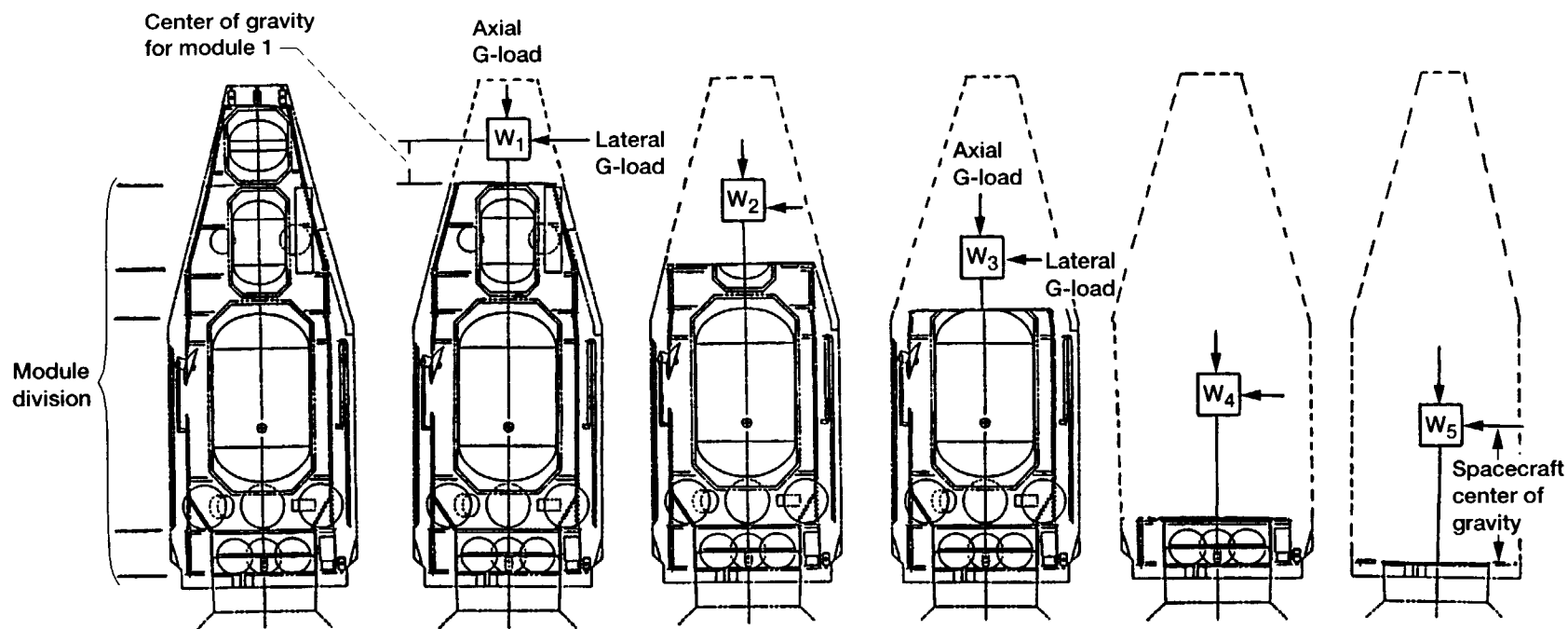


Figure 6.31.—Ball and stick models for module interfaces.

The weight of the ball is equal to the weight of that portion of the spacecraft above the interface (i.e., the weight of the small receiver tank module). Similarly, for the large receiver tank module, another ball and stick model is formed. This time the weight of the ball (lumped mass) is equivalent to the weight above the large receiver tank/electronics bay 2 interface (i.e., the weight of the large and small receiver tank modules combined). The height of the stick is equal to the height of the CG of all components in these two modules.

The reference plane for the stick model is always at the base of the module being analyzed. As one works down the spacecraft, a similar procedure is used for each module. For the last module (electronics bay 1), the ball and stick model is again formed at its base (the spacecraft's separation plane). The lump mass is equivalent to the spacecraft weight above this juncture (i.e., total spacecraft weight) and the stick height is equal to the CG of the weight above this juncture (i.e., the spacecraft CG).

The third step in the sizing analysis is to apply the total load factors (in the lateral and axial direction) to the ball and stick models which then produces the maximum axial force and bending moment for each model (see the resultant loads steps in fig. 6.32).

The fourth step in the sizing analysis is to determine the peak load on a longeron within each module. The axial load produces a uniform compressive load around the entire perimeter of the spacecraft structure. Each longeron equally resists the compression force so the load seen by each longeron is uniform and relatively straightforward. The peak load from the bending moment is a little less straightforward. The bending moment results in a force distribution that adds to one portion of the axial load and subtracts from another (see the distributed loads steps in fig. 6.32). For sizing, the worse-case loads are needed (axial combined with worst-case bending). The bending moment was integrated to find the peak load for a particular longeron. This load from the bending moment was added to the axial load to form the total compressive load acting on a longeron.

The fifth step of the sizing analysis determines the minimum longeron cross-sectional properties required to prevent failure based on the worse-case compressive load (calculated above). In effect, the minimum cross-sectional properties that prevent yielding and buckling are calculated for both the applied load and the longeron length and configuration. The sizing criteria used for these calculations are shown below.

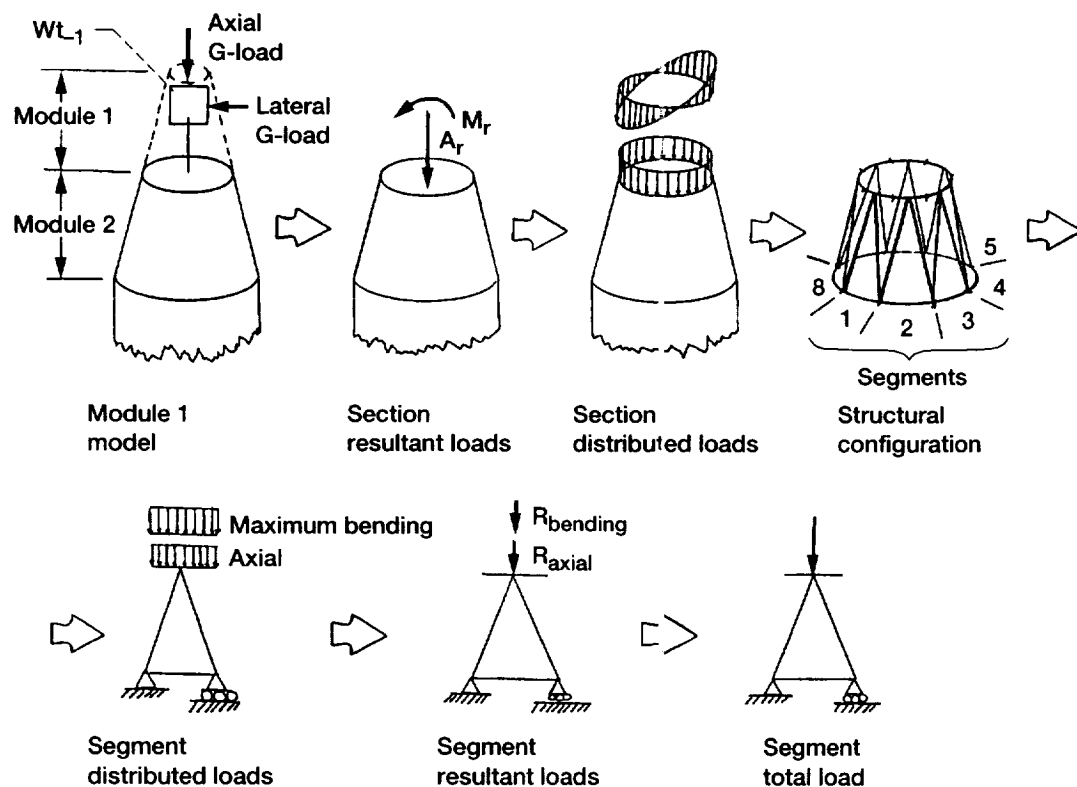


Figure 6.32.—Sizing methodology.

Yield/rupture:

$$A_{\min} = P/S_{YLD/ULT}$$

Buckling:

$$I_{\min} = P_{CR} (0.707L^2)/\pi^2(E)$$

where

A_{\min}	Minimum column area needed to sustain applied load
I_{\min}	Minimum column moment of inertia to resist buckling
P	Applied load to column
$S_{YLD/ULT}$	Allowable strength of column material, either yield or ultimate
P_{CR}	Theoretical maximum load that an initially straight column can support without buckling
$0.707L^2$	Effective column length that accounts for end conditions, assumed somewhere between fixed and pinned end constraints
π	3.14
E	Young's modulus

The criteria used to size the structure included an axial load criteria and an Euler buckling criteria. For the axial load criteria, the minimum cross-sectional area was determined for the worst-case compressive load on the longeron and allowable material property (yield or ultimate strength). For the buckling criteria, the minimum area moment of inertia that prevented buckling was determined from Young's modulus, the effective column length, and the column load. The effective column length was assumed to be 0.707. This is because the end conditions are somewhere between fixed and pinned. Because this assumption is not conservative, a more detailed investigation of the end conditions will occur in the next design phase.

The sixth step of the sizing analysis is to select the longerons with off-the-shelf cross-sectional properties that exceed the properties required to prevent yielding and buckling. A catalog of longerons was used that identified the cross-sectional properties of stock items. The results from this analysis are presented in figure 6.33.

The reader should note that the spacecraft structure has not been thoroughly analyzed and would not normally be during a feasibility study. Future work includes investigation of shear loads at the module interface, investigation of the kick loads between the supply module and the electronics bay 1 module, examination of load uniformity at the spacecraft adapter, investigation of COLD-SAT's fundamental modes of vibration, and extending the sizing analysis beyond a module basis to an integrated spacecraft approach. The hand calculations also need to be validated by a finite element analysis. Despite the work remaining, the author feels comfortable with the system's

present weight allocation, structural configuration, design conservatism, and possible work-arounds if the unexpected occurs. Therefore, the sizing of COLD-SAT's structural system demonstrates a feasible structural configuration and results in enough detail to derive a reasonable weight and complexity factor for the structural system.

6.5.5.4 Sizing of Hydrazine Tank Support Plate

A sizing analysis was performed for the hydrazine support plate located in electronics bay 1 (fig. 6.34). The function of this plate is to support the propulsion system's propellant and pressurant bottles. The plate was sized solely on the basis of axial fundamental frequency (15 Hz) and so on its stiffness in the out-of-plane direction because this was deemed the most significant sizing restraint. This direction is sensitive to vibration because the plate is mass loaded by several relatively heavy hydrazine propellant bottles and because the plate is most flexible in that direction. The plate was sized by hand calculations and the sizing was then verified by using finite element analysis (MSC/NASTRAN).

The octagonal plate is constructed from honeycomb to minimize weight. The plate spans essentially the width of the spacecraft and is perpendicular to the spacecraft's longitudinal axis. The plate's radius is 31 in. (to a flat) and the plate has four symmetric 22-in. recessed holes for mounting the hydrazine propellant bottles. The plate is attached to structural longerons at each corner and is supported along its perimeter with an angled member (fig. 6.34).

The objectives of the sizing analysis are to determine the honeycomb core and facesheet thicknesses required so that the vibration restraint is met, to estimate the plate's mass properties, and to calculate the plate's thickness so that it can be accounted for in the spacecraft configuration.

The hand calculations were made with a number of simplifying assumptions. The plate was assumed to be circular and to have uniform loading smeared over the entire plate (no recessed holes). The mass loading on the honeycomb plate was assumed to be twice the actual load.

Hand calculations determined the plate's fundamental frequency in two ways: (1) using a sandwich construction and (2) by using an equivalent solid plate. By using a sandwich construction, a conservative core thickness for COLD-SAT is 3 in. These calculations were checked by utilizing an equivalent solid plate. The out-of-plane plate frequency for an equivalent solid plate agreed with the one obtained with the sandwich construction.

To verify the hand-calculated vibration predictions, a finite element model was developed of the (equivalent solid) plate. In this case, an octagon configuration was employed rather than a circular plate. NASTRAN's predicted fundamental frequency is very similar to the hand calculations. NASTRAN predicted a first mode of 45 Hz, which was slightly below the hand calculations predicted, 52 Hz. In either case the fundamental

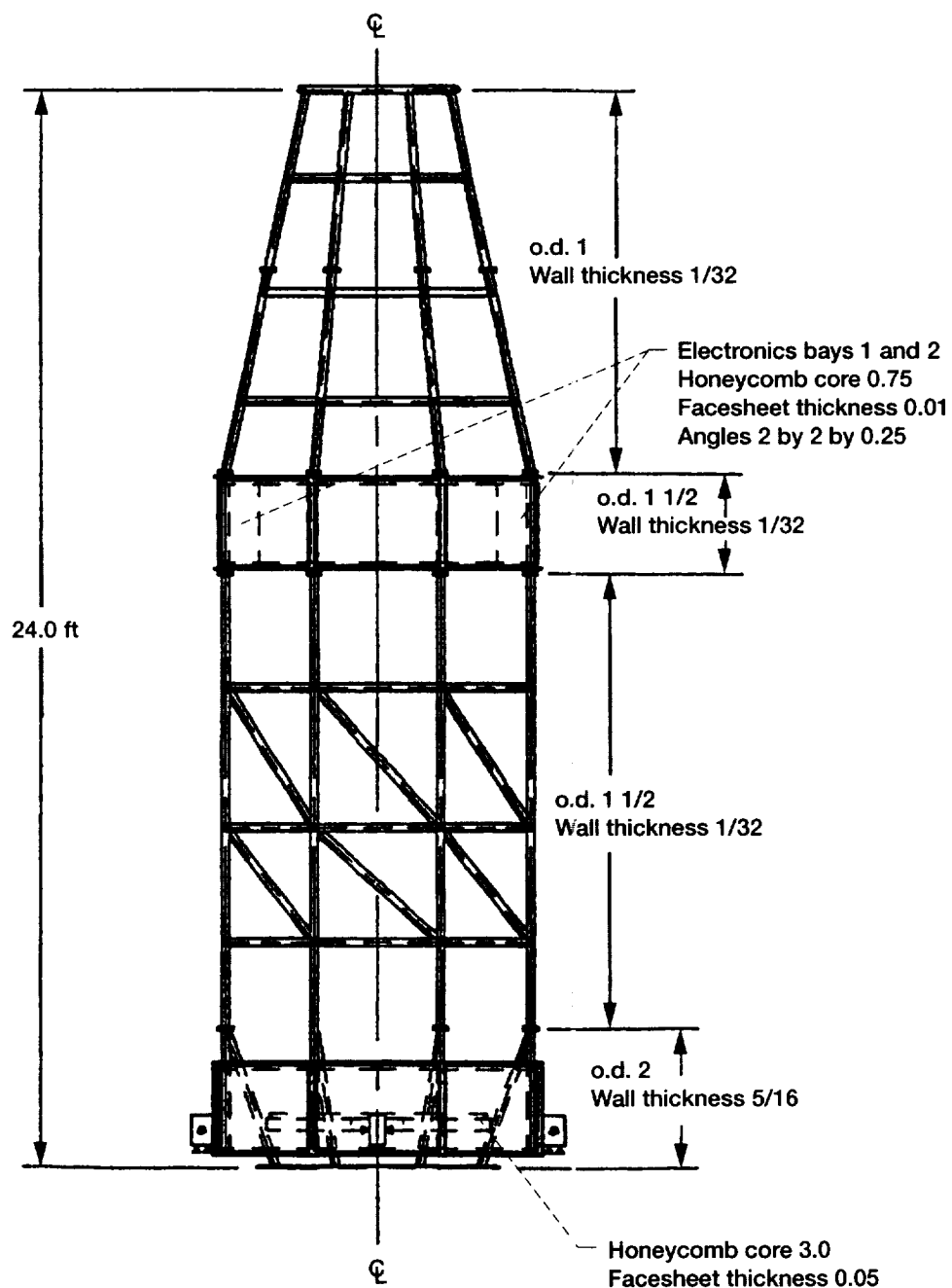


Figure 6.33.—Structural system member sizes (aluminum). Dimensions are in inches except where noted.

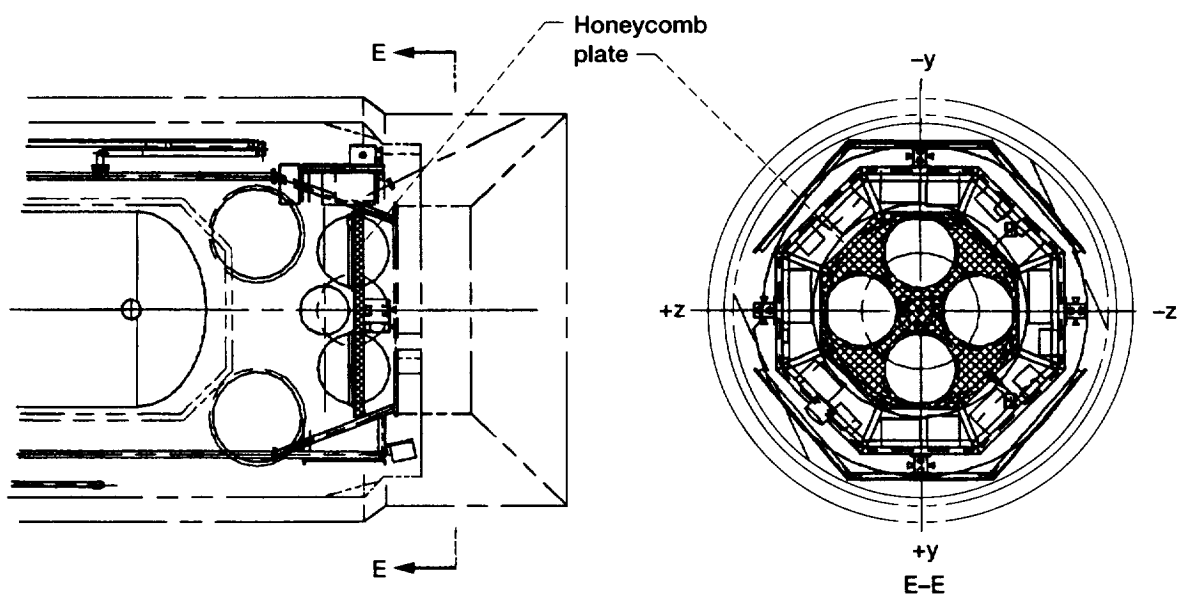


Figure 6.34.—Honeycomb plate.

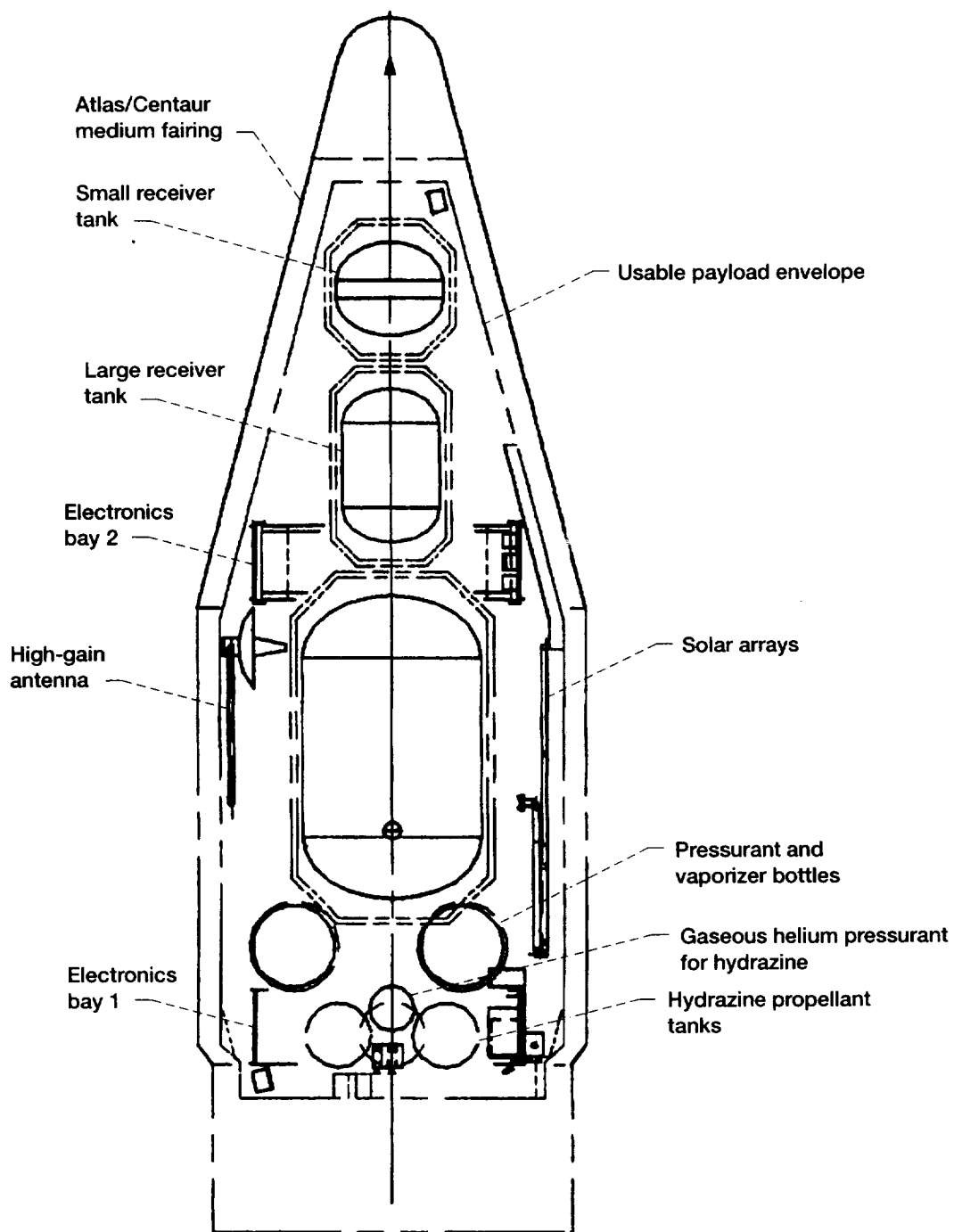


Figure 6.35.—COLD-SAT final configuration.

frequency of the plates significantly exceeds the launch vehicles minimum vibration requirement of 15 Hz. Thus a 23-lb honeycomb plate with a 3-in. core and 0.048-in. facesheets more than adequately meets the vibration requirement (with margin).

6.6 Selected Configuration

This section describes the final COLD-SAT conceptual configuration and structural system. Also included is a discussion of the principles which guided the development of the spacecraft configuration.

6.6.1 PRINCIPLES GUIDING THE CONFIGURATION

A number of ideas have guided the development of the COLD-SAT configuration. Historically, spacecraft have grown significantly in weight and volume from conceptual design to final delivery. To allow for this growth, a weight margin is always carried in the spacecraft mass estimates and the spacecraft layout allocates significant mounting area and volume margin for future growth. In addition, failures are a regular occurrence during assembly, integration, and test. Therefore accessibility and maintainability were constantly considered in defining the configuration. Items considered more likely to require access, such as electronics boxes, are located near the periphery of the spacecraft.

Thermal control is intimately associated with layout on a spacecraft of this type. Warm items such as the electronics boxes and hydrazine tanks are grouped together and isolated from the cryogenic systems. The cryogenic plumbing is grouped together on a cold side radiator tray to minimize heat leaks into the liquid hydrogen tanks.

For spacecraft, development costs regularly exceed hardware costs so maximum use of existing hardware and proven materials and techniques was always a major consideration. The remainder of this section covers, in more detail, some of the goals which strongly influenced the final spacecraft configuration.

6.6.1.1 Minimum Lateral Center of Gravity (CG) Shift

COLD-SAT is configured to minimize its lateral CG shift during spacecraft operations. On orbit, the spacecraft's CG shifts because of fluid movement (i.e., experimentation and/or propellant usage). COLD-SAT's configuration controls the lateral CG shift by component location. Components with consumables are either aligned on the spacecraft longitudinal axis (as in the case of the experiment tanks) or aligned symmetrically with respect to the longitudinal axis and with respect to each other (as in the case of the hydrazine propellant bottles).

This serves to minimize the lateral CG shift (notice that the propulsion system is designed to use its hydrazine supply from all four tanks equally and simultaneously).

6.6.1.2 Control of Axial Center of Gravity (CG) Location

COLD-SAT is configured with the lowest reasonable axial CG because of launch vehicle CG restraints. This goal is achieved by configuring COLD-SAT such that it has its highest density aft and becomes less dense as one proceeds forward in the spacecraft (fig. 6.27).

6.6.1.3 Minimization of Solar Pressure Torques

Solar pressure disturbance torques are minimized by locating the axis of the (deployed) solar arrays through the spacecraft CG. This also enhances the spacecraft symmetry and reduces gravity gradient torques.

6.6.1.4 Control of Moments and Products of Inertia

The gravity gradient torques acting on the spacecraft are proportional to the differences between the moments of inertia and the products of inertia. Differences between moments of inertia are minimized by increasing the mass symmetry of the spacecraft. The products of inertia are minimized by, among other things, the appropriate use of ballast.

6.6.1.5 Large Volume Margin

COLD-SAT tends to be a volume-limited spacecraft within the confines of existing payload fairings. COLD-SAT's configuration preserves a large volume margin for potential growth with respect to mounting surfaces for electronics boxes. Specific uncommitted locations in the electronics bays are carried through the design.

6.6.1.6 Simple Supporting Structure

The COLD-SAT structural configuration is designed to use common materials and proven fabrication and assembly techniques. Off-the-shelf hardware and traditional manufacturing and processes are employed throughout. This approach reduces program cost and risk.

6.6.1.7 Use of Spacecraft as a Sun Shield

COLD-SAT's configuration uses its aft end, electronics bay 1, as a Sun shield to block direct sunlight from impinging on the experiment tanks, particularly the supply tank. This approach minimizes heat leak into the cryogenic tanks and so minimizes liquid hydrogen boiloff.

6.6.1.8 Accessibility

COLD-SAT is configured to provide easy access to components which may require inspection or maintenance during ground testing and pad operations. Accessibility is accommodated by use of a modular design, open structure, valve panels located at the spacecraft's perimeter, removable mounting panels in the electronics bays, and solar arrays that do not completely envelope the spacecraft in the stowed configuration.

6.6.1.9 Summary

A configuration and structural system have been developed for COLD-SAT which meet all requirements and satisfy all interface compatibility constraints. The concepts developed provide a good basis for the continued development of the spacecraft.

6.6.2 FINAL DESIGN

The final spacecraft configuration, structural system, and mass properties are described in this section.

6.6.2.1 Final Configuration

COLD-SAT is 24.8 ft long and 9.6 ft in diameter and fits within the Atlas 11-ft medium payload fairing (fig. 6.35). The prominent components include three experiment tanks (supply, large receiver, and small receiver), four supply tank pressurant bottles, four hydrazine propellant tanks, two electronics bays, two deployable solar arrays, and one high-gain antenna. Additional component details are found in figure 6.36 coupled with table 6.27. In the remainder of this section COLD-SAT's configuration is described on a modular basis starting with the spacecraft adapter.

6.6.2.1.1 Spacecraft adapter.—The spacecraft adapter is the interface hardware between the launch vehicle (Centaur equipment module) and the spacecraft (electronics bay 1 module). The adapter is 23-in. long and slightly conical in configuration (fig. 6.37). COLD-SAT's adapter is a mission-peculiar piece of hardware that is a beefed-up version of an existing flight-qualified design developed by General Dynamics. COLD-SAT's adapter requires strengthening because of the spacecraft's weight and axial CG location. The adapter is of skin-stringer construction with rings at the upper and lower ends. The basic material is aluminum with the skin and stringers made from 2024-T81 sheet, and the rings from 2124-T851 plate.

The hardware device that physically holds the spacecraft adapter to the spacecraft is the vee-band clamp. At spacecraft separation, the vee-band clamp, when signaled, will release by firing pyrotechnic bolt cutters setting the separation springs free to give the necessary separation energy to the spacecraft.

COLD-SAT uses an existing vee-band clamp produced by Saab. The location of the vee-band clamp is at the separation plane shown in figure 6.37 and a typical vee-band clamp is shown in figure 6.9.

6.6.2.1.2 Electronics bay number 1.—Forward of the spacecraft adapter and the vee-band clamp is the COLD-SAT spacecraft itself. COLD-SAT consists of five vertically stacked modules: the electronics bay 1 module, the supply tank module, the electronics bay 2 module, the large receiver tank module, and the small receiver tank module (fig. 6.2).

The module located furthest aft (which interfaces with the spacecraft adapter) is electronics bay 1 (fig. 6.38). This module contains electronics bay 1 as well as the propulsion system (hydrazine propellant tanks, a gaseous helium pressurant bottle, and rocket engine modules). Electronics bay 1 houses a significant portion of the spacecraft's electronics boxes. The box layout is identified in figure 6.39, which includes an allocation for harnessing. Box removal can be achieved by removing the mounting panel (fig. 6.40). The panel labels (N, NW, SE, etc. shown in figure 6.39) are derived from directions with respect to COLD-SAT's attitude. The boxes in the bay (batteries, etc.) can be specifically identified from figure 6.39 coupled with table 6.27.

Physically, the electronics bay 1 module is 37.35 in. high and 88 in. in diameter. The electronics bay portion of the module is a 2-ft high octagonal framed structure that is 85 in. in diameter across a flat. The framed structure uses 21- by 30-in. detachable honeycomb panels for mounting electronics boxes. The volume enveloped by the electronics bay contains four 22-in. diameter hydrazine bottles which store propellant for the propulsion system. The bottles are supported on a 3-in. honeycomb plate that nearly spans the bay and has recessed holes to accommodate the hydrazine bottles. The propellant bottles are located low in the spacecraft because of their weight and within electronics bay 1 to take advantage of the heat radiated from the operating electronics boxes, which provides a warm thermal environment for the hydrazine. This arrangement protects against hydrazine freezing and minimizes required heater power. The bottles are located equal distances from the spacecraft longitudinal axis at 90° intervals to provide mass balance and to minimize lateral CG shift. The propulsion system also requires a 15-in. gaseous helium pressurant bottle for propellant expulsion and this bottle is located immediately adjacent to the hydrazine bottles. This location minimizes the pressurant line length and weight and consolidates the entire propulsion system within one module.

Also attached to the electronics bay 1 module are COLD-SAT's hydrazine thrusters. COLD-SAT has 20 individual thrusters that are used for experiment-induced accelerations and spacecraft attitude control. The thrusters are housed in five rocket engine modules (REM's) which have four thrusters each. Four of the REM's are located around the module's periphery on the spacecraft's $\pm z$ and $\pm y$ axes. The remaining REM is located on the spacecraft's (longitudinal) x-axis.

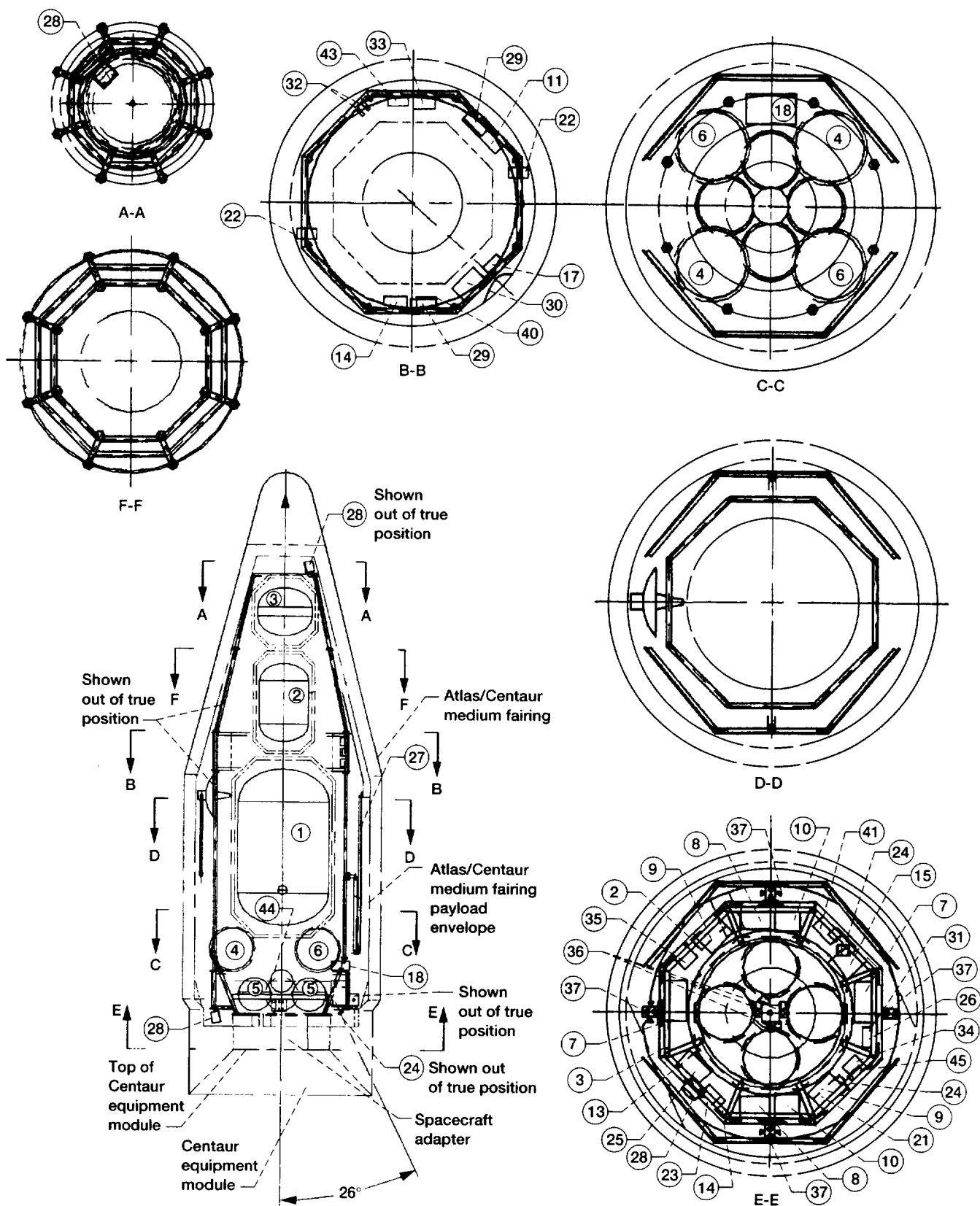


Figure 6.36.—Detailed COLD-SAT final configuration. See table 6.27 for a list of components identified by numbered circles in this figure.

TABLE 6.27.—COMPONENT CHARACTERISTICS FOR FINAL ATLAS CONFIGURATION

Item	Description	Size, in.	Volume	Weight, lb	Quantity
1	Supply tank	5-ft diameter by 8-ft-6.75-in. long ellipsoidal heads	145 ft ³	800 Tank 600 Liquid hydrogen	1
2	Large receiver tank	2-ft-8.5-in. diameter by 4-ft-3.5-in. long ellipsoidal heads; 2-in. insulation all around	21 ft ³	200	1
3	Small receiver tank	3-ft. diameter by 2-ft-7.5-in. long ellipsoidal heads; 2-in. insulation all around	13.5 ft ³	110	↓
4	Helium pressurant	2-ft-6-in. sphere, (2000 psia, 540 °R, 1.35 lb/ft ³)	5.7 ft ³	105 tank 7.4 Helium	2
5	Hydrazine sphere	1-ft-10.125-in. sphere	3.2 ft ³	14.0 tank 150 Hydrazine	4
6	Hydrogen pressurant (vaporizer)	2-ft-6-in. sphere (2000 psia, 540 °R)	5.7 ft ³	170 tank 3.7 Hydrogen gas	2
7	Batteries 1 and 2	16 by 15 by 9	2160 in. ³	85	↓
8	Sequencer 1 and 2	12 by 12 by 9	1296 in. ³	51	
9	Flight computer 1 and 2	12 by 11 by 9	1188 in. ³	35	
10	Data storage unit 1 and 2	10 by 16 by 10	1600 in. ³	28	↓
11	Command and telemetry unit	19 by 9 by 5	855 in. ³	17	1
12	-----	-----	-----	-----	-----
13	Radiofrequency processing box	10 by 4 by 10	400 in. ³	10	1
14	Remote command and telemetry units 1 and 2	12 by 9 by 5	540 in. ³	11	2
15	Power control	10 by 12 by 12	1440 in. ³	32	1
16	-----	-----	-----	-----	-----
17	Attitude control system interface electronics	8 by 15 by 4	480 in. ³	15	1
18	Propellant distribution assembly	12 by 20 by 6	1440 in. ³	15	↓
19	High-gain antenna	27.5-in. diameter by 16-in. deep	-----	16	
20	Antenna gimbal motor	6-in. diameter by 5-in. deep	141 in. ³	5	
21	Transponders 1 and 2	14 by 6 by 6	504 in. ³	14	2
22	Horizon sensors 1 and 2	4.1-in. diameter by 7.9-in. long	102 in. ³	2.5	2
23	Electrically gimbaled thruster	6.5 by 6.5 by 5	211.25 in. ³	4	1
24	Digital Sun sensor 1 and 2	3.3 by 4.3 by 0.94	13.3 in. ³	0.7	2
25	Inertial reference unit assemblies 3-2 DOF	12.25 by 9 by 9	993 in. ³	37	1
26	Motor drive electronics unit	8 by 11 by 6	528 in. ³	11	1
27	Solar panels	3 ft 8 in. by 8 ft 8 in.	31.8 ft ²	35	6
28	Low-gain antenna	7-in. diameter by 5-in. long	192 in. ³	3	2
29	Horizon sensor electronics	10.3 by 5.8 by 4	239 in. ³	7.5	2
30	Mixer motor inverter	12 by 15 by 7	1260 in. ³	7.5	1
31	Sun sensor electronics	4.5 by 7.8 by 2	70.2 in. ³	2.3	2
32	Magnetometers	1.25 by 1.375 by 4	6.93 in. ³	0.33	2
33	Experiment data units 1 to 3	9 by 5 by 5	225 in. ³	7	3
34	Signal condition	7 by 12 by 7	588 in. ³	12	1
35	Data acquisition	7 by 12 by 7	588 in. ³	20	1
36	Rocket engine modules (6 to 8) 1 thruster	3 by 3 by 6	54 in. ³	4	3
37	Rocket engine modules (1 to 4) 4 thrusters	8 by 6 by 10	480 in. ³	8	4
38	Rocket engine module (5) 1 gimbaled thruster	7 by 7 by 10	490 in. ³	15	1
39	-----	-----	-----	-----	-----
40	Power distribution box	8 by 12 by 5	480 in. ³	25	1
41	Ordnance control box	4 by 5 by 4	80 in. ³	5	1
42	-----	-----	-----	-----	-----
43	Accelerometer conditioner	8 by 5 by 4	160 in. ³	6	1
44	Hydrazine pressurant (gaseous helium)	15-in. sphere	1.03 ft ³	15	1
45	Redundancy control unit	6 by 6 by 3	108 in. ³	4	1

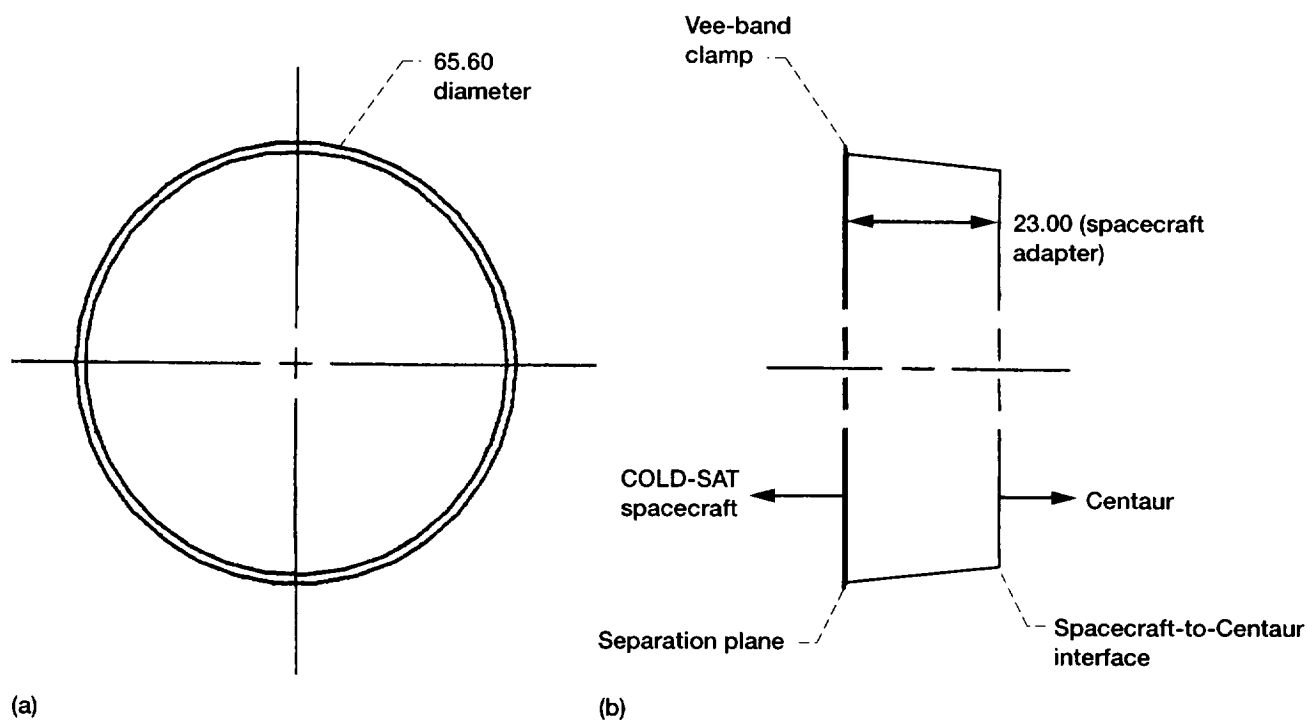


Figure 6.37.—Spacecraft adapter. (a) Top view. (b) Side view. Dimensions are in inches.

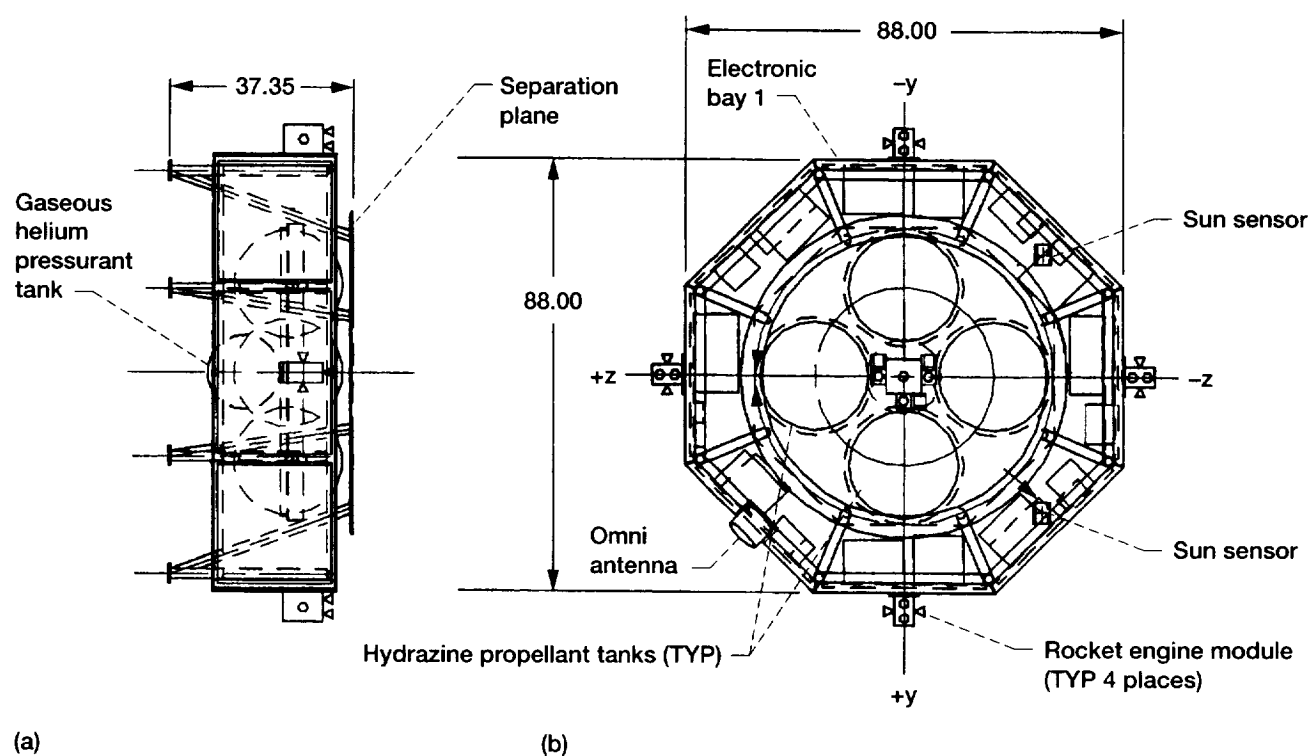


Figure 6.38.—Electronics bay 1 module. (a) Side view. (b) Bottom view. Dimensions are in inches.

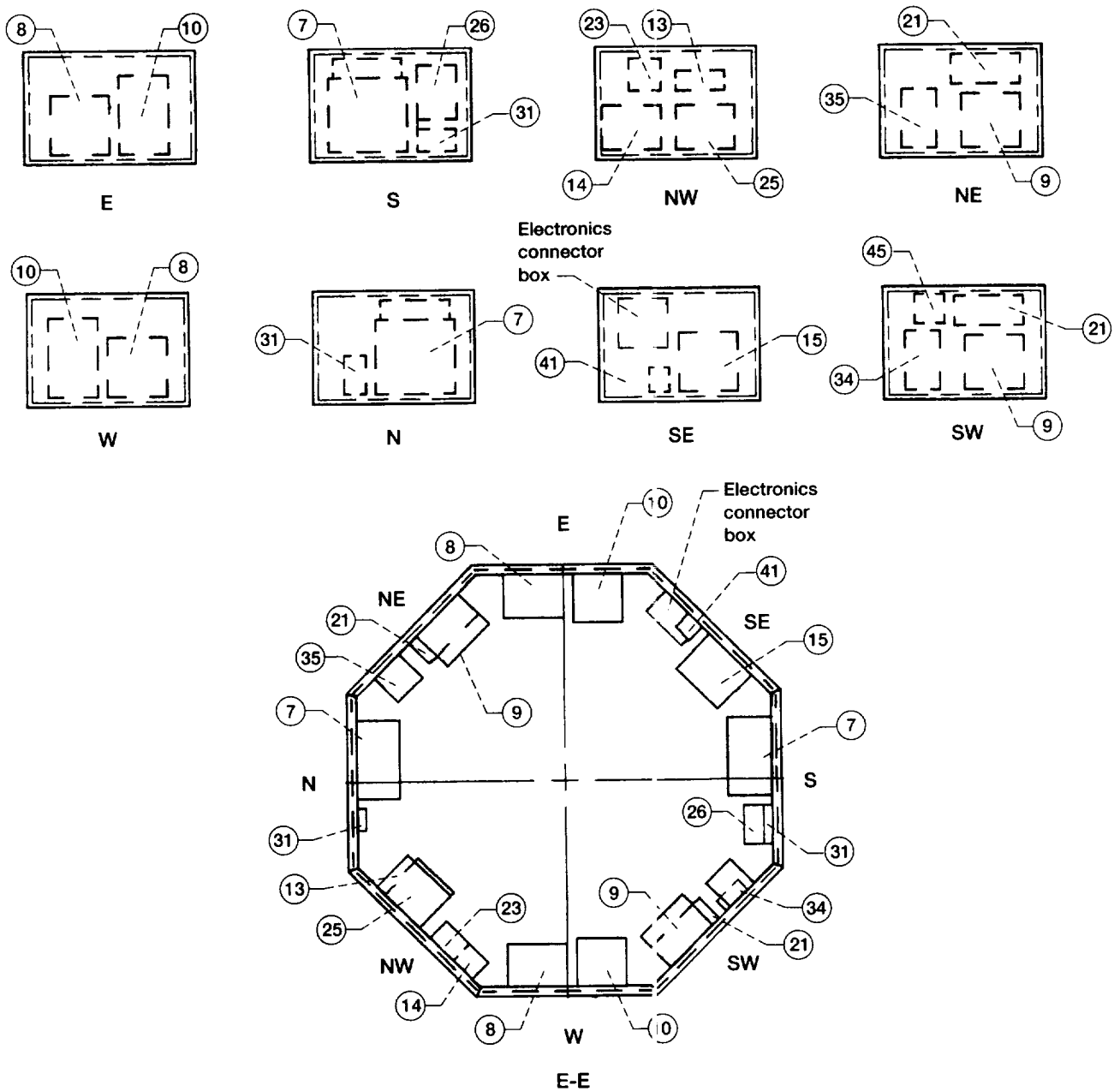


Figure 6.39.—Electronics bay 1. See table 6.27 for a list of components identified by numbered circles in this figure. See figure 6.37 for E-E location.

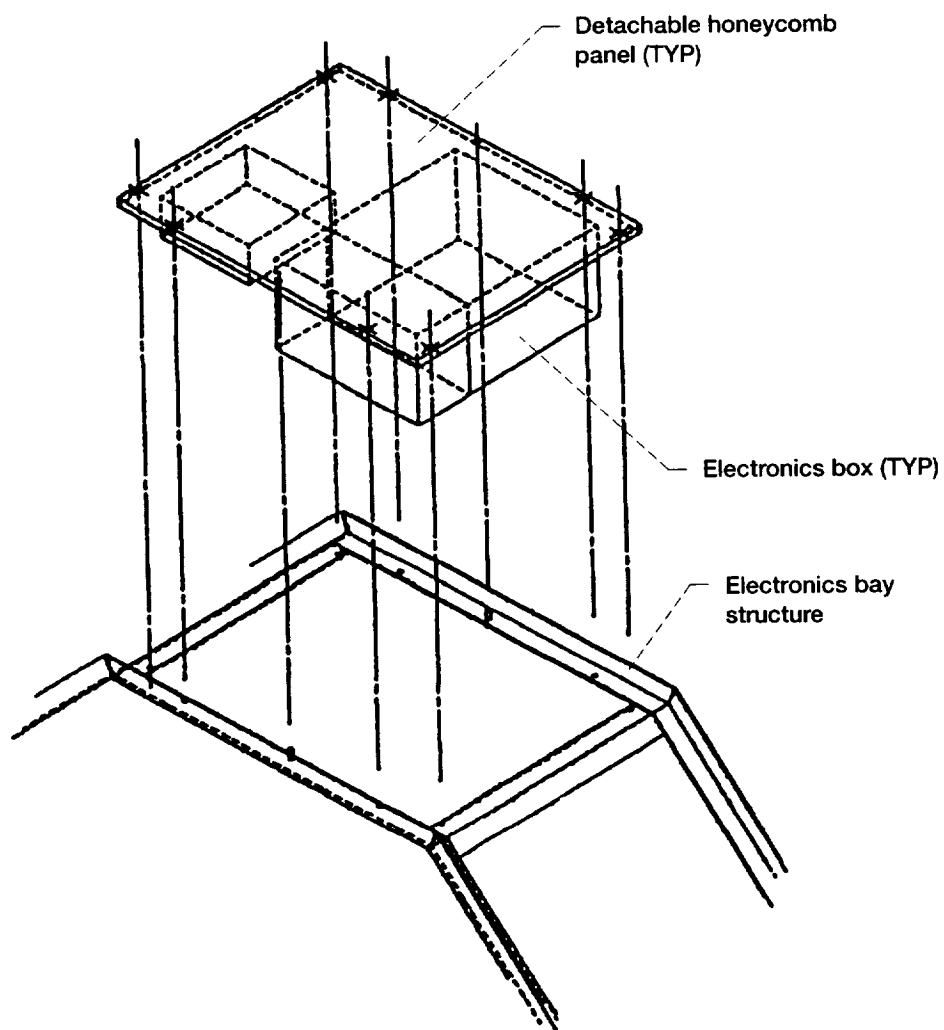


Figure 6.40.—Detachable electronics bay panel.

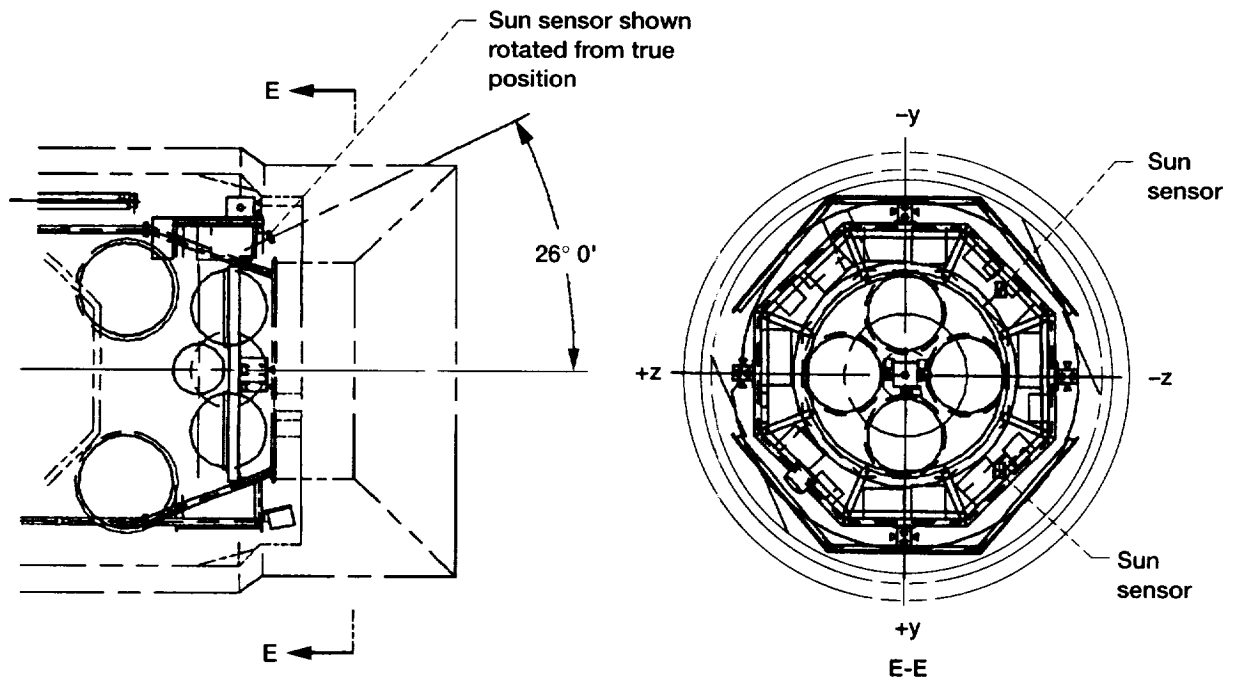


Figure 6.41.—Sun sensors.

Notice that the thrusters aligned along the x-axis are only directed in the $-x$ -axis direction (aft), whereas the other thrusters are directed in both the plus and minus y - and z -axes. To minimize the plume impingement, the thrusters are located on the spacecraft's aft end and on its perimeter. This location not only minimizes contamination, but also provides the largest moment arm, maximizes control torque, and minimizes hydrazine usage.

The electronics bay 1 module contains a hydrazine panel for servicing the propulsion system. The panel is located on the positive y -axis in the top portion of the electronics bay module (fig. 6.14).

The electronics bay 1 module also supports one of two omnidirectional antennas that are used when the high-gain antenna is not deployed or functional (the small receiver tank module houses the other). This low-gain antenna is located on the aft end of the spacecraft such that its operation is not hindered by the solar arrays prior to deployment and by spacecraft attitude. The module contains the two Sun sensors for spacecraft attitude control (fig. 6.41). The Sun sensors are located on the aft end of the spacecraft and are canted at 26.0° to bisect the path of the Sun.

6.6.2.1.3 Supply tank module.—Forward of the electronics bay 1 module is COLD-SAT's largest module, the supply tank module (fig. 6.42). This module is 121.6 in. long and 88.76 in. in diameter. The supply tank module houses the 145-ft³ liquid hydrogen supply tank and its associated pressurant bottles along with spacecraft deployables, a majority of the valve panels, and a portion of the plumbing tray. The four

30-in. diameter pressurant bottles located immediately aft of the supply tank provide pressurant for experiment fluid transfer. They are located aft of the supply tank because of their weight. They are also located symmetrically with respect to the spacecraft longitudinal axis and to each other for mass balance. Two of the pressurant bottles use gaseous helium pressurant and the other two use gaseous hydrogen. The gaseous hydrogen bottles have plumbing internal to their shell so they can generate pressurant gas from liquid hydrogen extracted from the supply tank while in-orbit and thus are referred to as vaporizers. The supply tank is enveloped by an MLI can that simplifies insulation layup. The supply tank and MLI can are located on the spacecraft's longitudinal centerline. Both the experiment tanks and propellant bottles are supported from the spacecraft's outside structure where hardpoints are provided for the tank's mounting struts.

The supply tank module also supports the spacecraft's deployable appendages: the high-gain antenna and the solar arrays. COLD-SAT's high-gain antenna is used to communicate to the ground through TDRSS. COLD-SAT's antenna dish is 27.5 in. in diameter and its final deployed location is over 4 ft from the spacecraft's perimeter where the antenna's line-of-sight to TDRSS is not obscured. The high-gain antenna is attached in the same (spacecraft) y - z plane as the solar arrays, but 90° away so that obstruction of the antenna by the solar arrays is minimized (fig. 6.18).

COLD-SAT's two solar arrays have a total surface area of 190 ft². In the stowed configuration, the arrays are body-wrapped around the spacecraft's perimeter such that their

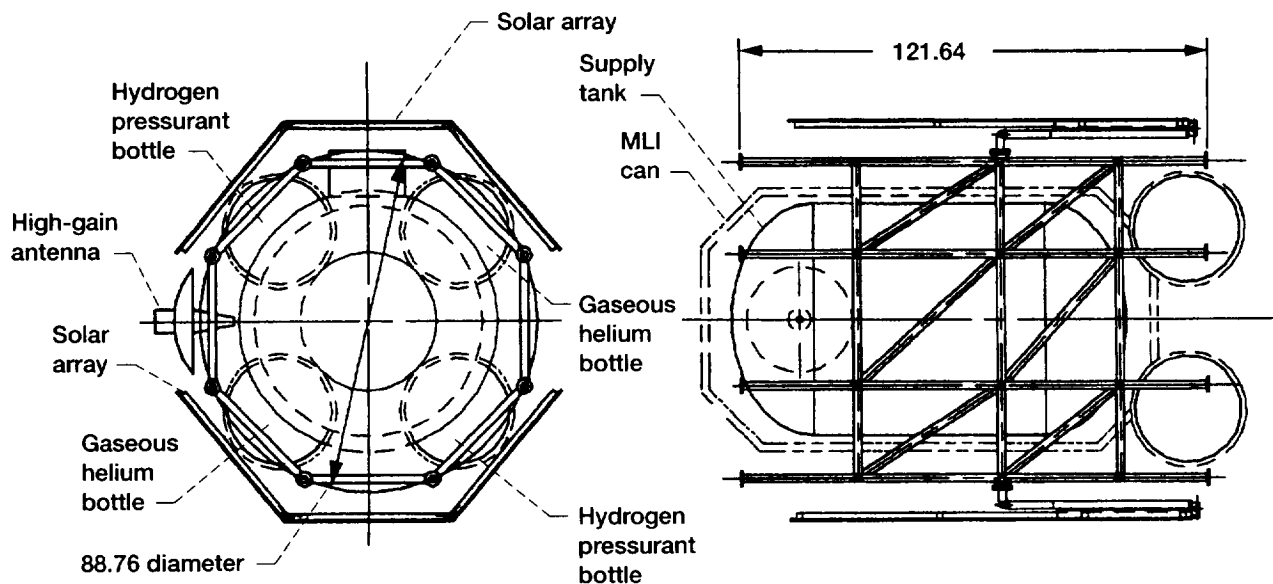


Figure 6.42.—Supply tank module. Dimensions are in inches.

on-orbit deployment is uninhibited. After deployment, the arrays extend a sufficient distance from the spacecraft to minimize the array's radiation view factor to the experiment tanks, particularly the supply tank.

COLD-SAT's solar arrays are based on the arrays used on FLTSATCOM and TDRSS. Similarities include: body-wrapped solar arrays (in the stowed position), two deployable arrays per spacecraft, three rectangular panels per array, and the deployment sequence. In fact, the array size between FLTSATCOM and COLD-SAT are remarkably similar. The arrays are constructed of aluminum honeycomb that is stiffened with a frame of aluminum hat sections on the side opposite the solar cells. Machined aluminum hinges and corner fittings are riveted to the hat sections and the entire frame-hinge-fitting assembly is fastened to the honeycomb with screws into threaded inserts. The differences between the arrays are: (1) FLTSATCOM/TDRSS arrays completely envelope the perimeter of the spacecraft, whereas COLD-SAT's arrays do not and thereby permit access to COLD-SAT's valve panels and plumbing tray located in the open areas (figs. 6.13 and 6.17), (2) FLTSATCOM/TDRSS solar arrays require a solar array drive for articulation, whereas COLD-SAT's arrays do not since they are fixed and, (3) COLD-SAT deployment sequence requires torsion spring motors for canting the arrays (to optimize the sunlight impinging on the arrays), whereas FLTSATCOM does not.

The supply tank module also contains a portion of the plumbing tray (fig. 6.13) and a number of valve panels, namely, vaporizer panels A & B, vent panel A, and the helium panel (a servicing panel) (fig. 6.14). Each one of these panels and trays are located on the spacecraft's perimeter and are accessible after the solar arrays have been mounted on the spacecraft.

6.6.2.1.4 Electronics bay number 2.—Forward of the supply tank module is electronics bay 2. This module is 27 in. high and 88 in. in diameter (fig. 6.43). The electronics bay portion of this module is identical in configuration and construction to electronics bay 1. However, the modules themselves differ significantly because the electronics bay 2 module does not house the propulsion system. In addition the electronics boxes and sensors associated with electronics bay 2 are different from those in electronics bay 1 (fig. 6.44). Electronics bay 2 houses the overflow boxes from electronics bay 1 and also provides a preferred location for some sensors and boxes (e.g., instrumentation data recovery boxes associated with the receiver tanks). Figure 6.44 shows a relatively large amount of unused mounting surface to accommodate spacecraft growth. Electronics bay 2 houses the Earth (horizon) sensors which are directed outward parallel to the spacecraft's z-axis and are required for spacecraft attitude control.

6.6.2.1.5 Large and small receiver tank modules.—Forward of electronics bay 2 are COLD-SAT's last two modules, the large receiver tank module and the small receiver tank module (figs. 6.45 and 6.46, respectively). The large receiver tank module is 54 in. long and 88.76 in. in diameter at its widest point and houses the 21-ft³ large receiver tank. This tank and its associated MLI can are aligned along the spacecraft's longitudinal axis. This module also houses vent panel B which is located on the spacecraft's perimeter along the spacecraft's -z-axis (fig. 6.14). Vent panel B contains valves and other small plumbing components.

The small receiver tank module is 58.55 in. long and 64.16 in. in diameter at its widest point and houses the 13.5-ft³ small receiver tank. This tank and its associated MLI can are aligned on the spacecraft's longitudinal axis. This module also

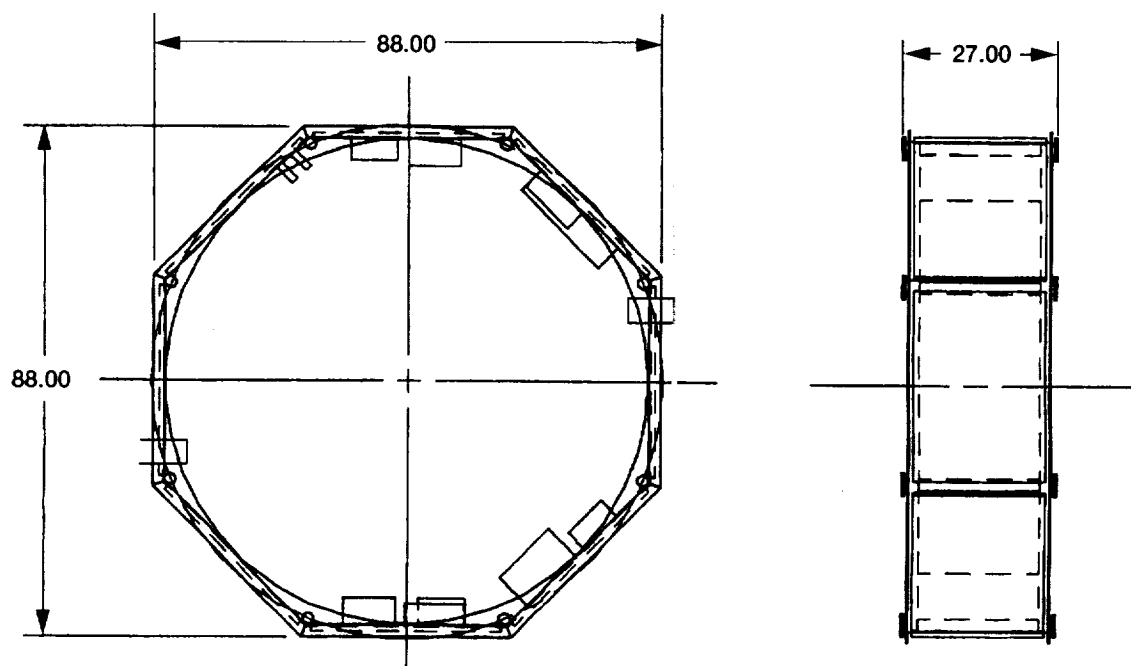


Figure 6.43.—Electronics bay 2 module. Dimensions are in inches.

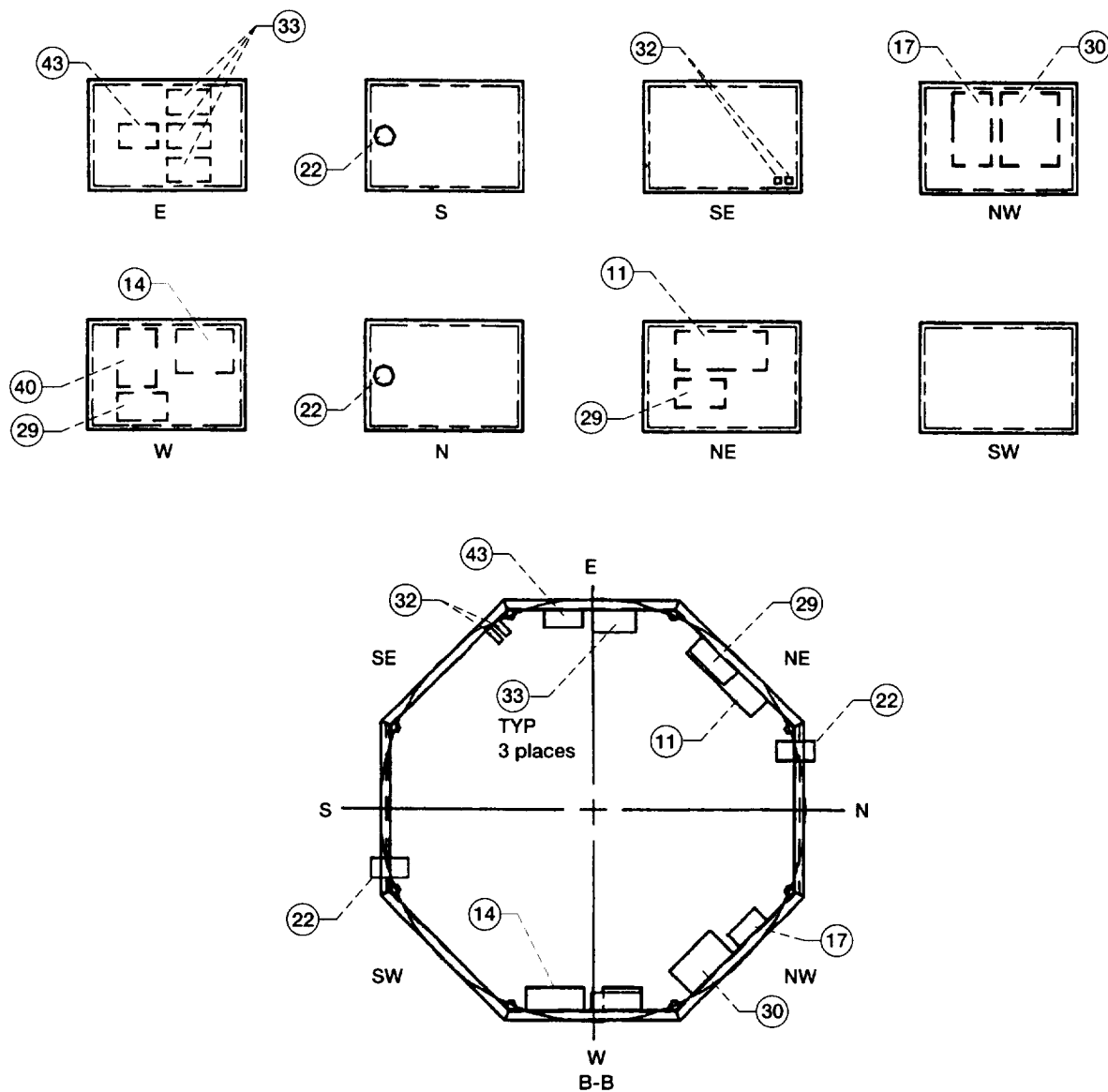


Figure 6.44.—Electronics bay 2 configuration. See table 6.27 for a list of components identified by numbered circles in this figure. See figure 6.37 for B-B location.

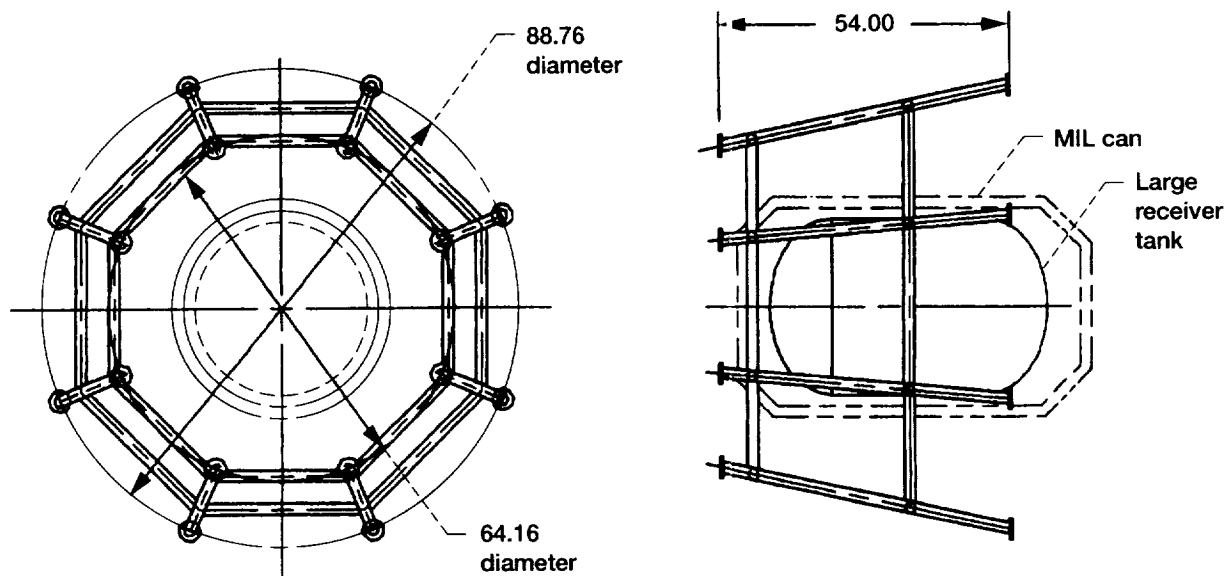


Figure 6.45.—Large receiver tank module. Dimensions are in inches.

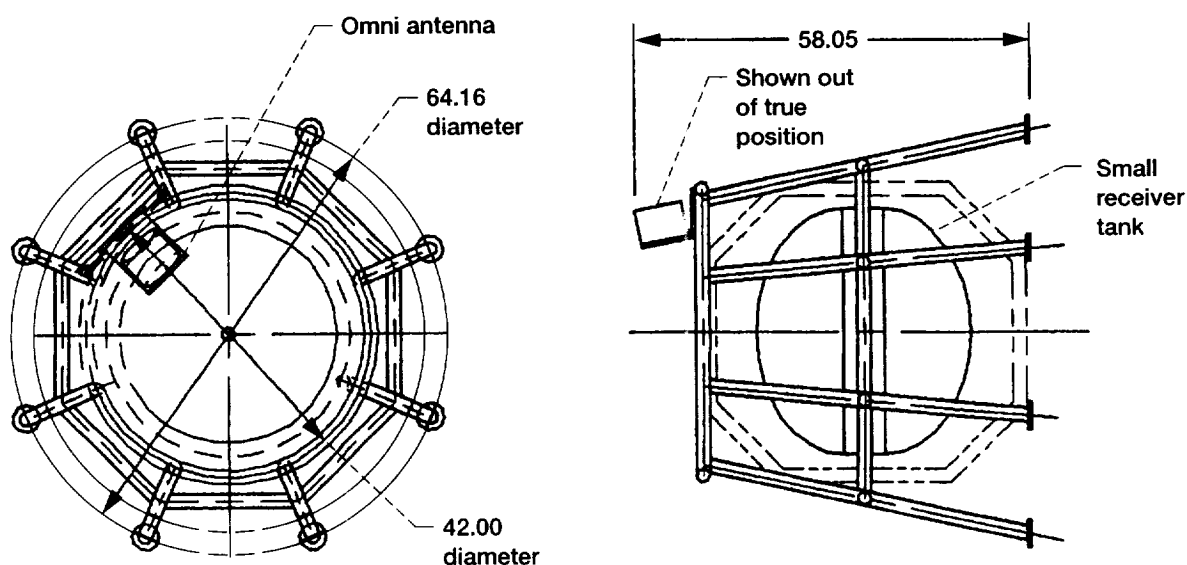


Figure 6.46.—Small receiver tank module. Dimensions are in inches.

houses one of two omnidirectional antennas that are used when the high-gain antenna is not deployed or functional. This low-gain antenna is located on the forward end of the spacecraft so that its operation is not hindered by the solar arrays prior to deployment and by spacecraft attitude.

Both receiver tank modules support a portion of the radiator tray that runs along the +z-axis at the spacecraft's perimeter (fig. 6.13). Also, both experiment tanks are supported by struts that extend from the tank to the spacecraft's outside structure.

The integration of the five aforementioned modules forms the COLD-SAT spacecraft (see fig. 6.1 for an artist's conception).

6.6.2.2 Structural System of Final Configuration

After the spacecraft configuration was firmly rooted, the spacecraft structural design was initiated. The structural system is required to provide the mechanical interface of the spacecraft with the launch vehicle, furnish mechanical support to all spacecraft systems, sustain launch loads, permit access for sensor alignment and component maintenance, comply with the launch vehicle constraints, provide a modular configuration that permits independent tank testing, use low-technology materials and manufacturing processes, minimize heat leak into the experiment tanks, and maximize the tanks' view factors

to deep space for thermal radiation. The structural system that meets these requirements is shown in figures 6.47 and 6.33.

From all these requirements, two were major drivers for the structural configuration, namely the experiment requirements pertaining to minimizing heat leak into the experiment tanks and maximizing experiment tank view factors to deep space. The minimum heat leak into the experiment tanks requirement (coupled with the low technology materials) drove the structural configuration to be an outside structure (i.e., one that envelopes the experiment tanks) thereby providing long conduction paths to the tanks. The other requirement, maximum view factors to deep space, drove the structural configuration to an open configuration, thereby allowing the tanks to "see" deep space. Thus, COLD-SAT's structural system can be referred to as an open-external structure that is constructed from longerons (see fig. 6.1 for artist's concept).

The structural system is required to provide the mechanical interface with the launch vehicle and does this by means of the spacecraft adapter. The adapter is a 23-in. piece of mission-unique hardware that mates between the launch vehicle and spacecraft. COLD-SAT's adapter is a stronger version of an existing General Dynamics design. Preliminary analysis by General Dynamics revealed no problems with COLD-SAT's adapter. Further adapter details can be found in sections 6.5.4.1, 6.3.1.4, and 6.6.2.1, of this report.

The structural system provides mechanical support to the other spacecraft systems. For example, a honeycomb plate is provided for mounting the hydrazine bottles; mounting panels and electronics bays are provided for the electronics boxes. An

outside structure supplies hardpoints for the experiment tank mounting struts, and so forth. The structural system is required to sustain launch loads and other dynamic environments during powered flight. COLD-SAT's structural system was sized to withstand the quasi-static load factors (static and dynamic) recommended for preliminary design. These load factors are expected to envelope maximum expected flight loads. However, in the event they do not, a conservative factor of safety was used to provide additional design margin. Additional details on the sizing analysis, load factors, and factors of safety can be found in sections 6.5.5.3, 6.3.1.6.1, and 6.2.5.4, respectively, of this report.

Figures 6.33 and 6.47 identify the structural system configuration and longeron size for each spacecraft module. The longeron size is derived from the launch loads and the sizing analysis (see section 6.5, Supporting Analyses, of this report). The structural system is sized based on yield strength, ultimate strength, and buckling of the longeron. Figure 6.33 illustrates size of the structural members that preclude these failures with safety factors (see table 6.2). The size of the longerons for the small and large receiver tank module is a 1-in. outside diameter with a 0.0312-in. wall thickness. The longeron size used for the electronics bay 2 module has a 1.5-in. outside diameter and a 0.0312-in. wall thickness. The supply tank module uses the same outside diameter as the electronics bay 2 module, but requires a greater wall thickness (0.1875 in.). The final module, electronics bay 1, uses 2-in. outside diameter longerons with a 0.3125-in. wall. The longerons that comprise the structural system are constructed from off-the-shelf sizes and shapes. The

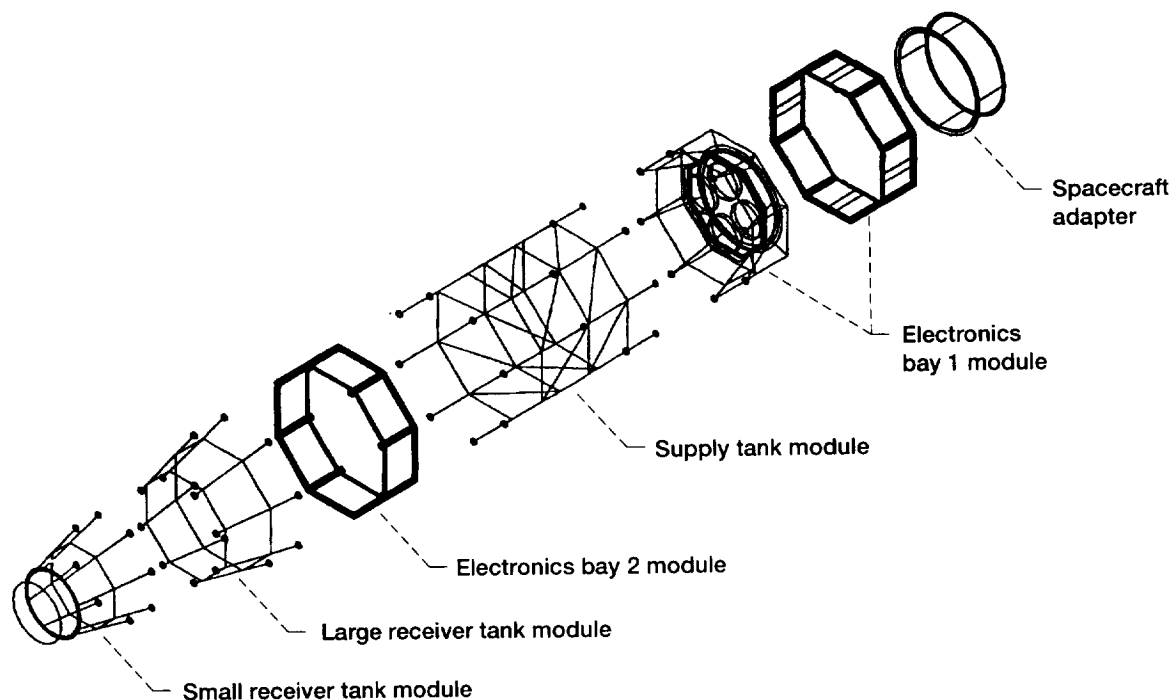


Figure 6.47.—COLD-SAT structural system.

intent was to develop a low-technology and low-cost structural system that fulfills the launch vehicle, program, and experiment requirements.

Included as part of the structural system is the honeycomb plate that supports the propulsion system's propellant supply in electronics bay 1 (figs. 6.47 and 6.34). This plate is octagonal in configuration, constructed from honeycomb, and located perpendicular to the spacecraft's longitudinal axis. The plate radius is 31 in. to a flat and has four symmetrical 22-in. recessed holes for mounting the propellant bottles. The plate is attached to structural longerons at each corner and is supported along its perimeter by an aluminum angled member.

The octagonal plate was sized solely on the basis of stiffness in the out-of-plane direction because this was deemed the most significant sizing restraint. This direction is sensitive to vibration because it is a rather large plate that is mass-loaded by several relatively heavy hydrazine propellant bottles.

The plate characteristics comply with the launch vehicle's minimum frequency requirements of 15 Hz. With a 3-in. thick core and 0.05-in. thick aluminum facesheets it exceeds the minimum vibration requirements. A completed description of the plate and method of analysis is found in section 6.5.5.4. Sizing of Hydrazine Tank Support Plate.

Structurally, the electronics bays are composed of an aluminum frame structure with detachable honeycomb windows (to accommodate box access and maintenance). The frame is constructed from aluminum 6061 and consist of welded support angles to accommodate the 30- by 21-in. detachable (bolted) honeycomb panels. The panels are constructed of aluminum 5052 honeycomb cores with aluminum 2024-T81 facesheets. The specific honeycomb and frame characteristics are summarize in table 6.28. The panel characteristics are based on the Advanced Communication Technology Satellite (ACTS).

The electronics bay frame structure has not been sized, but the weight estimate should be reasonable. The electronics bay frame is not considered part of the spacecraft's primary load path. The bays are attached to the primary structure.

TABLE 6.28.—ELECTRONICS BAY
STRUCTURAL CHARACTERISTICS

Honeycomb	
Cell size	0.125 in.
Cell shape	Hexagonal
Cell thickness	0.007 in.
Density	3.2 lb/ft ³
Plate thickness	0.75 in.
Facesheets	
Material	Aluminum
Size	0.01 in.
Weight	0.098 lb/in. ²
Support angles	
Material	Aluminum
Size	2- by 2- by 0.25-in.
Weight/ft	1.11 lb/ft

6.6.2.3 Mass Properties of Final Configuration

The mass properties of COLD-SAT's final configuration on an Atlas I are discussed below. Mass properties include spacecraft weight, CG location, and mass moment of inertia.

6.6.2.3.1 Weight.—COLD-SAT's launch weight is 6693 lb which includes a 20-percent margin on dry spacecraft weight (see table 6.29). The 20-percent margin is not applied to the consumables because the test fluid quantity is fixed by the experiment requirements, the spacecraft design, and the available volume within the payload fairing. The 20-percent margin was derived from historical data (i.e., the average growth of past flight programs) from conceptual design to final hardware. Notice that a 65-lb ballast weight is included in COLD-SAT's weight estimate. The ballast weight minimizes the spacecraft's disturbance torques. COLD-SAT's weight is described on a component level in table 6.30.

6.6.2.3.2 Center of gravity (CG).—COLD-SAT's CG is identified in table 6.31 (COLD-SAT's coordinate system is shown in figure 6.4). The reference plane for the spacecraft's axial CG is the top of the Centaur's equipment module.

COLD-SAT's weight and CG are required to be within the launch vehicle's allowable range. This range is dictated by the Centaur equipment module. Figure 6.48 shows that COLD-SAT falls within the allowable range and meets the launch vehicle (equipment module) requirement. In fact, figure 6.48 shows that COLD-SAT has an additional 20-percent margin by weight (assuming the same spacecraft CG) or 26-percent margin by CG (assuming the same spacecraft weight).

TABLE 6.29.—COLD-SAT MASS PROPERTIES

System	Weight, lb
Experiment (dry)	2206
Structure	680
Thermal	62
Power	690
Attitude control	79
Propulsion (dry)	158
TT&C	427
Ballast	65
Total, dry spacecraft	4367
20 percent margin (dry)	873
Hydrazine (maximum)	600
Propulsion pressurant (gaseous helium)	3.5
Liquid hydrogen	565
Gaseous hydrogen	7.4
Gaseous helium	17.4
Total, wet spacecraft	6434
Adapter and clamp	159
Total spacecraft weight	6593
Centaur batteries	75
Inadvertant separation destruct system	25
Total lift weight	6693
Vehicle allowable (18°)	7430
Launch margin	737

TABLE 6.30.—DETAILED COLD-SAT MASS PROPERTIES

Component or assembly	Hardware weight (dry), lb	Consumables (wet), lb	Component or assembly	Hardware weight (dry), lb	Consumables (wet), lb	Component or assembly	Hardware weight (dry), lb	Consumables (wet), lb
Experiment system			Propulsion system			Structural system		NA
Supply tank	890	565	Hydrazine propellant tank 1	14	150	Primary structure	581	
Large receiver tank module	207	NA	Hydrazine propellant tank 2			Antenna boom	9	
Small receiver tank module	178	NA	Hydrazine propellant tank 3	↓	↓	Solar array arms	20	
Gaseous hydrogen supply	426	7.4	Hydrazine propellant tank 4			Secondary structure	60	
Helium supply	188	17.4	Gimbal unit and electronics	10	NA	Array deployment mechanics	10	
Fluid interface system	271	NA	Hydrazine pressurant tank (15-in.)	23	3.5	Total structure weight	680	
Experiment system electronics			Propellant distribution assembly	19	NA			
Mixer motor	7.5		Rocket engine modules (2)	16		Thermal control system		
Experimental data unit 1	7		Rocket engine modules (2)	16		MLI blankets, velcro, adhesive	30	
Experimental data unit 2	7		Rocket engine module	8		OORS	5	
Experimental data unit 3	7		Miscellaneous hydrazine components	10		Thermal controllers	8	
Signal conditioner box	12		Subtotal	158	603.5	Temperature sensors, thermistors	5	
Accelerometer conditioner	6		Total propulsion weight	761.5	NA	Heaters and adhesives	2	
Subtotal	2206.5	589.8				Paint	3	
Total experiment weight	2796.3	NA	Telemetry, tracking, and command			Tape	1	
			Flight computer 1	35		Thermal interface (chotherm)	5	
Attitude control system			Flight computer 2	35		Thermal isolators (G-10)	3	
Horizon sensor 1	2.5		Sequencer 1	51		Total thermal weight	62	
Horizon sensor 2	2.5		Sequencer 2	51				
Sun sensor 1	0.7		Data storage unit 1	28		Power system		
Sun sensor 2	0.7		Data storage unit 2	28		Battery 1	85	
Inertial reference unit	37		RF processing box	10		Battery 2	85	
Horizon sensor electronics 1	7.5		Remote command and telemetry unit 1	9		Solar array 1	105	
Horizon sensor electronics 2	7.5		Remote command and telemetry unit 2	9		Solar array 2	105	
Sun sensor electronics 1	2.3		Command and telemetry unit	17		Power control box	32	
Sun sensor electronics 2	2.3		High-gain antenna	17		Power distribution box	25	
Attitude control system interface electronics	15		Antenna gimbal motor	5		Ordnance control box	5	
Magnetometer	0.33		Low-gain antenna 1	2		Harness/cables/connector	248	
Magnetometer	0.33		Low-gain antenna 2	2		Total power weight	690	
Total attitude control weight	78.66		Transponder 1	14		Miscellaneous		
			Transponder 2	14		Payload attach fitting	159	
			Motor drive electronics	11		Inadvertant destruct system	25	
			Redundancy control unit	4		Centaur batteries	75	
			TT&C harnessing	85.2		Ballast	65.4	
			Total TT&C weight	427.2				

TABLE 6.31.—COLD-SAT CENTER OF GRAVITY

Axis	CG location, in.
x	104
y	-0.02
z	0.18

TABLE 6.32.—COLD-SAT'S MASS MOMENTS OF INERTIA PROPERTIES
(in.-lb-sec²)

Configuration	I_{xx}	I_{yy}	I_{zz}	I_{xy}	I_{yz}	I_{xz}
Stowed	16908	85680	86400	371	-191	93
Beginning of life	35766	85814	102896	426	28	93
End of life	36840	75807	93707	452	46	97
Forward axial CG	30361	71962	86755	9	31	10

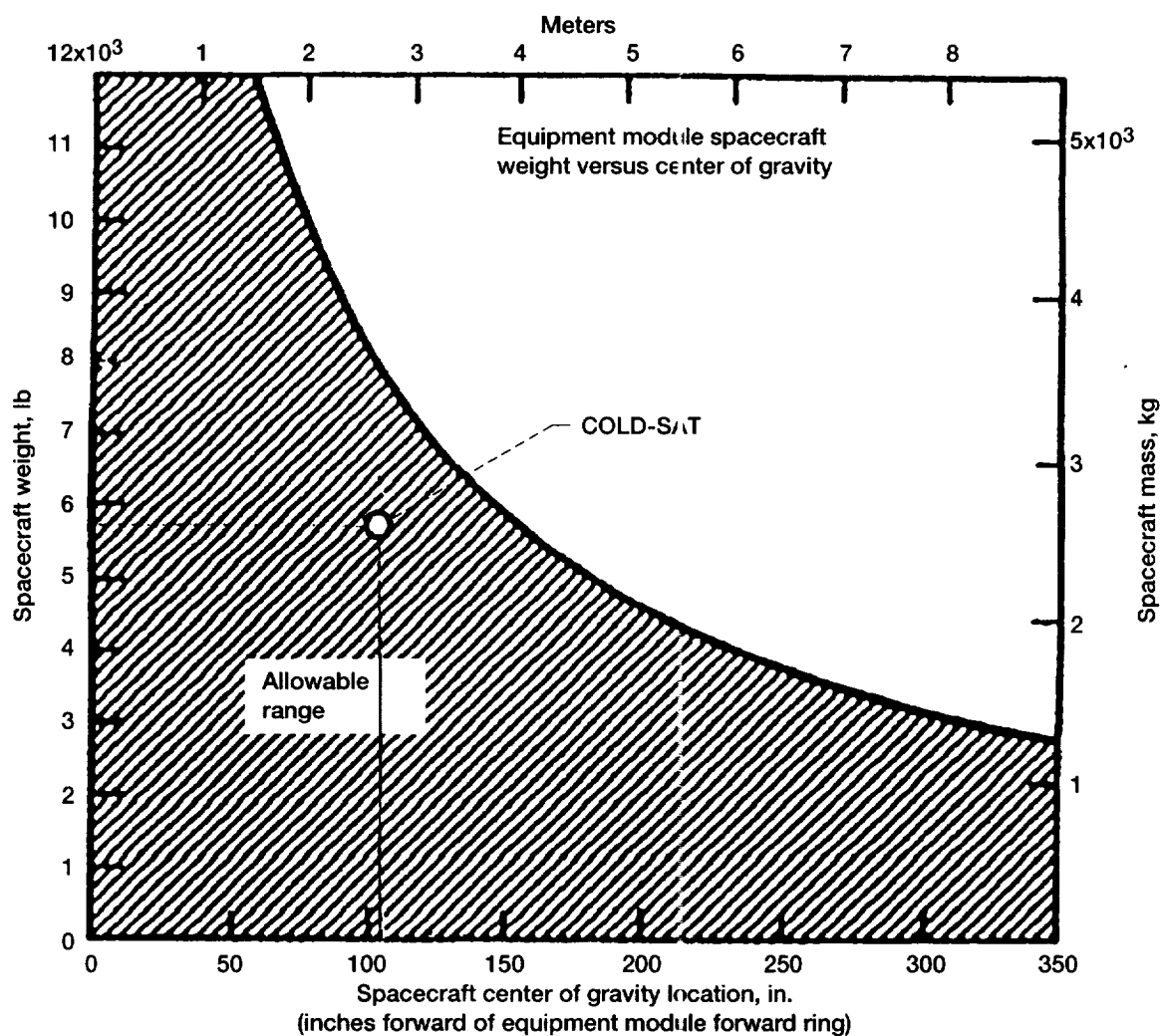


Figure 6.48.—COLD-SAT center of gravity restraint.

6.6.2.3.3 Moments and products of inertia.—COLD-SAT's final mass moment of inertia properties are shown in table 6.32. The table identifies the inertial properties for three different mission phases and one unrealistic condition (forward axial CG). The three mission phases include stowed, beginning of life (BOL), and end of life (EOL). The worst-case shift in the axial CG occurs when all the tanks (supply, pressurant, hydrazine) on COLD-SAT are empty except for the two receiver tanks, which are completely full. This (unrealistic) case was run to get the worst possible longitudinal CG shift for the attitude control system so they could size their system for control torque.

COLD-SAT's mass properties vary because of movement of the spacecraft deployables (antenna and solar arrays), propellant consumption (hydrazine), and because of the movement and venting of test fluid and pressurant (gaseous helium and gaseous hydrogen). In the stowed configuration, the arrays are body-wrapped around the spacecraft and the high-gain antenna is stowed. The supply tank, hydrazine bottles, and pressurant bottles are full. In addition, the two receiver tanks are empty except for a gaseous helium pad pressure to keep contaminants out. At the BOL, the arrays and the high-gain antenna are deployed and the fluid levels are similar to the stowed configuration. At the EOL, COLD-SAT's arrays and antenna are still deployed, but the fluid levels are depleted in the tanks.

6.7 Operation

During normal spacecraft operation, very little occurs from a spacecraft configuration and structural system viewpoint other than changes in the CG location caused by depletion of consumables. However, at the beginning of on-orbit activities, separation from the Centaur and deployment of appendages occur. These items are discussed below.

6.7.1 SEPARATION

The spacecraft separation sequence is under the control of the launch vehicle. It is initiated by redundant commands from the upper stage guidance system. Power for this event is supplied from the main vehicle battery. Positive spacecraft separation is detected through breakwires installed in the spacecraft rise-off disconnects and wired to the Centaur instrumentation system. The separation event is then telemetered to the ground by the launch vehicle.

The COLD-SAT separation system consists of a vee-band clamp set and the separation springs required to give the necessary separation energy after the clamp band is released. The clamp band set consists of a clamp band for attaching the satellite to the adapter structure plus devices to catch, extract, and retain the clamp band on the adapter structure after separation. The separation spring assemblies are mounted inside the spacecraft adapter. The springs are integrated with the space-

craft adapter and bear on supports fixed to the spacecraft rear frame. The springs will be sized appropriately for the COLD-SAT mission to provide the proper separation velocity between launch vehicle and spacecraft.

6.7.2 SOLAR ARRAY DEPLOYMENT

The deployment sequence of COLD-SAT's solar arrays from the body-wrapped stowed configuration to the final extended deployed configuration is largely based on an existing flight-qualified design used for the FLTSATCOM and TDRS spacecraft. Deployment occurs in three steps. First, three panels of each array are unwrapped from the spacecraft body into a single plane. This process is permitted by firing four ordnance devices. Second, the array booms are extended into their final position. Again, this is initiated by firing four additional ordnance devices. Finally, the arrays are rotated to their final canted position by spring motors. The final array deployment is verified by monitoring array output data and limit switches. The deployment sequence for the FLTSATCOM and TDRSS solar arrays is illustrated in figure 6.49.

6.7.3 VARIATION IN MASS PROPERTIES

Spacecraft mass properties change throughout the mission life for a variety of reasons including venting of boil-off from cryogenic fluids, transfer of test fluid, hydrazine propellant usage, and deployment of solar arrays and antenna. The range that the mass properties vary was calculated and supplied to the attitude control team so they could design that system properly. Mass properties from several exaggerated conditions were examined including the worst-case axial CG shift, the worst-case lateral CG location, and the mass moment of inertia properties.

The axial CG shift is summarized in table 6.33. The lowest axial CG condition occurs at spacecraft separation when the hydrazine propellant tanks and supply tank are full and the receiver tanks are empty. The other extreme occurs when the supply tank and hydrazine propellant tanks are empty and the two receiver tanks full. It was not evident if this case produced the worst-case axial CG shift or if it was produced by just the small receiver tank being full (and the large receiver tank being empty). However, after analyzing both alternatives, both receiver tanks full produces the worst-case shift. The worst-case CG shift was 12.4 in.

TABLE 6.33—COLD-SAT CENTER OF GRAVITY (CG) SHIFT

Configuration	X_{CG} , in.	Y_{CG} , in.	Z_{CG} , in.
Stowed, with 20 percent, loaded	103.9	-0.05	0.18
BOL, with 20 percent margin	103.7	-.05	-.16
EOL, with 20 percent margin	109.5	-.07	-.21
Most forward axial CG	115.3	-.07	-.21

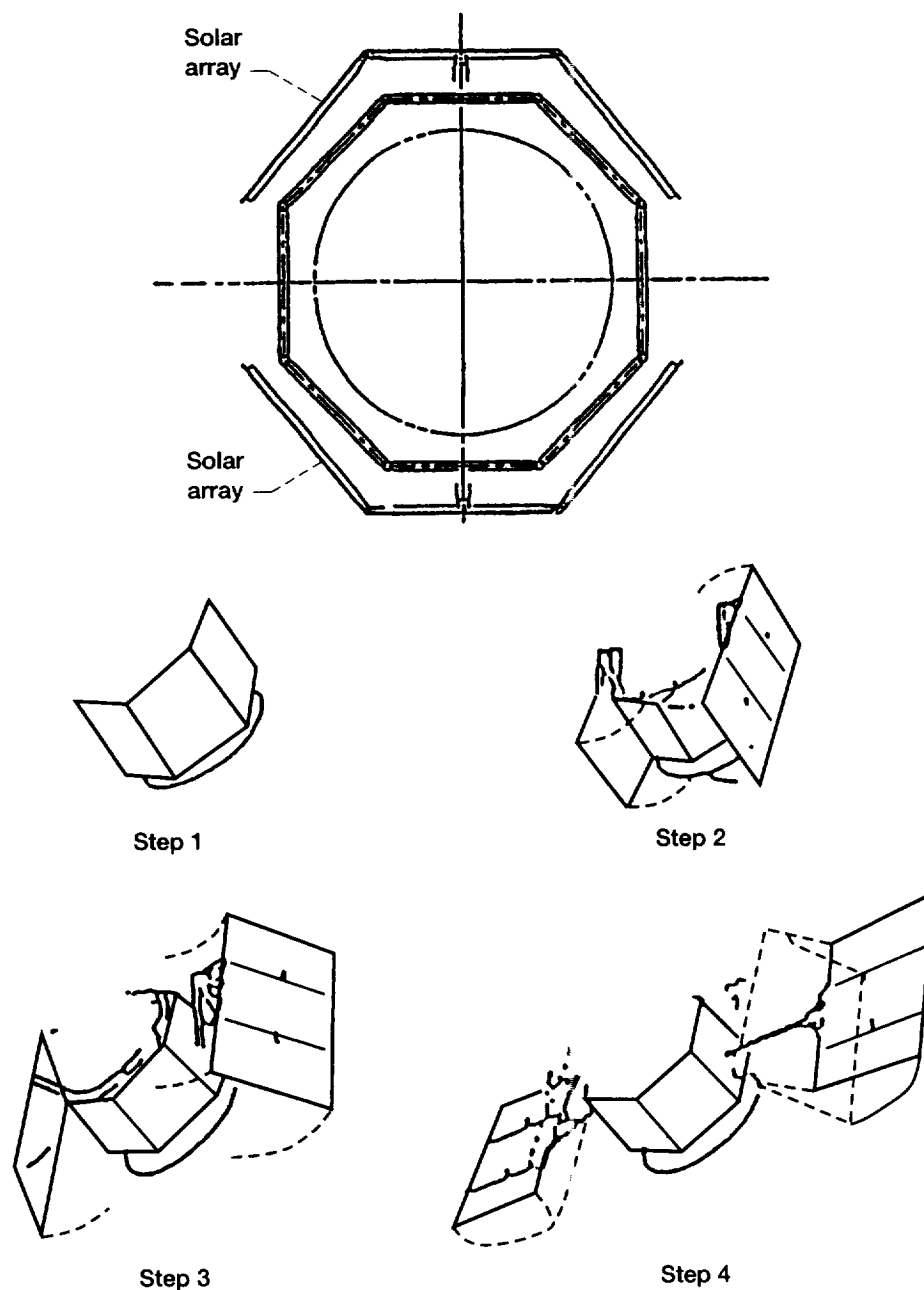


Figure 6.49.—FLTSATCOM and TDRS solar array deployment sequence.

The worst-case lateral CG is used to size the control torque required to counterbalance the torque produced by axial thruster misalignment. It is also used to determine the worst-case products of inertia terms which contribute to the gravity gradient torques (based on the greatest difference between the largest and smallest cross-product terms). The worst-case CG offset is 0.21 in. (table 6.33) and it complies with the launch vehicle alignment requirement as well as the attitude control system requirements.

6.8 Components

One of COLD-SAT's design goals is the use of existing designs and proven components. The spacecraft configuration and structural system uses flight-qualified solar array mechanisms as well as off-the-shelf hardware for the structural system.

6.8.1 SOLAR ARRAY MECHANISM

COLD-SAT baselined the solar array design, deployment sequence, and deployment mechanisms used on the TDRS and FLTSATCOM satellites. However, there are some minor differences. The COLD-SAT arrays are slightly larger than TDRS. Plus, COLD-SAT's solar arrays are fixed whereas the others articulate and require a solar array drive. The last difference is that COLD-SAT requires a torsional spring for canting where the others do not.

6.8.2 MATERIALS/STRUCTURAL SHAPES/STRUCTURES

COLD-SAT's structural system is composed of off-the-shelf hardware. The configuration lends itself to hand

calculations. The material used for the structural system is well known and has an extensive flight history. The longeron cross section is common in the aerospace industry and the sizes are off-the-shelf.

6.9 Reliability

The reliability goal for the entire COLD-SAT spacecraft is 0.92 or better. This overall objective was subdivided into allocations for each system that resulted in a reliability allocation for the structural system of 0.999. The reliability for the structural system was set equal to the reliability allocation. This equilibration was done in part because the failure of properly designed structure is deemed noncredible because of the conservative safety factors, well-known material properties, extensive testing, etc. The reader should note that reliability of solar array deployment and antenna deployment is included as part of the power and TT&C systems, respectively.

References

1. Mission Planner's Guide for the Atlas Launch Vehicle Family, General Dynamics Commercial Launch Services, Inc., 1989, Revision 1.
2. Delta II Commercial Spacecraft Users Manual, MDC H32.24, McDonnell Douglas Corporation, July 1987.
3. Schuster, J.R.; Russ, E.J.; Wachter, J.P. (General Dynamics Corp. Space Systems Division with Ford Aerospace Space Systems Division): Cryogenic On-Orbit Liquid Depot Storage, Acquisition and Transfer Satellite (COLD-SAT) Feasibility Study, NASA CR-185249, 1990.

Chapter 7

Attitude Control System

Dave Repas

Gary Bollenbacher

National Aeronautics and Space Administration

Lewis Research Center

Cleveland, Ohio

and

Neil Adams

Analex Corporation

Cleveland, Ohio

The attitude control system (ACS) provides for attitude determination, orientation, and stabilization of the COLD-SAT spacecraft during on-orbit operations.

7.1 Introduction

The COLD-SAT spacecraft will be placed into a circular low Earth orbit (LEO) at an initial altitude of 550 n mi and an inclination of 18° . During normal orbital operation, the spacecraft will maintain a pseudo-inertial attitude with the x- and y-axes in the orbit plane and the z-axis aligned with the orbit normal as shown in figure 7.1. The positive z-axis is on the side of the orbit opposite the Sun. The negative x-axis is pointed at the projection of the Sun vector in the orbit plane. The rationale for selecting this attitude is given in chapter 4, section 4.3 of this report.

The selected attitude causes the spacecraft to rotate very slowly with respect to inertial space. This motion consists of a counterclockwise rotation (as viewed from north) about the spacecraft z-axis at the rate of 1 rev/yr to track the Sun as illustrated in figure 7.2. Additional motion results as the spacecraft attitude is adjusted to keep the spacecraft x-y plane aligned with the rotating orbit plane.

The angle between the Sun vector and the orbit plane is called the β angle. The β angle varies continuously over the range of approximately $\pm 41^\circ$ for an 18° inclined orbit. The variation in β angle is due in part to the Earth's orbit about the

Sun and in part due to the rotation of the orbit plane caused by the Earth's oblateness. When the β angle crosses through zero, that is, when the Sun crosses the orbit plane, the spacecraft must be rotated 180° about the x-axis to keep the positive z-axis opposite the Sun.

In addition to maintaining the desired attitude, several factors unique to COLD-SAT need to be considered in the design of the ACS. These are

- (1) The large quantity of liquid hydrogen onboard with the potential for slosh
- (2) Long-term application of axial thrust in the spacecraft x-direction to satisfy experiment requirements
- (3) Spraying liquid hydrogen into the receiver tanks with tangential spray nozzles
- (4) Venting gaseous hydrogen
- (5) Fluid disturbances that are to be maintained below some specified level so as not to degrade scientific data.

Items (1) to (4) all cause disturbance torques on the spacecraft that the ACS must counteract to maintain the desired attitude. Item (5) places constraints on the ACS and influences the selection of ACS actuators.

Three levels of axial thrust are required for approximately 42 separate thrusting periods. The three thrust levels are 0.04, 0.16, and 0.52 lb. The cumulative time for axial thrust is 56 hr out of a total mission time of 6 months. The longest continuous application of axial thrust is 9 to 10 hr which occurs three times

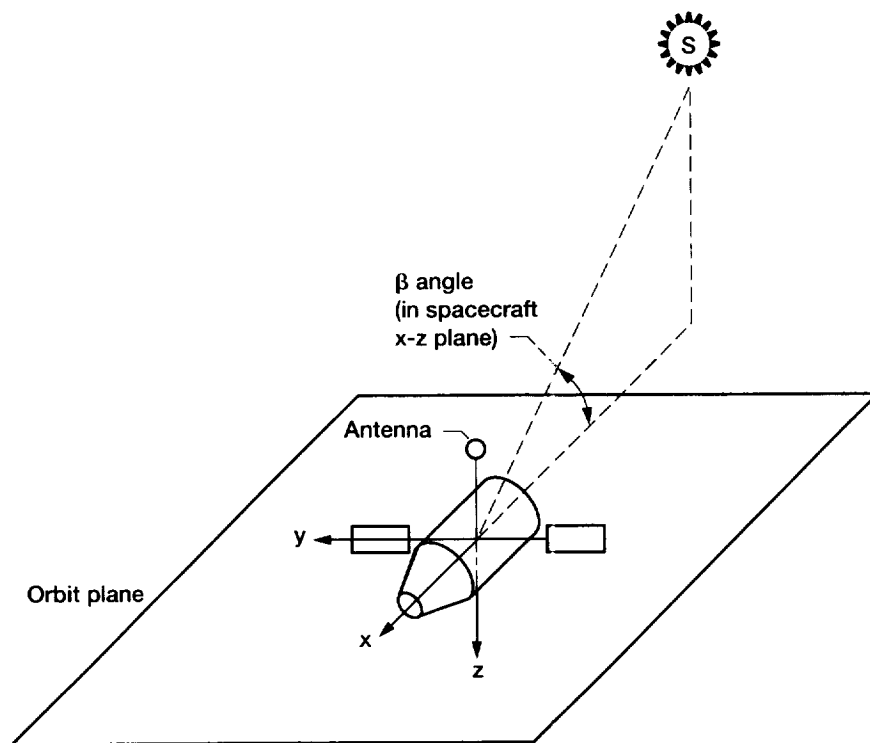


Figure 7.1.—COLD-SAT attitude. (COLD-SAT attitude is pseudo-inertial with x-axis in orbit plane, parallel to projection of Sun vector in orbit plane, and pointing away from Sun; y-axis in orbit plane; z-axis normal to orbit plane on opposite side from Sun.)

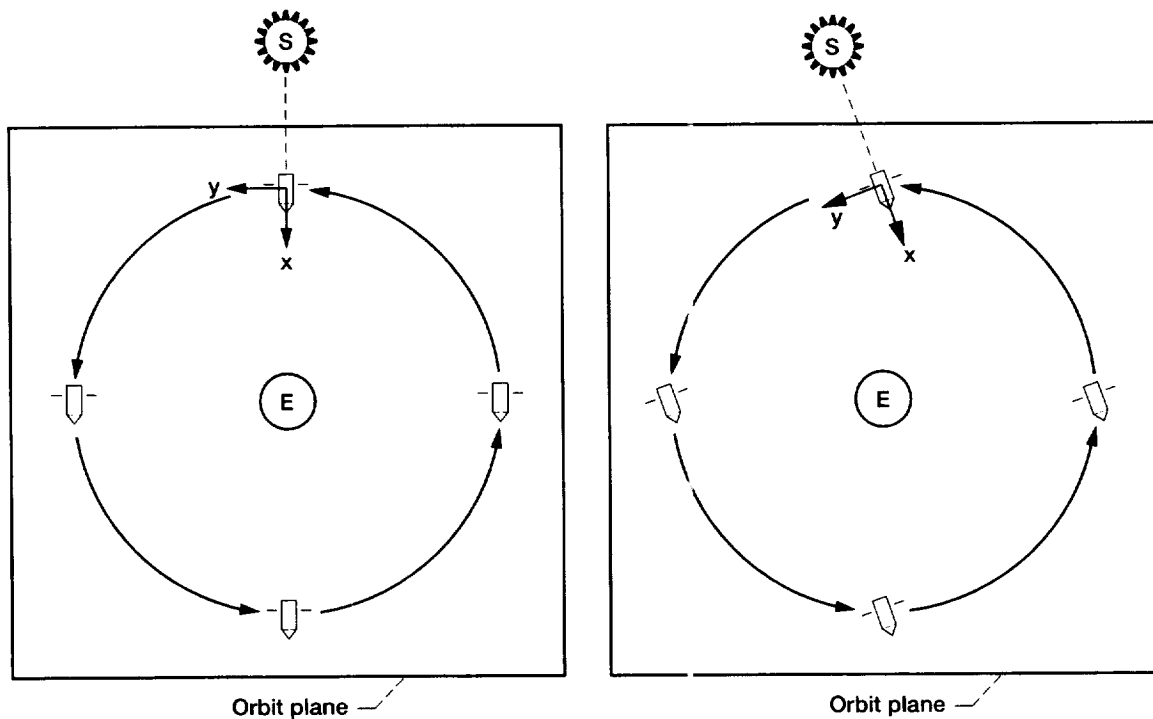


Figure 7.2.—Sun tracking with COLD-SAT attitude. (COLD-SAT spacecraft rotates counter clockwise about z-axis at 1 rev/yr to track Sun. COLD-SAT orbit plane rotates clockwise about polar axis at approximately 5.7 rev/yr due to nodal regression.)

in the course of the mission, once for each level of axial thrust. It is primarily during application of axial thrust that the fluid disturbances are to be minimized.

The ACS requirements, alternative designs considered, the selection process, and description and performance of the selected system are the subject of the remainder of this chapter.

7.2 Requirements

The pointing capabilities of the ACS are driven by the high-gain antenna pointing requirement. This antenna is required to be pointed toward the tracking and data relay satellite system (TDRSS) to an accuracy of $\pm 3^\circ$. For the purpose of the conceptual design, it was assumed that the contribution of the ACS sensor errors to pointing accuracy was $\pm 1^\circ$ and that the high-gain antenna could be pointed to within $\pm 1^\circ$ of the desired position. Accordingly, the ACS was designed to maintain the attitude to $\pm 1^\circ$ exclusive of sensor errors.

The ACS must have the capability to acquire the desired attitude from any arbitrary orientation. If the spacecraft is tumbling, the ACS is required to reduce the attitude rate to acceptable levels and then reorient the spacecraft to the desired attitude.

For some experiments the microgravity environment of the spacecraft needs to be controlled so as not to disturb the liquid hydrogen in the supply or receiver tanks. The ACS is one contributor to these deviations. Other contributors to microgravity disturbances are gravity-gradients, aerodynamic drag, axial experiment thruster misalignments, and disturbances caused by pumps, valve actuation, antenna slewing, and venting. The ACS must be designed such that the total disturbances do not exceed the maximum total allowance. The microgravity environment is of particular concern during application of axial thrust.

The ACS is also required to perform the 180° roll maneuver and to have a reliability of at least 0.997 for the 6-month mission life.

The ACS must meet all of the above requirements over a range of mass properties, center of gravity locations, and orbit altitudes as discussed below.

7.2.1 ORBIT ALTITUDE

The initial orbit altitude is planned to be 550 n mi. Analysis shows that, because of axial thrusting, the orbit altitude will reach a minimum of approximately 490 n mi. The eccentricity of the orbit ranges from 0 to 0.04.

7.2.2 MASS PROPERTIES

The ACS must function properly over the range of mass properties shown in table 7.1. The minimum inertias shown in the table are approximately 90 percent of the total estimated minimum inertias of the COLD-SAT spacecraft at the time the

TABLE 7.1.—COLD-SAT MASS PROPERTIES

Inertial properties, in. lb-sec ²					
I_{xx}	I_{yy}	I_{zz}	I_{xy}	I_{yz}	I_{xz}
Maximum					
39 343	94 395	113 186	469	31	102
Minimum					
27 544	64 766	78 080	0	0	0
Nominal					
33 265	74 366	90 366	226	23	49

ACS analysis was started; the maximum values shown are 10 percent higher than the highest estimate.

7.2.3 CENTER OF GRAVITY LOCATION

The ACS must be capable of normal operation over a range of center of gravity locations as follows:

X_{CG} (from rear of spacecraft), 79 to 92 in.

Y_{CG} (from spacecraft centerline), ± 0.5 in.

Z_{CG} (from spacecraft centerline), ± 0.5 in.

7.3 Disturbance Torques

For analysis purposes the disturbance torques have been divided into two categories, external and self-induced.

The external torques considered in the design of the ACS are

- (1) Gravity-gradient torque
- (2) Aerodynamic torque
- (3) Magnetic torque
- (4) Solar pressure torque

The self-induced disturbance torques that affect the ACS are

- (1) Axial experiment thruster misalignment torque
- (2) Control thruster misalignment torque
- (3) Slosh torque
- (4) Tangential spray torque
- (5) Antenna slewing torque
- (6) Pump turn-on and turn-off transient torques
- (7) Venting torque

All of the external and the first four self-induced disturbance torques have been analyzed. For the external disturbance torques, worst-case values for both nominal and random attitudes were determined. The worst-case disturbance torques are given in table 7.2. The assumptions for deriving the worst-case torques are given in tables 7.3 and 7.4 for external and self-induced torques, respectively. The self-induced disturbance torques were evaluated over the range of center of gravity locations; the worst-case self-induced torques are with the center of gravity in the most forward location.

TABLE 7.2.—WORST-CASE DISTURBANCE TORQUES

Disturbance torque	x-axis (in.-lb)	y-axis (in.-lb)	z-axis (in.-lb)
Nominal attitude without axial thrust			
Gravity-gradient	0.00071	0.00403	0.08520
Magnetic	.00650	.00750	.00590
Aerodynamic	0	0	.00210
Solar pressure	0	.00023	0
Axial thruster misalignment	0	0	0
Control thruster misalignment	.10052	.19686	.09634
Slosh	0	.00390	.01870
Tangential spray	<u>.31900</u>	<u>.03200</u>	<u>.03200</u>
Worst-case (arithmetic sum)	0.42673	0.24452	0.24024
Nominal attitude with axial thrust (gimballed thruster operating normally)			
Gravity-gradient	0.00071	0.00403	0.08520
Magnetic	.00650	.00750	.00590
Aerodynamic	0	0	.00210
Solar pressure	0	.00023	0
Axial thruster misalignment	0	.53800	.53800
Control thruster misalignment	0	.10052	0
Slosh	0	.06600	.05550
Tangential spray	<u>.31900</u>	<u>.03200</u>	<u>.03200</u>
Worst-case (arithmetic sum)	0.32621	0.74828	0.71870
Nominal attitude with axial thrust (failed gimballed thruster)			
Gravity-gradient	0.00071	0.00403	0.08520
Magnetic	.00650	.00750	.00590
Aerodynamic	0	0	.00210
Solar pressure	0	.00023	0
Axial thruster misalignment	0	.53800	.53800
Control thruster misalignment	.10052	.19686	.09634
Slosh	0	.08100	.06800
Tangential spray	<u>.31900</u>	<u>.03200</u>	<u>.03200</u>
Worst-case (arithmetic sum)	0.42673	0.85962	0.82754
Random Attitude			
Gravity-gradient	0.02910	0.11930	0.08520
Aerodynamic	0	.00330	.00330
Magnetic	.01111	.01111	.01111
Solar pressure	0	.00100	.00100
Axial thruster misalignment	0	0	0
Control thruster misalignment	.10052	.19686	.09634
Slosh	0	.00390	.01870
Tangential spray	<u>0</u>	<u>0</u>	<u>0</u>
Worst-case (arithmetic sum)	0.14073	0.33547	0.21565

TABLE 7.3.—ASSUMPTIONS FOR WORST-CASE EXTERNAL
DISTURBANCE TORQUES

Gravity-gradient	
Altitude	490 n mi
Mass properties	Maximum inertias
Magnetic	
Altitude	490 n mi
Spacecraft magnetic moment	30 A-m ²
Magnetic moment orientation	
Nominal attitude	Aligned with spacecraft y-axis
Random attitude	Arbitrary
Aerodynamic	
Altitude	490 n mi
Geomagnetic activity index	23
Daily 10.7-cm solar flux	193
81-Day mean solar flux	193
Solar pressure	
β angle	41°

TABLE 7.4.—ASSUMPTIONS FOR WORST-CASE SELF-INDUCED
DISTURBANCE TORQUES

Axial thruster misalignment torque	
Center-of-gravity offset	0.5-in. positive y; 0.5-in. positive z
Axial thrust vector angular misalignment	1/3°
Direction of angular misalignment	Chosen to maximize disturbance torque
Center-of-gravity distance from rear of spacecraft	92 in.
RCS thruster misalignment torque	
Angular thruster misalignment (two directions)	1.0°
Center-of-gravity distance from rear of spacecraft	92 in.
Slosh torque	
Tanks filled with liquid hydrogen	All
Tank fill level (all tanks)	80 percent
Center-of-gravity distance from rear of spacecraft	79 in.

The worst-case disturbance torques shown in table 7.2 are given for four scenarios as follows:

- (1) Nominal attitude without axial thrust
- (2) Nominal attitude with axial thrust (gimballed thruster operating normally)
- (3) Nominal attitude with axial thrust (failed gimballed thruster)
- (4) Random attitude

The last scenario assumes that attitude reference has been lost and that all experiments are shut down, that is, no axial thrust and no use of the tangential spray system.

7.3.1 EXTERNAL DISTURBANCE TORQUES

Each of these torques (except solar pressure torque) is a function of spacecraft altitude. Current analysis shows that the spacecraft altitude will range from an initial value of 550 n mi to a minimum altitude of 490 n mi.

The pseudo-inertial spacecraft attitude gives rise to a cyclical gravity-gradient torque predominantly about the spacecraft z-axis. This torque is nearly sinusoidal with a frequency equal to twice the orbital frequency. The gravity-gradient torque is the dominant external disturbance torque acting on the spacecraft.

For magnetic torque calculations, the spacecraft was assumed to be designed to Class III standards (ref. 1). This standard assumes that the spacecraft magnetic moment is greater than 10×10^{-3} A-m²/kg. The orientation of the spacecraft magnetic moment was assumed to be along the spacecraft y-axis. This orientation approximates the location of the spacecraft magnetic moment that results in the worst-case magnetic torque.

The worst-case atmospheric density was assumed for aerodynamic torques. Atmospheric density is computed using the Jacchia 1970 model (ref. 2).

The external disturbance torques were analyzed through the use of a computer model (see section 7.10 of this report) which simulates each of the torques. Reference 3 contains a detailed discussion of how each of the torques is modeled. Some representative curves of external disturbance torques are shown in figures 7.3 to 7.6. Each of the figures represents approximately one orbit.

7.3.2 SELF-INDUCED DISTURBANCE TORQUES

Each of the self-induced disturbance torques is discussed briefly in this section. The self-induced disturbance torques are independent of attitude.

It is assumed that the axial thrust vector is offset from the spacecraft center of gravity and in addition that a small angular

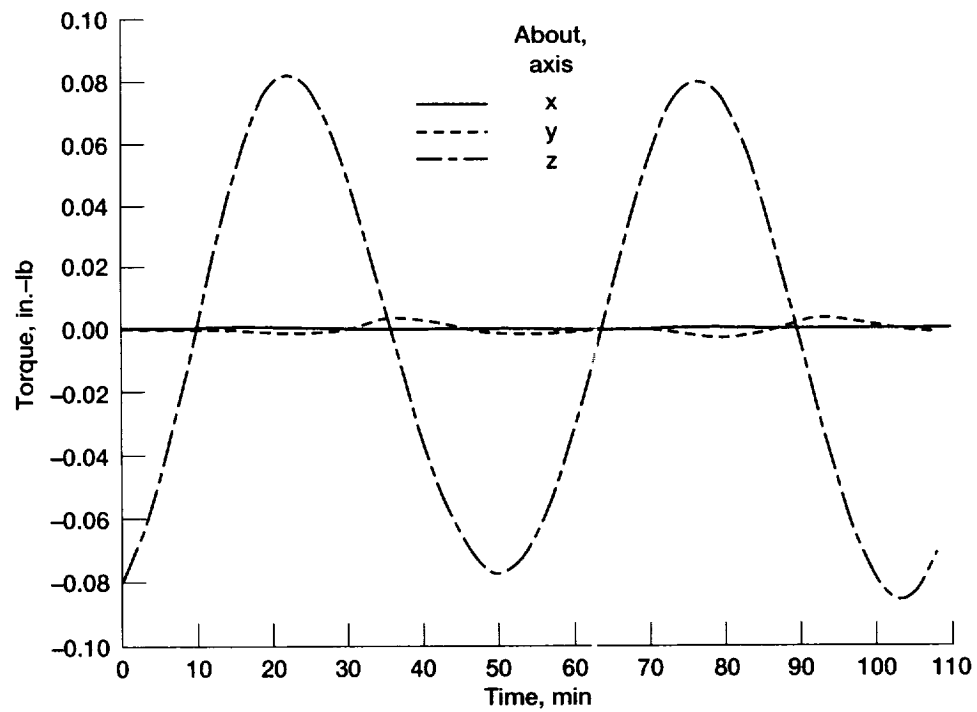


Figure 7.3.—Typical gravity-gradient torque.

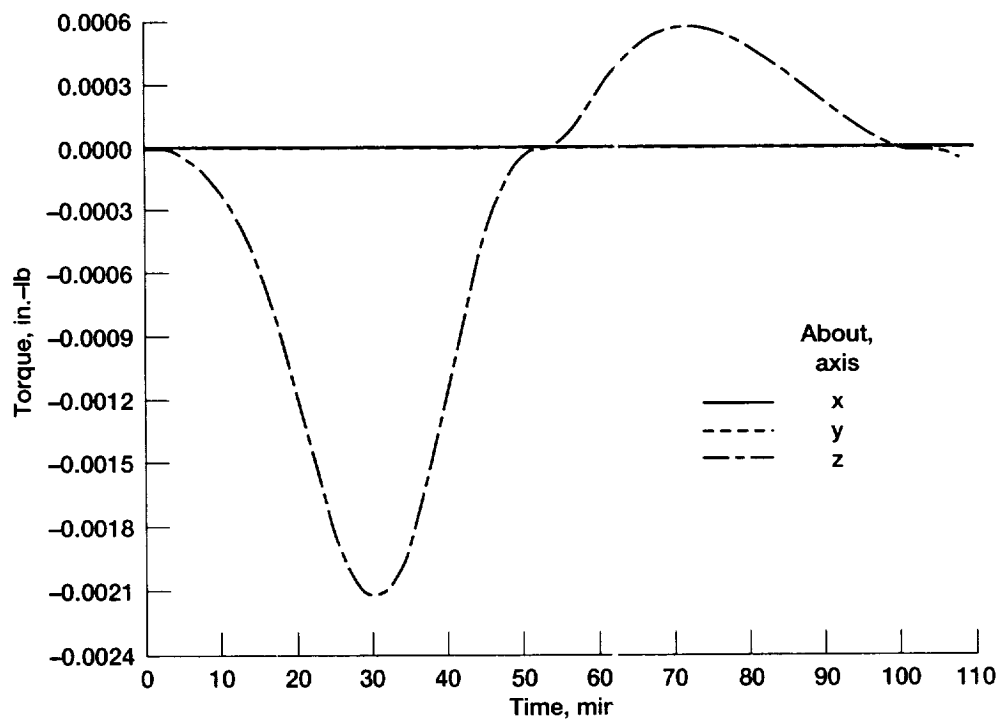


Figure 7.4.—Typical atmospheric drag torque.

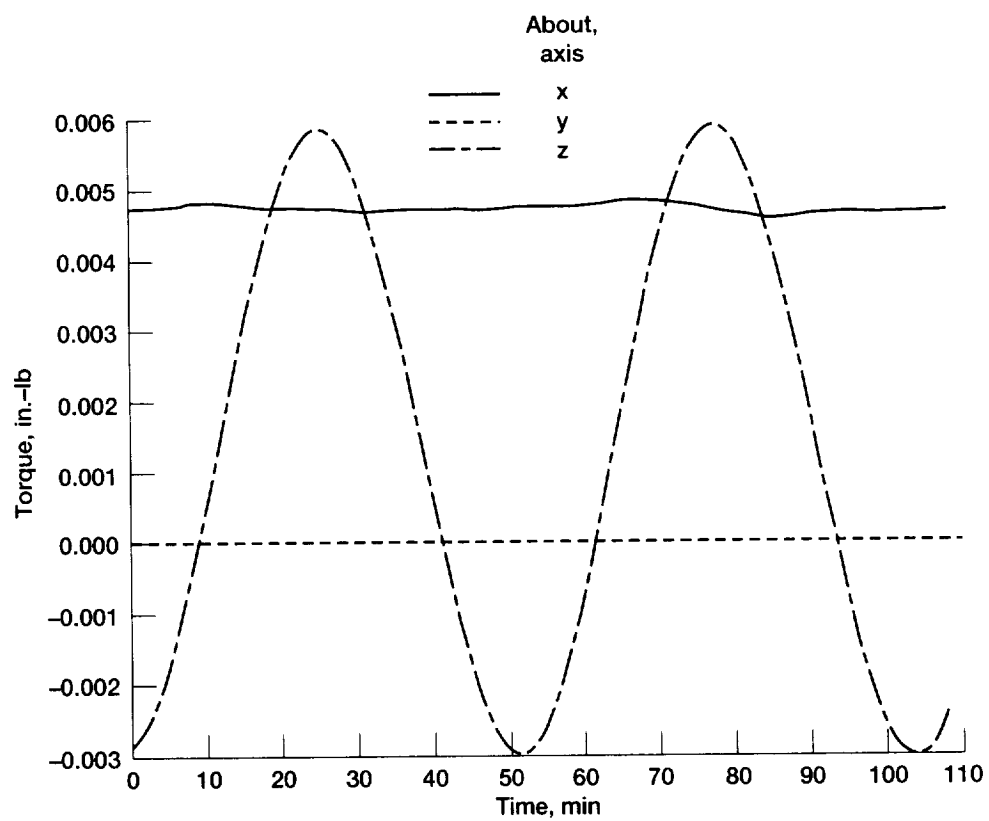


Figure 7.5.—Typical magnetic torque.

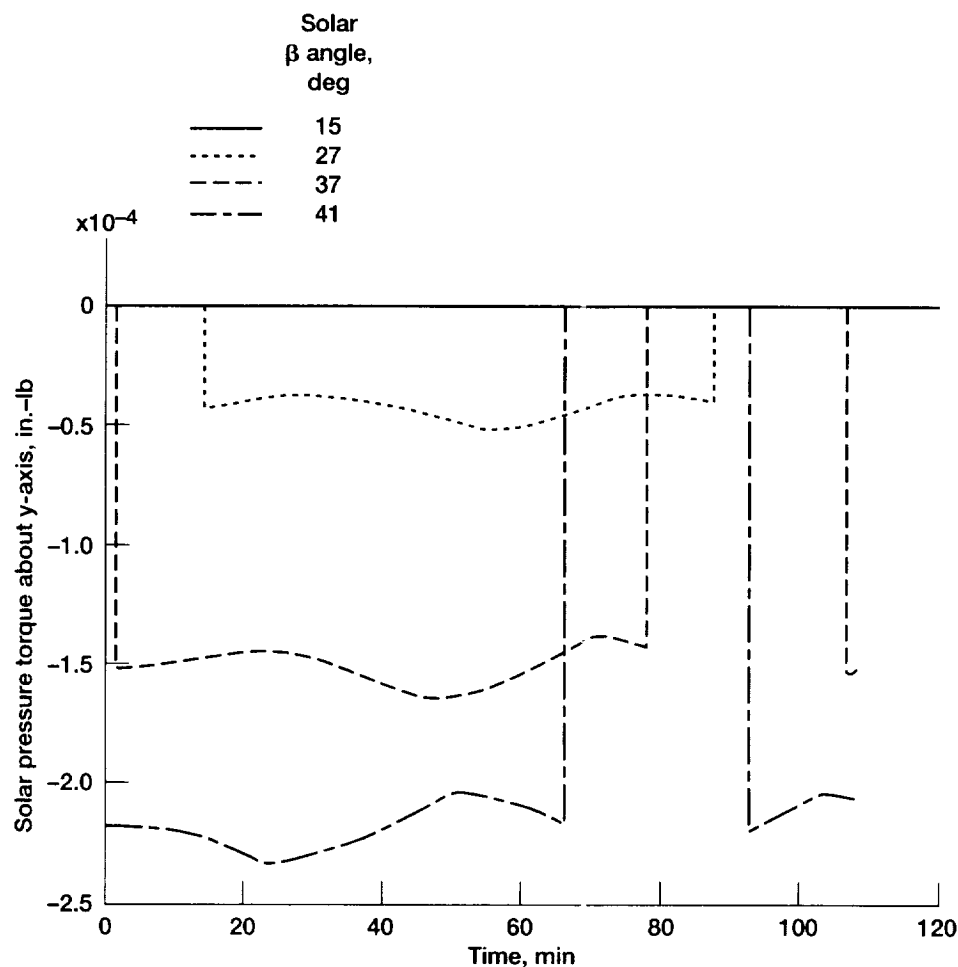


Figure 7.6.—Solar pressure torque for various β angles.

misalignment with respect to the spacecraft x-axis exists. The offset from the spacecraft center of gravity causes an undesirable, self-induced disturbance torque on the spacecraft whenever the experiment thrusters are in use. The angular misalignment causes undesirable microgravity accelerations in the spacecraft y and z directions.

The control thruster misalignment torque is produced by the angular misalignment of the attitude control system thrusters. Each thruster is assumed to be misaligned in both planes such that, for example, if the roll thruster is actuated to produce a control torque about the x-axis, small, undesirable torques about both the y- and z-axes are also produced.

The slosh torque is the result of liquid hydrogen sloshing in the supply tank and in both receiver tanks. For analysis purposes it was assumed that the sloshing liquids would only produce torques about the y- and z-axes and that the y and z torques would be independent. In addition only the fundamental slosh frequency was considered. The slosh model assumes cylindrical tanks and the slosh is modeled as a spring/mass/dashpot analogy. Computation of the slosh mass, slosh spring

constant, and the damping ratio are based on reference 4. The slosh model is described further in section 7.10 of this report.

To compute the worst-case slosh torque shown in table 7.2, slosh was modeled in all three tanks simultaneously. Each tank was assumed to be 80-percent filled with liquid hydrogen. From the simulations, the worst-case slosh torque from each tank was determined and the results were added arithmetically. In all slosh simulations initial attitude errors and slosh mass displacements were zero. Slosh torque generally peaks when there are rapid changes in spacecraft body rates, and decays thereafter.

Typical total slosh torque acting on the spacecraft is shown in figure 7.7.

Tangential spray torque results from the injection of liquid hydrogen into the receiver tanks by means of the tangential spray system. The reaction force from these nozzles is eventually opposed by an equal and opposite frictional drag of the fluid against the tank walls. The frictional drag is assumed negligible for purposes of evaluating the tangential spray torque. Thus, it is assumed that 100 percent of the torque

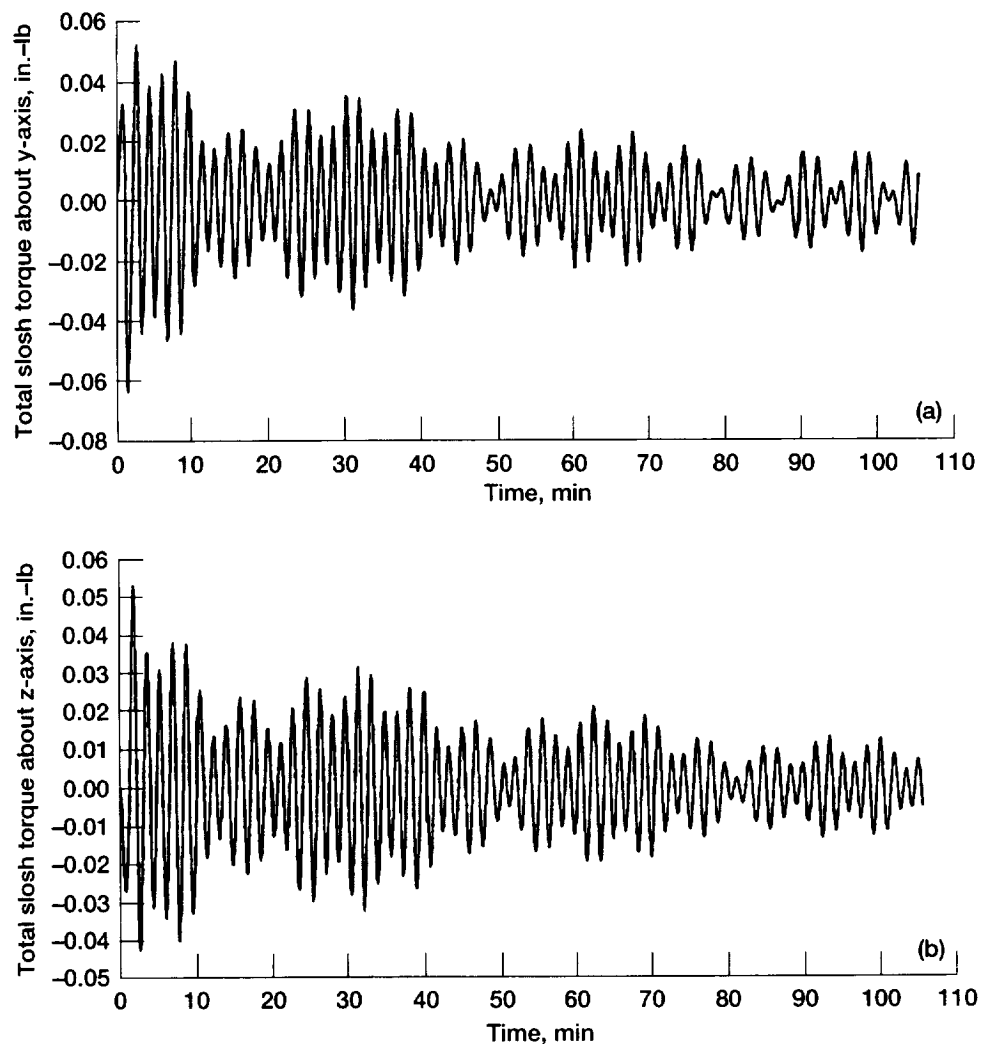


Figure 7.7.—Typical total slosh torque with liquid hydrogen in all tanks. (a) Torque about y-axis. (b) Torque about z-axis.

produced by the tangential spray nozzles has to be reacted to by the ACS for the duration of the tangential spray. The tangential spray torque may be present with and without axial thrust. The magnitude of the tangential spray torque shown in table 7.2 is taken from a General Dynamics analysis.

Venting of gaseous hydrogen overboard through a balanced, nonpropulsive vent system is planned. However, it is anticipated that some imbalance will exist for the duration of the venting which will produce a small, residual disturbance torque on the vehicle. The magnitude of this torque has not yet been estimated.

Pump torques, antenna slewing torques, and torques produced by valve actuation are transient in nature and occur whenever any of these devices are actuated. The magnitude or frequency of these torques has not yet been evaluated.

7.4 ACS Alternatives Considered

7.4.1 ATTITUDE DETERMINATION

In selecting an attitude determination system, the feasibility of the method, cost, and availability of components were considered.

An inertial reference unit (IRU) was selected as the primary attitude sensor. Gyro rate drift and IRU attitude data will be updated by information from two-axis digital Sun sensors and scanning horizon sensors. Star trackers were eliminated from consideration because of the associated hardware and software costs. Additionally, the accuracy provided by star trackers was not needed for COLD-SAT. Magnetometers were included for

use in attitude acquisition. No other alternatives for attitude determination were considered.

Exact algorithms for updating attitude from the Sun and horizon sensors were not determined. Discussions have been held with spacecraft contractors and horizon sensor manufacturers regarding possible methods. One sensor manufacturer stated that a method for an inertially oriented spacecraft had been developed on a previous program and algorithms were available although proprietary.

7.4.2 ATTITUDE CONTROL

Several systems for attitude control were studied. The most important consideration in choosing systems to study was the microgravity environment to be provided for the experiments.

The various alternatives considered are discussed in the following subsections.

7.4.2.1 Alternative 1

Alternative 1 is an all-thruster system using coupled thrusters for x-axis control and uncoupled thrusters for y- and z-axis control. The control thrusters are sized at 0.06 lb and produce a coupled torque of 5.76 in.-lb about the x-axis and an uncoupled torque of 2.88 in.-lb about the y- and z-axes.

7.4.2.2 Alternative 2

Alternative 2 is an all-thruster system which uses coupled thrusters on all three axes. The control thrusters are sized at 0.06 lb and produce a coupled torque of 5.76 in.-lb about the x-axis and 4.08 in.-lb about the y- and z-axes.

7.4.2.3 Alternative 3

Alternative 3 is an all-thruster system combined with a single reaction wheel with its spin-axis aligned with the spacecraft z-axis. The inertia of the reaction wheel is 0.144 in.-lb-sec² and the maximum developed torque is 4.43 in.-lb. Maximum wheel speed is 6685 rpm.

7.4.2.4 Alternative 4

Alternative 4 is an all-thruster system combined with a two-axis gimbaled thruster system. The system consists of a fixed nozzle thruster mounted on two single-axis antenna gimbals. The size of the thruster is 0.04 lb. Each gimbal is capable of rotating $\pm 20^\circ$.

7.4.2.5 Alternative 5

Alternative 5 is an all-thruster system combined with a single reaction wheel and a gimbaled thruster.

The thruster system used with alternatives 3 to 5 could use uncoupled thrusters as in alternative 1 or coupled thrusters as in alternative 2.

7.5 Tradeoff Analysis

Both qualitative and quantitative tradeoff analyses were performed for the five attitude control alternatives.

7.5.1 QUALITATIVE EVALUATION

Alternative 1 was the least complex option considered and had the lowest cost. All thrusters and propulsion system components would be located on the aft end (negative x-axis) of the spacecraft. Fewer thrusters are required and propellant line heaters would be eliminated. In addition to control torques, this system would produce linear accelerations. During zero-g operations, most control thruster activity produces torque about the spacecraft z-axis.

Alternative 2 would produce pure torques and eliminate linear accelerations. Thrusters would be required to be located on the forward end (positive x-axis) of the spacecraft in addition to the aft end, thus requiring additional propellant line heaters and associated power consumption. As in alternative 1, most control thruster activity produces torque about the spacecraft z-axis.

Alternative 3 would provide an improved microgravity environment during quiescent periods of experimentation. The reaction wheel would eliminate the control thruster firings about the z-axis, which is caused by gravity-gradient torques, by absorbing these torques and therefore reduce hydrazine usage. The reaction wheel would not be used during periods of axial experiment thrusting since it would quickly saturate because of the secular torque about the z-axis that is produced by axial experiment thruster misalignment.

Alternative 4 would provide an improved microgravity environment during the induced acceleration experiments. The gimbaled thruster provides a means of directing the thrust vector through the spacecraft center of gravity for the y- and z-axes, thus minimizing control thruster firings due to center of gravity offset. At the lowest g-level (0.04 lb thrust), the gimbaled thruster is the only thruster used. At the higher g-levels, the gimbaled thruster is used in conjunction with fixed axial thrusters.

The gimbaled thruster would use existing hardware but some development would be required for the interfaces between the thruster and the gimbals. A detailed discussion of the gimbaled thruster is given in chapter 8, Propulsion System, of this report.

Alternative 5 would provide an excellent microgravity environment during both induced acceleration experiments and quiescent periods. It is the most complex and costly of all the systems considered.

7.5.2 QUANTITATIVE EVALUATION

The purpose of the quantitative evaluation of the five alternatives was to determine the ability of each of the systems to maintain the desired attitude and to assess the impact on the microgravity environment. An accurate six-degrees-of-freedom model of the COLD-SAT spacecraft was created using EASY5 on the CRAY X-MP computer. All disturbance torques including slosh were included in the simulation. The model was run to determine ACS performance and the microgravity environment for the various options. Details of the model are given in section 7.10 of this report.

The ACS performance was evaluated by plotting attitude errors and attitude rates. Microgravity environment was evaluated by comparing the actual microgravity against the ideal. The ideal microgravity environment would be a constant acceleration in the spacecraft positive x direction and zero acceleration in the y and z directions. Two measures were defined to evaluate the microgravity deviations from the ideal:

(1) Maximum instantaneous deviation (MID)

$$\text{MID}(i) = \text{Max}[a_t(i) - a_o(i)]$$

where

Max Maximum value function

MID(i) Maximum instantaneous deviation along the *i*-th spacecraft axis

a_t(i) Instantaneous value of linear acceleration along the *i*-th spacecraft axis at time *t*

a_o(i) Desired level of acceleration along the *i*-th spacecraft axis taken to be the nominal axial thrust along the *i*-th axis divided by the spacecraft weight at the start of the experiment

(2) Root mean square deviation (RMSD)

$$\text{RMSD}(i) = \left\{ \left[\int (a_t(i) - a_o(i))^2 dt / T \right] \right\}^{1/2}$$

where the integration is over the orbit period *T* and *a_t(i)* and *a_o(i)* are as defined previously and *RMSD(i)* is the root mean square deviation along the *i*-th axis.

MID and RMSD were computed under conditions of applied axial thrust when the microgravity environment is of greatest concern. Alternatives 1, 2, and 4 were evaluated. Since the reaction wheel is not used during axial thrusting, alternatives 3 and 5 were not evaluated. The microgravity environment during thrusting for alternative 3 is the same as for alternatives 1 and 2; that for alternative 5 is the same as for alternative 4.

Computations were made for the high axial thrust level of 0.52 lb and for the assumed spacecraft weight of 5610 lb. For this case the value of *a_o* is 92.69 micro-g in the x direction. The value of *a_o* in the y and z directions is zero. The instantaneous linear acceleration *a_t* is the combination of the desired axial acceleration plus a number of disturbance accelerations. The value of *a_t* is a function of location relative to the spacecraft center of gravity. The disturbance accelerations included in the analysis are the following:

- (1) Gravity-gradient accelerations
- (2) Linear, tangential accelerations resulting from spacecraft angular accelerations (caused primarily by control thruster firings with contributions from all other torques acting on the spacecraft)
- (3) Linear, radial accelerations resulting from spacecraft angular rotations
- (4) Accelerations caused by the experiment axial thruster, which was assumed to have an angular misalignment of 1/3° (this angular misalignment causes acceleration in the spacecraft y and z directions)
- (5) Accelerations caused by the gimballed thruster, which causes accelerations in the spacecraft y and z directions with its gimbaling action
- (6) Aerodynamic drag
- (7) Variations in acceleration because of changes in spacecraft weight (caused by consumption of hydrogen and hydrazine)
- (8) Linear accelerations resulting from uncoupled control thrusters

Of these disturbance accelerations, the dominant contributor is the tangential acceleration resulting from spacecraft angular accelerations. Also significant are gravity-gradient accelerations and linear accelerations resulting from uncoupled control thrusters. Radial accelerations, aerodynamic drag, and changes in acceleration caused by spacecraft weight changes, are negligible. Linear accelerations due to uncoupled control thrusters are significant for alternative 1 but not for alternatives 2 and 4.

7.5.3 RESULTS OF EVALUATION

The performance of the ACS alternatives 1 to 5 is shown in figures 7.8 to 7.12. Each of these figures represents two complete orbits; the first orbit is without axial thrust and the second orbit is with 0.52 lb axial thrust. The figures show attitude errors, attitude rates, and microgravity accelerations at one representative point. For proper plotting, the microgravity pulses in these figures are time-stretched by a factor of 40. All simulations are with nominal inertial properties.

The coordinates of the point at which the microgravity accelerations were computed are as follows:

x, 142.0 in. forward of the spacecraft center of gravity

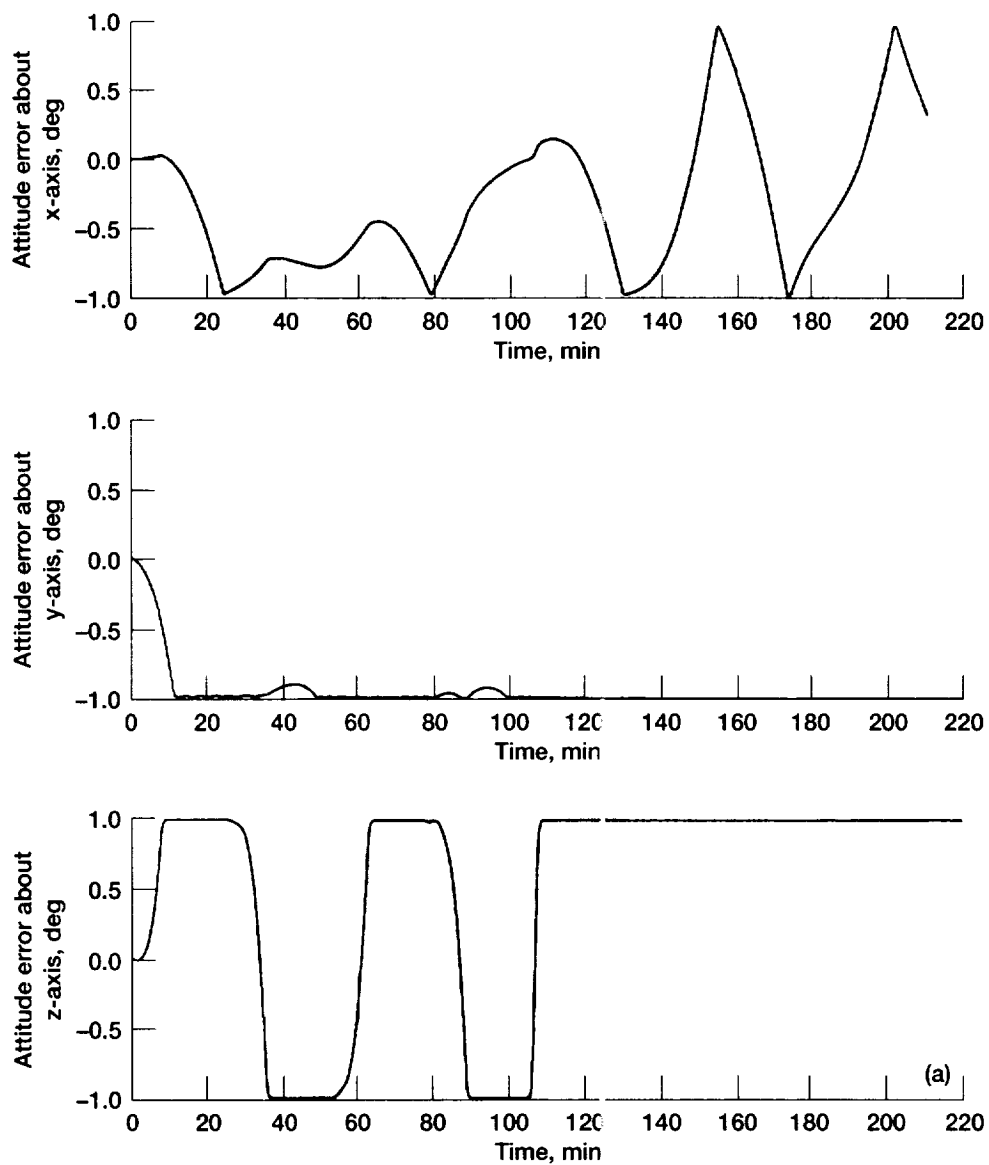


Figure 7.8.—Performance of ACS alternative 1. (a) Attitude errors. (b) Attitude rates. (c) Microgravity accelerations.

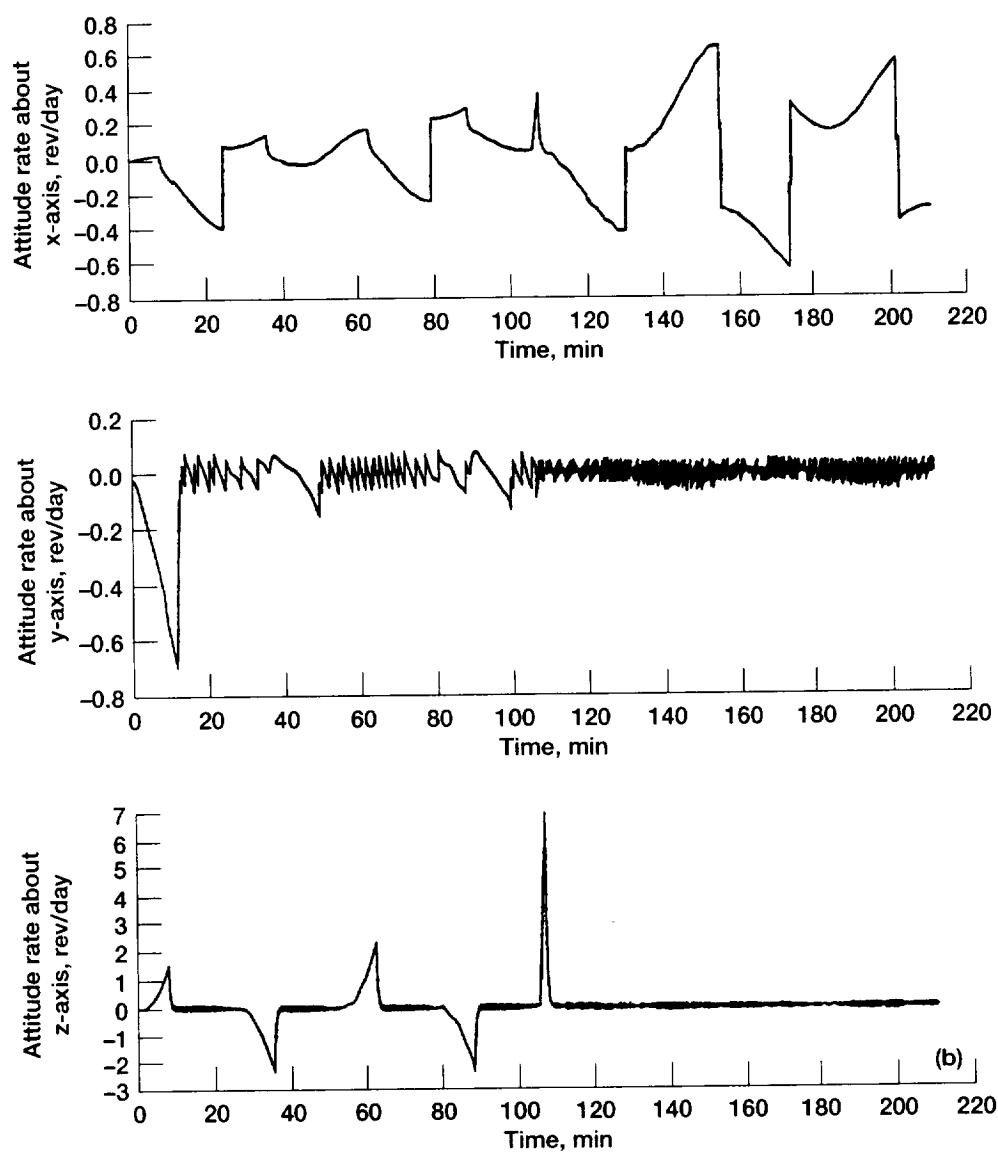


Figure 7.8.—Continued. (b) Attitude rates.

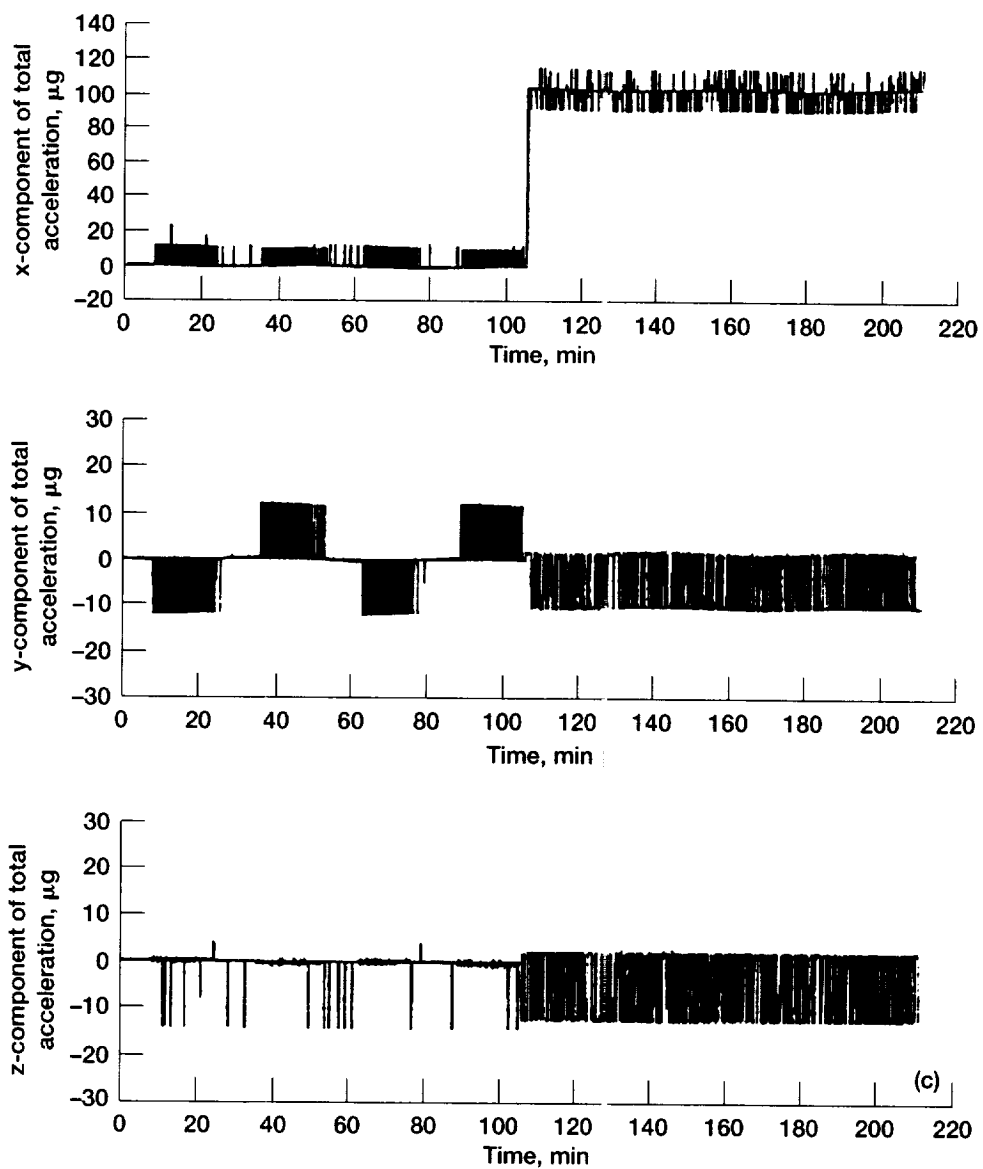


Figure 7.8.—Concluded. (c) Microgravity accelerations.

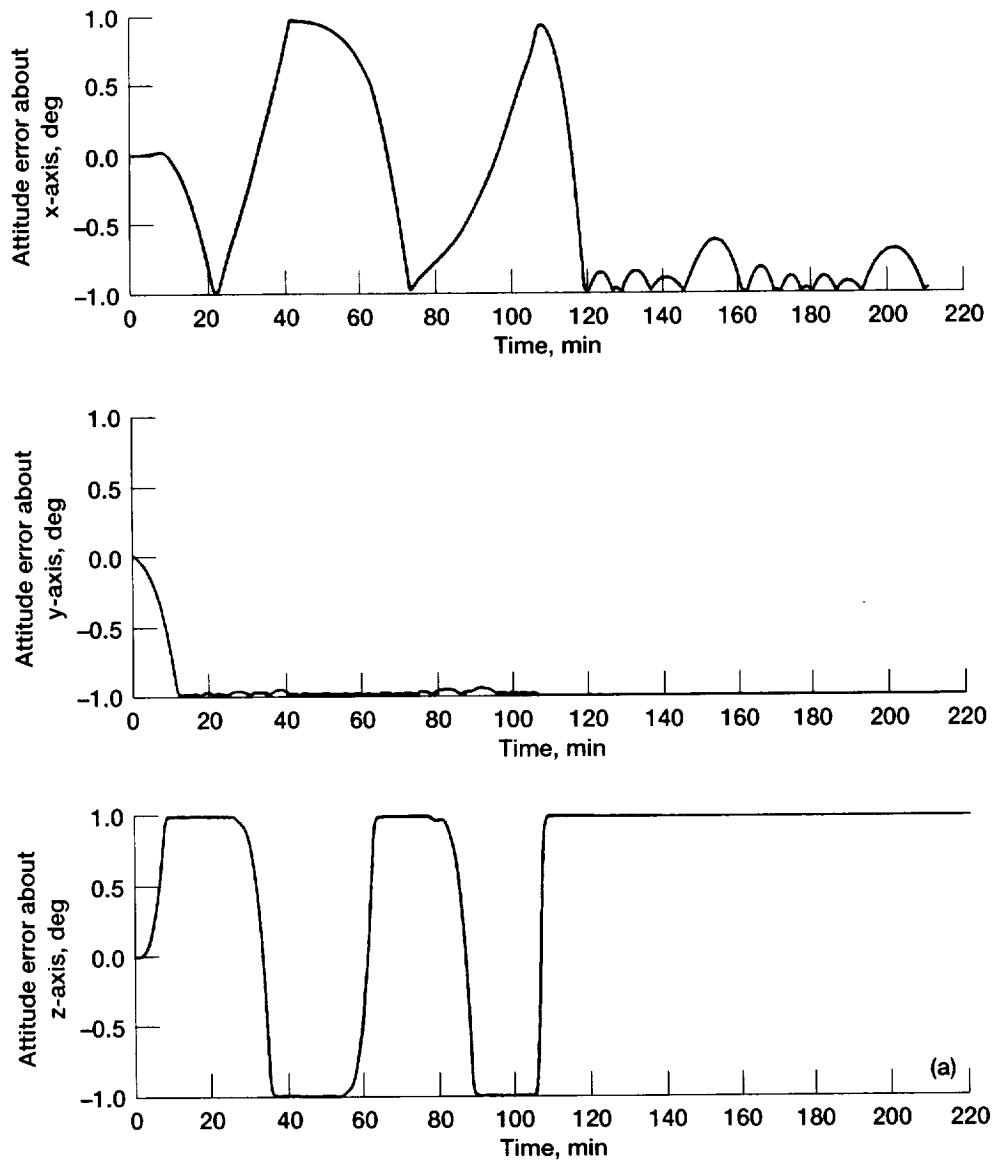


Figure 7.9.—Performance of ACS alternative 2. (a) Attitude errors. (b) Attitude rates. (c) Microgravity accelerations.

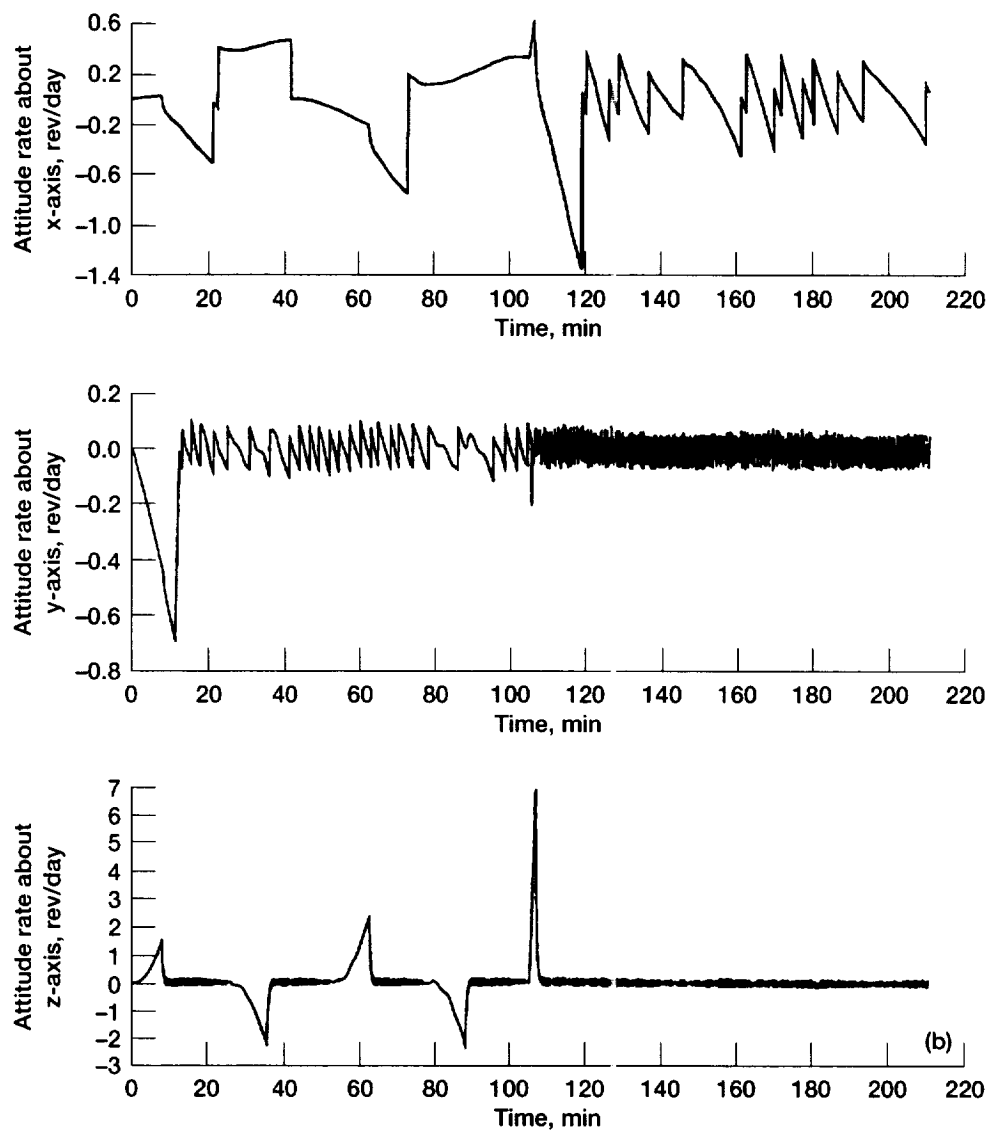


Figure 7.9.—Continued. (b) Attitude rates.

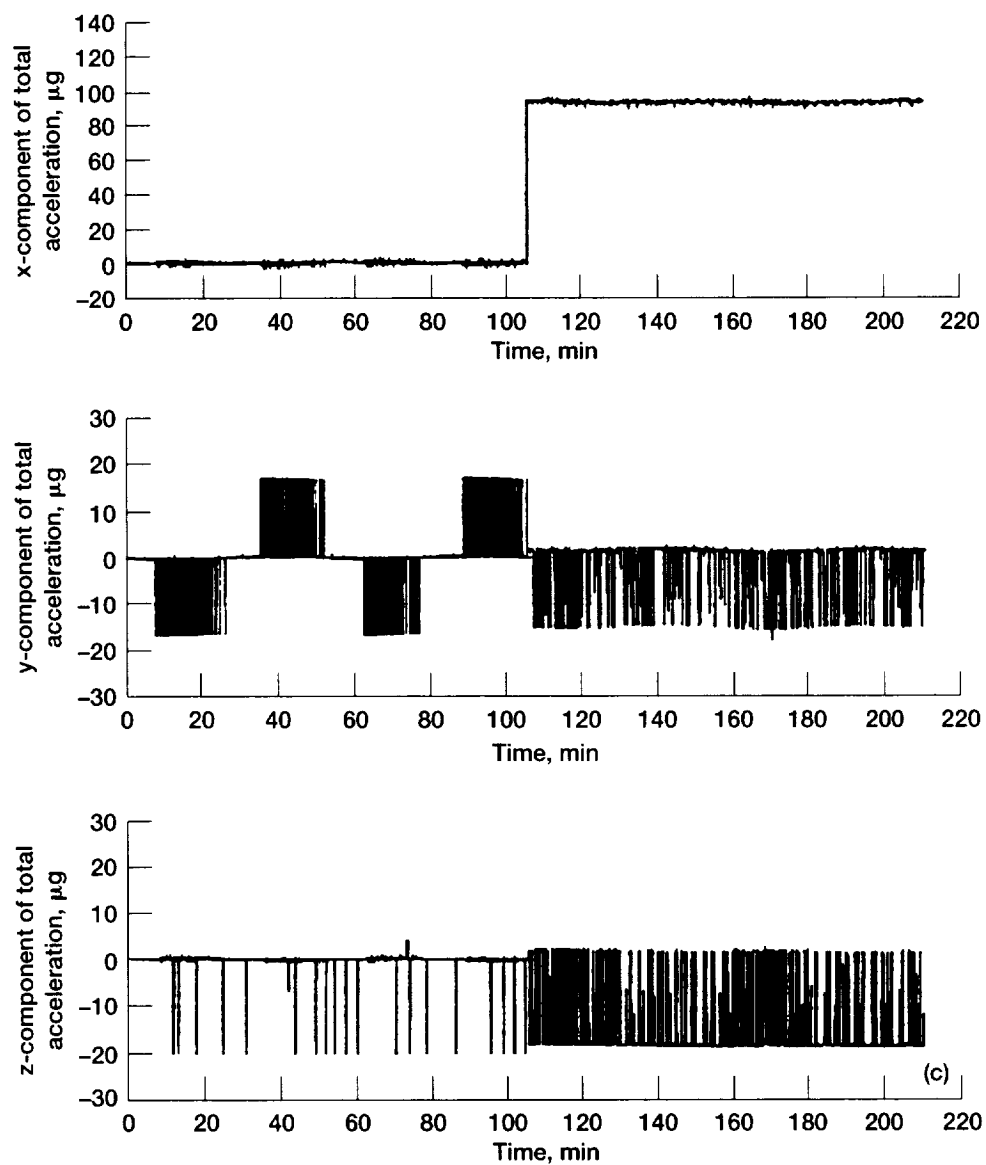


Figure 7.9.—Concluded. (c) Microgravity accelerations.

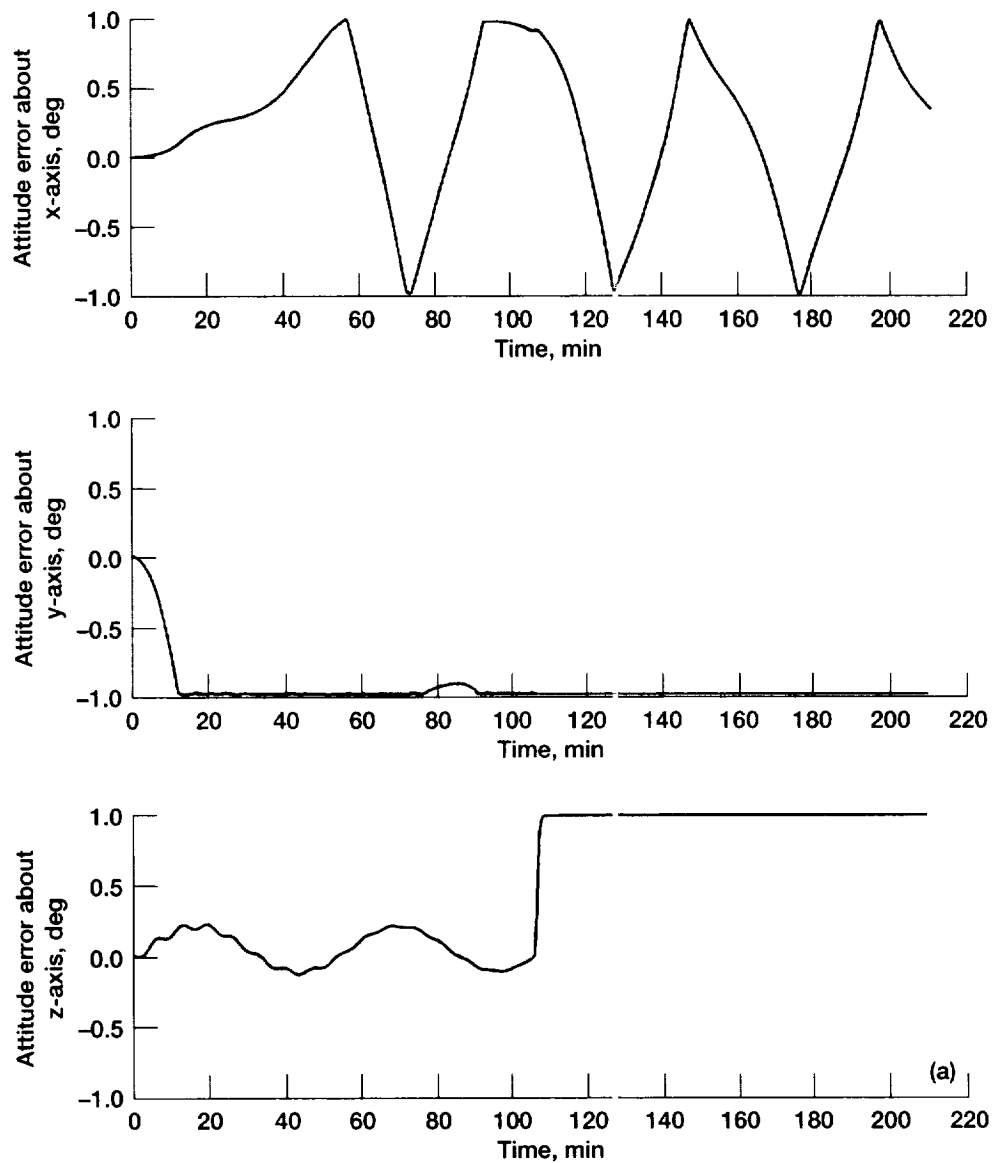


Figure 7.10.—Performance of ACS alternative 3. (a) Attitude errors. (b) Attitude rates. (c) Microgravity accelerations.

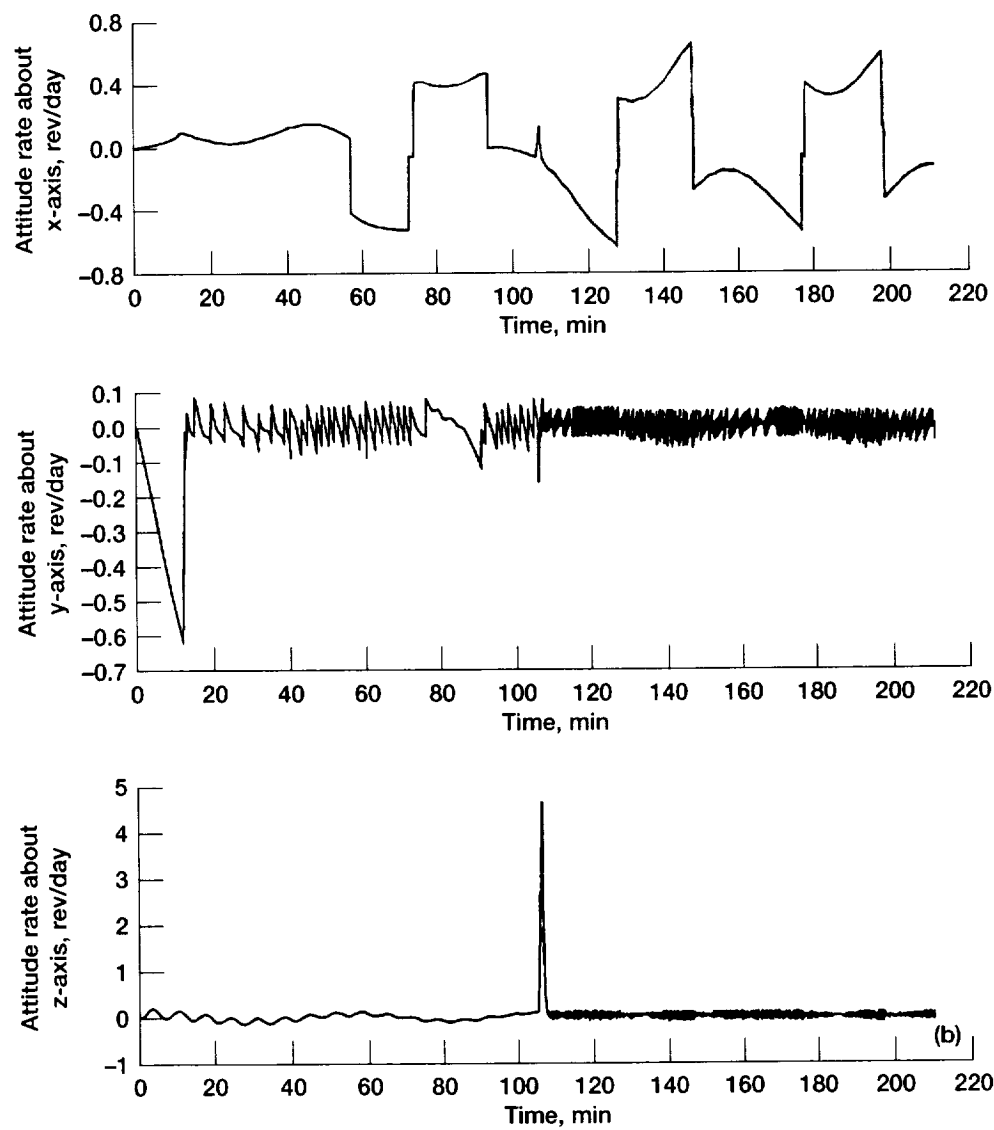


Figure 7.10.—Continued. (b) Attitude rates.

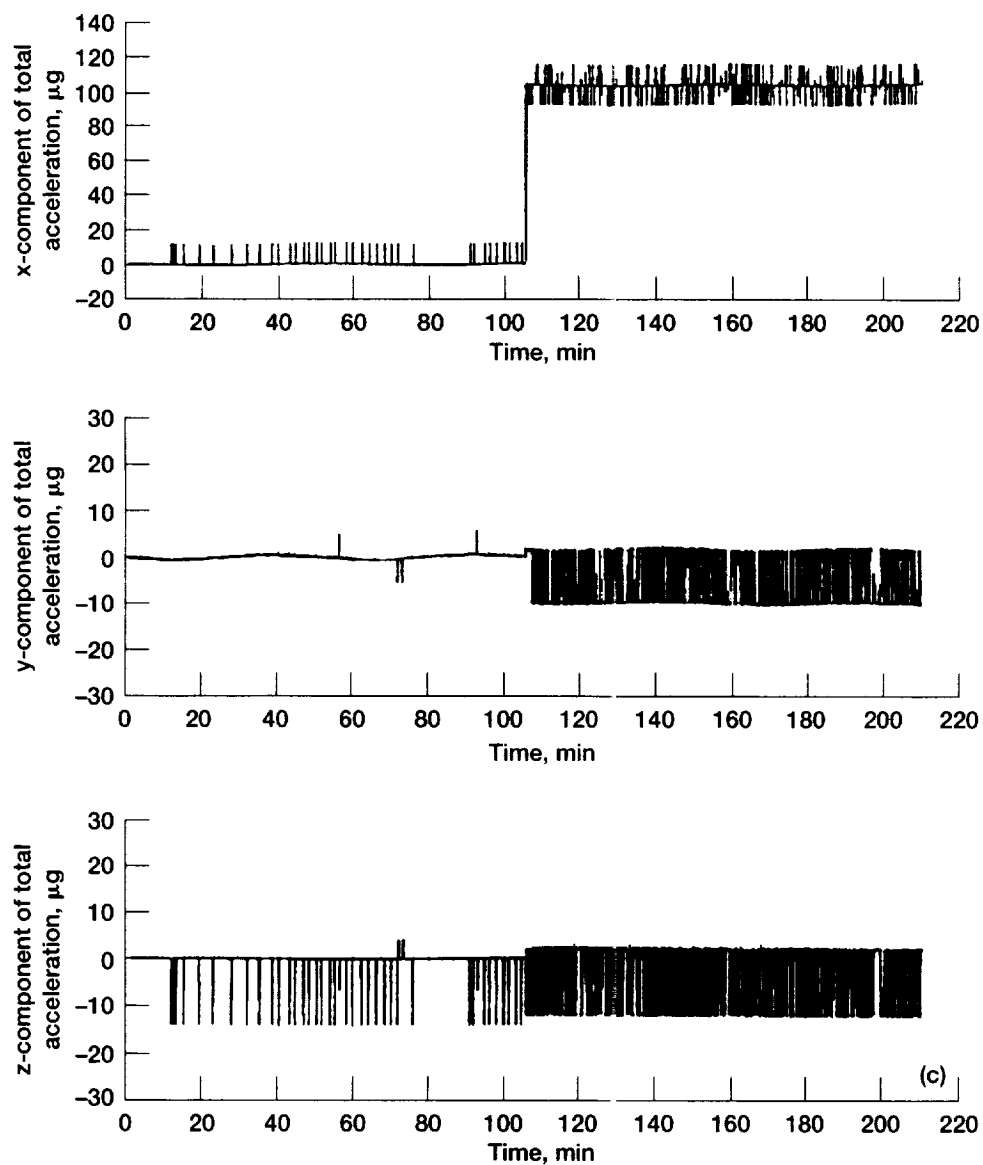


Figure 7.10.—Concluded. (c) Microgravity accelerations.

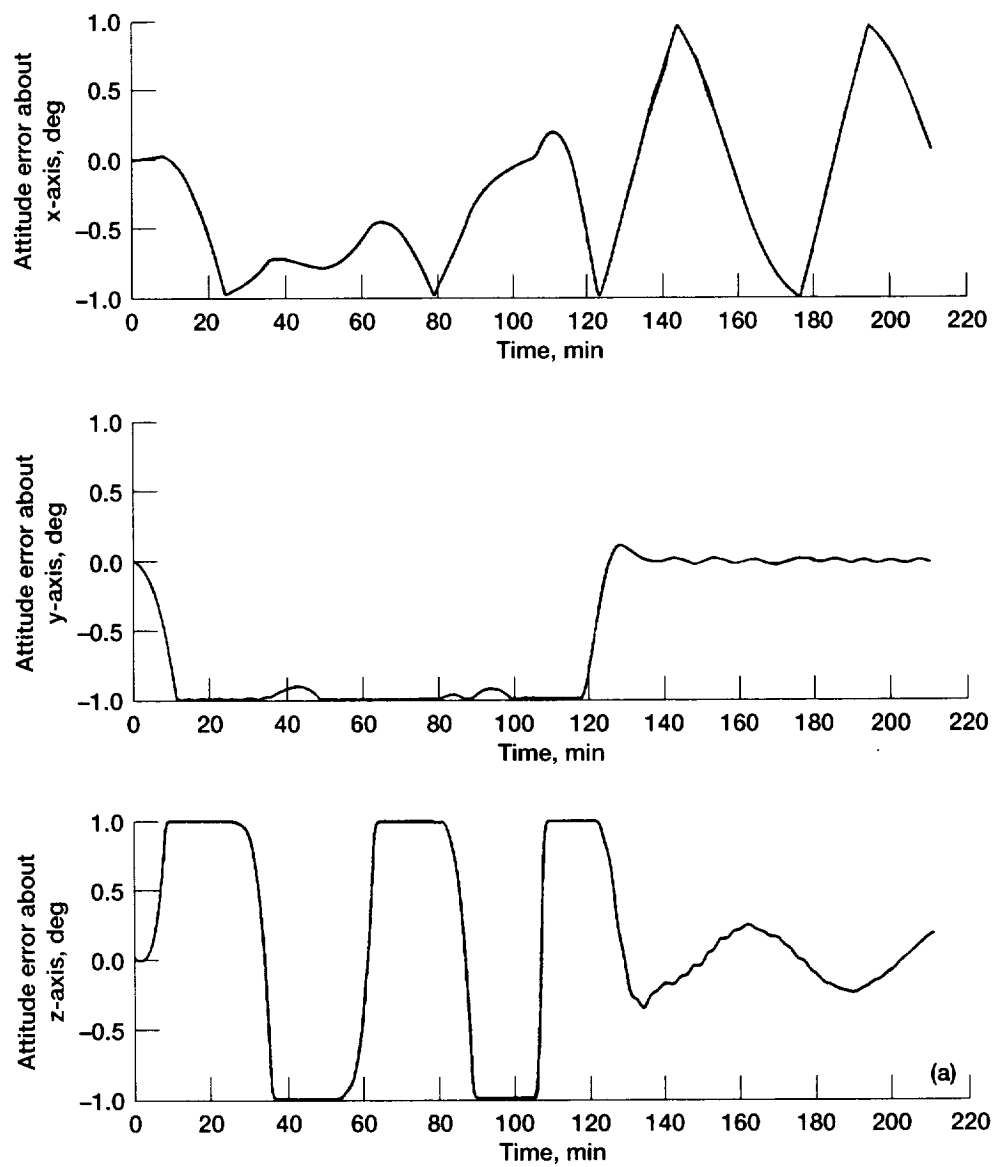


Figure 7.11.—Performance of ACS alternative 4. (a) Attitude errors. (b) Attitude rates. (c) Microgravity accelerations.

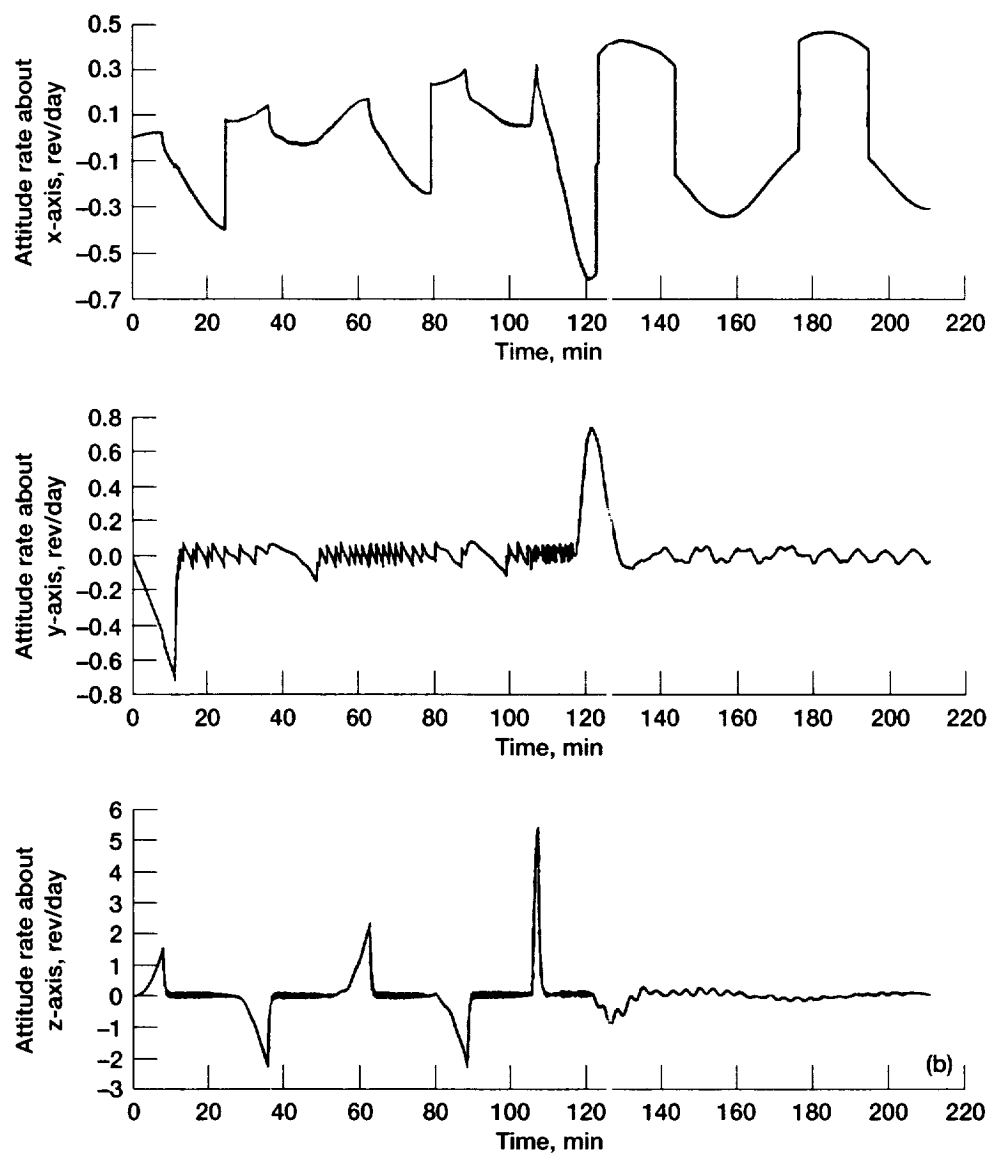


Figure 7.11.—Continued. (b) Attitude rates.

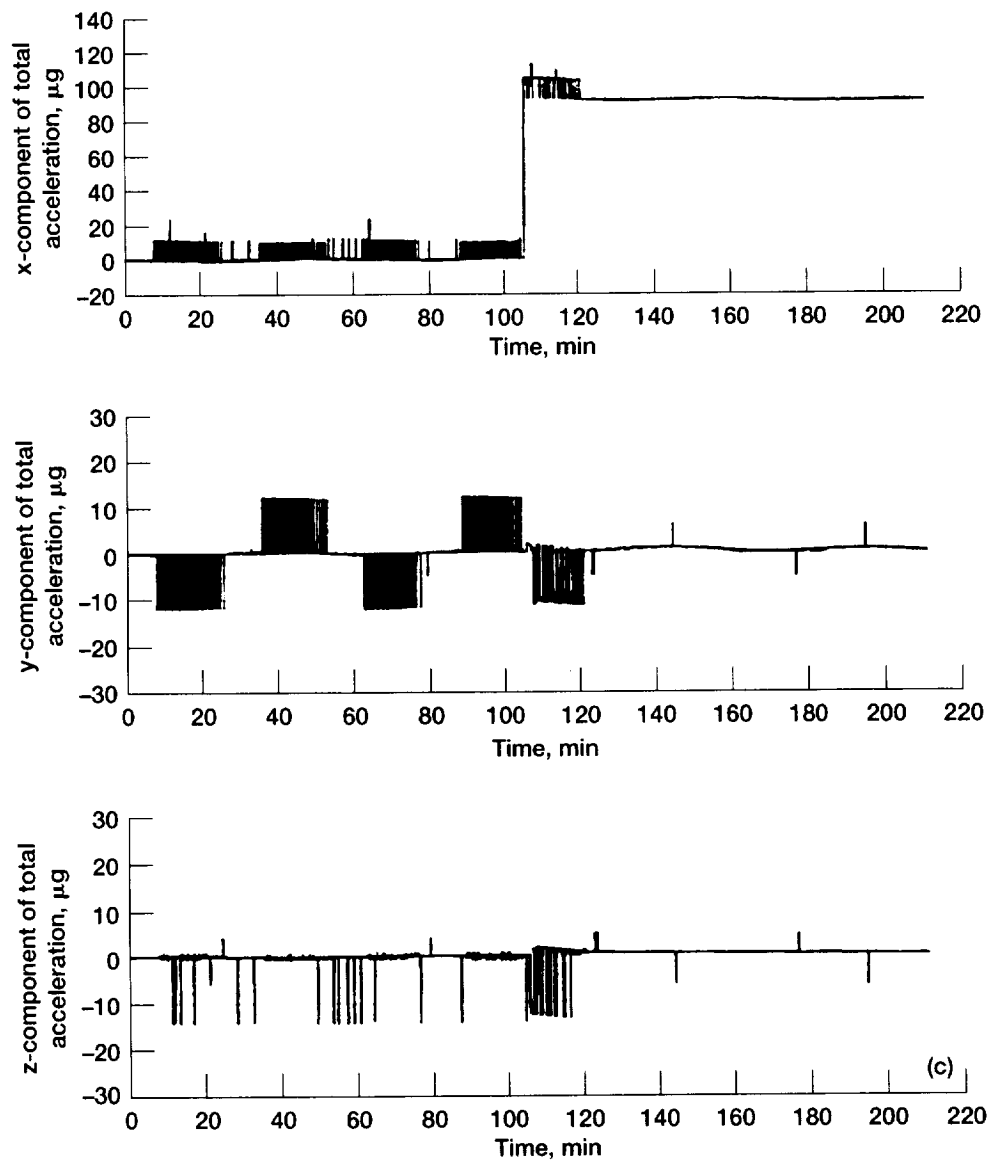


Figure 7.11.—Concluded. (c) Microgravity accelerations.

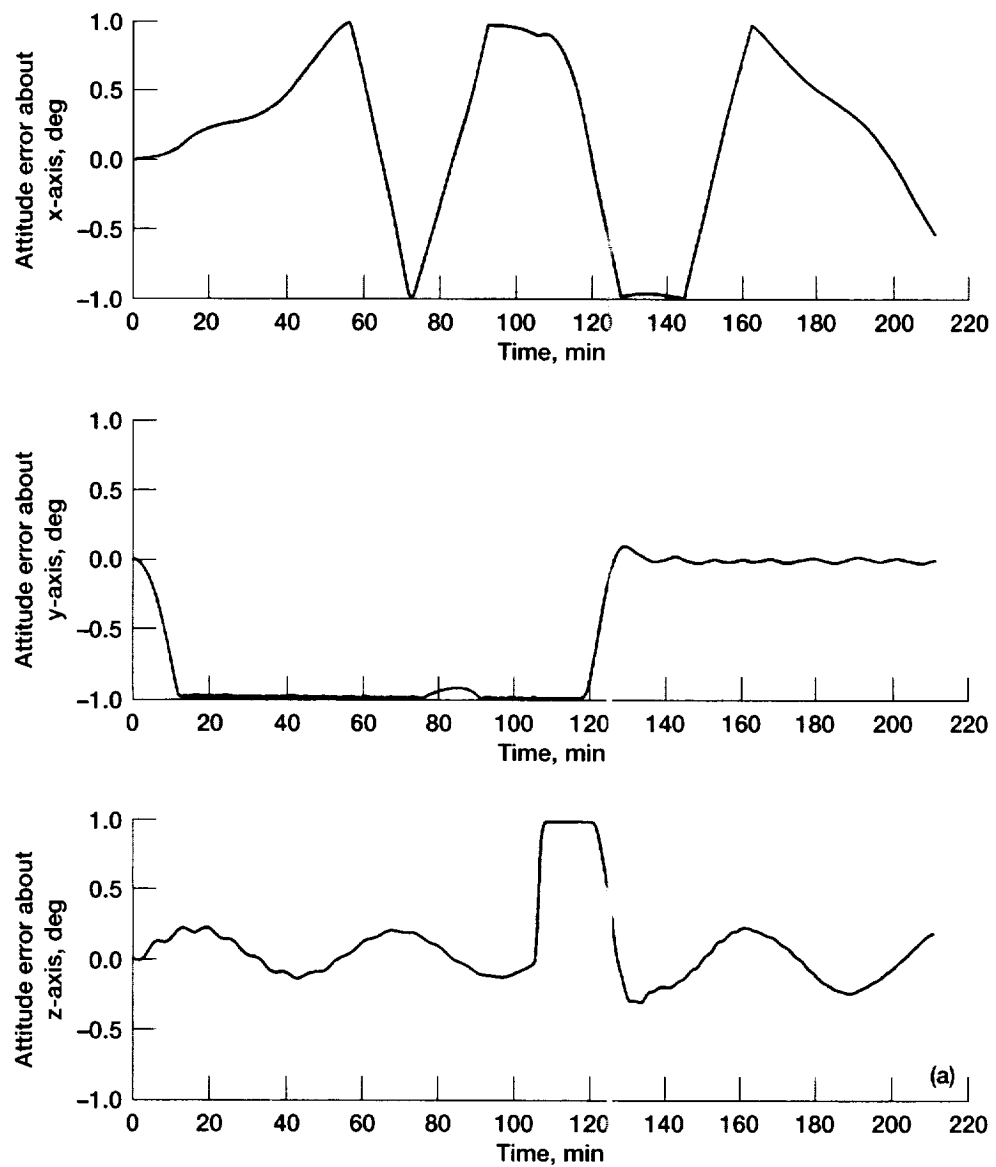


Figure 7.12.—Performance of ACS alternative 5. (a) Attitude errors. (b) Attitude rates. (c) Microgravity accelerations.

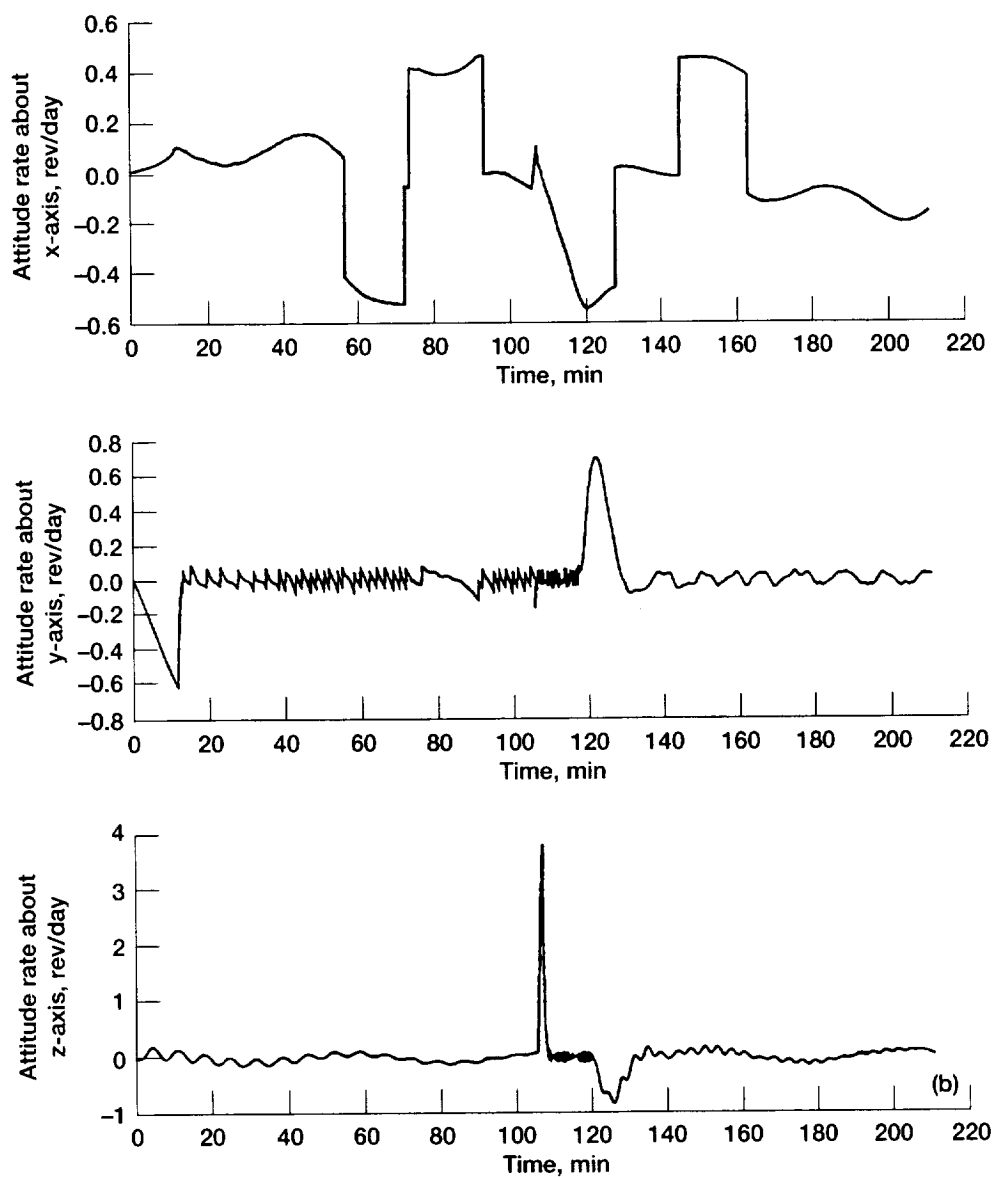


Figure 7.12.—Continued. (b) Attitude rates.

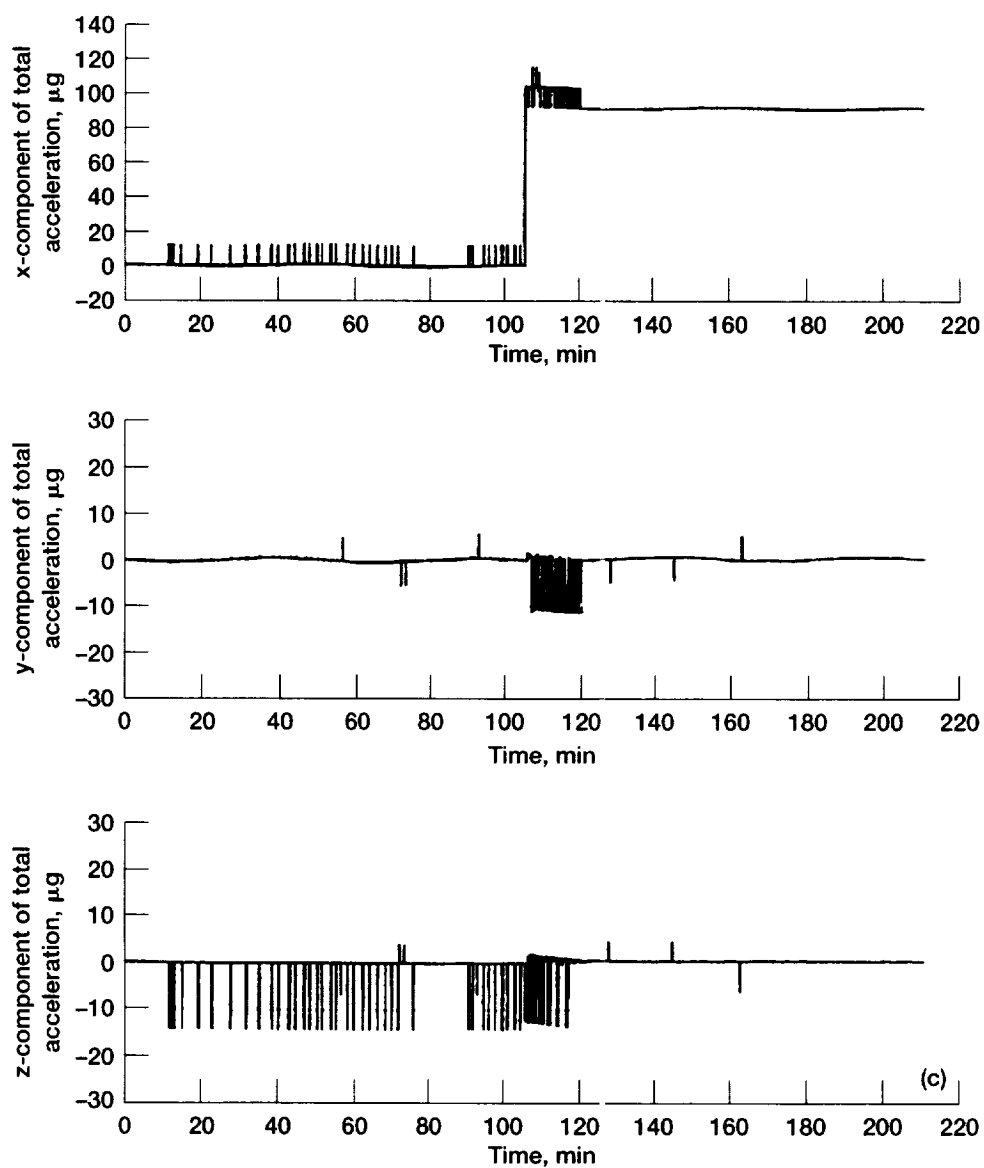


Figure 7.12.—Concluded. (c) Microgravity accelerations.

y, 11.5 in. from the spacecraft centerline
z, 11.5 in. from the spacecraft centerline.

This point is located on the large receiver tank wall at the forward end of the cylindrical tank section.

As these figures show, all ACS alternatives considered are able to maintain the desired attitude within the required accuracy.

For alternatives 4 and 5, the gimbal angles for the gimbaled thruster were nulled at the start of the simulation. Upon initiation of axial thrusting, a transient period of approximately 15 min is observed until the gimbal angles stabilize. During this period, the control thrusters assist in maintaining the proper attitude. Although not shown in the figures, the maximum gimbal angle required to maintain attitude was 10° on both axes.

The initial reaction-wheel speed for alternatives 3 and 5 was zero. During the simulations, the speed increased to a maximum of 400 radians/sec. At the start of the second orbit, when axial thrust was applied, the reaction wheel was allowed to coast. Because of friction, the wheel speed gradually decreased to near zero by the end of the second orbit.

The microgravity environment at the selected point described previously was analyzed in more detail for alternatives 1, 2, and 4 during application of 0.52 lb of axial thrust. The results of this analysis are shown in figures 7.13 to 7.15. Each figure represents one complete orbit which starts after the gimbal angle transient discussed previously has subsided. The time duration of the pulses in these figures is magnified by a factor of 20 to ensure consistent plotting by the graphics program. This stretching leads to a visualization of the microgravity disturbances that is highly exaggerated.

The MID's and the RMSD's were computed for the three cases shown in figures 7.13 to 7.15. The results of this analysis are presented in table 7.5.

7.5.4 SELECTED SYSTEM

Alternative 4 was selected, with input from the experimenters, after the quantitative results and qualitative evaluation were reviewed. Alternative 4 is a gimbaled thruster combined with an all-thruster system using coupled thrusters for x-axis control and uncoupled thrusters for y- and z-axis control.

While all the alternatives were fully capable of maintaining the spacecraft attitude within the required accuracy, alternative 4 was the least complex, lowest cost system that would satisfy the experiment requirements for minimal fluid perturbations during the application of axial thrust. Since the control of microgravity disturbances is not considered critical under zero-g conditions, alternatives 3 and 5 were eliminated from consideration to avoid the cost, weight, power consumption, and complexity of the reaction wheel. On the other hand, the improvement of the microgravity environment during axial thrusting of alternative 4 over alternatives 1 and 2 because of

the addition of the gimbaled thruster was judged to be worth the risk entailed in developing such a system. The risk of developing a gimbaled thruster system is mitigated through the use of off-the-shelf hardware.

7.6 Description of Selected System

7.6.1 ATTITUDE CONTROL SYSTEM (ACS) OVERVIEW

A functional block diagram of the ACS showing the various components and interfaces with other spacecraft systems is shown in figure 7.16. The ACS hardware consists of a complement of sensors and an interface electronics box. All data and command transfers between ACS sensors and actuators and the computers are provided by the TT&C system.

The primary attitude sensor is the inertial reference unit (IRU). Attitude data and gyro rate drift for the IRU will be updated by information from the digital Sun sensors and horizon sensors. Magnetometers are used to provide three-axis attitude information for on-orbit orientation during acquisition or tumble recovery.

During quiescent periods, hydrazine control thrusters will be used for attitude control. These thrusters provide coupled torque on the x-axis and uncoupled torques on the y- and z-axes.

During the induced acceleration experiments, the primary attitude control system will be a two-axis gimbaled thruster. The gimbaled thruster provides a means of directing the thrust vector through the spacecraft center of gravity for the y- and z-axes, thus minimizing control thruster firings for these axes. For x-axis control, the coupled thrusters will still be used. All thrusters are part of the propulsion system.

Algorithms for determining attitude and issuing commands from the ACS are implemented in the computers which are part of the TT&C system. The on-orbit flight software is responsible for spacecraft control and attitude determination.

7.6.2 HARDWARE DESCRIPTION

A description of the sensors, actuators, and ACS interface electronics is given in the following paragraphs. Key parameters of the ACS sensors and actuators are given in table 7.6. The approximate location of the various ACS components on the spacecraft is shown in figure 7.17.

7.6.2.1 Inertial Reference Unit (IRU)

The primary attitude sensor is the NASA standard dry rotor inertial reference unit (DRIRU II or IRU). The IRU is a strap-down rate-integrating system which supplies the rate and attitude information required for attitude control. The IRU has three independent gyro channels. Each channel supplies two

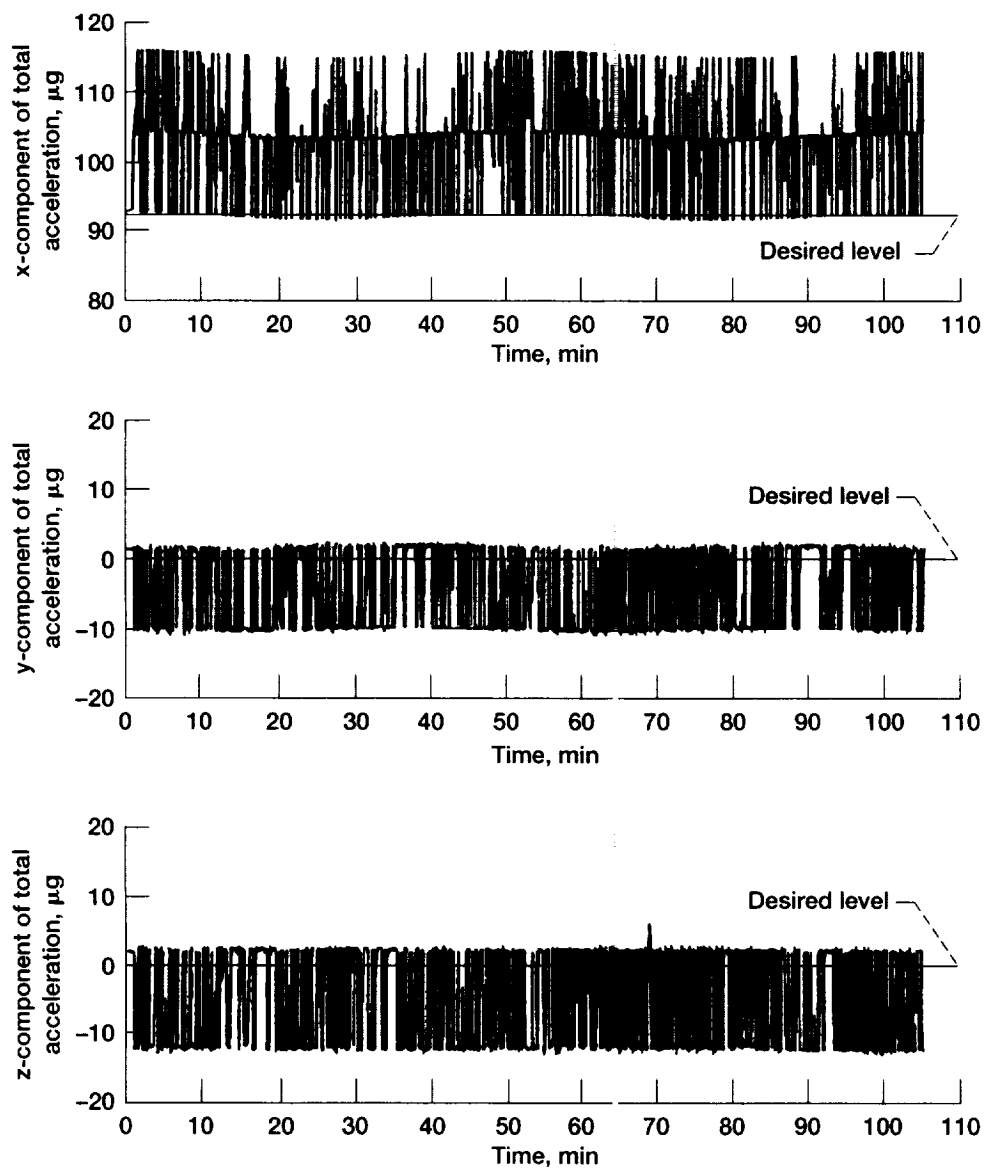


Figure 7.13.—Microgravity at selected point for ACS alternative 1 (uncoupled control thrusters).

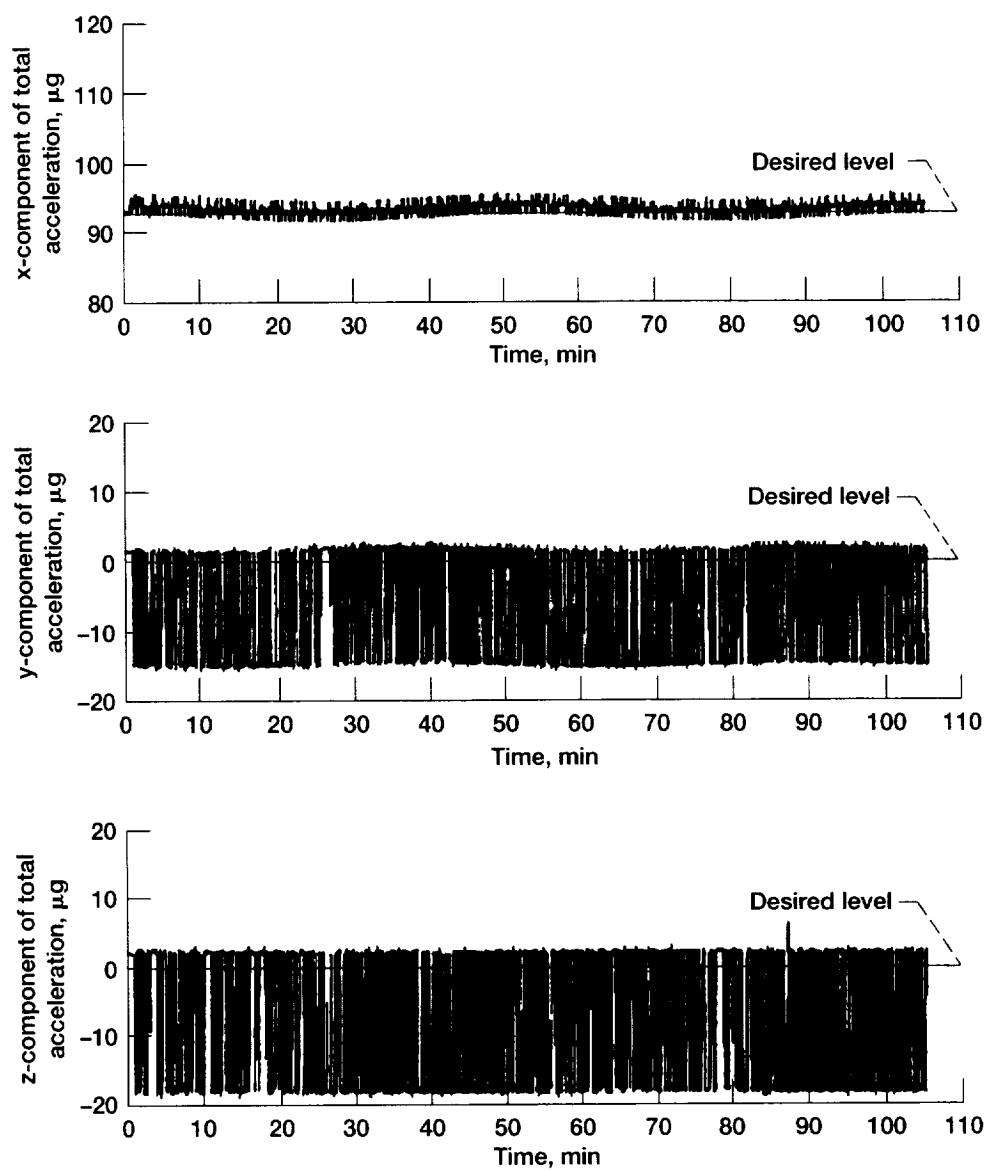


Figure 7.14.—Microgravity at selected point for ACS alternative 2 (coupled control thrusters).

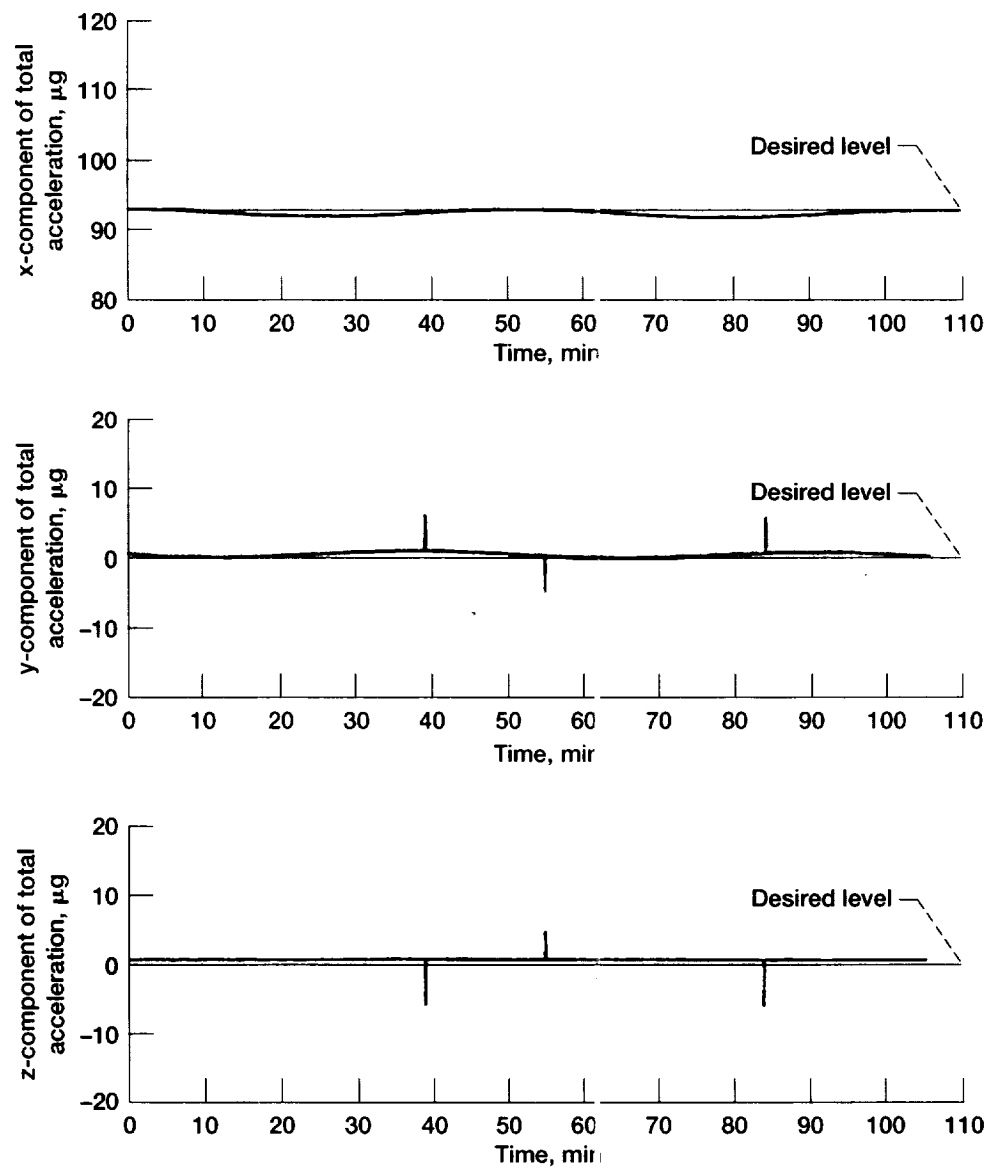


Figure 7.15.—Microgravity at selected point for ACS alternative 4 (with gimbaled thruster).

TABLE 7.5.—MICROGRAVITY DEVIATIONS^a

Maximum instantaneous deviation, $\mu\text{-g}$			
Alternative	Component		
	x	y	z
1	23.46	10.70	15.87
2	2.93	20.45	18.47
4	0.90	6.15	6.03
RMS deviation, $\mu\text{-g}$			
1	6.66	4.04	4.83
2	0.74	4.89	5.95
4	0.52	0.64	0.62

^aAt the point specified in section 7.5.3 with 0.52 lb axial thrust desired acceleration values are 92.69 $\mu\text{-g}$ in the positive x direction and 0 in the y and z directions.

TABLE 7.6.—COMPONENT PARAMETERS

Component	Key parameters
Inertial reference unit (IRU) (DRIRU II ^a)	Maximum rate High rate mode, 2 deg/sec Low rate mode, 400-arc-sec/sec Quantization High rate mode, 0.8 arc-sec/pulse Low rate mode, 0.05 arc-sec/pulse Acceleration insensitive drift rate stability (6 hr) High rate mode, NA Low rate mode, 0.003 deg/hr
Digital Sun sensor	Field of view, 64° by 64° Accuracy, $\pm 0.017^\circ$
Horizon sensor	Scan cone angle (half), 45° Rotation scan rate, 4 scan/sec Accuracy $\pm 0.07^\circ$
Magnetometer	Range, ± 600 mG Accuracy, 0.2 percent of full scale Orthogonality, $\pm 0.2^\circ$ axis-to-axis and axes-to-reference surface
Control thrusters	Size, 0.06 lb Torque x-axis, 5.76 in.-lb y- and z-axes, 2.88 in.-lb
Gimballed thruster	Size, 0.04 lb Gimbal angle, $\pm 20^\circ$ /axis maximum Torque Most forward center of gravity, 0.95 in.-lb Most aft center of gravity, 0.82 in.-lb

^aNASA standard dry rotor inertial reference unit.

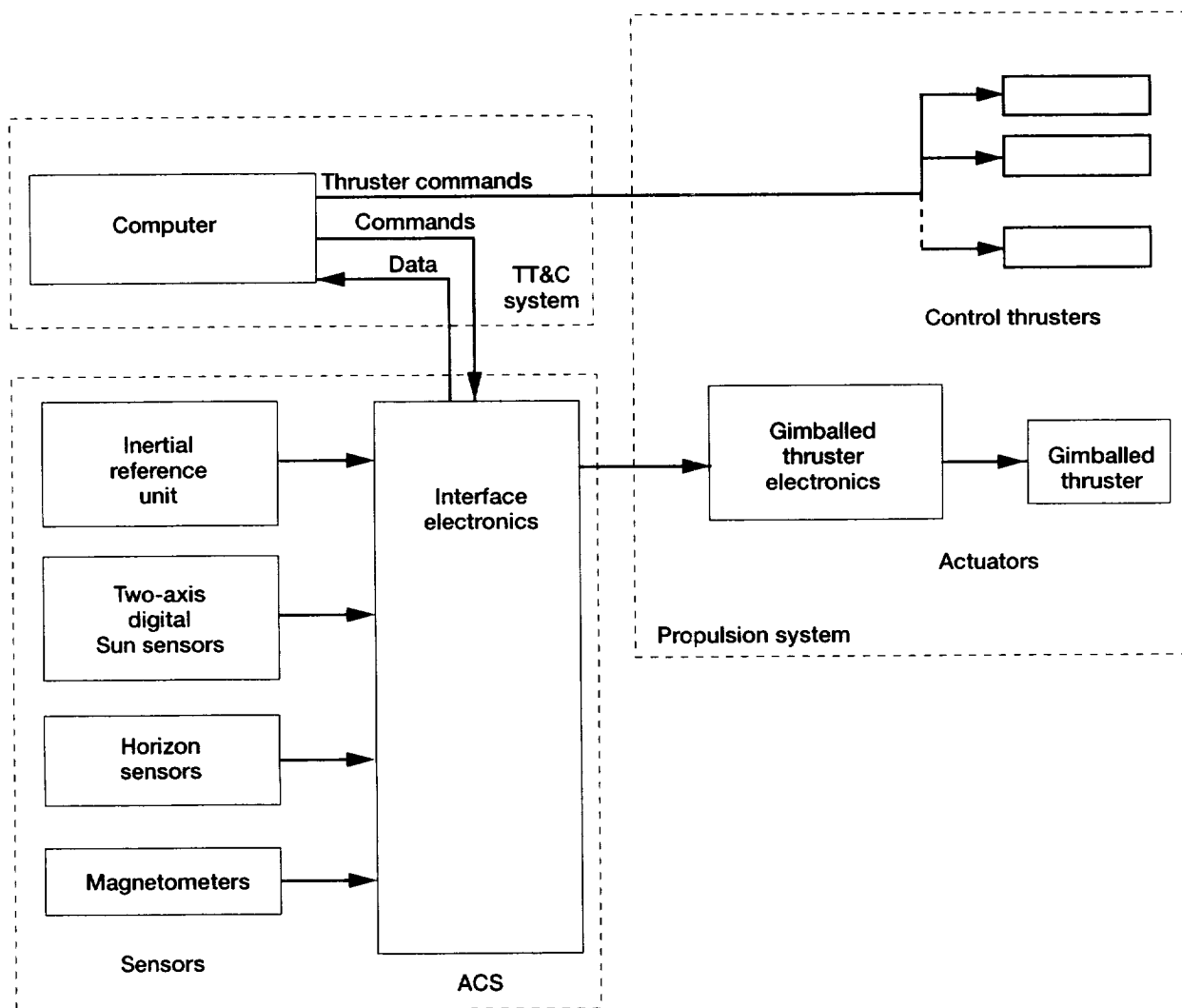


Figure 7.16.—Attitude control system (ACS) functional diagram.

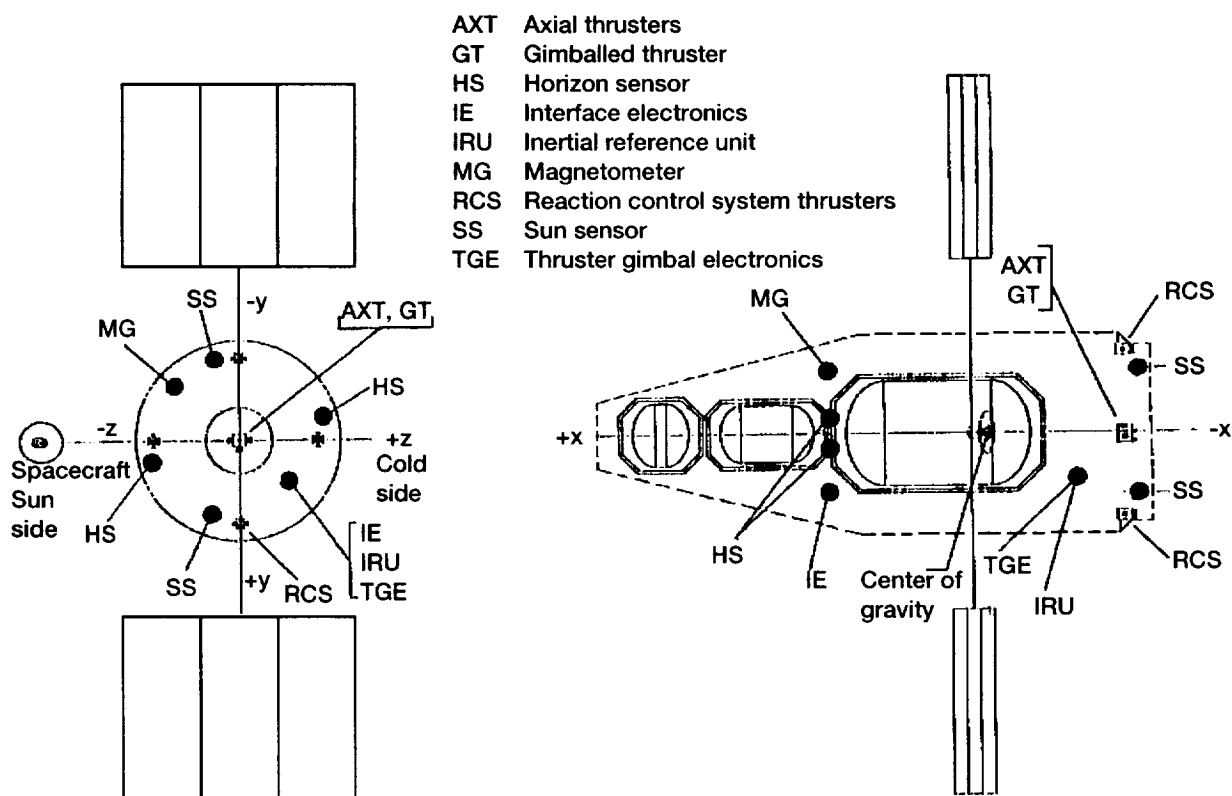


Figure 7.17.—Approximate location of attitude control system (ACS) components.

orthogonal axes of information derived from a dedicated gyro with two degrees of freedom.

Each gyro channel supplies the ACS interface electronics with positive and negative angle pulse trains for each axis and an associated reference clock. These gyro pulses are accumulated to give a count proportional to the incremental rotation about each gyro axis. The pulse count scale factor has two ranges selectable by discrete commands. The DRIRU II drift rate stability is within 0.003 arc-sec/sec over 6 hr.

7.6.2.2 Digital Sun Sensors

A digital Sun sensor system consists of a two-axis Sun sensor head and a package of signal processing electronics. The Sun sensor head uses two reticles for Sun-angle sensing, a Grey code reticle for coarse angles, and a periodic pattern reticle for fine-angle determinations. Conversion of the outputs of the Sun sensor head to series binary bits is performed in the signal processing electronics. The Sun sensor provides a $\pm 32^\circ$ field of view for each axis.

Redundant Sun sensor systems will be used on the spacecraft. The primary use of the Sun sensors will be to provide information to update the IRU data.

7.6.2.3 Horizon Sensors

A horizon sensor system consists of an optical head and an electronics package. The optical head contains a motor-driven scanner. The field of view of the sensor is deflected 45° and rotated continuously. When the scan path intersects the Earth, the infrared detector senses the difference between Earth and space. The electronics package contains the circuits needed to process the outputs of the infrared detector, a power supply, and the scanner motor drive circuits.

Redundant horizon sensors will be used on the spacecraft. The primary use of the horizon sensors will be to provide information to update the IRU data.

7.6.2.4 Magnetometers

Redundant magnetometers will be provided on the spacecraft. The magnetometers are a three-axis type with the magnetic sensor and the signal processing electronics packaged in one unit.

The magnetometers will be used to provide information about attitude for contingency acquisition.

7.6.2.5 Control Thrusters

The control thrusters are sized at 0.06 lb and produce a coupled torque of 5.76 in.-lb about the x-axis and an uncoupled torque of 2.88 in.-lb about the y- and z-axes. There are redundant and backup sets of control thrusters.

7.6.2.6 Gimballed Thruster System

This system consists of a fixed nozzle thruster mounted on two single-axis antenna gimbals. The first gimbal is mounted to the spacecraft with its rotation axis parallel to the spacecraft y-axis. The second gimbal is mounted on the first gimbal and its rotation axis is parallel to the spacecraft z-axis. To provide sufficient torque margin, a maximum gimbal angle of $\pm 20^\circ$ about both the y- and z-axes has been selected. The size of the thruster is 0.04 lb.

7.6.2.7 ACS Interface Electronics

The ACS electronics are shown in figure 7.18. An electronics box will provide an interface between the ACS sensors and

the CTJ (part of the TT&C system). This electronic box will also provide an interface with the high-gain antenna and thruster-gimbal electronics.

The ACS interface electronics provides the following circuits and functions:

- (1) DC/DC converter that converts unregulated spacecraft power to the secondary voltages required by the sensors, gimbals, and interface electronics.
- (2) Power switching electronics that provides power distribution and cross-strapping
- (3) Sensor processing/interface electronics, which accumulates gyro pulses; buffers serial digital data from the Sun and horizon sensors; digitizes analog outputs from the magnetometers; and digitizes analog data from the sensors and antenna and thruster-gimbals.
- (4) Bus interface electronics, which include telemetry address/reply bus interface; command bus interface telemetry processor; and command processor

The ACS interface electronics will be internally redundant. The bus interface electronics will be identical to those in the RCTU's.

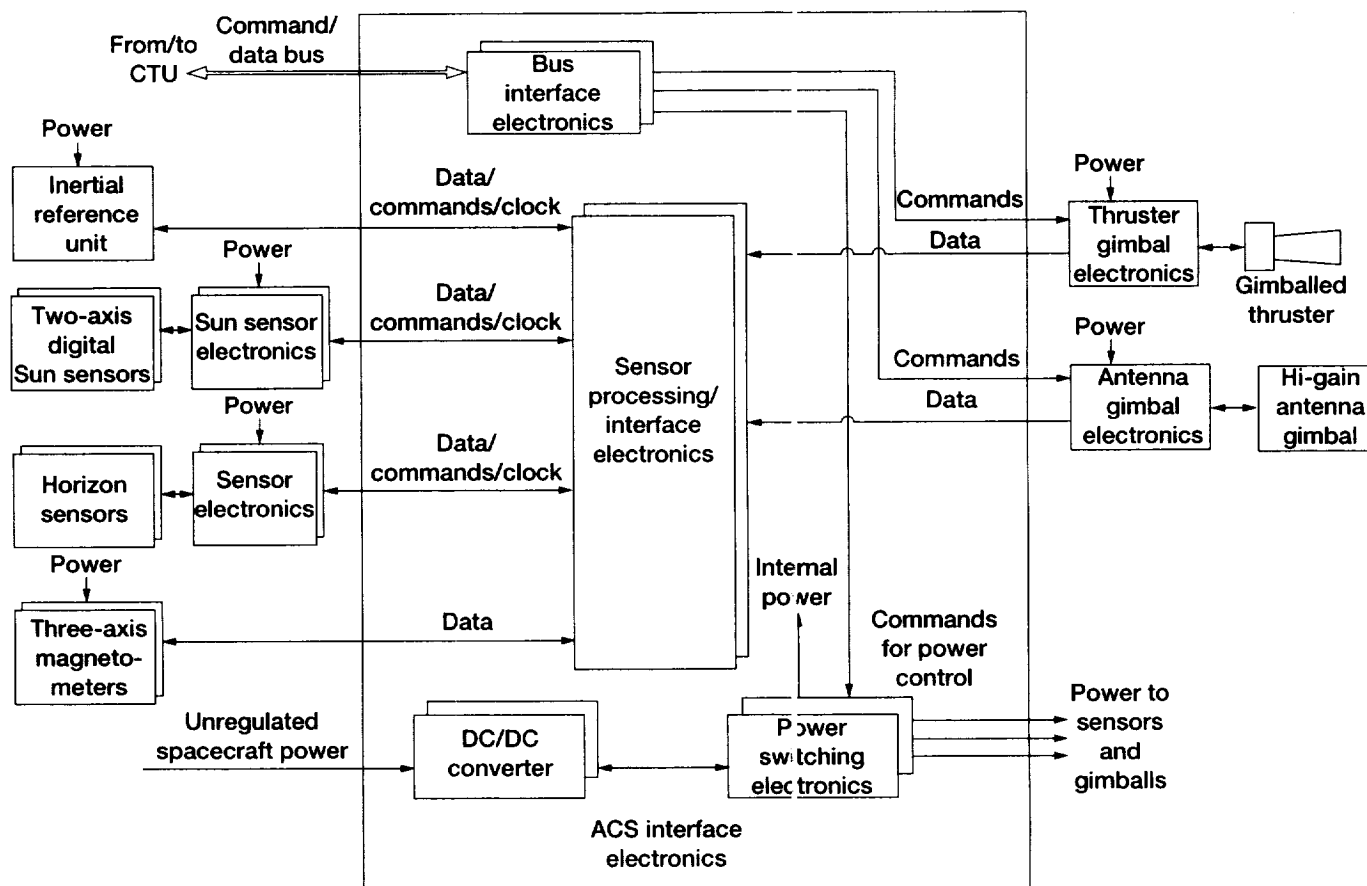


Figure 7.18.—Attitude control system electronics.

7.6.3 FUNCTIONAL DESCRIPTION

7.6.3.1 Attitude Determination for Normal On-Orbit Operational Mode

For the normal on-orbit mode, the primary attitude control sensor is the IRU. IRU data will be updated by information from the digital Sun sensors and horizon sensors.

Figure 7.19 shows the orientation and field of view of the Sun and horizon sensors.

The horizon sensors are mounted so that their spin axes are normal to the orbit plane, parallel to the spacecraft positive and negative z-axes. In the diagram, details of the horizon sensor whose spin axis is parallel to the +z axis are shown. The outputs of the horizon sensor are a chord and a phase. The chord is a measure of Earth width and the phase gives the distance from the sensor body reference to the midpoint of the chord. The scan cones of the horizon sensors can intercept the Earth over the entire orbit without any interference from the spacecraft structure, antenna, or solar arrays.

The Sun sensors are mounted so that the optical null is located parallel to the spacecraft x-z plane. As shown in figure 7.19, the Sun sensor is tilted with respect to the x-y plane at

an angle of 20.5° , one-half the maximum expected Beta (β) angle of 41° . This allows the sensor to be used over the $\pm 32^\circ$ field of view to cover the full range of β angles on the "hot" side of the spacecraft.

As shown in figure 7.20, IRU data will be processed to calculate gyro angular increments for the sampling period, corrected for gyro rate biases and axis misalignment. These compensated angular increments will be used to determine spacecraft attitude.

During Sun presence, data from the Sun and horizon sensors together with the actual spacecraft position and velocity, and the position of the Sun will be used to calculate the spacecraft attitude. This data will be used to update the attitude determined from the IRU data and the gyro rate biases. The Sun sensor data will be used to update information for the spacecraft y- and z-axes and the horizon sensor will be used to update information for the spacecraft x-axis.

The calculated attitude will be compared to the desired attitude in order to determine attitude errors. Spacecraft body rates will also be calculated. This data will be used to compute control law and thruster firing logic computations that will generate thruster firing commands. When the gimbaled thruster is being used, attitude error and body rate data are used to determine gimbal commands.

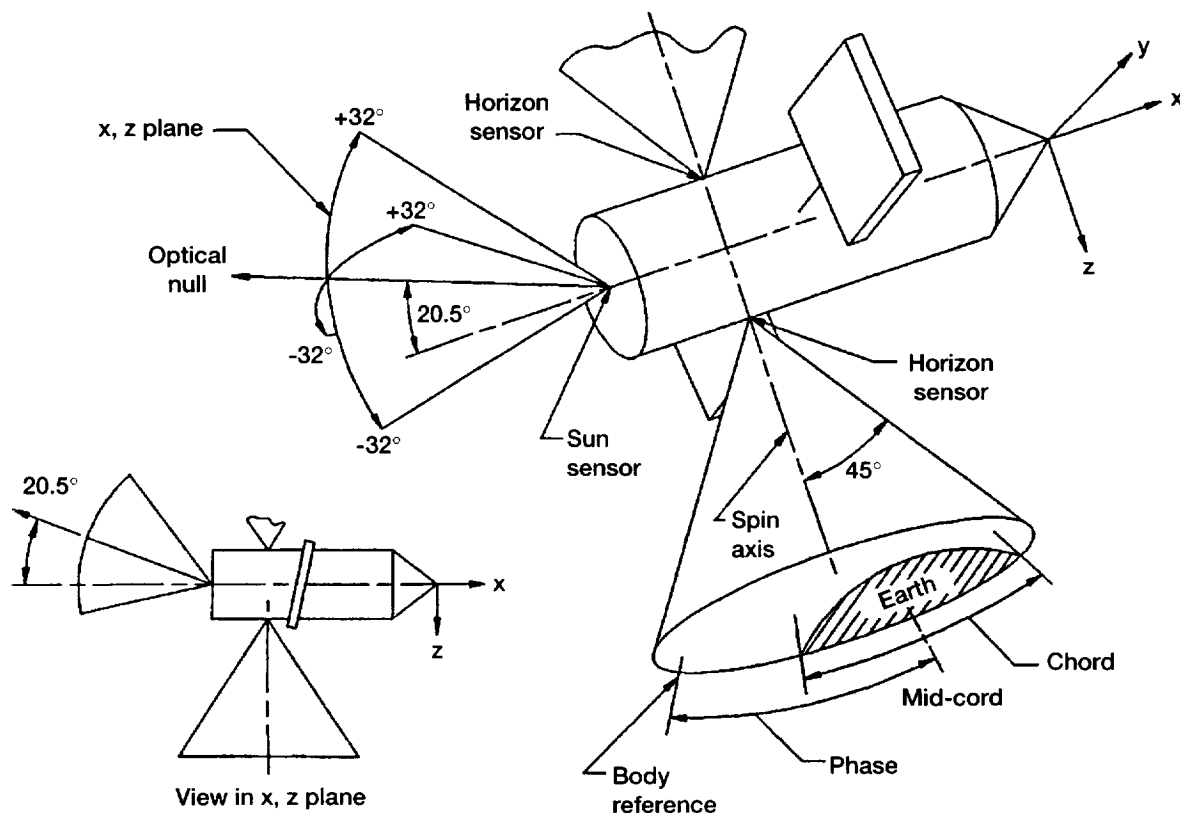


Figure 7.19.—Attitude control system (ACS) optical sensors.

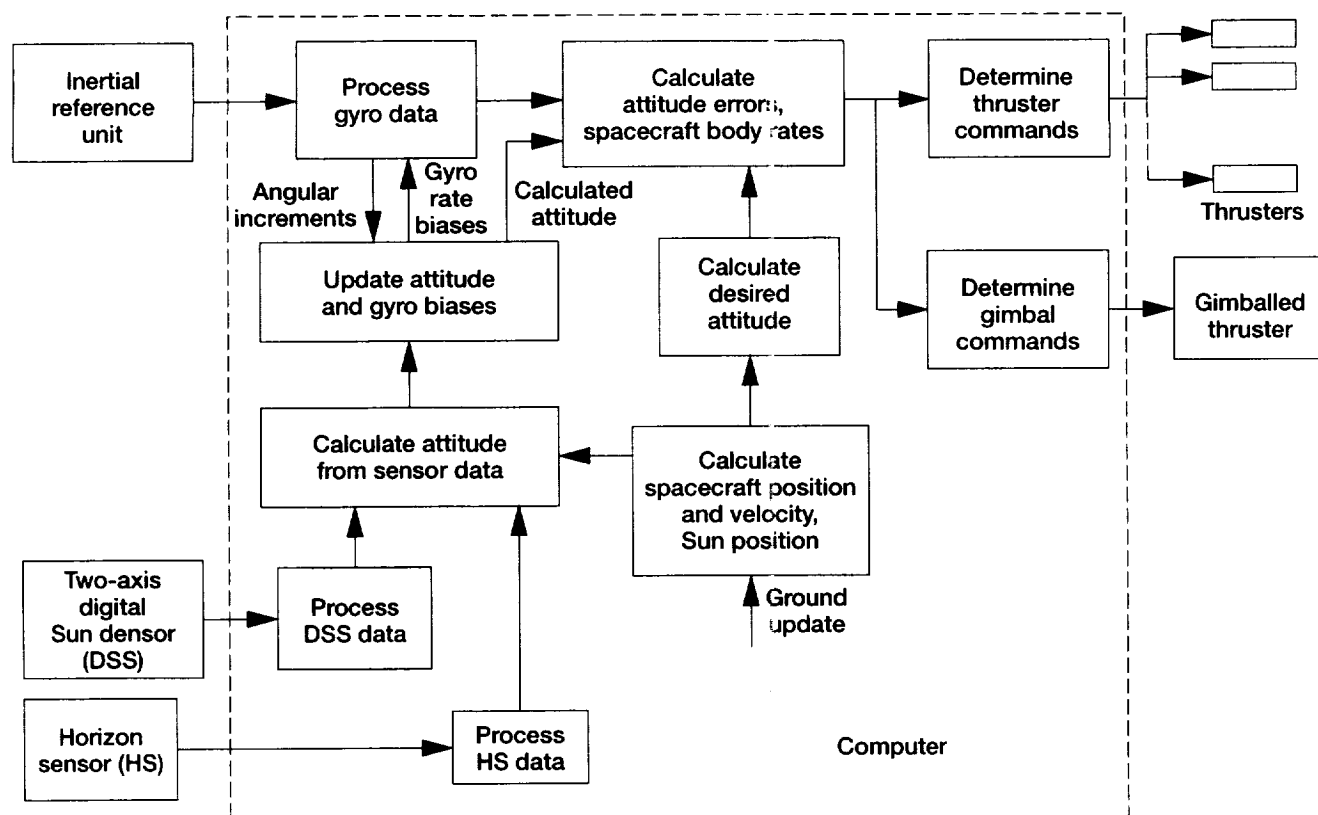


Figure 7.20.—Attitude determination in normal on-orbit mode.

Actual spacecraft position and velocity and Sun position will be computed onboard and updated periodically from the ground. Sun position will be provided by an onboard ephemeris.

7.6.3.2 Attitude Determination for Contingency Acquisition Mode

For contingency operations, such as, tumble recovery or acquisition from a spacecraft orientation where the Sun and Earth are out of view of the sensors, a technique is needed to allow the spacecraft to acquire the proper attitude. This will be accomplished onboard the vehicle for COLD-SAT by including a magnetometer.

The sequence of events for the acquisition system operation, which is described next, is illustrated in figure 7.21. The control system reduces the spacecraft rates to zero or near zero using data from the IRU. Once the rates are near zero, two magnetometer readings are taken 4.5 min apart (approximately 15° of orbit). These readings, in conjunction with knowledge of the spacecraft position and orbit parameters, an onboard Earth magnetic field model, and matrix orthogonality requirements, are used to determine the elements of the direction cosine matrix that relates the present spacecraft attitude to the desired attitude.

Given the elements of the direction cosine matrix, the quaternion relating the present spacecraft attitude to the desired

on-orbit attitude is computed. Once the quaternion has been determined, a command rate about the eigenaxis would be maintained on the spacecraft until the Sun and horizon sensors indicate that they have acquired the Sun and Earth, respectively. The attitude control system is then switched to its normal on-orbit mode.

7.6.3.3 Attitude Control

With the attitude errors and attitude rates determined as discussed in the previous section, the ACS determines the desired control thruster states and the appropriate thruster gimbal angles. The control thrusters and the gimbalanced thruster are two separate and independent attitude control systems and their control is achieved through different means. The following sections describe the proposed control logic for both systems.

7.6.3.3.1 Control Thruster Logic.—The control thrusters are enabled at all times throughout the mission. In the absence of axial thrust it is the primary system for attitude control. With axial thrust applied, the control thrusters provide primary attitude control about the spacecraft x-axis and serves as a backup system for attitude control about the y- and z-axes.

The thrusters are controlled by means of switch lines. A typical set of switch lines (for the spacecraft y-axis) are shown in figure 7.22. Separate sets of switch lines are used for each axis. The switch lines consist of two parallel lines plotted on the attitude rate versus attitude error plane. The two lines divide the

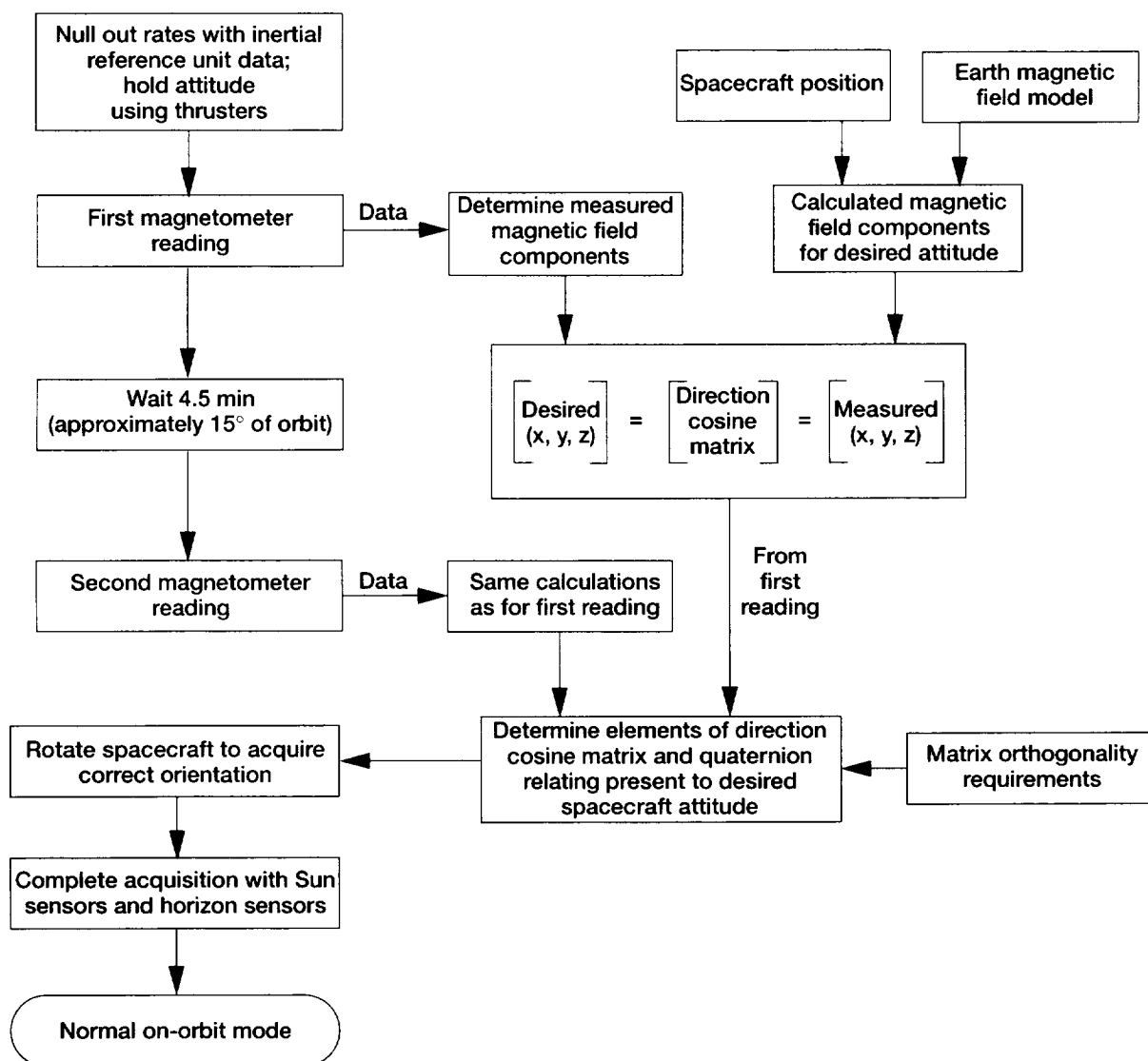


Figure 7.21.—Attitude determination in contingency acquisition mode.

plane into three regions. The attitude control logic determines in which region the spacecraft is operating by comparing the current attitude error and attitude rate against the switch lines. If the spacecraft is operating in the region above the upper switch line, then the thruster (or thrusters) that provide a negative torque about the axis in question is turned on. Positive torque is applied if the spacecraft is operating below the lower switch line. Whichever thruster(s) is turned on remains on as long as the operating point remains outside the two switch lines. When the operating point is within the switch lines, and provided that at least 200 m sec have elapsed since they were turned on, the thrusters are turned off. Once the thrusters are turned off, they remain off for as long as the spacecraft continues to operate between the two switch lines.

Two parameters are used to define the switch lines. They are the slope and the y intercept. The parameters are unique to each spacecraft axis and are a function of the moment of inertia and control torque about that axis. The slope and intercept are computed such that if, for example, the attitude error is -1° and the attitude rate is approximately 22 rev/day (see point A in fig. 7.22), then a single, continuous firing of the negative control thruster will reduce the attitude rate to zero at an attitude error of $+1^\circ$ assuming no other torques are acting on the spacecraft. The nominal inertias shown in table 7.1 are used to compute the switch line parameters. Switch line parameters for the three spacecraft axes are tabulated in figure 7.22.

7.6.3.3.2 Gimballed thruster control logic.—The gimballed thruster control logic employs a proportional/integral/rate

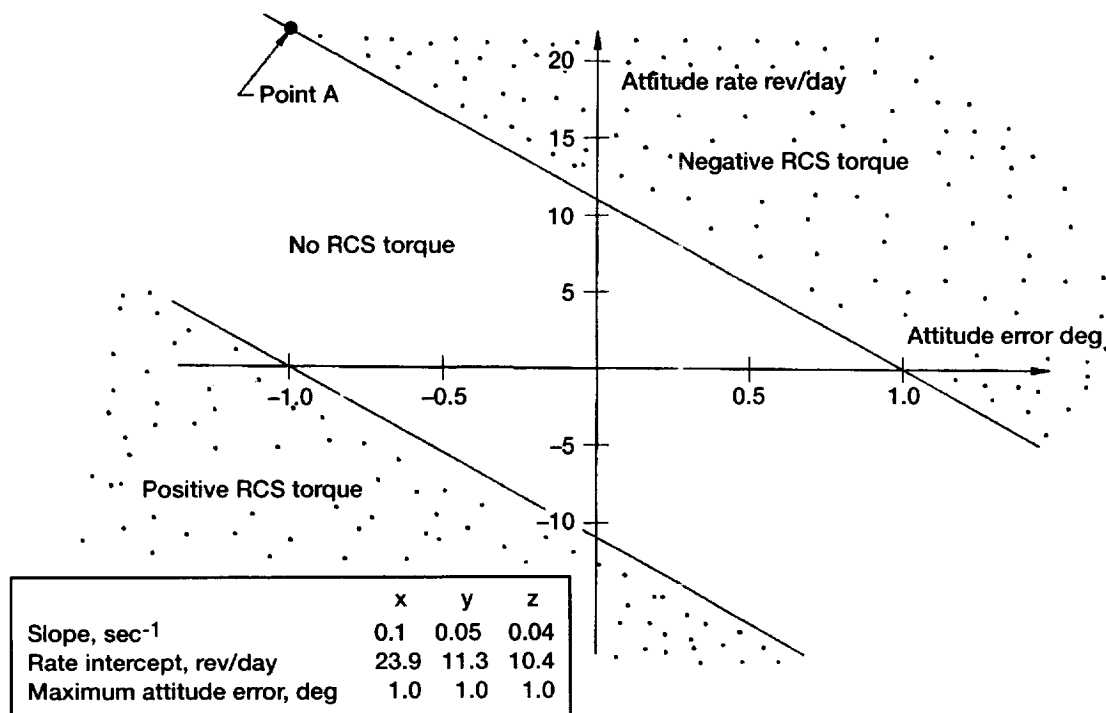


Figure 7.22.—Reaction control system (RCS) thruster switch lines (for spacecraft y-axis).

feedback loop. In this control scheme the attitude error, the integral of the attitude error, and the attitude rate are each multiplied by a suitable gain constant and combined. The resultant signal, limited to the range of $\pm 20^\circ$, represents the commanded gimbal angle as shown in figure 7.23. The integral term provides for a zero steady-state attitude error.

The same logic is applied to both the y- and z-axis controls independently.

7.6.4 ACS PERFORMANCE ANALYSIS

The ACS performance is evaluated in two parts. First, control torque margins are evaluated under worst-case conditions. Second, a dynamic spacecraft simulation is used to evaluate attitude errors, attitude rates, and microgravity disturbances as a function of time as the spacecraft orbits the Earth.

7.6.4.1 Control Torque Margins for Selected System

Comparisons of control torques with disturbance torques are made for four cases, outlined below, are compared in table 7.7.

- (1) Nominal attitude without axial thrust: for this case it is assumed that only the control thrusters are active
- (2) Nominal attitude with axial thrust (with gimballed thruster functioning normally): for this case it is assumed that the gimballed thruster is used for primary attitude control about the spacecraft y- and z-axes and the control

thrusters are used to control attitude about the spacecraft x-axis and as backup about the y- and z-axes

- (3) Nominal attitude with axial thrust (gimballed thruster assumed failed): for this case the control thrusters are assumed to provide all attitude control
- (4) Random attitude: for this case it is assumed that only the control thrusters are active

The torque margins shown in table 7.7 cover uncertainties in the disturbance torque and control torque calculations, and those disturbance torques that are not analyzed. The smallest torque margins occur when the gimballed thruster is used for attitude control on the spacecraft y- and z-axes. This margin results from comparing the worst-case disturbance torque with the lowest value of control torque which occurs when the center of gravity is in its most aft location. Additional margin is available since the control thrusters are operating in a backup mode to the gimballed thruster at all times.

7.6.4.2 Spacecraft Dynamic Simulation

The ACS performance was evaluated by using a six-degree-of-freedom computer simulation (described in more detail in section 7.10 of this chapter) of the COLD-SAT spacecraft. The simulation accurately modeled all disturbance torques, the attitude control system, the spacecraft rotational dynamics, and the translational motion of the spacecraft, in orbit about the Earth. All contributors to the microgravity environment were

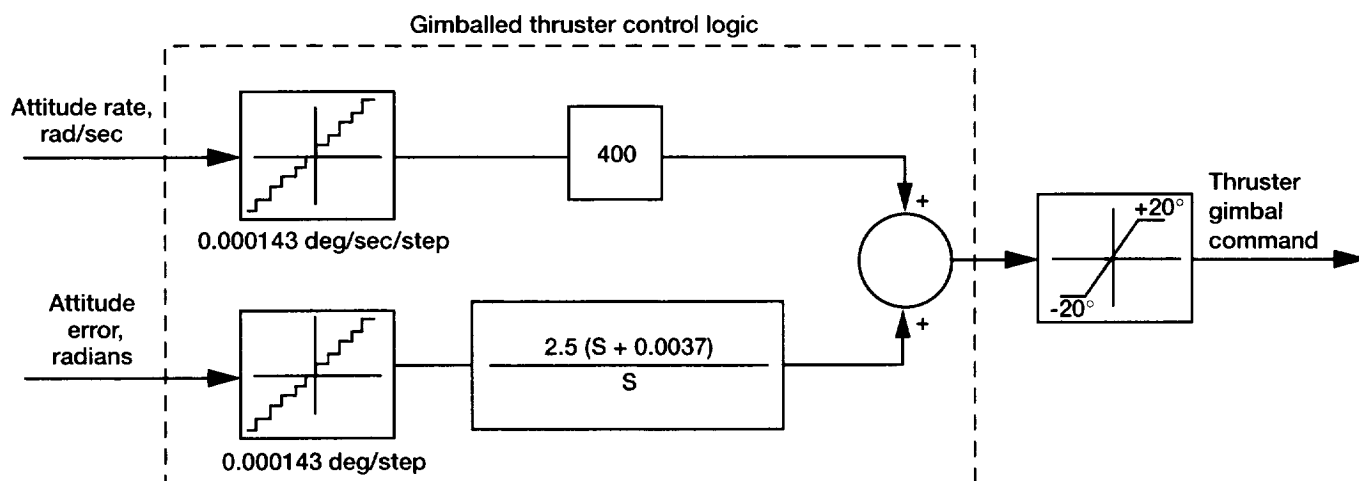


Figure 7.23.—Gimbaled thruster control logic (y- and z-axis).

TABLE 7.7.—COMPARISON OF DISTURBANCE TORQUES WITH CONTROL TORQUES

Torque	x-axis, in.-lb	y-axis in.-lb	z-axis in.-lb
Nominal attitude without axial thrust ^a			
Control torques	5.760	2.880	2.880
Worst-case disturbance torques	.427	.245	.248
Torque margin	5.333	2.635	2.632
Nominal attitude with axial thrust ^b (gimbaled thruster operating normally)			
Control torques	5.760	1.015 ^c	1.080 ^c
Worst-case disturbance torques	.326	.748	.719
Torque margin	5.434	.267	.361
Nominal attitude with axial thrust ^a (failed gimbaled thruster)			
Control torques	5.760	2.880	2.880
Worst-case disturbance torques	.427	.860	.828
Torque margin	5.333	2.020	2.052
Random attitude ^a			
Control torques	5.760	2.880	2.880
Worst-case disturbance torques	.141	.335	.216
Torque margin	5.619	2.545	2.664

^aCenter of gravity 92 in. from rear of spacecraft.

^bCenter of gravity 79 in. from rear of spacecraft.

^cTorque produced by gimbaled thruster with maximum gimbal angle of 20° and with most aft spacecraft center-of-gravity position.

TABLE 7.8.—POINTS FOR MICROGRAVITY COMPUTATION

Point number	Tank	x-Coordinate, in.	y-Coordinate, in.	z-Coordinate, in.
1	Supply	59.7	30.0	0
2	Supply	59.7	0	30.0
3	Supply	81.4	0	0
4	Large receiver	142.0	16.25	0
5	Large receiver	150.9	0	0

also modeled. The attitude determination system was not simulated but was assumed to provide perfect knowledge of the spacecraft attitude.

Major inputs to the model were the time and date at the start of the simulation, the initial orbital elements, the spacecraft mass properties, the ACS parameters, and the coordinates of points at which the microgravity environment was to be calculated.

Output from the computer simulation was principally graphical in nature. Any parameter computed by the simulation can be plotted. However, for the purpose of ACS performance evaluation, the parameters selected for graphical presentation were

- (1) Attitude error
- (2) Attitude rate
- (3) Microgravity environment at selected points
- (4) Slosh mass displacement
- (5) Gimbal angles
- (6) Total disturbance torque

The points selected for microgravity computation are given in table 7.8. The x coordinate was measured from the rear of the spacecraft and the y and z coordinates were measured from the spacecraft centerline.

Each of these points was located on the tank wall as shown in figure 7.24. Microgravity within the fluid away from the tank wall will be different from the microgravity calculated for points on the tank wall.

In addition to the graphics output, the model also provided numerical output of the number of firings of each control thruster, the total thruster ontime, and the maximum thruster ontime.

For the purpose of evaluating the ACS three cases were analyzed as follows:

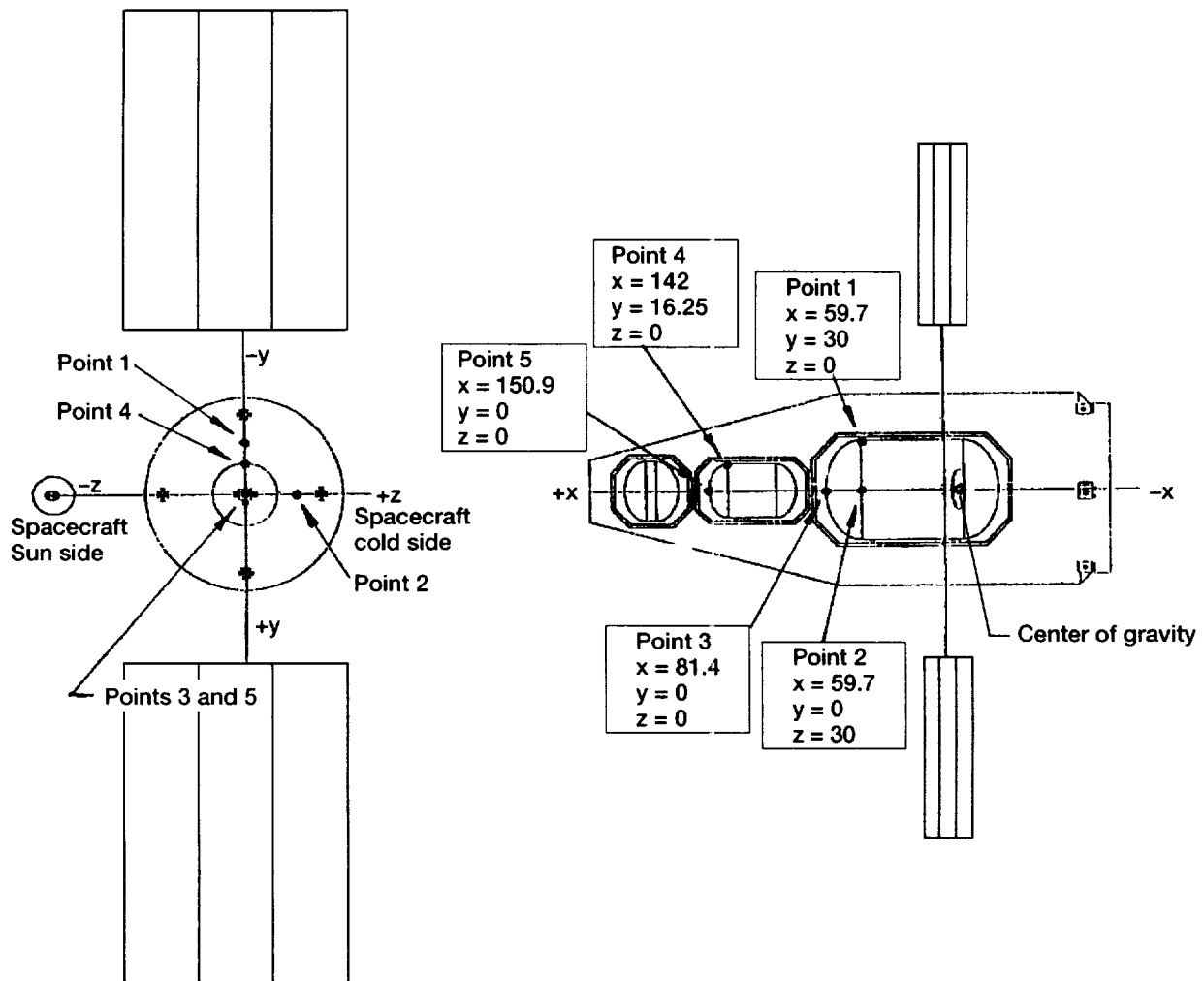


Figure 7.24.—Identification of points for microgravity computation.

- (1) Case 1 - Minimum spacecraft inertias
- (2) Case 2 - Maximum spacecraft inertias
- (3) Case 3 - Maximum spacecraft inertias with failed gimbaled thruster

Each case was simulated for two orbits; the first orbit was without axial thrust and was followed by a second orbit with high (0.52 lb) axial thrust. Table 7.9 lists the assumptions used in the analysis.

7.6.4.3 Simulation Results

The results of the analysis are shown in figures 7.25 to 7.40. An index to the various figures is shown in table 7.10. In figures 7.27 to 7.31, 7.37, and 7.40, pulses produced by the firing of a control thruster are visible. To ensure consistent plotting by the graphics program, the time duration of these pulses was exaggerated by a factor of 40. This stretching of the pulses leads to a visualization of the control thruster activity which is highly exaggerated. For a more accurate representa-

tion of thruster duty cycle and pulse duration, the numeric data presented in tables 7.11 to 7.13 should be consulted. These tables provide the following numeric data:

- (1) Number of thruster firings per orbit for each thruster (table 7.11)
- (2) Total "on" time per orbit for each thruster (table 7.12)
- (3) Maximum "on" time for each thruster (table 7.13)

The assumptions are the same as those given in table 7.8, and maximum inertias were used.

7.6.4.4 180° Roll Maneuver

The 180° roll maneuver was briefly analyzed and the pertinent results of that analysis are summarized in table 7.14. The numbers shown in the table assume a minimum time maneuver in which the spacecraft accelerates for the first 90° of rotation and then decelerates for the next 90°.

TABLE 7.9.—ASSUMPTIONS FOR ATTITUDE CONTROL SYSTEM
PERFORMANCE EVALUATION ANALYSIS

Orbit altitude, n mi	550
Orbit inclination, degree	18
Center-of-gravity location, (most rearward) in. from rear of spacecraft	79.0
β angle, degree	41
Disturbance torques included	all
External disturbance torque assumptions	(a)
Center-of gravity offset (along y- and z-axes), in.	0.5
Axial thruster angular misalignment (in x-y and x-z planes), degree	0.333
Control thruster angular misalignment (all thrusters; in two planes) degree	1
Slosh in supply tank	yes
Slosh in large receiver tank	yes
Slosh in small receiver tank	yes

^aSee table 7.3.

TABLE 7.10.—RESULTS MATRIX

Result	Case		
	1 (minimum inertia). figure number	2 (maximum inertia). figure number	3 (maximum inertia with failed thruster). figure number
Attitude errors	7.25	7.35	7.38
Attitude rates	7.26	7.36	7.39
Microgravity at point 1	7.27	7.37	7.40
Microgravity at point 2	7.28	---	---
Microgravity at point 3	7.29	---	---
Microgravity at point 4	7.30	---	---
Microgravity at point 5	7.31	---	---
Slosh mass displacement	7.32	---	---
Gimbal angle	7.33	---	---
Total disturbance torque	7.34	---	---

TABLE 7.11.—CONTROL THRUSTER FIRINGS PER ORBIT^a

Axial thrust, lb	+x	-x	+y	-y	+z	-z
With functional gimbaled thruster ^b						
None	2	0	39	0	214	199
0.04	1	0	0	0	0	0
.16	1	0	0	0	0	0
.52	2	1	0	0	0	0
With failed gimbaled thruster						
None	2	0	39	0	214	199
0.04	2	0	261	0	112	322
.16	3	4	1577	0	0	1511
.52	3	4	5474	0	0	4915

^aThese results are for an assumed center-of-gravity offset of 0.5 in. in the positive y and positive z directions and a 1/3° angular misalignment.

^bAfter steady-state gimbal angles are established.

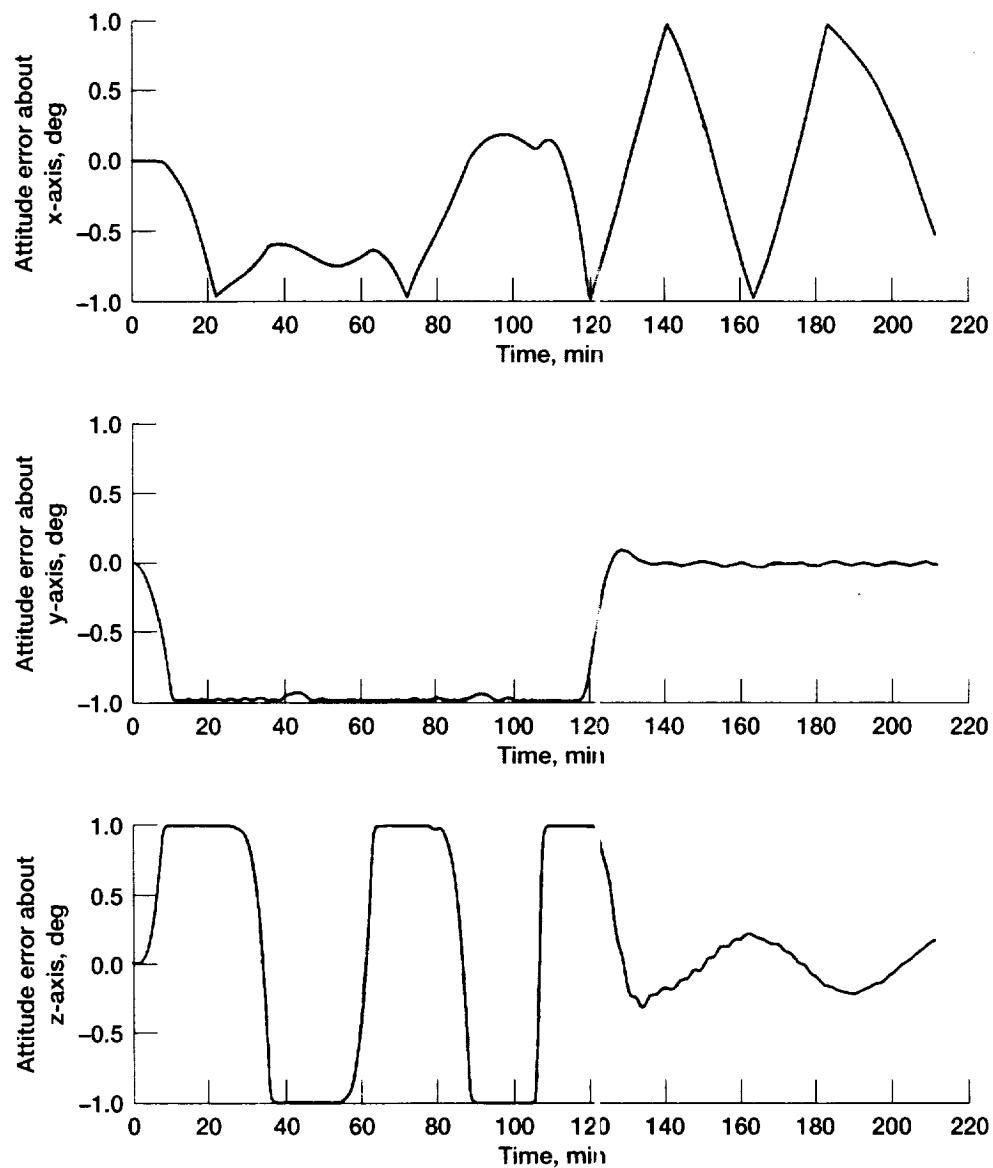


Figure 7.25.—Attitude errors for minimum inertia case.

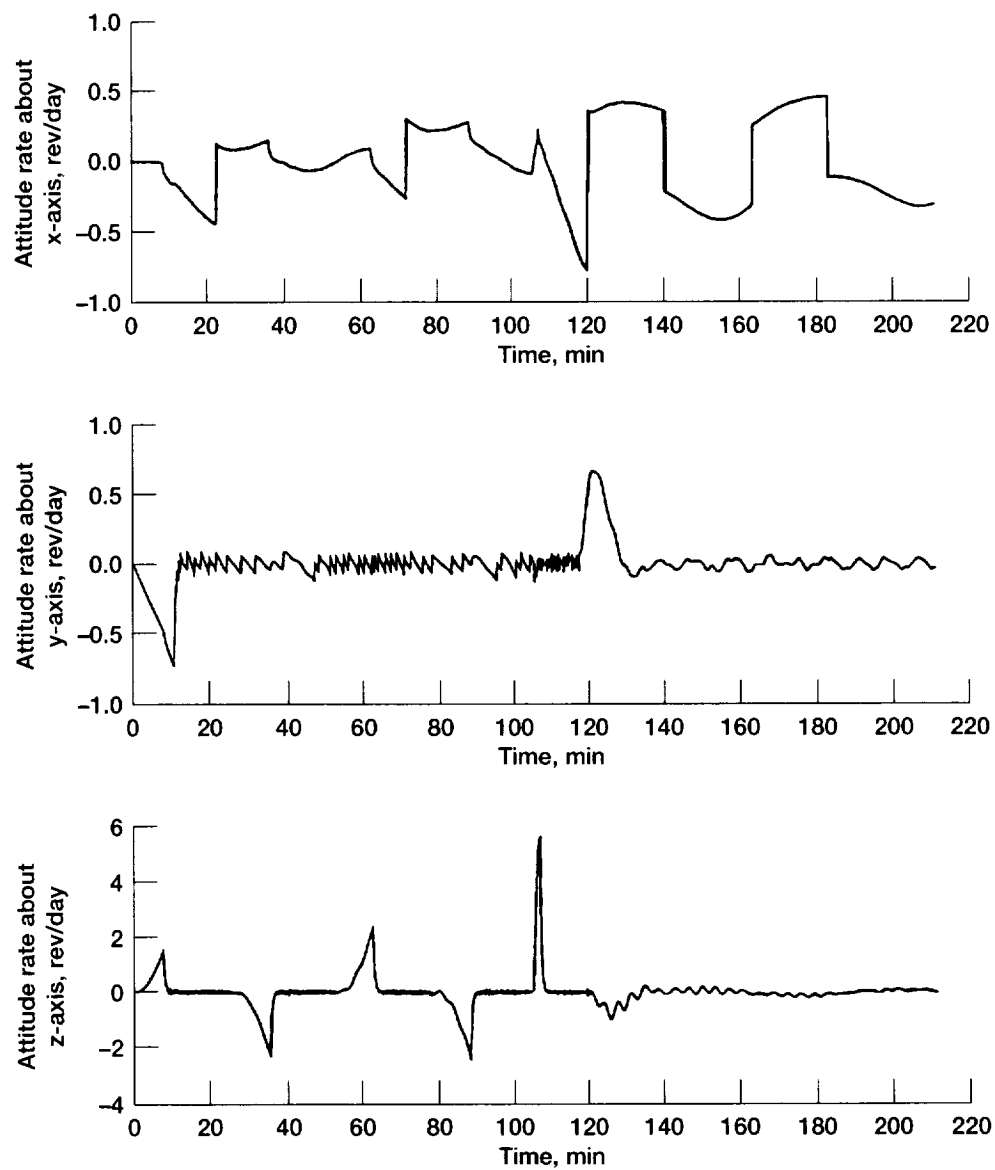


Figure 7.26.—Attitude rates for minimum inertia case.

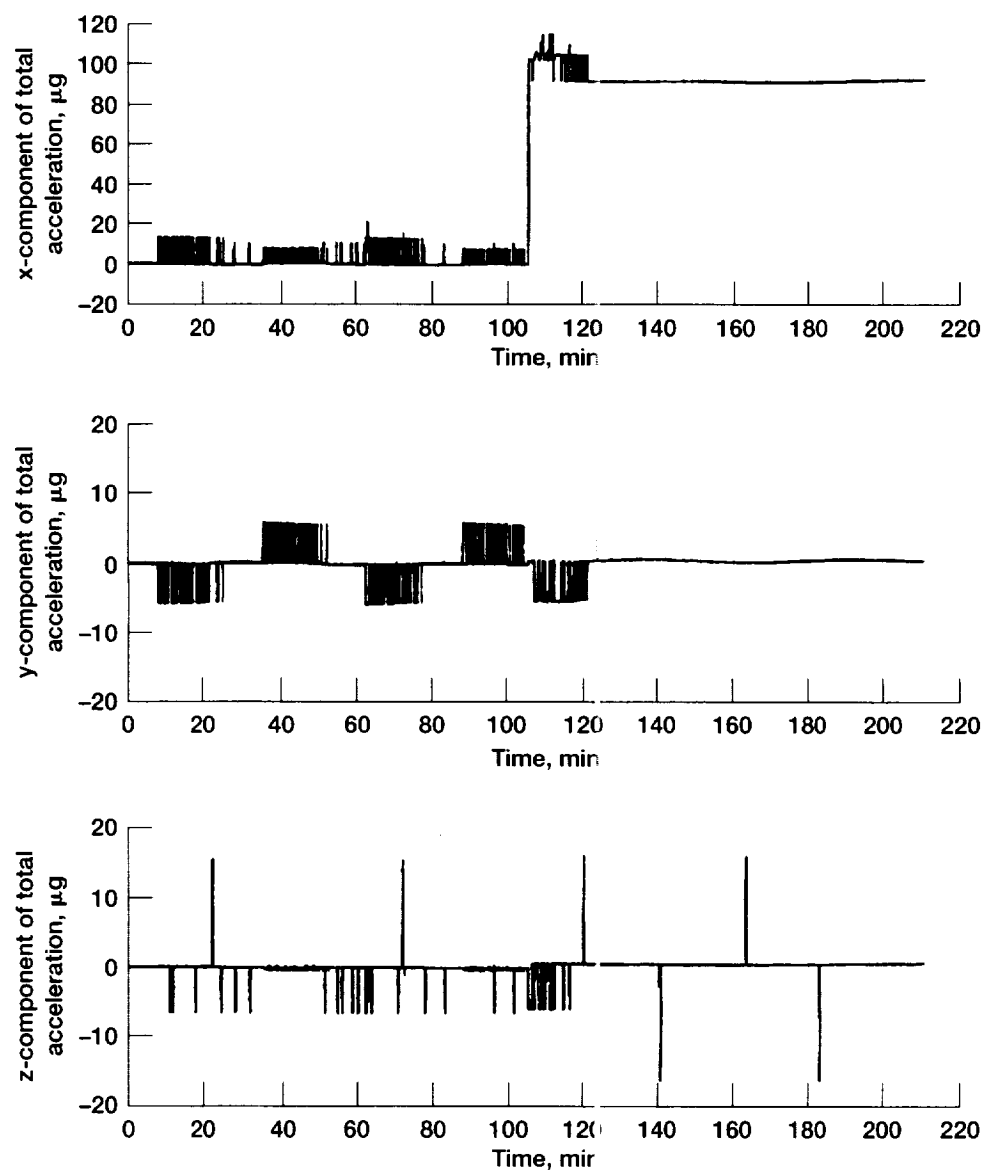


Figure 7.27.—Microgravity at point 1 (minimum inertia).

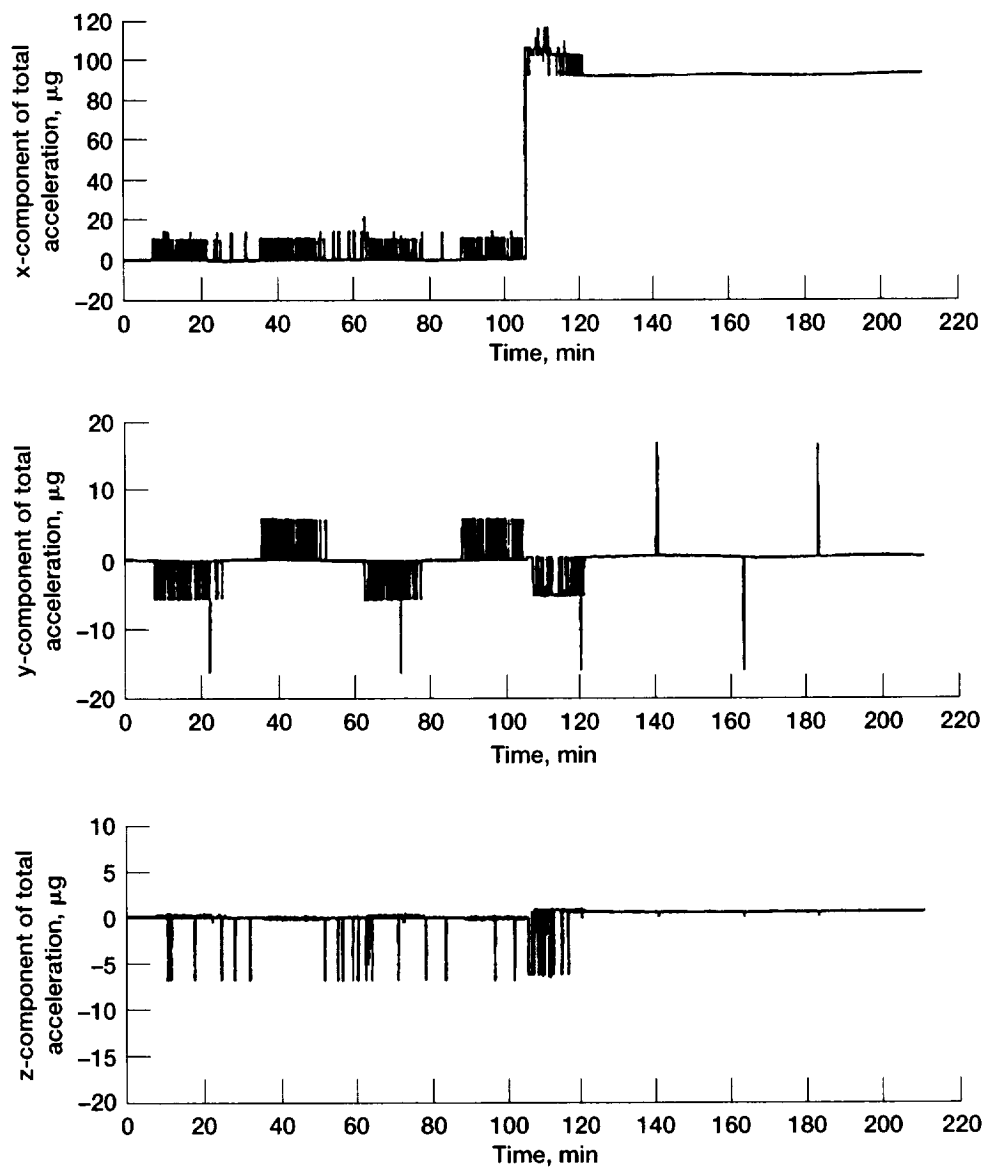


Figure 7.28.—Microgravity at point 2 (minimum inertia).

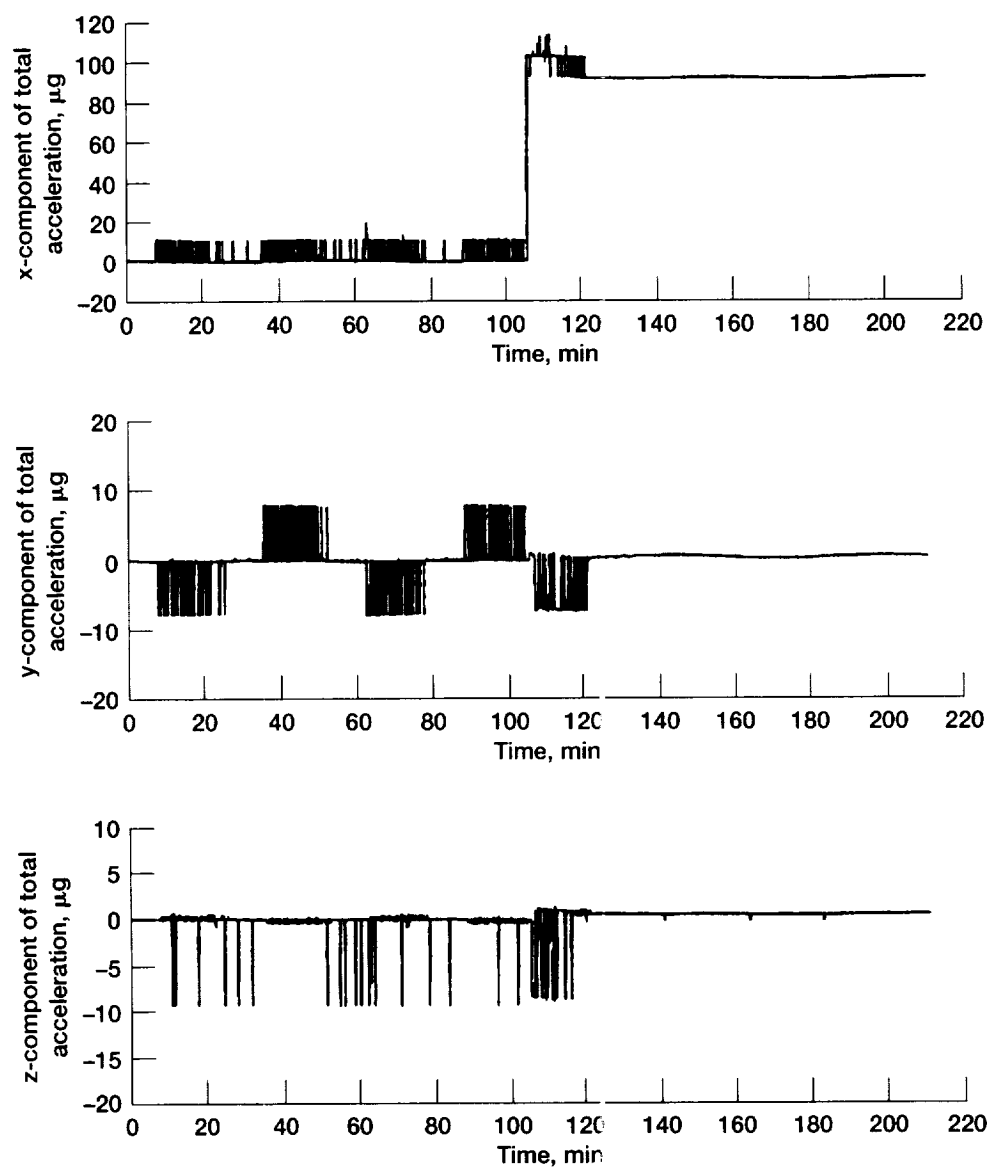


Figure 7.29.—Microgravity of point 3 (minimum inertia).

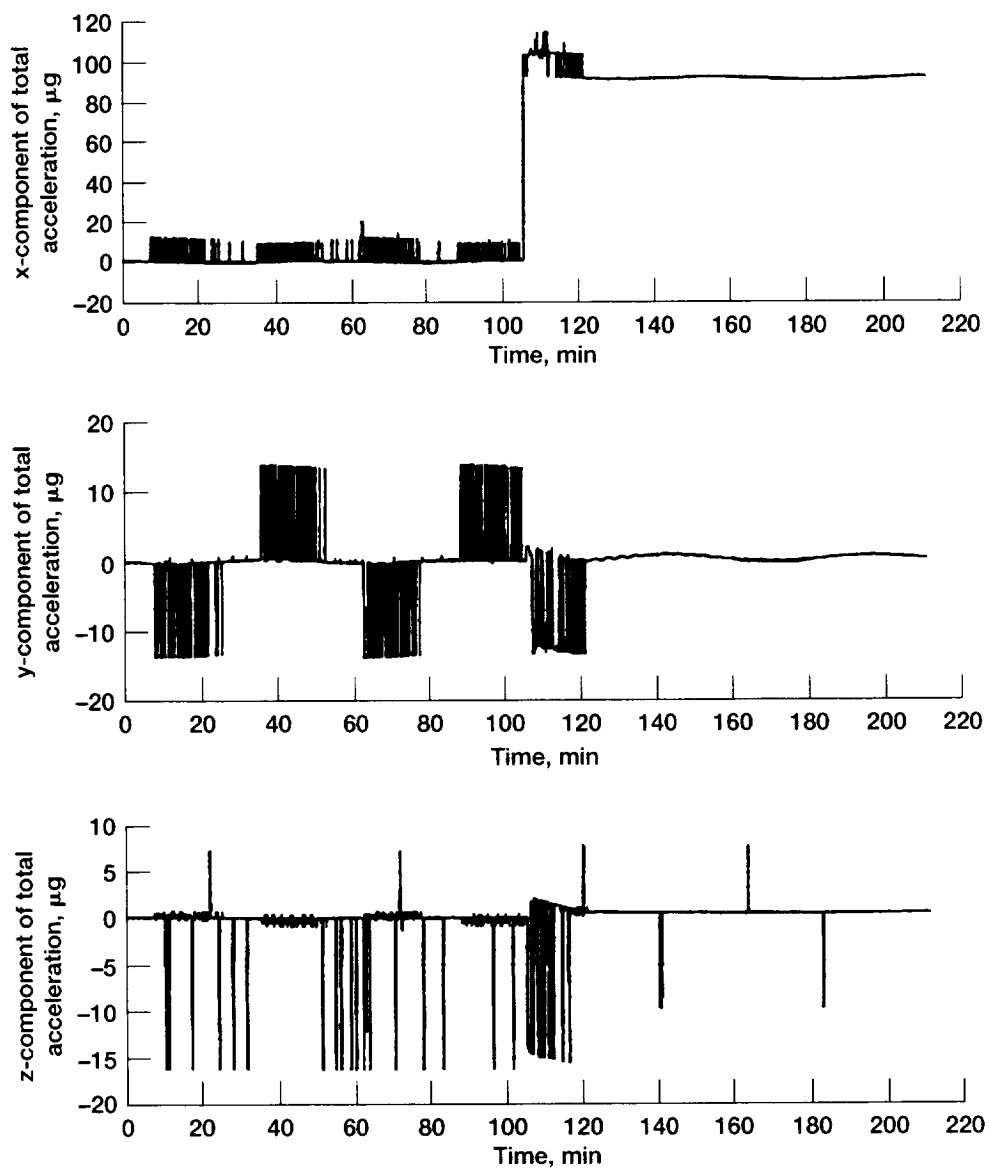


Figure 7.30.—Microgravity of point 4 (minimum inertia).

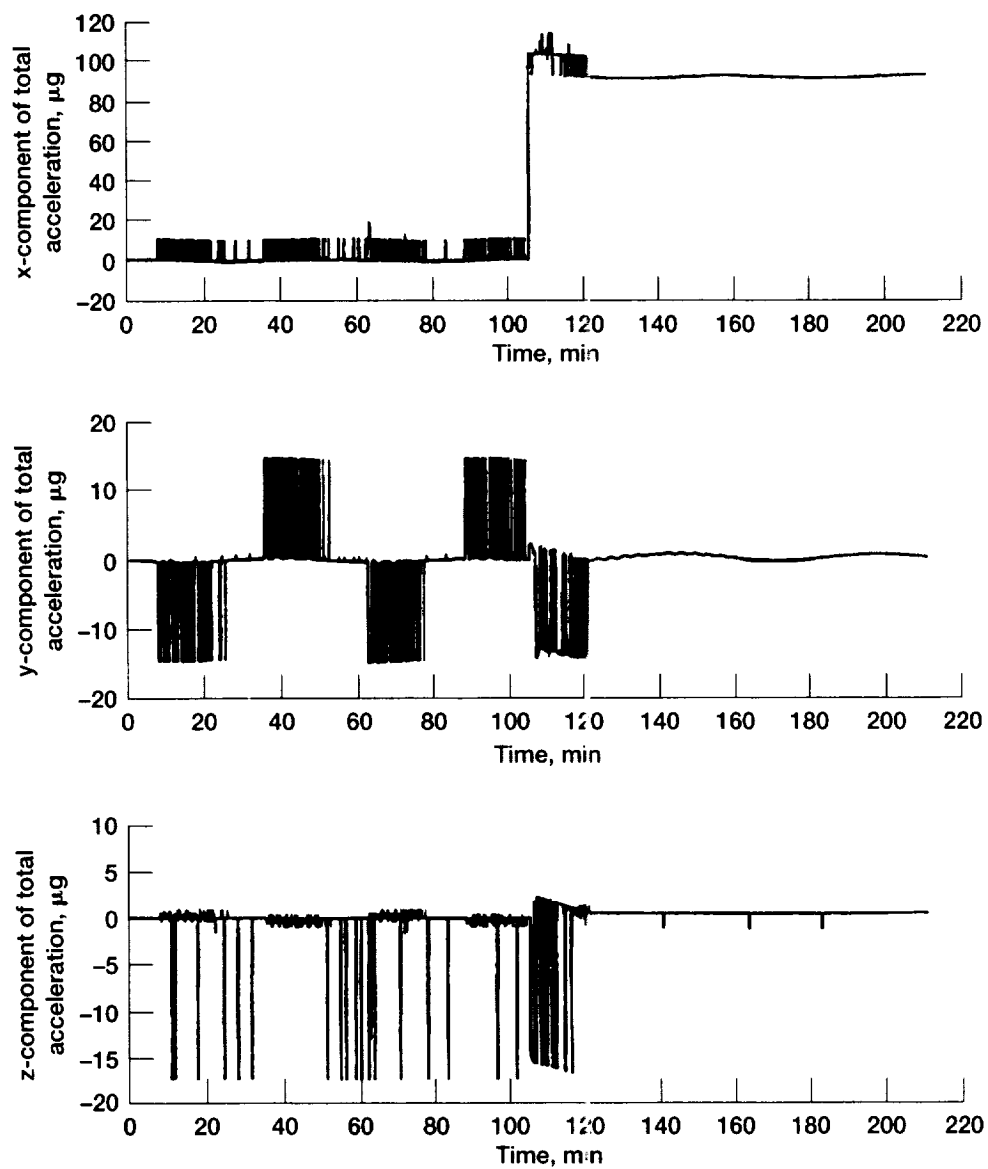


Figure 7.31.—Microgravity of point 5 (minimum inertia).

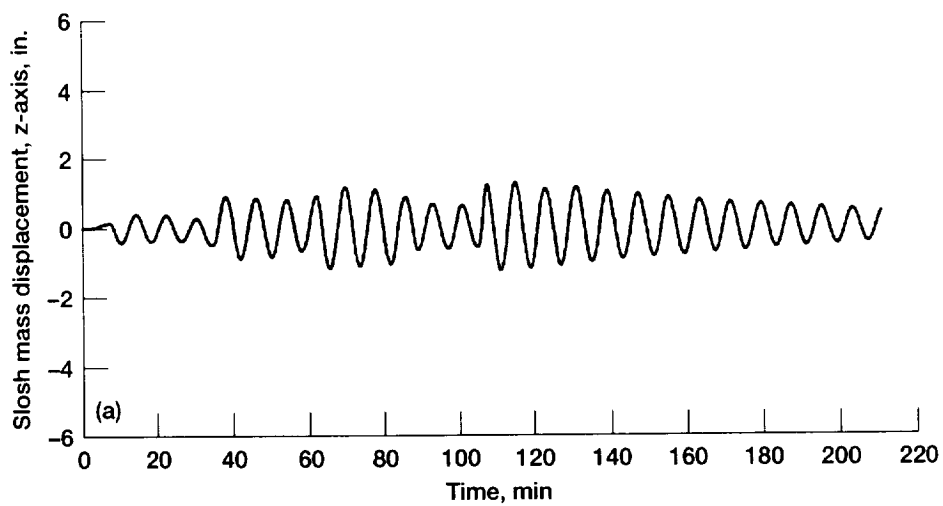
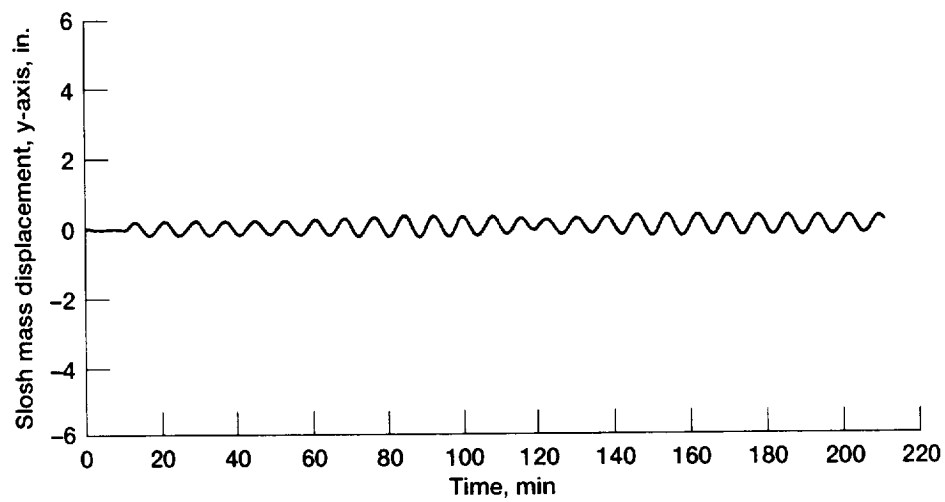


Figure 7.32.—Slosh mass displacement. (a) Supply tank. (b) Large receiver tank.
(c) Small receiver tank.

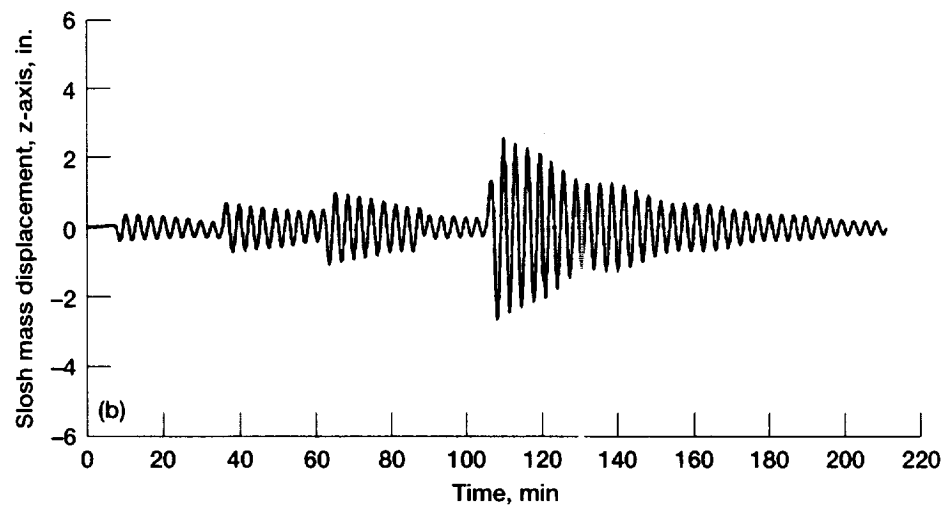
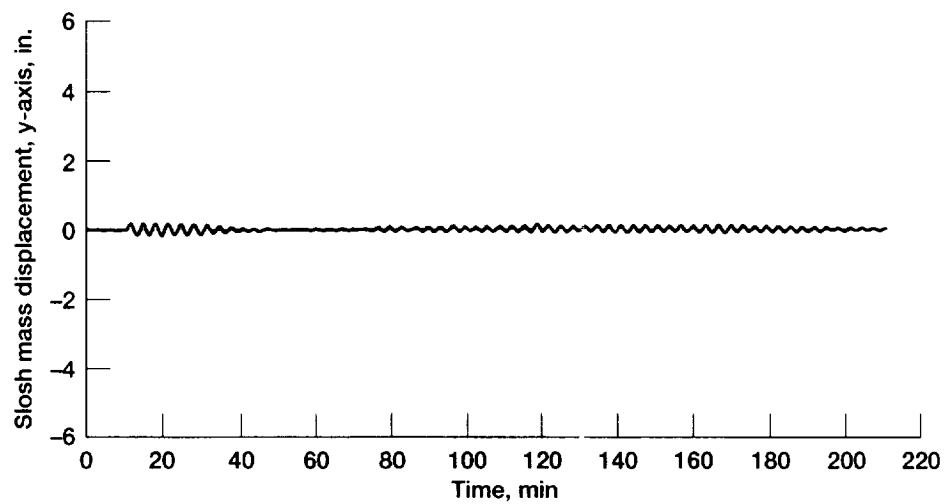


Figure 7.32.—Continued. (b) Large receiver tank.

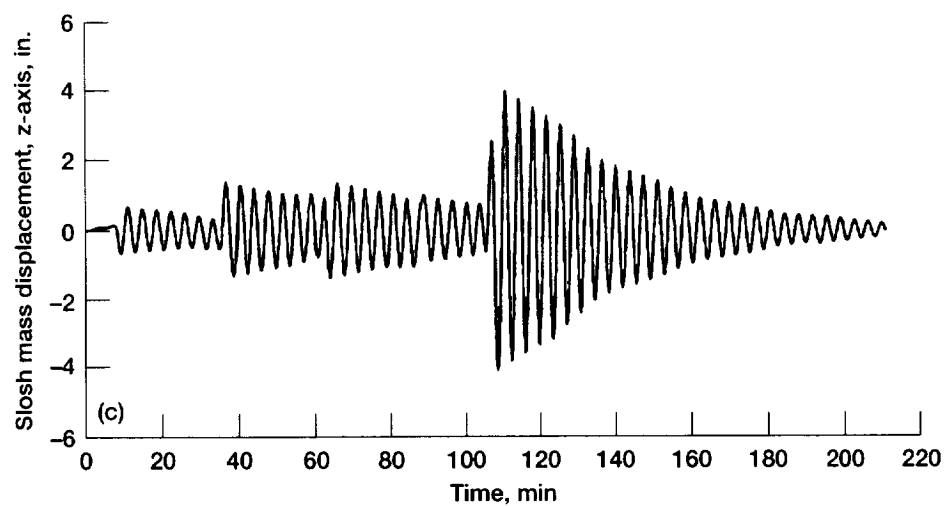
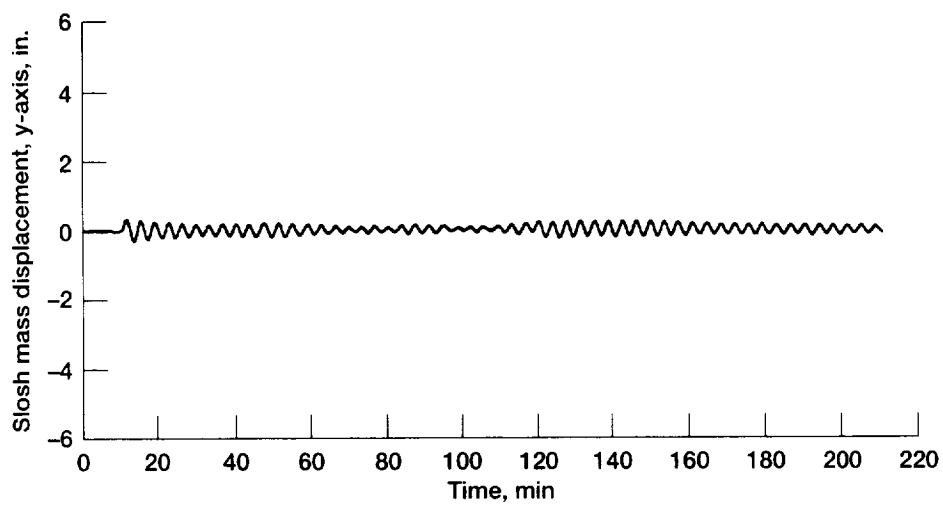


Figure 7.32.—Concluded. (c) Small receiver tank.

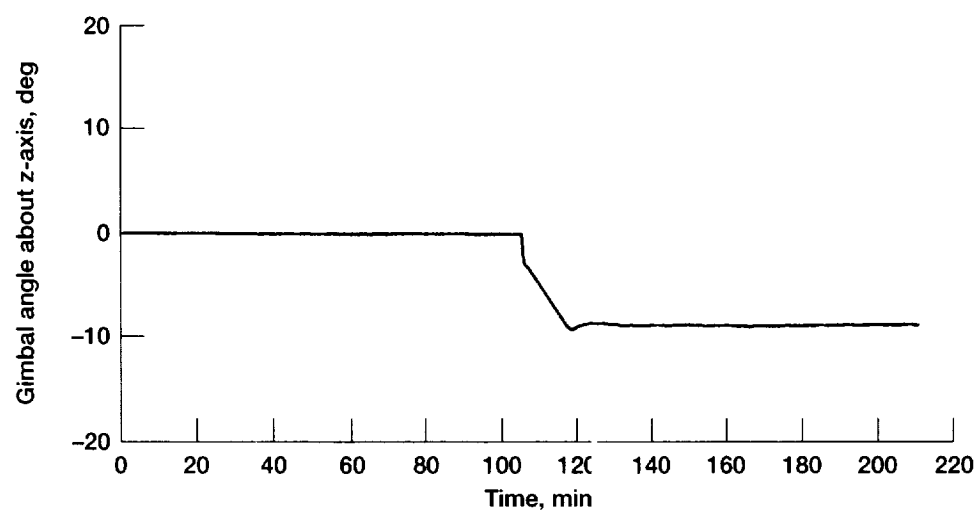
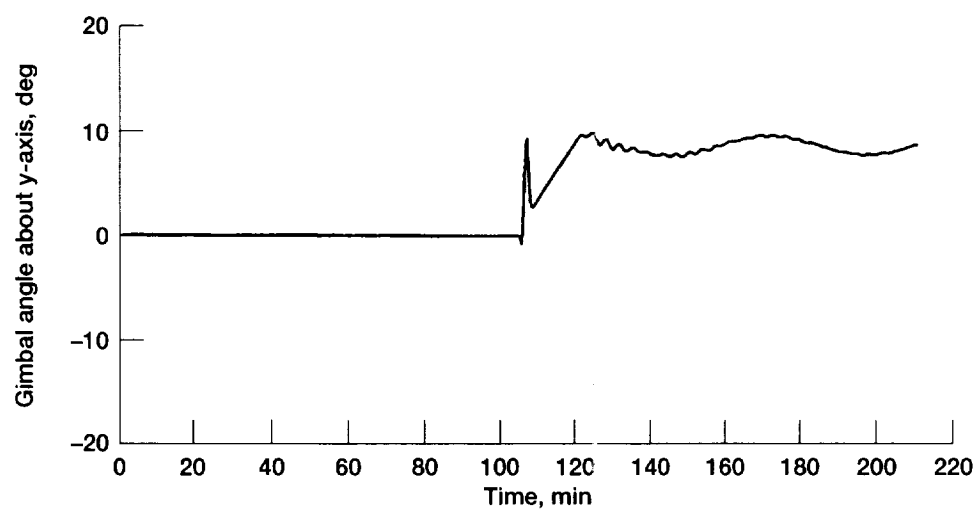


Figure 7.33.—Gimballed thruster angular displacement.

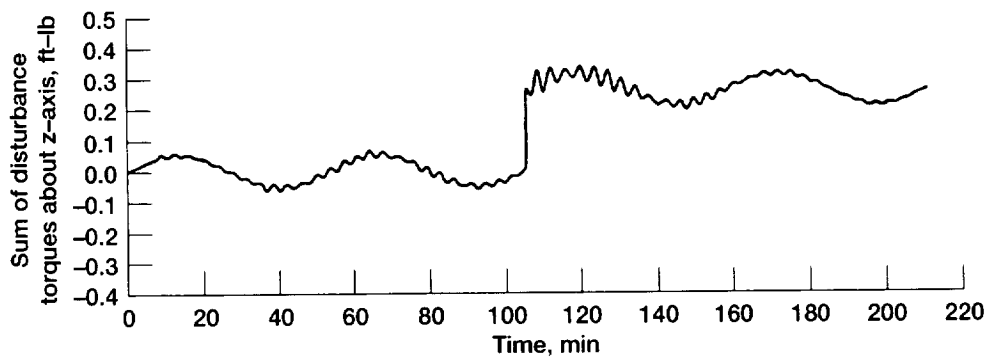
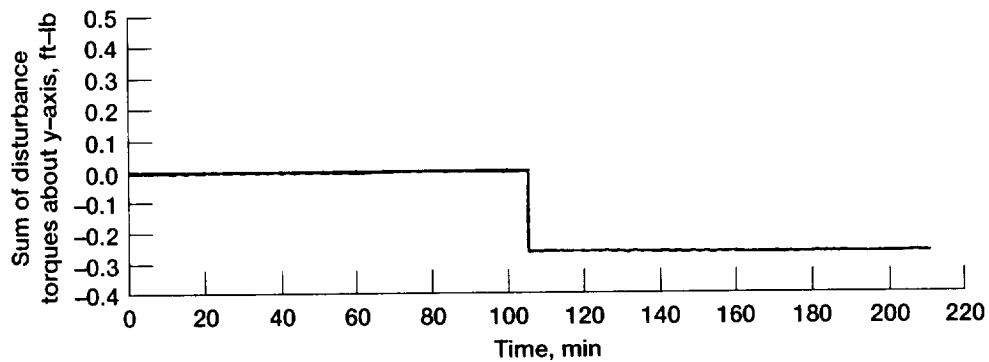
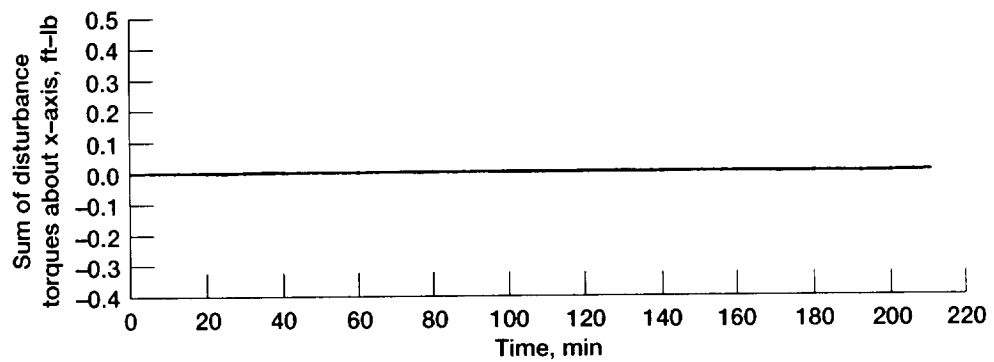


Figure 7.34.—Total disturbance torque (minimum inertia).

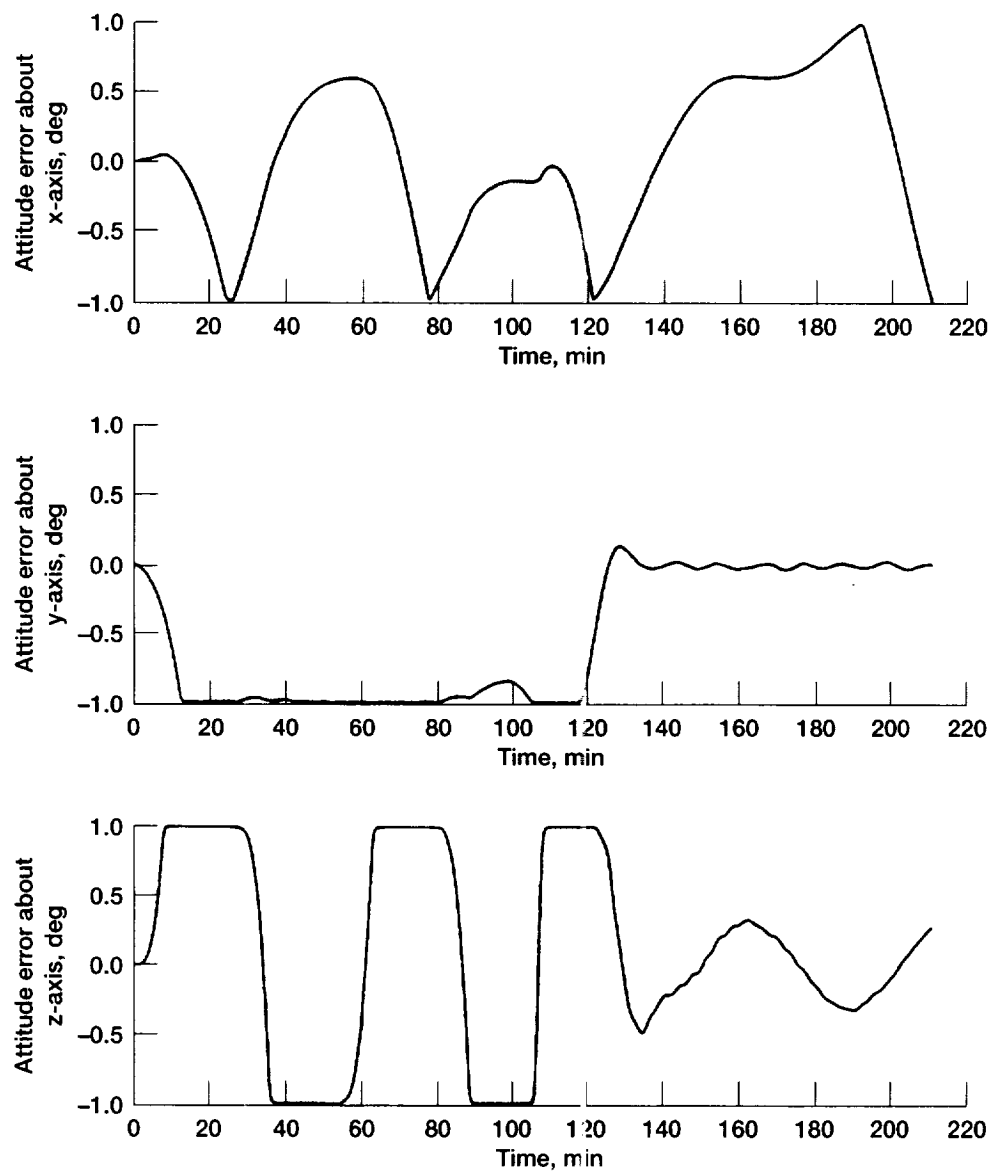


Figure 7.35.—Attitude errors for maximum inertia case.

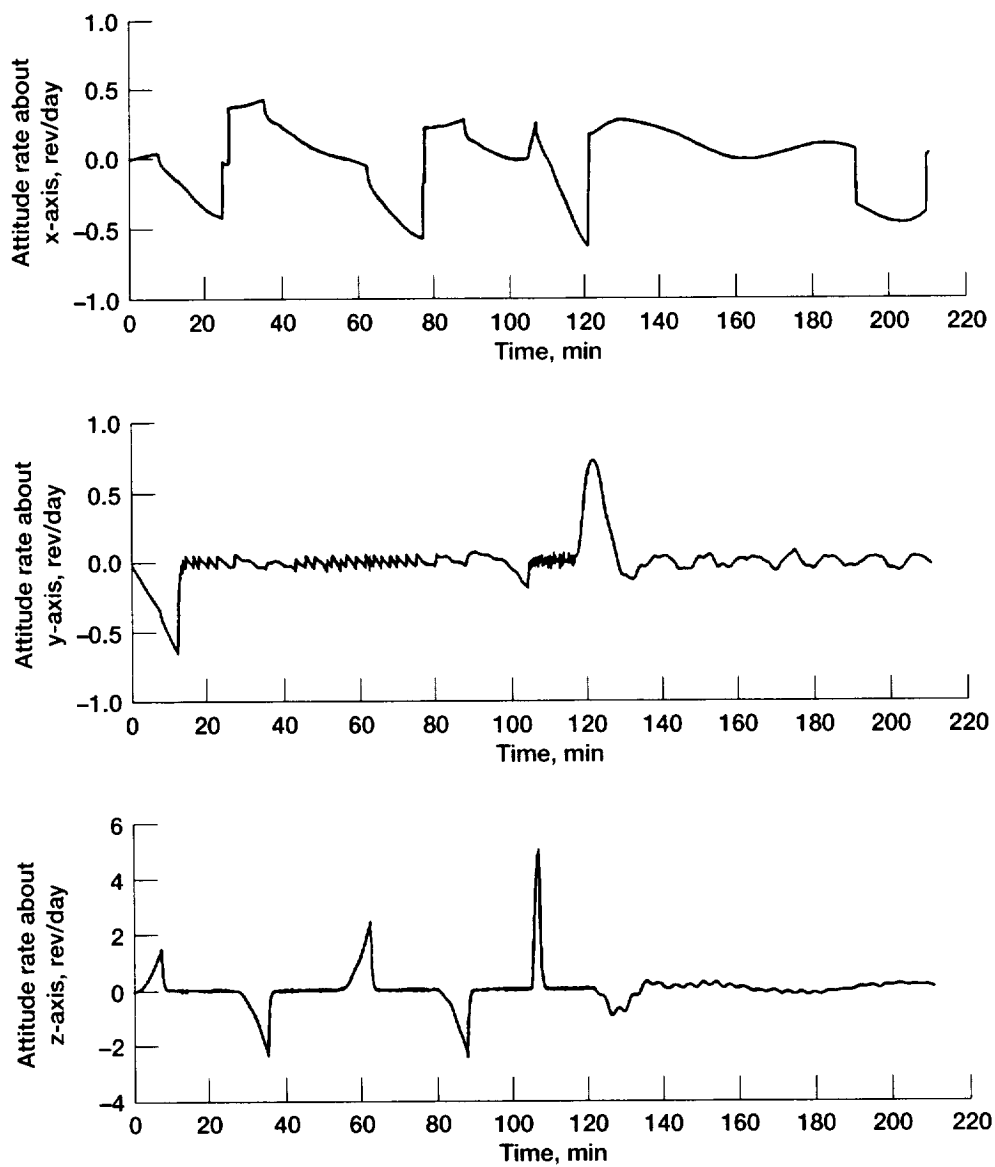


Figure 7.36.—Attitude rates for maximum inertia case.

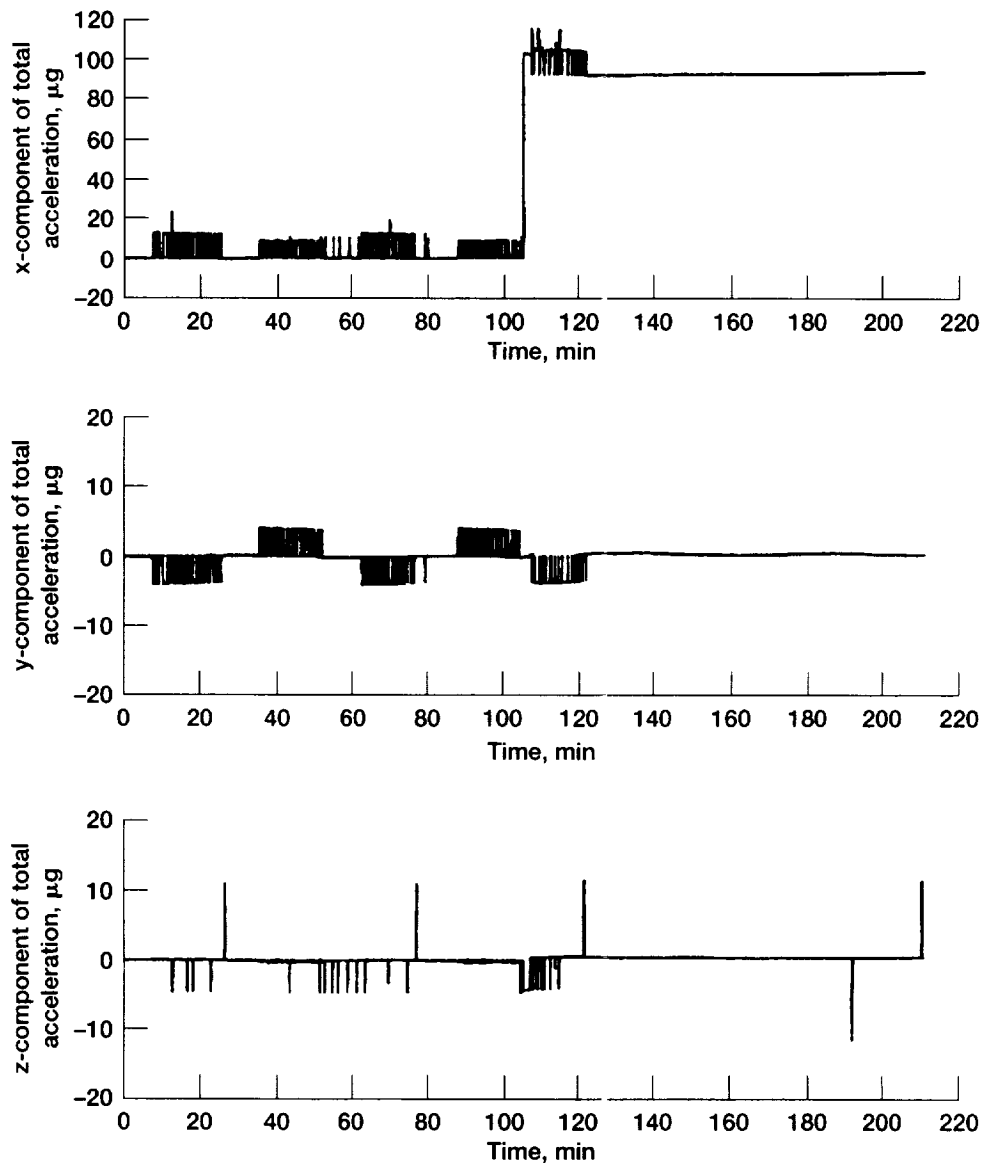


Figure 7.37.—Microgravity at point 1 (maximum inertia).

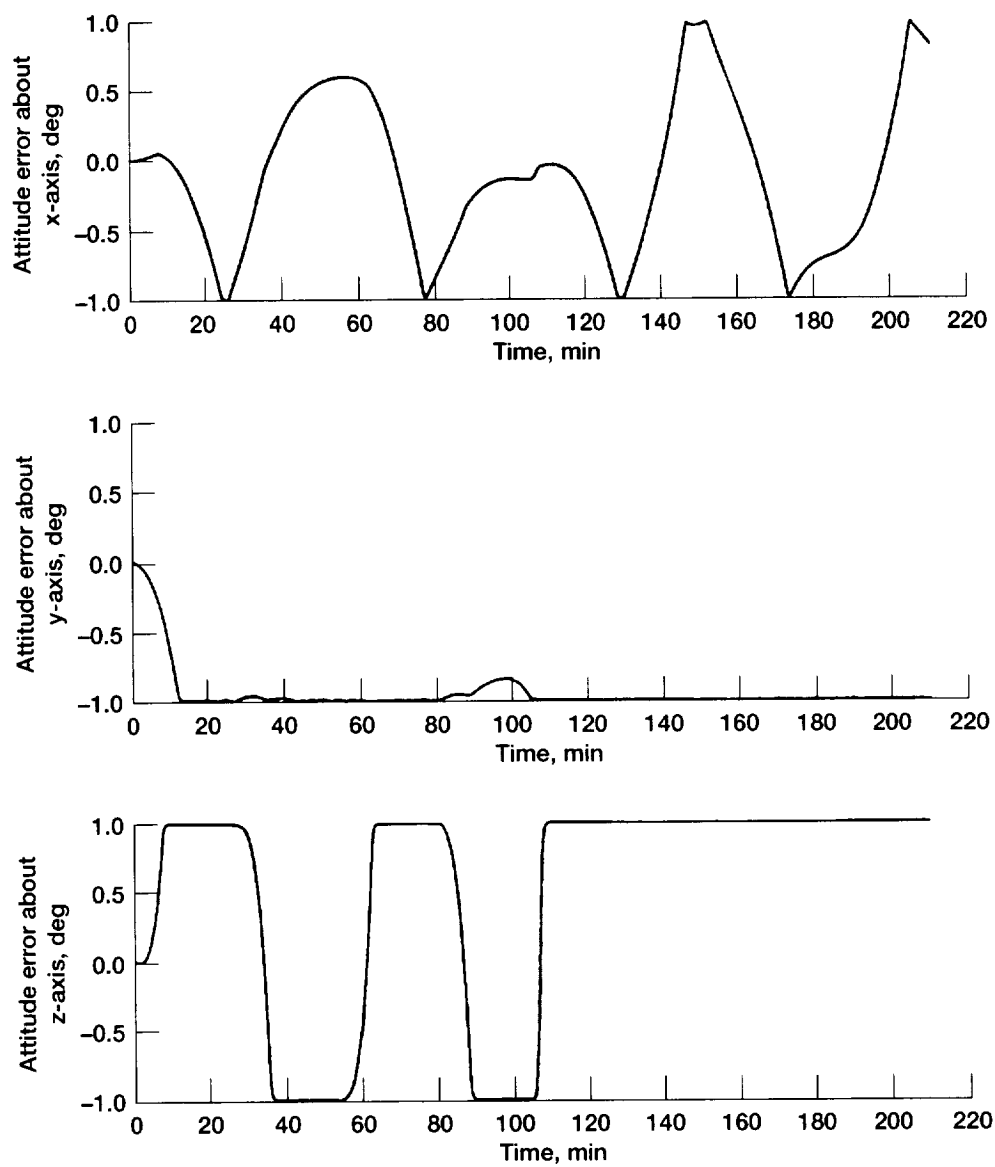


Figure 7.38.—Attitude errors with failed gimbaled thruster (maximum inertia).

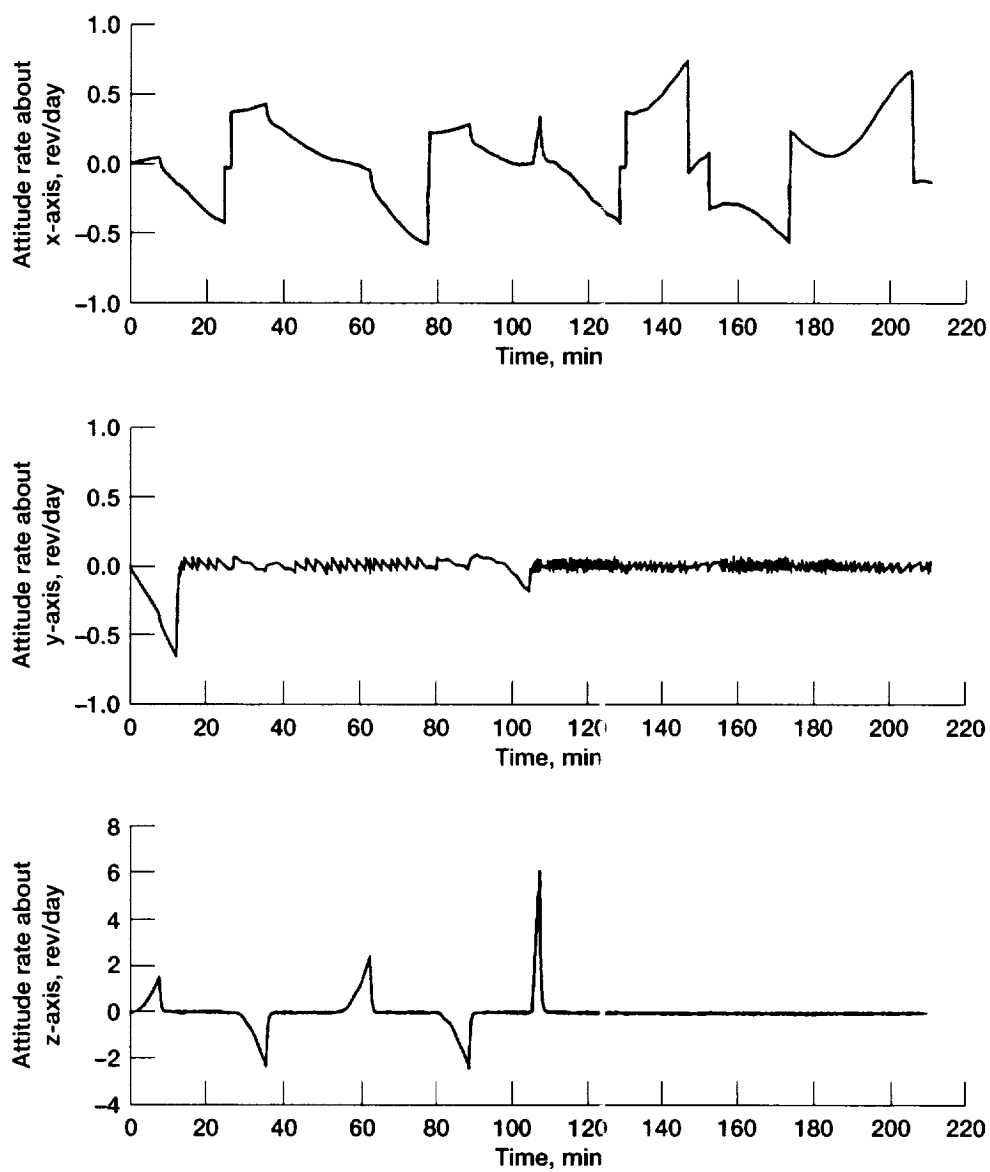


Figure 7.39.—Attitude rates with failed gimbaled thruster (maximum inertia).

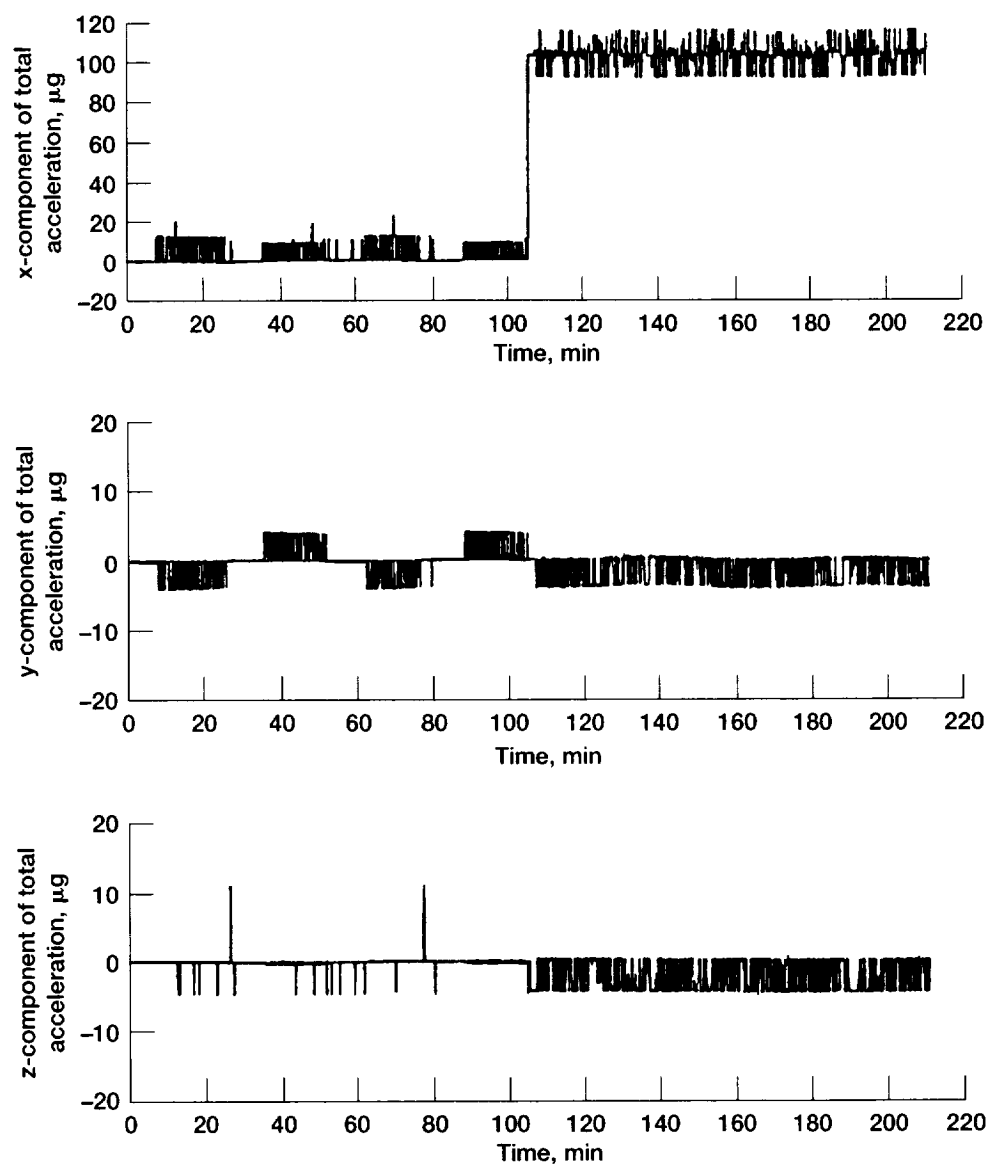


Figure 7.40.—Microgravity at point 1 with failed gimbaled thruster (maximum inertia).

TABLE 7.12.—CONTROL THRUSTER ON-TIME PER ORBIT^a

Axial thrust, lb	+x	-x	+y	-y	+z	-z
With functional gimbaled thruster, sec						
None	0.4	0	7.8	0	42.8	39.0
0.04	.2	0	0	0	0	0
.16	.2	0	0	0	0	0
.52	.4	.2	0	0	0	0
With failed gimbaled thruster, sec						
None	0.4	0	7.8	0	42.8	39.8
0.04	.4	0	52.2	0	22.4	64.4
.16	.6	.8	315.4	0	0	305.9
.52	.6	.8	1100.1	0	0	1090.0

^aThese results are for an assumed center-of-gravity offset of 0.5 in. in the positive y and positive z directions and a 1/3° angular misalignment.

TABLE 7.13.—MAXIMUM CONTROL THRUSTER ON-TIME PER FIRING^{a,b}

Axial thrust, lb	+x	-x	+y	-y	+z	-z
With functional gimbaled thruster, sec						
None	0.200	0	0.200	0	0.200	0.200
0.04	.200	.200	0	0	0	0
.16	.200	.200	0	0	0	0
.52	.200	.200	0	0	0	0
With failed gimbaled thruster, sec						
None	0.200	0	0.200	0	0.200	0.200
0.04	.200	0	.200	0	.200	.200
.16	.200	.200	.200	0	0	.225
.52	.200	.200	.224	0	0	.265

^aThese results are for an assumed center-of-gravity offset of 0.5 in. in the positive y and positive z directions and a 1/3° angular misalignment.

^b200 n sec was the minimum allowable thruster on-time.

TABLE 7.14.—180° ROLL MANEUVER CHARACTERISTICS

Characteristic	Minimum inertias	Maximum inertias
Time to complete maneuver, sec	245	293
Maximum roll rate, deg/sec	1.47	1.23
Angular acceleration, deg/sec ²	0.0120	0.0086
Hydrazine consumption, lb/maneuver	.178	.333

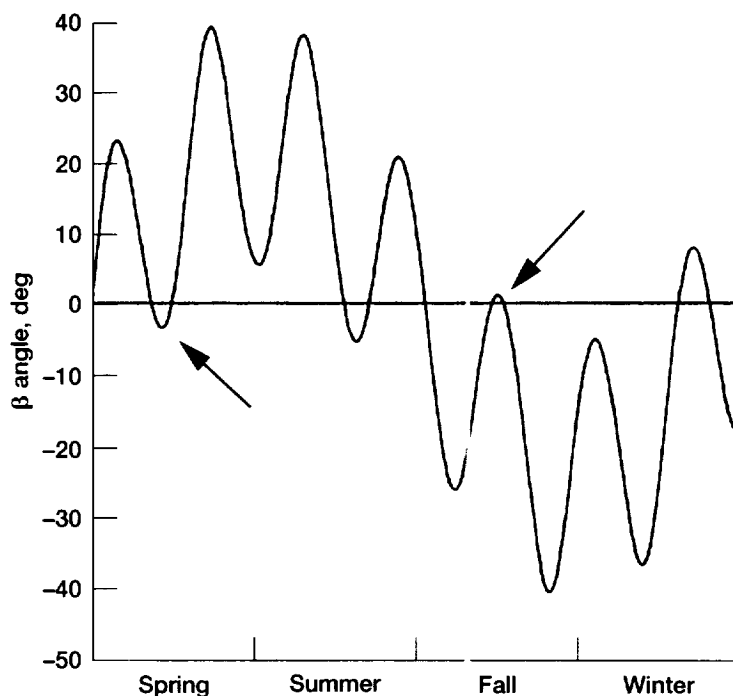


Figure 7.41.—Annual variation in β angle (Arrows indicate points when roll maneuver may not be necessary because the Sun crosses the orbit plane only briefly).

This maneuver, as discussed previously, is executed whenever the Sun crosses the orbit plane, that is, when the β -angle is zero. Figure 7.41 is a representative plot of the β -angle for a period of one year for an 18° inclined orbit. In this plot time zero is the vernal equinox and the right ascension of the orbit plane at time zero is 180° . Thereafter the right ascension changes at the rate of $-5.64^\circ/\text{day}$. During any 6-month period the maximum number of times that the β -angle passes through zero, and hence the maximum number of roll maneuvers required, is five. However, the time between crossings is not uniformly distributed throughout the year, being more frequent near the vernal and autumnal equinoxes, so that the exact number of roll maneuvers required will depend on the launch date and right ascension of the initial orbit.

On some occasions when the Sun crosses the orbit plane only briefly (as noted with arrows in fig. 7.41) the roll maneuver may not be necessary at all. Reversal of the β -angle without the associated 180° roll maneuver increases the temperature of the spacecraft cold side, reduces power output from the solar arrays, and moves the Sun close to the edge of the Sun sensor field of view. Analysis is required to determine the maximum cold side solar exposure that can be tolerated, but based on Sun sensor geometry alone, the maximum β -angle reversal that can be tolerated without a roll is 11.5° . In any case it is expected that the roll maneuver will be commanded from the ground, and since the timing is not critical, it will be scheduled at times when it will not interfere with the conduct of any experiment.

7.7 Components/Heritage

Table 7.15 shows the characteristics of components that could be used for the attitude control system. Manufacturers and models are listed for the sensors. These sensors are space-qualified components and have been used on other programs.

The ACS interface electronics have many of the characteristics of an RCTU and could be built by the same manufacturer.

7.8 Reliability

A reliability goal of 0.997 was assigned to the attitude control system (excluding the thrusters and the computers). The calculated reliability of the system is 0.998.

7.9 Summary and Conclusions

The requirements for the COLD-SAT ACS as described, were, in general, found to be fairly routine. The only unusual features are the requirement for minimizing disturbance accelerations and the potential for slosh. Five ACS alternatives were considered and an all-thruster system was selected. Two types of thrusters are used: control thrusters which provide coupled control torque about the spacecraft x-axis and uncoupled torque about the spacecraft y- and z-axes, and an axial gimbaled thruster which provides axial thrust for the experiments and control torque about the spacecraft y- and z-axes when axial thrust is required. The attitude determination system employs sensors that are space-qualified components and have been used on other programs.

The system selected is simple, reliable, and low-cost and it easily meets all the requirements. While the design is not optimized, it clearly demonstrates feasibility. The reliability of the ACS system (excluding the thrusters and computers) is 0.998 for the 6-month mission.

The potential for slosh was addressed and the results shown here, as well as numerous additional simulations specifically designed to elicit a slosh response, demonstrate that slosh is not a problem. The requirement for a low microgravity environment during axial thrusting was met by the inclusion of the gimbaled thruster.

The gimbaled thruster is itself unique for attitude control of a spacecraft although the concept of thrust vectoring for attitude control in other applications is time-tested. The gimbaled thruster uses only existing hardware, namely a fixed-nozzle.

TABLE 7.15.—ACS COMPONENTS

Component	Number	Manufacturer (model)	Unit weight, lb	Unit power, W	Unit reliability (6 mo)
Horizon sensor head	2	Barnes	2.5	"10	"0.9951
Horizon sensor electronics	2	(13-103)	7.5		
Sun sensor head	2	Adcole	0.7	"3	"0.9903
Sun sensor electronics	2	(20910)	2.3		
DRIRU II (gyros)	1	Teledyne (NASA standard)	37	25	.9985
Magnetometer	1	Schonstedt	0.33	1	.9985
ACS interface electronics	1	Custom built	15	20	.9999
Overall reliability	--	-----	---	--	0.998

*For sensor head and electronics functioning as a unit.

conventional hydrazine thruster mounted on a conventional, biaxial antenna gimbal mechanism. The thrust level of the gimballed thruster is very low, and the loads imposed on the antenna gimbal mechanism are not expected to be a problem. The total operational life required of the gimbal mechanism is less than 60 hr, which is far less than the design life for antenna gimbals.

7.10 COLD-SAT Dynamic Model

This description of the computer model used to analyze the spacecraft ACS is a qualitative overview limited to those capabilities of the model used to evaluate the COLD-SAT spacecraft. A detailed technical description of this model, including capabilities not discussed here, can be found in reference 3.

The model described here is implemented in EASY5 and was executed on the Lewis Research Center's Cray X-MP computer. The primary computational coordinate system used throughout the model is an Earth-centered, equatorial, inertial system. The x- and y-axes are in the equatorial plane with the positive x-axis in the direction of the vernal equinox; the z-axis is aligned with the Earth's rotation vector. Other coordinate systems are used as required such as spacecraft body coordinates and rotating Earth coordinates. Throughout most of the model the spacecraft attitude is expressed as a unit quaternion and all coordinate transformations between body and inertial coordinates, including the gravity-gradient torque model, use this quaternion.

An overview of the model is shown in figure 7.42. The model consists of three major segments: the translation model, the rotation model, and the slosh model. A more detailed block diagram of the three segments is given in figures 7.43 to 7.45. For simplicity, many of the details contained in the computer simulation are omitted from these diagrams.

7.10.1 TRANSLATION MODEL

The primary functions of the translation model (fig. 7.43) are to compute the Sun position and the instantaneous position and velocity of the spacecraft as it orbits the Earth. This information is then used to compute the desired spacecraft attitude. These and other functions of the translation model are described in more detail in the following paragraphs.

The translation model can be used alone for orbit analysis or, in conjunction with the other segments of the model, for attitude control system analysis.

User inputs to the translation model are as follows:

- (1) Initial orbit (and the location of the spacecraft in its orbit) given as orbital elements
- (2) Time and date at the start of the simulation
- (3) Characteristics and scheduling of the axial thrust

- (4) Hydrogen consumption schedule
- (5) Initial spacecraft weight
- (6) Spacecraft center of gravity location in spacecraft coordinates

7.10.1.1 Orbit Simulation

The orbit simulation propagates the initial spacecraft position and velocity, under the influence of an oblate Earth gravitational field, atmospheric drag, and the effects of spacecraft-produced linear thrust. The spacecraft-produced linear thrust consists of the thrust produced by the axial thrusters as well as the uncoupled control thrusters. The gravity model takes into account the first four zonal harmonics, which is sufficiently detailed to accurately simulate nodal regression and apsidal progression. The spacecraft-produced linear thrust, which is the sum of axial thrust and any linear thrust produced by the ACS, is first computed in spacecraft coordinates and then transformed into inertial coordinates by using the attitude quaternion computed by the rotation model. Weight changes of the spacecraft over time are taken into account when converting the thrust into acceleration. The thrust acceleration (from axial and control thrusters) is combined with the gravity acceleration and atmospheric drag and the resultant total acceleration is integrated twice to obtain the spacecraft velocity and position vectors, respectively. The velocity and position vectors can, if desired, be converted into orbital elements either for printing out or for plotting as a function of time.

7.10.1.2 Desired Attitude Computation

The direction cosine matrix for the desired attitude is computed as a function of the velocity, position, and Sun vectors. The direction cosine matrix is then converted to an attitude quaternion. The Sun vector is computed in inertial coordinates by using the time and date specified by the user. In addition to its use for the attitude computation, the Sun vector is also passed on to the rotation model for use in the disturbance torque calculations.

7.10.1.3 Axial Thrust Misalignment Torque

The axial thrust vector, combined with the spacecraft center of gravity location, is used to compute the axial thruster misalignment torque. This torque is passed to the rotation model.

7.10.1.4 Greenwich Hour Angle (GHA) Computation

The initial GHA is computed based on the user supplied time and date. The GHA is passed to the rotation model for use in transforming the Earth's magnetic field vector from rotating Earth coordinates into inertial coordinates. The rotation model continuously updates the GHA by the Earth's rotation rate as time advances.

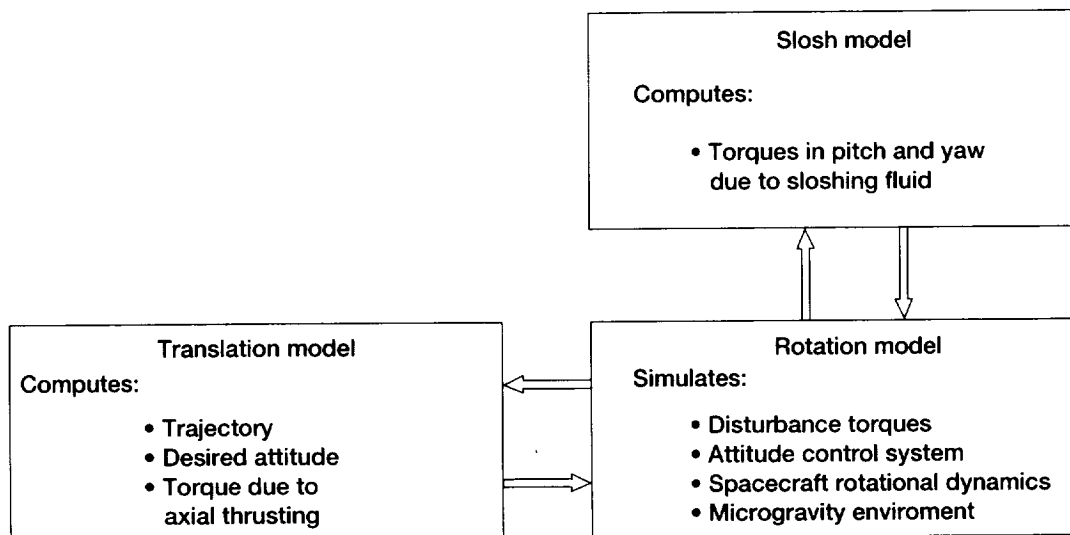


Figure 7.42.—COLD SAT model overview.

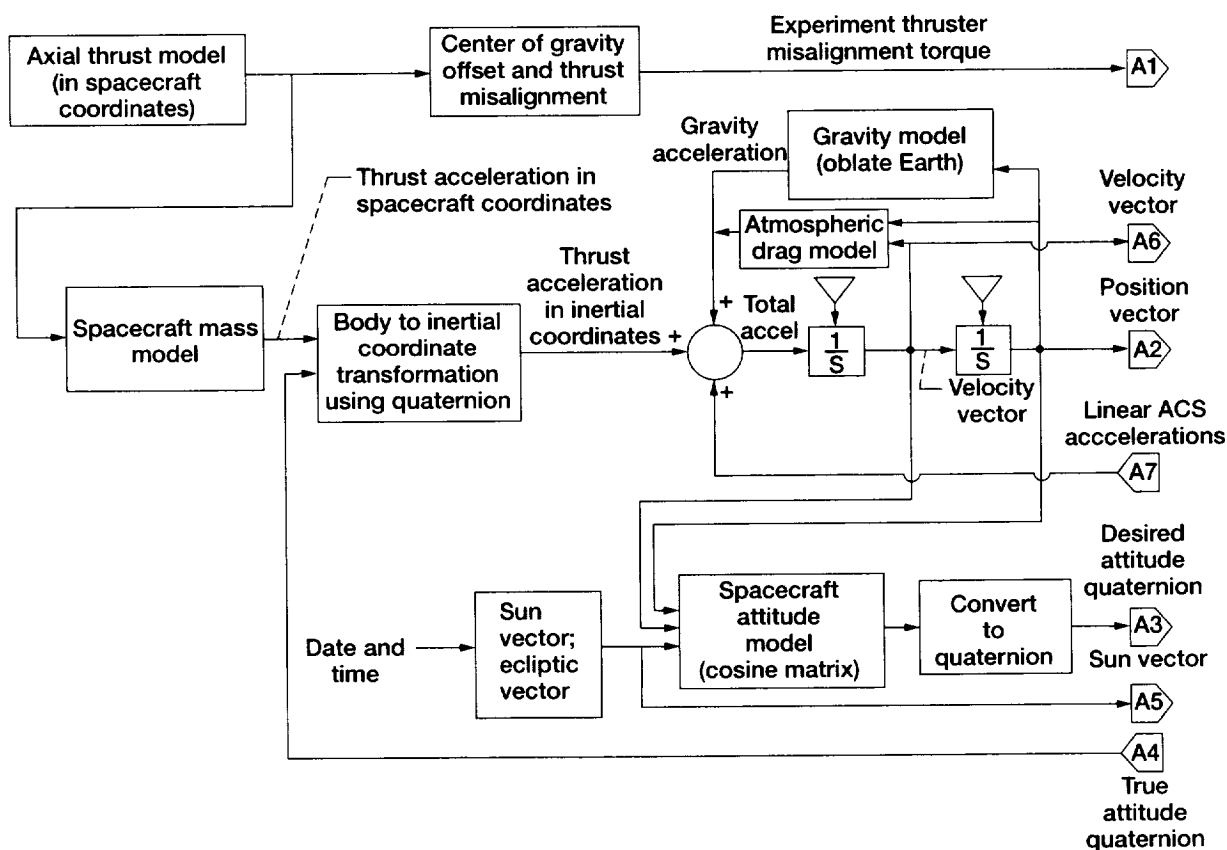


Figure 7.43.—Translation model block diagram. See figure 7.44 for identification of symbols.

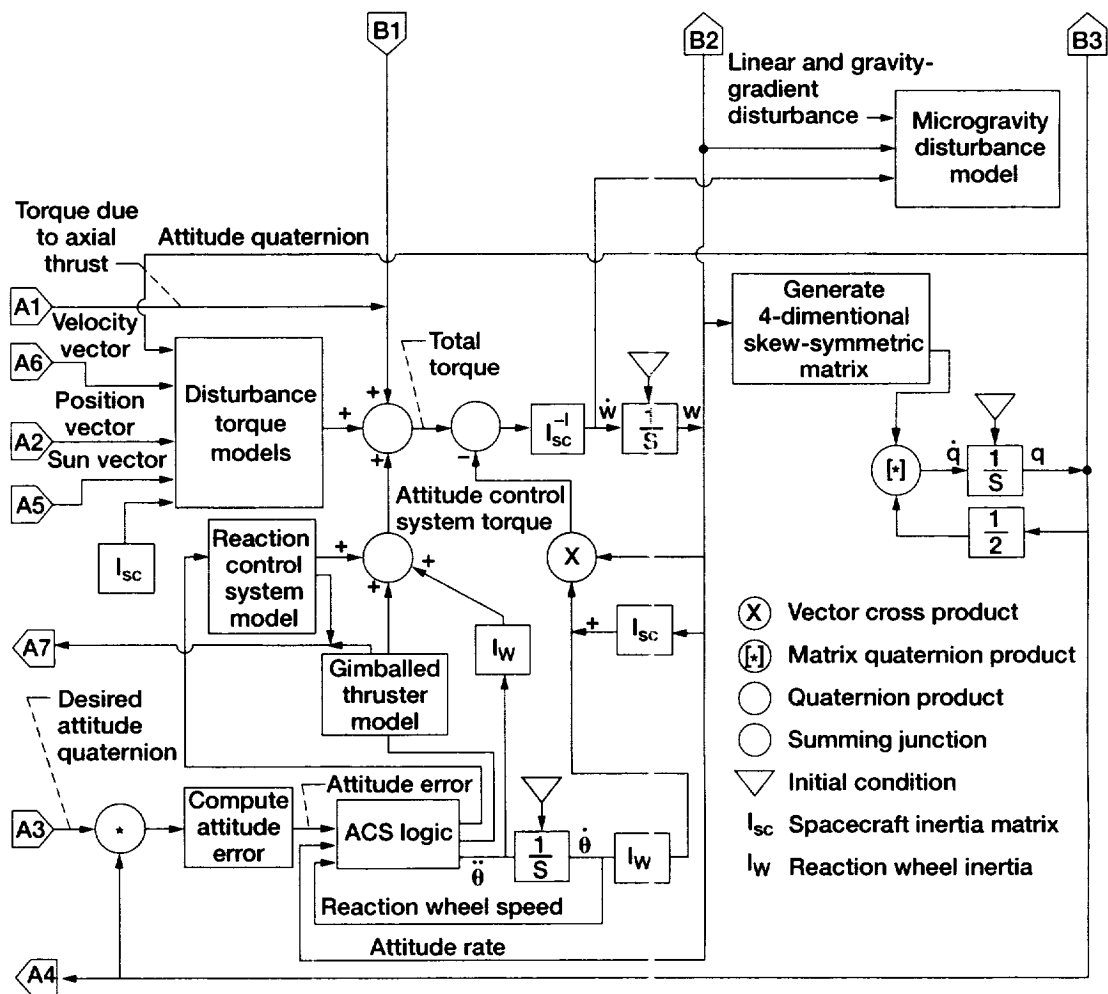


Figure 7.44.—Rotation model block diagram.

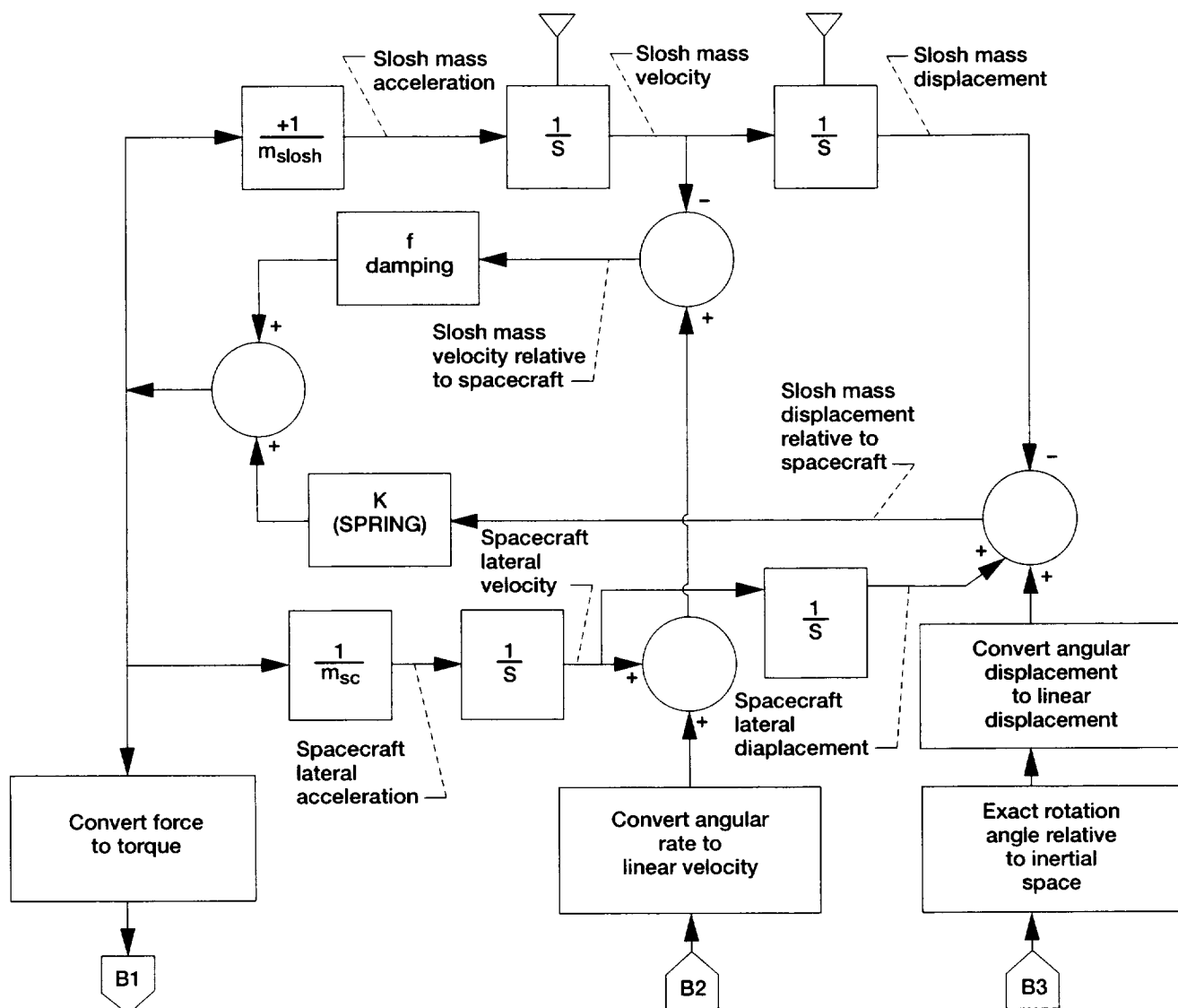


Figure 7.45.—Slosh model block diagram. See figure 7.44 for identification of symbols.

7.10.2 ROTATION MODEL

The rotation model (fig. 7.44) has as its primary function the computation of all disturbance torques (except slosh torque and axial misalignment torque), all ACS control torques, and the simulation of the spacecraft rotational dynamics. In addition the rotation model computes the microgravity disturbance accelerations.

User inputs to the rotation model are

- (1) Type of attitude control system to be modeled (that is coupled or uncoupled control thrusters, reaction wheel, gimballed thruster, etc.)
- (2) Spacecraft inertia matrix
- (3) Torque characteristics of the control thrusters
- (4) Initial attitude rates
- (5) Spacecraft magnetic moment in spacecraft coordinates
- (6) Gimballed thruster characteristics
- (7) Atmospheric density assumptions
- (8) Coordinates of points (in spacecraft coordinates) at which, disturbance accelerations are to be computed.

7.10.2.1 Gravity-Gradient Torque

The gravity-gradient torque computation assumes a spherical Earth gravity model. The computation takes into account both the moments and products of inertia of the spacecraft. Gravity-gradient torque calculation is for the actual spacecraft attitude as computed by the rotation model and for the actual spacecraft position as computed by the translational model.

7.10.2.2 Magnetic Torque

Magnetic torques are computed using a tilted dipole model of the Earth's magnetic field. The Earth's magnetic field is assumed to rotate with the Earth. As with the gravity-gradient torque, actual spacecraft position and attitude are used in the computations.

7.10.2.3 Aerodynamic Torque

The aerodynamic torque computation models the spacecraft as a solid cylinder with a solid, truncated cone attached on one end. The atmospheric density is computed using the Jacchia 1970 Model of the Earth's atmosphere. The spacecraft center of gravity is assumed fixed for all aerodynamic torque calculations.

7.10.2.4 Solar Pressure Torque

Solar pressure torque also uses a simplified geometric representation of the spacecraft. Individual surfaces are not modeled. Solar pressure torque is modeled as a simple function of β -angle. The program determines if the spacecraft is in the

Earth's shadow, in which case the solar pressure torque is assumed zero. As currently modeled, the solar pressure torque calculations are only valid for the attitude selected for COLD SAT.

7.10.2.5 Attitude Error Computation

Attitude error about each axis is determined by comparing the desired attitude quaternion with the actual attitude quaternion. No small angle approximations are made.

7.10.2.6 Control Thruster Torque Computation

The thrusters are controlled by the use of switch lines as described in section 7.6.3.3 of this report. Once it is determined (by comparing the current attitude errors and attitude rates against the three sets of switch lines) that a control torque needs to be applied, a two-step table lookup procedure is used. The program determines from the first user supplied table which thrusters are to be turned on to provide the required torque. Then, through the use of another user-supplied table, the program determines the amount of torque applied about each spacecraft axis by that thruster. The torques from all thrusters that are turned on are summed to arrive at the total, steady-state control torque. The steady-state torque determined in this way includes any torques resulting from any misalignment of control thrusters.

The model assumes that the steady-state torque is not reached instantaneously, but that there are startup and a shutdown transients. The actual torque applied to the spacecraft is simulated as shown in figure 7.46. The torque ramps up from zero to the steady-state value determined above, remains at the steady-state value until it is determined that the control torque is no longer required, and then ramps down to zero. The time for the rampup and rampdown are user supplied inputs. For all COLD SAT simulations these times were assumed to be 100 m sec. The time from the start of the startup transient to the start of the shutdown transient is constrained to be larger than some minimum on time. The minimum on time is a user selectable input which, for COLD-SAT, was selected to be 200 m sec.

Linear thrust resulting from the use of uncoupled control thrusters is determined and used by the translation model in its position and velocity computations.

7.10.2.7 Gimballed Thruster Simulation

The gimballed thruster is simulated as a second order system as shown in figure 7.47. The commanded position of the gimballed thruster is quantized to simulate the effect of a stepper motor drive.

For modeling purposes the gimballed thruster is assumed to be mounted on two single axis gimbal mechanisms. The first gimbal is mounted to the spacecraft with its rotation axis parallel to the spacecraft y-axis. The second gimbal is mounted on the first gimbal and its rotation axis is parallel to the

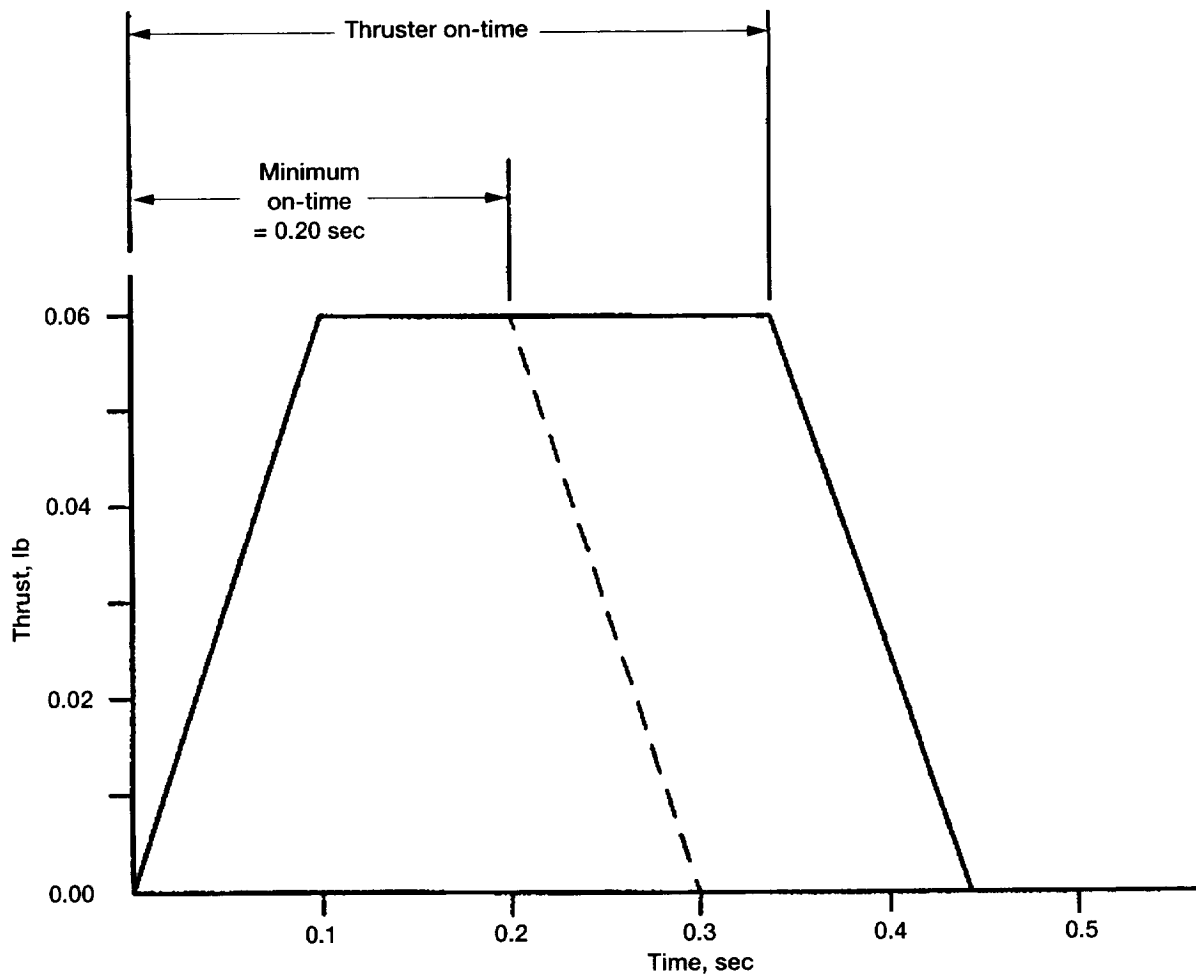


Figure 7.46.—Control thruster pulse profile.

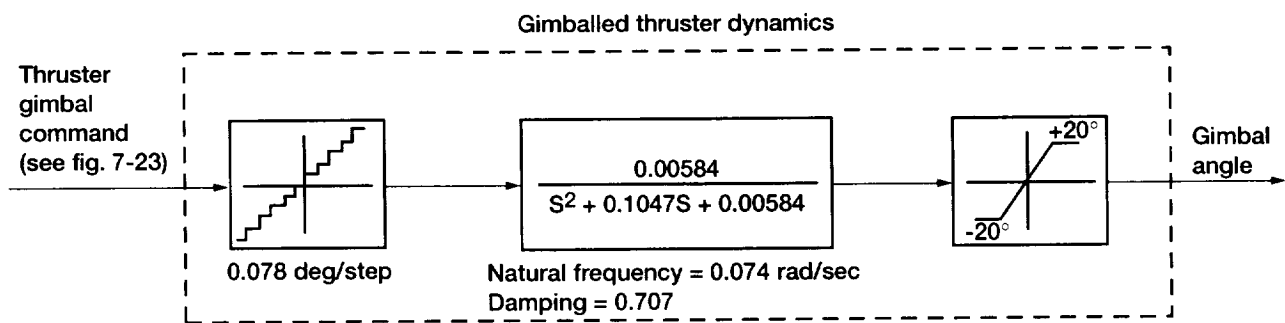


Figure 7.47.—Gimbal thruster model (y- and z-axis).

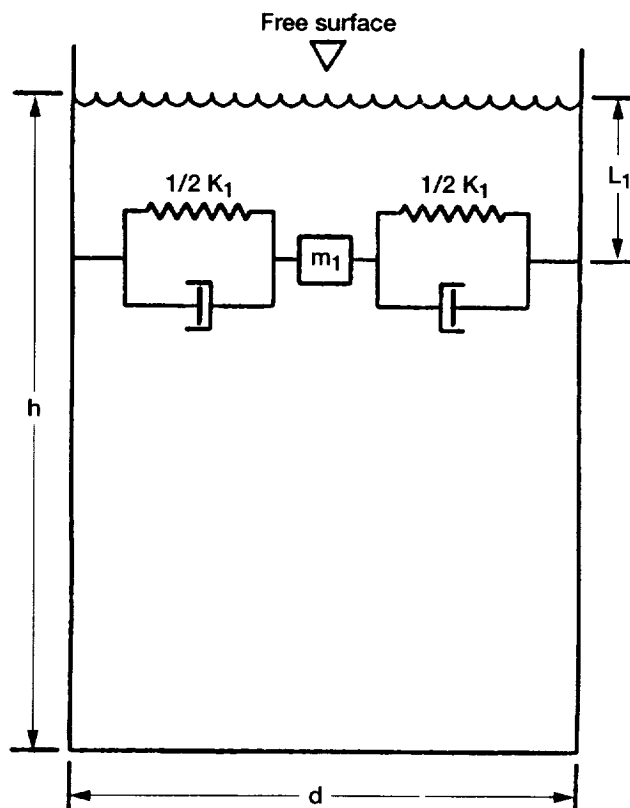


Figure 7.48.—Spring/mass/dashpot slush equivalence.

spacecraft z-axis. To provide sufficient torque margin, a maximum gimbal angle of $\pm 20^\circ$ about both the y- and z-axes has been selected. This arrangement results in torques about the spacecraft y- and z-axes as follows:

$$T_y = Fl(\sin \theta_y)(\cos \theta_z)$$

$$T_z = Fl(\sin \theta_z)$$

where θ_y is the gimbal angle of the first gimbal mechanism, θ_z is the gimbal angle of the second gimbal mechanism, F is the thrust, and l is the distance of the center of gravity from the rear of the spacecraft.

7.10.2.8 Kinematic Equations of Rotation

The disturbance torques and the control torques are summed to arrive at the total torque acting on the spacecraft. The gyroscopic torques for a rotating spacecraft are added. For COLD-SAT gyroscopic torques are very small since the spacecraft is in a nearly inertially fixed attitude. The total spacecraft torque is used to compute the angular acceleration and integrated once to obtain the angular rates. By using the kinematic equations, in quaternion form, the spacecraft rates are integrated to obtain the spacecraft attitude quaternion.

7.10.2.9 Disturbance Accelerations

The disturbance accelerations included in the analysis are the following:

- (1) Gravity-gradient accelerations
- (2) Linear, tangential accelerations resulting from spacecraft angular accelerations (caused primarily by control thruster firings)
- (3) Linear, radial accelerations resulting from spacecraft angular rotations
- (4) Accelerations caused by the axial thruster which was assumed to have an angular misalignment of $1/3^\circ$; this angular misalignment causes acceleration in the spacecraft y and z directions
- (5) Accelerations caused by the gimbaled thruster, which causes accelerations in the spacecraft y and z directions with its gimbaling action
- (6) Aerodynamic drag
- (7) Variations in acceleration due to changes in spacecraft weight (because of consumption of hydrogen and hydrazine)
- (8) Linear accelerations resulting from uncoupled control thrusters

7.10.3 SLOSH MODEL

The only function of the slosh model (fig. 7.45) is to compute the slosh-induced torque on the spacecraft. Any number of tanks may be modeled. For the COLD-SAT analysis the three tanks were either modeled individually or all three tanks were modeled simultaneously.

User inputs to the slosh model consist of:

- (1) Number of tanks
- (2) Tank dimensions
- (3) Tank location relative to the spacecraft center of gravity
- (4) Density of the fluid in the tank
- (5) Fill level of each tank

The fluid in the three hydrogen tanks is modeled as a mechanically equivalent system consisting of a spring, mass, and dashpot combination as shown in figure 7.48. The computations of the slosh mass size and location and of the spring constant are based on reference 4 for cylindrical tanks. To keep the slosh model reasonably simple only the fundamental slosh frequency is modeled and the slosh in the spacecraft x-y plane

is assumed independent of any slosh in the x-z plane. Slosh torques about the roll axis are neglected.

The slosh model computes the velocity and the displacement of the slosh mass relative to the spacecraft body. The relative velocities and displacements produce damping and spring forces, respectively. These forces are assumed to act equally but in opposite directions on the slosh mass and on the spacecraft body. The force acting on the spacecraft body causes the spacecraft to move laterally; the same force also creates a torque on the spacecraft which causes rotational motion.

References

1. Spacecraft Magnetic Torques. NASA SP-8018, p 6.14, 1969.
2. Models of Earth's Atmosphere (90 to 2500 km). NASA SP-8021. Revised Mar. 1973.
3. Adams, N.; and Bollenbacher, G.: COLD-SAT Dynamic Model. NASA TM-105185, 1992.
4. Abramson, N.: The Dynamic Behavior of Liquids in Moving Containers with Applications to Propellants in Space Vehicle Fuel Tanks. NASA SP-106.

Chapter 8

Propulsion System

Tony D. Shook
National Aeronautics and Space Administration
Lewis Research Center
Cleveland, Ohio

8.1 Introduction

Most spacecraft require a means of moving from one point to another or a means of maintaining a desired orientation while in orbit. These operations are often performed by the spacecraft's propulsion system. For COLD-SAT, the propulsion system must provide both three-axes spacecraft control and different levels of acceleration to create the desired experiment environment. This section will cover some of the concepts and ideas which led to the current design, but the majority of discussion will be about the current configuration and its operational characteristics.

8.2 Requirements

Requirements for the COLD-SAT propulsion system are grouped into three areas—spacecraft control, experiment, and reliability. The propulsion system works with the attitude control system to meet the spacecraft's control requirements. The initial function of the propulsion system is to stabilize and properly orient the spacecraft once it separates from the launch vehicle. The system must also provide three-axes spacecraft orientation to maintain proper Sun pointing requirements during orbit. This is done by controlling the torques on the spacecraft that are caused by environmental forces such as gravity-gradients and self-induced forces, such as those that result from misalignment of the experiment thrust vector with the spacecraft's center of gravity.

The experiment requirements for COLD-SAT provide the propulsion system with an interesting challenge. Many of the COLD-SAT experiments require a constant acceleration along the spacecraft's x-axis. These accelerations provide the necessary forces to orient the liquid hydrogen for transferring,

venting, and measuring liquid level. The experiments require a range of three induced-acceleration levels. This range of accelerations provides the necessary forces both to settle the liquid in the different sized tanks and to study affects on the liquid caused by varying these forces. Another important requirement based on experiment needs is to minimize the spacecraft disturbances during all induced-acceleration experiments. To properly conduct some experiments, their environments must be as stable as possible; this requires the induced-acceleration levels to be held constant and that all other disturbances to the spacecraft be minimized throughout the experiment.

The propulsion system has been designed with both safety and reliability goals in mind. Standard engineering practices and flight-proven hardware have been used to design a safe and reliable system. A reliability requirement of 0.998 was a design goal for the propulsion system.

8.3 Interfaces

The propulsion system interfaces with many of the spacecraft's major systems. The onboard computer system commands and controls many of the propulsion system components and operations. Propulsion system pressurization is controlled by the computer; system pressure signals are received by the computer to initiate commands sent to cycle valves which maintain a constant system pressure. In addition, the computer receives inputs from the attitude control system and provides both engine firing commands and gimbaled engine positioning commands. Another important function of the computer is to monitor all system health instrumentation and to initiate the proper commands if a problem is detected.

Because the COLD-SAT spacecraft must operate in the harsh environment of space, the thermal control of the propul-

sion system components is very important. The hydrazine propellant must be kept in a temperature range that does not lead to either freezing or boiling, which is accomplished by thermally controlling the components of the propulsion system. The thermal control system uses both heaters and insulation to maintain the system components in the desired temperature range.

Another system which interfaces with the propulsion system is the spacecraft configuration. All system components have been carefully configured to meet both the experiment and control requirements. The location of the engines on the aft end of the spacecraft helps to minimize effects of plume impingements, and at the same time provides both the required degree of torque authority for control and the proper levels of axial thrust for the experiments. In addition, engines are grouped together in modules that are thermally controlled as a unit, which minimizes the power required. Components have also been located with the goals of simple system integration and accessibility in mind.

8.4 Trade Studies

Concept trade studies focused on two system design areas—system pressurization and engine configuration. The strong and weak points were compared to choose the design which best satisfied the requirements of COLD-SAT.

8.4.1 SYSTEM PRESSURIZATION

There are two primary methods of pressurization for a hydrazine propulsion system—a blow-down type and a controlled type.

8.4.1.1 Blow-Down Pressurization

A blow-down type of pressurization requires a pressurant gas ullage to feed the propellant tanks. As the propellant is consumed, the ullage gas volume increases, while its pressure level decays (see fig. 8.1). A typical blow-down system starts with an initial system pressure of 300 psi, and when all propellant is depleted, an ullage pressure of 100 psi remains. A blow-down type of system is very common because it is simple, inexpensive, and reliable. However, a quick look at this type of system points out a few areas of concern. The thrust output of a hydrazine engine is directly related to the pressure level at which the propellant is fed; when the system pressure decays, the thrust decays. This characteristic thrust decay of a blow-down type of system presents two main concerns: (1) the experiment requirement of a constant acceleration is not possible, and (2) to maintain a high enough magnitude of thrust to meet the end-of-mission requirements, the thrust output must be oversized during the beginning of the mission. In an attempt to minimize the impact of these two concerns, the ratio of starting system pressure to ending pressure was reduced. But

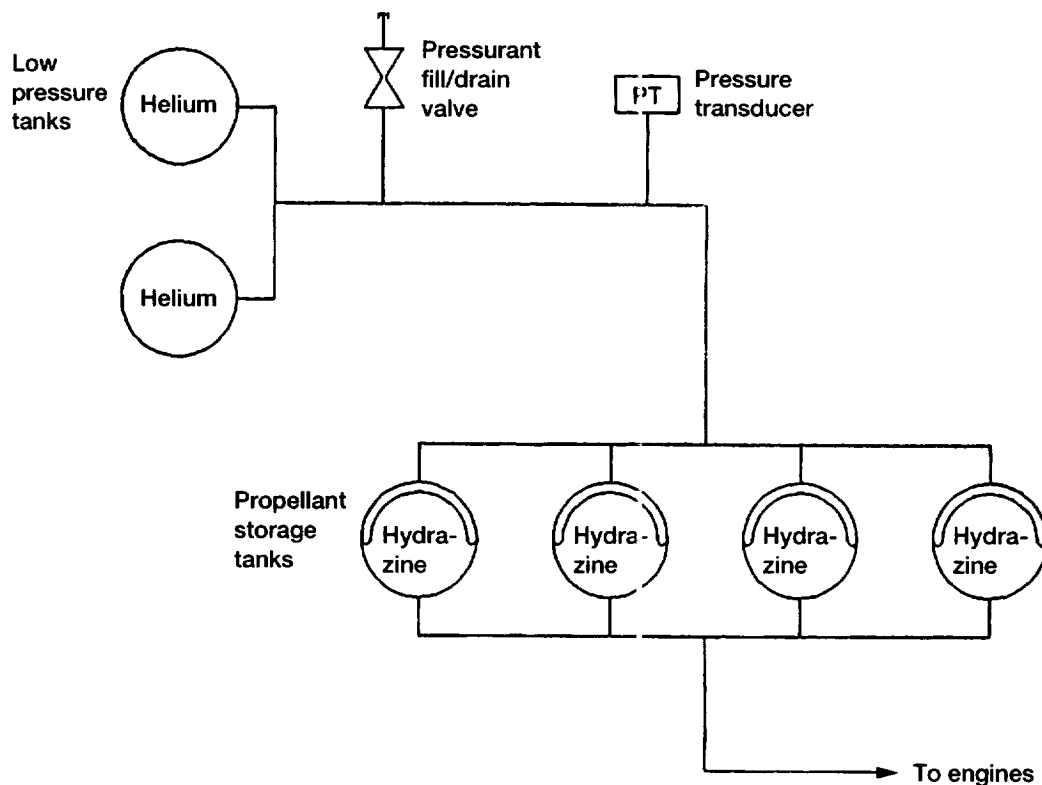


Figure 8.1.—Blow-down pressurization schematic.

while a smaller blow-down ratio produces less change in thrust from start to finish, the change in system size is extreme (see table 8.1). The system design must consider the launch vehicle constraints of weight and volume. Another attempt to reduce the blow-down ratio uses a modified system (see fig. 8.2). The operation uses pressurant supplied in cycles. The first cycle consists of a smaller volume of ullage pressurant at the high end of the blow-down range. The ullage pressure decays to the lower end of the blow-down ratio, and then, the next cycle, a

high-pressure bottle (2000 psi) supplies the system with a pressurant recharge to the upper end of the blow-down range. The high-pressure bottle for each cycle is sized so that its entire volume is released to the system upon opening of the valve. Although additional cycles do increase the complexity of the blow-down system, several other system characteristics are affected favorably. Table 8.2 shows a comparison between characteristics of different blow-down systems; the most important characteristics are system volume, total weight, and acceleration variation.

TABLE 8.1.—BLOW-DOWN PRESSURIZATION SYSTEM CHARACTERISTICS^{a,b,c,d}

Blow-down ratio	Propellant required, lb	System size, ft ³	System weight, lb	Thrust decay, percent
3:1	780.0	2.1	10.0	60
2:1	620.0	8.4	34.0	43
1.5:1	540.0	19.4	80.0	30
^e 1:1	460.0	1.0	23.0	0

^a100.0 psi is minimum operating pressure.

^b3:1 and 2:1 ratios require five propellant tanks.

^c1.5:1 and 1:1 ratios require four propellant tanks.

^dAll tank characteristics come from existing hardware designs.

^eThis ratio is for a pressure controlled system.

TABLE 8.2.—BLOW-DOWN PRESSURIZATION SYSTEM TRADE^{a,b,c,d,e}

Blow-down system	Propellant required, lb	System size, ft ³	System weight, lb	Thrust decay, percent
3:1	780.0	2.1	10.0	60
3:1 (2 cycles)	780.0	1.0	22.0	60
2:1	620.0	8.4	34.0	43
2:1 (2 cycles)	620.0	1.0	22.0	43
1.5:1	540.0	19.4	80.0	30
1.5:1 (2 cycles)	540.0	5.1	38.0	30
1.5:1 (3 cycles)	540.0	1.7	38.0	30
^f 1:1	460.0	1.0	23.0	0

^a100.0 psi is minimum operating pressure.

^b3:1 and 2:1 ratios require five propellant tanks.

^c1.5:1 and 1:1 ratios require four propellant tanks.

^dRecharge cycles are supplied by tanks at 2000 psi.

^eAll tank characteristics come from existing hardware designs.

^fThis ratio is for a pressure controlled system.

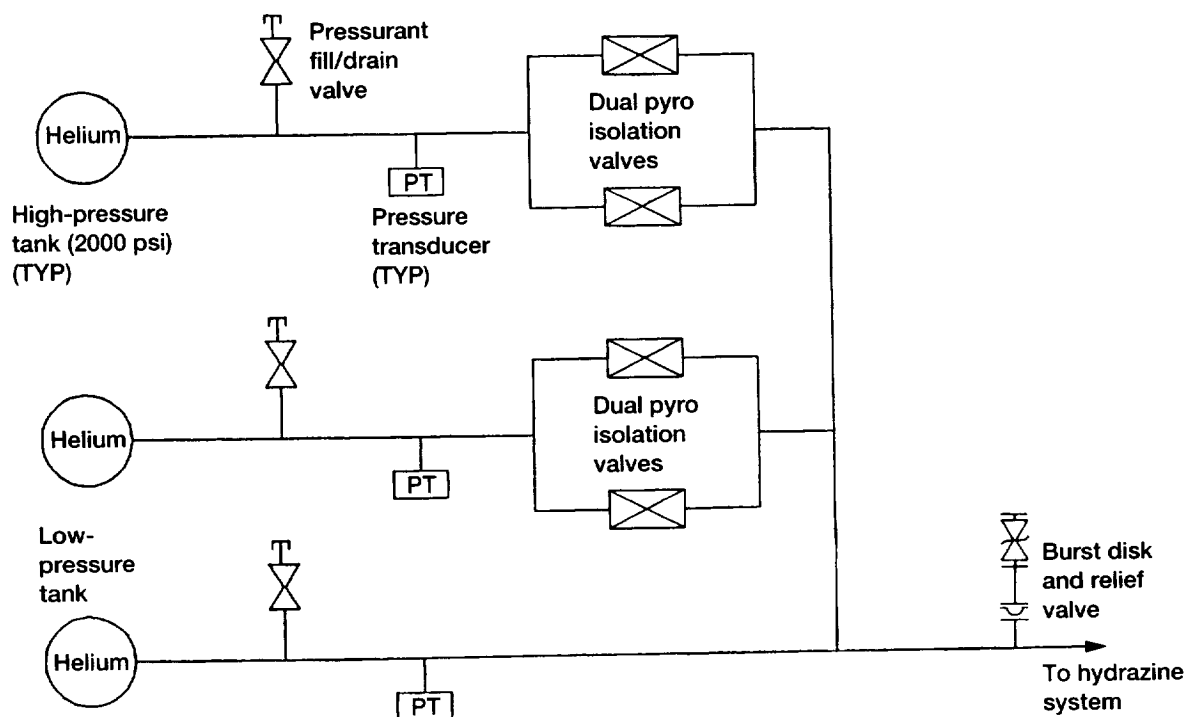


Figure 8.2.—Cycled blow-down pressurization schematic.

8.4.1.2. Controlled Pressurization

The other proposed method of system pressurization is a controlled pressure. A high-pressure gas supply (2000 psi) is used to pressurize the propellant tanks. The propellant tank pressure is maintained relatively constant by either a computer commanded valve or a pressure regulator (see fig. 8.3). There are several advantages of a controlled system pressure as opposed to a blow-down type of system. First, the overall system dry and wet weight can be reduced. Second, the system volume required for pressurant storage and plumbing is minimized. Third, a computer-controlled pressure provides the ability to upload software commands to the system for increasing the propellant tank pressure, thus increasing engine thrust output. Fourth, and most important, the experiment requirement of maintaining constant acceleration levels is most nearly accomplished with a controlled pressure system. These advantages largely outweighed the small increase in system complexity and their resulting affects on overall system reliability.

8.4.2 ENGINE CONFIGURATION

The second design area that used a trade study to analyze concepts is the control engine configuration. Since it was decided to use a hydrazine engine system to provide the axial acceleration levels for experimentation, the decision to expand that system to include engines for controlling the spacecraft's orientation seemed appropriate. Three configurations of control engines were reviewed—coupled engine pairs, a combination of coupled engine pairs and single engines, and a combination of coupled engine pairs and single engines with a gimballed engine. Each of these engine configurations provides the spacecraft with different control characteristics; these characteristics are summarized in table 8.3. The first control

engine configuration fires a pair of engines to produce torque about each of the three spacecraft axes. Engines are located on both the aft and forward ends of the spacecraft, which minimizes the engine plume effects on the spacecraft. A pair of engines, one on the forward and one on the aft end fire to provide control about the y- and z-axis. Two engines are located opposite each other on the circumference of the aft end of the spacecraft to provide control torque about the x-axis. The second engine configuration locates all engines on the aft end of the spacecraft; this simplifies system integration and reduces the number of engines required. Spacecraft orientation is controlled about the y-axis and z-axis by firing a single engine, while control about the x-axis is generated with a pair of engines. Because a single engine is used, the control torque about the y- and z-axis is reduced, thus increasing the control engine duty cycles. Also affected are the axial acceleration levels for the experiments; these levels will continually be disturbed by the control engines firing to maintain spacecraft orientation. The last engine configuration concept reviewed uses two separate control schemes for different phases of the mission. The first scheme is used for the majority of the mission when no induced-acceleration levels for experiments are required. Control is maintained about the y- and z-axis by firing a single engine, and control about the x-axis is maintained by firing a pair of engines; this scheme is the same as that used in the second configuration concept. The second scheme is used when the experiment requires an induced acceleration. A two-axis gimballed engine is fired throughout the duration of the experiment and maintains spacecraft control about the y- and z-axis. The x-axis control is produced as in the previous configurations, with a pair of engines firing. This configuration of control engines has the important advantage of providing the best induced-acceleration environments for the experiments with the fewest spacecraft disturbances.

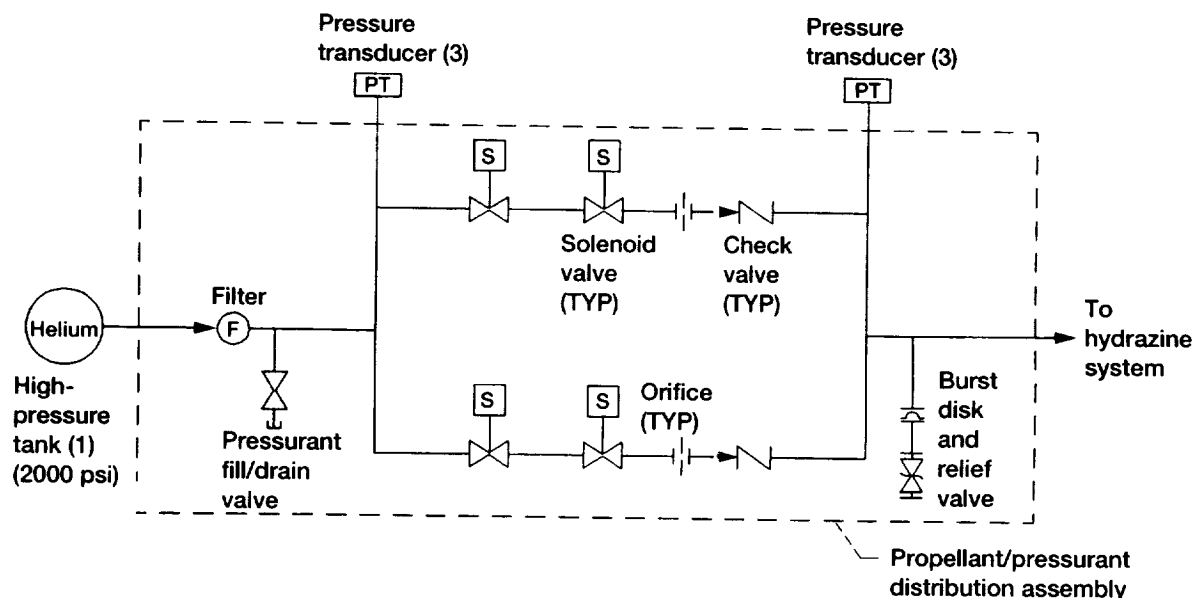


Figure 8.3.—Propulsion pressurization system schematic.

TABLE 8.3.—CONTROL ENGINE CONFIGURATION CHARACTERISTICS

Configuration	Advantages	Disadvantages
Coupled engine control	Axial thrust levels remain constant Good control torque authority	Maximum number of engines required Control engine disturbances during induced acceleration experiments Added system integration complexity
Coupled engine pairs and single engines	Simplified system integration Reduced number of engines required	Axial thrust levels increase with control engine firings Increased control engine duty cycles Added control disturbances during induced acceleration experiments
Coupled engine pairs, additional single engines and gimballed engine	Reduced number of engines required Simplified system integration Axial thrust levels remain constant Minimal control disturbances during induced acceleration experiments	Gimballed hydrazine engine concept not flight proven Gimballed engine requires computer interfacing

8.5 System Description

The COLD-SAT propulsion system is a monopropellant hydrazine system which provides thrust for two main functions: control of spacecraft orientation and experiment-required accelerations. A hydrazine engine system is well suited to satisfy the experiment requirements of low, sustained, and repeatable thrust levels. In addition, by implementing a few more engines, a very cost-effective approach to spacecraft attitude control is found.

8.5.1 PROPULSION SYSTEM CONFIGURATION

The propulsion system consists of four bladder-type propellant tanks each with the capacity of 150 lb. of propellant. Five rocket engine modules house four engines each and are located on the aft end of the spacecraft (see fig. 8.4). These modules protect the engine components from the space environment, while helping to maintain their thermal environment. A typical engine configuration is seen in figure 8.4. It consists of the following parts: a propellant feed valve, engine, catalyst bed thermocouple, valve heater, catalyst bed heater, and propellant line heater. These engines are grouped into three clusters which can be isolated from the propellant flow by a solenoid latching valve. The latching valve serves two functions. First, it provides a second level of propellant isolation from the engines while the spacecraft is on the ground; this protects against an inadvertent engine firing on the ground. Second, it allows a cluster to be completely isolated from propellant if a failure in that cluster occurs during the mission. The engines have been clustered so that only two of the three are needed to meet all the system control and experiment requirements. The three latching valves and fill/drain valve are grouped together on the

propellant/pressurant distribution assembly. This assembly is easily accessible, which simplifies testing of components, loading propellant, and draining propellant in case of an emergency.

8.5.2 PRESSURIZATION

The COLD-SAT propulsion system will maintain a constant thrust level throughout its mission by controlling the feed pressure to the propellant tanks. A trade study between a pressure-controlled and a blow-down type of system pressurization contributed to the decision to use a controlled pressure system (see fig. 8.3). Factors which led to this decision include, reduced system weight and volume, provision of constant system thrust, simplified system integration, and allowance for on-orbit thrust level increases.

The COLD-SAT propulsion pressurization system uses a 2000-psi pressurant supply to maintain the propellant tanks at a constant operating pressure of 100 psi. The pressure control method used is commonly referred to as a "bang-bang" type system. As propellant is consumed, the ullage pressure decays. This pressure decay is sensed by the computer which commands the solenoid valve to open, thus restoring the system pressure to 100 psi. The pressurization system valves are also located together on the propellant/pressurant distribution assembly, simplifying both system integration and checkout. System redundancy is provided by a parallel control leg, while system over-pressurization is protected against by a burst disk and relief valve combination. The system design also has the flexibility of increasing engine thrust level during the mission. By uploading software commands, the pressure can be controlled at a higher level, thus increasing the engine thrust output.

TABLE 8.4.—NOMINAL ACCELERATION LEVELS

Nominal acceleration, ^a g's	Thrust level, lb	Bond number		
		Supply tank	Small receiver tank	Large receiver tank
8.0×10^{-6}	0.04	1.6	0.6	0.5
3.2×10^{-5}	.16	6.5	2.3	1.9
1.0×10^{-4}	.52	20.9	7.5	6.1

^aNominal accelerations based on average spacecraft weight.

and misaligned thrust vectors must be controlled by the propulsion system. The control engine configuration trade study provided the information to help choose the best configuration for the COLD-SAT mission (table 8.3).

The configuration locates all of the engines on the aft end of the spacecraft, thereby simplifying system integration and reducing the number of engines. Two separate control schemes are used during different parts of the mission to maintain spacecraft orientation. The primary scheme is used during the majority of the mission for periods which do not require induced-acceleration levels for the experiments. The spacecraft's orientation is maintained about the y- and z-axes by firing a single engine, while for control about the x-axis a pair of engines are fired. The secondary control scheme is used during the 56 hr when the experiments require an induced-acceleration environment. A two-axis gimballed engine fires continuously during the experiment and maintains spacecraft orientation about the y- and z-axis, while a pair of engines are fired for control about the x-axis. It is during these 56 hr that the spacecraft would see its maximum frequency and magnitude of disturbance torques. By using a gimballed engine, the number of engine firings for control is significantly reduced, minimizing the disturbances to the experiment environment.

8.5.4 PROPULSION SYSTEM COMPONENTS

The propulsion system is designed with the goal of minimizing volume, weight, power, and complexity while meeting all the spacecraft control and experiment requirements. The propulsion system has a dry weight of 159 lb and a peak power estimate of 161 W. For additional component characteristics, see table 8.5.

The gimballed engine is an important part of the propulsion system design. This concept interfaces existing flight hardware to provide a function not commonly used with a hydrazine propulsion system. But, it is not often that a propulsion system must be designed to the unique requirements of COLD-SAT. Extensive dynamic modeling of the spacecraft has indicated that the gimballed engine provides the best experiment environment during the induced accelerations. The gimballed engine interfaces two flight qualified components—the hydrazine engine and the biaxial drives. Both of these components have an extensive flight history. In the past, these engines have been used for spacecraft control and the drives for positioning of instrumentation and antennas. The engine is a 0.04-lb, type MR-103, which is manufactured by Rocket Research. This engine is capable of providing the low, steady, and sustained thrust levels required for both control and experiment requirements. The engines have been tested and flown under operating conditions much more severe than those expected during the COLD-SAT mission. The biaxial drives are built by Schaeffer Magnetics, Inc. The capabilities of these drives far exceed the positioning and load carrying requirements expected for the propulsion system's gimballed engine. Although the gimballed hydrazine engine does not have a flight history and further development is required for interfacing its components, the gimballed engine design concept is based on existing technology and hardware.

TABLE 8.5.—PROPULSION SYSTEM COMPONENT CHARACTERISTICS

Description	Quantity	Dimensions, in. (length by diameter except where noted)	Unit weight, lb	Total weight, lb	Peak power, W
Fill/drain valve	2	4 by 2	1.0	2.0	---
Relief valve/burst disk	1	2 by 1	.5	.5	---
Check valve	2	2 by 1	.5	1.0	---
Propellant tank	4	22-in. sphere	14.0	56.0	---
Pressurant tank	1	15-in. sphere	23.0	23.0	---
Orifice	5	1 by 1	.3	1.5	---
Filter	2	2 by 1	.5	1.0	---
System lines/fittings	50 ft	0.5	10.0	10.0	---
Solenoid valve	7	4 by 2	2.0	14.0	25.0
Engine	20	8 by 4	2.0	40.0	36.0
Gimbal unit	1	10 by 6	10.0	10.0	10.0
Heaters:					
Catalyst bed	20				20.0
Engine valve	20				40.0
Propellant line	50 ft				5.0
Propellant tank	4				20.0
Propellant/pressurant distribution assembly	1				5.0
Total propulsion system dry weight				159.0	
Propulsion system peak power required					161.0

TABLE 8.6.—PROPELLANT USAGE

Function	Nominal usage, lb	Failed gimbal usage, lb
Experiments		
Tank chilldown	10.0	10.0
No vent fill	23.0	23.0
Pressure control	161.0	161.0
Vented fill	<u>40.0</u>	<u>40.0</u>
	234.0	234.0
Operations		
	104.0	104.0
Attitude control		
Spacecraft orientation (induced accelerations)	2.0	40.0
Spacecraft orientation (quiescent) ^a	<u>130.0</u>	<u>130.0</u>
	132.0	170.0
Total propellant required	470.0	508.0
Qualified tank capacity/margin	600.0/28 percent	600.0/18 percent

^aPeriods with no induced accelerations for experiment purposes.

The gimballed engine will operate continuously during the 56 hr of induced accelerations. The gimballed engine is located on the aft end of the spacecraft along the x-axis, and rotates around two axes to provide spacecraft control about the y- and z-axis. Extensive spacecraft dynamic modeling indicates that using a 0.04-lb thrust force with a maximum gimbal angle of 20° will control the spacecraft during the induced accelerations. The thermal control of the gimballed engine will be maintained by dissipating excess heat through a strap to the structure during engine operation and by generating heat with electric heaters during periods when the engine is idle. Because the gimballed engine has a very short operating life and the hardware requirements are not severe, the system design does not include a backup gimballed engine. Redundancy is provided by a fixed 0.04-lb engine, which results in a degraded experiment environment caused by the control engine firings.

8.6 Propellant Usage

Propellant usage is divided among three groups—experiments, operations, and attitude control (see table 8.6). The experiments require 234 lb of propellant to produce the acceleration levels. The experiment group using the largest percentage (69 percent) is pressure control, primarily because of a few long-duration tests (up to 10 hr). Engine thrust is also required for positioning the liquid hydrogen during pre- and post-test operations; these operations use 104 lb of propellant. The propellant required for maintaining the spacecraft's orientation is based on a 6-month mission duration; this nominal amount is 130 lb. An added contingency of 40 lb of propellant is necessary if the gimballed engine fails, requiring the y- and z-axis control

engines to fire during the induced-acceleration experiments. The 40 lb of propellant is based on a 1-in. thrust vector offset from the spacecraft's center of gravity. A nominal mission requires about 468 lb of propellant, leaving a 28 percent excess propellant margin based on the qualified tank capacity of 600 lb. If the failed gimbal engine contingency is included, a propellant amount of 508 lb is needed; this leaves about a 18 percent margin.

8.7 Safety and Reliability

A few important safety issues were identified during the design of the propulsion system. First, the propulsion system uses both high-pressure vessels for helium storage and low-pressure vessels for propellant storage. It is important that these vessels meet certain design standards to ensure a safe environment once they are loaded. The propulsion system design uses pressure vessels which are both flight-qualified and meet MIL-STD-1522A requirements. A second concern is a premature engine firing while the spacecraft is still on the ground. The engine can only fire when the propellant flow comes in contact with the engine's catalyst bed. The engines will not fire while on the ground because two valves, the engine valve and the latching solenoid valve feeding each cluster, provide isolation between the propellant and the catalyst bed. In addition, while work is still being done on or around the spacecraft, the latching solenoid valves will have their wiring leads disconnected to further ensure that the propellant remains isolated. Finally, the possible self-detonation of propellant once it is released to the system must be protected against. The propellant is contained in the storage tanks while on the ground and during the launch

TABLE 8.7.—FLIGHT-QUALIFIED PROPULSION SYSTEM COMPONENTS

Description	Failure rate (10 ⁻⁶)	Vendor	Heritage
Fill/drain valve	0.01	Pyrotechnics	ERBS/HEAO
Relief valve	.24	Vacco	Intelsat VI
Propellant tank	.025	PSI	Atlas Centaur
Check valve	.01	Vacco	Intelsat VI
Solenoid valve	2.3	Consolidated controls	Apollo
Pressurant tank	.03	PSI	European Program
Engine	1.8	Rocket Research	Satcom
Gimbal drive	.14	Schaefer Magnetics	-----
Line filter	.01	Vacco	Atlas Centaur
Propulsion system reliability allocation, 0.998.			
Propulsion system reliability, 0.998.			

phase of the mission. When the solenoid latching valves open and release the propellant to the system, precautions must be taken. The propellant flow will be released to the system at a low pressure and orificed to help provide a smooth fluid flow to the system.

A propulsion system design goal is to meet the reliability allocation of 0.998. The system is designed with reliability in mind, using flight-proven hardware and component redundancy. The two main areas of redundancy are the engine configuration and the pressurization control. Redundant

engines are included in the system to protect against both a failed "on" and a failed "off" engine. If an engine were to fail, the propulsion system could still meet all spacecraft control and experiment requirements. System pressurization has a redundant control leg to protect against a failure of the solenoid valve. The computer would detect the valve failure, isolate that control path, and actuate the redundant path. A reliability analysis (see table 8.7) has calculated a 0.998 system reliability, thus meeting the 0.998 system allocation goal.

Chapter 9

Telemetry, Tracking, and Command System

Christopher J. Pestak
Analex Corporation
Cleveland, Ohio

9.1 Introduction

The design of the COLD-SAT telemetry, tracking, and command (TT&C) system meets the data and control requirements of all the COLD-SAT spacecraft systems. The TT&C system gathers data in real time from all of the systems onboard the spacecraft including itself. This data consists of over 800 individual measurements that are used for evaluating the health and status of the spacecraft, monitoring the progress and results of the experiments being performed on-orbit, and as control inputs for closed loop control processes.

The TT&C system controls all systems onboard the spacecraft by actuating loads such as valves, heaters, hydrazine thrusters, and so forth. The logic for controlling these loads resides in software resident in the two flight computers (FC 1 and 2). Logic is executed based on data inputs to the computers. The number of measurements used as control inputs is a subset of the total spacecraft measurement complement which is serviced by the TT&C system. This design allows for autonomous operation of the COLD-SAT spacecraft for long periods of the mission.

The system is also designed to allow control of the spacecraft via ground commands. Operators on the ground can take control of the spacecraft whenever it is in view of a tracking and data relay satellite (TDRS). For COLD-SAT's 500-n mi circular orbit, a TDRS will be in view for over 95 percent of each orbit.

The TT&C system is designed to achieve a predicted reliability of at least 0.985. The system design, which is detailed in this section, accomplishes these objectives through the use of redundancy at the component (piece part), subassembly, or line replaceable unit (LRU) level where required. Cross-strapping of LRU's is also employed where practical. The TT&C system

is designed to reduce credible, single-point failures to an absolute minimum.

The design minimizes system weight, volume, and power consumption to the maximum extent possible and all LRU's are interconnected using standard multiplexed data busses to allow ease of interfacing, integration, and test. Existing designs which require little or no modification are used to the maximum extent possible in an effort to minimize system costs.

9.2 Major System Requirements

A number of requirements are imposed on the TT&C system by the overall system design. These requirements are discussed in this section. Detailed discussion of the interfaces through which these requirements are implemented are covered in section 9.3 of this chapter.

9.2.1 ON-ORBIT REQUIREMENTS

9.2.1.1 Telemetry

The TT&C system must perform the following telemetry acquisition, storage, and return functions for all spacecraft systems:

- (1) Acquire telemetry data from all spacecraft systems including itself. Sensor signal conditioning may be required. The overall spacecraft data rate of 3200 bps should be assumed
- (2) Store data between telemetry return passes for at least three orbits
- (3) Format and return all live and stored telemetry data for an orbit during one 13-min period per orbit by using the

Tracking and Data Relay Satellite System (TDRSS) multiple access service

(4) Provide for contingency return of real-time and stored data by means of the TDRSS single access service in the event of the loss of spacecraft attitude

(5) Allow the continuous return of all real-time spacecraft data by means of the TDRSS multiple or single access

9.2.1.2 Command and Data Uplink

The TT&C system must perform the following uplink functions by using TDRSS multiple access service:

(1) Load and reload flight computer software. It shall be possible to transmit and verify a complete flight computer software load in, at most, four 13-min TDRSS multiple access passes

(2) Process normal operational commands directed to the flight computer software

(3) Pass discrete commands directly to all spacecraft systems bypassing the flight computers

In the event of the loss of spacecraft attitude control or other contingency, it shall be possible to perform all functions using TDRSS single access service but at a potentially reduced data rate.

9.2.1.3 Tracking

The TT&C system shall provide for tracking of the spacecraft by means of the TDRSS system.

9.2.1.4 Spacecraft Control Computer

The TT&C system must provide a central spacecraft computer to execute software controlling all spacecraft subsystems. The basic computational requirements are as follows:

(1) Read-only memory, 46 Kbytes minimum

(2) Random access memory, 171 Kbytes minimum

(3) Computational throughput, 500 K instructions/sec

Telemetry data from all spacecraft systems must be available to control computer software, and the control computer must be capable of issuing commands to all systems.

9.2.1.5 Spacecraft Control

The TT&C system must provide control outputs to all spacecraft systems. When required by the system, this shall take the form of direct electrical load actuation.

9.2.2 LAUNCH, ASCENT, AND DEPLOYMENT REQUIREMENTS

There are three primary functions which the TT&C system must perform during the launch-ascent phase

(1) Autonomously control all spacecraft and experiment functions from liftoff through separation and deployment without ground intervention. If necessary, autonomously control the stabilization and attitude acquisition of the spacecraft.

(2) Acquire telemetry from all spacecraft systems and store for later playback. Format and transmit a selected subset of telemetry data to the launch vehicle via two 1000 bps serial data links for inclusion in the expendable launch vehicle (ELV) telemetry stream.

(3) Receive synchronizing commands from the launch vehicle and separation system to allow timely actuation of spacecraft functions.

9.2.3 PRELAUNCH REQUIREMENTS

On the pad prior to launch the TT&C system must be fully functional allowing complete checkout of all spacecraft systems other than the transponder. It must allow the upload, download, and checkout of the flight software. It must provide for the control of liquid hydrogen loading by way of a hardwire interface

9.2.4 SYSTEM TEST AND INTEGRATION REQUIREMENTS

During and following the integration of the spacecraft, the TT&C system must provide for the hardwire control of spacecraft systems currently installed and the return of telemetry data from them. This capability shall not be dependent on software or firmware resident in the flight computers.

9.2.5 RELIABILITY

The complete TT&C system shall have a computed reliability of 0.990 for a 6-month flight.

9.3 TT&C System Interfaces

The TT&C system provides the COLD-SAT spacecraft with the ability to communicate with the outside world through a number of external interfaces. It also provides command and data acquisition services to the other spacecraft systems. These two categories of interfaces, internal and external, are detailed in the following sections.

9.3.1 EXTERNAL INTERFACES

There are four TT&C system interfaces with other systems external to the COLD-SAT spacecraft: with TDRSS, the launch vehicle, the launch pad, and with COLD-SAT ground support equipment (GSE).

9.3.1.1 Tracking and Data Relay Satellite System (TDRSS) Interface

The spacecraft requires the following data rates to meet the system-imposed requirements:

Forward link (nominal), bps	1 000
Forward link (contingency), bps	250
Return link (nominal), bps	32 000
Return link (contingency), bps	6 000

The detailed characteristics of the TDRS forward and return links are covered in reference 1. Table 9.1 contains the significant characteristics for COLD-SAT operations.

Use of any of these services requires prediction of spacecraft position and range rate (for Doppler compensation) and prediction of spacecraft transmit frequency. Through the use of a suitable transponder, the TDRS system can provide tracking of the spacecraft as well as the aforementioned communications services. In addition the multiple access (MA) service requires the use of a unique pseudo-random noise coding by the transponder. Details are available in the TDRSS literature.

TDRSS MA service will be used for all normal communication with, and tracking of, the COLD-SAT spacecraft. S-band

single access (SSA) service will only be used during initial separation, deployment and acquisition, and during contingencies.

Figure 9.1 illustrates the flow of data and commands between the Payload Operations Control Center (POCC) and the COLD-SAT spacecraft through the TDRSS. For the return link, data is transmitted from COLD-SAT to the TDRS spacecraft in synchronous orbit. It is then relayed to the TDRSS White Sands Ground Station where it is decoded and sent to the NASCOM network control center at Goddard Space Flight Center. From there it is transmitted via NASCOM to the COLD-SAT POCC. The uplink occurs in reverse order.

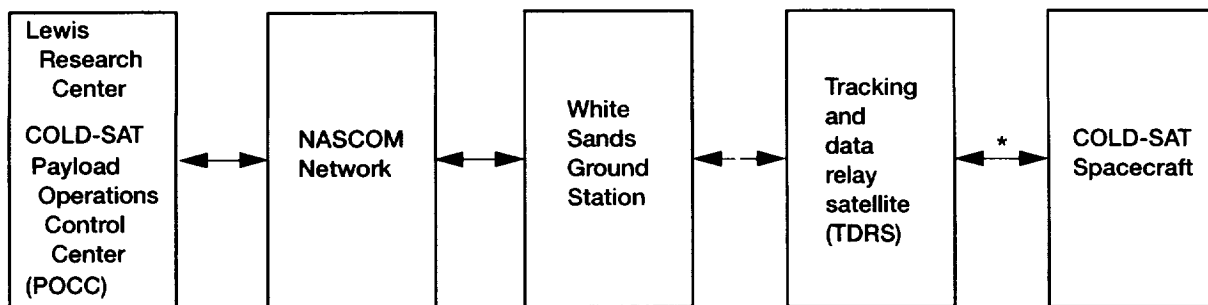
9.3.1.2 Launch Vehicle Interface

This section outlines the TT&C system interfaces with the Atlas I ELV. Details of this interface are discussed in reference 2.

During the powered flight (from T – 0 through spacecraft separation) the COLD-SAT TT&C system will be inhibited from transmitting data to the ground via the TDRSS link. However, telemetry data from the spacecraft during this critical phase is highly desirable. In order to obtain telemetry data during this time, the TT&C system provides two, 1-Kbps serial digital data lines from the command and telemetry unit (CTU) which are input to the Atlas/Centaur launch vehicle data acquisition system. One line shall be the primary, the other backup. These 75-Ω lines carry 1 Kbps of properly formatted COLD-SAT telemetry data which is interleaved into the Atlas/Centaur telemetry downlink. This data will be made available to the COLD-SAT POCC.

TABLE 9.1.—SIGNIFICANT TDRS CHARACTERISTICS FOR COLD-SAT OPERATIONS

Multiple access (MA) forward service	
Effective isotropic radiated power (EIRP), dBW	34
Polarization	Left-hand circular
Axial ratio, dB	1.5
Maximum data rate, Kbps	10
Frequency, MHz	2106.4
S-band single access (SSA) forward service	
EIRP, dBW	43.6
Polarization	Left- or right-hand circular (selectable)
Axial ratio, dB	1.5
Maximum data rate, Kbps	300
Frequency, MHz	2106.4
Multiple access (MA) return service	
Required isotropic receiver power (32 Kbps, 10^{-5} ber), dBW	-171.8
Polarization	Left-hand circular
Axial ratio, dB	1.5
Frequency, MHz	2287.5
S-band single access (SSA) return service	
Required isotropic receiver power (6 Kbps, 10^{-5} ber), dBW	-189.0
Polarization	Right- or left-hand circular (selectable)
Axial ratio, dB	1.5
Frequency, MHz	2287.5



*Return data primarily via multiple access link.

Figure 9.1.—Data and command flow between the Lewis Research Center POCC and the COLD-SAT spacecraft.

Eight sequence control discretes generated by the Atlas I launch vehicle must be sensed by the TT&C system. These discretes consist of contact closures to ground. They are capable of switching a nominal 28 V at 5 A.

Three discrete spacecraft separation breakwires must be sensed by the TT&C system. These are formed by circuits looped through the two COLD-SAT/Centaur rise-off disconnect electrical connectors. Since they are not dead-faced at separation, excitation current must be suitably limited.

The Centaur separation detection system (which relays the successful separation event to the POCC in the ELV telemetry data stream) requires the inclusion in the harnessing of two circuit loops through the rise-off disconnects.

In addition, the following signals are passed through the rise-off disconnects and the Atlas ELV to the T-4 sec umbilical for transmission to the control blockhouse and the COLD-SAT electronic ground support equipment (EGSE):

- (1) Primary COLD-SAT/EGSE data bus MIL 1553—75-Ω pair
- (2) Backup COLD-SAT/EGSE data bus MIL 1553—75-Ω pair
- (3) Primary COLD-SAT/EGSE telemetry stream PCM—75-Ω pair
- (4) Backup COLD-SAT/EGSE telemetry stream PCM—75-Ω pair
- (5) Spacecraft redundant computer switch Signal pair discrete
- (6) Spacecraft redundant computer switch Signal pair discrete

9.3.1.3 Ground Support Equipment (GSE) Interface

The TT&C system has three unique interfaces (I/F) to the GSE. Each of these interfaces is redundant. These three interfaces are

- (1) Flight computer number 1-to-GSE (FC1-GSE I/F)
Flight computer number 2-to-GSE (FC2-GSE I/F)
- (2) Primary command and telemetry unit-to-GSE (PCTU-GSE I/F)

Backup command and telemetry unit-to-GSE (BCTU-GSE I/F)

- (3) Redundancy control unit-to-GSE (primary) (PRCU-GSE I/F)

Redundancy control unit-to-GSE (backup) (BRCU-GSE I/F)

The FC1-GSE and FC2-GSE interfaces are used to load the appropriate ground checkout or flight software into the flight computers. This interface consists of a fully redundant MIL STD 1553 serial data bus. This bus allows data transfer rates of up to 1 mbps. The bus provides duplex (two-way) communication between the FC and the GSE allowing software to be uploaded and read back by means of the same interface. Data which indicates the health and status of the FC, such as checksums, memory reads, and results of internal computations is also provided to the GSE through this interface. This link is also used for control of the spacecraft on the ground.

The FCTU-GSE and BCTU-GSE interfaces consist of a simplex (one-way) serial data link each from the TT&C system to the GSE. Each link can transmit the full telemetry downlink of 32 Kbps to the GSE during ground checkout and prelaunch operations.

The FRCU-GSE and BRCU-GSE interfaces are each a simple, discrete uplink interface which is used to switch control between the primary and backup flight computer under ground command. Only one computer is in control of the spacecraft at a given time. The redundancy control unit (RCU) selects between the two computers.

For integration and test purposes an interface between the spacecraft internal data bus and the GSE is also required.

9.3.2 INTERNAL INTERFACES

The TT&C system must interface with each of the other spacecraft systems in order to collect data from, and to actuate electrical and electromechanical loads for, each system. The TT&C system must actuate many different types of loads and service a wide variety of measurements.

The TT&C must provide 8-bit analog-to-digital conversion capability for analog input voltages in the ranges of 0 to 5.1 V

dc and signal conditioning for a variety of sensors. It is required to provide sample rates of up to 20 samples/sec (SPS). For any measurement requiring resolution greater than 8 bits and sample rates greater than 20 SPS, the spacecraft system to which the measurement belongs is responsible for the signal conditioning and multiplexing of the measurement. A description of each system interface is included in the following paragraphs. A summary of the measurement servicing requirements for the TT&C system is listed in Tables 9.2 and 9.3. A summary of the

load actuation requirements for the TT&C system is listed in Tables 9.4 and 9.5.

9.3.2.1 TT&C-to-Spacecraft Structural System Interfaces

A description of the TT&C system interfaces with the structural system is included in the following sections. A functional block diagram of these interfaces is shown in Figure 9.2.

TABLE 9.2.—SPACECRAFT SYSTEM MEASUREMENT REQUIREMENTS
[COLD-SAT TT&C system measurement channel requirements.]

Measurement description	Range/unit	Quantity	Required sample rate, SPS
Box temperatures	-77 to +200 °F	50	1/5
Airframe temperatures	-240 to +200 °F	75	↓
Propulsion system temperatures	0 to +200 °F	24	
Propulsion system temperatures	0 to +2000 °F	20	
Box voltages	0 to 40 V	40	1
Box currents	0 to 5 A	40	1
Bus voltages	0 to 40 V	4	5
Bus currents	0 to 20 A	4	5
Spacecraft discretes	On/off (TOE)	8	1/5
Propulsion system pressures	0 to 200 psi	4	1
Propulsion system pressures	0 to 2000 psi	3	1
Pyro discretes	On/off (TOE)	14	1/5
Hydrazine valve positions	On/off	20	1

TABLE 9.3.—EXPERIMENT SYSTEM MEASUREMENT REQUIREMENTS
[COLD-SAT TT&C system measurement channel requirements.]

Measurement description	Range/unit	Quantity	Sample rate, SPS
Liquid/vapor detectors	Wet/dry	116	1/5
Tank temperatures	29 to 46	139	1/5
Tank temperatures	36 to 110	162	1/5
Valve positions	On/off (TOE)	57	1
High accuracy data	Serial digital	3	---
Electronics box temperatures	-77 to 200 °F	5	1/5
Electronics box currents	0 to 5 A	5	1
System pressures	5 to 5 Kpsia	33	1

TABLE 9.4.—LOAD ACTUATION REQUIREMENTS—SPACECRAFT SYSTEMS

Load type	Maximum load, A	Time duration, msec	Quantity
Hydrazine thrusters	0.2	Continuous	20
Hydrazine valves	3	250	11
Heater banks	5	Continuous	8
Pryotechnic firing circuit	2	100	14
Load shed relay reset	1	250	5
Electronic box on/off	10	Continuous	40
Antenna network select	3	250	1

TABLE 9.5.—LOAD ACTUATION REQUIREMENTS—EXPERIMENT SYSTEM

Load type	Maximum load, A	Time duration, msec	Quantity
Liquid hydrogen valve	5	250	56
Heaters	4	Continuous	11
Gas valve	2	250	12
Electronics unit on/off	5	Continuous	5

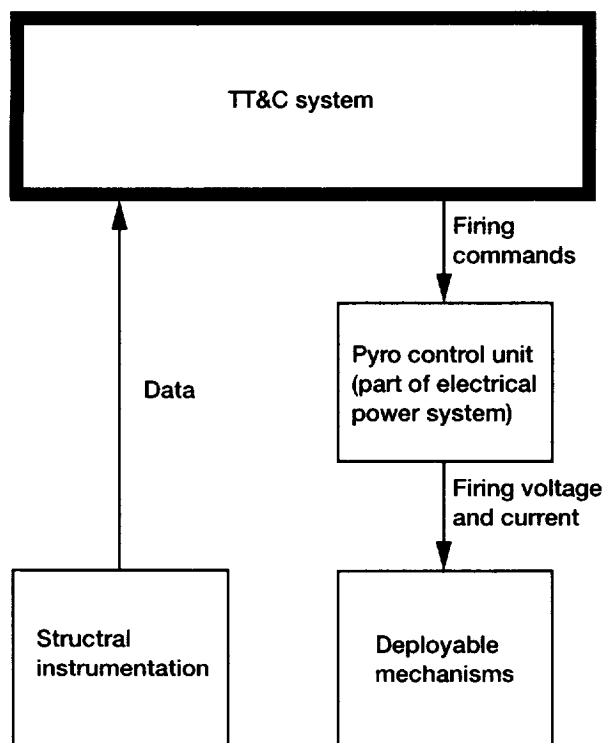


Figure 9.2.—Telemetry, tracking, and command (TT&C) system-to-structural system interface.

9.3.2.1.1 Data interface.—The TT&C system services data which is obtained from structural system instrumentation. This data includes structural member temperature and the status of mechanisms such as deployable booms.

9.3.2.1.2 Control interface.—While the TT&C system does not have a direct actuation interface to the spacecraft deployable mechanisms, the commands for deployment of all mechanisms originate in the active FC. Under command of the FC, the TT&C system actuates relays in the pyro control unit, which is part of the COLD-SAT electrical system. The pyro control unit provides the required voltage and current to actuate the various deployment mechanisms on the spacecraft.

9.3.2.2 TT&C-to-Attitude Control System Interface

A description of the TT&C system interfaces to the attitude control system is included in the following sections. A functional block diagram of these interfaces is shown in Figure 9.3. As can be seen from the figure, the attitude control system interface electronics (ACSIE) provides a data and control interface between the spacecraft gimbal systems, the various attitude sensors, and the TT&C system.

9.3.2.2.1 Data interface.—The TT&C system services data which is obtained from the ACSIE unit. The TT&C system communicates with this unit via a multiplexed serial command/response data bus. The ACSIE conditions and multiplexes data from two Sun sensors, two horizon sensors, two magnetom-

eters, the inertial reference unit, the thruster-gimbal electronics, and the high-gain antenna gimbal electronics. Gimbal position data are included in this stream. These data are retrieved by the TT&C system via the data bus.

9.3.2.2.2 Control interface.—Software resident in the TT&C system controls the spacecraft attitude using the data mentioned in the previous section as input parameters. The flight computers continually process this data to determine if attitude corrections and/or antenna gimbaling are needed.

The TT&C system performs attitude corrections by controlling the firing of propulsion system hydrazine thrusters. This control is performed by directly actuating the thruster hydrazine valves and catalyst bed heaters as required. Gimbaling of both the high-gain antenna and the gimballed thruster is also performed under TT&C system command. Antenna and thruster-gimbal commands are sent to the ACSIE through the multiplexed serial command/response data bus mentioned in the previous paragraph. The thrusters are directly controlled by relays in the TT&C system.

9.3.2.3 TT&C-to-Propulsion System Interfaces

A description of the TT&C system interfaces to the propulsion system is included in the following sections. A functional block diagram of these interfaces is shown in figure 9.4.

9.3.2.3.1 Data interface.—The TT&C system services data which is obtained from propulsion system instrumentation. These data include hydrazine tank and supply line temperatures and pressures, thruster catalyst bed temperatures, and thruster and system valve position indicators.

9.3.2.3.2 Control interface.—Attitude control software in the TT&C system controls the firing of the propulsion system thrusters based on information from the attitude control system (ACS) sensors and the experiment control software resident in the FC's. The TT&C system also controls both the operation of the propulsion system control and isolation valves which charge the hydrazine lines and the actuation of the solenoid valves that isolate each propulsion system thruster cluster. In each case the TT&C system provides the actuation power required to operate the valves at the proper time in the mission and/or experiment sequence.

9.3.2.4 TT&C-to-Electrical Power System (EPS) Interfaces

A description of the TT&C system interfaces to the electrical power system (EPS) is included in this section. A functional block diagram of these interfaces is shown in figure 9.5.

9.3.2.4.1 Power interface.—The EPS generates and provides electrical power for all of the electrical and electromechanical devices on the spacecraft. With the exception of the antennas, all of the TT&C system components require 28-Vdc electrical power from the EPS. The antennas themselves require no electrical power but the high-gain antenna gimbals require 28 Vdc.

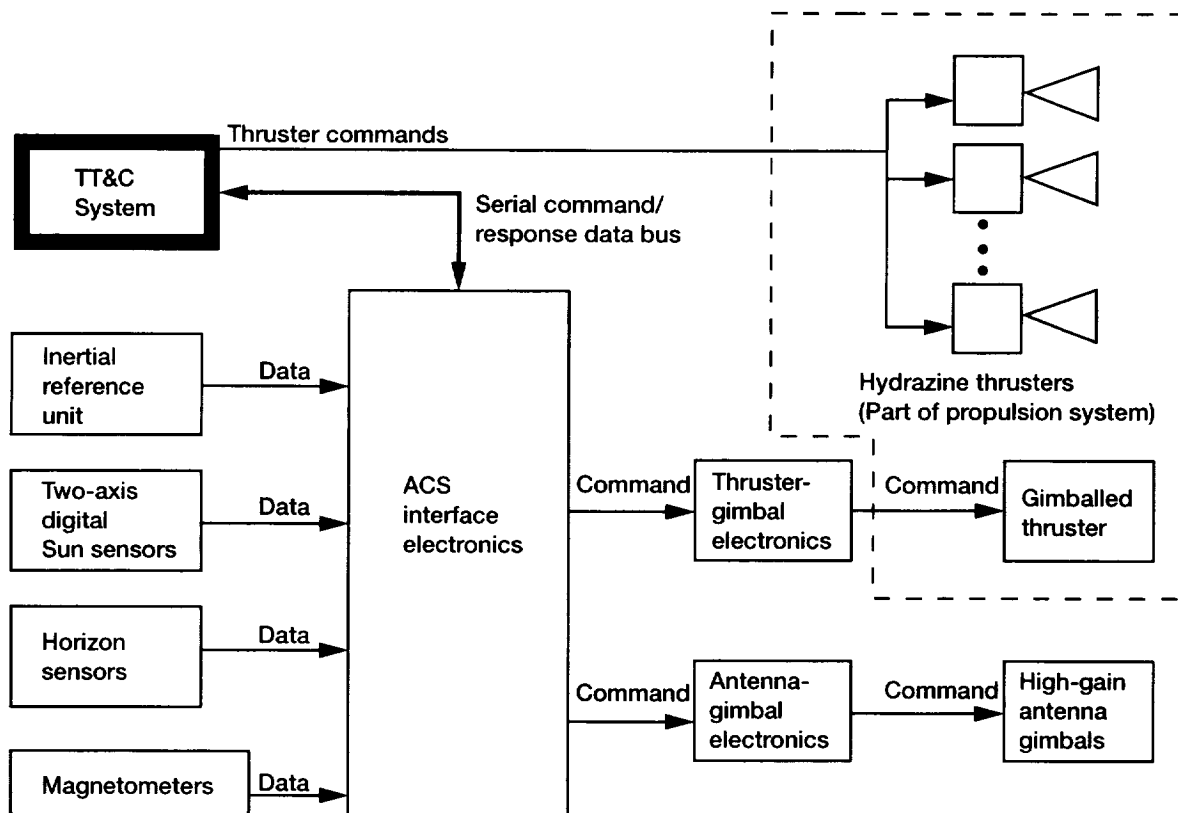


Figure 9.3.—Telemetry, tracking, and command (TT&C) system-to-attitude control system (ACS) interface.

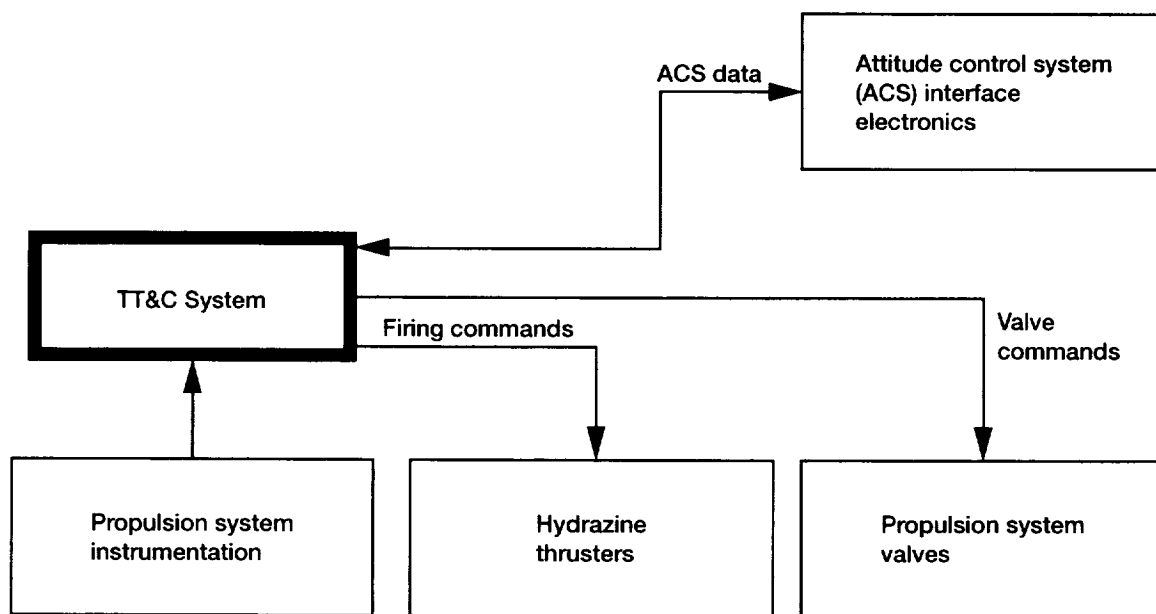


Figure 9.4.—Telemetry, tracking, and command (TT&C) system-to-propulsion system interface functional diagram.

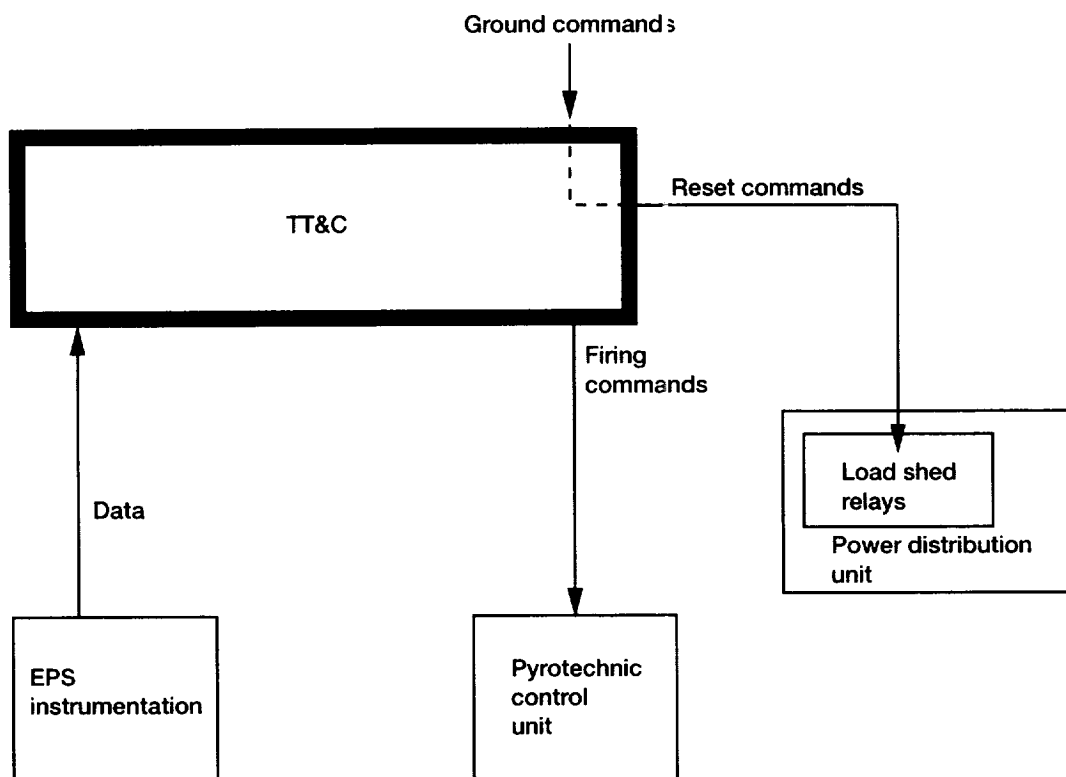


Figure 9.5.—Telemetry, tracking, and command (TT&C) system-to-electrical power system (EPS) interface.

The TT&C system actuates electrical and electromechanical loads for all spacecraft systems. The power required to actuate each load is provided to the TT&C system by the EPS and is routed and switched to the loads by the TT&C.

9.3.2.4.2 Data interface.—The TT&C system services data from each EPS unit, the solar arrays, batteries, and each power bus. The data consist of analog voltage and current measurements which are used for monitoring the health and status of the spacecraft by the COLD-SAT POCC team. They are also used for the control of the total spacecraft power load by software resident in the flight computers.

9.3.2.4.3 Control interface.—The TT&C system controls the firing of pyrotechnic devices by providing arm and fire commands to the pyro control unit which is part of the EPS system. The TT&C system also controls the resetting of the load shed relays which are located in the power distribution unit. Load shed relays are reset only under command from the COLD-SAT POCC.

9.3.2.5 TT&C-to-Thermal Control System (TCS) Interfaces

A description of the TT&C system interfaces to the thermal control system (TCS) is included in this section. A functional block diagram of these interfaces is shown in figure 9.6.

9.3.2.5.1 Data interface.—The TT&C system gathers data from over 160 sensors which measure the temperatures of each

electronic box on the spacecraft as well as the temperature of the spacecraft structure and propulsion system at selected locations.

9.3.2.5.2 Control interface.—TCS heater banks are switched on shortly after spacecraft separation by the TT&C system. After that, the heaters are thermostatically controlled.

9.3.2.6 TT&C-to-Experiment System Interfaces

The interfaces to the experiment system account for the largest number of all the TT&C system's data and control interfaces. A description of these interfaces is included in the following sections. A functional block diagram is shown in figure 9.7.

9.3.2.6.1 Data interface.—The TT&C system services over 500 measurements, which are part of the experiment system. This includes data generated by liquid hydrogen temperature and pressure sensors, hydrogen liquid/vapor sensors, accelerometers, flow meters, and valve position indicators. Table 9.3 lists the measurement requirements for the experiment system.

In table 9.3 there is a measurement description entitled "High Accuracy Data." This description refers to three serial digital channels which may each transmit up to 2 Kbps to the TT&C system. These channels carry data from measurement sensors which require resolution greater than the TT&C system's 8-bit ADC capability and/or a sampling rate greater than 20 SPS.

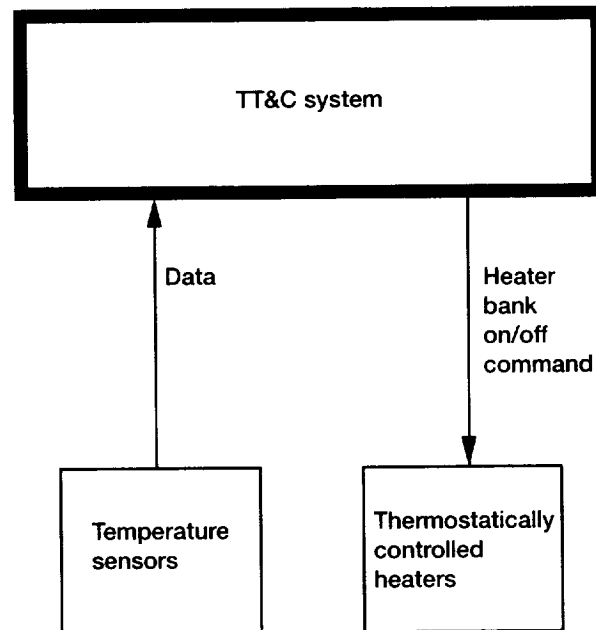


Figure 9.6.—Telemetry, tracking, and command (TT&C) system-to-thermal control system interface.

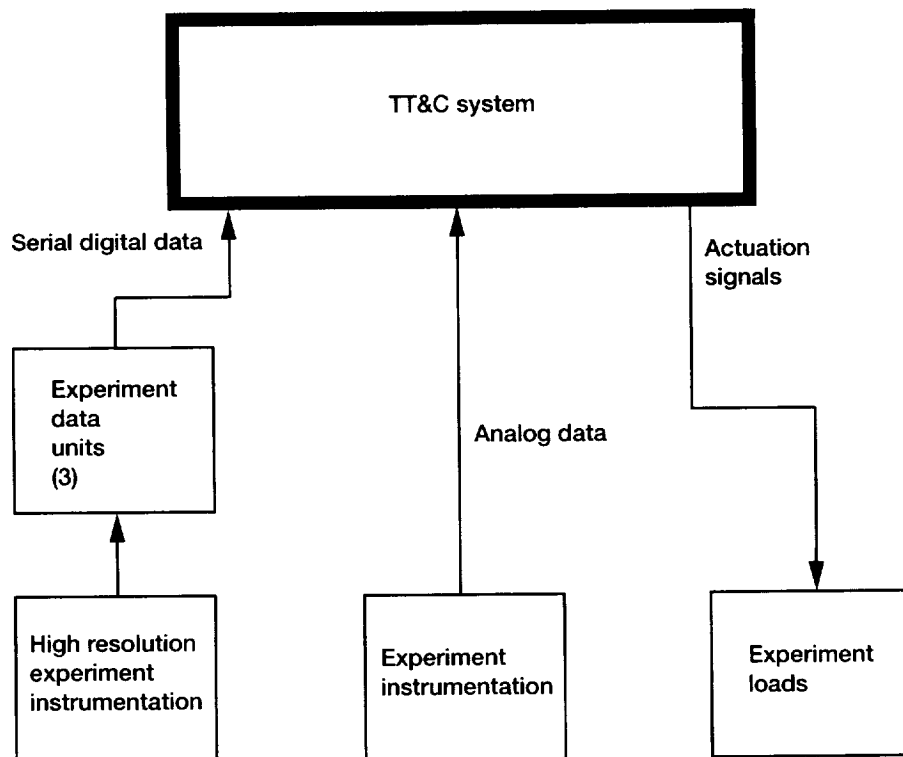


Figure 9.7.—Telemetry, tracking, and command (TT&C) system-to-experiment system interface.

9.3.2.6.2 Control interface.—The TT&C system controls all experiment operations by actuating the valves, pumps, and heaters which are part of the experiment system. The TT&C system controls experiment operations by using the data mentioned in the preceding section as input parameters to the flight software. The flight computers continually process these data in conjunction with the experiment timeline software to determine if a load, such as a valve, needs to be actuated. The load actuation requirements for the experiment system are listed in table 9.5.

9.4 TT&C System Design and Configuration

The TT&C System is designed to satisfy the data and control requirements detailed in section 9.2 across the interfaces described in section 9.3 while using available, flight-qualified hardware to the maximum extent possible. The use of custom-designed electronics units is kept to a minimum. Of the 13 electronics units that comprise the TT&C system (not including the antennas) only three units are custom-designed specifically for COLD-SAT. A detailed description of each unit within the TT&C system is provided in section 9.6.

An overall diagram of the TT&C system is shown in figure 9.8. The system is divided into four functional areas: external communications, data storage, computing, and internal communications. The antennas, radiofrequency (RF) processing unit, and the two transponders provide bidirectional communications with the TDRSS and Spaceflight Tracking and Data Network (STDN) systems. The solid-state recorders store data until it can be transmitted to the ground. The flight computers and associated redundancy control unit provide a central computing facility for all spacecraft systems. The remainder of the system is organized around a bidirectional data bus which provides internal communications for the spacecraft. The bus is controlled by the CTU which distributes commands and acquires data from all spacecraft systems either directly or through the use of other equipment interfaced to the bus.

In figure 9.8 boxes which are shadowed represent units which are in some way redundant. In the case of the transponders, solid-state recorders and flight computers, redundancy is implemented using two identical electronic units. In the case of the CTU and the remote command and telemetry units (RCTU'S 1 and 2), each unit is a single electronics box which is fully redundant internally. A detailed description of the TT&C system's redundancy implementation can be found in section 9.5.5. Boxes represented with dashed lines in figure 9.8 are not part of the TT&C system but are shown to provide a better understanding of how the system functions.

A number of bus-oriented spacecraft data handling systems are becoming available. For purposes of the COLD-SAT conceptual design, the T²C² (Telemetry, Timing, Command and Control) system manufactured by Gulton Industries Inc., Data

System Division, was used. Specific commercial units used in the COLD-SAT design are the CTU and RCTU'S 1 and 2. The two sequencers and the ACS interface electronics are designs which are unique to COLD-SAT. These units are modular in design and standard multiplexed busses are used for interconnection between units. Use of multiplexed data busses simplifies system interfacing and integration while the units' modular design provides an excellent level of adaptability for system changes if required. A more detailed description of this equipment is included in section 9.6.

9.5 TT&C System Operation

The operational characteristics of the TT&C system are best described in terms of the four distinct operations performed by the system. These four operations directly correspond to the four major requirements of the system which are detailed in section 9.2. The four distinct operations are

- (1) Telemetry downlink
- (2) Command uplink
- (3) Autonomous spacecraft control
- (4) Spacecraft tracking

Each of these functions will be described in the following sections (sections 9.5.1 to 9.5.4). Figures 9.9 to 9.12 are used to illustrate the functional flow for each of these functions. Figures 9.9 to 9.12 do not attempt to illustrate the levels of redundancy which exist in the TT&C system. A detailed description of the TT&C system's redundancy implementation and the effects of redundancy on the system's operation can be found in section 9.5.5.

9.5.1 TELEMETRY DOWNLINK OPERATION

The telemetry downlink operation involves the gathering, possible signal conditioning, formatting, storage, and transmission of data which is generated onboard the COLD-SAT spacecraft. Figure 9.9 illustrates the functional flow of the telemetry downlink operation, from sensor excitation through transmission of the digital data stream.

As shown in figure 9.9, telemetry data originates from transducers located throughout the spacecraft or from other data sources such as the flight computers or experiment data units. The CTU controls the acquisition of data via commands sent over the spacecraft's internal data bus. It causes data to be gathered to fit the requirements of telemetry formats stored within the RCTU's or similar circuit modules located within the CTU gather much of the data and provide the required signal conditioning and analog-to-digital conversion. Other data are obtained in digital form from external sources which are interfaced to the RCTU's. The ACS interface electronics are

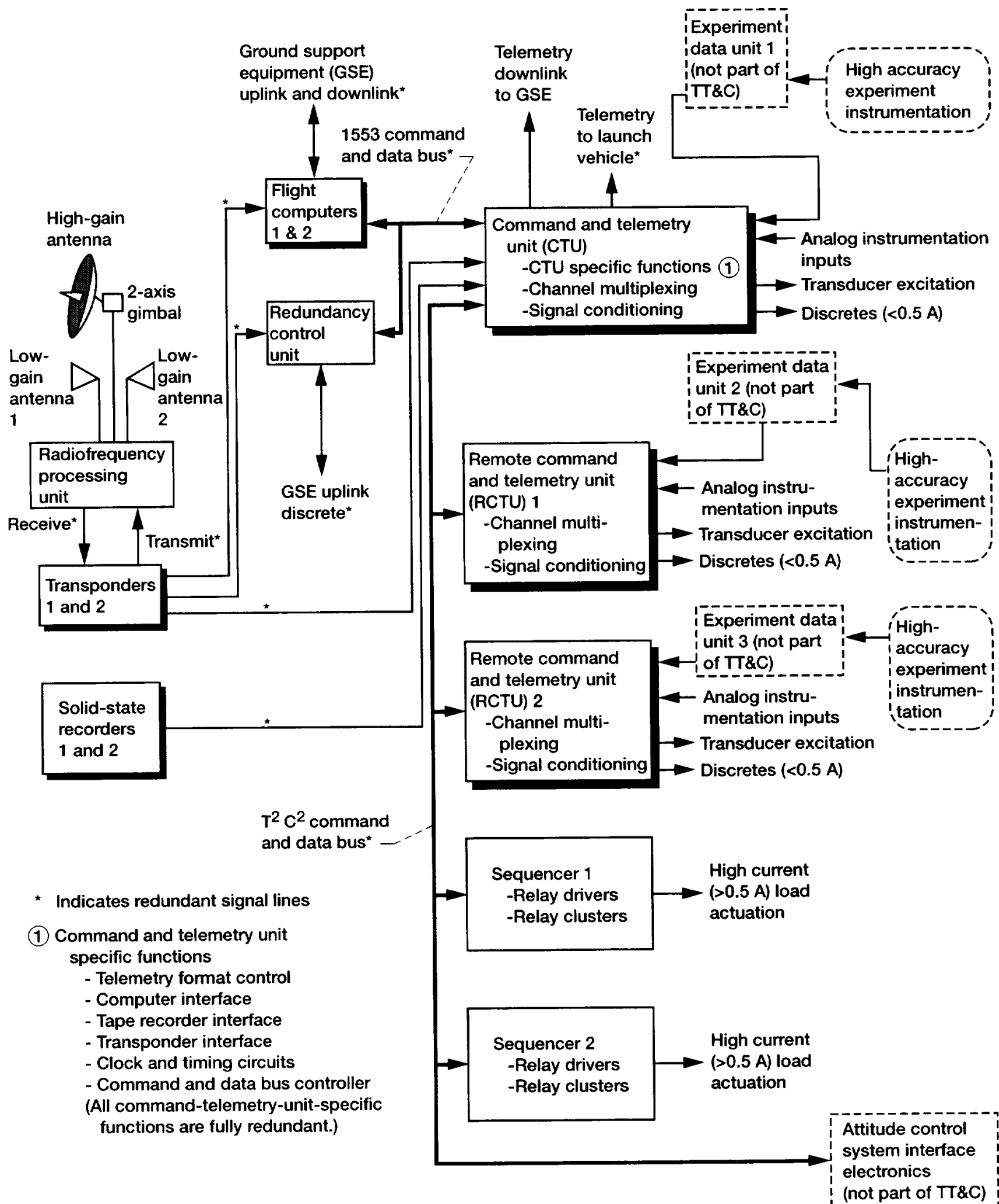


Figure 9.8.—COLD-SAT telemetry, tracking, and command (TT&C) system.

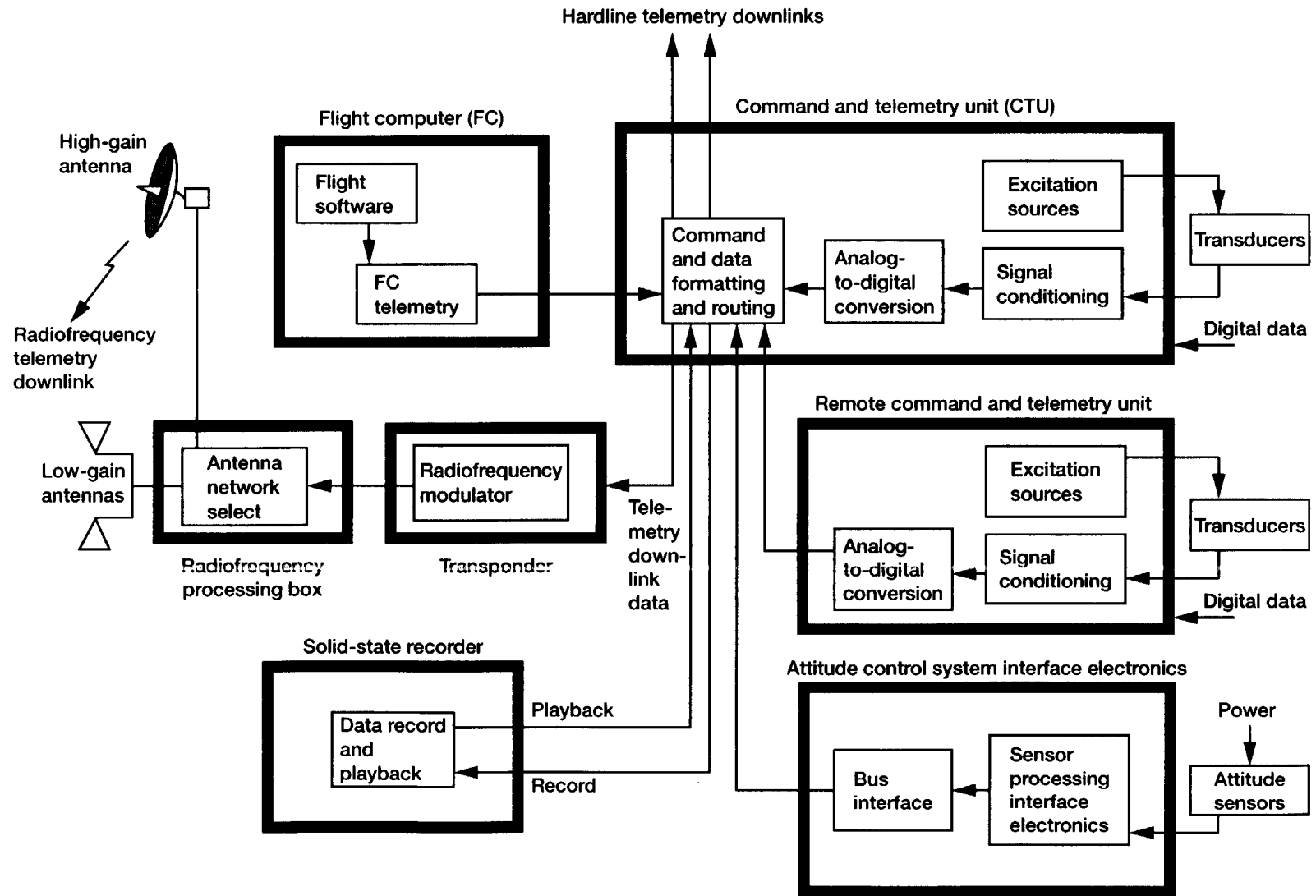


Figure 9.9.—Telemetry downlink functional flow.

interfaced directly to the internal data bus and receive commands and return data in a manner similar to the RCTU's. The flight computers are interfaced to the CTU through a separate data bus. All data are routed to the CTU where it is compiled into a telemetry format and then either stored in the solid-state recorder (SSR) or downlinked via RF or hardwire, depending on the mission phase.

Data from all phases of the mission, from prelaunch checkout through final on-orbit operations are required to evaluate spacecraft health and status and experiment results. The TT&C system accomplishes this by transmitting data via either hardwire interfaces directly from the CTU or via a RF link through the transponder, RF processing box, and the antenna(s).

The hardwire interfaces are used during both prelaunch checkout and the powered flight phases of the mission. The entire telemetry stream can be transmitted via hardwire to the GSE during prelaunch operations. During the powered flight phase, the CTU outputs two 1-Kbps serial data streams to the launch vehicle through a second hardware interface. This data stream is interleaved into the launch vehicle telemetry downlink and routed to the COLD-SAT POCC.

Once the COLD-SAT spacecraft is in orbit, the TT&C system transmits data via a RF link through the TDRSS to the COLD-SAT POCC using the TDRSS MA system. For nominal operations COLD-SAT will transmit data at a rate of 32 Kbps through its steerable high-gain antenna (HGA). The HGA is located at the end of a 55-in. boom which will be deployed shortly after separation from the launch vehicle. The antenna is steered by a two-axis gimbal on which it is mounted and tracks the TDRS it is scheduled to use.

COLD-SAT use of TDRSS is limited to 13 min/orbit and may not be available every orbit. According to prior schedule, contact is first established with the spacecraft using the TDRSS forward link and then, on command from the ground, the data stored in the spacecraft recorder are played back along with the current, real-time spacecraft data. Table 9.6 summarizes the parameters that determine the COLD-SAT data storage and playback requirements.

During contingency operations data are transmitted at a rate of 6 Kbps through two hemispherical low-gain antennas (LGA's) which are located at each end of the spacecraft structure. COLD-SAT may also use the STDN system during emergencies

9.5.2 UPLINK OPERATION

The uplink operation involves the receiving, decoding, and implementation of command messages sent from the POCC

to the COLD-SAT spacecraft. Figure 9.10 illustrates the functional flow of the command uplink operation. Uplink commands can be directed to either the FC, redundancy control unit (RCU), or the command and telemetry unit (CTU) depending on the nature of the command being sent and the state of the spacecraft at the time of the command uplink.

Command messages are sent to the FC to modify or reload flight software resident in the unit and to initiate or prematurely terminate an experiment run. Once a command has been uploaded to the FC, the execution of that command is performed in the same fashion as those generated by the FC software.

Commands are uplinked to the RCU to select which of the two FC's will control the spacecraft. Only one FC is enabled to execute control and issue control commands at a given time. A more detailed discussion of how the FC's and the RCU operate is included in section 9.5.3.

The TT&C system has been designed to operate in several extreme worst-case scenarios. One of those scenarios assumes total failure (hardware or software) of both flight computers. In order to accommodate this worst-case scenario, the capability exists in the TT&C system to bypass the flight computers and control discrete loads directly via command uplink. This is accomplished using a direct link through the transponder to the CTU.

Prior to T - 0, all commands are uplinked through hardwire links to the FC and RCU. No commands can be sent to the spacecraft during launch and ascent. After separation from the ELV, all uplink commands are transmitted by a RF link through the TDRSS. The RF signal is received by the HGA and routed through the RF processing box to the command receiver portion of the transponder. During contingency operations, the uplink is received through the LGA's at a reduced data rate. The command receiver in the transponder sends the uplink message to each of these units and the command is recognized by the appropriate unit.

9.5.3 AUTONOMOUS SPACECRAFT CONTROL OPERATION

During normal flight operations, the active FC controls almost all functions onboard the spacecraft. Figure 9.11 illustrates the functional flow of the data and commands which make up this closed-loop control system. Measurements, such as tank pressures, are collected from transducers located throughout the COLD-SAT spacecraft. These data are used as control inputs to the software resident in the FC. It should be noted that less than 20 percent of the transducers on the spacecraft are used

TABLE 9.6.—DATA PARAMETERS THAT DETERMINE STORAGE AND PLAYBACK REQUIREMENTS

Spacecraft data generation rate, bps	3900
Orbit period, min	100
Amount of TDRSS coverage, min/orbit	13 (conservative assumption)
Maximum allowable downlink rate, Kbps	50 (TDRSS S-band MA)

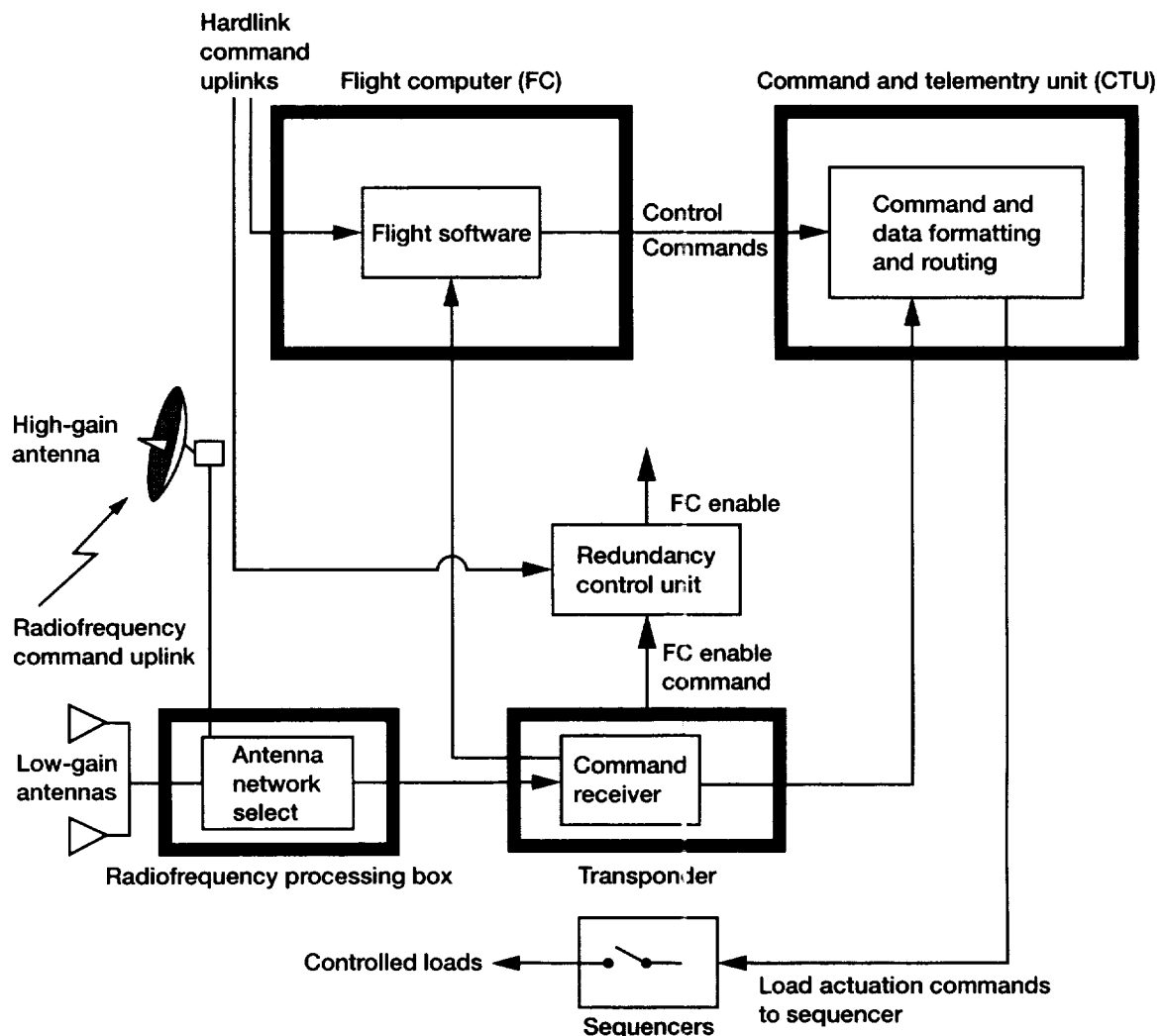


Figure 9.10.—Command uplink functional flow.

as control inputs to the FC. The majority of the sensors are used for telemetry data only. Any measurement which is used as a control input to the FC is serviced by both RCTU's and the CTU or by the ACSIE so that failure of any one of these units will not interfere with the control of the spacecraft. The FC software determines if a load, such as a valve, needs to be actuated based on the measurement information collected from the transducers. If the FC determines that a load needs to be actuated, a control command is generated.

The control command is sent from the FC to the CTU where it is formatted into a load actuation command and transmitted to the proper sequencer. The sequencer decodes the command and energizes the appropriate relay coils to close or open the electromechanical relays which in turn energize or deenergize a load.

The FC selected for this conceptual design is capable of processing data at rates up to 50 Hz. The most demanding functions in terms of the COLD-SAT control system's response rate are the attitude control functions, which require

processing data at a 10-Hz rate. Requirements for end-to-end response times were not levied on the TT&C system. The system will be designed to actuate a load within 500 msec of the control input from a transducer for any control function.

9.5.4 SPACECRAFT TRACKING OPERATION

The COLD-SAT TT&C system provides spacecraft range and range-rate information to the POCC by using the turn-around ranging capability built into the transponder. The turn-around ranging function in the transponder is available when the receiver is locked to a TDRSS forward link signal (uplink). Ranging is obtained by synchronizing the "all 1's" state in the transponder-generated return link pseudo-random noise (PN) code with the "all 1's" state in the received forward link PN code.

This operation is performed at the beginning of each scheduled uplink from the ground. The range and range-rate data are generated by the TDRSS White Sands Ground Terminal

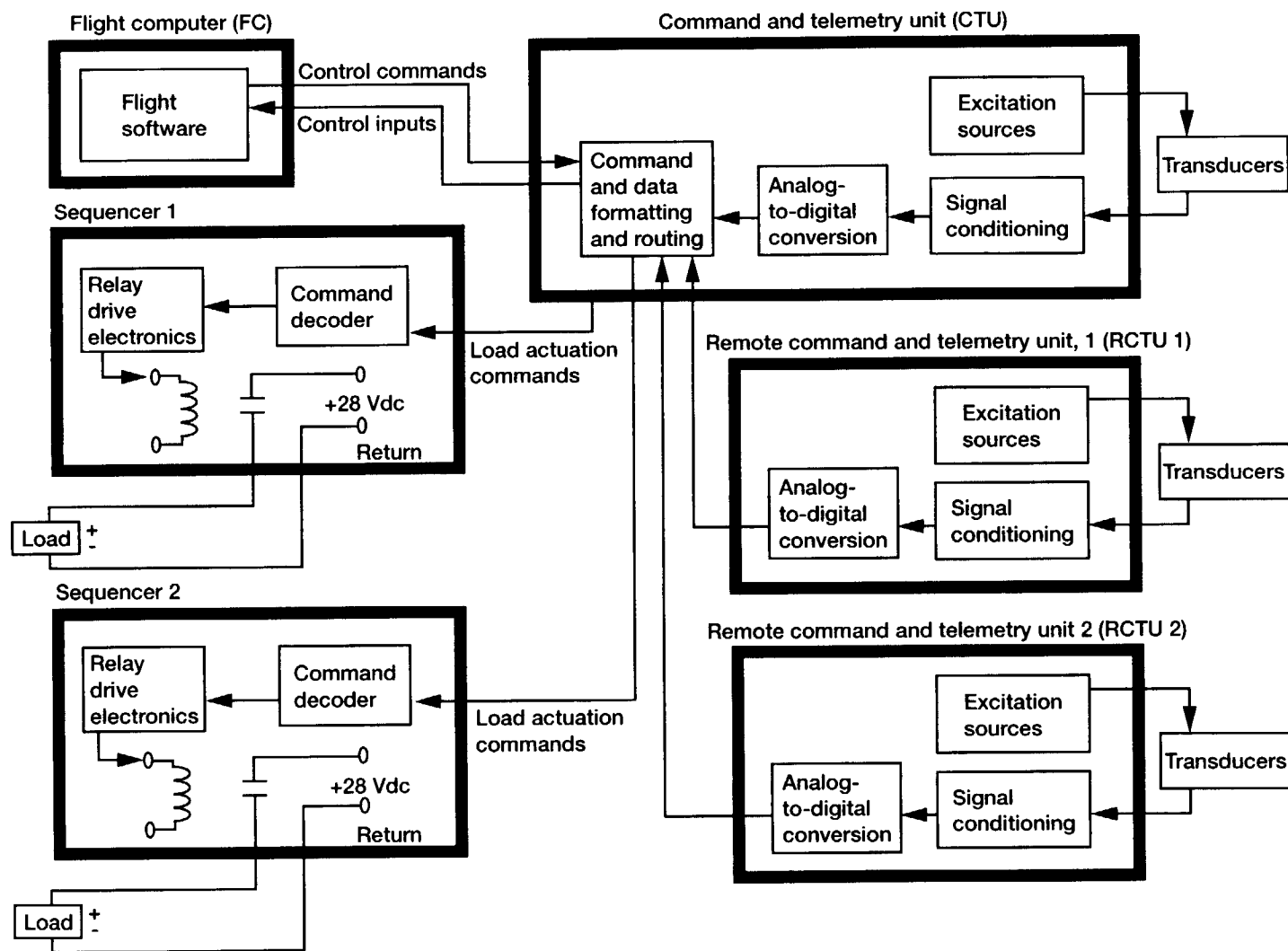


Figure 9.11.—Autonomous spacecraft control functional flow.

(WSGT) and passed on to the COLD-SAT POCC over NASCOM links between the two facilities. The entire tracking operation occurs independent of, and transparent to, all other spacecraft operations.

9.5.5 REDUNDANCY IMPLEMENTATION

The TT&C system uses redundancy to increase overall reliability and to specifically eliminate, wherever possible, any single-point failures in the system. The system is designed to be single-failure tolerant to all credible failures. The philosophy of the system design is to double up on the TT&C electronic units so that if a component or an entire unit fails, a backup unit will take the failed unit's place and the system will continue performing the required functions with no or only minimal degradation to system performance.

The CTU, the RCTU's, and sequencers 1 and 2 are units which are internally redundant. The CTU has two sides (A and B) which electrically function independently of each other. Only the unit's structure is shared between the two halves. The RCTU's are likewise internally redundant.

Sequencers 1 and 2 contain redundant electronics to decode commands and drive the electromechanical relays. The relays within each sequencer are configured so that the failure of a single relay within a given load actuation cluster will have a minimum impact on the operation of the loads in that cluster. Figure 9.12 illustrates one way which the relays can be configured to form a single failure-tolerant load actuation circuit.

System redundancy is implemented with the FC software. It will switch in a backup unit (in the case of the transponder and

SSR) or the backup side (in the case of the CTU, RCTU's, and sequencer 1 and 2 electronics) when a failure in the unit is detected. The FC controls all the switching between primary and back-up units (or sides). Information on the status of each unit is provided to the FC to allow the flight software to make the proper decision on when to switch out the primary and switch in the back-up.

There are two FC's. Both FC's receive and process control data in real time. Only one FC is in control at a given time, however. The redundancy control unit (RCU) enables one computer or the other based on checksum and execution status information which each FC provides to it.

If the primary flight computer never experiences a failure during the mission, the backup computer will never be switched in. If the primary computer does experience some type of failure, then it will either fail to generate its correct checksum or fail to execute a function which is required to write that checksum to the RCU. Uncorrected memory read errors will also cause the RCU to switch computers. Should a failure occur, the RCU will disable the communication link between the primary FC and the CTU and enable the backup FC-to-CTU communication link. Since the backup FC processes the same data as the primary FC throughout the mission and is synchronized with the other computer, it is a true "hot" spare capable of executing control in a continuous manner with no major interruption to spacecraft operations. The switch in computers will be signaled to the flight computers which will verify system status. Once the RCU enables the backup FC, the primary FC can only be re-enabled by an uplink command from the POCC to the RCU.

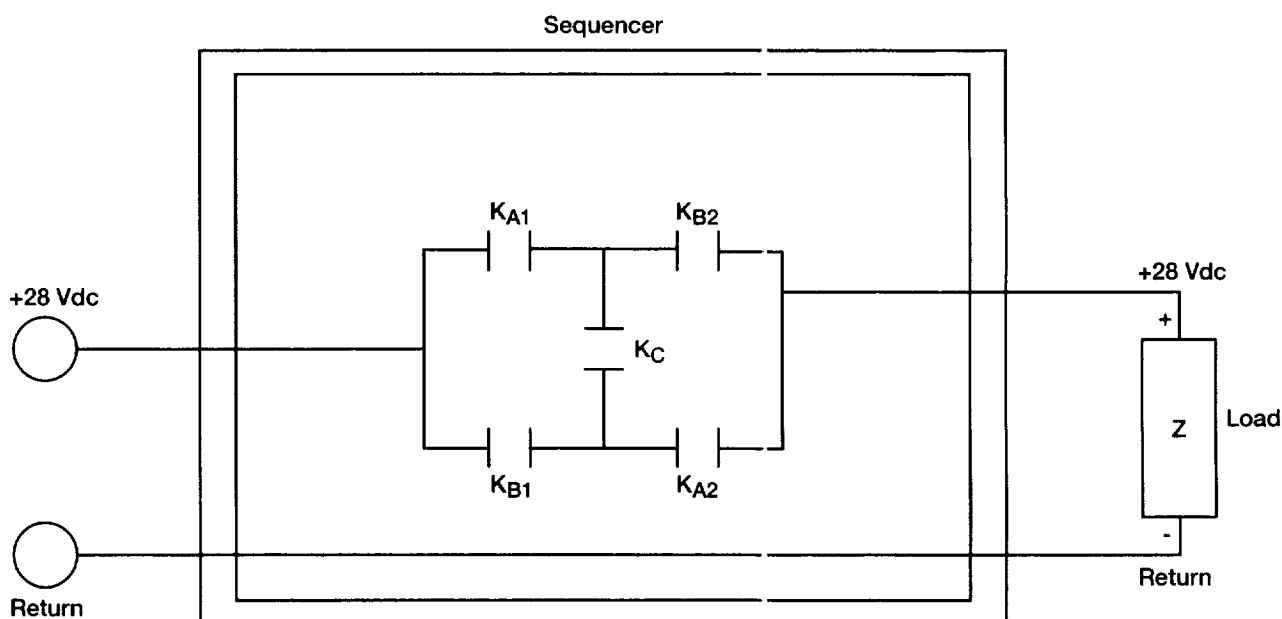


Figure 9.12.—Single-failure-tolerant load actuation circuit (relays K_A and K_B are double-pole, double-throw latching relays).

9.6 Components

This section provides a description of each of the components used for the conceptual design of the TT&C system. Table 9.7 summarizes key information pertaining to the system components. In many cases similar equipment is available from sources other than those indicated in the table.

9.6.1 FLIGHT COMPUTER

The FC selected for the TT&C system is based on the design of another unit which is manufactured by Honeywell. The computer is a derivative of the inertial navigation unit (INU) which is used for both the Atlas and Titan expendable launch vehicle programs. Significant features of the COLD-SAT FC include the following:

- (1) MIL STD 1750A instruction set
- (2) 25-MHz clock, 1-MIPS throughput
- (3) 1-million-word addressability
- (4) 22-bit words (6-bit EDAC)
- (5) Built in test capability
- (6) MIL STD 1553 I/O

The COLD-SAT FC contains seven unique card types. Six of these cards already exist and are used in the INU. A new card will need to be designed for the FC-to-transponder interface.

9.6.2 TRANSPONDER

The second-generation NASA standard transponder was selected for use on the COLD-SAT spacecraft. The unit is built by Motorola and is fully compatible with both the TDRSS and

the Space Flight Tracking and Data Network (STDN). This transponder is standard in design and will require no modifications for this application. The transponder is available with either a 2.5- or 5.0-W output power. The 5.0-W version is used in this design.

9.6.3 REMOTE COMMAND TELEMETRY UNIT (RCTU) AND COMMAND AND TELEMETRY UNIT (CTU)

The RCTU and the CTU are part of the Gulton Industries, Inc. T²C² system. Each unit is expandable and the size, weight, and power consumption of each RCTU and the CTU is dependent upon the number of measurements which each unit must service. Each unit services analog, digital, and bilevel inputs and provides 8-bit analog-to-digital conversion for analog inputs. The units were configured so that the number of measurements which need to be serviced by each of the two RCTU's and the CTU were split evenly between the three units.

The Gulton T²C² system has been qualified for spaceflight but has not been flown as of the time of this writing. There are 19 unique circuit-card types required for the COLD-SAT application. Of these 19 cards, 15 are fully developed.

9.6.4 SOLID-STATE RECORDER

The solid-state recorder (SSR) is built by Fairchild Space Company and is designed to replace the NASA standard tape recorder. The SSR is smaller, lighter, and, since it has no moving parts, more reliable than the tape recorder. The SSR is expandable up to 512 Mbytes of RAM. Both SSR's used in the COLD-SAT design employ the full 512-Mbyte capability.

TABLE 9.7.—COLD-SAT TT&C SYSTEM COMPONENT SUMMARY

Item	Manufacturer	Dimensions, in.	Weight, lbs	Power, W
Flight computer 1	Honeywell	12 by 11 by 9	35	40
Flight computer 2	Honeywell	12 by 11 by 9	35	40
Transponder 1	Motorola	14 by 6 by 5	16	44
Transponder 2	Motorola	14 by 6 by 5	16	18
RCTU 1	Gulton	5 by 9 by 12	11	17
RCTU 2	Gulton	5 by 9 by 12	11	17
CTU 1	Gulton	5 by 9 by 19	17	25
SSR 1	Fairchild	8 by 11 by 7	28	8
SSR 2	Fairchild	8 by 11 by 7	28	8
Sequencer 1	Custom design	12 by 12 by 9	51	15
Sequencer 2	Custom design	12 by 12 by 9	51	15
RF processing box	Custom design	10 by 8 by 4	10	10
HGA	Tecom	27.5 Diam by 16 long	16	0
LGA 1	Tecom	7 Diam by 5 long	3	0
LGA 2	Tecom	7 Diam by 5 long	3	0
Antenna deployment arm	Schaeffer Magnetics	55	8	0
Antenna 2-axis gimbal	Schaeffer Magnetics	5 by 6 by 5	10	12
Motor drive electronics unit	Schaeffer Magnetics	11 by 8 by 6	11	18
Redundancy control unit	Custom design	6 by 6 by 3	4	8
Total estimated system weight			364	
Total estimated system power consumption				295

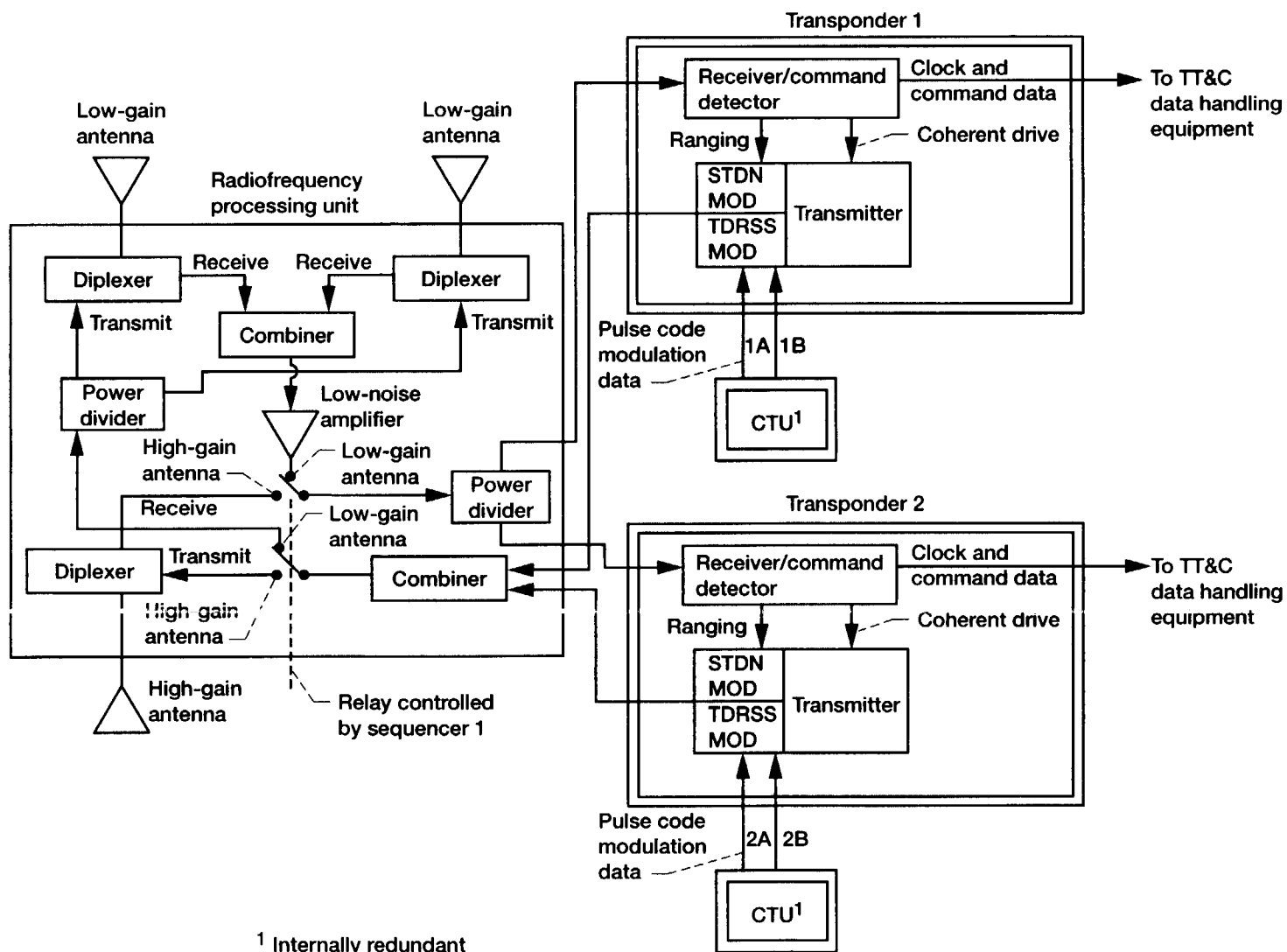


Figure 9.13.—COLD-SAT telemetry, tracking, and command (TT&C) system—radiofrequency portion.

9.6.5 SEQUENCERS

The sequencers perform load actuation by switching electrical power to and from electrical units or electromechanical devices onboard the COLD-SAT spacecraft. Power is switched to the loads by means of relays which are mounted in the sequencers. Each sequencer also contains the electronics necessary to decode load actuation commands from the FC and drive the relays to the set or reset position.

The sequencers will be a custom design specifically tailored to the load actuation requirements of the COLD-SAT spacecraft. The size, weight, and power estimates for the sequencers listed in table 9.7 are based on the assumption that double-pole-double-throw electromechanical relays are used throughout the units. One-, five-, and ten-Amp-sized relays are used in the design and are assigned to each actuation circuit depending on the current requirements of the load. Solid state relays were also considered but not used in this conceptual design. The final design of these units will most likely consist of a mixture of electromechanical and solid state relays.

For reliability purposes some of the loads driven by the sequencers are grouped into redundancy clusters. Each load in a given cluster serves as a backup for a load in another cluster. The individual loads within a cluster are selected by a single nonredundant relay. A fully redundant drive circuit then provides the excitation to any relay within the cluster which is selected. This implementation provides for greatly enhanced reliability while keeping the complexity (and parts count) of the electronics within reason.

9.6.6 RADIOFREQUENCY (RF) PROCESSING BOX

The RF processing box, like the sequencers, is a custom-designed unit, specifically tailored for the COLD-SAT spacecraft. This unit routes the uplink and downlink signals through the appropriate antenna networks. In the case of the uplink signal, low-noise amplifiers (LNA's) in the RF processing box boost the strength of the received signal for input to the transponder. Figure 9.13 illustrates the relationship between the antenna, RF processing box, and the transponders. All of the components in the box are standard flight-qualified items. Only the system implementation and packaging is new.

9.6.7 ANTENNAS

The HGA is a steerable 27.5-in. parabolic reflector with a gain of 20.9 dBi along the boresight. The HGA's half-power beam width is 18°. Many vendors are available to supply this antenna. Tecom Inc. was selected since a catalog version of this antenna is available from them.

The LGA's each have hemispherical coverage and are mounted at opposite ends of the spacecraft on the structure in order to maximize the view to a TDRS.

9.6.8 HIGH-GAIN ANTENNA (HGA) DEPLOYMENT ARM AND GIMBAL

Schaeffer Magnetics, Inc. manufactures a deployment arm and a fully redundant gimballing mechanism suitable for the COLD-SAT HGA. The size, weight, and power consumption estimates for these components is found in table 9.7.

9.6.9 REDUNDANCY CONTROL UNIT

The RCU is a custom designed unit specifically for the COLD-SAT spacecraft. The RCU consists of watchdog timers and hardwired logic gates. It determines which of the FC's command outputs are able to control the spacecraft. Each FC writes to the RCU a unique checksum generated by a software routine which verifies the integrity of the programs loaded in the computer's memory and the functioning of its processing unit. If the active FC generates an incorrect checksum or fails to write the correct checksum within the time allowed by the watchdog timer, the active FC is automatically switched. The same switch will take place if an uncorrected memory read error is detected in the memory of an FC through a hardware connection. The size, weight, and power consumption estimates were developed based on previous experience with checksum and watchdog timer units designed for other space-flight applications.

9.7 Supporting Analyses

Tables 9.8 and 9.9 summarize the RF link analysis which was performed for the normal, high-rate telemetry downlink, and the command uplink channels through the TDRSS. These analyses used conservative, worst-case values and illustrate that adequate margin exists in the design of the RF portion of the system.

Extensive error analyses of the TT&C data acquisition function have been performed. The results may be found in Chapter 5, the Experiment System section of this report.

9.8 Reliability

The TT&C system was assigned a reliability goal of 0.990 at the onset of the conceptual design. This system goal was part of the overall goal of achieving a reliability prediction of 0.92 for the entire COLD-SAT spacecraft.

The TT&C system design attempts to maximize system reliability while, at the same time, minimizing the total volume weight, power consumption, and cost of the system. Redundancy is selectively implemented in order to keep volume, weight, and power consumption within reasonable limits.

TABLE 9.8.—RADIOFREQUENCY (RF) LINK ANALYSIS FOR TELEMETRY DOWNLINK^{a,b,c}

Item	Description	Unit	Value	Comments
1	Transmitter power	dBW	+7.0	5-W option—NASA standard transponder
2	Circuit losses	dB	-3.0	Conservative estimate (cabling + RF processing box)
3	HGA ^d gain	dBi	+21.9	27.5-in. parabolic, $\mu = 0.55$
4	Antenna pointing loss	dB	-0.6	HPBW = 13°, pointing error = 3°
5	COLD-SAT EIRP	dBW	25.3	Items 1+2+3+4
6	Polarization loss	dB	-0.5	Worst-case alignment
7	Space loss	dB	-193.1	Range = 47 200 km (worst case)
8	Atmospheric loss	dB	-0.1	Worst-case estimate
9	Received power at TDRS	dBW	-168.4	Items 5+6+7+8
10	Required power at TDRS	dBW	-171.8	TDRSS users guide: 32 Kbps (10^{-5} ber)
11	Link margin	dB	+3.4	Item 9 minus item 10

^aRedundant telemetry downlink.^bData rate = 32 Kbps, frequency = 2287.5 MHz.^cTDRSS multiple access (MA) system.^dHigh-gain antenna.TABLE 9.9.—RADIOFREQUENCY (RF) LINK ANALYSIS FOR COMMAND UPLINK^{a,b,c}
[TDRSS (Tracking and Data Relay Satellite System)-to COLD-SAT LINK.]

Item	Description	Unit	Value	Comments
1	TDRS EIRP	dBm	+64.0	From TDRSS user's guide
2	Space loss	dB	-192.4	Range = 47 200 km
3	HGA ^d pointing loss	dB	-0.6	HPBW = 13.5°, pointing error = 3°
4	Polarization loss	dB	-0.5	Worst-case alignment
5	HGA ^d gain	dBi	+21.6	27.5-in. parabolic, $\mu = 0.55$
6	Circuit losses	dB	-3.0	Worst case
7	Power divider loss	dB	-3.0	-----
8	Power input to NST ^e	dBm	-113.9	Items (1+2+3+4+5+6+7)
9	Power required at NST ^e	dBm	-123.5	All worst-case receiver parameters for 1 Kbps (10^{-5} ber)
10	Link margin	dB	+9.6	Item 8 minus item 9

^aRedundant command uplink.^bData rate = 1 Kbps, frequency = 2206.4 Mhz.^cTDRSS multiple access (MA) system.^dHigh-gain antenna.^eNST-NASA standard transponder.

Also, when selecting a candidate unit, for example the FC, for use in the system, the predicted reliability of the unit was a major factor in the selection process.

The TT&C system design presented in this report was analyzed for its predicted 6-month mission reliability. The predicted value is 0.985 which is 0.005 short of the assigned goal. An analysis of the overall COLD-SAT spacecraft reliability determined that the 0.985 value was adequate to allow the spacecraft to achieve its overall goal of 0.92.

9.9 References

1. Goddard Space Flight Center, Space Network (SN) Users Guide, STUN No. 101.2, rev. 6, 1988.
2. Mission Planner's Guide for the Atlas Launch Vehicle Family, General Dynamics Commercial Launch Services Inc., rev. 1, 1989.

Chapter 10

Electric Power System

Todd A. Tofil

National Aeronautics and Space Administration

Lewis Research Center

Cleveland, Ohio

10.1 Introduction

The COLD-SAT spacecraft's electrical power system (EPS) provides power generation, storage and distribution, fault protection, and system data for the COLD-SAT satellite. Although it interfaces with all other COLD-SAT systems, it operates nearly independently from the other systems. The electrical power system is essential to the operation of the spacecraft. From the initial deployment of the solar arrays to the repeated charging and discharging of the batteries, the power system is responsible for many functions throughout the mission. Every onboard system depends on power, some more than others. A serious on-orbit power system failure will result in loss of the COLD-SAT mission.

The COLD-SAT spacecraft can be thought of as consisting of two main parts, the experiment system and the spacecraft systems. Experiment system functions requiring power consist of those associated with the cryogenic equipment; such as cryogenic tankage, valves, heaters, mixer, and experiment electronics units. Spacecraft systems' functions are those that are necessary to communicate with the spacecraft and keep the spacecraft in the correct orbit and attitude. These systems are the telemetry, tracking, and command (TT&C) system; propulsion system; attitude control system; and thermal control system. The generation and distribution of power for these systems is highly integrated. There is little separation of power functions based solely on the particular system being supplied with power.

The EPS also has a very important function that it performs only once. It actuates onboard pyrotechnic devices for deploying antennas, solar arrays, and opening and closing supply tank vent doors. These components must be secured during launch and must have a reliable method of deployment or actuation after launch.

The basic design philosophy for the COLD-SAT EPS is that the power system will control as many of its own functions as is practical. Throughout the design process, choices were made on dividing functions between the EPS and the TT&C system. Because there is no central processing unit in the power system, the TT&C system will contain software modules to control power switching to the loads. It is also possible to uplink commands through the TT&C system. One such input will reset relays in the power distribution unit after a fault. The solar panel and battery charge and discharge functions, as well as distribution and fault isolation functions, will be automatic. Control of these functions will reside in the power system.

Nominal bus voltage is unregulated 28 Vdc and average load power is 646 W. Special power conditioning requirements, such as a dc-to-dc conversion, are decentralized and will be provided by the respective system. Solar arrays are sized to supply load power and battery recharge power for over 6 months of on-orbit operation, while the batteries which supply load power during eclipse and additional power for pulse loads have a cycle life far exceeding the mission duration.

Figure 10.1 shows a simplified block diagram of the EPS, which consists of several main elements. They are the solar arrays, the two nickel-cadmium batteries, the power control unit, the power distribution unit, the power bus, and the pyro control unit. These elements interface with each other and form the EPS. The EPS contains voltage, current, temperature, and status sensors so sufficient system health data can be downlinked to indicate system performance to ground controllers. The interface for these data signals is the TT&C system.

Basic on-orbit operation of the EPS consists of using two solar array wings to generate power for loads and battery recharge. The EPS's power control unit controls battery charging and contains solar array protection circuits, as well as shunts to dissipate power during periods of low power usage. The

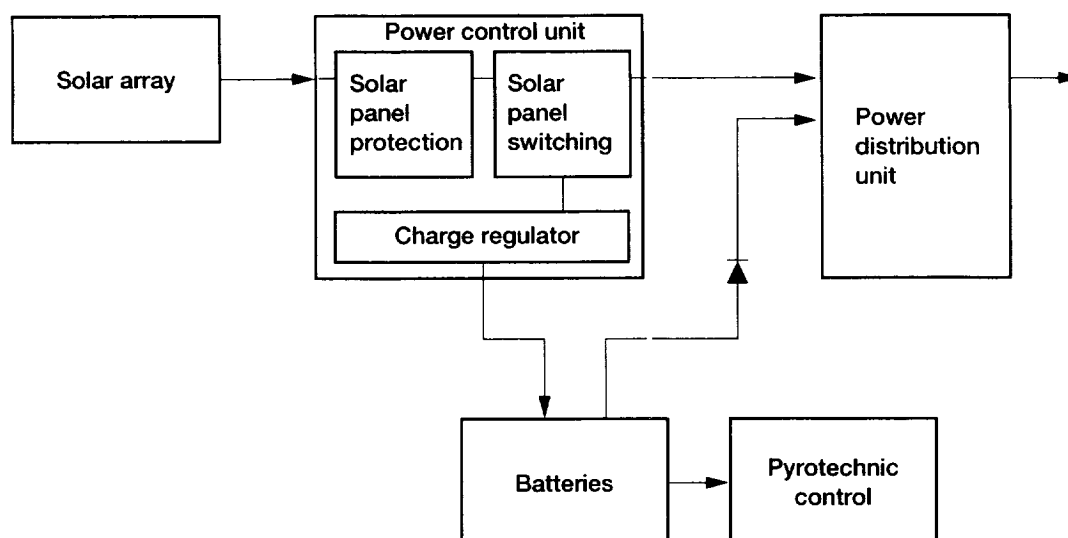


Figure 10.1.—Simplified electrical power system block diagram.

protection circuits consist of diodes to prevent reverse power flow from the battery to the solar array or from the power bus to the battery.

The system's power distribution unit provides top-level power distribution, including bussing, fault protection, and fault clearance. The sequencer units in the TT&C system control individual power switching to most of the spacecraft's electrical components. The EPS is an unregulated system and incorporates redundancy to achieve the desired reliability, which is 0.993. The design life is 6 months.

10.2 Requirements

The conceptual design of the EPS was driven by requirements from several sources. The primary driver was the spacecraft and experiment system's power profiles. Also affecting EPS configuration were the mission length, orbit inclination and altitude, and mission phases. The mission phases are prelaunch, ascent, orbit acquisition, on-orbit nominal, and emergency minimum. The EPS must provide power to meet all of the requirements. It is a system-level design decision that the spacecraft be powered by solar arrays.

Each of the mentioned mission parameters results in specific design criteria. For example, the mission length affects allowable battery depth of discharge and solar array degradation. The orbit parameters affect solar energy reaching the arrays, the length of time in sunlight and eclipse, and radiation and thermal environment. Each of the requirements are explained in the following paragraphs.

The EPS must survive the Earth and launch environments as well as operate to specifications in space for 6 months. Requirements for operating under specific temperature and humidity conditions prior to launch result from this requirement. The system must also withstand launch loads on an

expendable launch vehicle. For this study, an Atlas I launch vehicle was chosen, but requirements would be similar for other launch vehicles.

Orbital parameters also affect the EPS operation and drive the design. COLD-SAT will initially be in a 550-n mi circular orbit with an inclination of 18°. The orbit will change during the 6-month life to a slightly elliptical orbit. The orbit change will slightly affect the amount of time the spacecraft is in sunlight and eclipse. The change will not have a large impact on the EPS performance or design.

With an orbital inclination of 18°, the angle between the Sun line and the orbit plane, the β angle, can vary from +41.5° to -41.5°. However, the COLD-SAT spacecraft will be rotated so that Sun only illuminates one side, the warm side. This will limit the β angle relative to the spacecraft to a range of 0° to 41.5°.

COLD-SAT requires an average of 646 W of power during normal on-orbit operations. The highest expected power requirement is slightly less than 800 W. Power requirements for all mission phases are summarized in table 10.1. Figure 10.2 shows the power profile for the entire mission. Surge loads are not included in this profile.

The ascent phase, as identified in table 10.1, is defined as the time from the removal of ground power at T - 16 min until spacecraft separation from the Centaur upper stage at T + 2300 sec. During this phase, 443 W of power are required without the use of the solar arrays.

The attitude acquisition phase begins when the spacecraft separates from the launch vehicle and ends when the solar arrays are deployed and the Sun is acquired; 578 W are used by COLD-SAT systems in this phase. Up to 2.83 hr of operation are required before battery charging can begin.

On-orbit nominal power, which is 646 W, is the average power required to conduct the various experiments and power

TABLE 10.1.—SUMMARY OF COLD-SAT POWER BUDGETS

System	Ascent, W	Attitude acquisition, W	On-orbit nominal, W	On-orbit peak, W	Emergency minimum, W
Power	70	80	70	80	70
Propulsion	0	110	63	161	10
Experiment	45	60	125	536	0
Attitude control	73	73	73	73	0
Thermal control	0	0	10	100	0
TT&C	255	255	305	329	148
Total	443	578	646	1279	228

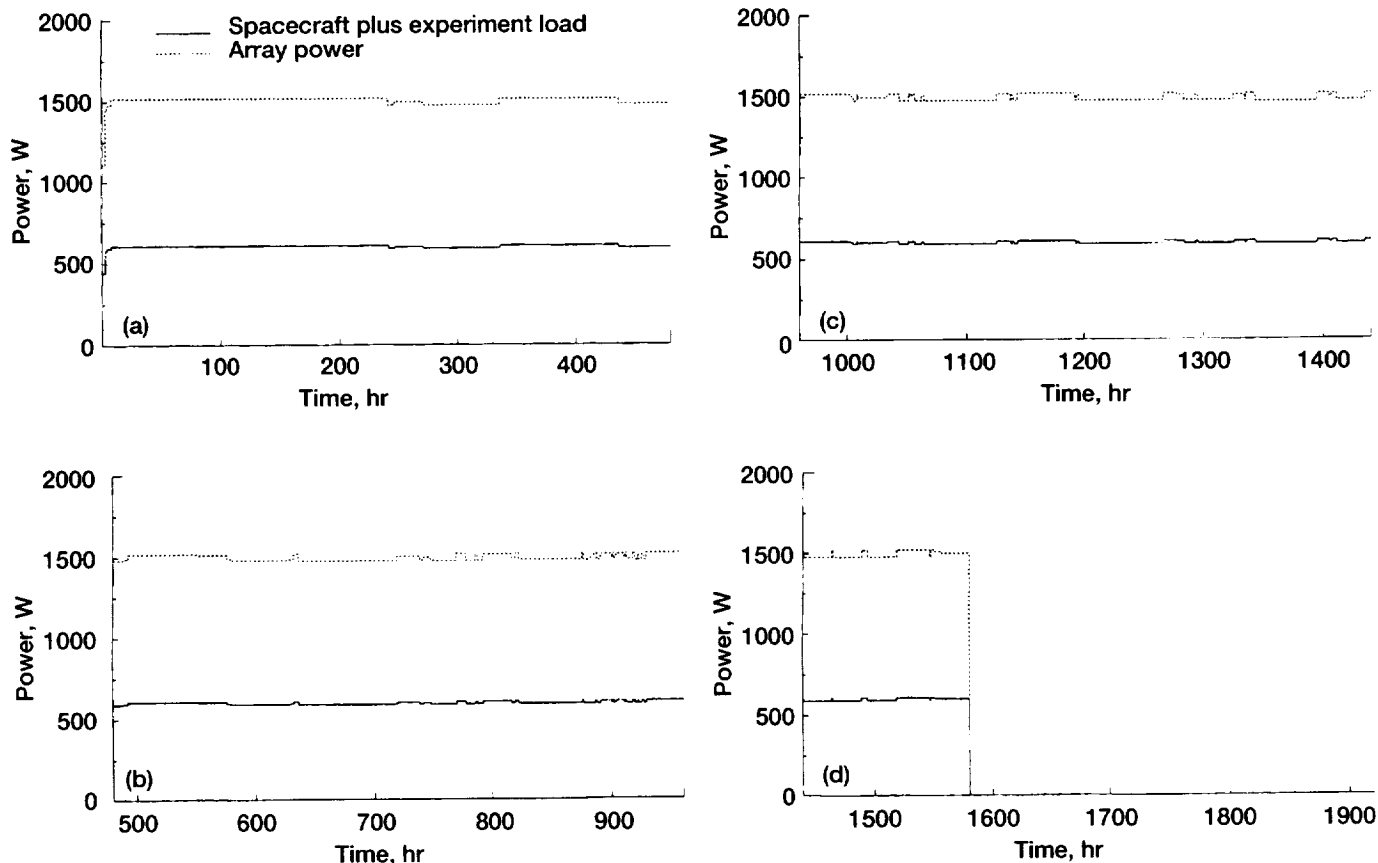


Figure 10.2.—COLD-SAT power profile. (Load power equals experiment plus spacecraft. Load power is based on minimum requirement. Array power is with 25 percent margin.) (a) Launch to day 20. (b) Day 20 to day 40. (c) Day 40 to day 60. (d) Day 60 to end of mission.

the spacecraft systems. The on-orbit peak column in table 10.1 is the sum of the power requirements for each component. It is very unlikely that all components will be operating simultaneously, and therefore, the peak power is a worst-case value, used for bookkeeping purposes only.

The emergency minimum column in the table is the power required to keep the spacecraft alive in the event of an anomaly that causes the available power to drop significantly. If this power level cannot be maintained, it is likely that the spacecraft will be lost. This applies to on-orbit problems only; it does not cover orbit acquisition anomalies. Two-hundred twenty eight

W are required to maintain the capability of the TT&C system to receive ground transmissions and to keep the attitude control system and propulsion system partially functioning.

In addition to the basic power requirements for flight, described previously, some additional conditions and restraints are imposed on the power system:

- (1) All power handling connectors must be dead-faced during spacecraft separation.
- (2) Provisions must be made for powering the spacecraft during test and integration on the ground.

(3) The control of pyrotechnic devices must conform to the requirements of MIL-STD-1512, Electroexplosive Subsystem, Electrically Initiated Design Requirements and Test Methods; specifically, means must be provided for safing the pyrotechnic devices until immediately prior to launch.

(4) Test connectors must be provided to allow simulation of the solar arrays.

10.3 Power System Interfaces

The EPS interfaces with a number of other systems including ground support equipment, the launch vehicle, and directly or indirectly with all other spacecraft systems. Figure 10.3 shows the EPS's electrical interfaces. In addition, the electrical power system has interfaces with the spacecraft structural and thermal control systems.

10.3.1 SPACECRAFT SYSTEMS ELECTRICAL INTERFACES

Onboard the COLD-SAT spacecraft, the EPS interfaces, directly or indirectly, with all other spacecraft systems. The EPS supplies power for all spacecraft functions and has direct power interfaces with three other spacecraft systems. They are the TT&C system, the propulsion system, and the attitude control system. The EPS power interfaces are shown in figure 10.3. Detailed power requirements for all mission phases are given in table 10.2. It should be noted that the table and figure contain components which are not present in the final COLD-SAT design. This occurs because the EPS design was unable to track design changes as they occurred during the later

portions of the feasibility study. The information presented here is that used to design the EPS.

The various spacecraft electrical loads are divided according to their priority for the operation of the spacecraft. There is a group of components which must be powered to allow the continued operation of the spacecraft. These are grouped onto one electrical bus, the essential bus, and include the spacecraft computers, and the telemetry transponders. If this bus loses power, it is likely that the spacecraft will be lost.

The second group of loads contains those components required to control spacecraft attitude. Loss of power to this group of loads, called priority bus 1, will result in loss of spacecraft attitude control and with it loss of solar array output and high-rate communications.

The remaining loads are primarily concerned with the operation of the experiments although some thermal control functions are also included. They are divided into two groups called priority bus 3 and priority bus 4. Loss of power to these loads does not have the immediate effect on the survival of the spacecraft that the first two groups of loads does. However, loss of power may compromise the experiment and, if it continues, may lead to thermally induced failure of the spacecraft. The loads grouped as bus 3 are somewhat more critical than those on bus 4.

Some loads on the essential bus and priority bus 2 interface directly with the EPS. However, most loads are coupled to the EPS through the sequencers in the TT&C system. These provide for the detailed control of these loads by ground command or the flight computers. Some sensor loads are interfaced to the EPS through the attitude control system interface electronics which provides similar control and power conditioning functions for them.

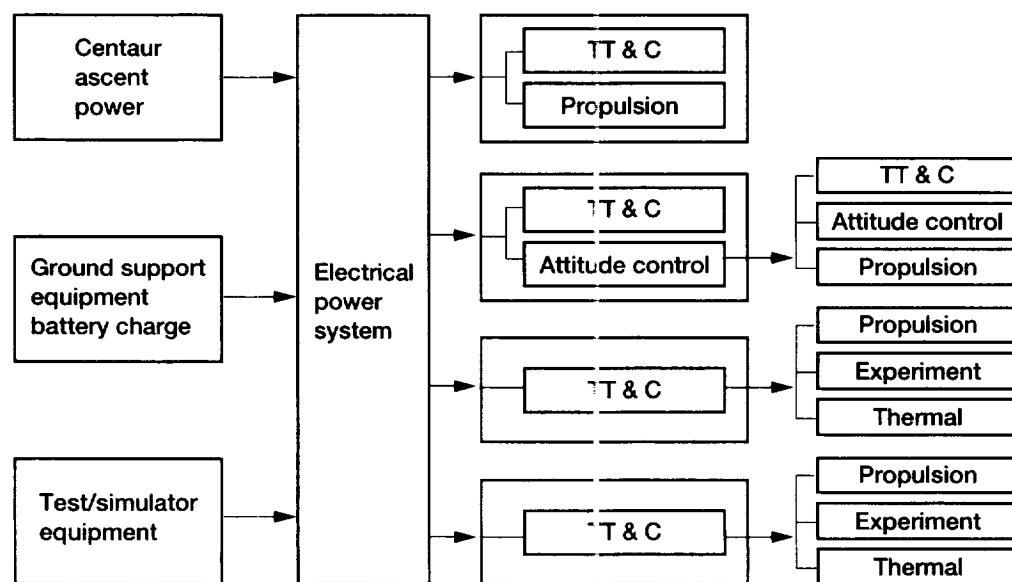


Figure 10.3.—Top level block diagram of the electric power system's interfaces.

TABLE 10.2.—COLD-SAT POWER BUDGET

Component	Ascent, W	Attitude acquisition, W	On-orbit peak, W	Duty cycle	On-orbit average, W
Propulsion					
Thruster valve heaters	0.0	40.0	40.0	0.75	30.0
Catalyst bed heaters	↓	18.0	20.0	.75	15.0
Propellant line heaters		5.0	5.0	1.00	5.0
Propellant distribution assembly		5.0	5.0	1.00	5.0
Propellant tank heaters		5.0	20.0	.25	5.0
Solenoid valve		25.0	25.0	.1	2.5
Thrusters		12.0	36.0	.02	.6
Gimbal unit		0.0	10.0	.01	.1
Subtotal	0.0	110.0	161.0	---	63.2
Attitude control					
Inertial reference unit	25.0	25.0	25.0	1.0	25.0
Horizon sensor electronics 1	7.0	7.0	7.0	↓	7.0
Horizon sensor head	3.0	3.0	3.0		3.0
Horizon sensor electronics 2	7.0	7.0	7.0		7.0
Horizon sensor head	3.0	3.0	3.0		3.0
Magnetometer 1	1.0	1.0	1.0		1.0
Magnetometer 2	1.0	1.0	1.0		1.0
Fine Sun sensor 1	3.0	3.0	3.0		3.0
Fine Sun sensor 2	3.0	3.0	3.0		3.0
Attitude control system interface electronics	20.0	20.0	20.0	---	20.0
Subtotal	73.0	73.0	73.0	---	73.0
Thermal control					
Electronics bay 1 heater	0.0	0.0	50.0	0.1	5.0
Electronics bay 2 heater	.0	0	50.0	.1	5.0
Subtotal	0.0	0.0	100.0	---	10.0
Power					
Battery 1					
Battery 2					
Solar array 1					
Solar array 2					
Power control unit					
Power distribution unit					
Pyrotechnic control unit					
Subtotal	70.0	80.0	80.0	---	70.0
TT&C					
Computer 1	40.0	40.0	40.0	1.0	40.0
Computer 2	40.0	40.0	40.0	↓	40.0
Transponder 1	18.0	18.0	44.0		44.0
Transponder 2	18.0	18.0	18.0		18.0
Radiofrequency processing box	10.0	10.0	10.0		10.0
Space shuttle recorder 1	16.0	16.0	16.0		16.0
Space shuttle recorder 2	16.0	16.0	16.0		16.0
Remote command and telemetry unit 1	17.0	17.0	17.0		17.0
Remote command and telemetry unit 2	17.0	17.0	17.0		17.0
Command and telemetry unit 1	25.0	25.0	25.0	↓	25.0
Command and telemetry unit 2	0.0	0.0	0.0		0.0
Sequencer 1	15.0	15.0	15.0		15.0
Sequencer 2	15.0	15.0	15.0		15.0
High-gain antenna	---	---	---		---
Low-gain antenna 1	---	---	---		---
Low-gain antenna 2	---	---	---		---
Drive motor electronics	0.0	0.0	18.0	0.2	3.6
Antenna gimbal motor	.0	0	12.0	0.2	2.4
Redundancy control	8.0	8.0	8.0	1.0	8.0
Command receiver	.0	0	18.0	1.0	18.0
Subtotal	255.0	255.0	329.0	---	305.0

Table 10.2.—Concluded.

Component	Ascent, W	Attitude acquisition, W	On-orbit peak, W	Duty cycle, W	On-orbit average, W
Experiment					
Experiment data unit 1	15.0	15.0	15.0	1.0	15.0
Experiment data unit 2	15.0	15.0	15.0		15.0
Experiment data unit 3	15.0	15.0	15.0		15.0
Accelerometer conditioner	0.0	0.0	10.0		10.0
Signal conditioner			15.0		15.0
Supply tank heater			21.0	0.1	2.1
Large receiver tank heater			50.0		5.0
Small receiver tank heater			50.0		5.0
Vaporizer A heater			100.0		10.0
Vaporizer B heater			100.0		10.0
Flight vent heater			7.0		0.7
TVS vent heater			7.0		.7
Vaporizer panel A heater			6.0	0.5	3.0
Vaporizer panel B heater			6.0		3.0
Connector panel A heater			2.0		1.0
Connector panel B heater			2.0		1.0
Latch valve			50.0	.1	5.0
Gas valve			50.0	.1	5.0
Mixer motor inverter		15.0	15.0	.25	3.75
Subtotal	45.0	60.0	536.0	---	125.25
Total	443.0	578.0	1279.0	---	646.45

In addition to power interfaces, the EPS also has control and data interfaces with the TT&C system. Control inputs from the TT&C system consist of commands to reset relays in the power distribution unit. Housekeeping data outputs from the EPS consist of temperature, voltage, and current sensors that are positioned throughout the system and interface with the TT&C system. They are monitored by software in the spacecraft computers and downlinked as part of the normal spacecraft housekeeping data.

A number of pyrotechnic devices powered by dual-bridgewire NASA standard initiators (NSI) must be triggered by the EPS. The required pyro devices include

- (1) The four pyrotechnic latches which sequence the vent doors on the supply tank MLI can
- (2) A minimum of 8 pyro devices for holddown and deployment of the solar arrays
- (3) A minimum of 2 pyro devices for deployment of the high-gain antenna

Each bridgewire of each NSI must be strapped and static-grounded until armed for operation. For initiation each bridgewire must be powered from a redundant source. Following actuation the firing current must be controlled.

10.3.2 OTHER SPACECRAFT INTERFACES

The solar arrays and their associated deployment mechanisms must be supported by the spacecraft structure and accommodated by the overall spacecraft configuration. The components of the EPS and especially the batteries require thermal control.

10.3.3 GROUND SUPPORT INTERFACES

The EPS has ground support interfaces for system test and prelaunch activities prior to beginning launch procedures while on the pad. These tests are part of the normal interface and functional verifications that take place prior to mating the spacecraft with the launch vehicle. System tests will also be performed throughout the development of COLD-SAT as well as at the launch site. Interfaces for system test include a solar array power simulator interface, a bus test interface, and a battery charge interface. The various interfaces and their functions are explained in the following sections.

The solar array power simulator interface allows an end-to-end check of the power system electronics and the remainder of the spacecraft without having the solar arrays connected. The solar array power simulator can supply voltages ranging between 0 and 80 V. This simulates the voltages produced at nominal operating conditions as well as voltage extremes caused by array temperature or solar intensity variation. The simulator interfaces with the power control unit where the solar array power would normally connect.

The bus test interface allows power to be supplied downstream of the batteries and solar arrays and is used for checkout of the power distribution functions. It can be used during development tests or prior to mating COLD-SAT to the launch vehicle. Spacecraft batteries and solar arrays are not connected during bus interface tests to permit isolation of the power distribution and load shedding capabilities. The ground support equipment (GSE) power system used for the bus interface checkout interfaces with the power distribution unit in the EPS. It simulates solar array power and battery power. Also, the voltage levels can be varied to test the automatic load shedding capabilities of the system.

10.3.4 EXPENDABLE LAUNCH VEHICLE (ELV) INTERFACES

Interfaces for launch pad operations include a battery charge interface and a cable to prevent inadvertent pyro actuation. The battery charge interface is between GSE battery chargers and the COLD-SAT spaceflight batteries. It is made through the Centaur upper stage, using rise-off disconnects in the spacecraft adaptor and the Atlas I payload umbilicals. The GSE will maintain the proper charge parameters. This function can be used any time during the system build and test, but is specifically for use on the launch pad. As the vehicle and spacecraft are prepared for launch, the spacecraft batteries will be charged to maintain full battery capacity for flight. The charge is terminated approximately 15 min before launch.

The pyro safing cable is connected to the EPS's pyro control box for use during ground operations when the pyros are installed in the spacecraft. This will prevent inadvertent actuation of the pyros. The cabling will be reconfigured for flight prior to launch.

In addition to interfaces with ground support equipment, the EPS also has a power interface with the launch vehicle. This interface is used to power the spacecraft both before launch and during ascent. The interface is between the power transfer unit on the equipment module of the Centaur and the power distribution unit on COLD-SAT. A functional diagram of the power transfer unit interface with the COLD-SAT power system is shown in figure 10.4. The power transfer unit is an electronics box that is provided as an optional service by the launch vehicle for use on the Centaur upper stage. It serves as the interface for ascent-phase battery power from the Centaur as well as the

interface for ground power. The power transfer unit contains circuitry to switch from ground power to Centaur battery power, as well as to switch from Centaur battery power to the COLD-SAT batteries just prior to separation. The Centaur provides a discrete command to the power transfer unit to initiate the switchover. The switch to spacecraft batteries is made just prior to separation from the launch vehicle battery.

10.4 System Alternatives Considered

10.4.1 GENERAL

After a review of the literature (refs. 1 to 3), several alternatives to the final EPS configuration were considered early in the design. The final selections were based on various criteria including cost, efficiency, reliability, availability, flight heritage, and simplicity. Many alternatives were considered but considerable effort was devoted to solar array configuration, battery selection, and power conditioning methodology.

10.4.2 SOLAR ARRAYS

The selection of solar array type depends on several criteria, including reliability, complexity, compatibility with spacecraft structural and thermal characteristics, spacecraft stabilization, cost, weight, serviceability, and space heritage. Solar array alternatives that were examined included rotating arrays versus fixed arrays, rollup arrays versus rigid arrays, flat-mounted cells versus shingle-mounted cells, and canted arrays versus noncanted arrays.

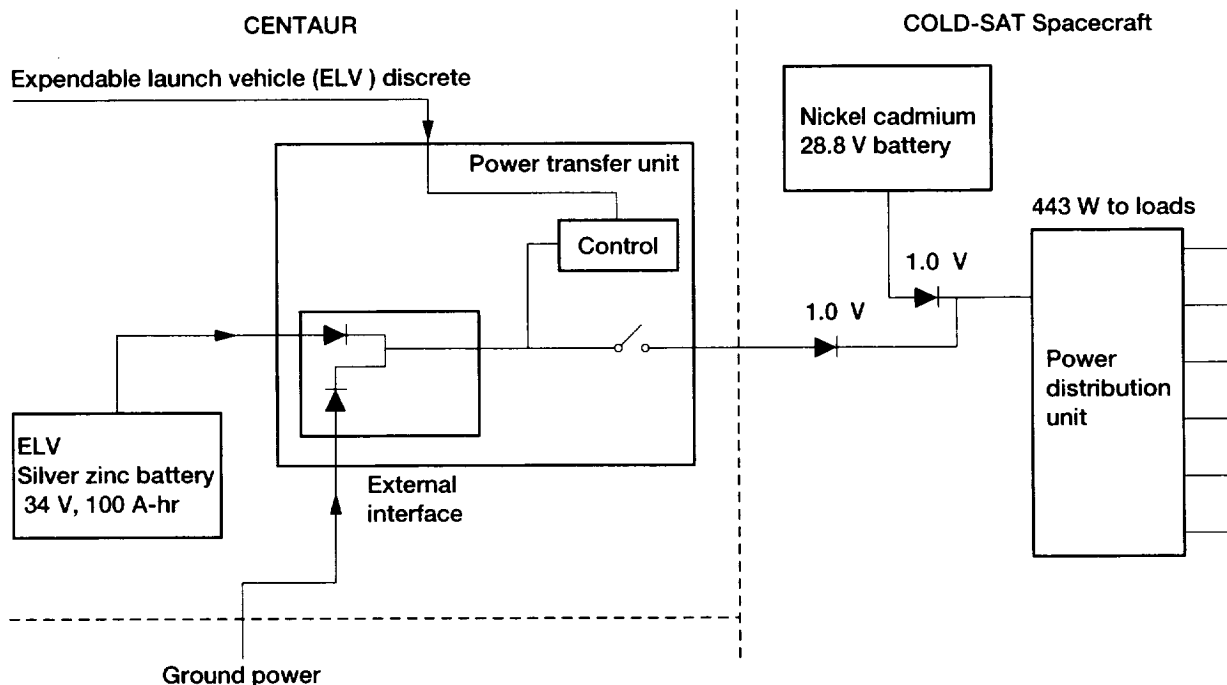


Figure 10.4.—Interfaces between COLD-SAT and the Centaur power transfer unit.

Solar arrays can be the body-mounted type or the deployable type. If they are deployable, they can be rigid or rollup arrays. Body-mounted arrays are mounted to the main body of the spacecraft and generally are used on spin-stabilized spacecraft. The advantage is they produce some power in almost all spacecraft attitudes. They are also useful during orbit acquisition. Body-mounted arrays were never seriously considered since COLD-SAT is not a spin-stabilized spacecraft and the power generated would be limited by the projected area of the spacecraft body. Also, body-mounted arrays generally are not advantageous for power requirements as high as that of COLD-SAT. Therefore, deployable arrays were selected. They can generate large quantities of power, and they are often used for similar types of missions.

Deployable arrays can be made by using rigid panels or rollup arrays. Rigid arrays are stored in panels and unfolded, whereas rollup arrays are stored in a cylindrical configuration and unrolled. Rigid arrays were selected because they have a much greater flight heritage. The cost and complexity are less. The rigid arrays do flex somewhat, and the design of the array must ensure that the mechanical frequencies of the array do not cause problems for the spacecraft's attitude control system.

Rigid arrays can be either fixed or rotating. The orientation of fixed arrays remains constant with respect to the spacecraft body once they are deployed, while the orientation of rotating arrays is controlled so that the solar cells point toward the Sun as the spacecraft moves through its orbit. The rotating array alternative was rejected but was not examined in depth. It was perceived as unnecessarily complex for the requirements of this mission. The savings in weight and volume for a given power output does not outweigh the need for added components. Rotating arrays require additional components compared with a fixed array, including a Sun tracker, control unit, and drive unit. Typically, the drive unit consists of a stepper motor, a gear assembly to transmit motor power to the array, a slip ring and brush assembly to transfer power and signals through the drive shaft to the spacecraft body, and shaft encoder to indicate array position relative to the spacecraft body. Fixed arrays were selected for the design because of their relative simplicity, space heritage, and lower cost.

Once fixed arrays were selected, their orientation relative to the spacecraft had to be determined. The alternatives receiving the most attention involved canting the arrays versus orienting them along the spacecraft axis. Canting the solar array reduces the loss of power in a fixed array because of the changing β angle caused by precession of the orbit and motion of the Sun along the ecliptic. By canting the arrays with respect to the spacecraft axis, the variation in maximum and minimum angle of incidence of solar energy can be reduced, thereby reducing the size of the arrays. The arrays can be made smaller because the canting reduces the power penalty imposed by the cosine law. However canting the arrays increases the complexity of the deployment mechanism. After analysis, canted solar arrays were selected.

A brief examination was done to determine how the cells would be mounted to the array. Flat-mounted cells are attached to the array substrate adjacent to each other with a small separation space. Shingle-mounted arrays are mounted such that the solar cells overlap each other like shingles on a house. Relative to shingle-type mounting, flat-type mounting has the advantages of better thermal properties, easier replacement of damaged cells, stronger bonding to the substrate, increased packing factor, and more freedom in making cell interconnections. Disadvantages of flat-type mounting are more physical connections per array and less cell area per unit projected area. Considering these comparisons and the high number of flat-mounted arrays that have been used in space, the decision was made to use flat-mounted arrays on COLD-SAT.

10.4.3 BATTERIES

Several battery types were compared to determine the best battery for the COLD-SAT mission. Each battery type has some favorable and some unfavorable characteristics (refs. 4 and 5). Basically, the final determination was influenced most heavily by spaceflight heritage. In all, three types of batteries were considered. They were nickel-hydrogen, silver-zinc, and nickel-cadmium. Several battery characteristics were considered in the selection process, including operating temperature range, discharge voltage, depth of discharge capability, cycle life, energy density, and space flight history. Spacecraft and mission factors such as orbit altitude, orbit inclination, eclipse power requirements, peak power requirements, operating temperature, and mission life determined which battery's characteristics would be acceptable.

Nickel-cadmium batteries were selected because of their proven flight record and their overall performance characteristics. Silver-zinc and nickel-hydrogen were also considered, but silver-zinc cannot undergo enough recharge cycles and nickel-hydrogen batteries do not, at this time, have a long history of use in low-Earth orbit. Along with their proven flight record, nickel-cadmium batteries have adequate performance characteristics such as voltage discharge profile, cycle life, energy density, depth of discharge, and operating temperature range. A comparison of battery types is shown in table 10.3. There is some doubt as to whether nickel-cadmium batteries will still be available at the time COLD-SAT is launched because of the lack of availability of the separator material. Another factor in the possible shortage of nickel-cadmium batteries is the trend toward use of nickel-hydrogen batteries. It may be necessary to reconsider battery selection in later stages of the COLD-SAT design.

Silver-zinc batteries offer the highest energy density and function well at high discharge rates. The discharge voltage can be as high as 1.85 V. They are not, however, a good choice for use on COLD-SAT because they can be recharged only several hundred times, depending on the depth of discharge. COLD-SAT requires 2500 recharges for a 6-month mission. Also,

TABLE 10.3.—SUMMARY OF CHARACTERISTICS FOR NICKEL-CADMIUM, NICKEL-HYDROGEN, AND SILVER-ZINC BATTERIES

	Nickel-cadmium	Nickel-hydrogen	Silver-zinc	COLD-SAT requirement
Operating temperature, °C	-40 to 45	0 to 50	-20 to 60	-----
Energy density, W-hr/kg W-hr/liter	30 80	55 60	90 180	-----
Discharge voltage, V	flat	flat	flat	flat
Recharge	Tolerates overcharge	Tolerates overcharge	Sensitive to overcharge	-----
Depth of discharge, percent	25 to 40	60 (intelsat, 6000 cycles)	High (relative to Nickel-cadmium)	-----
Discharge voltage, V	1.3	1.3	1.6	-----
Relative cycle life	High (thousands)	High (thousands)	Low (hundreds)	2500 to 5000
Charge measurement	Temperature sensors	Pressure property to charge	-----	-----
Miscellaneous	Most space flight history	Relatively new to space use	Activated just before use, little flight use	Flight proven

silver-zinc batteries are sensitive to overcharge, operate poorly at low temperature, and are expensive. Previous space applications include use in life support equipment used by Apollo astronauts, use in the Lunar Rover, and use in some space transportation system controls. Although this battery is not well suited for use as a source of power during eclipse on COLD-SAT, it has the potential for powering loads during ascent.

A nickel-hydrogen battery uses both battery and fuel cell technologies. Many of the applications of nickel-hydrogen batteries have been in the aerospace area, and they have characteristics that make them well suited for such applications. They have high energy density relative to nickel-cadmium. They can undergo up to 6000 charge/discharge cycles, depending on the depth of discharge. They can also function at high depth of discharge (60 percent), although for less cycles. The cell can tolerate overcharge and cell reversal. The major disadvantage for COLD-SAT applications are relatively high initial cost and relatively little space-flight experience compared with nickel-cadmium. There have been some spacecraft that have used this type of battery including NTS-2, launched in 1977 and INTELSAT V, launched in 1983. More recently, the Hubble Space Telescope is using nickel-hydrogen batteries in low-Earth orbit. The lack of extensive low-Earth orbit use translates into a lack of confidence, higher risk, and higher costs because of increased testing requirements. The cell discharge voltage is 1.2 V and is fairly constant over the discharge time. The cell temperature rise as the cells discharge depends on the discharge rate. Pressure also changes as the state of charge changes, and it can be used as a direct indication of battery state of charge.

Nickel-cadmium batteries have been the most widely used spacecraft batteries and have functioned well. The cells have a wide operating temperature range, acceptable energy density, long cycle life, and high allowable charge and discharge rates. The disadvantage is they have a relatively low depth of discharge capability if thousands of cycles are required. Other advantages are that the cells are sealed and contain no free

electrolyte. The batteries are designed to prevent excessive pressure buildup during charge. Nickel-cadmium cells can withstand overcharge reasonably well at relatively low rates, but at high charge rates excessive overcharge will result in high cell temperature. Also, the cell discharge voltage profile is flat which helps keep the bus voltage constant.

In summary, the nickel-cadmium battery appears to be the best choice for COLD-SAT because it meets the requirements. The nickel-hydrogen battery also meets many of the requirements and even appears to offer enhanced performance over the nickel-cadmium batteries. The major deficiency for the nickel-hydrogen is the lack of long-term space flight data, however, this may change by the time COLD-SAT is in the critical design phase and a final battery selection must be made.

10.4.4 POWER CONTROL AND DISTRIBUTION

Spacecraft electrical power systems can be dissipative or nondissipative. Dissipative systems can be either regulated or unregulated. An unregulated system was selected for COLD-SAT.

The power control and distribution functions the EPS must perform can become complex, especially if a system is desired that can detect and clear faults along with the more usual functions such as charging batteries and bus power. Several methods were considered to accomplish load shedding. Load shedding is necessary if the bus voltage drops significantly for a time longer than can be tolerated. This time was not precisely determined but depends on the specifications of the load. The voltage drop could be sudden because of a spacecraft component or EPS failure, or it could be gradual because of an attitude control failure. It must be determined when to shed loads and when to reconnect the loads.

The first alternative considered was to add a computer dedicated to EPS functions. A computer in the EPS would monitor several voltages on the buses and actuate relays to disconnect the loads if necessary. An electrical load priority

would be established so the least critical loads would be shed first. The computer could decide, based on sensor inputs, if the load shedding has relieved the undervoltage. If not, more loads would be shed. The computer could then monitor the system, possibly perform a self test, and then bring the loads back onto the bus. With a computer in the EPS, many additional EPS functions could be controlled locally. This would present alternatives to the overall system configuration. This alternative was rejected as being too complex and costly.

The second alternative considered was to use the flight computer in the TT&C system to monitor sensors in the EPS and command relays based on the sensor inputs. The computer would function much like the internal computer in the first alternative. Data are normally routed through the TT&C system for downlinking EPS status so the flight computer could use the data as the criteria for commanding bus relays. This method was rejected because it increased the work required of the flight computer. It placed dependence on software that may not be completely debugged and increased the complexity of the interfaces. As in the first alternative, this method was rejected because it is complex and costly.

The third alternative was to have analog instrumentation in the EPS detect low voltage and initiate load shed. There is no interface with the TT&C system for load shed, nor is there a dedicated EPS processor. Analog instrumentation in the EPS compares each of the voltages of the bus with the reference voltages. The EPS buses are configured so that loads of similar importance to the spacecraft are on the same bus. The reference voltage of the least important bus is set the highest so it would be the first bus to be shed. The second most important bus has the highest set point so it is the last bus to be shed. The most important components are on the "essential bus" and cannot be shed. This scheme assumes the voltage is decreasing slowly. The TT&C system is the only system that can reconnect the buses. A command from the ground and through the TT&C system controls the bus relays. This method of control was chosen because, if the same analog instrumentation were used to reconnect buses, it may be possible to start a toggling of the relays. If low voltage is detected and a bus is shed, the resulting effect may be to increase the bus voltage to a point where the analog instrumentation would sense a level high enough to reconnect the bus. This may again drop the bus voltage and restart the cycle. This method of shedding loads was selected and will be described in more detail in later sections.

Alternatives were also considered for spacecraft busing schemes, including busing power to loads that are grouped by system, by duty cycle and by relative importance. Busing power to loads that belong to the same system was considered and rejected because it meant many buses, and the amount of power carried by the buses differed significantly. The goal was to have similar amounts of power supplied by each bus. A second alternative involved grouping loads that were powered at the same time (had similar duty cycles) so that entire buses could be switched off when the loads on the bus were not being

used. This was rejected because most of the loads, except for the experiment loads, were always active. The number of loads with low duty cycles and amount of power switched was not large.

The bus scheme that was selected was to group the loads by order of importance for load shedding purposes. The result is shown in figure 10.5 Loads of least importance to spacecraft survival were placed on priority buses 3 and 4. These are mostly experiment system components and spacecraft heaters. These loads are switched by the sequencers, so it is also possible to switch loads on an individual basis. Priority bus 2 contains a nonessential TT&C system, an attitude control system, and propulsion system components. Priority bus 1, or the essential bus, contains EPS, TT&C, attitude control, and propulsion system components that are essential to communicating with the spacecraft.

10.5 Supporting Analyses

10.5.1 GENERAL

During the conceptual design of the power system, several trades were performed to select one option over other possible options. There are several ways to design a particular system to meet the performance specifications. In addition to performance, other factors, such as cost, reliability, availability, or flight heritage, figure into selecting a certain method or component. The EPS was initially assumed to require use of solar arrays, batteries, and power control and distribution components, but this was further examined to determine the way in which these were implemented. Solar array configuration, battery type, and power conditioning methods were examined.

Once the selection was made, the analyses to specify proper sizes, capacities, voltages, and currents were performed. The analyses required assumptions, and these are identified in the calculations that follow in this section. The references or rationale for the assumptions are also stated.

10.5.2 SOLAR ARRAY CANT ANGLE

For thermal and attitude control reasons, the COLD-SAT long axis will lie in the orbit plane with the aft end of the spacecraft aligned with the projection of the Sun line in that plane. The spacecraft will be rotated about its long axis so that the Sun only falls on one side, the Sun side. In this configuration the angle between the Sun line and the spacecraft long axis (the " β angle") can vary from 0° to 41.5° . The angle the plane of the solar arrays makes with the spacecraft long axis, the cant angle, must be determined for optimum performance.

The COLD-SAT orbit determines the angle that the arrays should be canted. Table 10.4 presents the results of preliminary calculations that show the comparison of array size for various

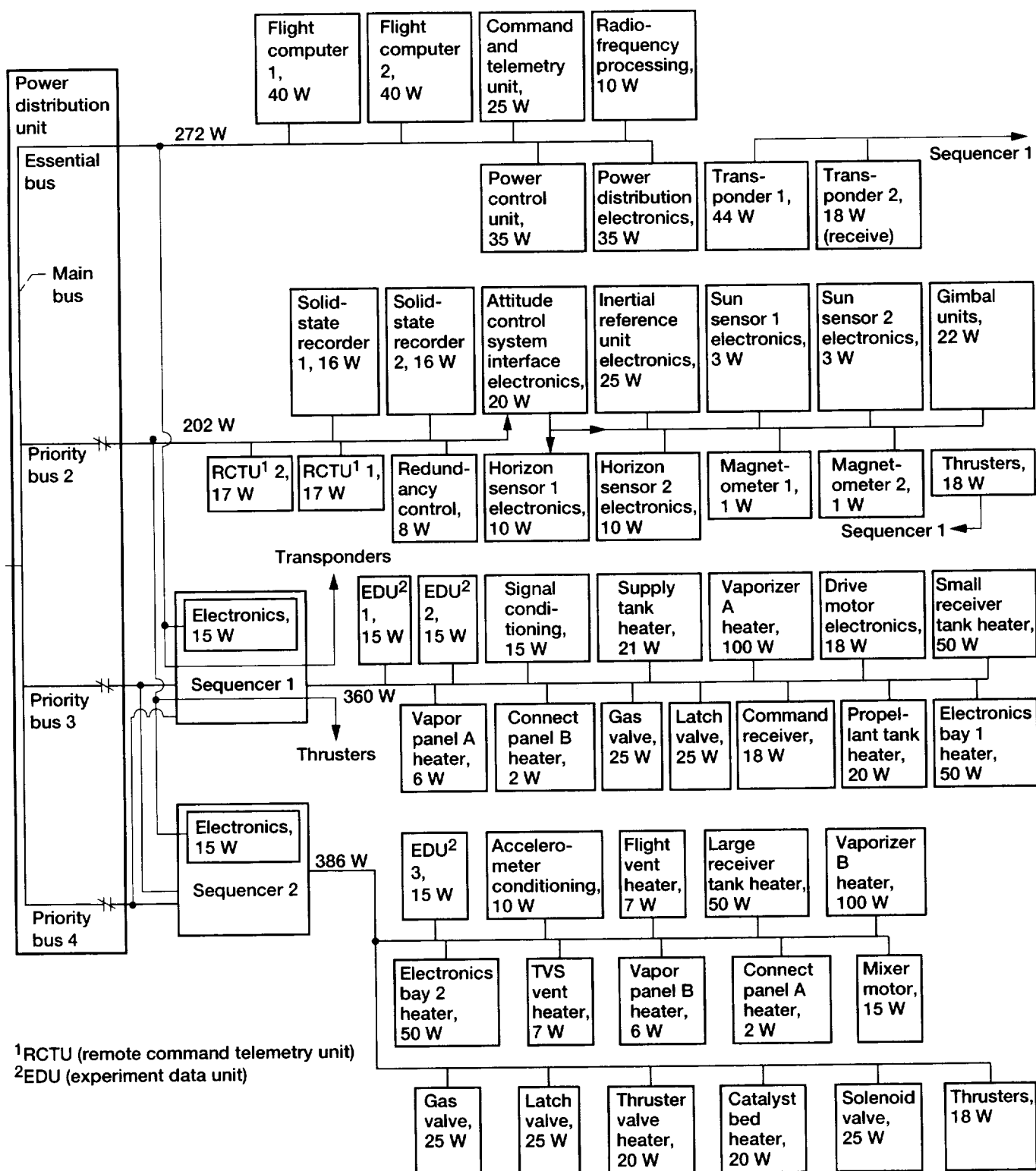


Figure 10.5.—Power distribution for COLD-SAT.

TABLE 10.4.—SOLAR ARRAY CANT ANGLE EFFECTS

Cant angle, degree	Power, W	θ , degree	$\cos\theta$	Number of parallel cells required, N_p	Number of series cells required, N_s	Area, ft ²	W/ft ²
0	^a 1815	0	1.000	83	102	170	10.67
	^b 1612	41	.755	98		200	8.06
8	^a 1815	8	0.990	84	102	172	10.55
	^b 1612	33	.838	88		181	8.90
10	^a 1815	10	0.984	84	102	172	10.55
	^b 1612	31	.857	86		176	9.15
11	^a 1815	11	0.981	84	102	172	10.55
	^b 1612	30	.866	86		176	9.15

^aBeginning at life.^bEnd of life.

cant angles. The calculations were performed iteratively, substituting the possible beta angles and eclipse times. The calculations were based on a 550-n mi orbit and 18° inclination. The table shows two results for a given cant angle. One result is for a β angle of 41°, the other is for a β angle of 0°. These represent the extreme cases.

In table 10.4, the power column represents the amount of power available at beginning of life and at end of life. These values differ slightly from the final array powers because the study was performed early in the design. The quantities were used to get an indication of cant angle effects. The extreme cases were considered. At beginning of life, the array produces the most power because of less degradation. At beginning of life, to generate 1815 W at 0° β angle, the arrays must be 170 ft². At end of life, to generate 1612 W at 41° β angle, the arrays must be 200 ft². The N_p column is the number of parallel cells required, the N_s column is the number of series cells required. The table shows examples for various cant angles and β angles. The table shows that a cant angle between 10° and 11° results in the smallest array size. A 10° cant angle was selected for the design study.

10.5.3 SOLAR ARRAY SIZING

The solar array electrical sizing analysis was performed based on the power requirements of other spacecraft systems and the operating characteristics of solar cells.

COLD-SAT will be launched into an 18° circular orbit from the Eastern Space and Missile Range. This indicates that the β angle varies from 0° to 41.5°. The β angle is the angle between the orbit plane and the Sun line and affects the solar array output because of reduced solar intensity. The efficiency of the solar arrays changes by a cosine of the β angle factor for angles below 40°. The deviation from the cosine law is insignificant for 41.5°.

The orbital period is 105 min. Also, the portion of the orbital period that COLD-SAT is in sunlight varies between 70 and 77 min, while the eclipse time varies between 28 and 35 min. These times depend on the altitude and β angle. Equation (10.1) is used to determine the orbital period and equation (10.2) is

used to calculate Sun and eclipse times. These times drive the design by affecting the time that the batteries will be discharged, and the available time per orbit for recharging the batteries. Also, for low-earth orbits, the number of battery charge-discharge cycles is high. Thus,

$$T^2 = \pi^2 r^3 / GM_e \quad (10.1)$$

where

T	period in sec
r	orbit altitude plus radius of Earth, R_e
G	gravitational constant
M_e	mass of the Earth
R_e	= 6.3783 × 10 ³ km
GM_e	= 3.98601 × 10 ¹⁴ m ³ /sec ²

and

$$t_s = \frac{1}{2} + \frac{1}{\pi} \sin^{-1} \left\{ \frac{\left[1 - \left(\frac{R_e}{r} \right)^2 \right]^{1/2}}{\cos \beta} \right\} \quad (10.2)$$

where

t_s	fraction of Sun time/orbit
R_e	radius of the Earth

The operating temperature range of the arrays was calculated by the COLD-SAT thermal analyst to be -80 to 135 °F. This plot is shown in figure 10.6. Array temperature affects the voltage output of the arrays, and this was taken into consideration for the sizing of the arrays. Voltage output ranges from 68.5 V at minus 80 °F to 36 V at 135 °F. A summary of the solar array characteristics is listed in table 10.5.

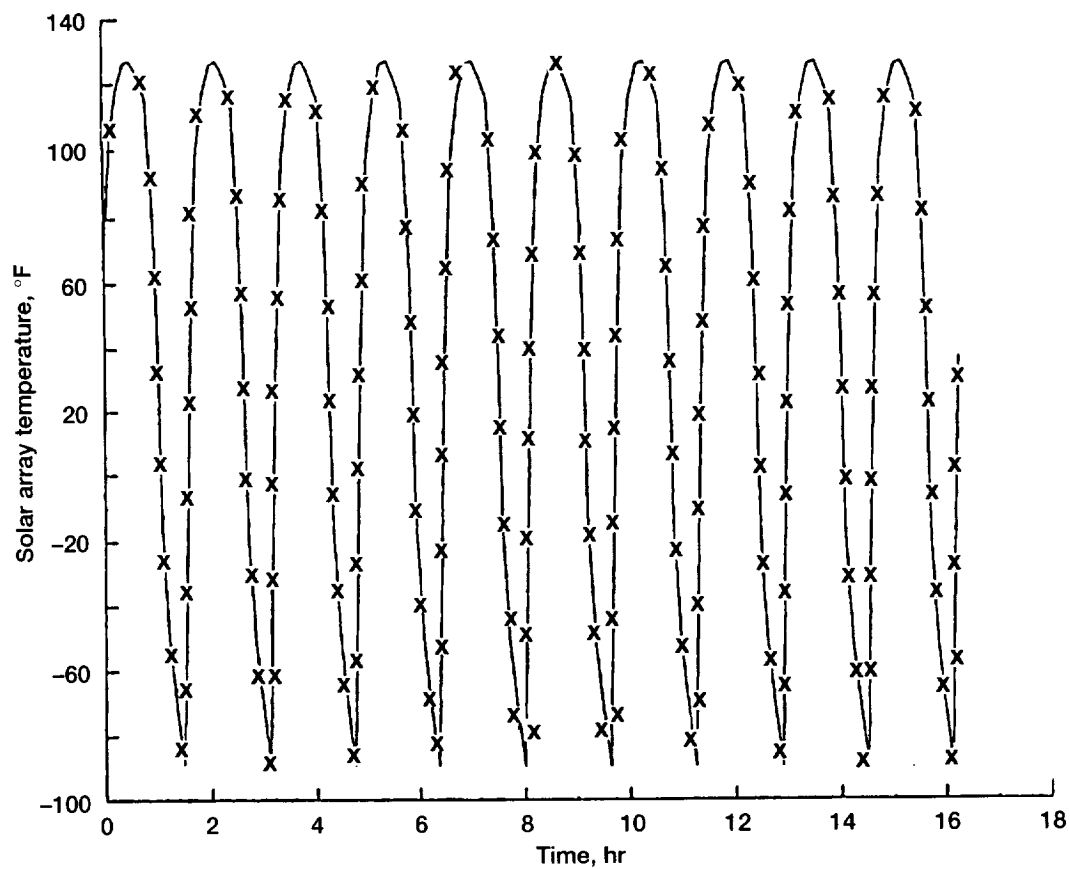


Figure 10.6.—Plot of solar array temperatures as the spacecraft travels through its orbit.

TABLE 10.5.—SUMMARY OF SOLAR ARRAY CHARACTERISTICS

Characteristics	Subsystem total
Beginning of life, W	1968
End of life, W	1643
Number of cells	17226
Output voltage, V BOL (V EOL)	39.5 (36.0)
Total area, ft ²	190
Active area, ft ²	148
Cell area, cm ²	8
Cell type	N/P silicon, 10 Ω
Total weight, lb	210
Operating temperature, °F	-80 to 135
Stacking factor, percent	83
Instrumentation	3 temperature/wing 1 deployment switch/wing
Watts/ft ² , BOL (EOL)	11.0 (9.2)

TABLE 10.6.—SOLAR ARRAY DEGRADATION FACTORS

Degradation factor	Current	Voltage
Assembly loss	0.98	0.98
Blocking diode drop	---	.8
Cell wiring loss	---	.005 V/cell
Thermal cycling	---	.99
UV radiation	.99	-----
Micrometeoroids	.99	-----
Particle radiation	.98	.97
Summer solstice	.968	-----
Vernal equinox	1.00	-----

Also considered were degradation factors that affect the efficiency of the arrays over the mission lifetime. The degradation factors considered include thermal cycling, ultraviolet radiation, micrometeoroids, and particle radiation. Additional design factors were assembly loss, blocking diode voltage drop, and cell wiring loss. These losses are encountered during assembly and do not change or reoccur during operation. A listing of the degradation factors is shown in table 10.6. The numbers that were used in sizing the arrays were from Solarex Aerospace (Private correspondence from E. Gaddy, Director of Aerospace Products, Solarex Aerospace Division dated July 19, 1989.) and solar array design articles (ref. 1). They are for an array operating life of 6 months. Considering the degradation factors and the physical size of the arrays, the beginning of life (BOL) power output is 1968 W and the end of life (EOL) power output is 1643 W. This works out to a power density of 11.0 W/ft² BOL and 9.2 W/ft² EOL.

Before the arrays can be sized, several other requirements have to be derived. Along with the orbit parameters and degradation factors already mentioned, the spacecraft power usage and battery recharge power need to be determined. The spacecraft power requirements were determined to the electrical component level, and then the batteries were electrically sized. After the batteries are sized and their recharge requirements are known, the array power output requirement is determined by summing the spacecraft loads and the battery recharge requirement. Since these loads do not decrease with time, the arrays must supply this power at the EOL.

To summarize, the following effects are considered by using the methods given in Agrawal (ref. 6)

- (1) Solar intensity variation
- (2) β angle variation
- (3) Solar cell degradation caused by environmental effects
- (4) Assembly inefficiencies
- (5) System inefficiencies

A 25 percent margin is applied to the load power requirement which then becomes 813 W. The inefficiencies of the power system's components are considered as well to determine the total solar array output requirement at EOL.

After calculating the array power requirement, the voltage and current of each cell is calculated by using solar cell output equations. Vendor data and the various degradation factors are

input in to the equations. Then the total spacecraft voltage and current requirements are divided by the individual cell outputs to get the number of series and parallel cells. The solar cell size is 2 by 4 cm, and the following cell characteristics are used:

$$\begin{aligned} I_{mp} &= 0.288 \text{ A} & I_{sc} &= 0.329 \text{ A} \\ V_{mp} &= 0.480 \text{ V} & V_{oc} &= 0.598 \text{ V} \end{aligned}$$

where I_{mp} is the cell current at maximum power operating point at BOL at 28 °C, V_{mp} is the cell voltage at maximum power operating point at BOL at 28 °C, I_{sc} is the cell short circuit current, and V_{oc} is the cell open circuit voltage.

Equations (10.3) and (10.4) are used with the previous values and design factors for calculating the voltage and current, respectively, of each cell.

$$v = [V_{mp} - V_d + C_v(T - 28)]K_a K_d \quad (10.3)$$

where

V_{mp}	BOL cell voltage at maximum power operating point
V_d	wiring loss per cell
C_v	temperature coefficient (voltage)
T	temperature
K_a	assembly loss
K_d	radiation and thermal cycling loss
v	cell voltage

$$\begin{aligned} v &= .48 - 0.005 - 0.0022(60 - 28)(0.98)(0.96) \\ v &= 0.381 \text{ V} \end{aligned}$$

At BOL, the cell voltage is $0.381/0.96 = 0.396 \text{ V}$.

Assuming that two blocking diodes are used on the array and that the voltage drop is 0.8V/diode, this number is added to the array output voltage (here 36 V) and divided by the voltage per cell to get the number of required series solar cells, N_s .

$$\begin{aligned} N_s &= (\text{array voltage} + \text{diode drop})/(\text{cell voltage}) \\ &= 91 \text{ cells} \end{aligned}$$

The cell current is given by the following equation:

$$I = [I_{mp} + C_i(T - 28)]K_a K_d K_s K_b \quad (10.4)$$

where

I_{mp}	BOL cell current at maximum power operating point
C_i	temperature coefficient (current)
T	temperature
K_a	assembly loss
K_d	radiation and micrometeoroid loss

K_s seasonal variation in solar intensity
 K_b cosine of incident angle of Sun line
 I cell current

$$I = [0.288 + 0.00013(60 - 28)](0.98)(0.96)(0.968)(0.985)$$

$$I = 0.262 \text{ A at EOL}$$

At BOL the current is $0.262/0.96 = 0.273 \text{ A}$. The required current per array, I_t , is

$$I_t = (\text{power/array voltage})$$

$$= 821.5/36$$

$$= 22.8 \text{ A}$$

The required number of cells in parallel, N_p , is calculated by dividing the current per array by the current per cell; that is,

$$N_p = (I_t/I)$$

$$N_p = 87 \text{ parallel cells}$$

COLD-SAT arrays require 99 series cells in each string and 87 parallel cell strings in each array. A total of 17 226 cells is required.

As the spacecraft enters the eclipse portion of the orbit, the array temperature drops to a minimum of -80°F . As it proceeds back into sunlight, the voltage of the array is increased for a short time because of the low temperature. At -80°C the voltage is 0.692 V per cell. This is an increase of 0.283 V compared with a cell at normal operating temperature. The solar array voltage is increased from 36.1 to 68.5 V at EOL. The cell current is not as significantly affected by a decrease in array temperature as the voltage.

An estimate of the area of the array can be made based on the cell size, cell spacing, and a small margin. The number of cells is 99 series by 87 parallel. The cell size is 2 by 4 cm, and 1 mm is allowed for spacing between cells. An additional 12-cm margin is allowed all around. If these sizes are used, the estimated area of a single array is 88 284 cm^2 or 95 ft^2 . The total array area is then 190 ft^2 .

10.5.4 BATTERIES

Following the selection of battery type, the desired depth of discharge was selected based on the number of cycles required, and mission life. The orbit parameters determined sunlight and eclipse periods, which, in turn, determined number of cycles required. For a nickel-cadmium battery requiring 2600 cycles, a depth of discharge greater than 40 percent can be used. This, in combination with power budgets, enabled electrical sizing of the batteries for normal on-orbit operation. Following this procedure, it was determined that a battery capacity driver was the orbit acquisition phase, rather than the normal on-orbit power profile. Because of this, the battery depth of discharge

TABLE 10.7.—SUMMARY OF COLD-SAT
BATTERY CHARACTERISTICS

Characteristic	Value
Type	Nickel-cadmium
Quantity	2
Capacity (each), A-hr	36
Dimensions, in.	16 by 15 by 9
Weight (each), lb	85
Number of cells	24
Discharge voltage, V	28.8
Charge voltage, V	36
Efficiency, percent	77
Operating temperature, $^\circ\text{C}$	0 to 30
Depth of discharge, percent	24.7
Number of cycles required	2503
Number of cycles capable	>8000

selected is less than is needed if on-orbit requirements are the design driver. Table 10.7 lists the battery performance characteristics.

An initial battery capacity selection was made, and it was adequate for nominal acquisition but did not have sufficient margin for keeping minimum spacecraft functions powered if another acquisition attempt was required. After analysis and discussions, the battery size was increased to 36 A-hr. This would permit additional acquisition time and provide larger margin for on-orbit operation. The minimum margin for acquisition time was established by examining the orbit acquisition sequence and power profile. In addition, the time required for corrective measures was determined. The total time was 2.8 hr. After this time, depending on the particular failure mode, the chances for recovery decrease. Some power can be generated by the folded arrays, even if the spacecraft is spinning, which will increase the available power. However, this is not a certainty because the spacecraft may be tumbling such that the arrays do not pass through the Sun line. The drawback of the larger batteries was additional weight compared to the initial selection.

Battery size calculations are based on a 6-month mission, a 550-n mi circular orbit, an inclination of 18° , a 850-W power requirement, and a nominal voltage of 28 V. The eclipse times range from 28 to 35 min and the Sun times range from 70 to 77 min each orbit. For a 6-month mission, a 25-percent depth of discharge will allow over 8000 charge/discharge cycles. Only 2500 cycles are required of the COLD-SAT batteries so an adequate margin is present with a 25-percent depth of discharge. The minimum discharge voltage at EOL for a nickel-cadmium battery cell is 1.2 V. To achieve a nominal 28-V battery voltage at EOL, 24 battery cells will be needed. If each battery supplies half of the required power, the battery capacity needed is given by the following equation:

$$C = \frac{Pt}{[(V_{db})(DOD)]} \quad (10.5)$$

where

C battery capacity, A-hr
 P load power, W
 t discharge time, hr
 V_{db} bus voltage, V
 DOD depth of discharge

$$C = (425 \text{ W})(0.583 \text{ hr}) / ((27.2 \text{ V})(0.25))$$

$$C = 36.4 \text{ A-hr}$$

Therefore, two 36-A-hr nickel-cadmium batteries were selected. This allows some margin for nominal operations because the capacity was calculated by using the longest eclipse time. Also, this battery capacity allows margin for extra orbit acquisition time. It would be possible to reduce the capacity of the batteries for on-orbit requirements; however, the attitude acquisition requirements drive the battery capacity to 36 A-hr.

After the desired spacecraft attitude is achieved and nominal operations begin, the batteries supply all power during eclipse. After discharging during eclipse, the solar arrays will completely recharge the batteries during daylight. A slightly higher voltage than the normal battery cell voltage is required to fully charge the batteries. The maximum allowable cell voltage is 1.5 V. Since there are 24 cells, the maximum charge voltage is 36.0 V at the battery terminals. To determine the recharge power that is required, it was assumed that battery efficiency is the product of the recharge factor and the ratio of the discharge voltage to charge voltage (ref. 2). The battery recharge factor BRF is assumed to be 0.96. The battery efficiency, η_b , is given by the following equation:

$$\eta_b = \left(\frac{V_{dc}}{V_{rc}} \right) (BRF) \quad (10.6)$$

where

V_{dc} cell discharge voltage, V
 V_{rc} cell recharge voltage, V
 BRF battery recharge factor

Substituting values into equation (10.6) results in a battery efficiency of 0.77.

If it is assumed that only 95 percent of the available time for recharging will be used to allow the solar array temperature and voltage to stabilize, the battery recharge power is calculated in equation (10.7) as follows:

$$P_{rc} = \frac{(P_{dc})(t_{dc})}{[(t_{rc})(\eta_b)]} \quad (10.7)$$

where

P_{dc} discharge power, W
 t_{dc} discharge time, min
 t_{rc} recharge time, min
 η_b battery efficiency

Substituting the appropriate values in equation (10.7) indicates that 291 W are required to recharge each battery or 582 W for both.

Next, the recharge current, I_{rc} , is calculated by using the following equation:

$$I_{rc} = \frac{P_{rc}}{V_{rb}} = 8.08 \text{ A / battery} \quad (10.8)$$

where

V_{rb} maximum battery recharge voltage, V

Equation (10.9) is used to determine charge rate. The charge rate depends on battery cycle life, temperature control limitations, and time available.

$$CR = C / I_{rc} \quad (10.9)$$

where

CR charge rate in terms of the battery capacity
 C battery capacity (A-m)

For COLD-SAT $CR = C / 4.45$.

The solar arrays must recharge the batteries but the system efficiency is less than 100 percent so some of the power generated by the arrays will be lost as heat in the electrical components. If a total of 582 W is required at the battery terminals, then considerably more power must be generated by the arrays to account for the inefficiencies. The array power to recharge the batteries is 735 W based on the estimates of the system inefficiencies as shown in figure 10.7.

For the part of the mission where the orbit is such that the eclipse is shortest, less recharge power is required. The shortest eclipse is 28 min, which leaves 77 min out of the 105 min for recharge. The required recharge power can be calculated for the new orbit parameters by using the previous method. This will yield a minimum recharge power requirement, (the previous recharge requirement was a maximum). When the orbit is such that eclipse is shorter and less power is needed for recharge, the β angle penalty is greater so the solar arrays generate relatively less power. The cant angle of the arrays takes advantage of the relationship of the eclipse times to β angle and minimizes the array size that is required for a given electrical load.

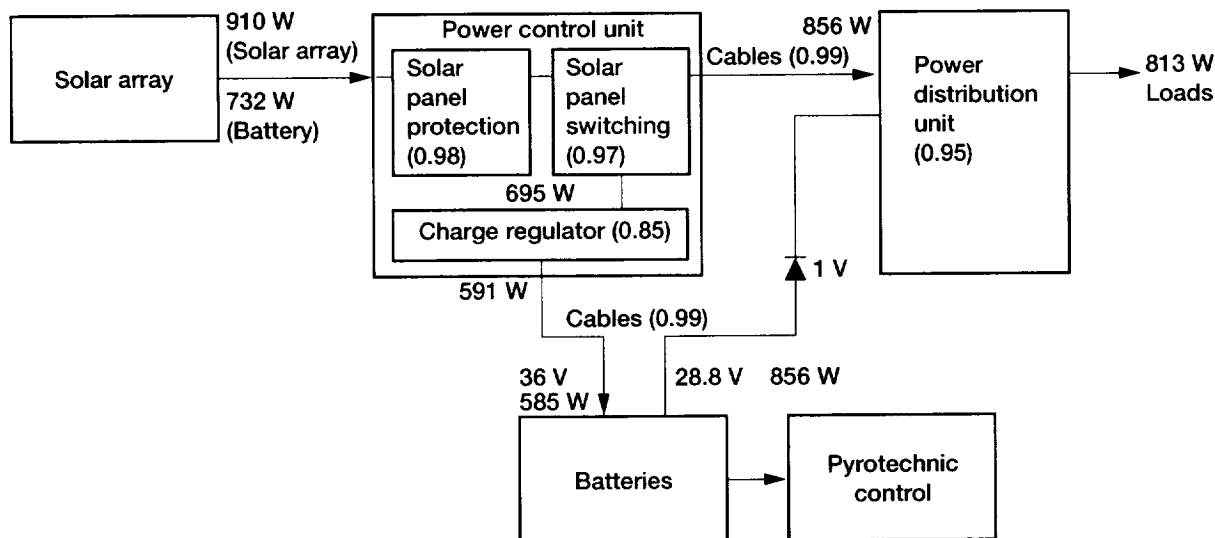


Figure 10.7.—Electrical power system inefficiencies. Parenthetical numbers indicate efficiency of item.

10.6 Power System Configuration

10.6.1 GENERAL

The electrical power system consists of two fixed solar arrays, two nickel-cadmium batteries, a power control unit, a power distribution unit, and a pyro control unit. The power system provides power generation, storage, distribution, and fault protection. It also supplies power and control for pyro firing.

The nominal bus voltage is 27 to 34 V at EOL, and the average load power requirement is 646 W. The solar arrays supply power to the loads and charge the batteries during the orbital day, while the batteries supply power during eclipse periods and supply pulse and peak loads as necessary. The solar panel power flow, battery charge and discharge functions, power distribution, and bus shedding will be controlled by the power control unit and power distribution unit. For system data, the EPS contains temperature, voltage and current sensors, and position switches on the arrays.

Figure 10.8 shows a block diagram of the EPS. The solar arrays interface with the power control unit, which contains array protection circuits, solar array string switching units, and the battery charge regulators. The power control unit interfaces with the batteries and the power distribution unit. The interface with the batteries provides power for battery charging as well as inputs from the battery for battery temperature and voltage data. The interface of the power control unit with the power distribution unit supplies array power to the main power bus.

The batteries interface with the power distribution unit where battery power connects to the main bus. Diodes prevent power flow from the main bus to the batteries. The batteries also

are connected to the pyro control unit, which will only be used at the beginning of the mission.

The power distribution unit interfaces both battery power and solar array power and distributes the power to the rest of the spacecraft. Load power is routed through the power distribution unit to components in the various spacecraft systems. However, much of the power is first interfaced with the sequencers in the TT&C system. It is the sequencers that handle most of the individual load switching. The EPS configuration will be described in more detail in the following sections.

10.6.2 SOLAR ARRAYS

Two solar array wings will be deployed during the attitude acquisition phase by firing pyros, which cause the release of the arrays. The arrays are positioned by a spring deployment mechanism. Upon deployment, the arrays are locked into place and are fixed to the spacecraft near the center of mass and 180° apart. Each array is canted 10° with respect to the axis of the spacecraft. The cant reduces the power penalty incurred because of the difference between the orbit plane and the ecliptic. Both arrays are illuminated for 70 to 77 min/orbit. Because their performance will degrade over time, the arrays are sized to generate enough power to supply load power and charge the batteries at EOL during summer solstice when incident solar energy is lowest.

The BOL capability of the arrays is 1968 W, but degradation causes the output to reduce to 1643 W at the end of the mission. The total area of both arrays is 190 ft²; each array is 95 ft². Based on similarly sized arrays for existing spacecraft, the estimate for total array weight is 210 lb. In order for the arrays to generate the correct voltage and current, the solar array cells

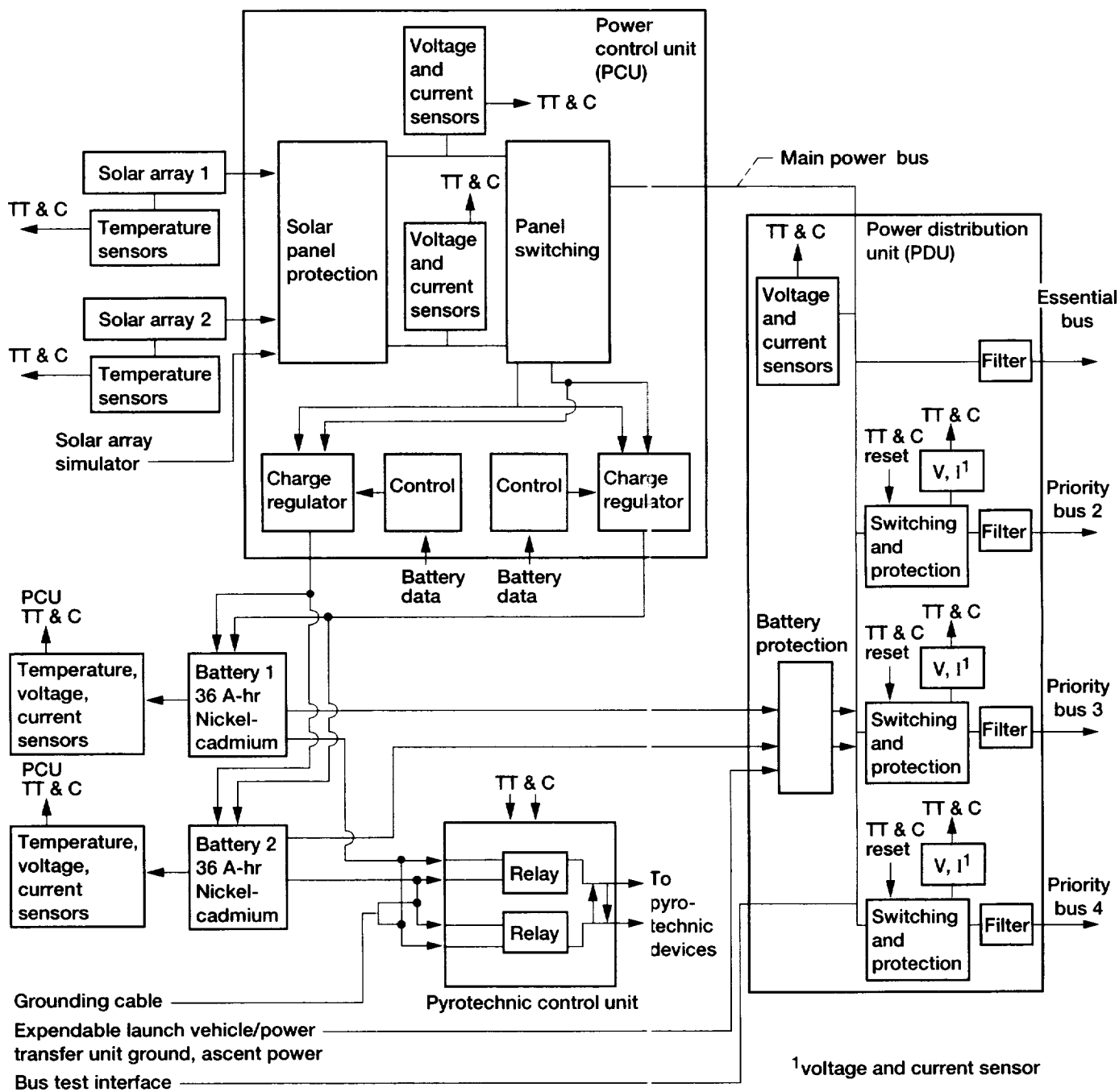


Figure 10.8.—Block diagram of the electrical power system.

are configured in series and parallel strings based on the output of the solar cells and the voltage and current requirements of the system. COLD-SAT arrays are baselined with 99 series cells and 87 parallel cells. With this design, the array voltage is nominally 37.7 V. Diode protection would be wired in parallel with groups of cells so that if a cell or cells in the group failed open or were shadowed, the diodes would permit current to continue to flow. With this configuration, the power for the entire string would not be lost, only the group of cells bypassed by the diode. The number of series and parallel solar cells in a group have not been determined.

Solar cells on COLD-SAT are silicon N/P cells with a base resistivity of 10 Ω . A typical array panel consists of a cover glass, solar cell, fiberglass insulator, substrate aluminum face sheet, honeycomb core, second face sheet, and thermal paint, in that order. Adhesives are used to fasten the various layers to each other, and solder is used to interconnect the cells.

10.6.3 BATTERIES

A battery on the equipment module of the Centaur upper stage of the ELV will provide 443 W for ascent power. The battery is a 100 A-hr silver-oxide battery, which is adequate during ascent but which cannot be operated prior to launch during extended holds. If a long launch delay is expected, the Centaur batteries will be switched off and ground power will be used. The battery use is dedicated to the COLD-SAT spacecraft, but it remains with the Centaur after the COLD-SAT separates from the Centaur. The interface between the Centaur battery and the COLD-SAT batteries is the power transfer unit, which is also located on the Centaur. This service is provided as an option by the Atlas I launch vehicle.

COLD-SAT battery operation will start just before separation from the Centaur upper stage. The operation of the batteries is critical during the attitude acquisition phase of the mission. Spacecraft batteries will power the COLD-SAT until solar array operation begins. During this time, the electrical load is 578 W.

Nominally, the solar arrays should be deployed and have acquired Sun within 48 min of switching from Centaur batteries to spacecraft batteries, which provides a margin of 2 hr. The actual time to acquire the correct attitude is approximately 13 min, but the total time of 48 min to Sun acquisition includes a possible worst-case eclipse delay that would occur if the arrays are deployed as the spacecraft was just entering into eclipse. This 48-min acquisition scenario results in a 23-percent depth of discharge. In the event that attitude cannot be acquired on the first attempt, the worst-case mission timeline indicates that backup scenarios to deploy the arrays and acquire the Sun will be accomplished within 2.8 hr. In this case, the battery does not provide margin, but the spacecraft can be switched to a low power "keep alive" mode which requires 228 W. The batteries are capable of supplying keep alive power for 8.8 hr. If Sun is not acquired by this time, the spacecraft

would lose all power. Also, the arrays will be configured so that, even if they are not deployed, they will generate partial power, which will enable at least partial load power and battery recharging. This can extend the time available to deploy the arrays and acquire the Sun, but it is difficult to calculate how much time this could add.

Two 36 A-hr sealed nickel-cadmium batteries are used to power COLD-SAT throughout the mission during the eclipse periods. The nickel-cadmium cells COLD-SAT will employ are sealed but incorporate pressure relief devices to preclude hazardous pressure increase. Nickel-cadmium battery cells have low internal resistance and a nearly constant discharge voltage of approximately 1.2 V. The required charge voltage is 1.5 V/cell. The cells are well suited for high discharge rates and pulse load applications. Each battery is composed of 24 cells. There are diodes in parallel with each cell so that charge and discharge functions would still be possible in case a cell fails open. COLD-SAT battery cells will operate over the temperature range of 0 to 30 °C.

The nominal depth of discharge is 24.7 percent, which will allow over 8000 charge and discharge cycles. Only 2500 cycles are required for a 6-month mission at an altitude of 550 n mi. A constant-current charge method will be used at a rate of C/4.7. A listing of battery characteristics is presented in table 10.7.

Along with supplying power to COLD-SAT during eclipses and periods of peak power demand, the spacecraft batteries also power the pyros. COLD-SAT has pyros for solar array and antenna deployment as well as for controlling the doors on the experiment system's supply tank purge bag. Separate and redundant power buses are used for pyro activation.

10.6.4 POWER CONTROL UNIT

As described earlier, the solar arrays and batteries are a large part of the power generation and storage, but the power control unit assists with those functions. The power control unit switches solar array circuits off when there is excess power, regulates the battery charge functions, and buses power to the power distribution unit.

The power control unit (PCU) connects to the solar arrays, the power distribution unit (PDU), and the batteries. It contains circuits for solar array protection, array switching, and battery charge regulation. It also contains data interfaces with the TT&C system and the batteries.

The PCU interfaces with the solar arrays by means of harnesses that carry the power to the PCU. The PCU contains diode circuitry to prevent reverse power flow to the arrays, which would damage cells.

The PCU also contains switching circuits that can switch off unneeded incoming power from the arrays. The solar arrays are divided into strings, based on cell characteristics, bus voltage, and current requirements. The strings are configured and interfaced in the PCU such that the bus and load requirements are met. Electronics in the PCU compare the array current to the bus

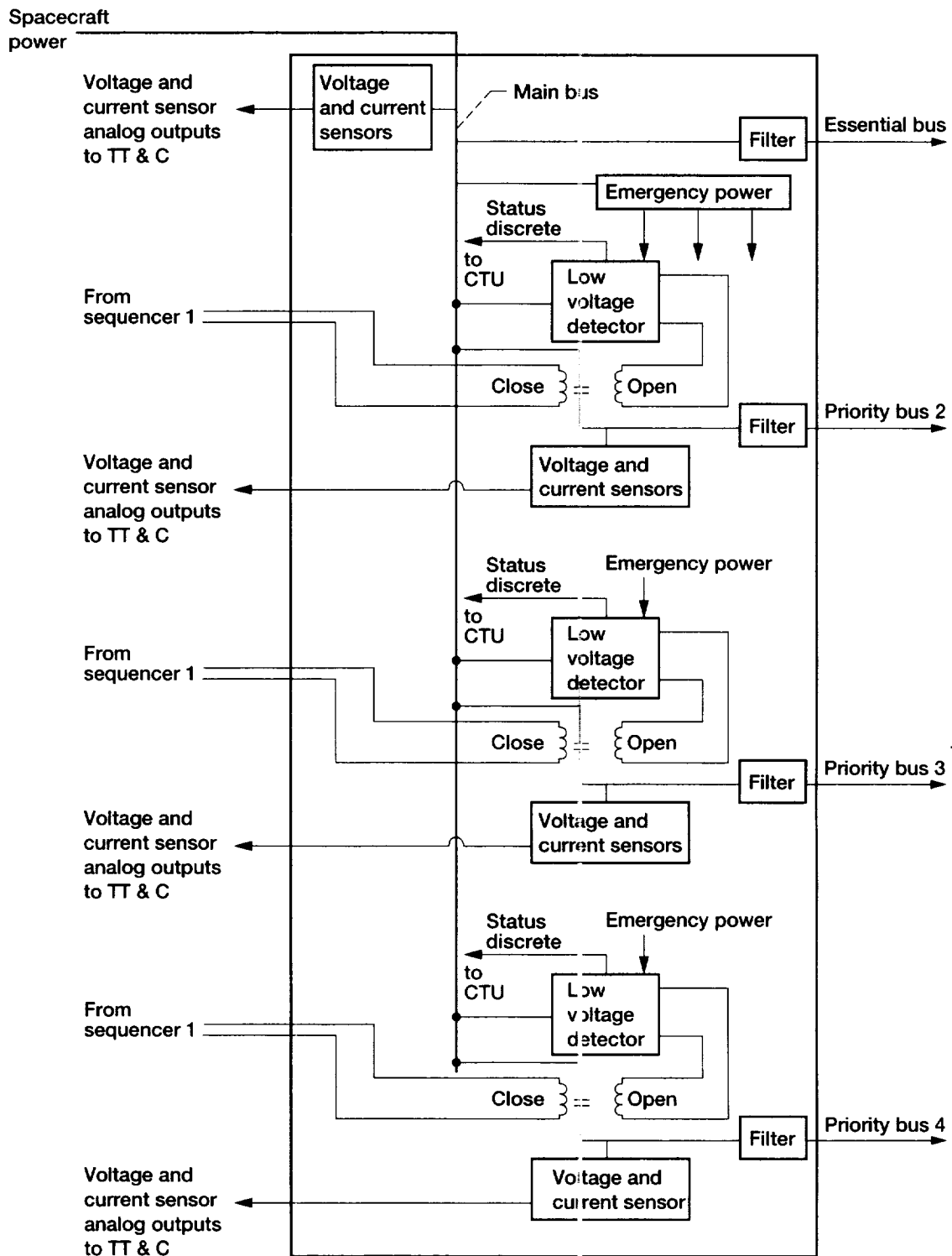


Figure 10.9.—Power distribution unit.

and shunt currents to determine when to switch out array circuits to reduce the available power. When the power generated by the arrays exceeds that required by the loads, the relays are opened, disconnecting the array circuits so the incoming power meets or slightly exceeds demand. The remaining excess power will be dissipated as heat in a resistive shunt.

The PCU also contains redundant regulators to control battery charging. The regulators will boost array voltage to match the voltage requirement for battery charge. The voltage from the arrays at the EOL will roughly match or be slightly less than the required battery charge voltage of 36.0 V. As the array voltage decreases over the mission life because of degradation, more regulation will be required.

Battery current, voltage, and temperature data are provided to circuits in the PCU to indicate charge state. Also, the current, voltage and temperature data is sent to the TT&C system for downlink.

10.6.5 POWER DISTRIBUTION UNIT

The design of the PDU includes capabilities to detect low bus voltage, measure bus current and voltage, switch off distribution buses from the main bus, receive commands from the TT&C system, send status signals to the TT&C system, and distribute power on four buses. Figure 10.9 shows the power distribution unit in more detail.

The PDU interfaces the battery buses and the solar array bus with the main power bus. The PDU also divides the main power bus into four buses that distribute power to the entire spacecraft. The four buses that form the distribution system are the essential bus, priority bus 2, priority bus 3, and priority bus 4. Figure 10.5 illustrates the individual buses and the loads they supply.

The essential bus powers the loads that are necessary to maintain communications capability on the spacecraft. Sequencer 1 is also powered by this bus. This is because at least one transponder is essential, and the capability to switch the transponders must be maintained by a sequencer. In the event that power demand is greater than power availability, individual components or even complete buses can be shed except for components on the essential bus. This bus must be powered at all times. The total power distributed by this bus is 272 W.

Priority bus 2 powers TT&C and attitude control components. This bus will enable attitude control functions to be performed. It can be shed, but only in extreme circumstances because, without this bus, the spacecraft will begin to drift. The attitude control system interface electronics box is powered from priority bus 2 and distributes power to attitude sensors and gimbal units. The total power distributed by this bus is 202 W.

For redundancy, priority buses 3 and 4 interface with both sequencers in the TT&C system. The sequencers provide switching to individual components in the experiment, propulsion, and thermal systems. The loads on these buses were divided so that each bus carries approximately the same power

and each sequencer contains approximately the same number of relays. Each sequencer has redundant power interfaces with the PDU. Bus 3 distributes 380 W, and bus 4 distributes 395 W.

Also contained in the PDU are load-shedding relays that are normally closed but can be opened to disconnect the main bus from one of the spacecraft load buses. Control of the relays is based on data from low voltage detectors. Each bus is monitored by a detector that inputs a signal to a controller to open the relay if low voltage occurs. A small emergency power source in the PDU, possibly capacitors or a battery, will provide power to open the relays if power drops rapidly. The unit can automatically and sequentially switch off buses, beginning with priority bus 4. A control interface exists with the TT&C for reconnecting buses after load-shed.

Data are sent to the TT&C system to provide temperature, voltage, and current measurements for downlink.

10.6.6 PYRO CONTROL UNIT

The pyro control unit is the interface between the batteries and the pyros. The unit contains arming circuits so each device can be isolated from the power supply until immediately before operation. Each battery sends 28 V power through redundant relays to actuate the pyros. Redundant inputs from the TT&C system control the firing of the pyros. During ground operations, a grounding cable is installed to prevent inadvertent actuation of the pyros. Manual access to this unit is required for connecting and disconnecting the grounding cable.

10.6.7 HARNESES

Electrical cables are used for input commands, data, power, and grounding. The cables are designed to withstand launch loads, temperature variations, vacuum, and other space effects. Flight-proven electrical connectors will be used. Where possible, each connector can only extend to its mating connector and cannot reach a mating connector of the same type. Connectors are keyed by a pair of toothed plugs and mating sockets to preclude mating errors.

10.6.8 INSTRUMENTATION

Instrumentation requirements are identified in table 10.8. Solar array instrumentation consists of temperature sensors on the arrays and position switches on the deployment mechanisms. Battery instrumentation requirements include temperature, current, and voltage. They are needed to indicate charge and discharge states. It is possible that each of the cells in the batteries will have a voltage sensor. The PCU has temperature, current, and voltage sensors. The current sensors will monitor input current from the solar arrays as well as output current of the PCU. The PDU also contains temperature, current and voltage sensors. All the data will be transmitted to ground controllers through the TT&C system.

TABLE 10.8.—ELECTRICAL POWER SYSTEM INSTRUMENTATION REQUIREMENTS

	Current		Voltage		Temperature		Pressure		Other	
	Each	Total	Each	Total	Each	Total	Each	Total	Each	Total
Solar array	1	2	--	--	3	6	--	--	^a 1	2
Battery	1	2	--	--	4	8	--	--	--	--
PCU	12	12	7	7	2	2	--	--	--	--
PDU	10	10	10	10	7	7	--	--	--	--
Pyro box	2	2	--	--	2	2	--	--	--	--
Total	28		17		25		---		2	

^aDeployment switch.

10.6.9 GROUNDING AND BONDING

Spacecraft grounding will be designed to comply with the requirements of MIL-STD-1541. The grounding scheme of the power system will consist of a balanced static drain to a single-point ground on the spacecraft structure. Prior to connection of equipment to the EPS, both power leads will have a minimum dc resistance of 1 m Ω to case or to any common or ground connection. The grounding and isolation of pyrotechnic circuits will conform to MIL-STD-1512 (Electroexplosive Subsystem, Electrically Initiated, Design Requirements and Test Methods).

Requirements of MIL-B-5087B (Bonding, Electrical and Lightning Protection for Aerospace Systems) will be observed with regard to bonding characteristics. The basic provisions are that structures supporting electrical equipment will be bonded by use of permanent metal-to-metal joints and semi-permanent metal-to-metal joints. Mating surfaces will be free of non-conductive film. To minimize problems of electrostatic charging, exposed dielectric surfaces will be coated with a conductive film. Electrical equipment will be bonded to its supporting structure with a maximum bonding resistance of 2.5 m Ω .

10.6.10 SAFETY

Safety considerations were included in the conceptual design. Potential hazards were identified in connection with the batteries and the ordnance, although any electrical power system components with current flowing could be a hazard.

Ordnance was identified as a safety concern during pre-launch servicing, countdown, launch, and ascent. The concern is inadvertent actuation causing harm to personnel or equipment. To preclude this event, physical inhibits are used prior to launch. After launch, software in connection with redundant inhibits will ensure that erroneous actuation will not occur.

Also of concern is handling and interfacing equipment during checkout procedures. Interfacing the wrong connectors can be hazardous to personnel and equipment. To prevent this, connectors will be keyed so that it will be impossible to connect the wrong components.

10.7 Electric Power System Function

10.7.1 POWER GENERATION AND STORAGE

The EPS supplies power at all times during the mission to the experiment and spacecraft systems. Prior to launch, during pad operations, ground power will be supplied to the EPS for distribution to necessary components and GSE will control the state of charge of the COLD-SAT flight batteries. At T-16 min ground power is terminated and a mission peculiar battery on the Centaur begins to power the spacecraft. A 100-A-hr, silver-zinc battery on the equipment module of the Centaur upper stage will provide 443 W for ascent power, but cannot operate prior to launch during extended holds. If a long launch delay is expected, the Centaur batteries will be switched off and ground power will be reconnected. The COLD-SAT spacecraft has dedicated use of the battery, but it remains with the Centaur after separation. The interface between the Centaur battery and the spacecraft is the Centaur power transfer unit. The launch vehicle will switch off power to the spacecraft just prior to separation.

The spacecraft battery is already connected to the main power bus so there is no power interruption when the battery on the Centaur is disconnected. The COLD-SAT batteries then power the necessary spacecraft functions until the arrays are deployed and the proper attitude is acquired. During this time, the electrical load is 578 W. This permits basic spacecraft acquisition functions and venting of the experiment tank. After separation from the launch vehicle, the solar arrays should be deployed and have acquired Sun within 48 min of switching from the Centaur battery to spacecraft batteries, which provides a margin of 2 hr. The nominal time to acquire the correct attitude is approximately 13 min, but the total time of 48 min to Sun acquisition includes a possible worst-case eclipse delay that would occur if the arrays were deployed as the spacecraft was just entering into eclipse. This scenario results in a 23-percent depth of discharge.

In the event that arrays cannot be deployed or attitude cannot be acquired on the first attempt, the worst-case mission timeline indicates that backup scenarios to deploy the arrays and acquire

the Sun will be accomplished within 2.8 hr, resulting in an 83-percent depth of discharge. In this case, the battery does not provide margin beyond the 2.8 hr, but the spacecraft can be switched to a low power "keep alive" mode which requires 228 W. The batteries are capable of supplying keep alive power for a total of 8.8 hr, or about 8 hr after attempting an acquisition sequence. If this were to occur, eight orbits will be required to fully recharge the batteries. This would be accomplished with the spacecraft power usage kept at the acquisition phase power level. After recharging the batteries, normal spacecraft functions would commence.

If the Sun is not acquired before the batteries are depleted, the spacecraft will lose all power. However, the solar arrays will be configured so that even if they are not deployed, they will generate partial power, which will enable at least partial load power and battery recharging. This can extend the time available to attempt to deploy the arrays and acquire the Sun, but it is difficult to calculate how much time this could add.

The arrays are deployed by firing pyros to release the arrays which are then positioned by a spring deployment mechanism. Upon deployment, the arrays are locked into place and are fixed to the spacecraft near the center of mass and 180° apart. Each array is canted 10° with respect to the spacecraft axis.

Both arrays are illuminated for 70 to 77 min/orbit out of a possible 105 min. No shadowing of any part of the arrays from the spacecraft body will occur at any time. Nominally, 36-V power is generated by the arrays and delivered to the PCU. There are voltage drops between the solar array output and the loads, so the voltage is reduced to approximately 34 V at the loads. The load voltage will decrease slightly as the solar cells degrade with time but will be in the range of 27 to 36 V.

The bus voltage is unregulated. If loads have special requirements, an appropriate converter or filter will be supplied by the system responsible for the load. The temperature of the arrays varies by over 210 °F because of cooling while in eclipse and heating while in the Sun. The cooler temperature of the array as it comes out of eclipse will cause the array voltage to increase to 68.5 V, but this voltage will decrease in several minutes as the temperature increases. The batteries will continue to power loads until the array voltage drops to an acceptable level.

The power control unit contains circuits to protect the arrays from reverse power flow (ref. 2) when the array output is low. The PCU also contains switches and shunts to match the bus power to the power demand. If the power being generated by the arrays exceeds the power demand, the regulator switches out array circuits until the supply meets the demand. Each section is connected to the bus through at least one switch. There is also a small dissipative shunt that provides control when the difference between power demand and power generated is less than the power controlled by the switches. For example, if the array generates much more power than is needed, the regulator switches out a circuit. If the power available is still greater,

another circuit is switched off. This continues until the available power is still greater than the power demand, but close enough to the power demand that switching off another circuit would make the available power less than the demand. When the power available is close to, but still greater than the demand, the analog shunt dissipates the extra power.

The bus voltage is maintained at the proper level by matching the current of the solar array circuits to the sum of the shunt current, battery recharge current, and load current. If it is assumed that the battery recharge current remains the same during recharge, a load current increase will result in a shunt current decrease. The load and shunt currents are compared, and if the load current increases resulting in a shunt current decrease below a certain minimum value, another array circuit will be switched on to meet the power demand. Similarly, if the shunt current increases above a specific maximum value, an array circuit is switched off. The shunt size and array circuit size were not determined for this study.

The PCU controls and monitors battery charging. For recharging the batteries, the 34-V charge power is boosted to the approximately 36 V needed to charge the batteries. Battery charging occurs once per orbit. The batteries do not require reconditioning since they are used for a small portion of their available life and depth of discharge is not that great. Voltage detectors indicate when solar array voltage is high and initiates battery charging after allowing time for the array temperature and voltage to stabilize. Charge control is accomplished by time integration of the battery charge and discharge currents, and measurement of battery cell voltage and temperature.

10.7.2 POWER DISTRIBUTION

The power flow from the PCU is to the batteries and to the PDU. The PDU distributes main power to the spacecraft and performs top-level switching functions. As indicated earlier, four buses distribute power to the spacecraft, the essential bus and priority buses 2, 3, and 4. The main bus is divided into these other buses in the PDU.

The bus scheme that was selected was to group the loads by order of importance for load shedding purposes. Loads of least importance to spacecraft survival were placed on priority bus 3 and 4. These are mostly experiment system components and spacecraft heaters. These loads are switched by the sequencers based on software in the TT&C system, so it is also possible to switch loads on an individual basis. Priority bus 2 contains TT&C system, attitude control system, and propulsion system components needed for maintaining spacecraft attitude. The essential bus contains the TT&C, attitude control, and propulsion system components that are essential to commanding the spacecraft from the ground. The PCU and PDU electronics are also on this bus.

10.7.3 DEGRADED PERFORMANCE

Several types of failures can occur in the EPS which will degrade performance. Solar cells can fail open, short, or short to ground. Cells are connected in strings consisting of series and parallel combinations of cells. A short circuit in a cell will cause a power loss from all cells in parallel and the string will deliver power at a reduced current; however, it is not catastrophic to the system. It is less likely for a cell to fail open. If it does occur, the current must flow through the other parallel cells. The string current is reduced, and the voltage across the functioning cells is decreased. The overall string power is significantly reduced. The arrays will be protected by placing a diode across one or more cells. This will limit the loss to only that section.

Battery cells can also fail as can a complete battery. A complete battery failure is unlikely, however, if a battery does fail, the remaining 36-A-hr battery can operate at a 49-percent depth of discharge for approximately 3000 cycles. This is acceptable for a 6-month mission. The charge rate of the remaining battery will increase to C/2.35. If the failure does not affect other power system functions, then all experiment objectives can still be met. An individual battery cell can fail open, short, or short to ground. If a cell fails open, a bypass diode across the cell will permit current to flow. A cell failure will result in a voltage drop, but several cells can fail before the voltage drops below 24 V.

Load shedding is based on the importance of the loads and is commanded either from the spacecraft computer or autonomously in the power system. Loads are dropped in the order of their importance until power demand is low enough to be supplied. Under-voltage is detected by the TT&C computer and the sequencers are commanded to switch off nonessential loads. The commands originate in the TT&C system. This is the normal manner in which loads are turned on or off, and it can also be used in a certain low voltage situation if the voltage decrease is small and slow. In most low voltage cases, this method of shedding loads will not be effective because the voltage decrease will be sudden and relatively large. In this case, low voltage detectors in the power distribution unit will open relays to disconnect buses. The lowest priority bus will be dropped first and then progressively higher priority buses will be shed if necessary.

Analog instrumentation in the power system compares each of the voltages of the bus with reference voltages. The buses of the power system are configured so that loads of similar importance to the spacecraft are on the same bus. The reference voltage of the least important bus is set the highest so it would be the first bus to be shed. The second most important bus has the lowest set point and longest time delay so it is the last bus to be shed. The most important components are on the "essential bus" and cannot be shed. This scheme assumes the voltage is decreasing slowly.

The TT&C system is the only system that can reconnect the buses. A command from the ground and through the TT&C

system controls the bus relays. This method of control was chosen because, if the same analog instrumentation were used to reconnect buses based strictly on bus voltage, it may be possible to start a toggling of the relays. If low voltage is detected and a bus is shed, the resulting effect may be to increase the bus voltage to a point where the analog instrumentation would sense a voltage high enough to reconnect the bus. This may again drop the bus voltage and restart the cycle.

Faults in the power system loads can be open circuits or short circuits. If the component has an open circuit failure there is little impact on the EPS. A short circuit is more harmful to the system. Two parallel redundant fuses are used in series with the component to clear such a failure.

A partial attitude control system failure could result in shadowing of the solar arrays. The impact of this cannot be exactly determined. It would result in inefficient operation of the illuminated portion caused by less cells and also because the dark cells in a string are a load for the operating cells in that string. As long as some of the array is illuminated, completion of at least some experiments could be expected.

10.8 Components/Heritage

Design goals for the EPS were to minimize weight, volume, cost, and risk. If possible, existing and proven flight hardware would be used in COLD-SAT systems. Table 10.9 shows the physical characteristics and heritage of the EPS components. Many of the EPS components, as currently specified, would require new or partially new designs. Several components exist that perform similar functions, but they are mission specific and not very flexible. Because of the way in which the COLD-SAT power system was baselined, a mostly new design for the power control and conditioning equipment is required. Re-examination of this area may result in locating components that can be used without much modification. One possible approach would be to start with a spacecraft bus that is available from industry. The advantage of doing this is the flight heritage and potential lower cost. The disadvantage is that some of the standard components in the bus may be over- or under-sized for particular applications.

Solar arrays are common items on spacecraft and have much heritage. The COLD-SAT arrays used would use established fabrication techniques and materials. Solar arrays on Cosmic Background Explorer and the Relay Mirror Experiment are examples of spacecraft using cells similar to those used in this design. The COLD-SAT arrays would require a specific electrical configuration to achieve the required voltage and current characteristics. Vendor data are available and design calculations used data from an array vendor. The industry is moving towards use of cells larger than the 2- by 4-cm cells used in this study. By the time COLD-SAT is built, larger cells may have become the industry standard which will increase the packing factor and decrease the array size.

TABLE 10.9.—ELECTRICAL POWER SYSTEM COMPONENT DESCRIPTION

Component	Size, in.	Weight, lb	Volume, in. ³	Reliability	Vendor/heritage	Status
Battery 1	16 by 15 by 9	85	2160	0.9985	Gates energy system	Slight modification
Battery 2	16 by 15 by 9	85	2160	-----	Gates energy system	Slight modification
Solar array 1	11 ft 1 by 9 ft 11	105	----	0.9999	SOLAREX	Slight modification
Solar array 2	11 ft 1 by 9 ft 11	105	----	-----	SOLAREX	Slight modification
Power control unit	12 by 10 by 12	32	1440	0.9970	-----	High mod to new design
Power distribution unit	8 by 12 by 5	25	480	0.9990	-----	New
Pyro control	4 by 5 by 4	5	80	0.9989	-----	New
Cables	-----	248	----	-----	Gore	-----
Current, volt sensor	-----	----	----	NA	American aerospace	-----
Total	-----	690	6320	0.9930	-----	-----

The solar arrays weigh 105 lb each, not including the deployment mechanism or supports. A specific deployment mechanism was not identified, but a spring device would be desired. However, very similar designs have been used on FLTSATCOM and TDRS. These are both rotating arrays so their solar array drives will have to be replaced with a simple one time spring motor to provide the proper cant angle for COLD-SAT.

Batteries are also common items on spacecraft and at least one vendor was identified. As mentioned previously, nickel-cadmium battery availability is questionable for the time frame in which COLD-SAT component procurements are expected to occur. The nickel-cadmium batteries currently baselined in the design weigh 85 lb each. The dimensions are 16 by 15 by 9 in. for each battery. Flight batteries could be purchased with very little, if any, modifications.

The PCU functions are similar to those of PCU's on other spacecraft; however, a new design is required. Existing technology and probably some existing electronic boards could be used. Using existing units as a guide, a weight estimate of 32 lb was made. The size estimate is 12 by 10 by 5 in. No new technology is required, but a new design is. Similarly, the PDU also requires a new design that uses existing technology. The weight estimate is 25 lb, and the size estimate is 8 by 12 by 5 in. The pyro control unit is new but similar in function to units used on many spacecraft. Full redundancy within the unit is required.

10.9 Reliability

The design life of the EPS is 6 months, and the reliability goal is 0.993 to perform at a level sufficient to meet all class 1 experiment requirements. This reliability goal was determined by the overall system design. A top level power system reliabil-

ity diagram was used to estimate the system's reliability. It exactly meets its goal. To achieve the reliability goal, flight proven components were used in the design where possible, and an attempt was made to keep the weight and system complexity as low as possible.

Redundancy is used in several places in the system, providing either full or partial backup in case one of the components fails. The use of redundancy was based on similar spacecraft systems. Two solar arrays and two batteries are used. A failure of one battery would not severely degrade performance, as long as the failure occurred after attitude acquisition. A solar array failure would significantly reduce the experiments that could be conducted, but the mission would still provide data.

The PCU contains redundant regulators and controllers for battery charging. The PDU has redundant buses for buses 3 and 4. The essential bus and bus 2 have are not redundant, but bus or redundant cable failures are considered unlikely. There is also redundancy in the pyro control unit. Redundant power and redundant control signals interface with redundant relays.

References

1. Rauschenbach, H.S.: Solar Cell Array Design Handbook, vol. 1, NASA CR-149364, 1976.
2. Chetty, P.R.K.: Satellite Technology and Its Applications. Tab Books Inc., Blue Ridge Summit, Pennsylvania, 1988.
3. Design Criteria For Spacecraft Solar Cell Arrays: Spacecraft Solar Cell Arrays. NASA SP-8074, 1971.
4. Linden, D.: Handbook of Batteries and Fuel Cells. McGraw-Hill, New York, 1984.
5. Gates Energy Products Applications Manual (Preliminary), Sealed Rechargeable Batteries, pp. 33-89, 101-112.
6. Agrawal, B.N.: Design of Geosynchronous Spacecraft. Prentice-Hall, Englewood Cliffs, 1986.

Chapter 11

Thermal Control System

Hugh Arif

National Aeronautics and Space Administration

Lewis Research Center

Cleveland, Ohio 44135

11.1 Introduction

The purpose of this chapter is to document the design features of the COLD-SAT spacecraft thermal control system (TCS), which maintains the temperature of the spacecraft systems and components within design limits. The TCS design is based on the boundary conditions, component dissipations, temperature requirements, duty cycles, and orbital and other parameters provided by the various COLD-SAT spacecraft systems. However, the spacecraft configuration used throughout this chapter reflects an earlier stage of the design.

The COLD-SAT spacecraft TCS provides active and passive design features for maintaining temperatures within requirements. The TCS has been customized for the temperature and thermal requirements of each of the five modules of the spacecraft, which are, beginning from the spacecraft aft end: electronics bay 1 (EB1), supply tank, electronics bay 2 (EB2), and receiver tank numbers 1 and 2. The exterior thermal design described herein, protects the spacecraft and its components from the orbital environmental fluxes while maximizing the use of these fluxes to reduce heater requirements. The use of the space heat sink has been maximized in the exterior thermal design of the cryogenic components. The interior thermal design of the electronics bays maximizes the use of power dissipation from each electronics box to reduce heater power.

Geometric and thermal math models have been developed for the exterior surface of the spacecraft and the interiors of the electronics bays. The thermal design has been analytically verified by the use of these math models. Temperature predictions have been made for all components and the capability of the TCS has been demonstrated to maintain the component temperatures within the specifications provided for the various systems. Four on-orbit mission conditions and phases have

been analyzed and the TCS viability verified for each. Heater power has been calculated for makeup and survival temperature conditions for each electronics component. Heater power has also been calculated for backup or load substitution conditions in case of loss of operation of an electronics box.

Special consideration was required in dealing with the thermal control of the experiment system because of the division of responsibilities between the thermal design of the spacecraft and of the experiment system tankage and other components. The interface between the spacecraft TCS and the experiment system was maintained at the hot-end boundary of each conductive and radiative path to the experiment component. This boundary was maintained within a specified temperature range by the spacecraft TCS. Although the division of responsibility was resolved, several trades were conducted to determine the effects of spacecraft thermal design on the experiment design before a final selection was made.

For an initial trade on the effects of the spacecraft thermal design on the heat leak into the supply tank, geometric and thermal math models were developed for the supply tank module. Parametric studies with various thermal control materials were performed to determine the impact on heat leakage before a final selection of the outer surface material for the tanks was made. Another trade was performed on the spacecraft attitude impacts on the thermal performance of the supply tank. The results of this study was one of the criteria by which the final COLD-SAT spacecraft attitude for this study was selected.

Materials for the spacecraft TCS were selected based on availability, heritage, cost, weight, and reliability. Vendors were contacted to obtain specific information for the above-mentioned specifications. The final thermal design is documented in this chapter.

11.2 Design Philosophy

The COLD-SAT TCS has a design philosophy of using simple, flight-proven, thermal control hardware to maintain acceptable component temperatures with adequate margins during all mission phases. Temperatures are controlled by techniques derived from previous spacecraft programs, featuring primarily conventional passive design elements augmented as required by controlled heaters. Passive design components include multilayer insulation (MLI) blankets, selected surface finishes, foils and tapes, conduction (coupled/decoupled mounting details), and optical solar reflectors. Louvers and heat pipes were not considered because of increased cost, decreased reliability, and complicated integration. Active components include resistance heaters, thermistors, and autonomous dual-temperature heater controllers. This approach provides simple, yet highly reliable temperature control for all mission conditions.

The TCS is designed to perform under the worst-case combination of external environment and equipment power dissipations to be experienced by the spacecraft. The system provides a margin of 35 °F above and 20 °F below the minimum and maximum component nonoperating temperatures, respectively, for operation under all mission conditions. These conditions account for end of life (EOL) electrical power availability and variation in environmental fluxes, as well as degradation in surface properties.

Since this is a cryogenic experimentation spacecraft, minimization of boiloff losses to enhance cryogen storage life is an important consideration. Every attempt was made to reduce the heat leaks into the liquid hydrogen supply and receiver tanks by lowering the hot-end boundary temperatures of these heat leak paths.

The heater power is minimized for all mission phases. Survival heaters for preoperational housekeeping heater power and makeup heater power during an eclipse are minimized. In addition, payload backup heaters do not add load to the power system. The TCS design approach does not require that restrictions be placed on the electronics operating duty cycles. Commandable backup heaters for load substitution are configured to accommodate a broad range of operational conditions for loss of power and seasonal conditions.

The performance of the MLI blanket design for cryogenic applications is based on previously flown and qualified hardware heritage configuration from the IRAS and COBE programs, rather than ground-based laboratory studies. The performance of the spacecraft thermal control blankets is based on data that is unpublished but verified by testing and flight performance by a major aerospace contractor. Beginning of life (BOL) data for optical thermophysical properties have been considered in the design because of the brevity of the mission.

11.3 Design Drivers and Requirements

11.3.1 CRITICAL DESIGN GOALS

While the TCS provides thermal control for all spacecraft components, control requirements for certain critical elements are key factors in the design, and are noteworthy.

11.3.1.1 Experiment System Supply Tank Module

For the experiment system supply tank module, total heat leak into the pressure vessel from all conductive and radiative sources has to be less than 0.1 Btu/hr-ft². To achieve this goal, the temperature of the purge diaphragm outer surface has to be maintained as cold as possible to reduce MLI radiative heat leaks. In addition, the temperature of the spacecraft structure, from which the supply tank is supported, has to be maintained as cold as possible to reduce parasitic conductive heat leaks through the tank support struts. The plumbing tray, from which all plumbing and wiring harnesses proceed to the supply tank, must have a temperature that is maintained as cold as possible to minimize parasitic conduction. The two receiver tanks of the experiment system also have heat-leak design goals of 0.5 Btu/hr-ft². Since these are higher than the supply tank heat-leak goal, the supply tank was considered to be the design driver for tankage outer-surface material selection.

11.3.1.2 Propulsion System

For the propulsion system, the hydrazine storage tanks and the gaseous helium pressurant bottles have to be maintained above 40 °F, allowing ample margin above the freezing point of hydrazine (34.8 °F). Temperature differences between interconnected tanks are maintained below 10 °F to preclude significant changes in spacecraft center of mass resulting from thermally induced flows. However, heater power requirements have to be minimized by tank layout and passive control, allowing for the maximum use of available power from the spacecraft electronics dissipation.

11.3.1.3 Power System

To maintain optimal performance and recharge capability throughout mission life, the nickel-cadmium batteries have to be maintained within their preferred operating temperature range of 30 to 85 °F.

11.3.1.4 Telemetry, Tracking, and Command (TT&C) System

For the TT&C system, thermal distortion of the high-gain antenna and its support must be minimized to reduce associated radiofrequency (RF) losses.

TABLE 11.1.—ON-ORBIT HEAT DISSIPATION SUMMARY

Component	Attitude acquisition, W ^a	On-orbit peak, W ^b
Telemetry, Tracking, and Command System		
Computer 1	40.0	40.0
Computer 2	40.0	40.0
Transponder 1	18.0	44.0
Transponder 2	18.0	18.0
Radiofrequency processing box	10.0	10.0
Solid-state recorder 1	16.0	16.0
Solid-state recorder 2	16.0	16.0
Remote command telemetry unit 1	17.0	17.0
Remote command telemetry unit 2	28.0	28.0
Remote command telemetry unit 3	28.0	28.0
Command and telemetry unit 1	25.0	25.0
Command and telemetry unit 2	15.0	15.0
Sequencer 1	15.0	15.0
Sequencer 2	15.0	15.0
High-gain antenna	0.0	0.0
Low-gain antenna 1	↓	0.0
Low-gain antenna 2	↓	0.0
Drive motor electronics	↓	18.0
Antenna gimbal motor	8.0	^c 12.0
Redundancy control unit	0.0	8.0
Command receiver	0.0	18.0
Subtotal	309.0	371.0
Experiment System		
Experiment data unit 1	15.0	15.0
Experiment data unit 2	15.0	15.0
Experiment data unit 3	15.0	15.0
Accelerometer conditioner	0.0	10.0
Signal conditioner	↓	15.0
Data acquisition unit	↓	15.0
Mixer motor inverter	↓	15.0
Liquid hydrogen valves	↓	^c 0.0
Experiment heaters	↓	^c 75.0
Gas generation heater	↓	^c 120.0
Gas valve	↓	^c 0.0
Subtotal	45.0	100.0
Propulsion System		
Thruster valves	^c 12.0	^c 36.0
Regulator	^c 25.0	^c 25.0
Solenoid valve	^c 0.0	^c 25.0
Subtotal	37.0	86.0
Attitude Control System		
Gyro assembly	25.0	25.0
Earth sensor 1 electronics	10.0	10.0
Earth sensor 2 electronics	10.0	10.0
Fine Sun sensor 1 electronics	3.0	3.0
Fine Sun sensor 2 electronics	3.0	3.0
Magnetometer 1	1.0	1.0
Magnetometer 2	1.0	1.0
Attitude control electronics	20.0	20.0
Subtotal	73.0	73.0
Power System		
Battery 1	25.0	25.0
Battery 2	25.0	25.0
Power control unit	35.0	35.0
Power distribution unit	35.0	35.0
Pyro control box	0.0	10.0
Subtotal	120.0	130.0

^aDissipation used for cold case ($\beta = 0^\circ$) analysis.^bDissipation used for hot case ($\beta = 41^\circ$) analysis.^cNot included in spacecraft thermal analysis

11.3.2 COMPONENT DISSIPATIONS AND TEMPERATURE REQUIREMENTS

Among all the mission phases that the COLD-SAT spacecraft will have to undergo, the attitude-acquisition phase and the on-orbit post deployment phase have been identified as the lowest and the highest power dissipation phases, respectively. Table 11.1 shows the on-orbit dissipation levels of the COLD-SAT spacecraft components for these two phases. The attitude-acquisition dissipations were used to perform the cold-case thermal analysis for $\beta = 0^\circ$ and the on-orbit peak dissipations were used for the hot-case analysis for $\beta = 41^\circ$. Some spacecraft components, such as the high-gain antenna gimbal motor and the propulsion system valves and plumbing components, have not been included in the math models developed for the thermal analysis. The gimbal motor is at the end of a support boom and away from the other spacecraft components, and therefore, does not have any thermal effects on them. Similarly, the propulsion valves are also remote and operate intermittently. However, these components do have thermal control to maintain them within their temperature specifications. Table 11.2 provides the totals of the lowest (attitude acquisition) and the highest (on-orbit peak) power dissipations of 547 and 674 W respectively, as used in the analysis, and for which the thermal system has been designed.

The design temperatures of the spacecraft components for operational and nonoperational conditions are shown in table 11.3. The minimum nonoperational temperature of -5°F was selected as the cold-start turn-on temperature for the electronics. It should be noted that the maximum temperatures for the vent and vaporizer panels are based on the condition when there is no liquid hydrogen flowing through them. In summation, the electronics boxes have to be maintained between 30 to 125°F , the batteries within 30 to 85°F , and the hydrazine components within 40 to 120°F . The experimental liquid hydrogen tank outer surfaces, supports, plumbing, and wiring should be as cold as possible. Some of the experiment panels should be as cold as possible, while others should be kept relatively warm in room-temperature conditions.

TABLE 11.2.—POWER DISSIPATION TOTALS

System	Attitude acquisition, W	On-orbit peak, W
Telemetry, tracking, and control	309	371
Experiment	45	100
Attitude control	73	73
Power	120	130
Total	547	674

TABLE 11.3.—DESIGN TEMPERATURE RANGES

Component	Operational range, °F		Nonoperational range, °F	
	Minimum	Maximum	Minimum	Maximum
Telemetry, Tracking, and Command System				
Computer 1	30	125	^a -5	145
Computer 2				
Transponder 1				
Transponder 2				
Radiofrequency processing box				
Solid-state recorder 1				
Solid-state recorder 2				
Remote command telemetry unit 1				
Remote command telemetry unit 2				
Remote command telemetry unit 3				
Command and telemetry unit 1				
Command and telemetry unit 2				
Sequencer 1				
Sequencer 2				
High-gain antenna	-100	200	-100	200
Low-gain antenna 1	30	125	-5	145
Low-gain antenna 2				
Drive motor electronics				
Antenna gimbal motor				
Redundancy control unit				
Command receiver				
High-gain antenna boom	-100	200	-100	200
Experiment System				
Gaseous helium bottle 1	-65	200	-320	200
Gaseous helium bottle 2	-65	200	-320	
Gaseous hydrogen bottle 1	-423	70	-423	
Gaseous hydrogen bottle 2	-423	70	-423	
T-0 panel	-423	-100	-423	150
Vaporizer panel A	40	^b 150	-40	
Vaporizer panel B	40	150	-40	
Helium panel	-40	150	-100	
Vent panel A	0	^b 150	-100	
Vent panel B	0	150	-100	
Plumbing tray/radiator	-423	-100	-423	
Connector panel A	0	100	-100	
Connector panel B	0	100	-100	
Supply tank purge diaphragm	-200	0	-300	300
Large receiver tank MLI outer surface	-200	0	-300	300
Small receiver tank MLI outer surface	-200	0	-300	300
Experiment data unit 1	30	125	-5	145
Experiment data unit 2				
Experiment data unit 3				
Accelerometer conditioner				
Signal conditioner				
Data acquisition unit				
Mixer motor inverter				
Propulsion System				
Valves	40	120	40	120
Catalyst beds	200	1000		
Propellant lines	40	120		
Thrusters				
Tanks				
Distribution assembly				
Regulator				
Solenoid valve				
Pressurant bottles				

^aAvionics minimum cold turn-on temperature is -5 °F.^bWithout liquid hydrogen.

TABLE 11.3.—Concluded.

Component	Operational range, °F		Nonoperational range, °F	
	Minimum	Maximum	Minimum	Maximum
Attitude Control System				
Inertial reference unit	30	105	65	165
Horizon sensor 1 electronics	30	125	-5	140
Horizon sensor 2 electronics	30	↓	-5	140
Fine Sun sensor 1 electronics	15	↓	-40	160
Fine Sun sensor 2 electronics	15	↓	-40	160
Magnetometer 1	30	↓	-5	145
Magnetometer 2	30	↓	↓	145
ACS interface electronics	30	↓	↓	145
Horizon sensor 1 optics	-5	140	↓	140
Horizon sensor 2 optics	-5	↓	↓	140
Fine Sun sensor 1 optics	15	↓	-40	160
Fine Sun sensor 2 optics	15	↓	-40	160
Power System				
Battery 1	30	85	30	85
Battery 2	30	85	30	85
Solar array 1	-95	160	-95	160
Solar array 2	-95	160	-95	160
Power control unit	30	125	-5	145
Power distribution unit	30	125	-5	145
Pyro control box	30	125	-5	145
Solar array booms	-100	200	100	200
Structural System				
Electronics bay 1 Panel N	30	125	-5	145
Electronics bay 1 Panel S	↓	↓	↓	↓
Electronics bay 1 Panel E	↓	↓	↓	↓
Electronics bay 1 Panel W	↓	↓	↓	↓
Electronics bay 1 Panel NE	↓	↓	↓	↓
Electronics bay 1 Panel NW	↓	↓	↓	↓
Electronics bay 1 Panel SE	↓	↓	↓	↓
Electronics bay 1 Panel SW	↓	↓	↓	↓
Electronics bay 2 Panel N	↓	↓	↓	↓
Electronics bay 2 Panel S	↓	↓	↓	↓
Electronics bay 2 Panel E	↓	↓	↓	↓
Electronics bay 2 Panel W	↓	↓	↓	↓
Electronics bay 2 Panel NE	↓	↓	↓	↓
Electronics bay 2 Panel NW	↓	↓	↓	↓
Electronics bay 2 Panel SE	↓	↓	↓	↓
Electronics bay 2 Panel SW	↓	↓	↓	↓
Struts	-100	50	-100	50
Supply tank longerons	-150	↓	-150	↓
Rings	-150	↓	-150	↓
Diagonals	-150	↓	-150	↓
Hydrazine tank plate	40	120	40	120

^aAvionics minimum cold turn-on temperature is -5 °F.

^bWithout liquid hydrogen.

11.3.3 SAFETY

The only safety hazard that was identified for the TCS was the buildup of electrostatic charge on MLI surfaces. Design details undertaken to avoid charge buildup are described in section 11.6.1.

11.4 Thermal Control Subsystem Description

The COLD-SAT TCS design was developed by tailoring component layouts, surface finish selection, mounting details, and active control-device (heater) sizing to maintain required spacecraft temperatures. The following sections describe the thermal control techniques employed in the design and the rationale behind implementing them.

11.4.1 EXTERIOR THERMAL CONTROL

The exterior thermal control has been applied to those surfaces and areas of the spacecraft exposed to heat gain on-orbit from direct solar flux and from Earth albedo and infrared radiation, and to heat loss by radiation to deep space. The exterior thermal control of the COLD-SAT spacecraft is shown in figure 11.1 and is described below.

11.4.1.1 Electronics Bays

The exterior surfaces of EB1 and EB2 are covered by specific combinations of optical solar reflectors (OSR's) and MLI to use the diurnal orbital environmental heat exchange for controlling the temperature of the components within the bays. Multilayer insulation is used to radiatively and conductively decouple the bays from heat gain and loss to the environment

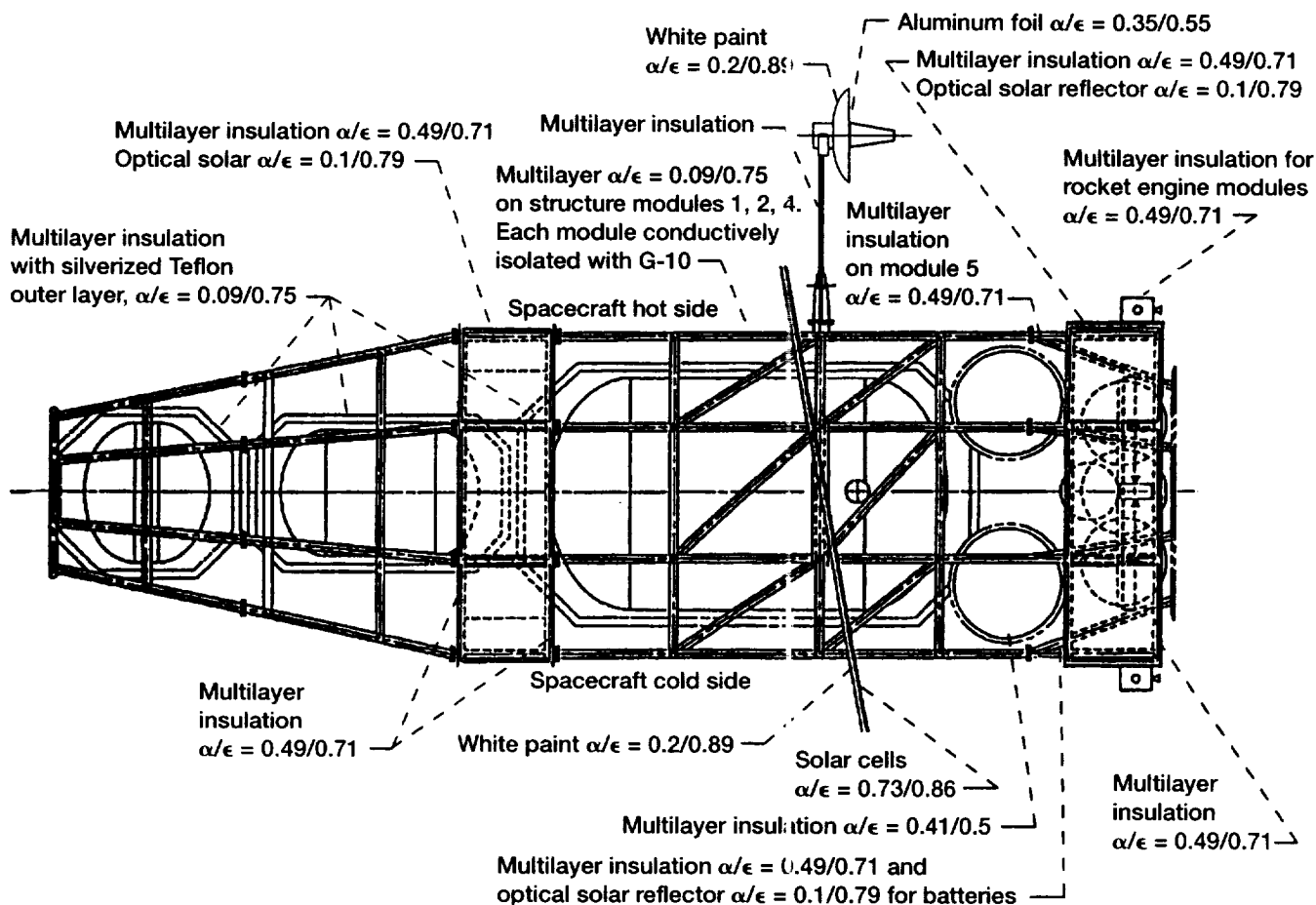


Figure 11.1.—COLD-SAT spacecraft external thermal control. Version 2700 of spacecraft was actually analyzed and is slightly different in configuration.

and to other portions of the spacecraft. Based on the selected on-orbit attitude of the spacecraft, the aft end of EB1 is fixed towards the Sun and is completely covered with MLI. Several small cutouts will have to be made in the aft MLI blanket in places where the ELV payload attach fitting bolts to the spacecraft. White paint will be used in these locations in lieu of MIL.

The side panels of the bays (E, W, N, S, NE, NW, SW, SE) include selective placement of OSR's beneath components having high heat dissipations. Optical solar reflector radiators on the external surfaces of these bays provide the means for the external radiation of excess heat generated by the components that cannot be used for temperature control by the bay internals. The front panel of EB1 has two additional OSR radiators for the two batteries. The OSR radiator surface area requirements were determined by analysis for the high-dissipation case (on-orbit peak) and are shown in table 11.4.

The remaining exterior areas of the two bays are covered with MLI. Spacecraft EB2 has been radiatively decoupled by using MLI from the large receiver tank which protrudes through the EB2 central cavity. The electronic bay modules are conductively decoupled for heat loss to the cryogenic modules via the spacecraft structure. This decoupling is achieved by the use of thermally isolating pads of G-10 fiberglass or Vespel located at the interfacing flanges of the structural longerons. Vespel is preferred because of its resistance to moisture absorption. The thermo-optical properties for each thermal control surface and finish is presented in table 11.5. All side, front, and aft panels of the two bays are highly conduction-coupled as a result of the use of aluminum honeycomb core with aluminum facesheets. This high conduction facilitates the diffusion of heat from any source to prevent localized temperature excursions.

11.4.1.2 Experiment Tankage

The experiment tankage consists of the liquid hydrogen supply tank, liquid hydrogen receiver tanks 1 and 2, two gaseous helium pressurant bottles, the gaseous hydrogen vaporizer, and the gaseous hydrogen accumulator. Each of the pressure vessels of the three liquid hydrogen tanks is surrounded by an aluminum honeycomb "can" which supports an MLI blanket. External to the MLI layers on the supply tank is a purge diaphragm which contains the gaseous helium used to purge the volume between the purge diaphragm and the pressure vessel, including the MLI. The purge diaphragm consists of two Kevlar-cloth-reinforced layers, separated by an embossed Kapton layer. The outer layer has a coating of second-surface silverized Teflon (SSST) to keep this outer layer at the lowest possible temperature. A lower temperature of the outer surface reduces the parasitic heat leak through the MLI to the can.

The two receiver tanks do not have a purge diaphragm since they are not loaded with liquid hydrogen at launch and, therefore do not require purging of the MLI or the pressure vessel on the ground. However, to reduce the parasitic heat leaks through the MLI while in orbit, both tanks have SSST as the outer layer of the MLI. An additional heat leak into the liquid hydrogen tankage is by conduction through tank support struts, power, and instrumentation wiring harnesses and plumbing lines. Each of these conduction paths have a hot-temperature boundary on the spacecraft which provides the necessary temperature difference for heat transfer into the cryogen. As explained in the Introduction to this chapter, the responsibility of the spacecraft TCS is to minimize this boundary temperature, which, for the tank support struts is the spacecraft structure temperature, and

TABLE 11.4.—RADIATOR SURFACE AREA REQUIREMENTS

Panel, electronics bay, (EB)	Low/high dissipation, W	Radiator	α/ϵ	Dimensions, in.
1 North	28/28	OSR	0.1/0.79 BOL ^a	10.0 × 16.0
1 South	28/46			10.0 × 16.0
1 East	31/31			8.75 × 12.0
1 West	31/31			6.75 × 12.0
1 Northeast	58/117			14.75 × 24.5
1 Northwest	35/45			16.75 × 22.5
1 Southeast	66/81			18.75 × 26.5
1 Southwest	77/77			9.75 × 13.25
1 Forward/battery 1	See EB 1 North			16.0 × 10.0
1 Forward/battery 2	See EB 1 South			16.0 × 10.0
2 North	3/3			2.0 × 2.0
2 South	3/3			2.0 × 2.0
2 East	70/70			18.0 × 20.0
2 West	45/55			10.0 × 12.0
2 Northeast	2/2			1.0 × 1.5
2 Northwest	20/35			10.0 × 12.0
2 Southeast	50/50			14.0 × 16.0
2 Southwest	0/0			-----

^aBOL, beginning of life.

TABLE 11.5.—PROPERTIES OF THERMAL CONTROL SURFACES AND FINISHES

Surface/finish	Composition	α	ϵ	Application
Multilayer insulation (MLI) (basic)	12 Layers double aluminized Kapton with Dacron net spacers, indium tin oxide (ITO) coating	0.49	0.71 (eff $\epsilon = 0.025$)	Electronics bay 1, electronics bay 2, structure (module 5), and rocket engine module
Silverized/Teflon outer layer (second surface)	1 layer outer-MLI surface, ITO coating	0.09	0.75	Experiment tanks, T-0 panel, plumbing tray/radiator, and structure (modules 1, 2, and 4)
Kapton/aluminum outer layer	1 layer outer-MLI surface, ITO coating	0.41	0.50	Gaseous helium, gaseous hydrogen experiment bottles, propellant distribution assembly, structure (ring 7 on module 1), vaporizer panels, helium panel, connector panels, and propulsion system gas bottles
Thick black film/Kapton/aluminum outer layer	1 layer outer-MLI surface, ITO coating	0.85	0.85	Vent panels
Thermally conductive interface	Silicone boron nitride sheet 0.125-in. thick	—	—	Between electrical boxes and panels in electronics bay 1 and electronics bay 2
Thermally isolating interface	G-10 fiberglass/Vespel spacer 0.5-in. thick	—	—	Between each structural module struts, gaseous helium and gaseous hydrogen bottles
Optical solar reflectors	Second surface fused silica mirror	0.1	0.79	Electronics bay 1 and electronics bay 2 radiators
Solar cells	Boron back-surface field cell with cerium dioxide cover	0.73	0.86	Solar array Sun side
Z-202 Chemglaze	White paint	0.2	0.89	Solar array anti-Sun side and high-gain antenna exterior
Z-306 Chemglaze	Black paint	0.85	0.85	Electronics bay 1 and electronics bay 2 inside panels and components
Aluminum foil	Vapor deposited aluminum	0.35	0.55	High-gain antenna reflective surfaces
Aluminized tape	First-surface aluminum Kapton tape	0.15	0.10	Wrapping for propellant lines and valves

for the wiring and plumbing, is the plumbing tray temperature. Thermal control of these items is described in the following two sections.

The gaseous helium and gaseous hydrogen bottles are each covered with an MLI blanket. The gaseous hydrogen bottles are located on the hot side of the spacecraft to reduce the heater requirements for vaporizing the liquid hydrogen to gas. In contrast, the gaseous helium bottles are maintained as cold as possible on the cold side of the spacecraft (this hot- and cold-side thermal bifurcation is defined in section 11.5.2.1). All four bottles are decoupled from their support structure by thermally isolating G-10 or Vespel pads.

11.4.1.3 Spacecraft Structure

Distortion of the spacecraft exterior support structure caused by changes in orbital fluxes at sunrise and sunset is minimized

by the use of MLI blankets. For the cryogenic modules to minimize parasitic strut conduction into the cryogen tankage, the structure is maintained at the lowest possible temperature by the use of SSST as the outer layer of the MLI. However, this low temperature of the structure can also act as a heat sink for the heat dissipated in the electronic bays, which, if not controlled, can cause the component temperature to go down drastically. Consequently, to avoid this situation, the structural longerons of the three cryogenic tank modules are conductively isolated from the electronic bay structure by the use of Vespel pads at each interfacing flange. The entire structure is composed of highly conducting aluminum, which prevents any temperature rise in the structure on the hot side of the spacecraft. The structure within each bay is considered as a part of the interior thermal control for the bay, and is described later in section 11.4.2.

11.4.1.4 Plumbing Trays and Panels

The plumbing tray is located just outside the spacecraft structure on the cold side of the spacecraft, which allows the plumbing and wiring penetrations of the liquid hydrogen tankage to get as cold as possible before they enter the tank MLI. A lower hot-end boundary temperature for these conductive paths lowers the parasitic heat leakage. The tray is attached to the spacecraft structure with stainless steel bolts and G-10 fiberglass spacers in an attempt to thermally isolate the tray from the spacecraft. The plumbing tray is covered that has an MLI blanket with an SSST outer layer.

In keeping with the modular concept of COLD-SAT spacecraft design, individual plumbing, and wiring, harness components are mounted on several panels based on functional requirements. Some of these panels have to be maintained in a warm environment, and therefore are located on the hot side of the spacecraft. Remaining panels are located on the spacecraft cold side to take advantage of the lack of solar flux to remain as cold as possible for cryogenic tankage parasitic heat leakage reduction. All panels are MLI-covered with individual thermal control outer layers, as shown in figure 11.2. Plumbing and

wiring from all panels proceed to the plumbing tray before penetrating the pressure vessels of the three liquid hydrogen tanks. The hot side panels also provide solar flux blockage to the supply tank. As in the case of the plumbing tray, all panels are conductively decoupled from the spacecraft structure. Thermal control heaters are located on the vent, vaporizer, and connector panels, as shown in table 11.6, but are budgeted to the experiment system. This table also shows the heater requirements of other components, with the heater requirements summary provided in table 11.7 by system.

11.4.1.5 Solar Arrays

Minimization of operational solar array temperature is achieved passively. Although the back of the solar array receives no direct solar flux, it does receive large levels of reflected solar radiation, and is finished with a high-emittance white paint to maximize heat rejection. Measured optical properties were obtained from the vendor for the Solarex boron silicate cesium solar cells selected. Each solar array hinge/damper will require a low-wattage, thermostatically controlled ground-enabled heater power approximately 30 min prior to

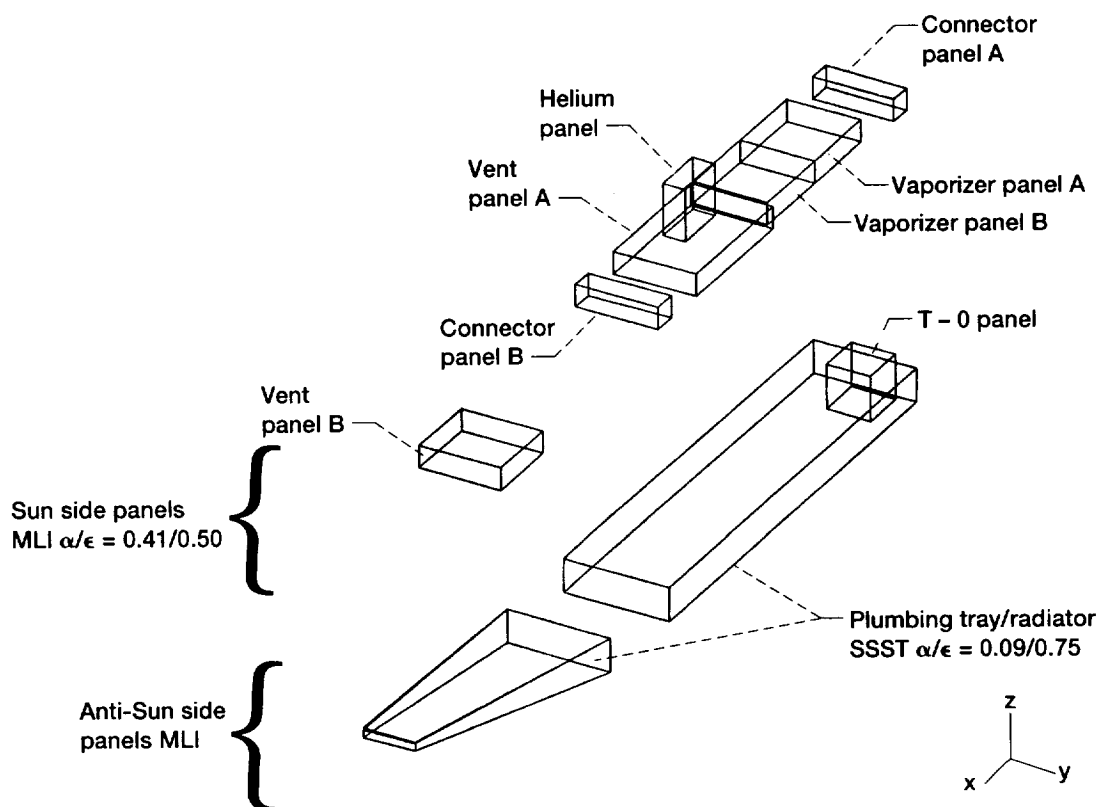


Figure 11.2.—Plumbing tray and panel thermal control. All components MLI covered. T-0 panel and plumbing tray has silverized teflon outer surface $\alpha/\epsilon = 0.09/0.75$ other panels have MLI with $\alpha/\epsilon = 0.41/0.50$. All components conductively isolated from spacecraft structure by G-10 pads, heaters on vent, vaporizer, and connector panels.

TABLE 11.6.—THERMAL SYSTEM HEATER REQUIREMENTS

Location	Power, W	Redundancy	Control	Setpoints, °F	Budgeted subsystem	
Propulsion System						
Propellant distribution assembly	6.0	Primary/backup	Makeup	60	Propulsion	
Pressurant bottle 1	7	↓	↓	↓	Thermal	
Pressurant bottle 2	7				Thermal	
Pressurant bottle 3	5				Thermal	
Pressurant bottle 4					Thermal	
Propellant tank 1	↓	↓	Dual-temperature controller	40–45	Propulsion	
Propellant tank 2			Dual-temperature controller	↓		
Propellant tank 3			Dual-temperature controller			
Propellant tank 4			Dual-temperature controller			
Propellant lines			Parallel			On/off
Thruster valves			Primary/backup	Dual temperature controller		
Catalyst bed	20.0	Parallel	On/off		↓	
Power System						
Batteries (2)	20.0 × 2	Primary/backup	Dual temperature controller	0–5	Thermal	
Solar array hinge damper (12)	12 × 2	Parallel	On/off	70.0	Thermal	
Telemetry, Tracking, and Command System						
High-gain antenna motor drive	5	Parallel	Makeup	70.0	Thermal	
Experiment System						
Vaporizer panel A	6.0	Primary/backup	Makeup	40.0	Experiment	
Vaporizer panel B	6	↓	↓	40	↓	
Vent panel A	7			0		
Vent panel B	7			↓		
Connector panel A	2					
Connector panel B	2					
Electronics Bay 2 Avionics						
Remote command and telemetry unit 2	2.0	Survival	On/off	–5	Thermal	
Horizon sensor 1 electronics	3.0	↓	↓	↓	↓	
Power distribution box	3.5					
Horizon sensor 1 optics	0.5					
Mixer motor inverter	1.0					
Attitude control system interface electronics	1.5					
Accelerometer conditioner	2.0					
Experiment data unit 1	1.0					
Experiment data unit 2	1.0					
Experiment data unit 3	1.5					
Horizon sensor 2 optics	0.5					
Command and telemetry unit 2	2.5					
Horizon sensor 2 electronics	4.5					
Remote command and telemetry unit 3	3.5					
Electronics Bay 1 Avionics						
No heaters required	—	—	—	—	—	

array deployment. The array booms are covered with an MLI blanket and finished with low-emittance tape on anti-Sun sides and low-absorbance, high-emittance tape on the Sun-facing sides to minimize boom distortion.

11.4.1.6 Antenna

Distortion of the high-gain antenna (HGA) and its support arm is minimized passively by the use of MLI blankets on the boom, aluminum foil on the dish Sun-facing side, and white paint on the dish anti-Sun side. The HGA motor is MLI covered and has a redundant, thermistor controlled makeup heater. The

HGA boom and its deployment hinge/damper has a similar treatment as the solar array boom. One low-gain antenna is conductively coupled to the EB1 panels, which are maintained in the 30 to 125 °F range. Multilayer insulation covering of the booms minimizes relative deflection and the aluminum foil minimizes focused solar reflection.

11.4.1.7 Components

The hydrazine rocket engine modules are conductively coupled to the EB1 side panels, have MLI blankets, and require heaters for the thruster valves and the catalyze beds, as shown

TABLE 11.7.—HEATER REQUIREMENTS SUMMARY

System	Heater type	Wattage
Propulsion	Makeup ^a	30
	Backup ^b	60
	Survival ^c	25
Power	Makeup	0
	Backup	40
	Survival	27.5
Telemetry, tracking and command	Makeup	5
	Backup	0
	Survival	8
Attitude control	Makeup	0
	Backup	0
	Survival	10
Experiment	Makeup	30
	Backup	0
	Survival	6.6
Totals	Makeup	65
	Backup	100
	Survival	77.1

^aThermistor controlled.^bDual temperature controller (DTC) controlled.^cThermistor controlled. Makeup heater duty cycle 50 percent or less.

in figure 11.3. These heaters provide temperatures of 40 °F or higher at ignition and are maintained by ground-commandable, redundant digital-temperature controllers (DTC's). Propellant lines will be partially wrapped in low-emittance tape (75 percent tape, 25 percent black) and will have heaters. The propellant distribution assembly will be MLI covered and will have thermostatically controlled heaters. The gimballed thruster is conductively coupled to the hydrazine tank support plate, which is located inside EB1.

The Sun sensor optics, which protrude through the MLI blanket of EB1, are an integral part of the sensor electronics; therefore, no separate thermal control of optics is required. The horizon sensor optics will be MLI-covered where the optical head protrudes from the EB2 mounting panel. A slit will be provided in the MLI for the mirror.

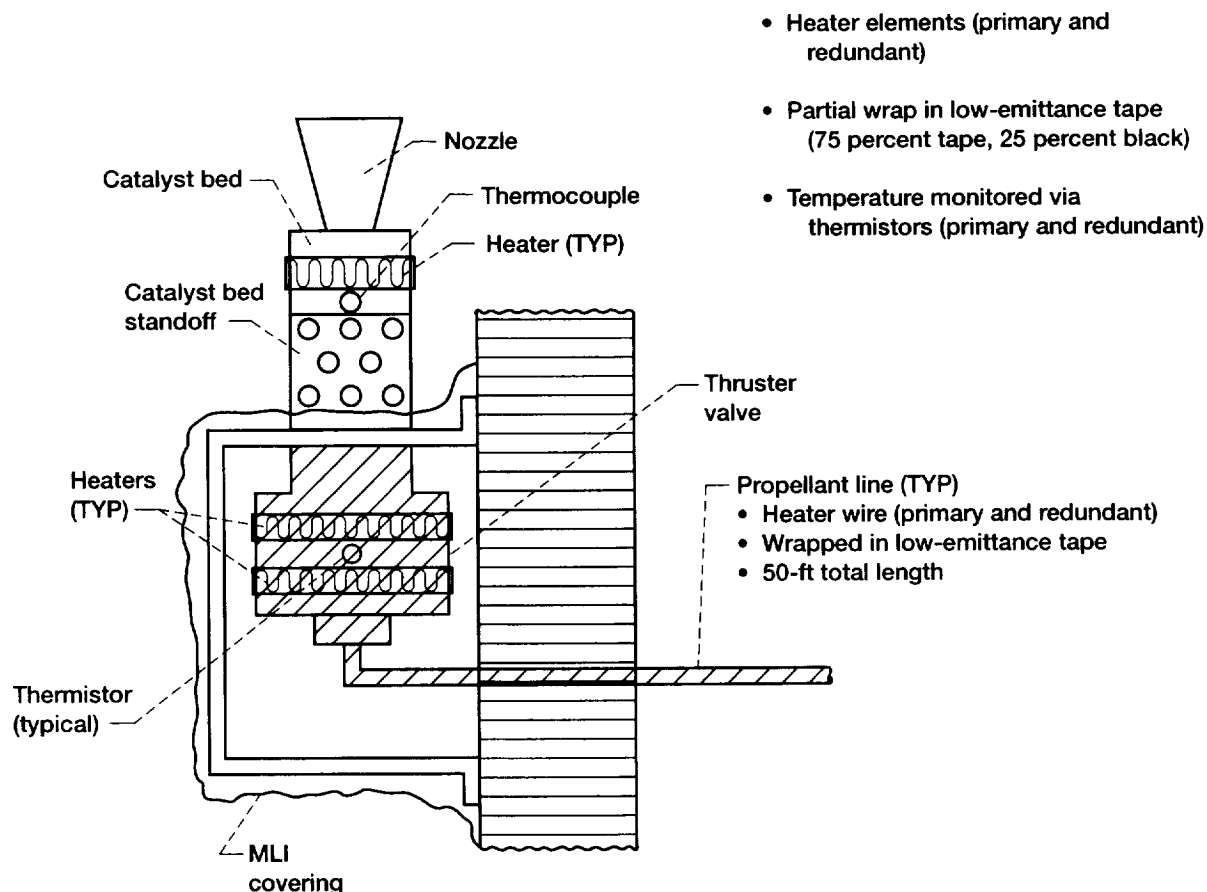


Figure 11.3.—Typical rocket engine module thermal control.

11.4.2 INTERIOR THERMAL CONTROL

The interior thermal control applies to the internals of the EB1 and EB2 enclosures and the electronics boxes, attitude control sensors, batteries, and propulsion components located within. The internal component layouts and passive surface finishes are described below.

11.4.2.1 Electronics Bays

In EB1, the TT&C system components such as the computers, transponders, RF processing box, solid-state recorders, command and telemetry units, and sequencers are mounted to the insides of the panels on the eight sides of the enclosure. In addition, there are the power, attitude control, and experiment

system boxes, which are similarly mounted. The panels provide an efficient means of spreading and rejecting the high-thermal dissipation loads of the electronics components, all of which have a duty cycle of 100 percent. The propulsion system hydrazine tankage is mounted on an aluminum honeycomb sandwich plate in the center of EB1. Additional electronics boxes belonging to the TT&C, experiment, and attitude control systems are contained in EB2.

The interior surfaces of the bays are painted with a high-emittance black paint to enhance radiative coupling and thus exchange heat between the boxes, panels, hydrazine tanks, and the support structure (fig. 11.4). The boxes, structure, tanks, and plate are also painted black to promote augmented heat rejection to the bay interior. To enhance conductive coupling from the base of each box to the OSR radiators on the outer

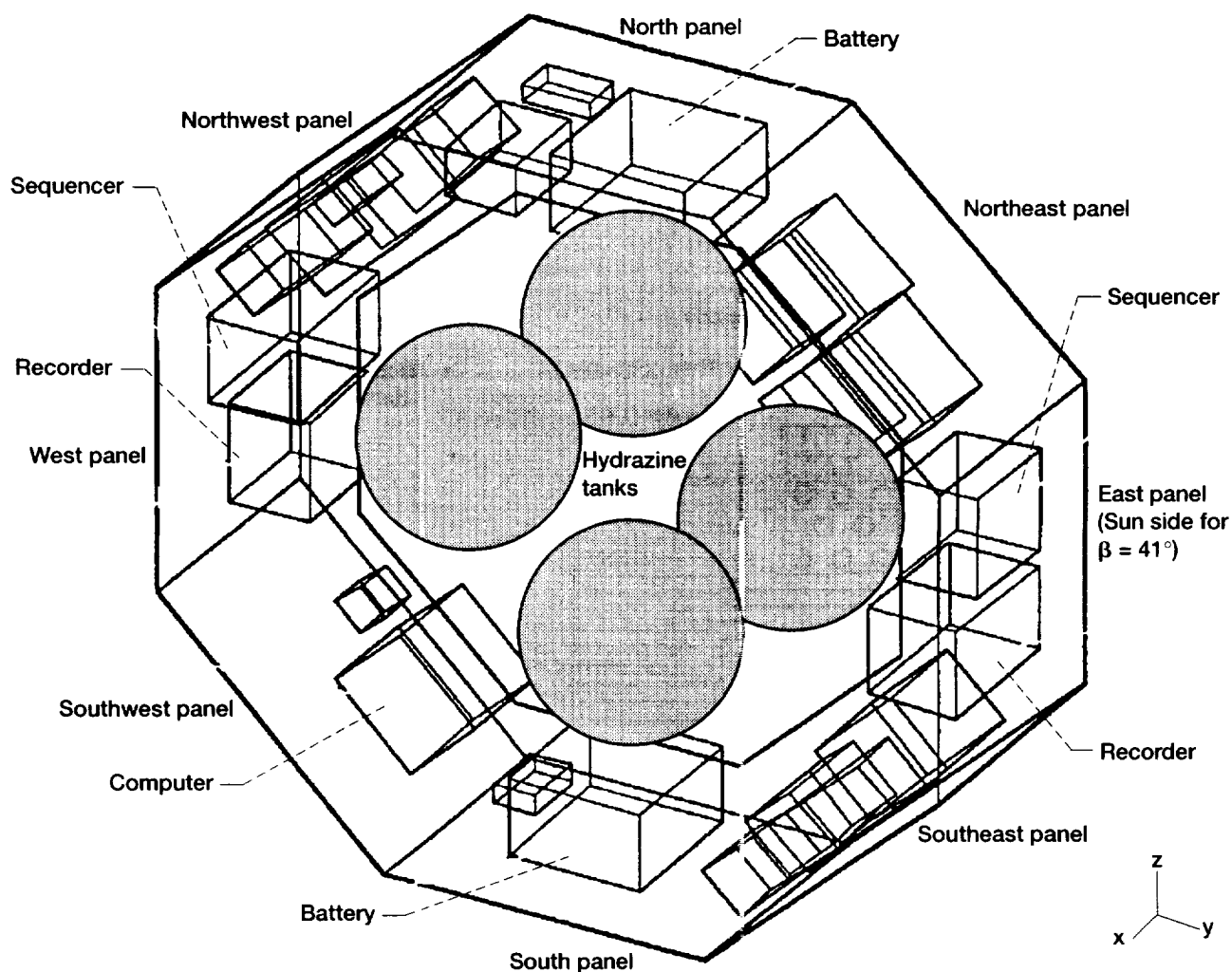


Figure 11.4.—Electronics bay 1, internal thermal control. Black paint ($\alpha/\epsilon = 0.85/0.85$) on honeycomb panels, avionics boxes, hydrazine tanks, tank support plate and struts. Conductive coupling enhanced from box to panel using Chotherm 1671. Tank support plate conductively isolated from honeycomb panels and tanks from plate using G-10.

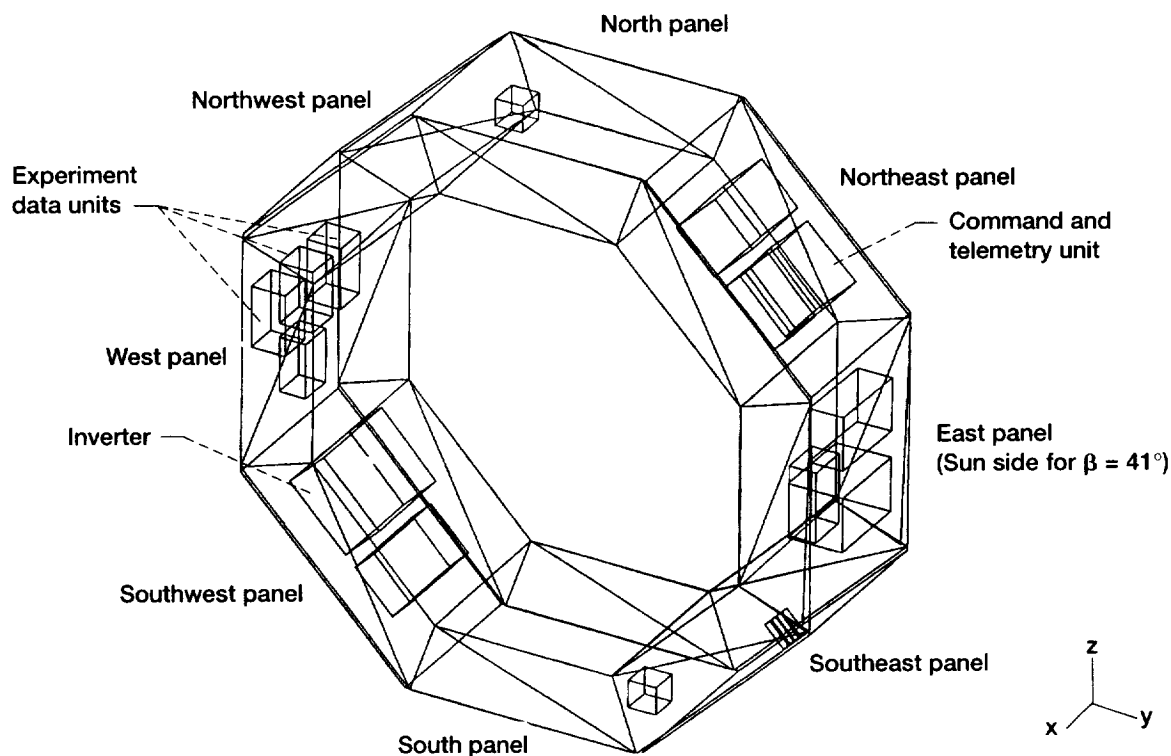


Figure 11.5.—Electronics bay 2, internal thermal controls. Black paint ($\alpha/\epsilon = 0.85/0.85$) on honeycomb panels, avionics boxes, and struts. Conductive coupling enhanced from box to panel using Clotherm 1671.

surface of the panels, silicone-boron-nitride Clotherm 1671 is used as a 0.125-in.-thick mounting sheet under each box. The tank support plate is conductively isolated from the side panels and the tanks are isolated from their support plate. A similar thermal control scheme of using high-emissivity black paint is used for EB2 (fig. 11.5).

There are no survival or backup heaters provided for the electronics boxes in EB1, since, in the case of power loss, the thermal mass of the hydrazine is sufficient to maintain the boxes within the operating-temperature range. This range is maintained longer than the capability of the batteries to supply power. Also, since the duty cycle of EB1 is 100 percent, the OSR's have been sized so that makeup heaters, are not needed for the low-power case (attitude-acquisition) and high-power case (on-orbit peak).

The temperature of the propulsion system's four hydrazine tanks is maintained above 40 °F by ground-commanded redundant heaters. The gaseous helium pressurant bottles (outside of EB1 for spacecraft version 2700) are maintained above 40 °F by DTC-controlled heaters with ground-commandable override redundant heaters. Temperature differences between interconnected hydrazine tanks are maintained within 10 °F by ground-commandable actuation of backup heaters as required.

In EB2, survival heaters are provided in redundant sets for maintenance of acceptable nonoperating temperatures for sur-

vival above -5 °F. These heaters are automatically enabled when electronics are made nonoperational.

11.4.2.2 Batteries

The power system components that require the most stringent thermal control are the nickel-cadmium batteries. Each battery dissipates 25 W during the charge and discharge cycles. Because battery life is inversely related to temperature, 85 °F maximum is desirable to ensure adequate operation throughout the mission. Consequently, each battery is located in two thermal control compartments in EB1, which are isolated from the hotter (125 °F) electronics compartment by structural bulkheads (fig. 11.6). The compartments are covered with MLI blankets on the inner and outer surfaces, both with a black outer layer and the battery is painted black on all sides. The forward panels of the compartments are covered with an OSR radiator, to which the batteries are radiatively coupled by the high-emissivity black paint.

Battery temperature is maintained above 30 °F by redundant DTC's and a heater with a ground override capability. As a result of the battery analysis, the EB1 was rotated 90° so that the east side is now the Sun-facing side, and batteries are not on the Sun-side anymore. Furthermore, both batteries are rotated 180° so their bases are in contact with the EB1 forward surface OSR

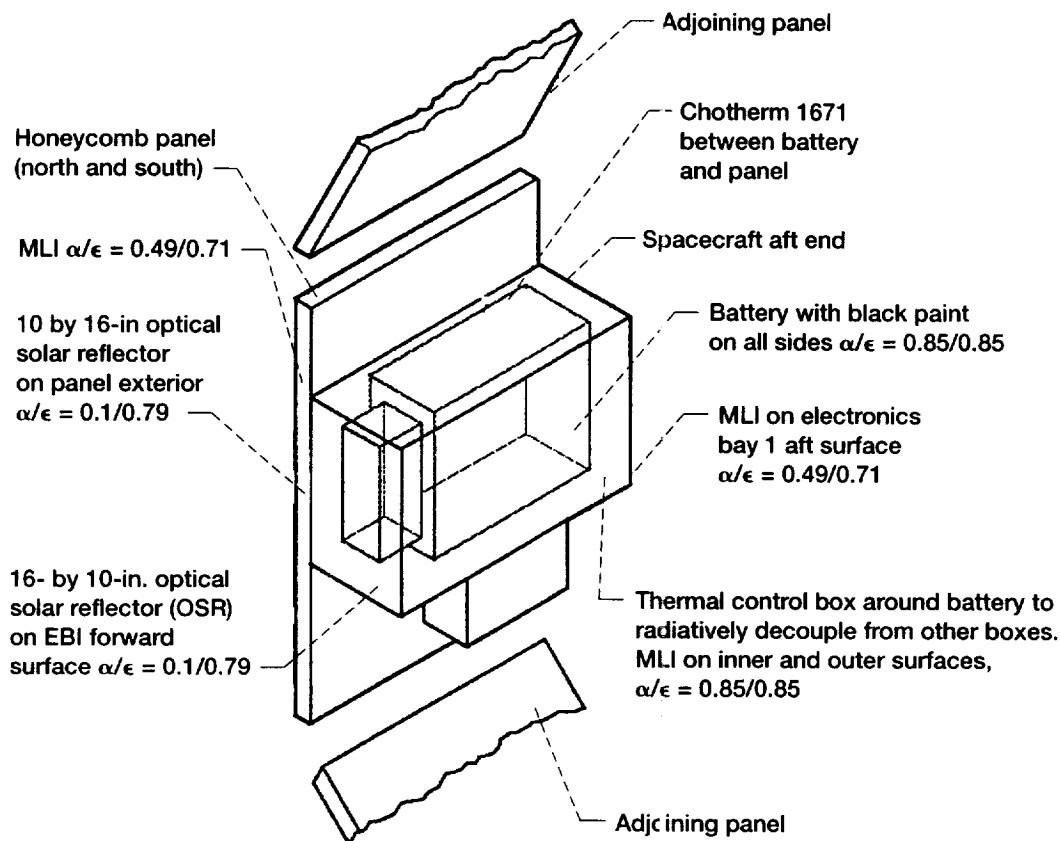


Figure 11.6.—Typical battery thermal control. As a result of the battery analysis, the electronics bay 1 was rotated 90°. The east side is now the Sun-facing side and batteries are away from the Sun. Furthermore, batteries were rotated 180° so their bases are in contact with the electronic bay 1 forward-surface radiators.

radiators. Additional information on battery thermal control is contained in reference 1.

11.5 Thermal Control Subsystem Analyses

11.5.1 ANALYSIS OVERVIEW

The COLD-SAT Spacecraft TCS was analyzed by using NASA standard computer codes. Using these codes, detailed geometric and thermal models were developed for the in-house spacecraft design version number 2700 dated January 31, 1990. The TRASYS-II code was used to calculate radiation-coupling factors for spacecraft exterior and interior surfaces. Also calculated were absorbed on-orbit heat fluxes due to solar radiation, Earth albedo, and Earth infrared radiation incident on the exterior surfaces for several β -angle orientations as described below. The spacecraft geometry was subdivided into six groups and a TRASYS-II geometric model was developed for the

radiation analysis of each group. These six groups are: all spacecraft exterior surfaces, EB1 exterior and interior, EB2 exterior and interior, and the structural system. The outputs from each of the six models were combined to form the inputs for the spacecraft-level thermal analysis.

Thermal analysis was performed using the SINDA85 code into which TRASYS-II inputs were provided to complete the physical design description of the spacecraft. Here, additional radiative couplings were combined with a mathematical description of the nodes for thermal capacitance, equipment thermal dissipation, and conductive couplings. This information permits spacecraft thermal balance computations to be made for the specific attitude and operational conditions of interest. The SINDA85 output includes both spacecraft and experiment component temperatures and heater power predictions based on equipment power dissipations and temperature ranges specified. From a manageability consideration, four SINDA85 thermal math models were developed: all spacecraft exterior surfaces; EB1 and EB2 interior and exterior; and the structural system. After debugging each model, the four were combined for final results at the spacecraft level.

Four spacecraft orbital conditions were evaluated to determine the viability of the thermal system design: hot case ($\beta = 41^\circ$), cold case ($\beta = 0^\circ$), loss-of-attitude case ($\beta = 0^\circ$, with the spacecraft long-axis normal to the orbit plane, and Sun incident on the battery panel), and load-shedding case ($\beta = 0^\circ$, with no power dissipation). Makeup heater power requirements were calculated to maintain components within their operating temperature range. Survival heater requirements were calculated to maintain electronics at cold-start temperature (-5°F) and hydrazine above freezing (40°F), in case of spacecraft bus-load-shedding situations. As described before, to increase conduction from the electronics boxes to the mounting honeycomb panels, Chotherm 1671 conduction enhancers were used and modeled. Also, EB1 and EB2 are conductively isolated at the spacecraft structure because of conflicting thermal control requirements and this too was modeled.

The spacecraft altitude was modeled as 550 n mi with an orbit inclination of 18° , at which the β angle range is 0 to 41° . For the $\beta = 41^\circ$, solar flux was modeled to be incident on the hot

side of the spacecraft only. The values of albedo, solar flux, and earth infrared were 0.3, 444 and 77 Btu/hr-ft², respectively. Solar arrays were modeled as canted at 13° to orbit normal. The design life of the spacecraft is 6 months, consequently, only BOL thermo-optical properties were considered in this analysis.

The area of each OSR radiator was sized according to maximum solar flux, OSR solar absorptivity (0.09), and maximum and minimum power dissipations. Initial estimates were obtained by hand calculations for thermal balance and parametric runs were performed to determine final areas. The heaters were sized by the HEATER subroutine in SINDA85 when given the desired temperature set points.

The analyses were performed with TRASYS-II and SINDA85 on the VAX8600 using ITPLOT, XPLOT, and GRAPHWRITER for preprocessing of input and postprocessing of results to develop presentation graphics. Analyzed spacecraft orbital conditions and the TRASYS model of the spacecraft exterior surfaces are shown in figure 11.7.

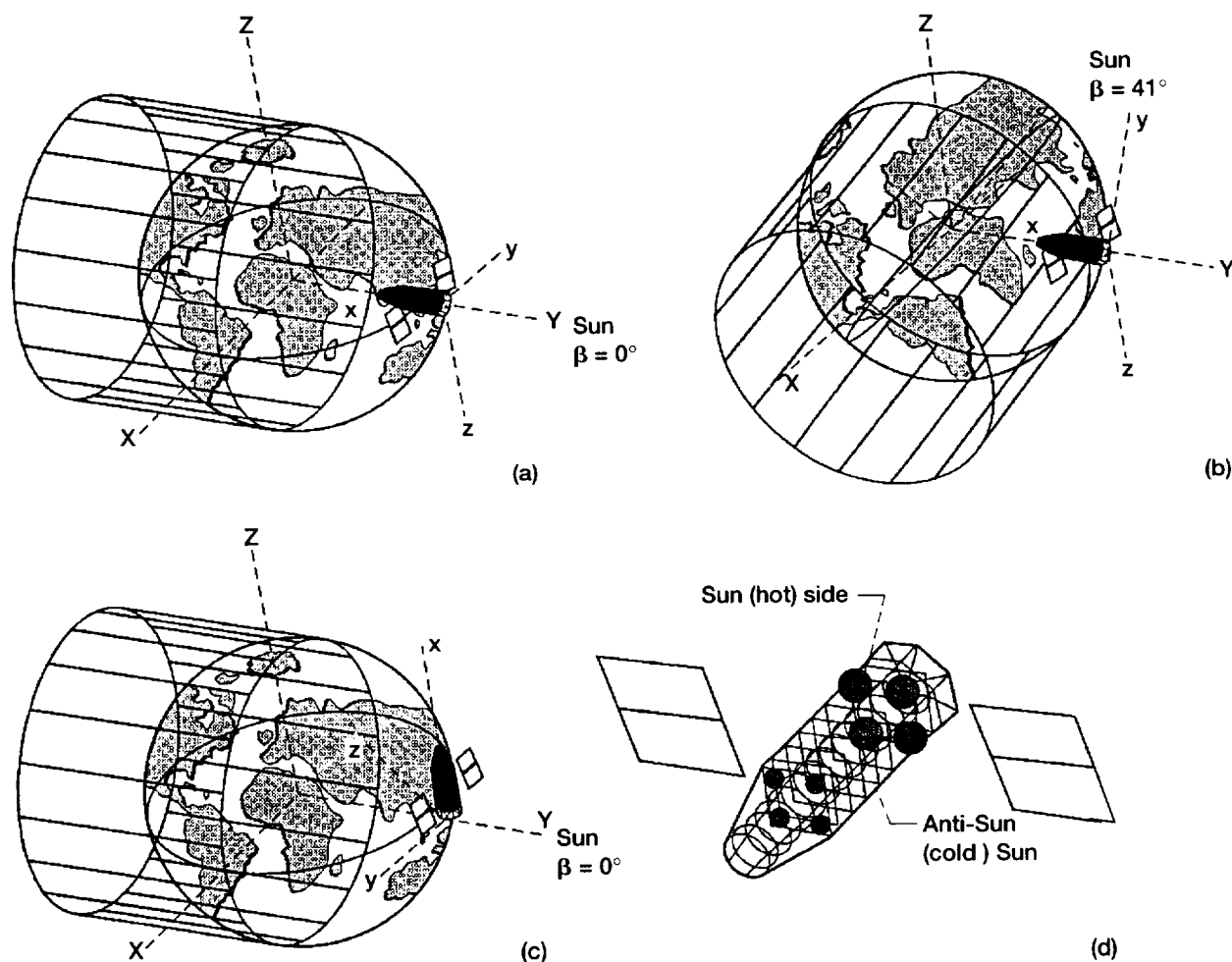


Figure 11.7.—Spacecraft orbital condition for thermal analysis. (a) Operational cold case and load shed case attitude. (b) Operational hot case attitude. (c) Loss of attitude case (Sun on battery panel). (d) Spacecraft external/exposed surfaces TRASYS model.

11.5.2 THERMAL DESIGN ISSUES AND TRADES

11.5.2.1 Spacecraft Thermal Bifurcation

Since the COLD-SAT spacecraft is comprised of cryogenic components, an important consideration in spacecraft thermal design was to minimize the parasitic heat leakage into the three liquid hydrogen tanks. Initial studies indicated that among the pressure vessel heat leak contributors for the supply tank, the manganin instrumentation wiring, aluminum power wiring, and SS304 plumbing lines are the major contributors. It was, therefore, decided to route all wiring and plumbing lines on a plumbing tray that will be located on a side of the spacecraft that is minimally impacted by solar flux and would thus be at the lowest-possible temperature. This tray will be conductively isolated from the spacecraft structure and will be radiatively cooled to space to achieve cold temperatures. Thus, the spacecraft was to be thermally bifurcated into a hot and a cold side.

Bifurcation was achieved by constraining the solar arrays to be of only a fixed design so that only Sun-tracking, quasi-inertial attitudes were possible. In these attitudes, the spacecraft is oriented to have the fixed arrays constantly face the Sun while rotating about one of its axes to track the Sun at one revolution per year. These attitudes resulted in large portions of the spacecraft becoming incident to the solar flux, thereby creating a hot side of the spacecraft. Considerably higher temperature excursions occur on this hot side as compared to the other, anti-Sun side. Because it is able to radiate to space and because it is only exposed to the comparatively lower Earth albedo and infrared fluxes, the anti-Sun side acts as a cold side and thus operates in a lower temperature range. Figure 11.8 depicts the temperature effects on the supply tank hot and cold sides for the COLD-SAT spacecraft attitude that was selected.

For the $\beta = 0^\circ$ case, since the solar flux is in line with the long axis of the spacecraft, there is no solar flux incident on the supply tank. Consequently, the average temperature profile of

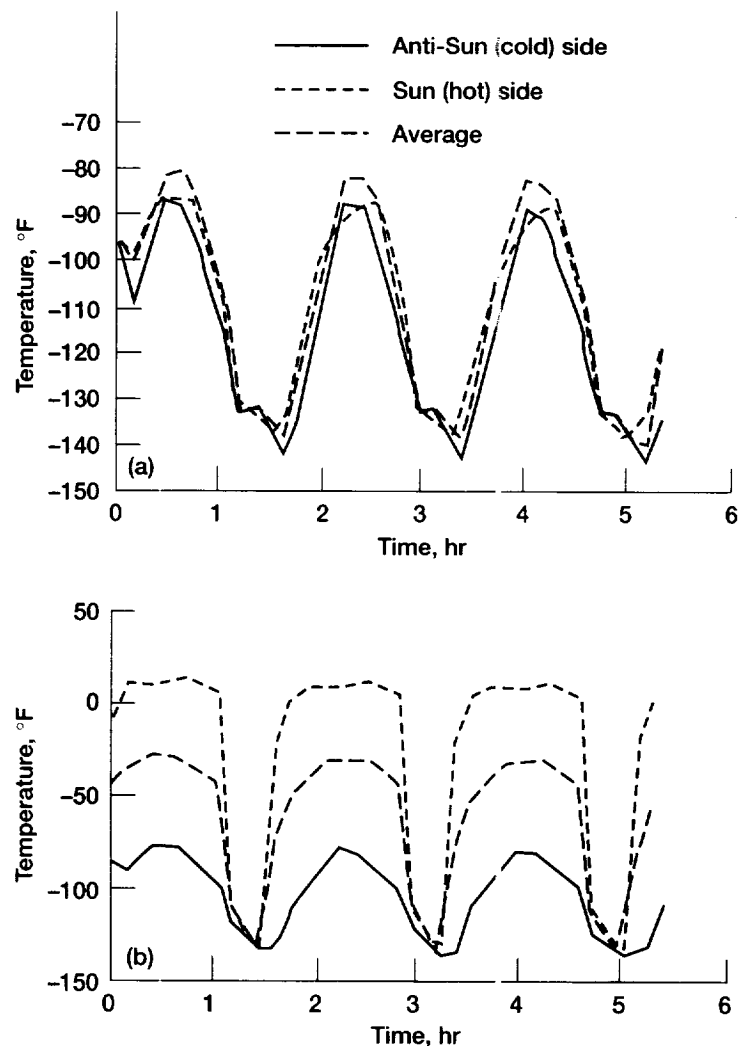


Figure 11.8.—Supply tank purge diaphragm Sun-facing and anti-Sun-facing temperatures. (a) $\beta = 0^\circ$. (b) $\beta = 41^\circ$.

the Sun-facing or hot side and the anti-Sun (cold) side are similar (-85 to -140 °F). However, for the $\beta = 41^\circ$ case, when the Sun is no longer colinear with the spacecraft long axis, the temperature of the Sun-facing side of the supply tank increases to as high as $+10$ °F, whereas the anti-Sun or cold side goes up to only -80 °F. Therefore, it is evident that by placing the plumbing tray on the spacecraft cold side, much less parasitic heat leakage through the plumbing lines and wiring into the supply tank would occur. As shown in figure 11.9, there is minimal (4 °F) change in the plumbing tray temperature regardless of the $\beta = 0$ or $\beta = 41^\circ$ orbital conditions.

It was calculated that in a 6-month period, given the COLD-SAT orbital parameters for any launch window, the Sun crosses the orbital plane a maximum of five times. To maintain the hot-and-cold-side restriction on the spacecraft periphery, the spacecraft will have to perform a 180° roll maneuver around its long axis whenever the Sun crosses the orbit plane. This is necessary

to ensure that the same side of the spacecraft remains in view of the Sun at $\beta = 41^\circ$, and to keep the arrays generally Sun-pointed.

11.5.2.2 Spacecraft Attitude Impacts

With only quasi-inertial attitudes as the optimum thermal orientation for the cryogenic tankage and components, two specific attitudes were considered, as indicated in figure 11.10. In one of the attitudes under consideration, named attitude "A", the long axis (x) of the spacecraft is co-planer with the orbit plane and the fixed solar arrays are canted at an optimized 13° to orbit normal. When the angle of the Sun line to the orbit plane (β angle) is 0° , the spacecraft EBI module shields the supply tank and other tanks from solar flux. This provides the coldest tank thermal condition for this attitude. As the Sun travels to the maximum of $\beta = 41^\circ$ (for the selected orbital inclination of 18°),

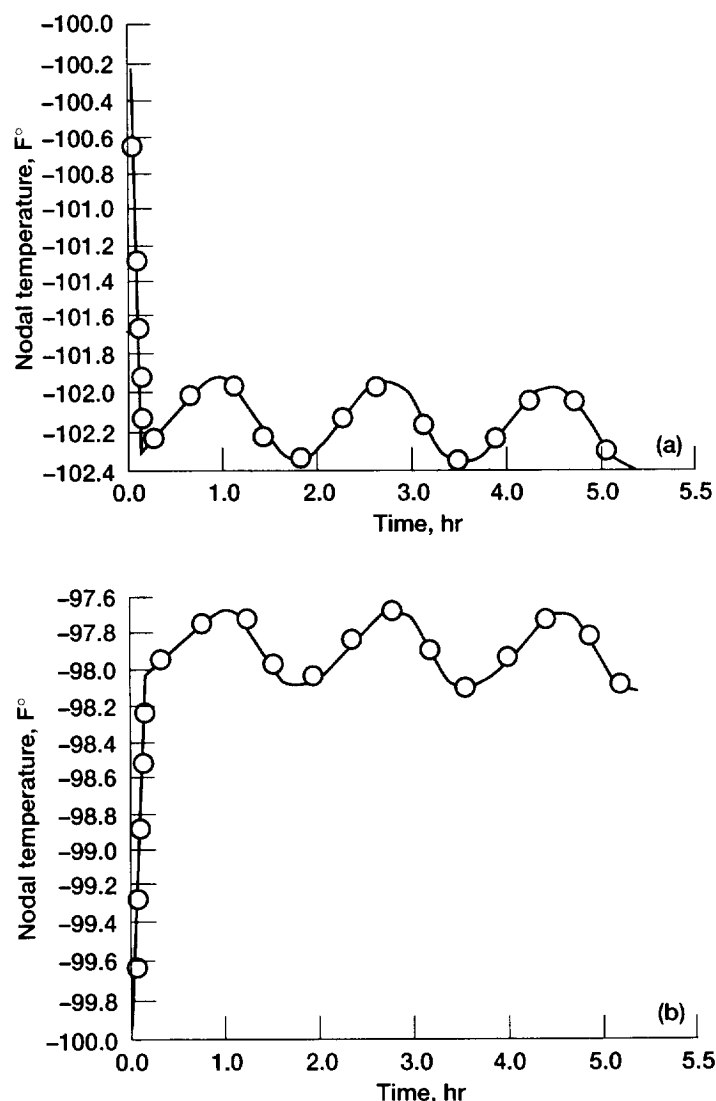


Figure 11.9.—Plumbing tray temperatures, (a) $\beta = 0^\circ$. (b) $\beta = 41^\circ$.

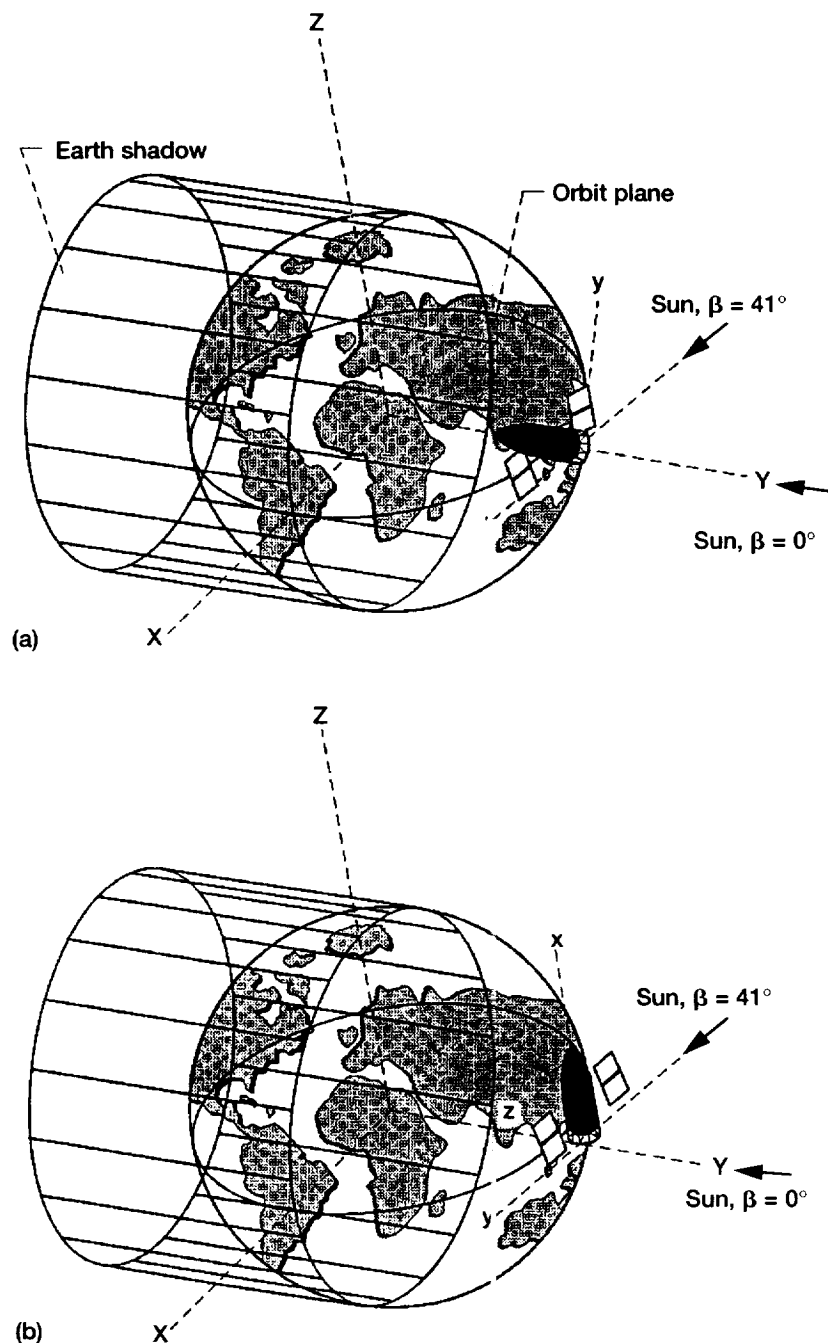


Figure 11.10.—Cold-SAT spacecraft attitudes considered in circular low-Earth orbit. At both attitudes, β angle in global y-z plane only. (a) Spacecraft attitude A. (b) Spacecraft attitude B.

the projected area of the supply tank to the Sun line is illuminated by solar flux. This creates the warmest environment for this attitude.

The other attitude investigated here is referred to as attitude "B" in which the spacecraft long axis is normal to the orbit plane. The fixed solar arrays are canted as before. By rotating the spacecraft around its z-axis, as shown in figure 11.10(b),

arrays remain Sun-pointed for $\beta = 41^\circ$. For this attitude, the supply tank has the smallest projected area normal to the Sun line when $\beta = \pm 41^\circ$, so this β angle provides the coldest conditions for the tank. A third attitude in which the same side of the spacecraft continuously faces the Earth was discounted. This was due to the necessity of including articulating arrays along with their inherent concerns described earlier.

For establishing spacecraft-attitude-dependent heat leaks into the tank, it is important to determine the hot boundary condition for each of the sources of heat: purge diaphragm for the MLI, spacecraft structure for the tank support struts, and the plumbing tray for the wiring and plumbing. The spacecraft and supply tank TRASYS-II and SINDA85 models were executed. The analysis results for the cases of interest are presented in figure 11.11 for the purge diaphragm where the surface temperature is plotted versus orbital time.

It can be seen that attitude A for a $\beta = 0^\circ$ has the lowest temperature due to the blocking of the solar flux by the aft end of the spacecraft. This temperature increases for the $\beta = 41^\circ$ cases, since the Sun is now impinging more directly on the supply tank. The temperature profile for attitude B, $\beta = 0$ and 41° is slightly higher at its peak than the $\beta = 0^\circ$ case. It can be surmised that this may be caused by the forward end of the purge diaphragm being heated through the central cavity of EB2 at this high β angle. It may also be a result of higher radiation contribution from the front MLI of EB1.

The average temperature of the eight structural longerons and also the plumbing tray was found to be constant. These values are tabulated in table 11.8.

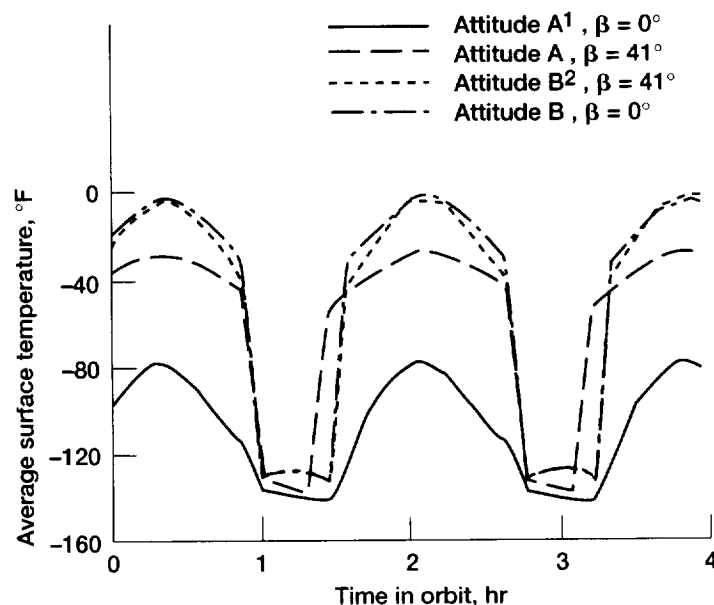
For attitude A, $\beta = 0^\circ$, because of the lack of solar flux, both the longerons and tray were identified at -102°F . However, as the Sun angle goes to $\beta = 41^\circ$, the longeron average temperature rises to -44°F . Since the tray is on the anti-Sun or cold side, it remains at a stable -98°F . Temperatures for both components increase tremendously for attitude B.

Total transient heat fluxes on the supply tank pressure vessel are presented in figure 11.12 for the four extreme cases. It is evident that for the thermal design used in this analysis, attitude A best case of $\beta = 0^\circ$ produces a 48 percent lower heat flux ($0.0559 \text{ Btu/hr-ft}^2$) relative to the $\beta = 41^\circ$ case for attitude B (0.0826). Comparably, the $\beta = 41^\circ$ worst-case for the attitude A (0.0728) produces a 22 percent lower heat flux than $\beta = 0^\circ$ for attitude B (0.0891). Further discussion is given in reference 2.

11.5.2.3 Supply Tank Purge Diaphragm Material

External to the MLI blanket, on the supply tank honeycomb can, is a purge diaphragm which contains the gaseous helium used to purge the volume between the purge diaphragm and the pressure vessel, including the MLI. To minimize the heat leak through the MLI blanket, the outer layer of the purge diaphragm requires a thermal control surface with the optimum α/ϵ , thermo-optical properties. For cryogenic tankage onboard the spacecraft, the goal is to reduce the α while maximizing ϵ , thereby reducing solar flux absorption and maximizing radiation to space for the outer surface. This produces the coldest temperature boundary for the MLI.

In the case of the COLD-SAT supply tank, three different materials were considered for the outer layer of the purge diaphragm, namely: aluminized Kapton with an α/ϵ of $0.49/0.71$, Beta cloth with an α/ϵ of $0.22/0.90$ and a SSST with an α/ϵ of $0.09/0.75$. White paint was not considered as an outer surface coating because of the requirement that this diaphragm be flexible, thereby precluding painted coatings.



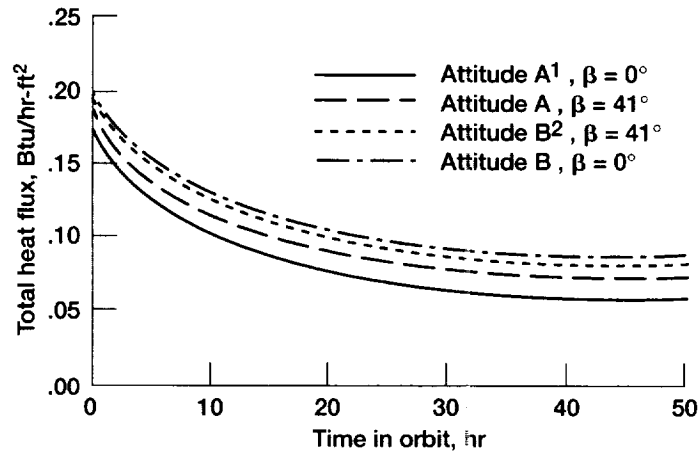
¹Attitude A: long axis in orbit plane.

²Attitude B: long axis normal to orbit plane.

Figure 11.11.—Effects of the spacecraft attitude on the average surface temperature of supply tank purge diaphragm.

TABLE 11.8.—SUPPLY TANK LONGERON AND PLUMBING TRAY
AVERAGE TEMPERATURES

Supply Tank Longeron and Plumbing Tray Temperature, °F				
Component	Attitude A, $\beta = 0^\circ$	Attitude A, $\beta = 41^\circ$	Attitude B, $\beta = 41^\circ$	Attitude B, $\beta = 0^\circ$
Longerons (average of 8)	-102	-44	-28	-8
Plumbing tray	-102	-98	-87	-71



¹Attitude A: long axis in orbit plane.

²Attitude B: long axis normal to orbit plane.

Figure 11.12.—Spacecraft attitude impacts on total heat flux
into pressure vessel.

Figure 11.13 provides analysis results for the purge diaphragm in these three cases. It can be seen that the SSST produces the lowest temperature profile with the aluminized Kapton being the warmest. On orbit, when the Sun is impinging on the purge diaphragm, the average surface temperature ranges from a minimum of -25°F for the SSST to a maximum of $+25^\circ\text{F}$ for the Kapton. Since the goal is to design the coldest purge diaphragm outer surface, the SSST was the material selected for the supply tank. Figure 11.14 shows the effects on the pressure vessel of varying the α/ϵ properties of the purge diaphragm outer surface on the total heat flux. As the α/ϵ increases, the temperature of the purge diaphragm increases. Being the thermal boundary for the heat leakage through the MLI, a higher diaphragm temperature produces a higher flux. For the materials considered for the purge diaphragm, the total heat flux varies from $0.0638 \text{ Btu/hr-ft}^2$ for the lowest case to the highest of $0.0765 \text{ Btu/hr-ft}^2$ producing an increase of 20 percent. Further discussion can be obtained in reference 3.

11.5.3 ANALYSIS RESULTS

As explained earlier in this report, four on-orbit cases of interest were analyzed

- (1) Operational on-orbit cold case with $\beta = 0^\circ$

- (2) Operational on-orbit hot case with $\beta = 41^\circ$

- (3) On-orbit load-shedding case with $\beta = 0^\circ$

- (4) On-orbit loss-of-attitude case with $\beta = 0^\circ$

Predicted temperature results of on-orbit thermal analysis for all systems and components are presented in table 11.9 and compared to the required operational temperature range. Where the predicted minimum temperature falls below the operational minimum, heaters were sized to maintain temperature. The minimum temperature was calculated for the worst on-orbit cold environmental conditions of $\beta = 0^\circ$ with the lowest power dissipation from the attitude-acquisition power profile. The maximum temperature was calculated for the worst hot case of $\beta = 41^\circ$ with the maximum on-orbit peak power dissipation.

Of specific interest are the temperature ranges of the outer surface of the supply tank purge diaphragm and the plumbing tray, which are presented graphically in figures 11.8 and 11.9, respectively, for the cold and hot cases. The propulsion system hydrazine tanks and the propellant distribution assembly temperature histories are plotted in figures 11.15 and 11.16, respectively. As can be seen, the PDA requires a 6 W makeup heater for both the hot and cold cases. For the case of load-shedding with no power dissipation in EB1 where the hydrazine tanks are

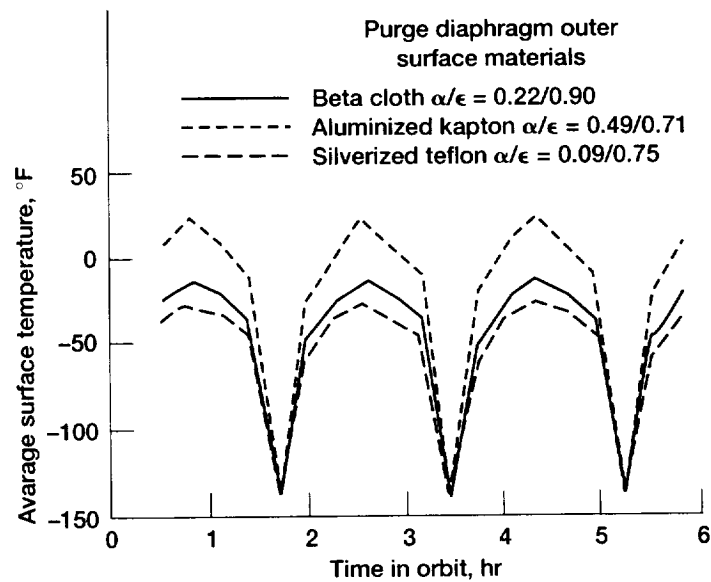


Figure 11.13.—Effects of different thermal treatments on purge diaphragm average temperature ($\beta = 41^\circ$).

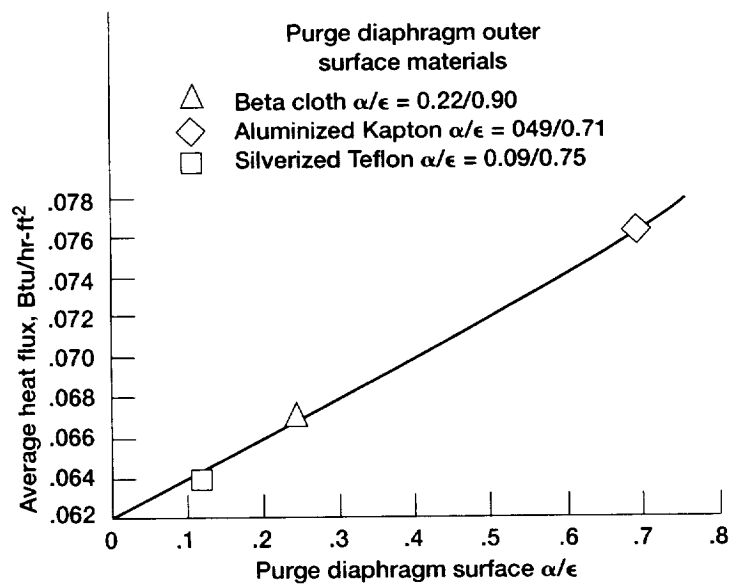


Figure 11.14.—Purge diaphragm surface effects on pressure vessel heat flux ($\beta = 41^\circ$).

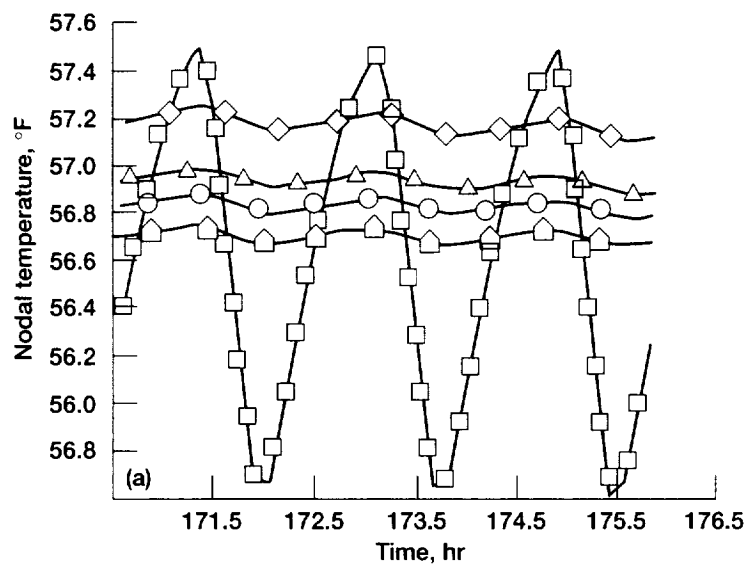
TABLE 11.9.—ON-ORBIT THERMAL ANALYSIS RESULTS

Component	Operational range, °F		Predicted range, °F			
	Minimum	Maximum	Minimum, $\beta = 0$	With heater	Maximum, $\beta = 41$	With heater
Telemetry, Tracking, and Command System						
Computer 1	30	125	51	—	92	—
Computer 2	↓	↓	58	—	85	—
Transponder 1	↓	↓	51	—	92	—
Transponder 2	↓	↓	58	—	85	—
Radiofrequency processing box	↓	↓	60	—	90	—
Solid-state recorder 1	↓	↓	59	—	90	—
Solid-state recorder 2	↓	↓	62	—	87	—
Remote command and telemetry unit 1	↓	↓	60	—	90	—
Remote command and telemetry unit 2	↓	↓	57	—	79	—
Remote command and telemetry unit 3	↓	↓	59	—	88	—
Command and telemetry unit 1	↓	↓	60	—	90	—
Command and telemetry unit 2	↓	↓	59	—	88	—
Sequencer 1	↓	↓	59	—	90	—
Sequencer 2	↓	↓	62	—	87	—
Drive motor electronics	↓	↓	50	—	79	—
Redundancy control unit	↓	↓	58	—	85	—
Command receiver	↓	↓	51	—	92	—
Experiment System						
Gaseous helium bottle 1	-65	200	-54	—	-54	—
Gaseous helium bottle 2	-65	200	-53	—	-53	—
Gaseous hydrogen bottle 1	-423	70	-54	—	24	—
Gaseous hydrogen bottle 2	-423	70	-52	—	26	—
T-0 panel	-423	-100	-96	—	-84	—
Vaporizer panel A	40	150	-88	40 (6W)	93	—
Vaporizer panel B	40	↓	-94	40 (6W)	82	—
Helium panel	-40	↓	-36	—	2	—
Vent panel A	0	↓	-94	0 (7W)	107	—
Vent panel B	0	↓	-82	0 (7W)	87	—
Plumbing tray/radiator	-423	-100	-102	—	-98	—
Connector panel A	0	100	-74	0 (2W)	94	—
Connector panel B	0	100	-96	0 (2W)	125	—
Supply tank purge diaphragm	-200	0	-115	—	-75	—
Large receiver tank MLI outer surface	-200	0	-110	—	-90	—
Small receiver tank MLI outer surface	-200	0	-130	—	-110	—
Experiment data unit 1	30	125	67	—	103	—
Experiment data unit 2	↓	↓	↓	—	↓	—
Experiment data unit 3	↓	↓	↓	—	↓	—
Accelerometer conditioner	↓	↓	58	—	85	—
Signal conditioner	↓	↓	50	—	92	—
Data acquisition unit	↓	↓	52	—	93	—
Mixer motor inverter	↓	↓	52	—	93	—
Propulsion System						
Distribution assembly	40	120	-57	60 (6W)	-35	60 (6W)
Pressurant bottle 1	↓	↓	-78	60 (7W)	-5	60 (7W)
Pressurant bottle 2	↓	↓	-74	60 (7W)	-60	60 (7W)
Pressurant bottle 3	↓	↓	-75	60 (5W)	-62	60 (5W)
Pressurant bottle 4	↓	↓	-76	60 (5W)	-5	60 (5W)
Tank 1	↓	↓	57	—	85	—
Tank 2	↓	↓	58	—	84	—
Tank 3	↓	↓	57	—	84	—
Tank 4	↓	↓	57	—	84	—
Propellant lines	↓	↓	*57	—	*85	—
Rocket engine module (REM) 1	↓	↓	77	—	101	—
Rocket engine module (REM) 2	↓	↓	73	—	98	—
Rocket engine module (REM) 3	↓	↓	73	—	96	—
Rocket engine module (REM) 4	↓	↓	77	—	97	—

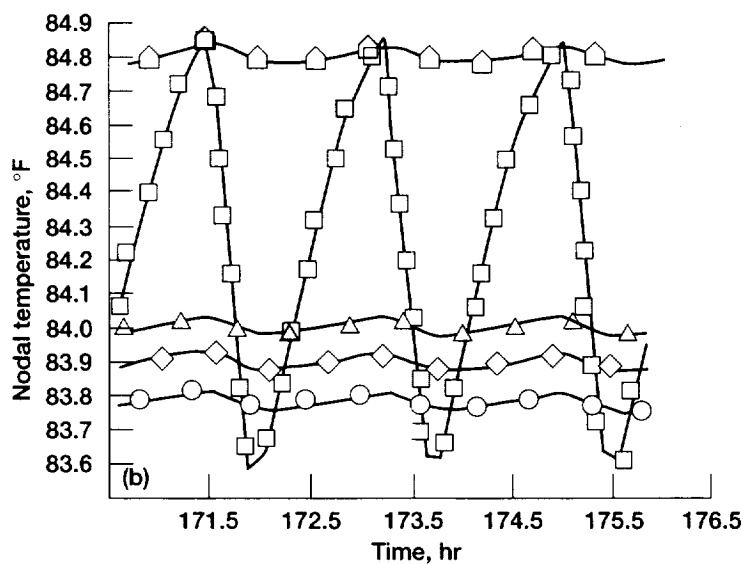
*Approximation.

TABLE 11.9.—Concluded.

Component	Operational range, °F		Predicted range, °F			
	Minimum	Maximum	Minimum, $\beta = 0$	With heater	Maximum, $\beta = 41$	With heater
Attitude Control System						
Inertial reference unit	30	105	60	-----	90	-----
Horizon sensor 1 electronics	30	125	57	-----	79	-----
Horizon sensor 2 electronics	30	↓	59	-----	88	-----
Fine Sun sensor 1 electronics	15		48	-----	72	-----
Fine Sun sensor 2 electronics	15		50	-----	79	-----
Magnetometer 1	30		49	-----	79	-----
Magnetometer 2	30		49	-----	79	-----
Attitude control system interface electronics	30		52	-----	93	-----
Horizon sensor 1 optics	-5	140	53	-----	90	-----
Horizon sensor 2 optics	-5	140	47	-----	84	-----
Fine Sun sensor 1 optics	15	140	77	-----	101	-----
Fine Sun sensor 2 optics	15	140	73	-----	98	-----
Power System						
Battery 1	30	85	48	-----	73	-----
Battery 2	30	85	50	-----	79	-----
Solar array 1	-95	160	-70	-----	135	-----
Solar array 2	-95	160	-70	-----	135	-----
Power control unit	30	125	61	-----	88	-----
Power distribution unit	30	125	57	-----	79	-----
Pyro control box	30	125	60	-----	88	-----
Structural System						
Electronics bay 1 panel N	30	125	48	-----	72	-----
Electronics bay 1 panel S	↓	↓	50	-----	79	-----
Electronics bay 1 panel E			59	-----	90	-----
Electronics bay 1 panel W			62	-----	87	-----
Electronics bay 1 panel NE			50	-----	91	-----
Electronics bay 1 panel NW			60	-----	87	-----
Electronics bay 1 panel SE			59	-----	89	-----
Electronics bay 1 panel SW			58	-----	84	-----
Electronics bay 2 panel N			47	-----	84	-----
Electronics bay 2 panel S			53	-----	90	-----
Electronics bay 2 panel E			57	-----	79	-----
Electronics bay 2 panel W			67	-----	103	-----
Electronics bay 2 panel NE			49	-----	79	-----
Electronics bay 2 panel NW			52	-----	93	-----
Electronics bay 2 panel SE			59	-----	88	-----
Electronics bay 2 panel SW			—	-----	—	-----
Struts	-100	50	-65	-----	-5	-----
Supply tank longerons	-150	↓	-110	-----	-44	-----
Rings	-150		-110	-----	-44	-----
Diagonals	-150		-110	-----	-44	-----
Hydrazine tank plate	40	100	58	-----	85	-----



Curve summary	Temperature, °F	
	Min	Max
□ = Tank support plate	55	58
⬠ = Tank 1	56	57
◇ = Tank 2	57	58
△ = Tank 3	56	57
○ = Tank 4	56	57



Curve summary	Temperature, °F	
	Min	Max
□ = Tank support plate	83	85
⬠ = Tank 1	84	85
◇ = Tank 2	83	85
△ = Tank 3	83	84
○ = Tank 4	83	84

Figure 11.15.— Electronics bay 1 hydrazine tank results for operational on-orbit case. (a) Worst-case cold; $\beta = 0^\circ$. (b) Worst-case hot; $\beta = 41^\circ$.

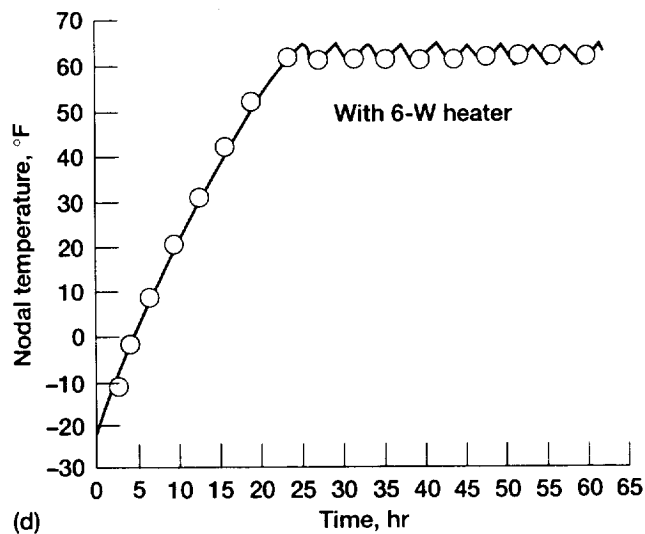
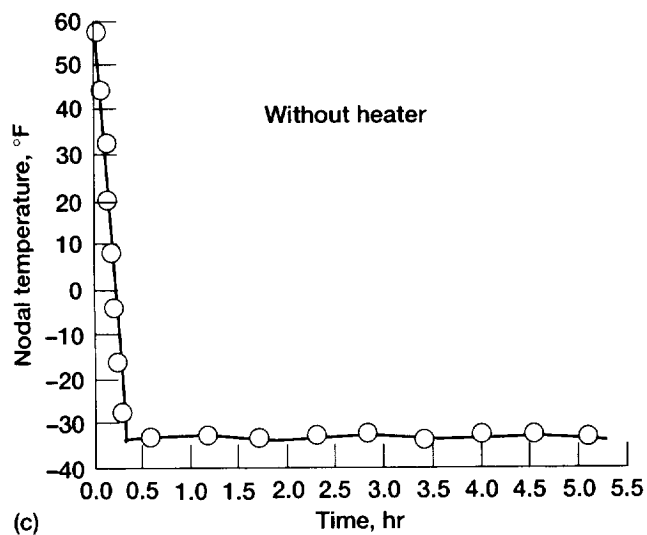
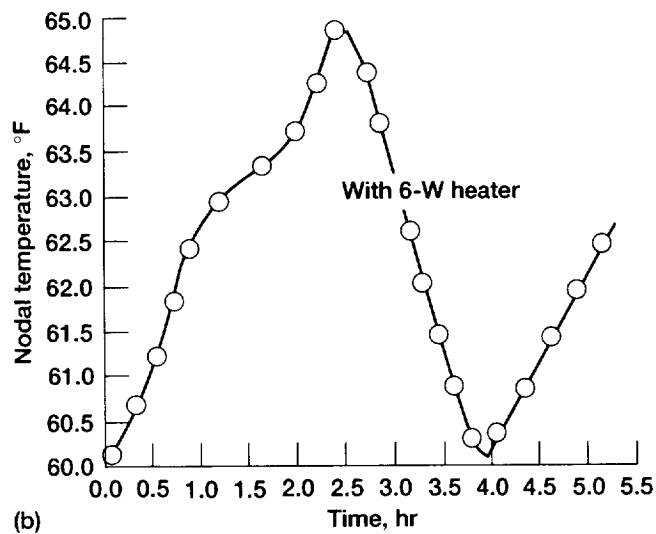
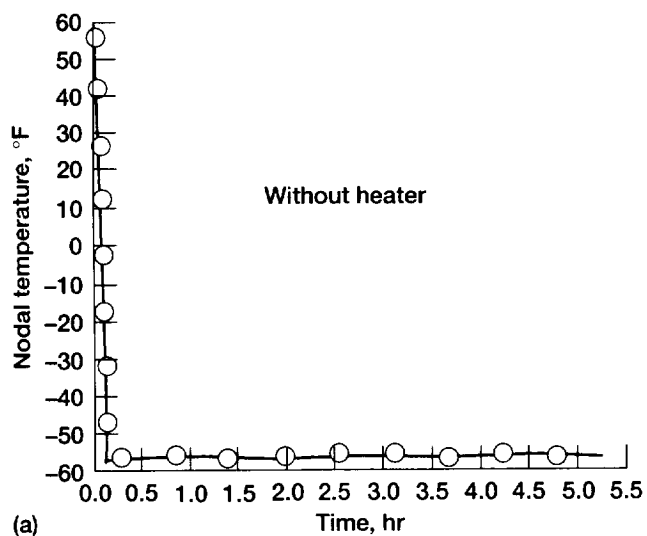


Figure 11.16.—Propellant distribution assembly results for operational on-orbit case; (a, b $\beta = 0^\circ$ cold; c, d $\beta = 41^\circ$ hot).

located, it will take 35 hr for the hydrazine to freeze at 34.8 °F, starting from the initial temperature of 75 °F (fig. 11.17). This case was analyzed for a $\beta = 0^\circ$ attitude with zero-power dissipation in EB1. As seen in figures 11.18 and 11.19, the thermal control system for the batteries maintains the temperature within an acceptable range for both the nominal hot and cold cases, and also for the loss-of-attitude case. The loss-of-attitude control case was considered when the spacecraft long axis is perpendicular to the orbit plane and solar flux is incident on the EB1 battery number 2 panel with maximum power dissipation from the rest of the electronics.

COLD-SAT heater-power requirements are summarized in tables 11.6 and 11.7. Makeup heaters are those that are necessary to maintain a component within operating range when the component is in normal operating mode and dissipating power. Backup heaters are required to maintain the component within the operating temperature range when the component is not operating. Survival heaters are needed for maintaining a cold-start turn-on temperature of -5°F for electronic components when these are shut down. Heaters are not required for EB1 components except for the batteries and the Propulsion Subsystem components. This is a result of the warm environment maintained in EB1 by the large thermal mass of the hydrazine tanks even when there is a sudden disruption of electrical power dissipation. This situation may arise when there is a loss of spacecraft attitude resulting in no power generation from the solar arrays. For the 4 hr that the batteries can supply power

without recharging, the temperature of the EB1 electronics boxes stays within operating range because of the hydrazine tanks.

Figure 11.20 shows predicted solar array transient temperature responses for $\beta = 0^\circ$ and $\beta = 41^\circ$ cases. Vendor-provided values of absorptivity and emissivity for the solar cell side of the array are 0.73/0.86.

11.5.4 ASCENT AERODYNAMIC HEATING

Aerodynamic heating during ascent causes a rise in the ELV fairing temperature. The increase in fairing temperature results in a rise in the temperature of low thermal-mass items located on the exterior of the spacecraft. Figure 11.21 shows data from the ANIK-E launch on the Ariane ELV. Similar results would be expected for COLD-SAT. The greatest temperature rise is experienced by the exterior layer of the MLI blankets. Internally mounted spacecraft components experience a temperature rise that is typically less than 3°C at fairing separation, because of a combination of their thermal mass and low thermal coupling to the fairing. Fairing separation occurs when the ELV is in the free-molecular-flow flight regime. The peak free-molecular heat flux after separation results in maximum temperature of selected equipment as shown in table 11.10. A separate thermal analysis for ascent has not been performed since the power dissipations for the ascent case is the same as in the attitude-acquisition case, for which analysis has been performed and results have been presented in this report.

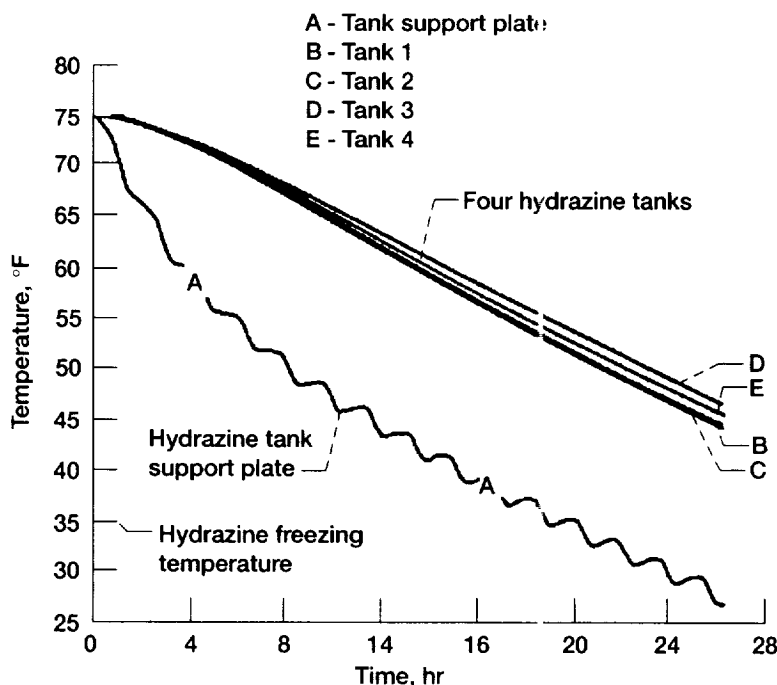
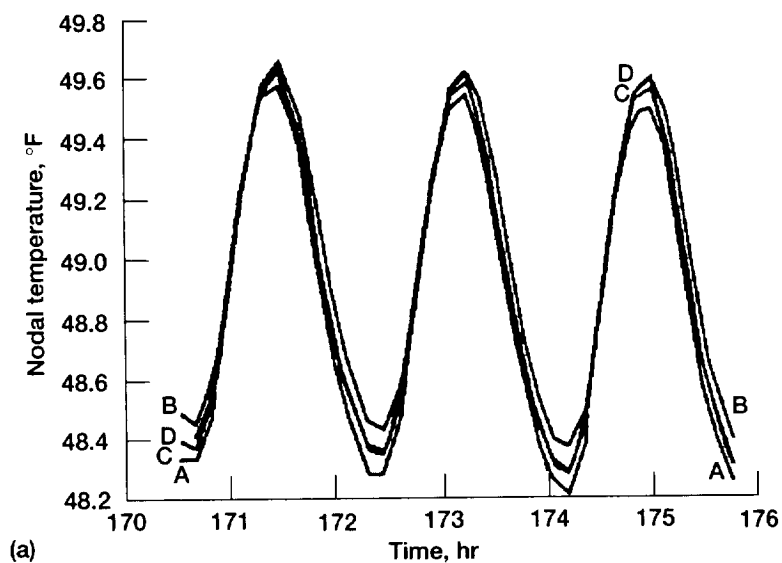
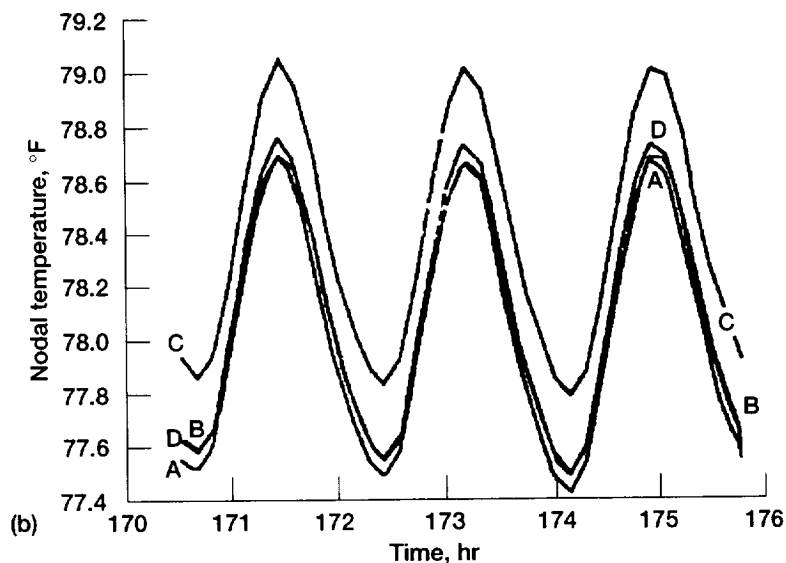


Figure 11.17.—Hydrazine tank results for load-shed case.

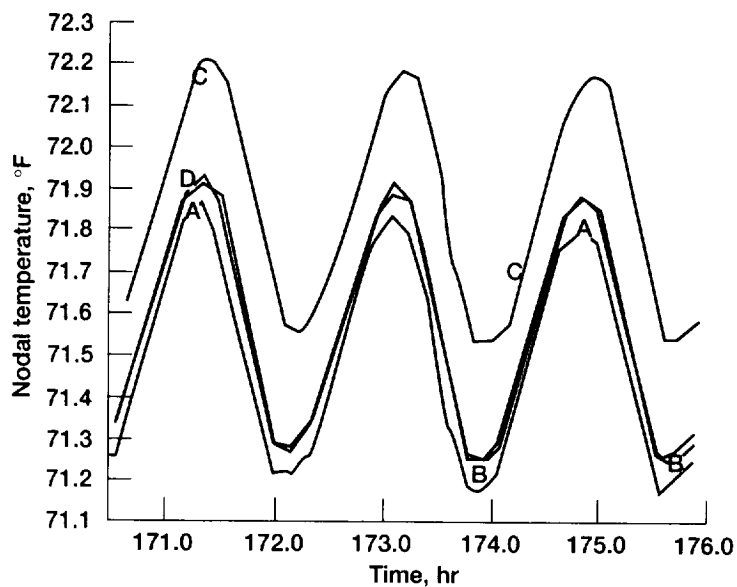


Curve summary	Temperature, °F	
	Min	Max
A = South panel	48	50
B = Battery 2	48	50
C = Motor drive electronics	48	50
D = Sun sensor 2 electronics	48	50



Curve summary	Temperature, °F	
	Min	Max
A = South panel	77	79
B = Battery 2	77	79
C = Motor drive electronics	77	79
D = Sun sensor 2 electronics	77	79

Figure 11.18.— Battery 2 results for operational on-orbit case. (a) Worst-case cold, $\beta = 0^\circ$. (b) Worst-case hot, $\beta = 41^\circ$.



Curve summary	Temperature, °F	
	Min	Max
A = South panel	71	72
B = Battery 2	71	72
C = Motor drive electronics	71	73
D = Sun sensor 2 electronics	71	72

Figure 11.19.— Battery 2 results for loss of attitude case.

TABLE 11.10.—MAXIMUM TEMPERATURE OF EQUIPMENT EXPOSED TO FREE-MOLECULAR HEATING

Exposed elements	Maximum temperature, °C
Outer MLI layer	^a 145
Low-gain antenna	^b 100
High-gain antenna reflector dish	^b 115

^aKapton survival temperature is 750 °C

^bCOLD-SAT low-gain antenna and high-gain antenna are MLI insulated.

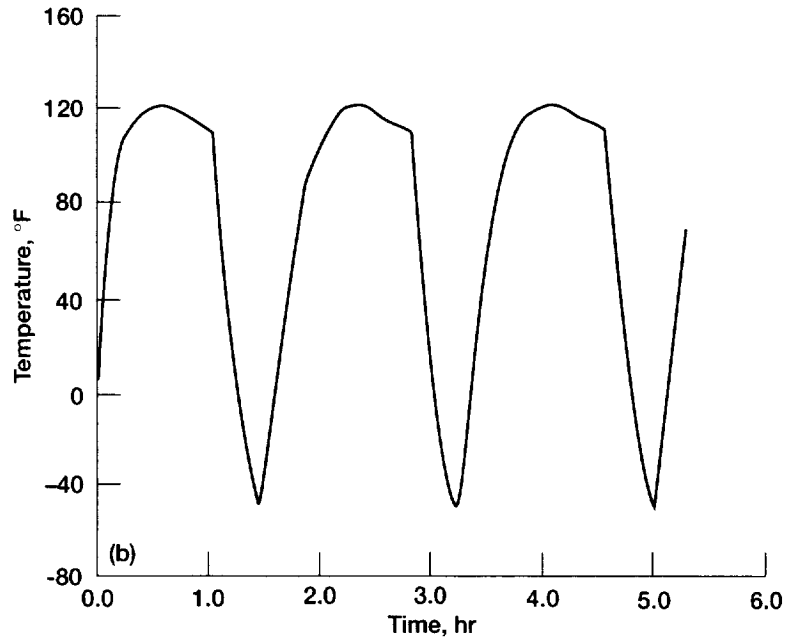
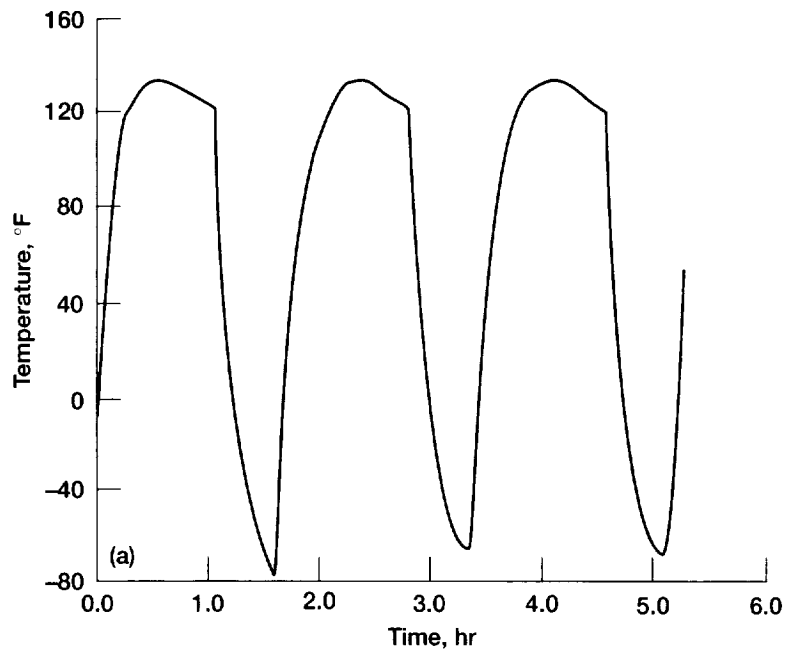


Figure 11.20.—Solar panel temperatures. (a) $\beta = 0^\circ$. (b) $\beta = 41^\circ$.

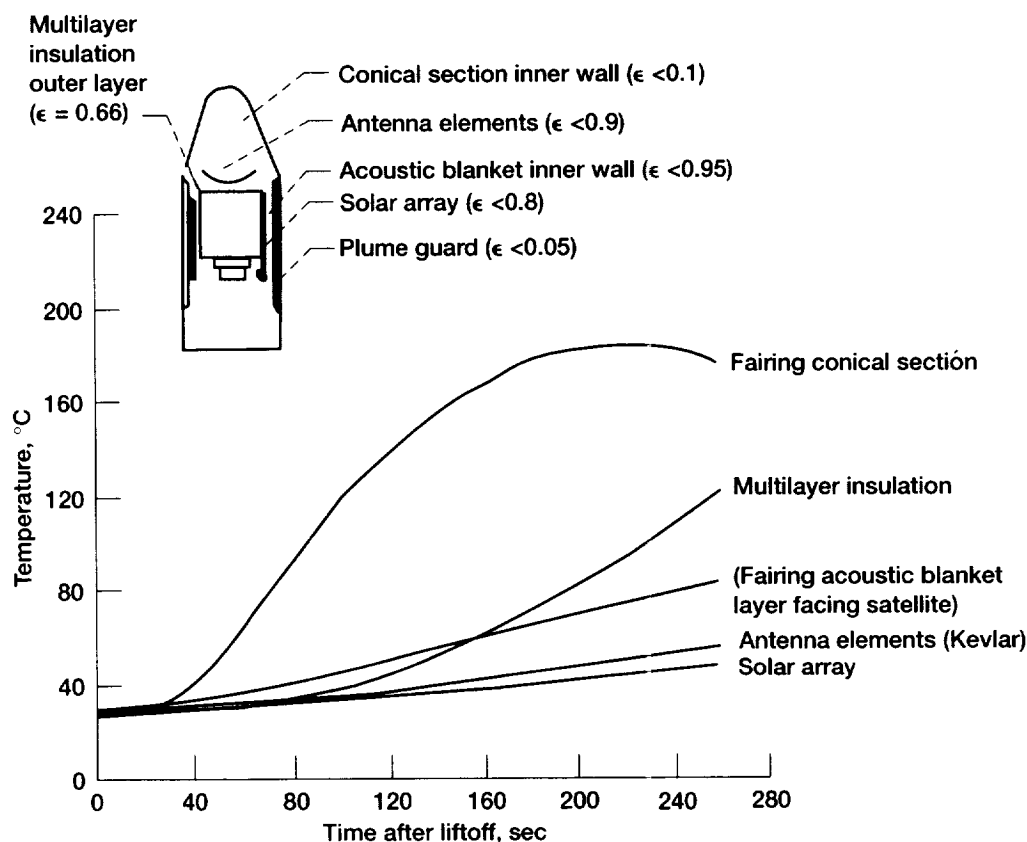


Figure 11.21.—Effect of fairing heating on satellite surfaces during ascent.

11.6 Thermal Control Subsystem Components

The heritage and qualification status of the COLD-SATTCS hardware is summarized in table 11.11. Availability and cost of components is shown in table 11.12. The composition and thermo-optical properties are tabulated in table 11.5. All properties used in the TCS analysis are BOL because in the short mission life no degradation for outgassing, solar illumination, plume effects and electrostatic charging, has been included. Key components of the TCS are described below.

11.6.1 MULTILAYER INSULATION

Spacecraft areas that require minimum interaction with the external environment are covered with MLI blankets. Details of blanket construction are shown in figure 11.22(a). Alternate layers of 1/4-mil double-aluminized Kapton and dacron net are sandwiched between outer layers of 2-mil reinforced Kapton with inner surface aluminized. The layers are sewn together with nylon thread, and large sections of blanket material are joined to each other and to the spacecraft using Velcro zipper material. To avoid charge buildup on MLI surfaces, several 2-mil-thick aluminum grounding straps are attached with soft aluminum rivets to aluminized surfaces, as shown in

figure 11.22(b). In addition, the outer surface of the outer layer is coated with indium tin oxide (ITO) to prevent electrostatic charge buildup.

Outgassing of volatile compounds for MLI blankets during the mission will be minimized by preflight thermal vacuum decontamination bakeout. Remaining residual outgassing during the mission will be directed away from the sensitive OSR radiator surfaces by preferentially located venting holes.

11.6.2 OPTICAL SOLAR REFLECTORS

Spacecraft surfaces which function as radiator surfaces are covered with OSR's. The reflectors are second-surface mirrors made from silver plated 0.006-in. fused silica. Individual 1-in.² mirrors are placed 15-mils apart and bonded with electrically conductive blue solithane to the outer aluminum facesheets of the EBI side panels. Of all potential radiation surfaces available for use in the COLD-SAT spacecraft, OSR's have been chosen because of the stability of their properties in the on-orbit environment for this critical application. Individual radiators have measured solar absorbance values of 0.06 at BOL. The OSR system, including gaps between individual mirrors, has an emissivity of 0.75 and a BOL absorbance of 0.09. Degradation in absorptivity results from ultraviolet radiation and particle fluence, as well as from induced contamination by thruster exhaust plumes and outgassing spacecraft materials.

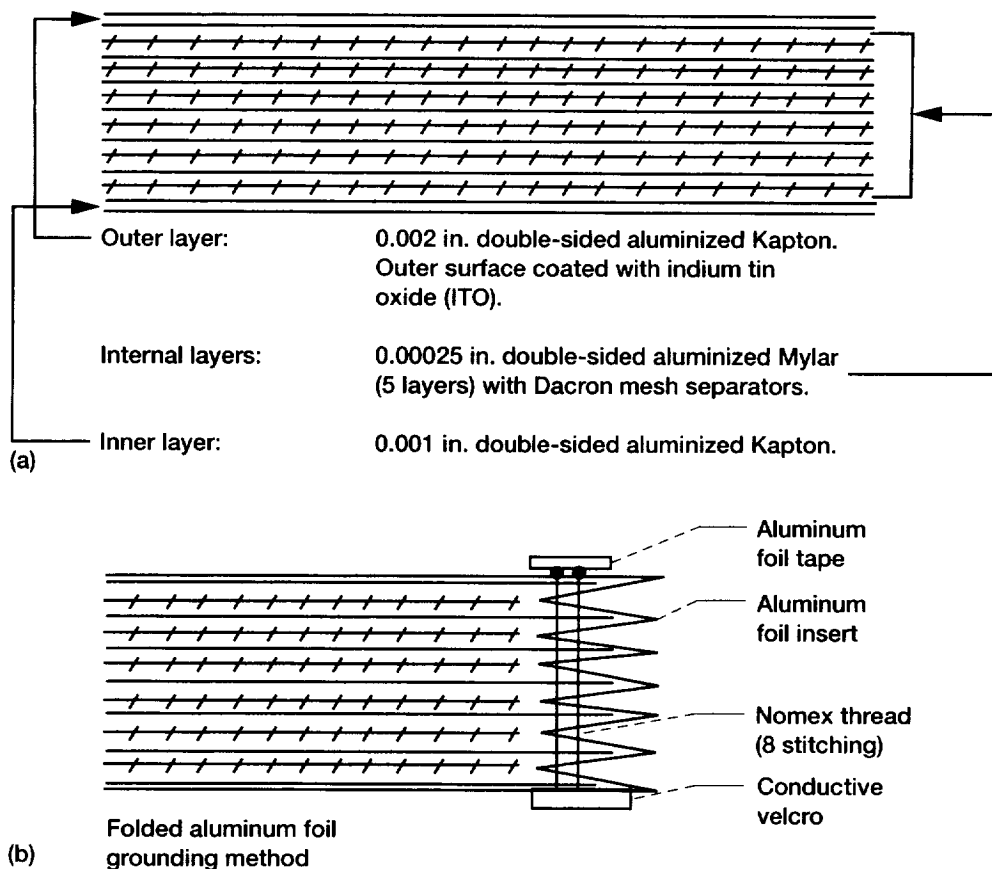


Figure 11.22.—Typical multilayer insulation blanket details. (a) Blanket configuration. (b) Blanket grounding configuration.

TABLE 11.11.—COLD-SAT THERMAL CONTROL SYSTEM COMPONENTS
HERITAGE AND QUALIFICATION STATUS

Component	Vendor	Heritage	Qualification status
Multilayer insulation (MLI) blanket materials	Sheldahl	IRAS, COBE, ERBS	Qualified ↓
Optical solar reflectors	Optical Coating Laboratory, Inc.	SATCOM, STC/DBS	
Heater and adhesives	MINCO	SATCOM	
Paints	Chemglaze	GSTAR, SPACENET	
Tape	Sheldahl	SATCOM	
Thermal interface	Chocterm	STS	
Thermal controllers	Elmwood	SATCOM, STC/DBS	
Temperature sensors	Elmwood	SATCOM, STC/DBS	
Velcro and adhesives	Velcro	GE SERIES 3000 and 4000	

TABLE 11.12.—THERMAL CONTROL SYSTEM COMPONENT AVAILABILITY AND COST

Component	Catalog number	Vendor	Cost	Comments
2.0-mil Kapton/VDA	G410620	Sheldahl	\$3394/sheet	4- by 10-ft sheet
5.0-mil Teflon/VDA	G401500		\$1554/sheet	4- by 10-ft sheet
Silver/VD Inconel				
0.5-mil Kapton/VDA	G410660		\$3263/sheet	4- by 10-ft sheet
Thick black film/0.5-mil	G143700		\$24/ft ²	250 to 500 ft ²
Kapton/SCRIM/VDA			\$20/ft ²	501 to 1000 ft ²
0.5-mil Kapton/VDA/	G407760		\$383/roll	108-ft-long roll tape
1.0-mil Silicone				
VDA/1.0 mil Kapton/	G407810		\$375/roll	108-ft-long roll tape
1.0-mil Silicone				
Optical solar reflector	6068002	OCLI	\$20/piece	1.5 by 1.5 in., 6 MIL thick
Conduction enhancer	Chothem 1671	Chomerics	\$178/piece	16 by 16 in.
White paint	Z-202	Lloyd Corporation	\$35/gal	\$525 minimum order
Black paint	Z-306	Lloyd Corporation	\$27/gal	\$525 minimum order
Heaters	Thermofoil SB 311C 79	MINCO	Various	
Velcro	Various	Velcro, USA	Various	

TABLE 11.13.—COLD-SAT THERMAL CONTROL SYSTEM WEIGHT SUMMARY

Component	Weight, lb
MLI blankets, velcro, and adhesives	30.0
Optical solar reflectors	5.0
Thermal controllers	8.0
Temperature sensors, thermistors	5.0
Heaters and adhesives	2.0
Paint	3.0
Tape	1.0
Thermal interface (Chothem)	5.0
Thermal isolators (G-10)	3.0
TOTAL	62.0

11.6.3 HEATERS AND CONTROLLERS

The active portion of the TCS is composed of Kapton film-strip heaters, DTC's, and temperature sensors. DTC's provide automatic control of heaters on the basis of sensor temperature. They have the following design features: proportional control of heater power, adjustable set point temperatures and heater output power, heater on/full-on temperature difference of 2 °F, and ground-commandable override capability.

11.6.4 PASSIVE SURFACES

The following passive surface treatments are employed to achieve specific radiative properties:

- (1) Black paint: Chemglaze Z-306 (Urethane), minimum $\epsilon = 0.85$
- (2) Aluminized Kapton Tape: Single aluminized, aluminized side out, $\epsilon = 0.10$; single-aluminized, aluminize second surface, $\epsilon = 0.55$
- (3) White paint: Chemglaze Z-202; $\epsilon = 0.89$, $\alpha = 0.2$

TABLE 11.14.—COLD-SAT THERMAL CONTROL SYSTEM COMPONENT RELIABILITY

Component	Duty cycle, percent	Probability of 2-year survival
Optical solar reflectors	100	0.999734
Multilayer insulation	100	.999825
Battery heaters	—	.999974
Thruster heaters	—	.999962
Fuel line heaters	—	.999999

11.6.5 CHOTHERM 1671

Chothem 1671 is a thermally conductive interface material designed for transferring heat from electronics components to heat sinks. It comprises a silicone binder with boron nitride as the thermally conductive filler. Unlike mica or beryllium oxide, Chothem does not require thermal grease. Greaseless application of Chothem precludes the contamination, cracking, migration, or drying out associated with greases. It is available in sheet sizes and meets NASA's outgassing requirements. The advantage of using Chothem is that it reduces the uncertainties in the determination of contact conductances between two surfaces for use in the thermal analysis models. Published values of thermal conductivity were used for Chothem for a 0.125-in.-thick sheet.

11.6.6 THERMAL CONTROL SUBSYSTEM WEIGHT

The weight of the TCS is summarized in table 11.13.

11.6.7 RELIABILITY

Reliability numbers for a probability of survival of two years are shown in table 11.14 for general TCS components. These are taken from the Advanced Communication Technology Satellite (ACTS) program.

TABLE 11.15.—THERMAL SYSTEM TEMPERATURE
TELEMETRY SUMMARY

Components	Number
Propulsion System	
Fill/drain valve	1
Relief valve/burst disk	1
Check valve	1
Solenoid valve	7
Hydrazine tanks	4
Fuel lines	--
Thruster valves	20
Nozzle shield	20
Gimbal unit	2
Gaseous helium tanks	1
Orifice	5
Line filters	2
Power System	
Batteries	8
Solar arrays	6
Power control unit	2
Power distribution unit	7
Pyro control box	2
Attitude Control System (ACS)	
Inertial reference unit	1
Horizon sensors electronics	2
Horizon sensors optics	2
Sun sensor assemblies	2
Magnetometers	2
ACS interface electronics	1
Telemetry, Tracking, and Command System	
Computers	2
Transponder	2
Radiofrequency processing box	1
Solid-state recorders	2
Remote command and telemetry units	2
Command and telemetry units	2
Sequencers	2
High-gain antenna drive motor electronics	2
High-gain antenna gimbal motor	1
Redundancy control unit	1
Command receiver	1
Low-gain antennas	1
Experiment System	
Supply tank	14
Large receiver tank	4
Small receiver tank	4
Gaseous helium and gaseous hydrogen bottles	4
Panels	10
Radiator/plumbing tray	4
Structure System	
Supply tank longerons	8
Large receiver tank struts	4
Small receiver tank struts	4
Electronics bay 1 and 2 panels	16
Total	189

TABLE 11.16.—THERMAL CONTROL HEATER ACTIVATION TECHNIQUES

Location	Activation technique	System monitoring
Batteries	Dual temperature control, ground-commandable override on backup redundant (2.01 ± 1 °F)	Redundant thermistors
Propellant tanks	Dual temperature control, ground commandable	Redundant thermistors
Pressurant tanks	Override on back-up redundant	Redundant thermistors
Propellant lines	Ground-commanded redundant heaters (10.0 ± 1 °F)	-----
Thruster valves	Dual temperature control, ground-commanded redundant (10.0 ± 1 °F)	Thermistors
Catalyst bed	Operated via ground-enable command, redundant heaters	Thermocouple
Propellant distribution assembly	Dual temperature control, ground-commandable override on backup redundant (10.0 ± 1 °F)	Redundant thermistors
Solar array hinge damper	Parallel redundancy, ground-commanded	None
High-gain antenna motor drive	Parallel redundancy, ground-commanded	Redundant thermistors
Experiment panels	Dual temperature control, ground-commanded redundant	Thermistors
Electronics bay 1 avionics	Computer on/off commandable survival heaters	Thermistors
Electronics bay 2 avionics	Computer on/off commandable survival heaters	Thermistors

TABLE 11.17.—THERMAL CONTROL SYSTEM (TCS)

Subsystem	TCS component
Structure	MLI OSR's Vespel pads Paint Chootherm 1671
Telemetry, tracking, and command	Paint Heaters Digital thermal controllers Chootherm 1671
Power	Solar array paint Paint Chootherm 1671 Heaters Digital thermal controllers Battery thermal enclosure
Attitude control	Paint Chootherm Heater Digital thermal controllers MLI
Propulsion	Paint MLI Tape Heaters Digital thermal controllers Thermal shorting strap
Experiment	Supply tank purge diaphragm outer surface Plumbing tray and panels outer surface Heaters Digital thermal controllers
Mechanism	Solar array damper/hinge heater High-gain antenna damper/hinge heater

11.7 Operational Characteristics

A summary of telemetry data requirements for the TCS is provided in table 11.15. The heater control, location, and activation techniques are summarized in table 11.16. Spacecraft heaters and associated controllers are functionally redundant, in cases where heated units themselves are not. Due to the closed-loop nature of DTC operation, uplink anomalies will not preclude nominal operation of heaters; however, ground commandable override capability is provided. Certain heaters are controlled by ground command only for components associated with ground-commanded events (e.g., solar array deployment and RCS thruster firings). Heater power is minimized for all mission phases. Preoperational housekeeping heater power for makeup is minimized. In addition, backup and survival heaters do not add load to the power system.

The TCS design approach does not require that restrictions be placed on the electronics operating duty cycle which for this analysis is assumed as 100 percent for all components. Commandable backup load substitution heaters may be configured to accommodate a broad range of operational conditions.

11.8 Interfaces

The TCS interfaces with all other spacecraft systems. The TT&C system provides data acquisition and heater power switching services to the TCS. Onboard software must be programmed to control TCS heaters and the electric power system must supply power to them. Protection of thermal control surfaces will place many stringent restrictions on ground and prelaunch activities. In addition, those items which constitute the TCS must be attached to the components of the other spacecraft systems which they protect. Table 11.17 provides a top level listing of types of TCS components required by the other parts of the spacecraft.

11.9 References

1. Knozok, H.-G., et. al.: Battery Thermal Design and Performance in European Geo-Satellite Programs. SAE Paper 871484, Proceedings of the 17th Intersociety Conference on Environmental Systems, 1987.
2. Arif, H.: Spacecraft Attitude Impacts on COLD-SAT Non-Vacuum Jacketed LH₂ Supply Tank Thermal Performance. AIAA Paper 90-1672, June, 1990 (also NASA TM-103158, 1990).
3. Arif, H.: Thermal Aspects of Design for the COLD-SAT Non-Jacketed Supply Tank Concept. AIAA Paper 90-2059, 26th AIAA/SAE/ASME/ASEE Joint Propulsion Conference and Exhibit, Orlando, Florida, July, 1990.

Chapter 12

Software

Daniel R. Vrnak

National Aeronautics and Space Administration

Lewis Research Center

Cleveland, Ohio

12.1 Introduction

This section of the report describes the COLD-SAT flight computer or onboard computer (OBC) software functions, requirements, and interfaces. The flight computer is part of the telemetry, tracking, and command (TT&C) system described in Chapter 9, Telemetry, Tracking, and Command System, of this report.

The COLD-SAT OBC is responsible for providing autonomous on-orbit computation and control capability in support of the spacecraft systems and experiment operation. The need for autonomy is greater in this application than in many previous spacecraft designs. During normal operations, Tracking and Data Relay Satellite System (TDRSS) forward link coverage will be limited to a 12-percent duty cycle or 13-min/105-min orbit. Yet many experiments are of long duration—up to 50 hr for some. Most experiments are placed in groups to be initiated by ground command and then proceed with minimal supervision. Therefore, the software must be written to anticipate and handle the many contingencies that may occur. Some possible contingencies include tank over-pressure or over-temperature, excessive attitude errors, battery failure, and thruster-heater failure.

12.2 Major Requirements

The top level requirements for the COLD-SAT flight computer software include the following:

- (1) Attitude determination and control
- (2) Navigation
- (3) Antenna pointing
- (4) Thermal system control

- (5) Propulsion system control
- (6) Electrical power system monitor
- (7) Respond to uplinked commands
- (8) Downlink spacecraft status and experiment data
- (9) Support ground, ascent, and post-separation operations
- (10) Comply with NASA and Department of Defense safety requirements
- (11) Store test sequences for all experiments
- (12) Monitor and control state of cryogen at all times
- (13) Place and maintain spacecraft in a safe-state mode during contingency operations
- (14) Periodically check integrity of the computer hardware and software
- (15) Switch to backup computer if a fault is detected in the primary computer

12.3 Description

The OBC is redundant. There is a primary computer and a secondary computer which acts as a hot backup. Each has the same software loaded. Both computers execute the same code in step, and receive the same input signals and data, with the output of the backup computer disabled. Each has its own spacecraft clock and they will periodically be resynchronized. A redundancy control unit monitors the activities of the two computers. Both computers periodically run a self-test which generates a specific result. If a fault is detected in the operation of the primary computer, the redundancy control unit will switch control to the backup and disable the outputs of the faulted computer. Possible faults include memory checksum error, clock failure, communications interface failure, and execution errors. Switching back to the primary computer can only take place by ground command.

The OBC software is required, upon power-up or reset, to run a self-test, the results of which are recorded for downlink. The last step of the self-test is to invoke the applications scheduler. The applications scheduler runs every basic spacecraft clock cycle and invokes the application programs or tasks according to a predefined schedule. The applications scheduler keeps track of the status of each task, updates its job control block upon job completion, and then selects the next task to execute based on the predefined schedule. The schedule may be modified by ground command.

A queue manager is used by the applications scheduler to queue tasks for future execution. The scheduler scans an array of job control blocks and submits the active ones to the queue manager. Some tasks will not be active during certain phases of the mission. Job control blocks provide scheduling information for each task including the following:

- (1) Next execution time
- (2) Priority level
- (3) Frequency of execution
- (4) Start cycle offset time
- (5) Queue status

Some tasks will not complete in their allotted time. These tasks will get interrupted to continue in the next processing cycle but only after the higher priority tasks have finished. The highest priority tasks will be designed to always finish in less than a basic clock cycle. Tasks that are likely to need more than one spacecraft clock cycle will have lower priorities and be scheduled to run less often.

After a task executes, it is rescheduled for its next execution time by the scheduler. While executing, a task may deactivate itself or other tasks. Communications between tasks is expected to take place mainly via shared memory. The basic spacecraft clock cycle is also used to update the onboard spacecraft clock which keeps absolute time. The spacecraft clock can be changed by ground command.

Built into the OBC is protection against single-event upsets (SEU's), which are a state change in a bit or cell of digital

memory caused by ionization when a high-energy cosmic ray particle passes through the integrated circuit transistor. The result of one or more SEU's occurring while the spacecraft is in active operation could be no effect or very serious. For example, the wrong valve could be opened during an experiment. The OBC uses the following three methods to minimize the possibilities of SEU's occurring:

- (1) integrated circuit technology that is extremely resistant to upset by cosmic rays
- (2) error detection and correction firmware with the extra six memory bits attached to every word
- (3) periodic running of the self-test which includes detection of errors caused by SEU's in specific hardware

Latch-up is another possible condition where a memory or register bit gets changed as a result of cosmic radiation. In this case the change of state is not reversible. The OBC will use components designed and tested to be latch-up immune.

12.4 Interfaces

The data flow between the OBC and the other components of the TT&C system are shown in figure 12.1. The OBC is comprised of a primary and a secondary computer. In all the interface listed in the following sections, each computer has its own link to the device.

12.4.1 COMMAND AND TELEMETRY UNIT (CTU)

The OBC exchanges data and commands with the CTU by using a 1553-serial-data link. This interface will have the most traffic.

12.4.2 REDUNDANCY CONTROL UNIT (RCU)

The OBC communicates status to and receives the switch-over command from the RCU.

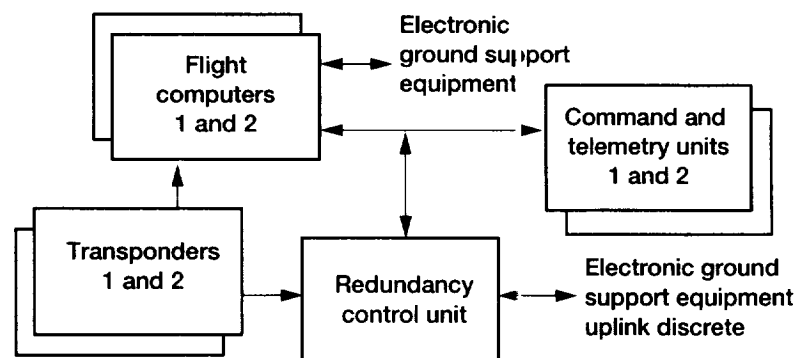


Figure 12.1.—Onboard computer interfaces.

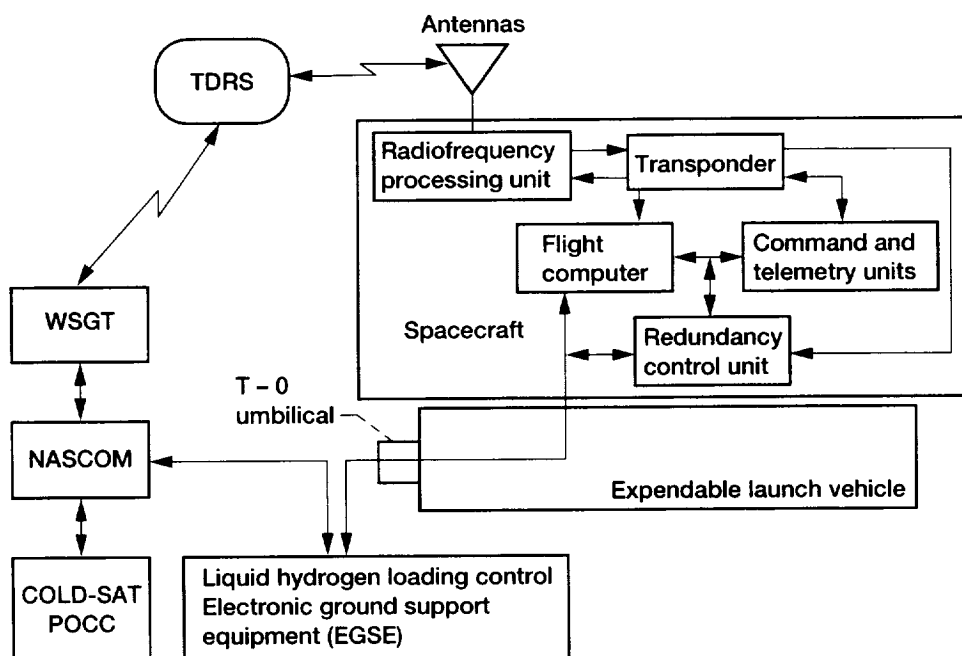


Figure 12.2.—External onboard computer interfaces.

12.4.3 TRANSPONDER

On-orbit software changes, when needed, will be loaded into the OBC read/write memory (RAM) using a data link to the transponder.

12.4.4 LAUNCH PAD ELECTRICAL GROUND SUPPORT EQUIPMENT (EGSE)

Figure 12.2 shows that there is a 1553-serial-data interface that exists only while the spacecraft is at the launch pad and mated to the launch vehicle, which connects the OBC to the electronic ground support equipment (EGSE). This link, which is cut at T-4 sec, is used for checkout of spacecraft systems, loading the RAM software, setting the spacecraft clock, and giving the OBC full control.

12.4.5 POCC TELEMETRY

Through the transponder, radiofrequency (RF) processing unit, and antennas, spacecraft telemetry and data are sent to and commands received from the TDRSS. Through White Sands Ground Terminal (WSGT) and NASCOM (NASA communications network), TDRSS data are sent to and received from the COLD-SAT payload operations control center (POCC). Computers at the POCC will be programmed so controllers will be able to safely control spacecraft operations and receive data and results. This link does not exist until spacecraft separation from the upper stage.

12.5 Software Description

There are 14 OBC tasks required for operating the spacecraft and conducting the experiments. These tasks are activated by the scheduler on a predefined plan. A conceptual diagram of the scheduler is shown in figure 12.3. The scheduler runs every basic spacecraft clock cycle of 62.5 msec. Most tasks do not need to run every cycle and therefore are scheduled to run every second cycle or third cycle, and so on. Some tasks are needed only for specific phases of the mission and are deactivated at all other times. The task "prelaunch operations" is an example. It is used from prelaunch startup until launch, after which it is never activated again. All tasks use input/output procedures of the operating system to access the spacecraft sensors and effectors via the TT&C system. The tasks are as follows:

- (1) Attitude determination and control
- (2) Ground command processing
- (3) Command and telemetry unit input/output (I/O)
- (4) Data formatting
- (5) Critical status monitor and safing
- (6) Electrical power monitor
- (7) Antenna pointing
- (8) Navigation
- (9) Thermal monitor and control
- (10) Propulsion system
- (11) Experiment monitor and control
- (12) Praelaunch operations
- (13) Ascent operations
- (14) Postseparation operations

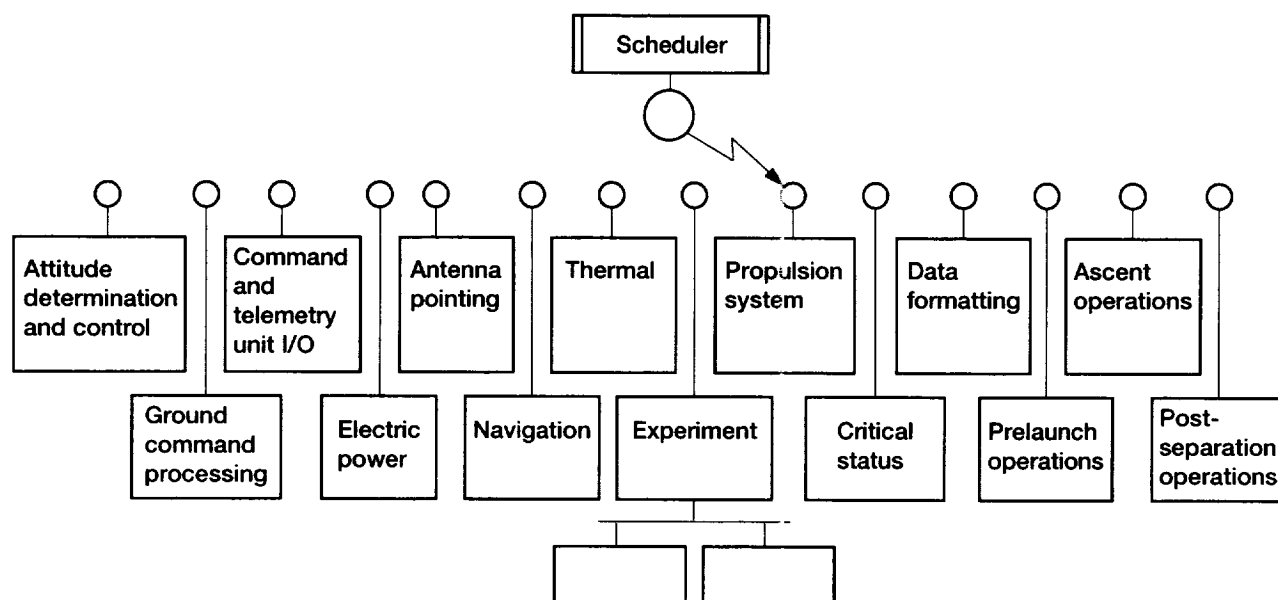


Figure 12.3.—Onboard computer task scheduler.

12.5.1 ATTITUDE DETERMINATION AND CONTROL

This task's main function is to maintain the desired spacecraft attitude within specific limits and to handle requests from the experiment task to provide induced accelerations at one of three levels. There is also an attitude acquisition mode and a contingency acquisition mode. Inputs to this task include data from the following: inertial reference (gyro), two-axis Sun sensor, horizon sensor, magnetometer sensor, position and velocity vectors, ephemeris, and requests for induced accelerations. Outputs include thruster valve commands, gimbaled thruster commands, and the attitude matrix. Processing includes calculating gyro angular increments, determining spacecraft attitude and body rates, determining attitude errors, computing gimbaled thruster commands, determining thruster firing logic, performing the 180° roll maneuver, and monitoring system health.

12.5.2 GROUND COMMAND PROCESSING

This task processes commands uplinked from ground controllers. Inputs to this task are ground commands received through the CTU. Outputs are decoded ground commands. Processing consists of decoding, verifying, and then executing the ground commands at the prescribed time. A partial list of ground commands includes the following:

- (1) Execute spacecraft 180° roll maneuver
- (2) Begin experiment X
- (3) Hold experiment X
- (4) Continue experiment X

- (5) Terminate experiment X
- (6) Set propulsion system pressure to X
- (7) Set valve X status to failed open/closed
- (8) Set sensor X status to failed
- (9) Switch to backup system X
- (10) Switch to primary system X
- (11) Modify flight software
- (12) Reload flight software

12.5.3 COMMAND AND TELEMETRY UNIT I/O

This task handles communications between the CTU and the OBC. Inputs include messages from the CTU and formatted messages from other OBC tasks for the CTU. Outputs consist of CTU messages and OBC messages. Processing consists of accepting, error checking, and buffering the messages from the CTU. It also buffers and sends OBC messages to the CTU.

12.5.4 DATA FORMATTING

This task assembles OBC data into blocks for downlinking. Inputs consist of OBC computation results, experiment results, and status data. The output is block-formatted data. Processing consists of assembling the OBC data into the proper formats for the CTU I/O task.

12.5.5 CRITICAL STATUS MONITOR AND SAFING

This task monitors spacecraft systems for safe operation. This includes the thermal, propulsion, and experiment systems. Inputs are sensor readings from certain critical areas of the

spacecraft. Outputs include commands to terminate, in an orderly manner, any experiments in progress and commands to control valves, mixers, heaters, and so forth. Processing consists of monitoring pressures and temperatures of the tanks. If parameters go out of safe limits, then any experiment in progress is shut down and the appropriate valves, heaters, mixers, and so forth, are activated to return the spacecraft to a safehold state and inform ground command of the situation.

12.5.6 ELECTRIC POWER MONITOR

This task monitors the spacecraft electric power system and continually assesses the reserve power available. Inputs include ground commands, bus and battery voltages, currents, temperature, and what loads, if any, have been shed. The outputs are a power availability status, and commands to put the spacecraft into the safehold state. Processing consists of monitoring the bus and batteries, determining the reserve power status and, upon detection of a load-shed condition, command the spacecraft to the safehold state. The resetting of load-shed relays to reactivate a bus is by ground command only.

12.5.7 ANTENNA POINTING

This task keeps the spacecraft high-gain antenna pointing at the most favorable tracking and data relay satellite (TDRS). This would be the nearest satellite with an unobstructed view. Inputs include the spacecraft attitude matrix, the spacecraft position, antenna position feedback, on/off status of the transmitter, and absolute time. The outputs are commands to the biaxial pointing system stepper-motors. Processing consists of the following:

- (1) Determine the position of both TDRSS satellites.
- (2) Determine if one or both are visible.
- (3) Select the most favorable if both are visible.
- (4) Compare current antenna position with desired.
- (5) Send stepper-motor commands to slew as needed.

12.5.8 NAVIGATION

This task works in conjunction with the attitude determination task. Its job is to continuously compute the position and velocity vector of the spacecraft, and to provide the Sun vector. These vectors are needed by the attitude determination task to compute the desired spacecraft attitude. The position vector is also used by the antenna-pointing task. Inputs to this task are the spacecraft attitude matrix, axial thrust vector, and absolute time. Outputs are a position vector and a velocity vector. Processing consists of computing position and velocity vectors for attitude determination.

12.5.9 THERMAL MONITOR AND CONTROL

This task controls certain spacecraft heaters. Inputs include temperature data from spacecraft housekeeping sensors and electric power system status. Outputs are electric heater control commands. Processing consists of the following:

- (1) Periodically compare sensor readings with preset limits.
- (2) Generate control commands.
- (3) Check that power is available before switching on any heaters.

12.5.10 PROPULSION SYSTEM

This task monitors the hydrazine tanks and lines and controls the propulsion pressurization system. Inputs are pressure and temperature data from the spacecraft hydrazine system. Outputs are valve commands to the system. Processing consists of the following:

- (1) Monitor hydrazine system pressure levels.
- (2) Generate valve commands to maintain the prescribed pressure level.
- (3) Monitor system health.
- (4) On-ground command set a new pressure level.

12.5.11 EXPERIMENT MONITOR AND CONTROL

This task runs all the tests of the experiments and gathers the results. Inputs include absolute time and sensor data from the experiment subsystem such as pressure, temperature, liquid/vapor, flow, and so forth. Outputs are requests for induced accelerations; commands to operate valves, pumps, heaters, and so forth; and computation results for downlink. Processing involves running the experiments by using the preprogrammed algorithms and termination criteria and to start, hold, continue, or terminate any experiment by ground command.

12.5.12 PRELAUNCH OPERATIONS

This task runs from initial OBC power on until spacecraft launch. Inputs include the RAM portion of the flight program, EGSE commands to exercise spacecraft valves, pumps, and so forth, through the EGSE communications link, spacecraft sensor readings, and a discrete signal from the launch vehicle. Outputs include EGSE commands passed to the CTU, and OBC-generated commands to operate spacecraft valves, pumps, and so forth. Processing consists of the following:

- (1) Pass to the CTU commands from EGSE to operate spacecraft effectors.

- (2) Monitor spacecraft sensors and send readings to EGSE.
- (3) Vent the supply tank as needed to relieve overpressure.
- (4) Accept and checksum test the RAM resident software.
- (5) On-command switch from EGSE slave mode to ascent operations.

12.5.13 ASCENT OPERATIONS

This task controls the spacecraft during the ascent phase. Inputs are spacecraft sensor readings and discrete signals from the launch vehicle passed from the CTU. Outputs are commands to spacecraft systems. Processing begins on command from the EGSE just prior to launch commit and includes the following operations keyed to further launch vehicle discretes:

- (1) Inhibit venting.
- (2) Vent as needed.
- (3) Activate the attitude determination and control task.
- (4) Activate the post-separation task.

12.5.14 POST-SEPARATION OPERATIONS

This task gets the spacecraft ready for normal operation after separation from the launch vehicle. Inputs are discrete signals from the launch vehicle and status data from spacecraft subsystems. Outputs include commands to activate spacecraft systems and commands to get spacecraft status. Processing begins at the separation discrete from the launch vehicle and includes the following operations:

- (1) Verify spacecraft health.
- (2) Stabilize and acquire attitude.
- (3) Deploy solar array.
- (4) Deploy the high-gain antenna.
- (5) Acquire telemetry.
- (6) Activate the antenna pointing task.

12.6 Sample Rates

For spacecraft systems there will be approximately 300 sensors total. For the experiment system there will be approximately 500 sensors total. From each, a subset of about 100 sensor readings will be used by the OBC for monitor and control. Sample rates for monitoring only will range from 1 per 10 sec to 5 per 1 sec. Sample rates for OBC control will be a minimum of 1 per second.

12.7 Safety

The software will have several safety-critical functions. These will concern mainly launch pad operations such as liquid

hydrogen loading, venting, and pressure control. There will also be a need for adequate guards and inhibits to prevent inadvertent thruster operation, ordnance firing, or antenna radiation. Many of these guards and inhibits will be implemented with hardware alone. The ones involving software will require careful design and extensive testing. Therefore, the software will be developed under a plan in accordance with NASA Management Instruction 2410.6, Software Management Requirements for Flight Projects.

12.8 Onboard Computer (OBC) Software Size Estimate

The total number of source lines of code was estimated for the flight software. The size and complexity of the software will be more than in many past designs because of the need for running experiments with minimal supervision. A large amount of failure detection/correction logic will be required.

The flight software will be written mostly in a high-order language. Some portions will need to be written in assembly language for speed purposes. This will be mainly in sections of the operating system software. The Ada computer language was assumed for making this estimate.

Software designs for several similar spacecraft were examined. From these an estimate of lines was determined for all the tasks except the experiment monitor and control task. This task is unique to COLD-SAT. Its size was estimated by using the following steps:

- (1) A representative five tests from two experiments were selected.
- (2) Flow charts were developed for each test.
- (3) Ada code was written for each test to get a number of source lines estimate.
- (4) The number of source lines for each of the remaining tests in all the experiments was determined based on relative complexity.
- (5) The total size of each test module was calculated by adding 50 percent for growth/contingency and 100 percent for failure detection/correction.
- (6) To the sum of all the tests were added lines for utility routines common to all the test modules.

An example of a conceptual flow chart for one test is shown in figure 12.4. The estimated lines of source code for each task are given in table 12.1.

12.9 Onboard Computer (OBC) Memory Requirements Estimate

The OBC has two types of memory: electrically erasable program nable read only memory (EEPROM), and read/write

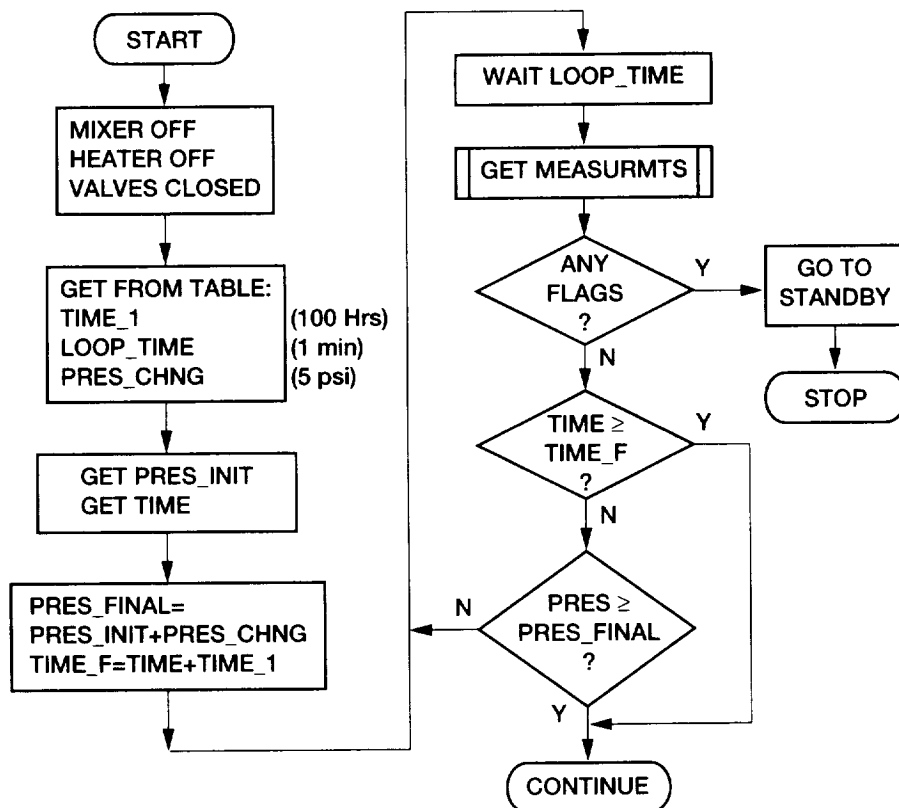


Figure 12.4.—Example flow chart.

TABLE 12.1.—ESTIMATED SOURCE LINES OF CODE

Task	Estimated source lines of code
Attitude determination and control	2600
Ground command processing	300
Command and telemetry unit I/O	130
Data formatting	200
Critical status monitor and safing	280
Electrical power monitor	230
Antenna pointing	650
Navigation	400
Thermal monitor and control	200
Propulsion system	200
Experiment monitor and control	6371
Prelaunch operations	160
Ascent operations	90
Postseparation operations	<u>200</u>
Subtotal	12 011
Operating system	<u>1200</u>
Total source lines	13 211

memory (RAM). RAM is loaded with a copy of all the software prior to launch. Only the software in RAM is executed. RAM also contains areas for the data base tables and task work space. ROM space is more limited and can only hold the software of a subset of the tasks. To ensure survival of the spacecraft in the event that RAM gets erased, the most critical and necessary tasks get loaded into ROM for copying into RAM. These are the tasks necessary to maintain attitude, receive and process ground commands, allow reloading of RAM software, and maintain a safe state. These tasks are the first five listed in table 12.2.

In making these estimates it was assumed that each line of code requires five assembly level lines and each assembly line requires two words of memory.

The OBC is baselined to have a total of 256K words of RAM and 64K words of ROM. This leaves about a 50-percent growth margin for RAM-resident software and about a 40-percent growth margin for ROM-resident software.

TABLE 12.2.—REQUIRED MEMORY
[WORDS]

Task	RAM	ROM
Attitude determination and control	41 360	26 000
Ground command processing	4 020	3 000
Command and telemetry unit I/O	2 320	1 300
Data formatting	4 050	2 000
Critical status monitor and safing	3 820	2 800
Electrical power monitor	4 350	
Antenna pointing	8 550	
Navigation	6 050	
Thermal monitor and control	3 020	
Propulsion system	3 020	
Experiment monitor and control	72 920	
Prelaunch operations	1 650	
Ascent operations	930	
Postseparation operations	<u>2 070</u>	
Operating system	14 020	1 200
Database/work space	<u>2 050</u>	
Total words of memory	174 200	47 100
Using 1k = 1024	171k	46k

12.10 Concluding Remarks

The design for the COLD-SAT spacecraft flight software must meet several requirements. The software must be able to control spacecraft systems with a large degree of autonomy. Extensive health monitoring of all spacecraft systems is required. If a problem is detected, the software must be capable of safely switching over to the backup system. Also, self-tests of the computer hardware and software will be run frequently to ensure their own integrity.

The experiments to be conducted must be carefully monitored through their duration with many lasting several hours. With TDRSS coverage expected to be only 13 min of every 105 min, much of the burden to handle unanticipated results falls on the flight computer. Also, the thermodynamic state of the cryogen in the tanks must always be controlled—even during quiescent periods.

Finally, the software design must allow for easy changes to experiment parameters and termination criteria. As the tests are conducted, experience will be gained that may require that later tests be conducted with parameter values different from those originally conceived.

Chapter 13

Launch Vehicle, Launch, and Ascent Operations

Edward Kramer and Don Perdue
National Aeronautics and Space Administration
Lewis Research Center
Cleveland, Ohio

and

Richard Jacobs and Jeff Samella
Analex Corporation
Cleveland, Ohio

13.0 Introduction

The COLD-SAT spacecraft must be mated to the Atlas launch vehicle. It must be checked out and serviced on the pad and filled with liquid hydrogen and other consumables. It must then be launched into its 550 n mi, 18°, nearly circular orbit, separated from the Centaur upper stage and stabilized in its proper attitude. While this is occurring the liquid-hydrogen-filled supply tank must be controlled, and along with the remainder of the spacecraft, must be monitored. This chapter details the spacecraft performance and interface requirements imposed on the launch vehicle, the operations which will be performed during the launch-ascent-stabilization phase, the capabilities of the launch vehicle to meet the spacecraft requirements, and the launch vehicle and launch site modifications needed.

It will be seen that the Atlas I expendable launch vehicle (ELV) has more than adequate capability to launch the spacecraft into the required orbit; that the required modifications to the pad and the ELV can be simply carried out; that all required control and telemetry interface requirements are satisfied; and that the necessary spacecraft operations have been identified and are feasible.

13.1 Spacecraft-ELV-Pad Interfaces

After completion of ground operations at Cape Canaveral Air Force Station (CCAFS) the COLD-SAT spacecraft will arrive at the launch pad mounted to the payload adapter inside the Atlas payload fairing. It will then be mated to the launch vehicle. Following mating, it will be checked out and serviced. Checkout of the spacecraft requires communication with the spacecraft which will take place via the Atlas provided T-4 sec umbilical. The flight batteries need to be connected and monitored and, if necessary, charged. Pyrotechnic devices must be armed, gaseous hydrogen loaded, and the spacecraft environment controlled. For loading of liquid hydrogen, the MLI must be purged with gaseous helium; those portions of the experiment system used for liquid hydrogen loading must be purged of gaseous helium and filled with gaseous hydrogen, and the supply tank must be filled with liquid hydrogen near the end of the launch count. Gaseous hydrogen must be vented from the spacecraft safely and, in the event of problems with the launch vehicle or spacecraft, it may be necessary to drain the liquid hydrogen and hydrazine propellant.

Following lift-off the pressure in the supply tank needs to be controlled. Telemetry data must be returned as the behavior of

cryogenic fluids in the supply tank in the launch environment are of technological and operational interest. Venting to control tank pressure has to be coordinated with the launch vehicle activities. Once in orbit, the spacecraft inertial reference must be aligned with those of the Centaur, and then the spacecraft must be separated from the launch vehicle.

All of these activities will occur through a variety of interfaces between the spacecraft, the launch vehicle, the launch pad, and the spacecraft Payload Operations Control Center (POCC). This section details these interfaces.

13.1.1 MECHANICAL INTERFACES

The spacecraft is attached to the launch vehicle by means of the payload adapter. In addition to the required mechanical fit, this interface also places requirements on weight, spacecraft center of mass, and dynamic properties. This interface accommodates the electrical connections between the spacecraft, the ELV, and the launch site. The adapter must separate the spacecraft from the launch vehicle upper stage with acceptable tip-off rates of less than 1.0 deg/sec.

A payload fairing is required to protect the spacecraft on the ground and during flight through the atmosphere. This constrains the dynamic envelope of the spacecraft. Access through the fairing is required on the pad to allow arming of the pyros, servicing of the hydrazine system, connection of flight batteries, filling with gaseous hydrogen, and loading with liquid

hydrogen. Details of these mechanical interfaces are covered in Chapter 6, Spacecraft Structure and Configuration, and are not considered further here.

13.1.2 ELECTRIC POWER SYSTEM INTERFACES

The spacecraft must be supplied with power while on the ground and during ascent. Figure 13.1 is a block diagram of these interfaces. Prior to lift-off the spacecraft will be supplied with power from ground-based electrical ground support equipment (EGSE) via the Centaur power transfer unit (PTU) and the T - 4 sec umbilical. During launch and ascent, power (443 W) will be supplied to the spacecraft by a mission-peculiar battery located on the Centaur upper stage. The source will be a silver-zinc primary battery supplying approximately 32 V to the spacecraft. This allows for a reduction in the capacity (and weight) of the spacecraft batteries which are sized by the power required from separation to acquisition. Prior to separation, the ELV will remove power from the spacecraft through the PTU to dead-front the interface connectors. Blocking diodes will assure that the transition occurs without interruption of power to the spacecraft buses and that the interface connector does not have voltage present when separation occurs.

While on the pad, the flight batteries must be monitored and possibly recharged. To accomplish this, circuits are required between the spacecraft and EGSE. Figure 13.2 illustrates this interface for one flight battery. Measurement of battery voltage

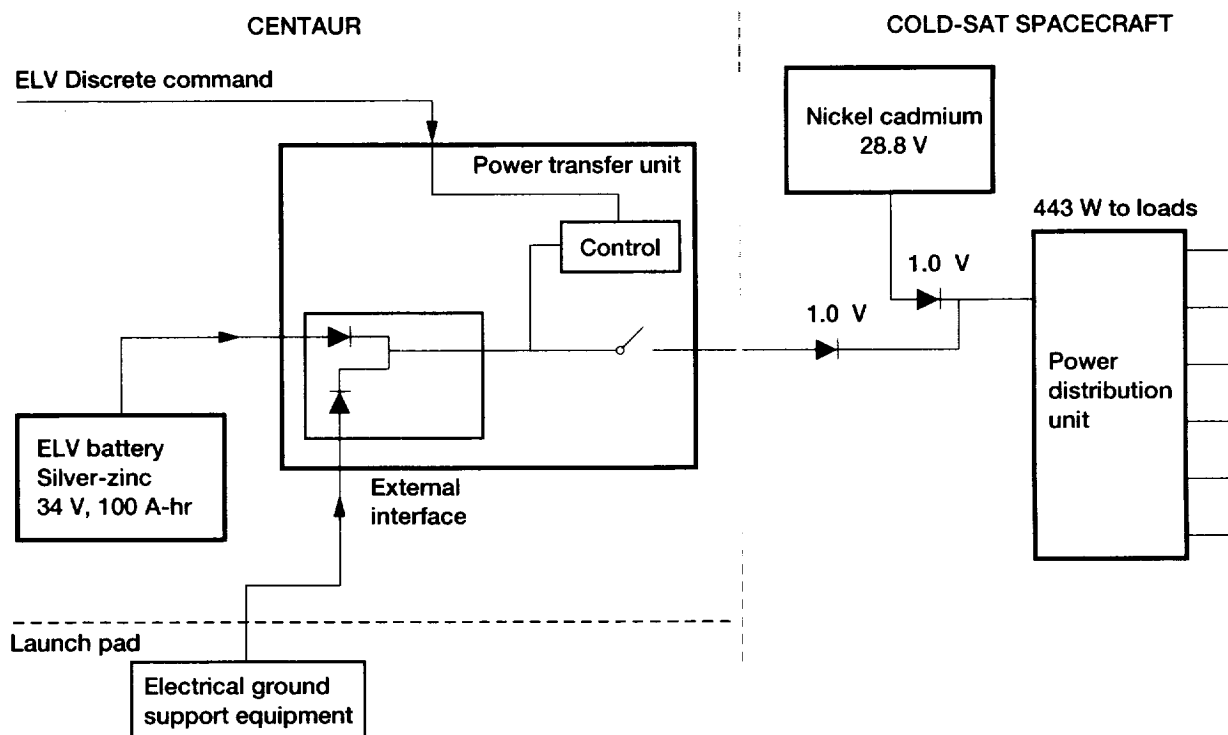


Figure 13.1.—Launch pad-expendable launch vehicle (ELV)-spacecraft power interfaces.

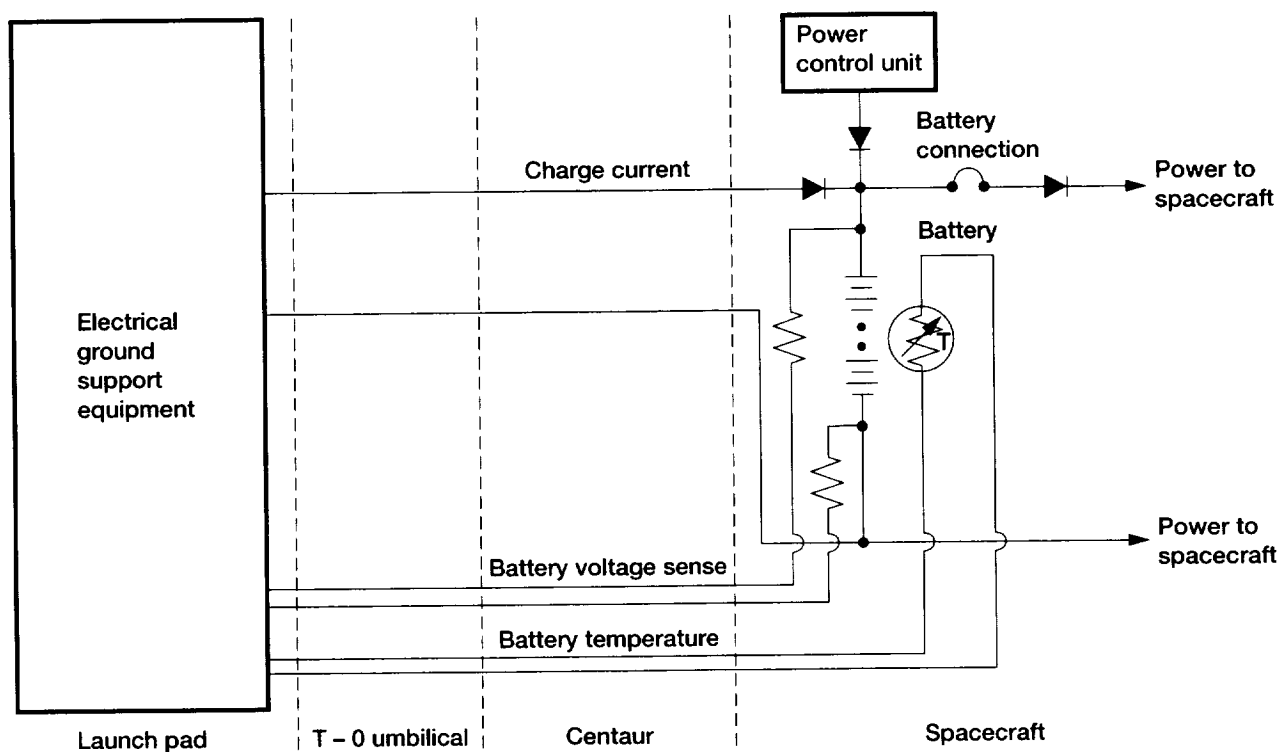


Figure 13.2.—Battery charge control interface.

and temperature allow the determination of the state of charge. If necessary it can be recharged through the indicated circuit. The circuits are routed through the Centaur harnessing and a spacecraft dedicated connector in the T - 4 sec umbilical to the EGSE. Identical circuits are used for the other spacecraft battery.

13.1.3 COMMAND AND TELEMETRY INTERFACES

Control of the spacecraft on the launch pad, including loading of liquid hydrogen, will occur via the flight computers. These computers must be loaded with ground and flight software and their operation verified. Figure 13.3 illustrates the command and control interfaces between the spacecraft and the EGSE while on the launch pad. Communication with each of the flight computers will take place via a MIL 1553 (ref. 1) half-duplex, bidirectional data bus. This bus will allow loading and checking of software, control of the computer and the spacecraft, and the return of status, telemetry, and software verification data. Two discrete commands run between the EGSE and the spacecraft redundancy control unit to allow the EGSE to force a switch in the active computer and to verify status. Two pulse code modulated data streams from the spacecraft command and telemetry unit supply continuous spacecraft telemetry data to the EGSE.

Data from the EGSE will be distributed to a special console in the Atlas blockhouse to allow control of liquid hydrogen loading and monitoring of the spacecraft. Duplex communication

with the flight computers and the continuous spacecraft telemetry streams will be routed to the COLD-SAT POCC to allow software uploads and downloads and spacecraft checkout.

From lift-off to separation communication must take place between the spacecraft and the launch vehicle. Figure 13.4 shows this interface. The spacecraft will be launched with the flight computers actively controlling the experiment system and monitoring the remainder of the spacecraft. The spacecraft transponder will be inactive so spacecraft telemetry, a subset of the complete telemetry frame, will be returned to the ground in the launch vehicle telemetry stream. This data will be communicated to the Centaur upper stage via two 1000 bps PCM channels.

Spacecraft hydrogen venting during ascent, and spacecraft inertial reference orientation immediately prior to separation, must be coordinated with the launch vehicle activities. This coordination is provided by eight Centaur contact closure discrete commands. The separation event itself will be signaled both to the spacecraft so that it may begin deployment, stabilization, and acquisition maneuvers and to the launch vehicle so that it can begin collision avoidance maneuvers. Separation is signaled by "breakwires" looped through the rise-off disconnects located in the payload adapter. Three are used for the spacecraft, and two are used for the ELV. The redundancy here is critical as premature activation of the spacecraft could result in its destruction.

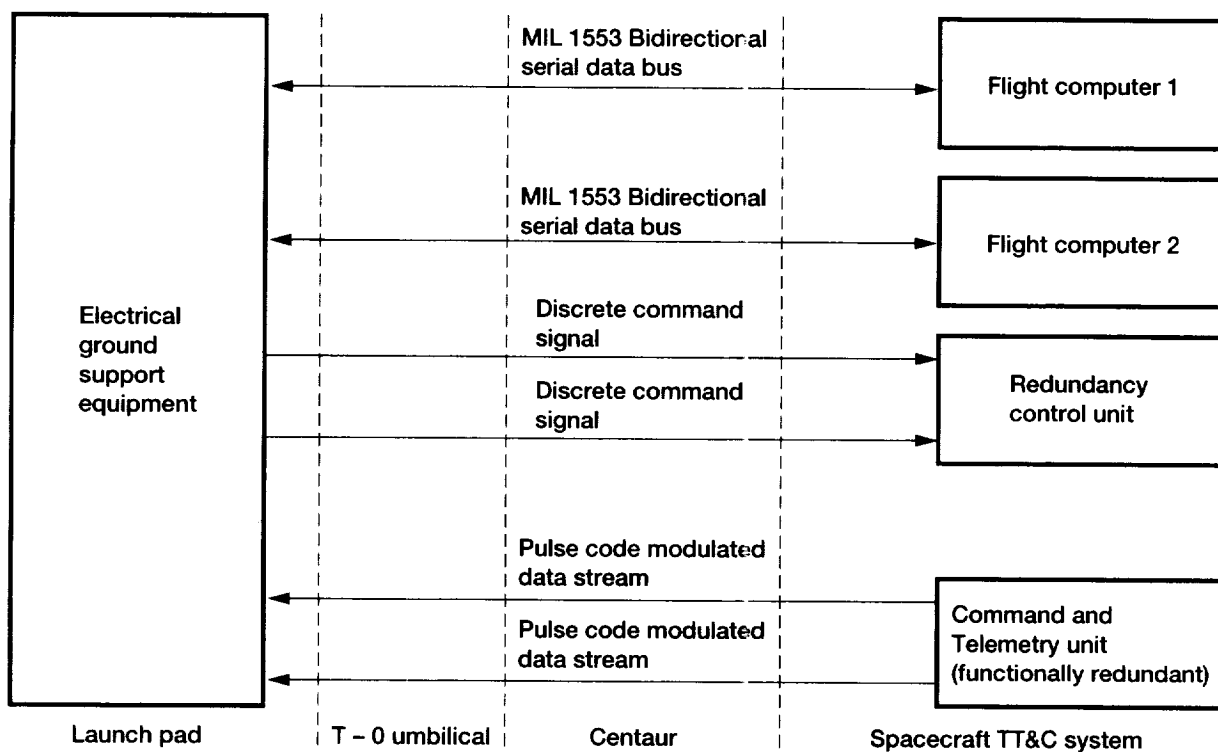


Figure 13.3.—Spacecraft-launch pad command and control interface.

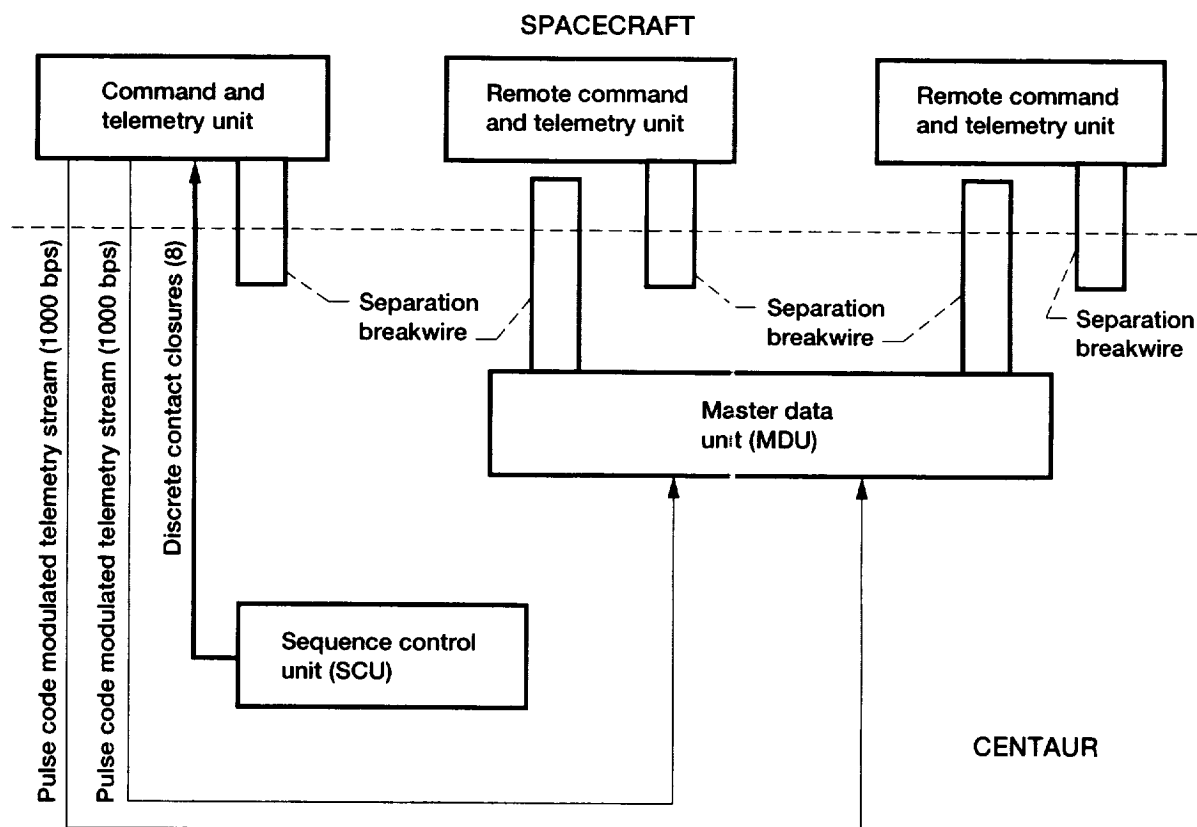


Figure 13.4.—Spacecraft/expendable launch vehicle command and telemetry interfaces.

13.1.4 FLUIDS INTERFACES

On the pad immediately prior to launch, the COLD-SAT experiment system must be loaded with liquid hydrogen and continuously topped off until launch to compensate for the 200-lbm/hr boiloff. Prior to loading, the system must be purged to clear it of air and contaminants with helium, and the helium must be purged from the system with gaseous hydrogen. Provisions will be made for venting the purge gases and the liquid hydrogen boiloff safely both on the pad and during ascent. In addition the supply tank MLI system requires a continuous purge with gaseous helium prior to, during, and following liquid hydrogen loading. Loss of purge can result in the condensation of nitrogen (or air) on the supply tank with boiloff potentially rising to 4600 lbm/hr, which would be a catastrophic event for the mission. Table 13.1 gives the required flow rates, fluid quantities, and thermodynamic states.

Filling and venting of hydrogen and purging of the supply tank MLI must continue until lift-off. This implies an umbilical which is pulled at launch. Without this there exists a potential unsafe state with no suitable vent for the hydrogen boiloff in the event of a launch delay.

The spacecraft will be loaded with up to 600 lb of hydrazine prior to transport to the launch pad. However, in the event of problems with the hydrazine system or other portions of the spacecraft, it may be necessary to offload the hydrazine and put the spacecraft propulsion system in a safe state. To allow this activity, access to the spacecraft on the pad, suitable ground support equipment, and trained personnel with protective equipment are required.

The experiment system accumulators must be filled with gaseous hydrogen prior to launch. It may also be necessary to

remove this hydrogen, purge the system, and put it in a safe state. It is intended that the connections for these operations will be made manually with loading and unloading operations being controlled remotely. Access to the spacecraft, suitable ground support equipment and trained personnel are required.

13.1.5 ENVIRONMENT

Prior to launch, the spacecraft must be protected from contamination and from temperature extremes. A conditioned, low-humidity purge with air is required while the spacecraft is within the payload fairing. The area within the fairing must be free from particulate matter. From the beginning of the liquid hydrogen loading process until launch, the area within the spacecraft fairing must be inerted to exclude air, in order to preclude explosion or fire in the case of a hydrogen leak and to exclude water and other condensibles. Temperature-controlled dry nitrogen is required for this purpose.

13.1.6 ELECTROMAGNETIC

Spacecraft transmitters will be inactive once the spacecraft is mated to the launch vehicle so there should be no electromagnetic compatibility (EMC) problems in that area. However, spacecraft computers and other electronics systems are operational both prior to launch and during ascent. They must operate satisfactorily both in the ambient radiation fields at the launch site and in the fields produced by the launch vehicle telemetry transmitters during launch and ascent. The spacecraft electronics cannot interfere with the operation of the nearby launch vehicle electronic systems. EMC standards and testing will be required to assure compatibility.

TABLE 13.1.—COLD-SAT LIQUID HYDROGEN LOADING FLUIDS REQUIREMENTS (COMPLEX 36)

Item	COLD-SAT line size, in.	Fluid	Flow rates, lbm/hr	Interface pressure, psia	Temperature, °R	Amount required
Liquid hydrogen fill/drain (145-ft ³ tank)	3/4	Liquid hydrogen	Fill 1200 ^a Top 100 to 400 ^{a,b} Chill 70 to 220 ^a	30 max 30 30	36 36 36	Liquid hydrogen 1300 lbm combined (565 lbm tank 92 percent full) Gaseous hydrogen, 25 lbm Gaseous helium, 25 lbm
		Gaseous hydrogen Gaseous helium	Purge 20 Purge 20	30 30	Ambient Ambient	
Hydrogen vent (ground and flight)	1.5	Gaseous hydrogen	Chill 220	17	36	
		Gaseous hydrogen	Fill 220	17	36	
		Gaseous hydrogen	Top 150	17	36	
		Gaseous hydrogen	Max 4200 ^c	30	36	
Insulation purge (Tested at HPF building)	Purge, 1/4	Gaseous helium	60 maximum	15	Ambient	120 lbm
	Maintain, 1/4	Dry gaseous nitrogen	5	15	Ambient	360 lbm
		Gaseous helium	20	15	Ambient	100 lbm

^aContinuously variable flow preferred.

^bContinue top-off to within 95 sec of launch or less.

^cWorst-case failure.

13.1.7 DESTRUCT SYSTEM

As currently envisioned, the launch vehicle must supply range safety and premature separation destruct capability for the spacecraft. Details of this requirement are covered in Chapter 17, Safety, of this report.

13.2 Launch Vehicle Capability

13.2.1 INTRODUCTION

This section documents the analysis and results of a preliminary launch vehicle performance study conducted for the COLD-SAT mission. The nominal COLD-SAT orbit is 550-n mi circular and inclined at 18°. Initially it was assumed that COLD-SAT would be launched on an Atlas I launch vehicle configured with the medium payload fairing. The COLD-SAT launch is scheduled to take place in the 1995-to-1999 timeframe. The final Atlas I launch is currently scheduled by General Dynamics for 1995. Therefore, it was decided to examine the performance of both the Atlas I and Atlas IIA launch vehicles. The Atlas IIA was chosen since it was the smallest Centaur-type commercial launch vehicle that was planned in the time frame of the COLD-SAT launch. The Atlas II launch vehicle may also be available in the 1995-to-1999 timeframe either commercially or through the Department of Defense. If so, its performance should be between that of the Atlas I and the Atlas IIA.

The object of this study was to determine the maximum payload weight that could be delivered to the COLD-SAT orbit. Direct ascent trajectories were examined, but it was found that parking orbit ascent trajectories provided significantly better performance. In the former case, the Centaur burns only once and places the spacecraft directly into the final orbit. In the latter case, the Centaur burns twice prior to final orbit injection with some parking orbit coast time between the burns. The study ground rules presented in the next section represent a generic set of assumptions which Lewis used to generate performance data for mission planning. These results do not include allocations for launch vehicle mission manager's reserve or a launch time reserve. In addition, these results do not account for any limits on the maximum payload weight that can be loaded on the launch vehicle. The application of mission-specific ground rules and the inclusion of the appropriate performance reserves will adversely affect performance. Therefore, the performance data presented here must be considered as preliminary.

13.2.2 ANALYSIS AND GROUND RULES

Atlas I and Atlas IIA launch vehicles were examined for this study. Both vehicles were configured with the medium payload fairing. The Atlas I model was taken from reference 2. Reference 3 was used to convert the GOES-I mission-peculiar Atlas I model given in reference 2 to a generic Atlas I configuration.

The Atlas IIA model was taken from reference 4. All of the launch vehicle mission-peculiar (LVMP) hardware assumed in these references was removed for this analysis.

The nominal mission targets were a 550-n-mi altitude circular orbit and an 18° inclination. In order to determine the performance impact of changing the final targets, circular altitudes between 300 and 800 n mi and inclinations between 10° and 26° were examined.

Launch was from the Eastern Test Range (ETR) at Complex 36 and the launch azimuth was optimized. During the ascent, the 11-ft-diameter payload fairing was jettisoned at a nominal free molecular heating rate of 59.17 lb/ft-sec for the Atlas I and 59.14 lb/ft-sec for the Atlas IIA. No range safety constraints were imposed in this analysis.

Two Centaur burns were modeled with a parking orbit coast between the burns. No constraints were imposed on the parking orbit. The parking orbit coast time was allowed to vary so that the location of the second Centaur burn could be optimized. All Centaur burns were constrained to be at least 30 sec in duration. The minimum burn time for the Centaur vehicle is limited because of considerations involving the guidance computer and injection accuracy. For study purposes, the 30-sec limit was chosen as a reasonable upper bound for the minimum burn time. If the mission requirements would demand greater performance for the trajectories where this minimum burn time were imposed, additional analyses would be required to determine the exact minimum value would be allowable.

The flight performance reserve (FPR) used for each vehicle was derived from reference 5. Flight performance reserve is the Centaur propellant reserve held to protect against 3 σ low vehicle performance. The FPR for the Atlas I was 250 lb and the FPR for the Atlas IIA was 325 lb. These reserves were larger than the respective FPR used in each reference case because the Centaur burnout weight had increased. The General Dynamics Launch Vehicle Contingency (LVC) was 150 lb for the Atlas I and 300 lb for the Atlas IIA. These values were taken from references 3 and 4, respectively. The LVC as defined here is the Centaur propellant reserve held out by General Dynamics to account for unplanned changes that affect nominal launch vehicle performance. No Lewis launch vehicle manager's reserve was assumed.

13.2.3 RESULTS AND CONCLUSIONS

The Atlas I performance for the nominal COLD-SAT mission is 7430 lb, and the Atlas IIA performance is 9200 lb. Launch vehicle performance as a function of circular orbit altitude can be seen in figure 13.5. The performance as a function of orbit inclination is shown in figure 13.6. Performance is stated in terms of payload systems weight. The payload systems weight includes the spacecraft, spacecraft adapter, and any spacecraft-required LVMP hardware.

In figure 13.6, the duration of the second Centaur burn was optimized except for cases in which the imposed minimum

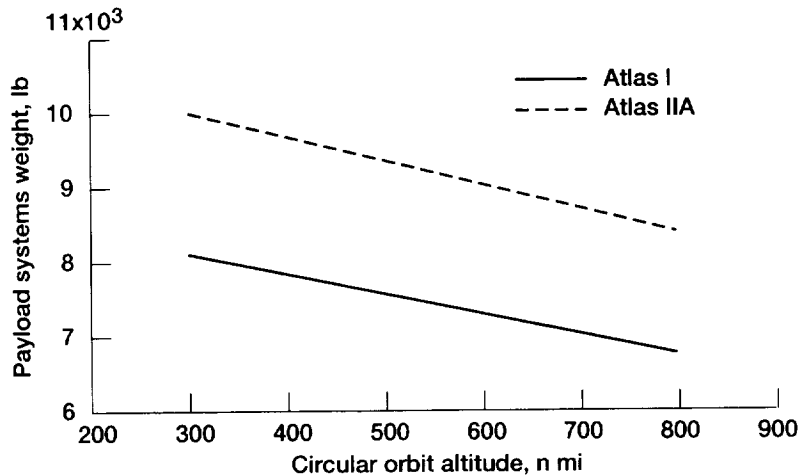


Figure 13.5.—Atlas performance for COLD-SAT (inclination, 18°).

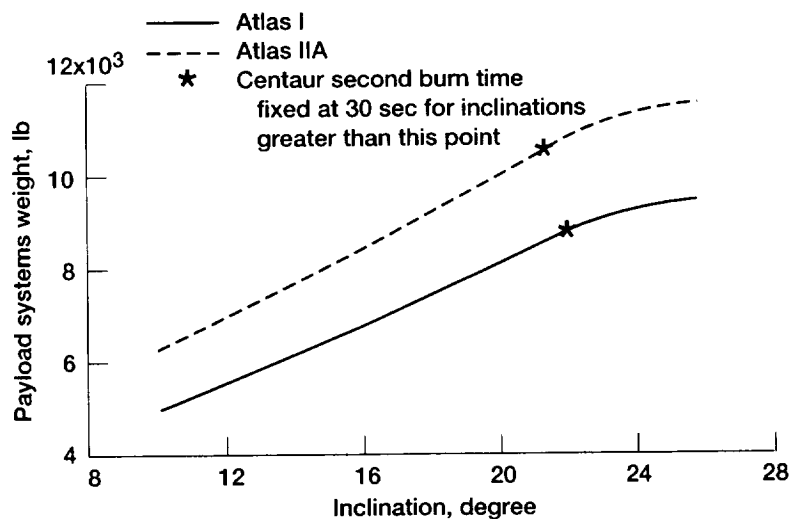


Figure 13.6.—Atlas performance for COLD-SAT (550 n mi circular orbit).

burn time limit of 30 sec was violated. The optimum burn time for the second Centaur burn continuously decreased as the orbit inclination increased. The point where each curve is marked with an asterisk is where the optimum burn time reached the 30-sec limit. Beyond this point, the duration of the second Centaur burn was fixed at 30 sec. Although the performance continued to increase after this constraint was imposed, it was less than it would have been with an optimum second burn time.

Although the vehicle is suborbital prior to the second Centaur burn, the altitude during the coast is such that no parking orbit constraints are needed. If the Centaur restart fails, however, the vehicle will re-enter. Impact will occur in the Indian Ocean. If the decision were made to have the spacecraft orbital at the end of the first Centaur burn, performance would be reduced. However, the advantage of having the Centaur and spacecraft orbital after the first Centaur burn is that some data could be gathered from the spacecraft in the event of a failed

restart. Although the spacecraft would not be in the proper final orbit and the mission would be short-lived, this may be preferable to the project in lieu of re-entering on the first orbit.

A plot of instantaneous impact points (IIP) is included as figure 13.7. The IIP trace near the bulge of Africa crosses the land mass for the nominal mission. This may be a range safety concern. Typically, a nominal IIP clearance of 150 n mi off the Ivory Coast is considered a safe distance by range safety. Modifying the trajectory in order to obtain 150 n mi of clearance would slightly reduce the launch vehicle performance. This safe clearance distance is not fixed and may be negotiated based on the performance margin and needs of the mission.

As can be seen from this analysis, the Atlas I and Atlas IIA launch vehicles are capable of placing the COLD-SAT spacecraft with a payload systems weight of 6715 lb into the required orbit. By implication the Atlas II launch vehicle would serve as well. There exists considerable excess performance capability

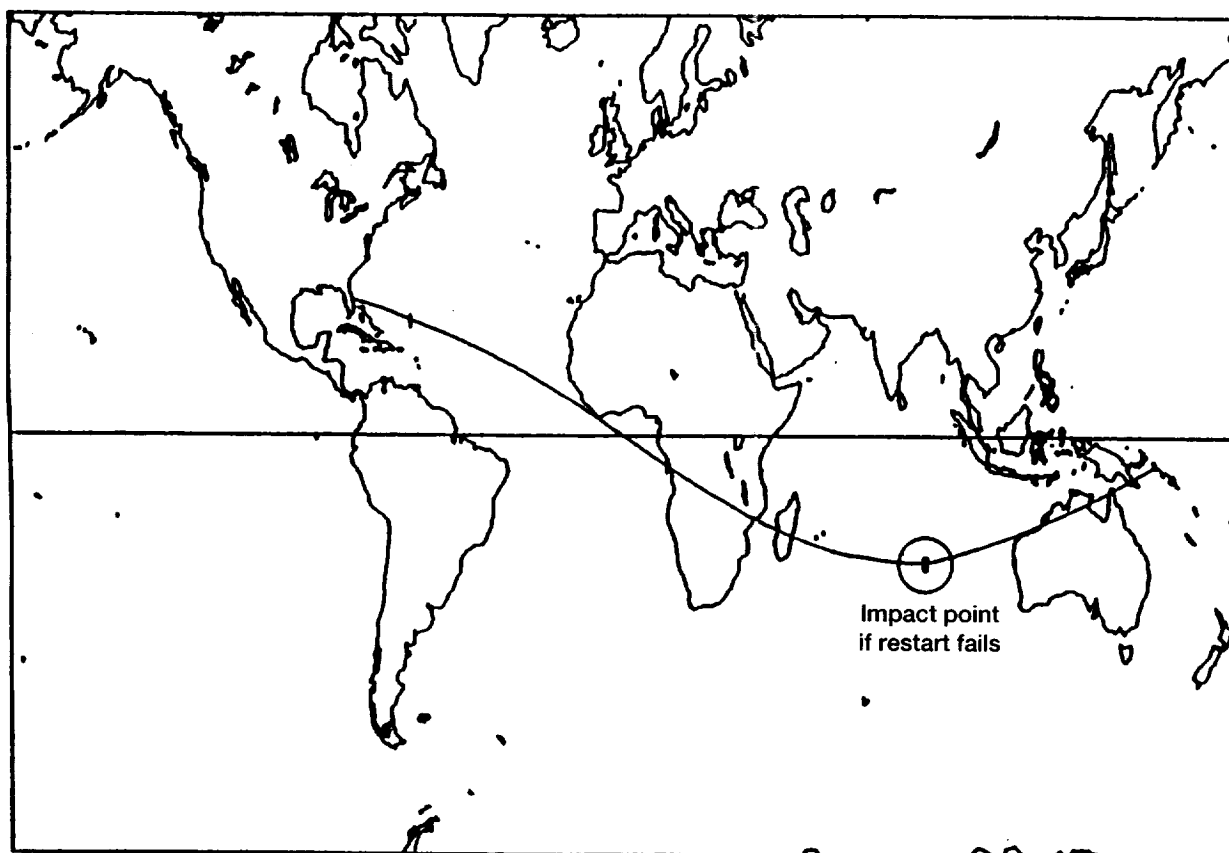


Figure 13.7.—COLD-SAT instantaneous impact point (550 by 550 n mi, inclination, 18°).

which could be used to lower the inclination even further, down to 12° with the Atlas IIA. This would result in improved thermal performance and a slight reduction in the size of the solar arrays.

13.3 Launch Vehicle/Launch Pad Modifications

13.3.1 INTRODUCTION

This section investigates some of the modifications and tasks necessary to launch a COLD-SAT spacecraft on an Atlas-I-type vehicle from Complex 36 at Cape Canaveral Air Force Station (CCAFS). The complexity of the modifications and tasks were assessed by using previous missions of the Atlas I as a basis. The modifications and tasks were categorized into three groups: standard, design, and developmental. Standard modifications use equipment or hardware already developed and used on previous missions. Design modifications are modifications to existing equipment or hardware that may require a partial requalification of ground support equipment (GSE) or flight hardware. Developmental modifications are modifica-

tions or tasks requiring a complete development program from conceptual design to qualification testing.

A straitman-type of approach was taken to assess the feasibility of using Complex 36 and the Atlas I vehicle. No attempt was made to perform trade studies on methods of loading the Centaur or spacecraft. Interface control documents (ICD) from the Combined Release and Radiation Effects Satellite (CRRES) and Geostationary Operational Environmental Satellite (GOES) missions were used as guidelines for this task.

13.3.2 SUMMARY

The required modifications to Complex 36 and the launch vehicle could be accomplished using standard modifications for electrical requirements and design modifications for mechanical and fluid requirements. All tasks can be accomplished by using standard engineering practices and technology. Modifications to Complex 36 and the launch vehicle for mechanical and fluid-type tasks were categorized as design modification types. The most complex tasks would be the design and installation of the spacecraft T-0 disconnect for the liquid hydrogen fill/drain system and the in-flight disconnect for the spacecraft gaseous hydrogen vent. Modifications to Complex

TABLE 13.2.—SPACECRAFT-EXPENDABLE LAUNCH VEHICLE-PAD
ELECTRICAL INTERFACES VIA RISE-OFF DISCONNECT
AND T – 4-SEC UMBILICAL

Description	Requirement
Spacecraft battery 1 charge (live and return)	5-A, 50-V maximum
Spacecraft battery 1 voltage sense (live and return)	0.1-A, 50-V maximum
Spacecraft battery 1 temperature (pair)	Signal pair
Spacecraft battery 2 charge (live and return)	5-A, 50-V maximum
Spacecraft battery 2 voltage sense (live and return)	0.1-A, 50-V maximum
Spacecraft battery 2 temperature (pair)	Signal pair
Spacecraft—EGSE data bus 1: spacecraft data and control (MIL 1553; bidirectional) (primary)	75-Ω pair
Spacecraft—EGSE data bus 2: spacecraft data and control (MIL 1553; bidirectional) (backup)	75-Ω pair
Spacecraft redundant computer switch discrete 1	Signal pair
Spacecraft redundant computer switch discrete 2	Signal pair
Spacecraft—EGSE telemetry stream (PCM)	75-Ω pair
Spacecraft—EGSE telemetry stream backup (PCM)	75-Ω pair

TABLE 13.3.—SPACECRAFT-EXPENDABLE LAUNCH VEHICLE-PAD ELECTRICAL INTERFACES VIA
RISE-OFF DISCONNECT TO CENTAUR

Description	Requirement
Spacecraft ground and ascent power from Centaur power transfer unit	36-V, 30-A maximum
Ground power from EGSE via T – 4-sec umbilical	
Ascent power to spacecraft via mission-peculiar battery	
Switchover/isolation via Centaur power transfer unit	
Spacecraft ascent data to Centaur MDU (channel 1)	1,000-bps pulse code modulation
Spacecraft ascent data to Centaur MDU (channel 2)	1,000-bps pulse code modulation
Spacecraft separation breakwire to spacecraft data system (1)	Loop through rise-off disconnect 1
Spacecraft separation breakwire to spacecraft data system (2)	Loop through rise-off disconnect 2
Spacecraft separation breakwire to spacecraft data system (3)	Loop through rise-off disconnect 1 and 2
Spacecraft separation breakwire to Centaur data system (1)	Loop through rise off disconnect 1
Spacecraft separation breakwire to Centaur data system (2)	Loop through rise-off disconnect 2
Control discrete signals via Centaur contact closure	
(1) T – 4-sec; launch commit; spacecraft liquid hydrogen fill/drain, gaseous helium electrical umbilical disconnected	
(2) T – 0; 2-in. motion by expendable launch vehicle (ELV)	
(3) OK-to-vent; used to inhibit venting during those portions of flight when undesirable because of effect on ELV (parallel Centaur venting).	
(4) ELV thrusting; closed during booster, sustainer, Centaur main engine burns; used to control venting of liquid hydrogen tank.	
(5) Payload fairing separation complete	
(6) Centaur settling between first and second main engine burns; used to control planned vent	
(7) Spacecraft separation in 5 min; spacecraft and Centaur stabilized in final orbit and attitude	
(8) Centaur and spacecraft stable in final attitude; at least 3 min after (7)	

36 and the vehicle for electrical interfaces are categorized as standard modifications. The electrical modifications and tasks appear similar to those performed for the CRRES and GOES missions. These electrical tasks or changes are ordinarily considered typical for Atlas I launches.

13.3.3 SPACECRAFT-PAD-EXPENDABLE LAUNCH VEHICLE INTERFACES

The interface requirements from the spacecraft to the electrical ground support equipment (EGSE) is listed in table 13.2. The COLD-SAT spacecraft electrical requirements are considered to be typical for most spacecraft. These requirements are very similar to electrical interface requirements for GOES and CRRES. Control consoles for operating and/or loading the COLD-SAT spacecraft will be installed in the blockhouse or other remote locations for spacecraft operations. These types of

interfaces were installed for CRRES and are planned for GOES. The T – 4 sec umbilical connectors and cables used for these missions would also have enough capacity for COLD-SAT. Figure 13.8 shows a typical path for data from the spacecraft to the EGSE. Existing cables for data, command signals, and electrical power could be used for COLD-SAT and would follow the same path to the blockhouse. The modifications for connecting and changing the wiring assignments from the spacecraft to the blockhouse is a standard modification and is typical for most missions. The only exception to this would be the design and installation of special loading panels for cryogenics onboard the spacecraft. This small task would be classified as design modification.

Electrical interface requirements for the spacecraft to the ELV are listed in table 13.3. All communications between the spacecraft and the ELV could use 2 rise-off disconnects as shown in figure 13.9. Disconnects planned for the GOES

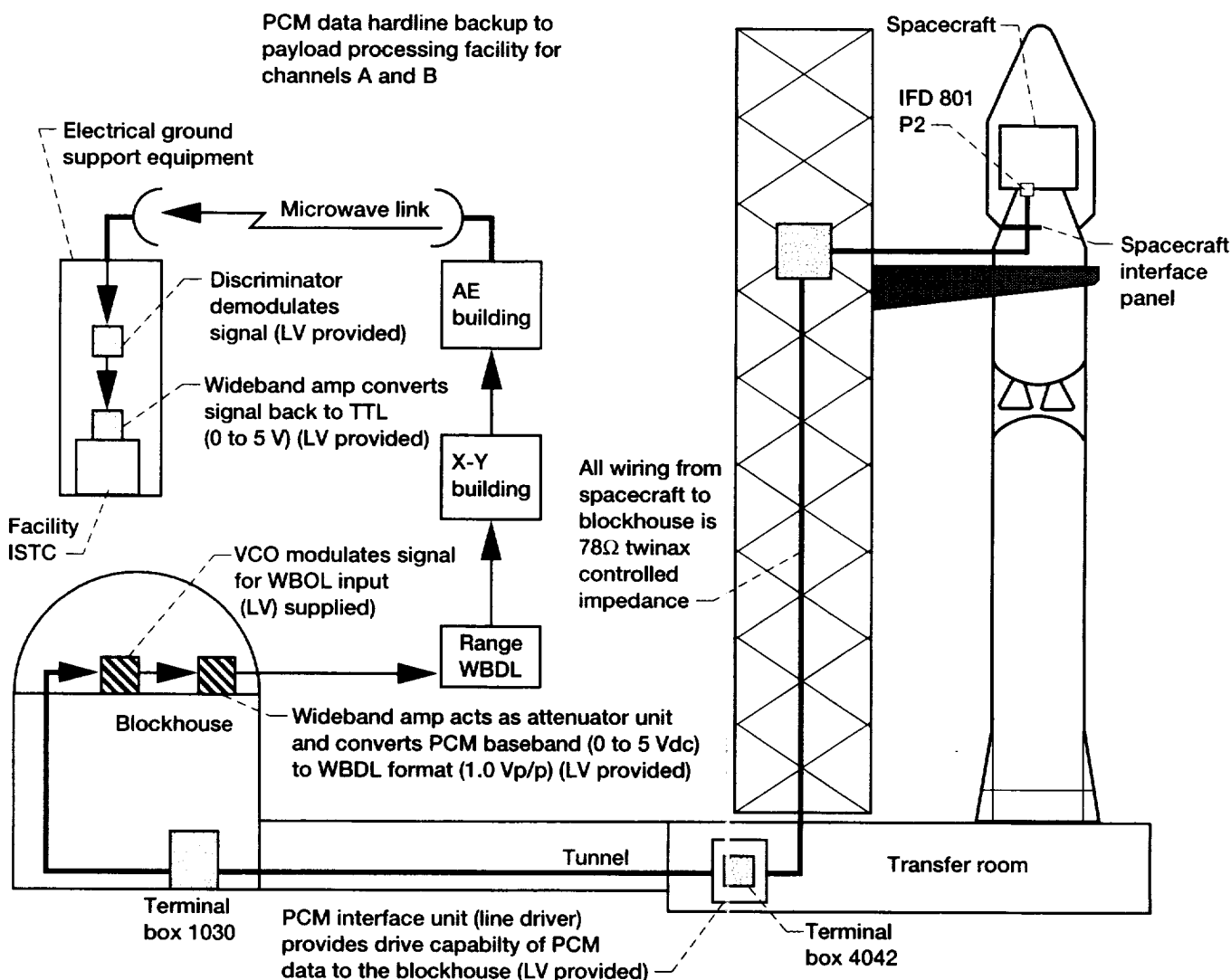


Figure 13.8.—Typical baseband telemetry system, Complex 36 spacecraft interface.

spacecraft have 31 pins each and could be used to meet the COLD-SAT requirements. A mission-peculiar harness would be fabricated to meet the unique requirements of each spacecraft. Again, these types of modifications are categorized as standard modifications. A summary of the electrical modifications for the vehicle and pad (Complex 36) is contained in table 13.4.

TABLE 13.4.—SUMMARY OF ELECTRICAL MODIFICATIONS

Modification/Task	Category
Flight harness	Standard
Centaur spacecraft battery	Standard
Electrical umbilical	Standard
Rise-off disconnects (2)	Standard
Power transfer unit (PTU)	Standard
Blockhouse spacecraft operations panels	Design
Vehicle-to-spacecraft software	Standard
Telemetry	Standard

13.3.4 VEHICLE AND PAD FLUID INTERFACES

Fluid interfaces with the vehicle (Atlas I) and the pad (Complex 36) are listed in table 13.5. Three tasks are categorized as design modifications and the remainder are standard modifications. The liquid hydrogen fill/drain and the vehicle gaseous hydrogen vent interfaces are the most complex and will require the greatest effort to design and install.

Some of the basic components of the liquid hydrogen fill/drain system for Complex 36 are shown in figure 13.10. The changes to the system include the addition of a flow control valve that connects upstream of the launch vehicle flow control valve, a shutoff valve, and a fluid disconnect for the liquid hydrogen fill/drain line. The capacity, flow rate, and supply pressure of the existing Dewar and lines could meet the requirements of the spacecraft. All liquid-hydrogen operations are performed remotely to meet safety requirements of

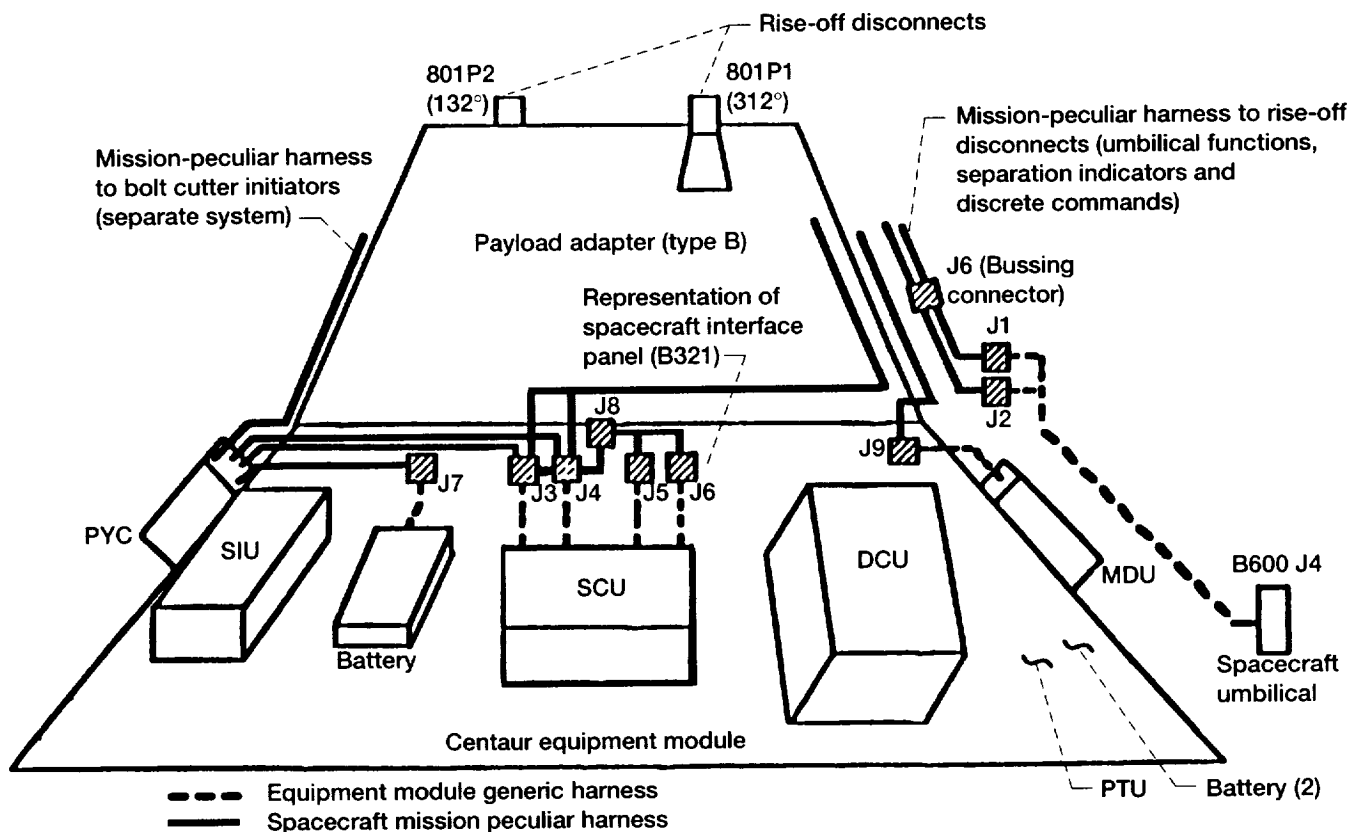


Figure 13.9.—Electrical interface harnessing.

TABLE 13.5.—VEHICLE AND PAD FLUID INTERFACES

Modification/Task	Category
Liquid hydrogen fill/drain (70 to 1200 lb/hr)	Design (new)
Gaseous helium blanket purge (20 to 60 lb/hr)	Design (new)
Gaseous hydrogen vent (vehicle) (70 to 4200 lb/hr)	Design (modify)
Gaseous hydrogen vent (pad) (70 to 4200 lb/hr)	Standard
Gaseous nitrogen purge to 11-ft fairing	Standard
Bottled gaseous hydrogen to vaporizers (2000 psia)	Standard
Gaseous hydrogen monitoring of payload fairing	Standard
Spacecraft operations panels in blockhouse	Standard

ESMCR 127-1. A loading panel for the spacecraft will have to be designed and installed in the blockhouse for remote propellant operations and checkouts. The spacecraft and vehicle can share the existing ground vent. Capacity and working pressure of the ground vent could meet the spacecraft requirements if selected loading sequences were followed. Figure 13.11 shows a basic schematic of the spacecraft and vehicle liquid hydrogen fill/drain/vent system. Some additional components required by the spacecraft are the self-sealing disconnects, and checkvalve/vent line connected to the vehicle flight/ground vent. The in-flight spacecraft vent line, checkvalve, and self-sealing disconnects are jettisoned during flight. The COLD-SAT supply tank insulation system is maintained with a gaseous helium atmosphere before and after liquid hydrogen operations

on the ground. The liquid hydrogen bypass line is used for chilldown and topping processes.

A basic schematic of the spacecraft gaseous hydrogen loading system is shown in figure 13.12. The loading operations will be accomplished at the launch site. This loading process was proposed to be a manual operation. For procedures using gaseous hydrogen, the atmosphere within the payload fairing would be inerted with gaseous nitrogen. Supply bottles used for gaseous hydrogen loading would be furnished by a commercial source. The "manual gaseous hydrogen loading cart" will be designed and fabricated to be transported to the loading area on the tower by means of existing personnel elevators. Potential leaks can be monitored with a gas detection system used for the launch vehicle. All the hardware and changes involved for the gaseous hydrogen loading process would not involve changes to the pad or tower. The hydrazine loading system was designed for manual operations for the GOES and CRRES missions using similar operating procedures for transport to the working levels on the tower.

Figure 13.13 shows a schematic of the supply tank MLI helium purge system. A quad set of valves, regulator, orifices, and filter are part of the skid-mounted system which is fed by the Complex 36 GSE helium supply. The valves and orifices

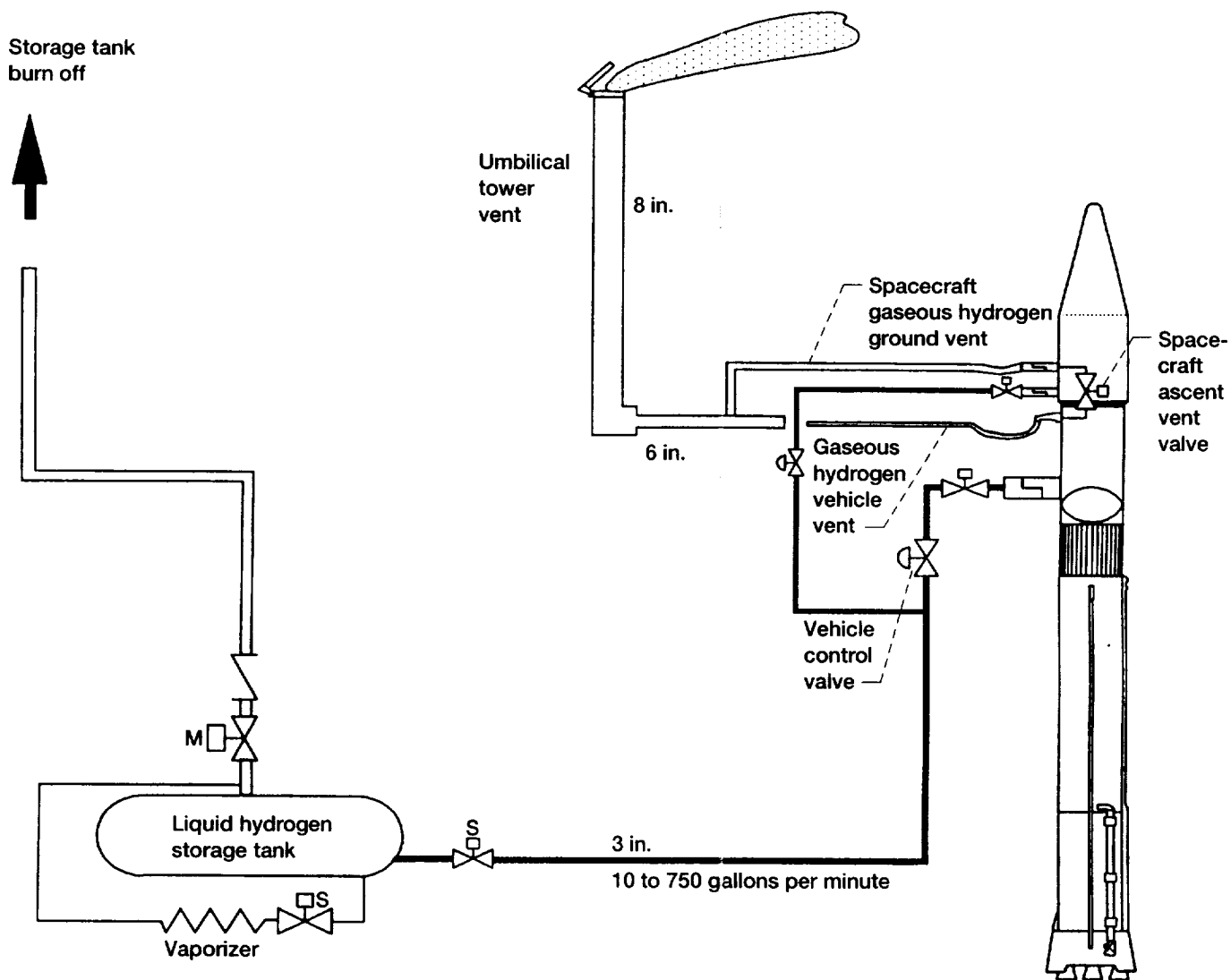


Figure 13.10.—COLD-SAT liquid hydrogen operations, Complex 36.

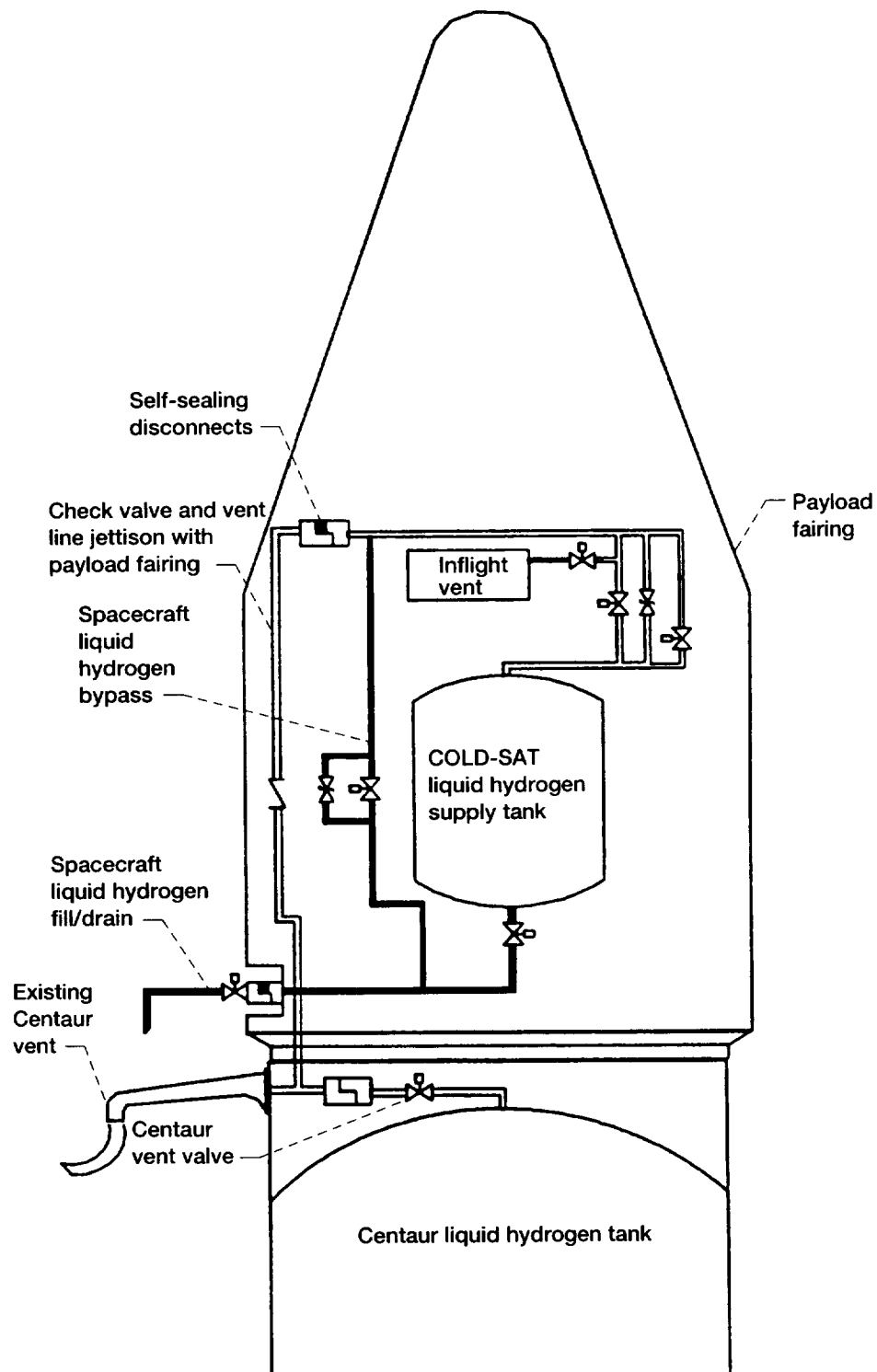


Figure 13.11.—COLD-SAT liquid hydrogen fill/drain/vent system.

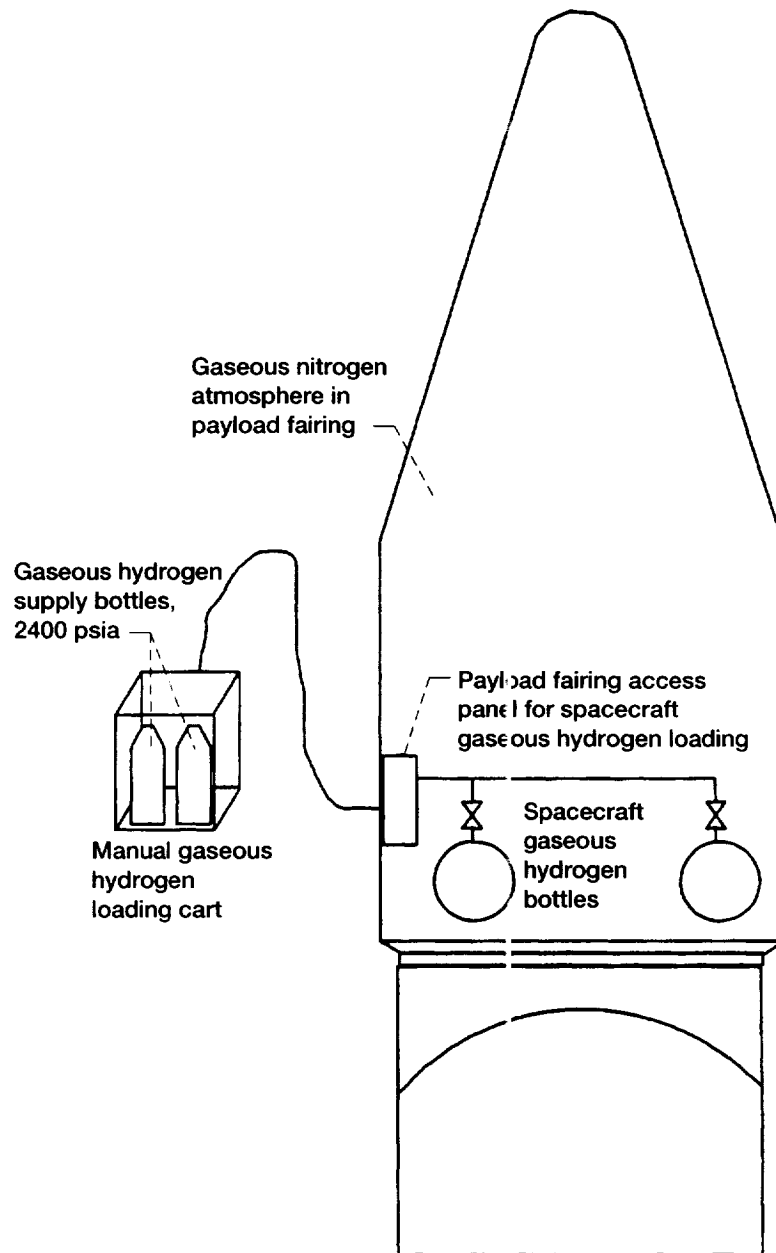


Figure 13.12.—COLD-SAT gaseous hydrogen loading system.

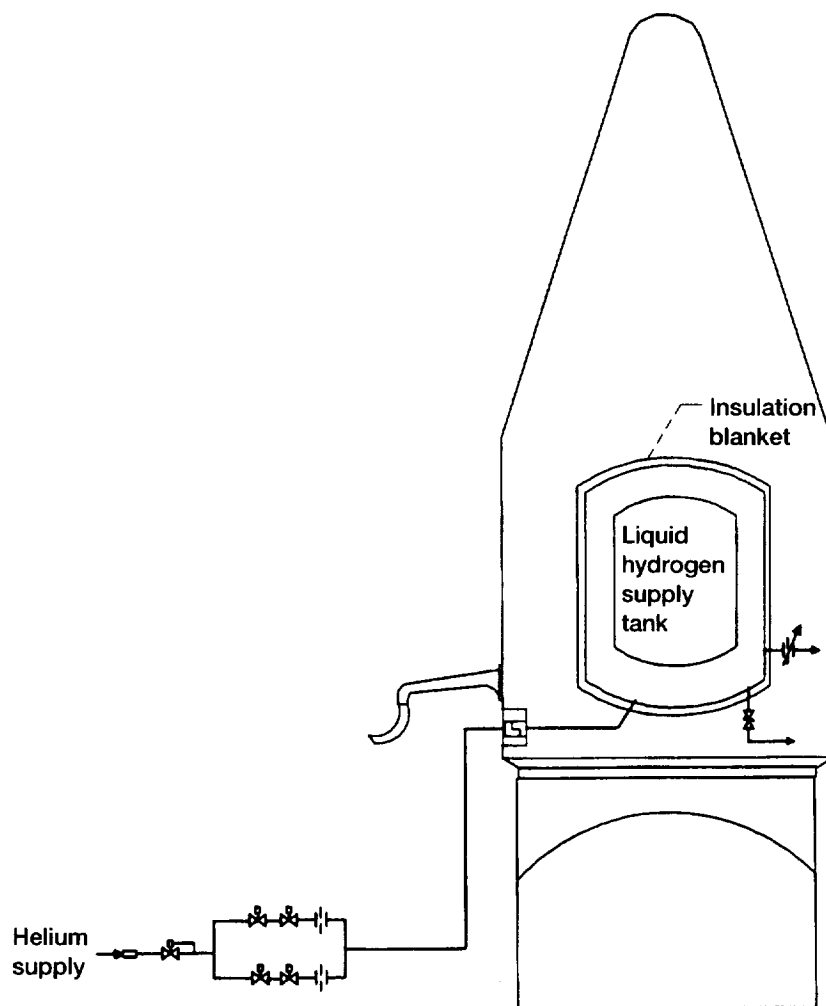


Figure 13.13.—COLD-SAT helium insulation purge system.

are redundant because loss of purge gas may result in condensation of air on the tank with resultant rapid loss of liquid hydrogen and operation of the relief valve on the spacecraft supply tank. The helium disconnect would be part of the T-0 umbilical along with the liquid hydrogen fill/drain disconnect. A helium purge panel could be installed in the blockhouse for purge control operations. Design and fabrication of the helium skid could be accomplished offsite to minimize inference with pad operations. The variable orifice and relief valve settings are set and verified at the spacecraft processing building prior to arriving at the launch site. The insulation helium purge system is also verified at the pad prior to liquid hydrogen loading.

Table 13.6 shows the capabilities of the pad air-conditioning for Complex 36. Figure 13.14 illustrates the location of the air-conditioning umbilical. If the requirements for CRRES and GOES missions are compared with the types of equipment used for the COLD-SAT spacecraft, it appears that the capabilities of the GSE air-conditioning would meet the needs of the space-

TABLE 13.6.—PAYLOAD FAIRING AIR-CONDITIONING CAPABILITIES FOR COMPLEX 36B

Parameter	Capability
Gaseous nitrogen flow range, lb/min	40 to 160
Minimum supply pressure, in.-H ₂ O (differential)	10
Temperature, range, °F	50 to 85
Dew point, °F	40 (maximum)
Cleanliness class	5000

craft. Requirements for spacecraft air-conditioning were not available at the time of writing this section.

13.3.5 MECHANICAL INTERFACES

The payload adapters and fairing proposed for the CRRES and GOES missions have similar requirements to COLD-SAT. Changes to the adapter and fairing are categorized as standard modifications. The adapter used for the GOES mission is being developed as the standard issue and recommended by the

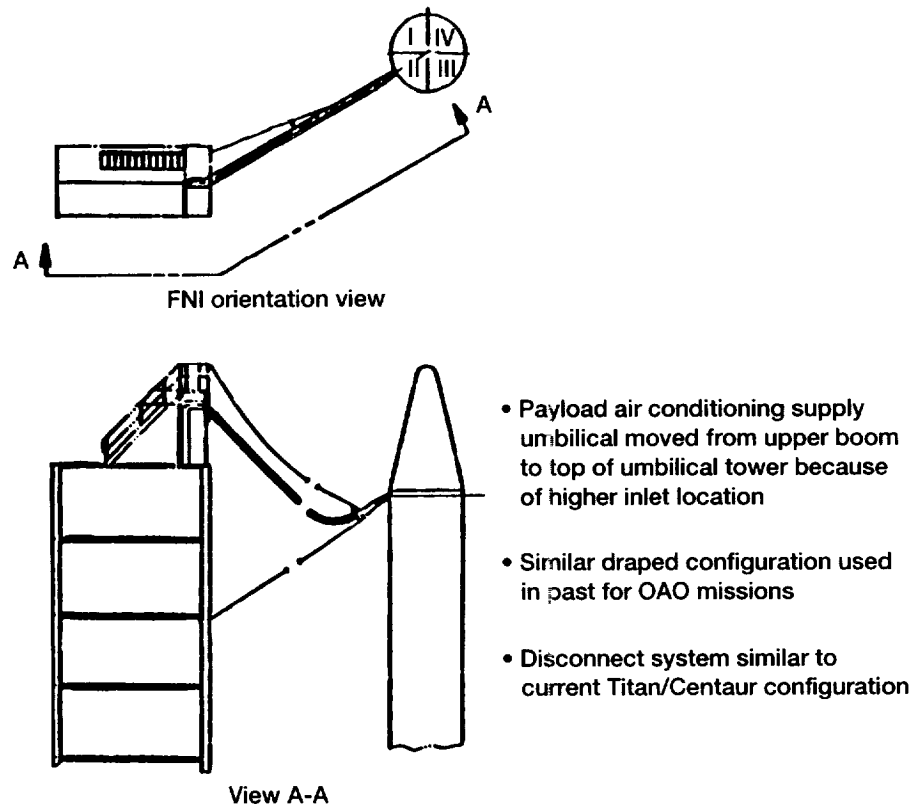


Figure 13.14.—Eleven-foot payload air conditioning draped umbilical at Cape Canaveral Air Force Station Launch Complex 36.

vehicle manufacturer. Attachment of the spacecraft to the vehicle adapter is accomplished through a separation system. The 47-in. system proposed for COLD-SAT is similar to the one developed by SAAB for Ariane vehicles. Access to the hydrazine fill/drain, gaseous hydrogen supply/vent, pyro-to-battery connector, and T - 0 panel could be accomplished through standard access doors in the payload fairing. Again similar tasks were planned for GOES and CRRES.

13.3.6 LIQUID HYDROGEN LOADING SEQUENCE

The bar chart in figure 13.15 depicts one of a number of possible COLD-SAT propellant loading sequences. In the illustrated sequence the spacecraft liquid hydrogen chill and fill is accomplished after the normally scheduled T - 90 min hold in the launch vehicle count and extends the normal count. After the spacecraft fill has stabilized and the boiloff is constant, the normal vehicle count is re-established. Spacecraft topping continues until T - 125 sec and spacecraft tank lockup occurs at T - 95 sec. This sequence is different from those used in the past for the Atlas, in that the Centaur liquid hydrogen tank is chilled and the chilled state maintained for about 145 min until loading. The normal sequence is to load the liquid hydrogen a short time period after chill during liquid oxygen tank filling.

The normal vehicle loading sequence would start to the right of the second vertical dashed line on the bar chart in figure 13.15. The reason for chilling first in the illustrated sequence is that sensible heat in the GSE piping is used to condition the first gaseous hydrogen from the GSE prior to its entering the Centaur tank for initial chill. Loading the spacecraft before the launch vehicle would use up some of this sensible heat, potentially allowing colder gas to enter the Centaur liquid hydrogen tank for the initial chilldown.

NASA Lewis feels that there is sufficient sensible heat in the piping downstream of the control valve shown in figure 13.10 to condition the gas. Analysis could be performed to determine if enough sensible heat is available. This would permit the spacecraft to be loaded without prechilling the vehicle tank first and shorten the loading time for the vehicle and spacecraft. The advantages of loading the spacecraft first are:

(1) The vehicle vent fin can handle the spacecraft worst-case predicted venting requirement of 4200 lbm/hr if the vehicle is not using the vent fin during initial chill and loading of the spacecraft.

(2) This latter loading sequence would allow verification of the spacecraft ground insulation system before vehicle tanking is initiated.

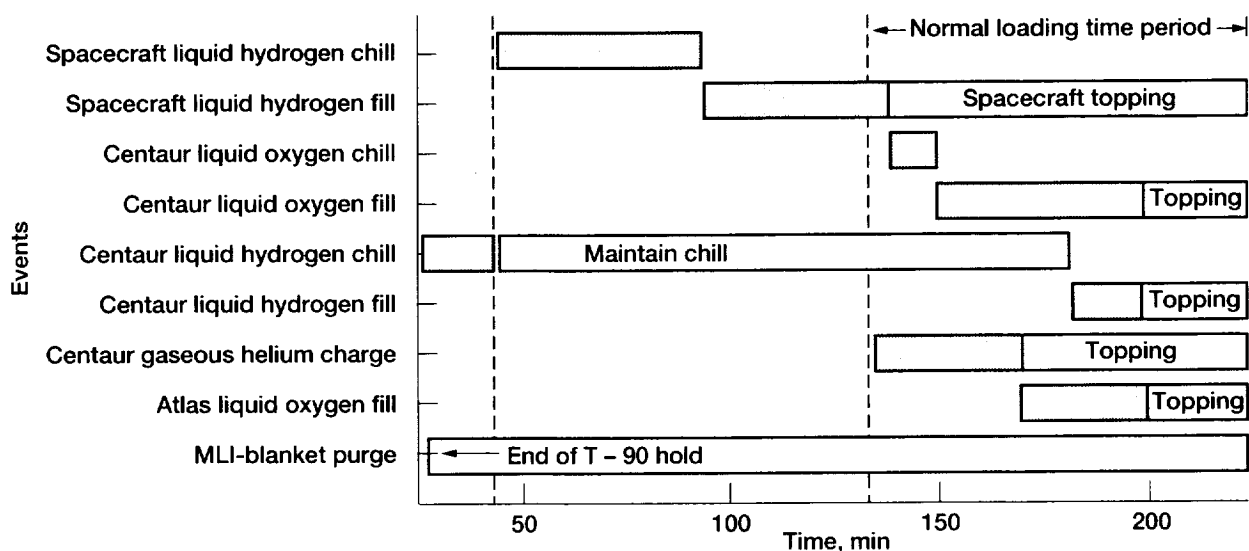


Figure 13.15.—COLD-SAT propellant loading sequence.

After the spacecraft boiloff has stabilized at approximately 200 lb/hr, spacecraft venting will not interfere with vehicle venting. A common liquid hydrogen vent for the spacecraft and vehicle eliminates the requirement for a dedicated vent for the spacecraft.

It is the NASA Lewis position that no technical reasons exist that would prevent the spacecraft from being loaded from Complex 36 if the loading sequence was adjusted to meet the requirements of the spacecraft and vehicle. A common gaseous hydrogen vent could then safely be used and prevent costly development of a dedicated spacecraft GSE/flight vent system.

13.4 Launch and Ascent Operations

13.4.1 INTRODUCTION

This section covers the operation of the spacecraft from immediately prior to launch until it is stabilized on orbit in the required attitude and has acquired the Sun. Until separation from the launch vehicle, the spacecraft, like the Centaur stage itself, cannot be commanded and returns its telemetry in the launch vehicle telemetry stream. Following separation communication will only be established when TDRSS single access coverage has acquired the spacecraft low-gain, omnidirectional antennas. This may not be possible if the spacecraft is tumbling at a high rate.

With its supply tank full of cryogenics, the spacecraft must remain active and control the thermodynamic state of the tank at all times. Inadvertent operation of the supply tank relief system could result in the loss of a major portion of the supply of liquid hydrogen. In addition, if a relief valve is forced to

operate, it may not seal completely on closure and result in a continuous low-level leak from the system to space.

The need to maintain active control consumes considerable power. Once power is lost, the backup mechanical relief systems on the cryogenic tanks will inevitably operate. There is little chance that random charging of the spacecraft batteries as the spacecraft tumbles would allow any kind of recovery before all cryogenics are lost. Failure to stabilize the spacecraft and acquire the Sun before the spacecraft batteries are discharged will probably result in failure of the entire mission.

For these reasons spacecraft operation from immediately prior to launch until stabilization and acquisition of the Sun by the solar arrays must be completely autonomous but coordinated with the operation of the launch vehicle. This section covers these operations and their interaction with the launch vehicle.

13.4.2 LAUNCH OPERATIONS

Table 13.7 provides a worst-case timeline for spacecraft operations from prelaunch until acquisition of the required attitude by the spacecraft. The reference time is the actual lift-off (2-in. motion) of the launch vehicle. Prior to launch, time is expressed as both "T" minus lift-off and "L" minus lift-off. The T time is the nominal launch vehicle count which contains a number of planned holds. The L time is the best estimate of the actual time to launch assuming that the launch vehicle count goes as planned. The table is based on a nominal set of launch vehicle operations and undoubtedly will vary somewhat for the actual flight. The following acronyms are used in table 13.7: BECO (booster engine cutoff); SECO (sustainer engine cutoff); MECO (main engine cutoff); and MES (main engine start).

TABLE 13.7.—LAUNCH/ASCENT OPERATIONS: WORST-CASE TIMELINE

Prior to T – 90 min (L – 295 min)	Final system checkout Spacecraft power from ground; flight battery backup Load flight software in spacecraft computer Spacecraft clock to UCT (or equivalent absolute time) Status spacecraft for liquid hydrogen loading Spacecraft control to flight software Spacecraft control by EGSE computer-serial data link-procedure in flight software Full spacecraft data stream to EGSE via separate serial data link
T – 86 min (L – 205 min)	Commence loading liquid hydrogen under ground control during scheduled T – 90 min hold
T – 86 min (L – 96 min)	Liquid hydrogen loading complete; begin topping off as required
T – 16 min (L – 26 min)	Spacecraft to ELV battery power (flight battery backup) Gyros on Control to flight software (with ground override for fill/drain control; software inhibits), vent closed, topoff inhibited
T – 15 min (L – 25 min)	Spacecraft go for launch (preliminary) Continue normal venting and topoff
T – 95 sec (L – 95 sec)	Final vent lockup Measure volume of liquid hydrogen
T – 45 sec (L – 45 sec)	Spacecraft go for launch (final)
T – 4 sec (L – 4 sec)	Centaur discrete signal Disconnect liquid hydrogen fill/drain umbilical Disconnect spacecraft electrical umbilical Remove software inhibits (full control to spacecraft computer)
T – 0 sec	Centaur discrete signal (2-in. motion), vent disconnected inhibit venting
T + 5 sec	Open purge bag doors by timer control
T + 17 sec	Centaur discrete signal—OK to vent as required
T + 130 sec	Begin Centaur liquid hydrogen pressure reduction
T + 156.8 sec	BECO: liquid hydrogen vent as required
T + 206.9 sec	Hydrogen venting inhibited; Centaur discrete signal
T + 208.7 sec	Payload fairing jettison; Centaur discrete signal
T + 210 sec	Switch to balanced vent; timer from fairing separation
T + 262.6 sec	SECO: inhibit hydrogen vent by Centaur discrete signal
T + 273.6 sec	MES 1; hydrogen vent as required by Centaur discrete signal
T + 626.8 sec	MECO 1; begin Centaur settling; low-g venting allowed by Centaur coast phase discrete signal
T + 1513.4 sec	Begin planned vent of supply tank to 25 psia; 300 sec maximum; by timer from coast phase discrete signal
T + 1813.8 sec	MES 2; hydrogen vent as required by Centaur discrete signal
T + 1864.0 sec	MECO 2; hydrogen venting inhibited until separation by Centaur discrete signal

TABLE 13.7.—Continued.

T + 2000 sec	Complete spacecraft-Centaur alignment: spacecraft-Centaur long axis (spacecraft x-axis) aligned with projection of Sun line in orbit plane; spacecraft y-axis in orbit plane Signal preliminary orientation. 5 min to separation by Centaur discrete signal Attitude sensors on
T + 2120 sec (approximately)	Centaur spacecraft orientated and stable by Centaur discrete signal Initial alignment for spacecraft gyros from known Centaur attitude
T + 2180 sec	2 min to separation by spacecraft timer: heat to hydrazine system; catalyst bed heaters on
T + 2300 sec	Spacecraft separation signaled by redundant breakwire Spacecraft on internal battery power Begin acquisition mode Spacecraft transponder on receive: Omni antennas; start initial acquisition by TDRSS single access
T + 2330 sec	Attitude control thrusters enabled; begin stabilization of spacecraft (Centaur 30 to 100 ft away)
T + 2630 sec	Spacecraft stabilized in presumed correct orientation Deploy solar arrays by internal command Stabilize spacecraft after deployment
T + 2930 sec (maximum)	Spacecraft stabilized Deploy high-gain antenna via external command Stabilize spacecraft after deployment
T + 3130 sec	Begin worst-case eclipse delay Spacecraft stabilized in presumed correct orientation Begin attitude determination via magnetometer Check for Earth presence via Earth sensor If not in eclipse, check for solar acquisition by Sun sensor (if Earth/Sun detected, adjust to final attitude, begin checkout)
T + 3970 sec	Complete attitude determination via magnetometer (14 min: 40° Δ true anomaly)
T + 5230 sec	End worst-case eclipse delay, check for solar acquisition (nominal end of acquisition phase)
T + 5290 sec	If Sun not acquired, reorient spacecraft to magnetometer determined attitude unless inhibited by ground command
T + 5890 sec	Reorientation complete, check for solar acquisition
T + 5950 sec	If no solar acquisition, begin search with Sun sensors unless inhibited by ground command (uninterrupted search time, 3780 sec)
T + 9388 sec	Begin eclipse: suspend search; allow spacecraft to continue to rotate
T + 11 476 sec	End eclipse: resume search for Sun (eclipse time, 35 min)
T + 12 496 sec	End search; begin battery recharge: 10 196 sec (2.83 hr) on battery, worst case Sun line normal to solar arrays
T + 37 696 sec	Complete battery recharge (4 orbits = 420 min)

TABLE 13.7.—Concluded.

T + 40 396 sec	End worst-case delay for optimum Sun-Earth configuration (45 min) Begin rotation about Sun line until horizon sensors acquire Earth with proper sense
T + 41 296 sec	Earth acquired (15-min worst case) Begin rotation about Earth line to obtain preliminary orientation
T + 41 896 sec	Complete reorientation, spacecraft in proper attitude (10 min) Continue attitude determination, wait for optimum Sun-Earth configuration
T + 43 456 sec	Final attitude determination/spacecraft orientation (26 min) Begin orientation of high-gain antenna to TDRSS
T + 44 056 sec	Establish TDRSS multiple access communications Begin spacecraft checkout (12.24 hr from launch worst case)

Prior to launch the integrated spacecraft will have been fully checked out. The spacecraft will be operating on ground power with the flight batteries connected and serving as a backup. All pyrotechnic devices and the hydrazine propulsion system will have been armed. The spacecraft will have been communicating with the COLD-SAT POCC through the launch site EGSE, telemetry and commands being passed between the spacecraft and the EGSE via cables in the T - 4 sec umbilical.

The spacecraft computers are operational and the initial flight software load will be checked out and functioning. Control of liquid hydrogen loading will be from the blockhouse through the spacecraft computers and special procedures written into the flight software. The COLD-SAT supply tank will be chilled and loaded with liquid hydrogen during the scheduled T - 90 min hold in the launch vehicle count. After loading the supply tank will be topped off as required to compensate for the 200 lbm/hr boiloff which occurs on the ground.

At T - 16 min the power source will be switched to the mission-peculiar spacecraft battery located on the Centaur second stage of the launch vehicle. The flight software will be activated, the gyros started, the hydrogen vent closed, and spacecraft operation verified in its launch configuration. If all is correct the spacecraft will issue a preliminary "go" for launch at T - 15 min. Normal top-off and venting of the supply tank will then be resumed.

At T - 95 sec top-off will be terminated and the supply tank locked up. The liquid hydrogen level will be measured. Successful sealing of the supply tank and proper functioning of the tank thermal insulation system will be verified by rate of pressure rise. The supply tank will remain locked until well into the ascent phase. At T - 45 sec the spacecraft will issue its final "go" for launch. Up until this point the launch can be scrubbed at any time if there are problems with the spacecraft. Later it can only be stopped if there are major problems before lift-off. At T - 4 sec the liquid hydrogen fill drain umbilical and the spacecraft electrical umbilical will be retracted. A discrete

signal from the launch vehicle will remove inhibits from the flight software which will assume full control of the spacecraft.

13.4.3 ASCENT OPERATIONS

Lift-off at T = 0 (2-in. motion) will be signaled to the spacecraft computers by a Centaur discrete signal. Five seconds later the vent doors in the supply tank purge bag will be opened by firing their pyros. Venting of the supply tank, if required, will be coordinated with the launch vehicle activities by discrete signals from the Centaur upper stage. In general, venting of the supply tank will not be required during ascent except for one planned vent used to restore thermodynamic state, not to maintain tank pressure within required limits.

At T + 208 sec the payload fairing will separate from the launch vehicle. This will disconnect the spacecraft vent system from the normal Centaur ascent hydrogen vent system by opening the disconnect between the spacecraft and the fairing. The event will be signaled to the spacecraft by a Centaur discrete signal and the spacecraft will switch its venting to its own balanced flight vent. Following the end of its first burn at T + 627 sec, the Centaur and the spacecraft will enter a coast phase in which the fluids onboard the launch vehicle are kept settled by its hydrazine propulsion system. This event is signaled to the spacecraft computer by a discrete signal and, following a timed delay, the supply tank will be deliberately vented to reduce the saturation pressure of the liquid hydrogen to 25 psi. This pressure reduction should remove the heat acquired by the cryogen during the initial launch ascent phase when the insulation system is inefficient because of the absence of adequate vacuum. No further venting should be required until deployment and acquisition maneuvers are initiated.

The coast phase will continue until the second Centaur burn at T + 1813 sec. Following completion of this burn at T + 1864 sec the spacecraft and launch vehicle second stage will be in the required orbit. Venting by the spacecraft will be inhibited

from this point on to prevent interference with the stabilization of the Centaur and spacecraft in preparation for separation.

13.4.4 SEPARATION, DEPLOYMENT, AND ACQUISITION

It is desirable to stabilize and orient the spacecraft as rapidly as possible. Because the Centaur upper stage is capable of accurate pointing in any desired attitude and separation with low tip-off rates, the Centaur is used to provide an initial orientation to the spacecraft inertial reference system. This approach is the first of three attitude-acquisition procedures for the COLD-SAT spacecraft. The Centaur will orient itself and the spacecraft in the desired attitude 5 min before separation and signal this event to the spacecraft by a discrete signal. The spacecraft attitude determination system will be activated. If this stable attitude has been held for approximately 2 min, a second discrete signal will be given to the spacecraft and the current attitude will be captured by the spacecraft inertial reference system.

By timer, 2 min before planned separation, the spacecraft will activate its propulsion system and turn on the thruster catalyst bed heaters. Prior to separation, the launch vehicle removes external power from the spacecraft. Separation occurs automatically and the event is signaled to the spacecraft by three redundant breakwires looped through the rise-off disconnects. The spacecraft adapter is capable of separation with tip-off rates of less than 1 deg/sec. The spacecraft gyros can track rates of up to 2 deg/sec and so should remain oriented through the separation event. The attitude control system is activated at separation, and then 30 sec are allowed to elapse to assure a clearance of at least 100 ft between the spacecraft and the launch vehicle before stabilization of the spacecraft is begun. Since the attitude control thrusters are located on the aft end of the spacecraft, and the spacecraft should not have rotated more than 30°, operation of the spacecraft attitude control thrusters should tend to increase the separation between the spacecraft and the launch vehicle upper stage. At this point the telemetry transponders are activated in the receive mode using the omnidirectional antennas. Initial acquisition of the spacecraft using TDRSS single-access coverage can begin.

Five minutes later when the Centaur is at least 1000 ft away and spacecraft stabilization is complete, the solar arrays are deployed by firing their pyrotechnic hold-down bolts and the spacecraft is restabilized. During this timeframe the Centaur is beginning its collision avoidance maneuvers to assure that it is adequately separated from the spacecraft. If communication is established with the spacecraft, the high-gain antenna may now be deployed by external command and the spacecraft restabilized. Approximately 14 min after separation, the spacecraft should be stabilized in the correct attitude and, unless it is in eclipse, both Sun and Earth sensors should be providing data. If this is true, the spacecraft will be rapidly stabilized in the required attitude and, after a possible delay for optimum Earth-

Sun orientation, final attitude determination made. This will be followed by establishment of TDRSS multiple-access communications and spacecraft checkout.

However, there may be a delay of up to 2100 sec because of eclipse. In any event, the first backup mode for attitude determination and acquisition will be initiated. This method uses a magnetometer to give the approximate attitude of a stabilized spacecraft. It requires approximately 15 min to get a reading as the spacecraft revolves through about 40° of its orbit. About 48 min after separation the worst case eclipse delay will be over and the Sun should be present to the Sun sensor. If the Sun is present, initial attitude determination will be made. If not, the spacecraft will be placed in its approximate correct attitude by using the attitude determined by the magnetometer and the presence of the Earth and Sun again will be determined.

If the sensors have still not detected the Sun, the second backup mode, direct search for the Sun, will be initiated. Search occurs by rotating the spacecraft about the initial z-axis of its inertial reference system and stopping if the Sun is detected. If not the spacecraft is rotated about its y-axis by two-thirds of the detection cone of the Sun sensor and then rotated about the z-axis. The process is assured to find the Sun in less than one hour and three minutes. The worst case for solar acquisition is 2.19 hr from separation. At this point, the spacecraft batteries are about 80 percent discharged.

In all events, or as soon as the Sun is acquired the spacecraft will be oriented to the Sun and the batteries recharged. Depending on depth of discharge, it may take up to 4 orbits (420 min) to recharge. If the Sun was acquired by the second backup mode, an additional search would have to be made for the Earth by rotating around the Sun line. In the worst case, in the absence of computer or gyro failure, final attitude, with fully charged batteries will be obtained within about 12 hr of separation. Following stabilization in the final attitude TDRSS multiple access communications will be established. The worst-case time to complete the acquisition phase and begin spacecraft checkout is 12.24 hr from launch. Other than the one planned vent during ascent, no venting of the supply tank for pressure control should be required.

References

1. MIL-STD-1553B, US Department of Defense, Naval Publications and Forms Center, Philadelphia (8 Sept. 1986).
2. GOES-I Configuration, Performance, and Weight Status Report: General Dynamics Space Systems Division, December, 1989.
3. Atlas I Configuration, Performance, and Weight Status Report (Reference GT0 Mission): General Dynamics Space Systems Division, March, 1988.
4. Atlas IIA Configuration, Performance, and Weight Status Report (Reference GT0 Mission): General Dynamics Space Systems Division, December, 1989.
5. Centaur Flight Performance Reserve Predictions: General Dynamics Space Systems Division Interoffice Memo 887-TP-86-078, from Trajectory and Performance, Dept 887-0 to J. Andrews, September 11, 1986.

Chapter 14

Ground Operations

Richard Jacobs
Analex Corporation
Cleveland, Ohio

14.1 Introduction

Prior to arrival at Kennedy Space Center (KSC)/Cape Canaveral Air Force Station (CCAFS), the spacecraft will be assembled and thoroughly tested. All components will be qualified for flight and pressure vessels will be proof-tested under simulated mission conditions. No further testing of the experiment system during ground operations at KSC/CCAFS is planned. Certain equipment will be removed for transportation and packing material added. The COLD-SAT spacecraft will arrive at CCAFS by plane inside its own transport trailer.

Upon arrival at KSC/CCAFS, the spacecraft will be transported to a payload processing facility (PPF). There, packing materials will be removed and checkout batteries installed. System functional, control, and data tests will be conducted. These include a mission power simulation test, a multilayer insulation (MLI) blanket purge test, and a flight-level pressure test with helium. After testing at the PPF is completed, the final spacecraft assembly will take place. This includes installation of solar arrays, high-gain directional antenna, flight batteries, and pyrotechnics for mechanism actuators. COLD-SAT will then be transported to the hazardous processing facility (HPF) for further processing.

Propellants and pressurants will be loaded at the HPF. After loading, removal of nonflight hardware and ground support equipment (GSE) used to service the spacecraft will be accomplished. Final weighing, center-of-gravity validation, and mass properties determination will be completed followed by final sensor alignment. Mating of the COLD-SAT to the Centaur payload adapter will precede encapsulation within the Atlas medium payload fairing (PLF). After encapsulation in the PLF, COLD-SAT will be transported to the launch complex for mating to the expendable launch vehicle (ELV) and prelaunch preparations.

Modifications to the launch pad will have been completed prior to the arrival of COLD-SAT. These modifications include the installation of the fluid systems necessary to service the spacecraft and the electrical lines necessary for power, control, and data transmission. The modified systems will have been tested to determine functionality for servicing COLD-SAT and communicating with the various control and data centers. Some launch complex systems required by COLD-SAT will not require modification. These systems, which mate with the Centaur upper stage and PLF, are used for all Atlas launches. Validation of the interfaces required for COLD-SAT will be required, however.

Upon arrival at launch Complex 36, the encapsulated COLD-SAT is mated to the ELV. After the spacecraft is mated, prelaunch readiness tests follow connection of the GSE required to service COLD-SAT for launching. The COLD-SAT vaporizers are then loaded with gaseous hydrogen from the GSE. A tanking test with liquid hydrogen will accompany the Atlas wet dress rehearsal (WDR), when the ELV (Centaur) upper stage is tanked. Two electrical tests follow to verify the ability of the ELV, spacecraft, electronic ground support equipment (EGSE), and launch control centers (LCC) to function properly to control the loading, launch, and ascent. These tests, the simulated flight test (SMFLT), and the composite electrical readiness test (CERT), are part of every Atlas prelaunch operation. Additional prelaunch readiness tests and spacecraft close-out will precede the launch. COLD-SAT will then be loaded with liquid hydrogen and launched into orbit.

The ground operations required for the COLD-SAT spacecraft at KSC/CCAFS are typical for spacecraft previously processed there. COLD-SAT is not a complex design requiring extensive prelaunch testing. The onboard systems, propellants, and pressurants are typical of many spacecraft. The unique requirement for this spacecraft is the loading of both liquid

hydrogen and gaseous hydrogen. The loading will take place at the launch complex, however, where handling of hydrogen for the ELV upper stage is normal.

14.2 Requirements

14.2.1 APPLICABLE DOCUMENTS

The ground operations will comply with applicable requirements for safety, transport and handling, test facility, and the launch complex. They are controlled by written test procedures. The requirements specific to COLD-SAT will be defined in a payload requirements document (PRD) formulated by a NASA launch services support manager (LSSM) assigned to COLD-SAT by the NASA KSC payload operations office.

A primary document for payload processing is K-STSM-14.1, Launch Site Accommodations Handbook For Payloads. This KSC handbook is not only a valued guide for processing payloads, but references many required documents in its appendix A. These include facility handbooks for all the KSC/CCAFS processing facilities, safety requirements, transportation requirements, and so forth.

The primary safety compliance requirements are given in

- (1) ESMCR-127-1 (USAF) Eastern Space & Missile Center, Range Safety
- (2) GP-1098, Vol. 1 (KSC) Ground Safety Plan, Safety Requirements
- (3) GP-1098, Vol. 2 (KSC) Ground Safety Plan, Safety Operating Procedures
- (4) NHB 1700.1 (V1-A) NASA Basic Safety Manual
- (5) U.S. DOT, Office of Commercial Space Transportation, Hazard Analysis of Commercial Space Transportation, Vols. 1, 2, and 3
- (6) 29 CFR (Federal) Occupational Safety and Health Administration, Department of Labor, Part 1910, Latest Issue

The primary transport and handling compliance requirements are given in

- (1) NHB 6000.1C (NASA) Requirements for Packaging, Handling, and Transportation
- (2) N3S/GO-1740.9 (NASA) Safety Standards for Lifting Devices and Equipment

14.2.2 FLUID LOADING

At the launch site, the COLD-SAT spacecraft must be loaded with a variety of consumables that include hydrazine propellant, helium pressurant for the propulsion and experiment systems, gaseous hydrogen pressurant for the experiment system, and the liquid hydrogen experiment fluid. Table 14.1 presents the quantities required of the various fluids for which the quantity of fluid is fixed. In addition, the supply tank must be loaded with 587 lbm of liquid hydrogen at lift-off. Much more will have to be supplied because of boiloff on the ground.

14.2.3 FACILITIES

A PPF is required for the reassembly and test of the delivered spacecraft. The facility must provide a clean protected space for this work along with a variety of ancillary services. Table 14.2 lists the requirements for this facility. In addition an HPF is required for the loading of hydrazine and similar more dangerous operations. Table 14.3 lists the requirements for the HPF.

14.2.4 COMMUNICATIONS

Full duplex communications at multiples of the spacecraft data rate (3200 bps) are required with the COLD-SAT Payload Operations Control Center (POCC) both during prelaunch testing as well as during the launch count. This will allow monitoring of the spacecraft by the POCC, checkout of the POCC operations, and download of software to the spacecraft.

14.2.5 ASSEMBLY

The spacecraft will arrive at the launch site without its solar arrays, without batteries, without its high-gain antenna, and with only some of the inaccessible NASA standard initiators

TABLE 14.1.—COLD-SAT GROUND LOADING REQUIREMENTS, HPF AND COMPLEX 36

Item	COLD-SAT line size, in.	Fluid	Interface pressure, psia	Temperature, °R	Amount required, lbm
Hydrogen pressurant, 2 (5.7 ft ³ bottles)	1/4	Gaseous hydrogen	>2(00)	540	7.4
Helium pressurant, 2 (5.7 ft ³ bottles)	1/4	Gaseous helium	>3(00)	540	17.4
Hydrazine propellant, 4 (3.2 ft ³ tanks)	1/2	Hydrazine	100	540	600.0
Helium pressurant, 1 (1 ft ³ tank)	1/2	Gaseous helium	>2(00)	540	1.4

TABLE 14.2.—COLD-SAT SPACECRAFT PAYLOAD PROCESSING FACILITY (PPF) REQUIREMENTS

Characteristic	Requirement
Dimensional	
Doorway (width × height)	12 by 16 ft
Airlock (length × width × height)	40 by 15 by 16 ft
High bay (length × width × height)	40 by 40 by 36 ft
Control room	
Storage	Desirable
Offices	Desirable
Cranes	
Capacity	5 ton
Hook height	36 ft
Lift required	5 to 10 ft
Environmental	
Temperature	75 °F
Humidity	50 percent
Cleanliness	100-K class
Emergency exhaust ventilation	-----
Electrical	
Power	120-V ac (single-phase) 208-V ac (three-phase)
Grounding	Building ground
Fluids	
Compressed air	115 psia
Gaseous nitrogen	Low pressure purge
Gaseous helium	Low pressure purge
Communications	
Telephone	X
OIS	X
OTV	X
Timing/count clocks	X
Antennas	X
Data lines	X
Radiofrequency transmit/receive	X
Facsimile	X
Safety	
Radiofrequency transmission	X
Installed PYRO NSI's	X
Security	Authorized personnel

(NSI) in its pyrotechnic devices. It will be packed for shipment and may be equipped with special transportation hardware. Shipping and packaging materials must be removed and the assembly of the spacecraft completed.

14.2.6 TESTING

Following arrival at the launch site, the spacecraft and its shipping container must be inspected and tested to assure that no damage has occurred in transit. As assembly proceeds, the status must be verified and then the completed spacecraft tested to assure that it is fully functional. This includes end-to-end communications tests through the Tracking and Data Relay Satellite System (TDRSS).

Communication between the launch site EGSE, the spacecraft, and the POCC must be validated. Following integration with the launch vehicle all interfaces between the spacecraft, the launch vehicle, the EGSE, the launch control complex, and the POCC must be verified. The procedures and equipment for

TABLE 14.3.—COLD-SAT SPACECRAFT HAZARDOUS PROCESSING FACILITY (HPF) REQUIREMENTS

Characteristic	Requirement
Dimensional	
Doorway (width × height)	12 by 36 ft
Airlock (length × width × height)	40 by 15 by 36 ft
High bay (length × width × height)	40 by 40 by 36 ft
Control room	X
Storage	X
Offices	X
Cranes	
Capacity	5 ton
Hook height	36 ft
Lift required	5 to 10 ft
Environmental	
Temperature	75 °F
Humidity	50 percent
Cleanliness	100-K class
Emergency exhaust ventilation	X
Electrical	
Power	120-V ac (single-phase) 208-V ac (three-phase)
Grounding	Building ground
Fluids	
Compressed air	115 psia
Gaseous nitrogen	Low pressure purge
Gaseous helium	>3000 psia and low pressure purge
Hydrazine	600 lb; >60 psia
Communications	
Telephone/facsimile	X
OIS	X
OTV	X
Timing/count clocks	X
Antennas	No radiofrequency test required
Data lines	X
Safety	
Hydrazine loading	X
Gaseous helium bottle charging	X
PYRO NSI's installation	X
Battery charging	X
Security	Authorized personnel

loading and de-tanking liquid hydrogen must be validated before the launch count begins.

Prior to its use on the spacecraft, all GSE and EGSE must be validated to assure that it is functioning correctly and will not damage the spacecraft. Table 14.4 provides a summary of the testing requirements.

14.3 Interfaces

The required interfaces for the COLD-SAT spacecraft will be presented in an interface requirements document developed by the COLD-SAT project office and the prime contractor with the concurrence of the NASA KSC LSSM. The interfaces presented herein are those required for ground operations at KSC/CCAFS. The interfaces required at the launch complex and ELV are presented in Chapter 13, Launch Vehicle, Launch and Ascent Operations, of this report.

TABLE 14.4.—GROUND PROCESSING REQUIREMENTS

- Ground operations—spacecraft
 - Systems functional tests
 - Mission power cycle simulation test
 - MLI blanket purge test
 - Flight level pressure test
 - Spacecraft final assembly
 - Propellant/pressurant loading
 - Payload adapter mate
 - Payload fairing encapsulation
- Ground tests and prelaunch operations—EGSE/LCC/POCC
 - Communication tests
 - NASCOM/TDRSS/GSTDN/POCC
 - Control tests
 - EGSE/LCC/PPF/HPF/Complex 36
 - Data and software management tests
 - EGSE/PPF/HPF/Complex 36/POCC transmit/receive
 - Spacecraft downlink
 - Engineering uplink
 - End-to-end tests
- Ground tests and prelaunch operations—Complex 36
 - Complex 36 systems modifications validation
 - Encapsulated spacecraft/ELV mate
 - GSE/EGSE and interface validation tests
 - EGSE/LCC TT&C and data communication tests
 - Umbilical tests
 - Spacecraft destruct package (FTS) installation
- Wet dress rehearsal (WDR)
- Launch vehicle simulated flight test (SMFLT)
- Composite electrical readiness test (CERT)
- Launch readiness tests and spacecraft closeout
 - Arm PYROS and FTS
- COLD-SAT final countdown and launch

14.3.1 ELECTRICAL INTERFACES

The electrical power system ground test interfaces provide for electrical servicing of the spacecraft from the EGSE power supplies. They provide for 24 to 34 Vdc ground/ascent power and distribution bus test power, 0 to 80 volt dc solar array simulator power, and electrical ground. The solar arrays are not connected at the same time as the simulator. Grounding is connected to the facility ground system.

The spacecraft electrical power interfaces are

- (1) Between the power distribution box and the ELV power transfer unit (24 to 34 Vdc) (ground/ascent power)
- (2) Power distribution box (24 to 34 Vdc) (bus test power)
- (3) Power control unit (0 to 80 Vdc) (solar array simulator)
- (4) Pyro control box (grounding cable)

Figure 14.1 provides a diagram of these interfaces.

14.3.2 CONTROL, COMMUNICATION, AND DATA INTERFACES

Interfaces with the spacecraft telemetry, tracking, and command (TT&C) system are required both for the checkout and

test of that system as well as for control and monitoring of the remainder of the spacecraft. The communication path is via redundant serial data links through dedicated land lines to the EGSE. The spacecraft TT&C interfaces are

- (1) Flight computers 1 and 2 (one MIL-STD 1553 bidirectional bus for each computer)
- (2) Redundancy control unit (EGSE uplink discrete commands)
- (3) Command and telemetry unit (serial telemetry downlink to EGSE)
- (4) Spacecraft TT&C internal data bus (MIL-STD 1553 bus)

There is an additional interface with the spacecraft high-gain antenna to allow end-to-end testing of the transponders with the TDRSS system. No radiofrequency testing of the low-gain antennas is planned.

There are additional command and data interfaces between the EGSE and both the launch control center and the COLD-SAT POCC via NASCOM (NASA worldwide communications network). Voice communication is required between personnel servicing the spacecraft, controlling the EGSE, directing the LCC and staffing the POCC. Normal business communications (Fax, TTY, phone, etc.) are required for personnel at KSC.

14.3.3 FLUID INTERFACES

The fluid interfaces for the COLD-SAT spacecraft provide for purging, propellant and pressurant loading, gaseous hydrogen loading, and liquid hydrogen fill and drain. The gaseous hydrogen and liquid hydrogen interfaces are intended for use only at the launch complex. The others are intended for use throughout the spacecraft processing. Control of the fluid valves is required to provide the proper flowpath, that is, proper purge and vent paths.

The spacecraft fluid interfaces are

- (1) Liquid hydrogen fill and drain, 0.75-in. flight umbilical
- (2) Gaseous hydrogen ground vent, 1.50-in. in-flight/umbilical
- (3) Gaseous helium/gaseous nitrogen MLI purge gas, 0.25-in. flight umbilical
- (4) Gaseous hydrogen vaporizer loading, 0.25-in. manual valve and cap
- (5) Experiment system gaseous helium pressurant, 0.25-in. manual valve and cap
- (6) Hydrazine fill/drain, 0.50-in. manual valve and cap
- (7) Propulsion system gaseous helium pressurant, 0.25-in. manual valve and cap
- (8) MLI purge vent, 1.50-in. relief valve, (a free vent)

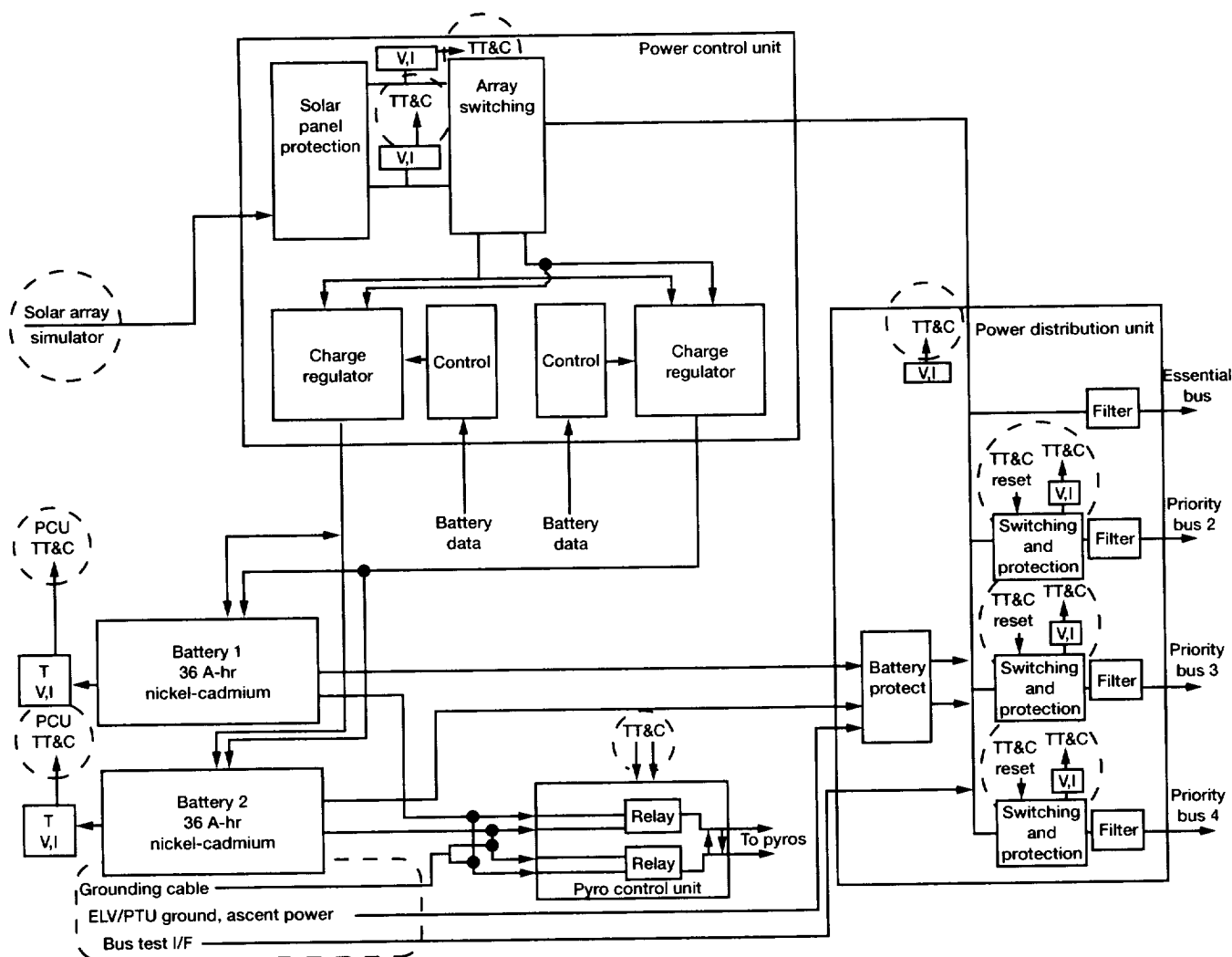


Figure 14.1.—Electrical power system ground test interfaces (interface items enclosed by dashed lines).

14.3.4 TRANSPORTATION AND HANDLING INTERFACES

The transport and handling interfaces (hardpoints) are dictated by the structural design of the spacecraft. Attachment points are required for the trunnion mounts of the handling dolly. Additional attachment points are required for lifting slings and strong backs. Nonflight (red) hardware attachments are dictated by spacecraft configuration.

14.4 Operations

This section covers the sequence of operations which must occur to prepare the spacecraft for launch. Figure 14.2 illustrates this basic processing flow from the KSC/CCAFS airstrip to the launch site. The details of the required operations are

presented in the following subsections that are keyed to the location at which the operations will take place.

14.4.1 OPERATIONAL TIMELINE

Table 14.5 presents the basic timeline for operations at the launch site. At least 120 days are required to prepare the spacecraft. The spacecraft is required at the launch complex a little earlier than is usual to allow for its participation in the launch vehicle's WDR to assure that liquid hydrogen loading and unloading will proceed as required at launch.

The basic processing flow is from the airstrip to the payload processing facility (PPF) for assembly and test as can be seen in figure 14.2. The spacecraft is then moved to a hazardous processing facility (HPF) for the more risky tests and operations. There the spacecraft is mated to the attach fitting, encapsulated in the payload fairing, and moved to launch

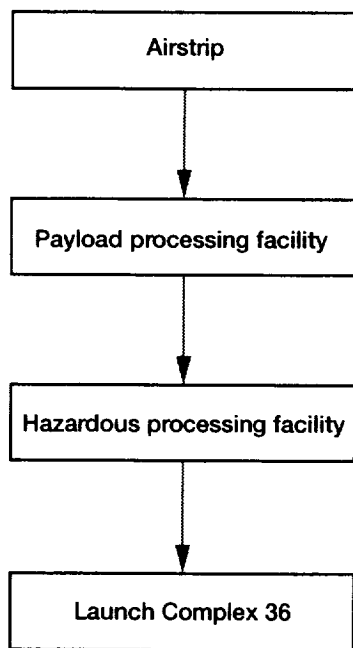


Figure 14.2.—KSC/CCAFS processing flow.

Complex 36. It is then mated to the launch vehicle, loaded, and launched. Table 14.6 summarizes the status of the spacecraft and principal activities at each location.

The time required for ground operations at KSC/CCAFS is 120 days. Two weeks (14 days) will be consumed in receiving, uncrating, and preparing for test. At this time, final preparations will be made at the EGSE and LCC in order to commence testing and data control. Processing at the PPF will commence on L – 105 days, and continue for 45 days. One month (30 days) will be used for processing at the HPF, which will start on L – 60 days. At L – 30 days, the COLD-SAT spacecraft will be mated to the ELV. The mating is about 20 days earlier than typical, because of the required liquid hydrogen tanking test. This test will occur at L – 24 days. The SMFLT at L – 21 days, and the CERT at L – 7 days, will complete the schedule milestones. After L – 7 days, the processing will follow the typical Atlas/spacecraft timeline. The Atlas launch count will start at L – 5 days, but the first scheduled COLD-SAT event will occur at L – 2 days (start payload gaseous helium purge).

The time required for development of the GSE and EGSE required for ground operations at KSC/CCAFS is not addressed here. It is assumed that the required hardware and control centers have been developed, fabricated, installed, and

TABLE 14.5.—KENNEDY SPACE CENTER (KSC)/CAPE CANAVERAL AIR FORCE STATION (CCAFS) GROUND OPERATIONS SCHEDULE

• L – 120 days	COLD-SAT spacecraft arrival at CCAFS skid strip
• L – 106 days	Start COLD-SAT spacecraft processing at PPF
• L – 060 days	Start COLD-SAT spacecraft processing at HPF
• L – 030 days	COLD-SAT spacecraft mate to Atlas ELV at Complex 36
• L – 024 days	COLD-SAT/Atlas tanking test (WDR) at Complex 36
• L – 021 days	Atlas simulated flight test (SMFLT) at Complex 36
• L – 007 days	COLD-SAT/Atlas electrical test (CERT) at Complex 36
• L – 000 days	Launch COLD-SAT on Atlas ELV at Complex 36

TABLE 14.6.—CONFIGURATION/HAZARDS STATUS

<ul style="list-style-type: none"> • Arrival at KSC/CCAFS <ul style="list-style-type: none"> • Primarily assembled except for solar arrays, directional antenna, and payload adapter • Some PYROS with “safed” NSI’s installed • Low-pressure gaseous helium/gaseous nitrogen in systems and plumbing • At PPF <ul style="list-style-type: none"> • Complete assembly • Battery charging • Spacecraft power/control tests • Spacecraft instrumentation and data tests • Radiofrequency testing • At HPF <ul style="list-style-type: none"> • Test gaseous helium insulation blanket • Flight level pressure check with gaseous helium • Install and “safe” PYROS with NSI’s • Load gaseous helium pressurants • Load hydrazine propellant • At launch Complex 36 <ul style="list-style-type: none"> • Arm PYRO NSI’s • Install/arm spacecraft destruct system • Load gaseous hydrogen in vaporizers • Purge gaseous helium insulation blanket • Load/vent liquid hydrogen

validated before the arrival of COLD-SAT at the airstrip. The EGSE and some GSE will have been used during the qualification and verification testing addressed in Chapter 18, System Development, Integration, and Test, of this report. Data communication with the POCC at Lewis during those tests will have also occurred. Prior to arrival of COLD-SAT at KSC/CCAFS, the EGSE and LCC control centers will have been installed and checked out. However some equipment used for spacecraft qualification testing will arrive at approximately the same time as the spacecraft and be installed as the spacecraft is being unpacked. The exact schedule will be influenced by other activities at the PPF and LCC, but installation should commence about a year ahead of needed time.

14.4.2 ARRIVAL

The COLD-SAT spacecraft will arrive at one of the KSC/CCAFS airstrips, and will be contained in its handling dolly inside the trailer transporter. The handling dolly will contain a strong back to support the spacecraft frame and assist in erecting it. The trailer transporter will be off-loaded from the airplane, and moved to the assigned PPF. Other spacecraft hardware and GSE will also be off-loaded and transported to the PPF.

At this time, the spacecraft solar arrays and high-gain antenna are not installed and the spacecraft will not be equipped with batteries. Only pyro devices, which are inaccessible at the launch site, will be installed, and these will be kept electrically safe. Additional delicate components may also be removed for shipment, and shipping or packing materials installed.

14.4.3 PAYLOAD PROCESSING FACILITY OPERATIONS

The spacecraft will first be removed from the trailer transporter and inspected. Shipping measurements will be reviewed for any excursions outside the specified transport measurements envelope. The installed pyrotechnics (MLI purge bag and can vent door actuators) will be verified as safe. Desiccants will be removed, gaseous helium pad pressure verified, shipping restraints removed, and the COLD-SAT spacecraft erected to vertical attitude in the high bay of the PPF. Workstands will be installed around the erected COLD-SAT for personnel access during testing.

The first operation required is to power-up the spacecraft. Before this is attempted, however, a spacecraft continuity and short circuit verification test must be completed. The EGSE used to power-up the spacecraft must be validated before connection. The EGSE power supplies for the spacecraft will be load-tested on dummy loads of the same power rating as COLD-SAT. The power supplies will then be connected to the spacecraft; these are the 24- to 34-V power supply to the spacecraft bus, and the 0- to 80-V power supply to the solar array input of the power control unit (PCU).

Tests of the isolation/operation of the pyro control box will be conducted with dummy loads in place of the pyrotechnic actuators. Control of the MLI purge blanket vent doors during ascent will be tested this way, as will the MLI can vent doors and deployment actuators for the solar arrays and high-gain directional antenna. The pyros will remain disconnected until prelaunch closeout at Complex 36.

After verifying that the spacecraft power system performs properly, the spacecraft batteries can be installed. The two batteries installed at this time will not be the flight batteries. Checkout (nonflight) ones will be used during the ground operations. The flight batteries will be installed later. The flight batteries have to be tested, however, to validate their functionality. Testing will include charging and load capability.

A functional interface test will be conducted to validate the bidirectional serial data link between the EGSE and the spacecraft computers. This link is used for commanding the spacecraft and for uploading and downloading spacecraft software. One test will verify the onboard computer's response to ground commands (EGSE uplink) and data from the computer to the ground (EGSE downlink). A similar test will verify the proper response of COLD-SAT to the launch network with EGSE discrete signals uplinked to the redundancy control unit (RCU). An instrumentation validation test will verify the spacecraft instrumentation response to the test values.

Control software residing in the ground operations computers of the EGSE control center will direct the tests conducted during COLD-SAT ground operations. There is also an interface with the LCC for test and launch direction while COLD-SAT is on the launch pad. Software will be uplinked from the EGSE to the spacecraft's flight computers via ground-line connection. Override of safety critical valves from the LCC via ground-line connection to the flight computers will be tested. Data will flow from the spacecraft via ground-line to the EGSE and LCC, and be transmitted to the POCC at Lewis for recording and analysis.

The ground control software will be thoroughly tested before use at KSC/CCAFS on a software simulator and again during the qualification and verification testing. The tested software used during ground operations will validate the ability to control the loading and venting of COLD-SAT while on the launch pad, as well as other ground test events.

The ability of the spacecraft transponders to communicate with the TDRSS-NASCOM-GSFC space network, and with the EGSE-LCC-POCC ground control centers will be tested. An antenna coupler will be installed on the high-gain antenna for transmission of radiofrequency (RF) signals. These signals will be received via TDRSS, GSTDN, and NASCOM at the three control centers (EGSE, LCC, and POCC). The telemetry downlink source is from the spacecraft's command and telemetry unit (CTU). Transmission from the low-gain antennas will not be tested at this time. A radiofrequency testing clearance has to be obtained from KSC/CCAFS safety organization before the communication tests can be run. After completion of

the communication tests in the PPF, COLD-SAT's radiofrequency system will be doubly inhibited, and no further radiofrequency testing is planned.

A series of functional tests will be conducted to validate the proper functioning of COLD-SAT's fluid systems, electrical systems, mechanisms, and sensors. Proper response to ground control initiated discrete commands uplinked to the RCU will also be verified. COLD-SAT will be tested to validate the ability of the spacecraft systems and subsystems to function according to the ground software program, with safety-driven overrides of critical hardware. The necessary control functions will be tested to verify loading, venting, and isolation of the liquid hydrogen and gaseous hydrogen portions of the experiment system. Verification that valves critical to those tasks can be operated properly by the ground software is safety critical. Monitoring of spacecraft instrumentation during gaseous hydrogen and liquid hydrogen loading, gaseous helium pressurant loading, and hydrazine propellant loading is also safety critical. The spacecraft instrumentation response will be verified during the functional tests.

The functional tests will be conducted with low-pressure helium in the spacecraft tanks and plumbing. The tests will be designed to verify proper control of the spacecraft systems before high-pressure or hazardous fluids are loaded.

The spacecraft's power control system will be tested by using the solar array simulator. The 0- to 80-V power supply connected to the PCU will be varied to simulate the output of the solar arrays as the spacecraft passes from sunlight to shadow on its orbit. The PCU will control the distribution of power to the spacecraft bus and charge the batteries.

The MLI helium purge bag functional testing requires several individual tests. These tests determine the functional characteristics of the purge system, and validate the proper operation of the purge bag's control devices. The devices to be tested are

- (1) The overpressure relief valve (set at 0.40 psid)
- (2) The adjustable vent bleed valve which determines the blanket pressure decay rate (should be set for approximately 3 to 4 times the pressurization rate)
- (3) The functional operation of the helium purge control skid. This skid maintains blanket pressure between 0.1 and 0.3 psid. Helium supply valves on the control skid open at 0.1, and close at 0.3 psid. The blanket pressure is sensed by connected DP transducers on the spacecraft

The flight level pressure test is conducted to verify the ability of the COLD-SAT spacecraft's tanks and plumbing to contain helium at flight operational level without leaking. Helium will be flowed into the spacecraft until the pressure equals the flight level value. The pressure will be increased in incremental steps until the flight level is reached. Evaluation of possible leakage will be done by the pressure decay method. Since design flight level pressures may vary throughout the spacecraft, control of

the fluid isolation valves is necessary. Ground software will be configured to control the test without overpressure of any component or system. This test is hazardous, and must be conducted within barricades and controlled remotely. Personnel will remain in a protected area during the test. Standard PPF procedures for this test will be adhered to.

The final assembly of the spacecraft includes installation of the solar arrays, high-gain antenna, flight batteries, and some pyrotechnics as well as removal of nonflight hardware. The antenna will be installed in the PPF. The solar arrays, flight batteries, and all remaining pyros will be installed in the HPF. Tests will be run to validate the electrical connections and functionality of the installed components. The pyrotechnics will be kept safe by not connecting the power cables from the pyro control unit to the pyros and by substituting shorting plugs. The pyrotechnics installed at this time are the mechanism pyros to control the deployment actuation of the solar arrays and high-gain antenna. The solar arrays will not be tested with solar-simulating lamps.

Preparation for transport will include disconnecting of the spacecraft batteries, verifying spacecraft fluid system configuration, and applying a gaseous helium pad pressure in the plumbing. The spacecraft will be lowered to horizontal attitude on the handling dolly, secured, and then installed in the transport trailer. The protective cover will be installed on the trailer and an inert (gaseous nitrogen) atmosphere applied for transport.

14.4.4 HAZARDOUS PROCESSING FACILITY OPERATIONS

The spacecraft ground processing will continue at the HPF. Loading of propellants and pressurants will be conducted in this facility, specifically designed for hazardous operations. After loading, verification of characteristics necessary for proper flight control will be determined. These include weight, center of gravity, and other mass properties. Final alignment of navigational sensors will be done before the spacecraft is mated to the payload adapter and encapsulated within the payload fairing.

All ground test operations at the HPF will be closely monitored by the spacecraft instrumentation system. The ground operations computer software will contain a redline file which will alert the test operators of any out-of-limits operation. All intrusions of the redlines will be logged and resolved before prelaunch closeout.

Loading of the up to 600 lb of hydrazine needed for spacecraft propulsion and attitude control is typical of most spacecraft. The hydrazine GSE service cart will be connected to the propellant fill/drain valve on the spacecraft. Helium pressurant from GSE will be connected to the gas fill/drain valve on the spacecraft. A gaseous helium cushion pressure of 3 atm will be installed in the four propellant tanks on the gas side of the separating bladder. Hydrazine will then be flowed into the

liquid side of the four propellant tanks until 150 lb is loaded in each tank. The isolating solenoid valves in the gas system will then be closed and latched prior to loading the pressurant bottle to 2000 psig from the helium GSE. The GSE connections will then be broken, tested for leakage, cleaned, and capped. No further operations with the propellant system are necessary, but hydrazine could be drained if the need arose.

The actuating electrical cables connected to the propellant latching solenoid valves, which isolate and preclude system actuation, will be disconnected before loading. These will be reconnected at spacecraft closeout on the launch pad on the day before launch. This safety measure prevents actuation of the propellant system before flight. Ground software will also contain inhibits to propellant system operation.

There are three helium pressurant bottles onboard the spacecraft. One bottle provides gaseous helium pressurant for the hydrazine system. The other two are loaded to 3000 psia with pressurant for the experiment system. The loading of the two gaseous helium bottles will be conducted in a similar fashion to the loading of the propulsion system bottle. The charging fitting will be connected to the GSE and helium flowed into the spacecraft bottles. The charging flow rate is limited by the temperature rise caused by the heat of compression. An orifice in the GSE helium supply and control skid limits the flow rate. The charging flow is terminated as the bottle temperature

approaches the redline value. After a cooling period, more gaseous helium is loaded until the bottle is full. The GSE is disconnected, the charging fitting on the spacecraft secured, and a pressure decay test conducted to verify that there is no leakage.

The final weight of the spacecraft can be determined now that most fluids are loaded onboard. The gaseous hydrogen in the two vaporizers (3.5 lb) and the liquid hydrogen in the supply tank (565 lb) are still to be loaded. Their weights have to be added to the weight determined here. The determined weight is compared to that in the mass properties report. Any overweight must be resolved.

The other mass properties will then be determined and a final alignment check made of the attitude control sensors. This will complete the spacecraft preparation and integration with the launch vehicle can begin.

14.4.5 ENCAPSULATION

The payload adapter connects the spacecraft to the equipment module of the Centaur upper stage of the ELV. The adapter has been tested previously for proper interface configuration with the ELV and the spacecraft. As illustrated in figure 14.3, the payload adapter is mated to a fixture and then the spacecraft is mated to the adapter. Finally the payload adapter

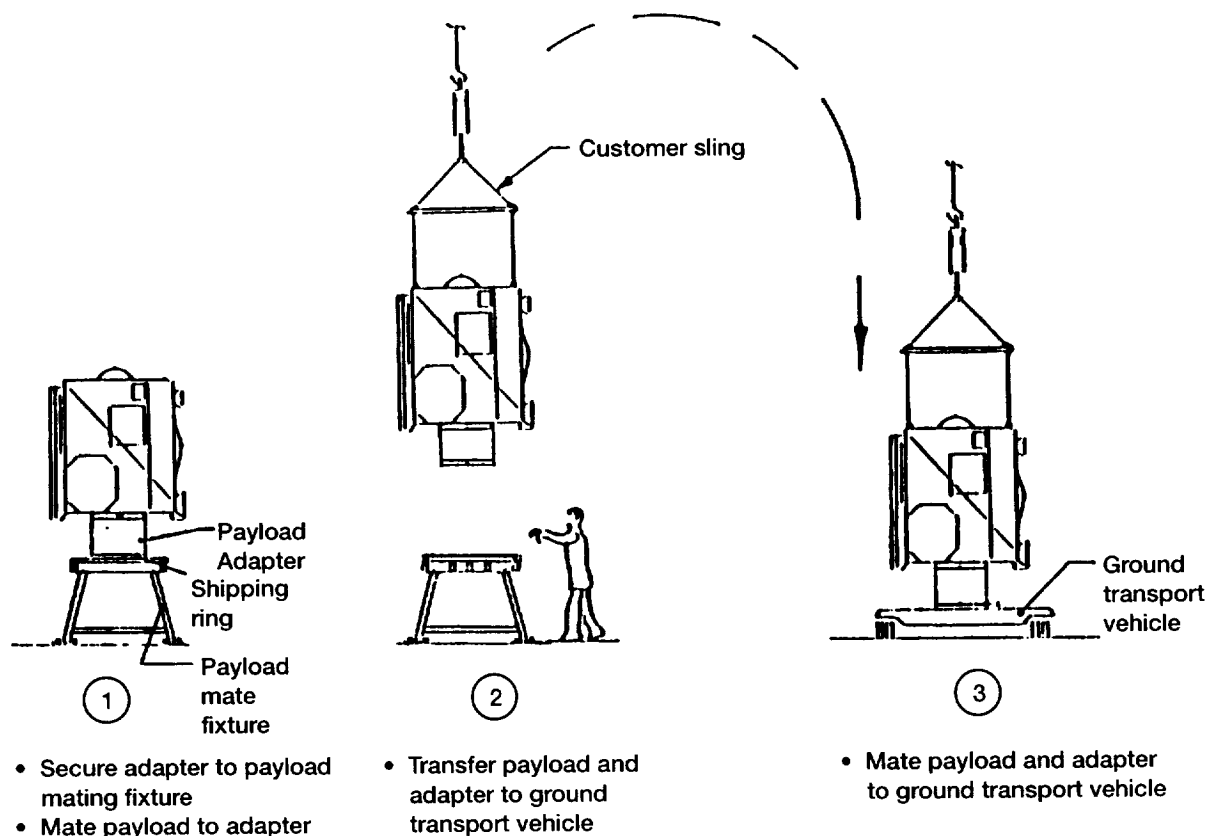


Figure 14.3.—Payload mate fixture usage procedure.

is mated to the ground transport vehicle (GTV). As an alternative, the payload adapter may first be mated to the GTV and the spacecraft then mated to it.

The spacecraft/payload adapter is now ready for encapsulation within the PLF. The fairing is first installed in a nose fairing access workstand. A Torus assembly mounted on a Torus handling cart is aligned to the GTV. The fairing is mated to the Torus and a fit check is made. After the fit check, the two PLF halves are separated and the spacecraft is positioned on the GTV. The PLF is then closed and secured after the payload hydrogen vent is connected. The four PLF access doors are then validated for fit and alignment, and installed. The four doors are

- (1) T – 4 umbilical panel
- (2) Hydrazine fill/drain panel
- (3) Electrical connection panel
- (4) Gaseous hydrogen vaporizer service panel

The complete assembly is then lifted onto the Centaur trailer for transport to Complex 36.

The encapsulated spacecraft is transported to launch Complex 36 on the Centaur trailer. This method of transport is typical for spacecraft scheduled for launch aboard the Atlas ELV. A low pad pressure of gaseous nitrogen inside the PLF will protect the spacecraft against contamination. A low pad pressure of gaseous helium will protect the spacecraft plumbing from contamination. GSE required for COLD-SAT processing at Complex 36 will be transported on a separate vehicle.

14.4.6 LAUNCH COMPLEX 36 OPERATIONS

The remaining ground operations will take place at one of the two Atlas launch pads. Here final integration with the launch vehicle will take place. This will be followed by check-out and test and the final launch of the spacecraft.

14.4.6.1 Launch Operations Timeline

As can be seen from table 14.5, the spacecraft will be moved to the launch pad 30 days prior to launch. Because of the need to load the spacecraft with liquid hydrogen, the spacecraft will be integrated with the launch vehicle earlier than is normal to allow participation in the various launch vehicle tests. The three principal tests prior to launch are the flight simulation test (SMFLT), the terminal countdown demonstration including wet dress rehearsal (WDR), and the composite electrical readiness test (CERT).

Table 14.7 lists the activities on the pad immediately prior to launch. After closeout of the spacecraft, the final communications checks and closeout of the launch vehicle are completed. The Centaur and spacecraft are then loaded with propellants and finally the launch itself occurs.

The launch complex operations timeline on launch day will depart from the standard Atlas mission plan to allow for chilldown and tanking of COLD-SAT. The Atlas mission plan launch count timeline starts at T – 615 min, has a 30-min hold at T – 95 min, and a 15-min hold at T – 5 min. The Atlas timeline from T – 615 min to T – 95 min is not changed.

The chilldown and tanking of both the ELV and the spacecraft occur after the T – 95 minute hold, when the moveable tower is removed and personnel are evacuated from the launch site. The chilldown of the spacecraft cannot proceed until the chilldown of the ELV's upper stage (Centaur) bulkhead has been accomplished. The bulkhead chilldown requires warmer vapor before liquid hydrogen to avoid thermal cracking. Since the same liquid hydrogen supply line used to service the ELV will be used to service COLD-SAT, the vapor from that line will be used to chill the Centaur's bulkhead first before the supply line is chilled to liquid hydrogen temperatures. After the Centaur bulkhead is chilled, enough liquid hydrogen will be loaded to keep it covered. The chilldown and tanking of COLD-SAT will then commence at T – 46 min in the Atlas launch count timeline. This will require at least 120 min. During this time, the Centaur operations will be in a hold maintaining liquid hydrogen above the bulkhead. The Atlas and Centaur tanking of liquid oxygen precedes the liquid hydrogen tanking in the Atlas launch count timeline. The liquid oxygen will have to be maintained in a topping mode for 2 hr during the COLD-SAT chilldown and liquid hydrogen tanking. The additional time required will impose added requirements on the liquid oxygen supply system at the launch complex.

After T – 46 min, the launch count will resume according to the Atlas mission plan. At this time, liquid hydrogen tanking of the Centaur will commence. The spacecraft will be maintained in a topping mode while the Centaur liquid hydrogen is tanked. The modified Atlas launch count timeline will include a hold for COLD-SAT chilldown and liquid hydrogen tanking at T – 46 min, or be retimed. Preferably, prelaunch operations required for COLD-SAT will be integrated into the Atlas timeline without launch count change.

14.4.6.2 Spacecraft Operations at the Launch Pad

Several Complex 36 tower modifications are required for servicing the COLD-SAT spacecraft. These include a modified ground vent system, loading skids for gaseous hydrogen and liquid hydrogen, and the typical spacecraft connections for the environmental conditioning system (ECS), gaseous helium purges, and umbilicals. Some modifications require tapping into existing Complex 36 systems. Tests are required to validate the functionality and safety of the modifications and the new fluid-loading skids. Configuration walkdowns will be followed with pressure and leak tests; these in turn will be followed by functional tests. The functional tests will be

TABLE 14.7.—LAUNCH COMPLEX 36 OPERATIONS

• Prelaunch readiness tests	
• F – 2 day	• Initiate spacecraft gaseous helium purge
• F – 1 day	• Arm spacecraft PYRO NSI's
	• Arm spacecraft flight termination system
	• Remove nonflight (red) hardware
	• Configure spacecraft for launch
	• Configure/test GSTDN and TDRSS voice/data
	• Spacecraft final access and closeout
• Final countdown and launch	
• T – 720 min	Voice/data transmit check
• T – 540 min	Spacecraft ground power on: TLM data on
• T – 300 min	SOCC/LCC/POCC checkout
• T – 240 min	Final briefing
• T – 220 min	Install PLF doors
• T – 190 min	Spacecraft health checks via TLM
• T – 150 min	Start gaseous helium MLI purge (gaseous nitrogen displacement)
• T – 120 min	Start gaseous helium MLI purge (control mode)
• T – 105 min	SOCC/LCC/POCC voice checks
• T – 090 min	Hold
	• Start test stand final preparations
	• Activate redline files
	• Start moveable tower removal
• Resume final countdown and launch (modified timeline)	
• T – TBD min	Complex 36 ECS from air to gaseous nitrogen
• T – TBD min	Start Centaur liquid hydrogen chilldown
• T – TBD min	Start COLD-SAT thermal conditioning
• T – TBD min	Start COLD-SAT liquid hydrogen tanking to 95 percent
T – TBD min	Maintain COLD-SAT liquid hydrogen at 95 percent
T – 043 min	Start Centaur liquid hydrogen tanking
T – 016 min	COLD-SAT to ELV battery power
T – 016 min	COLD-SAT spacecraft go/no-go for launch
T – 016 min	COLD-SAT control by flight software
T – 016 min	LCC fill/drain control if required
T – 006 min	Verify COLD-SAT at flight level
T – 005 min	Final hold (10 min)
• T – 125 sec	Secure COLD-SAT liquid hydrogen tanking
T – 095 sec	Lockup COLD-SAT liquid hydrogen tank vent valve
	Close COLD-SAT liquid hydrogen fill and drain valve
	Drain COLD-SAT liquid hydrogen umbilical and line
	Close Complex 36 liquid hydrogen supply valve for COLD-SAT
	Purge COLD-SAT fill/drain line with gaseous helium
T – 090 sec	Secure Centaur liquid hydrogen tanking
T – 045 sec	COLD-SAT final go/no-go for launch
T – 031 sec	Commence automatic launch sequence
T – 029 sec	Lock Centaur liquid oxygen and liquid hydrogen vent valves
T – 004 sec	Release COLD-SAT umbilicals (T – 4 panel)
T – 002 sec	Release Centaur T – 0 umbilicals
T – 0	2-in. motion
	Inhibit COLD-SAT venting until T + 17 sec

remotely controlled from the COLD-SAT control panel in the Complex 36 blockhouse. Launch pull tests may be required for the COLD-SAT umbilicals, particularly if the umbilicals are of new design. No PLF tests are envisioned, since the PLF is a standard Atlas configuration. These modifications and tests should be completed prior to the arrival of the spacecraft at the pad.

A receiving inspection and validation of the transport measurements will be conducted after the spacecraft arrives at the launch site. Inspection and validation of the required GSE to

support the prelaunch and launch operations will also be conducted. The arriving GSE consists of service hardware additional to the Complex 36 modifications discussed previously.

Validation of the spacecraft-ELV interfaces will precede the mating. The required support hardware for COLD-SAT will have been installed on the Atlas (Centaur) equipment module and validated. After the proper encapsulated spacecraft handling sling (GDSSD) has been attached, the spacecraft will be hoisted and mated to the Atlas ELV.

The mated spacecraft-ELV will be validated for the proper configuration. The validation will include PLF access doors, umbilical connections, and COLD-SAT to ELV interface connections. It will also include a match-mate of the spacecraft separation system.

Connection of the electrical GSE (EGSE) precedes the power up of the spacecraft. The mission-peculiar batteries on the Centaur equipment module and the spacecraft batteries will be connected. The electrical umbilical connection will provide connection to the Complex 36 landline. This will enable monitoring and control of the COLD-SAT spacecraft from the blockhouse. The spacecraft can now be powered up and the batteries charged. After charging, the batteries will be maintained at proper power level with a trickle charge.

Commands will be uplinked from the EGSE control center to the spacecraft by the ground computer. Control sequences required for ground operations will be verified. Data downlink to the EGSE control center and transmission to NASCOM will be verified. This will confirm spacecraft responses to the uplinked commands, assuring proper data for all prelaunch operations.

Connection of the ground support equipment (GSE) follows the electrical validation tests. The GSE required is

- (1) T - 4 umbilical (includes liquid hydrogen fill/drain)
- (2) Gaseous hydrogen ground vent umbilical to the Centaur vent fin
- (3) ECS supply duct to the PLF
- (4) Gaseous helium environmental purges

The two gaseous hydrogen vaporizers are loaded from a GSE service cart on the service tower. Limited personnel access will be required for this operation. The spacecraft valves are controlled by the ground computer from the EGSE control center. Monitoring of the vaporizer's pressure and temperature is done at the EGSE control center. Comparison to the redline file keeps the test within the proper limits. After the vaporizers are charged to 2000 psi, the manual loading valves are closed. The system is then leak-checked and the loading ports are capped. After loading is completed, the gaseous hydrogen vaporizers are benign. They are isolated from the rest of the spacecraft systems until after spacecraft-ELV separation.

The pre-WDR closeout will complete the spacecraft pre-launch configuration until 2 days before launch (L - 2 days). The spacecraft is now ready for liquid hydrogen tanking as part of the Atlas WDR.

14.4.6.3 Major On-Pad Tests

The WDR is the first of two major integrated tests required to achieve flight readiness for the Atlas launch vehicle. The spacecraft is typically not installed for this test but COLD-SAT will be, since it has to be loaded with liquid hydrogen immediately prior to launch. The liquid hydrogen loading of COLD-

SAT must be integrated with the launch countdown for the Atlas launch vehicle. Control of the spacecraft during liquid hydrogen tanking will be demonstrated during this test. The liquid hydrogen tanking and vent valves, and the gaseous helium purge valves on the launch service tower will be controlled by the spacecraft operator in the Complex 36 LCC (blockhouse). The spacecraft valves will be controlled by the ground operations computer from the EGSE control center. Monitoring and coordination functions will be executed by COLD-SAT's launch control team in the EGSE control center, and/or the POCC at Lewis.

The WDR simulates a major part of the launch countdown and demonstrates the capability of the ground and airborne systems to

- (1) Load and maintain Atlas and COLD-SAT propellant levels
- (2) Charge the Atlas airborne gaseous helium bottles to flight pressures
- (3) Perform liquid helium chilldown of the Centaur main engines
- (4) Verify proper operation of all vent valves
- (5) Verify the integrity of the Centaur intermediate bulk-head
- (6) Verify proper operation of the ECS and vehicle/spacecraft purges
- (7) Demonstrate proper operation of all systems under cryogenic conditions

The test is performed with the Atlas in a fully assembled configuration and the service tower withdrawn. The spacecraft and PLF will be installed for the test.

The launch vehicle SMFLT verifies, on an integrated basis, that all Atlas ground and airborne electrical systems are capable of properly combined operation throughout a simulated launch countdown and flight sequence. The Atlas SMFLT procedure will have to be amended to include the required COLD-SAT events. Only those events which directly affect the launch countdown and powered flight will be included. Post spacecraft-ELV separation events will be controlled directly from the POCC at Lewis.

The SMFLT demonstrates

- (1) Proper operation of the launch ladder release sequence
- (2) Capability to operate on internal power with the umbilicals pulled
- (3) Proper operation of all pyrotechnic circuits by use of squib simulators

The test is performed with the Atlas in a fully assembled configuration, which includes the spacecraft and PLF. The service tower is in place around the vehicle throughout the test. The umbilicals are pulled at T - 0 (Atlas) and T - 4 sec (COLD-SAT). Fluid loading and purging are not a part of this

test. The ECS and/or any gaseous helium environmental purges will operate as required.

The CERT verifies electrical readiness of the spacecraft and launch vehicle operating together through a simulation of the final minutes of countdown and the subsequent flight sequence of events. This is a standard Atlas test. The test is performed with the ELV and COLD-SAT fully assembled in the flight configuration. All systems on the spacecraft will be flight ready. Fluid loading and purging is not a part of this test. The ECS and/or any gaseous helium environmental purges will operate as required. The EGSE control center will coordinate the test with the Complex 36 LCC.

The prelaunch readiness tests and operations for the Atlas ELV start 5 days (L – 5) before launch. COLD-SAT prelaunch operations start 2 days before launch (L – 2 days). These tests are the final preparations for launch, all validation tests having been completed. A gaseous helium purge is initiated in the spacecraft liquid hydrogen insulation systems to remove moisture and any other gases. The pyro initiators and the flight termination system are armed on L – 1 day, before spacecraft closeout. At closeout all nonflight hardware is removed and access doors are closed.

14.4.6.4 Launch Operations

The launch countdown starts some 15 hours before lift-off. The Atlas countdown starts at T – 615 min, but an additional 2 to 3 hours have to be added for COLD-SAT liquid hydrogen tanking and conditioning. This time is inserted into the Atlas launch count after the T – 95 minute hold for service tower removal. The timeline is discussed in section 14.4.6.1.

On the pad the spacecraft computers are loaded with the initial flight software and the load verified. Those portions of the experiment system to be loaded with liquid hydrogen are purged with gaseous hydrogen to remove all traces of noncondensable gases. The supply tank multilayer insulation system is purged with helium to remove all condensable gases and so minimize the heat leak and the potential contamination of the insulation system. The flight batteries are fully charged and monitored until lift-off. The supply tank is loaded with liquid hydrogen in tandem with the loading of the Centaur upper stage and then continuously topped-off to make up for the 200 lbm/hr boiloff. Late in the count, spacecraft power is shifted from ground sources to a mission-peculiar battery on the ELV. At T – 90 sec the experiment system is locked up and at T – 45 sec a final go for launch is given. The launch vehicle then proceeds with an automatic count until lift-off. At T – 4 sec all spacecraft umbilicals are pulled. At launch, the hydrogen vent via the Centaur vent fin is pulled.

Lift-off of the Atlas ELV with the COLD-SAT spacecraft completes the ground operations. All subsequent events are part of flight operations. The functions of the LCC and the EGSE are terminated at this time. Flight operations are controlled from the POCC at Lewis.

Contingencies during ground processing will be planned for by the responsible COLD-SAT ground operations team. Procedures for the anticipated contingencies will be on hand. The spacecraft will be under the control of the ground operations computer during most operations at KSC/CCAFS. While the spacecraft is on the launch pad, the Complex 36 LCC will maintain safety override controls as needed. These controls will prevent the loading of fluids from the launch site supply systems, and enable draining of liquid hydrogen from the spacecraft, if needed. The fluid valves on the launch tower are directly controlled from the LCC. The valves on the spacecraft are controlled by the ground operations computer from the EGSE control center.

Blowdown of the high-pressure gaseous helium and/or gaseous hydrogen onboard the spacecraft is controlled by the ground operations computer through hardwire serial communications links to the spacecraft computer. Discharge will take place through the spacecraft hydrogen ground vent. Draining of hydrazine is a manual operation by Complex 36 personnel according to procedure. Control (arm/disarm) of the pyrotechnic initiators and the flight termination system is also handled by the launch complex personnel according to procedure.

The contingency operations are required by safety considerations in the event of a late-count launch abort, loss of spacecraft power, or any events which require access to the spacecraft after liquid hydrogen is loaded. The liquid hydrogen will be drained from the spacecraft supply tank, and the tank will be vented. The spacecraft supply tank and systems will then be purged with gaseous helium before launch complex personnel approach the spacecraft. This is the procedure currently used for the Atlas launch vehicle at Complex 36. If a spacecraft de-mate from the ELV is required, the high-pressure gaseous helium and gaseous hydrogen will be vented via the ground vent system. The gaseous hydrogen vaporizers will then be purged with gaseous helium before launch pad personnel approach the spacecraft to begin the de-mate procedure.

14.5 Alternative Processing Considered

Two alternate ground operations were considered for COLD-SAT at KSC/CCAFS. One was loading of the two gaseous hydrogen vaporizers at the HPF instead of at the launch complex. The other was the need for participation in the Atlas WDR at Complex 36.

The initial plan was to load the two gaseous hydrogen vaporizers in the HPF. It was determined with NASA KSC payload operations personnel that the hazardous processing facilities available were not equipped for gaseous hydrogen loading. The electrical and ventilation systems were not rated for hydrogen service. The alternate plan of loading at the launch complex from a GSE service cart was devised. The service cart concept is similar to the hydrazine service cart now in use at

Complex 36. The service tower of the launch complex is rated for hydrogen operations.

The WDR is a standard Atlas prelaunch test to achieve flight readiness of the launch vehicle. This test verifies the ability to complete the launch countdown under cryogenic conditions. All hardware and systems are tested under this dress rehearsal for the actual launch. Since the COLD-SAT spacecraft is also loaded with liquid hydrogen before launch, it requires similar prelaunch operations. The spacecraft will have been subjected to liquid hydrogen testing during the qualification and verification testing program; however, the WDR is the first opportunity to test a completely assembled spacecraft. The WDR is also the first opportunity to test the integrated Atlas/COLD-SAT launch countdown and to verify the planned liquid hydrogen conditioning and tanking. The WDR also provides a dress rehearsal for the spacecraft and ELV launch team.

The WDR will require about 3 hr more for COLD-SAT participation than would be required for the Atlas alone. The extended time will be duplicated on launch day. Considerable launch countdown procedure planning by COLD-SAT and ELV engineers will be required for either event.

An alternate plan would be to install the tested spacecraft on the ELV, modify the launch countdown, and tank COLD-SAT with liquid hydrogen for the first time immediately before launch. Any opportunity to resolve anomalies before launch day would not exist, however. The added cost and delay of a scrubbed launch would far outweigh the cost and effort of the WDR.

14.6 Ground Support Equipment

Ground support equipment (GSE) consists of all hardware needed to service COLD-SAT during ground operations at KSC/CCAFS. It includes mechanical lifting, handling, supporting, and transport equipment; and fluid loading, pressurizing, purging, and conditioning equipment. Electrical power, control, and communication equipment is defined as EGSE. The required GSE and EGSE will be provided by the COLD-SAT contractor(s) or the ELV contractor(s). Some of the equipment already exists for Atlas ground processing. This equipment is referred to herein as provided by the ELV contractor (GDSSD).

14.6.1 MECHANICAL GROUND SUPPORT EQUIPMENT

The mechanical support equipment consists of

- (1) Spacecraft shipping and handling equipment
- (2) Lifting and erecting slings
- (3) Workstands
- (4) Encapsulation equipment

- (5) Launch complex equipment
- (6) Launch complex contingency equipment

The COLD-SAT trailer transporter is the primary piece of mechanical GSE. The spacecraft will arrive at KSC/CCAFS in the transporter. Other GSE will arrive separately or be available from the ELV launch services contractor.

Figures 14.4 and 14.5 illustrate the COLD-SAT trailer transporter and associated handling dolly. The handling dolly supports the complete spacecraft for ground handling purposes. The trunnions on the dolly allow the spacecraft to be erected for servicing and placed in a horizontal position for shipping. The handling dolly also supports the spacecraft in the trailer transporter. The trailer transporter provides a controlled environment for the spacecraft during transportation.

14.6.2 FLUID SYSTEMS GROUND SUPPORT EQUIPMENT

The helium GSE needed to service the spacecraft consists of three separate supply and control systems; they are

- (1) Low-pressure gaseous helium (<20 psig) for pad pressure in the spacecraft plumbing
- (2) Very low-pressure gaseous helium (0.1 to 0.5 psig) for the MLI blanket purge
- (3) High-pressure gaseous helium (>3000 psig) for flight-level pressure test, and loading the pressurant bottles

The helium GSE will be built as a self-contained system complete with valves, regulators, gauges, transducers, and connections to interface with a helium supply source and the spacecraft. It will connect to the local helium supply at the PPF/HPF and regulate the pressure and control the flow to the spacecraft interface. Remote control by the ground operations computer will provide for loading the high-pressure bottles, and controlling the MLI blanket purge. A separate portable gaseous helium bottle supply will be used to supply the spacecraft plumbing systems with a low-pressure helium pad during transport. The helium GSE will be designed, fabricated, and flow-tested by a COLD-SAT contractor.

A nitrogen control system is required to provide low-pressure gaseous nitrogen for an inerting pad pressure and environmental control of the spacecraft and PLF. It connects to either the PPF/HPF gaseous nitrogen supply system or portable bottles.

A gaseous hydrogen service cart provides gaseous hydrogen for loading the two 2000-psi vaporizers. It will be a self-contained unit with commercial 2400-psi supply bottles, valves, regulators, and gauges. It connects to the vaporizer loading connection on the spacecraft with hoses. Operation will be manual, with a remote-controlled shutoff valve if required by CCAFS safety. The cart will also contain a mechanical vacuum

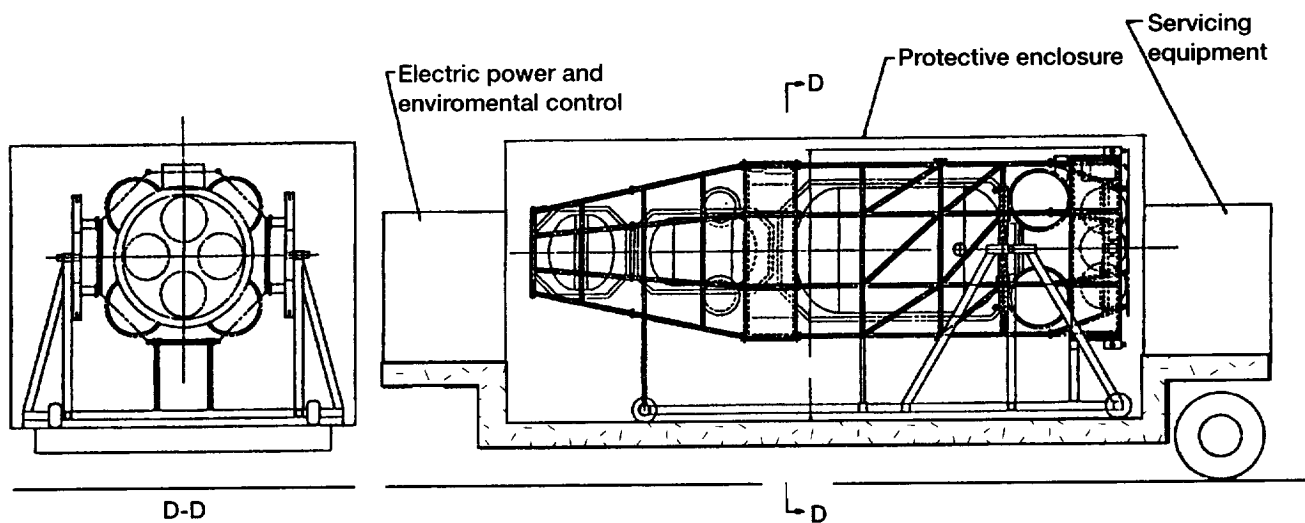


Figure 14.4.—COLD-SAT spacecraft installed on trailer transport in handling dolly.

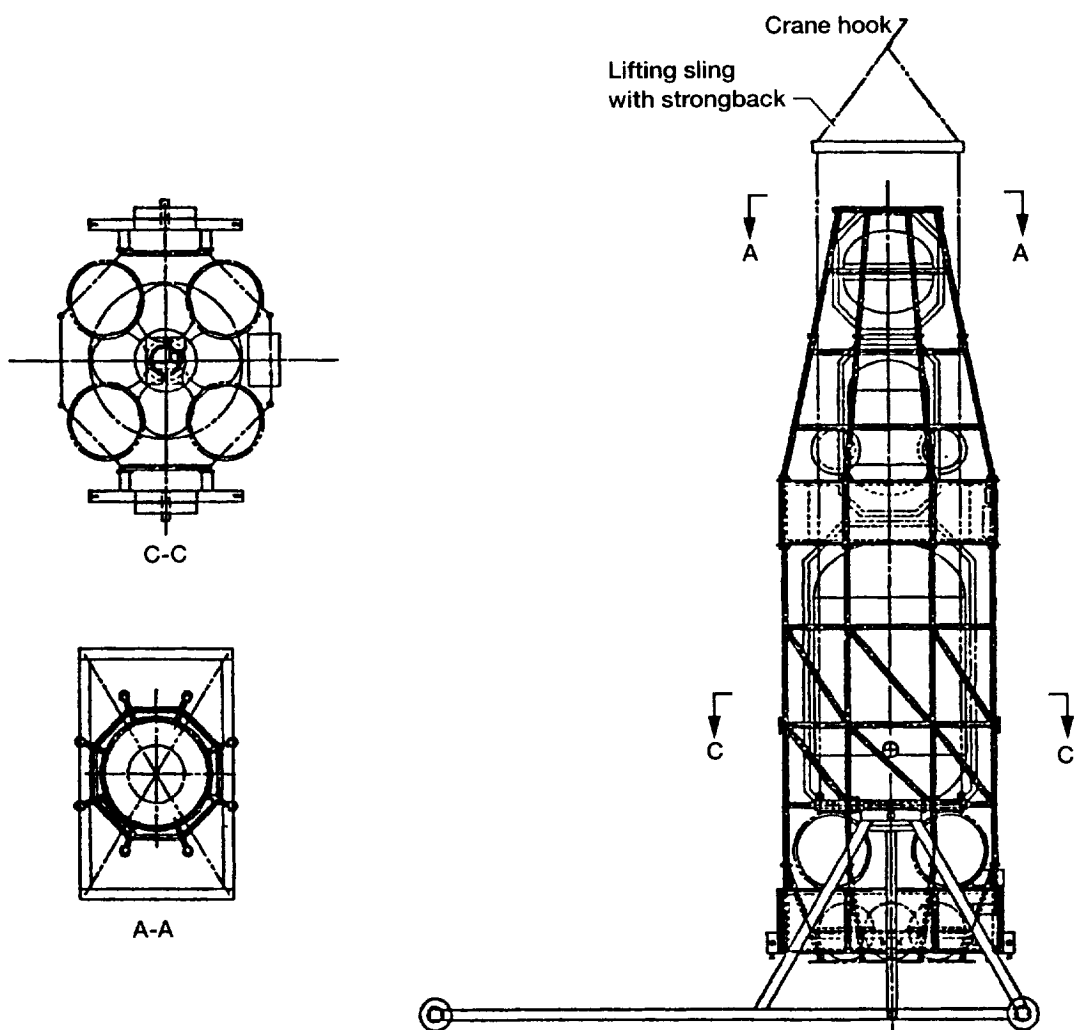


Figure 14.5.—COLD-SAT spacecraft erected on integrated trunnion support and handling dolly.

pumping system for evacuating the vaporizers prior to loading. The gaseous hydrogen service cart design is subject to safety approval by GDSSD, the Complex 36 launch services contractor, and ESMC.

The hydrazine service cart is existing equipment used for loading the Atlas (Centaur) hydrazine propellant system. It can also be used for filling (or draining) the COLD-SAT propulsion system. The cart is manually controlled by launch site personnel according to procedure. The cart is supplied from a hydrazine storage drum and is capable of either loading or draining the spacecraft. The hydrazine service cart will be supplied by GDSSD under the launch services contract.

14.6.3 ELECTRICAL GROUND SUPPORT EQUIPMENT

The electrical GSE consists of power supplies to provide spacecraft power; ground computer(s) to provide control of the spacecraft valves, heaters, and motors; a data system to monitor and record spacecraft information; a communication link to provide coupling of the spacecraft signals to the NASCOM network; and connecting cabling to spacecraft interfaces.

The spacecraft power electrical GSE consists of

- (1) 24- to 34-Vdc power source (ground/battery simulator)
- (2) 0- to 80-Vdc power source (solar array simulator)
- (3) Facility/spacecraft ground connection
- (4) Connecting cabling

The spacecraft control and data handling EGSE consists of

- (1) Ground operations computer and software
- (2) TT&C bus test set and ground connection
- (3) Sensors ground interface test set
- (4) Connecting cabling
- (5) Display CRT's, recorders, and panel meters
- (6) Connecting cabling to landlines interface
- (7) Antenna RF coupler for the spacecraft's high-gain antenna
- (8) Connecting communication EGSE for RF interface

A control center containing the ground operations and data computers will be established at KSC/CCAFS to provide the required interface with the spacecraft. This center will be set up in the PPF control center, or in a trailer adjacent to the PPF. Connections to the other test sites at KSC/CCAFS will be via landline.

A control panel for control of the launch complex servicing valves for COLD-SAT will be established in the Complex 36 blockhouse. The spacecraft operator will control the liquid hydrogen tanking and the MLI blanket purge from this panel. Connection to the launch service tower and the spacecraft will be via landlines. Landline connection to the EGSE control

center will enable communication and coordination with COLD-SAT engineers during operations at the launch complex.

The control of other spacecraft services, such as the ECS for the PLF, exists as part of the Atlas launch complex. Control of the fluid supplies at Complex 36 exists also. Tie-ins to those control systems may be required to accommodate the spacecraft servicing control skids. Required Complex 36 LCC controls are

- (1) MLI blanket gaseous helium purge skid
- (2) Liquid hydrogen tanking fill/drain valve skid
- (3) Gaseous hydrogen ground vent (monitoring only)

14.6.4 SAFETY GROUND SUPPORT EQUIPMENT

Safety monitoring equipment is required to properly monitor the spacecraft environment for leaking hazardous gases. Detectors for hydrogen and hydrazine are required, particularly during loading operations. A helium leak detector and a pressure recorder are required during pressure and leak tests. Low oxygen level detectors are required for personnel safety when using gaseous nitrogen for environmental conditioning and/or PLF inerting.

The KSC/CCAFS processing facilities and the launch complex regularly use this type of safety equipment. Arrangements must be made to assure its availability for COLD-SAT. Some of the GSE may be required for tests at other facilities before spacecraft arrival at KSC/CCAFS.

14.7 Personnel

A team of dedicated support personnel is required to conduct the ground operations and ready the spacecraft for launch. This team will conduct the required tests, record and analyze the data, coordinate the prelaunch activities with the ELV launch team, and manage the transport of the spacecraft between test sites. They are responsible for all ground operations activities at KSC/CCAFS. This team will consist of NASA Lewis, COLD-SAT contractor, and support services personnel. It is estimated that 3 to 4 dozen persons will be required.

Each COLD-SAT system will have its own engineering team responsible for all operations of that system. The system teams will be amalgamated into the spacecraft team. This includes required testing, test procedures, and test data. It also includes required GSE, lifting and handling, transport, and fluid loading. It also includes the required communication with all control systems and control centers. The COLD-SAT spacecraft team will interface with the NASA facility managers, payload support people, and safety personnel. The actual operations will be conducted by the spacecraft team, however, or its designated support service contractor(s).

The COLD-SAT ground operations team will require KSC/CCAFS training before the spacecraft arrives. This training will include required facility familiarization, safety orientation, communication procedures, and transport and handling procedures. The team will also provide spacecraft orientation training for the KSC/CCAFS facility personnel responsible for COLD-SAT. A team manager will provide direction of the ground operations effort including schedules and staffing.

Chapter 15

Flight Operations

Edward Kramer

*National Aeronautics and Space Administration
Lewis Research Center
Cleveland, Ohio*

and

Frank Zimmerman

*Analex Corporation
Cleveland, Ohio*

15.1 Introduction

The COLD-SAT experiment presents some unusual operational problems because of the volatile and wasting nature of the liquid hydrogen experiment fluid. Wherever it is contained, the liquid hydrogen will absorb heat and increase its pressure so that pressure control is a continuing problem. Reliance placed on mechanical relief valves presents the possibility that they will not reseal completely. The primary means of pressure control must use active, positive methods. In addition, in low gravity, fluid position cannot be guaranteed and so uncontrolled venting of a tank will likely result in the venting of liquid rather than vapor with the resultant loss of experimental capability.

When the liquid hydrogen supply is exhausted, experiment operations are over. In the best storage location, the experiment system supply tank, liquid hydrogen boils off at approximately 1.36 lb/day. That same tank will self-pressurize at greater than 0.1 psia/hr and thus may overpressure within a week depending on starting conditions unless active pressure control is maintained. The other experiment system tanks have significantly higher heat leaks and so present larger storage losses and faster self-pressurization rates. These numbers allow for comfortable operation of the system but they do not allow the luxury of stopping experiment operations and contemplating a work-around for some spacecraft or experiment problem.

All experiments involve the transfer, venting, and/or the change in thermodynamic state of liquid hydrogen. Transfers also may involve unavoidable residuals remaining in a tank. All of these situations represent a loss of liquid hydrogen. The various experiment tests must be combined in such a way as to provide the maximum experimental return from the available liquid hydrogen.

During some transfer and venting operations, the experiment system is susceptible to catastrophic failure. If certain valves remain open all of the liquid hydrogen can be lost overboard in a short period of time. However communications with the spacecraft are at best fragile. Failures in the Payload Operations Control Center (POCC) and in the TDRSS/NASCOM (Tracking and Data Relay Satellite System/NASA worldwide communications network) system are to be expected during the mission and spacecraft problems that result in loss of communication are possible. In addition, experiments continue over relatively long time periods (days) and the availability of continuous two-way communication via TDRSS is limited. For purposes of this study, TDRSS access is baselined at a maximum of 13 min/orbit of TDRSS multiple-access coverage.

For these reasons, the operation of the spacecraft and the experiment must be autonomous for periods of up to several days. Failures in the spacecraft systems must be detected and corrected and the experiment system must be protected from catastrophic loss of liquid hydrogen. To meet this latter require-

ment, a "safe state" has been defined for the experiment system which should preserve the bulk of the experiment fluid for at least a week.

Control of the spacecraft and experiment, including the operation of experiments and failure detection and correction, is vested in software that resides in the flight computers. Even failure detection in the computers themselves is essentially a software function through use of the redundancy control unit to switch flight computers in the event of a software or hardware failure.

Planning for on-orbit spacecraft operations must accommodate these constraints and provide for the efficient use of all resources. This chapter covers the methods, hardware, and personnel needed to operate the COLD-SAT spacecraft under these conditions.

15.2 Requirements

The basic requirement is to conduct all COLD-SAT experiments successfully without loss of data. There are also a number of subsidiary constraints on the operation of the spacecraft; they are the following:

- (1) Nominal communications with the spacecraft are limited to 13 min/orbit. All commanding of the spacecraft and return of telemetry data must occur during this period except for short term periods of continuous, single-access coverage.

- (2) Communications will take place through, and spacecraft tracking will be provided by, the TDRSS system. Use of the Spaceflight Tracking and Data Network (STDN) system is limited to spacecraft emergencies.

- (3) TDRSS operations must be scheduled in advance and conform to the capabilities of the system.

- (4) The spacecraft must be rotated periodically to maintain the solar flux on the warm side of the spacecraft and at the correct angle with respect to the solar arrays.

- (5) Experiments must be conducted expeditiously to prevent waste of the experimental fluid but must allow time for preliminary examination of the data and possible reaction to unanticipated phenomena. In addition, the number of available experts on the operation of the experiments is limited and so adequate provisions must be made for their human needs such as food, rest, and relaxation.

- (6) The spacecraft must be left in a safe condition with all fluids vented to preclude the possibility of explosion which would generate unnecessary debris in space.

- (7) The final spacecraft orbit must meet the final orbital lifetime requirement of 500 yr.

15.3 Interfaces

The spacecraft operations function interfaces with large segments of the project but the interfaces are human and documentary rather than physical. There will be continual interaction with the spacecraft subsystem and systems engineers and with the experimenters in planning the flight operations and preparing training and operations documentation. A significant amount of software development will be required for training and operational development. Participation in system testing requires coordination with the test engineers and monitoring of launch site operations requires interaction with spacecraft and launch vehicle personnel at Eastern Space and Missile Range. All communication with the spacecraft via TDRSS requires scheduling and coordination with personnel at Goddard Space Flight Center (GSFC) and White Sands Ground Terminal (WSGT).

During actual spacecraft operations, there will be continual interaction with the experimenters and, no doubt, frequent consultation with experts on the various spacecraft subsystems. Operations with TDRSS will have to be scheduled on a continuing basis. Following completion of operations, data must be distributed and archived and the usual reports written and distributed.

15.4 Nominal Operations

Table 15.1 presents the nominal COLD-SAT operational time line. It begins with the spacecraft stabilized on orbit in the desired attitude with all appendages deployed. Approximately 66 days later all experiment operations are complete. The remainder of the time is devoted primarily to preparing the spacecraft for final shutdown. After a variable delay to obtain the maximum increase in perigee from the available hydrazine, the spacecraft fluids are fully depleted and the spacecraft is shut down after a maximum of 142 days. Details of experiment operations are covered in Chapter 5, COLD-SAT Experiment System, of this report.

15.4.1 INITIAL CHECKOUT

The first 2 weeks of operations are devoted to checkout of the spacecraft and the experiment. All systems will be powered up and monitored, but no redundant systems will be switched in unless needed. Operation of the power system and attitude control system will be monitored. Data from all attitude sensors will be verified. Reception by both transponders will be veri-

TABLE 15.1.—NOMINAL COLD-SAT OPERATIONAL TIME LINE

Time	Operation
T - 0	Launch
T + 12 hr 14 min	End worst-case ascent/acquisition operations Begin on-orbit turn-on of all spacecraft systems Begin high-demand TDRSS multiple access or single access coverage
T + 14 hr	Close supply tank MLI can doors
T + 16 hr	Complete initial turn-on Turn on supply tank passive thermodynamic vent system (TVS) to begin collapse of liquid acquisition device (LAD) bubbles
T + 20 hr	Complete collapse of LAD bubbles Operate active TVS to reduce tank pressure to operational value (20 psi)
T + 1 day 1 hr	Complete supply tank pressure reduction (5 hr) Active and passive TVS off Control supply tank using active TVS as required (At this point, spacecraft and experiment should be stable and under control)
T + 2 days	Continue spacecraft checkout/observation Begin initial experiment leak check by observation of helium pad pressure
T + 4 days	Continue spacecraft checkout/observation Complete initial leak check Begin experiment system integrity check, valve operation check by sequentially venting helium to space and then repressurizing with gaseous hydrogen Begin verification of supply tank heat leak
T + 10 days	Complete spacecraft checkout/observation Complete experiment system integrity check, valve operation check Complete determination of supply tank performance End high-demand TDRSS multiple access/single access coverage Begin contingency period
T + 13 days	End contingency period
T + 13 days 12 hr	Roll spacecraft 180° (1 hr)
T + 14 days	Begin experiment operations Experiment group 1 (159 hr) ^a
T + 20 days 15 hr	End experiment group 1 Begin quiescent spacecraft operations (64.5 hr)
T + 23 days 7 hr	End quiescent spacecraft operations Begin experiment group 2 (85.5 hr)
T + 26 days 20.5 hr	End experiment group 2 Begin quiescent spacecraft operations (48 hr)
T + 28 days 20.5 hr	End quiescent spacecraft operations Begin experiment group 3 (26.5 hr)
T + 29 days 23 hr	End experiment group 3 Begin quiescent spacecraft operations (24 hr)
T + 30 days 23 hr	End quiescent spacecraft operations Begin experiment group 4 (107 hr)
T + 35 days 10 hr	End experiment group 4 Begin quiescent spacecraft operations (48 hr)

^aDetails of experiment groups found in experiment timeline/inventory.

TABLE 15.1.—Concluded.

Time	Operation
T + 37 days 10 hr	End quiescent spacecraft operations Begin experiment group 5 (143.5 hr)
T + 43 days 9.5 hr	End experiment group 5 Begin quiescent spacecraft operations (48 hr)
T + 45 days 9.5 hr	End quiescent spacecraft operations Begin 180° roll maneuver (1 hr)
T + 45 days 10.5 hr	End roll maneuver Begin quiescent spacecraft operations (23 hr)
T + 46 days 9.5 hr	End quiescent spacecraft operations Begin experiment group 6 (106 hr)
T + 50 days 19.5 hr	End experiment group 6 Begin quiescent spacecraft operations (68 hr)
T + 53 days 15.5 hr	End quiescent spacecraft operations Begin experiment group 7 (78.2 hr)
T + 56 days 21.7 hr	End experiment group 7 Begin quiescent spacecraft operations (50 hr)
T + 58 days 23.7 hr	End quiescent spacecraft operation Begin experiment group 8 (161 hr)
T + 65 days 16.7 hr	End experiment operations Begin vaporization of liquid hydrogen residuals (20 days)
T + 75 days	Perform 180° roll maneuver
T + 85 days	Complete vaporization of residuals Vent experiment system to space Delay until Sun line/thrust vector aligned with velocity vector near apogee (52 days maximum)
T + 105 days	Roll spacecraft 180°
T + 137 days (maximum)	Begin thrusting by using 0.52-lb thruster for 15.1 m per orbit (52°) around apogee until hydrazine is depleted (5.03 days to deplete planned 150-lbm margin)
T + 142 days (maximum)	End thrusting Open all hydrazine valves Shut down spacecraft End operations

fied. Spacecraft temperatures will be examined to assure that they are within the range of predicted values. The response of the spacecraft to the attitude control thrusters will be compared with that predicted in advance. Short periods of experimental thrusting will be performed to ascertain whether the system will operate as required during the conduct of experiments. Software loads in the flight computers will be verified.

A number of hours will be required to vent the residual gasses from the supply tank multilayer insulation. Until this occurs and the equilibrium temperature distribution is established, the heat leak will be off nominal. The doors in the MLI can must also be closed to reduce the direct radiation heat leak. This will occur 14 hr after launch but will not completely seal the MLI can so that additional venting can occur. During the remainder of the 2-week checkout period, the operation of the supply tank will be observed to verify its performance.

The boiling during launch and ascent will almost certainly leave bubbles in the supply tank liquid acquisition device (LAD). On the first day the vapor bubbles in the LAD will be collapsed by using the passive thermodynamic vent system (TVS). This activity should at most require less than an hour but four hours have been set aside for this critical operation; the LAD will not function if bubbles are present. Once it is assured that all vapor is removed from the LAD, the active TVS (which draws liquid from the LAD) will be used to reduce tank pressure to the initial experiment value of 20 psia. Following this initial pressure reduction, supply tank performance will be observed with the active TVS being used if necessary to control tank pressure.

The remainder of the experiment system will be launched with a pad pressure of helium. The pad pressure will be observed for several days to provide an initial leak check. The

helium will then be vented from the system through a slow, sequential opening of the experiment system valves, thereby providing an initial check on the operation of the valves and their integrity. Enough time will be allowed during each step in the process to allow observation of a pressure decrease in the event of a significant leak. Once the entire system (other than the supply tank) has been open to space long enough to assure that all helium has been vented, the system will be resealed and pressurized with hydrogen gas. The pressure of this gas will then be observed to assure that valves have resealed and that the system has an acceptable leak rate. In the event that a defective portion of the system is discovered, replanning of experiment activities to work around the problem will begin.

During this period, the spacecraft will be under close observation from personnel in the POCC. A high level of coverage will be required from the TDRSS system either for single-access coverage or for a significant portion of the available multiple-access coverage.

15.4.2 EXPERIMENT OPERATIONS

Operation of the experiment system from the ground is impractical. Frequently, valve operation must be closely timed. The opening or failure to open the correct valve can result in the rapid loss of the experiment fluid. Operator errors or loss of communications at an inopportune time could be catastrophic. For this reason the experiments will be conducted by well-tested software modules resident in the spacecraft computers and initiated by ground command.

To make the best use of the limited supply of experiment fluid, experiment tests will be arranged in coherent sequences which naturally follow one upon the other or are complementary. For example, an outflow test from one tank will be coupled with a fill test of another or a line chilldown will be coupled with a tank chilldown and fluid transfer. Depending on the sequence of tests in a group, it may last from 1 to 7 days. To allow for initial examination of the prior data and to allow rest periods for ground personnel, each group of experiments is separated by several days of quiescent spacecraft operations with essentially no experiment activity. The scheduling guideline used is 30 percent quiescent periods.

The results of each experimental test will be compared with prior predictions soon after the test is completed. If there are serious differences, the testing can be changed or a test rescheduled without major impact on the mission. If all of the liquid hydrogen is in the supply tank, delaying operations for a month will result in the wastage of about 40 lb of fluid. This is 7 percent of the initial stock. While this is a significant amount and may result in the cancellation of a few tests, it is not catastrophic.

The conduct of a number of tests requires thrusting by the spacecraft to generate the required acceleration field for the fluids. All required accelerations are along the long axis of the spacecraft. These thrusting periods will perturb the spacecraft orbit. However, the spacecraft axes are fixed in inertial space.

Since the duration of the thrusting is for at least an appreciable fraction of an orbit and the thrust levels are low, the effects on the spacecraft orbit tend to cancel out to a small final perturbation. Some minor adjustment to the timing of the thrusting periods may be used to further reduce the effects of experiment thrusting.

Active experimentation will be completed 66 days after launch. The residual fluids in the supply tank and receiver tanks will then be allowed to vaporize and vent while the amount of gas vented is carefully measured. This will allow a final mass balance to be completed and allow the efficiency of the LAD to be determined. It will also provide data on the thermal performance of the tank insulation systems. Vaporization of the last liquid residuals will be detected by the warmup of the tank.

After all liquid has been vaporized the entire experiment system will be vented to space and the remaining gaseous helium and gaseous hydrogen pressurant will be dumped to space through the experiment tanks. The experiment system is now in a condition which minimizes the possibility of explosion or rupture, which would result in the generation of more debris in space.

15.4.3 SPACECRAFT OPERATIONS

Following initial deployment, stabilization, and checkout, little in the way of specific spacecraft operations are planned. The exception is the periodic rotation of the spacecraft to maintain the solar flux on the warm side of the spacecraft. Simulations indicate that this operation can be accomplished in a fully controlled manner in less than an hour. Because of the nature of the operation, continuous TDRSS coverage is very desirable and single-access coverage may be required. The timing of this operation is not very critical and it can easily be scheduled in the quiescent periods between experiment groups.

The number and timing of the required roll maneuvers depends on the time and date of launch. For launches near the solstices at the right time of day, no roll maneuver may be required for the entire active experiment period. For initial planning purposes it was assumed the spacecraft would be rolled every 30 days. This rate is considerably faster than is likely in practice.

During the period of active experimentation, operation of all spacecraft systems will be monitored and corrections or work-arounds developed for any failures. However, because of the short duration of the mission and the redundancy of the spacecraft, this is not a likely event. The spacecraft systems will have been extensively analyzed in advance and the operators provided with planned responses for any of the more probable spacecraft system failures.

After the experimentation is complete and the remaining consumables have been vented, the spacecraft still must be prepared for shutdown. Because of allowances for contingencies, a significant amount of hydrazine propellant should remain onboard. The spacecraft will be allowed to stay in its

normal solar-oriented attitude and when the orbit has precessed sufficiently so the thrust axis is along the velocity vector at apogee, thrusting will be commenced in the vicinity of apogee, under ground command, to raise the perigee and so the orbital life. This will continue until the hydrazine propellant is depleted. This will remove the last significant source of internal energy which could fragment the spacecraft and lead to the creation of more space debris. All spacecraft systems will then be shutdown and the COLD-SAT mission will be over.

15.5 Redundancy Implementation and Spacecraft Autonomy

The dynamic nature of the liquid hydrogen experiment fluid, the practical limitations of available TDRSS coverage, the long duration of the interrelated experiment groups, and the potential for major loss of experiment fluid if an experiment sequence is interrupted by communications failure all require that spacecraft and experiment operate with a high degree of autonomy. Periodic control from the ground is not a feasible method of operation.

The pressure in the experiment tanks, especially the supply tank, must be controlled at all times or major loss of experiment fluid may occur. This requires that the thermodynamic vent systems be operated to assure pressure control under all conditions. The spacecraft frequently will be thrusting for long periods to provide low-level acceleration to the experiment system. This thrusting brings with it the possibility of tumbling the spacecraft; an eventuality which the spacecraft must detect and control. Hydrogen transfer and venting operations have the potential for dumping large quantities of liquid hydrogen if a valve inadvertently remains open. Experiment valve failures must be detected and controlled.

15.5.1 REDUNDANCY IMPLEMENTATION

Except for a few selected items (i.e., there is only one high-gain antenna) single-point failures have been eliminated from the spacecraft. All major subsystems are one out of two redundant. The telemetry, tracking, and command (TT&C) system has two transponders, two computers, and the remainder of the system is internally redundant. The propulsion subsystem has two complete, independent sets of attitude control thrusters. There are redundant attitude sensors and gyros. The electric power system has multiple strings on the solar arrays, two spacecraft batteries, and internal redundancy in its electronics. Only the structural subsystem is without redundancy but the large design margins used provide the same effect.

The experiment system is not fully redundant but effective redundancy (with reduced capacity) has been obtained. Fully redundant valving with fully redundant valve drive electronics has not been provided because of weight, cost, and pressure

drop considerations. However, there are always two valves in series between the experiment fluid and space. In addition to selective redundancy for critical functions, all valves and their associated electronics are divided into redundancy clusters (see fig. 15.1) which provide effective failure control for the experiment subsystem but at the potential cost of some experiment capability. Instrumentation is not fully redundant but the number and placement of sensors assures that significant data can still be acquired even if there is a failure of a sensor or even of a signal conditioning and data acquisition box.

The problem with one out of two redundant systems is the detection of failed systems and the subsequent replacement of them. In COLD-SAT failure detection and implementation is in general handled by software in the flight computers. This makes the computers especially critical since they too are only one out of two redundant.

In COLD-SAT there are two identical computers loaded with identical software other than an individualized self-test routine. Both operate continuously and monitor the state of the spacecraft but commands are only accepted from one computer, the active computer. Selection of the active computer is under the control of a redundancy control unit (RCU). Each computer will continuously perform self diagnostics on its hardware and software and write a resulting checksum to the RCU. If the RCU does not receive a correct "checksum" from the active computer within 10 sec, the RCU will switch control to the other computer. This change will be noted by the now active computer, which will confirm the status of the spacecraft and correct it if necessary. Each computer will also have its own error detecting and correcting memory which will cause a switch in active computers via hardware if an uncorrected bit error occurs. A second switch back to the initially active computer will only occur by ground command directly from the transponders.

15.5.2 FAILURE CORRECTION

Not all failures can be corrected by any reasonable set of flight software even if good backup hardware remains. To provide for cases which exceed the capabilities of the software an experiment system "safe state" has been defined. In this state all tanks are locked up, all lines are vented, all pumps and heaters are off, and passive TVS's are on. The experiment system can survive in this state for at least 24 hr which should be adequate time for ground intervention. Going to the safe state will of course disrupt any ongoing experimentation and may result in the permanent loss of some data because of the limitations on available experiment fluid, but it does prevent catastrophic loss.

Because there are redundant Earth and Sun sensors and redundant gyros, the first failure in these sensors can be detected and locked out in sunlight by three of four selection logics. In eclipse this is still true of the z-axis. There are three

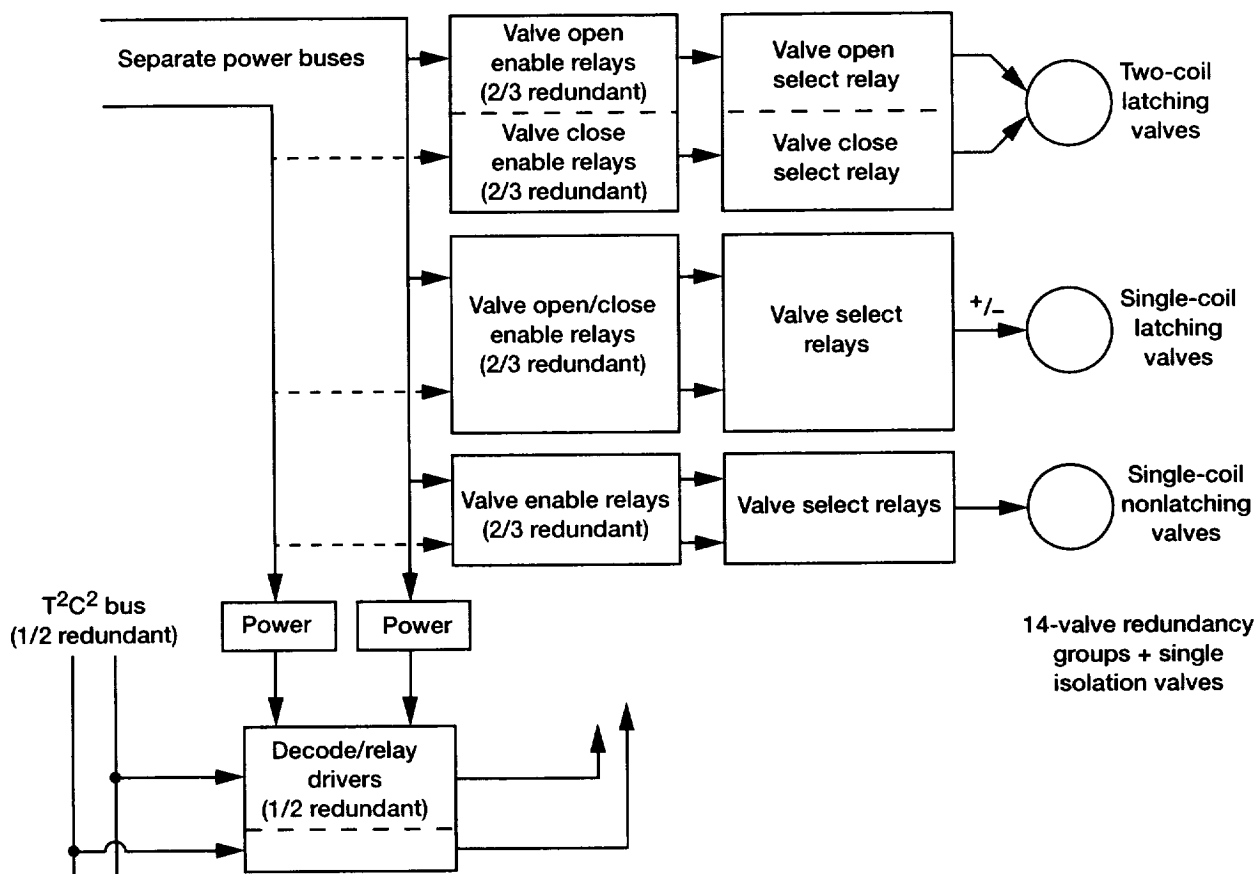


Figure 15.1.—Valve redundancy cluster implementation.

gyros which provide information on two orthogonal axes each. In eclipse, like axis outputs of the three gyros can be intercompared in an attempt to identify a single defective unit. Otherwise a major failure will have occurred.

Excessive attitude error or rates or excessive attitude thruster firing is most likely caused by an attitude control or propulsion thruster which has either failed on or stuck off. Checks on actual thruster temperature versus expected temperature and on thruster valve position should aid in identification of the defective thruster. If one is found, all propulsion thrusters will be shut down and a shift made to the backup set of attitude thrusters. The other potential cause of attitude errors is uncontrolled venting from the experiment system. If the initial procedure does not cure the attitude problem, the experiment system will be placed in the safe state and, if necessary, both sets of attitude control thrusters used to regain attitude control.

Should the Sun sensors and solar arrays fail to receive illumination when expected, there is a major problem with the attitude control system. However, if the gyros are still functional, the spacecraft can be approximately aligned to the Sun using the magnetometer provided for rapid initial attitude acquisition. This approach will result in reduced solar array

output but can keep the spacecraft alive at more moderate power consumption levels. Any experimental thrusting would of course be immediately terminated. A more serious problem is a bus undervoltage which does not trigger an immediate hardware load shed by the power system. In this case the experiment will immediately be placed in a safe state and nonessential bus 1 turned off. If this does not cure the problem, nonessential bus 2 will also be turned off.

It is possible that a major fault on the power system will cause a shutdown of the spacecraft computers. If power is restored and the computers restarted, a firmware routine will take emergency measures. The experiment will be placed in the safe state, spacecraft power consumption will be reduced to a low level, the transponders will be switched to the omnidirectional antennas, and the spacecraft will be stabilized using the gyros. The spacecraft z-axis will be oriented to Earth's magnetic field by using the magnetometer and a rotation about the z-axis commenced. If the Sun is not found after 360° of rotation (about 18 min), the spacecraft will be rotated 180° around the x-axis and the rotation about the z-axis resumed. With the approximate orientation provided by the magnetometer and the width of the Sun sensor's range, if not in eclipse, the Sun should

be acquired after two complete 360° rotations. If the Sun is acquired, the spacecraft will fly in a Sun-oriented mode at low power until ground operators intervene.

If the Sun is not acquired in one orbit or if any of the previous procedures fail to work, the spacecraft will be placed in a minimum power keep-alive mode. If not already there, the experiment will be placed in the safe state, the propulsion system will be shut down, the transponders will be switched to the omnidirectional antennas, and power consumption will be minimized. If the ground operators discover the problem and can diagnose it in time, it may be possible to save the spacecraft and the experiment.

Since the experiment may be operating autonomously, if the results of a given test are totally out of the expected range and may indicate the potential for damage or fluid loss, the experiment will be placed in the safe state until the ground operators can assess the problem. Similarly, since the high-gain antenna and its associated radiofrequency circuitry represent a single point failure, if communications are not established within a reasonable period after the scheduled time, the spacecraft transponders will be switched to the omnidirectional antennas. It is possible to operate the spacecraft by using the omnidirectional antennas if enough TDRSS time is available.

15.6 Payload Operations Control Center (POCC)

For planning purposes it is assumed that the COLD-SAT POCC will be constructed at the NASA Lewis Research Center. Facilities are available at other NASA centers and at some contractor locations. If these are available and if the correct logistics can be worked out, some cost savings may be possible. The design presented here is based on one used at the GSFC and presumes the use of available, NASA-owned software with some modifications. However, this design uses obsolescent computers which may not be available for use at the time of the COLD-SAT flight. The same problem will face all users, however, and other designs and software should be available if this one is not viable.

15.6.1 FUNCTIONS

The POCC must provide the facilities necessary for control of the COLD-SAT spacecraft and the recovery, recording, conversion, and distribution of the telemetry returned by it. It must also provide the physical facilities needed by the spacecraft controllers including appropriate displays. It must take incoming data from NASCOM and record the raw data, decommutate the telemetry, convert to engineering units, and then store, limit-check, and display the data. Personnel and

computers from POCC must analyze these data to monitor the operation of the spacecraft.

The day-to-day operation of the spacecraft must be planned and changes to the original operational plans (developed before the flight) must be made to accommodate responses to early experimental data. If tracking information supplied by GSFC is used, predictions of spacecraft position which incorporate the effects of any scheduled thrusting must be generated. Periodic contacts with the spacecraft via TDRSS must be scheduled with the network control center.

Command uplinks must be generated and their correctness verified before transmission. Modifications to the previously developed flight software may be required to accommodate changed experiment needs. Any software to be uplinked must be fully checked out and then assembled into blocks for transmission. After transmission to the spacecraft, but before execution, uplinked software must be verified.

Operations of the POCC must be scheduled on a 24-hr basis to assure that the right personnel and experimenters are available when needed. Processed data must be transmitted to contractor spacecraft personnel and experimenters at remote sites.

The POCC and its personnel must participate in the test and checkout of the spacecraft during final system test, assembly, test at the launch site, and during prelaunch checkout and loading. During launch and ascent, the telemetry stream received from the spacecraft via the Centaur upper stage of the launch vehicle must be monitored and analyzed.

15.6.2 INTERFACES

Figure 15.2 illustrates the various POCC interfaces. The primary mode of communication is via NASCOM but NASA video of the launch and normal voice and TTY communications will be transmitted by other routes. The primary route for COLD-SAT commands and telemetry is from the spacecraft to the TDRSS spacecraft then to the WSGT, then to GSFC and on to the POCC at Lewis via NASCOM. Communications with the spacecraft at the launch site will also use NASCOM.

Operators at all of these sites will also have voice communications. Use of the TDRSS system will be scheduled with the Goddard network control center via a special mission planning terminal at the POCC. The GSFC flight dynamics facility will obtain tracking data from the TDRSS system and communicate current orbital information and predictions to the POCC via NASCOM. The POCC will transmit digital data to remote terminals via leased lines.

15.6.3 DESIGN

Figure 15.3 presents a block diagram of the COLD-SAT POCC. The POCC is built around three minicomputers;

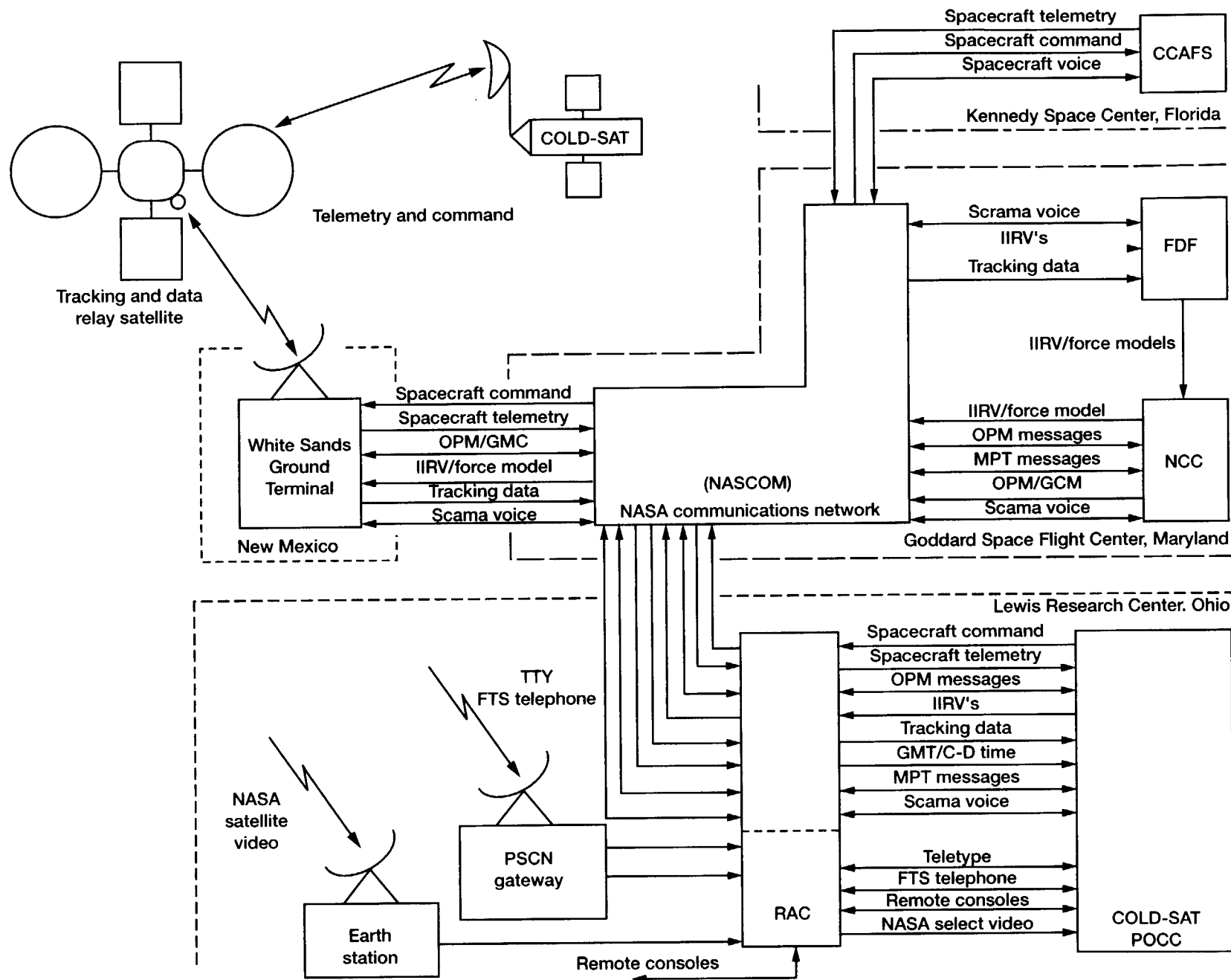


Figure 15.2.—COLD-SAT Communications and Payload Operations Control Center (POCC) interfaces.

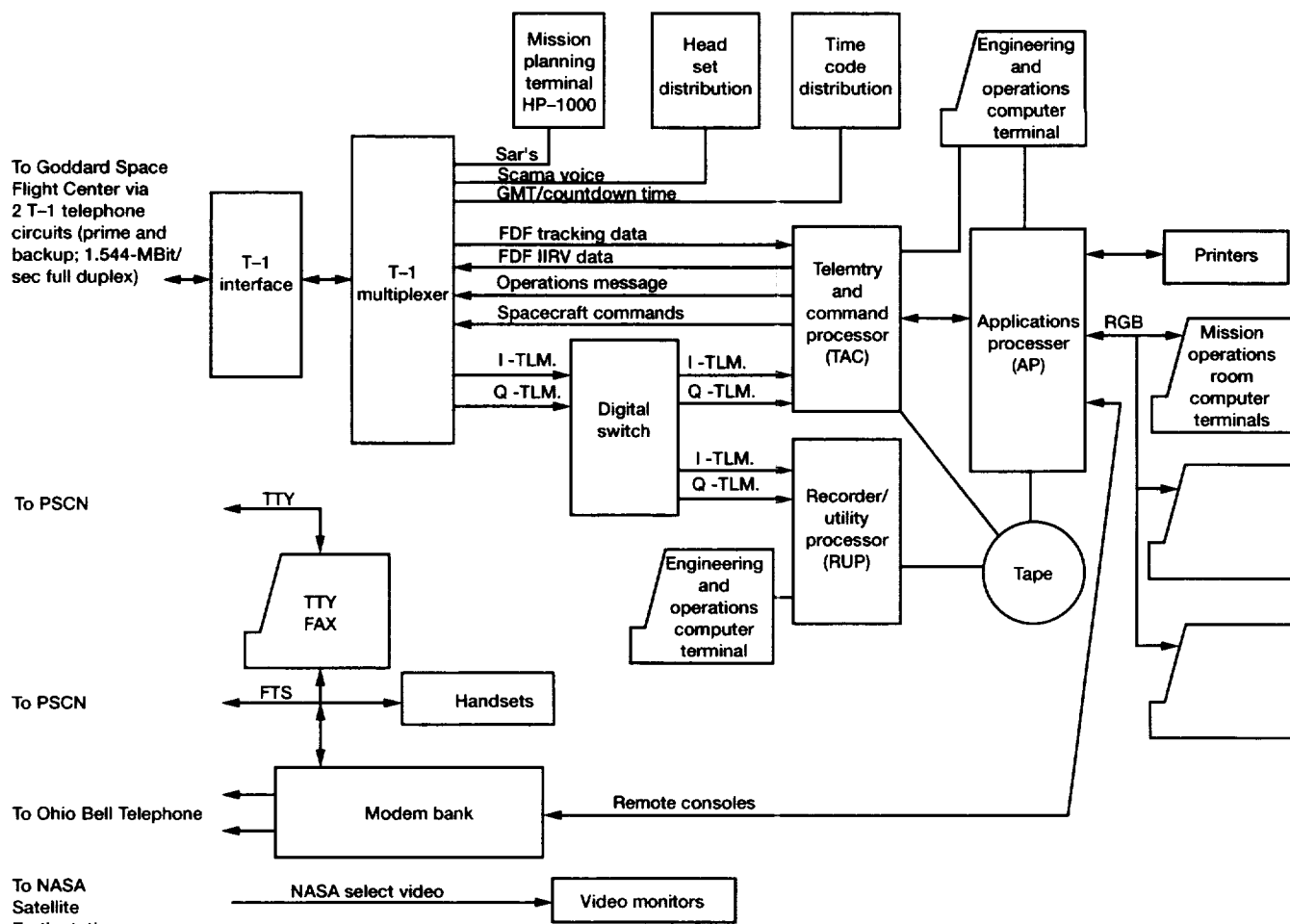


Figure 15.3.—COLD-SAT Payload Operations and Control Center (POCC) block diagram.

a telemetry and command processor (TAC), a recorder utility processor (RUP), and an applications processor (AP). The first two are Digital Equipment PDP 11/34, and the last is a DEC PDP 11/70. Communications with GSFC/NASCOM is via a full duplex, leased, 1.544-Mbyte T - 1 circuit. From the T - 1 interface communications will be routed to a T - 1 multiplexer and then to the various destinations in the POCC. The mission planning terminal (MPT), the POCC internal headset system, and the time code distribution system have separate interfaces with the T - 1 MUX. The primary interface is with the TAC.

The TAC receives telemetry data, tracking data, and operations data from NASCOM and transmits spacecraft commands and predictions to NASCOM. It sorts and logs all messages and checks the validity of, and deblocks data from, the NASCOM 4800-bit block format and also generates the required blocks for transmission. It provides frame synchronization for the telemetry data. The recorder utility processor serves as an online spare for critical TAC functions. It also prepares data for archiving to tape.

The applications processor is the heart of the system. It decommutates telemetry data, converts it to engineering units,

limit-checks it, and distributes it to the appropriate consoles; generates commands and processes software uploads for transmission to the spacecraft; generates operational messages; receives tracking data from the GSFC flight dynamics facility and processes it; has available online historical spacecraft data for display and analysis; and generates appropriate displays indicating status and out-of-limit conditions. It generates alarms for critical out-of-limit situations.

The POCC is also equipped with a mission planning terminal coupled with the GSFC computers for ordinary scheduling of contacts with the spacecraft. It has the necessary video display terminals (up to 16) for use by POCC personnel. Remote consoles are accessed via a modem bank and leased lines. It is also equipped with the usual headsets for voice communications and the ordinary means of communication (phone, fax, TTY, etc.). All equipment is powered by an uninterruptable power system.

Figure 15.4 provides a layout of the POCC. It is built around three rooms. The heart of the POCC is the mission operations room where the flight director and the operators responsible for the principal spacecraft systems have their consoles and work

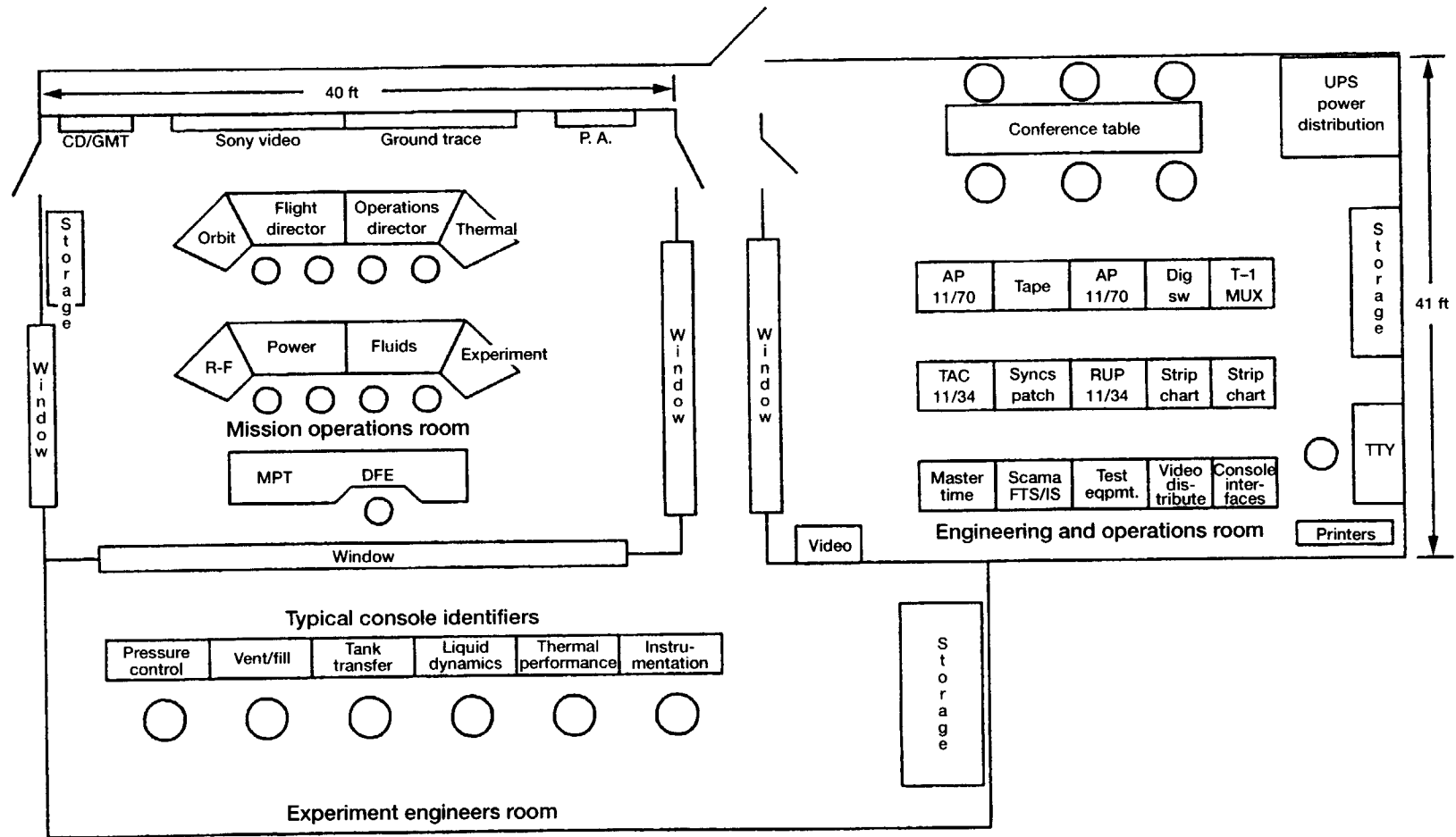


Figure 15.4.—COLD-SAT Payload Operations Control Center (POCC) layout.

as they control the spacecraft. It will be manned 24 hr a day while the spacecraft is in orbit. Behind the mission operations room is an area for the technologists responsible for the various experiments. They will have displays providing information germane to their interests. The third room will contain the equipment racks with the computers and electronics needed to support POCC operations. In addition those display devices which are noisy or disruptive such as line printers will be located here. This room will be staffed by the technicians responsible for the operation of the POCC equipment.

The POCC area will require the ordinary services; that is, security, heating, air conditioning, power, and other utilities. Special provisions will have to be made for installation of wiring such as a raised floor. Adequate soundproofing must be provided to prevent distraction by outside sources. POCC personnel will require office space and the usual facilities.

15.6.4 PERSONNEL

The POCC must be staffed from prior to spacecraft system test until the completion of all on-orbit operations. Staffing levels, however, will vary considerably from the few technicians needed to maintain the POCC equipment when there are no spacecraft operations up to the large number of personnel needed during launch, ascent, and attitude acquisition operations. The relatively short duration of COLD-SAT operations will make training and carrying a full, dedicated POCC staff from prior to system test noncost-effective. If a location is chosen with an available pool of technical personnel who could be trained to operate the spacecraft while performing other duties, considerable savings could result.

TABLE 15.2.—LAUNCH AND EARLY ORBIT PERSONNEL REQUIREMENTS

Mission operations room personnel
Flight director
Operations director
Orbit analyst
Thermal engineer
Radiofrequency engineer
Attitude control system engineer
Power systems engineer
Experiment system engineer
Experiment coordinator
Data flow engineer
Propulsion system engineer
Equipment and operations (E&O) room personnel
E&O manager
Systems programmer
Computer technician
Communications technician
Supporting personnel
Pressure control
Liquid dynamics
Mission planners (2)

TABLE 15.3.—ON-ORBIT PERSONNEL REQUIREMENTS DURING ACTIVE EXPERIMENTATION

Mission operations room personnel
Operations director
Thermal engineer
Radiofrequency engineer
Attitude control system engineer
Experiment system engineer
Power system engineer
Fluids engineer
Experiment coordinator
Data flow engineer
Equipment and operations (E&O) room personnel
E&O manager
System programmer
Computer technician
Communications technician
Experimenter evaluation room personnel (typical)
Pressure control
Tank analysis/transfer
Thermal performance
Vent fill
Liquid dynamics
Low-g performance/instrumentation

TABLE 15.4.—MINIMUM ON-ORBIT PERSONNEL REQUIREMENTS DURING QUIESCENT OPERATIONS

Mission operations room personnel
Operations director
Data flow engineer
Experiment system engineer
Spacecraft systems engineer
Equipment and operations (E&O) room personnel
E&O manager
Communications technician
Computer technician
Systems programmer (as required)
Supporting personnel
As required for experiment planning and post analysis
Mission planners (two on 8-hr day)

Table 15.2 lists the positions to be filled during the initial launch-ascent-acquisition operations of the spacecraft. It is estimated that this full level of staffing should not be required for more than 2 weeks so that only three shifts of 18 people each (54 total) will be required. Table 15.3 shows the potential personnel required during periods of active experimentation. Basically 13 positions need to be filled to operate the spacecraft and the FOCC with technologists being present as required to monitor their specific tests. Again three-shift operation should be satisfactory because of the short duration of the particular experiment groups. Table 15.4 shows the minimum personnel needed during quiescent on-orbit operations. These eight operating positions must be filled continuously and so four-shift operation with backup personnel (approximately 24 to 27 people) are required for the duration of the flight. In addition management and administrative support personnel will be required for the POCC and its personnel.

Preparation for flight operations and the training of POCC personnel will require a significant effort. Long before the spacecraft is complete, detailed operational plans and rules will have to be prepared and then modified as actual information from the spacecraft is obtained. A reasonable fidelity computer simulation of the spacecraft and the experiment system will be required for testing the POCC software and hardware and for training the personnel. It is highly desirable that POCC personnel participate in the conduct of the spacecraft systems test and the prelaunch testing at the launch site to give them some hands-on experience with the spacecraft before launch.

Other personnel will be involved in COLD-SAT operations in addition to the people at the POCC. Technical experts on all spacecraft systems must be available on-call for consultation in the event of anomalous operation. Project management personnel are required to oversee all operations and make or approve any major decisions regarding the spacecraft. The various technologists responsible for the several experiments will be involved fulltime in the preliminary analysis of experiment data and recommendation of changes to the planned testing in light of the early results. In a project of this size there will also be a certain number of public relations people involved.

Chapter 16

Reliability

W. James Dorcey

Science Applications International Corp.

Cleveland, Ohio

16.1 Introduction

The purpose of the COLD-SAT reliability program is to serve as a design tool to enhance the reliability of the spacecraft and experiment system and to assure that all NASA requirements are met (ref. 7). The role of the reliability function during the feasibility study is to provide an independent assessment and review of the design and to provide assistance to system designers with redundancy implementation and achievement of the system and spacecraft reliability goals.

Several reliability activities were undertaken during the COLD-SAT feasibility studies. The reliability goal of 0.92 was allocated to the separate spacecraft systems to provide system level reliability goals for the system designers to work toward. Component failure rates were compiled from a number of sources and evaluated to determine their applicability to this design. System reliability analyses and predictions were performed to evaluate design trades, to determine single-point failure tolerance, and for comparison to the system-level reliability goal. Assistance was provided to the system designers by identifying areas which could benefit from redundancy implementation. Spacecraft reliability analyses were conducted to review system interactions and for comparison to the spacecraft reliability goal. The reliability program and associated analyses were conducted using established aerospace methodologies (refs. 8 to 11).

The reliability prediction for COLD-SAT was found to equal the reliability goal of 0.92 for completion of all class I experiments during a 6-month mission. Table 16.1 shows the comparisons between the reliability allocation and the reliability prediction for each system. Since the reliability allocation was used in place of the reliability prediction for the structure and software systems, the difference between the two for these systems is not applicable.

The COLD-SAT conceptual design does not meet the goal of successful elimination of all potential single-point failures. The three areas in which the design falls short of this goal are the primary tanks (experiment system supply tank and propulsion system pressurant and propellant tanks), the telemetry, tracking, and command (TT&C) system radiofrequency (RF) processing switch, and non-class I experiments. An evaluation of trades involving the primary tanks revealed that these tanks have a low probability of failure and problems generated by the addition of redundant tanks (cost, weight, spacecraft performance) would outweigh the benefit of such an addition. The TT&C system RF processing switch is discussed in detail in section 16.5.4. The components associated with non-class I experiments are considered to be nonmission-critical items; therefore the additional cost and weight involved in the implementation of redundancy are not economical.

16.2 Requirements

A number of requirements were imposed on the reliability program. These requirements are discussed in this section.

16.2.1 SPACECRAFT RELIABILITY GOAL

A numerical reliability goal of 0.92 for the completion of all class I experiments within a 6-month mission time was established for COLD-SAT. This goal was based on reliability goals of other spacecraft programs and the COLD-SAT design goal of a reliable and economical design.

The reliability analysis performed during the feasibility study concerned only the operation of the spacecraft and experiment system for the 6 months following separation from the launch vehicle and the completion of all class I experiments

TABLE 16.1.—COMPARISON BETWEEN ALLOCATED AND PREDICTED RELIABILITY

System	Reliability		Difference
	Allocated	Predicted	
Structure	0.999	0.999	N/A
TT&C	0.990	0.985	-0.005
Attitude control	0.997	0.998	+0.001
Power system	0.992	0.993	+0.001
Software	0.985	0.985	N/A
Experiment	0.958	0.960	+0.002
Propulsion	0.998	0.998	0.000
Overall	0.920	0.920	0.000

within this 6-month period. It assumes autonomous spacecraft operation in a benign space environment free from any outside interference. The following ground rules were used during the reliability analysis:

- (1) The launch vehicle delivers COLD-SAT into the design baseline orbit and attitude with no damage to the spacecraft. No launch-induced failures occur to any of the spacecraft components during the course of the mission.
- (2) Micrometeoroids and orbital debris do not cause impact damage to the spacecraft during the 6-month mission.
- (3) The scope of communications is limited to the spacecraft's ability to transmit and receive data and commands. Any failures related to Tracking and Data Relay Satellite System (TDRSS) or ground communications were not considered during this study.
- (4) The mission is considered to be a success if no failure or failures occur which prevent the completion of all class I experiments within 4383 hr (6 months) following the separation of the spacecraft from the launch vehicle.
- (5) The allocated reliability of the structure and software systems will be used in developing the spacecraft reliability prediction.
- (6) Nonoperating or dormant failure rates are equal to 0.

In addition, the following items were assumed to be free from failures (reliability = 1):

- (1) All electrical, electronic, and instrumentation wires, cables, harnesses, busses, and connectors
- (2) Experiment tanks, vaporizers, and internal components (i.e., liquid acquisition devices, nozzles, etc.)
- (3) Experiment and propulsion system plumbing lines and fittings (including orifices and Joule-Thomson devices)

16.2.2 SINGLE-POINT FAILURE GOAL

One of the design goals during the feasibility study was to develop a design that eliminated the possibility of a single-point failure during the mission. A single-point failure is defined in MIL-STD-721C (ref. 1), as:

"The failure of an item which would result in failure of the system and is not compensated for by redundancy or alternative operating procedure."

The single-point failure goal for COLD-SAT was to identify and eliminate all potential critical single-point failures.

16.2.3 RELIABILITY ALLOCATION

The third reliability requirement was that the spacecraft reliability goal be allocated to each spacecraft system in a realistic manner. The "Feasibility of Objectives Technique" from MIL-HDBK-338-1A (ref. 2) was selected for performing this allocation because it fulfilled these requirements.

16.3 Reliability Activities

During the conduct of the feasibility study, a number of different reliability activities were performed. These activities are briefly discussed in this section.

16.3.1 SPACECRAFT DESIGN

The reliability activities on a spacecraft design level were to allocate the spacecraft reliability goal to the individual spacecraft systems and to review and resolve issues regarding inter-system reliability interactions.

16.3.2 SYSTEM DESIGN

The reliability activities on a system design level were to review the design, develop reliability predictions for comparison to the allocated reliability goal, and assist the system designers with redundancy implementation and component selection to improve system reliability.

16.3.3 FAILURE RATE DEVELOPMENT

One of the reliability activities was the compilation and review of component failure rates from the system engineers, manufacturer's data, spacecraft reports, and reports from the COLD-SAT conceptual design contractors. These failure rates were reviewed with the system engineers to determine their suitability for the COLD-SAT application and selected for incorporation in the COLD-SAT reliability models.

16.3.4 SINGLE-POINT FAILURE ANALYSES

Single-point failure analyses were conducted on both the system and spacecraft levels. The methodology used during the

feasibility study to work on potential single-point failures within the design was as follows:

- (1) Review the design and identify all potential single-point failures.
- (2) Determine the criticality of each potential single-point failure in relation to mission success.
- (3) Considering reliability, cost, power, performance, and weight, work with the system engineers to eliminate all potential single-point failures where possible.
- (4) Work with the system engineers to reduce the effect of remaining potential single-point failures through design enhancement and component selection.

16.4 Reliability Analysis Methodologies

A number of techniques were used to perform the required reliability analyses. The various methodologies used are described in this section.

16.4.1 SYSTEM RELIABILITY ALLOCATION

The "Feasibility of Objectives Technique" from MIL-HDBK-338-1A (ref. 2) was selected to allocate the COLD-SAT reliability goal to the spacecraft systems because it was specifically developed for allocating the reliability without repair for mechanical-electrical systems. This method, which is described in detail on pages 6-18 to 6-20 of MIL-HDBK-338-1A, develops allocation factors from ratings in four categories provided by each system engineer. The ratings for system intricacy, state-of-the-art, performance time, and environment are estimated by engineers on a scale of 1 to 10 based on their experience. The steps outlined in MIL-HDBK-338-1A were then followed to determine the relative complexity of each system and allocate the spacecraft reliability goal accordingly. These ratings, complexity factors, and reliability allocations are shown in table 16.2.

16.4.2 SYSTEM RELIABILITY ANALYSIS

All calculated reliability predictions are based on an exponential distribution, which assumes that any failures occur on a random basis. The equation used for this distribution is

$$R = e^{-\lambda dt}$$

where

- R reliability
- λ failure rate, failures per hour or failures per cycle
- d duty cycle or percentage of time used (ratio of operating time to total time)
- t life units (either time in hours or cycles)

This equation is derived from two equations in MIL-HDBK-338-1A (ref. 2), namely,

$$R = e^{-\lambda t}$$

where

- R reliability
- λ failure rate in failures per hour or failures per cycle
- t life units (either time in hours or cycles)

and

$$\lambda_T = \lambda_{op}d + (1 - d)\lambda_{nop}$$

where

- λ_T total failure rate
- λ_{op} operating failure rate
- λ_{nop} nonoperating failure rate

Since λ_{nop} was ground-ruled as zero, this simplifies to

$$\lambda_T = \lambda_{op}d$$

TABLE 16.2.—COLD-SAT RELIABILITY ALLOCATION METHODOLOGY^a
[Spacecraft requirements: reliability, 0.92; mission time, 4 383 hr; failure rate, 1.9×10^{-5} failures/hr.]

System	Intricacy	State-of-the-art	Performance time	Environment	Overall rating	Complexity	Allocated failure rate	Allocated reliability
Attitude control	8.00	2.0	10.0	2.0	320	0.04020	7.65×10^{-7}	0.997
Experiment	6.60	7.3	10.0	8.6	4143	.52053	9.90×10^{-6}	.958
Power	4.00	3.0	10.0	6.0	720	.09045	1.72×10^{-6}	.992
Propulsion	3.90	2.5	6.1	3.4	202	.02540	4.83×10^{-7}	.998
Software	9.00	8.0	10.0	2.0	1440	.18090	3.44×10^{-6}	.985
Structure	2.80	2.4	10.0	2.0	134	.16884	3.21×10^{-7}	.999
TT&C	10.00	5.0	10.0	2.0	1000	.12563	2.39×10^{-6}	.990
Spacecraft totals					7960	1.00000	1.90×10^{-5}	0.921

^aMIL-HDBK-338-1A (ref. 2).

By substituting λd for λ in the first equation, the equation $R = e^{-\lambda dt}$ was derived.

Unless otherwise noted, a duty cycle of 100 percent was used in computing component reliability. The minimum duty cycle used for any specific application is 1 percent.

Also used is the relationship between the failure rate and the mean time between failure (MTBF). The failure rate is the inverse of the MTBF as follows:

$$\lambda = \frac{1}{\theta}$$

where

λ failure rate, failures per hr
 θ MTBF, hours

Failure rate and MTBF information is displayed using scientific notation with two decimal places (e.g., 1.00×10^6). Reliability predictions are displayed to four decimal places (e.g., 0.9999). Components with reliability predictions of 1.0000 are the result of calculations rounded to the fourth decimal place.

16.4.3 SPACECRAFT RELIABILITY ANALYSIS

Since each spacecraft system is essential for mission success, the reliability of the spacecraft was assessed as consisting of each system in series as shown in figure 16.1. The predicted spacecraft reliability is the product of the system reliability predictions as shown in the following equation:

$$R_{\text{spacecraft}} = R_{\text{structure}} \times R_{\text{TT\&C}} \times R_{\text{ACS}} \times R_{\text{power}} \times R_{\text{software}} \times R_{\text{experiment}} \times R_{\text{propulsion}}$$

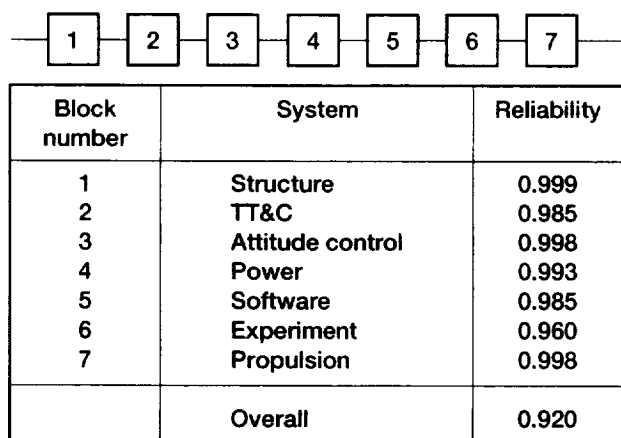


Figure 16.1.—Spacecraft reliability block diagram.

16.4.4 FAILURE RATE ESTIMATION METHODOLOGY

Because many of the COLD-SAT components are being or will be developed specifically for the COLD-SAT program, specific component failure rates for the COLD-SAT application were not available. The hierarchy used for sources of failure rate data incorporated into the COLD-SAT reliability predictions is as follows:

- (1) Flight history of specific components
- (2) Manufacturer-provided failure rates for specific components
- (3) Flight history of like components
- (4) Manufacturer-provided failure rates of like components
- (5) Engineering estimates based on information from component failure rate data bases (such as MIL-HDBK-217 (ref. 3) and NPRD-3 (ref. 4)).

16.5 Reliability Program Implementation

This section discusses in detail the results obtained during the reliability analysis of the various COLD-SAT systems.

16.5.1 INDIVIDUAL SYSTEM RELIABILITY ANALYSIS

Basically two steps were involved in analyzing the reliability of the various COLD-SAT systems. First, failure rate data for the various components were identified, and then reliability block diagrams were developed.

16.5.1.1 Development of Failure Rate Data

The failure rate data for individual components used in the reliability analysis were based on information from a number of sources. The component failure rates, sources, and resultant 6-month reliability predictions are as stated in the following sections.

16.5.1.1.1 Attitude control system

Horizon sensor: A combined MTBF of 9.00×10^5 hr for each Barnes Horizon Scanner Head and Horizon Scanner Electronics was provided by Barnes. This converts to a reliability of 0.9951 for a 4383-hr mission.

Sun sensor: A combined MTBF of 4.50×10^5 hr for each Adcole Sun Sensor Head and Sun Sensor Electronics was provided by Adcole. This converts to a reliability of 0.9903 for a 4383-hr mission.

Inertial reference unit (IRU): A MTBF of 1.9×10^5 hr for each channel (gyro) of the Teledyne DRIRU II was provided by Teledyne. This converts to a reliability of 0.9772 for a 4383-hr mission for each gyro.

Magnetometer: A MTBF of 3.00×10^6 hr for each Schonstedt Magnetometer was provided by Schonstedt. This converts to a reliability of 0.9985 for a 4383-hr mission.

Attitude control system electronics: For the purpose of this study, the reliability of the attitude control system electronics was assumed to equal the reliability of the remote command and telemetry units (RCTU's) in the TT&C system. The reliability of the Gulton RCTU for a 6-month mission, as provided by Gulton, is 0.9999.

16.5.1.1.2 Experiment system

Valve (liquid hydrogen, latching): A failure rate of 4.00×10^{-6} failures/cycle was used to predict the reliability of the valves within the experiment system. This failure rate was estimated by taking the failure rate of 6.70×10^{-7} failures/cycle provided by Moog and adjusting it by a factor of six to account for leakage, environment, and uncertainty regarding the Moog failure rate. There are three different life estimates for this valve, dependent on the specific application within the experiment system plumbing. The reliability predictions are given in table 16.3.

TABLE 16.3.—PREDICTED RELIABILITY OF LIQUID HYDROGEN VALVES

Life, cycles	Predicted reliability
100	0.9996
500	.9980
1000	.9960

Gas valve (gaseous hydrogen and gaseous helium, latching): A failure rate of 2.00×10^{-6} failures/cycle was used to predict the reliability of the gas valves within the experiment system. This failure rate was based on the failure rate of the propulsion system latching valves and assumes a cyclic use rate of 1 cycle/hr to convert the failure rate units. There are three different life estimates for these valve, dependent on the specific application within the experiment system plumbing. The reliability predictions are listed in table 16.4.

TABLE 16.4.—PREDICTED RELIABILITY OF GAS VALVES

Life, cycles	Predicted reliability
100	0.9998
500	.9990
1000	.9980

Valve relays: A failure rate of 3.00×10^{-6} failures/cycle was developed based on information provided by a number of vendors for the type of relays to be used to actuate the experiment system latching valves. There are three different life estimates for these relays, dependent on the specific application of the valve within the experiment system plumbing. Table 16.5 lists these reliability predictions.

TABLE 16.5.—PREDICTED RELIABILITY OF VALVE DRIVE RELAYS

Life, cycles	Predicted reliability
100	0.9997
500	.9985
1000	.9970

Relief valve: A failure rate of 7.00×10^{-6} failures/hour was used to predict the reliability of the experiment system relief valves. This failure rate was estimated based on relief valve failure rates contained within COLD-SAT contractor reports for propulsion system relief valves adjusted for the hydrogen environment and is within the range of failure rates for relief valves contained within NPRD-3 (ref. 4). The design-specified duty cycles for the relief valves were 1 and 5 percent, resulting in reliability predictions of 0.9997 and 0.9985, respectively.

Pressure regulator: A failure rate of 4.00×10^{-6} failures/hr was used to predict the reliability of the pressure regulators. This failure rate was estimated based on worst-case failure rates contained within COLD-SAT contractor reports for propulsion system pressure regulators and is within the range of pressure regulator failure rates contained within NPRD-3 (ref. 4). The design-specified duty cycle of 10 percent resulted in a reliability prediction of 0.9982 for each pressure regulator.

Check valves: A failure rate of 5.00×10^{-6} failures/hr was used to predict the reliability of the experiment system check valves. This failure rate was estimated based on failure rates contained within COLD-SAT contractor reports for propulsion system check valves adjusted for the hydrogen environment and is within the range of check valve failure rates contained within NPRD-3 (ref. 4). The design-specified duty cycle of 5 percent resulted in a reliability prediction of 0.9989 for each check valve.

Pump (liquid hydrogen): A failure rate of 4.85×10^{-7} failures/hr from the Martin Marietta CONE Review (ref. 5) was used to predict the reliability of each liquid hydrogen pump. A duty cycle of 1 percent is estimated for this pump, resulting in a reliability prediction of 0.9999 for each liquid hydrogen pump.

Turbine flowmeter: A failure rate of 4.85×10^{-7} failures/hr from the Martin Marietta CONE Review (ref. 5) was used to predict

the reliability of each flowmeter. This results in a reliability prediction of 0.9979 for each flowmeter.

16.5.1.1.3 Power system

Batteries: A reliability prediction of 0.9985 was developed by taking the average of the reliability predictions for the COLD-SAT power system batteries from General Dynamics and Ball Aerospace.

Solar arrays: A reliability prediction of 0.9999 for the solar arrays was developed from information supplied by SOLAREX Aerospace Division.

Power control unit: A reliability prediction of 0.9970 was developed for the power control unit based on COLD-SAT feasibility study contractor reports and historical data from other programs.

Power distribution unit: A reliability prediction of 0.9990 was developed for the power distribution unit based on COLD-SAT feasibility study contractor reports, historical data from other programs, and MIL-HDBK-217E (ref. 3).

Pyro control unit: A reliability prediction of 0.9989 was developed for the pyro control unit based on the lack of complexity of the unit and information contained within the COLD-SAT feasibility study contractor reports.

Pyro devices: A reliability prediction of 0.9997 was developed for the pyro devices based on the limited quantity and high reliability of these devices.

16.5.1.1.4 Propulsion system

Pressurant tank: A failure rate of 3.00×10^{-8} failures/hr was used to predict the reliability of the pressurant tank. This converts to a reliability of 0.9999 for a 4383-hr mission.

Gas filter: A failure rate of 1.00×10^{-8} failures/hr from General Dynamics was used to predict the reliability of the gas filter. This converts to a reliability of 1.0000 for a 4383-hr mission.

Gas fill/drain valve: A failure rate of 3.42×10^{-7} failures/hr from the Martin Marietta COLD-SAT Review (ref. 6) was used to predict the reliability of the gas fill/drain valve. This converts to a reliability of 0.9985 for a 4383-hr mission.

Pressure transducers: A failure rate of 1.96×10^{-7} failures/hr from General Dynamics was used to predict the reliability of each pressure transducer. The pressure transducers were modeled only for function and not leakage. This converts to a reliability of 0.9991 for a 4383-hr mission.

Solenoid valve: A failure rate of 2.00×10^{-6} failure/hr was used to predict the reliability of each helium solenoid valve. This failure rate is an estimate based on information from NPRD-3 (ref. 4). A duty cycle of 1 percent was assigned to the solenoid valves based on the limited number of cycles during the mission. This converts to a reliability of 0.9999 for a 4383-hr mission at a 1-percent duty cycle.

Check valve: A failure rate of 1.00×10^{-8} failure/hr was used to predict the reliability for each check valve. This converts to a reliability of 1.0000 for a 4383-hr mission.

Relief valve/burst disk: A failure rate of 2.4×10^{-7} failure/hr from Ball Aerospace was used to predict the reliability of the relief valve/burst disk. This converts to a reliability of 0.9989 for a 4383-hr mission.

Propellant tank: A failure rate of 3.0×10^{-8} failure/hr was used to predict the reliability for each propellant tank. This converts to a reliability of 0.9999 for a 4383-hr mission.

Heaters: The reliability for each heater within the propulsion system is based upon a failure rate of 1×10^{-8} failure/hr from General Dynamics. The duty cycles for the propellant tank heaters, patch heater, line heaters, and valve heaters are all estimated at 50 percent, while the duty cycle for the catalyst bed heaters is estimated at 10 percent. Each case results in a predicted reliability of 1.0000.

Hydrazine fill/drain valve: A failure rate of 3.42×10^{-7} failure/hr from the Martin Marietta COLD-SAT Review (ref. 6) was used to predict the reliability of the hydrazine fill/drain valve. This converts to a reliability of 0.9985 for a 4383-hr mission.

Hydrazine filter: A failure rate of 1.0×10^{-8} failure/hr from General Dynamics was used to predict the reliability of the hydrazine filter. This converts to a reliability of 1.0000 for a 4383-hr mission.

Hydrazine latching valve: A failure rate of 2.00×10^{-6} failure/hr was used to predict the reliability of each hydrazine latching valve. This failure rate is an estimate based on information from NPRD-3 (ref. 4). A duty cycle of 1 percent was assigned to the latching valves based on the limited number of cycles during the mission. This converts to a reliability of 0.9999 for a 4383-hr mission at a 1-percent duty cycle.

Thruster: A failure rate of 1.84×10^{-6} failure/hr from Ball Aerospace was used to predict the reliability of the thrusters. A duty cycle of 10 percent was assigned to the thrusters based on the preliminary estimate of thruster firings during the mission. This converts to a reliability of 0.9992 for each thruster.

Thruster gimbal: For the purpose of the feasibility study, a 2-axis antenna gimbal was used to model the thruster gimbal. A reliability estimate of 0.9998 for a 6-month (4383-hr) mission, provided by the TT&C system primary engineer for a 2-axis antenna gimbal, was used to predict the reliability of the thruster gimbal.

Thruster gimbal electronics: A reliability estimate of 0.9997 for a 6-month, 4383-hr mission, provided by the TT&C system primary engineer for the antenna gimbal electronics, was used to predict the reliability of the thruster gimbal electronics.

Valve and thruster relays: A failure rate of 3.00×10^{-6} failure/hr was used to predict the reliability of each relay used to control the solenoid valves, hydrazine latching valves, and the thrusters. This failure rate is an estimate based on information from NPRD-3 (ref. 4). A duty cycle of 1 percent was assigned to the valve relays based on the limited number of cycles during the mission. This converts to a reliability of 0.9999 for a 4383-hr mission at a 1 percent duty cycle. A duty cycle of 10 percent was assigned to the thruster relays based on the preliminary estimate of thruster firings during the mission. This converts to a reliability of 0.9987 for a 4383-hr mission at a 10-percent duty cycle.

16.5.1.1.5 Telemetry, tracking and command system

Flight computer: A reliability estimate of 0.9547 for a 6-month, 4383-hr mission for each Honeywell flight computer was provided by Honeywell.

Transponder: A reliability estimate of 0.9533 for a 6-month, 4383-hr mission for each Motorola transponder was provided by Motorola.

Remote command and telemetry units (RCTU's): A reliability estimate of 0.9999 for a 6-month, 4383-hr mission for the Gulton remote command and telemetry units was provided by Gulton.

Command and telemetry unit (CTU): A reliability estimate of 0.9997 for a 6-month, 4383-hr mission for each Gulton command and telemetry unit was provided by Gulton. This results in an overall reliability of 1.0000 for the CTU's.

Solid state recorder (SSR): A reliability estimate of 0.9950 for a 6-month, 4383-hr mission for each Fairchild solid state recorder was provided by Fairchild.

High-gain antenna: A reliability estimate of 0.9950 for a 6-month, 4383-hr mission for the TECOM high-gain antenna was provided by TECOM.

Low-noise amplifier: A reliability estimate of 0.9874 for a 6-month, 4383-hr mission was developed by using MIL-HDBK-217 (ref. 3).

2-Axis antenna gimbal: A reliability estimate of 0.9998 for a 6-month, 4383-hr mission for the Schaeffer Magnetics 2-axis antenna gimbal was provided by Schaeffer Magnetics.

Gimbal electronics: A reliability estimate of 0.9997 for a 6-month, 4383-hr mission for the Schaeffer Magnetics gimbal electronics was provided by Schaeffer Magnetics.

Low-gain antenna: A reliability estimate of 0.9999 for a 6-month, 4383-hr mission for each TECOM low-gain antenna was provided by TECOM.

Sequencers: The two sequencers within the TT&C system each contain two parallel strings of three components each. In addition, sequencer 1 contains two inverting power supplies in parallel. A list of these components with their reliability for a 6-month mission, developed by using MIL-HDBK-217E (ref. 3), is contained in table 16.6.

TABLE 16.6.—SEQUENCER CONNECT RELIABILITIES

Component	Reliability for 6 months
Bus interface	0.9995
Command decoder	.9925
Relay drive electronics	.9925
Inverting power supply	.9874

A reliability block diagram for the sequencers is shown in figure 16.2. The resulting overall reliability prediction for the sequencers is 0.9994.

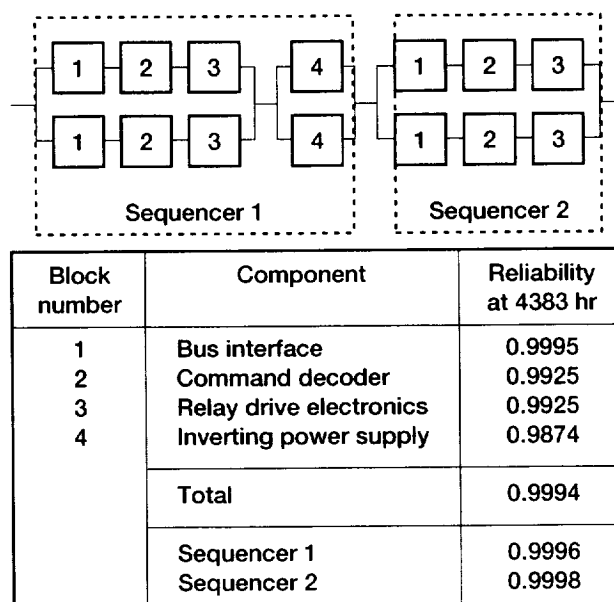


Figure 16.2.—Telemetry, tracking, and command system sequencer reliability block diagram.

Redundancy control unit: A reliability estimate of 0.9950 for a 6-month, 4383-hr mission was developed by using MIL-HDBK-217E (ref. 3) for the redundancy control unit.

Radiofrequency (RF) processing switch: A MTBF of 10 000 cycles for the RF processing switch was developed by taking the average of failure information from a number of vendors. Combination with an estimate of 100 total cycles for the 6-month mission results in a reliability prediction of 0.9900 for the RF processing switch.

16.5.1.2 System Block Diagram Development

In order to develop the reliability model, several assumptions regarding the mission operation of the spacecraft were made. Since one of the primary reasons for developing a reliability prediction for the spacecraft was for comparison to the reliability goal, the reliability model was developed based on the completion of all class I experiments within a 6-month mission time.

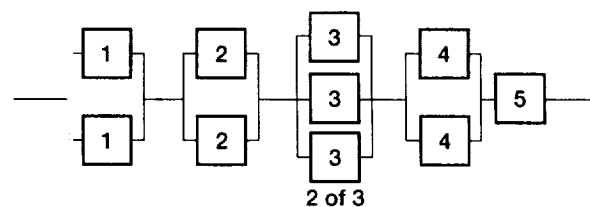
The first assumption is that class I experiments could take place at any time within the 6-month mission. The effect that this assumption has is that each of the supporting spacecraft systems are required to have a functional mission life of 6 months. Therefore, the attitude control, power, propulsion, and TT&C systems are each modeled for their reliability over a 4383-hr period of time, independent of which, if any, experiments are conducted during this period of time.

Since a clear definition of class I experiments and the functional requirements of the experiment system for these experiments were not available when the reliability prediction was made, a number of assumptions were made in order to develop the reliability model of the experiment system. This involved breaking the experiment system into seven subsystems: supply tank, large receiver tank, small receiver tank, vent, pressurization, instrumentation, and thermal. The assumptions for each spacecraft system are detailed separately in the following sections.

16.5.1.2.1 Attitude control system

The reliability block diagram for the attitude control system is shown in figure 16.3. The horizon sensors, Sun sensors, and magnetometers are each modeled in parallel for their individual functions, with each function modeled in series. The IRU gyros are modeled such that 2 of 3 are required. The attitude control system electronics, although internally redundant, is modeled as a single-string item.

The reliability prediction for the attitude control system is 0.9982, based on the reliability block diagram and component reliabilities.



Block number	Component	Failure rate (per hr)	Duty cycle, percent	Reliability at 4383 hr (each)
1	Horizon sensor	1.11×10^{-6}	100	0.9951
2	Sun sensor	2.22×10^{-6}	100	0.9903
3	Inertial reference unit gyro	5.26×10^{-6}	100	0.9772
4	Magnetometer	3.33×10^{-7}	100	0.9985
5	Attitude control system electronics			0.9999
	Total			0.9982

Figure 16.3.—Attitude control system reliability block diagram.

16.5.1.2.2 Experiment system

The experiment system was broken down into seven subsystems in order to simplify the modeling process. In the subsystem descriptions, the term "valve" refers to the liquid hydrogen latching valve and "gas valve" refers to the gaseous helium/gaseous hydrogen latching valve. The relays used to actuate these valves are not listed in the narrative descriptions but are contained in the reliability block diagrams and reliability predictions.

Supply tank subsystem: The following components were assigned to the supply tank subsystem for the purpose of modeling the subsystem: valves 1 to 5, 7 to 15, and 17; pumps 1 and 2; and flowmeter 1. The assumptions made regarding the supply tank subsystem include the following:

- (1) Valve 5 is required for all class I experiments that require pressurization of the supply tank.
- (2) The ground fill/drain liquid hydrogen disconnect is modeled as open after launch. This modeling requires both valves 3 and 4 to remain closed during the mission.
- (3) The pump circuit is modeled with three redundant legs. Leg 1 consists of valve 1 and pump 1, leg 2 consists of valve 2 and pump 2, and leg 3 consists of valve 17. It is assumed that only one of these three legs is required for the completion of class I experiments.
- (4) The circuit containing the Joule-Thomson (J-T) devices is modeled such that only one of the three control valves

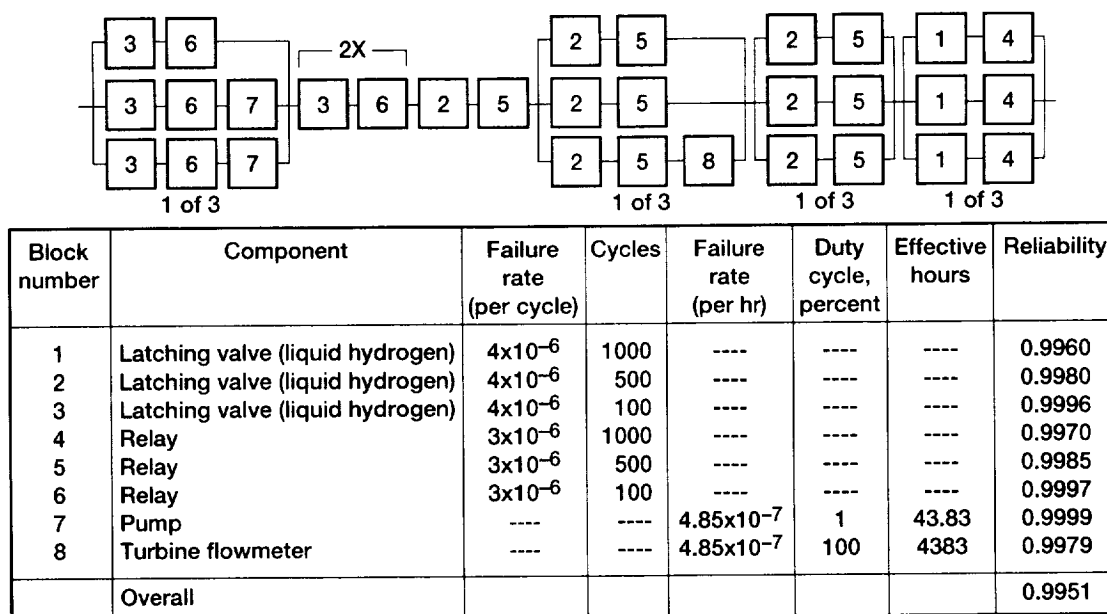


Figure 16.4.—Experiment system—supply tank subsystem reliability block diagram.

(valve 11, 12, or 13) is required for completion of class I experiments.

(5) The circuits containing valves 7 to 9 and valves 14 to 16 are modeled such that only one valve in each circuit is required for class I experiments.

The reliability block diagram for the supply tank subsystem is shown in figure 16.4. Valves 3 to 5 were modeled as single-string and are shown in series. The pump group is modeled such that 1 of the 3 legs are required. Leg 1 consists of valve 17, leg 2 consists of valve 1 and pump 1, and leg 3 consists of valve 2 and pump 2. The flowmeter group is modeled such that 1 of the 3 legs are required. Leg 1 consists of valve 7, leg 2 consists of valve 8, and leg 3 consists of valve 9 and turbine flowmeter 1. Valves 11 to 13 are modeled such that 1 of 3 is required. Valves 14 to 16 are modeled such that 1 of 3 is required.

The reliability prediction of the supply tank subsystem is 0.9951, based on the reliability block diagram and component reliabilities.

Large receiver tank subsystem: Valves 24 to 28 and 32 were assigned to the large receiver tank for the purpose of modeling the subsystem. The following assumptions were made regarding the large receiver tank subsystem:

(1) Each of the valves associated with the large receiver tank system is required for the completion of at least one class I experiment.

(2) Valve 24 is required for all fills of the large receiver tank.

(3) Valves 25, 27, and 28 are required for different types of class I fill experiments.

(4) Valves 26 and 32 are required for transfer of liquid hydrogen from the large receiver tank as part of class I experiments.

Based on these assumptions, all six valves assigned to the large receiver tank subsystem are required for the completion of class I experiments.

The reliability block diagram for the large receiver tank subsystem is shown in figure 16.5. Valves 24 to 28 and 32 were modeled as single-string items and are shown in series.

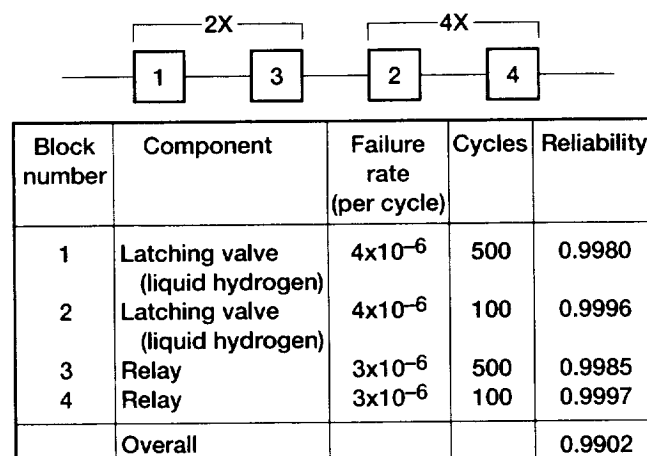


Figure 16.5.—Experiment system—large receiver tank subsystem reliability block diagram.

The reliability prediction of the large receiver tank system is 0.9902, based on the reliability block diagram and component reliabilities.

Small receiver tank system: Valves 29, 34 to 37, 41, and 46 were assigned to the small receiver tank for the purpose of modeling the system. The following assumptions were made regarding the small receiver tank subsystem:

- (1) Valve 29 is required for all fills of the small receiver tank.
- (2) Valves 34 and 35 are required for different types of class I fill experiments.
- (3) Either valve 36 or 37 is required for tangential spray, which is assumed to be part of at least one class I experiment.
- (4) Valves 41 and 46 are required for transfer of liquid hydrogen from the small receiver tank as part of class I experiments.

Based on these assumptions, six of the seven valves assigned to the small receiver tank system are required for the completion of class I experiments.

The reliability block diagram for the small receiver tank subsystem is shown in figure 16.6. Valves 29, 34, 35, 41, and 46 were modeled as single-string items and are shown in series. Valves 36 and 37 were modeled as parallel to each other.

The reliability prediction of the small receiver tank subsystem is 0.9909, based on the reliability block diagram and component reliabilities.

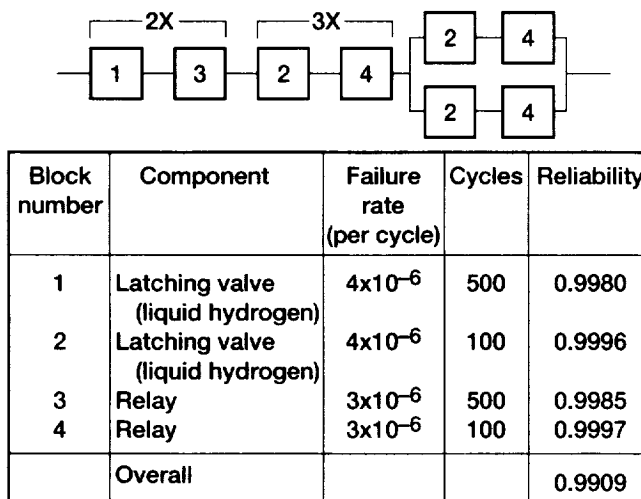
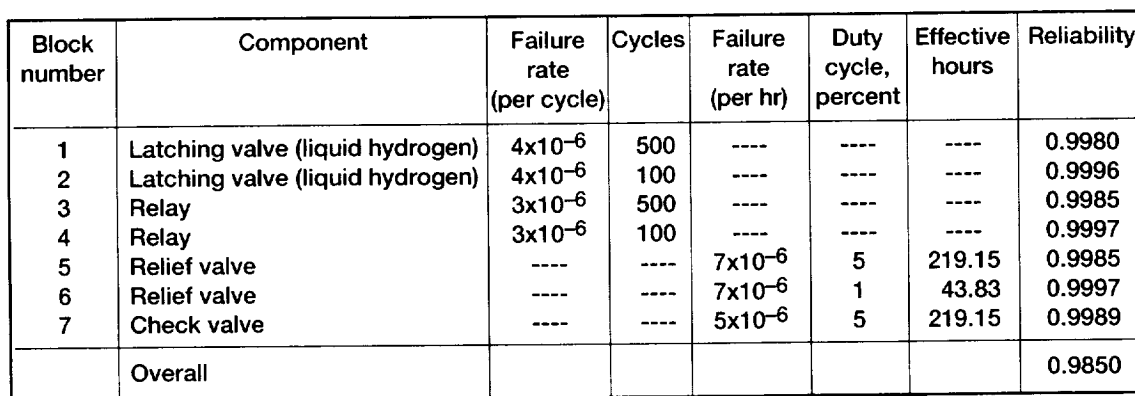


Figure 16.6.—Experiment system—small receiver tank subsystem reliability block diagram.

Vent sub system: The following components were assigned to the vent system for the purpose of modeling the system: valves 10, 18, 19, 31, 33, 39, 40, 42 to 45, 48 to 50; relief valves 2 to 6, 8, 9, and 11 to 19; and check valves 3 to 5. The assumptions made regarding the vent subsystem include:

- (1) A functional thermodynamic vent system (TVS) is required for each experiment system tank for the completion of all class I experiments.
- (2) The ground/ascent vent disconnect was assumed to be closed after spacecraft separation from the launch vehicle.
- (3) Protection of the tanks and plumbing lines from potential damage due to the expansion of trapped fluid or other "over-pressure" conditions is required throughout the mission to ensure mission success.
- (4) Valve 10 is required for the supply tank TVS function.
- (5) Check valve 3 and either valve 31 or relief valve 13 is required for the large receiver tank TVS function.
- (6) Valve 39 is required for the small receiver tank TVS function.
- (7) Either valve 42 and check valve 4 or valve 43 and check valve 5 are required for operation of the TVS.
- (8) Relief valves 2, 5, 6, 8, 9, 11, 12, 17, and 19 are required to protect the plumbing lines from potential damage caused by fluid expansion.
- (9) One of the following is required to protect the supply tank from potential damage caused by fluid expansion: relief valve 3, relief valve 4, valve 18, or valve 19.
- (10) Either valve 33 or relief valve 14 is required to protect the large receiver tank from potential damage caused by fluid expansion.
- (11) Either valve 38 or relief valve 45 is required to protect the plumbing lines from potential damage caused by fluid expansion.
- (12) Either valve 40 or relief valve 16 is required to protect the small receiver tank from potential damage caused by fluid expansion.
- (13) Either valve 44, 45, or relief valve 18 is required for operation of the flight balanced vent.
- (14) Either valve 48 or 49 is required to isolate the tank vent.
- (15) Valve 50 is required to isolate the small receiver tank from space prior to the dump experiment.

The reliability block diagram for the vent subsystem is shown in figure 16.7. Valves 10, 39, and 50, check valve 3, and relief valves 2, 5, 6, 8, 9, 11, 12, 17, and 19 were modeled as single-string and are shown in series. The following components were modeled in parallel: valves 48 and 49; valve 33 and relief valve 15; valve 40 and relief valve 16. Valve 42 and check valve 4 were modeled as parallel to valve 43 and check valve 5. Relief valve 3, relief valve 4, valve 18, and valve 19 were modeled such that one of the four is required. Relief valve 18, valve 44, and valve 45 were modeled such that one of the three is required.



The reliability prediction of the vent system is 0.9849, based on the reliability block diagram and component reliabilities.

pressurant subsystem is 0.9999, based on the reliability block diagram and component reliabilities.

Thermal subsystem: The reliability prediction of the thermal subsystem is based on an estimate of 0.9993 for the 6-month mission, based primarily on the reliability of the experiment system heaters.

Instrumentation subsystem: The reliability prediction of the instrumentation subsystem is based on an estimate of 0.9990 for the 6-month mission. This estimate considers the majority of the sensors to be at least partially redundant.

System reliability: The reliability block diagram for the experiment system is shown in figure 16.9. Since each subsystem is required, each subsystem is shown in series.

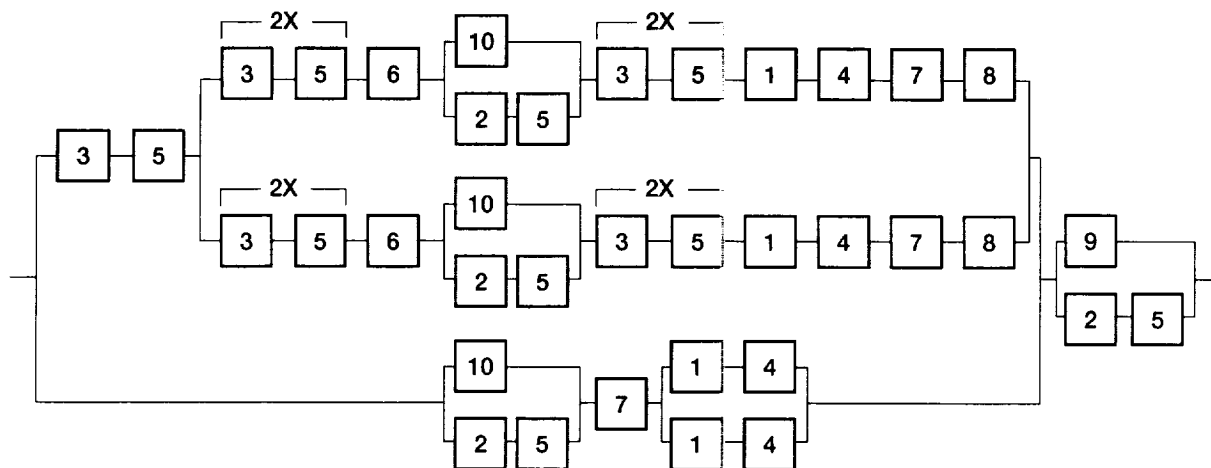
The reliability prediction for the experiment system is 0.9600, based on the reliability block diagram and the system reliabilities.

- (1) All class I experiments can be completed with either hydrogen or helium pressurant.
- (2) Either gas valve 12 or flowmeter 2 are required for supplying pressurant to the experiments.
- (3) All gas fill lines are capped prior to launch and the line caps have a reliability of 0.9999.
- (4) Valve 47 is required to supply liquid hydrogen to either vaporizer.
- (5) Vaporizer A requires valves 20 and 23, gas valves 6 to 8, pressure regulator 2, check valve 2, and either gas valve 5 or a line cap.
- (6) Vaporizer B requires valves 21 and 22, gas valves 2 to 4, pressure regulator 2, check valve 2, and either gas valve 5 or a line cap.
- (7) Pressure regulator 3 is required along with either gas valve 11 or a line cap. In addition, either gas valve 9 or gas valve 10 is required.

The reliability block diagram for the pressurant subsystem is shown in figure 16.8. The reliability prediction of the

The reliability block diagram for the power system is shown in figure 16.10. Each of the power system component types is required and are modeled in series.

The reliability prediction for the power system is 0.9930, based on the reliability block diagram and component reliabilities.



Block number	Component	Failure rate (per cycle)	Cycles	Failure rate (per hr)	Duty cycle, percent	Effective hours	Reliability
1	Latching valve (gas)	2×10^{-6}	1000	----	----	----	0.9980
2	Latching valve (gas)	2×10^{-6}	100	----	----	----	0.9998
3	Latching valve (liquid hydrogen)	4×10^{-6}	100	----	----	----	0.9996
4	Relay	3×10^{-6}	1000	----	----	----	0.9970
5	Relay	3×10^{-6}	100	----	----	----	0.9997
6	Relief valve	----	----	7×10^{-6}	1	43.83	0.9997
7	Pressure regulator	----	----	4×10^{-6}	10	483.30	0.9982
8	Check valve	----	----	5×10^{-6}	5	219.15	0.9989
9	Turbine flowmeter	----	----	4.85×10^{-7}	100	4383	0.9979
10	Cap	----	----	----	----	----	0.9999
	Overall						0.9999

Figure 16.8.—Experiment system—pressurant subsystem reliability block diagram.

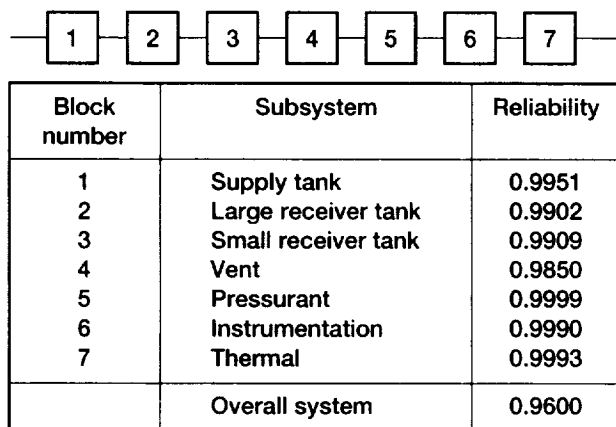


Figure 16.9.—Experiment system reliability block diagram.

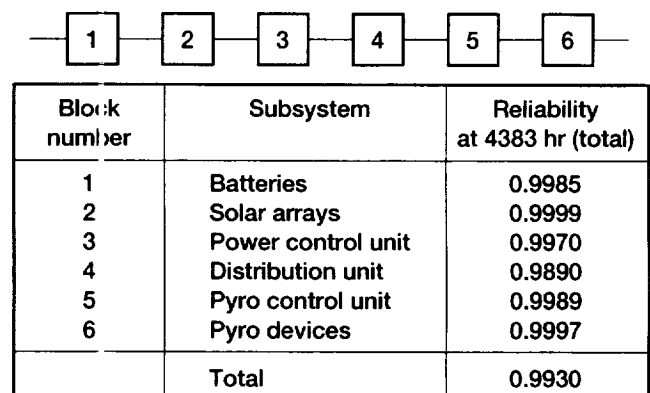
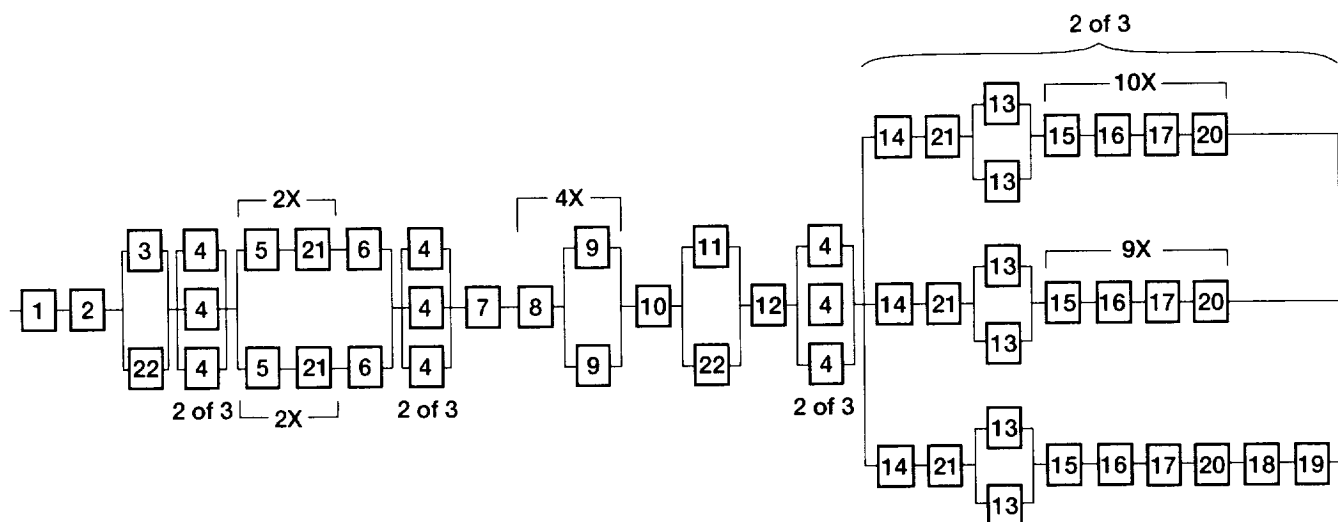


Figure 16.10.—Power system reliability block diagram.

16.5.1.2.4 Propulsion system

The reliability block diagram for the propulsion system is shown in figure 16.11. The pressurant tank, gaseous helium filter, relief valve/burst disc, propellant distribution (patch) heater, and hydrazine filter are each modeled as single-string items and are shown in series. The gas fill/drain valve and the hydrazine fill/drain valve are each modeled in parallel with a

line cap, which has an estimated reliability of 0.9999. The pressure transducers are modeled as 2 of 3 redundant and are shown in their relative position in respect to the propulsion system plumbing schematic. The pressurant valve cluster is modeled as two strings in parallel, with each string consisting of two solenoid valves, two valve relays, and one check valve. The propellant (hydrazine) tanks are modeled with each tank group consisting of one propellant tank and redundant tank



Block number	Component	Failure rate (per hr)	Duty cycle, percent	Reliability at 4883 hrs (each)
1	Pressurant tank	3.00×10^{-8}	100	0.9999
2	Gas filter	1.00×10^{-8}	100	1.0000
3	Gas fill/drain valve	3.42×10^{-7}	100	0.9985
4	Pressure transducers	1.96×10^{-7}	100	0.9991
5	Solenoid valve (gaseous helium)	2.00×10^{-6}	1	0.9999
6	Check valve	1.00×10^{-8}	100	1.0000
7	Relief/burst disk	2.40×10^{-7}	100	0.9989
8	Propellant tank	3.00×10^{-8}	100	0.9999
9	Tank heater	1.00×10^{-8}	50	1.0000
10	Patch heater	1.00×10^{-8}	50	1.0000
11	Hydrazine fill/drain	3.42×10^{-7}	100	0.9985
12	Hydrazine filter	1.00×10^{-8}	100	0.9999
13	Line heater	1.00×10^{-8}	50	1.0000
14	Latching valve (hydrazine)	2.00×10^{-6}	1	0.9999
15	Valve heater	1.00×10^{-8}	50	1.0000
16	Catalyst heater	1.00×10^{-8}	5	1.0000
17	Thruster	1.84×10^{-6}	10	0.9992
18	Gimbal	----	----	0.9998
19	Gimbal electronics	----	----	0.9997
20	Relay (thrusters)	3.00×10^{-6}	10	0.9987
21	Relay (valves)	3.00×10^{-6}	1	0.9999
22	Line cap	----	----	0.9999
	Total			0.9976

Figure 16.11.—Propulsion system reliability block diagram.

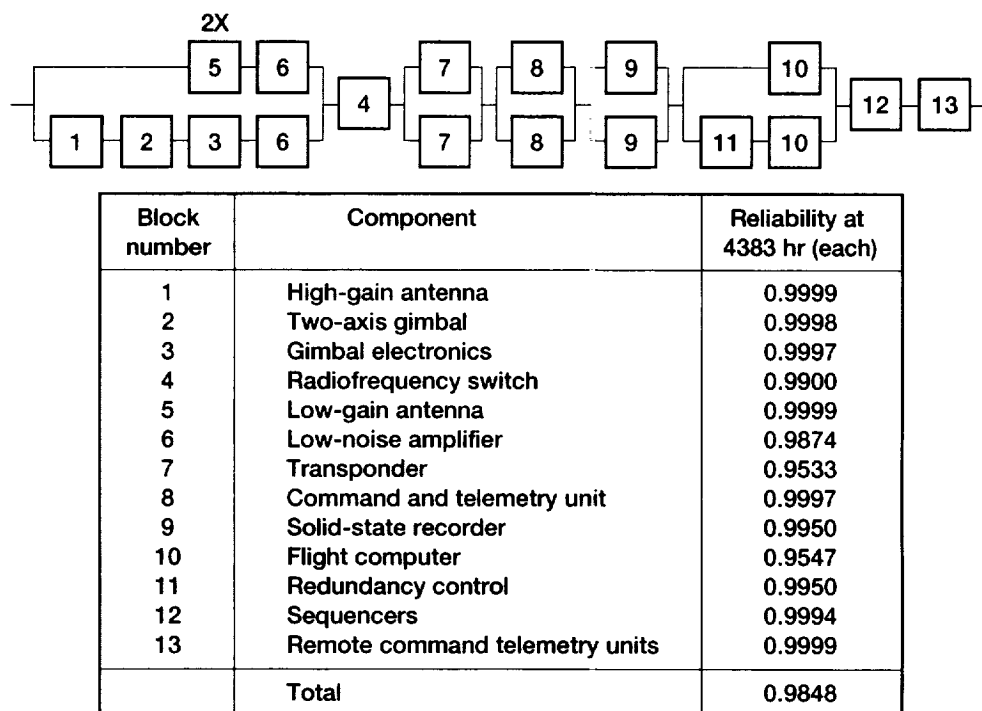


Figure 16.12.—Telemetry, tracking, and command system reliability block diagram.

heaters. The four tank groups are modeled in series. The thruster banks are modeled such that 2 of the 3 are required. Bank one consists of a latching valve, latching valve relay, redundant line heaters, ten valve heaters, ten catalyst bed heaters, ten thrusters, and ten thruster relays. Each of these items are in series with the exception of the line heaters, which are parallel. Bank two consists of a latching valve, latching valve relay, redundant line heaters, nine valve heaters, nine catalyst bed heaters, nine thrusters, and nine thruster relays. Each of these items are in series with the exception of the line heaters, which are parallel. Bank three consists of a latching valve, latching valve relay, redundant line heaters, one valve heater, one catalyst bed heater, one thruster, one thruster relay, the thruster gimbal, and the gimbal electronics. Each of these items are in series with the exception of the line heaters, which are parallel.

The reliability prediction of the propulsion system is 0.9976, based on the reliability block diagram and the component reliabilities.

16.5.1.2.5 TT&C system

The reliability block diagram of the TT&C system is shown in figure 16.12. The RF processing switch, sequencers, and RCTU are each modeled as single-string items and are shown

in series. The transponders, CTU's, and SSR's are each modeled in parallel for their individual function, with each function in series. The antenna group is modeled with a string consisting of two low-gain antennas in series and a low-noise amplifier in parallel with a string consisting of the high-gain antenna, 2-axis gimbal, gimbal electronics, and a low-noise amplifier in series. The flight computers are modeled with one flight computer in parallel with a string consisting of the redundancy control unit and a flight computer in series.

The reliability prediction for the TT&C system is 0.9848 based on the reliability block diagram and the component reliabilities previously discussed.

16.5.2 SPACECRAFT RELIABILITY ANALYSIS

Each spacecraft system is essential for mission success. As shown in section 16.4.3, the overall spacecraft reliability is given by

$$\begin{aligned}
 R_{\text{spacecraft}} &= R_{\text{structure}} \times R_{\text{TT\&C}} \times R_{\text{ACS}} \times R_{\text{power}} \times R_{\text{software}} \\
 &\times R_{\text{experiment}} \times R_{\text{propulsion}} = 0.999 \times 0.985 \times 0.998 \times 0.993 \times \\
 &0.985 \times 0.960 \times 0.998 = 0.920
 \end{aligned}$$

16.5.3 INTERSYSTEM RELIABILITY ISSUES

There are two intersystem reliability issues related to the COLD-SAT conceptual design that may require clarification. The thermal system, which is treated as a separate system on a design level, has been merged into the reliability analyses of the systems which require active thermal elements. The systems effected are the experiment and propulsion systems.

The valve relays described in the experiment and propulsion systems are actually part of the sequencer unit contained within the TT&C system. These are included in the experiment and propulsion systems for the purpose of reliability modeling and prediction as the functional time (either in hours or cycles), which these relays are subjected to, are equal the valves which they control.

16.5.4 SINGLE-POINT FAILURE ANALYSES

It was recognized during the COLD-SAT conceptual design that meeting a single-point failure goal of successful elimination of all potential single-point failures would result in a spacecraft that would exceed the program's cost and weight parameters. This led to the single-point failure methodology previously discussed. While the single-point failure analysis included all design functions, only those design functions that are required for the completion of class I experiments were assessed as critical. Redundant paths eliminated all critical single-point failures except the primary tanks (experiment system supply tank and the propulsion system pressurant and propellant tanks) and the TT&C system RF processing switch.

The potential single-point failure for the TT&C system RF processing switch, which is used to switch the communications link between the high-gain and low-gain antennas, is the possibility that the switch fails in an open position. If this occurred, communication to and from COLD-SAT would be lost. Failure history for this type of switch indicates that the primary failure mode is to fail in either closed position and the likelihood of failure in an open position is remote. The addition of a redundant switch path is not desirable because of the resultant loss of signal. This situation has been identified and is part of continued work on the COLD-SAT design.

16.6 Conclusion

The reliability evaluation of the COLD-SAT conceptual design indicates that the reliability goal of 0.92 can be met. Although the single-point failure goal is not met by the conceptual design, effective use of redundancy within the design provides a high level of spacecraft reliability without the high economic cost penalty which would be caused by excessive redundancy.

References

1. MIL-STD-721C (1981). Definitions of Terms for Reliability and Maintainability. US Department of Defense, Naval Publications and Forms Center, Philadelphia.
2. MIL-HDBK-338-1A (1988). Electronic Reliability Design Handbook. US Department of Defense, Naval Publications and Forms Center, Philadelphia.
3. MIL-HDBK-217E NOTICE 1 (1990). Reliability Prediction of Electronic Equipment. US Department of Defense, Naval Publications and Forms Center, Philadelphia.
4. Nonelectronic Parts Reliability Data (NPRD-3). Reliability Analysis Center, Griffiss AFB, NY 13441. Fall 1985.
5. Martin Marietta Space Systems, Inc.: Cryogenic Orbital Nitrogen Experiment (CONE) Design Study; NASA Contract NAS3-25063; September 19, 1990.
6. Bailey, W.J., et al. (Martin Marietta Space Systems, Inc., Denver, CO Astronautics Group): Cryogenic On-Orbit Liquid Depot Storage, Acquisition and Transfer Satellite (COLD-SAT) Feasibility Study, NASA CR-185247; 1990.
7. Reliability Program Requirements for Aeronautical and Space System Contractors. NASA NHB 5300.4(1A-1). 1987.
8. Juran, J.M.: Quality Control Handbook. 4th. Ed. McGraw-Hill, New York. 1988.
9. MIL-STD-756B (1981). Reliability Modeling and Prediction. US Department of Defense, Naval Publications and Forms Center, Philadelphia.
10. MIL-STD-785B NOTICE 1 (1986). Reliability Program for Systems and Equipment Development and Production. US Department of Defense, Naval Publications and Forms Center, Philadelphia.
11. O'Connor, P.D.T.: Practical Reliability Engineering. 2nd. ed. John Wiley & Sons, New York. 1985.

Chapter 17

Safety

Steven T. McHenry
Analex Corporation
Cleveland, Ohio

17.1 Introduction

The Cryogenic On-Orbit Liquid Storage, Acquisition, and Transfer (COLD-SAT) satellite presents some unique considerations from a safety perspective. The purpose of COLD-SAT is to perform subcritical liquid hydrogen storage and transfer experiments under low-gravity conditions in order to provide engineering data for future space transportation missions. Gaseous hydrogen and gaseous helium are also proposed for use in various components of the experiments.

In addition to the usual safety concerns involved with launching a space vehicle, COLD-SAT creates additional concerns because of its use of cryogenic hydrogen. Ground and launch operations are tremendously affected by this and will be modified in support of safety evaluations. The use of hydrazine, pyrotechnics, and pressure vessels on the spacecraft also provide the need for extensive safety input.

The approach used for this safety analysis is as follows. First, a hazard definition matrix was developed. Second, hazard definitions were defined in conjunction with this matrix. Next, each of the defined hazards was classified based on its applicability to the feasibility study. Finally, the hazards considered to be major concerns were evaluated by the system designers and safety engineers in order to identify proper design approaches and safety considerations. Each of these items will be discussed in detail in the following sections of this chapter.

The intent of this analysis is to provide a baseline for the COLD-SAT program safety efforts. The structure of the analysis is such as to be very thorough, yet general in nature. Thus, the analysis can be viewed as a complete analysis of the COLD-SAT system and yet be applicable for use by any organization that is selected to continue the effort. This analysis, as defined and presented in this report, should be used as the starting point for future preliminary design safety efforts. For more detailed information see reference 1.

17.2 Preliminary Hazards Analysis

17.2.1 HAZARD MATRIX DESCRIPTION

The hazard definition matrix developed for the COLD-SAT project is a three-dimensional matrix with the following matrix dimensions: cause category, hazard group, and operational phase. For an example of a single page (two dimensions) of the matrix see figure 17.1. The specific items, and their definitions relative to COLD-SAT are identified in tables 17.1 to 17.3.

The matrix was developed by applying the features of many different system safety hazard analysis procedures in a manner that makes them specific to COLD-SAT. The dimensions were chosen so as to be completely thorough. Therefore, there is overlap in a number of areas. The cause categories and hazard groups chosen are the items that are foreseeable as necessary for a complete evaluation on the COLD-SAT program from feasibility study through launch.

17.2.2 HAZARD DEFINITION APPROACH

The potential hazards were addressed by asking the generic question, "How can (cause category) cause (hazard group) during (operational phase)?" In each case a numbering system was developed to identify each matrix point according to the specific dimensions it encompassed. For example, the first hazard definition addresses the question "How can the structural/mechanical system cause collision/mechanical damage during launch site modifications?" From the matrix it is seen that "collision/mechanical damage" is the hazard group title for row 1; "structural/mechanical" is the cause category title for column A; and "launch site modifications" is designated as operational phase number 1. Therefore, this definition is given the title of 1.A.1.1, with the final "1" added to signify the first definition with others possibly being added.

COLD-SAT HAZARD MATRIX *LeRC Feasibility Study*

cause category: hazard group:	A. Structural/ Mechanical	B. Hazardous Materials	C. Environ- mental	D. Pneumatics/ Pressurants	E. Electrical/ Electronic	F. Ordnance	G. Propulsion	H. Non- Ionizing Radiation	I. Ground Support Equipment
Collision/ 1. Mechanical Damage									
2. Corrosion									
3. Contamination									
Electrical 4. Shock or Short									
5. Fire									
Explosion/ 6. Implosion									
Temperature 7. Extremes									

Operational Phases:

1. Launch site modifications
5. Element test
9. Countdown

2. Subsystem manufacture
6. System integration
10. Flight phase I

3. Transportation
7. System test
11. Flight phase II

4. Element Assembly
8. Pre-launch service
12. Payload separation

Figure 17.1.—Blank hazard matrix form.

TABLE 17.1.—CAUSE CATEGORIES

Category	Definition
Structural/mechanical	Any part of structure or any mechanical component or system
Hazardous materials	Liquid hydrogen/gaseous hydrogen, hydrazine, components or by-products of batteries, processing solvents, and so forth
Environmental	Shock/vibration, temperature extremes, uninhabitable atmospheres, excessive moisture (rain or condensation), salt air, lightning, and so forth
Pneumatics/pressurants	Gaseous helium, gaseous hydrogen, any ground operations pressurant, and so forth
Electrical/electronic	Any electrical or electronic component or system
Ordnance	Pyrotechnic valves, bolt/cable cutters (no shape charges), and so forth
Propulsion	Hydrazine, thrusters, and related plumbing and hardware
Nonionizing radiation	Generated by high-energy radio waves
Ground support equipment	Any equipment used on program that will not be launched

TABLE 17.2.—HAZARD GROUPS

Group	Definition
Collision/mechanical damage	A forceful impact of mechanical items
Corrosion	Structural degradation of metallic or nonmetallic equipment (including hydrogen embrittlement)
Contamination	The release, or cause of release, of toxic, flammable, corrosive, condensible, or particulate matter
Electrical shock/short	Personnel injury or equipment damage caused by improper passage of electrical current
Fire	Rapid oxidation of combustibles—combination of fuel, oxidizer, and ignition source
Explosion/implosion	A violent release or acceptance of energy caused by pressure differentials
Temperature extremes	Burning or freezing of skin or damage to equipment caused by departure of temperature from normal

TABLE 17.3.—OPERATION PHASES

Phase	Definition
Launch site modifications	Safety assessment to Launch site ready
Subsystem manufacture	Material receipt to pack and load complete
Transportation	Pack and load complete to arrival at CCAFS
Element assembly	Arrival at CCAFS to element test start
Element test	Element test start to system assembly start
System integration	System assembly start to system test start
System test	System test start to prelaunch servicing start
Prelaunch service	Prelaunch servicing start to countdown start
Countdown	Countdown start to launch
Flight phase I	Launch to arrive at park orbit
Flight phase II	Arrive at park orbit to arrive at final orbit
Payload separation	Arrive at final orbit to payload separation

The answer to the generic questions provided the substance of each hazard definition. The definitions were not developed until a deep understanding of the entire COLD-SAT system was obtained. The technical aspects of the definition were arrived at based on sound engineering knowledge and the acquired specific system knowledge. Each matrix point was viewed as an independent entity (i.e., the definition derived for one operational phase involving a certain cause category/hazard group did not affect the derivation of a definition for another operational phase). The definitions were then judged on their applicability to the COLD-SAT program. Certain definitions are not applicable while others are not a concern for a feasibility study (although they may need to be addressed during future program phases). The remaining definitions should be addressed during the preliminary design.

All of the hazard definitions are provided in reference 1. The coding system is as follows:

- + Not applicable to COLD-SAT
- Not a safety concern for the feasibility study
- * Safety concern that should be addressed during preliminary design

The structure of the matrix provides for 756 individual cause category/hazard group/operational phase definitions ($9 \times 7 \times 12$). All of these matrix points, however, are not applicable to COLD-SAT (see figure 17.2). Fourteen cause category/hazard group pairs were deemed to be not applicable during any operational phase. A total of 40 specific definitions were also deemed to be not applicable. Therefore, a total of 208 potential hazard definitions are not applicable to COLD-SAT

reducing the number of potential hazard situations evaluated to 588 definitions. Of these, 408 are not a safety concern for the feasibility study leaving 140 hazard definitions that are a safety concern and should be addressed during the preliminary design. These 140 hazard definitions are indicated on the matrix with the number that corresponds to the operational phase being addressed in that definition. The cause category/hazard group pairs that are marked with "N/A" do not have any definitions since it cannot be envisioned how such a situation could arise during the COLD-SAT program. The pairs marked with an "@" have definitions, but the definitions are either not a safety concern or they are not applicable to the COLD-SAT program. Table 17.4 contains a summary of all potential hazard definitions.

17.2.3 CLASSIFICATION APPROACH

At the feasibility study phase of the program, not all of the safety concerns have great impacts. Therefore, a classification system was developed in order to determine which of the hazards are major concerns for a feasibility study. The basic classification scheme was defined as (1) a major safety concern for preliminary design, (2) a minor safety concern for preliminary design, or (3) addressed during feasibility study.

The rationale for classifying a hazard definition into one of the categories was based on a number of factors. First, if an operation will be large in scope in the design effort, it was classified as a major concern. An example of this is the case of the ordnance used in this system. Although none of the proposed ordnance is believed to be of the "Category A" type (catastrophic in and of itself), the ordnance design effort is a major consideration due to the work involved in compiling the list of uses, evaluating the effects of operation on other functions, and evaluating power requirements and effects.

COLD-SAT HAZARD MATRIX *LeRC Feasibility Study*

20 December 1989

cause category: hazard group:	A. Structural/ Mechanical	B. Hazardous Materials	C. Environ- mental	D. Pneumatics/ Pressurants	E. Electrical/ Electronic	F. Ordnance	G. Propulsion	H. Non- Ionizing Radiation	I. Ground Support Equipment
1. Collision/ Mechanical Damage	8 9 10	N/A	e	e	e	e	8 9 12	N/A	e
2. Corrosion	e	8 9 10 11 12	8	1 8 9 10 11 12	e	N/A	8 9 10 11 12	N/A	e
3. Contamination	e	8 9	8 9 10 11 12	6 7 8 9	8 9 10 11	8	8	N/A	e
4. Electrical Shock	N/A	N/A	9 10 11 12	N/A	6 7 8 10 11 12	8 9	N/A	N/A	1 8 9
5. Fire	N/A	7 8 9 10 11 12	N/A	8 9 10 11 12	8 9 10 11 12	e	8 9 10	N/A	e
6. Explosion	8	7 8 9 10 11 12	e	5 7 8 9 10 11 12	1 8 9 10 11 12	7 8 9 10 11 12	e	N/A	8 9
7. Temperature Extremes	e	8 9 10 11 12	8 9 10 11 12	6 7 8 9 10 11 12	6 7 8 9 10 11 12	8 9 10 11 12	7 8 9 10 11 12	6 7 8	e

Operational Phases:

1. Launch site modifications
5. Element test
9. Countdown

2. Subsystem manufacture
6. System integration
10. Flight phase I

3. Transportation
7. System test
11. Flight phase II

4. Element Assembly
8. Pre-launch service
12. Payload separation

Note: Areas marked N/A have no safety concerns.

Figure 17.2.—COLD-SAT hazard matrix.

TABLE 17.4.—SUMMARY OF POTENTIAL HAZARD DEFINITIONS

Matrix points	Disposition
208	Not applicable for COLD-SAT (14 cause categories/hazard group; +40)
408	Not safety concern for feasibility study
140	Safety concern that should be addressed during preliminary design
756	Total matrix points

TABLE 17.5.—SUMMARY OF COLD-SAT HAZARDS ANALYSIS SAFETY CONCERNS

Category	Safety concerns
Addressed during feasibility study —incorporated into design	2
Minor safety concern for preliminary design Partially addressed; remainder is minor safety concern	106 <u>19</u> 125
Major safety concern for preliminary design Partially addressed; remainder is major safety concern	11 <u>2</u> 13
Total feasibility study safety concerns	140

Secondly, if an operation provides unique safety concerns, or is of catastrophic nature of itself or in its timing (i.e., during launch), it was classified as a major concern. The prime example of this is the use and handling of the liquid hydrogen. Thirdly, if an operation has safety requirements specifically mandated, it was considered to be one that must be addressed during the feasibility study. This is the case in the propulsion system design where it is required (by ESMCR 127-1 paragraph 3.11 (ref.2)) that two barriers be present between the hydrazine and the catalyst bed until after launch. Some of the hazards were only partially addressed in this manner and therefore have been dually classified. All remaining hazards were classified as a minor safety concern. This is not to say that these hazards are not of a programmatic concern, but that normal prelaunch safety analysis and review methods will address these items at future phases. Table 17.5 contains a summary of COLD-SAT hazard analyses safety concerns.

The reasons for classification as major safety concerns are as follows:

- (1) Effort needed to eliminate or control the hazard (design effort and/or safety effort)
- (2) Timing of potential hazard occurrence (i.e., during countdown or launch)
- (3) Scope of potential hazard (i.e., catastrophic result)
- (4) Unique safety requirements

All items identified as a safety concern are to be tracked throughout the program. This safety analysis is designed to be used at the various stages of the program as a method of thoroughly itemizing hazards and preparing for various safety reviews.

17.2.4 MAJOR SAFETY CONCERNS

A hazard was considered to be a major safety concern if it met any of the criteria presented in the preceding section. Hazards identified as a minor safety concern will be important during the various future design stages but are not considered to be "drivers" at the feasibility study phase of the program.

The following 13 definitions for a cause category/hazard group/operational phase were identified as areas that present major safety concerns:

- (1) The structural/mechanical system causing collision/mechanical damage during countdown (1.A.9.1)

* Any component on the spacecraft or associated ground support equipment could cause mechanical damage if it failed during countdown. The potential hazard is that the failure goes undetected and the launch occurs. The safety engineer would rely on adequate designs, testing, and quality assurance to assure that failures will not occur. Furthermore, it is critical that there are enough detection methods to alert the launch team to any failure.

(2) The structural/mechanical system causing collision/mechanical damage during flight phase I (1.A.10.1)

* During flight phase I, the greatest amount of stress and vibration will normally occur. Any of the satellite components could fail mechanically or structurally and cause collision or mechanical damage. The system safety engineer must rely on adequate design, testing, and quality assurance to assure that failures will not occur. If a failure occurs during flight phase I, there is no option for evasive or corrective actions.

(3) Ground support equipment causing an electrical shock/short during launch site modifications (4.I.1.1)

* The launch site is considered ground support equipment and there will be many uses of electrical power on the launch site. System safety will evaluate the proposed launch site modifications during preliminary design to determine the potential for electrical shocks/shorts during any operation.

(4) Pneumatics causing a fire during prelaunch service (5.D.8.1)

* Gaseous hydrogen is to be loaded prior to launch. This will require all electrical service in the area to be terminated or have only spark-proof electrical components in use during gaseous hydrogen loading. Pad/area safety plans will address the non-mission-unique safety requirements; ESMCR 127-1, chapter 5 (ref.2) is applicable. The mission-unique activities will be conducted via safety-approved procedures.

(5) The structural/mechanical system causing an explosion during prelaunch service (6.A.8.1)

* There will be many pressure vessels used during prelaunch services that could explode/implode as a result of structural/mechanical damage. The pressures and timelines, as well as the potential for structural/mechanical damage, need to be considered during preliminary design. Pad/area safety plans will address the non-mission-unique safety requirements; ESMCR 127-1, chapter 5 (ref.2) is applicable. The mission-unique activities will be conducted via safety-approved procedures.

(6) Pneumatics causing an explosion during element tests (6.D.5.1)

* There will be many element tests requiring pneumatics that have the potential for causing explosions/

implosions. Test plans/procedures will be required for all testing. Design factors of safety need to be considered during the preliminary design of the pressure vessels that will be included on the satellite. System safety will consider all tests for potential safety impacts. Upon determination that a test has potential for pneumatics causing explosions/implosions, the safety engineer will assure that appropriate safety measures are known and in place.

(7) Pneumatics causing an explosion during system tests (6.D.7.1)

* There will be many system tests requiring pneumatics that have the potential for causing explosions/implosions. Test plans/procedures will be required for all testing. Design factors of safety need to be considered during the preliminary design of the pressure vessels that will be included on the satellite. System safety will consider all tests for potential safety impacts. Upon determination that a test has potential for pneumatics causing explosions/implosions, the safety engineer will assure that appropriate safety measures are known and in place.

(8) The electrical/electronics system causing an explosion during launchsite modifications (6.E.1.1)

* The launch site will require explosion-proof electrical boxes on any level that may encounter liquid or gaseous hydrogen. This may require a major launch site modification to accommodate the handling of liquid and gaseous hydrogen.

(9) Ordnance causing an explosion during prelaunch service (6.F.7.1)

* A project list for the desired pyrotechnic applications needs to be compiled and the applications and installation sequence should be considered early in the design. System safety should be a primary contributor to this effort.

(10) Ordnance causing an explosion during countdown (6.F.8.1)

* The sequence of ordnance activation needs to be considered early in the design to assure an adequate supply of power and to evaluate whether the ordnance firing will impact other functions.

(11) Ordnance causing an explosion during flight phase I (6.F.9.1)

- * The sequence of ordnance activation needs to be considered early in the design to assure an adequate supply of power and to evaluate whether the ordnance firing will impact other functions.
- (12) Ordnance causing an explosion during flight phase II (6.F.10.1)
- * The sequence of ordnance activation needs to be considered early in the design to assure an adequate supply of power and to evaluate whether the ordnance firing will impact other functions.
- (13) Ordnance causing an explosion during payload separation (6.F.11.1)
- * The sequence of ordnance activation needs to be considered early in the design to assure an adequate supply of power and to evaluate whether the ordnance firing will impact other functions.

The next step was to identify the systems that each of these hazards applies to. Following the system identification, safety considerations for each hazard were identified.

17.3 System Design Approach to Major Safety Concerns

By combining the information in the preceding sections, a listing of the major safety concerns for each subsystem has been compiled. These lists follow.

17.3.1 STRUCTURAL SYSTEM

- * The structural system will be designed to withstand the stress and vibration encountered during flight phase I. In addition, the design will keep spacecraft bending within the allowable payload envelope, thus avoiding contact with the faring.
- * Adequate testing will be performed to assure that spacecraft structural or mechanical failures will not occur and that adequate controls will be mandated to assure conformance to the design.

17.3.2 GROUND SUPPORT EQUIPMENT

- * Non-mission-unique activities will follow the safety requirements of ESMCR 127-1 (ref.2).
- * Mission-unique activities will be conducted via safety-approved procedures.

- * Pressure vessels will be designed to the requirements of MIL-STD-1522A.
- * Adequate design, testing, and quality assurance will be performed to assure that mechanical ground support equipment failures will not occur.
- * Detection methods to alert the launch team to any failure will be provided.
- * All proposed launch site modifications will be evaluated by safety personnel to determine the potential for hazards during any operation.
- * All electrical service in the area will be terminated or have only spark-proof electrical components in use during gaseous hydrogen loading; liquid hydrogen will be remotely loaded.
- * The launch site will require explosion-proof electrical boxes on any level that may encounter liquid or gaseous hydrogen.

17.3.3 OPERATIONS

- * Non-mission-unique activities will follow the safety requirements of ESMCR 127-1 (ref.2).
- * Mission-unique activities will be conducted via safety-approved procedures.
- * Mission and ground pressures and timelines, and their hazard potential, will be evaluated by safety personnel and submitted to range safety for analysis.
- * The application and installation sequence of all pyrotechnic applications will be considered early in the design. Also, the sequence of ordnance activation will be evaluated to assure an adequate supply of power and to assess the impact of ordnance firing on other spacecraft functions.

17.3.4 EXPERIMENT SYSTEM

- * Mission-unique activities will be conducted via safety-approved procedures.
- * Mission pressures and timelines will be compiled.
- * Pressure vessels will be designed at a minimum to the requirements of MIL-STD-1522A.
- * All test plans and procedures will be evaluated and approved by safety for all testing.

- * A project list of the desired pyrotechnic applications will be compiled (including sequence of activation).

17.3.5 PROPULSION SYSTEM

- * Mission pressures and timelines will be compiled.
- * Pressure vessels will be designed to the requirements of MIL-STD-1522A.
- * All test plans and procedures will be evaluated and approved by safety for all testing.

17.3.6 POWER SYSTEM

- * A project list of the desired pyrotechnic applications will be compiled (including sequence of activation).

All of the previous safety considerations have become a part of the feasibility study design and the resulting baselined spacecraft. Obviously, there will be additional safety considerations as the program progresses—these should precipitate from this baseline analysis.

17.4 Specific Safety Issues

17.4.1 STRUCTURAL DESIGN CONSIDERATIONS

If the structural/mechanical system caused collision or mechanical damage at any point prior to the countdown, there would be the opportunity for corrective action at a later time. At countdown, however, this opportunity does not exist. Therefore, it is imperative that any hazard of this type be detected during the countdown. The timing of this event makes it a major safety concern. Thus, the structure system must have adequate design and testing to avoid any hazard, as well as adequate quality assurance programs. Secondly, the ground support equipment must provide adequate detection methods that will alert the launch team to any improper conditions.

The spacecraft and launch vehicle will encounter the greatest amount of stress and vibration during flight phase I. Therefore, this is the worst-case that must be designed for. The design must include accommodations for bending within the payload envelope as well as for the stress levels to be reached at this time. An adequate design and testing program and proper quality assurance provisions must be made.

17.4.2 LAUNCH SITE MODIFICATIONS

Because of the unique nature of COLD-SAT, extensive work will be done in the area of launch site modifications. The amount and duration of this work combine to make the launch site modifications a major safety concern. Since the bulk of this

work will be accomplished at later design phases, the only safety consideration that can be itemized at this time is that all modifications desired will be done in accordance with the requirements of ESMCR 127-1 (ref.2). Furthermore, all modifications will be approved by range safety and the launch site contractor.

17.4.3 GASEOUS HYDROGEN, GASEOUS HELIUM, AND HYDRAZENE LOADING CONSIDERATIONS

The loading of gaseous hydrogen, gaseous helium, and hydrazene during prelaunch servicing presents a major safety concern, in addition to requiring major launch site modifications. At the time of loading, either all electrical service in the area will have to be terminated, or all components in use at this time will be required to be spark-proof. Range safety (in accordance with ESMCR 127-1 (ref.2)) will approve all activities and will approve all plans and procedures. A significant effort is needed to design the modifications to assure safe operations.

The ground operations plan calls for the gaseous helium to be loaded in the hazardous processing facility (HPF) with existing facilities and servicing hardware. The hydrazene will also be loaded in the HPF. The hydrazene system consists of flight-qualified pressure vessels (at pressures higher than COLD-SAT is proposing) and will also use existing facilities and equipment. Access to the hydrazene is provided through the fairing should downloading of the propellant be required.

17.4.4 PRESSURE VESSEL DESIGN CONSIDERATIONS

The use of pressure vessels is a major safety concern. COLD-SAT uses pressure vessels in its experiment, its propulsion system, and in its ground support equipment. The major concern will occur during prelaunch service when the vessels are pressurized or during element and system tests. It is imperative that these vessels be designed with adequate factors of safety. Range safety has suggested designing to the requirements of MIL-STD-1522A. In addition, the pressure timeline must be evaluated and all procedures and plans must be approved by safety. Adequate safety measures will be followed, including those in ESMCR 127-1 (ref.2). The potential for structural or mechanical damage, and the resulting hazards, will also be evaluated. Table 17.6 contains pressure vessel design requirements.

17.4.5 LIQUID HYDROGEN HANDLING CONSIDERATIONS

The loading of the liquid hydrogen during prelaunch servicing presents probably the major safety concern, in addition to requiring major launch site modifications. Range safety (in accordance with ESMCR 127-1(ref.2)) will approve all

TABLE 17.6.—PRESSURE VESSEL DESIGN REQUIREMENTS

Pressure vessel	Quantity	Specification
Gaseous hydrogen vaporizers	2	MIL-STD-1522A
Gaseous helium bottles (experiment)	2	MIL-STD-1522A
Hydrazine bottles	4	MIL-STD-1522A, flight qualified
Gaseous helium pressurant tanks	2	MIL-STD-1522A, flight qualified
Liquid hydrogen supply tank	1	ASME Boiler and Pressure Vessel Code, section VIII, division 1
Liquid hydrogen small receiver tank	1	ASME Boiler and Pressure Vessel Code, section VIII, division 1
Liquid hydrogen large receiver tank	1	ASME Boiler and Pressure Vessel Code, section VIII, division 1

activities and will approve all plans and procedures. A significant effort is needed to design the modifications to assure safe operations.

The launch site will require explosion-proof electrical boxes and equipment on any level that may encounter liquid hydrogen. This is a feature that is provided by Complex 36, because of its Centaur facilities. In order to minimize safety concerns, Centaur systems will be used as much as possible. In addition, loading will be remotely monitored and controlled from the launch complex control room.

Although the liquid hydrogen supply tank will be "locked-up" at T - 95 sec, the capability to vent and drain will remain until the commit to launch.

17.4.6 PYROTECHNIC USAGE/CONTROL CONSIDERATIONS

Ordnance will be used in several COLD-SAT applications. It will be used as part of the power system (solar array deployment) and the experiment system (gaseous helium purge bag vent). Although no projected application involves high-explosive devices (irrespective of the flight termination system), the proper functioning of the respective pyrotechnics is essential to maintaining safety. Therefore, a list of all uses of ordnance is mandatory as is an evaluation that addresses the availability of adequate power, the sequence of activation, and the impact on other systems that the ordnance firing will have.

Because of the complexity of the COLD-SAT satellite, it was impossible to completely eliminate pyros that will not be accessible to ground personnel once the spacecraft is assembled. The occurrences were minimized to the activation of the gaseous helium purge bag vent. These pyros as well as any pyro that controls a hazardous function (i.e., liquid hydrogen flow) will be operated from a dedicated pyro control box. This box will isolate the pyros electrically until F - 1 day, at which time the flight actuation cable will be installed to arm the pyros. The pyro control box will be accessible through the fairing access doors.

17.4.7 FLIGHT TERMINATION SYSTEM

The requirements of ESMCR 127-1 chapter 4 (ref.2) specify the use of a flight termination system (FTS) unless a waiver is granted by range safety. For the COLD-SAT Feasibility Study, it was assumed that an FTS was needed and the spacecraft system was designed accordingly.

The need for an FTS arises based on two concerns: (1) an intact impact of a suborbital spacecraft following premature separation from the launch vehicle and (2) independent propulsive potential of the spacecraft. Because of the relative size of the propulsion system thrusters on COLD-SAT, it can be shown that the spacecraft will effectively have no independent propulsive potential. Therefore, the FTS concern is with an intact impact of the COLD-SAT liquid hydrogen and hydrazene vessels.

The FTS that is baselined for COLD-SAT is referred to as an inadvertent separation destruct system (ISDS). This type of system is attached to the launch vehicle and connected to the payload by breakwires. These breakwires will trigger the destruct mechanism if the payload should separate from the launch vehicle prior to the command to do so. The actual system baselined for COLD-SAT is the Martin Marietta Explosive Formed Projectile System. This system has flown on all the commercial Titans and will fly on the Titan IV/Centaur. The system is proposed to be mounted on the Centaur payload adapter thereby eliminating the concern of an inadvertent on-orbit firing.

17.5 Conclusion and Recommendations

The conclusion reached following this feasibility study safety analysis is that there do not appear to be any safety-related reasons that would make the COLD-SAT program nonfeasible. None of the major safety concerns are technical constraints. All of the safety considerations can be accomplished, albeit with some effort and cost, but do not appear to require extraordinary measures.

It is recommended that this analysis be used as the starting point for all future safety analyses. The analysis and database produced are designed to be used by other organizations involved with the COLD-SAT program.

However, some simple changes to the hazard matrix would be helpful in the future. First, the third dimension, operational phase, would be more accurate if described as program phase. Secondly, the program phases themselves would be more useful from a safety standpoint if they were changed as follows:

<u>From</u>	<u>To</u>
10. Flight Phase I	Launch
11. Flight Phase II	Payload Separation
12. Payload Separation	On Orbit

where launch would indicate the span from liftoff to payload separation. This would allow the evaluation of on-orbit safety issues such as end-of-life operations and space debris.

The only issue or concern that arose during the analysis dealt with the lack of concrete answers available from range safety. It is understandable that they cannot provide definite answers unless a firm design exists. Therefore, suggestions (not answers) received from range safety became answers to questions and part of the design. If all future work remains within the boundaries established by the feasibility study there should not be any additional safety issues. However, if the design is significantly altered, system safety personnel should evaluate the proposed changes for programmatic impacts. Therefore, it is imperative that all future work be done with both system safety's and range safety's knowledge, support, and approval.

References

1. McHenry, S.T., and Yost, J.M. (Analex Corporation): COLD-SAT Feasibility Study Safety Analysis. NASA CR-187042.; January, 1991.
2. Eastern and Western Range Safety Requirements (US Air Force 30th and 45th Space Wings). Range Safety Office, Patrick Air Force Base, Florida, March 31, 1995.

Chapter 18

System Development, Integration, and Test

Edward Kramer

National Aeronautics and Space Administration

Lewis Research Center

Cleveland, Ohio

18.1 Introduction

In spite of COLD-SAT's unusual payload, its development will generally follow the conventional path of most spacecraft. There will be no development of distinct experiment packages which will then be integrated onto a spacecraft bus because the experiment and spacecraft are highly integrated, integrated to the point where spacecraft structure is a part of the experiment modules. But the experiment system itself contains little developmental hardware. Instead it is composed of conventional tanks and plumbing with valves and instrumentation which are straightforward adaptations of existing designs and/or currently qualified hardware. During the design process every attempt was made to minimize development activities. The only aspect of COLD-SAT that is really new is the use to which the hardware is being put, long-term cryogenic operations in low gravity.

The unique features of COLD-SAT development are in the integration and test of the cryogenic system. An integrated system test with liquid hydrogen is required. However, delays and difficulties during final integration and test can be very expensive in both time and money. To reduce this risk, COLD-SAT will be constructed as a series of modules and each module will be extensively tested before final integration. This should at least reduce the time required for the sequential working of problems which can occur during final system integration and test.

18.2 System Development

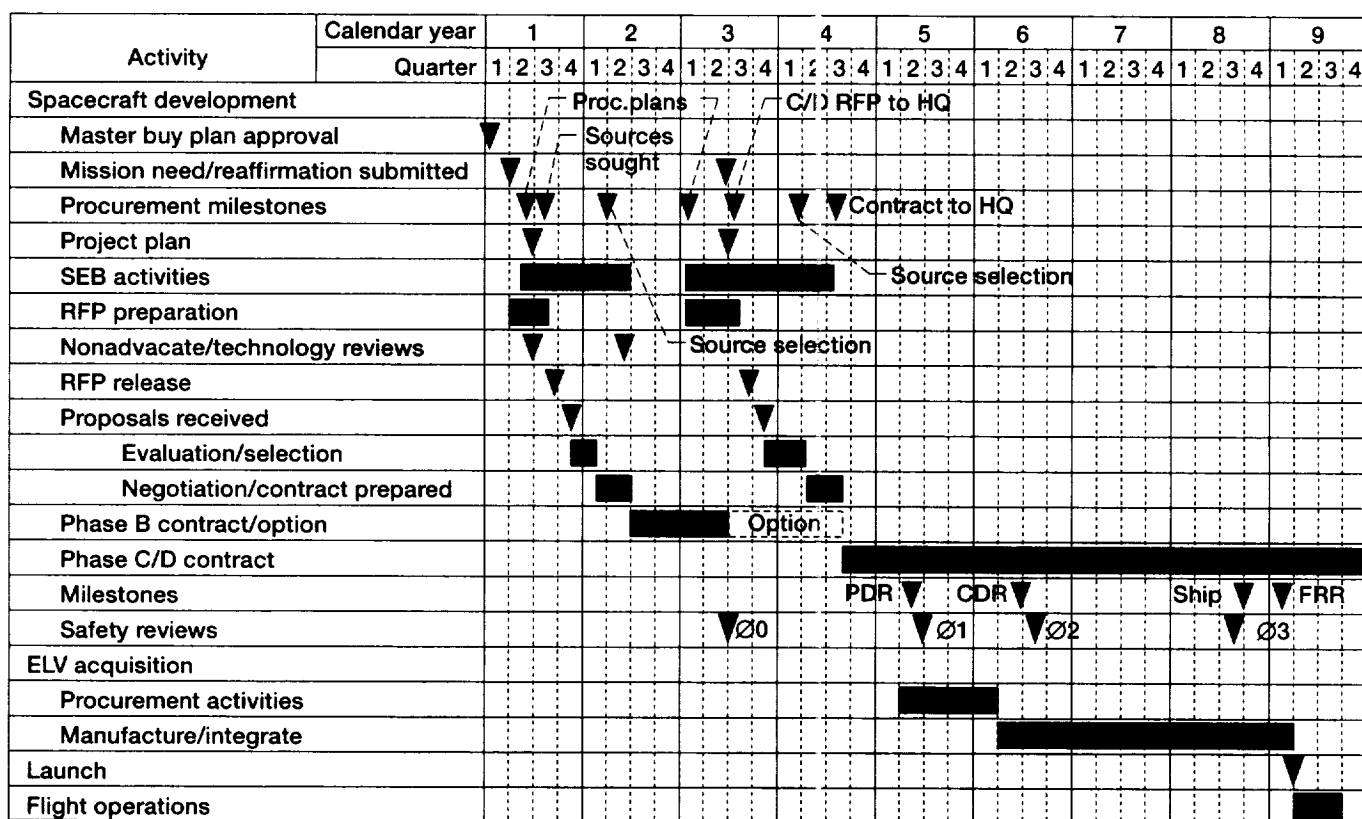
The pace of COLD-SAT development will be governed by the NASA policies which implement the requirements of Office of Management and Budget Circular A-109 and by the realities of government procurement regulations and practices.

Figure 18.1 presents a proposed schedule for the continued development of the spacecraft. Currently, four expanded phase A studies of COLD-SAT have been completed. This report covers the work performed in-house at the Lewis Research Center by NASA and support service contractor personnel. Studies have also been performed by Ball Aerospace Systems Group in cooperation with McDonnell Douglas Space Systems Company and Boeing Aerospace and Electronics (ref. 1), Martin Marietta Astronautics Group (ref. 2), and General Dynamics Space Systems Division with Ford Aerospace Space Systems Division (ref. 3). A variety of concepts have been developed, all of which are feasible designs to accomplish the COLD-SAT goals.

As can be seen from the schedule, at this point in the development process it is a little over eight years until launch. The next step is the solicitation and selection of one (or more) phase B contractors and the further development of a preliminary design. This effort will take a little over two years and should result in high-quality preliminary designs for COLD-SAT. At this stage, development of any critical components needed for the conceptual design will be initiated to reduce risk.

It should be pointed out that this development phase is not required for technical reasons but is mandated by regulations. The development time could be reduced by nearly two years by eliminating phase B. This phase is not required because of the extended nature of the phase A studies now completed and the relatively straightforward definition of what COLD-SAT must be. This would result in a reduction of development time by nearly two years. There would be a cost savings associated with the elimination of phase B as well.

Actual design, fabrication, integration, and test of the spacecraft will take place during phase C/D. Following the necessary procurement activities, the phase C/D work will consume slightly over four years followed by 6 months of preparation for



CDR = critical design review; FRR = flight readiness review; PDR = preliminary design review; RFP = request for proposal; SEB = source evaluation board.

Figure 18.1.—Proposed COLD-SAT schedule.

the launch. While there are only a few months of slack in this schedule, it is not especially tight because of the extensive provisions for integration and test built into it. The launch vehicle will be acquired and fabricated in parallel with the spacecraft phase C/D activities.

Following launch, on-orbit activities will take approximately 6 months. This will be followed by analysis of the flight data and publication of results. The spacecraft development contract will be carried forward past the end of the flight activities at a low level to provide assistance during these activities.

18.3 Development Philosophy

COLD-SAT is intended to be primarily a proto-flight spacecraft. The principle experiment tankage will be built to ASME Boiler and Pressure Vessel Code standards to further minimize risk and testing. In general, components which have been qualified for prior flights will not be requalified. Minor modifications to such designs will be qualified by similarity.

Full-up qualification testing using a qualification article will be limited to selected items which (1) are used repetitively in the system, (2) are judged to be especially critical to the safety or functionality of the system, or (3) are judged to be especially risky. A proto-flight testing approach will be used for new COLD-SAT designs or major modifications to existing designs.

Qualification for dynamic (launch) loads will be done primarily by analysis. Subassemblies such as electronic boxes or valve panels will be qualified by test or similarity. The completed spacecraft will only be subjected to static load testing and a modal survey (without liquid hydrogen loaded) to verify the dynamic model of the spacecraft. If analysis or engineering judgment indicate, selected subassemblies (i.e., instrument racks) will be tested. No vibrational testing with liquid hydrogen will be performed.

To allow for this qualification approach, certain constraints are placed on the design of the spacecraft. Large margins of safety, up to 1.5, will be used. All tankage which has not been previously qualified will be designed to the ASME Boiler and Pressure Vessel Code. This will eliminate burst testing. While this approach will impose a certain weight penalty on the

spacecraft, COLD-SAT is fundamentally volume-limited rather than weight-limited when using the selected launch vehicle, so the additional weight has no impact.

In addition, the design will be constrained to use conventional assembly techniques, methods, and materials. New development will be limited to absolutely essential items even if there is a certain loss of functionality.

Since the complete experiment system will not be assembled until final integration of the spacecraft, full-up system testing of the spacecraft with liquid hydrogen in a simulated thermal and vacuum environment is required. This is a major test which will be difficult to perform. A vacuum environment is required for the proper functioning of the cryogenic insulation systems. Cycling the complete spacecraft into and out of a hydrogen thermal vacuum facility for rework will impose major delays and must be minimized. Access to some portions of the fully assembled spacecraft will be difficult.

A principal area of risk is associated with the final integration and test of the experiment system and the spacecraft. The experiment and spacecraft systems are highly interrelated and ordinarily would not be tested together until final integration of the spacecraft. Problems may not surface until considerable testing occurs with liquid hydrogen. To minimize this risk, the spacecraft is designed as a series of modules. Each module forms as complete a functional unit as possible with relatively simple interfaces to the other modules. As the structure and the supports for the tankage and cryogenic plumbing are highly integrated, spacecraft structure is included in the modules. At final integration only plumbing and electrical interfaces will have to be mated.

Table 18.1 provides a listing of the major components in the five modules. Each module will be tested completely before final integration of the spacecraft. This will include thermal-vacuum cryogenic testing of the experiment modules. Major

portions of the spacecraft electronics will be integrated and tested prior to final assembly. This approach allows the various modules to be tested in parallel and the usual problems worked out before final integration. The success of this approach depends on the fidelity with which the various module interfaces are simulated during testing. The approach has the potential for reducing the time (and money) required for final integration and test, but most important, allows problems to be discovered much earlier when they can be worked without having a major impact on the rest of the spacecraft. This approach will also increase the amount of ground support equipment required but on balance this appears to be a good trade.

18.4 Integration and Test Flow

Flow charts have been developed detailing the major steps in the integration and test of the spacecraft. This flow will be discussed here. The charts all indicate the components, test facilities, and ground support equipment required at each step. In developing the integration and test flow it is assumed that fully qualified components and ground support equipment will be available as required.

18.4.1 ELECTRONICS INTEGRATION AND TEST

Figure 18.2 illustrates the off-spacecraft integration and test of the spacecraft electronics. The electronics boxes will be mounted to the module plates, the plates mounted to a mock-up of the electronics module structure, and the cables installed but not connected. Checkout will begin with the command and telemetry unit (CTU) using the appropriate electronic ground support equipment (EGSE) and the remaining units on the CTU bus will be sequentially connected and checked out. At this

TABLE 18.1.—SPACECRAFT MODULE DEFINITION

Electronics bay 1
Complete hydrazine propulsion system
Spacecraft—expendable launch vehicle adaptor
Sun sensors
Majority of electronics on board
OMNI antenna
Supply tank module
Liquid hydrogen supply tank with associated instrumentation, valving, and plumbing
Gaseous helium pressurant storage
Gaseous hydrogen pressurant storage
T - 4 sec liquid hydrogen fill/drain umbilical connections
Gaseous hydrogen vent connections
Solar arrays and HGA attach to, but not part of, module
Electronics bay 2
Earth sensors
Remainder of spacecraft electronics
Large receiver tank module
Large receiver tank with associated instrumentation, valving, and plumbing
Small receiver tank module
Small receiver tank with associated instrumentation, valving, and plumbing
OMNI antenna

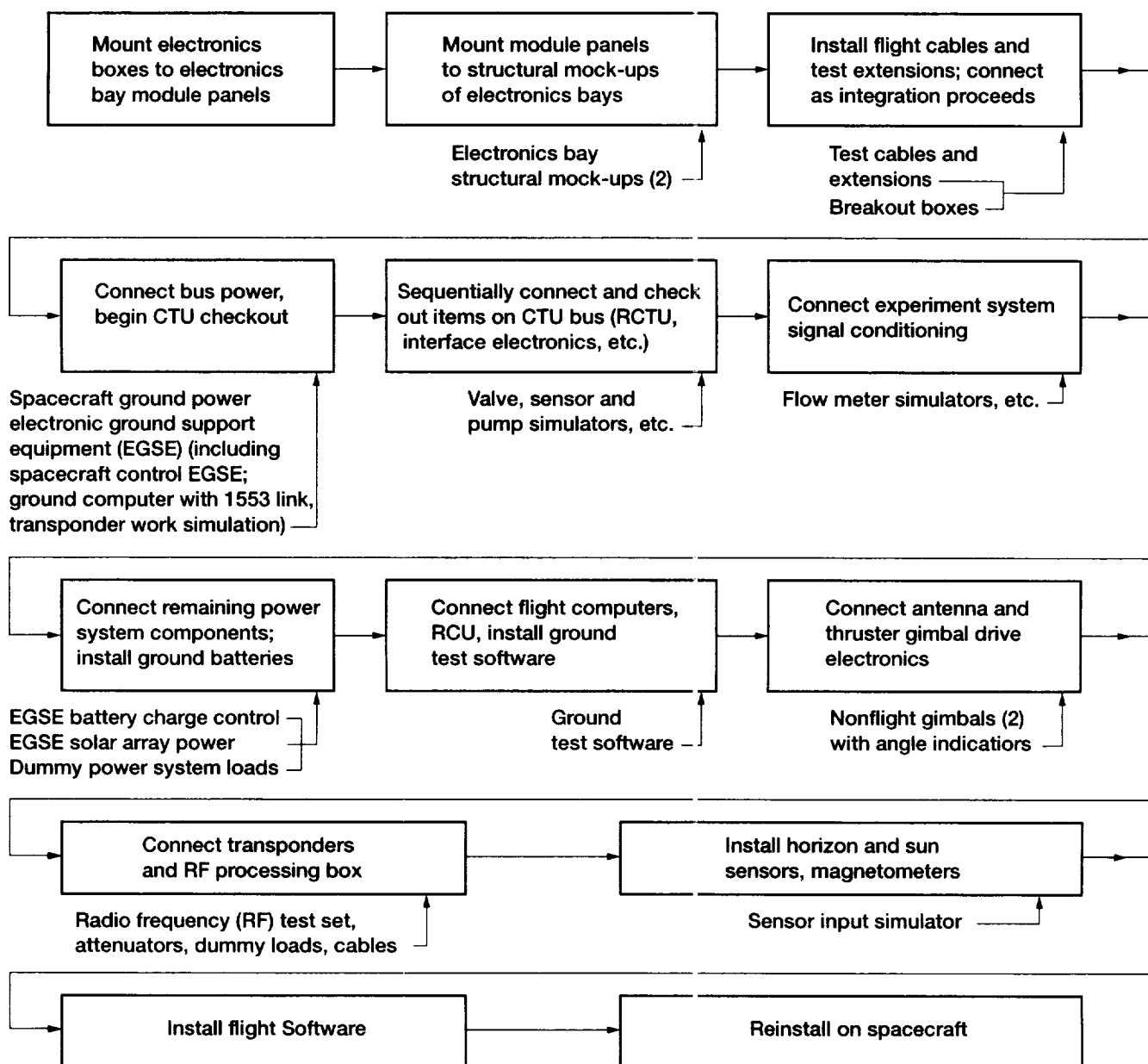


Figure 18.2.—Electronics integration and test (Flow assumes test/check-out of items recently integrated at each step.).

point the basic telemetry and control functions will be available. The experiment system signal conditioning units will then be connected. Next the power system boxes will be connected along with a set of test batteries. The spacecraft can now be operated from simulated solar array power. Next the flight computers, the redundancy control unit, and the ground test software will be installed and checked out.

The antenna and the thruster gimbal drive electronics boxes will be installed next, followed by the radiofrequency system components and the transponders. Now the system is fully functional and can be tested using simulated inputs to the transponders. Following integration of the attitude sensors, the

flight software can be checked out on the actual flight system. The cabling between the various module plates of the two electronics modules will then be removed and at an appropriate time be reinstalled as the spacecraft is being assembled.

18.4.2 ELECTRONICS BAY 1 ASSEMBLY AND TEST

The electronics bay 1 assembly and test sequence is illustrated in figure 18.3. First the structure of the bay will be assembled, suitably inspected, and mounted to the spacecraft vertical handling fixture. The hydrazine system tanks and lines will then be installed followed by a fit check with the supply

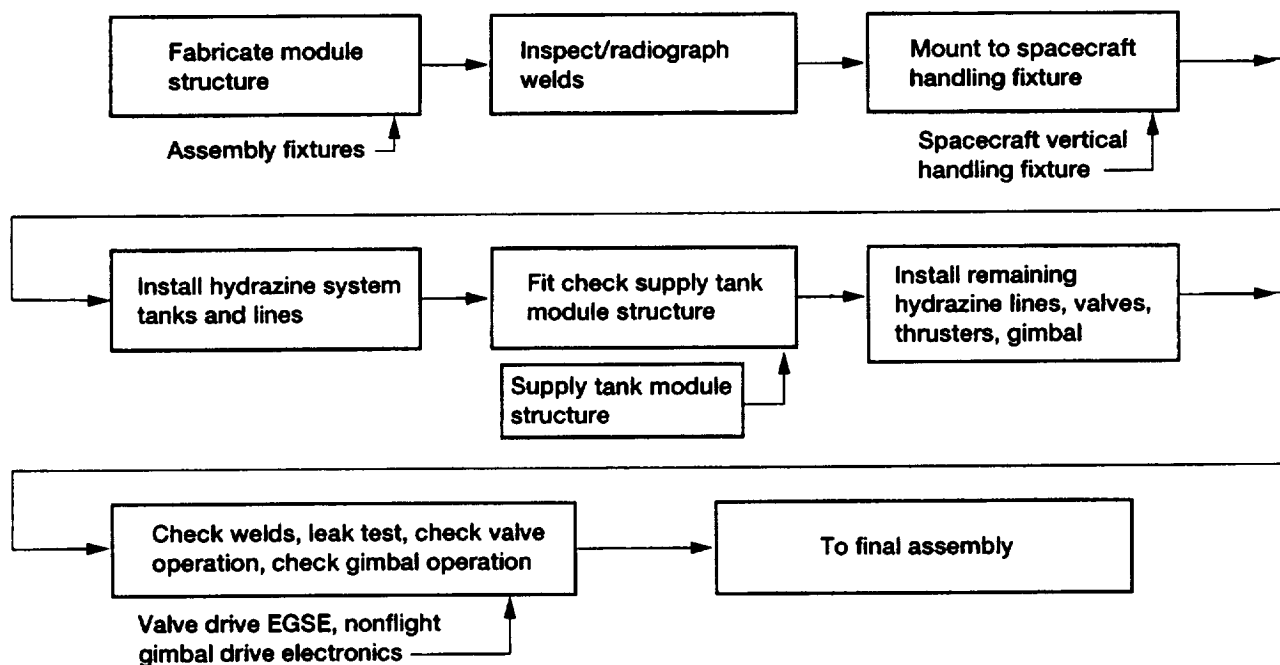


Figure 18.3.—Electronics bay 1 assembly and test.

tank module structure which stacks above it. The remaining propulsion components will be installed and checked out. The module, without electronics and harnesses, is now ready for final integration.

18.4.3 RECEIVER TANK MODULE ASSEMBLY AND TEST

Both the large and small receiver tank modules will undergo similar assembly and test procedures. The flow is shown in figure 18.4. First the tanks themselves will be partially assembled, by fabricating the barrel section and attaching one dome using suitable handling and assembly fixtures. Following a thorough cleaning, the tank internal structure, plumbing, and sensors will be installed in a clean room. Sensors will then be checked out at ambient and the tank will be closed out followed by inspection of the welds and leak checking. The pressure vessel assembly will then be completed by installation of the valve panels and external plumbing.

The complete assembly will be cold-shocked in liquid nitrogen followed by verification of sensor and valve operation at liquid nitrogen temperatures (77 K). Proof pressure testing followed by a through leak check will complete this phase of testing.

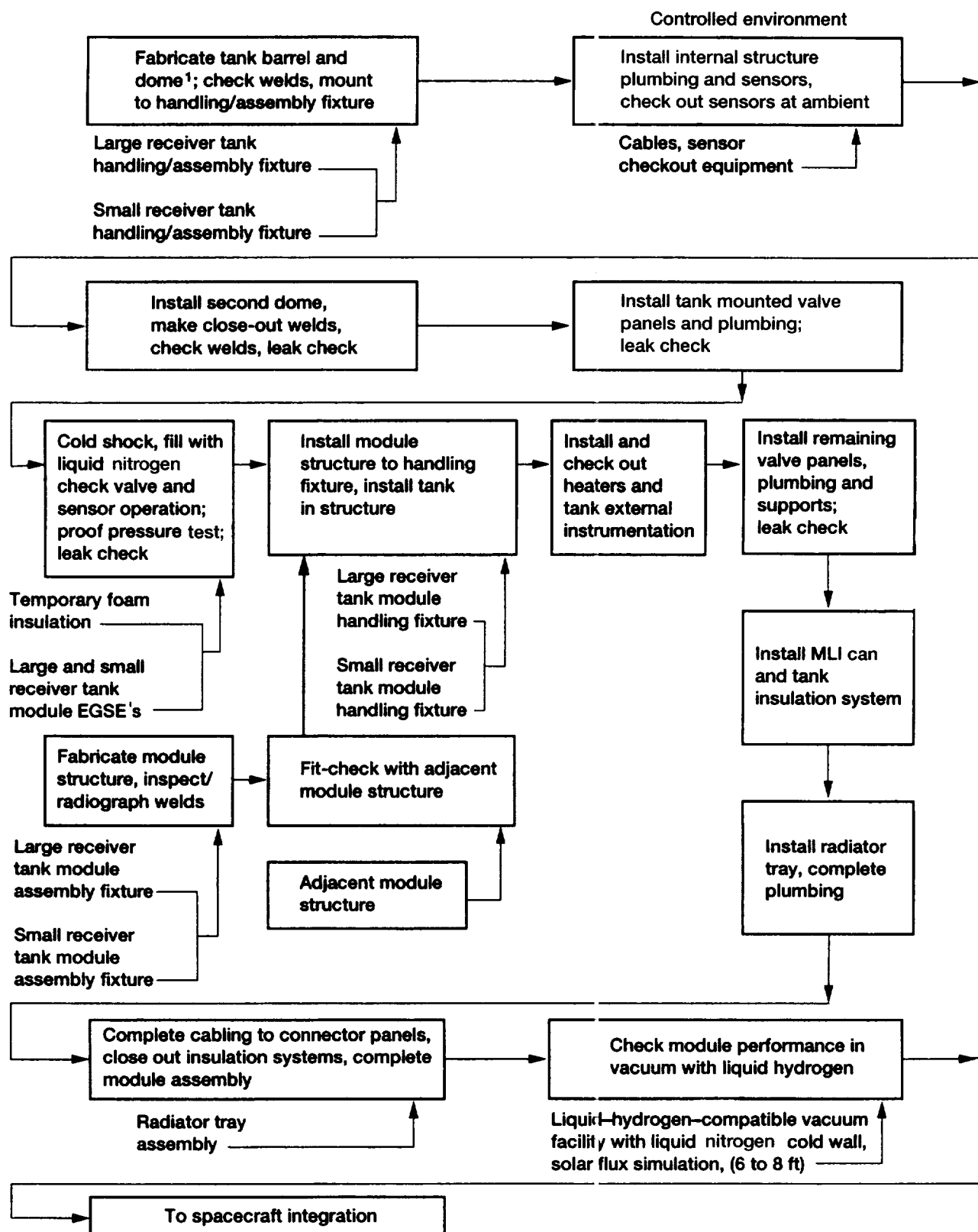
The module structure will have been fabricated and inspected in parallel with the tank assembly operations. They will now be mated with each other in the module handling fixture using the S-glass support struts. Tank heaters and external sensors will be installed and checked out at ambient. The remaining module valve panels and plumbing (those not mounted

to the tank) will then be installed and leak checked. Next the MLI can and the cryogenic insulation systems will be installed along with the module section of the radiator tray to complete the plumbing. Installation of cabling to connector panels and the close-out of insulation systems will complete assembly of the module.

The completed module will then be thoroughly tested in a thermal vacuum chamber with solar and deep space simulation using liquid hydrogen. All valves will be cycled repeatedly and sensor calibration checked. The system will be carefully monitored for leaks both into the vacuum chamber and internal to the plumbing. The system will be repeatedly cycled to ambient temperature by using the tank heaters. Thermal performance will be verified. When all bugs have been worked through and all tests passed, the modules are ready for integration with the spacecraft.

18.4.4 SUPPLY TANK MODULE ASSEMBLY AND TEST

The supply tank module is the most complex of the three experiment system modules so its assembly and test is correspondingly more involved. The assembly and test flow is shown in figure 18.5. Up until the installation of the gaseous hydrogen vaporizers, the sequence is the same as that used for the receiver tank modules and so will not be discussed further. Following closeout of the cryogenic insulation systems and the purge bag, the vaporizers will be installed. The vaporizers will have been cold-shocked with liquid nitrogen, proof-pressure tested, and leak-checked prior to installation. The remaining



¹Weld large receiver tank aft dome-to-barrel; weld small receiver tank forward dome-to-barrel.

Figure 18.4.—Large and small receiver tank modules assembly and test.

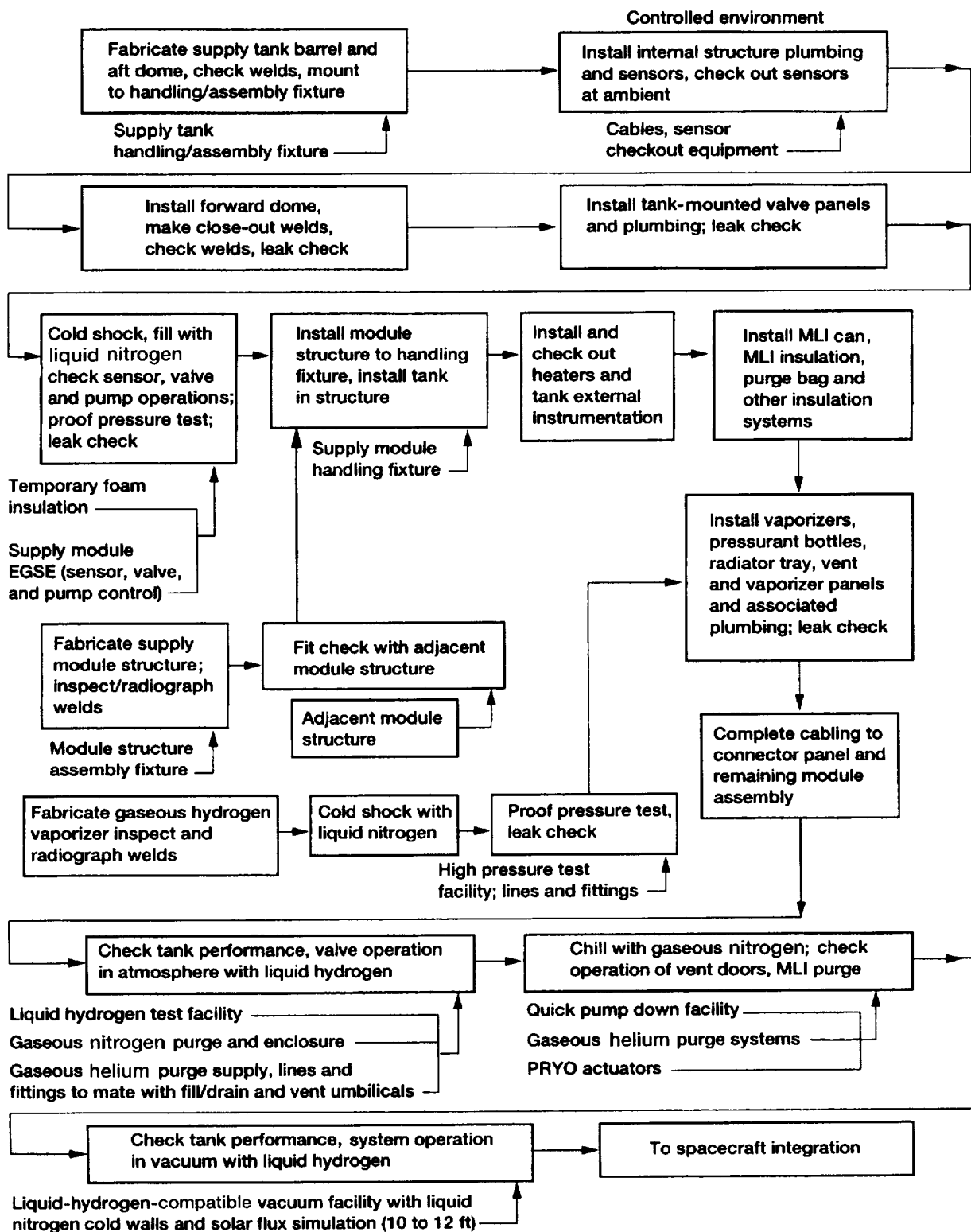


Figure 18.5.—Supply tank module assembly and test.

gaseous helium pressurant bottles, valve panels, and module plumbing will be installed along with the vaporizers. The module assembly will then be completed by the installation of cabling and the close out of insulation systems.

Initial testing will be performed in a gaseous nitrogen atmosphere using liquid hydrogen and the helium purge system. This will verify system integrity and thermal performance during ground hold and ascent. The module will then be moved to a quick pump-down facility and the operation of the purge system, vent doors, and pyro actuators will be verified in a simulated ascent environment. Next, on-orbit operation will be verified using liquid hydrogen in a simulated space environment. All components will be operated and the system repeatedly cycled from ambient to 20 K. Internal and external leakage will be monitored. Thermal performance of the cryogenic tankage will be verified. Following successful completion of the testing, the module is ready for integration with the remainder of the spacecraft.

18.4.5 SPACECRAFT ASSEMBLY, INTEGRATION, AND TEST

Figure 18.6 illustrates the final spacecraft assembly, integration, and test flow. At the beginning, all five spacecraft modules have been assembled and tested. The integration will be performed vertically and so the lowest module, electronics bay 1, will remain on the spacecraft vertical handling fixture. The remaining modules will then be stacked up in order and the relatively small number of plumbing interconnections will be welded and leak-checked. Next, intermodule cabling will be installed and all cryo insulation systems closed out. The spacecraft electronics boxes, on the electronics bay panels, will then be installed in the open position using the panel support brackets. Following that, the electronics will be sequentially reintegrated using the prior procedure and then integrated with the other spacecraft systems. The attitude sensors will be temporarily installed and checked out. After their removal, the solar arrays and their associated deployment mechanisms will be installed along with the high-gain antenna and required structural instrumentation. This will complete the initial integration of the spacecraft.

The spacecraft structure and dynamic characteristics will be qualified by analysis. The structural model will be verified by a lateral static load test and a modal survey. The spacecraft will then be placed in its transport and handling fixture and moved to an acoustic test facility. The following acoustic test will verify the integrity of a number of smaller, lighter, higher frequency items not likely to be well covered in the dynamic model. This will complete the structural testing of the spacecraft unless major problems are uncovered. The spacecraft will then be moved back to the integration and test facility and the solar arrays and accelerometers removed and packed for shipment to the launch site.

The spacecraft radiofrequency systems will be checked out using a variety of tests including a complete end-to-end test with the tracking and data relay satellite system (TDRSS). The high-gain antenna will then be removed and packed for shipment to the launch site. The spacecraft will be transported to a test facility for electromagnetic compatibility testing. The spacecraft will be tested for compatibility with the launch site, the launch pad, and the launch vehicle electromagnetic environments and susceptibilities. Tests will also be performed to verify the spacecraft internal electromagnetic compatibility (EMC) model.

The spacecraft will then be transported to the system test facility, a large liquid hydrogen-compatible thermal-vacuum chamber. After installation, the complete spacecraft will be tested to verify its functionality. A full mission simulation will be performed using the flight software with control from the COLD-SAT payload operations control center (POCC). Additional testing will be performed to verify degraded mode and off-nominal operation. The solar flux will be simulated to verify operation of the cryogenic thermal protection systems. In addition to validating the spacecraft, this test will also serve to provide a performance baseline for the experiment system, which can be compared with results obtained on-orbit in low gravity. The functionality of the POCC and its software and the training of the POCC personnel will also be confirmed.

Following successful completion of the system test, the spacecraft will be removed from the thermal vacuum chamber, mounted on the transport and handling fixture, and prepared for transportation. Batteries will be removed, sensors covered, fluid interfaces sealed, and electrical interface connectors protected. The spacecraft will then be placed in the shipping container in an inert atmosphere and shipped to the launch site.

18.5 Phase C/D Schedule

Figure 18.7 presents a proposed schedule for the COLD-SAT phase C/D (development, fabrication, and deployment) activities. The schedule time from authority to proceed (ATP) on the phase C/D contract until the final pre-ship review (PSR), which approves shipment of the spacecraft to the launch site, is 4 years and 6 months. This is a reasonably aggressive schedule but should be possible because of the extensive development work that precedes it and the parallel assembly and test of the major portions of the spacecraft.

The schedule is in general quite conventional. The only rather unique features are the relatively short time from ATP to critical design review (CDR) and the major parallelism that occurs during spacecraft module assembly and test. The 9 months to preliminary design review (PDR), which in fact only allows about 7 months of design following the contract startup activities, is reasonable because of the extensive development which will precede the phase C/D activities. The

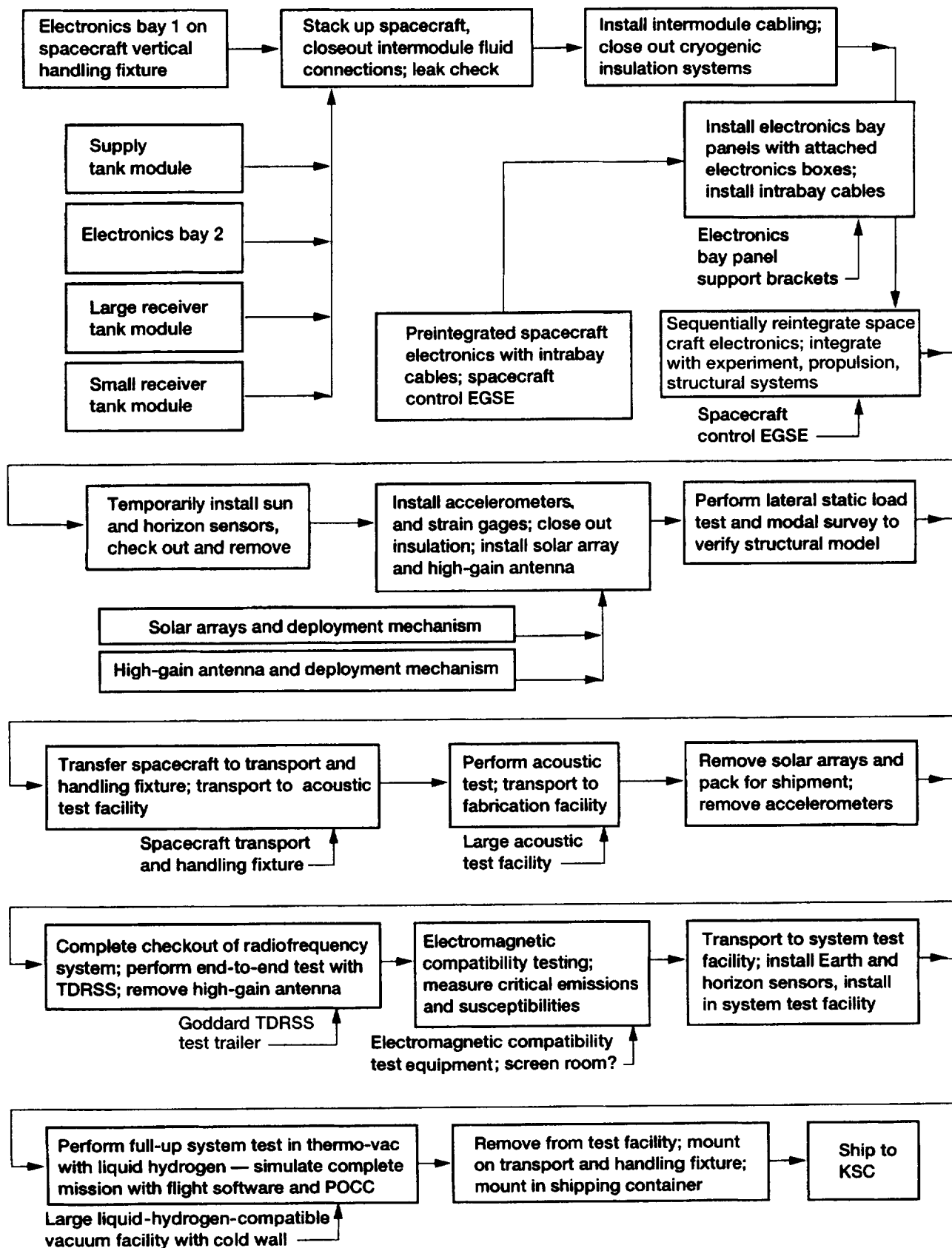
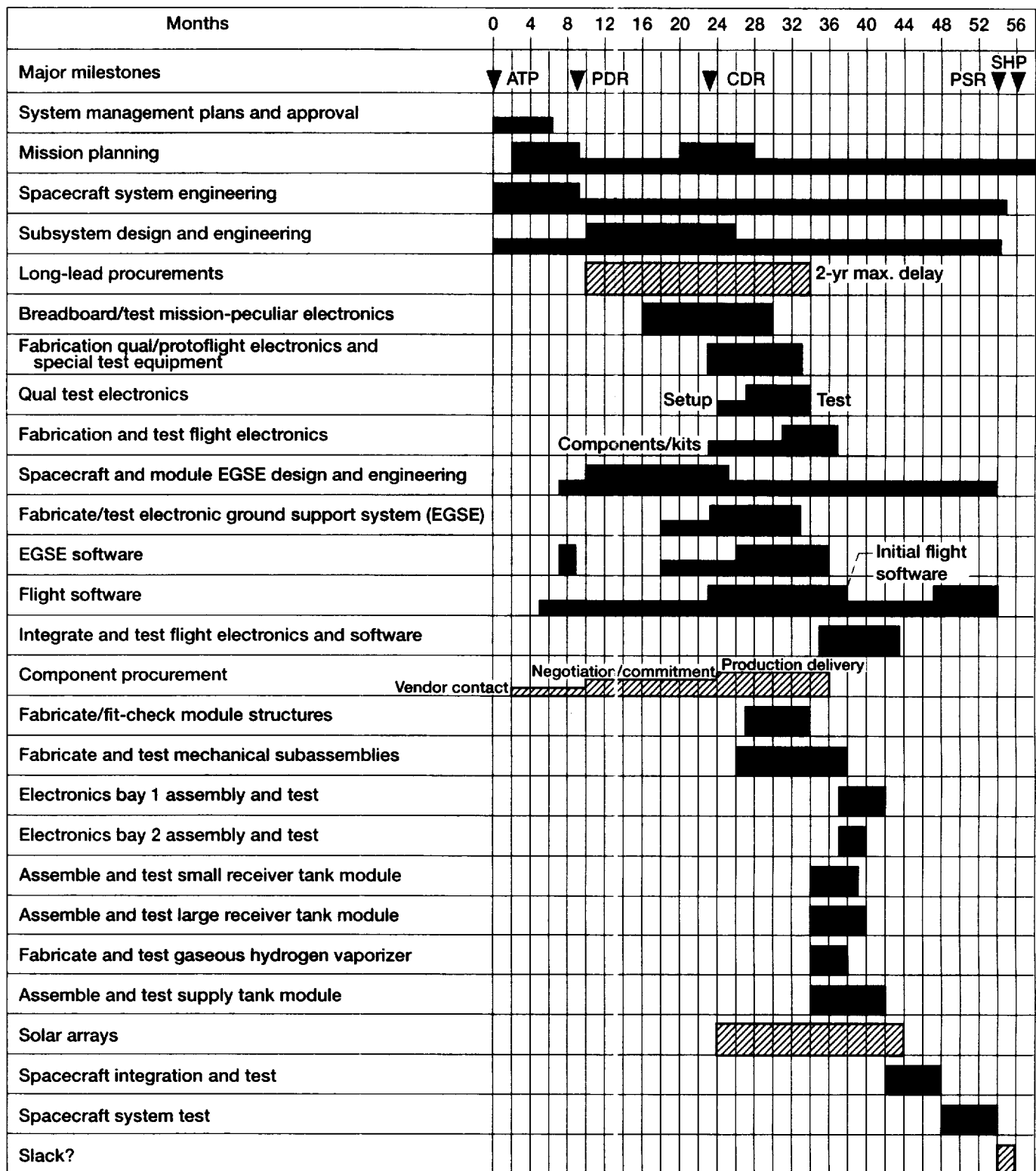


Figure 18.6.—Spacecraft assembly, integration, and test.



ATP = authority to proceed; CDR = critical design review; PDR = preliminary design review; PSR = pre-ship review; SHP = ship.

Figure 18.7.—COLD-SAT design, assembly, and test.

TABLE 18.2.—SPECIAL TEST FACILITIES

Facility required	Availability
Liquid-hydrogen-compatible vacuum facility with cold wall and solar flux simulation for system test	Lewis Plum Brook Station, B-2 Facility
Medium liquid-hydrogen-compatible vacuum facility with cold wall for module test	Lewis Plum Brook Station K-Site; several aerospace
Quick pump down facility for supply tank module testing	Several aerospace
Liquid hydrogen facility for supply tank module atmosphere testing	Several aerospace
Acoustic test facility capable of testing complete spacecraft	General Dynamics Kearny Mesa Facility

parallel fabrication and test of the various spacecraft modules is possible because of the relatively simple interfaces between the modules. The 6 months for final integration and system test is reasonable because of the testing which precedes it at the module phase.

18.6 Test Facilities

Most of the test facilities required for the development and test of the COLD-SAT spacecraft are conventional, the type ordinarily required for spacecraft development. However, some unique facilities are required for COLD-SAT development, principally for cryogenic testing. These have been identified in table 18.2. Also identified in table 18.2 are potential test facilities that meet COLD-SAT requirements. There is at least one facility available for each COLD-SAT test. For a number of tests several facilities have been identified and the search was not exhaustive. No special test facilities will have to be constructed for COLD-SAT.

18.7 Ground Support Equipment

A large amount of ground support equipment (GSE) and electrical ground support equipment (EGSE) will be required to support COLD-SAT operations both during assembly, integration, and test; for transportation to the launch site; and at the launch site. This section covers the GSE and EGSE, which has been identified to date. Some of the major items will be discussed briefly. The remaining items will only be tabulated.

18.7.1 ELECTRONIC GROUND SUPPORT EQUIPMENT (EGSE) TRAILER/SKID

The EGSE trailer/skid is required for spacecraft integration and test, spacecraft system test, and for spacecraft support at the launch site. It can also be used for the integration of the

spacecraft electronics. It will provide the control and data processing electronics and the interfacing required to communicate with the spacecraft electronics. It will be capable of simulating spacecraft transponder input and output (uplink and downlink). It will also be capable of operating directly the spacecraft internal data bus. It will interface with the spacecraft ground control interface and will simulate the Centaur side of the spacecraft/Centaur interface.

The COLD-SAT EGSE trailer/skid must have the computational capability to reasonably simulate launch, ascent and on-orbit operational inputs including the horizon and Sun sensor. It must generate command and software uploads and transmit them to the spacecraft. It must process spacecraft telemetry for engineering unit conversion, limit checking, display, and recording. It must also communicate externally with the spacecraft POCC and the launch site. The unit will duplicate many functions of the POCC and will probably benefit from commonality with the POCC software.

18.7.2 TRANSPORT TRAILER

The transport trailer is required to transport the completed spacecraft to the various facilities during system testing, to transport the tested spacecraft to the launch site, and to move the spacecraft around at the launch site. It will also be required to transport a certain amount of servicing equipment with the spacecraft. Figure 18.8 illustrates a concept for this transportation trailer. It shows the spacecraft mounted to its handling dolly on the trailer.

The trailer is basically required to provide a controlled, protected environment for the spacecraft during transportation. It will help to control the shock and vibration which occur during transportation to acceptable levels. When enclosed, the spacecraft will be maintained in a protected, clean, air conditioned, humidity controlled environment. Servicing equipment will be available to maintain proper pad pressure in the various spacecraft systems. The status of the spacecraft and its shock and vibration history will be monitored by systems on the transportation trailer.

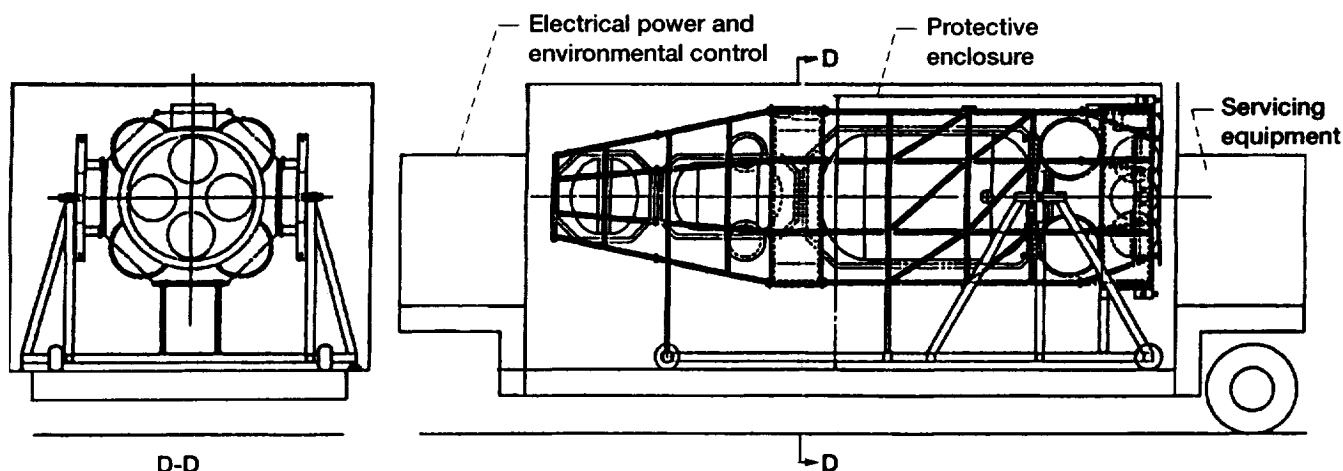


Figure 18.8.—COLD-SAT spacecraft installed on trailer transporter.

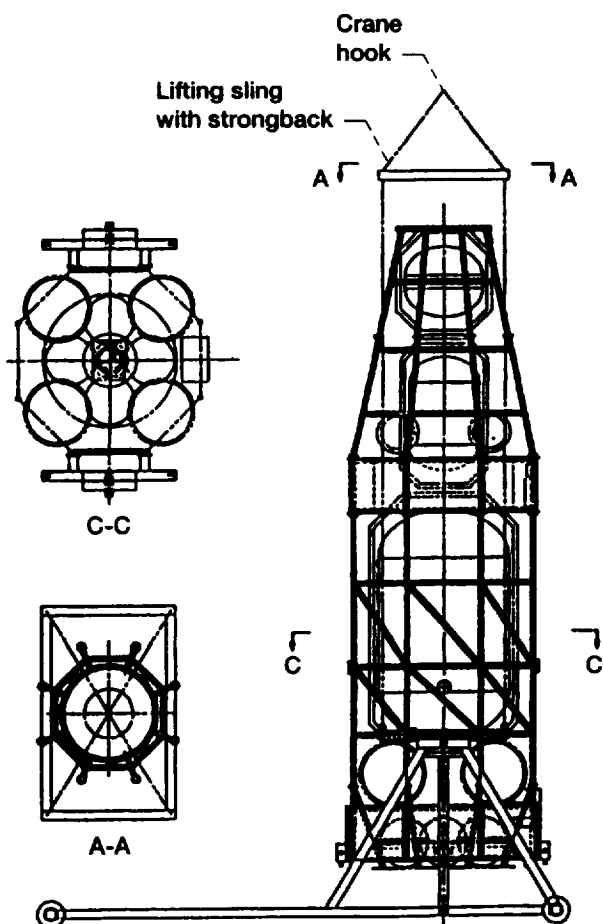


Figure 18.9.—COLD-SAT spacecraft erected on integrated trunnion support and handling dolly.

18.7.3 TRUNNION SUPPORT AND HANDLING DOLLY

The handling dolly is used to support and transport the spacecraft during a variety of assembly and test procedures. Figure 18.9 illustrates a concept for this dolly. The spacecraft is supported by trunnions located near its center of gravity. It can be rotated about these trunnions to the vertical position for testing, servicing and lifting and to the horizontal position for transportation. In both positions it will be supported by additional auxiliary supports attached to spacecraft hard points and the dolly. The transition from horizontal to vertical will be made using suitable lifting slings and supports. In general the spacecraft will always be lifted on and off the dolly in the vertical attitude. When on the transportation trailer the spacecraft is on the transportation dolly which forms its structural interface with the trailer.

18.7.4 SPACECRAFT MODULE EGSE

The modular assembly and test of the individual spacecraft modules will require additional electrical ground support equipment. For the electronics modules the spacecraft EGSE trailer should suffice if supplemented by simulation of the various sensor inputs. For the three experimental modules additional equipment will be required. The three items of module EGSE will be required to duplicate the sensor data acquisition and signal conditioning functions and valve and heater driver functions of the spacecraft electronics. In addition command input and data display will be required.

TABLE 18.3.—COLD-SAT GROUND SUPPORT EQUIPMENT

Equipment	Definition
Electrical ground support equipment (EGSE) trailer/skid	New: required for integration, test, and launch site operations
Trailer transporter	New: required for system testing, transport to launch site, and CCAFS operations
Spacecraft handling dolly	New: required for system test, transport to launch site, and CCAFS operations
Supply tank module EGSE	New: required for modular integration and test of supply tank module
Large receiver tank module EGSE	New: required for modular integration and test of large receiver tank module
Small receiver tank module EGSE	New: required for modular integration and test of small receiver tank module
Spacecraft power bus simulation	New: 24 to 32 V dc power to simulate spacecraft power bus. Required for electronic module test, system test, and launch site operations
Spacecraft solar array simulation	New: 0 to 80 V dc power to simulate spacecraft solar array. Required for electronic module test, system test, and launch site operations
Power system ground interface	New: cabling and interface electronics to control power system and connect to required power sources
Experiment and spacecraft sensor simulation	New: a variety of test boxes simulating sensors for electronic systems integration and test
Electronic systems ground interface	New: cabling and interface electronics required to connect various portions of the spacecraft electronics system to the EGSE trailer
Spacecraft radiofrequency test set	New: RF equipment and cabling required to test and calibrate the transponders and other onboard radiofrequency (RF) equipment
Spacecraft control consoles	New: consoles and associated computing facilities are required at launch site blockhouse to control spacecraft during prelaunch activities
Spacecraft/electronics bay 1 vertical handling fixture	New: required for assembly of electronics bay 1 and the spacecraft
Supply tank module handling fixture	New: required for assembly, integration and test of supply tank module
Large receiver tank module handling fixture	New: required for assembly, integration and test of large receiver tank module
Small receiver tank module handling fixture	New: required for assembly, integration and test of small receiver tank module
Supply tank handling fixture	New: required for assembly of supply tank and related items
Large receiver tank handling fixture	New: required for assembly of large receiver tank and related items
Small receiver tank handling fixture	New: required for assembly of small receiver tank and related items
Umbilical pull test hardware	New: required to test functioning of spacecraft umbilicals with liquid hydrogen
Gaseous helium loading system	New: includes pressurant supply, hoses, and controls needed to fill the gaseous helium pressurant bottles, test them and, if necessary, drain them
Gaseous hydrogen service cart	New: includes pressurant source, vacuum system, control, and monitoring equipment as well as interconnecting hoses for filling, draining, and testing hydrogen vaporizers during system test and at the launch site
Hydrazine service cart	Possibly existing: required to fill and, if necessary, drain propulsion system at launch site
Low-pressure helium service cart	New: required for testing supply tank insulation purge system and supplying pad pressure to spacecraft tanks during shipping
Spacecraft lifting slings	New: lifting slings with strongback for lifting spacecraft in the vertical position. Needed both before and after transport to launch site. Must be qualified at launch site.
Horizontal attitude workstand	New: required to allow access to spacecraft while in horizontal position on handling dolly and trailer

TABLE 18.3.—Conclusion

Equipment	Definition
Vertical attitude workstand	New: required to allow access to spacecraft while in vertical position while on handling dolly
Payload fairing workstand	Existing: needed for spacecraft encapsulation in fairing
Payload mating fixture	Existing: needed for payload adapter installation
Payload encapsulation equipment	Existing: nose fairing half carts, torus handling cart, and ground transport vehicle and associated facilities needed to encapsulate spacecraft in payload fairing, transport and mate it with ELV
Gaseous hydrogen detectors	Existing and new: required to monitor for leaks during all operations when gaseous or liquid hydrogen are present
Hydrogen flame detectors	Existing and new: required to monitor for invisible hydrogen flames whenever liquid or gaseous hydrogen are present
Hydrazine detectors	Existing: required to detect the presence of hydrazine leaks or contamination while the spacecraft is filled with propellant
Oxygen-level monitors	New and existing: required for personnel safety whenever gases or cryogenics are used
TDRSS test trailer	Existing: required for end-to-end test through TDRSS

18.7.5 OTHER GROUND SUPPORT EQUIPMENT

In addition to the equipment discussed above, a large amount of ground support equipment is required for COLD-SAT, some during assembly, integration, and test and some during launch site operations. Some of this equipment is unique to COLD-SAT and some is generic, of a type used by many spacecraft. In the COLD-SAT design every attempt will be made to use existing GSE, especially at the launch site. Table 18.3 is a tabulation of the GSE and EGSE which have been identified as required for COLD-SAT.

References

1. Rybak, S.C., et al. (Ball Aerospace Systems Group with McDonnell Douglas Space Systems Company and Boeing Aerospace and Electronics): Feasibility Study for a Cryogenic On-Orbit Liquid Depot-Storage, Acquisition and Transfer (COLD-SAT) Satellite. NASA CR-135248, 1990.
2. Bailey, W.J., et al. (Martin Marietta Space Systems, Inc., Denver, CO (Astronautics Group)): Cryogenic On-Orbit Liquid Depot Storage, Acquisition and Transfer Satellite (COLD-SAT) Feasibility Study. NASA CR-135247, 1990.
3. Schuster, J.R. (General Dynamics Corp. Space Systems Division with Ford Aerospace Space Systems Division): Cryogenic On-Orbit Liquid Depot Storage, Acquisition, and Transfer Satellite (COLD-SAT). NASA CR-135249, 1990.

Appendix A

Nomenclature

A/C	Atlas/Centaur rocket; air conditioning	CERT	composite electrical readiness test
ACS	attitude control system	CDR	critical design review
ACSIE	attitude control system interface electronics	CFMFE	Cryogenic Fluid Management Flight Experiment
ACTS	Advanced Communication Technology Satellite	CG	center of gravity
A/D	analog-to-digital	CHX	compact heat exchanger
ADC	analog digital converter	COLD-SAT	Cryogenic On-Orbit Liquid Depot-Storage, Acquisition, and Transfer (project, spacecraft, experiment)
Ag-Zn	silver-zinc (battery)	COM	center of mass
AP	applications processor	CTU	command and telemetry unit
ASME	American Society of Mechanical Engineers	CRES	stainless steel
ATP	authority to proceed	CRRES	Combined Release and Radiation Effects Satellite
AWG	American Wire Gage	CTU	command telemetry unit
AXT	axial thrusters	CV	check (one way) valve
BCTU	backup command and telemetry unit	dB	decibels
BECO	booster engine cutoff	dBm	decibels above a milliwatt
Bo	Bond number, dimensionless number, ratio of gravitational-to-surface tension forces	dBW	decibels above a Watt
BOL	beginning of life	DOD	depth of discharge; Department of Defense
BPJ	booster pod jettison	DOT	Department of Transportation
bps	bits/sec	DPT	differential pressure transducer
BRCU	backup redundancy control unit	DSS	digital Sun sensor
BRF	battery recharge factor	DTC	digital temperature controller
CCAFS	Cape Canaveral Air Force Station	EB	electronics bay

ECS	environmental conditioning system	GEOS	Geostationary Environmental Operational Satellite
EDAC	error detection and correction	GGT	gravity gradient torques
EDU	experimental data unit	GHe	gaseous helium
EEE	electrical, electronic, and electromechanical (parts)	GH ₂	gaseous hydrogen
EEPROM	electrically erasable programmable read only memory	GHA	Greenwich hour angle
EGSE	electrical/electronic ground support equipment	GMT	Greenwich mean time
EIRP	effective isotropic radiated power	gpm	gallons per minute
ELV	expendable launch vehicle	GRT	germanium resistance thermometer
EMC	electromagnetic compatibility	GSE	ground support equipment
EOL	end of life	GSFC	Goddard Space Flight Center
EPS	electrical power system	GSTDN	Ground Spacecraft Tracking and Data Network
ESEO	equivalent square-edged orifice	GT	gimballed thruster
ESMCR	Eastern Space and Missile Center Requirements (See now Eastern and Western Range Safety Requirements (U.S. Air Force 30 th and 45 th Space Wings) Range Safety Office, Patrick Air Force Base, Florida.)	GTV	ground transport vehicle
ETR	Eastern Test Range	GV	gas valve
F	flow meter	H/C	honeycomb
FC	flight computer	HGA	high-gain antenna
FDF	flight dynamics facility	HPF	hazardous processing facility
FLTSATCOM	Fleet Satellite Communications System	HS	horizon sensor
FOV	field of view	Hz	hertz
FPR	flight performance reserve	ICD	interface control documents
FTS	flight termination system	i.d.	inner diameter
GDSSD	General Dynamics Space Systems Division	IE	interface electronics
GEO	geosynchronous Earth orbit	I/F	interface
		IIP	instantaneous impact points
		INU	inertial navigation unit
		I/O	input/output

IRU	inertial reference unit	LVMP	launch vehicle mission-peculiar
ISDS	inadvertent separation destruct system	MA	multiple access
ITO	indium tin oxide	MAX	maximum
J-T	Joule-Thomson	MBPS	millions of bits/sec
Kbps	thousand of bits/sec	MBytes	millions of bytes
KBytes	thousands of bytes	MDU	master data unit
KIPS	thousands of instructions/sec	MECO	main engine cutoff
KSA	K-band single access	MEOP	maximum effective operating pressure
KSC	Kennedy Space Center	MES	main engine start
LAD	liquid acquisition device	MG	magnetometer
LCC	launch control center	micro-g	microgravity, $0(10^{-6}g)$
Lc/D	ratio of the length of cylindrical section of a tank to its diameter	MID	maximum instantaneous deviation
L/D	length-to-diameter ratio; equivalent length of a flow resistance in pipe diameter	MIL STD	Military Standard
LEO	low-Earth orbit	MIPS	millions of instructions/seconds
LeRC	NASA Lewis Research Center	MLI	multilayer insulation
Lewis	NASA Lewis Research Center	MOD	modulator
LGA	low-gain antenna	MOP	maximum operating pressure
LH ₂	liquid hydrogen	MPT	mission planning terminal
LHe	liquid helium	MTBF	mean time between failure
LNA	low-noise amplifier	MUX	multiplexer
LRT	large receiver tank	NASA	National Aeronautics and Space Administration
LR	large receiver (tank)	NASCOM	NASA worldwide communications network
LRU	line replaceable unit	NCC	network control center
LSSM	launch services support manager	Ni-Cd	nickel cadmium (battery)
LV	launch vehicle	Ni-H ₂	nickel hydrogen (battery)
LVC	General Dynamics Launch Vehicle Contingency	N ₂ H ₄	hydrazine (propellant)
		NSI	NASA standard initiator

OA0	orbiting astrophysical observatory	RCS	reaction control system
OBC	onboard computer	RCTU	remote command and telemetry unit
o.d.	outer diameter	RCU	redundancy control unit
OPM	operational message	Re	Reynolds number, dimensionless number
OSHA	Occupational Safety and Health Administration	REF	shown for reference only
OSR	optical solar reflector	REM	rocket engine module
PCM	pulse code modulation (modulated)	RF	radiofrequency
PCU	power control unit	RMSD	root mean square deviation
PDA	propellant distribution assembly	ROM	read only memory
PDR	preliminary design review	RSS	root sum square
PDU	power distribution unit	RTD	resistance temperature detector
PLF	payload fairing	RUP	recorder utility processor
PN	pseudorandom noise	RV	relief valve
POCC	Payload Operations Control Center	SA	single access
PPF	payload processing facility	S/C	spacecraft
PRD	payload requirements document	SCU	sequence control unit
PRT	platinum resistance thermometer	SECO	sustainer engine cutoff
PSR	pre-ship review	SEU	single-event upset
PT	pressure transducer	SHP	ship
PTU	power transfer unit	SMFLT	simulated flight test
P/V	pressure vessel	SPS	samples per sec
Q/A	heat flux; heat transfer rate/area of MLI blanket	SRT	small receiver tank
R	gas pressure regulator	SS	Sun sensor
RAC	Research Analysis Center at NASA Lewis Research Center	SSA	S-band single-access
RADK	radiation conductor	SSF	Space Station Freedom
RAM	random access memory; read/write memory	SSR	solid-state recorder
		SSST	second-surface silverized Teflon

ST	supply tank	TT&C	telemetry, tracking, and command system
S/T	supply tank	TTY	teletype
STDN	Spaceflight Tracking and Data Network	TVS	thermodynamic vent system
STS	space transportation system	TYP	typical or typically (illustration shown in detail only once on figure but typically appears in other locations)
T	temperature; transducer	V	valve
TAC	telemetry and command processor	VD	vapor deposited
T ² C ²	Telemetry, Timing, Command, and Control (manufactured by Gulton Industries, Inc.)	VDA	vapor deposited aluminum
TCS	thermal control system	Vdc	volts dc
TDRS	tracking and data relay satellite	WDR	wet dress rehearsal
TDRSS	Tracking and Data Relay Satellite System	WSGT	White Sands Ground Terminal
TFL	tank fill level		
TGE	thruster gimbal electronics		

Appendix B

Symbols

\hat{A}	total projected area of spacecraft [ch. 4]	C_v	temperature coefficient (voltage) [ch. 10]
A	area of MLI blanket; cross-sectional area; heat path cross-sectional area; flow area; heat transfer area; area [ch. 5]	c	radius of strut [ch. 5]
\hat{A}_B	effective area, spacecraft body [ch. 4]	$C(T)$	the specific heat of stainless steel as a function of temperature [ch. 5]
A_{\min}	minimum column area needed to sustain applied load [ch. 6]	D	diameter of cylinder [ch. 4]; liquid jet diameter at liquid-vapor interface; major diameter; characteristic dimension; diameter of cylindrical section [ch. 5]
\hat{A}_{sa}	average projected area [ch. 4]	D_h	hydraulic diameter [ch. 5]
A_I	area of surface 1 [ch. 5]	d	duty cycle or percentage of time used (ratio of operating time to total time)
a	acceleration; dimension along strut [ch. 5]	d_{MLI}	MLI blanket thickness, m [ch. 5]
$a_o(i)$	desired level of acceleration along the i -th spacecraft axis taken to be the nominal axial thrust along the i -th axis divided by the spacecraft weight at the start of the experiment [ch. 7]	DOD	depth of discharge [ch. 10]
$a_i(i)$	instantaneous value of linear acceleration along the i -th spacecraft axis at time t [ch. 7, 11]	E	weld efficiency [ch. 5]; Young's modulus [ch. 5, 6]
A/m	area to mass ratio [ch. 4]	e	roughness [ch. 5]
Bo	Bond number	F	nondimensional flow characterization parameter [ch. 5]; thrust [ch. 7]
BRF	battery recharge factor [ch. 10]	F_{ij}	gray body factor, node i to node j
b	specific surface tension [ch. 5]	F_{12}	view factor from surface 1 to surface 2, the fraction of the energy leaving surface 1 which reaches surface 2 [ch. 5]
C	battery capacity, A-hr [ch. 10]; specific heat	f	friction factor [ch. 5]
CR	charge rate in terms of the battery capacity [ch. 10]	G	mass velocity [ch. 5]; gravitational constant [ch. 10]
C_i	temperature coefficient (current) [ch. 10]	GM_e	Earth gravitational constant [ch. 4]; $3.98601 \times 10^{14} \text{m}^3/\text{sec}^2$ [ch. 10]
C_L	specific heat of liquid [ch. 5]	g	acceleration of gravity; gravity constant [ch. 5]
C_p	specific heat [ch. 5]		

gpm	liquid hydrogen flow rate, gallons per minute [ch. 5]	K_b	cosine of incident angle of Sun line [ch. 10]
H	pressure rise across pump in feet of liquid; enthalpy [ch. 5]	K_d	radiation and thermal cycling loss; radiation and micrometeoroid loss [ch. 10]
H_s	the change in enthalpy caused by sensible heating of the vapor [ch. 5]	K_{PINS}	thermal conductivity of MLI pins, W/m-K [ch. 5]
H_v	the enthalpy of vaporization [ch. 5]	K_s	seasonal variation in solar intensity [ch. 10]
h	heat transfer coefficient; specific enthalpy [ch. 5]	k	material thermal conductivity; thermal conductivity; constant; liquid conductivity; turbine flowmeter calibration constant [ch. 5]
h_g	two-phase heat transfer coefficient; convective heat transfer coefficient for hydrogen gas [ch. 5]	k_w	thermal conductivity [ch. 5]
h_L	convective heat transfer coefficient for hydrogen liquid; liquid heat transfer coefficient [ch. 5]	L	length of cylinder [ch. 4]
h_I	loss of static pressure head caused by fluid flow, feet of liquid [ch. 5]	L	heat path length; heat path length through MLI; length of strut [ch. 5]
I	moment of inertia [ch. 5]; cell current [ch. 10]	L/D	length-to-diameter ratio; equivalent length of a flow resistance in pipe diameter [ch. 5]
I_{min}	minimum column moment of inertia to resist buckling [ch. 6]	Lc/D	length of cylindrical section of tank (end caps excluded) [ch. 5]
I_{mp}	beginning of life cell current at maximum power operating point [ch. 10]	l	distance of the center of gravity from the rear of the spacecraft [ch. 7]
I_{rc}	recharge current [ch. 10]	M	total bending moment [ch. 5]
I_{SC}	spacecraft inertia matrix [ch. 7]; cell short circuit current [ch. 10]	M_p	pressurant mass
I_t	required current per array [ch. 10]	M_{eol}	end of life (EOL) mass [ch. 4]
I_W	reaction wheel inertia [ch. 7]	M_{max}	bending moment [ch. 5]
$I_{xx,yy,zz}$	spacecraft principal moments of inertia [ch. 4]	M_e	mass of the Earth [ch. 10]
$I_{xy,yz,yz}$	spacecraft products of inertia [ch. 4]	M_t	transfer line mass [ch. 5]
I_{xx}	area moment of inertia [ch. 5]	\dot{m}	mass flow rate [ch. 5]
K	resistance coefficient or velocity head loss; MLI conductivity; material thermal conductivity; MLI effective thermal conductivity [ch. 5]	Max	maximum value function [ch. 7]
K_d	assembly loss [ch. 10]	$MEOP$	maximum effective operating pressure [ch. 5]
		$MID(i)$	maximum instantaneous deviation along the i -th spacecraft axis [ch. 7]
		M/V	thermal-mass-to-volume ratio [ch. 5]
		mV/T	millivolts/degree [ch. 5]

N	blanket density, sheets/cm [ch. 5]	Q/A	heat flux, (Btu/hr-ft ²); heat transfer rate/area of MLI blanket
N_p	required number of cells in parallel [ch. 10]	R	radius of tank [ch. 5]; reliability
N_s	number of radiation shields [ch. 5]; number of required series solar cells [ch. 10]	R	magnitude of position vector [ch. 4]
P	design pressure; axial load on strut; internal pressure; pressure [ch. 5]; applied load to column; load power, W [ch. 10]	R_e	radius of Earth, 6.3783×10^3 km [ch. 10]
P_{CR}	theoretical maximum load that an initially straight column can support without buckling [ch. 6]	R_j	liquid jet radius at liquid-vapor interface [ch. 5]
P_{dc}	discharge power, W [ch. 10]	$R_{x,y,z}$	elements of spacecraft position vector [ch. 4]
P_{LR}	large receiver tank weight divided by four [ch. 5]	r_u	distance from wall to ullage [ch. 5]
P_{MLI}	MLI weight	r	characteristic length of the tank (usually tank radius); radial distance [ch. 5]; orbit altitude plus radius of Earth, R_e [ch. 10]
P_{rc}	battery recharge power [ch. 10]	Re	Reynolds number [ch. 5]
P_{SR}	small receiver tank weight divided by four [ch. 5]	$RMSD(i)$	root mean square deviation along the i -th axis [ch. 7]
P_{ST}	supply tank load on strut; vaporizer weight [ch. 5]	Ro	nozzle exit radius [ch. 5]
p_w	wetted perimeter [ch. 5]	Ro	ice point resistance [ch. 5]
Pr	Prandtl number [ch. 5]	S	stress [ch. 5]
Q	total heat flux; heat flux, W/m ² ; heat transfer rate [ch. 5]	$S_{YLD/ULT}$	allowable strength of column material, either yield or ultimate [ch. 6]
$Q_{CORRECTION}$	Q caused by pins through LMI + Q caused by seams [ch. 5]	T	orbit period [ch. 7]; period in seconds [ch. 10]; temperature
Q_{IDEAL}	Q caused by linear conduction + Q caused by radiation [ch. 5]	T_c	material cold side temperature; temperature of receiver MLI can (assumed equal to supply tank can temperature); blanket cold temperature [ch. 5]
Q_{PINS}	heat flux through pins [ch. 5]	T_f	final tank pressure [ch. 5]
Q_{RAD}	MLI heat flux via radiation [ch. 5]	T_H	material hot side temperature; blanket hot temperature; obtained from external spacecraft thermal modeling data [ch. 5]
Q_{SEAMS}	MLI seam heat flux via radiation [ch. 5]	T_i	initial tank temperature [ch. 5]
Q_{SOLID}	MLI heat flux due to conduction [ch. 5]	T_y	torque about the y-axis [ch. 7]
Q_{TOTAL}	total MLI heat flux [ch. 5]	T_z	torque about the z-axis [ch. 7]

T_1	initial transfer line temperature [ch. 5]	Z	section modulus [ch. 5]
T_2	final transfer line temperature [ch. 5]	α/ϵ	sunlight absorbtivity/infrared emmisivity
t	time: wall thickness [ch. 5]; discharge time, hr [ch. 10]; life units (either time in hours or cycles) [ch. 16]	β	beta angle (angle between orbit plane and Sun line [ch. 4]; specific surface tension [ch. 5]
t_{dc}	discharge time, min [ch. 10]	ΔT	hot-side to cold-side temperature difference [ch. 5]
t_s	fraction of Sun time/orbit [ch. 10]	ϵ	emissivity of surface 1 [ch. 5]
t_{rc}	recharge time, min [ch. 10]	ϵ_i	infrared emittance of node i [ch. 5]
U	overall heat transfer coefficient [ch. 5]	η_b	battery efficiency [ch. 10]
u	specific internal energy	θ	gimbal angle [ch. 7]; mean time between failure, hr [ch. 16]
V	velocity [ch. 5]	λ	failure rate per hour or cycle
V_d	wiring loss per cell [ch. 10]	λ_T	total failure rate
V_{dc}	cell discharge voltage [ch. 10]	λ_{op}	operating failure rate
V_{db}	bus voltage, V [ch. 10]	λ_{nop}	nonoperating failure rate
V_{oc}	cell open circuit voltage	μ	GM_e = Earth gravitational constant [ch. 4]; viscosity [ch. 5]
V_{mp}	BOL cell voltage at maximum power operating point [ch. 10]	μV	microvolts
V_{rc}	cell recharge voltage [ch. 10]	ρ	liquid density [ch. 5]
v	velocity of flow, ft/sec; nozzle exit radius [ch. 5]; cell voltage [ch. 10]	σ	surface tension; Stefan-Boltzmann constant [ch. 5]
W	load perpendicular to strut; width [ch. 5]	τ_w	wall thickness [ch. 5]
We	Weber number [ch. 5]	$\tau_{x,y,z}$	elements of spacecraft torque vector [ch. 4]
X	quality [ch. 5]	v	mean velocity of flow, ft/sec [ch. 5]
x	distance from heat exchanger internal to LAD [ch. 5]	v	nozzle exit velocity [ch. 5]

Appendix C

Bibliography

- Abramson, N.: The Dynamic Behavior of Liquids in Moving Containers with Applications to Space Vehicle Technology. NASA SP-106, 1996.
- Adams, N.; and Bollenbacher, G.: COLD-SAT Dynamic Model. NASA TM-105185, 1992.
- Agrawal, B.N.: Design of Geosynchronous Spacecraft. Prentice-Hall, Englewood Cliffs, 1986.
- Arif, H.: Preliminary Thermal Design of the COLD-SAT Spacecraft. AIAA Paper 91-1305, June 1991 (also NASA TM-104440, 1991).
- Arif, H.: Spacecraft Attitude Impacts on COLD-SAT Non-Vacuum Jacketed L_{H2} Supply Tank Thermal Performance. AIAA Paper 90-1672, June 1990 (also NASA TM-103158, 1990).
- Arif, H.: Thermal Aspects of Design for the COLD-SAT Non-Jacketed Supply Tank Concept. AIAA Paper 90-2059, 26th AIAA/SAE/ASME/ASEE Joint Propulsion Conference and Exhibit, Orlando, Florida, July 1990.
- Arif, H.; and Kroeger, E.W.: COLD-SAT: A Technology Satellite for Cryogenic Experimentation. NASA TM-102286, 1989.
- ASME Boiler and Pressure Vessel Code, Section VIII, Rules for Construction of Pressure Vessels, Division I. ANSI/ASME BPV-VIII-1. The American Society of Mechanical Engineers, New York, July 1980.
- Atlas I Configuration, Performance, and Weight Status Report (Reference GT0 Mission): General Dynamics Space Systems Division, March, 1988.
- Atlas IIA Configuration, Performance, and Weight Status Report (Reference GT0 Mission): General Dynamics Space Systems Division, December 1989.
- Aydellott, J.C.: Effect of Gravity on Self-Pressurization of Spherical Liquid Hydrogen Tankage. NASA TN D-4286, December 1967.
- Aydellott, J.C.: Modeling of Space Vehicle Propellant Mixing—Cryogenic Propellants. NASA TP-2107, 1983.
- Aydellott, J.C.: Normal Gravity Self-Pressurization of 9-inch (23 cm) Diameter Spherical Liquid Hydrogen Tankage. NASA TN D-4171, 1967.
- Aydellott, J.C.; Carney, J.J.; and Hochstein, J.I.: NASA Lewis Research Center Low-Gravity Fluid Management Technology Program. NASA TM-87145, 1985.
- Aydellott, J.C.; and Devol, W., eds.: Cryogenic Fluid Management Technology Workshop, vols. 1 and 2. NASA CP-10001 and NASA CP-10009, 1987.
- Aydellott, J.C.; and Rudland, R.S.: Technology Requirements to be Addressed by the NASA Lewis Research Center Cryogenic Fluid Management Facility Program. AIAA Paper 85-1229, July 1985 (also NASA TM-87048, 1985).
- Bailey, W.J.: The COLD-SAT Program: Advances in Cryogenic Experimentation, vol. 35B, Proceedings of the 1989 Cryogenic Engineering Conference, Plenum Press, 1990, pp. 1669-1680.
- Bailey, W.J.: COLD-SAT Program, presented at the Cryogenic Engineering Conference, Paper DC-03, Los Angeles, July 24-28, 1989.
- Bailey, W.J., et al.: Cryogenic On-Orbit Liquid Depot Storage, Acquisition and Transfer Satellite (COLD-SAT) Feasibility Studies (Martin Marietta Astronautics Group). NASA CR-185247, 1990.
- Barron, R.F.: Cryogenic Systems. Oxford University Press, New York, 1985.
- Bowles, E.B.; Dodge, F.T.; and Green, S.T.: Scaling Trades Study of the Cryogenic Fluid Management Flight Experiment. Final contract report, AC-86-002, Southwest Research Institute, October 1987.
- Bullard, B.R.: Cryogenic Tank Support Evaluation. NASA CR-72546, 1969.
- Cady, E.C.: Study of Thermodynamic Vent and Screen Baffle Integration for Orbital Storage and Transfer of Liquid Hydrogen. NASA CR-134482, 1973.
- Caine, G.H.; and Pradhan, A.V.: Pumps or Fans for Destratification of Hydrogen Liquid and Gas—Proceedings of the Advances in Cryogenic Engineering, vol. 13, Plenum Press, New York, 1968, pp. 728-738.
- Carter, J.S.; and Timberlake, T.E.: Filament Wound, Fiberglass Cryogenic Tank Supports. NASA CR-120828, 1971.
- Centaur Flight Performance Reserve Predictions; General Dynamics Space Systems Division Interoffice Memo 887-TP-86-078, from Trajectory and Performance, Dept 887-0 to J. Andrews, September 11, 1986.
- Chau, H.; and Moy, H.C.: Thermal Characteristics of Multilayer Insulation. AIAA Paper 70-850, 1970.
- Chen, J.C.: Boiling Heat—Transfer Coefficients for Saturated Nonmetallic Fluids in Convective Flow. ASME 63-HT-34, 1963.
- Chetty, P.R.K.: Satellite Technology and Its Applications. Tab Books Inc., Blue Ridge Summit, Pennsylvania, 1988.
- Crafts, J.L.; and Lindberg, J.P.: Procedure for Estimating Orbital Debris Risks. NASA TP-2507, 1985.
- Delta II Commercial Spacecraft Users Manual, MDC H3224, McDonnell-Douglas Astronautics Company, July 1987.
- Design Criteria For Spacecraft Solar Cell Arrays: Spacecraft Solar Cell Arrays. NASA SP-8074, 1971.
- DeWitt, R.L.; and Mellner, M.B.: Experimental Evaluation of a Purged Substrate Multilayer Insulation System for Liquid Hydrogen Tankage. NASA TN D-6331, 1971.
- Dittus, F.W.; and Boelter, L.M.K.: Heat Transfer in Automotive Radiators of the Tubular Type. University of California Publications in Engineering, vol. 2, no. 13, 1930, pp. 443-461.
- Drago, V.J.; and Edgecombe, D.S.: A Review of NASA Orbital Decay Reentry Debris Hazard, Appendix A. BMI-NLVP-TM-74-1, Battelle Columbus Laboratories, March 7, 1974.
- Eastern and Western Range ESMCR 127-1 Range Safety Requirements (US Air Force 30th Space Wing and US Air Force 45th Space Wing). Range Safety Office, Patrick Air Force Base, Florida, March 31, 1995.
- Eberhardt, R.N., et al. (Martin Marietta Aerospace, Bethesda, MD): Cryogenic Fluid Management Experiment. NASA CR-165495, 1981.
- Eberhardt, R.N., et al. (Martin Marietta Aerospace, Denver, CO): Cryogenic Fluid Management Facility Concept Definition Study (CFMF). NASA CR-174630, 1983.
- Eberhardt, R.N., et al. (Martin Marietta Aerospace, Denver, CO): Cryogenic Fluid Management Facility. AIAA Paper 84-1340, 1984.
- Edwards, L.G. (Analex Corp.) Cryogenic On-Orbit Liquid Depot Storage Acquisition and Transfer (COLD-SAT) Experiment Subsystem Instrumentation and Wire Harness Design Report. NASA CR-189172, 1992.
- Epstein, M.: Prediction of Liquid Hydrogen and Oxygen Pressurant Requirements. Adv. Cryo. Eng., vol. 10, Plenum Press, New York, 1965, p. 303.
- Flow of Fluids Through Valves, Fittings, and Pipe. Crane Co., Chicago, 1965.
- Fredrickson, G.O.; and Schweikle, J.D.: Project Thermo—Phase B Prime. NASA CR-88712, 1967.
- Gates Energy Products Applications Manual (Preliminary). Sealed Rechargeable Batteries, 1982, pp. 33, 89, 101, 112.
- Glover D.: NASA Cryogenic Fluid Management Space Experiment Efforts, 1960-1990. AIAA Paper 91-3538, 1991 (also NASA TM-103752, 1991).
- Goddard Space Flight Center, Space Network (SN) Users Guide, STDN no. 101.2, rev. 6, 1988.

- GOES-I Configuration, Performance, and Weight Status Report. General Dynamics Space Systems Division, December 1989.
- Hands, B.A. (ed.): *Cryogenic Engineering*. Academic Press, Orlando, 1986.
- Hawkins, K.: *Space Vehicle and Associated Subsystem Weight Growth*. SAWE Paper 1816, 1988.
- Hawks, K.H.: *A Radiometric Investigation of Emissivities and Emittances of Selected Materials*. University Microfilms, 1970.
- Hopkins, R.A.: *Design of a One-Year Lifetime, Spaceborne Superfluid Helium Dewar*. ASME Paper 79-ENAS-23, 1979.
- Hopkins, R.A., et al.: *Next-Generation Tension Strap Supports for Spaceborn Dewars*. AIAA 87-1500, 1987.
- Hopkins, R.A.; and Castles, S.H.: *Design of the Superfluid Helium Dewar for the Cosmic Background Explorer (COBE)*. *Cryogenic Optical Systems and Instruments Meeting Proceedings*. The International Society for Optical Engineering, San Diego, CA, August 23, 24, 1984, 1985, pp. 207-215.
- Hopkins, R.A.; and Payne, D.A.: *Optimized Support Systems for Spaceborn Dewars*. *Cryogenics*, vol. 27, Butterworth & Co., April 1987.
- Hopkins, R.A.; and Payne, D.A.: *Thermal Performance of the Cosmic Background Explorer Superfluid Helium Dewar, As Built and with an Improved Support System*. *Advances in Cryogenic Engineering*, vol. 33, Plenum Press, New York, 1988, pp. 925-933.
- Hydrogen Thermal Test Article, Thermal Design Report. NASA CR-147545, 1971.
- Jacobs, R.B.: *Liquid Requirements for the Cool-Down of Cryogenic Equipment*. *Adv. Cryo. Eng.*, vol. 8, Plenum Press, New York, 1963, p. 529.
- Jetty, R.L.; and Scarlotti, R.D.: *Space Station Experiment Definition: Long-Term Cryogenic Fluid Storage*. NASA CR-4072, June 1987.
- Jewett, R.P.; Walter, R.J.; Chandler, W.T.; and Frohberg, R.P.: *Hydrogen Environment Embrittlement of Metals*. NASA CR-2163, 1973.
- Johnson, V.J. (ed.): *A Compendium of the Properties of Materials at Low Temperature (Phase I)*. Wright Air Development Division Technical Report 60-56 Part II, October 1960.
- Juran, J.M.: *Quality Control Handbook*. 4th. Ed. McGraw-Hill, New York, 1988.
- Keller, C.W.; Cunningham, G.R.; and Glassford, A.P.: *Thermal Performance of Multilayer Insulation—Gas Evacuation in Characteristics of Three Selected Multilayer Insulation Composites*. NASA CR-13477, 1974.
- King-Hele, D.G.: *Satellite Orbits in an Atmosphere: Theory and Applications*. Blackie and Son, Ltd., Glasgow, 1987.
- Knight, M.; Schwartzberg, F.R., et al.: *Cryogenic Materials Data Handbook*, vol. 1. Air Force Materials Laboratory Technical Documentary Report, AFML-TDR-64-280, vol. 1 (Revised 1970), July 1970.
- Knoll, R.H.; MacNeil, P.N.; and England, J.E.: *Design, Development, and Test of Shuttle/Centaur G-Prime Cryogenic Tankage Thermal Protection Systems*. NASA TM-89825, 1987.
- Knozok, H.-G., et al.: *Battery Thermal Design and Performance in European Geo-Satellite Programs*. SAE Paper 871484, *Proceedings of the 17th Intersociety Conference on Environmental Systems*, 1987.
- Lee, J.H., et al.: *Cryogenic and Thermal Design for the Superfluid Helium On-Orbit Transfer (SHOOT) Experiment*. *Advances in Cryogenic Engineering*, vol. 33, Plenum Press, New York, 1988, pp. 901-908.
- Lee, J.H.: *Space Infrared Telescope Facility (SIRTF) Design and Thermal Analysis*. *Cryogenic Fluid Management Technology Workshop*, vol. 1, 1987, pp. 193-220.
- Linden, D.: *Handbook of Batteries and Fuel Cells*. McGraw-Hill, New York, 1984.
- Maloy, J.E.; and Sumner, I.E.: *Transient Thermal Performance of Multilayer Insulation Systems During Simulated Ascent Pressure Decay*. NASA TN D-6335, 1971.
- Martin Marietta Space Systems, Inc.: *Cryogenic Orbital Nitrogen Experiment (CONE) Design Study*. NASA Contract NAS3-25063; September 19, 1990.
- McCarty, R.D.: *Hydrogen Technology Survey: Thermophysical Properties*. NASA SP-3089, 1975.
- McCarty, R. D.: *Thermophysical Properties of Helium 4 from 4 to 3000°R with Pressures to 15000 psia*. NBS Tech. Note 622, September 1972.
- McHenry, S. T.; and Yost, J.M. (Analex Corporation): *COLD-SAT Feasibility Study Safety Analysis*. NASA CR-187042, 1991.
- MIL-HDBK-217E NOTICE 1 (1990). *Reliability Prediction of Electronic Equipment*. US Department of Defense, Naval Publications and Forms Center, Philadelphia.
- MIL-HDBK-338-1A. (1988). *Electronic Reliability Design Handbook*. US Department of Defense, Naval Publications and Forms Center, Philadelphia.
- MIL-STD-461D (1996) *Requirements for the Control of Electromagnetic Interference and Susceptibility*. US Department of Defense, Naval Publications and Forms Center, Philadelphia.
- MIL-STD-721C (1981). *Definitions of Terms for Reliability and Maintainability*. US Department of Defense, Naval Publications and Forms Center, Philadelphia.
- MIL-STD-756B (1981). *Reliability Modeling and Prediction*. US Department of Defense, Naval Publications and Forms Center, Philadelphia.
- MIL-STD-785B NOTICE 1 (1986). *Reliability Program for Systems and Equipment Development and Production*.
- MIL-STD-975M (2) (1995). *NASA Standard Electrical, Electronic, and Electromechanical (EEE) Parts List*. US Department of Defense, Naval Publications and Forms Center, Philadelphia.
- MIL-STD-1553B (8 Sept. 1986). *US Department of Defense, Naval Publications and Forms Center, Philadelphia*.
- Mission Planners Guide for the Atlas Launch Vehicle Family*. General Dynamics Commercial Launch Services, Inc., March 1989.
- Models of Earth's Atmosphere (90 to 2500 km)*. NASA SP-8021, Revised March 1973.
- Moore, R.W.; et al.: *Gas Pressurized Transfer of Liquid Hydrogen*. *Adv. Cryo. Eng.*, vol. 5, Plenum Press, New York, 1960, p. 450.
- Morris, E.E.: *Filament Wound Composite Thermal Isolator Structures for Cryogenic Dewars and Instruments*. ASTM, 1982.
- MSFC Specification: *Connector, Electrical, Circular, Cryogenic Environment Resisting*. Drawing Number 40M38294, Marshall Space Flight Center, May 25, 1973.
- NASA Safety Policy and Requirements Document. NHB 1700.1, vol. B. NASA Headquarters, June 1993.
- NASA Software Management Requirements for Flight Projects. NMI 2410.10, January 22, 1992.
- Nonelectronic Parts Reliability Data (NPRD-3), Reliability Analysis Center, Griffiss AFB, NY 13441, Fall 1985.
- O'Connor, P.D.T.: *Practical Reliability Engineering*. 2nd. ed. John Wiley & Sons, New York, 1985.
- Oxygen Thermal Test Article, Final Design and Test Report. NASA CR-140309, 1974.
- Parnley, R.T.: *Passive Orbital Disconnect Strut (PODS III) Structural Test Program*. NASA CR-177325, 1985.
- Rauschenbach, H.S.: *Solar Cell Array Design Handbook*, vol. 1. NASA CR-149364, 1976.
- Reliability Program Requirements for Aeronautical and Space System Contractors*. NASA, NHB 5300.4(1A-1), 1987.
- Rohsenow, W.M.; and Hartnett, J.P.: *Handbook of Heat Transfer*. McGraw-Hill, New York, 1973.
- Rudland, F.S.; Gille, J.P.; Eberhardt, R.N. (Martin Marietta Corporation, Denver, CO): *Liquid Hydrogen Pressurization, Venting, and Resupply in Low-g*. AIAA Paper 86-1251, 1986.
- Rybak, S.C., et al.: (Ball Aerospace Systems Group with McDonnell Douglas Space Systems Company and Boeing Aerospace and Electronics). *Depot-Storage, Acquisition and Transfer (COLD-SAT) Satellite, Feasibility Study*. NASA CR-185248, 1990.
- Schuster, J.R.; Bennett, F.O.; and Wachter, J.P.: *COLD-SAT Orbital Experiment Configured for Atlas Launch*, presented at the Cryogenic Engineering Conference, Paper DC-02, Los Angeles, July 24-28, 1989.

- Schuster, J.R.; Russ, E.J.; and Wachter, J.P.: (General Dynamics Space Systems Division with Ford Aerospace Space Systems Division), Cryogenic On-Orbit Liquid Depot Storage, Acquisition and Transfer (COLD-SAT) Feasibility Study Final Report. NASA CR-185249, 1990.
- Schuster, J.R.; Wachter, J.P.; and Powers, A.G.: COLD-SAT, An Orbital Cryogenic Hydrogen Technology Experiment. NASA TM-102303, 1989.
- Shah, M.M.: Prediction of Heat Transfer During Boiling of Cryogenic Fluids Flowing in Tubes. *Cryogenics*, 24, May 1984.
- Shuttle/Centaur Functional Requirements Document SC1114-2. General Dynamics Convair Division.
- Sorensen, G.L.; Niggemann, R.E.; Bassett, L.E.; and Sedillo, M.: A Zero-Gravity Thermodynamic Vent System for the Shuttle/Centaur Hydrogen Tank. Intersociety Conference on Environmental Systems, July 1984.
- Spacecraft Magnetic Torques, NASA SP-8018, pp. 6, 14, 1969.
- Steward, W.G.: Transfer Line Surge. *Adv. Cryo. Eng.*, vol. 10, Plenum Press, New York, 1965, p. 313.
- Stochl, R.J.; Masters, P.A.; DeWitt, R.L.; and Maloy, J.E.: Gaseous-Hydrogen Pressurant Requirements for the Discharge of Liquid Hydrogen from a 1.52-meter-(5-ft-) Diameter Spherical Tank. NASA TN D-5336, 1969.
- Stochl, R.J.; Masters, P.A.; DeWitt, R.L.; and Maloy, J.E.: Gaseous-Hydrogen Requirements for the Discharge of Liquid Hydrogen from a 3.96-meter-(13-ft-) Diameter Spherical Tank. NASA TN D-5387, 1969.
- Sumner, I.E.: Degradation of a Multilayer Insulation Due to a Seam and a Penetration. NASA TN D-8229, 1976.
- Sumner, I. E.: Liquid Propellant Reorientation in a Low-Gravity Environment. NASA TM-78969, 1978.
- Sumner, I.E.: Low-Density Foam for Insulating Liquid-Hydrogen Tanks. NASA TN D-5114, 1968.
- Sumner, I.E.: Thermal Performance of Gaseous-Helium Purged Tank-Mounted Multilayer Insulation System During Ground-Hold and Space-Hold Thermal Cycling and Exposure to Water Vapor. NASA TP-1114, 1978.
- Sumner, I.E.; and Maloy, J.E.: Transient Thermal Performance of Multilayer Insulation Systems During Simulated Ascent Pressure Decay. NASA TN D-6335, 1971.
- Swann, R.T.; and Pittman, C.M.: Analysis of Effective Thermal Conductivities of Honeycomb-Core and Corrugated-Core Sandwich Panels. NASA TN D-714, 1961.
- Symons, E.P.: Outlet Baffles: Effect on Liquid Residuals From Zero-Gravity Draining of Hemispherically Ended Cylinders. NASA TM X-2631, 1972.
- Symons, E.P.: Wicking of Liquids in Screens. NASA TN D-7657, 1974.
- Takeno, M., et al.: Thermal and Mechanical Properties of Advanced Composite Materials at Low Temperatures.
- Tegart, J.; and Dominick, S.: Collapse of Large Vapor Bubbles. D.H. Lecroissette, ed. *Proceedings of the Second International Colloquium on Drops and Bubbles*; NASA CR-168848, 1982.
- Thermal Performance of Multilayer Insulation. NASA CR-134477, 1974.
- Thermodynamic Models for Bounding Pressurant Mass Requirements of Cryogenic Tanks. *Advances in Cryogenic Engineering*, vol. 39B; P. Kittel, ed., Plenum Press, New York, 1994.
- Touloukian, Y.S., et al.: Tables of Thermophysical Properties of Materials. Final report, ML-TDR-64-184, 1964.
- VanDresar, N.T.: Two Simple Pressurization Analyses Applicable to Partially Filled and Emptied Liquid Hydrogen Tankage. NASA TM to be published.
- Van Gundy, D.A.; and Uglam, J.R.: Heat Transfer to an Uninsulated Surface at 20 K. *Advances in Cryogenic Engineering*, vol. 7; K.D. Timmerhaus ed., Plenum Press, New York, 1962, pp. 377-384.
- Vreeburg, J.B.; Delil, A.A.M.; and Heemskerk, J.F.: Handbook for the Thermal Modelling of Space Mechanisms by the Nodal Network Method. ESRO CR-219.
- Weast, Robert C. (ed.): *CRC Handbook of Chemistry and Physics*. CRC Press, Florida, 1986 (p. F-141, "US Standard Atmosphere (1976).", NOAA, NASA, USAF).
- White, F.M.: *Fluid Mechanics*. McGraw Hill, New York, 1979.
- Willen, G.S.; Riemer, D.H.; and Hustvedt, D.C. (Beech Aircraft Corporation, Boulder, CO): Conceptual Design of an In-Space Cryogenic Fluid Management Facility. NASA CR-165279, 1981.
- Williams, G.E.; and Schuster, J.R.: Thermal Design Considerations for the Cryogenic On-Orbit Liquid Depot Storage, Acquisition and Transfer Satellite (COLD-SAT). AIAA Paper 90-0057, 1990.
- Young, R.S.: *Formulas for Stress and Strain*. McGraw Hill, 1989.

REPORT DOCUMENTATION PAGE			Form Approved OMB No. 0704-0188	
Public reporting burden for this collection of information is estimated to average 1 hour per response, including the time for reviewing instructions, searching existing data sources, gathering and maintaining the data needed, and completing and reviewing the collection of information. Send comments regarding this burden estimate or any other aspect of this collection of information, including suggestions for reducing this burden, to Washington Headquarters Service, Directorate for Information Operations and Reports, 1215 Jefferson Davis Highway, Suite 1204, Arlington, VA 22202-4302, and to the Office of Management and Budget, Paperwork Reduction Project (0704-0188), Washington, DC 20503.				
1. AGENCY USE ONLY (Leave blank)	2. REPORT DATE December 1998	3. REPORT TYPE AND DATES COVERED Technical Paper		
4. TITLE AND SUBTITLE Cryogenic On-Orbit Liquid Depot-Storage, Acquisition and Transfer (COLD-SAT) Experiment Conceptual Design and Feasibility Study		5. FUNDING NUMBERS WU-506-48-00-00		
6. AUTHOR(S) Edward Kramer, Editor				
7. PERFORMING ORGANIZATION NAME(S) AND ADDRESS(ES) National Aeronautics and Space Administration Lewis Research Center Cleveland, Ohio 44135-3191		8. PERFORMING ORGANIZATION REPORT NUMBER E-9130		
9. SPONSORING/MONITORING AGENCY NAME(S) AND ADDRESS(ES) National Aeronautics and Space Administration Washington, DC 20546-0001		10. SPONSORING/MONITORING AGENCY REPORT NUMBER NASA TP-3523		
11. SUPPLEMENTARY NOTES Responsible person, Edward Kramer, NASA Lewis (now retired), (440) 734-5085.				
12a. DISTRIBUTION/AVAILABILITY STATEMENT Unclassified - Unlimited Subject Categories 15, 18, 20 and 28 This publication is available from the NASA Center for Aerospace Information, (301) 621-0390.			12b. DISTRIBUTION CODE Distribution: Non-standard	
13. ABSTRACT (Maximum 200 words) The cryogenic fluid management technologies required for the exploration of the solar system can only be fully developed via space-based experiments. A dedicated spacecraft is the most efficient way to perform these experiments. This report documents the extended conceptual design of the COLD-SAT spacecraft, capable of meeting these experimental requirements. All elements, including the spacecraft, ground segment, launch site modifications and launch vehicle operations, and flight operations are included. Greatly expanded coverage is provided for those areas unique to this cryogenic spacecraft, such as the experiment system, attitude control system, and spacecraft operations. Supporting analyses are included as are testing requirements, facilities surveys, and proposed project timelines.				
14. SUBJECT TERMS Cryogenic fluids; Cryogenic fluid storage; Cryogenic rocket propellants; Experiment design; Fluid dynamics; Microgravity applications; Liquid hydrogen; Spacecraft design			15. NUMBER OF PAGES 601	
			16. PRICE CODE A99	
17. SECURITY CLASSIFICATION OF REPORT Unclassified	18. SECURITY CLASSIFICATION OF THIS PAGE Unclassified	19. SECURITY CLASSIFICATION OF ABSTRACT Unclassified	20. LIMITATION OF ABSTRACT	